F 1103

ACADÉMIE DE LA RÉPUBLIQUE SOCIALISTE DE ROUMANIE

R

REVUE ROUMAINE DE CHIMIE

REFERÁLVA

TOME 27

N° 1

Janvier 1982

EDITURA ACADEMIEI REPUBLICII SOCIALISTE ROMÂNIA

Rev. Roumaine Chim.

RRCHAX, 27, *1*, p. 1–166 (1982), Bucarest

ACADÉMIE DE LA RÉPUBLIQUE SOCIALISTE DE ROUMANIE

COMITÉ DE RÉDACTION

Rédacteur en chef:

I. G. MURGULESCU, membre de l'Académie de la République Socialiste de Roumanie

Rédacteurs en chef adjoints:

A. T. BALABAN et V. EM. SAHINI, membres correspondants de l'Académie de la République Socialiste de Roumanie

Collège de rédaction:

EM. BRATU, ELENA CEAUȘESCU, ECATERINA CIORĂNESCU-NENITZESCU, CR. SIMIONESCU, membres de l'Académie de la République Socialiste de Roumanie ; P. SPACU, membre correspondant de l'Académie de la République Socialiste de Roumanie ; MARGARETA AVRAM, M. BANCIU, I. HAIDUC, D. I. MARCHIDAN, I. MOLDOVAN, G. NIAC et D. SĂNDULESCU

La Revue Roumaine de Chimie paraît 10 fois par an. Toute commande de l'étranger pour les travaux parus aux Editions de l'Académie de la République Socialiste de Roumanie sera adressée à ILEXIM, Departamentul Export-Import Carte (Livres)/Departamentul Export-Import Presă (Revues), P.O.B. 136—137, télex 11226, 3, str. 13 Decembrie, 79517 Bucarest, Roumanie

Les manuscrits, les livres et les revues proposés en échange, ainsi que toute correspondance seront envoyés à la rédaction :

REVUE ROUMAINE DE CHIMIE

125, Calea Victoriei 79717 Bucarest, Roumanie, téléphone 50 76 80

EDITURA ACADEMIEI REPUBLICII SOCIALISTE ROMÂNIA

125, Calea Victoriei, 79717 Bucarest, Roumanie, téléphone 50 76 80

ORSZÁGOS MŰSZAKI KÖNYVTÁR ÉS DOKUMENTÁCIÓS KÖZP.
1883

REVUE ROUMAINE DE CHIMIE

Tome 27, Nº 1 **Janvier, 1982**

A COLLECTION OF PAPERS DEDICATED TO PROFESSOR I. G. MURGULESCU ON HIS 80th BIRTHDAY JANUARY 27, 1982

Edited by Dr. D. I. MARCHIDAN, Prof. V. Em. SAHINI and Prof. A. T. BALABAN

Tribute to Professor I. G. MURGULESCU on his 80th birthday, 27th January 1982 3–6
Publications of Professor I. G. MURGULESCU . . . 7–17
M. BANCIU, M. ELIAN, PHAN LE THUY, C. DRĂGHICI and ECATERINA CIORĂNESCU, Synthesis and pyrolysis of dibenzo[*c*,*e*]tricyclo[5.3.0.$0^{2,10}$]deca-3,5,8-triene, a new dibenzo$(CH)_{10}$ hydrocarbon 19–26
EMIL CHIFU, MARIA TOMOAIA-COTIȘEL and ANCA IOANETTE, Mixed films of retinyl palmitate with lipids at the air – water interface . . . . 27–35 R
VASILE COCHECI, LUCIAN NEGULESCU, FRANCISC KLEPP, Contributions to the calculation of ion exchange equilibrium in water demineralization process 37–45
ELENA CONSTANTINESCU and HILDEGARD DENGEL, Thermogalvanic cells with aqueous rubidium chloride solutions (in German) . . . . . . 47–54 Bel
IULIA CONTINEANU, DAN BREȚCANU and D.I. MARCHIDAN, The enthalpies of combustion and formation of 3-amino-4-methoxyacetanilide and 3-(N-β-cyanoethyl)-amino-4-methoxyacetanilide 55–58
CR. CONȚESCU and M. I. VASS, On the dipole moment of Cu, Ag and Au atoms adsorbed on different tungsten planes 59–67
J. HERDAN, G. IORDACHE, N. NEGOIȚĂ, NICOLETA GRECU and A. T. BALABAN, New 2,4,6-trisubstituted phenols and their corresponding aroxyls 69–73
N. I. IONESCU and MONICA CĂLDĂRARU, Propylene oxidation on MoO_3/SiO_2 and Bi_2O_3/SiO_2 catalysts . . . . 75–79 R
SOFIA MARCHIDAN, IULIANA VARTIRES and N. D. TOTIR, Determination of trace quantities of the group V–A elements by anodic stripping voltammetry. II. Trace analysis of antimony . . . . 81–86 C

Revue Roumaine Chim. **27, *1*, 1–166 (1982) Bucarest**

LIANA MARTA, MARIA ZAHARESCU and C. GH. MACAROVICI, Thermal and structural investigation of some oxalato-niobic complexes II. Barium tris (oxalato) niobate 87–93

TATIANA ONCESCU, M. CONTINEANU and S. G. IONESCU, Model system to obtain photohydrogen . . . . 95–101 R

L. ONICIU and V. A. TOPAN, Investigation methods of the electrode processes 103–114

O. RADOVICI, BELARISA POPESCU and L. DIMA, The anodic oxidation of *n*-decane on platinum electrode in acid electrolyte . . . . 115–120 C

S. RADULY, M. MRACEC, D. CIUBOTARIU, ADELINA MUSTE and Z. SIMON, Arylamides of oxalic acid. III. Hückel molecular orbital and Del Ré calculations 121–128

V. E. SAHINI, C. BENDIC and L. VIRAG, Reactivity of *m*-nitrophenyl acetate in excited state . . . . 129–136 R

E. SEGAL, MARIA BREZEANU, ECATERINA SAFARICA, LUMINIȚA PATRON and TEODORA ROBU, An analysis of thermal decomposition of coordination polynuclear compounds in Fe(III), Mn(II), Ni(II) systems 137–140

CRISTOFOR I. SIMIONESCU and BOGDAN C. SIMIONESCU, Plasma-induced polymerization. VII. Some characteristics of this new method of polymer synthesis 141–146

S. STERNBERG and A. MASCAȘ, Thermal conductivity in $Ca(NO_3)_2 \cdot 4H_2O - nH_2O$ system 147–154

RODICA VÎLCU and FLORICA IRINEI, Thermodynamics of multicomponent electrolyte solutions. III. Ammonium persulfate activity coefficients in quaternary system, in solubility measurements 155–160

ȘTEFANIA ZUCA and MARIELA CONSTANTINESCU, Cationic self-diffusion coefficients in molten $(Tl-Ag)NO_3$ system 161–164

BOOK REVIEWS 165–166

I. G. Murgulescu

Revue Roumaine de Chimie, 27, 7, 3–17 (1982)

TRIBUTE TO PROFESSOR I. G. MURGULESCU ON HIS 80th BIRTHDAY, 27th JANUARY 1982

Professor Dr. I. G. Murgulescu, Member of the Academy of the Socialist Republic of Romania, Professor Emeritus of Physical Chemistry at the Bucharest University and formerly Director of the Center of Physical Chemistry, is eighty years old on January 27, 1982.

His scientific personality, his important contribution in creating a modern school of physical chemistry in Romania, and his multiple activities in teaching and scientific research have been unanimously recognized and appreciated.

His many students, colleagues, and friends felt the need to honor him at this stage of his scientific career with a special anniversary volume dedicated to the field of physical chemistry in recognition of his fundamental discoveries and achievements. Since, for practical reasons, the volume has to be limited in size, only a selected number of papers could be included, but the volume is still a tribute from all of us who have benefited from his work and friendship. The volume is striking evidence of the stimulating influence on the current research in the field of Professor I. G. Murgulescu's work, and also of the impact it will have in the future.

Professor Dr. I. G. Murgulescu was born at Cornu, Oltenia. He studied at the elementary school in his native village and followed the high school in Craiova. As a student at the Science Faculty of the Cluj University he has proven his ingenuity in numerous occasions.

He started his didactic activity at the Science Faculty of the Cluj University where he was appointed assistant in 1928, after having graduated from the same Faculty with the highest honours. In 1930 he obtained his Ph. D. degree, with a thesis on Copper Thiosulphate Complexes, which was approved with "Magna Cum Laude" by the Cluj University.

His scientific personality has been appreciated by the late Professor G. Spacu, head of the Chair of Inorganic Chemistry at the Cluj University. Professor I. G. Murgulescu spent the years 1932 – 1933 at the Institute of Physical Chemistry of the Leipzig University working with Professor F. Weigert on photochemical problems.

Returning home in 1934, Professor I. G. Murgulescu became reader in Analytical Chemistry and Physical Chemistry at the Timişoara Polytechnic Institute, and he hold this position until he was appointed full professor at the same Institute in 1945. In 1949 he was appointed professor of physical chemistry at the Bucharest University where he lectured until 1972.

Professor Murgulescu's research work covers a wide field : kinetics, thermodynamics, electrochemistry, spectroscopy, inorganic and analytical chemistry, molten salt chemistry.

Starting from the studies of complex combinations he identified new types of complex silver and copper thiosulphates in the presence of ammonium, potassium and sodium, and extended these investigations by spectrophotometric, cryoscopic, and conductimetric measurements; he determined thus the composition of Durrand's salt. He also investigated spectrophotometrically the copper and cobalt salts in solution and the type of the chemical bond of complex chromium, iron and cobalt oxalates.

The study of the refractometric properties of aqueous solutions of electrolytes allowed him to elaborate new methods for calculating the refractive index of electrolytes and the individual ionic refractions. One of these methods has been applied to obtain the refractive indices of ferricyanide and ferrocyanide ions.

In photochemistry, he studied the quantum efficiency and the mechanism of the photochemical decomposition of potassium cobaltic oxalate and of diphenyldiazomethane in solution. The kinetics of the thermal decomposition of diphenyldiazomethane has also been studied by Professor Murgulescu and his coworkers.

Professor I. G. Murgulescu studied the kinetics of the alcoholysis of some benzyl halides and decomposition of the cobaltic oxalate in aqueous solution.

Another problem in which Professor I. G. Murgulescu became interested was the anodic passivation of metals and alloys. His studies on the electrochemical behaviour of thin films and on the determination of electrode potentials are well known.

His contribution to chemical thermodynamics dealt mainly with thermal decomposition of calcium carbonate, thermodynamic activity of solutions and alloys and free energy of chemical substances. By ebullioscopy he obtained the dissociation constant of alpha-nitroso-beta-naphthol in solution. By calorimetry he obtained the heat of dissolution of sodium iodate, both anhydrous and hydrated.

In analytical chemistry Professor Murgulescu has elaborated new analytical methods for mercury and other elements, and he was the first to use *o*-chlorobenzoic acid in alkalimetry and acidimetry. He developed a new conductimetric method for titrating molybdates and wolframates using silver nitrate, and also for complex iron cyanides enriching the theory of precipitation processes in the physico-chemical analysis. He has published studies on the equivalence point in titrimetry, and the determination of normal electrode potential.

In 1957 Professor I. G. Murgulescu concentrated on the area of research for which he became best known, the phyical chemistry of molten salts. His contributions to this field are both theoretical and experimental. Professor Murgulescu's researches in molten salts cover a wide field : thermodynamic properties of binary mixtures of molten salts by the methods of electromotive forces; cryometry and vapour pressure measurements; transport properties of molten salts, namely viscosity, electric conductivity; optical properties of molten salts (refractive indices); heat of mixing, heat of melting, heat capacity of molten salts, etc.

The research program on chemisorption has focused on strong and weak interactions of gases with solid surfaces, aiming at elucidating the importance of the elementary act of adsorption in simple catalytic reactions.

The results of his scientific research have been published in over 200 articles in Romanian and foreign journals.

In addition, he has been an excellent and stimulating teacher, and his series of textbooks has proven to be of essential value in universities all over the country. In 1976 Professor Murgulescu started the publication of "Introduction to Physical Chemistry". The work is to be issued in three volumes subdivided into six parts whose topics are: I, 1 Atoms. Molecules. Chemical Bond; I, 2 Structure and properties of molecules; I, 3 Atomic nucleus. Nuclear reactions. Elementary particles; II. 1 Molecular theory of the states of matter: gas, solid, liquid and solutions; II, 2 Chemical kinetics. Catalysis; III Chemical thermodynamics. These volumes represent an extension and systematization of the lectures on physical chemistry given by the author, who has brilliantly led the Physical Chemistry Chair of the Department of Chemistry, University of Bucharest, almost a quarter of a century of teaching and scientific activity; these lectures have permanently been updated with the newest achievements in the field.

In 1948 Professor I. G. Murgulescu was elected Member of the Academy of the Socialist Republic of Romania. As a recognition of his merits he was elected Vicepresident between 1959–1963 and President of the Academy of the Socialist Republic of Romania between 1963–1966.

The Commission of Spectroscopy came into being in 1960 as part of the Chemical Sciences Branch of the Academy; its Chairman is Professor I. G. Murgulescu. This Commission has been promoting basic spectroscopy research in our country.

Since 1971 Professor Murgulescu is the Chairman of the editorial board of Revue Roumaine de Chimie.

The Centre of Physical Chemistry was formed in 1963 under Professor Murgulescu's leadership and he has been the Director of this institute until 1977.

At Professor Murgulescu's initiative, the Centre of Physical Chemistry assisted by central Government institutions (National Council for Science and Technology, the Academy of Socialist Republic of Romania, Ministry of Education, Ministry of Chemical Industry) has organized the five "National Conferences on Pure and Applied Physical Chemistry" between 1968 and 1976.

The stimulating atmosphere which prevails in Professor Murgulescu's activity at the Centre of Physical Chemistry and the Bucharest University has provided an excellent starting point for many young scientist who are now engaged in research and teaching in different fields of physical chemistry. The same atmosphere has been beneficial for a few young scientists from abroad during their affiliation with the Centre of Physical Chemistry.

Under his scientific guidance, overs 20 young researches have completed their graduate studies (Ph. D.).

As a recognition of his remarkable organizing aptitudes, Professor Murgulescu was nominated Rector of the Timişoara Polytechnic Institute (1947—1949), Rector of the Bucharest University (1949—1950), Deputy Minister, and later Minister of Education (1950—1956) and again Minister of Education (1960—1963).

In carrying out his duties, Professor Murgulescu has given an example of perseverance and tenacity to all his co-workers and pupils. His devotion to teaching and research, which he succeeded in combining throughout his career, was the most characteristic feature of his multilateral activity. Among the public offices he held in Romania, we would quote : member of the Grand National Assembly (1948—1965), Vice President of the State Council (1965—1967) and Vice President of the Grand National Assembly (1967—1975).

As an international recognition of his scientific merits, he was elected member of the USSR Academy of Sciences, of the Czechoslovak Academy of Sciences, of the Hungarian Academy of Sciences, of the Bulgarian Academy of Sciences and of the New York Academy of Sciences. He is a member of the editorial board of scientific journals : *Electrochimica Acta* and *Corrosion Science*. He is editor-in-chief of the chemical scientific journal *Revue Roumaine de Chimie* and was also editor-in-chief of *Studii şi Cercetări de Chimie — Academia R. S. România*.

He is also a Member of the American Chemical Society, of the International Society of Electrochemistry and of the American Association for the Advancement of Science.

For his scientific and public activity, Professor I. G. Murgulescu was awarded several distinctions, medals and prizes such as : Romanian State Prize (1963), Professor Emeritus (1964), Emeritus Scientist (1969), Gold Medal of the 39th International Congress of Industrial Chemistry (1970), Hero of Socialist Labour (1971).

Professor Murgulescu's personality is an example for the Romanian scientists who hold him in high esteem. With this anniversary volume, his many students, friends, and colleagues enclose the warmest wishes for many happy years to come. Vive valeque!

D. I. MARCHIDAN

Publications of Professor I. G. Murgulescu

I. PUBLICATIONS IN PERIODICALS

1. G. Spacu et I. G. Murgulescu: Étude sur les cupro-thiosulfates complexes d'ammonium, de potassium et de sodium. I, *Bull. Soc. Sci. de Cluj*, **5**, 61 (1929).
2. G. Spacu et I. G. Murgulescu: Étude sur les cupro-thiosulfates complexes d'ammonium, de potassium et de sodium. II, *Bull. Soc. Sci. de Cluj*, **6**, 254 (1930).
3. G. Spacu et I. G. Murgulescu: Étude sur les cupro-thiosulfates complexes d'ammonium, de potassium et de sodium. III, *Bull. Soc. Sci. de Cluj*, **8**, 79 (1932).
4. G. Spacu und I. G. Murgulescu: Über die Silberthiosulfate des Ammoniums, Kaliums und Natriums. I, *Z. anorg. Chem.*, **199**, 273 (1932).
5. G. Spacu und I. G. Murgulescu: Über die Silberthiosulfate des Ammoniums, Kaliums und Natriums. II, *Z. anorg. Chem.*, **207**, 150 (1932).
6. G. Spacu und I. G. Murgulescu: Über die Silberthiosulfate des Ammoniums, Kaliums und Natriums. III, *Z, anorg. Chem.*, **208**, 157 (1932).
7. G. Spacu, I. G. Murgulescu und M. Vancea: Über die komplexen Kobaltioxalate, *Z. anorg. Chem.*, **220**, 1 (1934).
8. I. G. Murgulescu: Die photochemische Zersetzung von Kaliumkobaltioxalates, *Bull. Soc. Sci. de Cluj*, **8**, 193 (1934).
9. G. Spacu und I. G. Murgulescu: Spektrophotometrische Untersuchungen der wässerigen Kobaltchloridlösungen, *Z. phys. Chem. (A)*, **170**, 62 (1934).
10. G. Spacu und I. G. Murgulescu: Spektrophotometrische Untersuchungen über die wässerigen Kupferchloridlösungen, *Z. phys. Chem. (A)*, **170**, 71 (1934).
11. G. Spacu et I. G. Murgulescu: Une nouvelle méthode potentiométrique pour le mercure, *Bull. Soc. Sci. de Cluj*, **8**, 562 (1934).
12. C. Cîndea et I. G. Murgulescu: Action du méthane sur le chlorure de sodium, *Chimie Industrie*, **34**, 1 (1934).
13. C. Cîndea und I. G. Murgulescu: Die konduktometrische Titration der Molybdate mit Silbernitrat, *Bul. Soc. Chim. din România*, **17**, 103 (1935).
14. C. Cîndea und I. G. Murgulescu: Die konduktometrische Titration der Wolframate mit Silbernitrat, *Bul. Soc. Chim. din România*, **17**, 229 (1935).
15. C. Cîndea et I. G. Murgulescu: Dosage volumétrique du plomb et des molybdates avec les indicateurs d'absorption, *Annales de Chimie Analytique*, **18**, 1 (1936).
16. C. Cîndea et I. G. Murgulescu: Action du gaz méthane sur les chlorures de lithium et de potassium, *Chimie Industrie*, **36**, 34 (1936).

17. C. Cîndea et I. G. Murgulescu: Action du méthane sur les chlorures de strontium et de baryum, *Chimie Industrie*, **38**, 1 (1937).
18. I. G. Murgulescu: Über die Lichtabsorption der wässeringen Kupferchloridlösung, *Bull. Sci. École Polytechnique Timişoara*, **7**, 3 (1937).
19. I. G. Murgulescu und C. Drăgulescu: Über die Abweichung des Äquivalentvolumes von dem Umschlagvolumen bei den potentiometrichen Titrationen. I, *Z. phys. Chem. (A)*, **185**, 375 (1939).
20. I. G. Murgulescu und C. Drăgulescu: Über die Abweichung des Äquivalentvolumes von dem Umschlagvolumen bei den potentiometrischen Titrationen. II, *Z. phys. Chem. (A)*, **190**. 174 (1940).
21. I. G. Murgulescu und E. Laţiu: Direkte konduktometrische Methoden. I, *Z. Elektrochem.*, **46**, 449 (1940).
22. I. G. Murgulescu und E. Laţiu: Direkte konduktometrische Methoden. II, *Z. Elektrochem.*, **48**, 60 (1940).
23. I. G. Murgulescu und C. Drăgulescu: Über die Verwendung der Hexaminokobalt III-Salze (Luteokobaltsalze) in der quantitativen Analyse. I, *Z. analyt. Chem.*, **123**, 272 (1941).
24. I. G. Murgulescu und M. Alexa: Über die Verwendung der Hexaminokobalt III-Salze (Luteokobaltsalze) in der quantitativen Analyse, II, Die konduktometrische Titration der Eisen II-Cyanide und Eisen III-Cyanide, *Z. analyt. Chem.*, **123**, 338 (1941).
25. I. G. Murgulescu und M. Alexa: Über die Verwendung der Hexaminokobalt III-Salze (Luteokobaltsalze) in der quantitativen Analyse, III, Die konduktometrische Titration der Vanadate, *Z. analyt. Chem.*, **123**, 341 (1941).
26. I. G. Murgulescu und C. Drăgulescu: Über die Verwendung der Hexaminokobalt III-Salze (Luteokobaltsalze) in der quantitativen Analyse, IV, Die potentiometrische Titration der Eisen II-Cyanide, *Z. analyt. Chem.*, **123**, 346 (1941).
27. I. G. Murgulescu: Die Löslichkeit und die freie Energie des Silberchromats, *Bull. Sci. École Polytechnique Timişoara*, **10**, 3 (1941).
28. I. G. Murgulescu: Über die Einordnung des Begriffes der Aktivität in die Thermodynamik der Lösungen, *Bull. Sci. École Polytechnique Timişoara*, **11**, 3 (1942).
29. I. G. Murgulescu und E. Laţiu: Die konduktometrische Bestimmung der Jodate mit starken Säuren, *Z. analyt. Chem.*, **125**, 256 (1942).
30. G. Spacu, I. G. Murgulescu und E. Popper: Refraktometrische Eigenschaften der wässeringen Lösungen von Elektrolytmischungen, *Z. phys. Chem. (B)*, **52**, 117 (1942).
31. I. G. Murgulescu und V. Alexa: *o*-Chlorbenzoesäure als Urtitersubstanz für die Acidimetrie, *Z. analyt. Chem.*, **125**, 260 (1943).
32. I. G. Murgulescu und E. Laţiu: *o*-Chlorbenzoesäure als Urtitersubstanz in der Jodometrie, *Z. analyt. Chem.*, **125**, 267 (1943).
33. I. G. Murgulescu: Sur la dissociation du carbonate de calcium, *Bull. Inst. Rech. Techn. Roumaine*, **1**, 21 (1946).
34. I. G. Murgulescu und E. Laţiu: Die konduktometrische Bestimmung der freien Säure im Aluminiumsulfat, *Z. analyt. Chem.*, **128**, 142 (1948).
35. I. G. Murgulescu und E. Laţiu: Refraktometrische Methoden für die Analyse von Lösungen, *Z. analyt. Chem.*, **128**, 193 (1948).
36. I. G. Murgulescu und F. Dobrescu: Die quantitative Fällung von Blei als basisches Bleisalicylat, *Z. analyt. Chem.*, **128**, 203 (1948).
37. I. G. Murgulescu: Despre refracţiile ionilor. I, *Bul. Acad. R. P. România, Secţia Şt. Tehnice şi Chimice*, **1**, 1 (1949).
38. I. G. Murgulescu şi E. Laţiu: Despre refracţiile ionilor. II, *Bul. Acad. R. P. România, Secţia Şt. Tehnice şi Chimice*, **4**, 410 (1952).

39. I. G. Murgulescu und S. Sternberg: Thermodynamische Eigenschaften binären Salzgemische im geschmolzenen Zustand. I, Das System AgCl + KCl, *Rev. Chim. Acad. R. P. Roumaine*, **2**, 251 (1957).
40. I. G. Murgulescu şi O. Landauer: Activitatea soluţiilor apoase de amestecuri de electroliţi, *Anal. Univ. Bucureşti. Seria Şt. Nat.*, **18**, 1 (1958).
41. I. G. Murgulescu şi F. Bărbulescu: Studiul cinetic al reacţiei dintre clorura de benzil şi isoamilatul de sodiu, *Anal. Univ. Bucureşti, Seria Şt. Nat.*, **18**, 22 (1958).
42. I. G. Murgulescu şi R. Vîlcu: Aparat pentru determinarea activităţii din măsurători ebulioscopice, *Anal. Univ. Bucureşti, Seria Şt. Nat.*, **18**, 39 (1958).
43. I. G. Murgulescu und D. I. Marchidan: Thermodynamische Eigenschaften binärer Salzgemische im geschmolzenen Zustand. Das System AgBr + AgCl, *Rev. Chim. Acad. R. P. Roumaine*, **3**, 47 (1958).
44. I. G. Murgulescu und S. Sternberg: Die Bestimmung der Aktivität aus den Schmelzdiagrammen von AgCl + $PbCl_2$, *Rev. Chim. Acad. R. P. Roumaine*, **3**, 55 (1958).
45. I. G. Murgulescu, S. Sternberg şi D. I. Marchidan: Asupra proprietăţilor termodinamice ale lichidelor ionice (în limba rusă), *Bul. nautchinyi informatsii*, nr. 3 (1958).
46. I. G. Murgulescu şi V. Em. Sahini: Despre refracţiile ionilor. III, *Studii şi Cercetări Chim. Acad. R. P. România*, **7**, 1 (1959).
47. I. G. Murgulescu et V. Em. Sahini: Spectres d'absorption dans l'infrarouge de quelques oxalates complexes, *Rev. Universelle de Mines*, **15**, 7 (1959).
48. I. G. Murgulescu: Aspecte din organizarea şi orientarea cercetărilor chimice din URSS, *Anal. Acad. R. P, România*, **9**, 253 (1959).
49. I. G. Murgulescu et E. Segal: La cinétique de la déshydratation des hydrates cristallins. II, *Rev. Chim. Acad. R. P. Roumaine*, **4**, 159 (1959).
50. I. G. Murgulescu et D. Cismaru: L'oxydation du cuivre aux températures élevées. Le système Cu—CO_2, *Rev. Chim. Acad. R. P. Roumaine*, **4**, 271 (1959).
51. I. G. Murgulescu şi S. Sternberg: Determinarea forţelor electromotoare şi potenţialelor de electrod la lichide ionice. In the volume dedicated to Acad. Traian Săvulescu, Ed. Academiei, Bucureşti, 1959, p. 115—124.
52. I. G. Murgulescu şi Ş. Zuca: Conductibilitatea electrică a amestecurilor de săruri topite. Sistemele: $KNO_3 + NaNO_3$, $Ba(NO_3)_2 + KNO_3$, $MnCl_2 + KCl$, *Studii şi Cercetări Chim. Acad. R. P. România*, **7**, 325 (1959).
53. I. G. Murgulescu şi D. I. Marchidan: Proprietăţile termodinamice ale amestecurilor binare de săruri topite. Determinarea activităţii termodinamice din forţele electromotoare ale pilelor de concentraţie, *Studii şi Cercetări Chim. Acad. R. P. România*, **7**, 461 (1959).
54. I. G. Murgulescu şi O. Radovici: Asupra pasivării anodice a unor oţeluri, *Studii şi Cercetări Chim. Acad. R. P. România*, **7**, 350 (1959).
55. I. G. Murgulescu und O. Radovici: Über die anodische Passivierung einiger Chrom—Nickel—Mangan—Stähle bei konstantem Strom, *Rev. Chim. Acad. R. P. Roumaine*, **4**, 287 (1959).
56. I. G. Murgulescu und T. Oncescu: Zur Kinetik der Zerzetzungsreaktionen von komplexen Kobalt (III) Oxalaten in wässerigen Lösungen, *Z. phys. Chem.*, **214**, 238 (1960).
57. I. G. Murgulescu et E. Segal: La cinétique de la déshydratation des hydrates cristallins. III, *Rev. Chim. Acad. R. P. Roumaine*, **5**, 5 (1960).
58. I. G. Murgulescu şi E. Tomuş: Căldura de dizolvare a iodatului de sodiu anhidru, monohidratat şi pentahidratat, *Anal. Univ. Bucureşti, Seria Şt. Nat.*, **9**, 213 (1960).
59. I. G. Murgulescu et D. I. Marchidan: Propriétés thermodynamiques des mélanges binaires de sels fondus. Le système $AgNO_3 + LiNO_3$ à l'état fondu, *Rev. Chim. Acad. R. P. Roumaine*, **5**, 17 (1960).

60. I. G. Murgulescu und D. I. Marchidan: Die Bestimmung der thermodynamische Aktivität in dem System $PbCl_2 + KCl$ aus Konzentration sketten, *Rev. Chim. Acad. R. P. Roumaine*, **5**, 299 (1960).
61. I. G. Murgulescu şi D. I. Marchidan: Determinarea activităţii termodinamice în sisteme binare de săruri topite din FEM a pilelor de concentraţie, *Zhur. fiz. Khim.*, **34**, 2534 (1960).
62. I. G. Murgulescu et D. Cismaru: Sur la nitruration du magnésium à des températures élevées. Le système $Mg-NH_3$, *Rev. Chim. Acad. R. P. Roumaine*, **5**, 289 (1960).
63. I. G. Murgulescu et D. Cismaru: Sur la nitruration du magnésium à des températures élevées. Le système $Mg-N_2$, *Rev. Chim. Acad. R. P. Roumaine*, *5*, 251 (1960).
64. I. G. Murgulescu şi I. A. Schneider: Despre descompunerea termică a metanului în condiţii dinamice, *Studii şi Cercetări Chim. Acad. R. P. România*, *8*, 482 (1960).
65. I. G. Murgulescu et D. Cismaru: Oxydation du zinc aux hautes températures. Cinétique de l'oxydation du zinc dans une atmosphère d'oxygène et de bioxyde de carbone, *J. Chim. phys.*, **58**, 181 (1961).
66. I. G. Murgulescu und R. Vîlcu: Die Assoziationskonstante des α-Nitroso-β-Naphtols aus ebulliometrischen Messungen, *Z. phys. Chem.*, **218**, 372 (1961).
67. I. G. Murgulescu et T. Oncescu: Étude cinétique sur la décomposition thermique du diphényldiazométhane en solution, *J. Chim. phys.*, **58**, 508 (1961).
68. I. G. Murgulescu şi E. Tomuş: Căldura de dizolvare a bromatului de sodiu, bromatului de litiu şi iodatului de litiu, *Anal. Univ. Bucureşti, Seria Şt. Nat.*, **10**, 13 (1961).
69. I. G. Murgulescu und S. Sternberg: Über die Mischungswärme binären geschmolzenen Salzgemische, *Rev. Chim. Acad. R. P. Roumaine*, **5**, 29 (1961).
70. I. G. Murgulescu und Ş. Zuca: Über die innere Reibung des Kryoliths, *Rev. Chim. Acad. R. P. Roumaine*, **6**, 21 (1961).
71. I. G. Murgulescu und Ş. Zuca: Die innere Reibung einiger einfacher geschmolzener Salze, *Z. phys. Chem.*, **218**, 379 (1961).
72. I. G. Murgulescu i Ş. Zuca: Viazkosti rasplavov sistemy $Na_3AlF_6 + BaCl_2$. *Tsvetnaja metalurghja*, **4**, 33 (1961).
73. I. G. Murgulescu et L. Marta: Tension de vapeur et activiţé thermodynamique des mélanges de sels fondus. Le système $PbBr_2 + KBr$, *Rev. Chim. Acad. R. P. Roumaine*, **6**, 317 (1961).
74. I. G. Murgulescu and C. Volanschi: Refractometric properties of binary mixtures of molten salts: $LiNO_3 + NaNO_3$ and $LiNO_3 + KNO_3$, *Rev. Chim. Acad. R. P. Roumaine*, **6**, 45 (1961).
75. I. G. Murgulescu şi C. Volanschi: Studiul spectrofotometric al sărurilor topite. Absorbţia sistemului bicromat-cromat de potasiu, *Studii şi Cercetări Chim. Acad. R. P. România*, **9**, 348 (1961).
76. I. G. Murgulescu und I. A. Schneider: Über die termische Zersetzung des Methans, *Z. phys. Chem.*, **218**, 338 (1961).
77. I. G. Murgulescu and O. Radovici: The potentiostatic behaviour of some Cr—Ni—Mn stainless steels, "First International Congress of Metallic Corrosion", London, 10—15 April, 1961.
78. I. G. Murgulescu: Frederic Jolliot—Curie, *Studii şi Cercetări Chim. Acad. R. P. România*, **10**, 36 (1962).
79. I. G. Murgulescu et T. Oncescu: Étude sur la décomposition photochimique du diphényldiazométhane en solution, *J. Chim. phys.*, **59**, 78 (1962).
80. I. G. Murgulescu and S. Sternberg: Experimental methods of measuring the thermodynamic activity in mixtures of molten salts, *Discuss. Faraday Soc.*, **32**, 197 (1962).
81. I. G. Murgulescu und S. Sternberg: Über die thermodynamischen Überschußgrößen binärer geschmolzener Salzgemische, *Z. phys. Chem.*, **219**, 114 (1962).
82. I. G. Murgulescu et L. Marta: Tension de vapeur et activité thermodynamique des mélanges de sels fondus. Le système $AgCl + KCl$, *Rev. Chim. Acad. R. P. Roumaine*, **7**, 1103 (1962).

83. I. G. Murgulescu und D. Topor: Die Bestimmung der Überführungszahlen für geschmolzenes Thallium I—Nitrat, *Z. phys. Chem.*, **219**, 134 (1962).
84. I. G. Murgulescu und I. A. Schneider: Die Methankrakung in Gegenwart von Mo und W, *J. prakt. Chem.*, **1962**, 2568.
85. I. G. Murgulescu und Z. Simon: Kinetische Untersuchung der thermischen cis-trans-Isomerisierung einiger α, β disubstituirter Äthylenderivate, *Z. phys. Chem.*, **221**, 29 (1962).
86. I. G. Murgulescu şi Z. Simon: Calcule de coeficienţi preexponenţiali ai unor reacţii monomoleculare, *Studii şi Cercetări Chim. Acad. R. P. România*, **10**, 382 (1962).
87. I. G. Murgulescu şi Z. Simon: Coeficientul preexponenţial şi energia de activare pentru descompunerea unimoleculară a ciclobutanului, *Studii şi Cercetări Chim. R. P. România*, **10**, 631 (1962).
88. I. G. Murgulescu et F. Bărbulescu: Étude cinétique sur la solvolyse du diphénylchlorméthane, *Rev. Chim. Acad. R. P. Roumaine*, **8**, 134 (1963).
89. I. G. Murgulescu und R. Vîlcu: Ebulliometrie bei Überdruck, I, Die thermodynamische Aktivität des Mannits in wässerigen Lösungen, *Z. phys. Chem.*, **234**, 241 (1963).
90. I. G. Murgulescu, V. Em. Sahini et L. Bolfa: Étude spectrale dans l'infrarouge de l'isométrie cis-trans, *Rev. Chim. Acad. R. P. Roumaine*, **8**, 65 (1963).
91. I. G. Murgulescu i E. Segal: Kinetika i termiceskaja razlozenja nekotoryh komplexnyh aminov. *Rev. Chim. Acad. R. P. Roumaine*, **8**, 51 (1963).
92. I. G. Murgulescu und E. Constantinescu: Bestimmung von Elektrodennormalpotentiale, *Rev. Chim. Acad. R. P. Roumaine*, **8**, 5 (1963).
93. I. G. Murgulescu şi E. Tomuş: Căldura de dizolvare a bromatului de bariu, *Anal. Univ. Bucureşti, Seria Şt. Nat.*, **41**, 97 (1963).
94. I. G. Murgulescu, S. Sternberg, L. Medinţev and C. Musteţea: Overvoltage and depolarisation in molten AgCl, AgBr, AgI, *Electrochim. Acta*, **8**, 65 (1963).
95. I. G. Murgulescu und Ş. Zuca: Die innere Reibung einiger einfacher geschmolzener Salze. II, *Z. phys. Chem.*, **222**, 300 (1963).
96. I. G. Murgulescu şi S. Sternberg: Energia liberă de exces a unor amestecuri binare de săruri topite, "Chimia fizică a electroliţilor topiţi", Ed. Academiei, Bucureşti, 1963, p. 43.
97. I. G. Murgulescu şi D. I. Marchidan: Despre determinarea căldurii de amestecare a sistemului $PbCl_2 + PbBr_2$ în stare topită, cu ajutorul unui calorimetru isoterm, "Chimia fizică a electroliţilor topiţi", Ed. Academiei, Bucureşti, 1963, p. 67.
98. I. G. Murgulescu şi Ş. Zuca: Studiul viscozităţii unor săruri topite, "Chimia fizică a electroliţilor topiţi", Ed. Academiei, Bucureşti, 1963, p. 209.
99. I. G. Murgulescu şi Z. Simon: Reacţii fotochimice şi tranziţii neradiative la cetone şi aldehide, *Studii şi Cercetări Chim. Acad. R. P. România*, **11**, 845 (1963).
100. I. G. Murgulescu et F. Bărbulescu: Sur la solvolyse du diphénylchlorméthane dans un mélange d'alcools, *Rev. Roumaine Chim.*, **9**, 12 (1964).
101. I. G. Murgulescu und R. Vîlcu: Ebulliometrie bei Überdruck. II. Die thermodynamische Aktivität des Kaliumbromids in wässerigen Lösungen, *Z. phys. Chem.*, **225**, 37 (1964).
102. I. G. Murgulescu, S. Sternberg et L. Medinţev: Processus aux électrodes pendant l'électrolyse de AgCl fondus, *Electrochim.* Acta, **9**, 219 (1964).
103. I. G. Murgulescu and D. I. Marchidan: Heats of mixing in binary fused salts systems, *Rev. Roumaine Chim.*, **9**, 793 (1964).
104. I. G. Murgulescu and D. I. Marchidan: Diffusion potential in molten salt systems, *J. Phys. Chem.*, **68**, 3086 (1964).
105. I. G. Murgulescu et D. Topor: Électromigration du lithium dans les nitrates alcalins fondus, *Rev. Roumaine Chim.*, **9**, 815 (1964).
106. I. G. Murgulescu, O. Radovici and S. Ciolac: The effect of some oxydizing substances on the behaviour of some alluminium alloys, *Corrosion Sci.*, **4**, 353 (1964).

107. I. G. Murgulescu, V. Em. Sahini, M. Segal and M. Damaschin: Vibrational spectra and structure of copper and silver thiosulfate complexes, *Rev. Roumaine Chim.*, **9**, 29 (1964).
108. I. G. Murgulescu, F. Bărbulescu, et A. Greff: Sur la conductivité de l'acide chlorhydrique dans des mélanges d'alcool-eau, *Rev. Roumaine Chim.*, **10**, 387 (1965).
109. I. G. Murgulescu and T. Oncescu: Kinetics and mechanism of thermal decomposition of Mn (III) complex oxalates in solution, *Rev. Roumaine Chim.*, **10**, 3 (1965).
110. I. G. Murgulescu et E. Segal: Les coefficients préexponentiels des constantes de vitesse, correspondant à l'ordre zéro pour les réactions solide-gaz, *Rev. Roumaine Chim.*, **10**, 307 (1965).
111. I. G. Murgulescu, E. Segal and D. Fătu: The thermal decomposition of pyridinic complexes of cobalt (II) and nickel (II) chlorides, *J. Inorg. Nuclear Chem.*, **27**, 2677 (1965).
112. I. G. Murgulescu, D. A. Isăcescu, E. Tomuș and F. Tomuș: Studies on furfurol. XXX. Heat of resinification of furfurol, mono- and difurfurylydene acetone of "Fa monomer" in acid catalysis, *Rev. Roumaine Chim.*, **10**, 269 (1965).
113. I. G. Murgulescu, D. A. Isăcescu, E. Tomuș and F. Tomuș: Studies on furfurol. XXXI. Heat of resinification of furfurol, mono- and difurfurylydene acetone of "Fa monomer" in acid catalysis, *Rev. Roumaine Chim.*, **10**, 583 (1965).
114. I. G. Murgulescu and S. Sternberg: "Contribution to the study of molten salts", Edited by EURATOM, 1965.
115. I. G. Murgulescu et Ș. Zuca: Viscosité des mélanges binaires de sels fondus. Les systèmes: KCl + NaCl, KCl + KBr, $PbBr_2$ + KBr, *Rev. Roumaine Chim.*, **10**, 120 (1965).
116. I. G. Murgulescu et Ș. Zuca: Viscosité de sels individuels à d'état fondu. III, *Rev. Roumaine Chim.*, **10**, 123 (1965).
117. I. G. Murgulescu, O. Radovici and M. Borda: Studies of the mechanism of anodic dissolution of Al-Zn binary alloys in alkaline solutions by potentiodynamic and potentiostatic pulse methode, *Rev. Roumaine Chim.*, **10**, 613 (1965).
118. I. G. Murgulescu et I. Cornea: Études galvanostatiques sur la passivité des aciers inoxydables du type 18Cr–8Ni, *Rev. Roumaine Chim.*, **10**, 809 (1965).
119. I. G. Murgulescu: John Dalton, *Studii și Cercetări Chim. Acad. R. S. România*, **14**, 587 (1966).
120. I. G. Murgulescu and E. Segal: Thermal decomposition of some complex amines. IV, *Rev. Roumaine Chim.*, **11**, 13 (1966).
121. I. G. Murgulescu. D. I. Marchidan et C. Telea: La chaleur de mélange des systèmes binaires de sels fondus, *Rev. Roumaine Chim.*, **11**, 1031 (1966).
122. I. G. Murgulescu, S. Sternberg and L. Bejan: The halogen carbon electrode. IV. Electrochemical determination of chlorine-adsorption on carbon, *Rev. Roumaine Chim.*, **11**, 447 (1966).
123. I. G. Murgulescu, S. Sternberg and M. Terzi: Potentiometric and thermodynamic study of molten PbI_2 + KI mixtures, *Electrochim. Acta*, **12**, 121 (1966).
124. I. G. Murgulescu et L. Marta: Les pressions de vapeur et l'association moléculaire des vapeurs du chlorure et du bromure de potassium fondu, "Thermodynamics", vol. I, Ed. IAEA, Viena, 1966, p. 345.
125. I. G. Murgulescu and L. Topor: Vapour pressure and molecular association of NaCl, NaBr vapours, *Rev. Roumaine Chim.*, **11**, 1353 (1966).
126. I. G. Murgulescu et Ș. Zuca: Viscosité des mélanges binaires de nitrates fondus en fonction du rayon ionique. *Electrochim. Acta*, **12**, 1383 (1966).
127. I. G. Murgulescu and G. Vasu: Cellular hole model for molten alkali halides, *Rev, Roumaine Chim.*, **11**, 681 (1966).

128. I. G. Murgulescu et D. Cismaru: La corrosion chimique de certains métaux à des températures élevées, dans une atmosphère de dioxyde de carbone, *Rev. Roumaine Chim.*, **11**, 671 (1966).

129. I. G. Murgulescu, D. Cismaru et E. Costeanu: Oxydation des couches minces de magnésium aux températures élevées, *Rev. Roumaine Chim.*, **11**, 769 (1966).

130. I. G. Murgulescu and M. Vass: Gas adsorption on metallic films. The surface potential in the oxygen-copper system, *Rev. Roumaine Chim.*, **11**, 299 (1966).

131. I. G. Murgulescu and N. I. Ionescu: The effect of oxygen chemisorption on the electric resistance of thin silver films, *Rev. Roumaine Chim.*, **11**, 1035 (1966).

132. I. G. Murgulescu and N. I. Ionescu: The effect of oxygen chemisorption on the temperature coefficient of the electric resistance of thin silver films, *Rev. Roumaine Chim.*, **11**, 1267 (1966).

133. I. G. Murgulescu und G. Comşa: Anderung des Hallefekts bei der Chemisorption von Sauerstoff an dünnen Kupferschichten, *Rev. Roumaine Chim.*, **11**, 1253 (1966).

134. I. G. Murgulescu und Z. Simon: Kinetische Untersuchungen der cis-trans Isomerisationen, *Rev. Roumaine Chim.*, **11**, 21 (1966).

135. I. G. Murgulescu und Z. Simon: Idem, III. Photochemische Isomerisationen, *Rev. Roumaine Chim.*, **11**, 35 (1966).

136. I. G. Murgulescu, T. Oncescu und Z. Simon: Redoxreaktionen der komplexen Oxalate einiger dreivvertigen Übergangsmetalle. I, *Rev. Roumaine Chim.*, **12**, 737 (1967).

137. I. G. Murgulescu, T. Oncescu und Z. Simon: Redoxreaktionen der komplexen Oxalate einiger dreivvertigen Übergangsmetalle. II, *Rev. Roumaine Chim.*, **12**, 755 (1967).

138. I. G. Murgulescu, T. Oncescu, J. Păun and I. Mihalcea: The radiolysis of the complex oxalates in aqueous solutions, *Rev. Roumaine Chim.*, **12**, 573 (1967).

139. I. G. Murguescu i I. Mihalcea: Deistvie γ izlucenja na vodnjie rastvory gheksaminkobalta, *Rev. Roumaine Chim.*, **12**, 763 (1967).

140. I. G. Murgulescu şi E. Segal: Studiul cinetic al reacţiilor eterogene cu ajutorul datelor termogravimetrice, *Studii şi Cercetări Chim. Acad. R. S. România*, **15**, 261 (1967).

141. I. G. Murgulescu et E. Constantinescu: Contribution à l'étude des potentiels normaux d'électrode. I, *Rev. Roumaine Chim.*, **12**, 199 (1967).

142. I. G. Murgulescu et E. Constantinescu: Contribution à l'étude des potentiels normaux d'électrode. II, *Rev. Roumaine Chim.*, **12**, 223 (1967).

143. I. G. Murgulescu et E. Constantinescu: Contribution à l'étude des potentiels normaux d'électrode. III, *Rev. Roumaine Chim.*, **12**, 339 (1967).

144. I. G. Murgulescu and L. Topor: Thermodynamical data of molten rubidium and caesium halides from vapour pressure determinations, *Rev. Roumaine Chim.*, **12**, 1077 (1967).

145. I. G. Murgulescu et D. Topor: Electromigration dans les nitrates alcalins fondus, *Rev. Roumaine Chim.*, **12**, 1279 (1967).

146. I. G. Murgulescu and G. Comşa: Comparative study of oxygen and carbon monoxyde adsorption influence on the Hall tension of thin copper films, *Rev. Roumaine Chim.*, **12**, 1171 (1967).

147. I. G. Murgulescu and N. I. Ionescu: The effect of oxygen chemisorption on the electric properties of unsintered thin silver films, *Rev. Roumaine Chim.*, **12**, 1395 (1967).

148. I. G. Murgulescu, O. Radovici and N. Totir: The determination of kinetic parameters of the reaction $Cd^{++} + 2e \rightleftharpoons Cd(Hg)$, *Rev. Roumaine Chim.*, **12**, 231 (1967).

149. I. G. Murgulescu, I. Vartires and O. Radovici: Electrochemical behaviour of silver thin films *Rev. Roumaine Chim.*, **12**, 215 (1967).

150. I. G. Murgulescu et I. Vartires: Sur le potentiel standard des films de cuivre minces, *Rev. Roumaine Chim.*, **12**, 1069 (1967).

151. I. G. Murgulescu, F. Bărbulescu et E. Constantinescu: Activités thermodynamiques déterminées à l'aide des éléments thermogalvaniques, *Rev. Roumaine Chim.*, **13**, 841 (1968).

152. I. G. Murgulescu, D. A. Isăcescu, E. Tomuş and F. Tomuş: Studies on furfurol, *Rev. Roumaine Chim.*, **13**, 297 (1968).

153. I. G. Murgulescu and M. Contineanu: Kinetics of the radiolysis of potassium oxalate and oxalic acid, *Rev. Roumaine Chim.*, **13**, 661 (1968).

154. I. G. Murgulescu: Present state and future prospects of the thermodynamics of fused salts, IAEA, Vienna, 1968.

155. I. G. Murgulescu and L. Topor: Molecular association of rubidium and caesium halides in gas phase, *Rev. Roumaine Chim.*, **13**, 1100 (1968).

156. I. G. Murgulescu et D. Topor: Détermination du nombre de transport dans le nitrate de rubidium fondu, *Rev. Roumaine Chim.*, **13**, 3 (1968).

157. I. G. Murgulescu et D. Topor: Electromigration dans les nitrates monovalents fondus. Les ions d'argent et de thalium, *Rev. Roumaine Chim.*, **13**, 979 (1968).

158. I. G. Murgulescu and G. Comşa: Halltension changes in thin silver films during oxygen chemisorption, *Rev. Roumaine Chim.*, **13**, 1261 (1968).

159. I. G. Murgulescu, G. Comşa and N. I. Ionescu: Influence of oxygen chemisorption on the thickness of thin silver films, *J. Catalysis*, **12**, 102 (1968).

160. I. G. Murgulescu and N. I. Ionescu: Effect of oxygen chemisorption on the electrical resistance of thin copper films, *Rev. Roumaine Chim.*, **13**, 1533 (1968).

161. I. G. Murgulescu and M. Vass: Gas adsorption on thin metallic films. Surface potential variation in oxygen-gold system, *Rev. Roumaine Chim.*, **13**, 373 (1968).

162. I. G. Murgulescu and M. Vass: Gas adsorption on thin metallic films. Variation of surface potential in the oxygen-silver system, *Rev. Roumaine Chim.*, **13**, 1521 (1968).

163. I. G. Murgulescu and I. Vartires: On the standard potential of thin gold films, *Rev. Roumaine Chim.*, **13**, 1397 (1968).

164. I. G. Murgulescu şi I. Vlagiu: Cinetica şi mecanismul polimerizării radiochimice, *Studii şi Cercetări Chim. Acad. R. S. România*, **16**, 317 (1968).

165. I. G. Murgulescu: Some physico-chemical properties of simple molten salts, *Rev. Roumaine Chim.*, **14**, 965 (1969).

166. I. G. Murgulescu: Viscosité et structure des sels fondus, *J. Chim. phys.*, Numero special, Oct. 1969, p. 43.

167. I. G. Murgulescu und G. Comşa: Chemisorption von Sauerstoff und Kohlenmonoxyd an vorbelegten Kupferschichten, *Rev. Roumaine Chim.*, **14**, 825 (1969).

168. I. G. Murgulescu, N. I. Ionescu und G. Comşa: Hallspannungsänderung bei der Chemisorption von Sauerstoff und Kohlenmonoxyd an dünnen Kupferschichten, *J. Catalysis*, **13**, 328 (1969).

169. I. G. Murgulescu and N. I. Ionescu: The effect of oxygen chemisorption on the temperature coefficient of the electrical resistance of thin copper films, *Rev. Roumaine Chim.*, **14**, 681 (1969).

170. I. G. Murgulescu and N. I. Ionescu: The effect of oxygen chemisorption on the temperature dependence of the variation of electrical resistance of the thin copper films, *Rev. Roumaine Chim.*, **14**, 1073 (1969).

171. I. G. Murgulescu and M. Vass: Calorimetric determination of the chemisorption heat of oxygen on thin copper films, *Rev. Roumaine Chim.*, **14**, 1201 (1969).

172. I. G. Murgulescu and I. Demetrescu: The kinetics of the reactions between benzoyl chloride and normal alcohols, *Rev. Roumaine Chim.*, **14**, 149 (1969).

173. I. G. Murgulescu und C. Potmischil: Die Reaktionen des Triphenylmethilchlorid mit Alkoholen, *Rev. Roumaine Chim.*, **14**, 1201 (1969).

174. I. G. Murgulescu, D. Fătu et E. Segal: Contributions à l'étude cinétique des décompositions endothermiques des systèmes solide-gaz à l'aide des données thermogravimétriques, *J. Thermal Analysis*, **1**, 97 (1969).

185. I. G. Murgulescu, D. Oancea and G. Mincu: Reactions between benzyl chloride and alkali alcoxides, *Rev. Roumaine Chim.*, **14**, 4 (1969).

176. I. G. Murgulescu and I. Vartires: On the standard potential of thin cadmium films, *Rev. Roumaine Chim.*, **14**, 1479 (1969).

177. I. G. Murgulescu et I. Vlagiu: Détermination des constantes $Q_{tr} - e_{tr}$ des valeurs des constantes de transport, dans le cas de la polymérisation radiochimique de l'acrylonitrile dans des solvants de filage, *Rev. Roumaine Chim.*, **14**, 411 (1969).

178. I. G. Murgulescu et I. Vlagiu: La cinétique de la polymérisation mixte de l'acrylonitrile sous l'action des radiations ionisantes et en présence de diaquodioxalomanganate de potassium, *Rev. Roumaine Chim.*, **14**, 1081 (1969).

179. I. G. Murgulescu: Some physico-chemical properties of simple molten salts. II, *Rev. Roumaine Chim.*, **15**, 1463 (1970).

180. I. G. Murgulescu and L. Vasu: Correlation between electrical conductivity and diffusion in molten salts, *Rev. Roumaine Chim.*, **15**, 837 (1970).

181. I. G. Murgulescu: Potentiels de diffusion, *Cronache di Chimica*, 30 Dec. 1970 (Carlo Erba — Milano — Italy).

182. I. G. Murgulescu, E. Popa et E. Ivana: Le spectre d'absorption des halogenures de plomb fondus. *Rev. Roumaine Chim.*, **15**, 669 (1970).

183. I. G. Murgulescu et L. Topor: L'association moléculaire des iodures alcalins en phase gazeuse, *Rev. Roumaine Chim.*, **15**, 997 (1970).

184. I. G. Murgulescu et D. Topor: Electromigration dans les nitrates monovalents fondus. Les ions de strontium et de baryum. *Rev. Roumaine Chim.*, **15**, 843 (1970).

185. I. G. Murgulescu und G. Comşa: Adsorption von Kohlenmonoxyd an dünnen Silberschichten, *Rev. Roumaine Chim.*, **15**, 987 (1970).

186. I. G. Murgulescu and M. Vass: Surface potential variation during nitrogen adsorption on thin copper films, *Rev. Roumaine Chim.*, **15**, 489 (1970).

187. I. G. Murgulescu and I. Demetrescu: Kinetics of the reactions between benzyl bromide and normal alcohols, *Rev. Roumaine Chim.*, **15**, 141 (1970).

188. I. G. Murgulescu şi I. Demetrescu: Influenţa solventului asupra reacţiilor dipol-dipol, *Studii şi Cercetări Chim. Acad. R. S. România*, **18**, 545 (1970).

189. I. G. Murgulescu und C. Potmischil: Die Kinetik der Reaktion zwischen Benzilidenbromid und Natriummetilat, *Bul. Inst. Politeh. Iaşi*, **16**, 23 (1970).

190. I. G. Murgulescu and I. Mihalcea: Radiolysis of the hexaminocobaltic nitrate in aqueous solutions, *Rev. Roumaine Chim.*, **15**, 3 (1970).

191. I. G. Murgulescu and D. Oancea: Nucleophilic substitutions. II. Reactions between benzyl bromide and alkali alcoxides, *Rev. Roumaine Chim.*, **15**, 858 (1970).

192. I. G. Murgulescu and D. Oancea: Nucleophilic substitutions. III. The kinetics of the reactions between benzyl iodide and sodium alcoxides, *Rev. Roumaine Chim.*, **15**, 1635 (1970).

193. I. G. Murgulescu, T. Oncescu et I. Vlagiu: Cinétique de la polymérisation de l'acrylonitrile initiée par $K[Mn(C_2O_4)_2(H_2O)_2] \cdot 3H_2O$, *J. Chim. phys.*, **10**, 148 (1971).

194. I. G. Murgulescu and N. I. Ionescu: The effect of oxygen chemisorption on electrical properties of thin copper and silver films, *Thin Solid Films*, **7**, 355 (1971).

195. I. G. Murgulescu and I. Demetrescu: Kinetics of reactions between benzhydryl chloride and primary isoalcohols, *Rev. Roumaine Chim.*, **16**, 781 (1971).

196. I. G. Murgulescu and I. Demetrescu: Kinetics of the reactions between benzyl bromide and primary isoalcohols, *Rev. Roumaine Chim.*, **16**, 1483 (1971).

197. I. G. Murgulescu and D. Oancea: The structure and nucleophilic reactivities of sodium alcoxides, *Rev. Roumaine Chim.*, **16**, 1625 (1971).
198. I. G. Murgulescu and J. Păun: Kinetics and mechanism of the radiolysis of some trans-oxalato complex in aqueous solutions, *Ber. Bunsenges. phys. Chem.*, **75**, 624 (1971).
199. I. G. Murgulescu and G. Mincu: The influence of hydrogen ion concentration on the thermal decomposition of the cis-dioxalato-diaquo-cobalt (III) complex in solution, *Rev. Roumaine Chim.*, **16**, 1023 (1971).
200. I. G. Murgulescu, T. Oncescu and G. Ionescu: On the photolysis of $[Mn(C_2O_4)_2(H_2O)_2]K$ in dimethylformamide, *Rev. Roumaine Chim.*, **17**, 423 (1972).
201. I. G. Murgulescu and E. Sălăgeanu: Some physico-chemical properties of simple molten salts. III, *Rev. Roumaine Chim.*, **17**, 602 (1972).
202. I. G. Murgulescu and L. Popescu: Thermodynamic properties from electromotive force measurements with formation cells in molten salts. AgBr + CsBr mixtures, *Rev. Roumaine Chim.*, **17**, 1287 (1972).
203. I. G. Murgulescu and M. Șerban: On the viscosity of molten metals, *Rev. Roumaine Chim.*, **17**, 432 (1972).
204. I. G. Murgulescu and I. Demetrescu: Kinetics of reactions of benzhydryl chloride and benzyl bromide with secondary alcohols, *Rev. Roumaine Chim.*, **17**, 595 (1972).
205. I. G. Murgulescu and M. Bozeșanu: Kinetics of the slow oxydation reaction of methane in dynamic system, *Rev. Roumaine Chim.*, **17**, 1637 (1972).
206. I. G. Murgulescu și S. Trestianu: Forțe și potențiale intermoleculare, *Studii și Cercetări Chim. Acad. R. S. România*, **20**, 757 (1972).
207. I. G. Murgulescu and L. Popescu: Diffusion potentials in molten salts, *Rev. Roumaine Chim.*, **18**, 737 (1973).
208. I. G. Murgulescu, E. Popa and E. Ivana: Electronic absorption spectra of silver halides in passing from solid to molten state, *Rev. Roumaine Chim.*, **18**, 189 (1973).
209. I. G. Murgulescu and E. Ivana: Absorption spectra of $PbCl_2$ and $PbBr_2$ in vapour phase, *Rev. Roumaine Chim.*, **18**, 1667 (1973).
210. I. G. Murgulescu and I. Demetrescu: The kinetics of reactions between benzhydryl bromide and normal alcohols, *Rev. Roumaine Chim.*, **18**, 355 (1973).
211. I. G. Murgulescu and I. Demetrescu: On the mechanism of the reactions between benzyl bromide and alcohols, *Rev. Roumaine Chim.*, **18**, 523 (1973).
212. I. G. Murgulescu and N. I. Ionescu: On the oxygen chemisorption on silver, *Thin Solid Films*, **15**, 15 (1973).
213. I. G. Murgulescu and A. Leibovici: An equation of state for metallic liquids, *Rev. Roumaine Chim.*, **19**, 799 (1974).
214. I. G. Murgulescu and M. Șerban: On the viscosity of molten metals. II, *Rev. Roumaine Chim.*, **19**, 1417 (1974).
215. I. G. Murgulescu and I. Bică: Pyrolysis and oxydative pyrolysis of isobutene, *Rev. Roumaine Chim.*, **19**, 1853 (1974).
216. I. G. Murgulescu and J. Păun: The radiolysis of the complex oxalates in aqueous solutions. II, *Rev. Roumaine Chim.*, **19**, 9 (1974).
217. I. G. Murgulescu and J. Păun: The radiolysis of the complex oxalates in aqueous solutions. III, *Rev. Roumaine Chim.*, **20**, 1196 (1975).
218. I. G. Murgulescu and M. Șerban: On the viscosity of molten metals. III. Activation Energy, *Rev. Roumaine Chim.*, **20**, 591 (1975).
219. I. G. Murgulescu i E. Segal: K vaprose o predexponentialnyh koefitsientov reactsii razloženia nekatoryh neorganiceskih veščest, "Gheterogennye Himiceskie Ravnovesia", Minsk, 1975, p. 37.

220. I. G. Murgulescu and E. Ivana: The absorption spectrum of PbI_2 in vapour phase, *Rev. Roumaine Chim.*, **21**, 169 (1976).

221. I. G. Murgulescu und M. Weissmann: Der Einfluß des Methans auf den thermischen Zerfall des Chloroforms, *Rev. Roumaine Chim.*, **21**, 1275 (1976).

222. I. G. Murgulescu und M. Weissmann: Der Einfluß des Methans auf den thermischen Zerfall des Chloroforms, II, *Rev. Roumaine Chim.*, **21**, 1435 (1976).

223. I. G. Murgulescu and C. Misdolea: A relation for the viscosity of ionic liquids, *Rev. Roumaine Chim.*, **22**, 1433 (1977).

224. I. G. Murgulescu and A. Leibovici: Internal pressure in liquid metals, *Rev. Roumaine Chim.*, **22**, 1279 (1977).

225. I. G. Murgulescu and M. Şerban: On the viscosity of molten metals IV. Dependence of viscosity of mean vibration frequency, *Rev. Roumaine Chim.*, **22**, 807 (1977).

226. I. G. Murgulescu and G. Mincu: Reaction of the bis-oxalato-diaquo Co (III) complex with iodide ion in acidic medium, *Rev. Roumaine Chim.*, **23**, 471 (1978).

227. I. G. Murgulescu and M. Şerban: Viscosity of liquids with quasispherical molecules,*Rev. Roumaine Chim.*, **24**, 1417 (1979).

228. I. G. Murgulescu and M. Terzi: Some physico-chemical properties of simple molten salts. IV. Surface tensions, *Rev. Roumaine Chim.*, **24**, 113 (1979).

229. I. G. Murgulescu, A. A. Borisov, C. Costea, C. Skachkov şi V.M. Zamanskii: Cinetica oxidării metanoice cu protoxid de azot. I. Consumul reactanţilor, *Rev. Chim. (Bucureşti)*, **31**, 43 (1980).

230. I. G. Murgulescu, G. Mincu and E. Jurconi: Catalysis by metal cation in the oxydoreduction of bisoxalatodiaquo Co (III) complex with iodide ion in acidic medium, *Rev. Roumaine Chim.*, **25**, 1033 (1980).

II. BOOKS IN THE SERIES "INTRODUCTION TO PHYSICAL CHEMISTRY":

1. I. G. Murgulescu, "Introducere în chimia fizică. Atomi. Molecule. Legătură chimică", vol. I. 1, Ed. Academiei, Bucureşti, 1976, 560 pp.
2. I. G. Murgulescu and V. Em. Sahini, "Introducere în chimia fizică. Structura şi proprietăţile moleculelor", vol. I. 2, Ed. Academiei, Bucureşti, 1978, 600 pp.
3. I. G. Murgulescu and J. Păun, "Introducere în chimia fizică. Nucleul atomic. Reacţii nucleare", vol. I. 3, Ed. Academiei, Bucureşti (in print).
4. I. G. Murgulescu and E. Segal, "Introducere în chimia fizică. Teoria molecular-cinetică a materiei", vol. II. 1, Ed. Academiei, Bucureşti 1979, 1030 pp.
5. I. G. Murgulescu, T. Oncescu and E. Segal, "Introducere în chimia fizică. Cinetică chimică şi cataliză", vol. II. 2, Ed. Academiei, Bucureşti, 1981, 1020 pp.
6. I. G. Murgulescu and R. Vîlcu, "Introducere în chimia fizică. Termodinamica chimică", vol. III, Ed. Academiei, Bucureşti (in print).

Revue Roumaine de Chimie, ,27 *1*, 19–26 (1982)

SYNTHESIS AND PYROLYSIS OF DIBENZO[*c,e*]TRICYCLO $[5.3.0.0^{2,10}]$ DECA-3,5,8-TRIENE, A NEW DIBENZO$(CH)_{10}$ HYDROCARBON

M. BANCIU[a)], M. ELIAN[b)], PHAN LE THUY[a)], C. DRĂGHICI[b)]
and ECATERINA CIORĂNESCU[a, b)]

a) Laboratory of Organic Chemistry ; Polytechnic Institute ; 76206, Bucharest, Romania.
b) Center of Organic Chemistry, ICECHIM ; Bucharest

Received June 1, 1981

The title hydrocarbon **3** ("3 : 4, 5 : 6-dibenzoisobullvalene") was obtained through the anionic Bamford-Stevens reaction of tosylhydrazone **12**. Pyrolysis or photolysis of the sodium salt of **12** afforded the dibenzo-enyne **13**. Pyrolysis of hydrocarbon **3** as well as pyrolyses of some derivatives of alcohol **2** (namely the acetate **8** and the ethylcarbonate **9**) gave triphenylene (**10**). The mechanisms of these reactions are discussed.

1. INTRODUCTION

The considerable interest concerning the syntheses and chemistry of $(CH)_{10}$ valence isomers was extended in the last years to the benzo $(CH)_{10}$ hydrocarbons[1–4] and dibenzo $(CH)_{10}$ isomers.[5] In spite of the replacement with aromatic rings of one or two double bonds of the parent hydrocarbon, the benzo $(CH)_{10}$-and dibenzo$(CH)_{10}$-valence isomers still retain an enhanced reactivity. In some cases, for example Nenitzescu's hydrocarbon[6] (tricyclo $[4.2.2.0^{2,5}]$ deca-3,7,9-triene), the mechanism of pyrolysis was completely understood only after the investigation of the benzoannelated derivatives.[7]

Continuing our interest in dibenzo $(CH)_{10}$ valence isomers[5c–f] we have recently considered[8] the ketone **1** and the alcohol **2** as precursors of a new dibenzo $(CH)_{10}$ valence isomer **3**. In this paper we describe the synthesis and pyrolysis of this hydrocarbon.

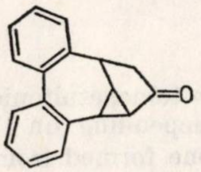

1

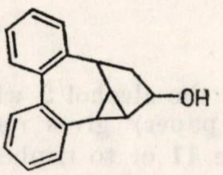

2

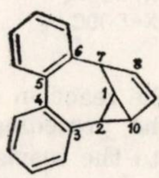

3

It should be noted that the parent compound 4 ("isobullvalene") was synthesized in 1970 independently by Masamune[9a] and Katz[9b] and all the three possible monobenzoderivatives 5[1a], 6[1c] and the unstable 7[1c] were described by Vedejs.

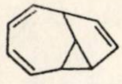

4

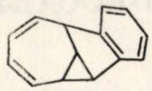

5

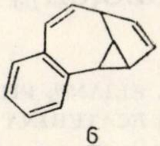

6

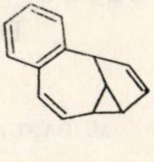

7

2. RESULTS

We reported recently[8] the five-step synthesis of dibenzo[*c*,*e*] tricyclo [5.3.0.$0^{2,10}$] deca-3,5-dien-9-one (**1**) starting from the known[10] 5*H*-dibenzo [*a*,*c*] cyclohepten-5-one. The corresponding alcohol **2** was obtained[8] on reduction of the ketone **1** with $LiAlH_4$. The conversion of these compounds into the dibenzoisobullvalene was attempted.

a. The tosylate of the alcohol **2** could not be obtained on treatment with tosyl chloride in pyridine. Consequently, the alcohol **2** was converted into its acetate **8** and ethyl carbonate **9**. Pyrolysis of the acetate **8** at 300° (10 mm Hg) or at 350° (atmospheric pressure) as well as pyrolysis of the ethyl carbonate **9** at 325° (atmospheric pressure) afforded in high yields triphenylene (**10**) as the single isolable product. Triphenylene was identified through its characteristic UV-[11a] and ^{1}H-NMR[11b] spectra. Triphenylene was also the single product isolated from the reaction of the alcohol **2** with boric acid at 200° and 2 mm Hg.

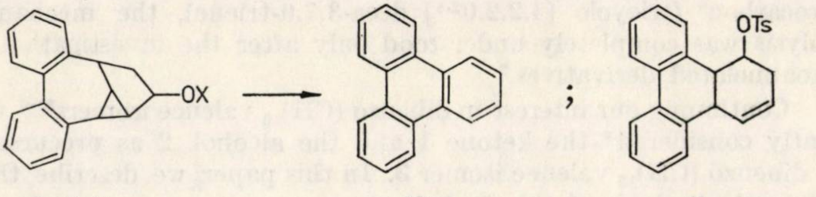

2, X=H
8, X=$COCH_3$
9, X=$COOC_2H_5$

10

11

Also the reaction of the alcohol **2** with *p*-toluenesulfonic acid, (described in the preceding paper)[8] gives rise, depending on the reaction conditions, to the tosylate **11** or to triphenylene formed from **11**. Thus, all reactions starting with alcohol **2** proceeded with rearrangement of the carbon skeleton and therefore failed to afford the desired hydrocarbon **3**.

b. The synthesis of hydrocarbon **3** through the Bamford-Stevens reaction of tosylhydrazone **12**, obtained from ketone **1** and tosylhydrazine, was then tried.

Pyrolysis of the anhydrous sodium salt of the tosylhydrazone **12** at 150° and 0.3 mm Hg, afforded a unitary product, **13**, in 80% yield. The IR spectrum of this product indicated the existence of a monosubstituted acetylene moiety ($\nu_{C\equiv C} = 2126$ cm^{-1} $\nu_{\equiv CH} = 3316$ cm^{-1}). The ^{1}H-NMR spectrum of **13** at room temperature (27°) presents a poorly resolved triplet at $\delta = 1.80$ ppm, wide signals at 2.5—3.4 and 5.8—6.3 ppm, a doublet at 6.65 ppm and a multiplet corresponding to aromatic protons at 7.1—7.9 ppm. The spectrum is temperature dependent and at 120° an averaged spectrum with sharp signals was obtained. At this temperature signals coresponding to the following protons can be observed: an acetylenic proton at 1.80 (t, J = 2.5 Hz) a CH_2 group at 2.65 (m), a CH group at 3.23 (q, J = 6.5 Hz) and the protons of a *cis*-disubstituted double bond at 6.10 (dd, J = 6.5 and 11 Hz) and 6.65 ppm (d, J = 11 Hz). The spectrum is in perfect agreement with the structure **13** (5(2′-propynil) 5*H*-dibenzo [*a*, *c*] cycloheptene).

It can be noted that the temperature dependence of the ^{1}H-NMR spectra was also observed[8] for other dibenzo [*a*, *c*] cycloheptenes substituted in position 5 with a CH_2X group, demonstrating thus the hindered rotation of the CH_2 group and/or the slow ring inversion.

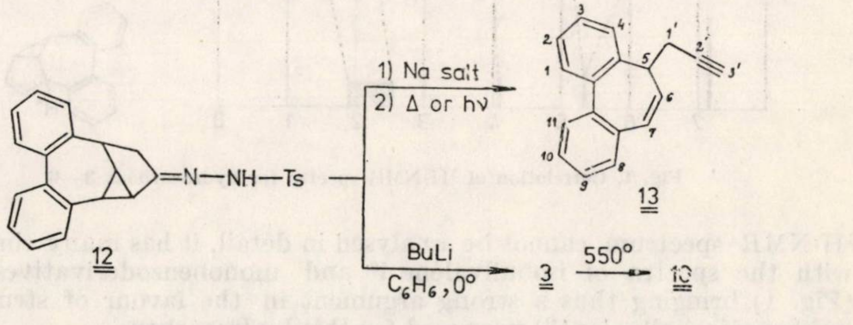

The photolysis of the sodium salt of **12** in tetrahydrofuran at —20° (with a medium — pressure UV Hg lamp) afforded the same acetylenic hydrocarbon **13** in 43% yield.

The product of the protic Bamford-Stevens reaction of tosylhydrazone **12** (sodium in ethyleneglycol at 140°) was again the acetylene **13** along with small quantities of ketone **1** and other minor unidentified compounds (different from a compound with formula **3**).

The treatment of the tosylhydrazone **12** with three moles of butyllithium in benzene at 0° gives rise, after the usual work-up followed by column chromatography on silica, to a new hydrocarbon, isolated in about 10% yield. In the infrared spectrum no characteristic absorptions of functional groups or of acetylenic compounds are visible. The hydrocarbon indicates in the UV spectrum (in methanol) two absorption maxima at 206.5(lg ε = 4.63) and 253nm(lg ε = 4.16) which demonstrate[12] that the dibenzo[*a*, *c*]cycloheptenic moiety from the starting compound **12** was preserved. The ^1H-NMR spectrum of this hydrocarbon presents signals at $\delta = 1.93 - 2.63$ (m; 3H); 4.05 (m; 1H); 5.30 (s, 2H) and 6.85–7.45 ppm (m; 8H). Even though the ^1H-NMR spectrum cannot be analysed in detail, it has many similarities with the spectra of isobullvalene **4**[9] and monobenzoderivatives **5**,**6**[1a,c] (Fig. 1) bringing thus a strong argument in the favour of structure **3** ("dibenzoisobullvalene") proposed for this hydrocarbon.

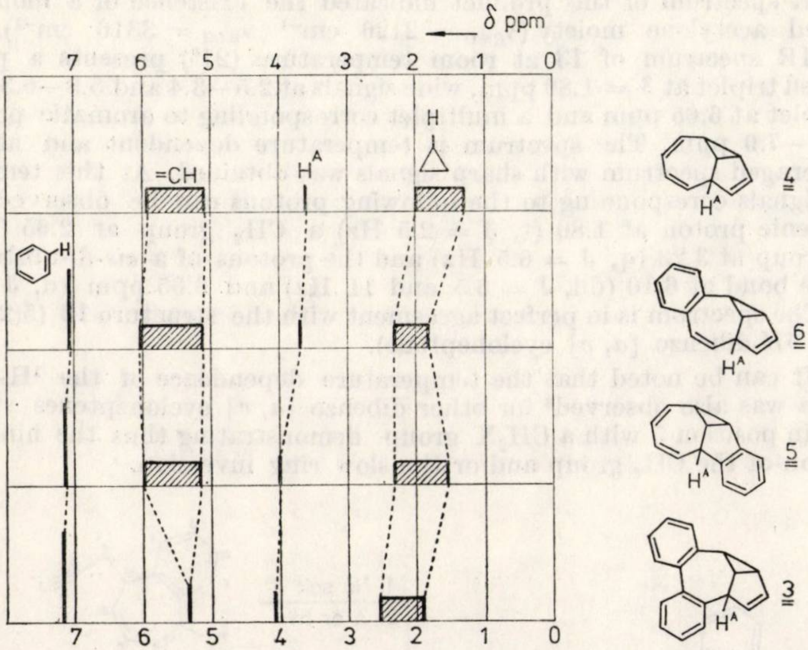

Fig. 1. Correlation of ^1H-NMR spectra for hydrocarbons **3**–**6**

3. DISCUSSION OF REACTION MECHANISMS

The generally agreed mechanism of ester pyrolysis through which a new double bond is created (without rearrangement) includes a cyclic transition state[13] from which the two leaving groups are simultaneously eliminated and linked together (E_i mechanism; *cis*-elimination). In the present case the olefin **3** should appear. Unfortunately, this strongly strained system rearranges probably during the pyrolysis into dihydrotriphenylene, **14**, a dibenzo $(CH)_{10}$ hydrocarbon, whose aromatisation leads easily to triphenylene. Similar aromatisations are well-known in the series of $(CH)_{10}$ valence isomers[14] and benzo $(CH)_{10}$ derivatives[2c]. Moreover, monobenzoisobullvalene **5** was transformed in pyrolysis conditions into a mixture of phenanthrene and dihydrophenanthrenes[1c].

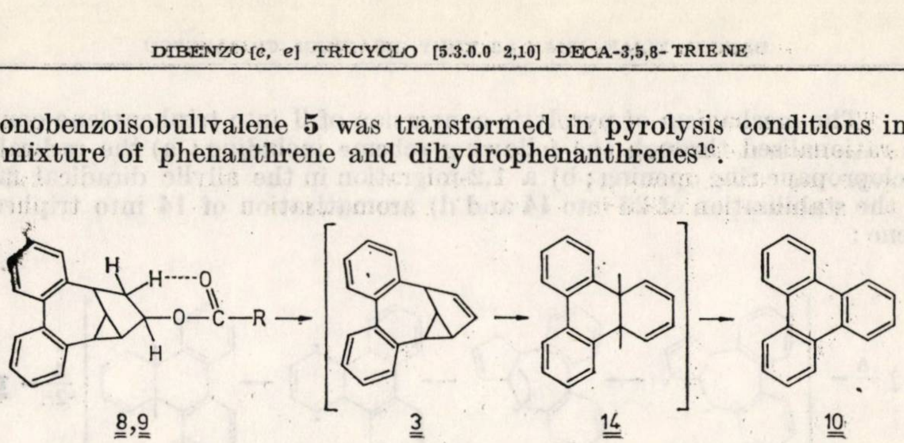

The formation of enynes in Bamford-Stevens reaction[15,16] was seldom described, being observed mainly when the generated carbenic centre possesses an α-cyclopropanic substituent.[17] In the present case the practically unstrained enyne **13** is formed through electron migration in the intermediate carbene **17** :

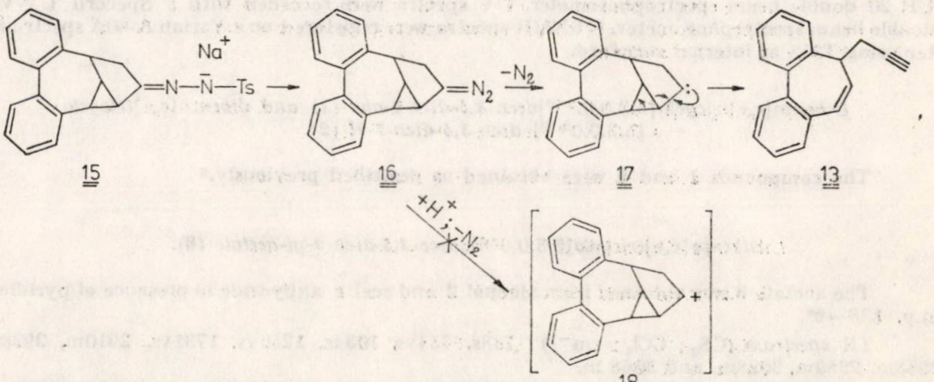

In protic conditions the elimination of a nitrogen molecule from the diazoderivative **16** seems to occur faster than the proton capture from a solvent molecule. Intervention of a carbocation **18** should give rise to compounds with a different skeleton (**11**) as it was shown previously.[8]

The formation of dibenzoisobullvalene **3** in the reaction of tosylhydrazone **12** with butyl-lithium could be explained by the anionic mechanism, including as succesive intermediates the tosylhydrazone anion **19**, the diimidic anion **20** and the vinylic anion **21** :

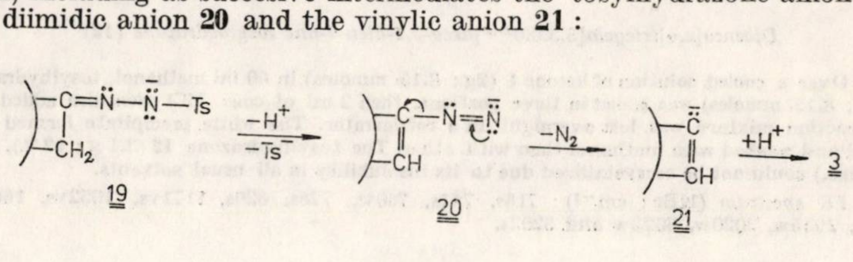

The mechanism of pyrolytic conversion of **3** into triphenylene could be rationalised through the following scheme including : a) the radicalic cyclopropane ring opening ; b) a 1,2-migration in the allylic diradical **22** ; c) the stabilisation of **23** into **14** and d) aromatisation of **14** into triphenylene :

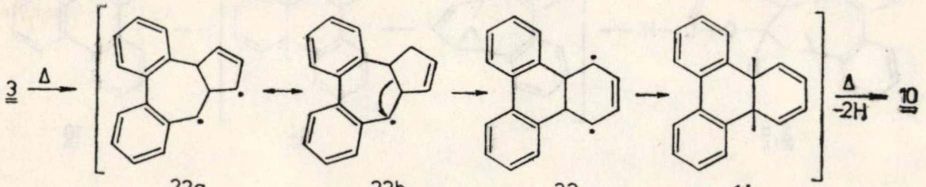

22a 22b 23 14

EXPERIMENTAL

Melting points are uncorrected. IR spectra were recorded with a Carl Zeiss-Jena UR 20 double beam spectrophotometer. UV spectra were recorded with a Specord UV-VIS double beam spectrophotometer. ^1H-NMR spectra were registered on a Varian A-60A spectrometer using TMS as internal standard.

Dibenzo[c,e]*tricyclo*[5.3.0.0.^{2,10}]*deca-3,5-dien-9-one* (**1**) *and dibenzo*[c,e]*tricyclo* [5.3.0.0^{2,10}] *deca-3,5-dien-9-ol* (**2**)

The compounds **1** and **2** were obtained as described previously.[8]

Dibenzo[c,e]*tricyclo*[5.3.0.0^{2,10}]*deca-3,5-dien-9-yl-acetate* (**8**).

The acetate **8** was obtained from alcohol **2** and acetic anhydride in presence of pyridine ; m.p. 138–9°.

IR spectrum (CS_2 ; CCl_4 ; cm^{-1}) : 738s, 754vs, 1034s, 1250vs, 1731vs, 2910m, 2928m, 2958m, 2989m, 3028m, and 3068 m.

^1H-NMR spectrum (CCl_4 ; δ ppm) ; 0.9–2.6 (m ; 5H ; $H^{8,8',1,2,10}$) ; 1.82 (s ; 3H ; $COCH_3$) ; 3.52 (m ; 1H ; H^7) ; 5.38 (m ; 1H ; H^9) ; 7.0–7.6 (m ; 8H ; H_{arom}).

Dibenzo[c,e]*tricyclo*[5.3.0.0^{2,10}]*deca-3,5-dien-9-yl-ethylcarbonate* (**9**)

The carbonate **9** was obtained from the alcohol **2** and ethylchloroformate in pyridine : m.p. 132–4°.

IR spectrum (CCl_4 ; cm^{-1}) : 1008m, 1265vs, 1738vs, 2855w, 2926m, 2960w, 2985w, 3026w and 3067w.

Dibenzo[c,e]*tricyclo*[5.3.0.0^{2,10}]*deca-3,5-dien-9-one tosylhydrazone* (**12**)

Over a cooled solution of ketone **1** (2g ; 8.15 mmoles) in 60 ml methanol, tosylhydrazine (1.5 g ; 8.15 mmoles) was added in three portions, then 2 ml of conc. HCl were also added and the reaction mixture was left overnight in a refrigerator. The white precipitate formed was filtered and washed with methanol then with ether. The tosylhydrazone **12** (3.1 g ; 92 %), m.p. 252° (dec.) could not be recrystallized due to its insolubility in all usual solvents.

IR spectrum (KBr ; cm^{-1}) : 716s, 741s, 760vs, 778s, 820s, 1171vs, 1352vs, 1667m, 2932w, 2955w, 3020w, 3073w and 3202s.

Pyrolyses of acetate **8** *and ethyl carbonate* **9** *of the alcohol* **2**

Pyrolyses were performed in a vertical quartz tube, electrically heated, filled with quartz chips. A stream of argon was admitted in pyrolysis tube, which was maintained under vacuum or at atmospheric pressure. Samples of 0.25 g **8** were pyrolysed ; at 250° and 10 mm Hg the acetate **8** was recovered unchanged, at 300° and 10 mm Hg the product consists (^{1}H-NMR spectrum) from triphenylene (**10**) and unreacted **8**, whereas at 350° and atmospheric pressure slightly impurified triphenylene (**10**) with a m.p. 182–195° was obtained (^{1}H-NMR and UV-spectra). Pyrolysis of **9** at 325° and atmospheric pressure affords triphenylene (**10**) impurified with small quantities of unreacted **9** (^{1}H-NMR spectrum).

Reaction of the alcohol **2** *with boric acid*

A finely powdered mixture of alcohol **2** (0.25 g ; 1mmole) and boric acid (0.25 g ; 4.05 mmoles) was sublimated at 180–200° and 2 mm Hg for 1–1.5 hrs. The sublimated thick uncoloured oil (0.135 g ; 58 %) was chromatographed on a Merck 60–SiO_2 column. On elution with petroleum ether white needles with m.p. 165–175° were obtained, consisting (^{1}H-NMR and UV-spectra) from slightly impurified triphenylene (**10**).

Bamford-Stevens reactions of tosylhydrazone **12**

a) *Aprotic pyrolysis of sodium salt of* **12**. In a sublimation apparatus over a suspension of tosylhydrazone **12** (0.420 g ; 1 mmole) in tetrahydrofuran (10 ml ; freshly distilled from $LiAlH_4$) a suspension of 40 % natrium hydride (0.08 g ; 1.32 mmoles ; washed twice with 4 ml tetrahydrofuran) in 10 ml tetrahydrofuran was added under argon atmosphere. After 1 hr., when the evolution of hydrogen ceased, the solvent was removed in vacuum and the dry sodium salt of **12** was heated at 150° and 0.3 mm Hg for 1.5 hrs. The sublimated oily product (0.188 g ; 80.7 %) represents the acetylenic olefine **13** in a practically pure state. It could be further purified by column chromatography on neutral alumina (elution with 3 : 7 ethyl ether : petroleum ether).

5(2′-propynyl)-5H-dibenzo[a,c]*cycloheptene* (**13**), uncoloured oil.

IR spectrum (CCl_4 ; cm^{-1}) : 911s, 1437s, 1483s, 2126m, 2851m, 2917m, 3027s, 3065s and 3316 vs.

^{1}H-NMR spectrum (CCl_4 ; δ ppm) : 1.80 (m ; 1H ; $H^{3'}$) ; 2.5–3.4 (m ; 3H ; $H^{1'}$, H^5) ; 5.8–6.3 (m ; 1H ; H^6) ; 6.65 (d ; $J_{7,6} = 11$ Hz ; 1H ; H^7) ; 7.1–7.9 (m ; 8H ; $H_{arom.}$).

b) *Aprotic photolysis of sodium salt of* **12**. A suspension of sodium salt of **12**,prepared as described above (*a*) from 0.420 g (1 mmole) **12** in 100 ml anhydrous tetrahydrofuran was irradiated at –20° with a medium pressure UV–Hg lamp (150 watt) for 3 hrs under argon atmosphere with magnetic stirring. After filtration of sodium toluene sulfinate and evaporation of the solvent the oily residue was chromatographed on neutral alumina. On elution with 3: 7 ethyl ether : petroleum ether the acetylenic olefine **13** was obtained (0.11 g ; 43.5 %) then, on elution with 1: 1 ethyl ether : petroleum ether the ketone **1** (0.04 g ; 16 %) was obtained.

c) *Protic Bamford-Stevens reaction of* **12**. Over a solution of sodium (0.035 g ; 0.015 gram atoms) in freshly distilled ethylene-glycol (5 ml) the tosylhydrazone **12** (0.420 g ; 1 mmole) was added and the mixture was heated under argon atmosphere at 130–140° for 2.5–3 hrs (after which time the evolution of nitrogen failed). The cooled reaction mixture was poured into water and ether extracted. The organic extract was washed with water, dried and evaporated affording a yellow oil (0.2 g) whose ^{1}H-NMR spectrum indicated the presence of enyne **13** beside ketone **1** and small quantities of unidentified components. Through column chromatography on neutral alumina the enyne **13** and the ketone **1** were obtained in small yields.

d) *Anionic Bamford-Stevens reaction of* **12**. Over an ice-cooled suspension of tosylhydrazone **12** (3.991 g ; 9.6 mmoles) in 200 ml anhydrous benzene a 15 % solution of *n*-butyllithium in *n*-hexane (17.6 ml ; 3: 1 molar ratio BuLi : **12**) was dropped with stirring under argon atmosphere during 15 minutes. In the first minutes an exothermic reaction occurs and the reaction mixture becomes a clear brownish-red solution. The reaction was maintained one hr at 0° then two hrs at room temp. The clear solution was poured into 200 ml ice-water (an insoluble yellowish precipitate was formed). The organic layer was separated and the aqueous one was extracted with benzene (3 × 30 ml). The combined benzenic solutions were washed with water, dried, filtered and evaporated in vacuum at room temp. The yellow thick oily residue (0.9 g) was dissolved in 2 ml benzene and chromatographed on a silica column. On elution with petroleum ether the hydrocarbon **3** was obtained (0.22g ; 10 %).

Dibenzo[c,e]*tricyclo* $[5.3.0.0^{2,10}]$*deca-3,5,8-triene* (**3**), ("dibenzoisobullvalene"), uncoloured thick oil.

IR spectrum (CS_2 ; CCl_4 ; cm^{-1}) : 725s, 735s, 754s, 770s, 785s, 3018 m, 3047m, and 3063m.

UV spectrum and *^{1}H-NMR spectrum* (see text).

Pyrolysis of dibenzoisobullvalene (3)

The pyrolysis of hydrocarbon **3** (0.1 g ; 0.5 mmoles) dissolved in 2 ml ethyl ether was performed in the apparatus described above (see pyrolyses of **8** and **9**), at 550° and 500 mm Hg. The product which was condensed in the final zone of the quartz tube was extracted with ether. The organic solution afforded after evaporation a crystalline product which, by UV- and ^{1}H-NMR spectral evidence, was triphenylene (**10**) in practically pure state.

REFERENCES

[1] a) E. Vedejs, *Tetrahedron Letters*, **1968**, 2633 ; b) E. Vedejs and T. Shepherd, *ibid.*, **1970**, 1863 ; c) E. Vedejs, R. A. Shepherd and R. P. Steiner, *J. Amer. Chem. Soc.*, **92**, 2158 (1970) ; d) E. Vedejs, *Tetrahedron Letters*, **1970**, 4963 ; e) E. Vedejs, *Chem. Comm.*, **1971**, 536 ; f) E. Vedejs, M. F. Salomon and P. D. Weeks, *J. Amer. Chem. Soc.*, **95**, 6770 (1973) ; g) E. Vedejs and R. P. Steiner, *Chem. Comm.*, **1973**, 599 ; h) E. Vedejs and E. S. C. Wu, *Tetrahedron Letters*, **1973**, 3793 ; i) E, Vedejs, M. F. Salomon and P. D. Weeks, *J. Amer. Chem. Soc.*, **95**, 6770 (1973) ; j) E. Vedejs, R. P. Steiner and E. S. C. Wu, *ibid.*, **96**, 4040 (1974).

[2] a) L. A. Paquette and J. C. Stowell, *Tetrahedron Letters*, **1970**, 2259 ; b) L. A. Paquette and J. C. Stowell, *J. Amer. Chem. Soc.*, **92**, 2584 (1970) ; c) L. A. Paquette, M. J. Kukla and J. C. Stowell, *ibid.*, **94**, 4920 (1972).

[3] a) I. Murata and Y. Sugihava, *Tetrahedron Letters*, **1972**, 3785 ; b) I. Muarta, Y. Sugihava and N. Ueda, *ibid.*, **1973**, 1183.

[4] L. Enescu, I. G. Dinulescu and M. Avram, *Rev. Roumaine Chim.*, **24**, 995 (1979).

[5] a) M. Avram, I. G. Dinulescu and C. D. Nenitzescu, *Liebigs Ann. Chem.*, **691**, 9 (1966) ; b) M. Stiles, U. Burkhardt and G. Freund. *J. Org. Chem.*, **32**, 3718 (1967) ; c) M. Banciu, M. Elian, E. Ciorănescu and C. D. Nenitzescu, *Tetrahedron Letters*, **1972**, 2573 ; d) M. Banciu, M. Elian, C. Drăghici and E. Ciorănescu, *Rev. Roumaine Chim.*, **19**, 1179 (1974) ; e) I. G. Dinulescu, M. Pop, F. Chiralcu, M. Avram and C. D. Nenitzescu, *ibid.*, **19**, 1197 (1974) ; f) M. Elian, M. Banciu, L. Stănescu and E. Ciorănescu, *ibid.*, **21**, 89 (1976).

[6] M. Avram, E. Sliam and C. D. Nenitzescu, *Liebigs Ann. Chem.*, **636**, 184 (1960).

[7] reviews, M. Banciu, *Rev. Roumaine Chim.*, **21**, 1083 (1976) ; A. T. Balaban, *ibid.*, **19**, 1185 (1974).

[8] M. Banciu, Phan Le Thuy, M. Elian, C. Drăghici and E. Ciorănescu, *Rev. Roumaine Chim.*, **26**, 1115 (1981).

[9] a) K. Hojo, R. T. Seidner and S. Masamune, *J. Amer. Chem. Soc.*, **92**, 6641 (1970) ; b) T. J. Katz, J. J. Cheung and N. Acton, *ibid.*, **92**, 6643 (1970).

[10] J. W. Cook, F. T. Dickson and J. D. Loudon, *J. Chem. Soc.*, **1947**, 746.

[11] a) E. Clar and L. Lombardi, *Ber. dtsch. chem. Ges.*, **65**, 1414 (1932) ; b) J. A. Pople, W. G. Schneider and H. J. Bernstein, "High Resolution Nuclear Magnetic Resonance", Mc Graw Hill, New York, 1959, p. 249.

[12] a) G. H. Beaven, G. R. Bird, D. M. Hall, E. A. Johnson, J. E. Ladburg, M. S. Leslie and E. E. Turner, *J. Chem. Soc.*, **1955**, 2708 ; b) E. Ciorănescu, M. Banciu, M. Elian, A. Bucur and C. D. Nenitzescu, *Liebigs Ann. Chem.*, **739**, 121 (1970).

[13] C. H. De Puy and R. W. King, *Chem. Rev.*, **60**, 431 (1960) ; G. G. Smith and F. W. Kelly, *Progr. Phys. Org. Chem.*, **8**, 75 (1971).

[14] W. V. E. Doering and J. W. Rosenthal, *J. Amer. Chem. Soc.*, **88**, 2078 (1966).

[15] W. R. Bamford and T. S. Stevens, *J. Chem. Soc.*, **1952**, 4735.

[16] see for example : R. H. Shapiro, in "Organic Reactions", vol. 23, J. Wiley, New York, 1976, p. 405 and the literature cited therein.

[17] J. W. Wheeler, R. H. Chung, Y. N. Vaisnav and C. C. Shroff, *J. Org. Chem.*, **34**, 545 (1969).

Revue Roumaine de Chimie, 27, 7, 27–35 (1982)

MIXED FILMS OF RETINYL PALMITATE WITH LIPIDS AT THE AIR–WATER INTERFACE

EMIL CHIFU and MARIA TOMOAIA-COTIŞEL

"Babeş-Bolyai" University, Department of Physical Chemistry; Str. Arany J., no. 11, 3400
Cluj-Napoca, Romania

Received April 14, 1981

Mixed films of all-*trans* retinyl palmitate with some lipids (stearic acid, tripalmitin or L-α-dipalmitoyl lecithin) at the air–water interface are studied by means of surface pressure *vs.* molecular area isotherms. The properties of the mixed films are interpreted in terms of molecular areas additivity and the surface phase rule. The findings enable us to conclude that the retinyl palmitate is immiscible either with stearic acid or tripalmitin, however it forms a quasi-ideal solution with dipalmitoyl lecithin in the monolayer—fact also revealed by close to zero values of the excess free energy of mixing. The different behaviour as regards miscibility of retinyl palmitate with various lipids may be accounted for by differences in the molecular structure of the latter.

With a view to investigating the interactions among the compounds of the biological membranes (e.g. carotenoids with lipids or phospholipids), the study of their miscibility in the mixed films spread at the air/water interface is of large interest,[1–9] taking into account certain resemblances of the natural membranes with the monomolecular films.[10–11]

Recently, we have reported some studies on miscibility of the carotenoid pigments with some lipids and phospholipids in mixed films at the air/water interface.[4–9]

This paper deals with the study on mixed films of all-*trans* retinyl palmitate (RP) and different lipids (stearic acid, tripalmitin or L-α-dipalmitoyl lecithin) at the air/water interface by means of the compression isotherms, surface pressure *vs.* area.

The complex problem regarding the miscibility of retinyl palmitate with the above mentioned lipids in two-dimensional state is interpreted in terms of the surface phase rule, the additivity rule of molecular areas, the collapse pressure of mixed monolayers and the excess free energy of mixing in the surface.

EXPERIMENTAL

The monolayers of pure components as well as of those of mixtures were studied by means of the compression isotherms, the surface pressure π as function of the molecular area A at the air/water interface. The compression curves were discontinuously recorded; the surface pressure was determined by the Wilhelmy method as we previously showed.[8,12]

Details on obtaining the mixed films have already been presented.[4,8] In our experiments the compression rate was 0.06 — 0.08 nm²/molecule min, what allowed for getting an isotherm within 15 — 20 min. The measurements were performed at ambient temperature (22 ± 2°C). The compression curves were reproducible within ±0.02 nm²/molecule and ±0.5 mN/m, as far as the area and the surface pressure measurements are concerned. Each of the isotherms ($\pi - A$) presented in the paper was chosen from a number of at least 10 experiments.

The retinyl palmitate in question was a synthetic product of cromatographic purity. The lipid components employed : stearic acid, tripalmitin and L-α-dipalmitoyl lecithin (dipalmitoyl lecithin : DPL) were synthetic products pro analysi, "Schuchardt", "Serva", respectively "Koch-Light".

Benzene "Reactivul" pro analysi was generally used for the film spread, however absolute ethanol — hexane mixture (2 : 98, *v/v*), commercial substances, pro analysi "Reactivul", respectively "Merck" were employed for the films bearing dipalmitoyl lecithin.

The films were usually spread on doubly-distilled water, while in the case of the stearic acid, in order to avoid its dissociation, this subphase was adjusted at pH = 2 with hydrochloric acid "Reactivul" volumetric solution.

RESULTS AND DISCUSSION

Compression curves. The experimental data obtained are plotted as surface pressure (π, mN/m) *vs.* molecular area (A, nm²/molecule) isotherms in Figs 1 and 2 for the mixed films of retinyl palmitate (RP) : stearic acid, respectively RP : tripalmitin, and RP : L-α-dipalmitoyl lecithin (DPL) in Figs 3 and 4, at the air/water interface for different mole fractions of retinyl palmitate (x_{RP}).

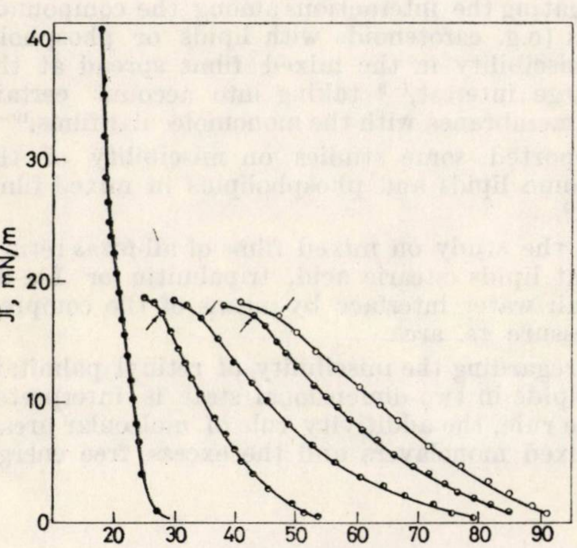

Fig. 1. — Surface pressure *vs.* area curves of monolayers of retinyl palmitate (RP) and stearic acid, on acidic solution (0.01 M HCl), at various mole fractions of RP. x_{RP} : ● :0.0 ; ◓ : 0.25 ; ◐ : 0.50 ; ◒ :0.75 ; ○ :1.0.

The isotherm (π *vs.* A (●), Fig. 1) obtained by us for pure stearic acid is similar to the one published in the reference literature.[13] In the case of tripalmitin, our data ((●), Fig. 2) are in accord with the ones obtained by other authors[14] for triglycerides.

As for the compression isotherms of DPL pure film ((●), Fig. 3) we have already published it;[15] it is to be noted that the DPL displays a phase transition in the pure monomolecular film at a surface pressure of about 8 mN/m. The DPL surface characteristics are in general agreement with those to be found in the literature.[16–19] The behaviour of retinyl palmitate in the monocomponent film (Fig. 3, (○)) was previously published by us.[4,8,9,20]

Considering the values of the compression moduli,[8,9,15] it may be noted that the lipids investigated display characteristic features of the typically condensed films, while RP exhibits properties of the liquid expanded films.[21]

The values of the collapse pressures show that RP is the easiest collapsable component ($\pi_c = 17$ mN/m, see the arrows in Figs. 1—4) out of all the substances studied.

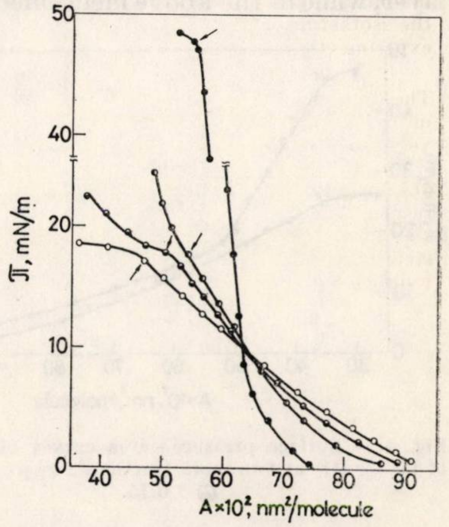

Fig. 2. — Surface pressure — area curves of monolayers of retinyl palmitate and tripalmitin, at the air-water interface at different mole frations of RP. x_{RP}: ● : 0.0; ◐ : 0.3; ◒ : 0.6; ○ : 1.0.

Following now, in Figures 1 and 2, the succession of the compression isotherms for different compositions of RP : stearic acid, respectively RP : tripalmitin monolayers, it is to be noted that the collapse pressure of the mixed films is constant and equals that of RP which has the lowest surface pressure. Thus the collapse pressure is independent of composition of the mixed monolayer.

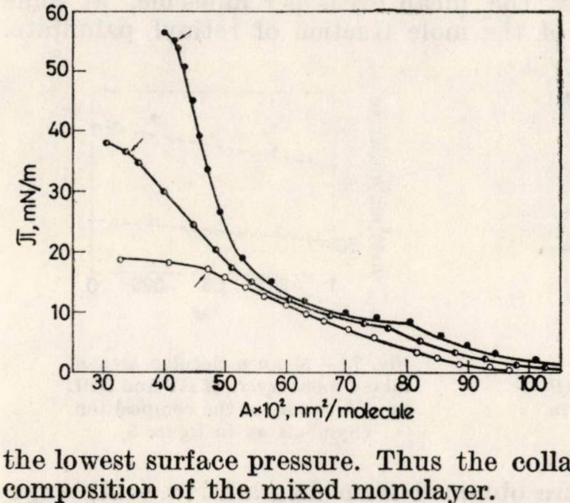

Fig. 3. — Surface pressure — area curves of dipalmitoyl lecithin (DPL) (●), retinyl palmitate (○) and DPL : RP mixture with x_{RP} : 0.5(◐).

Further on, considering in Figures 3 and 4, the compression isotherms corresponding to different surface mixture compositions of RP :

DPL, it is observed that the collapse pressure (see the arrows) varies continuously, ranging from one pure component to the other. Therefore, in this case the collapse pressure depends on composition of the mixed monolayer, while in the above mentioned ones (Figs 1 and 2) it remains constant.

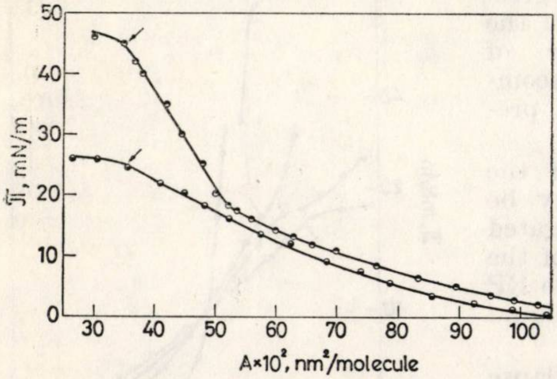

Fig. 4. — Surface pressure—area curves of mixtures of DPL : RP at two mole fractions : x_{RP} : ◓ : 0.25 ; ◒ : 0.75.

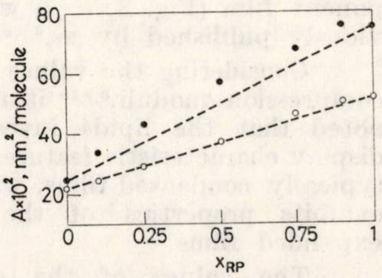

Fig. 5. — Mean molecular area of monolayers of RP and stearic acid as a function of the mole fraction of RP, x_{RP}, at two values of the surface pressure. π:5mN/m (●); 15 mN/m (○)

It is necessary to state first the degree of miscibility of the components in the monolayer, what will enable us to understand the nature of the molecular interactions that may occur in this mixed films.

In this respect, miscibility of RP with these lipids was put in question, utilizing the relation between the mean molecular area *vs.* composition in the mixed monolayers.

Figures 5, 6 and 7 show the mean areas per molecule, at some surface pressures as function of the mole fraction of retinyl palmitate.

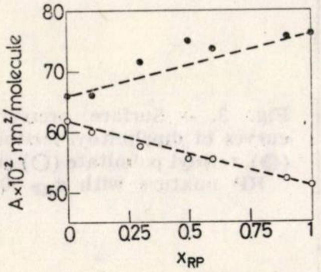

Fig. 6. — Mean molecular area — mole fraction, x_{RP}, plot of RP and tripalmitin. (Symbols as in figure 5).

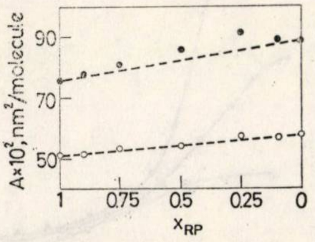

Fig. 7. — Mean molecular area of mixed monolayers of RP and DPL as a function of the composition. (Symbols as in figure 5).

The mean molecular areas were obtained from diagrams ($\pi - A$) experimentally recorded by graphical interpolation at the given surface pressures. It is to be noted that in all the cases RP : stearic acid, RP :

tripalmitin and RP : DPL, the diagrams show slightly positive deviations at low pressures, $\pi \leqslant 5$ mN/m, from the additivity rule (dotted line) given by equation:

$$A = x_1A_1 + x_2A_2 \tag{1}$$

In equation (1), A_i represents the molecular area of the ith component in the pure monolayer at one and the same fixed surface pressure, while x_i stands for the mole fraction of the ith component in the mixed monolayer.

On the diagrams (Figs 1–4), it is to be noted that the deviations are diminished by increasing the surface pressure, and at $\pi = 15$ mN/m (Figs 5–7) all the systems meet the requirements of the additivity rules.

As additivity of the molecular areas denotes either formation of an ideal two-dimensional solution or complete immiscibility of the components in the film,[22] the characteristics of the mixed films are interpreted from the standpoint of the surface phase rule[23] applied on the collapse pressure.[4–9,24,25]

Surface phase rule and the collapse pressure. For plane surfaces this rule reads:[23]

$$w = (c - r) + 2 - \varphi - (\psi - s) \tag{2}$$

where: w stands for the variance of the system, c the number of components, φ the number of bulk phases, ψ the number of surface phases, s the number of surface types, while r is the number of independent chemical reactions that may occur in the system. At constant external temperature and pressure, in the absence of chemical reactions ($r = 0$), the equation becomes:

$$w = (c - \varphi) - (\psi - s) \tag{3}$$

Generally, the two components in the monolayer may form either two surface phases if immiscible, or one single surface phase when their miscibility is complete.

The two-dimensional phase rule applied for discussion on the equilibrium between the surface film and the bulk collapse phase led us to the following conclusions:

(*i*) When the components are immiscible, in the film we have: $\psi = 4$, as one of the types of surface, namely the air/water interface, bears two surface phases (corresponding to each of the components), whereas any of the other two types of surface (collapsed phase/water, collapsed phase/air) bears only one surface phase. From equation (2) for the case $r = 0$, it results $w = 2$, respectively only temperature T and external pressure P may have arbitrary values. According to equation (3), at constant temperature and pressure, the variance of the system is $w = 0$. Thus, there is only one value of the collapse pressure compatible with coexistence of the two surface phases in the mixed films, and in consequence:

$$\pi_c = \text{const} \tag{4}$$

(*ii*) When the components are miscible, the air/water interface bears only one surface phase. It results, then, that $\psi = 3$, and from equation (2) correspondingly, we get $w = 3$, what shows that T, P and the collapse pressure π_c may be randomly fixed. At $T = \text{const.}$ and $P = \text{const.}$, according to equation (3), the variance of the system is $w = 1$, and in consequence the surface collapse pressure varies as function of the monolayer compositions:

$$\pi_c = \pi_c(x_i) \tag{5}$$

Case (*i*) is to be found with our systems, too: retinyl palmitate: stearic acid, and retinyl palmitate: tripalmitin (see Figs 1 and 2, and Eq. (4)), the components being immiscible in the monolayer at collapse nressure; it may be possible that at low surface pressures the compodents be miscible in the monomolecular film, while subsequent compression leads to phase separation, prior to collapse.[22,26]

Studying again in Figs 3 and 4, it may be noted that the continuous variation of the collapse pressure as function of the film composition reveals, in accord with the phase rule (Eqs (3) and (5), in the theoretical discussions for case (*ii*)), complete miscibility of the retinyl palmitate with dipalmitoyl lecithin.

For further information on miscibility, variation of the collapse pressure π_c of retinyl palmitate: dipalmitoyl lecithin mixed films as function of composition, plotted in Fig. 8, was put in question. The general equation on dependence of the collapse pressure as function of composition in the ideal case is:[27]

$$1 = x_1 \exp \frac{(\pi_c - \pi_{c1})A_{c1}}{kT} + x_2 \exp \frac{(\pi_c - \pi_{c2})A_{c2}}{kT} \tag{6}$$

where, π_{ci} is the collapse pressure of the *i*th component in the pure film, while A_{ci} — the corresponding collapse area, k and T — Boltzmann constant, respectively absolute temperature. When $(\pi_c - \pi_{ci})A_{ci} \ll \ll kT$, development of the exponentials in series leads to the following approximate relation:

$$\pi_c = x_1\,\pi_{c1} + x_2\,\pi_{c2} \tag{7}$$

According to equation (7), the experimental results in Fig. 8 point out an ideal surface solution behaviour of the retinyl palmitate: dipalmitoyl lecithin system.

Thus, for the mixed film of retinyl palmitate : dipalmitoyl lecithin, the collapse pressure method shows ideal miscibility (Fig. 8), but, by applying the additivity rule of molecular areas, small positive deviations from the ideal behaviour could be found (Fig. 7).

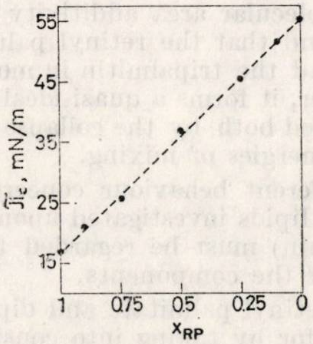

Fig. 8. — Collapse pressure of mixed RP : DPL monolayers as a function of the mole fraction of RP.

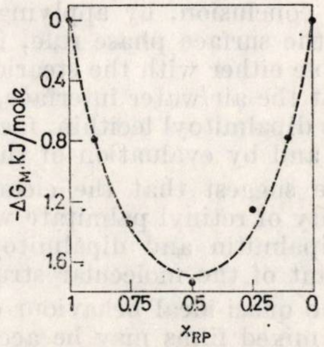

Fig. 9. — Free energy of mixing, ΔG_M kJ/mole, for mixtures of retinyl palmitate and dipalmitoyl lecithin at air/water interface.

In order to decide upon the behaviour of RP : DPL mixed films the free energy of mixing in the surface ΔG_M was determined,[22] by:

$$\triangle G_M = \triangle G_M^I + \int_0^\pi (A - x_1 A_1 - x_2 A_2) d\pi \tag{8}$$

where $\triangle G_M^I$ is the free energy of mixing for an ideal system and the A values have the known significances, with the only specification that in this case they are mole magnitudes. Equation (8) is applied to any surface pressure π, yet smaller than the one corresponding to the collapse of each pure component (see Figs 3 and 4); the values of the excess free energy of mixing in the surface were directly calculated graphically (the last term from Eq.(8)) from the compression isotherms for the pure and mixed monolayers, taking as integration limit $\pi = 17$ mN/m. Calculations showed that the values of excess-free energy of mixing in the film are practically zero (see Fig. 9), what points out a quasi-ideal behaviour of the retinyl palmitate : dipalmitoyl lecithin surface solution.

As for the small positive deviations from the additivity of areas (Fig. 7), respectively the slight expansion of dipalmitoyl lecithin films in the presence of retinyl palmitate, obtained at low pressures and small mole fractions of retinyl palmitate, they could be accounted for by a disturbance of interdigitation of the saturated chains in the film.

If interdigitation among the molecules of dipalmitoyl lecithin or between dipalmitoyl lecithin and retinyl palmitate were caused by the carotenoid pigment, then negative deviations from ideality would be stated. On the contrary, if interdigitation among the lecithin molecules is hindered by the retinyl palmitate, then positive deviations are obtained, of the same nature as those found by us.

We mention that in the literature[3] it has been reported the fact that the retinal may hinder or inhibit interdigitation of the phospholipids in the monolayers by the steric hinderance.

In conclusion, by applying the molecular area additivity rule, as well as the surface phase rule, it is found that the retinyl palmitate is immiscible either with the stearic acid and the tripalmitin in monolayers spread at the air/water interface, however, it forms a quasi-ideal solution with the dipalmitoyl lecithin, fact revealed both by the collapse pressure method and by evaluation of the free energies of mixing.

We suggest that the clearcut different behaviour concerning the miscibility of retinyl palmitate with the lipids investigated upon (stearic acid, tripalmitin and dipalmitoyl lecithin) must be regarded from the standpoint of the molecular structure of the components.

The quasi-ideal behaviour of the retinyl palmitate and dipalmitoyl lecithin mixed films may be accounted for by taking into consideration first a certain similitude in structure, respectively the existence of two hydrocarbon chains graphed on the polar group, one of the chains being of the same nature for the two components of the film.

In the case of retinyl palmitate : stearic acid, and retinyl palmitate : tripalmitin films, the difference in the molecular structure of different lipids (one hydrocarbon chain, respectively three chains) as compared with retinyl palmitate is noteworthy, and in lack of specific interactions, they are immiscible with retinyl palmitate at high surface pressures.

REFERENCES

[1] J. Aghion and R. M. Leblanc, *J. Membrane Biol.*, **42**, 189 (1978).

[2] O. A. Roels and D. O. Shah, *J. Colloid Interface Sci.*, **29**, 279 (1969).

[3] N. Yckowski and S. S. Brody, *Z. Naturforsch.*, **29** C, 327 (1974).

[4] E. Chifu and M. Tomoaia-Cotişel, *Rev. Roumaine Chim.*, **24**, 979 (1979).

[5] E. Chifu, M. Tomoaia-Cotişel and Z. Andrei, *Stud. Univ. Babeş-Bolyai Chem.*, **24** (2), 63 (1979).

[6] M. Tomoaia-Cotişel and E. Chifu, *Gazz. chim. Ital.*, **109**, 371 (1979).

[7] E. Chifu, M. Tomoaia-Cotişel and A. Ioanette, *Gazz. chim. Ital.*, **109**, 397 (1979).

[8] M. Tomoaia-Cotişel, *Ph. D. Thesis*, Babeş-Bolyai University of Cluj-Napoca, 1979.

[9] E. Chifu and M. Tomoaia-Cotişel, *Rev. Chim. (Bucureşti)*, in press.

[10] D. A. Cadenhead, *Recent Progr. Surface Sci.*, **3**, 169 (1970).

[11] G. L. Gaines, Jr., "Insoluble Monolayers at Liquid-Gas Interfaces", Interscience, New York, 1966, p. 348.

[12] E. Chifu, M. Tomoaia and A. Ioanette, *Gazz. chim. Ital.*, **105**, 1225 (1975).

[13] A. Matsubara, R. Matuura and H. Kimizuka, *Bull. Chem. Soc. Japan.*, **38**, 369 (1965); K. Motomura, A. Shibata, M. Nakamura and R. Matuura, *J. Colloid Interface Sci.*, **29**, 623 (1969); E. D. Goddard, S. R. Smith and O. Kao, *J. Colloid Interface Sci.*, **21**, 320 (1966); E. D. Goddard, O. Kao and H. C. Kung, *Ibbid.*, **24**, 297 (1967); H. E. Ries, Jr. and H. Swift, *J. Colloid Interface Sci.*, **64**, 111 (1978).

[14] D. A. Cadenhead, *Inds. Eng. Chem.*, **61**, 22 (1969).

[15] M. Tomoaia-Cotişel, I. Zsakó and E. Chifu, *Ann. Chim. (Rome)*, **71** 189 (1981)

[16] M. C. Phillips and D. Chapman, *Biochim. Biophys. Acta*, **163**, 301 (1968); F. Vilallonga, *Biochim. Biophys. Acta*, **163**, 290 (1968); M. Hayashi, T. Muramatsu and I. Hara, *Biochim. Biophys. Acta*, **225**, 98 (1972).

[17] J. C. Watkins, *Biochim. Biophys. Acta*, **152**, 293 (1968).
[18] P. Joos and R. A. Demel, *Biochim. Biophys. Acta*, **183**, 447 (1969).
[19] R. D. Smith and J. C. Berg, *J. Colloid Interface Sci.*, **74**, 273 (1980).
[20] I. Zsakó, E. Chifu and M. Tomoaia-Cotișel, *Gazz. chim. Ital.*, **109**, 663 (1979).
[21] J. T. Davies and E. K. Rideal, "Interfacial Phenomena", Acad. Press, New York, 1963, p. 265.
[22] G. L. Gaines, Jr., "Insoluble Monolayers at Liquid-Gas Interfaces", Interscience, New York, 1966, chapter 6.
[23] R. Defay, I. Prigogine, A. Bellemans and D. H. Everett, "Surface Tension and Adsorption", Longmans, Green, London, 1966, p. 77.
[24] M. C. Phillips and P. Joos, *Kolloid-Z. Z. Polym.*, **238**, 499 (1970).
[25] M. Nakagaki and N. Funasaki, *Bull. Chem. Soc. Japan.*, **47**, 2094 (1974).
[26] K. Tajima and N. L. Gershfeld, *Adv. Chem. Ser., (Monolayers)*, **144**, 165 (1975).
[27] P. Joos and R. A. Demel, *Biochim. Biophys. Acta*, **183**, 447 (1969); P. Joos, *Bull. Soc. Chim. Belges*, **78**, 207 (1969); **80**, 277 (1971).

Revue Roumaine de Chimie, 27, 7, 37—45 (1982)

CONTRIBUTIONS TO THE CALCULATION OF ION EXCHANGE EQUILIBRIUM IN WATER DEMINERALIZATION PROCESS

VASILE COCHECI*, LUCIAN NEGULESCU**, FRANCISC KLEPP*
* The Polytechnic, Bd. 30 Decembrie no. 2, Timişoara, Romania
** The Polytechnic, Faculty of Energetics, Spl. Independenţei, 202, Bucharest, Romania

Received June 18, 1981

The compositional variation isotherms, in the ion exchange processes, are of a great importance. The evolution of ion exchange process follows an isotherm defined by the molar ratio of the ionic species in the ion exchanger and in the effluent at a time τ. The present paper applying to the matrix modelling calculation presents an example for the ionic species transfer, in the case of different ion exchangers, which are used in water demineralization technology. Taking into account the ions leakage at the time τ, the composition of the effluent is represented by a line vector. As an immediate application, it is presented the case of water decarbonation with weakly acid exchangers, with a great content of bicarbonates and with a ratio of overunitary ion concentrations of $HCO_3^-/Ca^{+2} + Mg^{+2}$. Because the composition variation is that of the carbonic acid derivatives, these were plotted in a vector column and the stoichiometric coefficients in a vector line. Taking into account the fact that the concentrations of the carbonic acid derivatives existing in water depend on pH and on the dissociation constants, by applying the mass action law and mass conservation law we obtained a pratical calculation formula.

If we assume a homogenous chemical system formed of p elements, then the molecules and ions present in the system are to be composed of $X_1, X_2, \ldots, X_p$ elements. If the total number of molecular species and of ions respectively, is q, then for each Y_i species $(i = 1, 2 \ldots, q)$ we have:

$$Y_i = \alpha_{i1}X_1 + \alpha_{i2}X_2 + \ldots + \alpha_{ip}X_p \quad (i = 1,2,\ldots,q) \qquad (1)$$

which means that molecule or ion Y_i consist of α_{i1} atoms of element X_1, of α_{i2} atoms of elements X_2 and of α_{ip} atoms of element X_p. If $\alpha_{ij} = 0$, then the element X_j is not present in the molecule Y_i. Hence, molecule or ion Y_i could be written in the form of line vector:

$$\mathbf{Y}_i(\alpha_{i1}, \alpha_{i2}, \ldots, \alpha_{ip})$$

a vector which expresses the chemical formula of $\mathbf{Y}_i$.

Writing all the molecules and ions of the system in the form of a line vector, we obtain for the chemical system under consideration a matrix of the form:

$$\begin{Vmatrix} \alpha_{11} & \alpha_{12} & \alpha_{1p} \\ \alpha_{21} & \alpha_{22} & \alpha_{2p} \\ \hdashline \alpha_{q1} & \alpha_{q2} & \alpha_{qp} \end{Vmatrix}$$

As a rule, the number p of the chemical elements of the system is lower than the number of molecules and ions taken together, because some of the elements may belong to different components and therefore the number p of the matrix columns is smaller than the number q of the lines. In this case the matrix rank, i.e. the highest rank order of the non-null determinant that can be formed with matrix elements can be, at the most, p, that is: $r \leqslant p$. In this case $q - r$ matrix lines can be expressed as linear combinations of the other r lines. The relations of the chemical transformation are nothing but these linear combinations. As a consequence, if in a system, q chemical combinations (molecules and ions) exist and the chemical system matrix rank is $r < q$, then $q < r$ reactions could take place in that system.

The practical importance of this method lies in that it facilitates, in the case of more complex systems, the plotting of equilibrium concentration equations.

The equations expressing the linear combinations are of the form:

$$Y_k = \nu_{k1} Y_1 + \nu_{k2} Y_2 + \ldots + \nu_{kr} Y_r \quad K = r + 1, r + 2, \ldots, q$$

where values ν_{kl} $(k = r + 1, r + 2, \ldots, q;\ l = 1, 2, \ldots, r)$ represent the stoichiometric coefficients, some of which could be null.

To the $q - r$ linear combinations obtained in this way there correspond also $q - r$ thermodynamic equilibrium relations:

$$K = \frac{(m_1\gamma_1)^{k1}(m_2\gamma_2)^{k2}\ldots(m_r\gamma_r)^{kr}}{m_k\gamma_k}$$

where m is the molarity of the substances and γ the activity coefficient.

The neutralization equations of the electrolyte systems could be written as:

$$\sum_{i=1}^{q} z_{yi} \cdot m_{yi} = 0$$

where only ion concentrations are involved because z value is null in the case of molecules. For negatively charged ions z_{yi} will be written with minus sign.

The r relations used to obtain chemical compounds are of the form:

$$m_{yi} + \sum_{k=r+1}^{q} \delta_{kl} m_{yl} = w_l \quad (l = 1, 2, \ldots, r) \tag{2}$$

Indices yi designate r independent substances with magnitudes w_l being previously calculated from system :

$$Q_{yj} + \sum_{l=1}^{r} \alpha_{lj} w_l \quad (j = 1, 2, \ldots, p) \tag{3}$$

Further on, let us illustrate the matrix calculations for the ion exchange equilibrium.

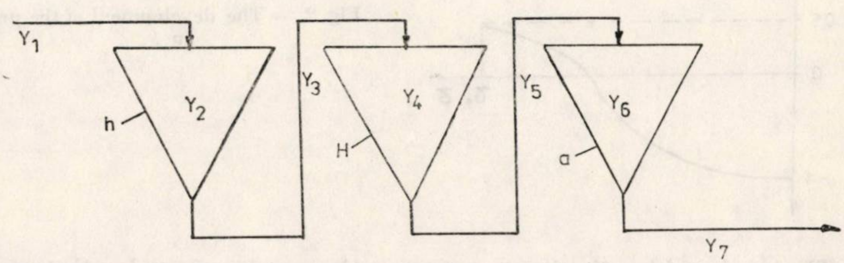

Fig. 1. — Demineralization installation.

We consider a water demineralization installation of the form shown in Fig. 1, where Y_1 is the inflow system reaching to the weak acid cation exchanger h ; Y_2 is the ionic mass charge system in h ; Y_3 is the effluent system of h and at the same time the inflow in the strongly acid cation exchanger H ; Y_4 is the ionic mass charge system in H ; Y_5 is the effluent system of H and the inflow in the weak basic anion exchanger a ; Y_6 is the ionic mass charge system in a and Y_7 is the effluent system of a.

Assuming the composition of raw water inflow to be :

Ca^{+2} Mg^{+2} Na^{+} K^{+} HCO_3^{-} Cl^{-} SO_4^{-2} SiO_3^{-2}

This composition can be illustrated in the following manner, as we stated above :

$$\mathbf{Y}_1(\alpha_{11}, \alpha_{12}, \alpha_{13}, \alpha_{14}, \alpha_{15}, \alpha_{16}, \alpha_{17}, \alpha_{18})$$

where :

$$\alpha_{11}X_1 + \alpha_{12}X_2 + \alpha_{13}X_3 + \alpha_{14}X_4 = \alpha_{15}X_5 + \alpha_{16}X_6 + \alpha_{17}X_7 + \alpha_{18}X_8$$

This water flows through h, charged with a weak acid cationic mass and changes its compositions into :

$$\mathbf{Y}_3 = (\alpha_{31}, \alpha_{32}, \alpha_{33}, \alpha_{34}, \alpha_{35}, \alpha_{36}, \alpha_{37}, \alpha_{38})$$

where :

$$\alpha_{31}X_1 + \alpha_{32}X_2 + \alpha_{33}X_3 + \alpha_{34}X_4 = \alpha_{35}X_5 + \alpha_{36}X_6 + \alpha_{37}X_7 + \alpha_{38}X_8$$

In this stage α_{15} turns into α_{35} in time τ_1, from $\alpha_{15} = -1$ to $\alpha_{35} = 0.5$, which represents the operation cycle of exchanger *h*. The process that takes place in *h* is shown in Fig. 2.

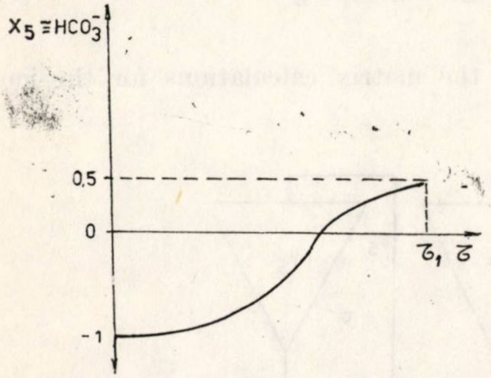

Fig. 2. — The development of the process in *h*.

The weak acid cationic mass retains the species given by line vector $\mathbf{Y}_2 = \mathbf{Y}_1 - \mathbf{Y}_3$.

The effluent from exchanger *h*, with the composition Y_3, flows through exchanger *H*, changing its composition in :

$$\mathbf{Y}_5(\alpha_{51},\ \alpha_{52},\ \alpha_{53},\ \alpha_{54},\ \alpha_{55},\ \alpha_{56},\ \alpha_{57},\ \alpha_{58})$$

where the sum of cations is equal to the sum of anions like in the preceding case.

In this stage $\alpha_{33} = 0$ turns into $\alpha_{35} = 0.2$ which represents the ion leakage from the device. The duration of this stage τ_2, represents the operation cycle of exchanger *H*. The process is shown in Fig. 3.

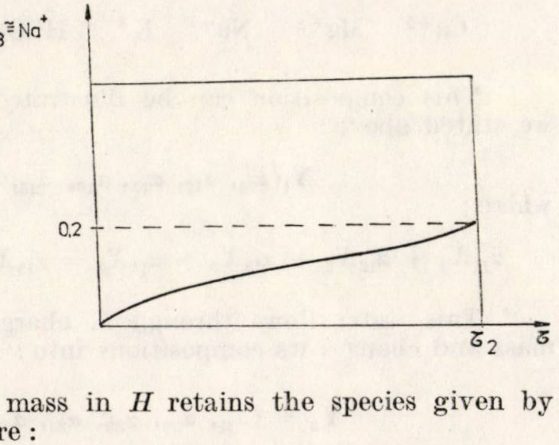

Fig. 3. — The development of the process in *H*.

The strongly acid ionic mass in *H* retains the species given by line vector $\mathbf{Y}_4 = \mathbf{Y}_3 - \mathbf{Y}_5$ where :

$\mathbf{Y}_4(\alpha_{41},\ \alpha_{42},\ \alpha_{43},\ \alpha_{44},\ \alpha_{45},\ \alpha_{46},\ \alpha_{47},\ \alpha_{48})$, where $\alpha_{4j} = \alpha_{3j} - \alpha_{5j}$ and $(j = 1, 2, \ldots, 8)$.

Exchanger *H* effluent with composition $\mathbf{Y}_5$ flows through exchanger *a*, equipped with a weak basic anionic mass and modifies its composition as follows :

$$\mathbf{Y}_7(\alpha_{71}, \alpha_{72}, \alpha_{73}, \alpha_{74}, \alpha_{75}, \alpha_{76}, \alpha_{77}, \alpha_{78}) \text{ where } \alpha_{71}X_1 + \alpha_{72}X_2 + \alpha_{73}X_3 + + \alpha_{74}X_4 = \alpha_{75}X_5 + \alpha_{76}X_6 + \alpha_{77}X_7 + \alpha_{78}X_8.$$

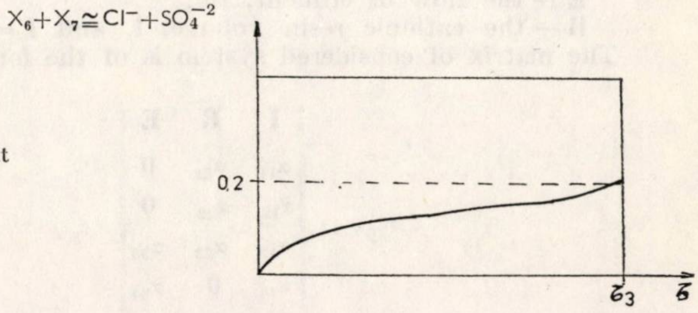

Fig. 4. — The development of the process in *a*.

In this stage $\alpha_{36} + \alpha_{37} = 0$ change into $\alpha_{56} + \alpha_{57} = 0.2$, which represents the ion leakage from the device in time τ_3, i.e. the operation cycle of the exchanger *a*. The proscess is shown in Fig. 4.

The weak basic anionic mass retains the species given by the line vector $\mathbf{Y}_6 = \mathbf{Y}_5 - \mathbf{Y}_7$ where :

$$\mathbf{Y}_6(\alpha_{61}, \alpha_{62}, \alpha_{63}, \alpha_{61}, \alpha_{65}, \alpha_{66}, \alpha_{67}\ \alpha_{68}), \text{ where } \alpha_{6j} = \alpha_{5j} - \alpha_{7j}.$$

In the following we relate, in detail, applying the matrix method, the practical case of ion exchange for a water which contains the next ionic species : Ca^{+2}, Mg^{+2}, Na^+, K^+, HCO_3^-, SO_4^{-2}, Cl^-.

The composition of this water may be mathematically presented as follows :

Ca^{+2}	α_{11}	HCO_3^-	α_{14}
Mg^{+2}	α_{12}	Cl^-	α_{15}
$Na^+ + K^+$	α_{13}	SO_4^{-2}	α_{16}

where :

$$\alpha_{11} + \alpha_{12} + \alpha_{13} = \alpha_{14} + \alpha_{15} + \alpha_{16}$$

and :

$$\alpha_{14} > \alpha_{11} + \alpha_{12}$$

Passing this water through a column with weak acid cationic resin, between the inflow, cationic resin and effluent, the ionic balance established is given by the following matrix relations :[1,2]

$$\mathbf{I} = \|\alpha_{11},\ \alpha_{12},\ \alpha_{13},\ \alpha_{14},\ \alpha_{15},\ \alpha_{16}\| =$$

$$= \mathbf{E}\|\alpha_{31},\ \alpha_{32},\ \alpha_{33},\ \alpha_{34},\ \alpha_{35},\ \alpha_{36}\| - \mathbf{R}\|\alpha_{21},\ \alpha_{22},\ \alpha_{23},\ \alpha_{24},\ \alpha_{25},\ \alpha_{26}\|$$

where : **I** is the flow of inflow, l/h,
E – the flow of effluent, l/h,
R – the cationic resin volume, l, and **I** = **E**

The matrix of considered system is of the form :

$$\left\| \begin{array}{ccc} \mathbf{I} & \mathbf{R} & \mathbf{E} \\ \alpha_{11} & \alpha_{21} & 0 \\ \alpha_{12} & \alpha_{22} & 0 \\ \alpha_{13} & \alpha_{23} & \alpha_{33} \\ \alpha_{14} & 0 & \alpha_{34} \\ \alpha_{15} & 0 & \alpha_{35} \\ \alpha_{16} & 0 & \alpha_{36} \end{array} \right\|$$

where : **I** = inflow, **R** = resin, **E** = effluent. Among the matrix elements the following relations exist :

$$\alpha_{11} - \alpha_{21} = 0 \qquad \alpha_{15} = \alpha_{35}$$

$$\alpha_{12} - \alpha_{22} = 0 \qquad \alpha_{16} = \alpha_{36}$$

$$\alpha_{33} = \alpha_{13} - \alpha_{23}$$

As only the cations Ca^{+2}, Ma^{+2}, Na^{+}, K^{+} are submitted to variations in their molar concentration, that is only these cations are changed, the following relation is reached :

$$\mathbf{I}\|\alpha_{11},\ \alpha_{12},\ \alpha_{13}\| = \mathbf{E}\|\alpha_{31},\ \alpha_{32},\ \alpha_{33}\| - \mathbf{R}\|\alpha_{21},\ \alpha_{22},\ \alpha_{23}\|$$

For evaluating the quantity of calcium and magnesium ions which are retained by resin we resort to the criterion $[HCO_3^-]$ in effluent.

In effluent the following ions will be present : HCO_3^-, CO_2 for equilibrium and the water ions OH^- and H^+. The ions HCO_3^- and CO_2 for equilibrium are included in $[CO_{3\ \mathrm{total}}]$, i.e. we obtain the column vector :[3]

$$\mathbf{A} = \left\| \begin{array}{c} [OH^-] \\ [CO_{3\ \mathrm{total}}] \\ [H^+] \end{array} \right\|$$

taking into account that $[OH^-] \cong [H^+]$

The ionic mass did not retain any of these ions, but modifications appear in the hydrogen ion concentration and in the structure of $[CO_{3\ total}]$ respectively, the hydrogen ions concentration of HCO_3^- falls and from ion exchange results also water :

$$R-COOH)_n+(Ca^{+2}, Mg^{+2}, Na^+, K^+)_m \rightarrow R-COO)_n(Ca, Mg, Na, K)_m+nH^+$$

and: $H^+ + HCO_3^- \rightarrow H_2O + CO_2$; $CO_2 + H_2O \rightleftharpoons H_2CO_3$

Owing to these reactions the effluent composition can be expressed by the column vector :

$$\mathbf{B} = \begin{Vmatrix} [H_2O] \\ [OH^-] \\ [H_2CO_3] \\ [HCO_3^-] \\ [CO_3^{-2}] \\ [H^+] \end{Vmatrix}$$

taking into account the relations :

$$[OH^-_{total}] = [H_2O] + [OH^-]$$

$$[CO_{3\ total}] = [H_2CO_3] + [HCO_3^-] + [CO_3^{-2}]$$

$$[H^+_{total}] = [H_2O] + 2[H_2CO_3] + [HCO_3^-] + [H^+]$$

Between column vectors of influent and of effluent there exists the relation :

$$\mathbf{B} = \mathbf{C}\cdot\mathbf{A} \tag{4}$$

where $\mathbf{C}$ is a matrix including the stoichiometric coefficients of influent species and has the form :

$$\mathbf{C} = \begin{Vmatrix} c_{11} & 0 & 0 \\ c_{21} & 0 & 0 \\ 0 & c_{32} & 0 \\ 0 & c_{42} & 0 \\ 0 & c_{52} & 0 \\ 0 & 0 & 0 \end{Vmatrix}$$

Applying the mass action law for a water including the carbonic acid derivates, the number of H^+ ions, made free by each chemical species is :

$$[H^+_{total}] = [H_2O] + 2[H_2CO_3] + [HCO_3^-] + [H^+]$$

The vector **E** relating to a single particle has one component part and to define it we use a linear combination of **B** vector components:

$$[H^+_{total}] = \Sigma_i n_i [D_i]$$

where n_i is a number of deliverable particles from donor D_i.

In this way it is possible to pass to a line vector **L** which allows to obtain the vector **E** by the matrix relation:

$$\mathbf{E} = \mathbf{L} \cdot \mathbf{B} \tag{5}$$

The elements of **L** are whole numbers of different donors particles of vector **B**:

$$\mathbf{L} = \| 1 \quad 0 \quad 2 \quad 1 \quad 0 \quad 1 \|$$

Taking into account relations (4) and (5), we obtain:

$$\mathbf{E} = \mathbf{L} \cdot \mathbf{B} = \mathbf{L} \cdot \mathbf{C} \cdot \mathbf{A}$$

if we note the product **L·C** with matrix **G** we have:

$$\mathbf{E} = \mathbf{G} \cdot \mathbf{A} \tag{6}$$

and for the carbonic acid derivates:

$$\mathbf{G} = \| g_{11}, \; g_{12}, \; g_{13} \| = \| c_{11} + 2c_{32} + c_{42} + 1 \|$$

Because in the effluent from weakly acid filters we have the couples donor-acceptor:

$$H_2CO_3 - HCO_3^- - CO_3^{-2}$$

the same like in raw water, the most important analytical size is the *m* alkalinity, i.e. the necessary of acid added to a sample since the pH of this is brought in the turning field of the indicator 4.3...4.6.

Also the analytical determination is nothing else but acidity variation *Ac* between the initial value (pH$_i$) and pH = 4.6:

$$m = [\Delta Ac]^{4.6}_{pH_i} = \Delta [H^+_{total}]^{4.6}_{pH_i}$$

and utilising relation (6) **E** = **G·A** we obtain:

$$m = [\Delta g_{11}]^{4.6}_{pH_i} \cdot [OH_{total}] + [\Delta g_{12}]^{4.6}_{pH_i} - [CO_{3\ total}] + [\Delta H^+]^{4.6}_{pH_i} \tag{7}$$

The **G** matrix elements are easy to calculate depending on pH (the temperature has no influence on the process because it is isotherm).

Because $[\mathrm{OH}^-_{\mathrm{total}}]$ is a constant value, the resolution of equation (7) allows the deduction of the $[\mathrm{CO}_{3\ \mathrm{total}}]$.

By applying to the relation (1), $\mathbf{B} = \mathbf{C}\cdot\mathbf{A}$ may be calculated:

$$[\mathrm{H_2CO_3}] = c_{32}[\mathrm{CO}_{3\ \mathrm{total}}]$$

$$[\mathrm{HCO_3^-}] = c_{42}[\mathrm{CO}_{3\ \mathrm{total}}]$$

$$[\mathrm{CO_3^{-2}}] = c_{52}[\mathrm{CO}_{3\ \mathrm{total}}]$$

In this way the *m* alkalinity determination allows to calculate not only $[\mathrm{CO}_{3\ \mathrm{total}}]$ but also the different available forms of $\mathrm{CO_2}$ derivates.

In the case of $\mathrm{CO_2}$ movement by ion exchange with weakly acid cationic resins appear a quantitative change of the alkalinity value and a qualitative change in the composition structure of carbonic acid derivatives.

Taking into account a water with an alkalinity $m = x_1$ and $\mathrm{pH} = 7$, the three carbonic acid derivatives are present. For calculating $[\mathrm{CO}_{3\ \mathrm{total}}]$ we use relation (7).

After passing through the weakly acid filter, the *m* alkalinity of water is reduced, reaching the breakpoint value x_2 and pH value is corresponding to that in relation (7).

For calculating the change of ion $\mathrm{HCO_3^-}$ concentration in effluent we have the relation:

$$[\mathrm{HCO_3^-}] = \frac{x_1 - g_{11}[\mathrm{OH}_{\mathrm{total}}] - g_{12}[\mathrm{CO}_{3\ \mathrm{total}}] - \frac{10^{-\mathrm{pH}}}{\gamma_1}}{g_{12}}$$

where γ_1 is the activity coefficient for monovalent ions.

The matrix method used in the case of studied water may be applied for other waters and other ion exchangers with the same efficiency. It is necessary to build for each case the mathematic model of the analysed situation.

REFERENCES

[1] H. Hömig, "Physikochemische Grundlagen der Speisewasserchemie," Ed. Vulkan, Essen, ed. II-a, 1963.

[2] N. Stepanov, M. Erlykina, and G. Filippov, "Metode ale algebrei liniare în chimia fizică", Ed. științifică și enciclopedică, București 1980.

[3] J. Hissel, *La tribune de Cebedeau*, no. 424, 1979, p. 55–61.

Revue Roumaine de Chimie, 27, 1, 47—54 (1982)

THERMOKETTEN MIT WÄSSRIGEN RUBIDIUMCHLORID LÖSUNGEN

ELENA CONSTANTINESCU * und HILDEGARD DENGEL **

* Polytechnisches Institut Bukarest, Institut für Chemie, Splaiul Independenţei 313
Cod 77206, Rumänien
** Universität Galatz, Bdul. Republicii 47, Rumänien

Eingegangen am: 7 April 1981

Anhand der potentiometrischen Methode wurden Soret-Koeffizienten und molare Überführungswärmen von wässrigen Lithiumchloridlösungen für sechs Konzentrationen bestimmt. Es wurde die Konzentrationsabhängigkeit der Soret-Koeffizienten und der molaren Überführungswärmen wiedergegeben.

By using potentiometric measurements to double thermogalvanic cells, the Soret coefficients and transfer molar heats to aqueous rubidium chloride solutions were determined. The dependence of Soret coefficients and transfer molar heats on concentrations were presented.

Unter dem zum Studium der Thermodiffusion angewanten potentiometrischen Messungen haben sich zwei Forschungsrichtungen ausgebildet.

Eine von diesen studiert einfache elektrolytische Thermoketten.[1-11] Diese Methode ist ziemlich kompliziert weil sie für die Errechung verschiedener thermodynamischer Größen außer den Anfangswerten und Endwerten der Thermokraft der Thermoketten das Kennen der Elektronenüberführhrungswärmen in den metalischen Leitern, der ionischen Überführungsentropien, die Konzentrationsabhängikeit der Überführungszahlen und anderer Größen welcher Bestimmung große Schwierigkeiten hervorruft, voraussetzt.

Die zweite Richtung welche sich im Studium der Thermodiffusion ausgeprägt hat, besteht in der Bestimmung der relativen Soret-Koeffizienten in Abhängikeit eines bekannten Soret-Koeffizientenwertes für das Bezugssalz. Dieses wurde durch die Korelierung der erhaltenen potentiometrischen Daten, anhand zwei verschiedenen Thermoketten,[12] einer Thermokette und einer isothermen elektrochemischen Kette,[13] als auch einer doppelten Thermokette,[14-17] verwirklicht.

In der gegenwärtigen Arbeit wurden doppelte Thermoketten der Form:

$$\underset{(T_1)}{\mathrm{Hg/Hg_2Cl_2}},\ \mathrm{KCl}(m),\ \underset{(T_2)}{\mathrm{Hg_2Cl_2/Hg/Hg_2Cl_2}},\ \mathrm{RbCl}(m),\ \underset{(T_1)}{\mathrm{Hg_2Cl_2/Hg}} \qquad (1)$$

studiert.

Man beobachtet, daß die doppelte Thermokette (1) durch das Verbinden von zwei einfachen Thermoketten mit identischen Kalomelelektroden entstanden ist. Die erste einfache Thermokette enthält die Bezugslösung mit bekanntem Soret-Koeffizienten, und die zweite die der Forschung unterworfene RbCl Lösung. Die extremen Elektroden besitzen die Temperatur T_1, welche kleiner ist als T_2.

Die Temperaturen T_1 und T_2 wurden so gewählt, daß die mittlere Temperatur stets 25,00°C beträgt:

$$\frac{T_1 + T_2}{2} = 25{,}00°\mathrm{C}$$

Die Molalitäten der beiden Elektrolytlösungen haben den gleichen Wert.

In verdünnten Lösungen wo die Bedingungen der Gleichheit der ionischen Überführungswärmen und der ionischen Überführungsentropien erfüllt sind, wie folgt:

$$Q^{*\mathrm{KCl}}_{\mathrm{Cl}^-} = Q^{*\mathrm{RbCl}}_{\mathrm{Cl}^-}; \quad S^{*\mathrm{KCl}}_{\mathrm{Cl}^-} = S^{*\mathrm{RbCl}}_{\mathrm{Cl}^-}$$

kann man für den Anfangswert der thermoelektrischen Kraft ε_0, unter welcher man das Verhältnis zwischen dem Anfangswert der E.M.K. der Thermokette und die Temperaturdifferenz ΔT versteht, folgende Gleichung schreiben:

$$\varepsilon_0 = \frac{E_0}{\Delta T} \tag{2}$$

$$\varepsilon_0 = \frac{2RT}{F}\left(t^{\mathrm{KCl}}_{\mathrm{K}^+} \cdot \sigma^{\mathrm{KCl}} \cdot B^{\mathrm{KCl}} - t^{\mathrm{RbCl}}_{\mathrm{Rb}^+} \cdot \sigma^{\mathrm{RbCl}} \cdot B^{\mathrm{RbCl}}\right) \tag{3}$$

wo:

$$\sigma^{\mathrm{KCl}} = -\left(Q^{*\mathrm{KCl}}_{\mathrm{K}^+} + Q^{*\mathrm{KCl}}_{\mathrm{Cl}^-}\right)/2RT^2B^{\mathrm{KCl}} \tag{4}$$

$$\sigma^{\mathrm{RbCl}} = -\left(Q^{*\mathrm{RbCl}}_{\mathrm{Rb}^+} + Q^{\mathrm{RbCl}}_{\mathrm{Cl}^-}\right)/2RT^2B^{\mathrm{RbCl}} \tag{5}$$

$$B^{\mathrm{KCl}} = 1 + \left(\frac{\mathrm{d}\ln\gamma^{\mathrm{KCl}}_{\pm}}{\mathrm{d}\ln m}\right)_{P,T} \tag{6}$$

$$B^{\mathrm{RbCl}} = 1 + \left(\frac{\mathrm{d}\ln\gamma^{\mathrm{RbCl}}_{\pm}}{\mathrm{d}\ln m}\right)_{P,T} \tag{7}$$

Aus diesen Gleichungen kann man den Ausdruck für den Soret-Koeffizienten und die molare Überführungswärme der RbCl Lösungen erhalten:

$$\sigma^{\mathrm{RbCl}} = \frac{2RTt^{\mathrm{KCl}}_{\mathrm{K}^+} \cdot \sigma^{\mathrm{KCl}} B^{\mathrm{KCl}} - F\varepsilon_0}{2RT \cdot t^{\mathrm{RbCl}}_{\mathrm{Rb}^+} \cdot B^{\mathrm{RbCl}}} \tag{8}$$

$$-Q^{*\mathrm{RbCl}} = \nu_{RT^2} B^{\mathrm{RbCl}} \cdot \sigma^{\mathrm{RbCl}} \tag{9}$$

Hierin bedeutet : R = die universelle Gaskonstante, F die Faradaysche Konstante, $t_{\mathrm{K}^+}^{\mathrm{KCl}}$ die Ionenüberführungszahl des Iones K^+ in der KCl Lösung, $t_{\mathrm{Rb}^+}^{\mathrm{RbCl}}$ die Ionenüberführungszahl des Iones Rb^+ in der RbCl Lösung, T die mittlere Temperatur (298, 14 K), σ^{KCl} — der Soret-Koeffizient der KCl Lösung, σ^{RbCl} — der Soret-Koeffizient der RbCl Lösung, ν die Ionenzahl in welche ein Molekül RbCl dissoziert, $Q_{\mathrm{K}^+}^{*\mathrm{KCl}}$, $Q_{\mathrm{Cl}^-}^{*\mathrm{KCl}}$, stellen die ionischen, Überführungswärmen der Ionen K^+ und Cl^- in der KCl Lösung dar, und $Q_{\mathrm{Rb}^+}^{*\mathrm{RbCl}}$ und $Q_{\mathrm{Cl}^-}^{*\mathrm{RbCl}}$ haben dieselbe Bedeutung für das Ion Rb^+ und Cl^- in der RbCl Lösung.

DER EXPERIMENTELLE TEIL

Die Arbeitszelle wurde in einer früheren Arbeit beschrieben.[18,19] Die Substanzen aus welchen die Elektroden und die Lösungen dargestellt wurden stammen direkt aus Jem Handel, wobei der höchstmögliche Reinheitsgrad gewählt wurde : (KCl-U. C. Belgien, $\mathrm{Hg_2Cl_2}$— Merck, RbCl — Riedel, Haën), das Quecksilber wurde im Vaccuum distilliert. Die Lösungen wurden aus dreifach distilliertem Wasser hergestellt.

Für die Bestimmung der Anfangswerte der E.M.K. wurde eine Feussnerbrücke welche eine Meßgenauigkeit von $1 \cdot 10^{-6}$ V gewährleistet, in Gebrauch genommen. Als Nullinstrument wurde ein Lichtgalvanometer von der Sensibilität $4 \cdot 10^{-9}$A/mm verwendet. Die Temperaturen wurden mit Termometern mit Zentelgraden gemessen. Die Temperierung wurde mit drei Ultrathermostaten nach Höppler unternommen.

ERGEBNISSE UND DISSKUSIONEN

Es wurden doppelte Thermoketten mit wässrigen RbCl — Lösungen im Konzentrationsbereich $5 \cdot 10^{-1} - 1 \cdot 10^{-3}$ $\mathrm{Mol \cdot kg^{-1}}$ für sieben Werte des Temperaturgradientes studiert.

In Tabelle 1 sind die mit dem Asymetriepotential korrigierten Anfangswerte der E.M.K., für drei experimentelle unabhängige Versuche, wiedergegeben.

Tabelle 1

Experimentelle Werte für die RbCl — Lösungen $E_0 \cdot 10^3$ (Volt)

ΔT°C	Konzentration $\mathrm{Mol \cdot kg^{-1}}$								
	0,500			0,100			0,050		
1	0,030	0,029	0,030	0,035	0,035	0,036	0,038	0,039	0,038
2	0,057	0,062	0,060	0,072	0,073	0,070	0,085	0,083	0,087
3	0,092	0,096	0,091	0,111	0,110	0,112	0,123	0,122	0,120
5	0,150	0,161	0,167	0,182	0,185	0,180	0,210	0,209	0,213
7	0,207	0,208	0,205	0,250	0,253	0,257	0,281	0,287	0,280
9	0,282	0,280	0,288	0,303	0,309	0,305	0,350	0,351	0,349
12	0,353	0,350	0,357	0,410	0,409	0,411	0,474	0,474	0,477
	0,010			0,005			0,001		
1	0,040	0,044	0,042	0,043	0,044	0,045	0,047	0,048	0,047
2	0,098	0,100	0,097	0,110	0,112	0,109	0,125	0,122	0,121
3	0,150	0,147	0,151	0,160	0,159	0,164	0,177	0,179	0,175
5	0,235	0,232	0,237	0,238	0,240	0,239	0,259	0,255	0,259
7	0,327	0,329	0,329	0,339	0,336	0,337	0,360	0,365	0,361
9	0,398	0,399	0,397	0,407	0,410	0,413	0,467	0,463	0,469
12	0,512	0,513	0,516	0,555	0,555	0,552	0,666	0,669	0,668

Die Daten aus Tabelle 1 zeigen eine gute Übereinstimmung für die in wässrigen RbCl – Lösungen gegebener Konzentration und demselben Temperaturgradienten, individuellen Zahlenwerte der Anfangswerte der E.M.K., was für ein gutes Entdecken des Anfangsstadium der doppelten Thermokette spricht und zugleich eine zufriedenstellende Konsistenzprüfung unabhängiger Messungen darbietet.

In Konformität mit der Vorzeichenvereinbarung, welche der E.M.K. ein positives Vorzeichen zuschreibt, wenn der Elektrod in der kühleren Seite der RbCl Lösung positiver ist, als der in der kühleren Seite der KCl-Lösung, wurden für alle Anfangswerte der E.M.K. der studierten Doppelketten, positive Werte gefunden. Die erhaltenen positiven Werte ordnen sich in das allgemeine Verhalten der wässrigen Alkali- und Erdalkalichloridlösungen ein.[4,11,14,15]

Die graphische Darstellung der Funktion $E_0 = f(\Delta T)$ führt zu Graden positiver Steilheit, was für einen linearen Anstieg der Anfangswerte der E.M.K. (E_0) mit dem Zunehmen der Temperaturdifferenz, für alle der Forschung unterworfenen wässrigen RbCl – Lösungen gegebener Konzentration, spricht.

In Abbildung 1 ist die Kurvenschar, mit der Molalität der RbCl-Lösungen als Parameter, wiedergegeben, welche eine lineare Abhängigkeit des Anfangswertes der E.M.K. (E_0) von der Temperaturdifferenz (ΔT) zeigt, und das charakteristische Gesetz für das Anfangsstadium der Thermoketten bestätigt.[20,21]

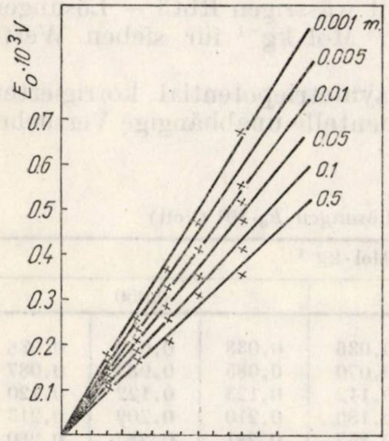

Abb. 1. – Die Veränderung des Anfangswertes der E.M.K. in Abhängigkeit vom Temperaturgradienten für verschiedene Konzentrationen der wässrigen RbCl Lösungen.

Die Thermokraft ε_0 wurde ausgehend von dem arithmetischen Mittelwert, als auch dem anhand der Gradegleichung linearisierten Wert errechnet.

Der Soret-Koeffizient σ^{RbCl} und die molare Überführungswärme $Q^{*\mathrm{RbCl}}$ der wässrigen RbCl – Lösungen wurden mit den Zahlenwerten von ε_0 bestimmt. Die Werte der Größen ε_0, σ^{RbCl} und $Q^{*\mathrm{RbCl}}$ für verschiedene Werte der Molalität des Elektrolyten sind in Tabelle 2 zusammengestellt.

Die zur Bestimmung des Soret-Koeffizienten und der Überführungs ärme notwendigen Hilfsgrößen als auch die entsprechenden Werte für das Bezugsalz, stammen aus der Literatur[14,22,23] und sind in Tabelle 3 eingeschrieben.

Die Zahlenwerte aus Tabelle 2 zeigen eine gute Übereinstimmung zwischen den Werten der Soret-Koeffizienten und der molaren Überführunswärmen die ausgehend von dem arithmetischen Mittel der Anfangsthermokraft ($\varepsilon_{0\,\mathrm{med}}$) und diejenigen, welche mit dem anhand der Gradegleichung linearisierten Werte, ($\varepsilon_{0\,Ec.dr}$) errechnet wurden.

Die für die Soret-Koeffizienten und molaren Überführungswärmen der wässrigen RbCl-Lösungen erhaltenen Zahlenwerte gliedern sich in den Bereich für die entsprechenden Werte der wässrigen Elektrolytlösungen ein. [24] Gleichfalls bemerkt man, daß die Zahlenwerte der Soret-Koeffizienten als auch der molaren Überfuhrungswärmen mit dem Anwachsen der Konzentration der RbCl-Lösung abnehmen. Änliche Abhänigkeiten wurden auch von anderen Forschern beobachtet[25] und zwar für ein-einwertige Elektrolyten als auch bei mehrwärtigen Elektrolyten bei kleinen Konzentrationen.

Tabelle 2

Anfangswert der Thermoelektrischen Kraft ε_0,
Soret — Koeffizienten σ^{RbCl} und molare Überführungswärmen $Q^{*\mathrm{RbCl}}$

Nr. crt.	m Mol·kg^{-1}	ε_0 $\mu V \cdot$ grad^{-1}		$-\sigma^{\mathrm{RbCl}} \cdot 10^3$ grd^{-1}		$Q^{*\mathrm{RbCl}}$ cal·Mol^{-1}	
		$\varepsilon_{0\,med.}$	$\varepsilon_0 \cdot Ec.dr.$	$\sigma^{\mathrm{RbCl}}_{med.}$	σ^{RbCl} $Ec.dr.$	$Q^{*\mathrm{RbCl}}_{med.}$	$Q^{*\mathrm{RbCl}}$ $Ec.dr.$
1	0,001	54,00	53,82	2,63	2,62	917,1	914,5
2	0,005	48,64	49,89	2,50	2,55	852,9	870,0
3	0,010	45,96	47,58	2,45	2,52	816,9	839,5
4	0,050	40,40	40,99	2,29	2,31	741,6	749,7
5	0,100	36,34	38,17	2,14	2,17	680,7	690,3
6	0,500	30,38	30,38	2,13	2,16	671,9	677,6

Tabelle 3

Überführungszahlen, Soret — Koeffizienten und die Zahlenwerte des Parameters B

m Mol·kg^{-1}	$t^{\mathrm{KCl}}_{\mathrm{K}^+}$	B^{KCl}	$-\sigma^{\mathrm{KCl}} \cdot 10^3$ grd^{-1}	$t^{\mathrm{RbCl}}_{\mathrm{Rb}^+}$	B^{RbCl}
0,001	0,4990	0,954	0,53	0,5020	0,987
0,005	0,4970	0,945	0,55	0,4990	0,967
0,010	0,4902	0,930	0,46	0,4970	0,945
0,050	0,4899	0,913	0,15	0,4950	0,920
0,100	0,4898	0,901	0,59	0,4940	0,901
0,500	0,4888	0,892	0,79	0,4920	0,891

Wenn man die Soret-Koeffizienten und die molaren Überführunswärmen in Abhänigkeit von der Quadratwurzel der Molalität aufzeichnet, erhält man Kurven die in Abbildung 2 und 3 wiedergegeben sind.

Bei kleinen Konzentrationswerten wird eine lineare Abhänigkeit der Soret-Koefizienten als auch der molaren Überführungswärmen von der Quadratwurzel der Molalität bemerkt, was für die RbCl — Lösungen eine analoge Gesetzmäßigkeit mit den von Agar[26] als auch Helfand und Kirkwood[27] demonstrierten Formeln bestätigt.

Bei größeren Konzentrationen der RbCl — Lösungen werden Abweichungen von der Linearität beobachtet. Dergleiche Abweichungen wurden im allgemeinen bei Alkali — und Erdalkalihalogenieden für Konzentrationen die größer als 0,5 m sind beobacht,[28] bei $CdCl_2$ — Lösungen[29] und bei einigen Polyelektrolytlösungen[30] erscheinen solche Abweichungen von der Linearität auch bei kleineren Konzentrationen. Diese Abweichungen der molaren Überführungswärme von der Linearität können den Veränderungen in der sekundären Hydratierungssphäre der Ionen die mit dem Ansteigen der Konzentration stattfinden, zugeschrieben werden. Diese Veränderungen in der sekundären Hydratierungssphäre sind um so begreifbarer je weniger das Ion primär hydratiert ist und je stärker es die Wasserstruktur auf größere Strecken zerstört, was der Fall des Iones Rb^+ ist.

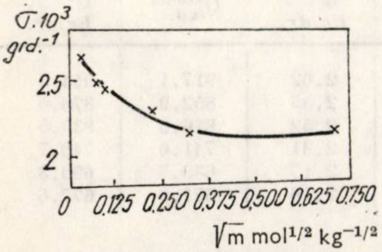

Abb. 2. — Die Abhänigkeit des Soret-Koeffizienten der RbCl Lösungen von der Quadratwurzel der Molalität.

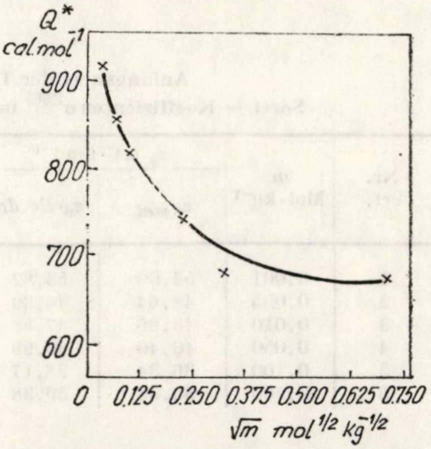

Abb. 3. — Die Abhänigkeit der molaren Überführungswärmen des RbCl von der Quadratwurzel der Molalität der Lösungen.

Mit Hilfe des Wertes der molaren Überführungswärme $Q^{*\mathrm{RbCl}}$ für die Konzentration 0,001 m, welcher als entsprechender Wert für die unendliche Verdünnung angenommen wurde,

$$Q^{*\mathrm{RbCl}} \approx {}^{*}Q^{0\,\mathrm{RbCl}}$$

hat man die konventionelle ionische Überführungswärme und die konventionelle ionische Überführungsentropie des Iones Rb^+ bestimmt.

Als Bezugsgröße wurde die ionische Überführungswärme für Cl^- nach Haase und Mitarbeiter

$${}^{*}Q^{0}_{\mathrm{Cl}^-} = 1700 \text{ cal}\cdot\text{Mol}^{-1} \text{ genommen.}$$

Die ionische Überführungswärme des Iones Rb^+ wurde mit folgender Formel bestimmt:

$${}^{*}Q^{0}_{\mathrm{Rb}^+} = {}^{*}Q^{0\,\mathrm{RbCl}} - {}^{*}Q^{0}_{\mathrm{Cl}^-}$$

Mit dem Zahlenwert der ionischen Überführungswärme wurde die ionische Überführungsentropie für unendliche Verdünnung mit dem Ausdruck

$${}^{*}S^{0}_{\mathrm{Rb}^+} = \frac{{}^{*}Q^{0}_{\mathrm{Rb}^+}}{T} + S^{0}_{\mathrm{Rb}^+}$$

errechnet, wo S^0 die ionische Überführungstandardentropie (29,7 cal·grd^{-1}·Mol^{-1}) darstellt.

Man bemerket eine gute Übereinstimmung zwischen unseren Rezultaten und Literaturwerten, welche von Messungen mit einfachen Thermoketten mit Ag/AgCl, Cl^- Elektroden stammen.[4]

Tabelle 4

Konventionelle ionische und molare Überführungswärmen und Überführungsentropien bei 25°C

m Mol·kg^{-1}	$^*Q^0_{Rb^+}$ cal·Mol^{-1}				$^*S^0_{Rb^+}$ cal·grd^{-1}Mol		
	Eigene Daten		Literaturdaten[4]		Eigene Daten		Literaturdaten[4]
	a	b	c	d	e	f	g
0,001	−783	−786	−915	−810	27,08	27,07	27,00

a und e — wurden mit den arithmetischen experimentellen Mittelwerten erhalten.
b und f — wurden ausgehend von den anhand der Gradegleichung linearisierten Werten erhalten.
c — experimenteller Wert
d — wurde mit den Werten der konventionellen ionischen und Standardentropien erhalten.

SCHLUẞFOLGERUNGEN

Die unternommenen E.M.K. Messungen an doppelten Thermoketten mit wässrigen RbCl – Lösungen bei einer mittleren Temperatur von 25,00°C, haben uns Daten zur Berechnung von Soret-Koeffizienten, molare Überführungswärmen dieser Lösungen, als auch für die Erhaltung der ionischen, konventionellen Überführungswärme und ionischen konventionellen Überführungsentropie des Iones Rb^+, geliefert.

LITERATURHINWEISE

[1] J. N. Agar und W. G. Breck, *Trans. Faraday Soc.*, **53**, 167 (1957).
[2] R. Haase, *Z. phys. Chem.*, *(Frankfurt)*, **13**, 21 (1957).
[3] J. Chanu, *J. Chem. Phys.*, **55**, 10 (1958).
[4] R. Haase und K. Hoch, *Z. phys. Chem. (Frankfurt)*, **46**, 63 (1965).
[5] L. Mousselin, *Compt. rend.*, **264**, 1541 (1967).
[6] I. Ryzlik und O. A. Korynshin, *Tr. Tambouskogo Inst. Khim. Mainostr.*, **4**, 179 (1970).
[7] R. Haase und H. Schönert, *Z. phys. Chem.*, *(Frankfurt)*, 25, 193 (1960).
[8] R. Haase, K. Hock und H. Schönert., *Z. phys. Chem.*, *(Frankfurt)*, **27**, 421 (1961).
[9] D. Rădulescu und Fl. Bărbulescu, *Bul. Soc. Chim. Rom.* **1936**, 137.
[10] Fl. Bărbulescu, E. Constantinescu und I. St. Popescu, *Rev. Roumaine Chim.*, **9**, 105 (1964).
[11] I. G. Murgulescu, Fl. Bărbulescu und E. Constantinescu, *Rev. Roumaine Chim.*, **13**, 841 (1968).
[12] H.J.V. Tyrrell und R. Colledge, *Trans. Faraday Soc.*, **50**, 1056 (1954).
[13] H. J. V. Tyrrell und R. Colledge, *Trans. Faraday Soc.*, **51**, 2834 (1955).
[14] T. Ideka, *Bull. Chem. Soc. Japan*, **38**, 407 (1965).

[15] T. Ideka, H. Ohe und S. Kawamura, *Bull. Chem. Soc. Japan*, **41**, 2858 (1968).
[16] T. Ideka und Y. Yamamoto, *Bull. Chem. Soc. Japan*, **47**, 838 (1974).
[17] T. Ideka, *Bull. Chem. Soc. Japan*, **48**, 2531 (1975).
[18] Fl. Bărbulescu, E. Constantinescu und H. Dengel, *Buletinul I.P.B. Seria Chimie-Metalurgie*, **XLI**, 19 (1979).
[19] Fl. Bărbulescu, E. Constantinescu und H. Dengel, *Rev. Chim. București*, **31**, 258 (1980).
[20] Ch. Moreau und G. Lepoutre, *J. Chem. Phys.*, **52**, 498 (1955).
[21] R. C. Srivastava, *J. Indian Chem. Soc.*, **40**, 585 (1963).
[22] T. Ideka, „Some Aspects of Electrochemistry in Non-isothermal Systems", Kaimeido Printing Co., Shizouka, 1961.
[23] H. S. Harned und B. B. Owen „The Physical Chemistry of Electrolytic Solutions" Reinhold Publishing Corp. New York, 1958.
[24] B. D. Butler und J. C. R. Turner, *J. Phys. Chem.*, **69**, 3598 (1965).
[25] P. N. Snowdon und J. C.R. Turner, *Trans. Faraday Soc.*, **56**, 456 (1960).
[26] L. G. Longsworth und J. N. Agar „The Structure of Electrolytic Solutions", Ed. Hamer, Wiley, New York, 1959, p. 213.
[27] E. Helfand un J. G. Kirkwood, *J. Chem. Phys.*, 32, 857 (1960).
[28] J. Chanu und L. Mousselin, *Electrochim. Acta.*, **14**, 207 (1969).
[29] J. Demichowicz-Piogoniowa, *Bull. Acad. Polon. Sci., Ser. Sci. Chim.*, **13**, 1 (1965).
[30] J. N. Agar und V.M.M. Lobo, *Electrochim. Acta*, **20**, 319 (1975).

Revue Roumaine de Chimie, 27, 1, 55–58 (1982)

THE ENTHALPIES OF COMBUSTION AND FORMATION OF 3-AMINO-4-METHOXYACETANILIDE AND 3-(N-β-CYANOETHYL)-AMINO-4-METHOXYACETANILIDE

IULIA CONTINEANU,* DAN BREȚCANU** and D. I. MARCHIDAN*

* Center of Physical Chemistry and ** Research Center for Dyes (ICECHIM), Splaiul Independenței 202, Bucharest 77208, Romania

Received April 28, 1981

The enthalpy of combustion of 3-amino-4-methoxyacetanilide and 3-(N-β-cyanoethyl)-amino-4-methoxyacetanilide has been determined in an oxygen static-bomb calorimeter. The enthalpy of formation has been derived using data from the available literature. The results obtained are as follows :

$C_9H_{12}N_2O_2(s) + 11\ O_2(g) = 9\ CO_2(g) + 6\ H_2O(l) + N_2(g)$

$\Delta cH^0(298.15\ K) = -\ 4702.5 + 5.75\ kJ/mol\ (-1123 \pm 1.37\ kcal/mol)$

$\Delta fH^0(298.15\ K) = -\ 554 \pm 5.75\ kJ/mol\ (-132.43 \pm 1.37\ kcal/mol)$

$C_{12}H_{15}N_3O_2(s) + 18\ 1/2\ O_2(g) = 12\ CO_2(g) + 71/2\ H_2O(l) + 1\ 1/2\ N_2(g)$

$\Delta cH^0(298.15\ K) = -\ 6600 \pm 1.73\ kJ/mol\ (-1577 \pm 0.41\ kcal/mol)$

$\Delta fH^0(298.15\ K) = -\ 265.85 \pm 1.73\ kJ/mol\ (-63.54 \pm 0.41\ kcal/mol)$

A comparison is given of the results of this investigation to those calculated by Handrick's method for both substances.

In order to determine the heat of formation of 3-amino-4-methoxyacetanilide ($C_9H_{12}N_2O_2$) (AMA) and 3-(N-β-cyanoethyl)-amino-4-methoxyacetanilide ($C_{12}H_{15}N_3O_2$) (NT), heats of combustion were measured. Use has been made of a calorimetric bomb and the procedure of processing data described elsewhere.[1] In this work the calorimeter constant was 10 460 J/K and the pressure of oxygen employed in the bomb 25 bars. The following values of heats of formation of carbon dioxide and water were utilized :[2]

$$\Delta fH^0(298.15\ K)\quad CO_2(g) = -\ 393.51 \pm 0.13\ kJ/mol$$

$$-94.051 \pm 0.031\ kcal/mol$$

$$\Delta fH^0(298,15\ K)\quad H_2O(l) = -\ 285.83 \pm 0.042\ kJ/mol$$

$$-\ 68.315 \pm 0.01\ kcal/mol$$

These values were obtained by critical evaluation of data in the literature[3] and are recommended as key values to be employed in scientific works. We have adopted the following values : $\Delta fH(HNO_3) = 219.488$ cal/g ; $\Delta fH(Fe_2O_3) = 1600$ cal/g and $\Delta cH(\text{cotton}) = 3885.15$ cal/g.

No data on heat of combustion of AMA, ($C_9H_{12}N_2O_2$), $C_6H_3(NHCOCH_3)\cdot(NH_2)(OCH_3)$, are available in the literature. As to the molecular mass a value of 180.2 has been used in calculations. The substance was 99% pure and its melting point ranged from 105 to 108 °C. The purity was determined by diazotation. The values obtained for the heat of combustion of AMA in solid state are listed in Table 1. The heat of formation of AMA in standard conditions was calculated by the equation :

$$C_9H_{12}N_2O_2(s) + 11\ O_2(g) = 9\ CO_2(g) + 6\ H_2O(l) + N_2(g)$$

and the value of -554 ± 5.75 ($\pm$ 0.122 %) kJ/mol was obtained. Neither are there data in the literature for the heat of combustion of NT, ($C_{12}H_{15}N_3O_2$), $C_6H_3(NHCOCH_3)\cdot(NHCH_2CH_2CN)\ (OCH_3)$; the molecular mass was taken as 233.25. NT purity was 99% and the melting point within 126 – 127°C. The results obtained for the heat of combustion of solid NT are listed in Table 2. The heat of formation of NT in standard conditions calculated by the equation :

$$C_{12}H_{15}N_3O_2(s) + 18\ 1/2\ O_2(g) = 12\ CO_2(g) + 7\ 1/2\ H_2O(l) + 1\ 1/2N_2(g)$$

amounted to $-265.86 \pm 1.73(\pm 0.03\ \%)$ kJ/mol.

Calculations of heat of combustion were also carried out for the substances under study. Thus, there are in literature several semiempirical methods of correlation and estimation which are underlaid by the following principle : within certain limits the structural groups of the molecule contribute the same amount to some thermodynamic quantity no matter the molecular structure of the substance. According to Handrick's method[4] the reaction of combustion of an organic compound of $C_mH_nN_pO_q$ general formula, is :

$$C_mH_nN_pO_q(\text{s or l}) + (m + n/4 - q/2)O_2(g) = mCO_2(g) + \\ + n/2H_2O(l) + p/2N_2(g)$$

hence the number of oxygen atoms required is :

$$x = (m + n/4 - q/2)$$

The basic principle of the method establishes that for an organic substance the heat of combustion is a linear function of x :

$$-\Delta cH^0(298.15\ \mathrm{K}) = \Sigma a' + x\Sigma b'$$

where a' and b' are coefficients that are tabulated for various structural groups.[4] The data yielded by this method are presented comparatively in Table 3.

To bring values obtained to standard state, calculations were the more intricate, the more complex the structure of the substance. In the case of compounds with carbon, hydrogen and oxygen of $C_mH_nO_q$ general formula the corrections of the procedure of reduction to standard state are summed by Washburn's equation : [5]

$$\pi = \frac{0.30 \times P \times m}{-\Delta U_B}\left[-1 + 1.1\left(\frac{2n - q}{4m}\right) - \frac{2}{P}\right]$$

TABLE 1

Heat of combustion of 3-amino-4-methoxyacetanilide

g substance	K ΔT	Joules ($\Delta T\times$calorim.const.)	ΔfH (Fe_2O_3)	ΔfH (HNO_3)	ΔcH (cotton)	J/g (ΔU_B)	kJ/mol (ΔU_B)
0.9187	2.396	25062.16	56.23	45.35	1078	25996.1	4686
0.8439	2.218	23200.29	50.21	43.72	1083	26097.1	4703
1.0842	2.844	29748.24	56.90	54.38	1272	26162.1	4714
1.2359	3.250	33995	55	44.35	1653	26088.4	4701.1

average value = 4701 kJ/mol

Standard deviation $\sigma = \sqrt{\Sigma \Delta^2/n(n-1)} = \pm 5.75$ kJ

$$\text{Washburn's correction } \pi = \frac{0.3\times 25\times 9}{-4701}\left[-1+1.1\left(\frac{12-4}{36}\right)-\frac{2}{30}\right] = -0.012\ \%$$

$$\text{hence } \Delta cU^0(298.15\ \text{K}) = \frac{-4\,701\times 99.988}{100} = -4700\ \text{kJ/mol}$$

For the reaction $C_9H_{12}N_2O_2(s) + 11O_2(g) = 9CO_2(g) + 6H_2O(l) + N_2(g)$ volume change is one unit so that $\Delta cH^0(298.15\ \text{K}) = -4700 - 1\ RT = -4700 - 2.48 = -4702.5 \pm$ $\pm\ 5.75(0.122\ \%)$ kJ/mol ; $-1123.9 \pm 1.37(0.122\ \%)$ kcal/mol

TABLE 2

Heat of combustion of 3-(N-β-cyanoethyl)-amino-4-methoxyacetanilide

g substance	K ΔT	Joules ($\Delta T\times$calorim.const.)	ΔfH (Fe_2O_3)	ΔfH (HNO_3)	J/g (ΔU_B)	kJ/mol (ΔU_B)
0.8572	2.324	24309	56	37	28250	6589
1.11	3.006	31443	56	47	28234	6586
0.8212	2.23	23326	56	61	28262	6592

average value = 6589 kJ/mol

Standard deviation $\sigma = \sqrt{\Sigma \Delta^2/n(n-1)} = \pm 1.73$ kJ

$$\text{Washburn's correction } \pi = \frac{0.3\times 25\times 12}{-6589}\left[-1+1.1\left(\frac{15-4}{48}\right)-\frac{2}{25}\right] = -0.012\ \%$$

$$\text{hence } \Delta cH^0(298.15\ \text{K}) = \frac{-6589\times 99.988}{100} = -6588\ \text{kJ/mol}$$

For the reaction $C_{12}H_{15}N_3O_2(s) + 18\ 1/2\ O_2(g) = 12\ CO_2(g) + 7\ 1/2\ H_2O(l) + 1\ 1/2\ N_2(g)$ volume change is five units so that

$$\Delta cH^0(298.15\ \text{K}) = -6588 - 5(2.48) = -6600 \pm 1.73(0.03\ \%)\ \text{kJ/mol} ; -1577 \pm 0.41(0.03\ \%)\ \text{kcal/mol}$$

TABLE 3

The enthalpies of combustion and formation of 3-amino-4-methoxyacetanilide and 3-(N-β-cyanoethyl)-amino-4-methoxyacetanilide

Substance		ΔcH^0(298.15 K)		ΔfH^0(298.15 K)	
		exp.	calc.	exp.	calc.
$C_9H_{12}N_2O_2$	kJ/mol	-4702.5	-4700.3	-554	-556
(AMA)	kcal/mol	-1123.9	-1123.4	-132.43	-132.86
$C_{12}H_{15}N_3O_2$	kJ/mol	-6600	-6585.62	-265.85	-280.12
(NT)	kcal/mol	-1577	-1574	-63.54	-66.95

where P stands for the initial oxygen pressure (in bars) and $-\Delta U_B$ for the heat of combustion; π is calculated in percents of experimental value. The above equation applies fairly well in the case of nitrogen compounds as well. The calculation of standard heat of combustion was effected after application of Washburn's corrections, by summation of the products RT (equal to $-$ 2.479 kJ/mol) times the number of volumes that entered and emerged from reaction. On combustion of organic compounds that do not contain nitrogen, nitric acid is formed by oxidation of nitrogen left as impurity in oxygen. On combustion of nitrogen-containing compounds, much more nitric acid is formed. However most of the nitrogen contained in these compounds emerges from combustion reaction as gas and usually only 10 % or less as nitric acid.

The data obtained were also utilized to calculate standard heat of reaction on formation of NT from AMA and acrylonitrile:

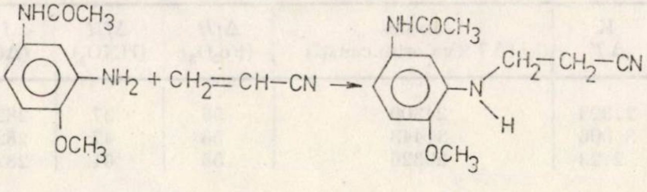

$$\Delta rH^0(298.15\ \text{K}) = -265.85 - [-554 + 151] = 137\ \text{kJ/mol}.$$

REFERENCES

[1] I. Contineanu and D. I. Marchidan, *Rev. Chim. (București)*, **30**, 1096 (1979).

[2] CODATA Bulletin no 28 (April 1978): "CODATA Recommended Key Values for Thermodynamics 1977".

[3] CODATA Task Group on Key Values for Thermodynamics. *J. Chem. Thermodynamics*, **4**, 331 (1972); *Teplofiz. Vys. Temperatur*, **9**, 657 (1971); CODATA Bulletin no 5 (1971).

[4] G. R. Handrick, *Ind. Eng. Chem.*, **48**, 1366 (1956) from R. C. Reid and T.K. Sherwood: "The Properties of Gases and Liquids. Their Estimation and Correlation". 2nd ed. McGraw-Hill, London, 1966, p. 221.

[5] E. W. Washburn, *J. Res. Nat. Bur. Standards*, **10**, 525 (1933).

Revue Roumaine de Chimie, **27**, *7*, 59–67 (1982)

ON THE DIPOLE MOMENT OF Cu, Ag AND Au ATOMS ADSORBED ON DIFFERENT TUNGSTEN PLANES

CR. CONŢESCU and M. I. VASS
Institute for Chemical Research, Center of Physical Chemistry
Splaiul Independenţei 202, Bucharest 77208, Romania

Received June, 8, 1981

Crystallographic variation of zero-coverage dipole moments of Cu, Ag and Au atoms adsorbed on tungsten single crystal planes is semiquantitatively explained by the simple model of a broad virtual level on adsorbed atoms, having different occupancy on various planes.

1. INTRODUCTION

Work function measurements by the Field Emission Microscopy (FEM) method revealed similar variations of the averge work function ($\overline{\varphi}$) during adsorption and growth of the copper,[1] silver[2–5] and gold [6,7] layers on tungsten, but a quite different behavior of the same adsorbates on various single crystal planes. Submonolayer amounts of copper[8–10] and gold [11,12] induce a decrease of the work function on the (110) plane (electropositive adsorption) but an increase on the other low index planes (electronegative adsorption) which is sometimes temperature (or coverage) dependent. [9,10,13] By using the same technique recently [14,15] we obtained similar results with silver on W (110) and on (211), (111) planes. This behavior which is therefore typical for all the I–B group metals adsorbed on tungsten is in an evident contrast with that of the alkali metals which are adsorbed with a drastic decrease of work function on all tungsten planes. Moreover, the values of the measured dipole moment extrapolated to zero coverage ($\mu^0_{\text{obs.}}$) for the noble atoms adsorbed on tungsten are extremely small (between -1.5 D and $+0.5$ D on various planes) compared with the corresponding values of the adsorbed alkali atoms (as large as $+(2-4)$D). This suggests a very low ionicity and a strong covalent character of the metallic chemisorption bonds formed by noble atoms on tungsten substrate.

The reason of the observed difference in the sign of work function changes between the smooth (110) and the other rough tungsten planes on adsorption of small amounts of noble metals is not clearly understood. Two explanations are usually resorted to. The first one[8,16,17] is based on the theory of the Smoluchowsky smoothing[18] (i.e. redistribution of surface electronic charges caused by adsorbate-induced changes in atomic surface structure of different planes). In the second one,[10-12] the dipole moments of the adsorbed atoms are assumed to be determined by the amount of the electronic charge transferred in the chemisorption bonds. The aim of the present work is to compare the consequences of both explanations and to substantiate the second one.

2. THE INFLUENCE OF ADSITE GEOMETRY ON THE WORK FUNCTION CHANGES

The work function changes induced by adsorption of alkali metals have been explained by the quantum theory of Lang[19] in relation with the surface density of metallic atoms. The same theory has also been used to explain both the work function increase and its decrease occurring in adsorption of noble metals on tungsten.[8,13,17,20] According to this explanation, atomic electronegativity of adsorbed atoms (either alkali or noble metals) has no influence on the character of work function variation on different substrate planes.[8,17] The unique surface property discussed herein is the surface density of metallic atoms, which increases upon adsorption of metallic atoms with low atomic radius on a rough tungsten plane (work function increases) and diminishes upon adsorption on the densely packed (110) plane (work function decreases). Since this approach makes no allowance either for charge transfer at small coverage in surface bonds or for polarization of adsorbed atoms in the surface electric field, the role of the geometric structure of the surface adsites seems to be overemphasized. However, by accepting the assumptions of the above explanation, it is obvious that the work function variation at constant coverage depends only on the radius of adsorbed atoms for a given plane. Because $r_{\mathrm{Cu}} < r_{\mathrm{W}} < r_{\mathrm{Ag}} = r_{\mathrm{Au}}$, it follows:

(a) $\Delta\varphi_{\mathrm{Ag}} = \Delta\varphi_{\mathrm{Au}}$ on the same (*hkl*) plane

(b) $\Delta\varphi_{\mathrm{Ag,Au}} < \Delta\varphi_{\mathrm{Cu}} < 0$ on the smooth (110) plane

(c) $\Delta\varphi_{\mathrm{Cu}} > \Delta\varphi_{\mathrm{Ag,Au}} > 0$ on the other rough planes

A comparison with available experimental data is not easy, because they generally refer to layers equilibrated at various temperatures. However, it is seen from table 1 that the effect of temperature is not as significant as that of surface orientation. It is found:

$$\Delta\varphi_{\mathrm{Cu}} < \Delta\varphi_{\mathrm{Ag}} \approx \Delta\varphi_{\mathrm{Au}} < 0 \quad \text{on W(110)}$$

$$\Delta\varphi_{\mathrm{Au}} \gtrsim \Delta\varphi_{\mathrm{Cu}} > \Delta\varphi_{\mathrm{Ag}} > 0 \quad \text{on W(211)}$$

$$\Delta\varphi_{\mathrm{Au}} > \Delta\varphi_{\mathrm{Ag}} > \Delta\varphi_{\mathrm{Cu}} > 0 \quad \text{on W(111)}$$

$$\Delta\varphi_{\mathrm{Au}} > \Delta\varphi_{\mathrm{Cu}} > 0 \quad \text{on W(100)}$$

TABLE 1

Available literature data on the work function variation and the corresponding zero-coverage dipole moments for the initial adsorption of Cu, Ag and Au on tungsten single crystal planes.

Adatom	I^a (eV)	Tungsten plane	φ^0_{hkl} (eV)	$\Delta\varphi_{hkl}$ (eV)	$\mu^0_{\text{obs.}}$ (Debye)	T (K)	Reference
Cu	7.72	(110)	5.35	−0.60	+0.51	77	10
				−0.55	+0.34	350	10
		(211)	4.75	−0.05	+0.02	77	10
				+0.20	−0.13	340	10
				+0.31	−0.26	700	10
		(100)	4.65	+0.40	−0.26	20	21,22
				+0.44	−0.26	78	9
		(310)	4.50	+0.37	−0.95	550	10
				+0.50	−1.43	650	10
		(111)	4.40	+0.42	−1.48	500	10
				+0.40	−1.06	700	10
Ag	7.57	(110)	5.35	−0.25	+0.17	550	14,15
		(211)	4.75	+0.11	−0.34	550	14,15
		(111)	4.40	+0.61	−1.33	550	14,15
Au	9.22	(110)	5.35	−0.35	+0.56	78	12
	8.09^b			−0.20	+0.30	160	12
		(211)	4.75	+0.40	−0.32	?	35
				+0.30	−0.24	78	12
				+0.45	−0.32	205	12
		(100)	4.65	+0.60	−1.06	20	21,23
				+0.50	−0.79	300	21,23
				+0.45	−0.40	78	12
				+0.40	−0.40	605	12
				+0.33	−0.60	?	11
		(111)	4.40	+0.70	−0.85	77	24

[a] First ionization potential corresponding to the ground state d^{10} s^1 configuration.
[b] The energy of the $5d^9$ $6s^2$ configuration of Au atoms.

where $\Delta\varphi$ is the maximum work function variation on a given plane. This is in a clear disagreement with the above mentioned predictions (a — c), showing that an explanation based only on the smoothing effects of surface charges is not satisfactory. Although the theory of the Smoluchowsky smoothing gives a good idea about the crystallographic anisotropy of work function of clean metallic surfaces, it cannot be applied in the same manner to metallic surfaces covered with foreign metallic atoms.

3. THE SURFACE DIPOLE LAYER OF ADSORBED ATOMS

A dipole layer is formed on the surface when foreign atoms are adsorbed on a metal substrate. The corresponding work function variations are produced by at least two major contributions:[25]

(i) adatom polarization by surface electric field (the sum of "smoothing" and "spreading" contributions) and (ii) charge transfer in chemisorption bonds. The net dipole moment per adsorbed atom may thus be expressed as:

$$\mu_{\text{actual}} = \mu_{\text{ch.tr.}} + \mu_{\text{pol.}} = \mu_{\text{ch.tr.}} + (\mu_{\text{spr.}} + \mu_{\text{sm.}}) \qquad (1)$$

where $\mu_{\text{spr.}} < 0$ (the spreading out of electronic charges gives negative surface dipoles) and $\mu_{\text{sm.}} > 0$ (the Smoluchowsky smoothing yields surface dipoles with positive end).

At present a quantitative estimation of (i) is not possible. However, $\mu_{\text{pol.}}$ should be positive in adsorption on an atomically smooth plane but smaller or even negative on a rough plane. Since surface polarization depends on the geometric arrangement of adsorbed atoms, it should be also temperature dependent. On substrate planes where a very small charge transfer is expected to occur, polarization effects play the leading role upon the work function changes observed. This may be the case with Cu on (100)[26] and (211)[8] planes or Ag on (100)[13] where changes of work function, small but with opposite sign, were observed at various temperatures. They are probably caused by the combined action of charge transfer and surface polarization of adatoms occupying different surface sites at different temperatures.[26] On the other hand, the changes in temperature do not appreciably change the work function of copper[26] or silver[27] monolayers on the flat (110) plane. It follows that the smoothing effects are small on a flat surface and that the observed decrease of φ_{110} is due mainly to charge transfer effects.

4. THE EFFECT OF CHARGE TRANSFER ON EXPERIMENTAL DIPOLE MOMENTS

When the adatom – substrate electronegativity difference is small, as in the case of I–B atoms on tungsten, the contribution of (ii) may be dominant on the overall behavior.[28] However, electronegativity is not a very useful quantity. More appropriate are the ionization potential (I) of adsorbed atoms and the work function value of clean surface planes (φ^0_{hkl}). The magnitude of $\mu_{\text{ch.tr.}}$ should depend on the surface crystallography in the same order of variation as φ^0_{hkl} values and on the nature of adsorbed atoms in the reverse order of electronegativities (or of ionization potentials). By plotting $\mu^0_{\text{obs.}}$ in table 1 against ($\varphi^0_{hkl} - I$), the above correlation is obtained as shown in figure 1,a. Supposing that charge transfer prevails over polarization effects, this could be rendered semiquantitative by using the virtual level approach of metallic chemisorption.

For an adsorbed atom with one valence electron, the dipole moment resulted through charge transfer between a resonance level at energy ε_v and metallic states below the substrate Fermi energy ($\varepsilon_F = 0$) may be estimated as:

$$\mu_{\text{ch.tr.}} = ed\Big(\sum_{\sigma} n_{a\sigma}^{\text{free}} - \sum_{\sigma} n_{a\sigma}^{\text{ads.}}\Big) = ed\left(1 - 2\int_{-\infty}^{0} \rho_{a\sigma}(\varepsilon)\,d\varepsilon\right) =$$

$$= (2ed/\pi)\tan^{-1}(\varepsilon_v/\Delta) \qquad (2)$$

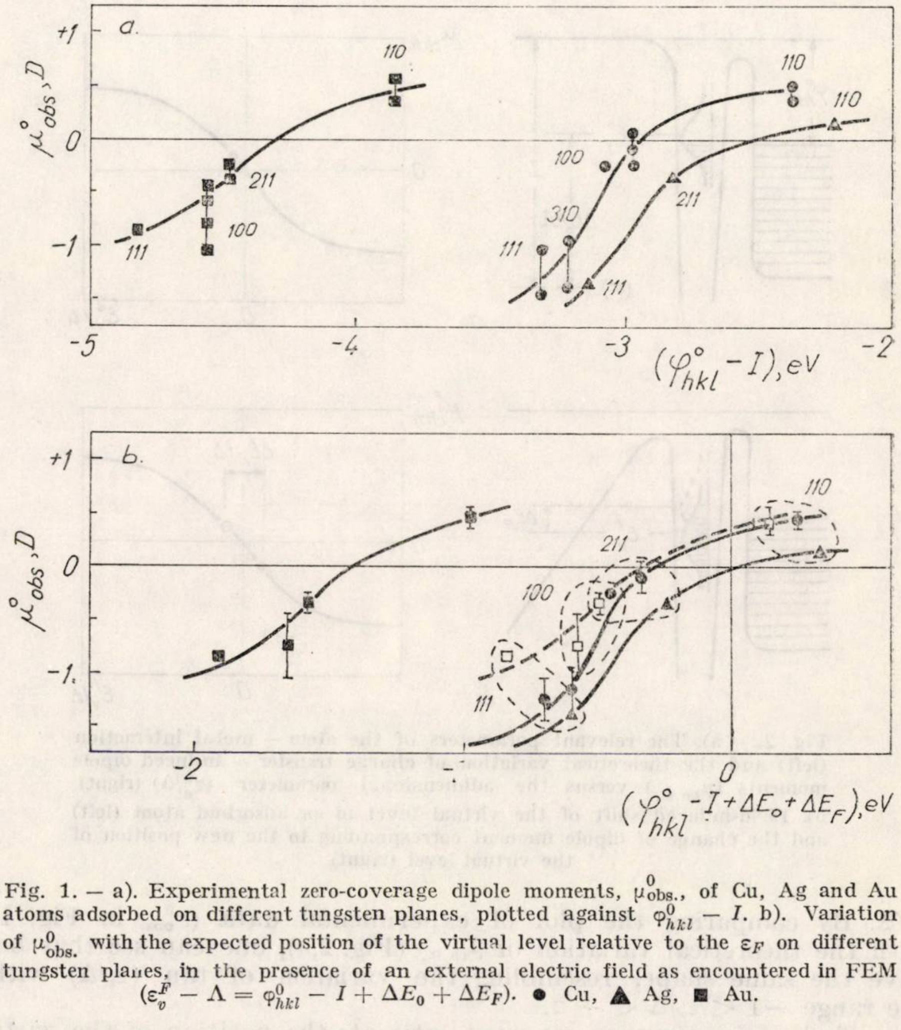

Fig. 1. — a). Experimental zero-coverage dipole moments, $\mu^{0}_{\text{obs.}}$, of Cu, Ag and Au atoms adsorbed on different tungsten planes, plotted against $\varphi^{0}_{hkl} - I$. b). Variation of $\mu^{0}_{\text{obs.}}$ with the expected position of the virtual level relative to the ε_F on different tungsten planes, in the presence of an external electric field as encountered in FEM ($\varepsilon_v^F - \Lambda = \varphi^{0}_{hkl} - I + \Delta E_0 + \Delta E_F$). ● Cu, ▲ Ag, ■ Au.

where $n_{a\sigma}^{\text{free}}$, $n_{a\sigma}^{\text{ads.}}$ are the electron occupancy numbers per spin (σ) in the free and adsorbed state respectively; a symmetrical Lorentz distribution was assumed[29] for the electron density per spin of adsorbed atom:

$$\rho_{a\sigma}(\varepsilon) = \frac{1}{\pi}\cdot\frac{\Delta}{(\varepsilon - \varepsilon_v)^2 + \Delta^2} \qquad (3)$$

where Δ is the half-width of the virtual level and the energy of the unperturbed virtual level is given by:

$$\varepsilon_v^0 = (\varphi_{hkl}^0 - I) + \Delta E_0 + \Lambda = \varepsilon_a + \Lambda \tag{4}$$

where Λ is the term of self-energy (usually small). In figure 2,a there is shown the expected variation of $\mu_{\mathrm{ch.tr.}}$ versus the adimensional parameter ε_v^0/Δ. By comparing the plot of experimental data ($\mu_{\mathrm{obs.}}^0$ in Fig. 1,a) with the theoretical variation of $\mu_{\mathrm{ch.tr.}}$ (Fig. 2,a), one can see that both have the same shape, resembling the variation of $\tan^{-1}(\varepsilon_v/\Delta)$ within the range $-1 < \varepsilon_r/\Delta < +2$.

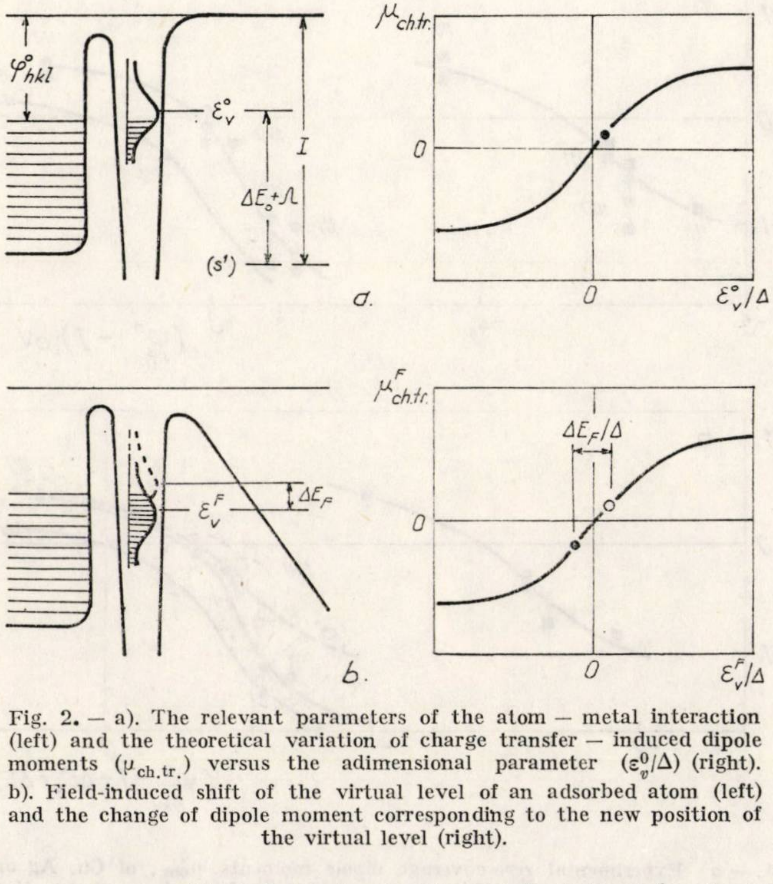

Fig. 2. — a). The relevant parameters of the atom — metal interaction (left) and the theoretical variation of charge transfer — induced dipole moments ($\mu_{\mathrm{ch.tr.}}$) versus the adimensional parameter (ε_v^0/Δ) (right). b). Field-induced shift of the virtual level of an adsorbed atom (left) and the change of dipole moment corresponding to the new position of the virtual level (right).

To be more rigurous, we must estimate the position of the virtual level on various planes and then compare the signs of $\mu_{\mathrm{obs.}}^0$ and ε_v. According to the virtual level model,[29] the level shift ΔE_0 of an electroneutrally adsorbed atom may be expressed in Hartree-Fock approximation by the simple relationship $\Delta E_0 = (1/2)(I - A)$, where A represents the electron affinity[30] of the isolated atom. Although $n_{a\sigma}^{\mathrm{ads.}}$ has actually small variations among different planes, the small values of

$\mu^0_{obs.}$ show that these variations are not greater than $\pm 5\,\%$. This gives a variation of about $0.1 - 0.2$ eV for ΔE_0 which is smaller than the difference of about 1.0 eV between φ_{110} and φ_{111}. It follows that ε_v depends mainly on the work function of different planes and ΔE_0 may be well assumed crystallographically independent at equilibrium separation.

The electric field used in FEM is a strong perturbation for the virtual level of the adsorbed atoms[31] which is shifted downwards at $\varepsilon_v^F = \varepsilon_v^0 + \Delta E_F$ where $\Delta E_F = - eFs_F$ and $s_F = r_a + k_s^{-1}$ (r_a = atomic radius, $k_s^{-1} = 0.6$ Å = Thomas-Fermi screening length). With $F = (0.35 - 0.40$ V/Å (values usually encountered in FEM), the field-induced level shift may be of $-(0.6 - 0.9)$ eV. If the half-width of the virtual level is of the same order,[14,15] this level shift produces a significant charge transfer to the adsorbate, as shown in the electronic scheme of figure 2,b. Supposing that the density of states for a field-perturbed virtual level can also be approximated by a symmetrical Lorentzian, equation (2) may be applied with ε_v replaced by ε_v^F.

5. RESULTS AND DISCUSSIONS

From the facts mentioned above we can estimate ε_v^F, the energy of the virtual level of the adsorbed atoms, considering the experimental conditions of FEM. By replotting the experimental data from Fig. 1,a, $\mu^0_{obs.}$ versus $(\varphi^0_{hkl} - I + \Delta E_0 + \Delta E_F) = \varepsilon_v^F - \Lambda$, the curves shown in figure 1,b have been obtained; in abscissa are figured the actual positions of the virtual level of different adsorbates on various tungsten planes. A satisfactory agreement with the theoretical curve (Fig. 2,b) is found for Cu and Ag. This is shown both by the similar shape of experimental and theoretical curves and by the close correspondance between the sign of $\mu^0_{obs.}$ and of $(\varepsilon_v^F - \Lambda)$. It follows that the crystallographic variations of $\mu^0_{obs.}$ can be well explained by changes on various planes of the relative position of the field-perturbed virtual level with respect to ε_F, which is a consequence of the work function anisotropy of clean tungsten crystal.

A short comment is needed for Au on W, where ε_v^F estimated with the energy of the ground state level ($5d^{10}\,6s^1$) is far below ε_F on all the tungsten planes. However, on account of the electronic structure of Au atoms (complete $4f^{14}$ subshell) and of the chemical properties of this element (stability of higher oxidation states) we may assume that the first excited configuration of free atoms ($5d^9\,6s^2$) is also effective in forming Au—W chemisorption bonds. An effective surface valency of 3 in gold adatoms was first postulated by Plummer and Rhodin[32] in order to explain the anomalously high adsorption energy of Au on W compared with Cu, Ag and the rest of 5d elements. To partially account for this change of electronic configuration we recalculated $\varepsilon_v^F - \Lambda$ starting from the energy of the $5d^9\,6s^2$ level.[33] By replotting $\mu^0_{obs.}$ in these possible positions of the virtual level, the dotted curve in figure 1,b was obtained. It is also in good agreement with the expected variation.

Therefore, our simple model gave the correct order of $\mu^0_{obs.}$ on various planes. The agreement is however semiquantitative since all the curves in figure 1, b are slightly shifted on the ordonate towards negative values, so that the inflexion is not exactly at $\mu^0_{obs.} = 0$ as equation (2) requires. This shift may be attributed to various reasons[34] as there are different dipole lenghts on various planes, polarization effects (neglected herein), electron-electron correlations and imperfect screening of surface charges. Still the most serious deviations from the theoretical model may be introduced by a non-symmetrical level resonance, including contributions from other excited levels of the adatoms. Indeed, the enhancement factors of resonance tunneling of the field emitted electrons have often narrow peaks superimposed over the broad resonance of the s-type electrons.[10,14,15,24,35,36] Then the integral giving $n^{ads.}_{a\sigma}$

$$n^{ads.}_{a\sigma} = \int_{-\infty}^{0} \rho_{a\sigma}(\varepsilon)\, d\varepsilon \tag{5}$$

no longer reduces to the simple $\tan^{-1}$ function and equation (2) has to be accordingly modified. When additional peaks of higher excited electronic levels are present besides a wide virtual level from the ground state level, the excess electrons filling up these states lead obviously to more negative $\mu^0_{obs.}$ values.

Nevertheless, the above observations do not affect our conclusions, since the exact computation of $\mu^0_{obs.}$ was beyond our aim. In our view, the electronegativity of adsorbed atoms (or more exactly, the value of their ionization potential) plays the dominant role in the character of work function variations on adsorption. This statement is equally valid in adsorption of alkali or noble metals on tungsten substrate. The crystallographic specificity of work function variations in adsorption of the first monolayer of Cu, Ag and Au on W was satisfactorily explained by using the picture of the surface dipoles arising from charge transfer in metallic-covalent chemisorption bonds. The effects of adatom polarization which depend on the geometry of adsorption sites, may also play a role, but of secondary importance, in the observed work function variations. We have shown that the values of $\mu^0_{obs.}$ for different adsorbates on various tungsten planes may be correlated with the actual position of the virtual level relative to the Fermi energy, taking also into account the conditions of the experimental procedure.

ACKNOWLEDGEMENT. We are indebted to Prof. R. Gomer from the James Franck Institute, University of Chicago, for a critical reading of the manuscript and valuable suggestions. Cr. Conțescu is also grateful to Prof. E. Segal, National Institute for Chemistry, Bucharest, for his theoretical guidance throughout this study.

REFERENCES

[1] J. P. Jones, *Proc. Roy. Soc.*, **A 284**, 469 (1965).
[2] J. P. Jones, *Surface Sci.*, **32**, 29 (1972).
[3] E. Sugata and K. Takeda, *Phys. Status Solidi*, **38**, 549 (1970).
[4] W. Wüstner and D. Menzel, *Thin Solid Films*, **24**, 211 (1974).

[5] M. I. Vass and Cr. Conţescu, *Rev. Roumaine Chim.*, **20**, 1253 (1974).
[6] J. P. Jones, in "Surface Phenomena of Metals", Monograph No. 28, Society of Chemical Industry, London, 1967.
[7] A. Cetronio and J. P. Jones, *Surface Sci.*, **44**, 109 (1974).
[8] J. Polanski and Z. Sidorski, *Surface Sci.*, **40**, 282 (1973).
[9] A. Cetronio, J. P. Jones and E. W. Roberts, *Surface Sci.*, **52**, 473 (1975).
[10] J. P. Jones and E. W. Roberts, *Surface Sci.*, **69**, 185 (1977).
[11] J. P. Jones and N. T. Jones, *Thin Solid Films*, **35**, 83 (1976).
[12] J. P. Jones and E. W. Roberts, *Thin Solid Films*, **48**, 215 (1978).
[13] Z. Sidorski, T. Szelwicki and Z. Dworecki, *Thin Solid Films*, **61**, 203 (1979).
[14] Cr. Conţescu, Thesis, National Institute for Chemistry, Bucharest, 1979.
[15] Cr. Conţescu and M. I. Vass, to be published.
[16] A. Mroz and Z. Sidorski, *Acta Phys. Polonica*, **A 49**, 437 (1976).
[17] J. Kolaczkiewicz and Z. Sidorski, *Surface Sci.*, **63**, 501 (1977).
[18] R. Smoluchowsky, *Phys. Rev.*, **60**, 661 (1941).
[19] N. D. Lang, *Phys. Rev.*, **B 4**, 4234 (1971).
[20] K. F. Wojciechowsky, *Surface Sci.*, **80**, 253 (1979).
[21] L. Richter and R. Gomer, *Surface Sci.*, **83**, 93 (1979).
[22] L. Richter and R. Gomer, *Appl. Phys.*, **13**, 303 (1977).
[23] L. Richter and R. Gomer, *Phys. Rev. Letters*, **37**, 763 (1976).
[24] P. L. Young and R. Gomer, *Surface Sci.*, **44**, 268 (1974).
[25] A. J. Sargood, C. W. Jowett and B. J. Hopkins, *Surface Sci.*, **22**, 343 (1970).
[26] E. Bauer, H. Poppa, G. Todd and F. Bonczek, *J. Appl. Phys.*, **45**, 5164 (1974).
[27] E. Bauer, H. Poppa, G. Todd and P. R. Davis, *J. Appl. Phys.*, **48**, 3773 (1977).
[28] E. Bauer, *J. Physique, Colloque C 4*, **38**, C 4 — 146 (1977).
[29] K. Lyo and R. Gomer, in "Interactions on Metal Surfaces", Ed. R. Gomer, Springer, New York, 1975.
[30] B. Edlen, *J. Chem. Phys.*, **33**, 98 (1960).
[31] B. Feuerbacher and B. Fitton, in "Electron Spectroscopy for Surface Analysis", Ed. H. Ibach, Springer, Berlin, Heidelberg, New York, 1977.
[32] E. W. Plummer and T. N. Rhodin, *J. Chem. Phys.*, **49**, 3479 (1968).
[33] C. E. Moore, "Atomic Energy Levels", NBS Circular No. 467, U. S. Government Printing Office, Washington D. C., 1958.
[34] J. W. Gadzuk, in "The Structure and Chemistry of Solid Surfaces", Ed. G. A. Somorjai, Wiley, New York, 1969.
[35] L. Richter and R. Gomer, *Surface Sci.*, **59**, 575 (1976).
[36] Cr. Conţescu and M. I. Vass, communicated to the International Seminar on Adsorption and Catalysis on Metals, paper No. 8, Institute of Catalysis, Novosibirsk, 1980.

Revue Roumaine de Chimie, 27, 1, 69—73 (1982)

NEW 2,4,6-TRISUBSTITUTED PHENOLS AND THEIR CORRESPONDING AROXYLS

J. HERDAN, [a*] G. IORDACHE, [a] N. NEGOIȚĂ, [b] NICOLETA GRECU, [b]
and A. T. BALABAN [c*]

a Institute of Technological Engineering, Research and Refinery Design (ICITPR) Ploiești, Romania
b Institute of Nuclear and Engineering Physics (IFIN), Bucharest, Romania
c Organic Chemistry Department, The Polytechnic, Bucharest, Romania
* To whom correspondence should be addressed

Received June 13, 1981

The syntheses of 2-*sec*-butyl-4,6-butylphenol (6) and 2-*sec*-butyl-4,6-diisopropylphenol (8) by Friedel-Crafts alkylation of *ortho-sec*-butylphenol are reported. The structures are confirmed by element analyses, IR and ^{1}H-NMR spectra. Oxidation of these phenols with lead dioxide in benzene yields persistent aroxyls (7 and 9, respectively) whose ESR spectra were determined; the coupling constants agree with the chemical structures. The new phenols may possess antioxidant properties.

Phenols possessing bulky groups in both *ortho* positions (**2**) have been long known to afford persistent free radicals, aroxyls **4**, whose stability makes them unable to carry on chain reactions.[1,2] This fact explains the wide use of such phenols as antioxidants, since the active peroxy radicals (**1**) are converted into hydroperoxides **3** and an inactive aroxyl radical **4**.

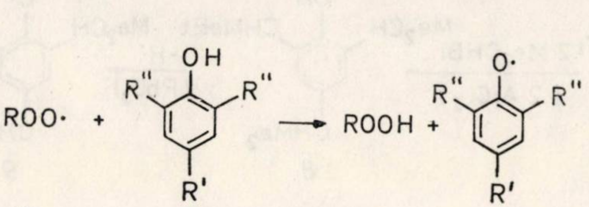

1 *2* *3* *4*

The efficiency as antioxidant depends on the rate of the above reaction, on the stability (non-reactivity) of the resulting aroxyl **4**, and on other factors.

Molecular orbital calculations by Davies et al.[3] for polycyclic phenols demonstrated that their activity as antioxidants is closely correlated with the resonance energy of the corresponding aroxyl free radical. However, the activity as antioxidant is not simply controlled exclusively by the stability of the aroxyl. Indeed, in the series of 2,6-di-t-butyl-4-R-phenols where R = Me, Et, i-Pr and t-Bu, the best antioxidant is the first phenol, despite the fact that the most stable aroxyl in this series is the last one.[2,4] Neither is the rate of the hydrogen abstraction from the phenol by the peroxy radical the only controlling factor, because in the above series, again the 2,4,6-tri-t-butylphenol undergoes the fastest hydrogen abstraction.[2,4]

Numerous electron spin resonance (ESR) studies were carried out for determining spin densities in a large variety of aroxyls.[2,5,6]

Most phenols used so far as antioxidants have in both *ortho* positions t-butyl groups. In order to investigate both the antioxidant activity and the hyperfine coupling constants for aroxyls with non-symmetrical 2 and 6 substituents, we studied 2,4,6-trisubstituted phenols with an *ortho-sec*-butyl group. Such a substituent has not been apparently investigated in 2,4,6-trisubstituted aroxyls (only *p-sec*-butylphenoxyl was studied by Stone and Waters[7]). We report the preparation of two new phenols, **6** and **8**, with one *ortho-sec*-butyl group in position 2, and two t-butyl or isopropyl groups (in positions 4 and 6), respectively. They were synthesized by Friedel-Crafts alkylation of *ortho-sec*-butylphenol (**5**) using isobutene and isopropyl bromide, respectively.

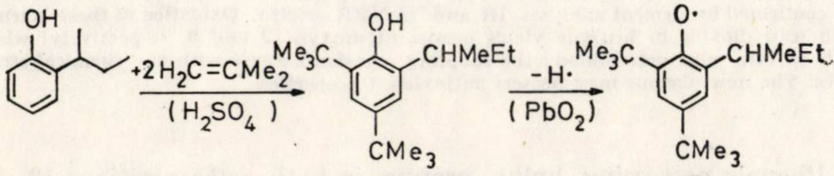

5 6 7

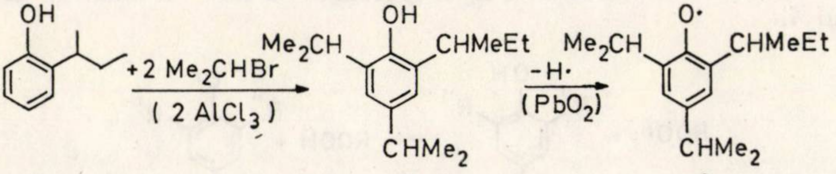

5 8 9

Both phenols **6** and **8** possess sufficient steric shielding around the phenolic oxygen, and both have no free *ortho* or *para* position, so that the corresponding aroxyl radicals can be isolated and studied by ESR. The structures of both phenols are confirmed by elemental analyses, ebulioscopic molar weight determinations, IR and ^1H-NMR spectra.

The ^1H-NMR spectrum of 2-*sec*-butyl-4,6-di-t-butylphenol **6** (in $CDCl_3$) has two different singlets for the t-butyl groups, and an AB quadruplet for the *meta*-protons. With the lanthanide shift reagent $Eu(fod)_3$, this phenol presents no complexation owing to the high steric hindrance around the oxygen. The ^{1}H-NMR spectrum of 2-*sec*-butyl-4,6-diisopropylphenol **8** also presents separate doublets for the isopropyl methyls.

Oxidation of **6** with lead dioxide in benzene leads to a persistent aroxyl **7** whose ESR spectrum (Figure 1) consists of a doublet of 1 :2 :1 triplets, indicating that the hyperfine coupling constant (hfc) with the CHMeEt benzylic proton in *ortho* is 0.62 mT (6.2 Gauss) and that the hfc's with the two *meta*-standing aromatic protons are equal, amounting to 0.22 mT (2.2 Gauss). Evaporation of the solvent leaves the liquid **7**, presenting strong ESR absorption. The difference between the hfc's of the two *meta*-standing protons is too small to be detected in the ESR spectrum.

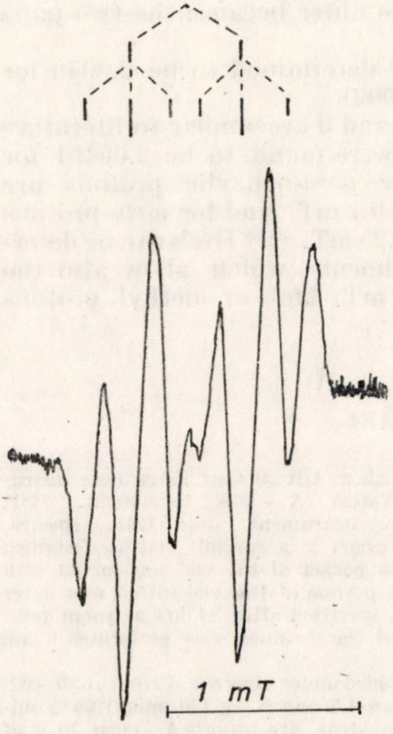

Fig. 1. — First-derivative ESR spectrum of the persistent aroxyl **7** obtained by oxidizing phenol **6** in degassed benzene.

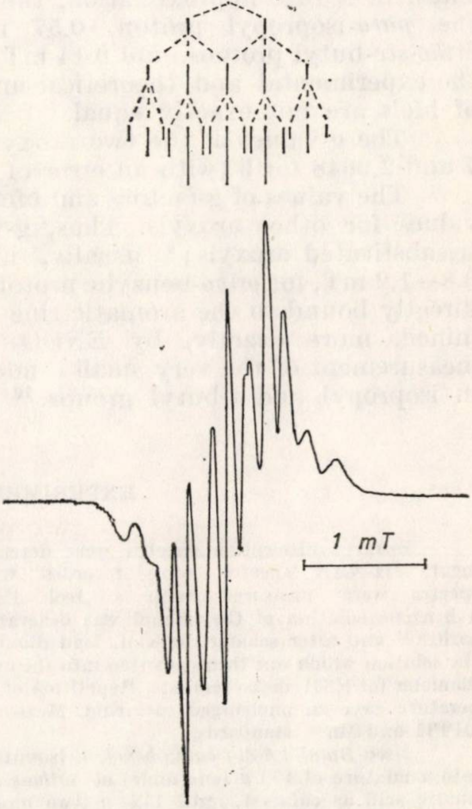

Fig. 2. — First-derivative ESR spectrum of the persistent aroxyl **9** obtained by oxidizing phenol **8** in degassed benzene.

The ESR spectrum of radical **9** obtained similarly from **8** (Fig. 2) is more complicated, presenting about eleven lines (the fifth and seventh lines are broader or evidence an additional splitting). Since in this radical no two coupling constants of the five protons which are coupled to the unpaired electron are exactly equal by reasons of molecular nonsymmetrical structure, the interpretation of the spectrum is rather difficult. However, one may assume that the two *meta*-protons will have approximately the same hfc's (as in **7**), and also that the hfc's of the two protons due to the *ortho-sec*-butyl and *ortho*-isopropyl groups will not be very different. This leaves only three different hfc's to be searched. Thus, in a first approximation, the hfc's of radical **9** are 1.15 mT for the *para*-isopropyl proton, 0.57 mT for the two *ortho*-isopropyl and *ortho-sec*-butyl protons, and 0.14 mT for the two *meta*-protons. Of course, the experimental and theoretical intensities differ because the two pairs of hfc's are not exactly equal.

The g-values of the two aroxyls were determined to be 2.0049 for **7** and 2.0048 for **9** (with an error of $\pm$ 0.0002).

The values of g-factors and hfc's in **7** and **9** are similar to literature values for other aroxyls. Thus, g-values were found to be 2.00451 for trisubstituted aroxyls;[8] usually, hfc's for *para*-benzylic protons are 0.8–1.2 mT, for *ortho*-benzylic protons 0.5–0.7 mT, and for *meta*-protons directly bound to the aromatic ring 0.1–0.25 mT.[2,6,7,9] Hfc's can be determined, more exactly, by ENDOR experiments which allow also the measurement of the very small (under 0.05 mT) hfc's of methyl protons in isopropyl and t-butyl groups.[10]

EXPERIMENTAL PART

Infrared absorption spectra were determined with a UR-20 Carl Zeiss Jena instrument. ^{1}H-NMR spectra were recorded with a Varian A – 60A instrument. ESR spectra were measured with a Jeol JES-ME-3X instrument. For ESR spectra, a benzene solution of the phenol was deaerated with argon in a special vial as described earlier,[11] and after sealing the vial, lead dioxide from a pocket of the vial was mixed with the solution which was then decanted into the cylindrical portion of the vial with 5 mm outer diameter for ESR measurements. Repetition of the ESR spectrum after 24 hrs at room temperature gave an unchanged spectrum. Measurements of the g-values were performed using DPPH and Mn^{2+} standards.

2-sec-*Butyl-4,6-di-t-butylphenol*, **6**. Isobutene is bubbled under vigorous stirring at 80–90° into a mixture of 150 g (one mole) of *ortho-sec*-butylphenol **5** and 5.1 g (50 mmol) 96% sulphuric acid as catalyst, until 112 g (two moles) of isobutene are absorbed. Then 20 g of anhydrous powdered sodium carbonate are added into the reaction mixture which is stirred for 5 hrs at 90° for neutralization of the acid. The mixture is filtered, the filtrate is washed with water, dried over anhydrous sodium sulphate, and distilled under reduced pressure, affording in about 90% yield a fraction with b.p. 136–140°/10 Torr, containing **6** in 80–85% relative amount (by g.l.c. analysis). By preparative column chromatography (on silica gel G, Merck, activated at 150° for 3 hrs., using petroleum ether for elution and rechromatographing the first fraction), the pure liquid phenol **6** was obtained. Found: C, 82.3; H, 11.5%. $C_{18}H_{30}O$ requires: C, 82.4; H, 11.4%. By ebullioscopy in carbon tetrachloride, the molecular weight was found 270 (calc. 262).

The IR spectrum in CCl_4 presents the free OH stretching band at 3640 cm^{-1}.

The ^{1}H-NMR spectrum in $CDCl_3$: $\delta = 0.75$ (3H, t, $C\mathbf{H}_3CH_2$, $J = 7$ Hz); 1.28 (3H, d, $C\mathbf{H}_3CHEt$, $J = 7$ Hz); 1.33 (9H, s, 2-t-Bu); 1.47 (9H, s, 4-t-Bu); 1.62 (2H, q, $C\mathbf{H}_2CH_3$, $J = 7$ Hz); 2.85 (1H, sextet, $C\mathbf{H}MeEt$, $J = 7$ Hz); 4.82 (1H, s, OH); 7.07 (1H, d, 3-H, $J = 2.5$ Hz); 7.23 (1H, d, 5-H, $J = 2.5$ Hz).

2-sec-*Butyl-4,6-diisopropylphenol*, **8**. In a four-necked flask with stirrer, reflux condenser and dropping funnel, 30 g (0.2 mol) *ortho-sec*-butylphenol (**5**) are placed. Then 53.4 g (0.4 mol) of anhydrous aluminium chloride are added from a flask protected against air moisture. Subsequently 49.2 (0.4 mol) of isopropyl bromide are added dropwise, at room temperature during 2 hrs. The flask is then heated at 60 – 70° continuing the stirring for 5 hrs till the evolution of hydrogen chloride ceases. The mixture is poured on 200 g crushed ice acidified with 20 ml conc. hydrochloric acid. The product is extracted with ethyl ether, the extract is washed with water and dried over anhydrous sodium sulphate. The ether is evaporated, then the product is distilled under reduced pressure affording in about 75% yield a fraction with b.p. 110 – 120°/10 Torr, which contains **8** in 89 – 93% relative amount (by g.l.c. analysis). By column chromatography as described above, pure liquid **8** is obtained. Found: C,82.1; H, 10.7%. $C_{16}H_{26}O$ requires: C, 82.1; H, 10.9%. Ebullioscopy in carbon tetrachloride evidences a molecular weight of 238 (calc. 234).

The IR spectrum (in CCl_4) presents the free OH bond stretching vibration at 3645 cm^{-1}.

^{1}H-NMR spectrum (CCl_4): $\delta = 0.85$ (3H, t, $\mathbf{CH_3}CH_2$, J = 7 Hz); 1.18 (3H, d, $\mathbf{CH_3}CHEt$, J = 7 Hz); 1.20 (6H, d, $\mathbf{Me_2}CH$, J = 7 Hz); 1.23 (6H, d, $\mathbf{Me_2}CH$, J = 7 Hz); 1.55 (2H, q, $\mathbf{CH_2}CH_3$, J = 7 Hz); 2.80 (3H, m, $\mathbf{CH}Me_2$ and $\mathbf{CH}MeEt$, J = 7 Hz); 4.23 (1H, s, OH); 6.62 (2H, broad, 3,5-H_2).

ACKNOWLEDGEMENT. Thanks are expressed to Dr. F. Chiraleu for recording the ^{1}H-NMR spectra.

REFERENCES

[1] J. L. Bolland, *Quart. Rev.*, **3**, 1 (1949).

[2] V. D. Pokhodenko, "Fenoxilnye radikaly", Naukova Dumka, Kiev, 1969.

[3] D. S. Davies, H. L. Goldsmith, H. K. Gupta and G. R. Lester, *J. Chem. Soc.*, **1956**, 4926.

[4] K. U. Ingold, *J. Phys. Chem.*, **64**, 1636 (1960).

[5] C. H. Clark and C. B. Kovens, *Plastics Technol.*, 41 (1959); J. K. Becconsall, S. Clough and H. G. Seo, *Proc. Chem. Soc.*, **1959**, 308; A. Rieker, K. Scheffler, R. Mager, B. Narr and E. Müller, *Liebigs Ann. Chem.*, **693**, 10 (1966).

[6] H. B. Stegmann and W. Uber, in "Landolt-Börnstein's Tabellen", vol. 9 (edited by H. Fischer and H. Hellweg), Springer Verlag, Berlin, 1979.

[7] T. J. Stone and W. A. Waters, *J. Chem. Soc.*, **1964**, 213.

[8] H. B. Stegmann and K. Scheffler, *Angew. Chem.*, **76**, 610 (1964).

[9] T. J. Stone and W. A. Waters, *J. Chem. Soc.*, **1964**, 2847.

[10] N. M. Atherton, A. J. Blackhurst and I. P. Cook, *Trans. Faraday Soc.*, **67**, 2510 (1971).

[11] A. T. Balaban, P. T. Frangopol, M. Frangopol and N. Negoiță, *Tetrahedron*, **23**, 4661 (1967).

Revue Roumaine de Chimie, 27, 1, 75–79 (1982)

PROPYLENE OXIDATION ON MoO_3/SiO_2 AND Bi_2O_3/SiO_2 CATALYSTS

N. I. IONESCU and MONICA CĂLDĂRARU
Center of Physical Chemistry, Spl. Independenţei 202, Bucharest, Romania

Received June 15, 1981

Propylene oxidation on the MoO_3/SiO_2 and Bi_2O_3/SiO_2 catalysts was studied using catalytic activity and electrical conductance measurements. A rate equation as :

$$r = k\ [C_3H_6]^x\ [O_2]^{0.5}$$

was obtained, where $x = 0$ for MoO_3/SiO_2 and $x = 1$ for Bi_2O_3/SiO_2. Some aspects of the electrical conductance changes for different reaction conditions are discussed.

In the previous papers[1-6] we have studied the temperature dependence of the catalytic activity and electrical conductance of a complex Bi-Mo catalyst for the propylene oxidation. All obtained data have indicated a change of the interaction of the catalyst with propylene at 300 – 310°C. Microgravimetric measurements have also evidenced two different types of interaction of propylene with the catalyst.

To correlate the experimental data with the complex structure or/and composition of the catalyst is a difficult task. So, it was interesting to study the same process using the main components (molybdenum oxide and bismuth oxide supported on silica) as catalysts ; the conditions of the reaction of the propylene oxidation were the same as for the complex catalyst.

The paper presents the results of this study.

EXPERIMENTAL

The measurements were performed in an integral reactor which allows the simultaneous measurements of electrical conductance and catalytic activity. All the experimental conditions have been described elsewhere.[5]

The MoO_3/SiO_2 and Bi_2O_3/SiO_2 samples were prepared containing 75% active phase on support (the same composition as for the complex catalyst).

MoO_3/SiO_2 was prepared by mixing at 60°C a solution of ammoniumparamolybdate with silicasol ; the product was dried at 90°C for 6 h, at 110°C for 16 h and then calcined in air flow at 400°C for 6 h and at 500°C for 6 h.

Bi_2O_3/SiO_2 was prepared by dissolving at 60°C bismuth nitrate in a HNO_3 aqueous solution and adding silicasol. The product was dried at 90°C for 6 h, at 110°C for 16 h, then calcined in air flow at 400°C for 6 h and at 500°C for 6 h.

In order to obtain accurate kinetic data, several precautions were taken. Flowing rate less than 2.6 ml/s were used to avoid the diffusional effects. Periodic activity checks were made to determine whether any deactivation had occurred. The catalysts were lined-out for 4 h to be sure a steady state reaction was reached before every kinetic data was taken.

Electrical conductance measurements were performed for flowing mixtures of different compositions : (a) propylene-argon mixtures from 1 : 5.3 till 1 : 1.8 ; (b) propylene-air mixtures from 1 : 15 till 1 : 8.

The initial reaction rates for the propylene oxidation on both MoO_3/SiO_2 and Bi_2O_3/SiO_2 were determined for the propylene-air mixtures as 1 : 10 and rates of feed between 0.33 and 2.58 ml/s.

The temperature range was 300 — 400 °C, the same as for the complex catalyst previously studied. [5]

RESULTS AND DISCUSSION

a. Electrical conductance measurements

The time dependence of conductance G of MoO_3/SiO_2 catalyst for 1 : 5.3 and 1: 1.8 propylene-argon flowing mixtures is given in Fig. 1 and Fig. 2, respectively.

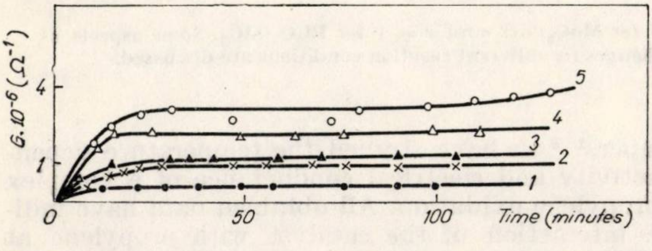

Fig. 1. — The time dependence of conductance G of MoO_3/SiO_2, sample, for propylene-argon mixture as 1: 3 ; feed rate 1.05 ml/s ; 1—260°C ; 2—300°C ; 3—320°C ; 4—335°C; 5 — 345°C.

The conductance increases faster for the first 30 minutes, then reaches an equilibrium value ; this value is higher, when the temperature is higher.

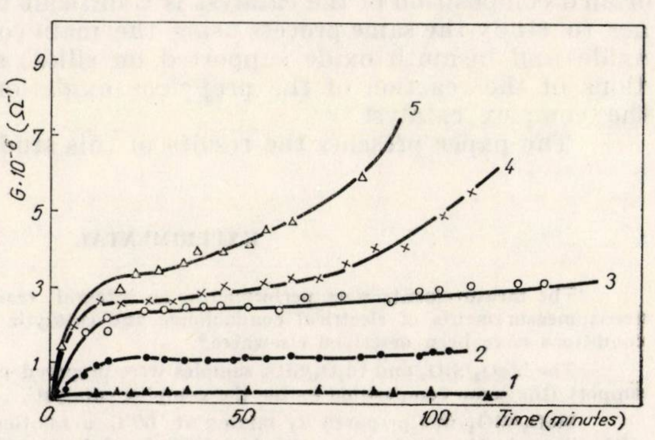

Fig. 2. — The time dependence of conductance G of MoO_3/SiO_2 sample, for propylene-argon mixture as 1 : 1.8 ; feed rate 1.05 ml/s ; 1—260°C ; 2 — 300°C ; 3 — 320°C ; 4 — 335°C ; 5 — 345°C.

At 260°C, the values of the equilibrium conductance are almost identical, regardless of the propene content in the feed, while starting with 300°C, they begin to be different : the higher the partial pressure of propylene, the higher the value of the equilibrium conductance. These results are in agreement with the previous conductance and microgravimetric measurements found on the complex Bi-Mo catalyst.[2,4,5]

A special behaviour is found for propylene contents higher than 1 : 3 (for example 1 : 1.8) and 335°C, when conductance increases sharply after 100 minutes (Fig. 2); for temperatures higher than 335°C one records a similar behaviour but with corresponding shorter times until the conductance presents its jump. The gas chromatographic analysis for these reaction conditions indicates the presence of hydrogen among the reaction products. If we explain the conductivity changes by the reduction of the catalyst, the appearance of H_2 means that MoO_3/SiO_2 sample became a partially reduced one, so that dehydrogenation[7,8] step leads only to H_2 formation instead of H_2O. No hydrogen was evidenced when the flowing mixture was propylene-air.

For Bi_2O_3/SiO_2 the time dependence of conductance G is different from that observed in the case of MoO_3/SiO_2 in propylene-argon flowing mixture (Fig. 3). No equilibrium conductance was obtained, indicating a continuous reduction of the sample during our experiments. The gas chromatographic analysis evidenced the presence of hydrogen (CO only as trace), the main products being CO_2 and H_2O.

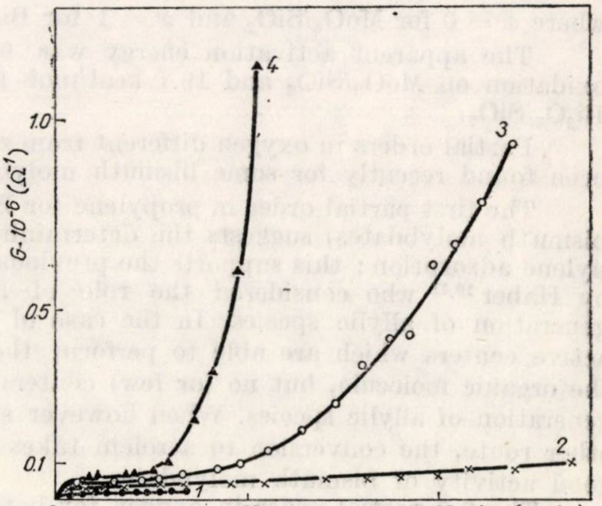

Fig. 3. — The time dependence of conductance G of Bi_2O_3/SiO_2 sample, for propylene-argon mixture 1 : 1.8; feed rate 1.05 ml/s; *1* — 300°C; *2* — 320°C; *3* — 350°C; *4* — 380°C.

The values of the Bi_2O_3/SiO_2 conductance depend strongly on the propylene concentration in the propylene-argon mixture.

For propylene-air mixtures, conductance of MoO_3/SiO_2 catalyst does not depend on the oxygen concentration, but on the propylene concentration.

No dependence of Bi_2O_3/SiO_2 conductance on the partial pressure of propylene or oxygen was found.

In the case of MoO_3/SiO_2, the main oxidation products of the oxidation reaction were CO, CO_2, acrolein and H_2O. For Bi_2O_3/SiO_2 the analysis indicated only CO_2 and H_2O among the reaction products (CO was found only as a small trace). This result indicates the higher oxidative power of Bi_2O_3/SiO_2 in comparison with MoO_3/SiO_2 catalyst.

b. Kinetic parameters measurements

The partial reaction order in propylene at 350°C for constant oxygen (in excess) concentration was determined.

Measurements for determining the partial order in oxygen are difficult because an excess of propylene might suddenly reduce the sample and lead to false results. So, the partial order in oxygen was determined by measuring the initial reaction rates for different oxygen concentrations at constant propylene (not in excess) concentration.

The initial rates, the rate constants and the apparent activation energies for MoO_3/SiO_2 and Bi_2O_3/SiO_2 have been calculated for the $300 - 400°C$ temperature range using the rate equation :

$$r = k[C_3H_6]^x [O_2]^{0.5} \tag{1}$$

where $x = 0$ for MoO_3/SiO_2 and $x = 1$ for Bi_2O_3/SiO_2.

The apparent activation energy was 9.6 kcal/mol for propylene oxidation on MoO_3/SiO_2 and 19.7 kcal/mol for propylene oxidation on Bi_2O_3/SiO_2.

Partial orders in oxygen different from zero as in these cases have been found recently for some bismuth molybdates[9] too.

The first partial order in propylene for Bi_2O_3/SiO_2 (the same as for bismuth molybdates) suggests the determining role of bismuth in propylene adsorption ; this supports the previous reaction scheme proposed by Haber [10,11] who considered the role of Bi centers as consisting in generation of allylic species. In the case of MoO_3, its surface contains active centers which are able to perform the insertion of oxygen into the organic molecule, but no (or few) centers are available for efficient generation of allylic species. When however such species are formed by other route, the conversion to acrolein takes place, this explaining the good activity of bismuth molybdates.

The 0.5 partial order in oxygen for both catalysts in this temperature range indicates a dissociative adsorption of oxygen on the catalyst surface.

For MoO_3/SiO_2 CO and CO_2 appear in comparable amounts, and also acrolein is among the reaction products, while for propylene oxidation on Bi_2O_3/SiO_2 only CO_2 is evidenced. This suggests that on MoO_3/SiO_2 and Bi_2O_3/SiO_2 two reaction paths could occur : one leading to total oxidation, the second to the partial one, but on Bi_2O_3/SiO_2 the total oxidation of acrolein is important.

Further experiments are in progress.

REFERENCES

[1] N. I. Ionescu and M. Căldăraru, *Reac. Kin. Catal. Lett.*, **8**, 477 (1978).
[2] N. I. Ionescu, M. Căldăraru and P. Banyai, "Proc. 4th International Symposium Heterogeneous Catalysis, Varna 1979", vol. 1, D. Shopov, A. Andreev, A. Palazov, L. Petrov eds., Publishing House of the Bulgarian Academy of Sciences, Sofia 1979, p. 229.
[3] R. Mănăilă, N. I. Ionescu, M. Căldăraru, S. Şerban, A. Belea, A. Weidenbecher and A. Rusu, "Proc. 4th International Symposium Heterogeneous Catalysis, Varna 1979", vol. 1, D. Shopov, A. Andreev, A. Palazov, L. Petrov eds., Publishing House of the Bulgarian Academy of Sciences, Sofia 1979, p. 223.
[4] N. I. Ionescu, P. Banyai, M. Căldăraru and M. Chirca, *Rev. Roumaine Chim.*, **26**, 681(1981).
[5] M. Căldăraru, P. Banyai and N. I. Ionescu, *Rev. Roumaine Chim.*, **26**, 837(1981).
[6] R. Mănăilă, N. I. Ionescu and M. Căldăraru, *Z. anorg. Chem.*, **466**, 221 (1980).
[7] J. Novakova, P. Jiru and V. Zavadil, *J. Catalysis*, **17**, 93 (1970).
[8] J. Novakova, P. Jiru and V. Zavadil, *J. Catalysis*, **21**, 143 (1971).
[9] L. D. Krenzke and G. W. Keulks, *J. Catalysis*, **64**, 295 (1980).
[10] J. Haber and B. Grzybowska, *J. Catalysis*, **28**, 489 (1973).
[11] J. Haber, *Pure Appl. Chem.*, **50**, 923 (1978).

REFERENCES

[1] N. I. Ionescu and M. Căldăraru, React. Kin. Catal. Lett., 9, 477 (1978).
[2] N. I. Ionescu, M. Căldăraru and E. Bâzgan, Proc. IIIrd International Symposium "Heterogeneous Catalysis, Varna 1975", vol. 1, D. Shopov, A. Andreev, A. Palazov, L. Petrov eds., Publishing House of the Bulgarian Academy of Sciences, Sofia 1979, p. 224.
[3] H. Knözinger, N. I. Ionescu, M. Căldăraru, S. Serban, A. Bedea, A. Weidenbacher and A. Petre, Proc. 4th International Symposium Heterogeneous Catalysis, Varna 1979", vol. I, D. Shopov, A. Andreev, A. Palazov, L. Petrov eds., Publishing House of the Bulgarian Academy of Sciences, Sofia 1979, p. 233.
[4] N. I. Ionescu, P. Bălan, M. Căldăraru and M. Chirea, Rev. Roumaine Chim., 26, 381(1981).
[5] M. Căldăraru, E. Georgescu and N. I. Ionescu, Rev. Roumaine Chim., 26, 857(1981).
[6] C. Mărcuță, N. I. Ionescu and M. Căldăraru, Z. anorg. Chem., 468, 231 (1980).
[7] J. Novakova, P. Jiru and V. Zavadil, J. Catalysis, 17, 93 (1970).
[8] J. Novakova, P. Jiru and V. Zavadil, J. Catalysis, 21, 143 (1971).
[9] I. D. Kremke and G. V. Keulks, J. Catalysis, 64, 295 (1980).
[10] J. Haber and B. Grzybowska, J. Catalysis, 28, 489 (1973).
[11] J. Haber, Pure Appl. Chem., 50, 923 (1978).

Revue Roumaine de Chimie, 27, 1, 81–86 (1982)

DETERMINATION OF TRACE QUANTITIES OF THE GROUP V–A ELEMENTS BY ANODIC STRIPPING VOLTAMMETRY. II

TRACE ANALYSIS OF ANTIMONY

SOFIA MARCHIDAN*, IULIANA VARTIRES and N. D. TOTIR
Centre of Physical Chemistry,
Splaiul Independenţei 202, Bucharest 77208, Romania

Received December 15, 1980

A new method for determining the antimony in the $10^{-6} - 10^{-8}$ M concentration range, with a variation coefficient less than 5 % has been worked out. There have been obtained a good sensibility and reproducibility for both antimony (III) and antimony (V) analysis on hanging mercury drop electrode, using 2 M HCl as supporting electrolyte. It has been established that large amounts of Cd, Pb, Zn, Ni, Fe, As and Cu do not disturb the stripping analysis of antimony.

Anodic stripping voltammetry has been employed by many authors for the determination of antimony in different samples.[1–10]

In this paper a procedure for trace analysis of antimony by anodic stripping voltammetry by using 2 M HCl as supporting electrolyte is described.

EXPERIMENTAL

Apparatus

All the information regarding the instrumentation and the quartz cell used in this work was given in a previous paper.[11] The proper working electrode for antimony ion analysis is the hanging mercury drop electrode (HMDE). As a counter electrode a platinum wire was used. All the potentials are referred to the saturated calomel electrode which was used as reference electrode.

Reagents

All the solutions were obtained from tetradistilled water[12] and Johnson Matthey standard spectrographic reagents.

In order to avoid experimental errors, all the solutions were prepared just before measurements. The mercury was tetradistilled in vacuum in a quartz apparatus and stored in argon atmosphere.

---

[*] Deceased on November 25, 1980.

Procedure

The general procedure for preparing the sample for anodic stripping analysis has been described previously.[13] All measurements were performed by using 2 M HCl as a supporting electrolyte and mercury drops of 3×10^{-2} cm^2. The potentials used for the cathodic deposition step were −400 mV or −250 mV vs. SCE.

By dissolving the Sb_2O_3 in a few milliliters of concentrated HCl and afterwards in 2 M hydrochloric acid the standard Sb^{3+} solutions were obtained.

For preparing Sb^{5+} standard solutions, $K[Sb(OH)_6]$ was dissolved in concentrated hydrochloric acid in the case of solution one and in tetradistilled water for solution two.

RESULTS AND DISCUSSION

Both the results from literature and our experimental measurements have shown that the best supporting electrolyte is 2 M hydrochloric acid. By using this experimental conditions a good sensibility and reproducibility for anodic stripping analysis of Sb^{3+} was obtained (Fig. 1).

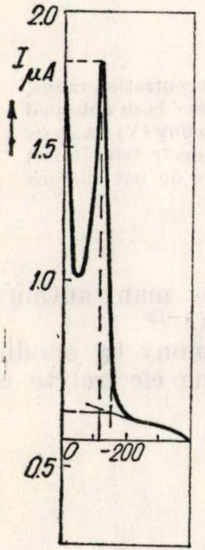

Fig. 1. — Stripping voltammogram of antimony in 2 M HCl : $\tau = 10$ min ; $E_d = -400$ mV ; $C_{Sb^{3+}} = 5 \times 10^{-7}$ M.

The dependence of peak current i_p on deposition potential E_d is given in table 1. The sensibility of the method is not affected by changing the potential from −200 mV to −600 mV. Most of the experiments were carried out with a deposition potential equal to −400 mV. When the sample was impurified with other cations, the −400 mV potential was preferred for deposition.

The influence of deposition time τ on peak current is given in table 2. The proper deposition time is five minutes for 10^{-6} M, ten minutes for 10^{-7} M and twenty minutes for 10^{-8} M concentration range.

There is a linear dependence between antimony concentration and the intensity of the peak current (Table 3).

As can be noticed from literature Sb^{5+} can be analysed by anodic stripping voltammetry only after a previous chemical reduction to Sb^{3+} with $2\ HCl \cdot NH_2-NH_2$ in presence of hydrochloric acid at 80−100° for about 15 minutes has taken place. On the other hand it is known from polarography that Sb^{5+} can be reduced from hydrochloric acid. To make clear this point we have used two different solutions, one prepared from $K[Sb(OH)_6]$ by dissolving it in concentrated hydrochloric acid (solution one) and the other prepared by dissolving the same substance in tetradistilled water (solution two). Separate samples from these solutions were prepared in the same manner as for the Sb^{3+} when using 2 M HCl.

The results obtained for 5×10^{-7} M Sb^{5+} in the case of solution one, without addition of $2\ HCl.NH_2-NH_2$, are given in Fig. 2 ; they appear in good agreement with that for Sb^{3+} (Table 4).

The behaviour of Sb^{5+} dissolved in water (solution two) is given in Fig. 3 where curve one is for the supporting electrolyte. Curbe two was recorded 60 minutes after dissolving the solution two in 2 M HCl and the other ones, from three to six, at 15 minute-intervals. The last voltammogram was recorded in the same conditions as the other ones after adding 0.5 g 2 HCl. NH_2-NH_2 to the sample and heating the solution to the boiling-point, the value of the current being identical with the one obtained for the other solution.

TABLE 1

Dependence of peak current i_p on deposition potential E_d ; $C_{Sb^{3+}} = 5 \times 10^{-7}$ M

E_d, mV	i_p, μA
−200	1.23
−300	1.24
−400	1.31
−500	1.33
−600	1.37

TABLE 2

Dependence of peak current i_p on deposition time τ.

$C_{Sb^{3+}} = 9 \times 10^{-6}$ M		$C_{Sb^{3+}} = 5 \times 10^{-7}$ M	
Deposition time, τ, min	i_p μA	Deposition time, τ, min	i_p μA
2.5	4.88	5.0	0.60
5.0	9.28	7.5	0.91
7.5	15.03	10.0	1.10
10.0	19.37	15.0	1.56
		20.0	1.85

TABLE 3

Dependence of peak current i_p on Sb^{3+} concentration

$C_{Sb^{3+}}$, M	i_p, μA	τ, min
9×10^{-6}	9.28	5.0
7×10^{-6}	7.51	
5×10^{-6}	4.74	
3×10^{-6}	2.62	
1×10^{-6}	0.99	
9×10^{-7}	2.23	10.0
7×10^{-7}	1.70	
5×10^{-7}	1.31	
3×10^{-7}	0.71	
1×10^{-7}	0.20	
9×10^{-8}	0.46	20.0
7×10^{-8}	0.38	
5×10^{-8}	0.26	
3×10^{-8}	0.13	
1×10^{-8}	0.03	

TABLE 4

Dependence of peak current i_p on Sb^{5+} and Sb^{3+} concentration. $E_d = -400$ mV ; $\tau = 10$ min

$C_{Sb^{5+}}$, M	$i_{p\,(Sb^{5+})}$ μA	$C_{Sb^{3+}}$, M	$i_{p\,(Sb^{3+})}$ μA	$i_{p\,(Sb^{5+})}/i_{p\,(Sb^{3+})}$
1×10^{-7}	0.32	1×10^{-7}	0.20	1.60
3×10^{-7}	1.03	3×10^{-7}	0.71	1.45
5×10^{-7}	1.62	5×10^{-7}	1.31	1.24
7×10^{-7}	2.04	7×10^{-7}	1.70	1.20
9×10^{-7}	2.77	9×10^{-7}	2.23	1.24

It can be concluded that instead of using 2 HCl.NH_2-NH_2 and heating the sample to the boiling-point it is better to dissolve initially the sample in concentrated hydrochloric acid, the results being the same.

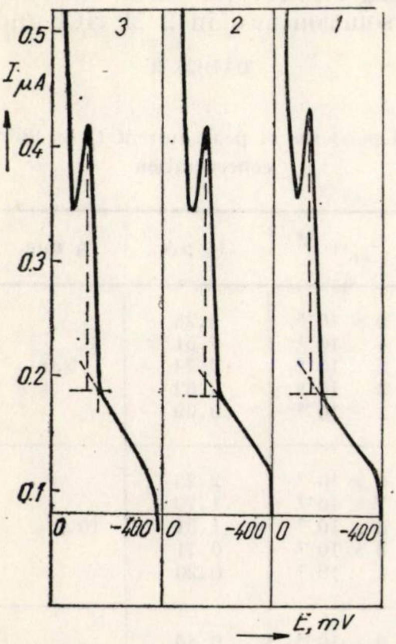

Fig. 2. — Stripping voltammograms of antimony in the presence of cadmium, lead, zinc, nickel and iron : 1. $C_{Sb^{3+}} = 1 \times 10^{-7}$ M ; 2. $C_{Sb^{3+}}/C_{cations} = 1/10$; 3. $C_{Sb^{3+}}/C_{cations} = 1/100$; $E_d = -400$mV ; $\tau = 10$ min.

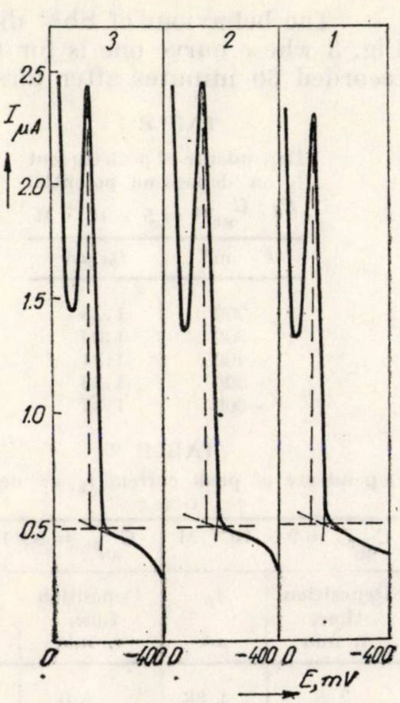

Fig. 3. — Stripping voltammograms of antimony in the presence of arsenic : 1. $C_{Sb^{3+}} = 5 \times 10^{-7}$ M ; 2. $C_{Sb^{3+}}/C_{As^{3+}} = 1/1$; 3. $C_{Sb^{3+}}/C_{As^{3+}} = 1/10$; $E_d = -400$ mV ; $\tau = 10$ min.

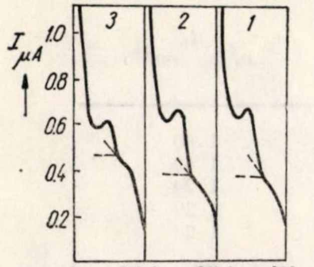

Fig. 4. — Stripping voltammograms of antimony in the presence of copper : 1. $C_{Sb^{3+}} = 1 \times 10^{-7}$M ; 2. $C_{Sb^{3+}}/C_{Cu^{2+}} = 1/10$; 3. $C_{Sb^{3+}}/C_{Cu^{2+}} = 1/100$; $E_d = -250$ mV ; $\tau = 10$ min.

The detection limit of the elaborated method is 5×10^{-9} M antimony.

The variation coefficient for four determinations in the concentration range 10^{-6}—10^{-8} M Sb (III) was 4%.

The influence of Cd^{2+}, Pb^{2+}, Zn^{2+}, Cu^{2+}, Ni^{2+}, Fe^{3+} and As^{3+} was also studied.

From the voltammograms shown in Fig. 4 one can notice that Cd^{2+}, Pb^{2+}, Zn^{2+}, Ni^{2+} and Fe^{3+} did not interfere. It is possible to explain this behaviour by taking into consideration the deposition potentials of these cations and the influence of the supporting electrolyte.

The influence of the cations with deposition potentials closer to that of antimony is presented in Fig. 5 and 6. In Fig. 5 the voltammogram of antimony and arsenic is given.

As it can be seen, arsenic interferes at the ratio 1 :100 of Sb : As. By changing the electrodeposition potential from −400 to −250 mV the interference was avoided even for a ratio of 1 :100 of Sb : As, the current being modified only by 5%.

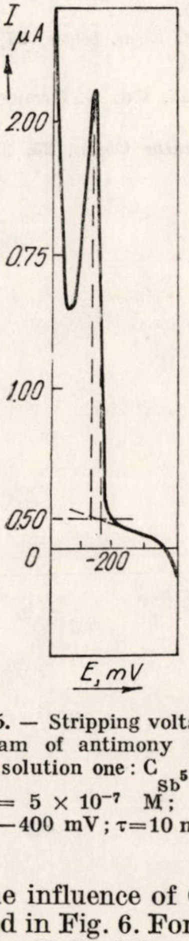

Fig. 5. — Stripping voltammogram of antimony (V) from solution one : $C_{Sb^{5+}} = 5 \times 10^{-7}$ M; $E_d = -400$ mV ; $\tau = 10$ min.

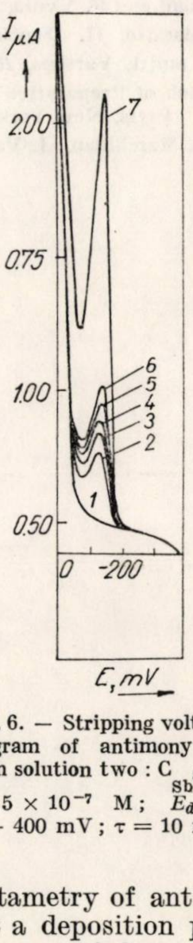

Fig. 6. — Stripping voltammogram of antimony (V) from solution two : $C_{Sb^{5+}} = 5 \times 10^{-7}$ M ; $E_d = -400$ mV ; $\tau = 10$ min.

The influence of Cu on anodic stripping voltametry of antimony is presented in Fig. 6. For the ratio 1 :10 of Sb :Cu at a deposition potential of −250 mV Cu did not interfere. For a higher amount of Cu an interference appears, the peak current for antimony being lower by 50%.

The method elaborated can be used for anodic stripping trace analysis of antimony in different organic and inorganic reagents of high purity.

REFERENCES

[1] R. Neeb and F. Wahdat, *Z. analyt. Chem.*, **260**, 239 (1972).

[2] T. M. Florence, *J. Electroanalyt. Chem.*, **35**, 237 (1972).

[3] T. R. Gilbert and N. D. Hume, *Analyt. Chim. Acta*, **65**, 451 (1973).

[4] D. C. Johnson, *Analyt. Chem.*, **45**, 1755 (1973).

[5] G. Van Dyck and F. Verbeek, *Analyt. Chim. Acta*, **66**, 251 (1973).

[6] Kh. Z. Brainina and A. B. Cheryshova, *Talanta*, **21**, 287 (1974).

[7] Ya. E. Neiman and M. F. Sumenkov, *Zhur. analit. Khim.*, **30**, 1625 (1975).

[8] Ya. E. Neiman and Kh. Z. Brainina, *Zhur. analit. Khim.*, **30**, 1073 (1975).

[9] T. V. Naghi and F. Vydra, *Analyt. Chim. Acta*, **80**, 267 (1975).

[10] H. Verplaestse, H. Donche and E. Temmerman, *Bull. Soc. chim. belges*, **87**, 85 (1978).

[11] N. Totir and I. Vartires, *Rev. Roumaine Chim.*, **20**, 23 (1975).

[12] "Handbook of Preparative Inorganic Chemistry", vol. I, Ed. II, Ed. G. Brauer, Academic Press, New York, 1963, p. 118.

[13] Part I: S. Marchidan, I. Vartires and N. D. Totir, *Rev. Roumaine Chim.*, **25**, 33 (1980).

Revue Roumaine de Chimie, **27**, *1*, 87–93 (1982)

THERMAL AND STRUCTURAL INVESTIGATION OF SOME OXALATO-NIOBIC COMPLEXES. II.[1]

BARIUM TRIS(OXALATO)NIOBATE

LIANA MARTA*, MARIA ZAHARESCU** and C. GH. MACAROVICI***

* Politechnic Institute, str. Gh. Bariţiu 25, Cluj-Napoca, Romania
** Center of Physical Chemistry, Spl. Independenţei 202, Bucharest, Romania
*** Chemistry Department, University of Cluj-Napoca, str. Arany J. 11, Cluj-Napoca, Romania

Received February 26, 1980

The synthesis and thermal stability of barium tris(oxalato)niobate were investigated. The compound was characterised by elemental analysis, infrared spectroscopy and X-ray diffraction. The mechanism of thermal decomposition was established by differential thermal analysis and the conditions of barium metaniobate formation were established.

INTRODUCTION

The literature on niobium complexes, especially if compared with other transition metals, seems relatively scarce. In recent years, considerable attention was paid to organometallic and related niobium compounds.[2,3]

The carboxylic acid complexes,[4–11] especially oxalato-complexes are particularly important in the chemistry of niobium. Until now, the alkali-metal oxalato-niobates with different niobium-oxalate ratios were investigated, in solution as well as in solid state.[12–15]

The tris(oxalato)niobic acid,[16] ammonium tris(oxalato)niobate[17] and caesium bis(oxalato)niobate[18] structure have been established by X-ray diffraction.

The alkali-metal and magnesium bis(oxalato)niobates have been obtained,[19,20] as well as ethylenediammonium[21] and tetraphenyl-phosphonium and arsonium tris(oxalato)niobates.[22]

Some attempts to obtain the alkaline-earth oxalato-niobates have been made. Russ[23] precipitated for the first time tris(oxalato) niobic anion with several cations : Ca^{2+}, Sr^{2+}, Ba^{2+}, Pb^{2+}, Cu^{2+} Fe^{2+}, Ni^{2+}, etc., but the composition of these salts was not determined. Brnicevic and Djordjevic,[22] Limar et al.[24] confirmed the precipitation of these salts, but made no attempt to determine their composition and structure.

In a previous paper[1] we have reported the synthesis, structure and thermal decomposition mechanism of the potassium tris(oxalato)niobate.

In this paper, the synthesis and characterisation of barium tris(oxalato)niobate is reported. The thermal decomposition mechanism of this compound was investigated with the purpose of establishing the formation conditions of the perovskite type barium metaniobate, which exhibits some interesting ferroelectrical and electrooptical properties.

RESULTS AND DISCUSSION

The synthesis and the isolation of the oxalato-niobic complexes in a pure form are somewhat difficult, as we have mentioned in a previous work,[1] because of the tendency of niobium to hydrolyse and to precipitate niobic acid.

An attempt has been made to obtain barium oxalato-niobate from water soluble potassium salt, by precipitating with barium cations, as mentioned in the literature.[22–24] It has been impossible to isolate the complex in pure form by this way, because it was impurified by barium oxalate. The tendency of niobic acid to separate has also been observed.

The direct synthesis of barium tris(oxalato)niobate has been successfully attempted by treating the barium salts with tris(oxalato)niobic acid.

The compound occurs as a fine, white powder, insoluble in water and ethanol, and soluble in oxalic acid and hydrochloric acid (1: 1).

The composition established by chemical analysis corresponds to $Ba_3[NbO(C_2O_4)_3]_2 . 8H_2O$.

Infrared spectra

The infrared spectrum of barium tris(oxalato)niobate is listed in Table 1, where the absorption bands and their assignment are given. The spectrum is compared with that of barium oxalate.

TABLE 1

IR spectra

BaC_2O_4 (cm^{-1})	$Ba_3[NbO(C_2O_4)_3]_2 . 8H_2O$ (cm^{-1})	Assignment
490	485	(O−C=O), (Nb−O_{ox})
	525	(C=C), (O−C=O)
	550	(Nb−O_{ox}), (C−C)
660		
725	735	
760		
	810	(O−C=O)
890	920	(Nb=O), (C−C), (C−O)
	960	
1030	1260	(C−O), (O−C=O)
	1280	
1315		
	1425	(C−O), (C=C)
1640	1650	(C=O), (H_2O)
	1670	
	1700	(O=C)
	1720	
	3460	(H_2O)

The barium tris(oxalato)niobate spectrum is different from that of barium oxalate. In the IR spectrum of the complex no bands of the free oxalate ions ($C_2O_4^{2-}$ or $HC_2O_4^{-}$) are observed and the bands due to oxalato groups coordinated to niobium atom are present, at a wave number of 550 cm^{-1}, near to those of the analogous potassium salt.

In the spectrum of the barium salt the bands are generally shifted towards a higher wave number compared with the potassium salt. This is probably due to the influence of the heavier barium atom. The bands at 1260 — 1280 cm^{-1} represent probably not only a change of the force constant, therefore not only the influence of the heavier atom, but a change in the local molecular symmetry.

The characteristic $\nu(Nb=O)$ band occurs as a doublet at 920 — 960 cm^{-1}, which indicates a lower molecular symmetry of barium complex than in alkali-metal salts.[12,25] The IR spectrum also contains bands due to the ν(Nb-oxalate) groups at 485 and 550 cm^{-1}. It has been shown that the Nb-oxalate bond is partially covalent,[12] which results in a shortening of the $C = O$ bond in the complex compared to the free oxalate ion (the wave number increases from 1640 cm^{-1} in the free oxalate ion, to 1670 cm^{-1} in barium tris(oxalato) niobate). The $C—O$ bond becomes longer in the complex and the wave number decreases from 1315 cm^{-1} and 1320 cm^{-1} in the free oxalate group, to 1260 cm^{-1} and 1280 cm^{-1} in the barium tris(oxalato)niobate complex.

X-ray diffraction

The characteristic X-ray diffraction lines of barium tris(oxalato) niobate are shown in Table 2.

TABLE 2

X-ray diffraction lines

$Ba_3[NbO(C_2O_4)_3]_2 \cdot 8H_2O$			
dÅ	I/I_0	dÅ	I/I_0
6.7422	10	3.0353	8
6.5148	100	2.9644	12
5.8315	25	2.9079	20
5.7339	7	2.8323	16
5.0576	36	2.8012	19
4.8807	14	2.7280	19
4.6330	27	2.6496	13
4.5253	31	2.6136	7
4.4622	94	2.5473	8
4.3495	10	2.4402	21
4.1717	7	2.3852	21
3.8969	15	2.3587	7
3.8634	20	2.3029	14
3.6507	18	2.2285	16
3.5364	18	2.1710	16
3.4501	9	2.0650	18
3.3091	20	2.0116	11
3.1184	20	1.9457	9

The presence of a spectrum with a large number of lines (like in the case of potassium tris(oxalato)niobate[1]) indicates a low symmetry structure of the complex, which can be monoclinic or triclinic.

Thermogravimetric (TG) and differential thermal analysis (DTA)

The TG and DTA curves of barium tris(oxalato)niobate are given in Fig. 1. A scheme for the thermal decomposition of barium tris(oxalato) niobate is suggested in Table 3.

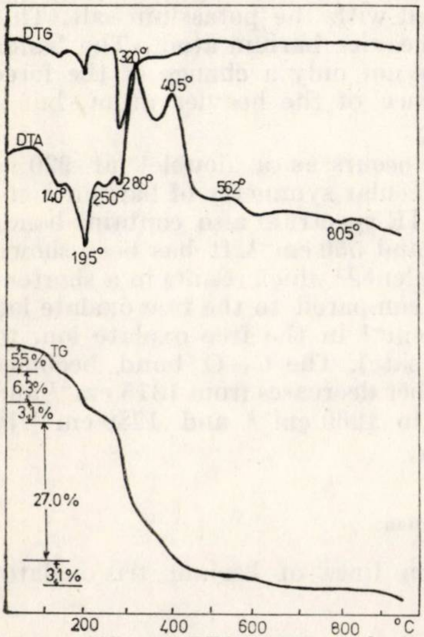

Fig. 1. — TG and DTA curves of barium tris(oxalato)niobate.

The barium complex containing eight molecules of crystallisation water releases them in two steps, as indicated by the two weight losses at 150°C and 205°C, associated with two endothermic effects at 140°C and 195°C, respectively (DTA curve). This suggests two different ways of attachment of the water molecules.

Above 200°C, the complex begins to decompose, with elimination of carbon oxides. As mentioned in our previous paper,[1] the thermal decomposition of simple or complex oxalates occurs with formation of CO and CO_2, which remain in intermediate phase, adsorbed on the solid products. The desorption occurs stepwise. This behaviour is known in the literature.[25]

TABLE 3

Thermal analysis data for $Ba_3[NbO(C_2O_4)_3]_2 \cdot 8H_2O$

Weight loss			Thermal effects		Compounds
Temperature °C	% loss	Lost species	*Endo*	*Exo*	
					$Ba_3[NbO(C_2O_4)_3]_2 \cdot 8H_2O$
20–150°	5.5	$3.5\ H_2O$	140°		$Ba_3[NbO(C_2O_4)_3]_2 \cdot 4.5H_2O$
150–205°	6.3	$4.5\ H_2O$	195°		$Ba_3[NbO(C_2O_4)_3]_2$
205–265°	3.1	$CO, (1-x)CO_2$	250°		$2\ BaC_2O_4 + Ba[NbO_2C_2O_4]_2 \cdot xCO_2$
265–330°	16.9	$3CO,\ 2CO_2$	280°		
				320°	
330–455°	10.2	$2CO,\ CO_2$		405°	
455–950°	3.1	xCO_2		562°	$2\ BaCO_3$(rhombic) + $BaNb_2O_2 \cdot xCO_2$ ads.
			610°		
				805°	$2\ BaCO_3$(hexagonal) + $BaNb_2O_6$

The decomposition of the tris(oxalato)niobate complex occurs with the mono(oxalato)niobate complex and with barium oxalate formation, revealed by endothermal effects at 250°C and 280°C. The decomposition occurs stepwise, slowly in the beginning, then fast between

265 and 455°C, when a pronounced weight loss is observed, totalling 27.0 % of the initial weight. This corresponds to a loss of five CO molecules and three CO_2 molecules in two steps; first five between 265 and 330°C, then three molecules between 330 and 445°C. At 320°C begins the decomposition of the 1: 1 complex, associated with a marked exothermal effect.

Between 390 and 470°C the decomposition of barium oxalate occurs with formation of barium carbonate,[26,27] associated with an exothermal effect at 405°C.

At 550°C begins the formation of barium metaniobate,[26] $BaNb_2O_6$, revealed by an exothermal effect at 562°C. Between 455 and 660°C the adsorbed carbon dioxide is eliminated.

The last endothermal effect, at 805°C without weight loss, is due to a polymorphous transformation of barium carbonate, from the rhombic to the hexagonal form.

Finally, the product of the thermal decomposition of barium tris (oxalato)niobate is a mixture of barium carbonate and barium metaniobate, in 2 : 1 molar ratio. From the mixture, the barium metaniobate can be readily separated, by dissolving barium carbonate in hydrochloric acid (1 : 1), in which the metaniobate is scarcely soluble.

In the infrared spectrum of the final product of thermal decomposition the characteristic bands of barium carbonate[28] are readily observed at 700, 865, 1435 cm^{-1}, along with a weak band at 670 cm^{-1} due to the presence of metaniobate.[29] After washing with hydrochloric acid, in the final product the characteristic carbonate bands disappear completely from the infrared spectrum, and only the bands due to metaniobate are observed.

TABLE 4

X-ray diffraction data for the final product of thermal decomposition of $Ba_3[NbO(C_2O_4)_3]_2 \cdot 8H_2O$

Complex heated at 900°C			Complex heated at 900°C and washed with HCl 1 : 1		
dÅ	I/I_0	Assignment	dÅ	I/I_0	Assignment
3.2757	100	$BaCO_3$			
3.0805	50	$BaNb_2O_6$	3.0805	100	$BaNb_2O_6$
2.9473	98	$BaCO_3$	3.0639	29	$BaNb_2O_6$
2.8969	56	$BaNb_2O_6$	2.8950	65	$BaNb_2O_6$
2.5615	10	$BaCO_3$			
2.3659	6	$BaCO_3$			
2.1912	53	$BaCO_3$			
2.1281	13	$BaCO_3$			
2.1138	30	$BaNO_2O_6$	2.1157	41	$BaNb_2O_6$
1.9641	10	$BaCO_3$			
1.7602	23	$BaCO_3$			
1.7263	13	$BaNb_2O_6$	1.7263	15	$BaNb_2O_6$
1.7060	27	$BaNb_2O_6$	1.7060	26	$BaNb_2O_6$
1.6332	7	$BaCO_3$			
1.4775	10	$BaCO_3$			

The results are confirmed by X-ray diffraction data in Table 4, where the X-ray diffraction patterns for the final product of thermal decomposition as well as for the product washed with HCl 1 : 1 are presented.

EXPERIMENTAL PART

Synthesis of barium tris(oxalato)niobate

From Nb_2O_5. Niobium pentaoxide (1 g) is mixed with cca 1.5 g potassium carbonate in a platinum crucible and the mixture is heated in a furnace at 1000°C for 6 hours. After cooling, the product is dissolved in water and filtered if the solution is not perfectly clear. The solution will be treated as described below.

From metallic niobium. A powder of metallic niobium (0.5 g) and 2 g KOH are mixed in a nickel crucible and heated in a gas-burner flame for cca 1 hr, until a clear melt is formed. After cooling the product is dissolved in hot water.

The aqueous solution of potassium niobate obtained by one of the procedures mentioned above, is treated with conc. HCl until $pH = 2$ is reached, then concentrated ammonia is added, until $pH = 6$. Under these conditions niobic acid precipitates quantitatively, as an amorphous white precipitate. The precipitate is filtered under suction, washed with hot water and dried.

From the hydrated niobic acid thus obtained, after drying, an amount of cca 1 g is dissolved in a hot solution containing 2.46 g oxalic acid in 100 ml water. As the water content of niobic acid can vary, the amount of acid to be weighed should always be such as to lead to the 1: 3 mole ratio with respect to 2.46 g of oxalic acid. If the dissolution is not complete at the boiling temperature, a few drops of conc. HCl are added. The solution thus obtained is treated with 2.55 g $Ba(NO_3)_2$ dissolved in the minimal amount of water and the mixture is heated for another 30 min. A white crystalline precipitate of barium tris (oxalato)niobate is formed. The product is filtered, washed with hot water, then with alcohol and dried at 105°C.

Analysis

The niobium content was determined gravimetrically by one of the following procedures:

a) Precipitation as niobic acid in the solution left after the permanganometric determination of oxalate, followed by conversion to Nb_2O_5.

b) Precipitation with 8-hydroxyquinoline and decomposition to Nb_2O_5.

c) The complex is heated with conc. H_2SO_4 to white fumes, until a dry residue is left. The niobium is determined by difference.

Barium was determined gravimetrically, by precipiation as sulfate, after the dissolution of the complex in 1 : 1 hydrochloric acid. Alternatively, barium was determined by flame photometry.

The oxalate was determined by permanganometric titration. The carbon content was also determined by microcombustion.

The results of the chemical analysis are as follows :

	Nb	Ba	C_2O_4	C	H_2O
Found (%)	14.70	32.13	42.17	11.40	11.80
Calculated (%)	14.20	32.40	41.60	11.06	11.06

The data are in agreement with the composition $Ba_3[NbO(C_2O_4)_3]_2 \cdot 8H_2O$.

Equipment

The infrared spectra were recorded with an UR-20 Carl Zeiss Jena (DDR) spectrophotometer, in the range 4000—4000 cm^{-1}, in KBr pellets.

The TG, DTG and DTA curves were recorded with a Paulik-Paulik Erdey (MOM) Budapest Derivatograph, in the presence of air, with a heating rate of 5°C/min.

X-ray diffraction analysis was carried out on a TUR-M 62 diffractometer with a proportional counter, using Cu_{K_α} radiation.

REFERENCES

[1] Part I : L. Marta, M. Zaharescu and C. Gh. Macarovici, *Rev. Roumaine Chim.*, **24**, 1115 (1979).
[2] R. C. Mehrotra, A. K. Rai, P. N. Kapoor and R. Bohra, *Inorg. Chim. Acta*, **16**, 237 (1976).
[3] A. A. Pasynskii, *Metody Elementorg. Khim.*, **1**, 434, 453 (1974).
[4] F. Fairbrother and J. B. Taylor, *J. Chem. Soc.*, **1956**, 4946.
[5] B. V. Ptitsin and L. N. Sheronov, *Izvest. Sibirsk. Otdel. Akad. Nauk S.S.S.R., Ser. Khim. Nauk*, **1965**, 68.
[6] A. V. Lapitskii, Pin-Hsi-Sao and L. G. Vlasov, *Radiokhimiya*, **7**, 241 (1965).
[7] A. N. Nevzorov and N. S. Onoprienko, *Zhur. neorg. Khim.*, **13**, 2131 (1968).
[8] V. V. Grigorieva and I. V. Golubeva, *Zhur. neorg. Khim.*, **20**, 941 1254 (1975).
[9] V. V. Grigorieva and I. V. Golubeva, *Ukrain. Khim. Zhur.*, **42**, 1027 (1976).
[10] J. E. Land and C. V. Osborne, *J. Less-Common Metals*, **14**, 349 (1968).
[11] A. T. Pilipenko, L. I. Savranskii and A. J. Samchuk, *Zhur. neorg. Khim.*, **14**, 739 (1969).
[12] M. Müller and J. Dehand, *Bull. Soc. chim. France*, **1971**, 2837.
[13] L. G. Vlasov, A. V. Lapitskii and B. V. Strijkov, *Vestn. Moskovsk. Univ.*, **1**, 57 (1961).
[14] L. G. Vlasov, A. V. Lapitskii, M. A. Salimov and B. V. Strijkov, *Zhur. neorg. Khim.*, **7**, 2534 (1962).
[15] B. V. Ptitsin and A. N. Sheronov, *Izvest.Sibirsk. Otdel. Akad. Nauk S.S.S.R., Ser. Khim. Nauk*, **1961**, 44.
[16] M. Galesic, B. Matkovic, M. Herceg and M. Sliukic, *J. Less-Common Metals*, **25**, 234 (1974).
[17] G. Mathern, R. Weiss and R. Rohmer, *Chem. Commun.*, **1969**, 70.
[18] B. Kojik-Prodic and R. Liminga, *Acta Crystallogr.*, **B 29**, 864 (1973).
[19] N. Brnicevic and C. Djordjevic, *J. Less-Common Metals*, **45**, 55 (1976).
[20] N. Brnicevic and Z. Despotovic, *Therm. Anal., Proc. Int. Conf. 3rd*, **2**, 705 (1971).
[21] J. F. Dietsch, M. Müller and J. Dehand, *Compt. rend.*, **272**, 541 (1971).
[22] Brnicevic and C. Djordjevic, *Inorg. Chem.*, **7**, 1936 (1968).
[23] F. Russ, *Z. anorg. Chem.*, **31**, 42 (1902).
[24] T. F. Limar, U. G. Slatinskaya and O. P. Sikora, *Zhur. neorg. Khim.*, **9**, 2381 (1964).
[25] J. T. Yates, *J. Phys. Chem.*, **65**, 617, 746, 901 (1961).
[26] C. Duval, "Inorganic Thermogravimetric Analysis", Elsevier, Amsterdam, 1963.
[27] E. G. Derouane, Z. Gabelice, R. Hubin and M. J. Hubin-Franskin, *Thermochim. Acta*, **11**, 287 (1975).
[28] K. Nakamoto, "Infrared Spectra of Inorganic and Coordination Compounds", Wiley, New York, 1962.
[29] C. Rocchiciolli-Deltcheff and R. Frank, *Ann. Chim. (France)*, **9**, 43 (1974).

Revue Roumaine e Chimie, **7**, *1*, 95–101 (1982)

MODEL SYSTEM TO OBTAIN PHOTOHYDROGEN

TATIANA ONCESCU, M. CONTINEANU and S. G. IONESCU
Department of Physical Chemistry and Electrochemical Technology, The Polytechnical Institute of Bucharest, Bd. Republicii 13, Romania

Received June 18, 1981

This paper describes a photochemical system for hydrogen generation by water reduction under visible light from aqueous solutions containing : $Ru(bipy)_3^{+2}$ as photosensitizer (Phs), the Co(II)-bipyridine complex as relay species which mediates water reduction process, an amine TEOA as electron donor, and sometimes a redox catalyst facilitating H_2 formation. The influence of each component concentration on the H_2 generation, in the presence and in the absence of atmospheric O_2 was investigated. On the ground of the results obtained a tentative reaction mechanism was proposed.

I. INTRODUCTION

The processes for the photochemical generation of H_2 and O_2 from water in artificial systems represent a model for photosynthesis and consequently a means of solar energy storage and fuel production. Some results concerning hydrogen production have been presented in the recent literature.[1–4]

Ru(II) complexes, usually $Ru(bipy)_3^{+2}$ have been generally used as light absorbing species, namely as photosensitizer of electron transfer processes. [4–7] The production of H_2 by direct electron transfer to proton has never been observed, so that the photochemically activated transformation may not involve water directly but takes place between species relating to the reactions which involve water.

The present paper describes a system generating H_2 via catalytic cycles from aqueous solutions of metal complexes under continuous irradiation with visible light ; it involves the photochemical production of a reducing species which thermally reduces water as was already shown[6] for the system : $Ru(bipy)_3^{+2} - Rh(bipy)_3^{+3}$. By taking into account the suggestion of these authors we changed the relay species Rh(III) complex with the coresponding Co(II) one and used H_2PtCl_6 or $(NH_4)_2PtCl_6$ as catalyst.

II. EXPERIMENTAL

As irradiation source we used a 400 W mercury lamp which emitted visible light. The samples disposed around the Hg-lamp were irradiated at 55° in glass phials of 2–7 ml. For the degassed samples the phials provided for had two necks, one for Argon bubbling and the other one for air evacuation, in both cases through syringe needles.

$Ru(bipy)_3Cl_2$ was prepared according to literature[8] and the Co(II) bipyridine complex by dissolution of the desired amount of cobalt chloride and bipyridine in hot water.

The electronic absorption spectra of the complexes were recorded at a Pye Unicam SP 8000 spectrophotometer and the emission spectra were registered with a Pye Unicam SP 90 atomic absorption apparatus adapted for emission measurements.

The amounts of H_2 generated during irradiation of the sample were determined by gas-chromatography (Carlo Erba).

The pH values of the solutions were measured at a Radiometer pH-meter.

III. RESULTS AND DISCUSSION

In our experiments, with or without catalyst, the system investigated $Ru(bipy)_3^{+2}$—$Co(bipy)_3^{+2}$—TEOA generated hydrogen. By using heavy water, the experiments with other similar systems[3] demonstrated that hydrogen comes from water. $Ru(bipy)_3^{+2}$ is the absorbing species — the photosensitizer (Phs) with a strong absorption band in visibile[9,10] ($\lambda=452$ nm) leading to a dπ* LMCT excitated state of about 2.1 eV higher energy[11] which may luminesce or produce electron transfer by reductive or oxidative quenching[6]. The phosphorescence spectrum of $^*Ru(bipy)_3^{+2}$ presents an emission maximum at $\lambda = 640$ nm. In order to specify what kind of quenching mechanism takes place in our system we carried out quenching experiments by adding Co(II) complex — the relay species (R) — to the solutions containing the Ru $(bipy)_3^{+2}$ ion. One observed the diminution of its emission intensity simultaneously with the increase of the Co(II) bipyridine complex absorption resulting from the increase of its concentration. In this case the most plausible mechanism *is the oxidative quenching*, in good agreement with the redox potential of $Ru(bipy)_3^{+3}/{}^*Ru(bipy)_3^{+2}$ and $Co(II)^{+2}/Co(I)^{+1}$, that is :

$$\begin{tikzcd} Ru(bipy)_3^{+2} \arrow[r, "h\nu", "\text{visible}"'] & {}^*Ru(II)^{+2} \arrow[r, "k_e"] \arrow[d, "k_q\ +Co(II)^{+2}"] & Ru(II)^{+2} + h\nu' \\ & Ru(III)^{+3} + Co(I)^{+1} & \end{tikzcd} \qquad (1)$$

We also tested the reductive quenching because we deliberately added TEOA to the system as an electron donor (D) to $Ru(III)^{+3}$ in order to recycle it, according to the reaction :

$$Ru(bipy)_3^{+3} + TEOA \rightarrow Ru(bipy)_3^{+2} + TEOA^{\cdot -} \qquad (2)$$

Therefore, to make sure that TEOA is not an electron donor also for the excited $Ru(II)^{+2}$ complex we performed quenching experiments separately with the system $Ru(II)^{+2}$ — TEOA ; the luminescence of $^*Ru(bipy)_3^{+2}$ is unaffected by the TEOA concentration in aqueous solutions, so that we opted for the oxidative quenching and investigated it.

The spectral data obtained are summarized in table 1. They permitted the calculation of the quenching rate constant k_q, that is of the electron transfer process, by means of the Stern-Volmer equation:

$$\frac{I_0}{I} = 1 + k_q \tau_{\mathrm{Phs}}[\mathrm{R}] \tag{3}$$

TABLE 1

Phosphorescence quenching of Ru(bipy)$_3^{+2}$ by Co(II) complex
[Phs] = 5.1×10^{-5} M ; $I_0 = 0.89$; $A_{\mathrm{Phs}} = 0.542$; $\lambda_{\mathrm{ex}} = 436$ nm ;

Co(II) × 10^3 M	I (arb. units)	$(I_0/I)_{\mathrm{obs}}$	A_R^{436}	$(I_0/I)_{\mathrm{cor}}$
1	0.780	1.185	0.080	1.102
2	0.645	1.434	0.220	1.181
3	0.560	1.964	0.356	1.450
4	0.430	2.151	0.524	1.404
5	0.360	2.625	0.586	1.620
6	0.220	3.136	0.804	1.680
7	0.190	3.789	0.896	1.920

I_0 and I being the emission intensities of the photosensitizer Ru(bipy)$_3^{+2}$ in the absence and in the presence of the relay species, the Co(II) bipyridine complex respectively. The values of the ratio I_0/I were corrected by taking into account the relay R absorption for the excitation wavelength $\lambda = 436$ nm:

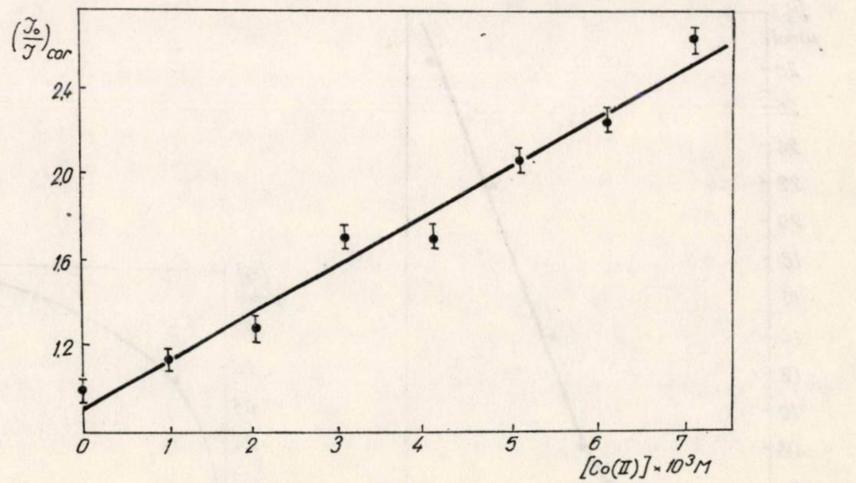

Fig. 1. — Stern-Volmer plot for the phosphorescence quenching of *Ru(bipy)$_3^{+2}$ by Co(II) bipyridine complex at the natural pH of the solution.

$$\left(\frac{I_0}{I}\right)_{\mathrm{cor}} = \left(\frac{I_0}{I}\right)_{\mathrm{obs}} \frac{1 - 10^{-(A_{\mathrm{Phs}} + A_R)}}{1 - 10^{-A_{\mathrm{Phs}}}} \frac{A_{\mathrm{Phs}}}{A_{\mathrm{Phs}} + A_R} \tag{1}$$

Fig. 1 presents the plot of equation (3).

By using a value of 6.6×10^{-7} s for the radiative life τ_{Phs} reported in the literature,[9] one obtained from the slope the quenching rate constant : $k_q = (3.14 \pm 0.14)\ 10^8\ \mathrm{M^{-1}\ s^{-1}}$, comparable to $(3.5 \pm 0.5)\ 10^8\ \mathrm{M^{-1} s^{-1}}$ for the quenching emission of $^*\mathrm{Ru(bipy)_3^{+2}}$ by $\mathrm{Rh(bipy)_3^{+3}}$.

From the maximum values of the emission intensities one calculated also the critical distance R_c for which the electron transfer from the excited Phs molecule to the relay one takes place with equal probability with the phosphorescence emission, and found 46.5 Å; this relatively high value shows the efficiency of the electron transfer process (k_q) as compared with the emission one (k_e).

As a result of the electron transfer process, Co(I) species appear in the irradiated system (see eq.1), probably as $\mathrm{Co(bipy)_2^{+1}}$ and $\mathrm{Co(bipy)_3^{+1}}$, both known in the literature.[12,13] Their presence was qualitatively revealed by the appearance of the characteristic absorption bands at 540 nm and 620 nm respectively, and of the free bipyridine band at 280 nm, after irradiation of the deaerated samples. The Co(I) complexes are relatively air sensitive, which correlates well with other experiments in which the consumption of O_2 during irradiation was evident.

We also investigated the role of each component concentration on the H_2 generation from the system Ru(II)—Co(II)-TEOA-Pt catalyst. Initially one explored the effect of the photosensitizer concentration main-

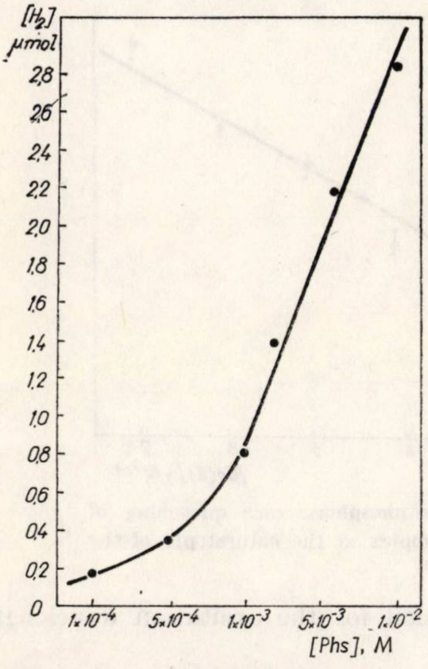

Fig. 2. — Dependence of the H_2 generation on the photosensitizer Ru $\mathrm{(bipy)_3^{+2}}$ concentration : $[\mathrm{R}]=2\times10^{-3}\mathrm{M}$; $[\mathrm{Cat}] = 2.8 \times 10^{-4}$ M ; [TEOA] = = 0.67 M ; $t_{\mathrm{irr}} = 3$ hours.

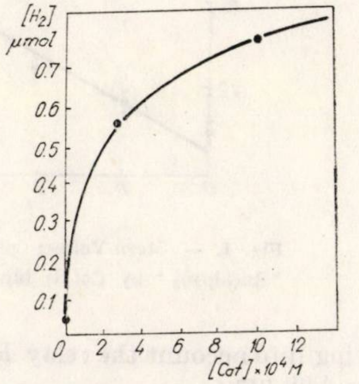

Fig. 3. — Dependence of the H_2 amount evolved on the catalyst concentration : $[\mathrm{Phs}] = 6\times10^{-3}$ M ; [R]= $= 2 \times 10^{-3}$ M; [TEOA] = 0.67 M ; $t_{\mathrm{irr}} = 220$ minutes.

taining constant the concentration of the other component. Fig. 2 gives the results obtained in the concentration range used.

When adding a redox catalyst, the increase of its concentration favours H_2 formation as figure 3 shows.

When testing the influence of the irradiation time the behaviour pointed out in figure 4 was obtained. It was noticed that the induction period is shorter in the presence of the catalyst. At the same time it is evident that a very prolonged irradiation is not necessary. We also investigated if the amount of the hydrogen generated is the same on continuous or interrupted irradiation, and obtained identical behaviour as table 2 shows.

TABLE 2

Comparative results of the H_2 generation, between a continuous and an interrupted irradiation.
$[Cat] = 2\times10^{-3}$ M; $[Phs] = 2\times10^{-3}$ M; $[R] = 2\times10^{-3}$ M; $[TEOA] = 0.67$ M

t, hours interrupted irradiation	H_2, μ mole	*t*, hours continuous irradiation	H_2, μ mole
3	1.4	10	2.46
3	0.91		
4	0.18		
10	2.49		

The influence of the ligand excess was also tested. The system needs at least three (bipy) groups per Co(II) cation and the ligand excess (up to its solubility limit) accelerates H_2 generation so that one can conclude that it has a catalytic effect.

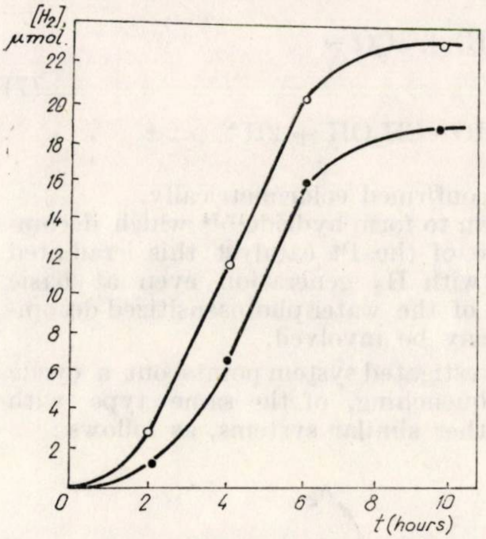

Fig. 4. — Dependence of the hydrogen generation on the irradiation time: $[R] = 5\times10^{-4}$ M; $[Fs] = 10^{-3}$ M; $[TEOA] = 8.4 \times 10^{-2}$ M; ○ $[Cat] = 3.5 \times 10^{-4}$ M;

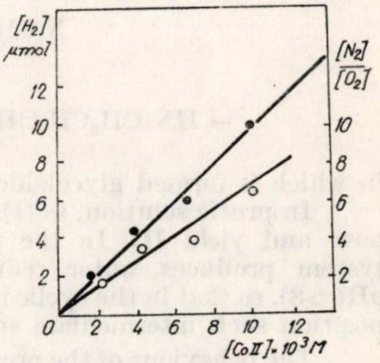

Fig. 5. — ● Dependence of the hydrogen amount on th $Co(bipy)_3^{+2}$ concentration: $[TEOA] = 8.4 \times 10^{-2}$ M; $[Cat] = 3\times10^{-4}$ M; $t_{irr} = 140$ minutes. ○ Dependence of $[N_2]/[O_2]$ on Co(II) concentration.

In other experiments the increase of the relay concentration at constant [Phs], [TEOA] and [PtCat] shows also an increase of the H_2 amount evolved from this system. By measuring gas chromatographic

N_2, O_2 and H_2, one noticed an increase of the ratio $[N_2]/[O_2]$, which means that oxygen is consumed in secondary reactions. As mentioned before, this result is in good agreement with the air sensitivity of the solutions irradiated which contain Co(I) species resulting from the electron transfer process from the $^*Ru(II)^{+2}$ photosensitizer to the $Co(II)^{+2}$ complex. To verify this assumption we performed three parallel experiments: in the presence of atmospheric O_2, by bubbling O_2 in the sample and by bubbling Argon to deaerate the solution, under the following experimental conditions: $[CoCl_2] = 3 \times 10^{-2} M$; $[bipy] = 9 \times 10^{-2}$ M; $[Ru(bipy)_3Cl_2] = 3 \times 10^{-3}$ M; $[TEOA] = 0.67$ M and $[Ptcat] = 7 \times 10^{-4}$ M; one obtained the results:

$$\frac{[H_2]_{Ar}}{[H_2]_{atm.\,O_2}} = 3.5 \text{ and } \frac{[H_2]_{Ar}}{[H_2]_{O_2}} = 7 \qquad (5)$$

which establishes the following series in terms of the H_2 generated amount:

$$[H_2]_{Ar} > [H_2]_{atm.\,O_2} > [H_2]_{O_2} \qquad (6)$$

An other observable effect is the slight decrease of the pH after irradiation. This result can be due to the overall oxidative decomposition of TEOA according to the reaction:

$$\begin{gathered} N(CH_2CH_2OH) + H_2O \rightarrow \\ \rightarrow HN(CH_2CH_2OH) + CHO-CH_2OH + 2H^+ + 2e \end{gathered} \qquad (7)$$

in which is formed glycolaldehyde, confirmed colorimetrically.

In protic solution, Co(I) is known to form hydride[12,14] which decompose and yield H_2. In the presence of the Pt catalyst this irradiated system produces water reduction with H_2 generation even at basic pH(>8), so that in the cyclic reaction of the water photosensitized decomposition such intermediate species may be involved.

The behaviour of the present investigated system points out a cyclic mechanism with oxidative Ru(II) quenching, of the same type with those proposed in literature[3-6] for other similar systems, as follows:

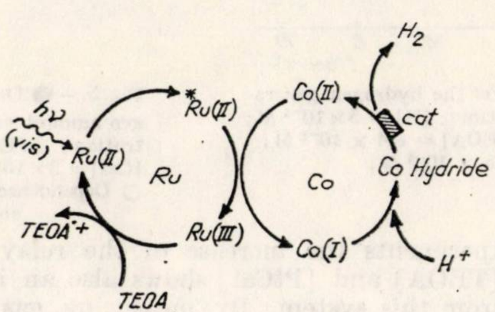

(8)

One calculated the number of catalytic cycles described by the parameter TO (turnover number) which evaluates the efficiency of the system for a given irradiation experiment. For one of the usual conditions used (not the best one) during five hour- irradiation, we calculated the following in terms of the photosensitizer :

$$(\mathrm{TO})_{\mathrm{Phs}} = 2\,\frac{n\,\mathrm{H_2\,mol}}{n_0\,\mathrm{Phs\,mol}} = 40 \tag{9}$$

This value is lower than in the case of the system Ru(II)—Rh(III)—TEOA[4,6] but improvements in the reaction condition are still possible.

REFERENCES

[1] S. Clarsson and L. Engström Eds., "Solar Energy, Photochemical Conversion and Storage", NE 1977 : 6 (project 5562071).

[2] J. R. Bolton, "Solar Power and Fuels", Academic Press, 1977, p. 146.

[3] A. Moradpour, E. Amouyal P. Keller and H. Kogan, *Nouv. J. Chim.*, **2**, 546 (1978).

[4] J. M. Lehn and P. J. Sauvage, Demande B.I. nr. pub. 2409262 (1979).

[5] J. M. Lehn and J. P. Sauvage, *Nouv. J. Chim.*, **1**, 449 (1977).

[6] M. Kirsch, J. M. Lehn and J. P. Sauvage, *Helv. Chim. Acta*, **62**, 1345 (1979).

[7] G. M. Brown, B. S. Brunschwig, C. Creuzt, J. F. Endicott and N. Sutin, *J. Amer. Chem. Soc.*, **101**, 1298 (1979).

[8] J. N. Braddock and T. J. Meyer, *J. Amer. Chem. Soc.*, **95**, 3158 (1973).

[9] J. N. Demas and A. W. Adamson, *J. Amer. Chem. Soc.*, **95**, 5159 (1971).

[10] C. T. Lin, W. Böttcher, M. Chou, C. Creutz, and N. Sutin, *J. Amer. Chem. Soc.*, **98**, 6536 (1976).

[11] G. A. Crosby, *Accounts Chem. Res.*, **8**, 231 (1975).

[12] G. M. Waind and B. Martin, *J. Inorg. Nuclear Chem.*, **8**, 551 (1958).

[13] S. Margel, W. Smith and F. C. Anson, *J. Electrochem. Soc.*, **125**, 241 (1978).

[14] G. N. Schrauzer, E. Deutsch and R. G. Windgassen, *J. Amer. Chem. Soc.*, **90**, 2441 (1968).

Revue Roumaine de Chimie, 27, 7, 103–114 (1982)

INVESTIGATION METHODS OF THE ELECTRODE PROCESSES

L. ONICIU and V. A. TOPAN
Babeş-Bolyai University, Department of Physical Chemistry, Str. Arany Janos, 11,
3400-Cluj-Napoca, Romania

The article is a review of the most important stationary and nonstationary electrochemical methods for investigating the electrode kinetics.

1. INTRODUCTION

A study of electrode kinetics has as final purpose the determination of the reaction mechanism and the rate as a function of the concentration of the reactants, intermediates, conditions etc. In the electrode kinetics the reaction rate is expressed by the current density which is simply measurable with an ampermeter. This feature is a considerable advantage of the electrochemical kinetics.[1] Also, there is the possibility to change the activation energy of the process by the potential sweep across the electrode–electrolyte interface. In this way, the electrochemist has the opportunity to calculate the activation energy – overpotential relation and to identify the steps of the process, without changing the nature of the studied process.

As in any kinetics, a previous identification of the active species, stoechiometry and, in general, of all the parameters involved, is very useful. A termodynamical characterization is also necessary.

More than the description of the various chemical steps, a complete electrochemical study has to include some data about the mass transport to and from the electrode – electrolyte interface, the electrosorption of the system components etc.

Due to the presence of the electric charges, the ions are randomly distributed in the system, especially on the surface of the electrode, where the concentrations are higher than in bulk with several magnitude orders and thus, the behaviour of the system is strongly influenced by this double layer.

Therefore, the electrochemical investigation of the process has the following main purposes :

a). the reaction order n_j related to the j species ;

b). the rate constant k_j, respectively k_j^0 (standard conditions) ;

c). the symmetry coefficient β (for monoelectronic transfer), the transfer coefficient α respectively (for polyelectronic transfer);

d). the stoechiometric number ν;

e). the exchange current density, i_0.

For an electrochemical reduction, described by the equation

$$n_A A + n_B B + \ldots + n_i I + ne^- \rightleftharpoons n_m M + n_n M + \ldots + n_j J \qquad (1)$$

the reaction rate is expressed by:

$$\frac{\mathrm{d}n}{\mathrm{d}t} = \frac{i}{zF} = \vec{k} \prod (a_i)^{n_i} - \vec{k} \prod (a_j)^{n_j} \qquad (2)$$

where a_i and a_j are the activities for reagents and products, respectively. The rate constants are:

$$\vec{k} + \vec{k}^0 \left\{ \exp\left[- \frac{F \sum n_i z_i}{RT} Ø_2 \right] \exp\left[\frac{-\vec{\alpha} zF}{\nu RT} (\Phi_S - \Phi_2) \right] \right\} \qquad (3)$$

and

$$\overleftarrow{k} = \overleftarrow{k}^0 \left\{ \exp\left[- \frac{F \sum n_j z_j}{RT} \Phi_2 \right] \exp\left[\frac{\overleftarrow{\alpha} zF}{RT} (\Phi_S - \Phi_2) \right] \right\} \qquad (4)$$

where the terms in the first brackets are corrections for double layer effect, Z_i and Z_j the electric charges for i and j species respectively, Φ_2 is the potential of the solution in PHE relative to the bulk of the solution and Φ_s the potential of the electrode surface relative to the bulk region of the solution.

Equations (3) and (4) do not take into consideration the electrosorption, which may lead to fundamental modifications in the double layer and, thus in the reaction rate.

Introducing the simplifying assumptions, that the system is an equilibrium, without double layer effects, the wellknown Butler—Volmer equation results:

$$i = i_0 \left\{ \exp\left(- \frac{\vec{\alpha} zF}{\nu RT} \eta \right) - \exp\left(\frac{\overleftarrow{\alpha} zF}{\nu RT} \eta \right) \right\} \qquad (5)$$

The Butler—Volmer equation is correct only if the exchange current density, i_0, is constant; that is only in solutions of high ionic strength (> 2M) in the absence of polyvalent ions and not far from the ZCP. The Buttler—Volmer equation allows the calculation of some important parameters, such as the reaction order, transfer coefficient, activation energy, the exchange current density etc. However, there is no possibility to obtain any information about transient state, which is of the highest interest in describing the cell behaviours in practical use. Such data could be the double layer capacity, the coating rate, diffusion parameters etc.

2. CLASSIFICATION OF THE METHODS

The study of the electrode processes is based on relaxation methods. Taking into account the particularities of the electrochemical methods, the perturbation can be achieved by one of the following ways :

— potentiostatically, when the potential is perturbed in a controlled way and the relaxation of the system in terms of current or charge is being observed ;

— galvanostatistically, when the current is perturbed and the potential answer observed ;

— culostatically, when the charge through the system is varied and the potential or the current is measured ;

The investigation procedures can be classified in steady state and nonsteady (or dynamic) methods. At the time, more than **100** methods are described. The most important of them are listed in table 1.

TABLE 1

Electrochemical methods of investigating the electrode kinetics

No	Method	Variable controlled	Variable followed	k cm.s^{-1}	Observations
A. 1	*Steady state* Potentiostatic	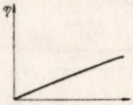	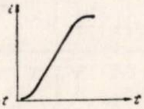	10^{-2}	Simple instrumentation. The scan should be made slow enough for avoiding transient states
2.	Galvanostatic, direct	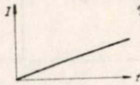	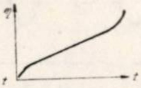	10^{-2}	Idem. Reproductibility of the surface is critical.
3.	Galvanostatic, indirect	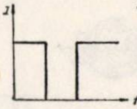	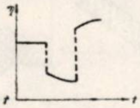	10^{-2}	Idem. Interrupting the current, the IR drop can be identified and compensated
B. 4.	*Non steady state* Single potential step.	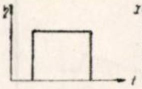	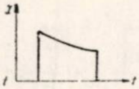	10^{0}	The IR drop should be small. Requires double layer charge effect corrections
5.	Double potential step.	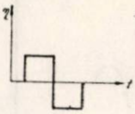	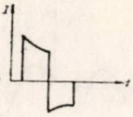	10^{0}	Processes with short-lived intermediates can be studied

TABLE 1 (continued)

0	1	2	3	4	5
6.	Periodical potential step.	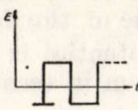	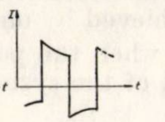	10^0	Theoretical treatment difficult. Parallel reactions can be studied.
7.	Cyclic voltammetry	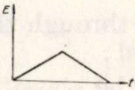	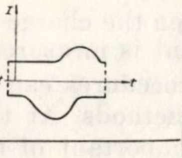	10^{-1}	Theoretical treatment difficult. Reactions with various intermediates can be studied.
8.	Single current step	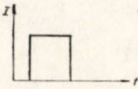	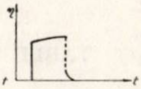	10^0	Simple instrumentation. Double layer effect corrections required.
9.	Double current step.	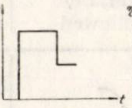	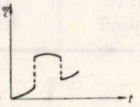	10^1	More accurate than the previous method. Needs more complicated instrumentation.
10.	Impedance measurement at reversible potential	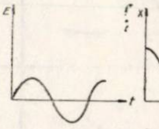	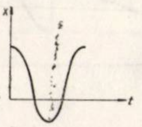	10^1	Middle instrumentation. Frequencies of about 10^6 Hz can be reached.
11.	Impedance measurements in alternative current on the ramp.	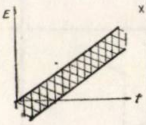	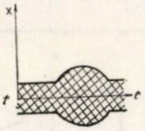	10^0	Theoretical analysis very difficult. Allows obtaining of information about adsorption variations in double layer
12.	Intermitent reflectometry	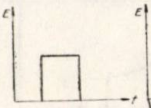	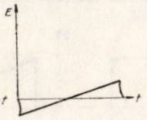	10^1	Frequencies of 10^8 reached. Requires sophisticated electrochemical cells.
13.	Faradaic rectification and distortion	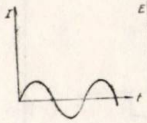	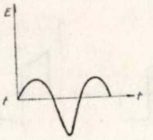	10^1	Very sophisticated equipment required.

TABLE 1 (continued)

0	1	2	3	4	5
14.	**Pressure step.**	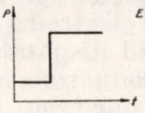	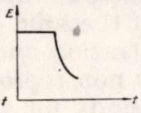	**10^0**	**Very quickly reactions at very low conductivities can be studied.**
15.	**Concentration perturbation**	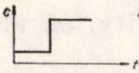	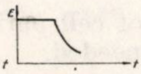	**10^{-1}**	**Idem**

3. PURIFICATION OF THE INVESTIGATED ELECTROCHEMICAL SYSTEM

The accuracy of the results is conditioned by the purity of the system. In order to illustrate the importance of this problem it must be mentioned that a monolayer ($10^{12}-10^{15}$ molecules/cm^2) is enough to cover completely the surface, as to be detected by most of electrochemical investigation methods. In terms of usual chemicals, the above mentioned figure represents $10^{-6}-10^{-9}$ moles/l. Somewhat higher concentrations of impurities are admitted only in thin layer electrochemistry, and in the methods based on dropping mercury electrode whose surface is continuously regenerated.

The purification involves the electrolyte, the electrodes and the cell.

a). Purification of the electrolyte.

— primary: it is made by one of the largely used methods, such as recrystallization, distillation, extraction etc.

— finally: the concentration of the impurities is lowered by preelectrolysis performed at suitable potentials (either more negative or more positive than the studied processes).

The preelectrolysis will occur for 10 – 1 000 h, on inert electrodes, separated or not by a semipermeable membrane. The electrodes used for preelectrolysis are the same as those used in this study, or inert electrodes. Many authors have observed some strange catalytic effects after a preelectrolysis on platinum. The explanation was the presence in solution of Pt in a concentration of $10^{-6} - 10^{-7}$%, which can induce the observed effects. The latter improvement in this way was the utilisation of 2 or more electrodes. The preelectrolysis time can be calculated by the Bockris and Conway model.[3]

For purifying the electrolyte from inoxidable or unreducible impurities, Soxhlett processing with ultrapure conc. HCl for 6 months is indicated.

b). The electrodes, except mercury usage, represent the main problem of the study.

Indeed, after HNO_3 washing and triple distillation, Hg is pure enough for obtaining reproducible results. The problem presents completely different aspects in the case of the solid electrodes; not only the "history" of the metal, but the concentration and disposition of the metal crystal defects can be responsible for non reproductible results. Many authors[4-8] have proposed different methods for purifying the surface in order to obtain comparable results.

c). Some requirements of cell purity, on which we do not insist in this paper, are also needed.

4. SHORT REVIEW OF INVESTIGATION METHODS

4.1. DIRECT METHODS

Chronologically, these are the first methods used in the electrochemical kinetics, based on the perturbation of one parameter of the surface at a rate; this allows the system to follow equilibrium states. The main methods, which have to be named both by the perturbed parameter and the followed (relaxed) one, are:

Perturbed variable	method	Variable followed (relaxation variable)	Method
Potential	Potentiostatic	Current charge	Chronogalvanometry Chronocoulometry
Current	Galvanostatic	Potential Charge	Chronopotentiometry Chronocoulometry
Charge	Culostatic	Potential Current	Chronopotentiometry Chronogalvanometry

There are several synonyms not indicated in the table.

The use of one method or of another is a function of several variables such as the shape of the function of the two variables, the nature of studied process, the scientific equipment available etc; irrespective of the method used, the cell has 3 electrodes (Fig. 1). When the total current which passes through the cell is low enough for maintaining the reversible state of the reference electrode, this can be also used as counter electrode.

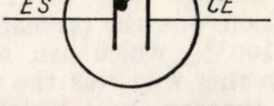

Fig. 1. — Electrochemical cell. ES — Working electrode; CE — Counter electrode; ER — Reference electrode.

For lowering the influence of the working electrode —Luggin capillary distance on the results, many authors recommend the determination of the values for several distances and extrapolation to zero.

In some situations, when a Luggin capillary is undesirable because of hydrodynamic reasons, the cell is built such as the interpolar distance is of only a few microns. In this way the volume of electrolyte is 10^{-5}—10^{-6} l.

Because of geometrical and hydrodynamical hindrances, if present, the position of the reference electrode differs from that in the normal electrochemical cell.[9] This method allows the use of solutions with higher impurities concentration. The theoretical base of the thin layer chemistry is rather simple and it is well applicable in complex processes with a high degree of irreversibility.

4.1.2. Indirect method

4.1.2.1. *Interruption method*

In a solution with a high ohmic drop or when the Luggin is undesirable due to various reasons, the ohmic overpotential can be compensated by periodical curent interruptions. Indeed, the ohmic drop disappears very fast ($\sim 10^{-12}$ s),[10] while the activation and concentration overpotentials disappear *only* after $10^{-5} - 10^{-6}$ s. This way, a fast oscilloscope allows the visualisation of the difference, which can be compensated by a usual ohmic drop electronic compensator.

The interruption can be made once or, better, periodically, for better results. This method cannot be applied for porous electrodes because of irregular current distribution on their surface. The overpotential — time correlation after interruption is:

$$\Delta\eta = \eta - \eta_0 = \frac{\nu RT}{\alpha zF}\ln(Kt+1), \tag{6}$$

where η_0 is the overpotential in the moment of interruption, t — time and

$$K = \frac{i}{C}\cdot\frac{\alpha zF}{\nu RT} \tag{7}$$

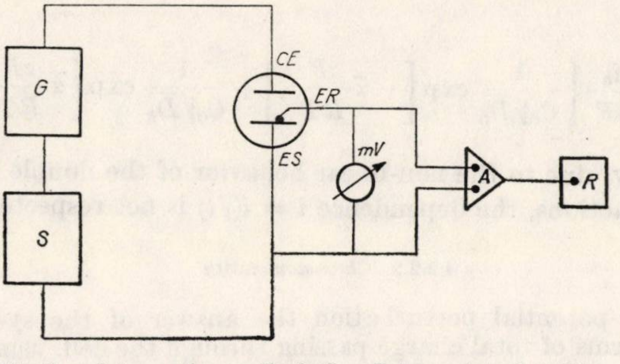

Fig. 2. — Interruption method. G — Galvanostat; S — Electronic switch; CE — Counter electrode; ER — Reference electrode; ES — Working electrode; A — Differential amplifier; mV — High input electronic milivoltmeter; R — High speed recorder or oscilloscope.

where i is the current density and C — the double layer capacity; the used circuit is given in Fig. 2.

4.2. NON STEADY STATE METHODS

4.2.1 Double layer charging effects

In non-steady state conditions, a good fraction of the total current is due to the charging of the double layer. In earlier works, many authors have calculated the non faradaic charging current $\left(I_{nf} = C\dfrac{\mathrm{d}E}{\mathrm{d}t}\right.$ where C is the double layer capacity$\left.\vphantom{\dfrac{\mathrm{d}E}{\mathrm{d}t}}\right)$ and deduced it from the total current. Delahay [11] has invalidated the supposed additivity, the parameter-time dependence being more complicated.

4.2.2. Potential perturbation methods

4.2.2.1. *Chronogalvanometry*

If the potential is shifted very quickly from equilibrium, the current passing through the cell should be infinite, because charging the double layer.

In fact, the current is limited by the potentiostat power-limit.

The current—time dependence after a potential perturbation was studied by several authors[11–14] for the case of linear diffusion on planar electrodes. The current density during the transient period following relaxation, is described by the equation :

$$i = i_0 \left\{ \exp\left[-\frac{\vec{\alpha} zF}{\nu RT}\eta \right] - \exp\left[\frac{\overleftarrow{\alpha} zF}{\nu RT}\eta \right] \right\} A(t) \tag{8}$$

where :

$$A(t) = \exp(\lambda^2 t)\,\mathrm{erfc}(\lambda\, t^{1/2}) \tag{9}$$

and

$$\lambda = \frac{i_0}{zF}\left\{ \frac{1}{C_{\mathrm{O}}\sqrt{D_{\mathrm{O}}}} \exp\left[-\vec{\alpha}\frac{zF}{RT}\eta \right] + \frac{1}{C_{\mathrm{O}}\sqrt{D_{\mathrm{R}}}} \exp\left[\overleftarrow{\alpha}\frac{zF}{RT}\eta \right] \right\} \tag{10}$$

Unfortunately, due to the non-linear behavior of the double layer, in the case of fast reactions, the dependence $i = i(\sqrt{t})$ is not respected.

4.2.2.2. *Chronocoulometry*

After a potential perturbation the answer of the system can be followed in terms of total charge passing through the cell, using, for example, a coulometer or an integrator circuit.

The equation describing the charge passing through the cell after a potential perturbation, is :

$$Q = \frac{b}{\lambda^2}\left\{ \exp(\lambda^2 t)\,\mathrm{erfc}\,(\lambda t^{1/2}) + 2\lambda\sqrt{\frac{t}{\pi}} - 1 \right\}, \tag{11}$$

where :

$$b = zF\,k_0\,C_O \exp\left[-\vec{\alpha}\,\frac{zF}{RT}(\varepsilon - \varepsilon_0)\right], \tag{12}$$

and

$$\lambda = k_0 \left\{\frac{1}{\sqrt{D_O}} \exp\left[-\vec{\alpha}\,\frac{zF}{RT}(\varepsilon - \varepsilon_0)\right] + \frac{1}{\sqrt{D_R}} \exp\left[\overleftarrow{\alpha}\,\frac{zF}{RT}(\varepsilon - \varepsilon_0)\right]\right\} \tag{13}$$

where D_O and D_R are the diffusion coefficients for the oxidated and respectively reduced forms.

For higher t values, the following simplified equation can be used :

$$Q = \frac{2b}{\lambda}\sqrt{\frac{t}{\pi}} - \frac{b}{\lambda^2} \tag{14}$$

In practice the arrangement shown in Fig. 3 can be used.

4.2.2.3. *The cell potential step*

Vielstich and Delahay [15] have developed a simpler method consisting in application of a potential sweep of no higher than 5 mV between working electrode and a much larger counter-electrode ; in these conditions it could be assumed that the whole potential sweep is applied only to the working electrode. The answer of the system is followed in terms of current as a function of time :

$$i = -\triangle V\left[\Omega + \frac{RT}{zFi_0}\right]^{-1} \exp\left[\lambda^2 t\right] \operatorname{erfc}\left(\lambda\sqrt{t}\right), \tag{15}$$

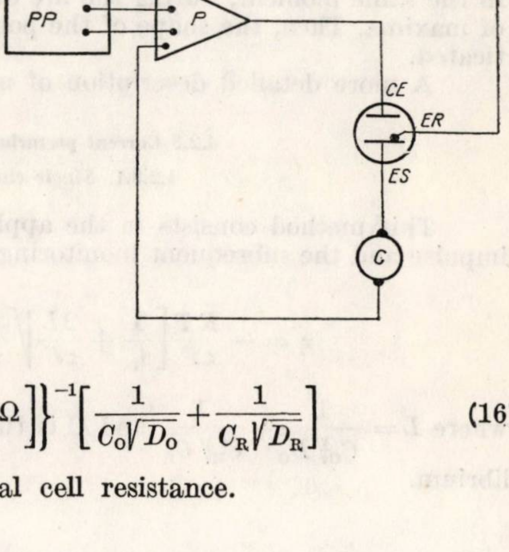

Fig. 3. — Cronocoulommetry. PP — Potential programmer ; P — Potentiostat ; ES — Working electrode ; ER — Reference electode ; CE — Counter electrode ; C — Coulometer.

where

$$\lambda = \left\{zF\left[\frac{1}{i_0} + \frac{zF}{RT}\Omega\right]\right\}^{-1}\left[\frac{1}{C_O\sqrt{D_O}} + \frac{1}{C_R\sqrt{D_R}}\right] \tag{16}$$

and $\triangle V = \eta - i\Omega$; Ω is the total cell resistance.

4.2.2.4. *Linear and cyclic voltammetry*

By this method a scan of constant speed is applied between two limits, in only one direction (linear voltammetry) or with returning back to the initial value (cyclic voltammetry).

The method is to be considered as a semiquantitative technique only, because of the limitations involved by the work with solid electrodes. According to our observations made during the study of electrodeposition and electrodissolution of Pb and Zn with cyclic voltammetry, the results obtained were very reproducible and allowed the understanding of some interesting aspects of electrode processes.

For example, in this way, we could indentify a form of lead, existing for a short time, on which the hydrogen overpotential does not exist. On the other hand, by finding an appropriate scan rate, the quantity of previously adsorbed ions can ve determined by calculating the area under the voltammetric peak.

In our opinion, the linear or cyclic voltammetry has capabilities yet unemployed and in some cases, it can become a good quantitative investigation method.

4.2.2.5. *The dropping electrode voltammetry. Polarography*

Polarography is the oldest non steady-state investigation method. For its elaboration, Heyrowsky won the Nobel prize in 1959.

In the original form of this method a linear potential scan is applied between a dropping mercury electrode and a mercury pool as counter electrode. The current passing through the cell increases suddenly each time when the ions present in the solution begin, one by one, their electrode processes. The method is strongly affected by the occurrence of polarographic maxima of different orders, whose origin is not well understood yet.

In order to avoid this hindrance, the polarography has been much improved. Thus, if the measurement of the current is made only once, in the same moment, during the life of each drop, the polarogram is free of maxima. Then, the shape of the potential function is also very sophisticated.

A more detailed description of modern polarography is given in.[16]

4.2.3 Current perturbation methods

4.2.3.1. *Single current step*

This method consists in the application of a single square current impulse and the subsequent monitoring of the potential-time dependence.

$$\eta = -\frac{RT}{zF}\left[\frac{1}{i_0} + \frac{2L}{zF}\sqrt{\frac{t}{\pi}} - RT\left(\frac{L}{zF}\right)^2 C\right]i \qquad (17)$$

where $L = \frac{1}{C_O\sqrt{D_O}} + \frac{1}{C_R\sqrt{C_R}}$ and C is the double layer capacity at equilibrium.

The simplest device which can be used for the study of electrochemical systems by means of single current step method is given in Fig. 4.

The most important drawback of the method consists in the strong influence of the double layer charging current on the global shape of the monitored time function. Thus, the method is not applicable for the study of fast reactions. This hindrance is solved by applying a double pulse; the first one is used for charging the double layer and the second acts as a measurement pulse. The same device might be used.

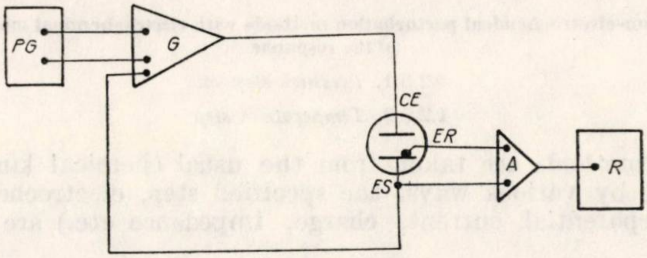

Fig 4. — Current step method. PG — Pulse generator; G — Galvanostat; CE — Counter electrode; ER — Reference electrode; ES — Working electrode; A — Differential amplifier; R — High speed recorder.

The overpotential-time relation is always of the $\eta = \eta(\sqrt{t})$ type.

4.2.3. Coulombian perturbation methods

In this family of methods the total charge passing through the cell is perturbed.

The relaxation equation has the following form:

$$\eta = \eta_0 \exp - \frac{t}{\tau} \tag{18}$$

where the relaxation time $\tau = \dfrac{C\,RT}{i_0\,zF}$

If the time t is very short, it can be assumed that Q used for charging the double layer is very small, and $\eta = Q/C$.

4.2.4. Other investigation methods

4.2.4.1. *Impedance measurements*

These are among the latest methods of investigation and consist in following the variation of the impedance of the cell, variation triggered by suddenly modifying one of the parameters. This kind of methods is particularly useful for the study of very fast processes, but the theoretical basis is not enough developed.

4.2.4.2. *Faradaic rectification and distortion*

The method uses the "semiconducting" behaviour of irreversible electrochemical systems. The theoretical basis is rather complex. Faradaic distorsions appear in the systems with a given irreversibility degree.

4.2.5. Non-electrochemical perturbation methods with electrochemical monitoring of the response

4.2.5.1. *Pressure step and*

4.2.5.2. *Temperature step*

These methods are taken from the usual chemical kinetics. After determining, by various ways, the specified step, electrochemical parameters (overpotential, current, charge, impedance etc.) are followed.

4.2.6. Conclusions

Nowadays there is a very rich lot of methods for investigating electrochemical systems.

The variety of methods reflects the variety in the behaviour of the systems.

There are enough methods and the most important task is now the enlargement of the theoretical basis.

The most important methods are the non-steady-state ones since they describe more accurately the functioning electrochemical systems.

REFERENCES

[1] L. Oniciu, "Chimie Fizică, Electrochimie", Editura Didactică — Pedagogică, București, 1977, ed. 2, sect. 5.

[2] E. Yeager and A. J. Salkind, "Techniques of Electrochemistry", Wiley, New York, 1972, vol. 1, p. 152.

[3] J. O'M. Bockris, B. E. Conway, *J. Sci. Instr.*, **25**, 283 (1948).

[4] A. N. Arshinov, *Elekrokhimiia*, **13**, (8), 1134 (1978).

[5] F. G. Will, *Electrochim. Acta*, **14**, 749 (1969).

[6] L. Oniciu and V. A. Topan, to be published.

[7] N. D. Tomashov and L. P. Vershinina, *Electrochim. Acta*, **15**, 501 (1970)

[8] H. Ewe, *Chem. Ing. Tech.*, **45**, 207 (1973).

[9] V. Cermak, *Coll. Czech. Chem. Commun.*, **24**, 831 (1959).

[10] L. Oniciu, "Pile de combustie", Ed. Științifică, București, 1971, p. 53.

[11] P. Delahay, *J.Electrochem. Soc.*, **113**, 967 (1966).

[12] W. Vielstich, H. Gerischer, *Z. Physih. Chem.*, **4**, 10 (1955).

[13] A. G. Kicheev et. al., *Elektrokhimiia*, **5**, 202 (1975).

[14] B. Nesterov, N. Korovin, *Elektrokhimiia*, **2** (11), 1296 (1976).

[15] W. Vielstich and P. Delahay, *J. Am. Chem. Soc.*, **79**, 4824 (1957).

[16] L. Oniciu and L. Mureșan, to be published.

Revue Roumaine de Chimie, 27, 1, 115—120 (1982)

THE ANODIC OXIDATION OF n-DECANE ON PLATINUM ELECTRODE IN ACID ELECTROLYTE

O. RADOVICI, BELARISA POPESCU and L. DIMA
Polytechnic Institute of Bucharest, Department of Physical Chemistry and Electrochemical Technology, Faculty of Chemical Engineering, Bdul Republicii 13, Bucharest, Romania

Received June 16, 1981

The mechanism of anodic oxidation of n-decane was studied using electrochemical pulse technique. The first charge transfer reaction is the rapid electrochemical oxidation of hydrogen. The second charge transfer reaction is the electrochemical oxidation of the previously chemosorbed hydrocarbon on the metallic surface.

The performances obtained with saturated hydrocarbons in fuel cells using phosphoric acid as electrolyte are quite encouraging, as shown by results obtained on n-decane-oxygen fuel cell in H_3PO_4 14.7 M at 150°C on platinum-teflon catalyst electrode. [1] An advantage of using a liquid hydrocarbon as fuel is that it facilitates the removal of gaseous products and furthermore, liquid hydrocarbons are available in large quantities (decane is one of the main constituents of diesel oil).

Our research in this area focused on the mechanism of anodic oxidation of n-decane by means of the electrochemical pulse techniques.

EXPERIMENTAL

The electrochemical cell consists of three compartments for the reference, working and counter electrode separated by porous frits. A hydrogen electrode was used as reference, working and counter electrodes consisted of smooth platinum. All solutions were prepared from spectral grade reagents and tridistilled water.

The electrochemical measurements were performed under potentiostatic control using a Tacussel PR-20 electronic potentiostat in a combination with an ORION EMS/1117 function generator.

The voltamograms were recorded on X—Y recorders (ORION 7981) or a TESLA BM/450 oscilloscope.

Pretreatment of the electrodes

In order to obtain reliable data and a good reproducibility of results, the platinum electrode was cleaned in a bichromate sulfuric acid mixture intensively flushed with distilled water. Then the surface of the working electrode was electrochemically treated in agreement with the potential time function applied on the metallic surface, as shown in Fig. 1.

This purification procedure of the electrode surface is largely described in the literature.[2–4] Steps A and B in this potential time function applied on the electrode correspond to the formation and stabilisation of an adsorbed oxygen surface layer ; step C corresponds to the reduction of adsorbed oxygen and adsorption of hydrogen on the surface of the electrode. Step D corresponds to the oxidation of the hydrogen and the formation of a clean surface of the electrode ready for the adsorption of the hydrocarbon, which is adsorbed at this value of the potential. The time of adsorption was selected between 10 seconds and 30 minutes.

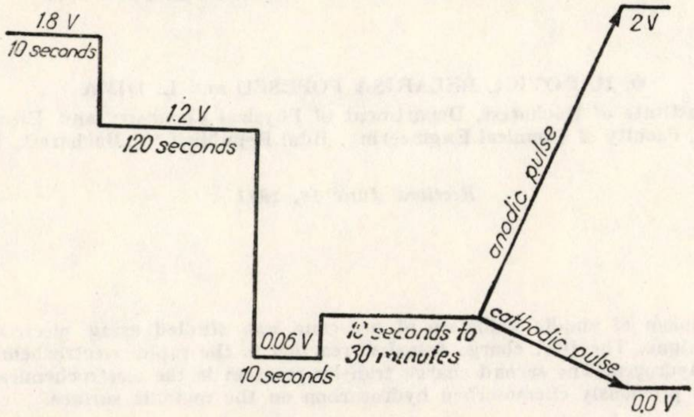

Fig. 1. — The programme of electrochemical treatment of the electrode.

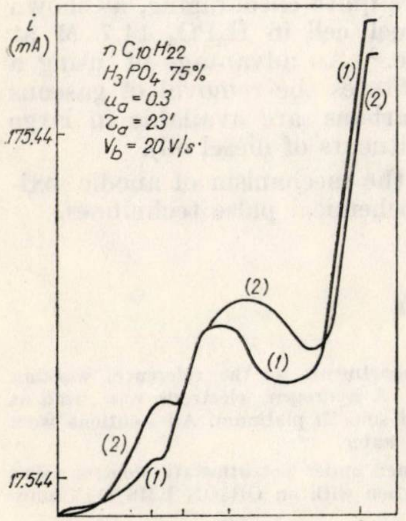

Fig. 2. — Polarisation curve of *n*-decane in H_3PO_4 : (1) without *n*-decane ; (2) with *n*-decane.

Adsorption measurements

In order to investigate the adsorption mechanism of *n*-decane on platinum, the fast anodic potentiostatic pulse proposed by Breiter and Gilman[5] was used.

To test the application of this technique to our electrolyte and fuel, current-potential curves were recorded with different scan rates. It was found that at a sweep rate of 20 V/s, the diffusion of the organic compound from the solution during the pulse can be neglected.

A comparison of the curve obtained in the presence of the fuel to the curve for the pure electrolyte without fuel (blank curve) allows the determination of the amount of the charge consumed in the anodic oxidation of the fuel. Although the adsorption equilibrium of the fuel at 0.300 V is established after a short time of adsorption, a period of 10 s to 30 minutes was chosen as mentioned before. The shape and course of the anodic curve can be seen in Fig. 2.

On comparing the curve of Fig. 2 to the curves obtained by different authors for other hydrocarbons[4,6–10] the same type of oxidation products of *n*-decane can be observed, i.e. at 0.8 V the formation of species of the so-called type I, at + 1.2 V the formation of species of type II and at a higher potential the species of type III. The amount of charge (in microcoulombs) utilized for the oxidation of the species of type I(Q_I), II(Q_{II}) and the charge utilized for the oxidation of *n*-decane (Q_{Hc}) for various times of adsorption (τ_a) (s), are presented in Table 1.

TABLE 1

The charge necessary for anodic oxidation of species I, II

τ_a(s)	Q_{Hc}(μC)	Q_I(μC)	Q_{II}(μC)	Q_{Hc}(μC/cm^2) real surface	Q_I(μC/cm^2) real surface	Q_{II}(μC/cm^2)
10	346.3	87.1	258.3	107.9	27.2	80.7
30	556.7	10.8	449.9	174	33.4	140.6
60	749.7	187.7	562	234.3	58.6	175.7
150	905	248.7	656.3	282.8	77.7	205.1
300	1,066.3	325.5	740.3	333.3	101.7	231.6
480	1,103.5	398.5	715	348	124.5	223.5
720	1,142.1	438.2	703.9	357	127	220
1020	961.9	377.2	584.7	300.6	118	182.6
1320	1,101	438.2	662.8	347.2	137	210.2
1800	983	422	561	307.2	131.8	175.4

In order to obtain the degree of coverage (θ) of Pt with *n*-decane and the species I, II and III, we performed cathodic polarisation of Pt electrode by sweep technique (sweep rate 100 V/s) in the potential range 0.3—0.0 V in 75% H_3PO_4 *n*-decane solution.

From these curves we obtained data which allow us to calculate the degree of coverage of the hydrocarbon θ_{Hc} and the different oxidation products θ_I, θ_{II} θ_{III}, as shown in Table 2.

TABLE 2

The values of θ at different times of adsorption

τ_a(s)	$\theta_{Hc}=\left(\frac{Q_H-Q_{Hc}}{Q_H}\right)_{100V/s}$	$\theta_I=\left(\frac{Q_H-Q_{Hc}}{Q_H}\right)_{20V/s}$	$\theta_{II}=Q_{Hc}-Q_I-Q_{III}$	$\theta_{III}=\frac{(i_H)^{2V}-(i_c)^{2V}}{(i_H)^{2V}}$
10	0.0758	0.0172	0.0585	—
30	0.329	0.106	0.223	—
60	0.412	0.167	0.245	—
150	0.632	0.342	0.290	—
300	0.754	0.400	0.331	0.023
480	0.782	0.459	0.290	0.031
720	0.769	0.477	0.241	0.051
1020	0.789	0.486	0.246	0.057
1380	0.825	0.486	0.270	0.069
1800	0.817	0.486	0.235	0.096

DISCUSSION

As was shown by different authors [3,6,11] the adsorption of the hydrocarbons on the platinum electrodes is in agreement with a Langmuir adsorption isotherm, to which corresponds the following kinetic equation:

$$\frac{d\theta_{Hc}}{dt} = k_{ads}c_{Hc}(1 - \theta_{Hc})^m \tag{1}$$

where *m* is the reaction order in respect of the free surface and practically corresponds to the number of the active centres of the surface involved in the determining step of the adsorption reaction.

If equation 1 is rewritten in the logarithmic form we have:

$$\ln\left(\frac{\mathrm{d}\theta_{Hc}}{\mathrm{d}t}\right) = \ln K_{\mathrm{ads}} c_{Hc} + m \ln (1 - \theta_{Hc}) \qquad (2)$$

The graphical representation of this equation is a straight line which has the slope equal to *m*.

We have calculated the values of $(1 - \theta_{Hc})$ and of $\mathrm{d}\theta_{Hc}/\mathrm{d}t$ using the data from table 2 and from the curves θ_{Hc} versus τ_a (because $\mathrm{d}\theta_{Hc}/\mathrm{d}t$ represents the slope of this curve at the point τ_a) as shown in Table 3.

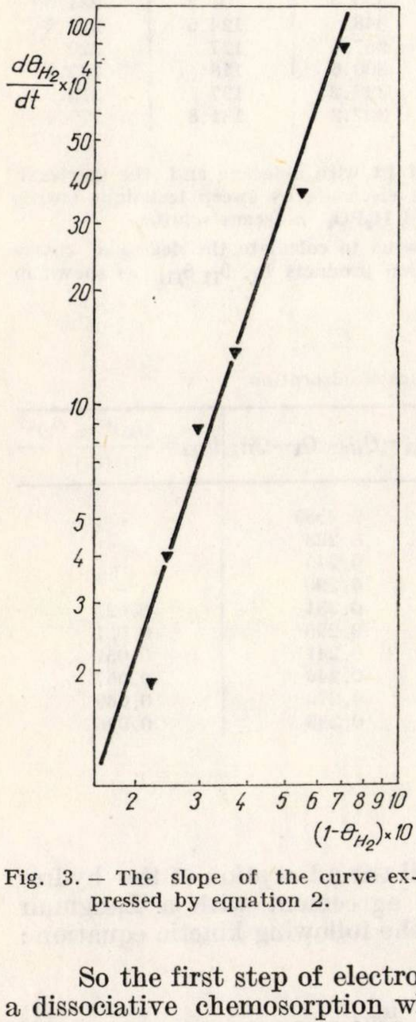

Fig. 3. — The slope of the curve expressed by equation 2.

TABLE 3

The variation of the ratio $\frac{\mathrm{d}\theta}{\mathrm{d}t}$ calculated from the slope of the curve in Fig. 3

τ'_a(s)	θ_{Hc}	$1 - \theta_{Hc}$	$\mathrm{d}\theta_{Hc}/\mathrm{d}t$
30	0.3	0.7	0.0088
60	0.44	0.56	0.00361
90	0.525	0.475	0.00258
150	0.632	0.368	0.00138
210	0.7	0.3	0.000857
300	0.754	0.246	0.0004
390	0.775	0.225	0.000185

Fig. 3 represents equation 2 applied to the adsorption of *n*-decane. The slope of the curve is $m = 2.98 \cong 3$, which corresponds to the number of active centers of the surface of platinum involved in the process of adsorption of *n*-decane.

Taking into account this result, the structure of *n*-decane and the surface arrangement of platinum (face-centered cubic crystal), we propose the following mechanism of adsorption of this hydrocarbon:

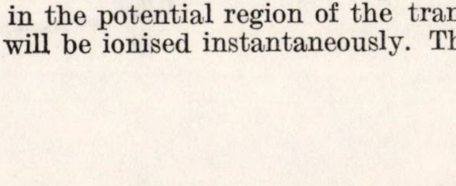

$$nC_{10}H_{22} + 3M \longrightarrow R_8-\underset{M}{\overset{H}{C}}-\underset{M}{\overset{H}{C}}-H + \underset{M}{H}$$

$$\underset{M}{H} \longrightarrow M + H^+ + e$$

So the first step of electrochemical oxidation of *n*-decane represents a dissociative chemosorption where, in the potential region of the transfer reaction, the adsorbed hydrogen will be ionised instantaneously. This dissociative adsorption process is the rate determining step of the anodic oxidation of *n*-decane.

The adsorbed species formed in the first step is afterwards oxidized in subsequent steps to other oxidation species of type I, II or III.

The maximum degree of coverage was found to be $\theta_{\text{I}} = 0.5$ at 1000 s for species of type I; $\theta_{\text{II}} = 0.33$ at 300 s for species of type II and $\theta_{\text{III}} = 0.1$ at 1800 s for species of type III.

The species of type I oxidize at + 0.8 V and the maximum amount of charge involved in this process $Q_{\text{I}} = 137\ \mu\text{C/cm}^2$, and 1 : 2 electron per active site.

The active species of type II oxidize at 1.2 V with $Q_{\text{II}} = 231\ \mu\text{C/cm}^2$ and need 3 : 4 electron per active site. The inactive species of type II oxidize at 1.3 V.

The species of type III do not oxidize even at 2V.

Based on these results we propose the following mechanism for dissociative chemosorption of *n*-decane: OH^- ions present in the double layer will be discharged under chemosorption, and formation of Pt—OH on free surface is possible. The decisive rate determining step represents a reaction of adsorbed and dehydrogenated *n*-decane with Pt—OH species.

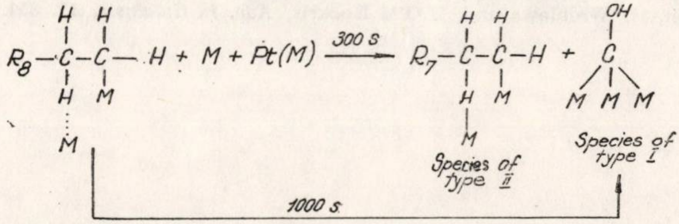

The species of type III appear very slowly from the inactive type II species by a dehydrogenation process

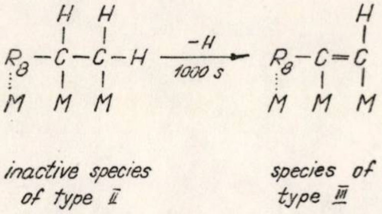

The general oxidation mechanism is as follows:

1. Adsorption step is slow: 300 — 1800 s.

2. Electrochemical oxidation of H first charge transfer reaction (rapid).

3. Electrochemical oxidation of the adsorbate is rapid.

Second charge transfer reaction is :

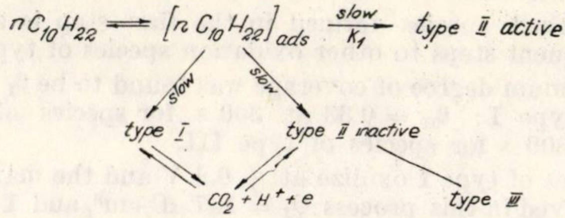
$nC_{10}H_{22}$
$[nC_{10}H_{22}]_{ads}$
slow
K_1
type II active
slow
slow
type I
type II inactive
$CO_2 + H^+ + e$
type III

REFERENCES

[1] W. R. Eppesly, *Proc. Ann. Power Sources Conf.*, **19**, 46 (1965).
[2] S. Gilman, *J. Phys. Chem.*, **67**, 78 (1963).
[3] S. B. Brummer, J. I. Bond and M. Y. Turner, *J. Phys. Chem.*, **69**, 3424 (1965).
[4] L. W. Niedrach and M. Tachner, *J. Electrochem. Soc.*, **114**, 17 (1976).
[5] M. W. Breiter and S. Gilman, *J. Electrochem. Soc.*, **109**, 622 (1962).
[6] E. J. Cairns and A. M. Breitenste, *J. Electrochem. Soc.*, **114**, 764 (1967).
[7] E. J. Cairns, A. M. Breitenste and A. J. Scorpelins, *J. Electrochem. Soc.*, **115**, 597 (1968)
[8] S. Gilman, *J. Electrochem. Soc.*, **113**, 1036 (1966).
[9] L. W. Niedrach, S. Gilman, J. W. Eirtock, *J. Electrochem. Soc.*, **112**, 1061 (1965).
[10] L. W. Niedrach, *J. Electrochem. Soc.*, **113**, 645 (1966).
[11] S. Srinivasan, H. Wroblowa and J. O'M Bockris, *Adv. in Catalysis*, **17**, 351 (1967).

Revue Roumaine de Chimie, 27, 7, 121–128 (1982)

ARYLAMIDES OF OXALIC ACID. III[1,2]. *HÜCKEL* MOLECULAR ORBITAL AND *DEL RÉ* CALCULATIONS

S. RADULY*, M. MRACEC**, D. CIUBOTARIU***, ADELINA MUSTE****
and Z. SIMON****

* University of Timişoara, Department of Natural Sciences
** Petrochemical Works "Solventul". Research Department, Timişoara
*** "Traian Vuia" Polytechnic Institute of Timişoara, Organic Chemistry Department
**** Institute of Medicine, Timişoara, Department of Biochemistry, Piaţa 23 August 2, Timişoara 1900, Romania

Received February 3, 1981

Electronic structure calculations were performed for oxalic acid, oxamic acid, oxamide, oxanilic acid, oxanilide and for the corresponding esthers. The ω-HMO method was used for the π-electronic systems, and the Del Ré-method for the σ-bonds. Molecular diagrams and frontier orbitals are listed, allowing a perturbational treatment for substitution derivatives. The frontier orbitals indicate a rather strong reducing character, most pronounced for oxanilic acid.

INTRODUCTION

In two preceding notes [1,2] the synthesis and characterisation of several new substituted oxanilides are given. Several oxanilides are used as antioxidants, or have interesting biological properties, especially bacteriostatic.[3] This note is a study of the electronic structure of these compounds, in order to obtain electronic parameters to be used in QSAR (quantitative structure activity relations) studies related to the biological activity of these compounds.

A combination of ω-HMO method [4] for the π-electronic system and of the Del Ré method [5] for the σ-bonds is used in this paper, a method considered to yield realistic values for QSAR studies, at least as a first step for considering electronic parameters.[6,7] Calculations were performed for oxanilic acid, the corresponding oxanilides and also oxalic acid and its amide-simple molecules are used as standards to compare influences of phenyl cycles and other substituents. The results obtained here will be used in note IV in a study of electronic spectra for substitution derivatives of oxanilic acid, the ethyl ester and the oxanilide.

CALCULATION METHOD AND PARAMETERS

The iterative ω-HMO method was used for π-electronic systems, a method that avoids too large nonuniformities in electronic distribution as it considers repulsion of π-electrons localised at the atom. The systems of secular equations were solved on the computer of the Territorial Computing Centre in Timişoara on the basis of a programme written by one of us (M. Mracec), for oxalic acid (I), oxamic acid (II), oxamide (III), oxanilic acid (IV) and the oxanilide (V).

The influence of substituents in the phenyl cycle was considered by a modified variant of first and second order perturbational method.[8] The substituent R at atom q of the phenyl cycle will modify energy $\varepsilon_i = \alpha + \lambda_i\beta$ of the molecular orbital Φ_1 of the unperturbed system by:

$$\Delta\varepsilon_i'' = \frac{c_{qi}^2 \cdot \eta_{CR}^2 \cdot}{\lambda_i - \delta_R + \eta_{CR} \cdot \mathrm{sign}(\lambda_i - \delta_R)} \tag{1}$$

The energy of the orbital φ_R of R is $\alpha_R = \alpha + \delta_R\beta$, the exchange energy integral, $\beta_{CR} = \eta_{CR} \cdot \beta$. The coefficient c_{Ri} which gives the mixing of φ_R to Φ_i is:

$$\Phi_i = \frac{1}{\sqrt{1 + c_{Ri}^2}} (\Phi_i + c_{Ri} \cdot \rho_R);$$

$$c_{Ri} = \frac{c_{qi} \cdot \eta_{CR}}{\lambda_i - \delta_R + \eta_{CR} \cdot \mathrm{sign}(\lambda_i - \delta_R)} \tag{2}$$

For an inductive effect $\delta_x \cdot \beta$ at atom q the energy $\Delta\varepsilon_i'$ is changed by:

$$\Delta\varepsilon_i = c_{qi}^2 \cdot \delta_x \cdot \beta \tag{3}$$

The parameters used are those recommended by Streitwieser[4,8,9]:

$$\alpha_{-O^{\theta}} = \alpha + 2\beta;\ \alpha_{=O} = \alpha + \beta;\ \alpha_{-NH-} = \alpha + 1.5\beta;\ \beta_{C=O} = \beta;$$

$$\beta_{C-O} = 0.8\beta;\ \beta_{C-N} = 0.8\beta;\ \beta_{C-C} = 0.9\beta\ (\text{single C}-\text{C bond});$$

while for the substituents:

$$\alpha_{CH_3O} = \alpha + 2\beta;\ \beta_{C-O} = 0.8\beta;\ \alpha_{Cl} = \alpha + 1.8\beta;$$

$$\beta_{C-Cl} = 0.4\beta;\ \alpha_{N(CH_3)_2} = \alpha + 1.2\beta;\ \beta_{C-N} = 0.8\beta;$$

$$\alpha_{-NO_2} = \alpha - 0.4\beta;\ \beta_{C-NO_2} = 0.7\beta.$$

All substituents were considered with one π-orbital φ_R and 2 π-electrons, except $-NO_2$ considered with one empty π-orbital.[9] For R: $-N(CH_3)_2$, $\alpha = \alpha + 1.2\beta$ was considered instead of $\alpha + 1.5\beta$ to account for the more electron donating character of the dimethylamino group as compared to the amino group. The ionisation of the carboxyl group is accounted for by changing from $\alpha_{OH} = \alpha + 2\beta$ to $\alpha_{-O^{\theta}} = \alpha + \beta$, considered as inductive effect ($\delta_O = -1$ for eq. (3)). No other inductive effects are considered.

The calculations for the Del Ré method were performed also on the computer of the Territorial Computing Centre in Timișoara, the programme written by Raduly. For atomic valence orbitals the following electronegativities were considered[5,10]:

$$\delta^0_{H} = 0.0\,;\ \delta^0_{C(sp^3)} = 0.07\,;\ \delta^\theta_{C(sp^2)} = 0.12\,;\ \delta^0_{O(sp^3)} = 0.40\,;$$

$$\delta^0_{O(sp^2)} = 0.28\,;\ \delta^0_{N(sp^2)} = 0.24\,;\ \delta^0_{Cl} = 0.35,$$

the inductive effect $\gamma_{q(p)}$ of atom p on atom q:

$$\gamma_{C(C)} = \gamma_{C(N)} = \gamma_{C(O)} = 0.1\,;\ \gamma_{N(H)} = \gamma_{O(H)} = \gamma_{C(H)} = 0.3\,;$$

$$\gamma_{N(C)} = \gamma_{O(C)} = 0.1\,;\ \gamma_{H(N)} = \gamma_{H(O)} = \gamma_{H(Cl)} = 0.4\,;\ \gamma_{C(Cl)} = 0.2$$

the exchange integrals:

$$\eta_{CH} = \eta_{CC} = 1.0\,;\ \eta_{CO(sp^3)} = 0.95\,;\ \eta_{CO(sp^2)} = \eta_{CN} = 0.7\,;$$

$$\eta_{NH} = \eta_{OH} = 0.45\,;\quad \eta_{CCl} = 0.65.$$

THE π-ELECTRONIC STRUCTURE OF MOLECULES

Molecular diagrams of the five basis-(unsubstituted) molecules are illustrated in Fig. 1, the frontier orbitals and delocalization energies ΔE in Table 1.

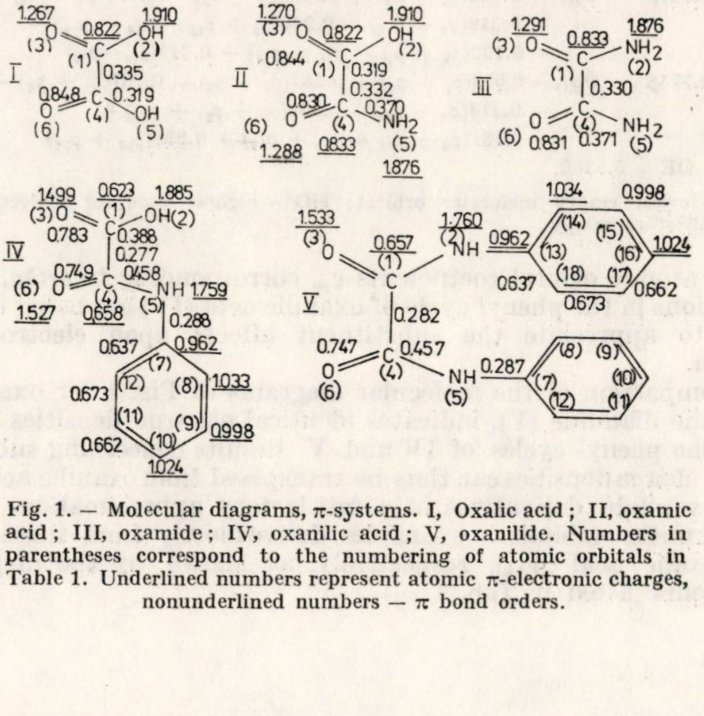
I
II
III
IV
V
1.267
0.822
1.910
0.335
0.848
0.319
1.270
0.844
0.319
0.332
0.830
0.370
1.288
0.833
1.876
1.291
0.833
1.876
0.330
0.831
0.371
1.499
0.623
1.885
0.783
0.388
0.277
0.749
0.458
1.759
1.527
0.658
0.288
0.637
0.962
0.673
1.033
0.998
0.662
1.024
1.533
0.657
1.760
0.962
1.034
0.998
1.024
0.637
0.673
0.662
0.282
0.747
0.457
0.287

Fig. 1. — Molecular diagrams, π-systems. I, Oxalic acid; II, oxamic acid; III, oxamide; IV, oxanilic acid; V, oxanilide. Numbers in parentheses correspond to the numbering of atomic orbitals in Table 1. Underlined numbers represent atomic π-electronic charges, nonunderlined numbers — π bond orders.

TABLE 1

Frontier molecular orbitals and energy levels

I — Oxalic acid

$$\varepsilon_{LE} = \alpha - 0.255\beta \qquad \Phi_{LE} = 0.458(\rho_1 + \rho_4) + 0.154(\rho_2 + \rho_5) - 0.516(\rho_3 + \rho_6)$$

$$\varepsilon_{HO} = \alpha + 1.062\beta \qquad \Phi_{HO} = 0.268(\rho_1 - \rho_4) - 0.201(\rho_2 - \rho_5) + 0.623(\rho_3 - \rho_6)$$

$$DE = 0.554\beta$$

II — Oxalic acid monoamide (oxamic acid)

$$\varepsilon_{LE} = \alpha - 0.281\beta \qquad \Phi_{LE} = 0.472\rho_1 - 0.157\rho_2 - 0.519\rho_3 + 0.444\rho_4 - 0.181\rho_5 - 0.503\rho_6$$

$$\varepsilon_{HO} = \alpha + 1.015\beta \qquad \Phi_{HO} = 0.206\rho_1 + 0.148\rho_2 + 0.532\rho_3 - 0.281\rho_4 + 0.338\rho_5 - 0.678\rho_4$$

$$DE = 0.932\beta$$

III — Oxalic acid diamide (oxamide)

$$\varepsilon_{LE} = \alpha - 0.307\beta \qquad \Phi_{LE} = 0.457(\rho_1 + \rho_4) + 0.184(\rho_2 + \rho_5) - 0.507(\rho_3 + \rho_6)$$

$$\varepsilon_{HO} = \alpha + 0.984\beta \qquad \Phi_{HO} = 0.236(\rho_1 - \rho_4) - 0.271(\rho_3 - \rho_5) + 0.609(\rho_3 - \rho_6)$$

$$DE = 0.970\beta$$

IV — Oxalic acid monoanilide (oxanilic acid)

$$\begin{aligned}\varepsilon_{LE} = \alpha - 0.230\beta \qquad \Phi_{LE} &= 0.526\rho_1 - 0.189\rho_2 - 0.427\rho_3 + 0.508\rho_4 - 0.220\rho_5 - 0.414\rho_6\\ &- 0.032\rho_7 + 0.092(\rho_8 + \rho_{12}) + 0.011(\rho_9 + \rho_{11}) - 0.094\rho_{10}\end{aligned}$$

$$\begin{aligned}\varepsilon_{HO} = \alpha + 0.771\beta \qquad \Phi_{HO} &= 0.011\rho_1 - 0.007\rho_2 - 0.046\rho_3 + 0.067\rho_4 + 0.416\rho_5 - 0.292\rho_6\\ &- 0.448\rho_7 - 0.339(\rho_8 + \rho_{12}) + 0.186(\rho_9 + \rho_{11}) + 0.483\rho_{10}\end{aligned}$$

$$DE = 3.228\beta$$

V — Oxalic acid dianilide (oxanilide)

$$\begin{aligned}\varepsilon_{LE} = \alpha - 0.245\beta \qquad \Phi_{LE} &= -0.509(\rho_1 + \rho_4) + 0.218(\rho_2 + \rho_5) + 0.408(\rho_3 + \rho_6) +\\ &+ 0.034(\rho_7 + \rho_{13}) - 0.091(\rho_8 + \rho_{12} + \rho_{14} + \rho_{18}) -\\ &- 0.011(\rho_9 + \rho_{11} + \rho_{15} + \rho_{17}) + 0.094(\rho_{10} + \rho_{16})\end{aligned}$$

$$\begin{aligned}\varepsilon_{HO} = \alpha + 0.767\beta \qquad \Phi_{HO} &= 0.041(\rho_1 - \varphi_4) + 0.304(\rho_2 - \rho_5) - 0.175(\rho_3 - \rho_6) +\\ &+ 0.319(\rho_7 - \rho_{13}) + 0.244(\rho_8 + \rho_{12} - \rho_{14} - \rho_{18}) -\\ &- 0.132(\rho_9 + \rho_{11} - \rho_{15} - \rho_{17}) - 0.345(\rho_{10} - \rho_{16})\end{aligned}$$

$$\begin{aligned}\varepsilon_{HO} = \alpha + 0.774\beta \qquad \Phi_{HO} &= 0.053(\rho_1 + \rho_4) + 0.287(\rho_2 + \rho_5) - 0.237(\rho_3 + \rho_6) -\\ &- 0.314(\rho_7 + \rho_{13}) - 0.236(\rho_8 + \rho_{14} + \rho_{18}) +\\ &+ 0.131(\rho_9 + \rho_{11} + \rho_{15} + \rho_{17}) + 0.338(\rho_{10} + \rho_{16})\end{aligned}$$

$$DE = 5.530\beta.$$

LE — lowest empty molecular orbital; HO — highest occupied molecular orbital; DE — delocalisation energy

The atomic orbital coefficients c_{pq} corresponding to *ortho*, *meta* and *para* positions in the phenyl cycle of oxanilic acid (IV) are listed in Table 2, allowing to appreciate the substituent effects upon electron density repartition.

A comparison of the molecular diagrams of Fig. 1 for oxanilic acid (IV) and the dianilide (V), indicates identical electron densities and bond orders in the phenyl cycles of IV and V. Results concerning substituents' effects on charge densities can thus be transposed from oxanilic acid derivatives to oxanilide derivatives in a satisfactory approximation.

The frontier orbitals in oxanilides derive mostly from those of aniline (Φ_{HO}) or oxalic acid (Φ_{LE}), respectively, as shown by the inspection of c_{pq}-coefficients listed in Tab. 1.

TABLE 2

Atomic orbital coefficients in *ortho, meta* and *para* positions of the phenyl cycle in oxalic acid (IV) ; π-system, $\varepsilon_1 - \varepsilon_7$ correspond to the occupied orbital

ε_i	c_{oi}	c_{mi}	c_{pi}
$\varepsilon_{12} = \alpha - 2.039\beta$	−0.409	−0.386	−0.376
$\varepsilon_{11} = \alpha - 1.509\beta$	−0.019	0.103	−0.137
$\varepsilon_{10} = \alpha - 1.072\beta$	0.240	0.302	−0.563
$\varepsilon_9 = \alpha - 1.000\beta$	0.500	−0.500	0.000
$\varepsilon_8 = \alpha - 0.230\beta$	0.092	0.011	−0.094
$\varepsilon_7 = \alpha + 0.771\beta$	−0.339	0.186	0.483
$\varepsilon_6 = \alpha + 1.000\beta$	0.500	0.500	0.000
$\varepsilon_5 = \alpha + 1.323\beta$	−0.022	0.118	0.578
$\varepsilon_4 = \alpha + 1.486\beta$	0.031	0.221	0.297
$\varepsilon_3 = \alpha + 1.888\beta$	0.290	0.350	0.370
$\varepsilon_2 = \alpha + 2.308\beta$	0.230	0.161	0.139
$\varepsilon_1 = \alpha + 2.574\beta$	0.110	0.061	0.047

ATOMIC CHARGE DISTRIBUTION

The distribution of total ($\pi + \sigma$) atomic charges is given in Fig. 2 These distributions are rather insensitive to distant structural modifications, especially if they concern only the σ-bonds. Atomic charges in the

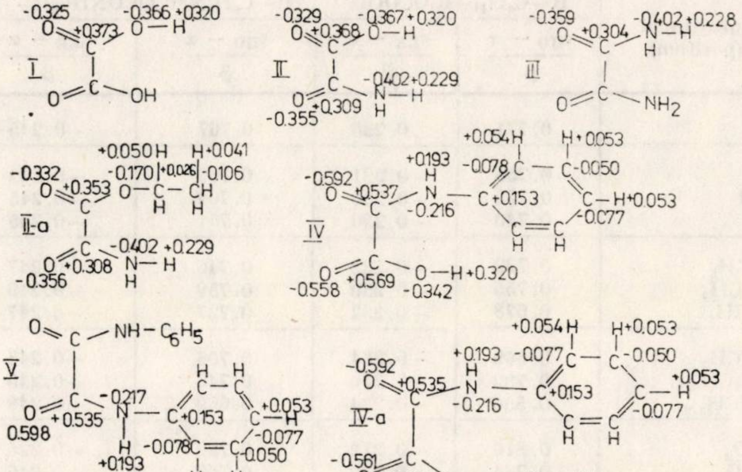
I
-0.325
+0.373
-0.366
+0.320
OH
II
-0.329
+0.368
-0.367
+0.320
-0.402
+0.229
+0.309
-0.355
III
-0.359
+0.304
-0.402
+0.228
NH2
II-a
-0.332
+0.353
+0.050 H
H +0.041
-0.170
+0.026
-0.106
-0.402
+0.229
+0.308
-0.356
IV
-0.592
+0.537
+0.193
-0.216
+0.054 H
H +0.053
-0.078
-0.050
+0.153
H +0.053
-0.077
+0.569
-0.558
-0.342
H +0.320
V
NH − C6H5
-0.217
+0.535
0.598
+0.193
+0.153
+0.053
-0.077
-0.078
-0.050
+0.054
+0.053
IV-a
-0.592
+0.535
+0.193
-0.216
+0.054 H
H +0.053
-0.077
-0.050
+0.153
+0.053
-0.077
-0.561
+0.545
-0.145
+0.026
-0.106
H +0.050
H +0.041

Fig. 2. — Total ($\sigma + \pi$)-atomic charges. Significance of I—V as in Fig. 1 ; II-a : ethyl ester of oxamic acid ; IV-a : ethyl ester of oxamic acid.

C_2H_5 group, for example, are the same in ethyl esters of oxalic acid (II-a) and of oxanilic acid (IV-a). Substitution of H by C_2H_5 does not change distributions within the single C—C bond in the oxalic acid residue (compare II and II-a or IV and IV-a).

INFLUENCE OF SUBSTITUTION IN PHENYL CYCLES

The influence of substitution in phenyl cycles was considered by the perturbational method described in a previous paragraph as concerns the π-electronic systems and by Del Ré calculations on the substituted molecules, for the σ-bond systems.

Variations in the energy of frontier orbitals (ε_{HO}, ε_{LE}) were calculated by eq. (1) while the shift of π-electronic charges from the substituent to the parent molecule were calculated by formula (2). In case of the CH_3O—, Cl—, $(CH_3)_2N$— substituents, considered with one atomic orbital with 2 π-electrons, this shift is given by the interaction of the substituent with the unoccupied molecular orbitals of the unsubstituted molecule. For substitution by the —NO_2 group, considered with one empty atomic orbital, the shift results by interaction with the occupied molecular orbitals of the unsubstituted molecule.

The frontier orbitals of substitution derivatives of oxanilic acid and of the oxanilide are listed in Table 3. The total electric charge of the substituent resulted by interaction with the unsubstituted molecule, Δq, and separately the effect of π-interactions Δq_π and of σ-interactions Δq_σ are listed in Table 4. The effect of one substituent upon the frontier orbi-

TABLE 3

Frontier orbital energies in substitution derivatives of oxanilic acid and oxanilides

Substituent (position)	$R-C_6H_4NHCOCOOH$		$R-C_6H_4NHCOCONHC_6H_4-R$	
	$\frac{\varepsilon_{HO}-\alpha}{\beta}$	$\frac{\varepsilon_{LE}-\alpha}{\beta}$	$\frac{\varepsilon_{HO}-\alpha}{\beta}$	$\frac{\varepsilon_{LE}-\alpha}{\beta}$
H	0.771	0.230	0.767	−0.245
o-Cl	0.755	−0.231	0.759	−0.245
m-Cl	0.766	−0.230	0.764	−0.245
p-Cl	0.740	−0.230	0.751	−0.245
o-OCH_3	0.722	−0.232	0.740	−0.247
m-OCH_3	0.755	−0.230	0.759	−0.245
p-OCH_3	0.678	−0.232	0.727	−0.247
o-$N(CH_3)_2$	0.669	−0.234	0.706	−0.248
m-$N(CH_3)_2$	0.732	−0.230	0.746	−0.245
p-$N(CH_3)_2$	0.586	−0.234	0.659	−0.249
o-NO_2	0.810	−0.212	0.789	−0.226
m-NO_2	0.784	−0.230	0.760	−0.245
p-NO_2	0.847	−0.212	0.812	−0.225

tals of monoanilides is about 2 times larger than for dianilides because the atomic orbital coefficients c_{qi} (for substituted atoms) in the phenyl cycle are about $\sqrt{2}$ times larger for monoanilides than for oxanilides. The π-charge shift on the substituent, Δq_π, must be about the same in both cases, the previous effect being compensated by an almost doubled number of molecular π-orbitals for oxanilides.

TABLE 4

Substituent charges due to interaction with the electronic system of oxanilic acid. Δq : total substituent charge ; Δq_π — part due to π-electronic interactions ; Δq_σ — part due to σ-bond interactions

Substituent	Δq_π	Δq_σ	Δq
R	0.000	0.053	+0.053
$o-Cl$	+0.030	−0.155	−0.125
$m-Cl$	+0.032	−0.155	−0.123
$p-Cl$	+0.026	−0.155	−0.129
$o-OCH_3$	+0.051	−0.125	−0.074
$m-OCH_3$	+0.053	−0.125	−0.072
$p-OCH_3$	+0.045	−0.125	−0.080
$o-NO_2$	−0.129	−0.188	−0.317
$m-NO_2$	−0.103	−0.188	−0.291
$p-NO_2$	−0.144	−0.188	−0.332
$o-NMe_2$	+0.078	—	—
$m-NMe_2$	+0.074	—	—
$p-NMe_2$	+0.074	—	—

The total electric charge, Δq of substituents is the result of the electron attracting effect in the σ-bond system and of the electron donor effect in the π-system (except for $-NO_2$). The π-charge shift, Δq_π was calculated only for oxanilic acid derivatives, while the σ-charge shift Δq_σ, also for some oxanilide derivatives, but as discussed above, the total shift Δq must be about the same for a substituent both on oxanilic acid and on oxanilide derivatives. The π-effect, Δq_π depends rather strongly upon the *ortho*, *meta* or *para* position of the substituent with respect to the anilide N-atom, but the σ-effect Δq_σ is insensitive to the substituents' position. Distribution of σ-charges in CH_3O- and $-NO_2$ are given in Fig. 3.

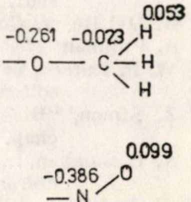

Fig. 3. — Atomic σ-charges in the methoxy and nitro groups.

All substituents are negatively charged, the σ-effect predominates, but as it decreases strongly with the distance, the π-effect will be more important for reactivity.

The substituent effect upon the lowest empty orbital, Φ_{LE} is low, as the Φ_{LE}'s of anilides correspond approximately to those of oxalic acid or oxamide, with only a small admixture of benzenic orbitals (Table 1).

The effect upon highest occupied orbitals, Φ_{HO} is large, the Φ_{HO}'s of anilides corresponding approximately to Φ_{HO} of aniline. The $-NO_2$ orbital ($\alpha_{NO_2} = \alpha - 0.40\beta$) is above the Φ_{LE} of oxanilic acid ($\varepsilon_{LE} = \alpha - 0.23\beta$) and of the oxanilide ($\varepsilon_{LE} = \alpha - 0.2458\beta$). This order is maintained even in the *meta* substituted derivative where the energy of the NO_2-orbital is decreased by $\Delta\varepsilon \cong 0.13\beta$.

CONCLUSIONS

The ω-HMO calculations indicate a rather low ε_{LE}-value for oxalic acid and all its derivatives, i.e. a reducing character which must increase in the order: oxamide < oxamic acid < oxalic acid < oxanilide < oxanilic acid. Of the substituents, NO_2 in *ortho* and *para* positions will enhance the reducing character. The energy of the highest occupied orbital, ε_{HO} increases sensibly from oxalic acid to oxalamides and oxanilides; a bathochromic effect in the electronic spectra is thus expected. The calculated charge distribution is not changed from acid to ethyl-esters, except the atoms in first and second vicinity to the C_2H_5 group. The substituents $Cl-$, CH_3O-, NO_2 become negative charges as a result of the combined π and σ-electronic interactions, but Cl- and especially CH_3O-donate electrons in the π-bond system.

REFERENCES

[1] A. Muste, R. Nuţiu and C. Csunderlik, *Analele Univ. Timişoara, Serie Fiz. Chim.*, **18(2)**, 53 (1979).
[2] A. Muste, C. Csunderlik and R. Nuţiu, *Analele Univ. Timişoara, Serie Fiz. Chim.*, **19(1)**, 2 (1980).
[3] A. Muste, Doctoral Thesis, in preparation.
[4] A. Streitwieser Jr., "Molecular Orbital Theory for Organic Chemistry", Wiley, New York, 1961.
[5] G. Del Ré, *J. Chem. Soc.*, **1958**, 4031.
[6] A. Pullman, *Modern Quantum Chemistry*, **3**, 283 (1965).
[7] W. P. Purcell, in "Biological Activity and Chemical Structure", Jane A. Keverling Buisman editor, Elsevier, Amsterdam, 1977, p. 281.
[8] Z. Simon, "Biochimie Cuantică şi Interreacţii Specifice", Ed. ştiinţifică, Bucureşti, 1973, chap. 2.
[9] A. T. Balaban, L. Birlădeanu, J. Bally, P. T. Frangopol, M. Mocanu and Z. Simon, *Tetrahedron*, **19**, 2199 (1963).
[10] G. Del Ré and B. Pullman, *J. Chem. Phys.*, **62**, 942 (1965).

Revue Roumaine de Chimie, 27, 1, 129–136 (1982)

REACTIVITY OF *m*-NITROPHENYL ACETATE IN EXCITED STATE

V. E. SAHINI, C. BENDIC and L. VIRAG

Department of Physical Chemistry and Electrochemical Technology, Polytechnic Institute,
Bd. Republicii 13, Bucharest, Romania

Received March 10, 1981

The acid and base photohydrolyses of *m*-nitrophenyl acetate, irradiated with $\lambda=254$ nm in $0.5-4$ mol l^{-1} $HClO_4$ and in a buffered solution at pH = 9.36 respectively, were studied. The products of photochemical reactions were the same as for the hydrolysis in the ground state. The quantum yields were determined in the presence of the inner filter effect and the simultaneous thermal reaction using an iterative method. A mechanism was proposed to explain the linear dependence of the reciprocal values of the quantum yield and acid concentration. The specific *meta* activation by nitro group was correlated with the change in the electronic structure induced by excitation. The charge densities for the ground state and for the first excited singlet and triplet states were calculated using the SCF-CI method.

The aromatic heterolytic photosubstitution reactions became a subject of large interest after the observation of R.O. de Jongh that nitrophenyl esters and ethers, stable in aqueous solution in the dark, undergo a striking smooth light-induced hydrolysis in neutral or alkaline solutions.[1] The photosubstitution was soon found to occur with other aromatic esters, ethers, halogeno-compounds, polycyclic and some heterocyclic compounds, in reaction with a variety of nucleophiles,[2,3] opening interesting new possibilities for the organic synthesis.

From the study of these heterolytic processes the following empirical classification could be ruled out[4]: a) nucleophilic photosubstitution of aromatic compounds activated by electron attracting substituents ($-NO_2$, $-COCH_3$, $-NO$, $-CN$). In these reactions a *meta* or *meta/ortho* activation is observed in contrast to the well-known *ortho/para* activation of the normal ground state reactions; b) nucleophilic photosubstitution of aromatic compounds activated by electron donating groups ($-OH$, $-OR$, $-NR_2$, $-R$), when *ortho/para* activation is observed; c) α-reactivity in polycyclic aromatics and d) merging resonance stabilization in product formation.

It may be remarked that while the reaction pattern observed in this category of heterolytic photosubstitution reactions does not exhibit a relation to the calculated localization energies in the S_1 state,[2,5] in some cases there is a direct correspondence to the charge densities in the excited singlet state of the molecule,[4,5,6] or in the radical cation formed by loss of an electron.[4] Beside quantum yield determination, numerous attempts were made to find the nature of the reacting excited species by the sensitization, quenching and flash techniques.[7–11]

The purpose of the present work is to study the acid and base hydrolysis of *m*-nitrophenyl acetate in the first excited state and to correlate its reactivity with the change in the electronic structure induced by excitation.

EXPERIMENTAL

The acid hydrolysis of *m*-nitrophenyl acetate (5×10^{-4} mol l^{-1}) both in the ground and excited state was carried out in aqueous solutions containing two per cent methanol and perchloric acid in a concentration range 1–4 mol l^{-1}. For the base hydrolysis only a buffered solution at pH = 9.36 was used. The ester solutions were irradiated at 254 nm in a silica cell (1 cm) using a low-pressure Hg-lamp (Original-Hanau, 77 w). The intensity of the incident light was measured with potassium ferrioxalate actinometer and was found, for the appropriate geometry, to be $Q_0 = 5.63 \times 10^{-4}$ einstein l^{-1} min^{-1}. In order to calculate the quantum yield for a photochemical reaction accompanied by a thermal one, the total absorption condition at each moment of the reaction was required; the initial concentration and the pathway length used make possible the achievement of this condition.

The hydrolysis was followed to practical total conversion of the ester and the only reaction product was identified to be *m*-nitrophenol, by means of thin-layer chromatography (silicagel Merck GF 254).

The kinetics of the reaction was studied spectrophotometrically, the chemical change in the system being monitored by the ultraviolet absorption spectra recorded at various moments during the irradiation, using a spectrophotometer SPECORD UV-VIS. The following values for the molar absorption coefficients of *m*-nitrophenyl acetate (ε_A), *m*-nitrophenol (ε_P) and *m*-nitrophenoxide ion (ε_{P-}) were obtained at 254, 330 and 392 nm: $\varepsilon_A^{254} = 6.91 \times 10^3$ l mol^{-1} cm^{-1}, $\varepsilon_A^{330} = 5.15 \times 10^2$ l mol^{-1} cm^{-1}, $\varepsilon_P^{254} = 3.28 \times 10^3$ l mol^{-1} cm^{-1}, $\varepsilon_P^{330} = 1.91 \times 10^3$ l mol^{-1} cm^{-1}, $\varepsilon_{P^-}^{254} = 1.02 \times 10^4$ l mol^{-1} cm^{-1} and $\varepsilon_{P^-}^{393} = 1.48 \times 10^3$ l mol^{-1} cm^{-1}.

RESULTS AND DISCUSSION

The kinetics of the acid hydrolysis of *m*-nitrophenyl acetate was followed using the spectrophotometric measurements on the *m*-nitrophenol band at 330 nm which is only slightly superposed over the broad band of *m*-nitrophenyl acetate centered at 265 nm. The amount of reacted *m*-nitrophenyl acetate can thus be determined monitoring the increase in the optical density at 330 nm due to *m*-nitrophenol formed during the thermal and photochemical reaction; the absorbance of *m*-nitrophenol at this wavelength was corrected for the absorbance of *m*-nitrophenyl acetate.

For the base hydrolysis the increasing absorbance of *m*-nitrophenoxide at 392 nm was recorded.

The absorption spectra recorded during the photochemical hydrolysis present the same sharp isosbestic points as those corresponding to the thermal reaction (Fig. 1).

This feature is an additional evidence in the favour of *m*-nitrophenol formation in the photochemical reaction. In the neutral and very low acid concentrated solutions there are not longer true isosbestic points due to some secondary photoreactions (probably photo-Fries rearrangements *via* a radicalic mechanism) which become preponderant; this fact points out the role of the proton in the mechanism of the photochemical heterolytic process.

One may conclude that in the ground state as well as in the excited state the main process is the hydrolysis of *m*-nitrophenyl acetate to *m*-nitrophenol, but in the excited state the substrate undergoes hydrolysis

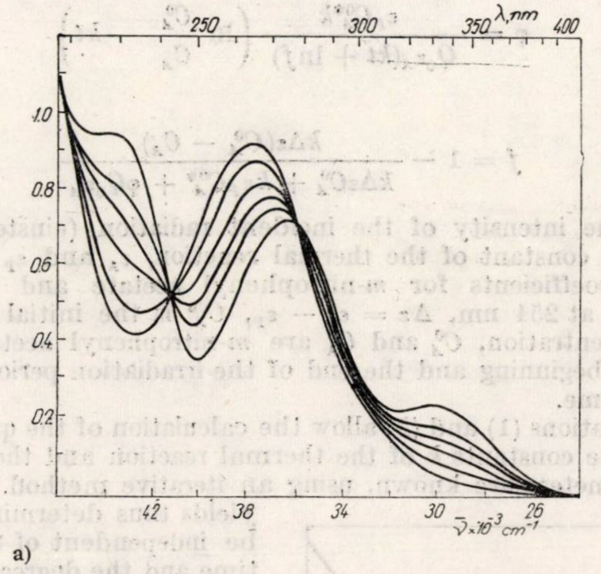

Fig. 1. — Ultraviolet absorption spectra taken at various moments during the irradiation: a) Acid photohydrolysis of *m*-nitrophenyl acetate; b) Base photohydrolysis of *m*-nitrophenyl acetate (pH = 9.36).

much more rapidly. The acid photohydrolysis is thus seventy times faster than the reaction in the ground state for 1 mol^{-1} acid concentration.

The accurate values of the quantum yield in the presence of the inner filter effect and simultaneous thermal reaction can be obtained, as was shown in another work, [12] only under the total absorption condition; in this case the integration of the rate equation led to the following relation:

$$\varphi = \frac{\varepsilon_P C_A^{0*} k}{Q_0 \varepsilon_A (kt + \ln f)} \left(\ln \frac{C_A^0}{C_A} - kt \right) \qquad (1)$$

where:

$$f = 1 - \frac{k \Delta\varepsilon (C_A^0 - C_A)}{k \Delta\varepsilon C_A^0 + k \varepsilon_P C_A^{0*} + \varphi Q_0 \varepsilon_A} \qquad (2)$$

and Q_0 is the intensity of the incident radiation (einstein.l^{-1}. min^{-1}), k is the rate constant of the thermal reaction, ε_A and ε_P are the molar absorption coefficients for *m*-nitrophenyl acetate and *m*-nitrophenol, respectively, at 254 nm, $\Delta\varepsilon = \varepsilon_A - \varepsilon_P$, C_A^{0*} is the initial *m*-nitrophenyl acetate concentration, C_A^0 and C_A are *m*-nitrophenyl acetate concentrations at the beginning and the end of the irradiation period, and t is the irradiation time.

The relations (1) and (2) allow the calculation of the quantum yields, when the rate constants k of the thermal reaction and the other experimental parameters are known, using an iterative method. The quantum yields thus determined proved to be independent of the irradiation time and the degree of conversion.

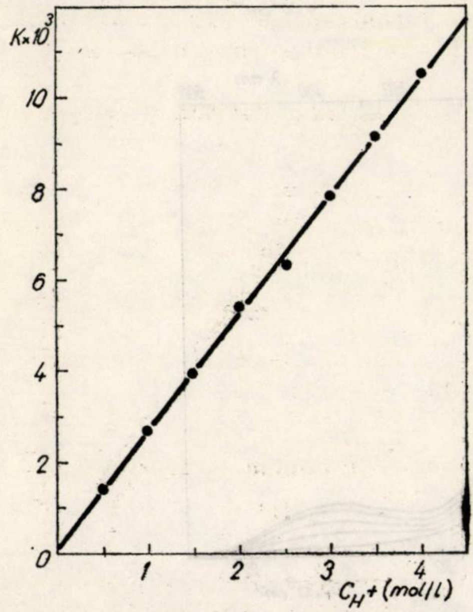

Fig. 2. — Observed rate constants for the acid hydrolysis of *m*-nitrophenyl acetate as function of the hydronium ion concentration.

The observed pseudo-first order rate constant k for the acid hydrolysis of *m*-nitrophenyl acetate in the ground state may be expressed as function of the hydronium ion concentration (perchloric acid) by the equation:

$$k = k_{H_2O} + k_{H^+} C_{H^+} \qquad (3)$$

where k_{H_2O} is the pH-independent rate constant, k_{H^+} is the rate constant for the hydronium ion catalysed reaction and C_{H^+} is the hydronium ion concentration. From the intercept and slope of the plot of the observed rate constants k (determined for different perchloric acid concentrations) *vs.* C_{H^+} (Fig. 2), it were obtained $k_{H_2O} = 7.5 \times 10^{-5}\ \mathrm{min}^{-1}$ and $k_{H^+} = 2.59 \times 10^{-3}\ \mathrm{l\ mol^{-1}\ min^{-1}}$, respectively.

These values allow the calculation of the rate constant for any desired acid concentration.

For the alkaline hydrolysis the rate constant at $\mathrm{pH} = 9.36$ was $k = 1.74 \times 10^{-1}\ \mathrm{min}^{-1}$.

Relevant data were obtained from the study of the acid concentration influence. In order to obtain a substantial quantum yield the acid has to be present in a high concentration (1 to 4 mol l^{-1} or higher). This is consistent with the idea of a bimolecular process in which one of the partners has a short-lived excited state. The quantum yield determined in the manner described above increases with the increasing acid concentration and tends towards a constant upper value at a very high acid concentration as is shown in figure 3 (when acid concentrations higher than 4 mol l^{-1} were used, the quantum yield determination was very difficult, and the obtained values are uncertain due to the very fast thermal reaction).

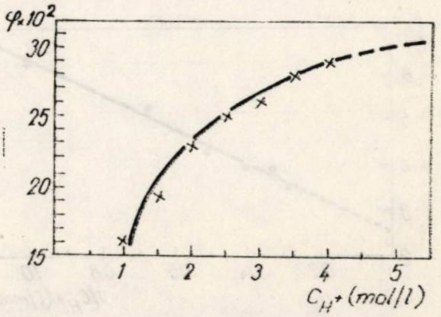

Fig. 3. — Quantum yields for the acid photohydrolysis of *m*-nitrophenyl acetate as function of the acid concentration.

The result suggests a competition between the spontaneous deactivations of the excited molecules and their encounters with the proton. However, even if the acid is present in a high concentration, the quantum yield remains significantly below 1 ; this means that the encounters between the excited molecule and proton lead either to reaction or to quenching.

In order to explain the experimental data the following reactino scheme was proposed :

$$\mathrm{A} \xrightarrow{h\nu} A^*$$

$$\mathrm{A}^* \xrightarrow{k_Q} \mathrm{A}$$

$$\mathrm{A}^* + \mathrm{H}^+ \xrightarrow{k'_Q} \mathrm{A} + \mathrm{H}^+$$

$$\mathrm{A}^* + \mathrm{H}^+ \xrightarrow{k_H} (\mathrm{AH}^+)^* \left| \begin{array}{l} \xrightarrow{k_P} \text{Products} \\ \xrightarrow{k_D} \mathrm{A} + \mathrm{H}^+ \end{array} \right.$$

According to this scheme an excited molecule may undergo the following processes : a) deactivation by fluorescence or internal conversion (k_Q) ; b) quenching (k'_Q) or protonation (k_H) by the encounter with the proton. The excited protonated species lead either to the product formation (k_P) or to the dissociative quenching (k_D).

Applying the steady state approximation it was obtained the following relation between the reciprocal values of the quantum yield and the proton concentration :

$$\frac{1}{\varphi} = \frac{(k_P + k_D)(k'_Q + k_H)}{k_P k_H} + \frac{k_Q(k_P + k_D)}{k_P k_H} \cdot \frac{1}{C_{H^+}} \qquad (4)$$

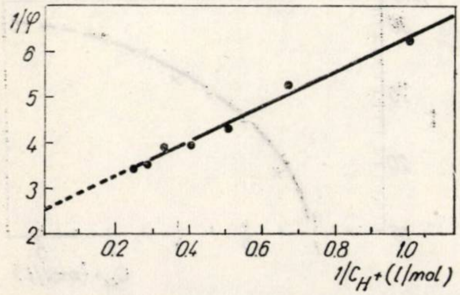

Fig. 4. — Reciprocal of quantum yield *versus* reciprocal of the acid concentration for the photohydrolysis of *m*-nitrophenyl acetate.

This linear relationship is consistent with the constant quantum yield value at the very high acid concentration and is also in agreement with the experimental data ; the plot $1/\varphi$ *vs.* $1/C_{H^+}$ (Fig. 4) gives a linear correlation given by the equation :

$$\frac{1}{\varphi} = 2.252 + 3.80 \frac{1}{C_{H^+}} \qquad (5)$$

From the relations (4) and (5) one can obtain some information about the reaction rates involved in the scheme (3). The ratio of the intercept and the slope is $(k'_Q + k_H)/k_Q = 0.66\ \mathrm{l\,mol^{-1}}$. Therefore, for an acid concentration of $1.5\ \mathrm{mol\,l^{-1}}$ the reactions with the proton and the spontaneous deactivation are in balance. This means that out of two excited molecules one encounters a proton and the other deactivates.

The ratio $k'_Q/k_H = \alpha$ ascertains the ratio between the rate constants for the dissociative quenching and the product formation of the excited protonated species $k_D/k_P = (1.52 - \alpha)/(1 + \alpha)$, where $0 \leqslant \alpha \leqslant 1.52$. For $\alpha \simeq 0$ $(k_H \gg k'_Q)$, this ratio has a maximum value $k_D/k_P = 1.52$ and $k_Q/k_H = 1.52\ \mathrm{mol\ l^{-1}}$, while for the other limit value $\alpha = 1.52$, the dissociative quenching of the excited protonated species is negligible $(k_P \gg k_D)$ and $k_Q/k_H = 3.82\ \mathrm{mol\ l^{-1}}$.

The base photohydrolysis of *m*-nitrophenyl acetate was carried out only at pH = 9.36. The very fast thermal conversion of the substrate in the base hydrolysis did not allow the use of the more alkaline solutions, the quantum yield determination being difficult and affected by important errors. The same acceleration of the hydrolysis was observed, but the quantum yield ($\varphi = 0.014 \pm 0.002$) was much greater than the extrapolated value at the corresponding acid concentration in the acid catalysed reaction.

CALCULATIONS

In order to correlate the reactivity of *m*-nitrophenyl acetate with the change in the electronic structure induced by excitation, the charge densities for the ground state and for the first excited singlet and triplet states were calculated by the SCF-CI method using a computer program written in **FORTRAN IV.** [13]* The results of this calculation are given in figure 5.

One may notice that $S_0 \rightarrow S_1$ transition is accompanied by a large charge transfer from the aromatic ring and esteric oxygen to the nitro group, leading to an important decrease of the charge density of the *meta* position. This decrease is more pronounced in the singlet state than in the triplet one. As a result of this process, in the excited protonated

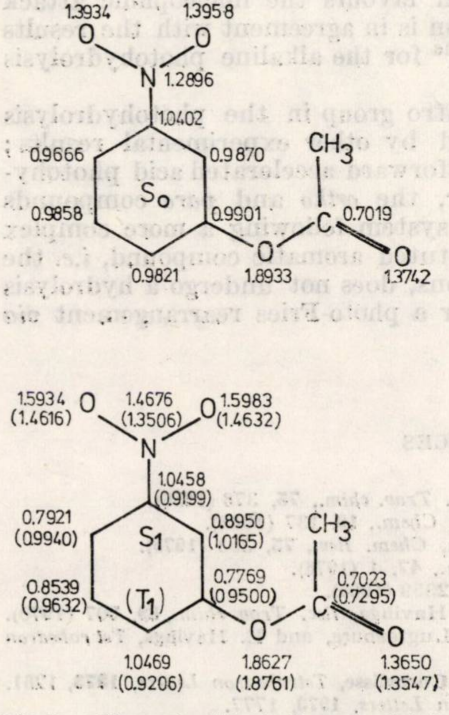
1.3934
1.3958
O
O
N 1.2896
1.0402
0.9666
0.9870
CH3
S0
0.9858
0.9901
C 0.7019
O
O
0.9821
1.8933
1.3742
1.5934 (1.4616)
1.4676 (1.3506)
1.5983 (1.4632)
N
1.0458 (0.9199)
0.7921 (0.9940)
S1
0.8950 (1.0165)
CH3
0.8539 (0.9632)
(T1)
0.7769 (0.9500)
0.7023 (0.7295)
C
1.0469 (0.9206)
1.8627 (1.8761)
1.3650 (1.3547)

Fig. 5. — Charge densities in the ground state and first excited singlet and triplet states of *m*-nitrophenyl acetate.

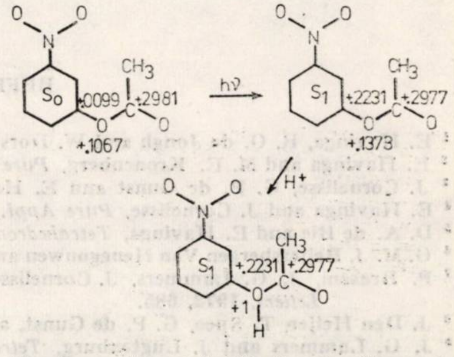
S0
CH3
.0099
+.2981
+.1067
hν
S1
+.2231
+.2977
+.1373
H+
+1
H

Fig. 6. — Charge distribution in the reaction centre before and after protonation.

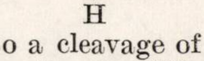

species the group $-\mathrm{C}-\underset{\displaystyle \mathrm{H}}{\overset{+}{\mathrm{O}}}-\mathrm{C}\lessdot$ is the centre of a great electrostatic repulsion leading to a cleavage of one C—O bond in the product-forming step before the deactivation (Figure 6).

These theoretical results support the singlet state of *m*-nitrophenyl acetate as reacting species in the acid photohydrolysis (by irradiation with 254 nm, the first singlet state is reached by internal conversion of the second singlet state). Some experimental data seem also to be consistent with the hypothesis that the acid photohydrolysis proceeds *via* the first excited singlet state. Thus, the photohydrolysis is not sensitized by benzophenone (using 313 nm radiation) and is not diminished by the presence of the oxygen in the system. Besides, the acid has to be present in a high concentration in order to obtain a substantial quantum yield, suggesting a bimolecular step (protonation) in which one of the partners has a short-lived excited state.

---

* The ionization energies and affinities according to Hinze and Jaffé [14] were used and the two-centre bielectronic repulsions were calculated by the Nishimoto-Mataga approximation. [15]

In the base photohydrolysis of *m*-nitrophenyl acetate, the decrease of the charge density in *meta* position favours the nucleophilic attack of OH^- at this position. This assumption is in agreement with the results of the isotopic study of Havinga et al.[16] for the alkaline photohydrolysis of *m*-nitroanisole.

The specific *meta* activation by nitro group in the photohydrolysis of *m*-nitrophenyl acetate is supported by other experimental results; thus in contrast to the simple, straightforward accelerated acid photohydrolysis exhibited by the *meta* isomer, the *ortho* and *para* compounds yield a variety of photoproducts, the system following a more complex reaction pattern. Besides, the unsubstituted aromatic compound, *i.e.* the phenyl acetate under the same conditions, does not undergo a hydrolysis *via* a heterolytic mechanism but rather a photo-Fries rearrangement *via* a radicalic mechanism.[17]

REFERENCES

[1] E. Havinga, R. O. de Jongh and W. Dorst, *Rec. Trav. chim.*, **75**, 378 (1956).
[2] E. Havinga and M. E. Kronenberg, *Pure Appl. Chem.*, **16**, 137 (1968).
[3] J. Cornelisse, G. P. de Gunst and E. Havinga, *Chem. Rev.*, **75**, 353 (1975).
[4] E. Havinga and J. Cornelisse, *Pure Appl. Chem.*, **47**, 1 (1976).
[5] D. A. de Bie and E. Havinga, *Tetrahedron*, **21**, 2359 (1965).
[6] G. M. J. Beijersbergen Van Henegouwen and E. Havinga, *Rec. Trav. chim.*, **89**, 907 (1970).
[7] P. Brasem, J. G. Lammers, J. Cornelisse, J. Lugtenburg, and E. Havinga, *Tetrahedron Letters*, **1972**, 685.
[8] J. Den Heijer, T. Spee, G. P. de Gunst, and J. Cornelisse, *Tetrahedron Letters*, **1973**, 1261.
[9] J. G. Lammers and J. Lugtenburg, *Tetrahedron Letters*, **1973**, 1777.
[10] G. P. de Gunst and E. Havinga, *Tetrahedron*, **29**, 2167 (1973).
[11] E. Ullmann and P. Singh, *J. Amer. Chem. Soc.*, **94**, 5077 (1972).
[12] C. Bendic and V. E. Sahini, *Rev. Roumaine Chim.*, to be published.
[13] C. Bendic, Mihaela Hillebrand and V. E. Sahini, *Rev. Roumaine Chim.*, **23**, 3 (1978).
[14] J. Hinze and H. H. Jaffé, *J. Amer. Chem. Soc.*, **84**, 540 (1962).
[15] K. Nishimoto and N. Mataga, *Z. phys. Chem. (Frankfurt)*, **13**, 140 (1957).
[16] R. O. de Jongh and E. Havinga, *Rec. Trav. chim.*, **85**, 275 (1966).
[17] C. Bendic and V. E. Sahini, unpublished data.

Revue Roumaine de Chimie, 27, 1, 137–140 (1982)

AN ANALYSIS OF THERMAL DECOMPOSITION OF COORDINATION POLYNUCLEAR COMPOUNDS IN Fe(III), Mn(II), Ni(II) SYSTEMS

MARIA BREZEANU, ECATERINA SAFARICA*,**
E. SEGAL*, LUMINIŢA PATRON* and TEODORA ROBU*****

*** Chair of Physical Chemistry and Electrochemical Technology, Polytechnical Institute of Bucharest, Bd. Republicii 13, Romania**
**** Chair of Inorganic Chemistry and Technology, Polytechnical Institute of Bucharest, Spl. Independenţei 202, Bucharest 77208, Romania**
***** Center of Physical Chemistry, Spl. Independenţei 202, Bucharest 77028, Romania**

Received April 8, 1981

The nonisothermal kinetic investigations of the thermal decomposition of coordination polynuclear compounds of Fe(III), Mn(II), Ni(II) is reported.

INTRODUCTION

The decomposition of solid coordination compounds belongs to the large class of endothermal decompositions in solid-gas systems and may be represented by the general chemical equation:

$$A(s) \rightarrow B(s) + C(g)$$

The decomposition reactions may be investigated both under isothermal and nonisothermal conditions. The latter ones have proved to be more efficient due to their rapidity and to the possibility to pursue a succession of processes which occur in a large temperature range.

The present paper contains the results of the investigations concerning the thermal stability of some coordination polynuclear compounds and a nonisothermal kinetic study of their thermal decomposition.

EXPERIMENTAL

The thermal stability of the following coordination polynuclear compounds in Fe(III), Mn(II), Ni(II) systems has been investigated:

$$(NH_4)_2[Fe_2(Mn,\ Ni)\ (CH_3COO)_6(OH)_4]\ (s) \qquad (1)$$

$$(NH_4)_8[Fe_2(Mn,\ Ni)\ (C_2O_4)_8]\ (s) \qquad (2)$$

$$(NH_4)_2[Fe_2(Mn,\ Ni)\ (C_2O_4)_2(OH)_6]\ (s) \qquad (3)$$

which were analysed according to the methods indicated in literature.[1] The substances have been ground and sieved, retaining the grains with a 90—95 μm diameter.

The thermal decomposition has been analysed under nonisothermal conditions by means of a MOM Budapest Paulik-Paulik-Erdey type derivatograph, in static air atmosphere at three different values of the heating rate: 2.5, 5 and 10 °C/min. The thermal decomposition has also been investigated under isothermal conditions in an electric thermostated furnace.

The IR spectra of the intermediates have also been studied by means of a 71 IR Specord.

RESULTS AND DISCUSSIONS

The experimental data show that the thermal decomposition of the investigated coordination compounds takes place in more than one stage as suggested by the thermogravimetric TG and the derivative thermogravimetric DTG curves. The processes of thermal decomposition are followed by phase transformation phenomena as pointed out on the differential thermal analysis DTA curve.

The kinetic analysis of the decomposition processes involved four methods different in principle.

1. the Coats-Redfern method[2] — an integral thermogravimetric method using only one thermogram for the evaluation of the kinetic parameters. For this method a FORTRAN program[3] has been used.
2. the Ozawa[4], Flynn-Wall[5] method—also an integral thermogravimetric method using more than one thermogram at different heating rates.
3. the Freemann-Carroll[6] method — a difference-differential method
4. the Kissinger[7] method — a differential thermogravimetric method applied to the maximum point of the derivative thermogravimetric curve.

a) The thermal decomposition of $(NH_4)_2\ Fe_2(Mn, Ni)(CH_3COO)_6(OH)_4]$

By progressive heating the thermal decomposition of the coordination compound exhibits three stages. The first stage which takes place with maximum rate at 95°C corresponds to a single process and, consequently, the kinetic parameters may be evaluated.

$$(NH_4)_2[Fe_2(Mn,\ Ni)(CH_3COO)_6(OH)_4]\ (s) \rightarrow$$

$$\rightarrow 2H_2O(g) + NH_3\ (g) + (NH_4)[Fe_2(Mn,\ Ni)(CH_3COO)_6\ (OH)O]\ \ (s)\quad (I)$$

1.1 intermediate

The determination of the 1.1 intermediate was achieved by means of the thermogravimetric data and by identifying the products emitted in the first stage of the thermal decomposition.

The kinetic parameters obtained are presented in table 1.

b) The thermal decomposition of $(NH_4)_8[Fe_2(Mn,\ Ni)\ (C_2O_4)_8]$

The thermogravimetric data indicate for this coordination compound a process of thermal decomposition in two stages. The former may be represented by the following chemical equation:

$$(NH_4)_8[Fe_2(Mn,\ Ni)\ (C_2O_4)_8]\ (s) \rightarrow$$

$$\rightarrow (NH_4)_6[Fe_2(Mn,\ Ni)\ (C_2O_4)_7]\ (s) +$$

2.1 intermediate

$$+ 2NH_3(g) + CO_2\ (g) + CO(g) + H_2O(g) \qquad (II)$$

This process of thermal decomposition takes place with maximum rate at 140°C. The results obtained are given in table 2.

The composition of the 2.1 intermediate was confirmed by means of the thermogravimetric data and qualitative analysis of the products evolved during the first stage of the thermal decomposition.

TABLE 1

Kinetic parameters value of reaction (I)

Method	n	E(kJ/mol)	$A(s^{-1})$
Coats-Redfern	0	45.6	2.45×10^{5}
Ozawa, Flynn-Wall	0	43.9	—
Freemann-Carroll	0	44.7	
Kissinger	—	46.4	—

By analysing tables 1 and 2 it is easy to see that all the methods used for the evaluation of the kinetic parameters of reaction (I) and respectively reaction (II) led to similar results within the limit of experimental errors.

c) The thermal decomposition of $(NH_4)_2[Fe_2(Mn, Si)\,(C_2O_4)_2\,(OH)_6]$

According to the results of the thermogravimetric analysis, the thermal decomposition of this coordination compound takes place in five stages: the maximum rates corresponding to the first four stages are recorded at 60°C, 95°C, 200°C and 245°C. The chemical equations corresponding to these processes are given below:

TABLE 2

Kinetic parameters values of reaction (II)

Method	n	E(kJ/mol)	$A(s^{-1})$
Coats-Redfern	0	57.5	6.03×10^{6}
Ozawa, Flynn-Wall	0	58.9	—
Freemann-Carroll	0	62.3	—
Kissinger	—	60.6	—

$$(NH_4)_2\ [Fe_2(Mn, Ni)(C_2O_4)_2(OH)_6](s) \xrightarrow{(III)}$$

$$\longrightarrow H_2O(g) + (NH_4)_2[Fe_2(Mn,\ Ni)(C_2O_4)_2(OH)_4O]\ (s) \xrightarrow{(IV)}$$

3.1 intermediate

$$\longrightarrow 2\ NH_3(g) + H_2O(g) + [Fe_2(Mn, Ni)(C_2O_4)_2(OH)_4\ (s) \xrightarrow{(V)}$$

3.2 intermediate

$$\longrightarrow H_2O(g) + [Fe_2(Mn, Ni)(C_2O_4)_2(OH)_2O]\ (s) \xrightarrow{(VI)}$$

3.3 intermediate

$$\longrightarrow [Fe_2(Mn, Ni)(C_2O_4)O_3]\,(s) + H_2O(g) + CO_2(g) + CO(g)$$

3.4 intermediate

The formulas of the intermediates were confirmed by means of the thermogravimetric data and the analysis of the gaseous reaction products. For the the 3.3 intermediate only the thermogravimetric data were used because of the difficulties encountered in isolating it. To establish the formulas of the 3.2 and 3.4 intermediates the IR spectra of the initial compound, the intermediates and the final compound were used. These spectra were interpreted according to the literature.[8-9]

For the evaluation of the kinetic parameters of (III) — (VI) reactions the thermogravimetric data at low heating rate were used, with a better resolution of the peaks corresponding to these processes. Consequently, no methods that required thermograms recorded at different heating rates were used, nor, did we use methods based on the difference of differentials, where more pairs of values (α, T) were needed.

The kinetic parameters of the (III)—(VI) reactions were evaluated using the Coats-Redfern method and they are presented in table 3.

The value experimentally obtained for the preexponential factor of the process (III) agrees satisfactorily with the expected value, based on the transition state theory.[10]

TABLE 3

Kinetic parameters values of reactions (III)—(VI)

Reaction	n	E(kJ/mol)	A(s^{-1})
(III)	1	98.6	6.78×10^{14}
(IV)	0	71.5	2.37×10^{9}
(V)	0	115.8	1.08×10^{12}
(VI)	0	72.3	1.03×10^{6}

CONCLUSIONS

1. The thermal decomposition of (1)—(3) coordination compounds has been investigated, outlining the specific character of each intermediate.

2. The kinetic parameters of (I) — (II) reactions were evaluated by four different methods.

3. A kinetic nonisothermal investigation of the coordination compound (3) decomposition has been performed.

REFERENCES

[1] Gh. Macarovici, "Chimie analitică cantitativă-Gravimetria", Ed. tehnică, București, 1979, p. 58.

[2] A. W. Coats and J. Redfern, *Nature*, **21**, 68 (1964).

[3] V. Marcu and E. Segal, *Rev. Chim. (București)*, **28**, 33 (1977).

[4] T. Ozawa, *Bull. Chem. Soc. Japan*, **38**, 1981 (1965).

[5] J. H. Flynn and L. A. Wall, *J. Res. Nat. Bur. Stand.*, **70**, 487 (1966).

[6] E. S. Freemann and B. Carroll, *J. Phys. Chem.*, **62**, 394 (1958).

[7] H. E. Kissinger, *J. Res. Nat. Bur. Stand.*, **57**, 217 (1956).

[8] I. G. Murgulescu, V. Em. Sahini and L. Bolfa, *St. și cerc. Chim. Acad. R.P.R.*, **9**, 585 (1961).

[9] P. D. Garn, *J. Thermal Anal.*, **13**, 581 (1978).

[10] K. Laidler, "Chemical Kinetics", McGraw Hill, London, 1966, p. 166.

Revue Roumaine de Chimie, 27, 7, 141–146 (1982)

PLASMA-INDUCED POLYMERIZATION. VII.*

SOME CHARACTERISTICS OF THIS NEW METHOD OF POLYMER SYNTHESIS**

CRISTOFOR I. SIMIONESCU and BOGDAN C. SIMIONESCU
Department of Organic and Macromolecular Chemistry, Polytechnic Institute, 6600 Jassy, Romania

Received August 14, 1981

The paper deals with plasma-induced homo- and copolymerizations, insisting on specific features of this new approach to polymer synthesis. Experimental results show the existence of "living" macroradicals; their use as macromolecular initiators in polymerization processes is exemplified.

INTRODUCTION

In the last years, numerous papers dealt with chemical reactions carried out in plasma conditions. The possibility of generating mono- and multifunctional radicals under the influence of electrical discharges created new highways for the transformation of practically all organic and elemento-organic compounds in macromolecular structures.

Macromolecular plasma-chemistry oriented in the following main directions:

— polymerization of common monomers

— polymerization of unconventional monomers (saturated hydrocarbons, aromatic derivatives, saturated cycles, etc.)

— surface grafting and/or modification of polymers (films, natural and synthetic fibres, fabrics).

— synthesis of biopolymer-like structures in simulated primeval Earth conditions.

Plasma polymerization presents, however, a number of limitations. So, irrespective of the nature of predominantly active species, side reactions take place simultaneously with the main process, and the structure and properties of plasma-obtained polymers considerably differ from those of the conventional ones, these polymers being generally amorphous and highly crosslinked.

---

* Part VI in *Polymer Bull.*, **5**, 61(1981).

** Part of the conference presented at the First Freiburg-Jassy Seminar on Polymer Chemistry, Freiburg, March 8–12, 1981

Plasma-induced polymerization (copolymerization)[1,2] is a new direction in macromolecular plasma-chemistry. In this particular case, the initiation reaction takes place in the gas phase and can be easily controlled; the molecular weight and polydispersity of the resulting polymers are directly related to the reaction conditions; and, at the same time, the activity of the propagating species appears to be unusually high and very stable in time, even at room temperature. One has to underline also that ultrahigh molecular weight polymers are yielded and that polymerization reactions occur at room temperature.

The present paper deals with some homopolymerization, copolymerization and block copolymerization reactions performed by plasma induction, underlining some features and advantages of the method.

EXPERIMENTAL

The general experimental procedure was previously described.[3,4] The monomers were purified with great care before use, introduced in Pyrex ampoules, frozen in liquid nitrogen after degassing, evacuated to $10^{-3} - 10^{-4}$ Torr and sealed. Electrical discharges were then operated between two electrodes situated on each ampoule at 4.0 and 6.5 cm from the sample (monomer or comonomer mixtures) and coupled to a high frequency discharge generator (frequency — 2.5 MHz, power — 100 W). The discharges were operated during 30 — 180 seconds. The samples were kept at room temperature, in dark, and opened after different periods of time.

The molecular weights of the obtained polymers were determined either by viscosity measurements (M_{LV}), using the limiting viscosity number — molecular weight relationship, or by light scattering (M_{LS}).

RESULTS AND DISCUSSION

1. Plasma-Induced Homopolymerizations and Copolymerizations

The results on plasma-induced bulk homopolymerization of styrene, acrylic acid, methacrylic acid, ethyl acrylate, methyl methacrylate and on plasma-induced solution homopolymerization of N-vinyl carbazole, styrene and acrylamide are presented in Table 1.

TABLE 1

Plasma-induced homopolymerizations

Polymerization conditions	Polymer
bulk homopolymerization	
— styrene, 180 s discharge, 45 days (post polym. period)	18 % yield, $M_{LS} = 3.87\cdot10^{7}$
— acrylic acid, 60 s, 3 hours	100 % yield, $M_{LS} = 2.21\cdot10^{6}$
— methacrylic acid, 60 s, 10 days	1.2 % yield, $M_{LV} = 1.35\cdot10^{7}$
— ethyl acrylate, 60 s, 9 days	1.8 % yield, $M_{LV} = 9.32\cdot10^{6}$
— methyl methacrylate, 60 s, 5 days	2.7 % yield, $M_{LS} = 1.63\cdot10^{7}$
solution homopolymerization	
— N-vinyl carbazole/benzene, 60 s, 30 days	3.8 % yield, $M_{LV} = 1.81\cdot10^{4}$
— styrene/benzene, 60 s, 10 days	0.3 % yield, $M_{LV} = 4.95\cdot10^{4}$
— acrylamide/water, 60 s, 10 days	7.9 % yield, $M_{LS} = 1.37\cdot10^{7}$

Both bulk and solution homopolymerization led to ultrahigh or high molecular weight polymers. Even if small amounts of polymers are yielded in some cases, the results on bulk polymerization of acrylic acid and on solution polymerization of acrylamide show that yields can be considerably improved.

Data on bulk copolymerization of some vinylic monomers are presented in Table 2. The copolymerization systems considered were methyl methacrylate (MMA, M_1) — styrene (S, M_2); methacrylonitrile (MAN, M_1) — styrene (M_2); methyl methacrylate (M_1) — alpha-methyl styrene (MS, M_2) and acrylonitrile (AN, M_1)—alpha-methyl styrene (M_2). Copolymer compositions were determined by ^{1}H-NMR spectroscopy; the data were processed according to the Kelen — Tüdös method (Figure 1).

TABLE 2

Copolymerization data

Copolymerization system		r_1	r_2
M_1	M_2		
MMA	S	0.41	0.57
MAN	S	0.21	0.34
MMA	MS	0.42	0.22
AN	MS	0.03	0.14

The copolymers obtained by plasma-induced polymerization have compositions very close to those obtained by classical radical copolymerization. Considering, in addition, that the presence of radical polymerization inhibitors impede the development of the reaction, while the presence of water does not, one can presume that a radical mechanism of polymerization has to be taken into account in studying plasma-induced polymerization.

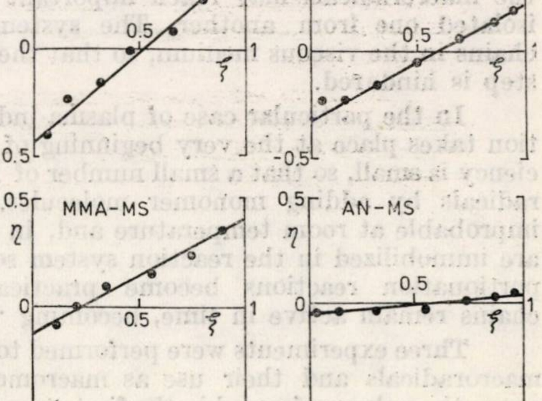

Fig. 1. — The Kelen — Tüdös plots of the studied copolymerization systems.

2. "Living" Macroradicals. The Mechanism of Plasma-Induced Polymerization

In all studied cases, an increase of the molecular weight of polymers, in time (post-polymerization period), was noticed; for instance, in the particular case of low conversion bulk polymerization of styrene, the molecular weight (M_{LS}) increased to $2.0 \cdot 10^7$ in about 400 hours, while the relative viscosity of the reaction system increased about 200 times in the same period.[5] These observations led to the idea of the existence of "living" (long-lived) macroradicals in such systems.

The classical kinetic model of free radical polymerization kinetics involves the unimolecular decomposition of the initiator, to produce free radicals, a fraction of which then add to the monomer, to initiate the active polymer chain. The active chain either propagates and grows by adding more monomer, or stops its growth by undergoing chain transfer with different species (initiator, monomer, polymer, solvent, impurity, deliberately added chain transfer agent) or by terminating in a bimolecular reaction with another active chain.

This model assumes that the reactivities of the growing chains are independent of their lengths and that the termination rate constant is also independent of the chain length. However, theoretical and experimental work has shown, last years, that, in diffusion controlled reactions, the termination rate constant is function of the chain length.[6,7]

Two different cases can be considered in radical polymerization processes :

i) when the resulting polymer is not soluble in the reaction medium, the growing macroradicals precipitate and form a second phase together with the "dead" polymer. The interaction of two growing chains may be very slow, these being coiled and occluded in dead polymer particles[8];

ii) when the resulting polymer is soluble in the reaction medium, the milieu may become very viscous due to conversion to polymer and to the increase of the molecular weight ; at a small initiator concentration, the macroradicals may reach important lengths and become practically isolated one from another. The system may immobilize the growing chains in the viscous medium, so that the diffusion controlled termination step is hindered.

In the particular case of plasma-induced polymerization, the initiation takes place at the very beginning of the reaction. The initiation efficiency is small, so that a small number of radicals become growing macroradicals by adding monomer molecules. Transfer reactions are highly improbable at room temperature and, in time, part of the macroradicals are immobilized in the reaction system so that recombination or disproportionation reactions become practically impossible. The ultralong chains remain active in time, becoming "living" macroradicals.

Three experiments were performed to prove the existence of "living" macroradicals and their use as macromolecular initiators. In all three cases, the polymer formed in the first stage was kept at room temperature for long periods of time and then a new amount of monomer was added, under vacuum conditions. The results are schematically represented in Figure 2.

CONCLUSIONS

Plasma-induced polymerization is a new method of polymer synthesis which leads to ultralong macromolecular compounds. The process occurs at room temperature, by a radical mechanism. The experimental

c. 1625

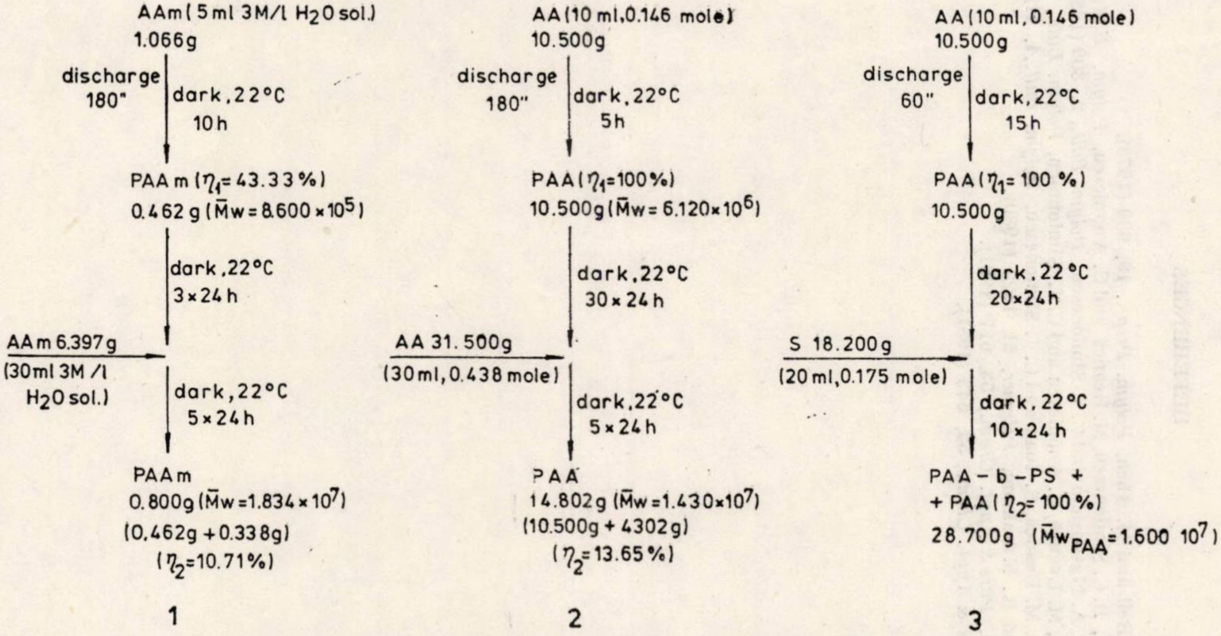
AAm (5 ml 3M/l H2O sol.)
1.066g
discharge
180"
dark, 22°C
10 h
PAAm (η1 = 43.33 %)
0.462 g (M̄w = 8.600 × 10^5)
dark, 22°C
3 × 24 h
AAm 6.397g
(30ml 3M/l
H2O sol.)
dark, 22°C
5 × 24 h
PAAm
0.800g (M̄w = 1.834 × 10^7)
(0.462g + 0.338g)
(η2 = 10.71%)
1
AA (10 ml, 0.146 mole)
10.500g
discharge
180"
dark, 22°C
5h
PAA (η1 = 100%)
10.500g (M̄w = 6.120 × 10^6)
dark, 22°C
30 × 24 h
AA 31.500g
(30 ml, 0.438 mole)
dark, 22°C
5 × 24 h
PAA
14.802g (M̄w = 1.430 × 10^7)
(10.500g + 4302g)
(η2 = 13.65 %)
2
AA (10 ml, 0.146 mole)
10.500g
discharge
60"
dark, 22°C
15h
PAA (η1 = 100 %)
10.500g
dark, 22 °C
20 × 24h
S 18.200g
(20 ml, 0.175 mole)
dark, 22°C
10 × 24 h
PAA - b - PS +
+ PAA (η2 = 100 %)
28.700g (M̄w PAA = 1.600 10^7)
3

Fig. 2. — Schematic representation of experiments performed to prove the existence of "living" macroradicals. AAm — acrylamide; AA — acrylic acid; S — styrene.

data, theoretically justified, prove the existence of "living" macroradicals, appearing in plasma-induced polymerization conditions, both in homogeneous and heterogeneous media.

REFERENCES

[1] Y. Osada, A. T. Bell and M. Shen, *Polym. Prepr.*, **19**, 639 (1978).
[2] C. I. Simionescu, B. C. Simionescu, M. Leancă and C. Ananiescu, *Polym. Bull.*, **5**, 61(1981).
[3] B. C. Simionescu, A. Natansohn and C. I. Simionescu, *Polym. Bull.*, **2**, 809 (1980).
[4] B. C. Simionescu, M. Leancă, C. Ananiescu and C. I. Simionescu, *Polym. Bull.*, **3**, 437 (1980).
[5] B. C. Simionescu, M. Leancă, S. Ioan and C. I. Simionescu, *Polym. Bull.*,**4**, 415 (1981).
[6] T. Yasukawa and K. Murakami, *Polymer*, **21**, 1423 (1980).
[7] K. F. O'Driscoll, *Pure & Appl. Chem.*, **53**, 617 (1981).
[8] A. Chapiro, *Pure & Appl. Chem.*, **53**, 643 (1981).

Revue Roumaine de Chimie, 27, 1, 147–154 (1982)

THERMAL CONDUCTIVITY IN $Ca(NO_3)_2 \cdot 4H_2O - nH_2O$ SYSTEM

S. STERNBERG* and A. MASCAŞ**

* Polytechnic Institute, str. Polizu no. 1, Bucharest, Romania
** Physical Chemistry Laboratory, Higher Education Institute, str. Armatei Roşii no. 5, Oradea — Romania

Received December 23, 1980

The thermal conductivity in $Ca(NO_3)_2 \cdot 4H_2O - nH_2O$ system was studied over an $n = 0 \div 60$ concentration range and a 313–343 K temperature range. The equipment employed was devised by the authors. For n within 3–60 range the dependence of thermal conductivity on molarity is linear while at higher concentrations considerable deviations from linearity are present. The relative thermal conductivity does not depend on temperature in the former concentration, C_I range and the concentration dependence is described by the expression $\lambda_r = 1 + \beta C$. At higher concentrations the relative thermal conductivity depends on temperature while its concentration dependence is exponential : $\Delta\lambda = A . \exp\,[-B.n/C]$, where A and B are empirical constants.

INTRODUCTION

Hydrated melts have recently been approached in many investigations, due to both their theoretical importance and applications among which energy storage is the most remarkable.[1-9]

Scientific literature is rich in data regarding electric conductance, viscosity and diffusion of the system in question but information on thermal conductivity is scarce.

This contribution deals with thermal conductivity of calcium nitrate tetrahydrated as well as of $Ca(NO_3)_2 \cdot 4H_2O$ — water system. The temperature range was 313–343 K while calcium nitrate concentration between 69.481 % (corresponding to the tetrahydrate) and 14.229 % (for $Ca(NO_3)_2 \cdot 4H_2O + 60\ H_2O$ system).

EXPERIMENTAL

Chemicals. Reagent grade $Ca(NO_3)_2 \cdot 4H_2O$ and twice distilled water degreased by boiling were employed. Calcium content of tetrahydrate was determined by flame photometry and water content by dehydration in vacuum at 160°C. The two techniques yielded values that agreed.

Equipment. Various methods have been applied in the determination of thermal conductivity of liquids of which most often those based on parallel plates,[10,14] concentric cylinders[10,11,15-18] and hot wire.[10,11,19] This study has made use of the apparatus shown in Fig. 1.

The constant resistors R_1, R_2, R_3 and the measuring cell, RM, were thermoset to within ±0.05°.

The cell (Fig. 2) was immersed into the thermostated bath whose temperature was t_m. The cell thermistor was fed with constant d.c. The temperature drop across the liquid layer $\Delta T = t_c - t_m$ represents the difference between the temperature of the thermistor lower surface, t_c (measured by a copperconstantan thermocouple applied directly on the surface) and that of the thermostated cell bath, t_m. A galvanometer (sensitivity $0.7.10^{-9}$ A. mm/m) allowed to monitor any bridge unbalance caused by thermal conduction of liquids in the measuring cell. This device extends the principle of katharometer[18,19] employed as detector in gas chromatography. Thermal conductivity of liquids was determined by the cell shown in Fig. 2.

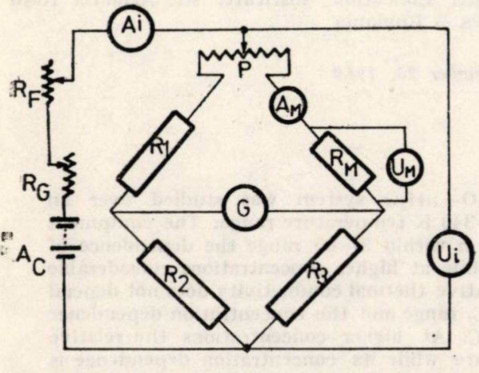

Fig. 1. — The apparatus employed for the determination of thermal conductivity of liquids: AC — Stabilized d.c. supply; RG — Variable resistor for rough adjustment; RF — The same for fine adjustment; P — Helical potentiometer. $R_1 R_2 R_3$ — Constant resistors; RM — The resistance of the measuring cell (thermistor); AM — Milliampermeter for the measuring cell (resistor); UM — Millivoltmeter for the measuring cell (resistor); U_i — Voltmeter for the voltage applied to the bridge; A_i — Milliampermeter for the bridge current; G — Galvanometer.

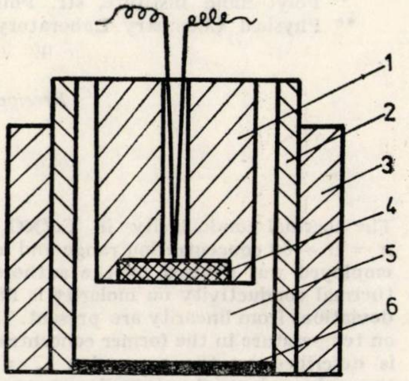

Fig. 2. — The measuring cell: 1 — Synthetic copolymer; 2 — Glass tube; 3 — Thermal insulator; 4 — Thermistor; 5 — Container of the liquid to be measured; 6 — Metal plate (Pt).

Since this device is different from those presented in literature, its operation is described here briefly. The standard liquid I of known thermal conductivity λ_I is contained in the carefully washed and dried cell. After thermosetting the thermistor is fed with constant d.c. whose value depends on the working temperature and the convenient temperature gradient. Potentiometer P is so chosen that the shift of the galvanometer spot stays within the scale. The stationary state is reached in 60—90 minutes and then the G_I reading of the galvanometer is recorded. Then the standard sample II replaces I and G_{II} trading is made for the same position of P and the same current fed into the thermistor.

The apparatus constant is then:

$$K = \frac{\Delta\lambda}{\Delta G} = \frac{\lambda_I - \lambda_{II}}{G_I - G_{II}} \tag{1}$$

where λ_I, λ_{II} stand for thermal conductivities of the two standard substances, G_I, G_{II}, for the two galvanometer readings.

To determine thermal conductivity of a given liquid, λ_x, the above procedure is repeated for that liquid at the same temperature and G_x is measured so that :

$$\lambda_x = \lambda_e - K \cdot \Delta G \tag{2}$$

where λ_x and λ_e are the thermal conductivities of the unknown substance and of one of the standard substances, respectively.

The device described above combines higher accuracy and sensitivity with the advantage of a simple cell which is easy to build and handle ; besides, a classical Wheatston bridge is suitable for detection.

RESULTS AND DISCUSSION

The values of thermal conductivity of tetrahydrated calcium nitrate without or with water addition are listed in Table 1. Thermal conductivities are plotted *versus* molar concentration for four temperatures in Fig. 1 ; use has been made of the densities of calcium nitrate solutions determined by Ewing and Mikovsky.[20]

The solid lines in Fig. 3 show the dependence of thermal conductivity on molar concentration according to the Riedel equation[21,22] (with the Riedel coefficients) :

$$\lambda = \lambda_a + \sum_{i=1}^{n} \alpha_i C_i \tag{3}$$

where λ, λ_a stand for thermal conductivity of electrolyte solution and water respectively, α_i is the coefficient of contribution of i-th ionic species to thermal conduction and C is the molar concentration of the solution. This figure shows that measured thermal conductivities observe a linear

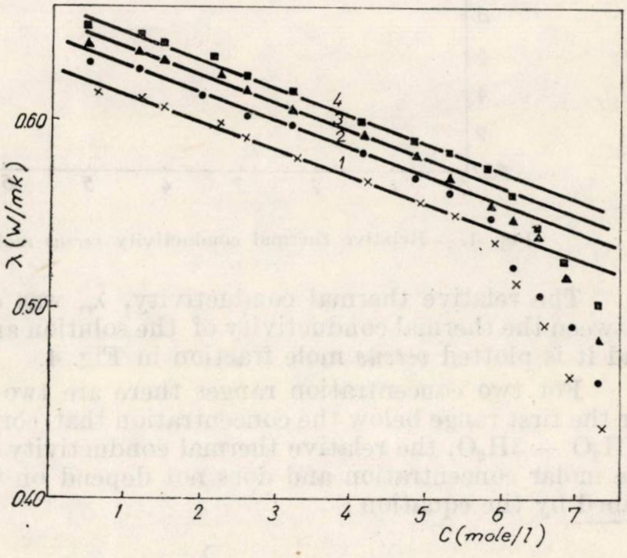

Fig. 3. — Thermal conductivity of calcium nitrate aqueous solutions *versus* molar concentration. (1) : 313 K ; (2) : 323K ; (3) : 333K (4) : 343 K.

dependence only up to a concentration that corresponds approximately to $Ca(NO_3)_2 . 4H_2O + 3H_2O$ system; at higher concentrations, deviations from linearity are large.

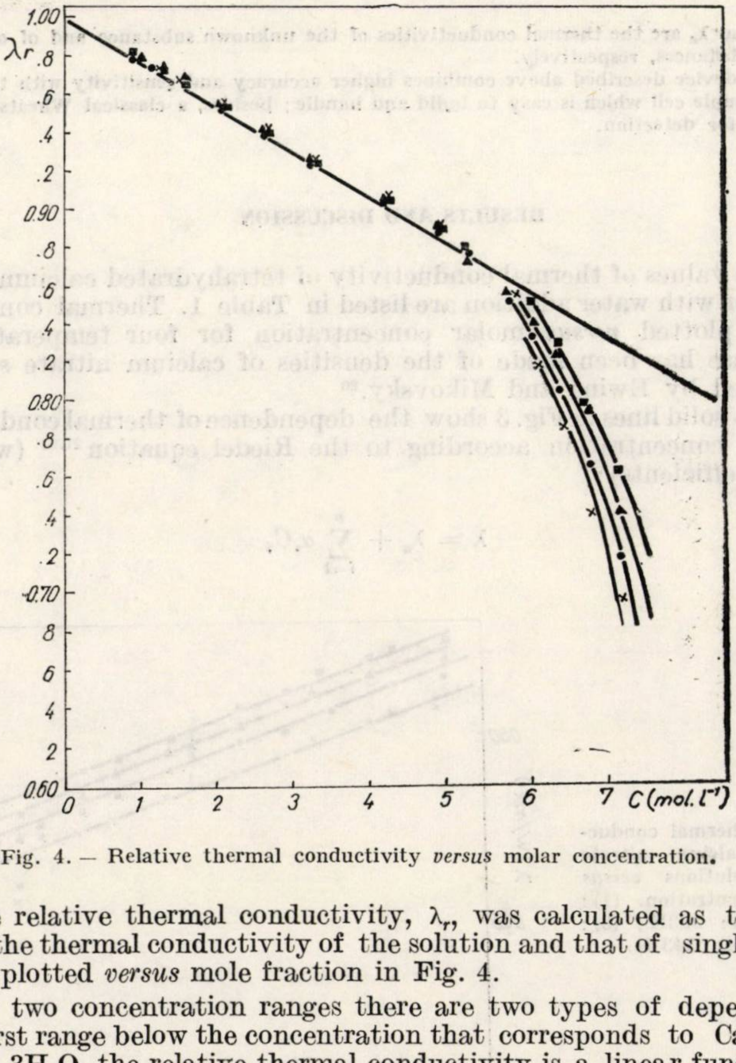

Fig. 4. — Relative thermal conductivity *versus* molar concentration.

The relative thermal conductivity, λ_r, was calculated as the ratio between the thermal conductivity of the solution and that of single water and it is plotted *versus* mole fraction in Fig. 4.

For two concentration ranges there are two types of dependence: for the first range below the concentration that corresponds to $Ca(NO_3)_2 . 4H_2O + 3H_2O$, the relative thermal conductivity is a linear function on the molar concentration and does not depend on temperature. It is described by the equation:

$$\lambda_r = \frac{\lambda}{\lambda_0} = 1 - \beta C \qquad (4)$$

where λ and λ_0 are the thermal conductivites of the solution and water, respectively, C is the molar concentration, β is a constant which depends only on the electrolyte. In case β is known for a certain electrolyte, eq. (4) allows the calculation of thermal conductivity of any concentration and temperature within the linearity range.

The experimental values in Table 1 were employed to calculate λ_r for calcium nitrate and the following equation was established:

$$\lambda_r = \frac{\lambda}{\lambda_0} = 1 - 0.02263 . C \qquad (4')$$

TABLE 1

The experimental values of thermal coductivity

No.	System	$\lambda(W \cdot m^{-1} \cdot K^{-1})$			
		313 K	323 K	333 K	343 K
1	$Ca(NO_3)_2 . 4H_2O + 0.0H_2O$	0.4373	0.4617	0.4838	0.5036
2	$Ca(NO_3)_2 . 4H_2O + 0.5H_2O$	0.4652	0.4919	0.5175	0.5257
3	$Ca(NO_3)_2 . 4H_2O + 1.0H_2O$	0.4931	0.5175	0.5396	0.5431
4	$Ca(NO_3)_2 . 4H_2O + 1.5H_2O$	0.5140	0.5350	0.5478	0.5606
5	$Ca(NO_3)_2 . 4H_2O + 2.0H_2O$	0.5361	0.5478	0.5547	0.5745
6	$Ca(NO_3)_2 . 4H_2O + 3.0H_2O$	0.5501	0.5629	0.5687	0.5827
7	$Ca(NO_3)_2 . 4H_2O + 4.0H_2O$	0.5571	0.5716	0.5803	0.5885
8	$Ca(NO_3)_2 . 4H_2O + 6.0H_2O$	0.5675	0.5827	0.5920	0.5989
9	$Ca(NO_3)_2 . 4H_2O + 10.0H_2O$	0.5803	0.5966	0.6059	0.6146
10	$Ca(NO_3)_2 . 4H_2O + 14.0H_2O$	0.5896	0.6048	0.6152	0.6234
11	$Ca(NO_3)_2 . 4H_2O + 20.0H_2O$	0.5978	0.6129	0.6234	0.6315
12	$Ca(NO_3)_2 . 4H_2O + 30.0H_2O$	0.6059	0.6210	0.6309	0.6396
13	$Ca(NO_3)_2 . 4H_2O + 40.0H_2O$	0.6106	0.6257	0.6350	0.6443
14	$Ca(NO_3)_2 . 4H_2O + 60.0H_2O$	0.6141	0.6292	0.6385	0.6478

Eq. (4′) was used to calculate λ_c which were then compared to λ_m; the deviation is expressed by the equation:

$$\Delta = \frac{\lambda_m - \lambda_c}{\lambda_m} 100 \qquad (5)$$

whose values are listed in Table 2.

TABLE 2

Verification of eqs. (4) and (4′)

No.	n	313 K			323 K		
		λ_m	λ_c	%Δ	λ_m	λ_c	%Δ
14	60	0.6141	0.6143	+0.03	0.6292	0.6286	−0.10
13	40	0.6106	0.6112	+0.10	0.6257	0.6260	+0.05
12	30	0.6059	0.6067	+0.13	0.6210	0.6214	+0.06
11	20	0.5978	0.5989	+0.18	0.6129	0.6134	+0.08
10	14	0.5896	0.5906	+0.17	0.6048	0.6050	+0.03
9	10	0.5803	0.5819	+0.10	0.5966	0.5962	−0.06
8	6	0.5675	0.5684	+0.16	0.5827	0.5825	−0.03
7	4	0.5571	0.5584	+0.23	0.5727	0.5723	−0.06

TABLE 2 (continued)

N°.	n	333 K			343 K		
		λ_m	λ_c	Δ %	λ_m	λ_c	Δ %
14	60	0.6385	0.6384	−0.01	0.6478	0.6471	−0.11
13	40	0.6351	0.6351	+0.01	0.6443	0.6439	−0.06
12	30	0.6309	0.6305	−0.06	0.6396	0.6392	−0.06
11	20	0.6234	0.6225	−0.14	0.6315	0.6311	−0.06
10	14	0.6152	0.6141	−0.18	0.6234	0.6226	−0.13
9	10	0.6059	0.6052	−0.11	0.6146	0.6135	−0.18
8	6	0.5920	0.5913	−0.12	0.5989	0.5996	+0.12
7	4	0.5803	0.5809	+0.06	0.5885	0.5892	+0.12

The very good agreement between the calculated and experimental thermal conductivity supports the validity of eqs. (4) and (4′); they may be regarded in fact as a simplified form of the Jones-Dolle relation for relative viscosity [23,24]:

$$\eta_r = 1 + A\sqrt{C} + B\cdot C \tag{6}$$

In case of relative thermal conductivity, the nonlinear term in Jones-Dolle equation vanishes.

The following equation is advanced to describe the behaviour of the system under study in the higher concentration range ($n < 3$):

$$\Delta\lambda = A \exp\left[-B\cdot\frac{n}{c}\right] \tag{7}$$

which was checked by experiments carried out in this investigation. In eq. (7) $\Delta\lambda$ stands for the difference between the thermal conductivity of water λ_0 and that of calcium nitrate solution, λ; c is the molar concentration, n is the number of moles of water in $Ca(NO_3)_2.4H_2O + nH_2O$ and A and B are constants. In $(\Delta\lambda)$ versus $\frac{n}{c}$ ratio is plotted in Fig. 5 for 313 and 343 K.

The dependence is linear in the range of high concentrations ($n<3$).

The A and B constants were calculated from experimental data and their values were employed to recalculate thermal conductivity.

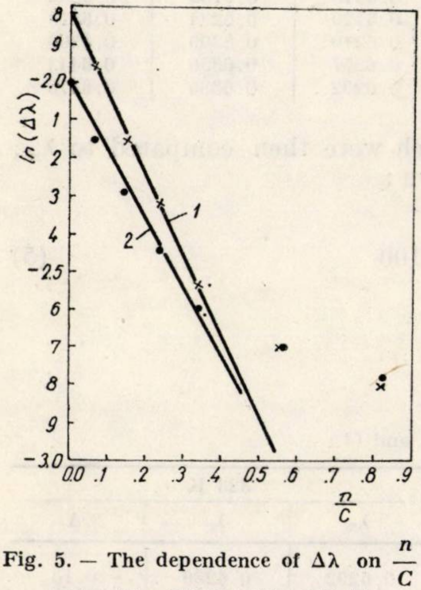

Fig. 5. — The dependence of $\Delta\lambda$ on $\frac{n}{C}$ ratio. (1) : 313 K ; (2) : 343 K.

The calculated values as well as their agreement with the experimental ones are listed in Table 3.

The table proves the good agreement between the calculated and measured values.

TABLE 3

The values of thermal conductivity calculated by eq. (7) and $\Delta\lambda = \lambda_0 - \lambda$. A and B constants were calculated from experimental data by the least square method*

No.	n	313 K				343 K			
		λ_m	λ_c	Δ	$\%\Delta$	λ_m	λ_c	Δ	$\%\Delta$
1	0.0	0.376	0.376	0.000	0.00	0.433	0.433	0.000	0.00
2	0.5	0.400	0.400	0.000	0.00	0.452	0.4504	0.0016	−0.35
3	1.0	0.424	0.423	−0.001	−0.24	0.467	0.4672	+0.0002	+0.04
4	1.5	0.442	0.443	+0.001	+0.23	0.482	0.483	+0.001	+0.21
5	2.0	0.461	0.462	+0.001	+0.23	0.494	0.497	+0.003	+0.60

* Thermal conductivities are given in kcal $m^{-1}h^{-1}K^{-1}$

CONCLUSIONS

The existence of two concentration ranges was evidenced. From $n \simeq 60$ to $n \simeq 3$ of $Ca(NO_3)_2.H_2O + nH_2O$ a linear relation between thermal conductivity and molar concentration is observed. Within this concentration range, relative thermal conductivity may be calculated by a Jones-Dolle type relation wherein the nonlinearity term is practically zero and the proportionality constant does not depend on temperature. The linearity range of thermal conductivity extends over a concentration domain which is wider than for other transport properties, e.g. viscosity and equivalent conductance.[25−27]

For the range of high concentrations ($n \simeq 3$ to $n = 0$) the dependence of thermal conductivity on composition is exponential. An equation is advanced which allows the calculation of conductivity as a function of concentration in the range of very high concentrations, in terms of constants A and B, at a given temperature.

REFERENCES

[1] C. A. Angell, *J. Phys. Chem.*, **69**, 2137 (1965); **70**, 2793, 3988 (1966).

[2] C. T. Moyniham, *J. Phys. Chem.*, **70**, 3399 (1966).

[3] C. A. Angell and R. D. Bressel, *J. Phys. Chem.*, **71**, 2759 (1967); **76**, 3244 (1972).

[4] C.A. Angell and E. J. Sare, *J. Phys. Chem.*, **52**, 1058 (1970).

[5] C. T. Moyniham and C. A. Angell, *J. Phys. Chem.*, **74**, 736 (1970).

[6] J. Novák, I. Slamá and Z. Kodejs, *Coll. Czech. Chem. Comm.*, **41**, 2838 (1976).

[7] J. Malá, J. Novák, Z. Kodejs and I. Slamá, *Coll. Czech. Chem. Comm.*, **43**, 183 (1978).

[8] J. Novák, I. Slamá and Z. Kodejs, *Chem. Zvesti*, **31**, 29 (1977).

[9] S Zuca and N. Ene, *E.E.A. – Electrotechnica*, **27**, 15 (1979).

[10] N. V. Tsederberg, "Thermal Conductivity of Gases and Liquids", Copyright, 1965.

[11] L. Farády and L. Bencze, *Magyar Kém. Lapjá*, **31**, 347 (1976).

[12] H. Charmook, *J. Amer. Chem. Soc.*, **44**, 313 (1961).

[13] R.C.L. Bosworth, "Processes in Applied Chemistry", Wiley, London, 1956.

[14] J.E.S. Venart, *J. Sci. Instr.*, **44**, 727 (1964).

[15] R. P. Tye, "Thermal Conductivity", Academic Press, New York, 1968.

[16] N. B. Vargaftik and Yu. P. Osminin, *Teploenergetika*, **1956**, 7.

[17] H. S. Gregory and C. I. Archer, *Phil. Mag. and J. Sci. Ser.* 7, **15**, 201 (1933).

[18] M. Singliar, "Practica Cromatografiei de Gaze", Ed. tehnică, Bucureşti, 1963.

[19] O. Piringer and E. Tărău, "Cromatografia în fază gazoasă", Ed. tehnică, Bucureşti, 1969.

[20] W. W. Ewing and J. R. Mikovsky, *J. Amer. Chem. Soc.*, **72**, 1390 (1950).

[21] L. Riedel, *Chem. Ing. Tech.*, **22**, 54 (1950).

[22] A. Missenard, « Conductivité Termique des solides, liquides, gas et de leurs mélanges », Ed. Eyroles, Paris, 1965.

[23] G. Jones and M. Dolle, *J. Chem. Soc.*, **51**, 2950 (1929).

[24] G. Jones and S. K. Talley, J. *Amer. Chem. Soc.*, **55**, 624, 4124 (1933).

[25] J. Mc. Donald and H. T. Davis, *J. Phys. Chem.*, **74**, 725 (1970).

[26] L. Werblan, A. Rotowska and S. Minc, *Electrochim. Acta*, **16**, 41 (1971).

[27] I. G.Murgulescu and S. Zuca, *Electrochim. Acta*, **11**, 1383 (1966) ; **14**, 519 (1969).

Revue Roumaine de Chimie, **27**, *7*, 155–160 (1982)

THERMODYNAMICS OF MULTICOMPONENT ELECTROLYTE SOLUTIONS. III.[1,2]

AMMONIUM PERSULFATE ACTIVITY COEFFICIENTS IN QUATERNARY SYSTEM, IN SOLUBILITY MEASUREMENTS

RODICA VÎLCU and FLORICA IRINEI

The Polytechnic, Physical Chemistry and Electrochemical Technology Departments,
Bucharest, Romania

Received June 10, 1981

The present paper reports on the thermodynamic behaviour of ammonium persulfate in quaternary solution $(NH_4)_2S_2O_8 + (NH_4)_2SO_4 + H_2SO_4 + H_2O$ studied by means of the activity coefficients calculated from its solubility data at high concentrations. The regularities specific of electrolyte solutions of medium concentrations could be extended, in the case of multicomponent concentrated solutions, by the substitution of effective ionic strength for normal ionic strength.

Previous investigations [1-3] studied the thermodynamic and electrochemical conditions for obtaining ammonium persulfate by electrolysis of an aqueous solution of sulfuric acid and ammonium sulfate. Electrochemical measurements showed that a good yield of the synthesis is obtained in acid solutions in which electric conductibility is high.

The activity coefficients of ammonium persulfate in the $(NH_4)_2S_2O_8 + H_2O$; $(NH_4)_2S_2O_8 + (NH_4)_2SO_4 + H_2O$; $(NH_4)_2S_2O_8 + H_2SO_4 + H_2O$ systems were calculated from solubility measurements in concentrated solutions.

Using the same experimental method, the present paper, with the help of activity coefficients, reports on the thermodynamic behaviour of $(NH_4)_2S_2O_8$ in $(NH_4)_2S_2O_8 + (NH_4)_2SO_4 + H_2SO_4 + H_2O$ quaternary mixture in the region of high concentrations.

The activity coefficients of persulfate were calculated using equation (1).

$$\frac{1}{\nu_p}\log K_p = \frac{1}{\nu_p}\log (S_p)_0 + \log\,[(\gamma_\pm)_p]_0 = \frac{1}{\nu_p}\log S_p + \log\,(\gamma_\pm)_p \quad (1)$$

where $(S_p)_0$ and (S_p) are the salting products of amonium persulfate in water and the multicomponent solution respectively, and $[(\gamma_\pm)_p]_0$ and $(\gamma_\pm)_p$ are the corresponding ionic medium molal activity coefficients.

In[1] it was shown that $\frac{1}{\nu_p} \log (S_p)_0 + \log [(\gamma_\pm)_p]_0 = 0.2169$ at the solubility limit of ammonium persulfate in water (3,478 molal), hence, relation (1) becomes

$$\log (\gamma_\pm)_p = 0.2169 - \frac{1}{3} \log 4 \cdot (m_p + m_s)\, m_p \qquad (2)$$

where m_p and m_s represent the molalities of ammonium sulfate and persulfate, respectively.

EXPERIMENTAL

Solubility of ammonium persulfate was calculated in solutions of varied concentrations of sulfuric acid and ammonium sulfate at 293 K. Working conditions for the correct determination of the equilibrium between ammonium persulfate crystals and the solution saturated in persulfate in the presence of sulfate and sulfuric acid have been presented in earlier papers.[1−4]

Table 1 shows the concentrations (expressed in molality and molar fractions) of $(NH_4)_2S_2O_8 + (NH_4)_2SO_4 + H_2SO_4 + H_2O$ solution components in equilibrium with persulfate crystals and also the total ionic strength of the solutions.

TABLE 1

Activity coefficients of $(NH_4)_2S_2O_8$ in the $(NH_4)_2S_2O_8 + (NH_4)_2SO_4 + H_2SO_4 + H_2O$ system

	$m_{H_2SO_4}$	$x_{H_2SO_4}$	$m_{(NH_4)_2S_2O_8}$	$x_{(NH_4)_2S_2O_8}$	$m_{(NH_4)_2SO_4}$	$x_{(NH_4)_2SO_4}$	I	$(\gamma\pm)_p$
	5% H_2SO_4		m_p		m_s			
1	0.905	0.223	2.788	0.686	2.369	0.090	18.19	0.3319
2	0.931	0.196	2.202	0.465	1.605	0.338	14.21	0.3272
3	0.989	0.165	1.154	0.193	3.848	0.642	17.97	0.3383
4	1.039	0.156	0.799	0.120	4.804	0.723	19.93	0.3546
5	0.970	0.127	1.106	0.145	5.524	0.726	22.80	0.2844
	10% H_2SO_4							
6	1.802	0.391	2.244	0.487	0.565	0.122	13.83	0.3983
7	2.066	0.297	1.864	0.268	3.019	0.434	20.84	0.2930
8	2.095	0.268	0.965	0.123	4.766	0.609	23.48	0.3280
9	2.207	0.250	0.757	0.086	5.864	0.664	26.48	0.3230
10	2.177	0.241	0.149	0.016	6.722	0.743	27.14	0.5417
	15% H_2SO_4							
11	2.694	0.524	1.796	0.349	0.651	0.127	15.42	0.4703
12	2.611	0.338	1.246	0.161	1.255	0.500	15.34	0.5235
13	3.018	0.406	0.966	0.130	3.452	0.464	22.31	0.3900
14	3.618	0.334	0.567	0.053	6.646	0.614	32.49	0.3359
15	3.510	0.333	0.184	0.017	6.838	0.950	31.59	0.4977
	20% H_2SO_4							
16	3.699	0.596	1.215	0.196	1.287	0.207	18.60	0.5278
17	4.353	0.471	0.640	0.069	4.246	0.459	27.72	0.4320
18	5.102	0.410	0.325	0.026	7.003	0.563	27.29	0.4766
19	5.006	0.409	0.098	0.008	7.116	0.582	36.66	0.6030
	25% H_2SO_4							
20	4.732	0.674	0.928	0.142	1.355	0.193	20.04	0.6138
21	5.019	0.617	0.649	0.079	2.460	0.303	24.38	0.5628
22	6.615	0.491	0.415	0.031	6.435	0.478	40.39	0.3858
23	7.042	0.468	0.166	0.011	7.815	0.520	45.07	0.4729

Solutions from the same group have the same percentage acid concentration, whereas persulfate concentration varies with the added sulfate concentration. The last column of the table includes the values of the activity coefficients of ammonium persulfate, calculated by relation (2).

The complexity of the system — due both to the great number of uni-bivalent components and to concomitant variation of the total ionic strength of the solution that changes with the molality of each component — rendered interpretation of the activity coefficient values very difficult.

Graphical representations, including activity coefficient variation of ammonium persulfate with total ionic strength of the system and also with molar fractions of the components are not conclusive because of the great dispersion of the points. This, because the behaviour of multicomponent electrolyte solutions is not subordinated to the total ionic strength of the solution but to the effective ionic strength.^{5}

A first information, lending support to this assumption, is furnished by the marked variation of the total ionic strength of the solution under the conditions mentioned.

Effective ionic strength is not a simple concentration factor but includes the deviation terms of the solution components with respect to ideality, owing both to hydration and to mutual interactions between ions.

For a solution containing dissolved electrolytes i and j, the following can be written in keeping with the Harned rule

$$\log\,(\gamma_i)_{ij} = \log\,(\gamma_i)_0 - \alpha_{ij} I_j \tag{3}$$

where α_{ij} is the Harned coefficient of electrolyte i and I_j is the ionic strength of electrolyte j. The activity coefficient of electrolyte i in its binary solution depends on the ionic strength of the solution according to equation (4)

$$\log\,(\gamma_i)_0 = a + b_i I_i \tag{4}$$

(Relation (4) is a generalized form of the Debye—Hückel equation). Under these conditions, relation (3) becomes

$$\log\,(\gamma_i)_{ij} = a + b_i I_i\ (b_i - \alpha_{ij}) I_j \tag{5a}$$

or

$$\log\,(\gamma_i)_{ij} = a + b_i I_e \tag{5b}$$

where $I_e = I_i + \beta_j I_j$ is the effective ionic strength of the solution. For multicomponent electrolyte solutions

$$I_e = I_i + \sum_j \beta_j I_j \tag{6}$$

Corrective coefficients β_j in relation (6) are defined by relation (7)

$$\beta_j = 1 - \frac{\alpha_{ij}}{b_i} \tag{7}$$

These coefficients were calculated from experimental data using relation (8) which expresses the dependence of the product of ionic activities on the concentration of the components^6

$$\log K = C_0 + \sum_k C_k m_k \tag{8}$$

$$k = i, j \ldots$$

Using the least square method, the coefficients C_k were calculated for ammonium persulfate, ammonium sulfate and sulfuric acid in solution. The respective values are shown in table 2.

Relation (8) can also be written

$$\log K = C_0 + B[I_i + \Sigma\,(I_e)_j] \tag{9}$$

$$= C_0 + B(I_i + \Sigma\beta_j I_j)$$

$$= C_0 + BI_e$$

where $B = \dfrac{C_i m_i}{I_i}$; $(I_e)_j = \dfrac{C_j m_j}{B}$; $\beta_j = \dfrac{C_j m_j}{BI_j}$

In the quaternary solution studied, the reference electrolyte (i) is ammonium persulfate. The salt effects of the added electrolytes on persulfate solubility are reflected in their β_j coefficients shown in columns 4 and 5, table 2.

TABLE 2

Corrective coefficients of ammonium sulfate and sulfuric acid in quaternary solution

	$C_{(NH_4)_2S_2O_8}$	$C_{(NH_4)_2SO_4}$	$C_{H_2SO_4}$	$\beta_{(NH_4)_2SO_4}$	$\beta_{H_2SO_4}$
1 2 3 4 5	0.0223	0.0075	0.2567	0.34	11.6
6 7 8 9 10	−0.0683	−0.0396	0.2688	0.58	−3.93
11 12 13 14 15	−0.0702	−0.0409	0.1714	0.58	−2.44
16 17 18 19	−0.0730	−0.0413	0.1219	0.57	−1.67
20 21 22 23	−0.0663	−0.0399	0.0896	0.60	−1.35

DISCUSSIONS

In all cases, $\beta_{(NH_4)_2SO_4}$ coefficients have low, positive values, which reflect the slight salt effect of ammonium sulfate on ammonium persulfate.

In contrast, H_2SO_4 has a strong influence on the dissolution of ammonium persulfate. If the values of coefficient β_j, in table 2, are introduced in relation (6), then $\beta_{H_2SO_4} > 1$ for solutions with low acid concentrations (about 5 %), therefore the presence of the acid increases the ionic strength of the multicomponent solution. With increase in the acid concentration, $\beta_{H_2SO_4} < 1$, the contrary effect takes place, lowering the effective ionic strength of the solution. For solutions (1 — 5) where acid concentration is low, the effective ionic strength of the multicomponent solution varies around 44. For all the other solutions(6 — 23) where H_2SO_4 in excess exists, the total effective ionic strength is virtually constant (≈ — 13).

If in relation (9), ammonium sulfate is considered as reference electrolyte, the salt effect of H_2SO_4 on $(NH_4)_2SO_4$ is of the same order of magnitude as that on $(NH_4)_2S_2O_8$.

Therefore, it was considered relevant to determine (Fig. 1) the dependence of the reactivity coefficients of ammonium persulfate in multicomponent solution on the effective ionic strength of the solution, expressed in ammonium sulfate and persulfate.

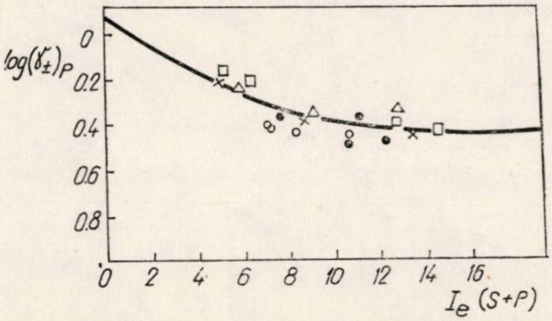

Fig. 1. — Variation of the activity coefficients of ammonium persulfate in $(NH_4)_2S_2O_8 + (NH_4)_2SO_4 +$ $+ H_2SO_4 + H_2O$ solution with the effective ionic strength of ammonium sulfate and persulfate.

The monotonous variation of the activity coefficients of ammonium persulfate with the effective ionic strength of ammonium sulfate and persulfate confirms the justness of substituting normal ionic strength, in the case of concentrated multicomponent solutions of electrolytes by the effective ionic strength.

Figure 1 shows an increase of the activity coefficients of persulfate in multicomponent solution with lowering of the effective ionic strength of ammonium persulfate and sulfate, that is with increase in the effective ionic strength of the acid.

Therefore, it results that extension of the regularities of the multicomponent electrolyte solutions of medium concentrations imposes, in case of high concentrations, the substitution of normal ionic strength bv effective ionic strength.

On the other hand, for practical purposes, interpretation of the values obtained, both for the activity coefficients of ammonium persulfate and for the β corrective coefficients, suggests the use of some slightly acid $(NH_4)_2SO_4 + H_2SO_4$ solutions for obtaining concentrated ammonium persulfate solutions by electrochemical methods.

REFERENCES

[1] R. Vîlcu, Fl. Irinei, A. Gref and R. Condei, *Bull. Inst. Polit. București*, **17**, 2, 39 (1980).
[2] Part II. R. Vîlcu and Fl. Irinei, *Bull. Inst. Polit. București*, in press (1980).
[3] R. Vîlcu, A. Gref and F. Irinei, *Bull. Inst. Polit. București*, in press (1981).
[4] J. Balej, *Cool. Czech. Chem. Comm.* **30**, 2663 (1965).
[5] A. M. Rozen, *Zhur. Fiz. Khim*, **8**, 2012 (1976).
[6] K. Schwabe, H. Kelm, and Chr. Queck, *Z. phys. Chem. (Leipzig)*, **255**, 1149 (1974).

Revue Roumaine de Chimie, 27, 1, 161–164 (1982)

CATIONIC SELF-DIFFUSION COEFFICIENTS IN MOLTEN (Tl–Ag)NO_3 SYSTEM

ŞTEFANIA ZUCA and MARIELA CONSTANTINESCU
Center of Physical Chemistry, Splaiul Independenţei 202, Bucharest, Romania

Received June 16, 1981

The cationic self-diffusion coefficients in molten (Tl–Ag)NO_3 system were investigated as a function of temperature and concentration. The diffusion isotherms were discussed in terms of various types of anion-cation interactions on mixing and of their relative contribution.

According to Raman spectra,[1–3] the nature of anion-cation interactions in single fused nitrates depends directly on the nature of metal species involved. Thus in molten alkali nitrates the interaction forces are predominantly coulombic in nature. The $AgNO_3$ and $TlNO_3$ melts are characterized by a pronounced covalency due to a stronger ion-pair interaction which originated in the so-called "chatt-effect"[4] (back donation of electrons from the *d* orbital of cation into the π-system of NO_3^-). Consequently, a higer degree of disorder prevails in $AgNO_3$ and $TlNO_3$ melts, which accounts for their low melting points, high diffusion coefficient and low activation energy E_{D^+}.[5,6] Moreover, some ionic "agglomerates" are assumed in $TlNO_3$ melt, whose thermal dissociations accompanied by the correspondent change in the size of diffusion governing unit on heating (> 280°) was signaled on log D_{Tl^+} + *vs.* $1/T$ curve. [6]

All these findings suggest that mixing of such melts should be accompanied by important changes in anion-cation bond energy and by the consequent alteration of the diffusion process. Some of the informations thus obtained have been already discussed. [5,7–9].

Aiming at a more complete characterization of the nature of ionic interactions in binary molten nitrates, in addition to the previously studied (Ag–Alk)NO_3 [5,7] and (Tl – Alk)NO_3 [8,9] mixtures, (Ag–Tl)NO_3 system for which no diffusion data are available in literature, has been investigated. According to Raman spectra which do not indicate any frequency shifts or intensity changes [1] and to the ideal behaviour of viscosity isotherms,[1] the force field in the mixture does not differ significantly from that in the melt of parent components. A clearer insight into the behaviour of this system should be supplied by the diffusion coefficients as they characterize not the melt in the bulk but the motion of each constituting species of the medium.

RESULTS AND DISCUSSIONS

The "diffusion into the capillary method" previously[10] described was employed for measurements. The self-diffusion coefficients of both cations were determined over the entire concentration range from pure $AgNO_3$ to pure $TlNO_3$ at temperatures ranging between 100–340°. The nitrates and the tracers were the same as those used in our earlier works.[6,10] The obtained experimental data are listed in Table 1.

TABLE 1

Cationic self-diffusion coefficients in molten $(Tl-Ag)NO_3$ system

x_{TlNO_3}	t°	$D_{Tl}\cdot 10^5$ $cm^2\cdot s^{-1}$	t°	$D_{Ag^+}\cdot 10^5$ $cm^2\cdot s^{-1}$
0.75	260	1.29 ± 0.01	238	1.58 ± 0.01
	270	1.36 ± 0.01	268	2.04 ± 0
	298	1.68 ± 0.03	269	2.08 ± 0.01
	340	2.30 ± 0.01	290	2.32 ± 0.05
			320	2.52 ± 0.02
			321	2.59 ± 0.01
0.50	93	0.89 ± 0.02	127	0.90 ± 0.01
	114	1.09 ± 0	131	0.94 ± 0.02
	121	1.17 ± 0.05	153	1.07 ± 0.03
	200	1.38 ± 0.03	167	1.14 ± 0.02
	214	1.30 ± 0.01	206	1.44 ± 0.01
0.25	160	1.04 ± 0.03	150	1.18 ± 0.03
	161	0.95 ± 0	160	1.26 ± 0
	260	1.53 ± 0.06	171	1.24 ± 0.04
	309	1.72 ± 0.03	233	1.46 ± 0.04
	340	2.08 ± 0.04		
0.10	210	1.06 ± 0		
	230	1.30 ± 0.06		
	247	1.37 ± 0.03		
	269	1.56 ± 0.01		

In all studied compositions the temperature dependence of self-diffusion coefficients was of non-Arrhenius type which proves that mixtures bear the same covalency as single $TlNO_3$ melt.[6] Regarding the composition dependence, as illustrated by the isotherms in Fig. 1, it is directly influenced by the temperature. While at high temperature both D_{Ag^+} and D_{Tl^+} isotherms are quasi-linear, large positive deviations from linearity arc noticeable on D_{Tl^+} isotherm at lower temperature. The high temperature behaviour clearly proves that mixing occurs now with no important energy changes. Although the sizes of the two uncommon cations differ significantly, (Pauling radius $r_{Tl^+} = 1.40$ Å and $r_{Ag^+} = 0.95$Å in the melt [5,11–13]), the competitive attractions of anion environment are negligible, most probably due to own polarizability of both cations and of their consequent low polarizing strength.

However, to account for the large positive deviations from linearity of D_{Tl^+} isotherm at lower temperature, additional facts must be considered. Indeed, the more pronounced covalency of $TlNO_3$ melt and the consequent closer cation-anion pairs packing in this temperature region favour a repulsive effect in the nearest neighbours Tl^+ and Ag^+ within the coordination sphere of NO_3^- ion. Thus, a hindrance of π-interaction between $Tl^+ - NO_3^-$ ion pairs accompanied by the decrease of melt covalency takes place when $AgNO_3$ is added to the $TlNO_3$ melt. According to the data in Fig. 1, the phenomenon diminishes significantly with temperature raising, which reminds the behaviour observed in single $TlNO_3$ melt.[6]

The peculiarity of $(Ag\text{-}Tl)NO_3$ mixture is better emphasized if present D_{Tl^+} values are compared to those obtained in $(Tl - Na)\,NO_3$ system.[8] It is generally accepted that both Ag^+ and Na^+ cations are almost similarly sized in their melts[5,11-13] and, therefore, according to the common anion polarization model of Lumsden,[14] the mixing should occur in similar conditions in the above named systems. However, as evidenced by the data in Table 2, D_{Tl^+} in $(Tl-Ag)NO_3$ system takes systematically, at comparable temperatures, higher values than in $(Tl-Na)NO_3$ system. In our opinion, this behaviour is due to the much lower polarizing strength exerted on the common anion NO_3^- by Ag^+ compared to that of Na^+.

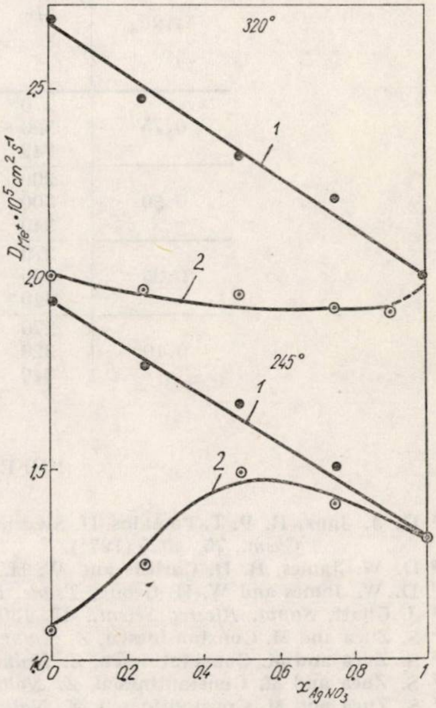

Fig. 1. — Cationic self-diffusion coefficient isotherms in the molten $(Tl-Ag)NO_3$ system, 1 ● D_{Ag^+}; 2. ⊙ D_{Tl^+}.

In fact, due to the high polarizing strength of Na^+ and to the more easily polarized NO_3^- in $TlNO_3$ melt,[1-3] the formation of some ionic agglomerates with Na^+ laying in the second coordination sphere was suggested[8] in $TlNO_3$ reach region of $(Tl-Na)NO_3$ system.

In conclusion, from our systematic investigation of the diffusion coefficients in binary molten nitrates mixtures, it is evident that the mass-transport process is directly influenced by the nature of various types of ionic interactions and by their relative contribution. According to the obtained data, the anion-cation polarization interactions prevail in $(Ag-Alk)NO_3$ and $(Tl-Alk)NO_3$ systems while small but finite cation-cation repulsive contributions appear in $(Tl-Ag)NO_3$ melt.

TABLE 2

D_{Tl^+} in molten (Tl—Ag)NO$_3$ and (Tl—Na)NO$_3$ systems

x_{TlNO_3}	$t°$	$D_{Tl^+} \cdot 10^5 cm^2 \cdot s^{-1}$	
		(Tl — Ag)NO$_3$	(Tl — Na)NO$_3$
0.75	270	1.20	1.36
	300	1.48	1.68
	340	1.96	2.30
0.50	200		1.38
	300	0.96	1.50
	340	1.93	2.05
0.25	270	1.00	1.57
	300	1.26	1.68
	340	1.83	2.08
0.10	270	0.95	1.56
	320	1.40	1.90
	340	1.63	2.05

REFERENCES

[1] G. J. Janz, R. P. T. Tomkins, H. Siegenthal, K. Balasubrahmanian and W. Lurie, *J. Phys. Chem.*, **75**, 4025 (1971).

[2] D. W. James, R. D. Carlisle and W. H. Leong. *Austral. J. Chem.*, **23**, 1779 (1970).

[3] D. W. James and W. H. Leong, *Trans. Faraday, Soc.*, **66**, 1948 (1970).

[4] J. Chatt, *Suppl. Ricerca Scient.*, **28**, 130 (1958).

[5] S. Zuca and M. Constantinescu, *Z. Naturforsch.*, **28a**, 51 (1973).

[6] S. Zuca and M. Constantinescu, *Z. Naturforsch.*, **32a**, 1433 (1977).

[7] S. Zuca and M. Constantinescu, *Z. Naturforsch.*, **29a**, 497 (1974).

[8] S. Zuca and M. Constantinescu, *Z. Naturforsch.*, **32a**, 1435 (1977).

[9] S. Zuca and M. Constantinescu, *Rev. Roumaine Chim.*, **23**, 995 (1978).

[10] S. Zuca and M. Constantinescu, *Rev. Roumaine Chim.*, **17**, 385 (1972).

[11] S. Zuca and R. Borcan, *Electrochim. Acta*, **15**, 1817 (1970).

[12] R. W. Laity, J. *Amer. Chem. Soc.*, **79**, 1849 (1957).

[13] B. de Nooijer, Thesis, Amsterdam, 1965.

[14] J. Lumsden, *Discuss. Faraday Soc.*, **32**, 138 (1961).

Revue Roumaine de Chimie **27**, *1*, **165** (1982)

COMPTES RENDUS

I. G. MURGULESCU, TATIANA ONCESCU and E. SEGAL, "Introducere în chimia fizică" (Introduction to physical chemistry), vol. II, 2. Cinetică chimică și cataliză (Chemical Kinetics and Catalysis). Editura Academiei, Bucharest, 1981, 1022 p.

Designed as an extensive work to be issued in several volumes, "Introduction to Physical Chemistry" by Acad. Prof. I. G. Murgulescu, is much more than just a treatise of physical chemistry; it is a window opened to physical chemistry, to basic knowledge required for smoothing out the way to handbooks, to articles in journals,to improving the qualification of those involved in any kind of chemistry. The work is to be issued in three volumes subdivided into six parts.

These volumes represent an extension and systematization of the lectures on physical chemistry given by the author, who has brilliantly led the Physical Chemistry Chair of the Department of Chemistry, University of Bucharest, almost a quarter of a century of teaching and scientific activity; these lectures have permanently been updated with the newest achievements in the field.

The second part of volume II (in collaboration with Prof. Tatiana Oncescu and Prof. E. Segal), is dedicated to the reaction rate and its dependence on concentration temperature, catalysts, etc.

The general principles and methods for the kinetic analysis of chemical reactions (including catalytic and fast reactions) are presented. Much space is devoted to the theoretical problems of chemical kinetics (modern theories of activation), as well as to the practical ones (kinetics of homogeneous and heterogeneous catalytic reactions). Many examples illustrate different theories, facilitating thus an easy understanding of chemical kinetics.

The book is meant to meet the requirements of the students and teaching people interested in physical chemistry, as well as to the research workers involved in this field.

D. I. Marchidan

Revue Roumaine de Chimie, 27, 7, 165 (1982)

COMPTES RENDUS

I. G. MURGULESCU, TATIANA ONCESCU and E. SEGAL, "Introducere în chimia fizică" (Introduction to physical chemistry), vol. II, 2. Cinetică chimică şi cataliza (Chemical Kinetics and Catalysis). Editura Academiei, Bucureşti, 1981, 1022 p.

Designed as an extensive work to be issued in several volumes, "Introduction to Physical Chemistry" by Acad. Prof. I. G. Murgulescu, is much more than just a treatise of physical chemistry; it is a window opened to physical chemistry, to basic knowledge required for smoothing out the way to handbooks, to articles in journals, to improving the organization of those involved in any kind of chemistry. The work is to be issued in three volumes subdivided into six parts.

These volumes represent an extension and systematization of the lectures on physical chemistry given by the author, who has brilliantly led the Physical Chemistry Chair of the Department of Chemistry, University of Bucharest, since a quarter of a century of teaching and scientific activity; these lectures have permanently been updated with the newest achievements in the field.

The second part of volume II (in collaboration with Prof. Tatiana Oncescu and Prof. E. Segal), is dedicated to the reaction rate and its dependence on concentration, temperature, catalysts, etc.

The general principles and methods for the kinetic analysis of chemical reactions (including catalytic and fast reactions) are presented. Much space is devoted to the theoretical problems of chemical kinetics (modern theories of activation) as well as to the practical ones (kinetics of homogeneous and heterogeneous catalytic reactions). Many examples illustrate different theories, facilitating thus an easy understanding of chemical kinetics.

The book is meant to meet the requirements of the student and teaching people interested in physical chemistry, as well as to the research workers involved in this field.

D. I. Marchidan

NOTE POUR LES AUTEURS

La Revue Roumaine de Chimie publie des articles en anglais, français, russe, allemand ou espagnol. Les auteurs sont priés d'envoyer des articles et des comptes rendus inédits.

Les manuscrits seront dactylographiés à double interligne. La bibliographie, les tableaux et la légende des figures seront placés après le texte.

Si l'article fait partie d'une série numérotée, la partie précédente sera donnée comme première référence.

Chaque article sera précédé d'un résumé comprenant quinze lignes au maximum.

Les références bibliographiques dans le texte seront faites par des exposants sans parenthèses et paraîtront à la fin de l'ouvrage.

Les publications périodiques mentionnées dans la bibliographie seront présentées suivant les prescriptions internationales : le nom de l'auteur précédé de l'initiale du prénom, le titre du périodique abrégé conformément à « Chemical Abstracts » et souligné par une ligne, le numéro du tome indiqué par des chiffres arabes et souligné par deux lignes, suivi de la première page de l'article ; à la fin, l'année de la parution sera placée entre parenthèses. Le numéro de la revue ne sera pas indiqué si les pages du volume sont numérotées consécutivement.

Les textes des livres ou traités inclueront : le nom des auteurs, précédé de l'initiale du prénom, le titre du livre entre guillemets et sans être souligné, le numéro du tome précédé par l'abréviation « vol. » (ou « Bd. »), le numéro de l'édition, les éditions (the publisher), la localité de la parution du livre, l'année de la parution et la page de la référence précédée(s) par l'abréviation «p ». (ou « S. »).

Les brevets seront indiqués comme suit : l'auteur ou la firme, le pays et le numéro du brevet, la date et la revue (Chem. Abstr.).Par ex. : M. Jones (to Union Carbide Co), *Brit. Pat.* 601 238, 2 Sept, 1959, *Chem Abstr.*, 54, 12808 (1960).

Si la référence n'a pas été lue en original, on indiquera aussi la revue de références consultée.

Les diagrammes seront tracés à 'encre de Chine sur papier calque. Les tableaux et les figures (en nombre strictement nécessaire) ainsi que les courbes dans les figures seront numérotés par des chiffres arabes. Leur explication sera donnée dans la légende des figures. Prière de ne pas inscrire les mêmes données dans les tableaux et les figures. Chaque tableau aura un titre. On indiquera dans le texte la place approximative des tableaux et des figures. Les formules chimiques seront incluses dans le texte ; en outre, elles seront transcrites sur papier calque, à l'encre de Chine.

Les auteurs sont priés d'indiquer les caractères italiques (en soulignant les lettres au crayon), ainsi que toute autre caractère spécial ; les préfixes *ortho*, *meta*, *para*, *cis*, *trans*, etc. seront soulignés pour indiquer leurs caractères italiques et ne seront jamais écrits avec des majuscules.

Aucune correction à la main ne sera admise sur le manuscrit. Les corrections seront frappées à la machine. Les lettres grecques ou autres symboles spéciaux seront insérés à la main à l'encre clairement.

Le manuscrit sera signé par l'auteur.

Le colonne-titre aura 50 lettres au maximum.

L'entière responsabilité du contenu des articles appartient aux auteurs.

Sur demande on peut obtenir une note plus complète.

PRINTED IN ROMANIA

KÖNYVTÁR ÉS KÖZPONT DOKUMENTÁCIÓS 1983

NOTE POUR LES AUTEURS

La Revue Roumaine de Chimie publie des articles en anglais, français, russe, allemand ou espagnol. Les auteurs sont priés d'envoyer des articles et des comptes rendus inédits.

Les manuscrits seront dactylographiés à double interligne. La bibliographie, les tableaux et la légende des figures seront placés après le texte.

Si l'article fait partie d'une série numérotée, la partie précédente sera donnée comme première référence.

Chaque article sera précédé d'un résumé comprenant quinze lignes au maximum.

Les références bibliographiques dans le texte seront citées par des exposants mis entre parenthèses et paraîtront à la fin de l'ouvrage.

Les publications périodiques mentionnées dans la bibliographie seront présentées suivant les prescriptions internationales : le nom de l'auteur précédé de l'initiale du prénom, le titre du périodique abrégé conformément à «Chemical Abstracts» et souligné par une ligne, le numéro du tome indiqué par des chiffres arabes et souligné par deux lignes, suivi de la première page de l'article ; à la fin, l'année de la parution sera placée entre parenthèses. Le numéro de la revue ne sera pas indiqué si les pages du volume sont numérotées consécutivement.

Les textes des livres ou traités indiqueront : le nom des auteurs, précédé de l'initiale du prénom, le titre du livre entre guillemets et sans être souligné, le numéro du tome précédé par l'abréviation «vol.» (ou «Bd.»), le numéro de l'édition, les [illegible] (the publishers), la localité de la parution du livre, l'année de la parution et la page de la référence précédée(s) par l'abréviation «p.» (ou «S.»).

Les brevets seront indiqués comme suit : l'auteur ou la firme, le pays et le numéro du brevet, la date et la réf. «Chem. Abstr.». Par ex. : M. Jones, (to Union Carbide Co), Brit. Pat. 691 238, 2 Sept. 1953, Chem. Abstr., 48, 13203 (1954).

Si la référence n'a pas été lue en original, on indiquera aussi la revue de références consultée.

Les diagrammes seront tracés à l'encre de Chine sur papier calque. Les tableaux et les figures (en nombre strictement nécessaire) ainsi que les courbes dans les figures seront numérotés par des chiffres arabes. Leur explication sera donnée dans la légende des figures. Il faut de ne pas inscrire les mêmes données dans les tableaux et les figures. Chaque tableau aura un titre. On indiquera dans le texte la place approximative des tableaux et des figures. Les formules chimiques seront insérées dans le texte ; en outre, elles seront transcrites sur papier calque, à l'encre de Chine.

Les auteurs sont priés d'indiquer les caractères italiques (en soulignant les lettres au crayon), ainsi que toute autre caractère spécial ; les préfixes ortho, méta, para, cis, trans, etc. seront soulignés pour indiquer leurs caractères italiques et ne seront jamais écrits avec des majuscules.

Aucune correction à la main ne sera admise sur le manuscrit. Les corrections seront frappées à la machine. Les lettres grecques ou autres symboles spéciaux seront insérés à la main à l'encre clairement.

Le manuscrit sera signé par l'auteur.

Le colonne-titre aura 50 lettres au maximum.

L'entière responsabilité du contenu des articles appartient aux auteurs.

Sur demande on peut obtenir une note plus complète.

PRINTED IN ROMANIA

1982 JUN 2 4

TRAVAUX PARUS AUX ÉDITIONS DE L'ACADÉMIE DE LA RÉPUBLIQUE SOCIALISTE DE ROUMANIE

ELENA CEAUŞESCU, **Noi cercetări în domeniul compuşilor macromoleculari** (Nouvelles recherches dans le domaine des composés macromoléculaires), 1981, 536 p.

I. GĂLĂŢEANU, **Procese şi metode radiochimice aplicate în energetica nucleară** (Processus et méthodes radiochimiques appliqués dans l'énergétique nucléaire), 1981, 234 p.

I. G. MURGULESCU, TATIANA ONCESCU, E. SEGAL, **Introducere în chimia fizică. Vol.II.2. Cinetică chimică şi cataliză** (Introduction à la chimie physique. Vol. II.2. Cinétique chimique et catalyse), 1981, 1024 p.

V. DRĂGUŢAN, A. T. BALABAN, M. DIMONIE, **Metateza olefinelor şi polimerizarea prin deschidere de inel a cicloolefinelor** (La métathèse des oléfines et la polymérisation par ouverture annulaire des cyclo-oléfines), 1981, 254 p.

O. IORDACHE, **Procese polistocastice aplicate la fenomenele de transfer** (Processus polystochastiques appliqués aux phénomènes de transfert), 1981, 187 p.

CR. SIMIONESCU, VALERIA GORDUZA, **Polimeri biocompatibili şi biologic activi** (Polymères biocompatibles et biologiquement actifs), 1980, 497 p.

Ş. MOLDOVEANU, A. SAVIN, **Aplicaţii în chimie ale metodelor semiempirice de orbitali moleculari** (Applications en chimie des méthodes semi-empiriques d'orbitaux moléculaires), 1980, 286 p.

ELENA CEAUŞESCU, **Polimerizarea stereospecifică a izoprenului** (La polymérisaton stéréospécifique de l'isoprène), 1979, 307 p.

M. FLORESCU, **Metode ştiinţifice în dezvoltarea industriei chimice moderne** (Méthodes scientifiques dans le développement de l'industrie chimique moderne), 1979, 256 p.

A. T. BALABAN, I. GALĂŢEANU, G. GEORGESCU, LIGIA SIMIONESCU, **Compuşi marcaţi şi radiofarmaceutici cu aplicaţii în medicina nucleară** (Composés marqués et radiopharmaceutiques à application en médecine nucléaire), 1979, 495 p.

CONST. GH. MACAROVICI, **Analiza chimică cantitativă anorganică** (L'Analyse chimique quantitative inorganique), 1979, 457 p.

I. G. MURGULESCU, E. SEGAL, **Introducere în chimia fizică, vol. II.1. Teoria molecular cinetică a materiei** (Introduction à la chimie physique, vol. II.1. La théorie moléculaire-cinétique de la matière), 1979, 1036 p.

I. E. TEODORESCU, MARIA FITI, **Iradierea tehnologică** (L'Irradiation technologique), 1979, 216 p.

S. STERNBERG, FL. DANEŞ, **Termodinamica chimică aplicată** (La thermodynamique chimique appliquée), 1978, 400 p.

I. G. MURGULESCU, V. EM. SAHINI, **Introducere în chimia fizică, Vol. I.2. Structura şi proprietăţile moleculelor** (Introduction à la chimie physique. Vol. I.2. La structure et les propriétés des molécules), 1978, 604 p.

C. DRĂGULESCU, E. PETROVICI, **Chimie structurală modernă. Chimia coordinanţei 8** (La chimie structurale moderne. La chimie de la coordinence 8), 1977, 947 p.

I. ZUGRĂVESCU, MAGDA PETROVANU, **N-ylid chemistry**, coédition avec McGraw Hill International Book Company, U.S.A., 1977, 396 p.

I. G. MURGULESCU, **Introducere în chimia fizică. Vol. I.1. Atomi, molecule, legătură chimică** (Introduction à la chimie physique, vol. I.1. Atomes, molécules, liaison chimique), 1976, 560 p.

CONST. GH. MACAROVICI, D. MACAROVICI, **Chimia oxizilor dubli şi utilizările lor** (La chimie des oxydes doubles et leur utilisation), 1975, 195 p.

ELENA CEAUŞESCU, **Research work on synthesis and characterization of macromolecular compounds.** Contributions, 1974, 251 p.

I.P.INFORMAŢIA c. 1625

43426

Lei 25.—

$ 70 (pour un abonnement annuel)

F 1103

REFERÁLVA

ACADÉMIE DE LA RÉPUBLIQUE SOCIALISTE DE ROUMANIE

R

REVUE ROUMAINE DE CHIMIE

TOME 27
N° 2
Février 1982

EDITURA ACADEMIEI REPUBLICII SOCIALISTE ROMÂNIA

Rev. Roumaine Chim.

RRCHAX, 27, 2, p. 167–310 (1982), Bucarest

ACADÉMIE DE LA RÉPUBLIQUE SOCIALISTE DE ROUMANIE

COMITÉ DE RÉDACTION

Rédacteur en chef:

I. G. MURGULESCU, membre de l'Académie de la République Socialiste de Roumanie

Rédacteurs en chef adjoints:

A. T. BALABAN et V. EM. SAHINI, membres correspondants de l'Académie de la République Socialiste de Roumanie

Collège de rédaction:

EM. BRATU, ELENA CEAUŞESCU, ECATERINA CIORĂNESCU-NENITZESCU, CR. SIMIONESCU, membres de l'Académie de la République Socialiste de Roumanie ; P. SPACU, membre correspondant de l'Académie de la République Socialiste de Roumanie : MARGARETA AVRAM, M. BANCIU, I. HAIDUC, D. I. MARCHIDAN, I. MOLDOVAN, G. NIAC et D. SĂNDULESCU.

La Revue Roumaine de Chimie paraît 10 fois par an. Toute commande de l'étranger pour les travaux parus aux Editions de la République Socialiste de Roumanie sera adressée à ILEXIM. Departamentul Export-import Carte (Livres), Departamentul Export-Import Presă (Revues), P.O.B. 136—137, télex 11226, 3, str. 13 Decembrie, 79517—Bucarest, Roumanie.

Les manuscrits, les livres et les revues proposés en échange, ainsi que toute correspondance seront envoyés à la rédaction :

REVUE ROUMAINE DE CHIMIE
125, Calea Victoriei 79717, Bucarest, Roumanie, téléphone 50 76 80

EDITURA ACADEMIEI REPUBLICII SOCIALISTE ROMÂNIA
125, Calea Victoriei, 79717 Bucarest, Roumanie, téléphone 50 76 80

REVUE ROUMAINE DE CHIMIE

ORSZÁGOS MŰSZAKI KÖNYVTÁR ÉS DOKUMENTÁCIÓS KÖZPONT 1983

Tome 27, N° 2 Février, 1982

RODICA VÎLCU and ELENA DIMITRIU, Nickel electroless plating in ultrasonic field . . . . 169–174 R

A. CĂLUȘARU and M. APOSTOL, Charge transfer by quantum tunneling across the separation interface of two media using perturbation formalism 175–190

Z. FINTA, E. CHIFU, EUGENIA GAVRILA and M. SALAJAN, Surface oxidation of some sulphurous minerals by the hypochlorite ion . . . . 191–198 C

R. MISHRA, Excess surface tension of binary liquid mixtures 199–203

IULIA CONTINEANU, LUMINIȚA WAGNER, LIDIA STĂNESCU and D. I. MARCHIDAN, The enthalpies of combustion and formation of *o*-phenylenediamine urea, and 2-hydroxy benzamidazole (in German) 205–209

J. D. PANDEY and R. P. PANDEY, On generalized pair potential. Evaluation of crystal properties 211–215

S. STERNBERG and V. BRÂNZOI, Polarization behaviour of Armco iron in anhydrous solution of R—OH + HCl 217–223

RADU VÂLCEANU and IOAN MOȚOC, Steric effects in effector—receptor interactions. The steric difference method and applications (in German) 225–233

MAMDOUH S. MASOUD, T. M. SALEM and M. H. AMER, Studies on iron (III), cobalt (II) and nickel (II) azido complexes 235–242

AL. IVANOV and D. I. HERȚIA, Stationarity in quantum theory of molecules. I. General formalism 243–255

R. P. VARMA and R. DAYAL, Characterization of strontium soaps and studies of their viscosity in aqueous isopropanol. 257–260

N. BARAKAT, F. ABOU EL-NOUR and N. SHAHEEN, Quantitative spectrographic estimation of zirconium by chemical enrichment . . . . 261–264 R

S. C. AGARWAL, SMT. P. L. AGARWAL, V. B. AGARWAL and VIBHAKAR DWIVEDI, Kinetics and mechanism of Cu(II)—catalysed oxidation of acetone by the peroxodisulphate ion 265–272

I. SIMITI and AURELIA MĂRIE, Contribution to the study of some heterocycles. LI. Preparation of some 2-phenyl-5-R-thiazolo [3, 2-*b*]-1, 2, 4-triazoles (in French) 273–279

BHARATI V. BADAMI and GURUBASAV S. PURANIK, Reactions of sydnones . . . . 281–284 BC

Rev. Roumaine Chim. **27**, *2*, 167–310 (1982) Bucarest

MANUEL RUBIO, RAÚL CETINA and MANUEL SALMÓN, Conformational calculations of some azobilirubin isomers. II. 3′-Methyl-4′-vinyl derivative (in Spanish) 285–290

FL. POPESCU, LIDIA ROSESCU, SIMONA PERCEC and OANA PETREUŞ, Study of hydrolytic behaviour of certain polyesters and polyamides containing phosphorus in the chain (in French) . . . . 291–299 R

LUMINIŢA VLĂDESCU and ARIADNA HARLES, Utilization of chromotropic acid in separation of titanium with ion exchange resins. I. Cation exchange behaviour . . . . 301–304 R

BOOK REVIEWS 305–309

Revue Roumaine de Chimie, **27**, *2*, 169–174 (1982)

NICKEL ELECTROLESS PLATING IN ULTRASONIC FIELD

RODICA VÎLCU* and ELENA DIMITRIU**

* Chair of Physical Chemistry and Electrochemical Technology, National Institute of Chemistry, Bd. Republicii 13, Bucharest, Romania

** ICEFIZ, Institute of Physics and Technology of Materials, Măgurele, Bucharest, Romania

Received April 21, 1981

The nickel chemical deposition on various substrata (dielectrics and metalics) becomes possible if on their surfaces a thin layer of aluminium is deposited by vacuum evaporation. An improvement of the properties of the nickel films deposited in this manner is observed if during deposition an ultrasonic field is applied. The structure becomes more uniform, the electrical sheet resistance decreases, the Rockwell hardness and the adherence of the film on the substratum increases.

INTRODUCTION

There are several methods for the chemical deposition of nickel[1–5] on dielectric substrata. They consist of an activation of the dielectric substratum surface (by depositing tin chloride and palladium chloride 1)), followed by the chemical deposition of nickel. The adherence of the nickel films obtained by these methods is generally much better than the one obtained by vacuum deposition. But neither of these procedures is adequate when the films are subjected to sudden temperature changes.

In order to improve the adherence of the Ni films on the substrata we activated the surface by deposition of a thin aluminium layer and investigated the process of the nickel chemical deposition on an alumina substratum in the presence of an ultrasonic field. [6,7]

EXPERIMENTAL

The nickel films were chemically deposited on sintered alumina plates (0.5 mm thick) with square shape (4, 27, and 108 mm one side). The roughness of the substratum surface was about 2–3 μm. The plates were thoroughly washed for two minutes in a solution of HNO_3 and HF (12 : 1), followed by rinsing in double distilled water and finally in acetone.

In order to activate the substratum surface a very thin layer of aluminium (about 0.45 μm) was deposited in vacuum (10^{-5} torr) on the surface. The nickel film was then chemically deposited by introducing the substrata into a plating bath for 8 minutes, at a temperature of 95–100°C.[2] This procedure was carried out both in the absence and in the presence of an ultrasonic field, supplied by an Ultramet® III sonic cleaner from Buehler Ltd Co. (frequency = 20 kHz ; transducer power = 50 W).

The thickness of the films ranged between 8 and 12 μm. The structure of the films was investigated by means of an ISM 20 type scanning electron microscope and the hardness was tested by means of a πMT 3 type microhardness tester. The sheet resistance[8,9] and the adherence of the Ni films on the substratum were also determined.

RESULTS AND DISCUSSIONS

Figures 1a and 1b show the structure of the Ni films deposited in the absence and in the presence of the ultrasonic field, respectively. It

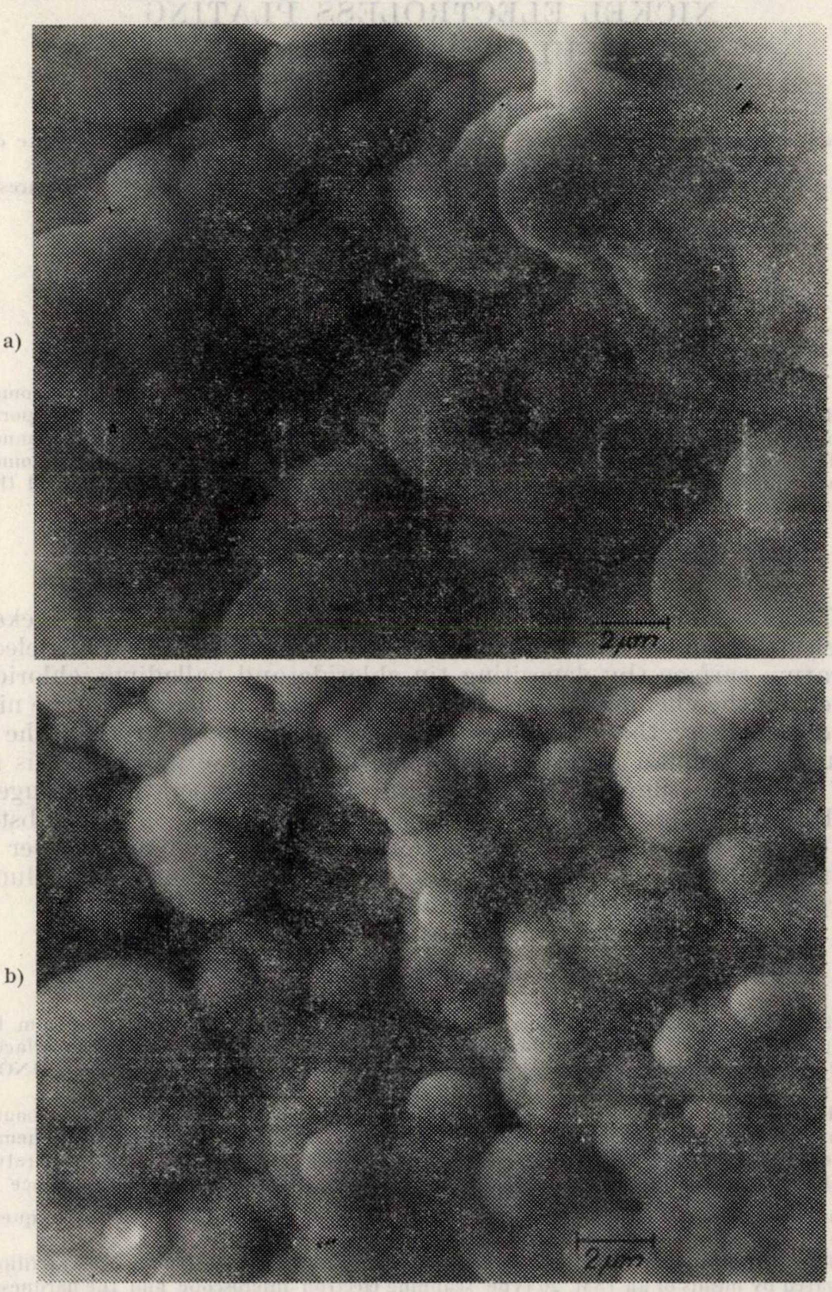

Fig. 1. — Scanning electron micrograph of electroless Ni films deposited on an alumina substratum · a) without ultrasonic field ; b) with ultrasonic field.

can be seen that the film structures, in both cases, consist of nearly spherical particles with various diameters ranging from 0.2 to 2.0 μm, though in the second case small size particles are predominant. This can be seen in figures 2a and 2b, where the relative frequency of the particle size, f_i vs. the particle diameter is ploted. The maxima of the frequency poligon are differently centred for both types of deposition. In the absence of the ultrasonic field it is situated around 0.8 – 0.9 μm, while in the presence of the ultrasonic irradiation it is shifted toward lower values: 0.4 – 0.5 μm. In the former case, the lowest limit of the particle size is about 0.4 μm, while for the latter, particles of that size represent 21%, and those of 0.5 μm diameter – nearly 58%. Fig. 2b shows that the presence of the ultrasonic field during Ni deposition has a beneficial effect on the particle size distribution, making a film with a more uniform structure and smaller particle size as compared to the simple chemical deposition.

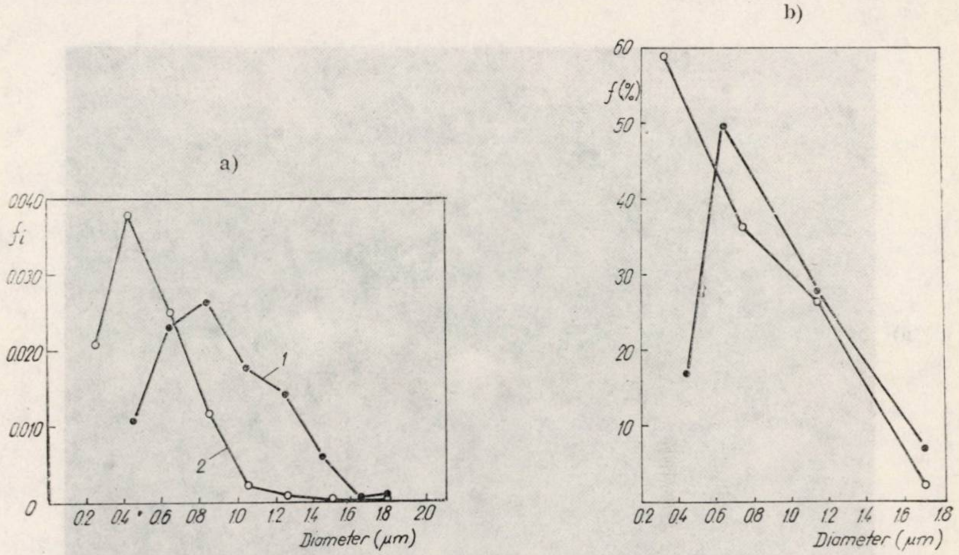

Fig. 2. – Relative frequencies poligon of nickel particles: a) the interval of the diameters used for drawing the hystogram is of 0.2 μm; b) the intervals of the diameters used for drawing the hystogram are: 0.2 – 0.5 μm, 1.0 – 1.3 μm, 1.4 – 2.0 μm. 1. without ultrasonic field; 2. with ultrasonic field.

This effect did not depend on the nature of the substrata. Experiments made on copper, graphite or barium titanate substrata gave entirely similar results (figs 3a and 3b).

It was experimentally found that the optimum results are obtained for a deposition time of 8 minutes, during which the ultrasonic field was applied for 3 minutes. Higher intervals can damage the films as it can be seen in figure 4 (for an irradiation time of 5 minutes). The same structure can be also obtained for the 180 W transducer power. When this power exceeds 250 W the nickel layer initially formed on the substratum is destroyed.

Not only the structure but also some properties of the nickel films were affected by the presence of the ultrasonic field during deposition. Thus an improvement of the sheet resistance, adherence and hardness was observed. The comparative results of these parameters are given

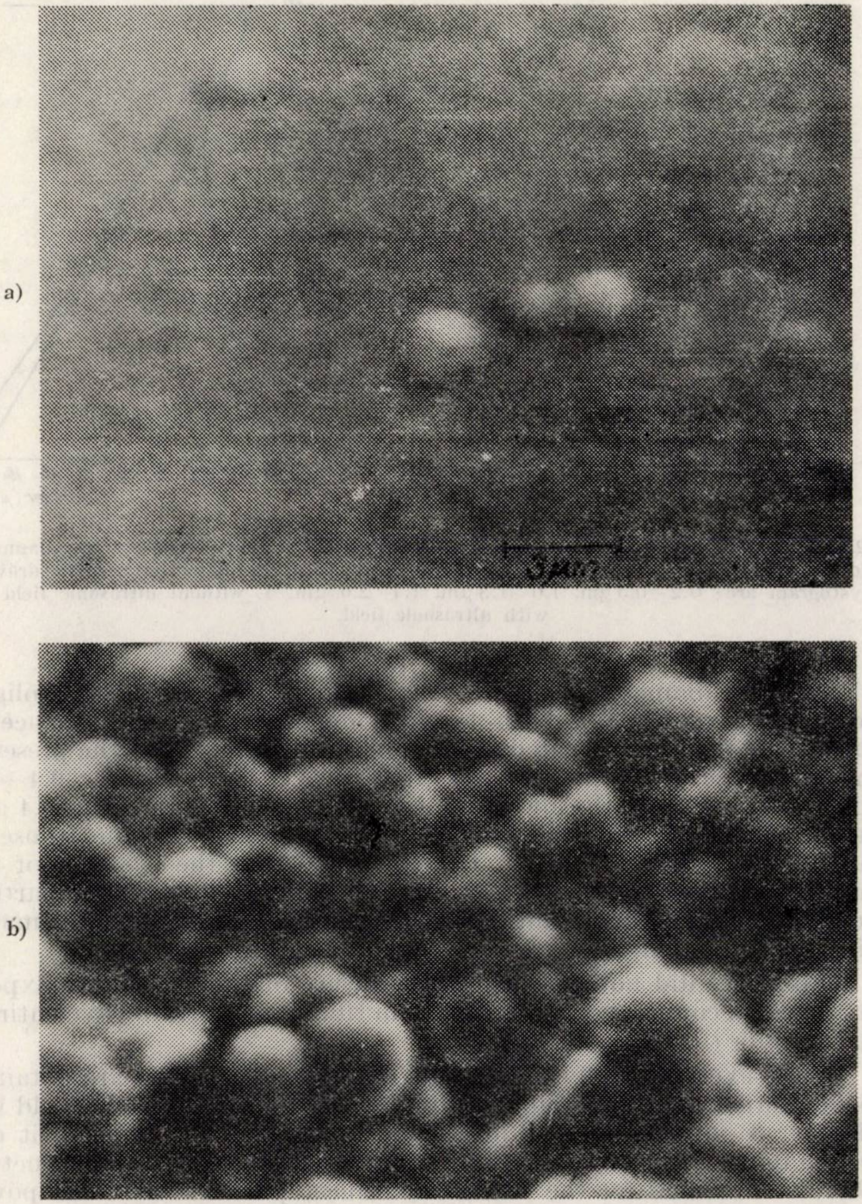

Fig. 3. — Scanning electron micrograph of electroless nickel films on a copper substratum; a) without ultrasonic field; b) with ultrasonic field.

in tables 1 and 2. The sheet resistance of the nickel films deposited in the presence of the ultrasonic field is about 2.4 times lower than that of the films deposited in the absence of the ultrasonic field. A slight increase of the irradiation time over the optimum value of three minutes brings about an important increase of the sheet resistance. This is due to the formation of islands within the films, as it was observed in Fig. 4.

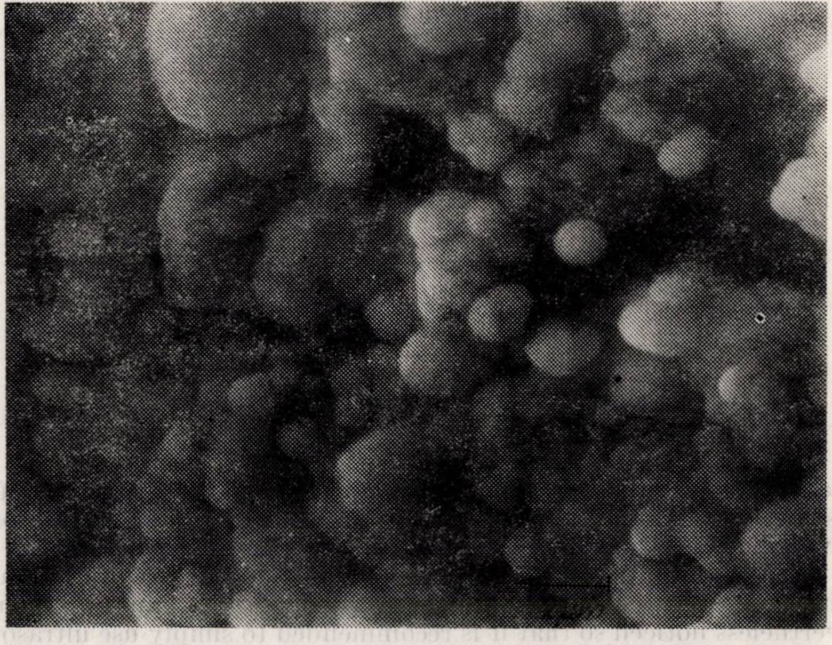

Fig. 4. — Scanning electron micrograph of electroless Ni film on the alumina substratum for a five minute irradiation with ultrasounds.

TABLE 1

The seet resistance $R_\square$ and the traction force F for peeling off the nickel films deposited on alumina

Plating	Time of irradiation (min)	R (Ω)	F (kg cm^{-2})
Electroless	—	5.3	112.5
Electroless in ultrasonic field	3	2.2	>175.0
	5	8.0	115.0 ; 162.5 175.0

The adherence of the film was determined by measuring the traction force which is necessary in order to peel off the nickel layer from the substratum. In order to do this the film was divided in squares of 4 mm².

A copper wire was sealed with a Bi — Sn euthectic alloy in each square and the traction force was measured by means of a dynamometer fixed at the end of the wire. From table 2 it can be seen that the adherence substantially increased for the films deposited in the presence of the ultrasonic field. At the same time an approx. three times increase of the Rockwell hardness was also observed in the case of such films.

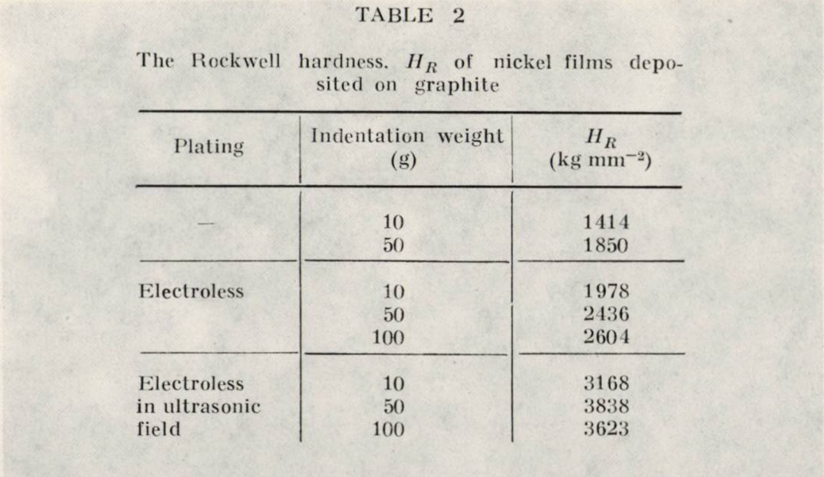

TABLE 2

The Rockwell hardness. H_R of nickel films deposited on graphite

Plating	Indentation weight (g)	H_R (kg mm^{-2})
—	10 50	1414 1850
Electroless	10 50 100	1978 2436 2604
Electroless in ultrasonic field	10 50 100	3168 3838 3623

Though the properties of the nickel films do not essentially change by the application of ultrasounds during deposition, an improvement is nevertheless noticed so that it is recommended to simply use ultrasounds when better nickel films are to be obtained by chemical deposition on various substrata.

The authors are deeply indebted to Igor Nazarenco for his help in the vacuum deposition of aluminium on various substrata.

REFERENCES

[1] Ch. R. Brumett, *Official Gazette of the United States, Patents and Trademark Office*, **941**, 1901 (1975).

[2] Fr. E. Costello, *ibid*, **965**, 303 (1977).

[3] H. F. Bell, D. W. Rich and M. C. Smith, *ibid*, **913**, 916 (1973).

[4] G. A. Miller, *ibid*, **915**, 1421 (1973).

[5] H. E. Bellis, *ibid*, **911**, 609 (1973).

[6] T. Takahashi and H. Itoh, *J. Mater. Sci.* **14**, 1285 (1979).

[7] T. Takahashi and H. Itoh, *J. Electrochem. Soc.*, **124**, 797 (1977).

[8] L. I. Maisel and R. Glang. "Handbook of Thin Film Technology", McGraw — Hill, London, 1970.

[9] D. R. Zrudsky, H. D. Bush and J. R. Fasset, *Rev. Sci. Instrum.*, **37**, 885 (1966).

Revue Roumaine de Chimie, 27, 2, 175–190 (1982)

CHARGE TRANSFER BY QUANTUM TUNNELING ACROSS THE SEPARATION INTERFACE OF TWO MEDIA USING PERTURBATION FORMALISM

A. CĂLUŞARU* and M. APOSTOL

Central Institute of Physics, Dept. of Theoretical Physics, P.O. Box 5206, Bucharest, Romania

Received June 5, 1981

The quantum tunneling is studied in the present paper, using the elastic scattering approximation of the electrons on the potential barrier at the separation interface of two media. In the description of the model four hamiltonian components were considered for both the tunneling and reflexion processes. On the basis of this model the exact one-particle Green functions were analytically deduced. The problem is treated in the framework of time dependent perturbation theory, therefore using the Feynman-Dyson hamiltonian and S-matrix. The equations obtained allow to deduce the formula corresponding to the flow of the electrical current through the interface. At the same time the energy loss undergone by the electrons annihilated and created during tunneling transition was calculated. Finally, it is shown that the energy adsorbed by the tunneling process can be measured by the surface of the barrier; this energy loss represents the effect of the hamiltonian corresponding to the tunneling phenomena.

The calculation of the reflected or penetrated fraction, in the form of the transparence coefficient, appeared in the first state of the development of quantum mechanics as very complicated. That is why only the approximate calculations were possible at that time, the most known being the so-called W.K.B.-approximation. In this case appears that the tunneling occurs with maximum probability in conditions of resonant transition only, when the tunneling takes place from one level to another with equal energy. Owing to the fact that the result obtained by the W.K.B.-method [1] is an approximate one, the apparent conclusion was that the tunneling occurs without energy consumption and the particle undergoes no change during the transition.

The aim of the present work is to consider the deeper aspects of the quantum tunneling and to try to find a more realistic solution for the expression of transition probabilities.

The problem of the tunneling is treated in the elastic scattering approximation of the electrons on the potential barrier of the interface. But as we have already emphasized, the tunneling transition cannot be possible without any change in the energetical state of the system. In a real picture of the phenomenon, the electron transition from a milieu into another is accompanied by energy loss as a consequence of the electron collisions with the components of the interface, so that the eneryg levels which can be occupied by electrons after collision are not identical with those before collision as in the older approximations. In addition the electron flux which is scattered on the interface passes partially through it and the remained part is reflected or adsorbed, participating in other physico-chemical processes. So, finally, the model used in this work is to describe the electron flow across the interface in the case of the inelastic scattering and the absorption or generation of charge carriers.

---

* Permanent address: Institute of Chemical Research, Spl. Independenţei 202, 79611 Bucharest, Romania

1. THE MODEL

The one-electron wave functions are denoted by $\varphi^{(1)}(p)$ and $\varphi^{(2)}(p)$, corresponding to the milieu (1) and (2) respectively. The variable p represents all the quantum numbers that describe the one-electron state with free energy levels $\varepsilon_p^{(1,2)}$.

In order to carry out the calculation we assume that in the approximation of the quasi-free electrons, these lasts are described by the wave function of the plane wave type and the one-particle energies are given by the expressions :

$$\varepsilon_p^{(1)} = p^2/2m_1 \tag{1 a}$$

and :

$$\varepsilon_p^{(2)} = p^2/2m_2 \tag{1 b}$$

where p is the electronic momentum and m_1 and m_2 the effective masses of the quasi-free electrons in the (1) and (2) media respectively (for sake of simplicity the Planck constant is taken equal to unity). Here the one-dimensional model only is considered, the relative coordinate x of the electron motion being on the direction of the external electrical field; this simplification is only geometrical and the final conclusion is not affected.

The potential difference (voltage) U created by the applied electrical field displaces the energy levels occupied in the electron fundamental state in the milieu (1), whose displacement is in opposite direction as compared with the electrical field applied. Considering N electrons on the unit length in the milieu (1), the Fermi momentum is (the electron spin is omitted) :

$$k_F^0 = \pi N \tag{2}$$

without consideration of the electrons on the other directions. The variable λ_1 of the Fermi momentum is given by the equation (Fig. 1) :

$$k_{F_1}^{(1)} = k_F^0 + \lambda_1 \tag{3 a}$$

and :

$$k_{F_2}^{(1)} = k_F^0 - \lambda_1 \tag{3 b}$$

The energy of the fundamental state is:

$$E = \frac{1}{2\pi}\int_{0}^{k_{F_1}^{(1)}} \mathrm{d}k\,\frac{k^2}{2m_1} + \frac{1}{2\pi}\int_{-k_{F_2}^{(1)}}^{0} \mathrm{d}k\,\frac{k^2}{2m_1} = \frac{1}{2\pi}\int_{-k_F^0}^{k_F^0} \mathrm{d}k\,\frac{k^2}{2m_1} + NeU \tag{4}$$

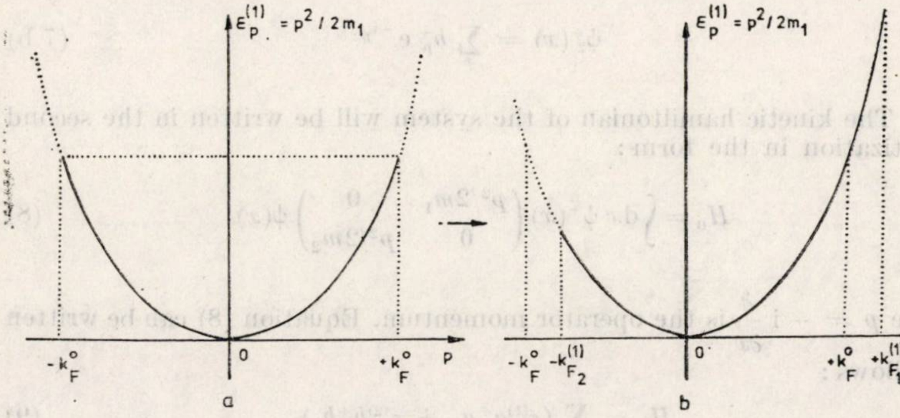

Fig. 1. — Energy levels as a function of the electron momentum. a — free electrons; b — with an applied voltage.

from which it follows:

$$\lambda_1 = (2m_1 eU)^{1/2} \tag{5 a}$$

Similarly, for the milieu (2) we obtain:

$$\lambda_2 = (2m_2 eU)^{1/2} \tag{5 b}$$

where U is the potential difference (electrical voltage) at the interface.

We denote by a_p and a_p^+ the annihilation and creation operators respectively of the one-electron states in the milieu (1) and by b_p and b_p^+ the same operators corresponding to the milieu (2); the electronic field can be represented by the vector with two components:

$$\psi(x) = \begin{pmatrix} \psi_1(x) \\ \psi_2(x) \end{pmatrix} \tag{6}$$

where

$$\psi_1(x) = \sum_p a_p \mathrm{e}^{\mathrm{i}px} \tag{6 a}$$

$$\psi_2(x) = \sum_p b_p \mathrm{e}^{\mathrm{i}px} \tag{6 b}$$

The creation and annihilation operators satisfy the well-known anticommutation fermionic relations.

The hermitian conjugate of the field operator $\psi(x)$ is by definition:

$$\psi^+(x) = (\psi_1^+(x),\ \psi_2^+(x)) \tag{7}$$

where:

$$\psi_1^+(x) = \sum_p a_p^+ \,\mathrm{e}^{\mathrm{i}px} \tag{7 a}$$

$$\psi_2^+(x) = \sum_p b_p^+ \,\mathrm{e}^{-\mathrm{i}px} \tag{7 b}$$

The kinetic hamiltonian of the system will be written in the second quantization in the form:

$$H_0 = \int \mathrm{d}x\, \psi^+(x) \begin{pmatrix} p^2/2m_1 & 0 \\ 0 & p^2/2m_2 \end{pmatrix} \psi(x) \tag{8}$$

where $p = -\mathrm{i}\dfrac{\partial}{\partial x}$ is the operator momentum. Equation (8) can be written as follows:

$$H_0 = \sum_p (\varepsilon_p^{(1)} a_p^+ a_p + \varepsilon_p^{(2)} b_p^+ b_p) \tag{9}$$

The presence of the interface is signified by the potential $V(x)$ (a real and even function, $V(x) = V(-x) = V^{*}(x)$, conditions imposed evidently by the physics of the problem) in which move the two kinds of electrons. Since in the present two-component formulation of the electric field, equation (6), in the (2) milieu there are no more electrons of the b type, it results that the effect of the interface must be manifested by absorption and creation of electrons. More precisely electrons of the "a" type annihilated by the interface will be created in the (1) milieu by shutting the electrical circuit and the electrons of the "b" type created in the interface will be annihilated in the milieu (2) by shutting the same electrical circuit. Consequently, the current flow process through the interface must be expressed by a pure imaginary potential:

$$W(x) = \mathrm{i}V(x) \tag{10}$$

which, as it is known from the nuclear physics (the optical model) [2] is responsible for the absorption and creation of particles in a collision process. The interaction hamiltonian can be written in the second quantization in the form:

$$H_1 = \int \mathrm{d}x\, \psi^+(x) W(x) \psi(x) = \sum_{pk} (W_k b_p^+ a_{p-\kappa} + W_{-k} a_p^+ b_{p-b}) \tag{11}$$

where:

$$W(x) = \begin{pmatrix} 0 & W(-x) \\ W(x) & 0 \end{pmatrix} \tag{12}$$

The choice of the interaction matrix $W(x)$ in this form is imposed by the necessity to describe the current flow across the interface and also to obtain the corresponding process which completes the energy levels in the two media by shutting the circuit, in order to have a real current flow and not an electrical double layer only. Obviously, the introduction of the pure imaginary potential $W(x)$ in the problem hamiltonian renders this into a nonhermitian one, a property which describes just the loss and formation of particle due to the interface.

We denote by $\mathrm{i}\, t_k$ (from tunneling) the Fourier W_k components of the $W(x)$ potential. Assuming that $W(x)$ is chosen in such a manner that W_{-2p+k} is independent of p, at least in the Fermi surface region, where the states implying the highest weight in the current flow are located, we have $W_{-2p+k} = \mathrm{i}\, r_k$ (from reflexion); the interaction hamiltonian (11) can be written in the form:

$$H_1 = H_t^1 + H_t^2 + H_t^{1C} + H_t^{2C} + H_r^1 + H_r^2 + H_r^{1C} + H_r^{2C} \tag{13}$$

The indexes t, r and C, denote the terms "tunneling", "reflexion" and "compensation" respectively. The term expressions from (13), as it can be obtained from equation (11), are the following:

$$H_t^1 = \sum_{\substack{p>0 \\ p+k>0}} \mathrm{i}\, t_k b_{p+k}^{+} a_p \tag{14 a}$$

$$H_t^2 = \sum_{\substack{p<0 \\ p+k<0}} \mathrm{i}\, t_k a_p^{+} b_{p+k} \tag{14 b}$$

$$H_t^{1C} = \sum_{\substack{p>0 \\ p+k>0}} \mathrm{i}\, t_k a_p^{+} b_{p+k} \tag{14 c}$$

$$H_t^{2C} = \sum_{\substack{p<0 \\ p+k<0}} \mathrm{i}\, t_k b_{p+k}^{+} a_p \tag{14 d}$$

$$H_r^1 = \sum_{\substack{p>0 \\ -p+k<0}} \mathrm{i}\, r_k b_{-p+k}^{+} a_p \tag{14 e}$$

$$H_r^2 = \sum_{\substack{p<0 \\ -p+b>0}} \mathrm{i}\, r_k a_p^{+} b_{-p+k} \tag{14 f}$$

$$H_r^{1C} = \sum_{\substack{p>0 \\ -p+k<0}} \mathrm{i}\, r_k a_p^{+} b_{-p+k} \tag{14 g}$$

$$H_r^{2C} = \sum_{\substack{p<0 \\ -p+k>0}} \mathrm{i}\, r_k b_{-p+k}^{+} a_p \tag{14 h}$$

The processes described by these terms are presented schematically in Figs 2 and 3, which give an image of the physical significance of the interaction hamiltonian H_1.

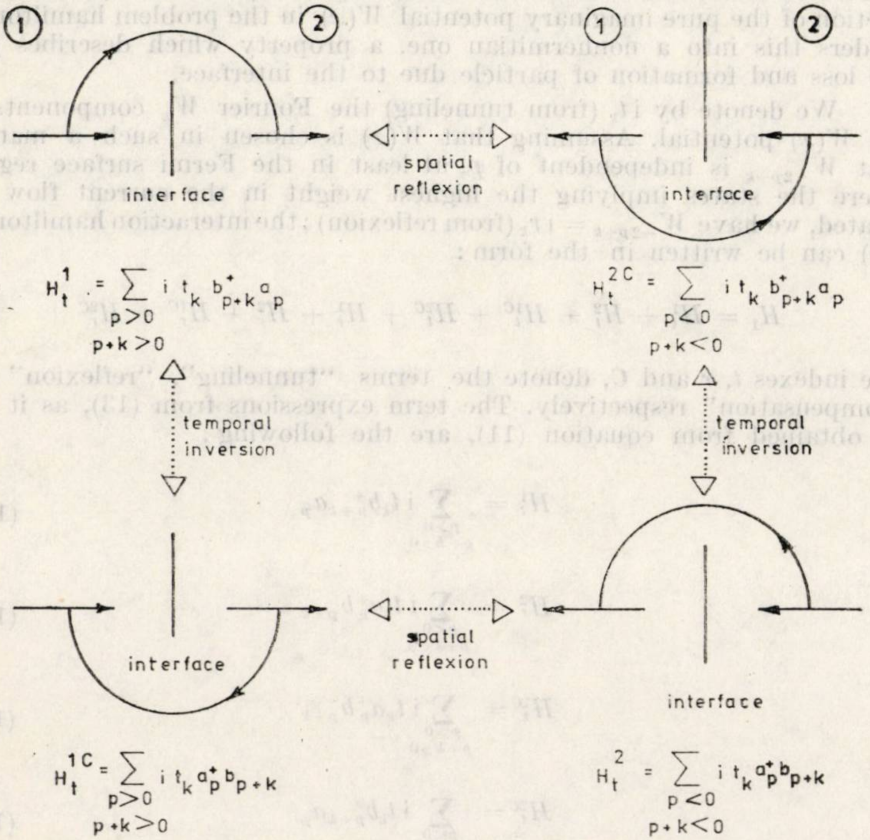
1
2
interface
spatial reflexion
1
2
interface
$H_t^1 = \sum_{\substack{p>0 \\ p+k>0}} i\, t_k\, b^+_{p+k} a_p$
$H_t^{2C} = \sum_{\substack{p<0 \\ p+k<0}} i\, t_k\, b^+_{p+k} a_p$
temporal inversion
temporal inversion
interface
spatial reflexion
interface
$H_t^{1C} = \sum_{\substack{p>0 \\ p+k>0}} i\, t_k\, a^+_p b_{p+k}$
$H_t^{2} = \sum_{\substack{p<0 \\ p+k<0}} i\, t_k\, a^+_p b_{p+k}$

Fig. 2. — Tunneling phenomena and the corresponding components.

The introduction of the $W(x)$ pure imaginary potential allows us to treat the problem of the inelastic scattering of the electrons on the interface as a formal inelastic scattering problem, the fraction of the "lost" electrons in inelastic "channels" being controlled by parameters t_k and r_k. Therefore, in equations (14 a—h) it is allowed to take $k = 0$ and at the same time $\varepsilon_p^{(1)} = \varepsilon_p^{(2)}$. Obviously, the parameters $t_{k=0} \equiv t$ and $r_{k=0} \equiv r$ do not longer satisfy in this case the well-known relation of normation $|t|^2 + |r|^2 = 1$, applicable in the case of true elastic scattering only. The parameter t will control the electron fraction lost by tunneling through the inelastic collision "channels" and r is the reflected electron fraction in the same inelastic "channels". The exact physical significance of these values will be discussed in section 4.

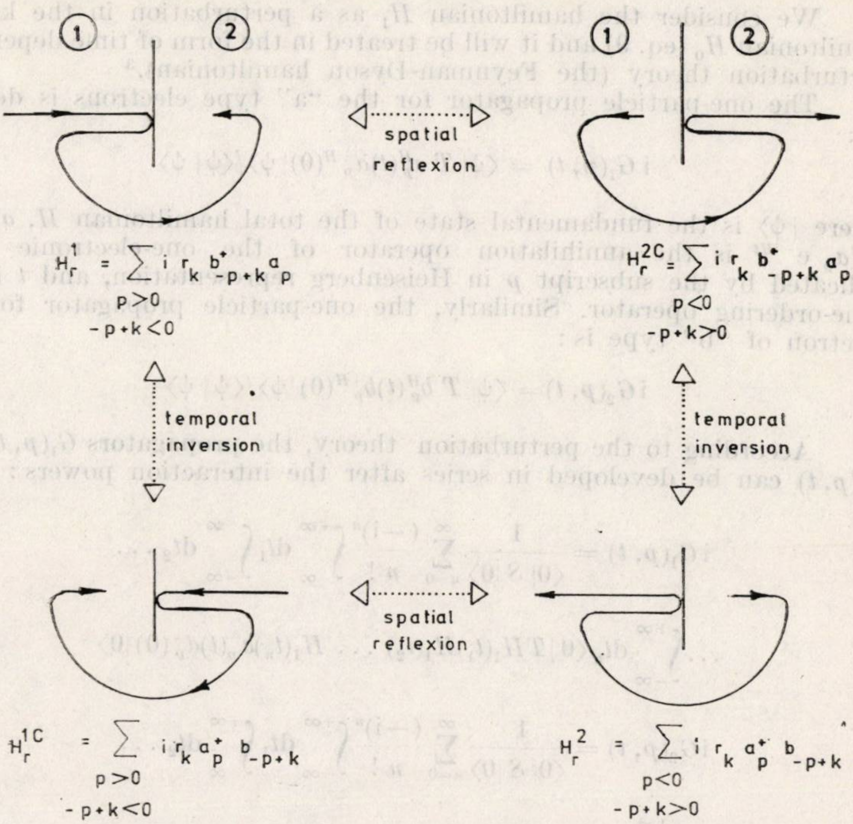
①
②
spatial reflexion
①
②
$H_r = \sum i\, r_k\, b^+_{-p+k}\, a_p$
$p>0$
$-p+k<0$
$H_r^{2C} = \sum i\, r_k\, b^+_{-p+k}\, a_p$
$p<0$
$-p+k>0$
temporal inversion
temporal inversion
spatial reflexion
$H_r^{1C} = \sum i\, r_k\, a_p^+\, b_{-p+k}$
$p>0$
$-p+k<0$
$H_r^2 = \sum i\, r_k\, a_p^+\, b_{-p+k}$
$p<0$
$-p+k>0$

Fig. 3. — Reflexion phenomena and the corresponding components.

2. ONE-PARTICLE GREEN FUNCTION

In the first state of this treatment we can neglect the reflexion terms from the hamiltonian (eqs. (14 d—h)). According to the discussion at the end of the previous section, the interaction hamiltonian has the form:

$$H_1 = H_t^1 + H_t^2 + H_t^{1C} + H_t^{2C} \tag{15}$$

$$H_t^1 = \mathrm{i}\, t \sum_{p>0} b_p^+ a_p \tag{16 a}$$

$$H_t^2 = \mathrm{i}\, t \sum_{p<0} a_p^+ b_p \tag{16 b}$$

$$H_t^{1C} = \mathrm{i}\, t \sum_{p>0} a_p^+ b_p \tag{16 c}$$

$$H_t^{2C} = \mathrm{i}\, t \sum_{p<0} b_p^+ a_p \tag{16 d}$$

We consider the hamiltonian H_1 as a perturbation in the kinetic hamiltonian H_0 (eq. 9) and it will be treated in the form of time dependent perturbation theory (the Feynman-Dyson hamiltonian).[3]

The one-particle propagator for the "a" type electrons is defined as :

$$\mathrm{i}\, G_1(p, t) = \langle\psi|\, T\, a_p^H(t) a_p^{+H}(0)|\,\psi\rangle / \langle\psi\,|\,\psi\rangle \tag{17}$$

where $|\,\psi\rangle$ is the fundamental state of the total hamiltonian H, $a_p^H(t) = \mathrm{e}^{\mathrm{i}Ht} a_p\, \mathrm{e}^{-\mathrm{i}Ht}$ is the annihilation operator of the one-electronic state indicated by the subscript p in Heisenberg representation, and t is the time-ordering operator. Similarly, the one-particle propagator for the electron of "b" type is :

$$\mathrm{i}\, G_2(p, t) = \langle\psi|\, T\, b_p^H(t) b_p^{+H}(0)\,|\psi\rangle / \langle\psi\,|\,\psi\rangle \tag{18}$$

According to the perturbation theory, the propagators $G_1(p, t)$ and $G_2(p, t)$ can be developed in series after the interaction powers :

$$\mathrm{i}\, G_1(p, t) = \frac{1}{\langle 0|\, S\,|0\rangle} \sum_{n=0}^{\infty} \frac{(-\mathrm{i})^n}{n\,!} \int_{-\infty}^{+\infty} \mathrm{d}t_1 \int_{-\infty}^{+\infty} \mathrm{d}t_2 \ldots$$

$$\ldots \int_{-\infty}^{+\infty} \mathrm{d}t_n \langle 0\,|\, T H_1(t_1) H_1(t_2) \ldots H_1(t_n) a_p(t) a_p^{+}(0)\,|0\rangle \tag{19 a}$$

$$\mathrm{i}\, G_2(p, t) = \frac{1}{\langle 0|\, S\,|0\rangle} \sum_{n=0}^{\infty} \frac{(-\mathrm{i})^n}{n\,!} \int_{-\infty}^{+\infty} \mathrm{d}t_1 \int_{-\infty}^{+\infty} \mathrm{d}t_2 \ldots$$

$$\ldots \int_{-\infty}^{+\infty} \mathrm{d}t_n \,\langle 0\,|\, T H_1(t_1) H_1(t_2) \ldots H_1(t_n) b_p(t) b_p^{+}(0)\,|\,0\rangle \tag{19 b}$$

where $|0\rangle$ is the fundamental state of the system without interaction, S the operator of evolution in the remote past to the far future (S-matrix) :

$$\langle 0\,|S\,|0\rangle = \sum_{n=0}^{\infty} \frac{(-\mathrm{i})^n}{n\,!} \int_{-\infty}^{+\infty} \mathrm{d}t_1 \ldots \int_{-\infty}^{+\infty} \mathrm{d}t_n \langle 0\,|\, T H_1(t_1) \ldots H_1(t_n)\,|\,0\rangle \tag{20}$$

The averages in equations (19 a, b) and (20) are calculated. The nominator of the right side of equation (19 a) in zero order of perturbation theory is just the free Green function (the propagator) :

$$\langle 0\,|\, T a_p(t) a_p^{+}(0)\,|0\rangle = \mathrm{i}\, G_1^0(p, t) \tag{21}$$

The next contribution is given by the second order of the perturbation theory and has two terms :

$$(\mathrm{i}\ t)^2\, \mathrm{d}t_1\, \mathrm{d}t_2 G_2^0(p_1 t_2 - t_1) G_1^0(p_1 t_1) G_1^0(p_1 t - t_2) \tag{22 a}$$

$$-(\mathrm{i}\ t)^2\, \mathrm{d}t_1\, \mathrm{d}t_2\, G_2^0(p_1 t_2 - t_1) G_1^0(p_1 t_1 - t_2) G_1^0(p, t) \tag{22 b}$$

The terms (22 a, b) can be represented by the diagram in Figs. 4 and 5.

In the Feynman diagrams for the perturbation representation of the exact Green functions, the continuous right lines represent the 1-type propagators, the dotted right lines the 2-type propagators

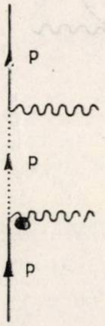

Fig. 4. — Feynman diagram for eq. (22).

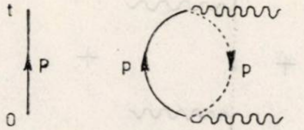

Fig. 5. — Unlinked Feynman diagram.

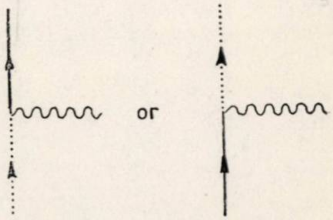

Fig. 6. — Fundamental vertex in the Feynman diagrams.

and the wavy lines represent the interaction (the "i t" value). The fundamental vertex in the Feynman diagrams is represented in Fig. 6. This represents, therefore, the interaction which is bound to two lines representing the particle propagation (particle lines) from which one is of the 1-type and the other of the 2-type (one is continuous and the other is dotted). It can also be seen that the interaction is not accompanied by the transport of the "momentum-energy" in the manner that the momentum and energy variables of the electronic propagators are the same in the entire diagram.

Developing the denominator of the right side of equation (19 a) the diagramatic expression until the second order of the perturbation

Fig. 7. — Diagramatic expansion of $\langle 0|S|0\rangle$.

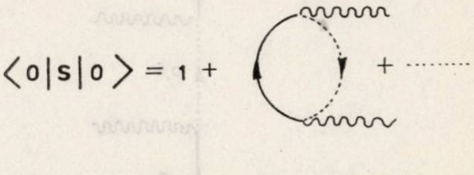

theory is obtained, which is shown in Fig. 7. In this way the Green function $G_1(p, t)$ can be expressed diagramatically to the second order in the form represented in Fig. 8.

We can see that the unlinked diagrams of the type represented in Fig. 5 do not contribute to electronic propagators.

When a Fourier transformation referred to time is considered, the following relation is obtained :

$$G_{1,2}(p, t) = \int \frac{d\varepsilon}{2\pi} G_{1,2}(p, \varepsilon) e^{-i\varepsilon t} \tag{23}$$

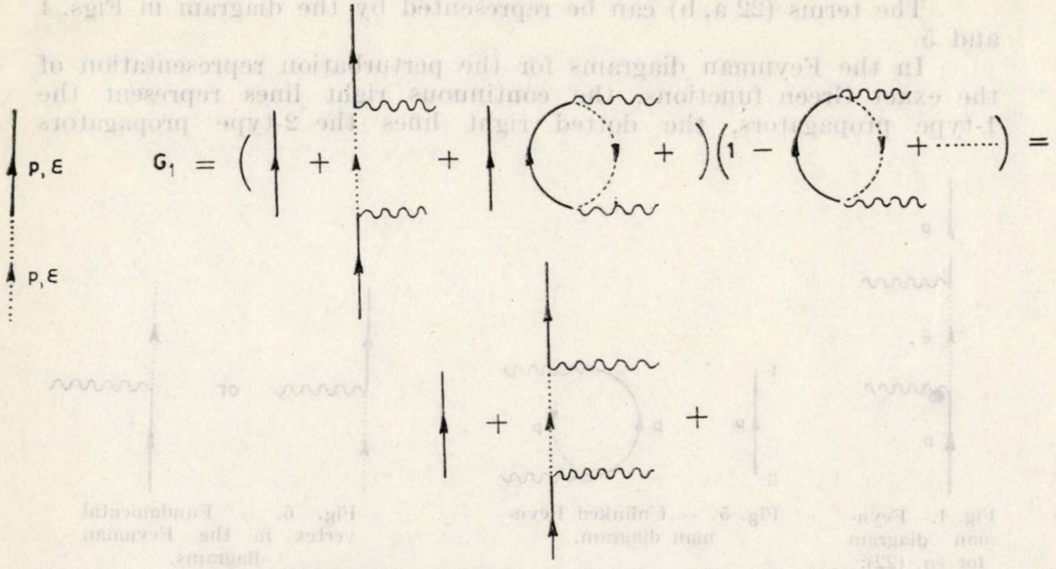

Fig. 8. — Diagramatic expression of the Green function $G_1(p, t)$.

With this relation equation (22) becomes :

$$(\mathrm{i}\,t)^2 G_2^0(p, \varepsilon) G_1^{0^2}(p, \varepsilon) \tag{24}$$

The corresponding diagram is given in Fig. 9. The next diagram, contributing to $G_1(p, \varepsilon)$, is of the fourth order of the perturbation theory and

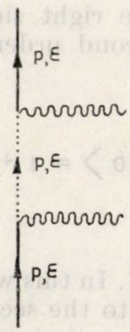

Fig. 9. — Diagram corresponding to eq. (24).

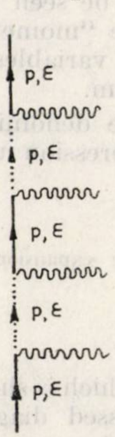

Fig. 10. — Diagram of the fourth order of the perturbation theory, eq. (25).

has the form represented in Fig. 10. The analytical expression is :

$$(\mathrm{i}\,t)^4 G_2^{0^2}(p, \varepsilon) G_1^{0^3}(p, \varepsilon) \tag{25}$$

The weight with which appears the 2 n order diagram in perturbation development (19 a) is related to the weight g_{n-1} with which appears the 2 $(n-1)$ diagram by the following recurrence relation:

$$2g_{n-1}(2n-1+C^2_{2n-1}) = g_n , \quad n = 2, 3, \ldots \tag{26}$$

$$g_1 = 2$$

Then, we can find:

$$g_n = (2n)\,! \tag{27}$$

Therefore, the rules to find an analytical expression for the 2 n linked diagram are as follows:

1. The value i $G_1^0(p, \varepsilon)$, with the p, ε variables is attached to each continuous line;

2. The value i $G_2^0(p, \varepsilon)$, with the p, ε variables, is attached to each dotted line;

3. To each interaction line the value "i t" is attached;

4. All is multiplied by $(-\mathrm{i})^{2n+1}$. This factor arises from both the interaction and i coefficient on the left part of equation (19 a); a multiplication with $(-1)^F$ is carried out where F is the number of closed electron lines (these latter do not appear in the linked diagrams of the propagators).

We can deduce the general expression for the $2n$ order diagram of the propagator $G_1(p, \varepsilon)$:

$$G_1^{(n)}(p, \varepsilon) = (\mathrm{i}\,t)^{2n} G_2^{0^n}(p, \varepsilon) G_1^{0^{n+1}}(p, \varepsilon) \tag{28}$$

The Dyson equation for $G_1(p, \varepsilon)$ can be represented as it is shown in Fig. 11. The heavy lines represent the exact propagators. The analytical expression of Fig. 11 is:

$$G_1(p, \varepsilon) = G_1^0(p_1, \varepsilon) + (\mathrm{i}\,t)^2 G_1^0(p, \varepsilon) G_2^0(p, \varepsilon) G_1(p, \varepsilon) \tag{29}$$

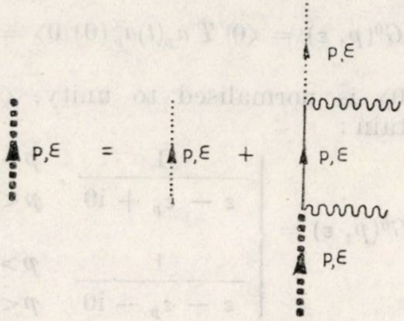

Fig. 11.—Dyson equation for $G_1(p, \varepsilon)$.

from which:

$$G_1(p, \varepsilon) = \frac{G_1^0(p, \varepsilon)}{1 + t^2\, G_1^0(p, \varepsilon) G_2^0(p, \varepsilon)} \tag{30}$$

a expression which can also be obtained by direct summation of the terms from (28):

$$G_1(p,\,\varepsilon) = \sum_{n=0}^{\infty} (\mathrm{i}\,t)^{2n} G_2^{0^n}(p,\,\varepsilon) G_1^{0^{n+1}}(p,\,\varepsilon) \tag{31}$$

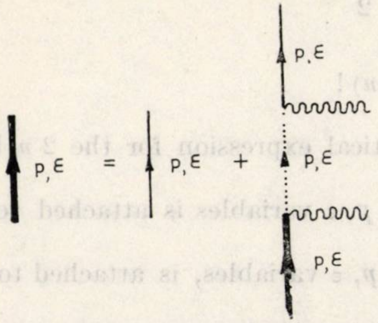

Fig. 12. — Dyson equation for the propagator $G_2(p,\,\varepsilon)$.

Similarly, the propagator $G_2(p,\,\varepsilon)$ can be obtained:

$$G_2 = \frac{G_2^0(p,\,\varepsilon)}{1 + t^2\, G_1^0(p,\,\varepsilon) G_2^0(p,\,\varepsilon)} \tag{32}$$

whose Dyson equation can be represented in the diagram form given in Fig. 12.

Considering the hypothesis assumed at the end of the first section we obtain:

$$G_1^0(p,\,\varepsilon) = G_2^0(p,\,\varepsilon) \equiv G^0(p,\,\varepsilon)$$

and, therefore:

$$G_1(p,\,\varepsilon) = G_2(p,\,\varepsilon) \equiv G(p,\,\varepsilon)$$

The free propagator $G^0(p,\,\varepsilon)$ can be calculated using its definition:

$$\mathrm{i}\, G^0(p,\,\varepsilon) = \langle 0|\, T\, a_p(t) a_p^+(0)\, |0\rangle = \langle 0|\, T\, b_p(t) b_p^+(0)\, |0\rangle \tag{33}$$

The state $|0\rangle$ is normalised to unity, $\langle 0 | 0\rangle = 1$.
We obtain:

$$G^0(p,\,\varepsilon) = \begin{cases} \dfrac{1}{\varepsilon - \varepsilon_p + \mathrm{i}0} & \begin{array}{l} p>0,\ \varepsilon_p > \mu_1 = k_{F1}^2/2m \\ p<0,\ \varepsilon_p > \mu_2 = k_{F2}^2/2m \end{array} \\[2ex] \dfrac{1}{\varepsilon - \varepsilon_p - \mathrm{i}0} & \begin{array}{l} p>0,\ \varepsilon_p < \mu_1 = k_{F1}^2/2m \\ p<0,\ \varepsilon_p < \mu_2 = k_{F2}^2/2m \end{array} \end{cases} \tag{34}$$

From equations (30) and (32), we can obtain:

$$G(p,\,\varepsilon) = \frac{\varepsilon - \varepsilon_p}{(\varepsilon - \varepsilon_p)^2 + t^2} = \frac{\varepsilon - \varepsilon_p}{(\varepsilon - \varepsilon_p + \mathrm{i}\,t)(\varepsilon - \varepsilon_p - \mathrm{i}\,t)} \tag{35}$$

We can see that the one-electronic levels suffer a decay with the rate t (the lifetime is $1/t$).

At the same time with the one-particle propagators $G_1(p, \varepsilon)$ and $G_2(p, \varepsilon)$, of the type 1 and 2, crossed Green functions can be defined by the relations :

$$\mathrm{i}\, G_{ab}(p, t) = \langle \psi | T a_p^H(t) b_p^{+H}(0) | \psi \rangle / \langle \psi | \psi \rangle \tag{36 a}$$

$$\mathrm{i}\, G_{ba}(p, t) = \langle \psi | T b_p^H(t) a_p^{+H}(0) | \psi \rangle / \langle \psi | \psi \rangle \tag{36 b}$$

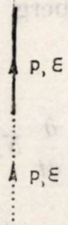

Fig. 13. — First order diagram of the crossed Green function G_{ab}.

The first contribution to these propagators appears in the first order of the perturbation theory and is expressed by the diagram given in Fig. 13, whose analytical expression is :

$$\mathrm{i}\, t G_1^0(p, \varepsilon) G_2^0(p, \varepsilon) \tag{37}$$

By carrying out the same analysis as for the propagators of the types 1 and 2, we obtain :

$$G_{ab}(p, t) = G_{ba}(p, t) = \bar{G}(p, t)$$

$$\bar{G}(p, \varepsilon) = (\mathrm{i}\, t) \sum_{n=1}^{\infty} (\mathrm{i}\, t)^{2(n-1)} G_1^{0^n}(p, \varepsilon) G_2^{0^n}(p, \varepsilon) =$$

$$= \mathrm{i}\, t \frac{G_1^0(p, \varepsilon) G_2^0(p, \varepsilon)}{1 + t^2 G_1^0(p, \varepsilon) G_2^0(p, \varepsilon)} \tag{38}$$

Considering that $G_1^0(p, \varepsilon) = G_2^0(p, \varepsilon) = G^0(p, \varepsilon)$, it results :

$$\bar{G}(p, \varepsilon) = \mathrm{i}\, t \frac{G^{0^2}(p, \varepsilon)}{1 + t^2 G^{0^2}(p, \varepsilon)} = \mathrm{i}\, t \frac{1}{(\varepsilon - \varepsilon_p)^2 + t^2} =$$

$$= \mathrm{i}\, t \frac{1}{(\varepsilon - \varepsilon_p + \mathrm{i}\, t)(\varepsilon - \varepsilon_p - \mathrm{i}\, t)} \tag{39}$$

As we can see the model proposed here allows to find an exact solution considering the perturbation theory formalism which makes possible a more exact treatment of the problem.

3. FLOW OF THE ELECTRICAL CURRENT THROUGH THE INTERFACE AND ENERGY LOSS

The electrical current flowing across the interface is given by the variation of the number of the type "a" or "b" electrons in time unit :

$$N_a = \sum_p a_p^+ a_p \tag{40}$$

This variation is given by the terms H_t^1 and H_t^2 from the equations (16 a, b). In Heisenberg representation :

$$N_a^{(t)} = \mathrm{e}^{\mathrm{i}Ht} N_a \, \mathrm{e}^{-\mathrm{i}Ht} \tag{41}$$

We have :

$$\frac{\partial}{\partial t} N_a(t) = \mathrm{i}[H_t^1 + H_t^2, \, N_a(t)] =$$

$$= -t \sum_{p>0} b_p^+(t) a_p(t) + t \sum_{p<0} a_p^+(t) b_p(t) \tag{42}$$

If we make the average on the fundamental state and use the definitions (39 a, b), we have :

$$I = \mathrm{i}\, e t [\sum_{p>0} \vec{G}(p, \bar{0}) - \sum_{p<0} \vec{G}(p, \bar{0})] \tag{43}$$

where :

$$\vec{G}(p, \bar{0}) = \int \frac{\mathrm{d}\varepsilon}{\mathrm{d}\pi} \vec{G}(p, \varepsilon) \tag{44}$$

the integration being carried out over the half-plane.

By using equation (39) and considering the analytical structure of the one-particle Green function, as given by equation (34), we obtain :

$$I = \mathrm{i}\, e t \left[\sum_{0<p<k_{F_1}} \mathrm{i}\, t \frac{1}{2t} - \sum_{-k_{F_2}<p<0} \mathrm{i}\, t \frac{1}{2t} \right] = -\frac{et}{2\pi} \lambda \tag{45}$$

Hence :

$$I = -\frac{e\, t}{2\pi} (2\, m\, e\, U)^{1/2} \tag{46}$$

The loss of energy in time unit arises from the kinetic energy variation of the electrons of the "a" type due to the term H_t^1 and from the variation of the kinetic energy of the "b" type electrons owing to the term H_t^2 :

$$\frac{\partial E}{\partial t} = \mathrm{i}[H_t^1, \, \sum_p \varepsilon_p a_p^+(t) a_p(t)] + \mathrm{i}[H_t^2, \, \sum_p \varepsilon_p b_p^+(t) b_p(t)] =$$

$$= \mathrm{i}\, t [\sum_{p>0} \varepsilon_p b_p^+(t) a_p(t) + \sum_{p>0} \varepsilon_p a_p^+(t) b_p(t)] \tag{47}$$

Taking into account the average on the fundamental state and with the notation :

$$P = \left\langle \psi \left| \frac{\partial E}{\partial t} \right| \psi \right\rangle$$

we have :

$$P = \mathrm{i}\, t [\sum_{p>0} \varepsilon_p \vec{G}(p, \bar{0}) + \sum_{p<0} \varepsilon_p \vec{G}(p, \bar{0}) \tag{48}$$

Using the above results for calculation we have :

$$P = \mathrm{i}\, t \left[\sum_{0<p<k_{F_1}} \varepsilon_p \mathrm{i}\, t \frac{1}{2t} + \sum_{-k_{F_2}<p<0} \varepsilon_p \mathrm{i}\, t \frac{1}{2t} \right] = - \frac{t}{12\, \pi\, m} (k^3_{F_0} + 3 k_{F_0} \lambda^2) \tag{49}$$

Hence :

$$P = - \frac{tN}{12m} (\pi^2 N^2 + G\, m\, e\, U) \tag{50}$$

4. DISCUSSION

Equation (45) can be written in the form :

$$I = - e t^2 \left(\sum_{0<p<k_{F_1}} \frac{1}{2t} - \sum_{-k_{F_2}<p<0} \frac{1}{2t} \right) \tag{51}$$

We can see that the sums in brackets represent the number of states accessible for electron transition from a medium to another. It is well known that the probability of transition from the state i in the state j, under the influence of a V perturbation acting in a finite short interval, is :

$$w_{me} = \frac{| V_{ij} |^2}{(E_i - E_j)^2} \tag{52}$$

or for a continuous spectrum :

$$\mathrm{d}w = 2\pi | V_{ij} |^2 \delta | E_i - E_j \, \mathrm{d}\nu_e \tag{53}$$

where $\mathrm{d}\nu_e$ is the number of acceptor states and V is constant in time. $| V_{ij} |$ is the matrix element of perturbation between the states i and j. By summing all available states in equations (52) or (53), including in this sum also the denominator $(E_i - E_j)^{-2}$, we can understand the meaning of equation (51). It follows that t^2 can be taken as an average value of the sum :

$$\sum_e | V_{ij} |^2 = \int \mathrm{d}x \, | V(x) |^2 \tag{54}$$

$V(x)$ is the function in real coordinates which describes the interface barrier.

For a rectangular barrier with a width and V height, we have:

$$t^2 = Va \tag{55}$$

which is the geometrical area of the barrier having a defined form. In general, t^2 must be equaled with the area S of the barrier having a particular shape. Therefore, t^2 is defined as the integral of the function describing the form of the barrier such as: rectangular, parabolic, Schotky, etc (Fig. 14). The integration limits are located within the width of the corresponding barrier:

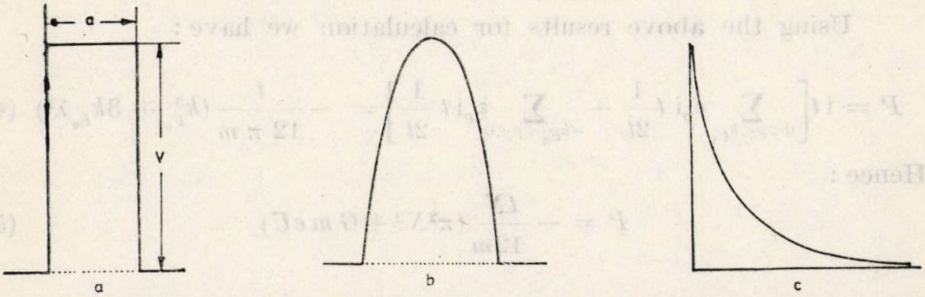

Fig. 14. — Common types of the potential barriers; the surface delimited by the barrier shape corresponds to t_2: a — rectangular; b — parabolic; c — Schotky barrier.

$$t^2 \equiv S$$

This interpretation of the parameter t is justified as a first approximation. A more exact calculation should take into account all the components t_k from equations (14 a-d) and also the reflexion terms from equation (14 e-h). Such treatment of the problem appears as more advantageous in the frame of the perturbation theory, considering the inelastic collisions of the electrons on the interface barrier.

REFERENCES

[1] L. D. Landau and E. M. Lifshitz, "Mecanica Cuantică (Teoria nerelativistă)", Editura tehnică, Bucureşti, 1965, pp. 156, 162.
[2] A. Bohr and B. Mattelson, "Nuclear Structure", vol. 1, Benjamin Inc., New York, 1969.
[3] A. L. Fettev and J. D. Walecka, "Quantum Theory of Many-Particle Systems", McGraw-Hill Book Company, New York, Part 2, 1967.

Revue Roumaine de Chimie, 27, 2, 191–198 (1982)

SURFACE OXIDATION OF SOME SULPHUROUS MINERALS BY THE HYPOCHLORITE ION

ZOLTÁN FINTA, EMIL CHIFU, EUGENIA GAVRILA and MARIUS SALAJAN
Department of Physical Chemistry, Babeş-Bolyai University, Str. Arany J. 11, 3400 Cluj-Napoca, Romania

Received March 2, 1981

The kinetics of the surface oxidation of galena, blende and chalcopyrites with the ClO^- ion has been studied and the activation parameters of the reaction were derived. On the basis of IR spectra of the oxidated mineral powders and of the chemical analysis of the solutions found in contact with them, the state of the surfaces submitted to oxidation was investigated in a large pH range. The results suggest that galena might have a specific behaviour in the selective flotation of oxidated complex sulphurous ores in weakly acidic media, due to the different state of its surface as compared to that of blende and chalcopyrites.

The specific behaviour manifested by the surface of different sulphurous minerals against oxidant agents is used for separating these minerals from complex ores by selective flotation. Among the phenomena giving support to selective flotation technologies, the basic one is surface oxidation. That is why the state of oxidated surfaces is very important to be known, as a determinant element in the selectivity of the flotation process. A series of fundamental works [1-10] have dealt with this subject, making use of air or pure oxygen as the oxidation agent.

Yet, from the practical point of view, the problem of employing some strong oxidizers, in order to assure rapid oxidation in well monitored conditions, is also as much important. So that an easily procurable oxidizer, such as calcium hypochlorite, can be of interest due to its relatively low price and to the rather simple methods involved in purifying the residual water.

In the present work some kinetic data are reported concerning the surface oxidation of galena, blende and chalcopyrite. At the same time, the state of their surfaces is studied after completion of the oxidation process. But the properties of technical calcium hypochlorite do not assure proper conditions for an accurate kinetic study. Therefore, we used natrium hypochlorite, the alkaline solutions of which are relatively stable and possess the same oxidizing species (ClO^-, Cl_2, ClO_3^-, dissolved O_2) as in the case of calcium hypochlorite, the main oxidation agent being the hypochlorite ion.

EXPERIMENTAL

Kinetic measurements. The oxidizer solutions of differing concentrations have been prepared from a concentrated NaClO solution, the active chlorine content of which was 12.5%. In order to obtain the desired pH and a constant ionic strength of approximately 0.2 M, determined quantities of NaOH and HCl were added to the solutions. 200 ml aliquots of the prepared solutions were thermostated at the working temperature with an accuracy of 0.1°C.

The mineral crystals obtained by manual selection from the natural ores were ground and sorted shortly before the use, and the fraction having a granulation less than 100 μ was chosen. The start of the reaction was considered the moment when a determined quantity (0.5—2.0 g) of powder was introduced into the oxidizer solution previously brought at the working temperature.

In the course of the oxidation the solution was well stirred, to assure a kinetic regime by reducing to the minimum the role of diffusion in determining the reaction rate. The evolution of the surface oxidation process was pursued by determining the concentration of the SO_4^{2-} ions in the solution and, in some cases, also by determining the concentration of the ClO^- ions. The SO_4^{2-} ions were dosed by an indirect spectrophotometric method namely by measuring, at 430 nm, the extinction caused by the occurrence of CrO_4^{2-} ions as a result of precipitating the SO_4^{2-} ions with a $BaCrO_4$ suspension. The concentration of the ClO^- ions was determined iodometrically.

Determination of the specific surface. The Blaine method was applied on the freshly ground powders, in the conditions imposed by the in force industrial standards. [11]

The IR spectra of the fresh powders and of those subjected to surface oxidation have been recorded at a UR—10 (Carl Zeiss, Jena) spectrophotometer, using KBr pellets. The surface of the samples destined to IR-spectrophotometry was oxidated in the same conditions as in the case of the kinetic studies, and after oxidation they were thoroughly washed with large quantities of distilled water, then dried in air.

RESULTS AND DISCUSSION

The Kinetics of Surface Oxidation. Due to the ClO^- ion instability in acid and even in neutral media, the explorable pH range at the service of the proposed kinetic study is limited. Thus, the kinetic measurements have been made in alkaline solutions, but the use of buffer solutions was avoided in order not to cause secondary reactions on the surface of minerals.

For establishing the rate law and the activation parameters, the influence of the surface size, the concentration of the ClO^- ions, the pH and the temperature on the reaction rate was studied, at a constant ionic strength of approximately 0.2 M. The ratio of the concentration of the consumed ClO^- ions to the concentration of the resulted SO_4^{2-} ions has a value close to 20 at the beginning, then it gradually diminishes up to the constant value 13. But all the time during the process this ratio is still too large as compared to that expected from the overall reaction

$$\begin{aligned} &2\,CuFeS_2 + 17\,ClO^- + 8\,OH^- + H_2O \rightarrow \\ &\rightarrow 2\,Cu(OH)_2 + 2\,Fe(OH)_3 + 4\,SO_4^{2-} + 17\,Cl^-. \end{aligned} \tag{1}$$

The fact suggests that, parallelly with the surface oxidation, a disproportionation of the oxidizer ion also takes place — probably under the catalytic action exerted by the solid surface of the mineral powder —, because in the given experimental conditions the oxidizer solution is stable enough. This assumption was tested and confirmed by measuring, from time to time, the concentration of ClO^- ions in a solution found in contact with an inert powder (SiC) of a granulation similar to the studied mineral. The decomposition of the oxidizer was ascertained again and the rate of the process was comparable to that measured in the presence of the mineral.

In the case of galena and blende a phenomenon similar to the above one was noticed.

In conditions in which the oxidizer was not stable, and the pH varied because of the too slight buffer capacity of weak alkaline solutions, the continual observation of the reaction during its course could not lead to quantitative results. In situations like that, the determination of the reaction rate was done in the very moment when the reaction began:

$$v_0 = (\mathrm{d}c/\mathrm{d}t)_{t\to 0} \tag{2}$$

where c represents the concentration of the SO_4^{2-} ions yielded in the solution; this rate was evaluated from the tangents at the origin of the $c = c(t)$ curves, obtained for different initial values of the powder surface and of both the ClO^- and the OH^- ion concentration, at a given temperature. From these data the influence of the above parameters on the reaction rate could be established (Figs 1 — 3).

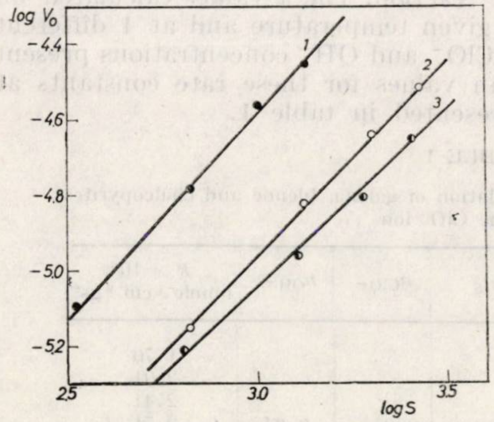

Fig. 1. — Dependence of the initial oxidation rate v_0 on the magnitude of the mineral surface. 1 : galena, 20°C, pH = 12.80 ; 2 : blende, 40°C, pH = 12.37 ; 3 : chalcopyrites, 40°C, pH = 12.34. Concentration of the oxidizer : 0.203 mole l^{-1}.

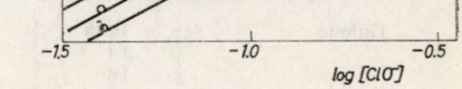

Fig. 2. — Dependence of the initial oxidation rate v_0 on the oxidizer concentration. 1 : galena, 20°C, $S = 1.34 \times 10^3$ cm^2g^{-1} ; pH = 12.80 ; 2 : blende, 40°C, $S = 2.67 \times 10^3$ cm^2 g^{-1} ; pH = 12.37 ; 3 : chalcopyrites, 40°C, $S = 2.55 \times 10^3$ cm^2g^{-1}, pH = 12.34.

For all the minerals studied, the initial rate v_0 varies linearly with the magnitude S of the solid surface, and with the concentration of ClO^- and of OH^- ions. The partial reaction order with respect to these three magnitudes (n_S, n_{ClO^-} and n_{OH^-}) was determined from the slope of the straight lines represented in Figs 1 – 3 and obtained by the least squares method. As can be seen from the data in table 1, values close to unity were obtained for all the three partial reaction orders.

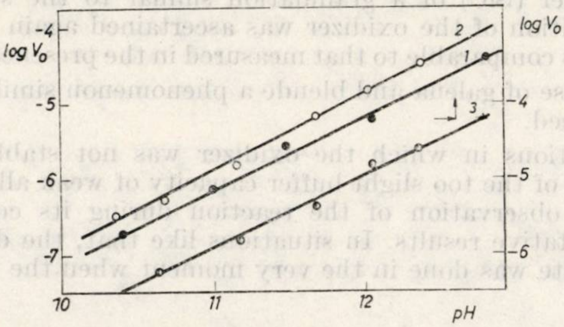

Fig. 3. – Dependence of the initial oxidation rate v_0 on the pH. 1 : galena, 20°C, $S = 1.34 \times 10^3$ cm^{2}g^{-1} ; 2 : blende, 40°C, $S = 2.67 \times 10^3$ cm^2 g^{-1} ; 3 : chalcopyrites, 40°C, $S = 2.55 \times 10^3$ cm^2 g^{-1}. Concentration of the oxidizer : 0.203 mole l^{-1}.

Consequently, the rate of the surface oxidation reactions studied here can be expressed by a kinetic law of the following form :

$$v = kS[\mathrm{ClO}^-]\,[\mathrm{OH}^-] \tag{3}$$

where k is the rate constant of the reaction. The k values calculated on the basis of this relationship at a given temperature and at 4 different values of S and 5 – 6 values of the ClO^- and OH^- concentrations present a satisfactory dispersion. The mean values for these rate constants at different temperatures are also presented in table 1.

TABLE 1

Kinetic data obtained for surface oxidation of galena, blende and chalcopyrites with the ClO^- ion

Mineral	Temp., °C	n_S	n_{ClO^-}	n_{OH^-}	$k \times 10^6$, l mole^{-1} cm^{-2} gs^{-1}
Galena	10.5				1.70
	14				2.01
	18				2.41
	20	1.08	0.95	0.94	2.71
	21				2.82
	25				3.29
Blende	40	1.07	1.06	1.01	6.32
	45				8.20
	50				10.0
	55				13.2
	60				16.1
Chalcopyrites	40	0.97	1.03	0.94	5.22
	45				6.55
	50				8.28
	55				10.3
	60				12.7

The activation parameters of the studied reactions were calculated on the basis of the known relation of the theory of absolute rates. The linear variation of the values $\ln(k/T)$ with $1/T$ is good in all cases, as can be seen in Fig. 4.

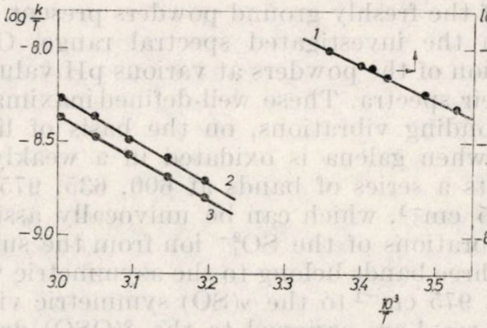

Fig. 4. — Determination of the activation parameters for the surface oxidation reactions. 1 : galena, 2 : blende, 3 : chalcopyrites.

The values of the activation parameters obtained by the least squares method are presented in table 2.

The activation enthalpies of the three oxidation reactions are fairly close to one another, that for galena being a little lower. Their magnitudes correspond to redox reactions of the same type.

The activation entropies, practically equal for the three cases, indicate a pronounced drop of entropy in the transition state. This fact, according to the rate law (3) found above, suggests that the rate-determining step of the studied reactions might be the adsorption of ClO^- and OH^- ions on the mineral surface. The adsorption preceding the proper electron exchange had been noticed also in the case of galena oxidation with air in alkaline solutions.[1,2]

TABLE 2

Activation parameters of the surface oxidation reactions

Mineral	$\Delta H^{\neq}$, kJ mole^{-1}	$\Delta S^{\neq}$, J mole^{-1}k^{-1}
Galena	30.1 ± 2.5	-247 ± 13
Blende	38.5 ± 1.7	-243 ± 8
Chalcopyrites	$36\ 0 \pm 2.5$	-251 ± 13

The State of Oxidated Surfaces. The state of mineral powders oxidated with ClO^- ions was studied by examining their IR absorption spectra, accompanied by the qualitative analysis of the solutions found in contact with the oxidated powders.

As a result of some preliminary tests it was noticed that, at a sufficiently small granulation (below 100 μ), the powders of the studied sulphurous minerals are transparent in the spectral range between 400 and 4000 cm^{-1}. This fact allowed to record the absorption spectra of unoxidated powders, as well as those of powders oxidated at different pH values between 6 and 13. On the basis of these spectra, due to the transparence of the mineral grains, the presence of any IR-active product gathered on the surface could be found out without resorting to special reflexion techniques.

The spectra of the freshly ground powders present no characteristic absorption band in the investigated spectral range. On the contrary, after surface oxidation of the powders at various pH values, characteristic maxima arise in their spectra. These well-defined maxima could be assigned to the corresponding vibrations, on the basis of literature data.

In this way, when galena is oxidated in a weakly acidic medium its spectrum exhibits a series of bands at 600, 635, 975, 1055, cca 1090 (shoulder) and 1185 cm^{-1}, which can be univocally assigned to valence and deformation vibrations of the SO_4^{2-} ion from the sulphates of heavy metals.[12] The last three bands belong to the asymmetric valence vibration ν (SO), the band at 975 cm^{-1} to the ν(SO) symmetric vibration, and the maxima about 600 cm^{-1} are assigned to the δ(OSO) deformation vibration. But, the spectrum is lacking in another characteristic band of the SO_4^{2-} ion which, about data in the literature, also belongs to an IR-active deformation vibration and should lie between 400 and 500 cm^{-1}. Taking into account the low intensity of this band,[12] its absence in the spectra recorded in the conditions of this work is not surprising.

In a weakly alkaline medium the vibration bands characteristic of the SO_4^{2-} ion gradually disappear from the spectrum of oxidated galena, with simultaneous appearance of another band at 1410 cm^{-1} and of a series of very weak bands about 1000 and 700 cm^{-1}. These bands can be assigned to valence and deformation vibrations of the CO_3^{2-} ion found in the crystalline net of heavy metal carbonates.[13] In the conditions of this study the formation of carbonates is not unexpected, if we make allowance for the rather high content of carbonate in the oxidant solution.

Besides these bands, beginning with pH ~ 13, an intense and wide band arises which appears to represent an overlap of at least two maxima in the range 400 – 500 cm^{-1}; and another one, also wide, at approx. 3400 cm^{-1}. By using certain analogies,[14] the latter can be assigned to the valence vibration of some OH groups affected by coordination effects, and the band between 400 and 500 cm^{-1} appears to belong to M—O valence vibrations in molecules of the type of basic carbonates or of hydroxocomplexes.

In neutral and acidic media, the surface oxidation of blende causes no modification of the IR spectrum. In weakly alkaline solutions a series of weak bands appear, indicating the presence of CO_3^{2-} ions on the oxidated surface. The position of these bands is a little shifted from that in the spectrum of galena. In a strongly alkaline medium, the bands corresponding to the CO_3^{2-} ion decrease in intensity and, simultaneously, wide bands at 400—500 and at cca 3400 cm^{-1} arise, like in the case of galena. In comparison with the similar band in the spectrum of galena, the former is shifted towards higher frequencies, what agrees with the above assignment of this band to M—O valence vibrations.

In the case of chalcopyrites, before pH = 9 the vibration spectrum appears as not being affected by surface oxidation. In strongly alkaline solutions the wide bands in the 400—500 and 3400 cm^{-1} ranges arise again, with lower intensities than in the case of galena and blende. It seems therefore probable that, in a strongly alkaline medium (pH ~ 13), the oxidated surface of chalcopyrites is covered with sparingly soluble hydroxo-compounds, as well.

The qualitative analysis of the solutions found in contact with the oxidated minerals revealed the presence of the SO_4^{2-} ions in all cases except the galena oxidation in acidic medium, when this ion is present only as traces. The corresponding metal ions also appear in these solutions but at galena oxidation in acidic and neutral medium the Pb^{2+} concentration is very low. The Fe^{3+} and Cu^{2+} concentration also drops drastically in the strongly alkaline solutions resulted at oxidation of chalcopyrites.

In the strongly alkaline solutions (pH ~ 13) resulted after oxidation of galena and blende, the Pb^{2+} and Zn^{2+} ions are partly blocked under the form of soluble hydroxo-complexes. The existence of these species has been noticed by the recovery of the metal ions on acidulating the solutions. On the other hand, it is indirectly confirmed also with increasing pH, when a well-marked decrease is found for the carbonate or basic carbonate quantity occurred on the galena and blende surfaces, oxidated in a weakly alkaline medium. This decrease was remarked in the IR spectra.

The elementary sulphur as well as its ionic species corresponding to inferior oxidation states (SO_3^{2-}, $S_2O_3^{2-}$, $S_4O_6^{2-}$, etc.), reported for the air-oxidated minerals, [4-7,10] have not been found in sensible quantities in the solutions investigated in the present work. The fact is not surprising if we take into consideration the strongly oxidant character of the ClO^- ion.

The results obtained by interpreting the IR spectra of oxidated mineral surfaces and the chemical analysis of the solutions found in contact with these surfaces are presented in table 3.

TABLE 3

The state of mineral surfaces oxidated with the ClO^- ion in various media and the ions arising in the solution after oxidation

Mineral	Medium	State of the surface	Ions in solution
Galena	Acidic, neutral	$PbSO_4$	Pb^{2+} (traces) SO_4^{2-} (traces)
	Weakly alkaline	$PbSO_4$, $PbCO_3$, $Pb(OH)_2$	Pb^{2+} (traces), SO_4^{2-}
	Strongly alkaline	$PbCO_3$, $Pb(OH)_2$	Pb^{2+} (traces), SO_4^{2-}, $[Pb(OH)_4]^{2-}$
Blende	Acidic, neutral	—	Zn^{2+}, Fe^{3+} (traces), SO_4^{2-}
	Weakly alkaline	$ZnCO_3$, $Zn(OH)_2$, $Fe_2(CO_3)_3$ (traces), $Fe(OH)_3$ (traces)	Zn^{2+} (traces), Fe^{3+}(traces), SO_4^{2-}
	Strongly alkaline	$ZnCO_3$, $Zn(OH)_2$, $Fe_2(CO_3)_3$ (traces), $Fe(OH)_3$ (traces)	SO_4^{2-}, $[Zn(OH)_4]^{2-}$
Chalcopyrites	Acidic, neutral	—	Cu^{2+}, Fe^{3+}, SO_4^{2-}
	Alkaline	$CuCO_3$, $Cu(OH)_2$, $Fe_2(CO_3)_3$, $Fe(OH)_3$	SO_4^{2-}

CONCLUSIONS

The experimental results obtained in this work indicate that the behaviour of galena is different from that of blende and chalcopyrite, when found together in complex ores under the conditions of flotation. As show the kinetic data, the mentioned difference is not the result of a selective oxidation of the minerals by the ClO^- ion, but it is due to the unlike states of the oxidated surfaces, determined by the nature of the oxidation products or of other species resulted in subsequent reactions.

On this basis, our results lead to the conclusion that the convenient medium for selective flotation is the weakly acidic one, in which the occurrence of a sparingly soluble layer of $PbSO_4$ on the surface of the oxidated galena makes it to behave differently against surface-active agents. In alkaline solutions, the surface oxidation leads to the covering of all the studied sulphurous mineral surfaces with sparingly soluble compounds, maybe hydroxides, carbonates and hydroxo-carbonates which have a more hydrophilic character than the surfaces of the unoxidated minerals.

REFERENCES

[1] F. R. McFeely, S. Kowalczy, L. Ley, R. A. Pollak and D. A. Shirley, *Phys. Rev., B*, **7**, 5228 (1973).

[2] K. Kishi and M. W. Roberts, *J. Chem. Soc., Faraday Trans.*, **1**, 1721 (1975).

[3] H. Nagihara, *J. Phys. Chem.*, **56**, 510 (1952).

[4] R. G. Greenler, *J. Phys. Chem.*, **66**, 879 (1962).

[5] G. W. Poling and J. Leja, *J. Phys. Chem.*, **67**, 2121 (1963).

[6] B. Reuter and R. Stein, *Z. Elektrochem.*, **61**, 440 (1957).

[7] P. Eagington and A. P. Prosser, *Trans. Instr. Mineral Met., C*, **78**, 74 (1969).

[8] A. S. Manocha and R. L. Park, *Appl. Surface Sci.*, **1**, 129 (1977).

[9] I. A. Kakovski and E. M. Kosikov, *Obogoshenie Rud*, **1974**, 28 ; **1975**, 18.

[10] A. A. Abramov, V. M. Avdolin and E. M. Dzugkoeva, *Tsvetn. Metaly*, **1975**, 83.

[11] STAS 4223/1 (1970).

[12] K. Nakamoto, "Infrared Spectra of Inorganic and Coordination Compounds", Wiley, New York, 1962, p. 154.

[13] Idem ref 12, p. 132.

[14] D. Scargill, *J. Chem. Soc.*, **1961**, 4440.

Revue Roumaine de Chimie, 27, 2, 199–203 (1982)

EXCESS SURFACE TENSION OF BINARY LIQUID MIXTURES

R. MISHRA
Department of Chemistry, P. B. Degree College (affil. Avadh University), Pratapgarh City — 230 002 (U.P.), India

Received November 29, 1979
Revised September 12, 1981

Excess surface tension of binary mixtures-cyclohexane — *o*-xylene, cyclohexane — *m*-xylene and cyclohexane — *p*-xylene have been calculated over a wide range of composition at 298.16 K. Brock and Bird's relation has been used and extended to the surface tension of the mixtures by making use of pseudo critical constants. It is found that though Brock and Bird's relation underestimates excess surface tension values, it predicts correctly the variation of excess surface tension with composition. The excess surface tension values calculated using Brock and Bird's relation are also seen to be in better agreement with experimental values as compared to those obtained by Flory's theory and average potential model (APM) theory by the earlier workers.

INTRODUCTION

Several investigators [1–17] have successfully attempted to calculate theoretically the surface tension of liquids and liquid mixtures. Ono and Kondo [18] and recently Gubbins and Haile [19] have given a thorough review of these theoretical approaches. Flory's theory [20,21] recently extended [16,17] to enable the calculation of the surface tension of pure liquids and liquid mixtures and average potential model (APM) theor of Prigogine [11] are the most sophisticated methods used so far. Singh et. al. [22] examined the APM theory as applied to calculate excess surface tension for a number of binary mixtures at 15°C, whereas Jain et. al. [23] tested Flory's theory at a temperature of 25.16°C. Pandey et. al. [24] studied the relative merits of the two theories as applied to the calculation of excess surface tension over a wide range of temperature and whole range of composition. The increasing importance of surface tension in oil recovery and dam enginnering draws the attention of the present author towards its theoretical evaluation in mixtures following a simple but efficient and correct method due to Brock and Bird.[25] The relation has been successfully applied for the calculation of excess surface tension of three binary mixtures: cyclohexane-*o*-xylene, cyclohexane—*m*-xylene and cyclohexane—*p*-xylene over a wide range of composition at 298.16 K. The calculations are based on the data of Jain et. al. [26] and other necessary constants were taken from the literature.[27]

THEORETICAL

According to Brock and Bird [25] the surface tension σ is given by the relation :

$$\frac{\sigma}{(P_c^2 T_c)^{1/3}} = \left(-0.951 + \frac{0.432}{Z_c}\right)(1 - T_r)^{11/9} \tag{1}$$

Here P_c, V_c, T_c, Z_c and T_r stand for critical pressure, critical volume, critical temperature, critical compressibility factor and reduced temperature respectively.

Critical compressibility factor and reduced temperature are given by :

$$Z_c = \frac{P_c V_c}{R T_c} \tag{2}$$

$$T_r = \frac{T}{T_c} \tag{3}$$

T stands for absolute temperature and R for the gas constant. However, it does not work well for associated liquids. This technique has been claimed to give errors of less than 7 % for many non-aqueous solutions. [28] Eq (1) when extended to mixtures may be written as

$$\frac{\sigma_{\text{mix}}}{(P_{cm}^2 T_{cm})^{1/3}} = \left(-0.951 + \frac{0.432}{Z_{cm}}\right)(1 - T_{rm})^{11/9} \tag{4}$$

The characteristic parameters P_{cm}, T_{cm} and V_{cm} for the mixtures are calculated from the critical constants of pure liquids. The simplest procedure is to assume that P_{cm}, T_{cm} and V_{cm} are all the mole fraction averages, i.e.,

$$P_{cm} = \sum_{i=1}^{2} X_i P_{c_i}, \text{ etc.} \tag{5}$$

In the case of a binary mixture :

$$\begin{aligned} P_{cm} &= X_1 P_{c_1} + x_2 P_{c_2} \\ V_{cm} &= x_1 V_{c_1} + x_2 V_{c_2} \\ T_{cm} &= x_2 T_{c_1} + x_2 T_{c_2} \end{aligned} \tag{6}$$

where x_1 and x_2 are the mole fractions of the pure components. T_{rm} and Z_{cm} are given by

$$T_{rm} = \frac{T}{T_{cm}} \text{ and}$$

$$Z_{cm} = \frac{P_{cm} V_{cm}}{R T_{cm}} \tag{7}$$

Excess surface tension σ^E is calculated by using the expression :

$$\sigma^E_{\text{calc}} = \sigma_{\text{mix(calc)}} - \sum_{i=1}^{2} x_i \sigma_i \tag{8}$$

where ($i=1, 2$) stands for components 1 and 2 of the mixture respectively.

RESULTS AND DISCUSSION

Table 1 enlists the surface tension values of pure liquids evaluated by using Brock and Bird's relation. The calculated σ value for cyclohexane is smaller than that measured experimentally (deviation $\approx 2.5\,\%$), whereas the theoretical σ values for isomeric xylenes are found to be greater than the observed values. The deviation is around 5.5 to 8.7 per cent. The greater discrepancy in the case of isomeric xylenes may be attributed to the fact that in comparison to cyclohexane, the isomeric xylenes do not obey strictly the theorem of corresponding states which has been used as a base in the derivation of the relation under investigation. A perusal of columns 2 and 4 of table 2 shows that the calculated values of surface tension of the mixture are in better agreement with the experimental values at higher mole fractions of cyclohexane. It is thus the concentration of isomeric xylenes which causes the greater discrepancies in the σ_{mix} values. As it is obvious from columns 5 and 6 of table 2, the sign of σ^E values and their trend of variation with composition are correctly predicted by Brock and Bird's relation.[25] However, theoretical σ^E values are smaller in magnitude than experimental values for all the mixtures under present study. The discrepancies in the magnitude of σ^E values may be attributed partly to the pure components not following the theorem of corresponding states[2] and partly to the fact that dispersive forces do also operate between the components of the mixtures. A further examination of columns 5 and 6 of table 2 shows that probably the dispersive forces become prominent at higher concentrations of xylene molecules. In other words, the dispersive forces are found to be the characteristics of the flat molecules like benzene and its homologues and such forces are less in the case of flexible molecules like cyclohexane and other aliphatic compounds which undergo random coiling due to greater internal rotation about C—C bond.

TABLE 1
Surface tension of pure liquids at 298.16 K and related parameters

Compound	T_r	Z_c	σ (10^{-3} Nm^{-1})	
			Calc (by Eq 1, Ref. 25)	Expt Ref. 26
Cyclohexane	0.53916	0.27160	23.820	24.36
o-xylene	0.47177	0.25387	32.013	29.48
m-xylene	0.48168	0.25686	29.678	28.14
p-xylene	0.48245	0.25268	30.260	27.84

TABLE 2

Surface tension and excess surface tension values of liquid mixtures at 298.16 K

x_1	σ_{mix} $(10^{-3}\ Nm^{-1})$			σ^E $(10^{-3}\ Nm^{-1})$	
	Calc. by Eq (4) (Ref. 25)	add. (by Eq (1) Ref. 25)	Expt. (Ref. 26)	Calc. (Ref. 25)	Expt. (Ref. 26)
I cyclohexane $-o$-xylene					
0.122	30.92	31.01	28.56	−0.09	−0.30
0.173	30.48	30.60	28.19	−0.12	−0.40
0.244	29.87	30.01	27.73	−0.15	−0.50
0.343	29.03	29.20	27.03	−0.17	−0.70
0.404	28.51	28.70	26.70	−0.19	−0.71
0.419	28.39	28.58	26.49	−0.19	−0.85
0.499	27.73	27.92	26.27	−0.19	−0.65
0.547	27.34	27.53	25.87	−0.19	−0.82
0.661	26.43	26.60	25.57	−0.17	−0.53
0.736	25.84	25.98	25.31	−0.14	−0.43
0.778	25.51	25.64	25.00	−0.13	−0.50
0.867	24.79	24.91	24.93	−0.12	−0.12
II cyclohexane $-m$-xylene					
0.129	28.79	28.92	27.39	−0.13	−0.28
0.151	28.65	28.79	27.23	−0.14	−0 36
0.235	28.10	28.30	26.78	−0.20	−0.50
0.285	27.78	28.01	26.51	−0.23	−0.59
0.299	27.69	27.93	26.42	−0.24	−0.63
0.315	27.59	27.83	26.32	−0.24	−0.67
0.418	26.96	27.23	25.89	−0.27	−0.73
0.470	26.65	26.93	25.62	−0.28	−0.81
0.580	26.01	26.28	25.39	−0.27	−0.64
0.708	25.30	25.53	25.10	−0.23	−0.46
0.830	24.66	24.82	24.78	−0.16	−0.34
0.896	24.33	24.43	24.57	−0.10	−0.31
III cyclohexane$-p$-xylene					
0.076	29.67	29.77	27.30	−0.10	−0.28
0.168	28.98	29.18	26.93	−0.20	−0.33
0.179	28.90	29.11	26.86	−0.21	−0.36
0.194	28.79	29.01	26.81	−0.22	−0.36
0.285	28.12	28.42	26.41	−0.29	−0.44
0.343	27.73	28.05	26.20	−0.32	−0.44
0.453	27.01	27.34	25.72	−0.33	−0.55
0.519	26.57	26.92	25.48	−0.35	−0.55
0.602	26.05	26.38	25.27	−0.33	−0.48
0.698	25.47	25.76	25.01	−0.29	−0.41
0.789	24.95	25.18	24.89	−0.23	−0.21
0.889	24.40	24.53	24.62	−0.13	−0.13

CONCLUSION

Brock and Bird's method for calculation of excess surface tension values is useful in that, with the knowledge of the critical constants of the pure components, only an adhoc study of the excess surface tension of the mixtures (particularly of non-aqueous solutions) may be made successfully. Furthermore, the excess surface tension values obtained by this method are found to be in far better agreement with the experimental values and strictly follow the same trend of variation with composition as observed experimentally, whereas with other methods (Flory's theory and APM theory) a quantitative disagreement is considerable. Moreover, the method is simpler to operate and only a knowledge of critical parameters is needed.

ACKNOWLEDGEMENT. The author is grateful to Dr. J. D. Pandey for his kind advice and interest. He also records his thanks to Dr. R. L. Mishra for his keen interest and support during the course of this work.

REFERENCES

[1] A. Schuchowitsky, *Acta physicochim. U. S. S. R.*, **19**, 176, 508 (1944).
[2] J. W. Belton and M. G. Evans, *Trans. Faraday Soc.*, **14**, 1 (1945).
[3] E. A. Guggenheim, *Trans. Faraday Soc.*, **41**, 151 (1945).
[4] J. A. V. Butler, *Proc. Roy. Soc.*, **41**, 150 (1945).
[5] R. Defay and I. Prigogine, *Trans. Faraday Soc.*, **46**, 199 (1950).
[6] J. H. Hildebrand and R. L. Scott, "Solubility of Non-electrolytes". Reinhold, New York, 1950.
[7] R. Defay and I. Prigogine "Tension Superficielle et Adsorption". Liège 1951, Chap. XII.
[8] E. A. Guggenheim. "Mixtures", Oxford, 1952, Chap. IX.
[9] I. Prigogine and I. Saraga, *J. Chim. Phys.*, **49**, 399 (1952).
[10] T. P. Hoar and D. A. Melford, *Trans. Faraday Soc.*, **53**, 315 (1957).
[11] I. Prigogine, "Molecular Theory of Solutions", North-Holland, Amsterdam, 1957.
[12] A. Englert-Chwoles and I. Prigogine, *Nuovo Cimento.*, **9**, 347 (1958).
[13] A. Chwoles-Englert and I. Prigogine, *J. Chim. Phys.*, **55**, 16 (1958).
[14] J. G. Eberhart, *J. Phys. Chem.*, **46**, 199 (1966).
[15] F. B. Sprow and J. M. Prausnitz, *Canad. J. Chem.*, **45**, 25 (1967).
[16] D. Patterson and A. K. Rastogi, *J. Phys. Chem.*. **74**, 1067 (1970).
[17] V. T. Lam and G. C. Benson, *Canad. J. Chem.*, **48**, 3773 (1970).
[18] S. Ono and S. Kondo, "Handbuch der Physik", Vol. X, "Structure der Flüssigkeiten", Ed. Flügge, Springer Verlag, Berlin, 1960, p. 134.
[19] K. E. Gubbins and J. M. Haile, "Molecular Theories of Interfacial Tension", Reprinted from Improved Oil Recovery by Surfactant and Polymer Flooding, Academic Press, New York, 1977, p. 148.
[20] a) P. J. Flory, R. A. Orwoll and A. Vrij, *J. Amer. Chem. Soc.*, **86**, 3507 (1964); (b) A. Abe and P. J. Flory, *J. Amer. Chem. Soc.*, **87**, 1838 (1965).
[21] P. J. Flory, *J. Amer. Chem. Soc.*, **87**, 1833 (1965).
[22] B. S. Mahl, S. L. Chopra and P. P. Singh, *Z. phys. Chem. (Leipzig)*, **249**, 337 (1972).
[23] D. V. S. Jain, S. Singh and R. K. Wadi, *Trans. Farady Soc.*, **70**, 961 (1974).
[24] R. L. Mishra and J. D. Pandey, *Chemica Scripta*, **11**, 117 (1977).
[25] J. R. Brock and R. B. Bird., *A. I. Ch. E. J.*, **1**, 174 (1955).
[26] D. V. S. Jain and S. Singh, *Indian J. Chem.*, **12**, 714 (1974).
[27] Handbook of Chemistry and Physics, CRC Press Ohio, 58 Ed. PF-90, 1977–78.
[28] R. C. Reid and T. K. Sherwood, "The Properties of Gases and Liquids". 2nd Edition, Mc Graw Hill, New York, 1966. Chap. 8.

Revue Roumaine de Chimie **27**, *2*, 205–209 (1982)

DIE VERBRENNUNGS- UND BILDUNGSWÄRMEN DES *o*-PHENYLENDIAMINS, HARNSTOFFS UND BENZIMIDAZOLONS-2

IULIA CONTINEANU, LUMINIȚA WAGNER, LIDIA STĂNESCU und D. I. MARCHIDAN
Zentrum für physikalische Chemie und Forschungszentrum für Farbstoffe, (ICECHIM), Splaiul Independenței 202, Bukarest 77208, Rumänien

Eingangen am 28. April 1981

Es wurde die Verbrennungswärme des *o*-Phenylendiamins, Harnstoffs und Benzimidazolons-2 mit Hilfe einer statischen kalorimetrischen Sauerstoffbombe bestimmt. Die Bildungs-wärme wurde durch Literaturdaten gerechnet. Es wurden folgende Daten erhalten :

$$C_6H_8N_2(f) + 8\,O_2(g) = 6\,CO_2(g) + 4\,H_2O\,(fl) + N_2(g)$$
$$\Delta cH^0\,(298{,}15\ K) = -\,3543{,}5 \pm 5{,}67\ kJ/mol\ (-\,847 \pm 1{,}36\ kcal/mol)$$
$$\Delta fH^0\,(298{,}15\ K) = -\,39{,}12 \pm 5{,}67\ kJ/mol\ (-\,9{,}35 \pm 1{,}36\ kcal/mol)$$
$$CH_4ON_2(f) + 3/2\,O_2(g) = CO_2\,(g) + 2H_2O(fl) + N_2(g)$$
$$\Delta cH^0\,(298{,}15\ K) = -\,645 \pm 2kJ/mol\ (-\,154{,}16 \pm 0{,}5\ kcal/mol)$$
$$\Delta fH^0\,(298{,}15\ K) = -\,320{,}17 \pm 2kJ/mol\ (-\,76{,}52 \pm 0{,}5\ kcal/mol)$$
$$C_7H_6ON_2(f) + 8\,O_2(g) = 7\,CO_2(g) + 3\,H_2O(fl) + N_2(g)$$
$$\Delta cH^0\,(298{,}15\ K)) = -\,3527{,}51 \pm 3{,}16\ kJ/mol\ (-\,843 \pm 0{,}76\ kcal/mol)$$
$$\Delta fH^0\,(298{,}15\ K) = -\,85{,}06 \pm 3{,}16\ kJ/mol\ (-\,20{,}33 \pm 0{,}76\ kcal/mol)$$

Es wurden such die durch Handrickrechnungsmethode erhaltenen Daten mit den experimentellen Daten verglichen.

The enthalpy of combustion of benzene-1,2-diamino (1,2-Phenylenediamine), urea and benzimidazole, 2-hydroxy (1,2-Phenylene urea) has been determined in an oxygen static-bomb calorimeter. The enthalpy of formation has been derived using data from the available literature. A comparison is given of the results of this investigation with those calculated by Handrick's method.

Zwecks Erhaltung der Bildungswärme des o-Phenylendiamins (OFDA), Harnstoffs und Benzimidazolons-2 (BZION-2) wurden Messungen der Verbrennungswärmen durchgeführt. Die verwendete kalorimetrische Bombe so wie die verwendete Rechnungsmethode wurden in einer früheren Arbeit beschrieben. [1]

In der vorliegenden Arbeit waren die Kalorimeterkonstante 10460 J/K und der in der Bombe verwendete Sauerstoffdruck 25 bar.

Für die Bildungswärmen des Kohlenstoffdioxyds und Wassers wurden die vorgetragenen Werte der ICSU – CODATA [2] die durch kritische Bewertung der vorliegenden Daten aus der Spezialliteratur entstanden verwendet. Wir haben folgende Werte vereinigt :

$$\Delta fH(HNO_3) = 219{,}488\ \ cal/g;\ \ \Delta fH\,(Fe_2O_3) = 1600\ \ cal/g\ \ und$$
$$\Delta cH\ (Baumwolle) = 3885{,}15\ \ cal/g$$

Für OFDA, $C_6H_4(NH_2)_2$, sind in der Spezialliteratur keine Verbrennungswärmedaten bekannt. Für des Molekulargewicht wurde der Wert 108,14 in Rechnungen genommen. Die untersuchte Substanz war Fluka — Herkunft und hatte eine höhere Reinigkeit als 99% und ein Schmelzpunkt von 101—103°C.

Die erhaltenen Ergebnisse für die Verbrennungswärme des OFDA in festem Zustand sind in Tabelle 1 vorgestellt.

Für die Bildungswärme des OFDA in Standardbedingungen laut Reaktion :

$$C_6H_8N_2(f) + 8\,O_2(g) = 6\,CO_2(g) + 4\,H_2O(fl) + N_2(g)$$

wurde das Wert 39,12 ± 5,67 (± 0,16%) kJ/mol erhalten.

TABELLE 1

Verbrennugswärme des *o*-Phenylendiamins

g Substanz	K ΔT	Jouli ($\Delta T \times$ Kalorim. konst.)	ΔfH (Fe_2O_3)	ΔfH (HNO_3)	ΔcH (Baumwolle)	J/g (ΔU_B)	kJ/mol (ΔU_B)
1,0542	3,388	35 439	55	46	877	32 689	3535
1,0114	3,245	33 943	56	67	605	32 841	3551
0,7038	2,205	23 064	56	49	—	32 622	3528
0,9849	3,167	33 127	56	72	670	32 825	3550

Mittelwert = 3541 kJ/mol

Standarddeviation $\sigma = \sqrt{\Sigma\Delta^2/n(n-1)} = \pm 5{,}67$ kJ

$$\text{Washburnskorrektion } \pi = \frac{0{,}3 \times 25 \times 6}{-3541}\left[-1 + 1{,}1\left(-\frac{8}{24}\right) - \left(\frac{2}{25}\right)\right] = -0{,}0092\,\%$$

$$\text{woraus } \Delta cU^\circ\ (298{,}15\ \text{K}) = \frac{-3541 \times 99{,}9908}{100} = -3541$$

Für Reaktion : $C_6H_4(NH_2)_2\,(f) + 8\,O_2\,(g) = 6\,CO_2\,(g) + 4\,H_2O\,(fl) + N_2\,(g)$;
Die Volumänderung ist 1, woraus :

$$\Delta cH^\circ (298{,}15\ \text{K}) = -3541 - RT = -3541 - 2{,}48 = -3543.5 \pm 5{,}67\ (\pm 0{,}16\,\%)\ \text{kJ/mol}$$
$$= -847 \pm 1{,}36\ (\pm 0{,}16\,\%)\ \text{kcal/mol}$$

Für Harnstoff, NH_2CONH_2, sind Domalskisdaten[3] bekannt die —150,97 kcal/mol für Verbrennungswärme und —79,71 kcal/mol für Bildungswärme sind. Für das Molekulargweicht hat man mit dem Wert 60,06 gerechnet.

Die Reinigkeit der Substanz war 99,8% und der Schmelzpunkt 132,7°C. Die von uns erhaltenen Ergebnisse für Verbrennungswärme des Harnstoffs in festem Zustand sind in der Tabelle 2 vorgestellt.

Für die Bildungswärme des Harnstoffs in Standardbedingungen laut Reaktion :

$$CH_4ON_2(f) + 3/2\,O_2(g) = CO_2(g) + 2\,H_2O\,(fl) + N_2(g)$$

wurde das Wert — 320,17 ± 2 (± 0,31%) kJ/mol erhalten.

TABELLE 2

Verbrennungswärme des Harnstoffs

g Substanz	K ΔT	Jouli ($\Delta T \times$ Kalorim.konst.)	ΔfH (Fe_2O_3)	ΔfH (HNO_3)	ΔcH (Baumwolle)	J/g (ΔU_B)	kJ/mol (ΔU_B)
1,3900	1,502	15 711	58	29	773	10 684	642
1,4498	1,576	16 485	56	34	741	10 797	648
1,5979	1,724	18 033	56	41	849	10 693	642

Mittelwert = 644 kJ/mol

Standarddeviation $\sigma = \sqrt{\Sigma\Delta^2/n(n-1)} = \pm 2$ kJ

Washburnskorrektion $\pi = \dfrac{0{,}3 \times 25 \times 1}{-644}\left[-1 + 1{,}1\left(\dfrac{2}{4}\right) - \left(\dfrac{2}{25}\right)\right] = -0{,}006\,\%$

woraus $\Delta cU^\circ\,(298{,}15\ K) = \dfrac{-644 \times 99{,}994}{100} = -644$ kJ/mol

Für Reaktion: $NH_2CONH_2\,(f) + 3/2\ O_2\,(g) = CO_2(g) + 2H_2O\,(fl) + N_2\,(g)$; Die Volumänderung ist 0,5 woraus:

$\Delta cH^0\,(298{,}15\ K) = -644 - 0{,}5\ RT = -644 - 1{,}24 = -645 \pm 2\ (\pm 0{,}31\,\%)$ kJ/mol

$= -154{,}16 \pm 0{,}5\ (\pm 0{,}31\,\%)$ kcal/mol

Für BZION-2 (o-Phenylenharnstoff) C_6H_4 (NHCONH) sind in der Literatur keine Daten für die Verbrennungswärme bekannt. Für das Molekulargewicht wurde mit dem Wert 134,14 gerechnet.

Die erhaltene Substanz hatte eine Reinigkeit von 99% und einen Schmelzpunkt zwischen 310°C und 312°C. Die erhaltenen Ergebnisse für die Verbrennungswärme des BZION-2 in festem Zustand sind in der Tabelle 3 vorgestellt.

Für die Bildungswärme des BZION-2 in Standardbedingungen laut Reaktion:

$$C_7H_6ON_2(f) + 8\ O_2(g) = 7\ CO_2(g) + 3\ H_2O\ (fl) + N_2(g)$$

wurde der Wert $-85{,}06 \pm 3{,}16\ (\pm 0{,}09\,\%)$ kJ/mol erhalten.

Für die studierten Substanzen wurden sowohl Rechnungen der Verbrennungswärmen laut Handricksmethode [4] durchgeführt.

Laut dieser Methode, die Verbrennungsreaktion einer organischen Verbindung mit der allgemeinen Formel $C_mH_nN_pO_q$ ist:

$$C_mH_nN_pO_q\ (f\ oder\ fl) + (m + n/4 - q/2)O_2(g) = m\ CO_2(g) +$$
$$+ n/2H_2O\ (fl) + p/2\ N_2(g)$$

woraus die nützliche Sauerstoffatomanzahl resultiert:

$$x = (m + n/4 - q/2)$$

TABELLE 3

Verbrennungswärme des Benzimidazolons-2

g Substanz	K ΔT	Jouli ($\Delta T \times$ Kalorim. konst.)	ΔfH (Fe_2O_3)	ΔfH (HNO_3)	ΔcH (Baumwolle)	J/g (ΔU_B)	kJ/mol (ΔU_B)
0,8302	2,149	22 478	55	45	597	26 237	3520
0,7030	1,827	19 110	56	43	533	26 285	3526
0,7897	2,052	21 464	56	49	548	26 353	3535
0,8137	2,109	22 060	56	45	549	26 312	3530

Mittelwert = 3528 kJ/mol

Standarddeviation $\sigma = \sqrt{\Sigma\Delta^2 n(n-1)} = \pm 3{,}16$ kJ

Washburnskorrektion $\pi = \frac{0{,}3 \times 25 \times 7}{-3528}\left[-1 + 1{,}1\left(\frac{6-2}{28}\right) - \left(\frac{2}{25}\right)\right] = -0{,}0138\%$

woraus $\Delta cU^0\,(298{,}15\text{ K}) = \frac{-3528 \times 99{,}9862}{100} = -3527{,}51$ kJ/mol

Für Reaktion : $C_6H_4(NH-CO-NH)\,(f) + 8O_2\,(g) = 7CO_2(g) + 3H_2O(fl) + N_2(g)$;
Die Volumänderung ist 0, woraus :

$$\Delta cH^0\,(298{,}15\text{ K}) = -3527{,}51 \pm 3{,}16\ (\pm 0{,}09\%)\ \text{kJ/mol}$$

$$= -843 \pm 0{,}76\ (\pm 0{,}09\%)\ \text{kcal/mol}$$

Das Grundprinzip der Methode ist, daß für eine organische Substanz, die Verbrennungswärme eine Liniarfunktion des x ist :

$$-\Delta cH^0(298{,}15\text{ K}) = \Sigma a' + x\Sigma b'$$

worin a′ und b′ tabellierte Indikatoren für verschiedene strukturelle Gruppierungen sind.

Die durch diese Methode erhaltenen Daten sind in der Tabelle 4 komparativ vorgestellt.

TABELLE 4

Die Verbrennungs- und Bildungswärmen des o-Phenylendiamins, Harnstoffs und Benzimidazolons-2

Substanz		ΔcH^0(298,15 K)		ΔfH^0(298,15 K)	
		exper.	gerechn.	exper.	gerechn.
OFDA $C_6H_4(NH_2)_2$	kJ/mol	−3543,5	−3501	39,12	3,29
	kcal/mol	−847	−836,72	9,35	0,786
HARNSTOFF NH_2CONH_2	kJ/mol	−645	−629,4	−320,17	−336
	kcal/mol	−154,16	−150,43	−76,52	−80,221
BZION−2 C_6H_4 (NH.CO.NH)	kJ/mol	−3527,51	−3519,16	−85,06	−92,68
	kcal/mol	−843	−841,1	−20,35	−22,15

Nun merkt man, daß die errechneten Werte den experimentellen näher sind. Die Große Differenz die bei der Bildungswärme des o-Phenylendiamins erscheint, konnte dadurch erklärt werden, daß die Methode den Eingang einer Korrektion durch eine eventuelle intramolekulare Interaktion zwischen den enthaltenden $-NH_2$ Gruppen hier in der orto-Stellung nicht erlaubt ist.

Die Behauptung ist vertieft auch durch die errechneten Werte die sehr nahe von den experimentellen[5] die für *p*-Phenylendiamin erhalten. sind : ΔcH^0 (298,15 K) = − 838,3 ± 0,15 kcal/mol und b.z.w. ΔfH°(298,15 K) = 0,73 ± 0,17 kcal/mol.

Die erhaltenen Daten wurden auch bei der Errechnung der Reaktionswärme in Standardbedingungen des *o*-Phenylenharnstoffbilddung verwendet :

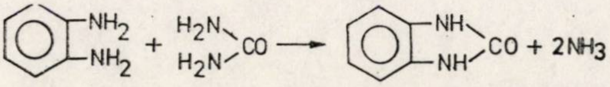

$$\Delta rH^0(298{,}15\ K) = [-85{,}06 - (2\times 45{,}94)] - [39{,}12 - 320{,}17] =$$
$$= 104{,}11\ kJ/mol$$

LITERATURHINWEISE

[1] I. Contineanu und D. I. Marchidan, *Rev. Chim. (București)*, **30**, 1096 (1979).

[2] CODATA Bulletin nr. 28 (April 1978) : „CODATA Recommended Key Values for Thermodynamics 1977". Ins Rumänische übersetzt in *Revista de Chimie*, *București*, **32**, 396 (1981).

[3] E. S. Domalski, *J. Phys. Chem. Ref. Data*, **1**, 221 (1972).

[4] G. R. Handrick, *Ind. Eng. Chem.*, **48**, 1366 (1956).

[5] J. D. Cox., „Thermochemistry of Organic and Organometallic Compounds". Academic Press, London, 1970, p. 290.

Revue Roumanie de Chimie, 27, 2, 211–215 (1982)

ON GENERALIZED PAIR POTENTIAL. EVALUATION OF CRYSTAL PROPERTIES

J. D. PANDEY and R. P. PANDEY
Department of Chemistry, University of Allahabad, Allahabad – 211 002.

Received November 8, 1979
Revised June 1, 1981

The generalised pair potential of Woodcock (*J. Chem. Soc., Faraday Trans. II*, 70, 1405 1974) has been used to compute various crystal properties of twenty alkali metal halides. These properties include cohesive energy, atomization energy and electron affinity. The agreement between experimental and theoretical value is quite satisfactory showing the validity of generalised pair potential.

INTRODUCTION

Theoretical evaluation of crystal properties of alkali metal halides using interaction potential has received the attention of a number of workers [1-11] during recent years. The aim of such calculations is to test the validity of the specific form of interaction potential by comparing the computed properties with experimental ones. Secondly, the relative merits of various empirical interionic potential functions can also be assessed.

The crystal and related properties of alkali metal halides have been generally computed using Born [12], Born-Meyer [13], Gaussian [14], modified Gaussian [15] and logarithmic [16-17] potential functions. Calculations were made with the inclusion of the Van der Waals and other short range forces in these potential functions. Purely empirical methods have also been used to compute the properties of alkali metal halides. Sangster [5] and coworkers reported a consistent set of shell parameters for alkali metal halides and derived a set of interionic potentials of the Born-Mayer form.

Since two term potentials corresponding to a simple ionic model are inadequate for experimental data on gaseous alkali halide ion pairs, Woodcock [18] proposed a generalised three term pair potential which has been used to parametrise experimental data for gaseous alkali metal halide ion pairs. For alkali halide crystals, the generalised pair potential can be written as

$$\Phi(R) = C.A.R.^{-m} \exp.\ [-B\,(R^{n} - 1)] - M \cdot e^{2} \cdot R^{-1} \qquad (1)$$

where, C is the coordination number of the lattice, e is the electronic charge, R is the internuclear separation, A and B are potential parameters and M is the Madelung constant. The values of m and n are different for different crystals. In the present paper, we have evaluated cohesive energy, atomization energy and electron affinity of alkali metal halide crystals using the generalised pair potential of Woodcock.[18]

THEORY

Applying the following stability and compressibility conditions,

$$\Phi'_{(R)} = 0$$

$$\text{and } \Phi''_{(R)} = \frac{q,\, Cr_0}{\beta} \text{ at } R = r_0 \tag{2}$$

to equation (1), we obtain the expressions for potential parameters A and B

$$A = \frac{M \cdot e^2}{r_0^{1-m}\, C \exp[-B(r_0^n - 1)]\, (m + nBr_0^n)} \tag{3}$$

$$B = \frac{-x + \sqrt{x^2 - 4yz}}{2y} \tag{4}$$

where,

$$x = r_0^n \left\{ 2mn - n^2 - \frac{nr_0}{M \cdot e^2} \left(\frac{9Cr_0^3}{\beta} + \frac{M \cdot e^2}{r_0} \right) \right\}$$

$$y = n^2 r_0^{2n}$$

$$z = m^2 - \frac{mr_0}{M \cdot e^2} \left(\frac{9Cr_0^3}{\beta} + \frac{M \cdot e^2}{r_0} \right)$$

where β, r_0 and C are the compressibility, nearest neighbour distance and structural constant respectively. The cohesive energy W, can be computed from the relation

$$W = -[N\Phi(r_0) + \varepsilon] \tag{5}$$

where,

$$\Phi(r_0) = -\frac{M \cdot e^2}{r_0} \left(1 \frac{1}{(m + nB\; r_0^n)} \right) \tag{5}$$

and ε is the zero point energy. N is the Avogadro number. The atomization energy, E_a, which gives better insight of crystal stability than the cohesive energy, can be obtained from the relation

$$E_a = W + E - I \tag{6}$$

where E is the electron affinity of anion and I is the ionization potential of cation.

RESULTS AND DISCUSSION

In order to compute the various crystal properties of alkali metal halides, the experimental values of r_0 and β are taken from different sources,[19-20] the values of m and n are taken from the work of Woodcock [22]. Table 1 enlists the results of calculation of cohesive energy. The values of the potential parameter, $\boldsymbol{B}$, computed for twenty alkali metal halides according to equation (4), are given in the second column. In the third column of table 1, cohesive energy of the metal halides obtained from equation (5) is recorded. For comparison, the experimental values are also recorded in the fourth column. Theoretical values of cohesive energy derived from older potentials have also been included which have been compiled from different sources. It is evident from table 1 that the average percentage errors between the theoretical and experimental

TABLE 1

Theoretical and experimental values of the cohesive energy of alkali halide crystals (KJ mol^{-1})

Crystal	$B \times 10^{+n}$	W Calc) eq. (5)	W exp.	W Born-Lande (Ref. [2])	W Born-Meyer (Ref. [6])	W Kapustinski (Ref. [10])	W (Ref. [6])
LiF	0.03924	1031.3	1004.58	1004.6	1000.0	952.7	924.5
NaF	0.0060709	939.3	892.87	899.5	894.1	884.9	858.9
KF	0.072808	813.3	792.03	796.6	792.4	788.7	794.9
RbF	0.052429	759.0	759.81	760.6	756.0	760.2	774.0
CsF	−0.20817	720.1	726.76	723.0	714.2	712.9	747.7
LiCl	0.00185	833.1	843.08	808.7	818.0	803.7	810.9
NaCl	0.000895	768.6	772.78	754.8	756.0	752.7	761.7
KCl	0.0005724	699.6	684.5	687.8	687.4	680.7	713.0
RbCl	0.0003745	667.3	684.5	664.8	660.6	661.9	692.9
CsCl	0.000359	631.8	660.24	623.0	620.5	625.1	673.6
LiBr	0.00121	780.3	801.24	766.1	671.9	792.9	778.6
NaBr	0.000702	729.7	735.97	718.4	719.2	734.3	733.5
KBr	0.000396	664.8	677.81	660.2	659.4	674.9	687.9
RbBr	0.000194	635.5	661.07	638.1	635.1	626.3	671 5
CsBr	0.000256	607.5	637.22	600.4	597.5	602.1	651.9
LiI	0.000678	716.6	753.12	714.2	710.4	712.9	731.8
NaI	0.000477	675.7	695.80	672.8	670.3	673.6	695.7
K	−0.000004	612.1	639.32	623.4	620.5	614.2	654.4
RbI	0.000154	599.6	626.34	603.3	599.6	590.0	639.8
CsI	0.000169	573.6	608.35	569.4	565.2	563.6	620.9
Average % error		3.04	—	2.97	3.13	3.31	2.4

values of W from present method are 3.04 percent. The average percentage error from the present method is greater than the Born-Lande, Sinha and Thakur and less than the Born-Mayer, Kapustinski values. Thus the agreement between the calculated and experimental values appears to be satisfactory. Table 2 enlists the results of calculation of atomization energy and electron affinity of alkali metal halide crystals. Equations (5) and (6) are employed to compute the atomization energies of these crystals. The theoretically computed and Sanderson's [21] experimental values are presented in the second and third columns of table 2. Similar values, derived from potential energy functions employed by earlier workers, have also been included in table 2 for comparison. For calculating the values of E_a, the experimental values of E and I were taken respectively from the work of Bocking et al. [23] and Massay. [24] The mean percentage error between experimental and calculated values for atomization energy is 4.9 only. It can be seen that the present values compare well with the experimental and other theoretical values. The electron affinity of halogen atoms was obtained from equation (6) and is recorded in the seventh column of table 2. The mean values of electron

TABLE 2

Atomization energy and electron affinity of alkali halide crystals at 2.98.18K (kJ mol^{-1})

Crystal	E_a (calc) eq. (6)	E_a (exp.) Sanderson (Ref. [21])	E_a Born-Lande (Ref. [2])	E_a (Born-Mayer (Ref. [2])	E_a (Ref. [6])	E (cal.) eq. (6)	E average	E_a(exp)
LiF	838.4	849.4	848.1	806.6	780.0	338.09		
NaF	770.6	757.3	738.6	742.8	739.1	313.8		
KF	721.7	732.2	719.5	729.2	752.1	337.6	337.3	327.1*
RbF	683.2	711.3	706.0	706.0	746.6	355.2		324.4+
CsF	671.7	686.2	697.4	695.8	749.7	341.6		
LiCl	666.2	690.4	686.1	661.1	658.4	444.2		
NaCl	625.9	640.2	639.2	635.3	633.9	267.4		
KCl	634.0	648.5	637.1	637.1	662.2	367.6	385.2	353.1*
RbCl	617.5	635.9	631.8	632.0	657.5	371.6		348.1+
CsCl	609.4	631.8	629.9	630.2	667.6	375.5		
LiBr	555.5	623.4	561.2	557.3	595.3	363.1		
NaBr	529.1	581.6	535.4	577.2	574.9	347.7		
KBr	541.3	594.1	553.9	533.9	606.3	348.0	353.2	295.2*
RbBr	527.8	585.8	544.8	548.7	605.3	353.2		324.3+
CsBr	527.2	585.8	546.9	547.0	615.1	353.8		
LiI	507.3	539.7	521.4	517.4	512.8	342.1		
NaI	489.6	502.1	499.9	503.7	501.4	322.2		
KI	503.1	523.4	526.7	526.8	537.1	329.6	328.2	309.7*
RbI	506.4	518.8	525.9	529.8	537.9	322.1		295.4+
CsI	507.8	523.0	523.7	532.2	548.4	324.9		
Average % error	4.9	—	2.9	3.2	3.8			

* From the experimental values of Schmidt et al.
+ From the experimental values of Berry et al.

affinity are compared with the reliable experimental values of Berry-Reimann [22] and Schmidt-Bocking-Bethge. [23] The agreement between theoretical and experimental values of electron affinity is also satisfactory.

ACKNOWLEDGEMENT. One of the authors (R.P.P.) is grateful to University Grants Commission, New Delhi for the financial assistance.

REFERENCES

[1] R. Narayan and S. Ramasashan, *J. Phys. Chem. Solids*, **37**, 395 (1976).

[2] K. P. Thakur, *Austral. J. Phys.*, **29**, 46 (1976), **30**, 325 (1977).

[3] C. M. Kachhava and S. C. Saxena, *J. Chem. Phys.*, **44**, 986 (1966).

[4] J. D. Pandey, *J. Phys. Soc. Japan*, **26**, 579 (1969).

[5] M. J. L. Sangster, V. Schrodes and R. M. Atwood, *J. Phys. chem.*, **11**, 1523 (1978) : **11**, 1541 (1978).

[6] A. K. Sinha and L. Thakur, *Ind. J. Pure and Appl. Phys.*, **15**, 115 (1977).

[7] J. Sherman, *Chem. Rev.*, **11**, 93 (1932).

[8] J. D. Pandey, *J. Phys. Chem.* B., **3**, 925 (1970).

[9] T. C. Waddington, "Advances in Inorganic Chemistry and Radiochemistry", vol. 1, Academic, New York, 1959, p. 159.

[10] A. P. Kapustinski, *Acta Physico Chim, USSR*, **18**, 370 (1943).

[11] R. T. Sanderson, "Chemical Bonds and Bond Energy", Academic Press, London, 1971, pp. 133–175.

[12] M. Born and G. Mayer, "*Handbuch der Physik*", **24**, 623 (1933).

[13] M. Born and J. Meyer, *Z. Physik*, **75**, 1 (1932).

[14] Y. P. Varshni and R. C. Shukla, *J. Chem. Phys.*, **35**, 582 (1961).

[15] M. M. Patel, V. B. Gohel and M. D. Trivedi, *Indian J.Phys.*, **41**, 235 (1967).

[16] K. P. Thakur, *J. Inorg. Nuclear Chem.*, **36**, 2171 (1974).

[17] K. P. Thakur, *Indian J. Pure Appl. Phys.*, **11**, 549 (1973).

[18] L. V. Woodcock, *J. Chem. Soc., Faraday Trans., II*, **70**, 1405 (1974).

[19] R. P. Jain, S. Saxena and J. D. Pandey, *J. Inorg. Nuclear Chem.*, **36**, 203 (1974).

[20] M. Born and K. Hung, "Dynamical Theory of Crystal Lattice", Oxford-Clarendon Press, 1956.

[21] R. T. Sanderson, "Inorganic Chemistry" Reinhold, New York, 1967.

[22] R. S. Berry and C. W. Reimann, *J. Chem. Phys.*, **38**, 1540 (1963).

[23] H. Schmidt-Bocking and K. Bethge, *J. Chem. Phys.*, **58**, 3244 (1973).

[24] A. G. Massay, "The Typical Element", Penguin, London, 1972.

Revue Roumaine de Chimie, 27, 2, 217–223 (1982)

POLARIZATION BEHAVIOUR OF ARMCO IRON IN ANHYDROUS SOLUTIONS OF R–OH + HCl

SOLOMON STERNBERG and VIOREL BRÂNZOI

Department of Physical Chemistry and Electrochemistry, National Institute of Chemistry, Str. Polizu 1, Bucharest, Romania

Received April 16, 1981

Using the potentiostatic method, the polarization behaviour of Armco iron in anhydrous solutions of R–OH + HCl (where R=CH_3 ; C_2H_5 ; C_3H_7 ; C_4H_9 ; C_5H_{11}) was studied. The increase of HCl concentration as well as temperature leads to an increase of corrosion rate, while the increase of the hydrocarbonate chain length leads to a decrease of the corrosion rate.

INTRODUCTION

The corrosion in organic solvents is of increasing practical interest due to the large number of organic systems used in technics.

However, the number of papers referring to the corrosion in organic liquids is very reduced as compared to the similar studies in aqueous solutions. In the last years, several monographic papers appeared $^{1-6}$ showing that from physico-chemical point of view the corrosion in protic organic solvents occurs at the metal/ liquid interface in the same way like in aqueous solution. Since there is a large variety of organic liquids, a large number of metal/ organic solvent systems can be investigated. It must be emphasized that the corrosion in these media is usually due to the presence of impurities originating either in the manufacturing procedure or in the sidereactions after a longer period of using these solvents.

The most frequent impurities are water, acids and halides of higher valence metallic ions. This implies a good knowledge of the relationship between the corrosion rate and the impurity concentration. The present paper reports on the influence of temperature and HCl concentration on the Armco iron polarization in anhydrous R–OH (where R = CH_3 ; C_2H_5 ; C_3H_7 ; C_4H_9 ; C_5H_{11}).

EXPERIMENTAL

The polarization curves have been obtained using the potentiostatic method. In all experiments the electrochemical polarization was started about 30 minutes after the working electrode was immersed in solution, to allow the stabilization of the stationary potential. The working electrode potential was always measured with reference to the saturated calomel electrode and was plotted against the current in the external circuit, obtaining the anodic or cathodic curves according to the variation of the working electrode potential.

In order to reduce ohmic resistance caused by the low conductivity of the organic solvents, we used a single compartment cell (Fig. 1) in which the working electrode was situated in the cell center and surrounded by the auxiliary electrode, made of a bright platinum gauze. This position allows the formation of a uniform and high electric field during the anodic or cathodic polarization.

The connection between the cell compartment and the reference electrode was made through a Haber-Luggin capillary and the solution was continuously stirred by bubbling purified argon introduced through the lower part of the cell.

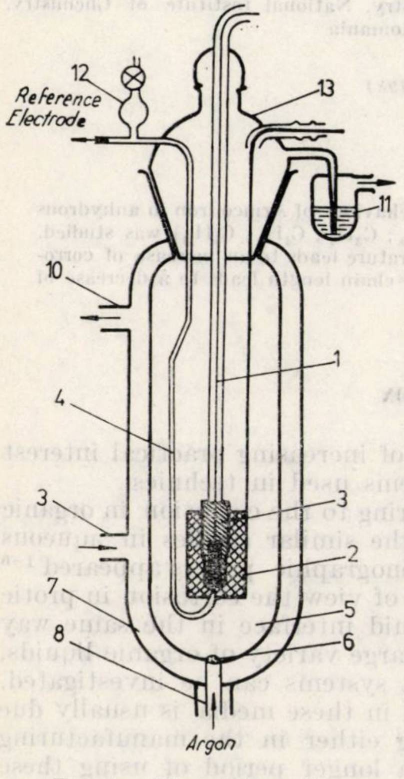

Fig. 1. —Electrolytic cell.

All these precautions contribute to the lowering of the ohmic resistance of the cell.

The reagent grade alcohols were distilled over organo-magnesium compounds to remove the water traces and checked up by Karl-Fischer method. The anhydrous solutions of HCl in R—OH have been obtained by bubbling anhydrous gaseous HCl freshly prepared through alcohol until saturation. These solutions were then diluted to the desired concentration of HCl by adding anhydrous R—OH, measuring the final concentration by titration with aqueous NaOH in the presence of phenolphtaleine as indicator. The gaseous HCl was obtained from Merck R. G. concentrated H_2SO_4 and concentrated HCl solution. The working electrode made of Armco iron (99.93 %Fe) had a surface of 1 cm^2. Before each measurement the working electrode was polished with fine emery, then it was immersed in boiling benzene for five minutes to remove the remaining fat traces and the abrasive dust on the electrode surface after polishing. The samples were subsequently electropolished according to the method used for different metals.[7,8] After electropolishing, the working electrode was washed with anhydrous alcohol, then with the working solution and finally immersed in the cell. The working solution had been previously degased by bubbling argon for one hour, continuing this procedure during the measurement.

The temperature in the cell was kept constant using a UM—210 thermostat with the precision of ± 0.1 °C. The recording of the polarization curves was always made starting from the stationary potential. Several measurements were carried out for each solution until a good reproducibility was attained. It is known that a long lasting anodic polarization may generate some modifications of the surface structure, thus leading to a displacement of Tafel regions. This behaviour can be avoided[9,10] plotting the cathodic polarization curves in the first stage and then the anodic ones.

RESULTS AND DISCUSSION

The anodic and cathodic polarization curves are shown in Figs 2, 3 and 4 for Armco iron in anhydrous solutions of HCl in CH_3OH.

The increase of HCl concentration leads to a displacement of the polarization curves towards more negative potentials (almost parallel displacement), an increase of the corrosion rate and of the limiting diffusion current.

The shown polarization curves indicate that there is no active-passive transition up to very high currents. This behaviour can be explained by the presence of HCl which hinders the formation of the passive film and accelerates the anodic dissolution proportionally to the concentration of Cl^- ions. It is likely that the halide ions participate to the reactions at the metal—electrolyte interface by a competitive adsorption

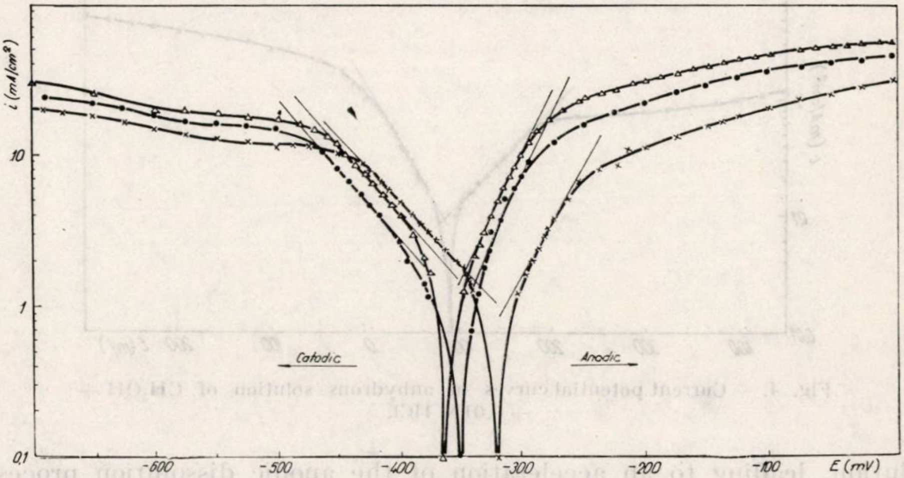

Fig. 2. — Current potential curves in anhydrous solution of CH_3OH + HCl : (Δ) CH_3OH + 2.5N HCl ; (●) CH_3OH + 1.5N HCl ; (×) CH_3OH + 1N HCl.

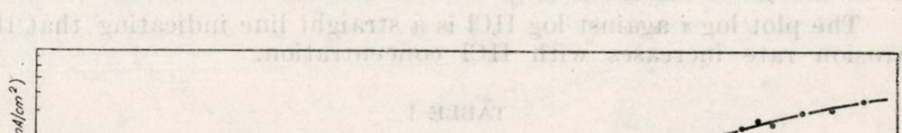

Fig. 3. — Current-potential curves in anhydrous solution of CH_3OH + HCl ; (●) CH_3OH + 0.5N HCl ; (×) CH_3OH + 0.1N HCl.

forming chemisorbed films which satisfy the surface affinity for the oxygen atoms or alcohol molecules. [11,12]

The specific adsorption of these anions results in a lowering of the potential energy associated with the transition from the metal to the solution, leading to an acceleration of the anodic dissolution process. The kinetic parameters of corrosion calculated from the polarization curves are given in table 1.

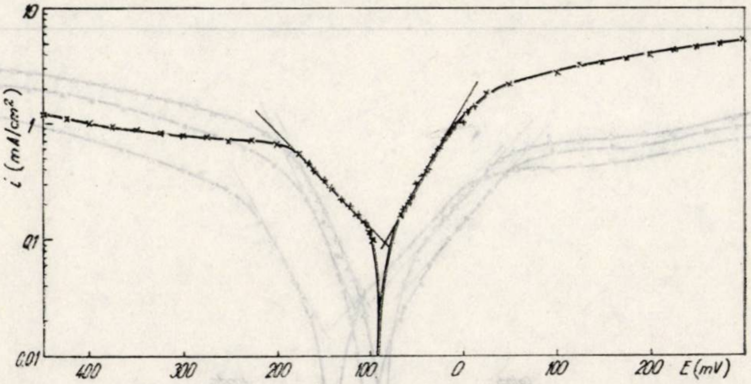

Fig. 4. — Current potential curves in anhydrous solution of CH_3OH + + 0.01N HCl.

The plot log *i* against log HCl is a straight line indicating that the corrosion rate increases with HCl concentration.

TABLE 1

The kinetic parameters of Armco iron in anhydrous solutions of R—OH + HCl at 20°C (i_{LD} = = the limiting diffusion current)

Solution	i_{corr} mA/cm²	P_{mpy}	Tafel b_a mV	Slopes $-b_c$	$-E_{corr}$ mV SCE	i_{LD} mA/cm²
CH_3OH + 2.5 N HCl	1.54	718.56	62.5	114	355	26.5
CH_3OH + 1.5N HCl	1.15	536.59	59.5	117.5	345	18.7
CH_3OH + 1N HCl	0.94	438.6	64	121	317	12
CH_3OH + 0.5N HCl	0.8	373.28	60	122.5	290	10
CH_3OH + 0.1N HCl	0.27	126	65	119	280	5
CH_3OH + 0.01N HCl	0.095	44.33	70	120	82.5	2.2

An analysis of the current density—potential curves shown in Figs 2, 3 and 4 indicates that at the low overpotential the Tafel relationship is followed, showing that both anodic and cathodic reactions are activation controlled.

At higher overvoltages a limiting diffusion current appears on the anodic polarization curves showing that at higher current densities the transport of HCl towards electrode surface becomes the rate determining step (concentration polarization).

The electrode surface cannot be completely covered with adsorbed Cl^-ions in this case and thus it is possible for the solvent molecules to participate directly in the mechanism of metal dissolution through its oxidation products on the free regions of the electrode surface. The methanol oxidation on these free regions, together with participation of the oxidation products in the metal dissolution as well as the increase of the transport rate of Cl^- ions to the electrode surface due to the potential increase could explain why the limiting diffusion current is not always well defined.

At the same time, these facts explain why the limiting diffusion current decreases when the HCl concentration decreases (see table 1).

THE INFLUENCE OF THE HYDROCARBONATE CHAIN ON THE POLARIZATION BEHAVIOUR OF ARMCO Fe

The polarization curves of Armco iron in anhydrous solutions of lower alcohols at the same HCl concentration have also been recorded. Since the shapes of these curves are the same with those shown in Figs 2, 3 and 4, only kinetic parameters of corrosion are given in table 2. It can be seen that there is a lowering of the corrosion rate of Armco Fe when the hydrocarbonate chain increases. This behaviour could be explained as follows :

The organic solvent is the carrier of the corrosion agents and of the products resulted during the corrosion reaction.

A higher mobility of the organic solvent molecules facilitates the transport of the corrosion agents increasing the corrosion rate.

The increase of the hydrocarbonate chain length leads also to an increase in solvent viscosity, a decrease of the diffusion coeficient and of the specific conductivity as well as to a decrease of the dielectric constant. All these effects contribute to the decrease of the corrosion rate when the hydrocarbonate chain increases. On the other hand, it is well known that the alcohols are protic solvents associated by hydrogen bonds.

The formation of these hydrogen bonds leads consequently to the autodissociation resulting in the formation of solvated protons $R-OH_2^+$; these being the main corrosion agents. As the hydrocarbonate chain length increases, a steric hindrance of the autodissociation occurs and the concentration of the solvated proton decreases as well as its mobility, leading finally to a lowering of medium aggressivity. This explanation is in good agreement with the corrosion potential shift towards more positive values and also with the lowering of the corrosion current density (see table 2).

TABLE 2

Corrosion parameters of Armco iron in anhydrous solutions 1N HCl in R–OH at 20°C

Solution	i_{corr} mA/cm²	P_{mpy}	Tafel b_a	Slopes $-b_c$	$-E_{corr}$ mV SCE	i_{LD} mA/cm²
CH_3OH + 1N HCl	0.94	438.6	64	121	317	12
C_2H_5OH + 1N HCl	0.52	242.63	65	124	325	8.5
C_3H_7OH + 1N HCl	0.44	205.3	62.5	135	197	3.8
C_4H_9OH + 1N HCl	0.2	93.32	57.5	135	120	2.4
$C_5H_{11}OH$ + 1N HCl	0.15	70	50	123	57.5	1.4

It can be also seen a significant decrease of the diffusion limiting current density with the increase of the hydrocarbonate chain length increasing.

TEMPERATURE EFFECT

The behaviour of Armco iron in anhydrous solution 1N HCl in CH_3OH during polarization was studied at different temperatures. The

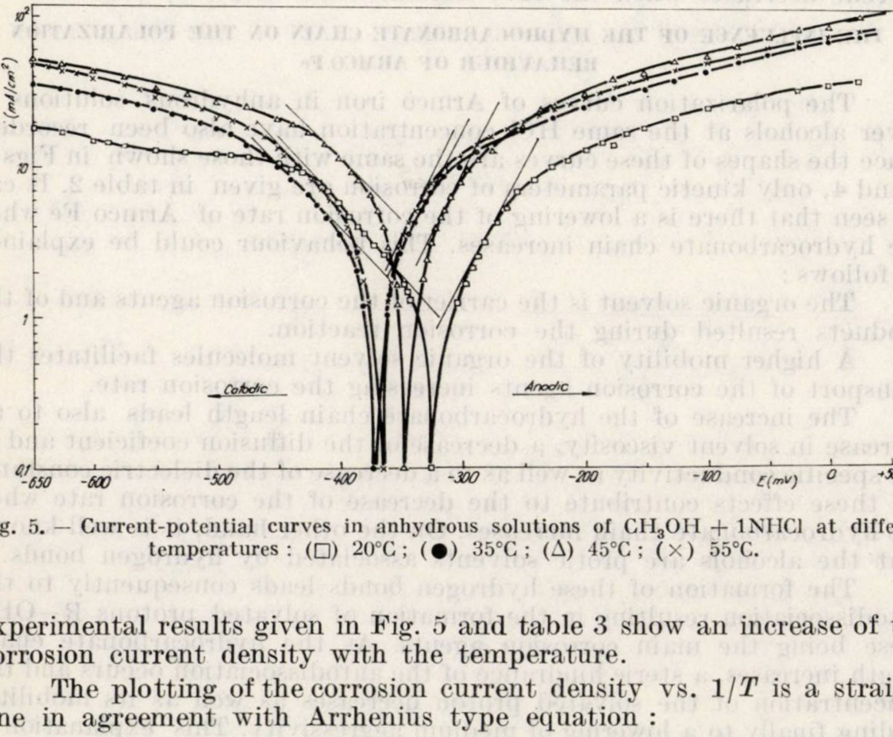

Fig. 5. — Current-potential curves in anhydrous solutions of $CH_3OH + 1NHCl$ at different temperatures : (□) 20°C ; (●) 35°C ; (Δ) 45°C ; (×) 55°C.

experimental results given in Fig. 5 and table 3 show an increase of the corrosion current density with the temperature.

The plotting of the corrosion current density vs. $1/T$ is a straight line in agreement with Arrhenius type equation :

$$i_{\text{corr}} = A \exp(-E/RT)$$

$$\text{or } \ln i_{\text{corr}} = \ln A - E/RT$$

The apparent activation energy obtained from this plot is given in table 3. The ratio i_t/i_{20} indicates the increase of the corrosion rate with reference to 20°C.

Finally, it can be concluded that in anhydrous alcohols the increase of HCl concentration as well as of temperature leads to an increase of corrosion rate, while the increase of the hydrocarbonate chain length leads to a decrease of the corrosion rate.

TABLE 3

Corrosion rate dependence upon temperature in anhydrous solution 1N HCl in CH_3OH

Anhydrous solution of $CH_3OH + 1N\ HCl$	t °C	$(1/T) \cdot 10^3$	i_{corr} mA/cm²	i_t/I_{20}	Apparent activation energy cal/mol
	20	3.45	0.94	1	
	35	3.25	1.8	2	6313
	45	3.144	2.3	2.45	4580
	55	3.05	2.8	3	4163

REFERENCES

[1] K. Schwabe, "Acid Corrosion of Metals in Nonaqueous Solvents", Verlag Technik, Berlin, 1952.

[2] A. Bukowiecki, *Metall*, **13**, 536 (1959).

[3] W. Schmidt, *Zashchita Metall*, **5**, 608 (1969).

[4] J. J. Demo, *Chem. Eng. World*, **7**, 115 (1972).

[5] E. Heitz, "Corrosion of Metals in Organic Solvents", Adv. Corr. Science Technol., Vol. 4, Edited by M. G. Fontana and R. W. Staehle, 1974, p. 150–225.

[6] E. Heitz, *Oberfläche-Surface*, **15**, 331 (1974).

[7] W. J. McG. Tegart, "The Electrolytic and Chemical Polishing of Metals in Research and Industry", Pergamon Press, London, 1959.

[8] E. McCafferty and N. Hackerman, *J. Electrochem. Soc.*, **119**, 999 (1972).

[9] E. Heitz and W. Schenk, *Werkst. u. Korr.*, **27**, 241 (1976).

[10] E. Heitz, *Werkst. u. Korr.*, **19**, 773 (1968).

[11] N. D. Stolica and H. H. Uhlig, *J. Electrochem. Soc.*, **110**, 1215 (1968).

[12] E. J. Kelly, *J. Electrochem. Soc.*, **112**, 124 (1965).

Revue Roumaine de Chimie, **27**, *2*, 225–233(1982)

STERISCHE EFFEKTE IN EFFEKTOR–REZEPTOR INTERAKTIONEN. DIE METHODE DER STERISCHEN DIFFERENZEN UND ANWENDUNGEN.

RADU VÂLCEANU und IOAN MOȚOC

Chemie-Forschungszentrum,
Bd. Mihai Viteaz 24,
1900 Timișoara, Rumänien

Eingegangen am: 12. Februar 1981

Vorliegende Arbeit enthält die endgültige Version der Methode der sterischen Differenzen (abgekürzt SD*, *S*teric *D*ifference). Die SD*-Methode wurde ausgearbeitet, um die sterischen Effekte in den Effektor-biologischer Rezeptor-Interaktionen quantitativ behandeln zu können. Charakteristisch für diese Methode ist die Tatsache, daβ sie sowohl die Topologie des Effektormoleküls, als auch die Topologie des Rezeptorhohlraums in Betracht zieht. Die SD* – Methode hat praktisch folgende Vorleile : 1) die sterischen Parameter $SD^* = [SD_c^*, SD_w^*]$ sind leicht zu berechnen ; ii) sie kann sowohl für strukturell verwandte Verbindungen (mit einem gemeinsamen Molekülskelett), als auch für sehr verschiedene Strukturreihen angewendet werden ; iii) da die sterischen SD* – Parameter zwei an der Zahl sind, für jedwelche Reihe bioaktiver Verbindungen, ist die Methode auch für kurze Serien anwendbar. Die SD* – Methode wird auch zur Voraussage neuer physiologisch aktiver Strukturen benützt. Die SD* – Methode wird erfolgreich in den Hapten-Antikörper Interaktionen angewendet.

The paper presents the improved version of our Steric Difference method (i.e., SD* version). The SD* – method has the following advantages :

i) the $SD^* = [SD_c^* ; SD_w^*]$ steric parameters are easily to compute ; ii) the method applies both to congener and non-congener series ; iii) the steric dissimilarity within any series of bioactive compounds is expressed by two figures (i.e., $SD_c^*$and SD_w^*). Accordingly, the method may be applied to short effector series. The SD* – method is useful in QSAR and drug design. The method here discussed is applied with good results to hapten – antibody interactions.

1. EINLEITUNG

Die quantitative Behandlung der sterischen Effekte in den Effektor-biologischer Rezeptor-Interaktionen ist ein schwieriges Problem, da es scheinbar in den biologischen Systemen zwei Ursachen für sterische Effekte gibt [1] : i) ein repulsives sterisches Potential, ähnlich den sterischen Effekten die in chemischen Reaktionen wirken ; ii) ein attraktives sterisches Potential, durch London'sche Kräfte, die infolge der Bildung des Effektor-biologischer Rezeptor-Komplexes wirken. Aus diesem Grund können die sterischen Substituentkonstanten (also die Taft-Konstanten vom E_S-Typ und die topologischen Indexe – für eine allgemeine Übersicht, siehe

Lit. [2]) der organisch-physikalischen Chemie nicht immer mit den Interaktionen aus biologischen Systemen in Zusammenhang gebracht werden.

Der Zweck der vorliegenden Arbeit ist die für die quantitative Bewertung der sterischen Interaktionen in biologischen Systemen entwickelte Methode der sterischen Differenzen systematisch zu behandeln. In der ersten Version der Methode [3] nahm man an, daß alle Atome dasselbe Volumen besitzen (diese übertriebene Vereinfachung war der Tatsache zuzuschreiben, daß in der Methode Begriffe verwendet wurden, wie *Nichtbesetzung des Rezeptorhohlraums* und *Besetzung der Rezeptorwände*). Diese Unzulässigkeit wurde dann später beseitigt [4] durch die Einführung der *Besetzung* anstatt *Nichtbesetzung des Rezeptorhohlraums* und durch die Benützung der k_i-Werte (berechnet von Austel und Mitarb. — siehe weiter). Die letzte Version der Methode wird mit SD* (*S*teric *D*ifference) bezeichnet.

Im folgenden wird die SD*-Methode detailliert vorgestellt und es werden die SD*-Gleichungen für die sterischen Effekte der Hapten-Antikörper-Interaktionen berechnet.

2. DIE SD*-METHODE

Die SD*-Methode stützt sich auf folgende zwei Hypothesen:

1) der biologische Rezeptor wird als ein Hohlraum angesehen, der von isotropischen und relativ deformierbaren Wänden und dem Raum außerhalb des Rezeptorhohlraums, ein sterisch irrelevanter Raum, definiert wird.

2) die Affinität des Rezeptors für Effektoren ist eine Funktion von zwei Veränderlichen: die Rezeptorbesetzung, SD^*_c (*c* von „cavity“) und die Besetzung der Rezeptorwände, SD^*_w (*w* von „walls“). SD* bedingt die Aktivität durch die London'schen Kräfte (SD^*_c ist ein Maß für das attraktive sterische Potential), während SD^*_w die Affinität bedingt, die durch die konformationalen Modifikationen im Biomakromolekül und/oder die intermolekularen sterischen Effekte, ähnlich denen aus chemischen Reaktionen hervorgerufen wird (SD^*_w ist ein Maß für das repulsive sterische Potential).

Wir werden folgenderweise vorgehen: es sei die Reihe bioaktiver Moleküle $S_1, S_2, \ldots, S_n$ gegeben, die eine bestimmte biologische Reaktion, durch einen einzigen Mechanismus hervorruft. Die Struktur S, *Standard* genannt, wird dem Hohlraum als komplementär angenommen. Wir berechnen die Funktion:

$$\mathrm{SD}^* : \{S\} \times \{S_i\}_{i=1,\ldots,n} \to R \times R \qquad (1)$$

wobei X das karthesische Produkt bezeichnet und R die Menge der reellen Zahlen darstellt.

Also, mit Hilfe der Funktion (1) wird die Form des bioaktiven Moleküls mit der Form des Rezeptorhohlraums, mit dem dieses Molekül interaktioniert, verglichen.

Die oben angeführten Hypothesen (1) und (2) unterstützen dei Berechnung der SD*-Funktion, auf Grund des folgenden Algorythmus:

1) Wenn keine andere Möglichkeit besteht, wird als Standard S, das aktivate Molekül der gegebenen Reihe (Biomoleküle $S_1, \ldots, S_n$) angenommen, das heißt, dieses Molekül ist, laut Annahme, komplementär dem Rezeptorhohlraum. Im Falle der Hapten-Antikörper-Interaktion ist bekannt,[6] daß der Rezeptorhohlraum des Antikörpers relativ komplementär der Antigengruppe als Standard S benützt werden.

2) Es wird S mit S_i überlagert, $i = 1, 2, \ldots, n$, laut der Überlagerungsregel der Pharmakonen aus S und S_i. Die Differenzen von ungefähr ± 0,20 A und ± 20^0 zwischen den Bindungslängen, bzw. den Valenzwinkeln, können vernachlässigt werden. Wir empfehlen sogar diese Vernachlässigung, damit die geometrischen Kongruenzen ohne Komplikationen verwirklicht werden können. Gleichzeitig scheint es sinnvoll, daß die Vernachlässigung dieser Differenzen die biologische Reaktion nicht semnifikativ beeinflußt, weil dadurch ja nur kleine Deformationen der Valenzwinkel im Biomakromolekül entstehen. Diese Deformationen benötigen kleine Energiemengen (laut,[7] benötigt die Deformation des C—C—C-Winkels von einem Wert von $\Delta\theta$ bis zu $\pm 20^0$, $0{,}01 \cdot (\Delta\theta)^2$ kcal. Grd^2. Mol^{-1} ; d. h. $\Delta\theta = \pm 10^0$ entspricht 1 kcal/Mol).

Im allgemeinen ist die Festlegung des Pharmakons (d. h. die Atomgemeinschaft die das Erscheinen der biologischen Reaktion bedingt) eine schwere Aufgabe. Diese kann aber gelöst werden, wenn z.B., der von Lesk[8] entwickelte Algorythmus benützt wird (für eine ausführliche Darlegung in diesem Sinn, siehe[10] und besonders[9]).

3) Es werden die Atome aus S_i, $1, 2, \ldots, p$, gezählt, die sich mit S überlagern, $i = 1, 2, \ldots, n$. Man berechnet die Summe $\sum_{j=1}^{p} k_j = \mathrm{SD}_c^*$. k_j sind die von Austel und Mitarb[5] berechneten Werte, wo das Volumen des Atoms j in Betracht gezogen wird. $k_j = 1$ für die Atome j der Elemente der zweiten Periode (eine Ausnahme bildet Fluor, $k_F = 0{,}1$) und $k_j = 1{,}2$; 1,7 für die Atome j der Elemente der dritten, vierten und fünften Periode. Für Wasserstoff wird $k_H = 0$ angenommen.

4) Es werden die Atome aus S_i $1, 2, \ldots, q$ gezählt, die sich mit S nicht überlagern. Dann berechnet man die Summe $\sum_{j=1}^{q} k_j = \mathrm{SD}_w^*$.

Die von einer Reihe bioaktiver Verbindungen hervorgerufene biologische Reaktion, BR ist von den sterischen Parametern: $\mathrm{SD}^* = [\mathrm{SD}_c^* ; \mathrm{SD}_w^*]$ laut folgender Gleichung bedingt:

$$\mathrm{BR} = a + b\ \mathrm{SD}_c^* + c\,\mathrm{SD}_w^*,\ b > 0,\ c < 0 \tag{2}$$

a, b und c werden durch die Methode der kleinsten Quadrate berechnet.

Da BR nicht nur von sterischen Faktoren, sondern auch von elektronischen, hydrophoben usw. Faktoren abhängt, wird die Gleichung (2) entsprechend ergänzt:

$$\mathrm{BR} = a' + b\ \mathrm{SD}_c^* + c\,\mathrm{SD}_w^* + \sum_i d_i\ \sigma_i \tag{3}$$

wo σ_i die Substituentkonstante bedeutet, die quantitativ die elektronischen, hydrophoben usw. Faktoren ausdrücken.

Es folgt, daß das geordnete Dublett $SD^* \ (S, S_i) = [SD_c^* ; SD_w^*]$, $i = 1, 2, \ldots, n$ ein Maß der sterischen Dissimilarität zwischen S (Rezeptorhohlraum) und S_i (Effektor) darstellt.

Zum Beispiel, für die Verbindungen :

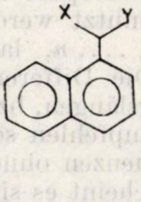

$S_1 (\equiv S)$

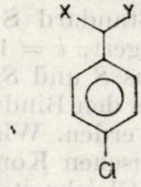

S_2

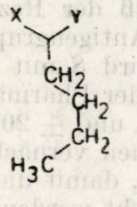

S_3

hat SD* folgende Werte :

$$SD^*(S, S_1) = [10 ; 0], \ SD^* \ (S, S_2) = [6 ; 1{,}2], \ SD^* \ (S, S_3) = [4 ; 0]$$

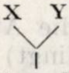

bedeutet das Pharmakon, dessen Atome nicht in Betracht gezogen wurden. Für die Verbindung S_3 wurde die Konformation, die SD_w minimalisiert, angenommen, eine Tatsache die sich vom physikalischen Standpunkt aus leicht rechtfertigen läßt.

3. ANWENDUNGEN : HAPTEN-ANTIKÖRPER-INTERAKTIONEN

Im folgenden wird die SD*-Methode für die Haoten-Antikörper-Interaktionen angewendet. Die berechneten Gleichungen werden vom statistischen Standpunkt durch den Korrelationskoeffizienten (r), die Standardabweichung (s), die Fischer-Statistik (F) charakterisiert, während die Existenz der Multikoliniarität durch die Berechnung des Interkorrelationskoeffizienten, $r(SD_c^*, SD_w^*)$ testiert wird; wenn $r^2(SD_c^*, SD_w^*) < < 0{,}40$, wird angenommen, daß die Multikoliniarität nicht besteht.[11] Die verwendeten experimentellen Befunde, K_{rel} (die relative Gleichgewichtskonstante) sind aus Lit.[6] zu entnehmen.

3. 1. Das Benzoation/anti-p-(p′-azophenylazo)-Benzoat-System

Die Interaktion der Haptene **1** mit dem vom Immunogen erzeugten Antikörper der antigenischen Struktur **2**, wird durch die K_{rel}-Werte aus Tabelle 1, charakterisiert.

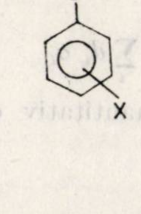

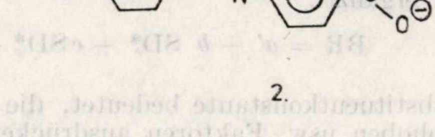

2.

TABELLE 1[a]

Hapten **1**/ Antikörper *anti*-**2** Interaktion

X	K_{rel}	SD_c^*	SD_w^*
m-Cl	0,43	9	1
p-Cl	5,30	10	0
m-NO_2	0,12	9	3
p-NO_2	1,80	11	1
3—NO_2, 4—Cl	0,41	10	3
3—NO_2, 5—Cl	0,07	9	4
3,5-di-NO_2	0,024	9	6

E_S(Cl : $-0{,}97$; NO_2 : $-2{,}52$; H : 0,00),
ν(Cl : 0,55 ; NO_2 : 1,39 ; H : 0,00)

[a] die K_{rel}-Werte wurden aus [6], S. 60 entnommen.

Mit Hilfe der sterischen SD*-Parameter (berechnet für **2** als Standard) (Tabelle 1) wurden folgende Gleichungen berechnet:

$$\log K_{\text{rel}} = -7{,}789 + 0{,}762\ \text{SD}_c^* \tag{4}$$

$$(r = 0{,}738\ ;\ s = 0{,}548\ ;\ F = 2{,}392)$$

$$\log K_{\text{rel}} = 0{,}449 - 0{,}368\ \text{SD}_w^* \tag{5}$$

$$(r = 0{,}937\ ;\ s = 0{,}284\ ;\ F = 14{,}310)$$

$$\log K_{\text{rel}} = -2{,}962 + 0{,}338\ \text{SD}_c^* - 0{,}298\ \text{SD}_w^* \tag{6}$$

$$(r = 0{,}976\ ;\ s = 0{,}176\ ;\ F = 20{,}130)$$

$$r(\text{SD}_c^*,\ \text{SD}_w^*) = -0{,}54)$$

Die Gleichungen (4)—(6) beschreiben einen starren Rezeptorhohlraum, dessen Struktur der Struktur **2** komplementär ist. Jedes Nichtwasserstoffatom aus der *orto-* oder *meta*-Stellung des Haptens **1** verkleinert den log K_{rel} mit ungefähr 0,30 logarithmischen Einheiten, während jedes auf **2** überlagerende Nichtwasserstoffatom log K_{rel} mit ungefähr 0,34 logarithmischen Einheiten vergrößert. Diese Ergebnisse sind in übereinstimmung mit den neusten Ergebnissen, die auf Grund der NMR-Spektroskopie [12] erhalten wurden.

Um die SD*-Methode mit den üblichen Methoden zu vergleichen, wurde die Gleichung (6) unter Verwendung der E_S-Taft Parameter [13] und ν-Charton [14] neu berechnet. Die erhaltenen Ergebnisse sind folgende:

$$\log K_{\text{rel}} = 0{,}202 + 0{,}372\ E_S^m - 0{,}109\ E_S^p \tag{7}$$

$$(r = 0{,}953\ ;\ s = 0{,}246\ ;\ F = 9{,}869\ ;$$

$$r(E_S^m, E_S^p) = -0{,}64)$$

$$\log K_{\text{rel}} = 0{,}203 - 0{,}674\, \nu^m + 0{,}217\, \nu^p \qquad (8)$$

$$(r = 0{,}954\,;\; s = 0{,}243\,;\; F = 10{,}154\,;$$

$$r(\nu^m, \nu^p) = -0{,}57)$$

Vergleicht man die Gleichung (6)—(8) stellt man fest, daß sie prinzipiell in Übereinstimmung sind, aber auf Grund der Fischer-Statistik geht hervor, daß die Gleichung (6) den Gleichungen (7) und (8) überlegen ist.

3.2. Das Carboxylation/anti-*p*-Azobenzoat — System

Die Werte der SD*-Parameter für die Carboxylationen (Tabelle 2) wurden unter Annahme von **3** als Standard berechnet.

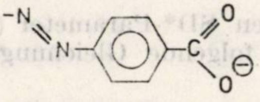

3.

TABELLE 2

Carboxylation/Antikörper *anti*-**3** Interaktion

Hapten	K_{rel}	SD_c^*	SD_w^*
Benzoat	1,00	9	0
Phenylacetat	0,002	6	4
Phenylpropionat	0,005	9	2
Cyclohexancarboxylat	0,002	7	2
Acetat	0,0001	4	0
Propionat	0,0001	5	0

[a] Die K_{rel}-Werte wurden aus [6], S. 51 entnommen.

Es wurden die Gleichungen berechnet:

$$\log K_{\text{rel}} = -6{,}636 + 0{,}603\; SD_c^* \qquad (9)$$

$$(r = 0{,}848\,;\; s = 0{,}778\,;\; F = 3{,}839)$$

$$\log K_{\text{rel}} = -\,6{,}580 + 0{,}617\; SD_c^* - 0{,}113\; SD_w^* \qquad (10)$$

$$(r = 0{,}857\,;\; s = 0{,}757\,;\; F = 1{,}844)$$

Da die Fischer-Statistik der Gleichung (10) ($F = 1{,}844$) einen kleineren Wert hat als die F-Statistik der Gleichung (9) ($F = 3{,}839$, Semnifikationsbereich $> 0{,}95$), kann man den Schluß ziehen, daß die Hapten/Antikörper-Interaktion nicht von der Interaktion mit den Wänden des Rezeptorhohlraums bedingt ist. Diese Schlußfolgerung hat einen Sinn, wenn man die konformationelle Flexibilität der angenommenen Hapten-Strukturen in Betracht zieht, sowie auch die Tatsache, daß diese Strukturen im allgemeinen ein kleineres Van der Waals Volumen besitzen als die Struktur **3**.

3.3. Das Arsonation/anti-*p*-(*p′*-Azophenylazo)benzenarsonat System

Die Werte der SD*-Parameter für die Arsonationen (Tabelle 3) wurden unter Annahme von **4** als Standard, berechnet.

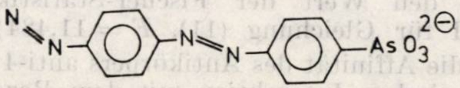

4.

TABELLE 3[a)]

Arsonation/Antikörper anti-**4** Interaktion

Hapten	K_{rel}	SD_c^*	SD_w^*	σ	I
Benzolarsonat	1,0	10	0	0,00	0
m-Nitrobenzolarsonat	3,6	10	3	0,71	0
m-Methylbenzolarsonat	1,1	10	1	−0,07	0
p-(p′-Hydroxiphenylazo)-benzolarsonat	30,0	19	0	0,25	1
p-(p′-Aminophenylazo)-benzolarsonat	26,0	19	0	0,15	1
p-Iodbenzolarsonat	6,8	11,7	0	0,18	0
p-Benzoylaminobenzolarsonat	4,8	18	1	0,00	0
p-Nitrobenzolarsonat	4,4	12	1	0,78	0
p-Acetaminobenzolarsonat	3,3	13	1	0,00	0
p-Brombenzolarsonat	3,1	11,3	0	0,23	0
p-Chlorbenzolarsonat	2,9	11,2	0	0,23	0
p-Methylbenzolarsonat	2,7	11	0	−0,17	0
p-Hydroxybenzolarsonat	1,2	11	0	−0,37	0
p-Aminobenzolarsonat	1,0	11	0	−0,66	0
p-Carboxybenzolarsonat	0,9	12	1	0,00	0

[a)] Die K_{rel}-Werte wurden aus [6], *S.* 90–91 entnommen.

Die Parameter σ und I aus Tabelle 3 bedeuten die Hammett-Konstante (σ) und die folgenderweise definierte Indikator-Veränderliche: $I = 1$, wenn das Hapten eine $-N{=}N-$ Funktion besitzt und $I = 0$, im entgegengesetzten Fall. Es wurde folgende Gleichung berechnet:

$$\log K_{rel} = 0{,}423 + 0{,}069\ SD_c^* - 0{,}095\ SD_w^* + 0{,}446\ I + 0{,}603\sigma \quad (11)$$

$$(r = 0{,}930\,;\ s = 0{,}174\,;\ F = 11{,}484\,;\ r(SD_c^*) = 0{,}798\,;$$

$$r(I) = 0{,}805\,;\ r(\sigma) = 0{,}459\,;\ r(SD_w^*) = 0{,}100).$$

Die Bedeutung der durch die unabhängigen veränderlichen der Gleichung (11) modellierten Faktoren nimmt mit der Verkleinerung des Wertes der partiellen Korrelierungskoeffizienten ab. Besonders wichtig für den Feststellungsprozeß der Hapten-Antikörper sind SD_c^* und *I*. Diese zwei Faktoren erklären die Varianz der experimentellen Daten in über 67 %:

$$\log K_{\mathrm{rel}} = -\,0{,}382 + 0{,}063\ SD_c^* + 9{,}176 + 0{,}622\ I \qquad (12)$$

$$(r = 0{,}845\,;\ s = 0{,}253\,;\ F = 0{,}176).$$

Die Ergänzung der Gleichung (12) mit den Veränderlichen SD_w^* und σ wird durch den Wert der Fischer-Statistik ($F = 9{,}176$ für Gleichung (12) und für Gleichung (11), $F = 11{,}484$) gerechtfertigt.

Es folgt, daß die Affinität des Antikörpers anti-4 für die Arsonationen von der London'schen Interaktion mit dem Rezeptorhohlraum bedingt wird. Die semnifikative Abhängigkeit des K_{rel}-Wertes von der Veränderlichen I unterstreicht die auch von Pressmann und Grossberg[6] festgestellte Tatsache, daß der Antikörper die Anwesenheit der Azo-Funktion anerkennt, daß aber die Charakteristika die diese Funktion individualisieren, nicht ohne eine detaillierte quanten-chemische Berechnung festgestellt werden können.

Das SD*-Glied fällt nicht schwer ins Gewicht, da die studierten Haptene nicht stark von der Struktur 4 abweichen. Diese Glied kann als eine Korrektur füür das SD_w^*-Glied angesehen werden.

Das σ-Glied zeigt an, daß Haptene mit elektronenanziehenden Substituenten Aktiver sind als jene mit elektronenspendenden Substituenten. Daraus geht die Bedeutung der elektrostatischen Interaktion zwischen dem Arsonation und dem Rezeptor hervor.

4. SCHLUßFOLGERUNGEN

Die in der dieser Arbeit vorgeschlagene Methode der sterischen Differenzen (SD*) wird für die Festlegung der quantitativen Beziehungen zwischen der chemischen Struktur und der biologischen Aktivität benützt. Unsere Methode hat den wichtigen Vorteil, daß sie sowohl zum Studium strukturell verwandter bioaktiver Verbindungsreihen geeignet ist (in diesem Falle sind die üblichen Methoden, die sterische Taft-Konstanten vom E_S-Typ benützen, nicht anwendbar). Die SD-Methode wurde im Falle der Hapten-Antikörper-Interaktion getestet. Diese Interaktion eignet sich besonders gut zu diesem Zweck, weil in diesem Fall bekannt ist, daß der Rezeptorhohlraum dem Antigenanteil des Immunogens relativ komplementär ist. Die berechneten SD*-Gleichungen besitzen eine zufriedenstellende statistische Semnifikation und beweisen so die Gültigkeit der SD*-Methode.

LITERATURHINWEISE

[1] M. Charton und B. I. Charton, *J. Org. Chem.*, **44**, 2284 (1979).
[2] A. T. Balaban, A. Chiriac, I. Moţoc und Z. Simon, ,,Steric Fit in QSAR", Lecture Notes in Chemistry, vol. 15, Springer, Berlin, 1980.
[3] I. Moţoc, *J. Chim. Phys. Biol.*, (unter Druck).
[4] I. Moţoc, *Arzneim. Forsch.*, **31**, 290 (1981).
[5] V. Austel, E. Kutter und W. Kalfbleisch, *Arzneim. Forsch.*, **29**, 585 (1979).
[6] D. Pressmann und A. L. Grossberg, ,,Structural Basis of Antibody Specificity", Benjamin, New York, 1968.
[7] K. Mislow, ,,Introduction to Stereochemistry", Benjamin, New York, 1966, S. 33–42.
[8] M. Lesk, *Comm. ACM*, **22**, 219 (1979).
[9] P. Gund, ,,Pharmacophoric Pattern Searching in Receptor Mapping", in ,,Annual Reports in Medicinal Chemistry", ed. H. J. Hess, Academic, New York, 1979.
[10] E. J. Barrantes, *Ann. Rev. Biophys. Bioeng.*, **8**, 287 (1979).
[11] J. C. Topliss und R. J. Costello, *J. Med. Chem.*, **15**, 1066 (1972).
[12] R. J. P. Williams, *Angew. Chem. Intern. Ed.*, **16**, 766 (1977).
[13] R. W. Taft, in ,,Steric Effects in Organic Chemistry", ed. M. S. Newman, Wiley, New York, 1956, S. 597.
[14] M. Charton, *J. Amer. Chem. Soc.*, **91**, 615 (1969).

Revue Roumaine de Chimie, 27, 2, 235–242 (1982)

STUDIES ON IRON(III), COBALT(II) AND NICKEL(II) AZIDO COMPLEXES

MAMDOUH S. MASOUD *, T. M. SALEM and M. H. AMER
Chemistry Department, Faculty of Science, Alexandria, Egypt

Received October 5, 1979

Investigation on the interaction of sodium azide with iron(III), cobalt(II) and nickel(II) were followed spectrophotometrically. The species formed and their stabilities were determined to depict the mechanism of complexation and the geometries of the complexes.

A great deal of attention has been paid to the chemistry of organic azides in contrast to the coordinated azides that had received little attention until the early sixties. [1-6] This was undoubtedly due to the explosive nature of metal azides and their extreme sensitivity to shocks.[4] Shock resistance and thermal stability became apparent for azido complexes that contained large counter ions or a central metal whose oxidation state was stabilised by certain ligands. This area of chemistry has gained impetus. We investigated the most suitable reaction conditions and the stabilities of Fe(III), Co(II) and Ni(II) azido complexes.

EXPERIMENTAL

All chemicals were of Analar grade.

I. Preparation of solutions

i. *Stock solution of NaN_3 :* 0.1 N-stock solution was prepared by dissolving 6.5 g of the salt in one litre of doubly distilled water. The solution was analyzed argentometrically using K_2CrO_4 as indicator. More dilute solutions were prepared by dilution of the stock.

ii. *Stock metal solutions :* 0.1 M-stock solutions were prepared by dissolving the required weight of the metal salt in one litre of doubly distilled water. The analyses were done applying the usual analytical methods.

iii. *Buffer solutions :* Experiments were measured in acetate, borate, phthalate and universal buffer solutions. The pH's of the buffer solutions were checked using a radiometer pH meter, type 28 with a sensitivity of ± 0.01 pH unit.

---

* To whom all correspondence should be addressed.

II. Working procedure

The room temperature absorbance measurements were carried out on Unicam Spectrophotometer Model SP 200 covering a range of 325 to 800 nm. Two matched 1 cm cells were used one for the blank and the other for the solution.

RESULTS AND DISCUSSIONS

The interaction between the linear triatomic azide ion having 16 valence electrons as an inorganic ligand and ironIII, cobaltII and nickelII gave different complexes. The stoichiometry was traced by electronic spectral methods and the stability constants were computed. This is used to shed a clear picture upon the reaction mechanisms in these systems. Throughout this paper we shall write ionic aggregates with their net charge, for convenience, and this should not imply a special distribution of charge in the complex ion.

Iron azide reaction

A mixed solution composed of 5×10^{-4}Me–FeIII and 1×10^{-3} M–NaN_3 at different pH values, in the range 1.42 and 3.09, gave different colours. At pH 1.42 the colour of the mixed solution was pale rose and at pH 3.09 the colour became yellow. This was accompanied by a blue shift with increasing the pH. In phthalate buffered media, immediate discharge of colour occurred. In the wavelength range 450 to 550 nm and at the concentration of FeIII and N_3^- employed, neither the ligand nor the metal ion showed an appreciable absorbance. The change in absorbance as the concentration of the reactions and/or pH of the system vary was attributed solely to complex formation. The absorbance (A_s) – pH plot, Fig. 1A, showed that the intensity decreased at pH 2 in a minimum absorbance value, then started to increase again till saturation, pointing again to the existence of different stoichiometric ratios. Solutions in 1M-$HClO_4$ which all contain the most intense Fe^{3+} species have been observed to obey Beer's law while diluted samples by water which contain different species have been found not to obey Beer's law. The fading of the red colour of ferric azide solutions could be related to a kinetic mechanism of different steps. However, this point needs further work.

By successive changes of either $[N_3^-]$ or [Fe (III)] and measuring the absorbance of the resulting solution, the stability constant of the formed complexes could be calculated. Assume this reaction to proceed in the following:

$$m\mathrm{Fe}^{3+} + n\mathrm{N}_3^- \rightleftharpoons \mathrm{Fe}_m(\mathrm{N}_3)_n$$

If the values of m and n are known, the charges on the complex could be determined. However, these parameters could be omitted for clarity. The concentrations of both Fe^{3+} and N_3^- were calculated as follows:

$$C_{\mathrm{Fe}^{3+}} = [\mathrm{Fe}^{3+}] + [\mathrm{FeN}_3^{2+}] \quad (1)$$

$$C_{\mathrm{N}_3^-} = [\mathrm{HN}_3] + [\mathrm{N}_3^-] + [\mathrm{FeN}_3^{2+}] \quad (2)$$

This was based on the fact that the predominating complex was of the stoichiometry 1 : 1. If β is the stability constant of the FeN_3^{2+} species and K_a is the dissociation constant of the hydrazoic acid (1.95×10^{-5}), then:

$$HN_3 \rightarrow H^+ + N_3^- ; \quad K_a = [H^+][N_3^-]/[HN_3] \tag{3}$$

$$Fe^{3+} + N_3^- \rightarrow FeN_3^{2+} ; \quad \beta = [FeN_3^{2+}]/[Fe^{3+}][N_3^-] \tag{4}$$

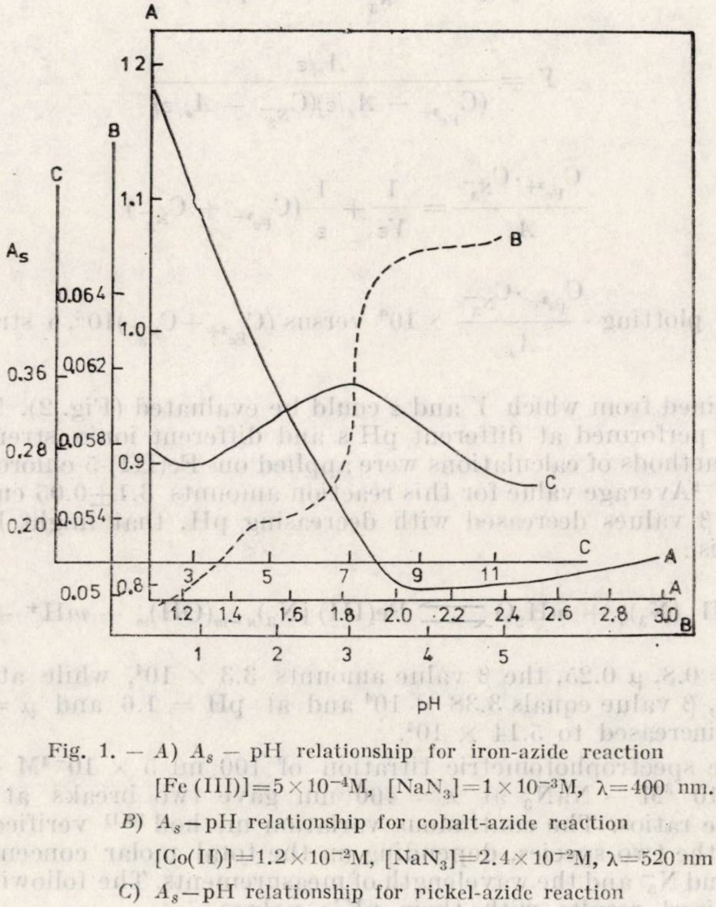

Fig. 1. — *A*) A_s — pH relationship for iron-azide reaction
$[Fe(III)] = 5 \times 10^{-4}M$, $[NaN_3] = 1 \times 10^{-3}M$, $\lambda = 400$ nm.
B) A_s — pH relationship for cobalt-azide reaction
$[Co(II)] = 1.2 \times 10^{-2}M$, $[NaN_3] = 2.4 \times 10^{-2}M$, $\lambda = 520$ nm
C) A_s — pH relationship for nickel-azide reaction
$[Ni(II)] = 4 \times 10^{-2}M$, $[NaN_3] = 0.2$ M, $\lambda = 560$ nm.

One can reach the conclusion that:

$$\frac{\beta}{1 + [H^+]/K_a} = [FeN_3^{2+}]/[Fe^{3+}]\,[HN_3] + [N_3^-] \tag{5}$$

If the reaction is measured at constant pH, the left hand side of the latter equation is constant (Y). If Beer's law is obeyed, then :

$$[\mathrm{Complex}] = \frac{A_s}{\varepsilon} \tag{6}$$

$$[\mathrm{Fe}^{3+}] = \mathrm{C}_{\mathrm{Fe}^{3+}} - [\mathrm{complex}] \tag{7}$$

$$[\mathrm{N}_3^-] = \mathrm{C}_{\mathrm{N}_3^-} - [\mathrm{complex}] \tag{8}$$

and

$$Y = \frac{A_s/\varepsilon}{(\mathrm{C}_{\mathrm{Fe}^{3+}} - A_s/\varepsilon)(\mathrm{C}_{\mathrm{N}_3^-} - A_s/\varepsilon)} \tag{9}$$

So,

$$\frac{\mathrm{C}_{\mathrm{Fe}^{3+}} \cdot \mathrm{C}_{\mathrm{N}_3^-}}{A_s} = \frac{1}{Y\varepsilon} + \frac{1}{\varepsilon}(\mathrm{C}_{\mathrm{Fe}^{3+}} + \mathrm{C}_{\mathrm{N}_3^-}) \tag{10}$$

On plotting $\dfrac{\mathrm{C}_{\mathrm{Fe}^{3+}} \cdot \mathrm{C}_{\mathrm{N}_3^-}}{A_s} \times 10^6$ versus $(\mathrm{C}_{\mathrm{Fe}^{3+}} + \mathrm{C}_{\mathrm{N}_3^-})10^3$, a straight line was obtained from which Y and ε could be evaluated (Fig. 2). This reaction was performed at different pH's and different ionic strengths (μ). Similar methods of calculations were applied on Fe(III)-5-chlorosalicylate system. [7-9]Average value for this reaction amounts 3.1 ± 0.05 cm^{-1}mole^{-1} l^{-1}. The β values decreased with decreasing pH, that might be due to hydrolysis :

$$\mathrm{Fe(III)}\,(\mathrm{N}_3)_n + m\mathrm{H}_2\mathrm{O} \rightleftharpoons \mathrm{Fe(III)}\,(\mathrm{N}_3)_{n-m}(\mathrm{OH})_m + m\mathrm{H}^+ + m\mathrm{N}_3^-$$

At pH $= 0.8$, μ 0.25, the β value amounts 3.3×10^4, while at pH $= 1$, $\mu = 0.15$, β value equals 3.38×10^4 and at pH $= 1.6$ and $\mu = 0.5$, the β value increased to 5.14×10^4.

The spectrophotometric titration of 100 ml 5×10^{-4}M – Fe (III) against 10^{-3}M – NaN$_3$ at $\lambda = 460$ nm gave two breaks at 1 : 1 and 1 : 2 mole ratios. The continuous variation method [10,11] verified the existence of the two species, depending on the total molar concentration of Fe(III) and N$_3^-$ and the wavelength of measurements. The following depicts the obtained results with their pK's values.

Total molar concentration of Fe(III) and N_3^-	λ_{nm}	Stoichiometry	pK
2×10^{-3}M	460, 550	1 : 1	4.57 ± 0.12
0.8	675, 700	1 : 2	4.12 ± 0.02

Iron(III) formed a large number of complexes, mostly octahedral ones, and the octahedron might be considered its characteristic coordination polyhedron. A few tetrahedral complexes were formed of which $FeCl_4^-$ was the most important, and its salt with large cations might be isolated. The complexes with SCN^- similar to N_3^- are intense red that might be extracted into ether.[12] The intense red iron azido complexes of $p\pi-d\pi$ interaction were discharged in the presence of fluoride ions leading to the preferential formation of the fluoride complexes. The octahedral geometry for the azido complexes was preferred to take place using water molecules to complete the coordination sites. In our lab,[13] monooctyl-α-anilinobenzyl phosphonate was found to be a very good extractant for the iron azido complexes through adduct formation.

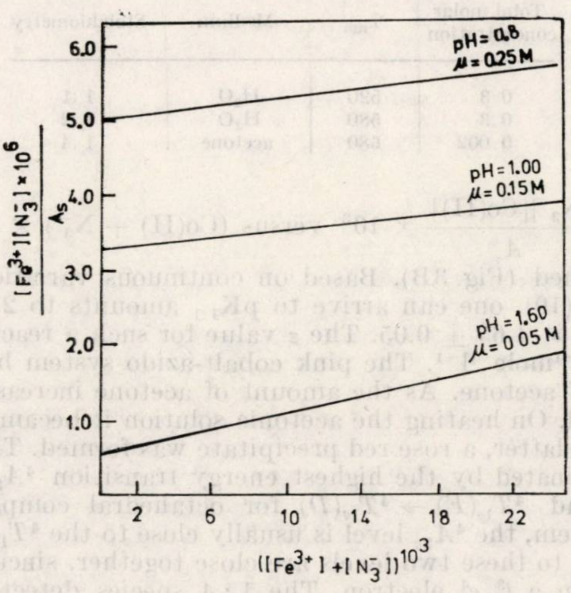

Fig. 2. — Effect of pH and ionic strength on the stability constant of iron azide reaction, λ = 460 nm.

Cobalt azide reaction

The intensity of the spectral bands for the pink cobalt azido system obtained by mixing $1.2 \times 10^{-2}M-Co(II)$ and $2.4 \times 10^{-2}M-NaN_3$ in the wavelength range 460 to 580 nm (Fig. 1B) with λ_{max} at 520 nm was found to be pH dependent, and not affected by light or time. The colour was slightly discharged in buffered media, that might be due to some sorts of interaction of the buffer constituents with the formed complexes. The continuous variation method[10,11] traced different complexes, depending on the total molar concentration, wavelength of measurements and the medium used for the studies as follows:

Total molar concentration	λ_{nm}	Medium	Stoichiometry
0.3	520	H_2O	1 :1
0.3	580	H_2O	1 :2
0.002	680	acetone	1 :4

On plotting $\frac{[N_3^-][Co(II)]}{A_s} \times 10^3$ versus $(Co(II) + N_3^-) \times 10^3$, a straight line was obtained (Fig. 3B). Based on continuous variation method[10,11] and equation (10), one can arrive to $pK_{1:1}$ amounts to 2.67 ± 0.05 and that for $pK_{1:2}$ is 1.65 ± 0.05. The ε value for such a reaction was found to be 12.5 $cm^{-1}mole^{-1}l^{-1}$. The pink cobalt-azido system became blue on the addition of acetone. As the amount of acetone increased, slight turbidity occurred. On heating the acetonic solution it became more turbid. On cooling the latter, a rose red precipitate was formed. The visible spectrum was dominated by the highest energy transition $^4A_2 \rightarrow {}^4T_1\,(P)$ for tetrahedral and $^4T_{1g}(F) \rightarrow {}^4T_{1g}(D)$ for octahedral complexes. In the octahedral system, the $^4A_{2g}$ level is usually close to the $^4T_{1g}(P)$ level and the transitions to these two levels are close together, since the $^4A_{2g}$ state is derived from a $t_{2g}^3\,e_g^4$ electron. The 1 : 4 species detected in acetonic media is of tetrahedral geometry (Fig. 4). It was r eported that the coordination of the azide in the corresponding azido pentamine cobalt(III) complex was found to be linear and asymmetric with a relatively large

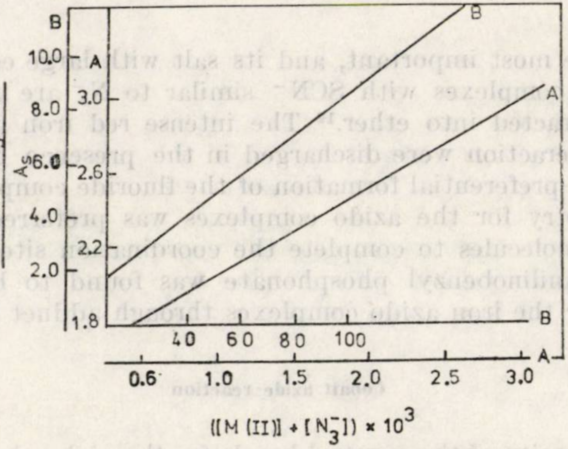

Fig. 3. — Evaluation of ε and pK values of:
A) Nickel-azide system, $\lambda = 490$ nm
B) Cobalt-azide system, $\lambda = 540$ nm.

Co-N_3 angle.[14] In the formed binuclear complexes, it was assumed that the azide group might function as a bridging group[15-17] with two possible structures. The four-membered ring structure with an increase in the non-bonded repulsion owing to the coordination sphere was unfavourable. The intermediate polarizability of the azide ligand[18-20] gave a most convenient skeleton in an eight-membered ring structure.

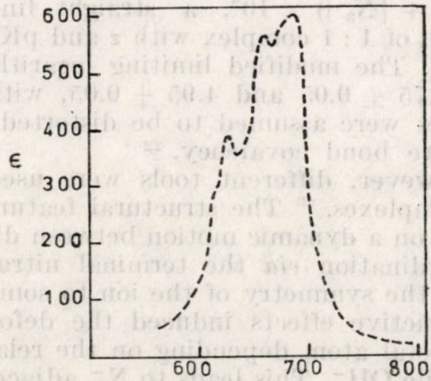

Fig. 4. — Absorption spectra of cobalt-azide system in acetone.

Nickel azide reaction

Spectra of the metal azido system were not substantially different from those of the metal salts under the same conditions. Addition of high concentration of azido to a relatively low concentration of Ni(II) showed an increase in band intensity verifying the presence of complex compounds. The A_s-pH relationship for the nickel-azido system verified that most media for complexation lay in the neutral range (Fig. 1 C). The solutions became turbid above pH 9, which might be due to the formation of a basic colloidal compound, resulting from hydrolysis.

The spectrophotometric titration of 4×10^{-2}M–Ni(II) against NaN_3 at $\lambda = 490$ nm showed a maximum in the curve at 1.25 mole ratio for the azide to Ni(II), verifying the existence of 1 : 1 complex species. For 0.1 M–Ni(II), precipitation of colloidal particles occurred before the formation of 1 : 1 species. Therefore, more dilute solutions less than 0.1 M–Ni(II) were used during the course of this investigation. The continuous variation method[10] for this system verified that the tracing of a complex compound was both concentration and wavelength dependant, as follows :

Total molar concentration of Ni(II) and N_3^-	λ_{nm}	Stoichiometry
0.04 M	490	1 : 2, 2 : 1
	520	1 : 1, 1 : 2, 2 : 1
	540	1 : 2, 3 : 2
0.4 M	490	1 : 1, 2 : 1
	520	1 : 1, 1 : 2

The polymeric nature for these complexes was assumed to explain why Beer's law was not applied. On plotting $\frac{[\mathrm{Ni(II)}][\mathrm{N}_3^-]}{A_s} \times 10^4$ *versus* $([\mathrm{Ni(II)}] + [\mathrm{N}_3^-]) \times 10^2$, a straight line was obtained, depicting the formation of 1 : 1 complex with ε and pK values of 214.44 and 2.61 respectively. The modified limiting logarithmic method [24] gave two pK's values 2.75 ± 0.05 and 4.95 ± 0.05, with possible association.[21] These complexes were assumed to be distorted from simple cubic symmetry with more bond covalency. [22]

However, different tools were used for tracing transition metal azido complexes. [23] The structural feature for the formed species could be based on a dynamic motion between different resonating structures. [22] The coordination *via* the terminal nitrogen atom of the azide ligand destroys the symmetry of the ion to some extent. The orienting ligands with inductive effects induced the deformation of the electron shells of the metal atom depending on the relative position of the N_3^- to the nucleophile OH^-. This leads to N_3^- adjacent to the metal repels OH^- i.e. the azido complexes are of instantaneous formation[23] and the most suitable media for complexation lie in neutral or acidic solutions.

REFERENCES

[1] B. L. Evans, A. D. Yoffe and P. Gray, *Chem. Rev.*, **39**, 515 (1959).

[2] P. Gray, *Quart. Rev.*, **17**, 441 (1963).

[3] J. L. Leed, F. Wang and F. Bascal, *J. Amer. Chem. Soc.*, **94**, 7173 (1972).

[4] R. Ziolo, J. Thick and Z. Dori, *Inorg. Chem.*, **11**, 626 (1972).

[5] R. Bereman, *Inorg. Chem.*, **11**, 1149 (1972).

[6] Z. Dori and R. Ziolo, *Chem. Rev.*, **73**, 191 (1973).

[7] S. Moulik and K. Gupto, *J. Indian Chem. Soc.*, **49**, 447 (1972).

[8] M. Chattopadhyaya and R. Singh, *Analyt. Chim. Acta*, **70**, 49 (1974) ; *Indian J. Chem.*, **14A**, 118 (1976).

[9] M. Chattopadhyaya, *J. Inorg. Nuclear Chem.*, **38**, 569 (1976).

[10] H. El-Shamy and F. G. Sherif, *Egypt. J. Chem*, **2**, 217 (1959).

[11] T. Musgrare and R. Keller, *Inorg. Chem.*, **4**, 12 (1965).

[12] A. G. Maddock and L. O. Medeiros, *J. Chem. Soc. A*, **1969**, 1946.

[13] M. S. Masoud and B. R. Elhaj, *Indian J. Chem.*, **20A**, 101 (1981).

[14] G. H. Palenik, *Acta Cryst.*, **17**, 360 (1964).

[15] H. P. Fritzer and K. Torkar, *Monatsh.*, **99**, 2333 (1968).

[16] I. E. Maxwell, *Inorg. Chem.*, **10**, 1782 (1971).

[17] W. P. Fehlhammer and L. D. Dable, *J. Amer. Chem. Soc.*, **94**, 3377 (1972).

[18] A. P. Lever, "Inorganic Electronic Spectroscopy", Elsevier, Amsterdam, 1968.

[19] H. P. Fritzer and W. Dobramsyl, "Proceeding Collection International Spectroscopy XVII", Firenze, 1973.

[20] H. P. Fritzer, D. T. Clark and I. S. Wodsey, *Inorg. Nuclear Chem. Lett.*, **10**, 247 (1974).

[21] R. C. Das, M. K. Mistra and B. K. Nanda, *Indian J. Chem.*, **14A**, 624 (1976).

[22] R. Abou-Eittah and S. El-Mekabary, *J. Inorg. Nuclear Chem.*, **35**, 291 (1973).

[23] L. Lightig and G. de Oliveira Neto, E. A. Neves and E. Oliveria, "XVIII International Conference on Coordination Chemistry", Sao Paulo, Brazil, July 1977.

[24] M. S. Masoud, T. M. Salem and M. M. Elessawi, *J. Chem. Eng. Data.*, **23**, 12 (1978).

Revue Roumaine de Chimie, 27, 2, 243–255 (1982)

STATIONARITY IN QUANTUM THEORY OF MOLECULES. I

GENERAL FORMALISM

AL. IVANOV and D. I. HERŢIA
Center of Physical Chemistry, ICECHIM, Spl. Independenţei 202, Bucharest, Romania

Received August 14, 1980

The quantum dynamics of the systems described by mixed states with special emphasis on the stationarity time is given. The possible relations of this theory with quantum chemistry are stressed.

1. INTRODUCTION

The main problem of the quantum theory of isolated molecules is to find good approximations for the eigenfunctions of molecular Hamiltonians. In other words, we try to solve approximately the so-called stationary Schrödinger equation. Almost all mathematical methods of quantum chemistry use the extremal properties of the energetic functional $\varphi \rightarrow (H\varphi, \varphi)/(\varphi, \varphi)$ (here φ is a square integrable function, H is the Hamiltonian of the molecule and (,) denotes the scalar product of the wave functions). Looking for the minimum of the energetic functional, more or less good approximations ξ for the exact fundamental state ψ are found, i.e. one gets such functions ξ that the distance $\| \psi - \xi \| (\| \varphi \| = (\varphi, \varphi)^{1/2})$ is sufficiently small. What means "sufficiently small" depends on the physical quantities which are calculated using the function ξ. The problem of the "stationarity" of these approximate solutions is not discussed — presumably because it is considered irrelevant for the quantum chemistry of isolated molecules. We think this fact is not allways true. In order to explain our doubts let us examine carefully the metric (distance) $d(\varphi, \psi) = \| \varphi - \psi \|$ (φ and ψ are elements of the Hilbert space of the wave functions). This is indeed a metric, since $\| \varphi - \psi \| = 0$ implies the coincidence almost everywhere of the functions φ and ψ (let us remind that two square integrable functions which coincide almost everywhere represent the same element of the L^2-space). Suppose now that $\| \varphi - \psi \| < \varepsilon$, where $\varepsilon > 0$ is fixed. If ε is sufficiently small, the values of the energetic functional for φ and ψ may be very close. On the other hand, this fact does not mean that the differences between the values of the functions φ and ψ are small for all elements of the configuration space. Translating this affirmation into the familiar language of quantum chemistry, we can say that there are domains of the configuration space where the electronic charge densities calculated with the functions φ and ψ are quite different. For instance, it would be easy to construct one-dimensional examples of normalized φ and ψ functions whose values on some intervals are significantly different and for which the $\|\varphi - \psi\|$ distance is arbitrarily small. Consequently, the quantities which depend directly on the electronic charge density may be affected by this phenomenon. We must note that in quantum chemistry the distance $d(\varphi, \xi)$ between the exact fundamental wave function φ and a function ξ can not be evaluated because the function φ is unknown. An approximation is usually verified by comparing the calculated energies of the electronic transitions with the experimental data. In this situation, it is clear that the local charge densities remain quite uncontrollable quantities. All methods of quantum chemistry offer nevertheless, the possibility to define charge densities on the atoms of a molecule and other quantities which correspond to the real charge densities in different regions of the molecule, and to calculate some physical quantities using them. Having in view the above mentioned property of the distance d, the success or failure of such calculations is rather a question of hazard. The question arising now is : is there a possibility to decide whether an approximation of a true stationary wave function describes correctly the local charge density? In our opinion, the answer is strongly correlated with the "degree of stationarity" of the wave functions. In order to explain this statement, let us observe first that no approximation of a given stationary wave function, obtained by standard methods, is stationary. Suppose we know what it means that a wave function is more stationary than another function. In this situation it is normal to assume that the greater the "stationarity" of a given approximate function ξ, the better the description of the real charge density by the function ξ. If we want to transform this assumption into a working hypothesis, we have to define precisely the notion of stationarity. More precisely, we must find a measure of stationarity. Such a measure was proposed by Eberly and Singh in a short paper.[1] We think that this measure is good for our purposes and we will use it. In fact, in this paper we intend to begin a mathematically rigorous analysis of the stationarity problem and of its implications in quantum chemistry. We want to give in a coherent form a series of exact results which may constitute a rigorous basis for calculations in various situations interesting for quantum chemistry.

This first paper exposes a more or less complete theory of stationarity for the mixed states of general quantum systems. The central part of the theory is the analysis of the stationarity time which was defined by Eberly and Singh in their aforementioned paper. These authors included in their work only a formal proof of the relation between the stationarity time and the mean square dispersion of the Hamiltonian. Our paper contains proofs for some basic properties of the stationarity time, mean square dispersion, etc. We include also a "preparatory" part (the second paragraph), where some old and new problems concerning the stationarity mixed states are listed (the mathematical apparatus used in the paper is fully contained in the general book of Prugovečki [2]). We decided to write an extended theory of the stationarity because we are convinced that it presents a great interest for quantum chemistry. For instance, we work with mixed states because the most general states of the subsystems of a given system are mixed — even if the system is in a pure state.

2. GENERAL DYNAMICS OF THE CONSERVATIVE QUANTUM SYSTEMS

We will discuss from the dynamical point of a view a system described by a Hilbert space $\mathscr{H}$, a Hamiltonian H and a mixed state ρ. We give first some usual notations.

The scalar product and the norm of the space $\mathscr{H}$ will be denoted by "$(\cdot, \cdot)$" and "$\|\cdot\|$", respectively. If $A : \mathscr{H} \to \mathscr{H}$ is a linear operator, $\mathscr{D}(A)$ and $\mathscr{R}(A)$ denote, respectively, the domain and the range of A. A and B being two linear operators (bounded or not), we can set up a new operator $[A, B] = AB - BA$, called the comutant of A and B. The operator $[A, B]$ is not always defined in the whole space $\mathscr{H}$. Each linear selfadjoint operator A defines a family of projectors in $\mathscr{H}$, $\{E_\lambda\}_{\lambda\in\mathbb{R}}$ ($\mathbb{R}$ is the set of real numbers, $\mathbb{N}$ is the set of natural numbers), called the spectral family of A, which is characterized by the following properties:

E i) $E_\lambda E_\mu = E_{\min(\lambda,\mu)}$

E ii) $\displaystyle s\text{-}\lim_{\lambda\to\infty} E_\lambda\varphi = \varphi$

$$s\text{-}\lim_{\lambda\to-\infty} E_\mu\varphi = 0 \qquad \forall\varphi\in\mathscr{H}$$

E iii) $\displaystyle s\text{-}\lim_{\mu\downarrow\lambda} E_\mu\varphi = E_\lambda\varphi$

E iv) $\displaystyle (\varphi, A\varphi) = \int_{-\infty}^{\infty} \lambda \mathrm{d}\,(\varphi, E_\lambda\varphi), \quad \varphi\in\mathscr{D}(A)$

The notation $s\text{-}\lim\limits_{n\to\infty} \varphi_n = \varphi$ means $\lim\limits_{n\to\infty} \|\varphi_n - \varphi\| = 0$. The integral from E iv) is a Stieltjes integral with respect to the real function $\lambda \mapsto (\varphi, E_\lambda\varphi)$ and we will use the shortened notation

$$A = \int_{-\infty}^{\infty} \lambda\, \mathrm{d}E_\lambda$$

We say that the function $t \mapsto \varphi(t) \in \mathscr{H}$ is differentiable at t_0 if the limit

$$s\text{-}\lim_{t\to t_0} \frac{\varphi(t) - \varphi(t_0)}{t - t_0}$$

exists. The limit is called the derivative of the function $\varphi(t)$ at the point t_0.

We can begin now the study of a system described by the Hamiltonian H. It is well known that H defines a family of unitary operators $\{U_t\,; t \in \mathbb{R}\}$, called the one-parametric evolution of the system. More precisely,

$$U_t \overset{\text{def}}{=} \int_{-\infty}^{\infty} \exp(i\lambda t)\, \mathrm{d}E_\lambda \equiv \exp(iHt)$$

(here $\{E_\lambda\}$ is the spectral family of H).

The one-parametric evolution of a system has the properties:

U i) $U_0 = 1$ (1 is the identity of $\mathscr{H}$)

U ii) $U_{t_1+t_2} = U_{t_1} U_{t_2} = U_{t_2} U_{t_1}$

U iii) $t \mapsto U_t\varphi$ is differentiable at $t = 0$ if and only if $\varphi \in \mathscr{D}(H)$; in this situation

$$\mathrm{i}H\varphi = s\text{-}\lim_{t\to 0} \frac{1}{t}(U_t\varphi - \varphi).$$

For any mixed state ρ (which is a positive trace-class operator such that $\mathrm{Tr}\,\rho = 1$), can define an operator-valued function $t \mapsto \rho(t) = U_t \rho U_{-t}$. If ρ is considered as the state at the moment $t = 0$, $\rho(t)$ appears as the state at the moment t. To investigate the dynamics of a system means in fact to study the set of all functions $t \mapsto \rho(t)$, when ρ runs the set of all states of the system.

Since U_t is a unitary operator, a function $\rho(t)$ may be defined for any ρ. But we want $\rho(t)$ to have derivatives for any physically interesting vector of $\mathscr{H}$ (i.e. for $\varphi \in \mathscr{D}(H)$). The following definition delimitates the class of the so-called admissible states.

DEFINITION 1. *A state* ρ *is said* U_t*-admissible if the function* $\rho(t)\varphi$ *is differentiable at* $t = 0$ *for every* $\varphi \in \mathscr{D}(H)$.

The first theorem of this work characterizes the admissibility of the mixed states.

THEOREM 1. *A state* ρ *is* U_t*-admissible if and only if* $\rho\mathscr{D}(H) \subseteq \mathscr{D}(H)$. *In these conditions*

$$\left.\frac{\mathrm{d}\rho(t)}{\mathrm{d}t}\varphi\right|_{t=0} = \mathrm{i}[H, \rho]\,\varphi, \quad \forall \varphi \in \mathscr{D}(H).$$

$\left(\text{here } \left.\frac{\mathrm{d}\rho(t)}{\mathrm{d}t}\varphi\right|_{t=0} \text{ denotes the derivative of } \rho(t)\varphi \text{ at } t = 0\right)$.

Proof. Observe first that, if $t \mapsto A(t)$ is an operator-valued function with the property

$$\lim_{t\to 0} \|A(t)\varphi - \psi\| = 0,$$

then

$$\lim_{t\to 0}\| U_t A(t)\,\varphi - \psi\| = 0.$$

Indeed,

$$\| U_t A(t)\varphi - \psi\| = \| A(t)\,\varphi - U_{-t}\psi\| \leqslant \| A(t)\varphi - \psi\| + \| U_{-t}\psi - \psi\|$$

and the result is a straightforward consequence of the fact that

$$\| U_{-t}\psi - \psi\| \xrightarrow{t\to 0} 0.$$

Suppose now that $\rho\mathscr{D}(H) \subseteq \mathscr{D}(H)$. For $\varphi \in \mathscr{D}(H)$ we can write

$$\frac{1}{t}(U_t\rho U_{-t} - \rho) = \frac{1}{t}(U_t\rho U_{-t} - U_t\rho + U_t\rho - \rho) =$$

$$= U_t\rho\left[\frac{1}{t}(U_{-t} - 1)\right] + \frac{1}{t}(U_t - 1)\,\rho$$

Using the above mentioned property of the operator-valued functions and the boundedness of ρ, we obtain:

$$\lim_{t\to 0} U_t\rho\left[\frac{1}{t}(U_{-t} - 1)\right]\varphi = \rho\left[\lim_{t\to 0}\frac{1}{t}(U_{-t} - 1)\,\varphi\right] = -\mathrm{i}\rho H\varphi$$

Since $\rho\varphi \in \mathscr{D}(H)$, we get finally

$$\lim_{t\to 0}\frac{1}{t}(U_t - 1)\,\rho\varphi = \mathrm{i}H\rho\varphi$$

and

$$\lim_{t\to\infty}\frac{1}{t}(U_t\rho U_{-t} - \rho)\varphi = \mathrm{i}\,[H, \rho]\,\varphi$$

Conversely, suppose that $\rho(t)\varphi$ is differentiable at $t = 0$ for $\varphi \in \mathscr{D}(H)$. For $\varphi \in \mathscr{H}$ the equality

$$\frac{1}{t}(\rho\,(t) - \rho)\varphi - U_t\rho\left[\frac{1}{t}(U_{-t} - 1)\,\varphi\right] = \frac{1}{t}(U_t - 1)\,\rho\varphi$$

holds. Since $\rho(t)\varphi$ is differentiable at $t = 0$, the left part of this equality has a limit for $t \to 0$. Therefore, the right hand side has also a limit and from U iii) we get $\rho\varphi \in \mathscr{D}(H)$ ✳

COROLLARY

$$\left.\frac{\mathrm{d}\rho\,(t)}{\mathrm{d}t}\,\varphi\right|_{t=t_0} = U_{t_0}\left(\left.\frac{\mathrm{d}\rho(t)}{\mathrm{d}t}\,U_{-t_0}\varphi\right|_{t=0}\right)$$

for every $\varphi \in \mathscr{D}(H)$.

Proof. It is sufficient to observe that, if $\varphi \in \mathscr{D}(H)$, we have

$$\lim_{t\to 0} \frac{\rho(t_0 + t) - \rho(t_0)}{t} \varphi = U_{t_0} \left[\lim_{t\to 0} \frac{\rho(t) - \rho}{t} U_{-t_0}\varphi \right]$$

and we get the proof using Theorem 1 and the equality $U_t\mathscr{D}(H) = \mathscr{D}(H)\ \forall t \in \mathbb{R}$. ✳

By combining these facts we obtain the well-known Schrödinger equation for mixed states:

$$\frac{\mathrm{d}\rho(t)}{\mathrm{d}t} = \mathrm{i}[H, \rho(t)] \tag{1}$$

Now we can say that equation (1), with the initial condition $\rho(0) = \rho$, has a solution if and only if ρ is admissible; the solution, if it exists, has the form $\rho(t) = U_t \rho U_{-t}$. We known that any mixed state ρ may be written in the form

$$\rho = \sum_{i=1}^{\infty} p_i P_{\varphi_i},$$

where p_i, $1 \leqslant i \leqslant n$, are the eigenvalues of ρ and P_{φ_i} is the projector onto the subspace of $\mathscr{H}$ spanned by the vector φ_i. It is often useful to know whether the admissibility of a mixed state ρ results from the admissibility of all pure states P_{φ_i}. This is not always true. The next proposition gives a sufficient condition for the admissibility of ρ when we know that P_{φ_i}, $1 \leqslant i \leqslant n$, are admissible.

PROPOSITION 1. *If P_{φ_i} is admissible for all i such that $p_i \neq 0$ and the series $\sum_{i=1}^{\infty} p_i \|H\varphi_i\|$ is convergent, then ρ is admissible.*

Proof. In fact, we will prove that $\rho\mathscr{H} \subseteq \mathscr{D}(H)$. Indeed, if $\rho \in \mathscr{H}$, we can write $\varphi = \varphi' + \sum_{i=1}^{\infty} \alpha_i \varphi_i$, where $\rho\varphi' = 0$, and

$$\rho\varphi = \sum_{i=1}^{\infty} \alpha_i p_i \varphi_i = \lim_{n\to\infty} \sum_{i=1}^{n} \alpha_i p_i \varphi_i \equiv \lim_{n\to\infty} \psi_n$$

Obviously $\psi_n \in \mathscr{D}(H)$, $\forall n$. We have

$$(\psi, H\psi_n) = (H\psi, \psi_n) \to (H\psi, \rho\varphi), \forall \psi \in \mathscr{D}(H)$$

and

$$\|H\psi_n\| = \left\| \sum_{i=1}^{n} p_i \alpha_i H \psi_i \right\| \leqslant \|\varphi\| \sum_{i=1}^{n} p_i \|H\varphi_i\| \leqslant \|\varphi\| \sum_{i=1}^{\infty} p_i \|H\varphi_i\|$$

It follows that $H\psi_n$ converges weakly to a vector $\xi \in \mathscr{H}$. Since H is selfadjoint, we find that $\rho\varphi \in \mathscr{D}(H)$ and $\xi = H\rho\varphi$. ✳

The most important class of admissible states is that of the so-called stationary states.

DEFINITION 2. *A state ρ is said stationary if there exists $t_0 \in \mathbb{R}$ such that*

$$\left.\frac{\mathrm{d}\rho(t)}{\mathrm{d}t}\right|_{t=t_0} = 0$$

Since equation (1) may be written in the form

$$\left.\frac{\mathrm{d}\rho(t)}{\mathrm{d}t}\right|_{t=t_0} = \mathrm{i}U_{t_0}[H, \rho]\, U_{-t_0},\ \forall t_0 \in \mathbb{R}$$

we see that the derivative of $\rho(t)$ is zero at any moment t. Hence, it is zero at $t = 0$ and this means that $[H, \rho] = 0$. Conversely, if $[H, \rho] = 0$, ρ is stationary. Therefore we can formulate

PROPOSITION 2. *ρ is stationary if and only if* $[H, \rho] = 0$. It is very important to known which is the general structure of a stationary state. We remind that we say that $[H, \rho] = 0$ (or H and ρ commute) if the following two conditions are satisfied:

C i) $\rho\mathscr{D}(H) \subseteq \mathscr{D}(H)$

C ii) $\rho H\varphi = H\rho\varphi,\ \forall \varphi \in \mathscr{D}(H)$

We need the following result: H and ρ commute if and only if $E_\lambda\rho = \rho E_\lambda$, $\forall\lambda$, where $\{E_\lambda;\ \lambda \in \mathbb{R}\}$ is the spectral family of H (here ρ may be replaced by any bounded selfadjoint operator). The following proposition characterizes completely the stationary states.

PROPOSITION 3. *A state ρ is stationary if and only if it is a convex combination of pure eigenstates of the Hamiltonian H.*

Proof. Suppose that the state ρ is stationary and has the spectral decomposition (i.e. the representation in terms of the projectors P_i, where P_i is the projector onto the subspace spanned by the eigenvectors corresponding to the eigenvalue $p_i \neq 0$)

$$\rho = \sum_{i=1}^{\infty} p_i P_i$$

Then the spectral family of ρ, $\{P_\mu\}$, is defined in an obvious way:

$$P_\mu = \sum_{p_i<\mu} P_i$$

Since ρ and H commute we have

$$\rho E_\lambda = E_\lambda\rho,\ \forall\lambda \in \mathbb{R}$$

Using similar consideration we get

$$P_i E_\lambda = E_\lambda P_i, \quad \forall i, \ \lambda$$

(note that P_i is the difference of two projectors from the spectral family $\{P_\mu\}$). Consequently P_i and H commute. In this situation, the restriction of H to the subspace $P_i\mathscr{H} \equiv \mathscr{H}_i$ is a selfadjoint operator in $\mathscr{H}_i$. Since $\mathscr{H}_i$ is of finite dimension (ρ is a trace-class operator) H has a complete set of eigenvectors in $\mathscr{H}_i$, let us denote them by $\{\varphi_{ij}\,;\ 1 \leqslant j \leqslant \dim \mathscr{H}_i\}$. It is easy to verify that the set of all vectors φ_{ij} is a basis in $\mathscr{R}(\rho)$ when $i \in \mathbb{N}$. It results that we can write

$$\rho = \sum_{i=1}^{\infty} p_i P_{\varphi_i}$$

where φ_i are eigenvectors of H (we consider that $\{\varphi_i\}$ is an orthonormal set). This means that ρ is a convex combination of pure eigenstates of H (generally, by convex combination of states $\{\rho_n\}_{n\in\mathbb{N}}$ we mean any state of the form $\sum\limits_{n=1}^{\infty} \alpha_n \rho_n$, where $\alpha_n \geqslant 0$ and $\sum\limits_{n=1}^{\infty} \alpha_n = 1$). The converse implication is obvious, so that the proposition is completely proved. ✳

3. MEASURE OF STATIONARITY. STATIONARITY TIME

In order to define the stationarity time we need the general definitions of the average value and of the mean square dispersion of an observable, described by a selfadjoint operator, in a state ρ. Note that, if $\{E_\lambda\}_{\lambda\in\mathbb{R}}$ is the spectral family of A, $\lambda \mapsto \operatorname{Tr}(\rho E_\lambda)$ is an increasing real function with the properties $\lim\limits_{\lambda\to-\infty} \operatorname{Tr}(\rho E_\lambda) = 0$ and $\lim\limits_{\lambda\to\infty} \operatorname{Tr}(\rho E_\lambda) = 1$. We can therefore write the Stieltjes integrals

$$\bar{A}_\rho = \int_{-\infty}^{\infty} \lambda \, \mathrm{d}\operatorname{Tr}(\rho E_\lambda)$$

$$\Delta^2 A_\rho = \int_{-\infty}^{\infty} (\lambda - \bar{A}_\rho)^2 \, \mathrm{d}\operatorname{Tr}(\rho E_\lambda)$$

which are the average value and the mean square dispersion of the operator A in the state ρ, respectively.

All the theorems we shall prove below are based on the following lemma:

Lemma. *Let H be a selfadjoint operator bounded from below and ρ a state. Then, if $\overline{H}_\rho < \infty$ and $\varphi_i \in \mathscr{D}(H)$ for all φ_i with the property $\rho\varphi_i = p_i\varphi_i$, $p_i \neq 0$, the equality*

$$\overline{H}_\rho = \sum_{i=1}^{\infty} p_i \int_{-\infty}^{\infty} \lambda \, \mathrm{d}(\varphi_i, E_\lambda \varphi_i) = \sum_{i=1}^{\infty} p_i (\varphi_i, H\varphi_i)$$

holds.

Proof. With no loss in generality, we can consider that H is positive. Then,

$$\overline{H}_\rho = \lim_{\alpha\uparrow\infty}\int_0^\alpha \lambda\,\mathrm{d}\mathrm{Tr}(\rho E_\lambda) = \lim_{\alpha\uparrow\infty}\int_0^\alpha \lambda\,\mathrm{d}\left(\sum_{i=1}^{\infty} p_i(\varphi_i, E_\lambda\varphi_i)\right) =$$

$$= \lim_{\alpha\uparrow\infty}\sum_{i=1}^{\infty} p_i\int_0^\alpha \lambda\,\mathrm{d}(\varphi_i, E_\lambda\varphi_i)$$

Since $\varphi_i\in\mathscr{D}(H)$ the integrals $\int_0^\infty \lambda\,\mathrm{d}(\varphi_i, E_\lambda\varphi_i)$ exist and we write

$$\overline{H}_\rho = \lim_{\alpha\uparrow\infty}\sum_{i=1}^{\infty} p_i(E_\alpha\varphi_i, H\varphi_i)$$

The obvious inequality $\sum_{i=1}^{n} p_i(\varphi_i, H\varphi_i)\leqslant \overline{H}_\rho$ implies the convergence of the series $\sum_{i=1}^{\infty} p_i(\varphi_i, H\varphi_i)$ and the fact that its sum is smaller than $\overline{H}_\rho$. Since

$$\overline{H}_\rho = \lim_{\alpha\uparrow\infty}\left(\lim_{n\to\infty}\sum_{i=1}^{n} p_i(E_\alpha\varphi_i, H\varphi_i)\right)$$

the theorem would be proved if we can show that the two limits in the last equality may be inverted. But the series $\sum_{i=1}^{\infty} p_i(E_\alpha\varphi_i, H\varphi_i)$ are uniformly convergent in α, i.e. for any $\varepsilon>0$ we can find $n_\varepsilon\in\mathbb{N}$ such that

$$\sum_{i\geqslant n} p_i(E_\alpha\varphi_i, H\varphi_i)\leqslant\varepsilon,\ n\geqslant n_\varepsilon,\ \alpha>0.$$

Indeed, all these series are smaller than the convergent series $\sum_{i=1}^{\infty} p_i(\varphi_i, H\varphi_i)$ and the lemma is completely proved. *

Before defining the concept of stationarity time, we shall first present an important application of the lemma.

THEOREM 2. *Let H be a selfadjoint operator and ρ a state. Then $\Delta^2 H_\rho=0$ if and only if $H\varphi=\overline{H}_\rho\varphi$ for every eigenvector of ρ corresponding to a nonvanishing eigenvalue. In these conditions,* $[H, \rho]=0$.

Proof. Suppose that $H\varphi_i=\overline{H}_\rho\varphi_i$ for every φ_i with the property $\rho\varphi_i=p_i\varphi_i$, $p_i\neq 0$. Then we have $[H, P_i]=0\ \forall i$ and, since it is selfadjoint, H leaves invariant the kernel of ρ. Therefore $[H, \rho]=0$. Let us write the definition of $\Delta^2 H_\rho$:

$$\Delta^2 H_\rho=\int_{-\infty}^{\infty}(\lambda-\overline{H}_\rho)^2\,\mathrm{d}\,\mathrm{Tr}(\rho E_\lambda).$$

$[H, \rho] = 0$ implies that $\mathrm{Tr}(\rho E_\lambda)$ is a function of the form $\mathrm{Tr}(\rho E_\lambda) = \sum\limits_{\substack{i \\ P_i \subseteq E_\lambda}} p_i$ ($P_i \subseteq E_\lambda$ means $P_i\mathcal{H} \subseteq E_\lambda\mathcal{H}$). Therefore

$$\int_{-\infty}^{\infty} (\lambda - \overline{H}_\rho)^2 \, \mathrm{dTr}(\rho E_\lambda) = \sum_{i=1}^{\infty} p_i (E_i - \overline{H}_\rho)^2 = 0$$

Conversely, suppose that $\Delta^2 H_\rho = 0$. Then, since $(\lambda - \overline{H}_\rho)^2 \geqslant 0$, $\lambda \in \mathbb{R}$, and $(\lambda - \overline{H}_\rho)^2 > 0$ for $\overline{H}_\rho \neq \lambda$, it follows that on the interval $(\overline{H}_\rho, \infty)$ the function $\mathrm{Tr}(\rho E_\lambda)$ is constant. Since $\lim\limits_{\lambda \to \infty} \mathrm{Tr}(\rho E_\lambda) = 1$ we find that $\mathrm{Tr}(\rho E_\lambda) = 1$, $\forall \lambda > \overline{H}_\rho$. This equality holds if we have $P_{\mathcal{R}(\rho)} \subseteq E_\lambda$ for every $\lambda > \overline{H}_\rho$. ($P_{\mathcal{R}(\rho)}$ is the projector onto $\mathcal{R}(\rho)$). Indeed, if there exists $\lambda_0 > \overline{H}_\rho$ such that $\mathcal{R}(\rho) \notin E_\lambda \mathcal{H}$, we can find for every basis $\mathcal{B}$ of $\mathcal{R}(\rho)$ a vector $\varphi \in \mathcal{B}$ and $\varphi \notin E_{\lambda_0}\mathcal{H}$. Taking the basis $\{\varphi_i\}$, $\rho\varphi_i = p_i\varphi_i$, $p_i \neq 0$, we find that $\mathrm{Tr}(\rho E_{\lambda_0}) < 1$, since there exist $\varphi_i \notin E_{\lambda_0}\mathcal{H}$. Consequently, $[P_{\mathcal{R}(\rho)}, H] = 0$, then $[\rho, H] = 0$ and $\rho\mathcal{D}(H) \subseteq \mathcal{D}(H)$. By using the lemma, we obtain easily

$$\sum_{i=1}^{\infty} p_i(\varphi_i, (H - \overline{H}_\rho)^2 \varphi_i) = 0, \text{ or } \|(H - \overline{H}_\rho)\varphi_i\| = 0 \ \forall i$$

and finally $H\varphi_i = \overline{H}_\rho \varphi_i$, $\forall i$. ✻

Now we can define and study the stationarity time for admissible states. Take a system in a state ρ, whose evolution is generated by the Hamiltonian H. The operator

$$T = i[H, \rho] \tag{2}$$

is called the time operator associated to the state ρ (the Hamiltonian H is fixed).

DEFINITION 3. *We call stationarity time of an admissible state* ρ *the number*

$$T_S(\rho) = (\overline{T^2_\rho})^{-\frac{1}{2}}$$

Here $\overline{T^2_\rho}$ is the average value of the operator T^2 in the state ρ. From (1) it results that

$$\overline{T^2_\rho} = \overline{\left(\frac{\mathrm{d}\rho(t)}{\mathrm{d}t}\bigg|_{t=0}\right)^2}_\rho$$

The derivative of $\rho(t)$ can be taken at any moment t_0 because

$$\frac{\mathrm{d}\rho(t)}{\mathrm{d}t}\bigg|_{t=t_0} = U_{t_0}\left(\frac{\mathrm{d}\rho(t)}{\mathrm{d}t}\bigg|_{t=0}\right)U_{-t_0},$$

so that $T_S(\rho)$ characterizes the state — it does not depend on time. The next two theorems justify the fact that $T_S(\rho)$ may be a good measure of the stationarity. For the sake of convenience we will use the notation $S(\rho) \equiv T_S(\rho)^{-2}$.

THEOREM 3. *$S(\rho) = 0$ if and only if ρ is stationary.*

Proof. We saw that ρ is stationary if and only if $[H, \rho] = 0$, i.e. $T=0$. Hence the stationarity implies $S(\rho) = 0$. Conversely, let $\{E_\lambda\}_{\lambda \in \mathbb{R}}$ be the spectral family of the positive operator T^2. We can write

$$S(\rho) = \int_0^\infty \lambda \mathrm{d}\mathrm{Tr}(\rho E_\lambda) = 0$$

Following a procedure already used in proving Theorem 3 we find that $[\rho, T^2] = 0$. Applying the lemma, we get

$$\sum_{i=1}^{\infty} p_i(\varphi_i, T^2\varphi_i) = 0$$

that is $\| T\varphi_i\|^2 = 0$ and $T\varphi_i = 0$ for all φ_i with the property $\rho\varphi_i = p_i\varphi_i$, $p_i \neq 0$. Since the subspace spanned by $\{\varphi_i ; p_i \neq 0\}$ is dense in $\mathscr{R}(\rho)$, for $\varphi \in \mathscr{D}(H) \cap \mathscr{R}(\rho)$ there exists $\psi_n \to \varphi$, where ψ_n are linear combinations of φ_i. It follows immediately that $T\varphi = 0$. Finally, since T Ker $\rho \subseteq$ Ker ρ, we get $T\psi = 0$ for $\psi \in \mathscr{D}(H)$ and the fact that ρ is stationary. ⋇

We shall give now a theorem which proves that $T_S(\rho)$ satisfies an "uncertainty relation" with respect to the mean square dispersion of H in the state ρ, i.e.

$$T_S(\rho)^2 \cdot \Delta^2 H_\rho \geqslant 1 \tag{3}$$

In order to prove this relation we shall replace it by the equivalent inequality $S(\rho) = \Delta^2 H_\rho$.

THEOREM 4. *Suppose that $S(\rho)$ and $\Delta^2 H_\rho$ exist. Then $S(\rho) \leqslant \Delta^2 H_\rho$. When ρ is a pure state, the equality holds.*

Proof. Since $\varphi_i \in \mathscr{D}(T)\ \forall\ i$, the integral $\int_{-\infty}^{\infty} \lambda^2 \mathrm{d}(\varphi_i, E_\lambda\, \varphi_i)$, where $\{E_\lambda\}_{\lambda \in \mathbb{R}}$ is the spectral family of T, exists. Therefore we can write

$$S(\rho) = \int_{-\infty}^{\infty} \lambda^2 \mathrm{d}\mathrm{Tr}(\rho E_\lambda) = \sum_{i=1}^{\infty} p_i \int_{-\infty}^{\infty} \lambda^2 \mathrm{d}(\varphi_i, E_\lambda\, \varphi_i) = \sum_{i=1}^{\infty} p_i \| T\varphi_i \|^2.$$

Denoting $(H\varphi_i, \varphi_j)$ by H_{ij} and making simple calculations, we get

$$\| T\varphi_i \|^2 = \sum_{\substack{j=1 \\ j \neq i}}^{\infty} (p_i - p_j)^2 H_{ij} H_{ji}$$

and

$$S(\rho) = \sum_{\substack{i,j=1\\ i\neq j}}^{\infty} p_i(p_i - p_j)^2 H_{ij}H_{ji}$$

On the other hand,

$$\Delta^2 H_\rho = \overline{H^2_\rho} - (\overline{H}_\rho)^2$$

where

$$\overline{H^2_\rho} = \sum_{i=1}^{\infty} p_i(H\varphi_i, H\varphi_j) = \sum_{i,j=1}^{\infty} p_i H_{ij}H_{ji}$$

$$\overline{H^2_\rho} = \sum_{i,j=1}^{\infty} p_i p_j H_{ii}H_{jj}$$

Since $p_i - p_i^2 = p_i \sum_{\substack{j\\ j\neq i}} p_j$

we get finally

$$\Delta^2 H_\rho = \sum_{\substack{i,j=1\\ i\neq j}}^{\infty} p_i H_{ij}H_{ji} + \sum_{i<j} p_i p_j (H_{ii} - H_{jj})^2$$

But $(p_i - p_j)^2 \leqslant 1$. Therefore

$$S(\rho) \leqslant \sum_{\substack{i,j=1\\ i\neq j}}^{\infty} p_i H_{ij}H_{ji}$$

On the other hand, the above obtained relation for $\Delta^2 H_\rho$ implies that

$$\Delta^2 H\rho \geqslant \sum_{\substack{i,j=1\\ i\neq j}}^{\infty} p_i H_{ij}H_{ji}$$

and we thus obtain the desired inequality:

$$S(\rho) \leqslant \Delta^2 H_\rho$$

If $\rho = P_\varphi$, i.e. if ρ is a pure state, we may write

$$S(\rho) = (H\varphi, H\varphi) - (H\varphi, \varphi)^2 = \Delta^2 H_\rho$$ ✳

Note that if $S(\rho) = \Delta^2 H_\rho = 0$, the state ρ can be a mixed one (see Theorems 2 and 3). For the case $\Delta^2 H_\rho \neq 0$ we can prove an interesting proposition

PROPOSITION 4 *If* $S(\rho) = \Delta^2 H_\rho \neq 0$, *then* ρ *is a pure state.*

Proof. From the proof of Theorem 5 we known that $S(\rho) = \Delta^2 H_\rho$ means

$$\sum_{i=1}^{\infty} p_i \left(\sum_{\substack{j=1 \\ j \neq i}}^{\infty} [1 - (p_i - p_j)^2] |H_{ij}|^2 \right) = 0$$

where

$$p_i \geqslant 0, \quad \sum_{\substack{j=1 \\ j \neq i}}^{\infty} [1 - (p_i - p_j)^2] |H_{ij}|^2 \geqslant 0.$$

Since $\rho \neq 0$, there exists $p_i > 0$ and for this i

$$\sum_{\substack{j=1 \\ j \neq i}}^{\infty} [1 - (p_i - p_j)^2] |H_{ij}|^2 = 0$$

Further $\Delta^2 H_\rho > 0$ implies the existence of a j, $j \neq 1$, such that $|H_{ij}|^2 > 0$ and we get

$$(p_i - p_j)^2 = 1$$

If $p_j > 0$, from the inequalities $0 \leqslant p_i, p_j \leqslant 1$ it results that $(p_i - p_j)^2 < 1$, i.e. a contradiction.

Therefore $p_i = 1$ and from the condition $\mathrm{Tr}\,\rho = 1$ we find that $\rho = P_{\varphi_i}$. The proposition is thus proved. ✳

REFERENCES

[1] J. H. Eberly and L. P. S. Singh, *Phys. Rev.*, D, **7**, 359 (1973).
[2] E. Prugovecki, "Quantum Mechanics in Hilbert Space", Academic Press, New York, 1971.

Revue Roumaine de Chimie, 27, 2, 257–260 (1982)

CHARACTERIZATION OF STRONTIUM SOAPS AND STUDIES OF THEIR VISCOSITY IN AQUEOUS ISOPROPANOL

R. P. VARMA and R. DAYAL

Department of Chemistry, D.A.V. College, Muzaffarnagar–251001, India

Received June 21, 1979

Revised April 20, 1981

Strontium soaps of *n*-fatty acids (C_5-C_8) have been analysed by elemental and infrared studies and are found free from water of crystallization. Viscosity data show that two kinds of micelles are formed in the soap solutions and that the change in the nature of hydrophilic oleo micelles to lipophilic hydromicelles occurs at about 50–60% isopropanol. Vand and Moulik's equations are applicable only above CMC of the soaps. The parameters of these equations have been evaluated. These may be used to calculate the viscosity of soap solutions in the concentration range in which the equations hold good.

INTRODUCTION

Infrared studies like so many instrumental techniques can provide efficient information concerning the structure of the substances. The first reported collection of valuable IR spectra pertaining to surfactants was made by Delsemme [1]. The use of IR spectra for identifying surfactants was made public by Sadtler. [2] Recently, IR spectra of iron and cobalt [3] and magnesium soaps [4] of lower fatty acids have showed that these soaps are free from water of crystallization.

In the present investigation, strontium soaps were prepared and characterized. Viscosities of these soap solutions in aqueous isopropanol at 35° were measured in order to test the applicability of some viscosity equations and to confirm the results obtained by conductivity measurements. [5]

EXPERIMENTAL

The chemicals were purified and the soaps were prepared by the method described in a previous communication. [5] The elemental analysis was carried out by standard methods and IR spectra were recorded in Beckman IR 20 spectrometer by using the Nuzol technique. An Ostwald viscometer was used to determine the viscosity of soap solutions in a thermostatically controlled ($35 \pm 0.05°$) bath. The densities were measured with a dilatometer constructed of pyrex glass having a reservoir volume of 15 ml. The measuring section was constructed of precisely bored graduated capillaries. The dilatometer was calibrated with conductivity water and the accuracy of the measurements was checked against some test solutions of known density. The density data obtained agreed with literature values within ± 0.001 to 0.003%.

RESULTS AND DISCUSSION

Characterization of soap:

Wurzschmitt [6] based his excellent qualitative analytical system for surfactants on the quantitative analysis of the unknown samples for C, H, O, N etc. Strontium soaps have been analysed and the proportions of the elements present (Table 1) suggest that these soap molecules are free from water of crystallization.

TABLE 1

Analysis of strontium soaps

Soap	Molecular formula	%							
		Sr		C		H		O	
		Theor.	Pract.	Theor.	Pract.	Theor.	Pract.	Theor.	Pract.
Valerate	$(C_5H_9O_2)_2Sr$	30.26	30.32	41.43	41.34	6.21	6.22	22.10	22.12
Caproate	$(C_6H_{11}O_2)_2Sr$	27.58	27.58	45.34	45.42	6.93	6.82	20.15	20.18
Caprylate	$(C_8H_{15}O_2)Sr$	23.45	23.48	51.39	51.22	8.03	8.10	17.13	17.20

The IR spectra of soaps serve to indicate typical I.R. absorptions and some of the characteristic absorption frequencies are given in table 2. It is observed that there is no peak in the region of 3030 – 50 cm^{-1} but a peak due to c = 0 group is found at 1510–1560 cm^{-1} instead of 1710 cm^{-1} from its corresponding acids. This is because of the formation of soaps which is also confirmed by the presence of the peak of —COOH anion near 1400 cm^{-1}. These spectra show no peak in between 3590 – 3650 cm^{-1} due to the absence of water of crystallization which corresponds to the results obtained by elemental analysis.

TABLE 2

Some of the characteristic absorption frequencies (cm^{-1}) of strontium soaps

Soap	Tentative assignements			
	C—H stretching vibrations	C=0 stretching vibrations	CH_2 stretching vibrations	COOH stretching vibrations
Valerate	2900 (s)	1530 (s)	1450 (m)	1370 (m)
Caproate	2880 (s)	1560 (s)	1440 (m)	1370 (m)
Caprylate	2890 (s)	1540 (s)	1450 (m)	1390 (m)

s = strong ; m = medium.

Viscosity:

The viscosity of soap solutions increases with increasing soap concentration. The values of CMC obtained from the plots of viscosity vs. soap concentration are 0.015, 0.010 and 0.008M for valerate, caproate and caprylate, respectively at all concentrations of isopropanol which are in close agreement with the values reported earlier.[5] The extrapolated values of viscosity η_0 are in agreement with the corresponding experimental values of water-isopropanol mixtures and are independent of the chain length of the soap. It is also observed that the larger molecules impart greater viscosity. This is due to an increase in the size of the micelles with the increasing number of carbon atoms in the soap.

It may be pointed out that the viscosity of soap solutions in aqueous isopropanol increases linearly up to 50% of isopropanol and then decreases. A similar change in the behaviour of strontium soaps in solutions containing 50 – 60% isopropanol has been also observed by conductivity measurements.[1]

The viscosity of strontium soap solutions in water and isopropanol mixtures has been satisfactorily represented in the wide range of concentrations by the following[7,8] equations.

$$\text{Vand}: 1/C = (0.921/\overline{V})^{-1} 1/\log(\eta/\eta_0) + Q\overline{V} \qquad \text{(i)}$$

where Q and $\overline{V}$ are the interaction coefficient and molar volume of the solute in litre mole^{-1}, C is the concentration of the solute in mole litre^{-1} and η_0 is the viscosity of the solvent.

$$\text{Moulik}: (\eta/\eta_0)^2 = M + K^1C^2 \qquad \text{(ii)}$$

where M and K^1 are constants.

The values of $\overline{V}$ do not remain constant but a sudden increase in the values for a solution of 60% isopropanol suggests that a change in the behaviour occurs at this alcohol concentration. A perusal of table 3 shows that the values of $\overline{V}$ present the following order :

Caproate > caprylate > valerate

The interaction coefficient, Q (Table 3) also shows a change at 60% isopropanol concentration which supports the results of $\overline{V}$. It may be mentioned that the parameter $\overline{V}$ is perfectly defined but the interaction coefficient Q is only approximately obtained.[9] It is evident[10] that probably Q is a specific property of a solute and not a general property.

The constants, M and K^1 have been calculated from equation (ii) and are given in table 3. It has been observed that these constants also show a change at 60% isopropanol concentration.

Both the equations reveal that a change in the nature of the micelles from hydrophilic oleo micelles to lipophilic hydromicelles[11] occurs at about 50–60% isopropanol. The evaluated parameters can be used to calculate the solution viscosity in the concentration range in which the equations hold good.

ACKNOWLEDGEMENTS. The authors thank Dr. K. N. Mehrotra, Reader in the Department of Chemistry, University of Jodhpur, Jodhpur for his keen interest in the work and to the college authorities for providing laboratory facilities.

TABLE 3

Viscosity parameters for strontium soap solutions in water isopropanol mixtures at 35°C.

Vol. % of isopropanol	Tested conc. limit (mole/ litre)	Valid conc. zones (mole/litre)	$\bar{V}$	Q	M	K^1
		Valerate				
10	0.004–0.05	0.02–0.05	0.39	17.93	1.047	37
20	0.004–0.05	0.02–0.05	0.32	12.41	1.030	28
30	0.004–0.05	0.02–0.05	0.29	10.47	1.026	25
40	0.004–0.05	0.02–0.05	0.25	7.89	1.025	18
50	0.004–0.05	0.02–0.05	0.23	4.40	1.023	15
60	0.004–0.04	0.02–0.04	0.34	− 2.92	1.024	24
70	0.004–0.04	0.02–0.04	0.30	−10.21	1.022	20
80	0.004–0.04	0.02–0.04	0.26	−19.74	1.020	14
		Caproate				
10	0.002–0.02	0.010–0.020	0.50	25.65	1.018	105
20	0.002–0.02	0.010–0.020	0.50	−25.65	1.016	70
30	0.002–0.02	0.010–0.020	0.46	−32.57	1.015	55
40	0.002–0.02	0.010–0.020	0.42	−41.02	1.012	50
50	0.002–0.02	0.010–0.020	0.40	−50.00	1.011	45
60	0.002–0.02	0.010–0.020	0.63	− 3.19	1.020	100
70	0.002–0.02	0.010–0.020	0.60	−16.70	1.020	80
80	0.002–0.02	0.010–0.020	0.44	−13.66	1.008	65
		Caprylate				
10	0.002–0.015	0.006–0.015	0.49	48.25	1.013	170
20	0.002–0.015	0.006–0.015	0.44	40.71	1.011	135
30	0.002–0.015	0.006–0.015	0.39	25.24	1.009	125
40	0.002–0.015	0.006–0.015	0.38	18.54	1.008	115
50	0.002–0.015	0.006–0.015	0.33	8.33	1.007	110
60	0.002–0.015	0.006–0.015	0.51	38.71	1.009	250

REFERENCES

[1] A. H. Delsemme, *Mendedeel Vlaam. Chem. Ver.*, **13**, 152 (1951.
[2] P. Sadtler, *Am. Soc. Testing Materials Bull.*, **190**, 55 (1953).
[3] R. P. Varma and H. K. Bhargava, *Ann. Chim.*, **66**, 773 (1976).
[4] R. P. Varma and K. Kumar, *J. Indian Chem. Soc.*, **LV**, 675 (1978).
[5] R. P. Varma and R. Dayal, *J. Chim. Phys. Physico. Chim. Biol.*, **74**, 443 (1977).
[6] B. Wurzschmitt, *Chem. Ztg.*, **74**, 16 (1950).
[7] V. Vand, *J. Phys. Colloid. Chem.*, **52**, 277 (1948).
[8] S. P. Moulik, *J. Phys. Chem.*, **72**, 4682 (1968).
[9] "International Encyclopedia of Physical Chemistry and Chemical Physics" Topic 16, Pergamon Press, Oxford, England, 1965, Vol. 2, p. 4f.
[10] S. P. Moulik, *J. Indian Chem. Soc.*, **49**, 483 (1972).
[11] J. H. Schulman and D. P. Riley, *J. Colloid Sci.*, **3**, 383 (1948).

Revue Roumaine de Chimie, 27, 2, 261–264 (1982)

QUANTITATIVE SPECTROGRAPHIC ESTIMATION OF ZIRCONIUM BY CHEMICAL ENRICHMENT

N. BARAKAT *, F. ABOU EL-NOUR** [a] and N. SHAHEEN ***
* Faculty of Science, Ain Shams University, Cairo, Egypt
** Atomic Energy Establishment, Cairo, Egypt
*** Faculty of Science, Asiut University, Aswan, Egypt

Received 12 June 1980

A chemical preenrichment procedure for determination of Zr in soil samples is described. Such a procedure minimizes the interference of Zr spectral lines with that of other elements present in the samples. Thus there is no need for preparation of standard samples on special matrices. The sensitivity of the method was found to be 1 ppm with relative deviation of $\pm 2.5\,\%$.

INTRODUCTION

The importance of Zr comes from its use as a structural material in thermal reactors. It fulfils the requirements of such reactors as it has an extremely low thermal neutron cross-section combined with exceptional corrosion resistance. In addition, it has relatively high strength at the moderately elevated temperatures obtained in thermal reactors.

Several difficulties arise in the emission spectrographic analysis of Zr, because of poor precision and low sensitivity resulting from the interference of its very large number of spectral lines. For the sake of precision and high sensitivity the signal to noise ratio in the spectrographic set up should be as high as possible.

A variety of enrichment procedures [1] have been employed to increase the spectral line intensities of Zr present in the samples. Chemical methods [2,3] depend on the dissolution of the samples followed by precipitation on a suitable carrier, while other enrichment procedures depend on the use of spectro-chemical operations such as double arc furnace [4,5] and the boiler electrode technique. [6] In addition ashing techniques may be considered as an enrichment procedures. [7]

PREVIOUS WORK

Strock [8] has shown that ZrO_2 is difficult to vaporize. Its release from the electrode is probably further impeded by reduction to ZrC which when molten dissolves Zr and changes to a very stable ZrN. Eeckhout [9] used Na_2CO_3 as a buffer in the determination of Zr. Churchill[10] described various techniques including the use of carbon over ammonium salts. Jaycox[11] used CuO as a buffer; carbon was also used as an additional one. Hamaguchi[12] studied the addition of $BaCl_2$ to silicates in determining Zr. Addink et al.[13] used C, SiO_2, Ni and Na_2CO_3 as buffers. Rusanow et al.[14] illustrated a method for the determination of Zr using C and $BaCO_3$ buffers. Roca et al.[15] used Sr_2CO_3 and C buffers. Moroshkina and Vanaeva[16] applied acid condensation of pyrogallol formaldehyde resine for prechemical enrichment of Zr in the samples.

---

[a] Present address of correspondence: Chemistry Department, College of Science, Riyadh University, Riyadh, Saudi Arabia.

The present study represents an efficient, precise and sensitive method by which it is possible to estimate Zr in soil samples by chemical preenrichment and precipitation on a suitable carrier.

EXPERIMENTAL

1. *Preparation of the soil samples :*

Soil samples were dried, sieved to pass through 2-mm sieve and ignited at 450°C. $\frac{1}{2}$ g of the sample was boiled in an aliquot of 20 ml aqua regia and left to be digested till a cake was obtained. It was then cooled and another aliquot of 20 ml aqua regia was added. The process was repeated 10 times. The solution was then filtered and the residue was well washed. The filtrate containing Zr was evaporated to 5 ml and mixed with $\frac{1}{4}$ g spec. pure carbon containing Mo as internal standard element. It was then dried, grounded and loaded in the electrode crater (28 g).

2. *Preparation of the standards :*

The used matrix composed of 1000 ppm Mo internal standard added as MoO_3 dissolved in dilute ammonia with the ratio of 1 : 1 to the spec. pure carbon powder. This matrix was dried at 110°C and well mixed in an agate mortar. Zr was then added as ZrO_2 to the matrix with concentration of 1000 ppm. Subsequent dilutions with the base matrix were made to obtain concentrations of 100, 50, 25, 10, 5 and 1 ppm.

RESULTS

The selected line pair used in constructing the working curve was Zr (II) 2571.39 Å and Mo 2572.34 Å. These spectral lines were inspected by using Jarrell-Ash Plane Grating Spectrograph.

A working curve representing the relation between log I and log C was constructed, C being the concentration of Zr and I the intensity of spectral lines being given by $(I_{E+B1} - \mathrm{I}_{B1}/(I_{I\cdot S\cdot+B2} - I_{B2})$. Here I_{E+B1} is the combined intensity of the element spectral line and its background, I_{B1} is the intensity of the neighbouring background, $L_{I\cdot S\cdot+B2}$ is the intensity of Mo internal standard line and its background and I_{B2} is the intensity of the neighbouring background.

Figure 1 gives the graphical representation of the working curve. It covers the concentration range between 1 and 100 ppm. Its slope is 0.479 and the index value is 22.909 ppm. This curve can be represented by the equation:

$$Y = 0.479 \log C - 0.65$$

Such an equation provides an accurate and convenient method for Zr determination. Y is the logarithm of the intensity ratio of the element and the internal standard.

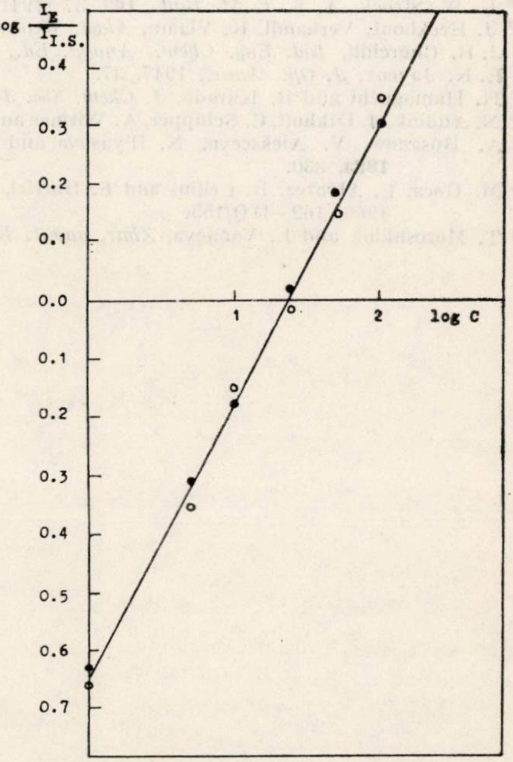

Fig. 1. — The working curve for determination of Zr in soil (○ — and ● — represent different experiments).

The sensitivity of the method for Zr determination in soil was found to be 1 ppm with relative deviation of ± 2.5 %.

CONCLUSION

The chemical enrichment procedure of Zr in soil samples using aqua regia followed by precipitation on spec. pure carbon powder as carrier material was found to be suitable for its emission spectrographic analysis. Interference of Zr spectral lines with that of the elements present in the matrix was minimized. Preparation of standard matrices of the same composition as that of the analyzed samples was not required. The sensitivity of the method for determination of Zr in soil samples of 1 ppm is acceptable in quantitative spectrographic analysis.

REFERENCES

[1] L. H. Ahrens and S. R. Taylor, "Spectrochemical Analysis", Addison Welsey, London, 1961.

[2] C. Lorenz, German Patent No. 536, 549, 31 (1921).

[3] J. W. Marden and M. N. Rich, *Bull. U.S. Bur. Min.*, **186**, 31, 32, 39, 40 (1921).

[4] D. M. Shaw, O. I. Joensuu and L. H. Ahrens, *Spectrochim. Acta*, **4**, 233 (1950).

[5] K. H. Wedepohl, *Geochim. et Cosmochim. Acta*, **3**, 93 (1953).

[6] R. H. Hall and H. L. Lovell, *Analyt. Chem.*, **30**, 1665 (1958).

[7] R. E. Thiers, "Separation, Concentration and Contamination", Wiley, New York, 1957.

[8] L. W. Strock, *A. S. T. M. Bull.*, **109**, 37 (1941).

[9] J. Eeckhout, Verhandl. K. Vlaam, *Akad. Wetensch. Lett. Schonne Kunst Belg.*, **7**, 1(1945).

[10] J. R. Churchill, *Ind. Eng. Chem., Analyt. Ed.*, **17**, 66 (1945).

[11] E. K. Jaycox, *J. Opt. Amer.*, 1947, 37.

[12] H. Hamaguchi and R. Kurado, *J. Chem. Soc. Japan*, **76**, 524 (1955).

[13] N. Addink, J. Dikhoff, C. Schipper, A. Witmer and T. Groot, *Spectrochim. Acta*, **7**, 45 (1955).

[14] A. Rusanow, V. Alekseeva, N. Il'yasova and V. Khitrov, |*Redkozemel'nye Elementary*, **1963**, 330.

[15] M. Roca, F. Alvarez, R. Cellini and F. Burriel, "Spanish Atomic Energy Report", JEN, 1966, 162—D Q/155.

[16] T. Moroshkina and L. Vanaeva, *Zhur, analit. Khim.*, **25**, 2374 (1970).

Revue Roumaine de Chimie, **27**, *2*, 265–272 (1982)

KINETICS AND MECHANISM OF Cu(II)–CATALYSED OXIDATION OF ACETONE BY THE PEROXODISULPHATE ION

S. C. AGARWAL, SMT. P. L. AGARWAL*, V. B. AGARWAL and
VIBHAKAR DWIVEDI**
Chemical Laboratories, Agra College, Agra – 282002, India

Received May 23, 1980

Preliminary experiments show that the reaction between acetone and potassium peroxodisulphate is very slow. The reaction rate becomes measurable at 55°C by introducing Cu(II) ion as catalyst. The total order of the reaction is nearly unity. The rate law $-d[S_2O_8^{2-}]/dt = k_1[S_2O_8^{2-}]\,[\text{acetone}]^{-0.1}\,[\text{Cu(II)}]^{0.25}$ has been interpreted in terms of a most likely mechanism involving oxidation of the Cu(II)-acetone complex by the $SO_4^{-}\cdot$ and $OH\cdot$ radical ions by parallel reaction pathway. Allyl acetate an effective scavenger, inhibits the reaction. H^+ ion and oxygen gas also have depressing action on the rate of reaction.

INTRODUCTION

Catalysis by copper (II) in peroxodisulphate oxidation has been reported for thiosulphate,[1,2] oxalate,[3] arsenic,[4] antimony,[5] hydrazine,[6] hydrogen peroxide,[7] alcohols,[8–10] glycollic acid,[11] malic acid,[12] lactic acid,[13] succinic acid[14] and in a few other cases. Insufficient kinetic data do not provide evidence for the mechanism of the catalytic action.[15]

Uncatalysed and Ag (I) – catalysed oxidation of acetone has been studied by various workers,[16,17] but this work is the first attempt to oxidize a member of ketone series in the presence of copper catalyst by $S_2O_8^{2-}$ ion with the aim to elucidate the catalytic role of Cu (II) in the oxidation mechanism.

RESULTS

Stoichiometry

To verify the stoichiometry of the Cu (II)-catalysed reaction, a kinetic run was followed up to the final stage of reaction at 55° C. A blank was also run simultaneously. Experiments were repeated with different molar concentrations of peroxodisulphate, acetone and constant quantity of $CuSO_4$. The results showed that one molecule of acetone reacted with two molecules of peroxodisulphate. Stoichiometric equation is as follows :

---

* Department of Chemistry, Rajasthan University, Jaipur (India)
** Department of Chemistry, R. B. S. College, Agra (India)

$$2CH_3COCH_3 + 4K_2S_2O_8 + 4H_2O + 3CH_3COOH + 8KHSO_4$$

Identification of acetic acid

The main reaction product, acetic acid, was identified by spot test[19]. However, carbon dioxide is also present as a minor product.

The rate law of catalysed reaction

Table 1 gives the results of kinetic run at 55°C.

TABLE 1

First order rate constant in Cu (II)—catalysed oxidation of acetone

Time (s)	Volume of 0.04N $Na_2S_2O_3$ (ml)	$(a - x)$ (ml)	$[S_2O_8^{2-}]$ (moles/l)	10^7R moles l^{-1} (S^{-1})	10^5k_1 (S^{-1})
0	5.12	5.00	0.0200	—	—
1800	4.97	4.85	0.0194	3.33	1.70
3600	4.84	4.72	0.0188	3.10	1.66*
7200	4.58	4.46	0.0178	3.00	1.59
10800	4.39	4.27	0.0171	2.70	1.46
14400	4.18	4.06	0.0162	2.60	1.45
18000	3.97	3.85	0.0154	2.55	1.46
21600	3.72	3.60	0.0144	2.58	1.52
25200	3.52	3.40	0.0136	2.53	1.53
28800	3.40	3.28	0.0131	2.38	1.46
32400	3.12	3.00	0.0120	2.47	1.58
36000	3.00	2.38	0.0115	2.35	1.53
39600	2.82	2.70	0.0108	2.32	1.56
43200	2.60	2.48	0.0099	2.33	1.62
Mean				2.63	1.59
Slope value					1.52

* Mean calculated hereafter

$(Acetone)_0 = [K_2S_2O_8]_0 = 0.02M$; $[CuSO_4]_0 = 1 \times 10^{-3}M$, Temp. 55°C

A fair constancy of the first order rate constants obtained with equimolar concentration of the reactants suggests that the overall order of the reaction is one. First order plots were found to be linear for almost the entire reaction and the velocity constants were calculated from the slope of these lines.

Peroxodisulphate dependence

Table 2 includes the rate data of runs obtained with different initial concentrations of peroxodisulphate and constant acetone concentration.

The slight decrease in the values of k with increase in $[S_2O_8^{2-}]_0$ is due to the inhibition of K^+ ions which is characteristic of most peroxodisulphate reactions.[20]

TABLE 2

Rate dependence on peroxodisulphate

$[K_2S_2O_8]_0$ M	0.005	0.01	0.015	0.02	0.03	0.04
$10^5 k_1 (S^{-1})$	1.61	1.58	1.53	1.52	1.51	1.50

$[\text{Acetone}]_0 = 0.02$ M ; $[CuSO_4] = 1.0 \times 10^{-3}$M ; Temp. 55°C.

Acetone dependence

Table 3 records the rate data at 55°C in the concentration range of 0.005 — 0.05M acetone and constant peroxodisulphate concentration.

The value of k_1 is observed to decrease with the increase in acetone concentration. Evidently, the rate of reaction is slightly dependent on the concentration of reducing ions. The order, when calculated by the differential method for any two acetone concentrations (Table 3, column 3) comes out to be -0.1. This negative order suggests inverse fractional proportionality of the rate to acetone concentration and the value of $\text{rate}/[\text{acetone}]^{-0.1}$ i.e. $R \times [\text{acetone}]^{0.1}$ should be constant for different $[\text{acetone}]_0$. This is shown in column 4 of table 3.

TABLE 3

Rate dependence on [Acetone]

$[\text{Acetone}]_0$ M	10^7R moles l^{-1} S^{-1}	$[\text{Acetone}]^{-0.1}$	$10^7 R \times [\text{Acetone}]^{0.1}$
0.005	2.96	0.59	1.75
0.010	2.81	0.63	1.77
0.015	2.72	0.66	1.80
0.020	2.63	0.68	1.79
0.030	2.45	0.70	1.72
0.040	2.28	0.72	1.64
0.050	2.18	0.74	1.61

$[K_2S_2O_8]_0 = 0.02$M, $[CuSO_4]_0 = 1.0 \times 10^{-3}$ M, Temp. 55°C

Copper (II) dependence

Table 4 summarises the results showing the influence of varying concentration of Cu (II) on the rate of reaction.

Thus, a fractional power dependence in copper sulphate concentration is encountered. The same value for order in Cu (II) has been obtained by 'Van't Hoff's differential method' between the two copper concentrations i.e. 0.001M and 0.002M. The plot between k_1 and $[\text{Cu (II)}]^{0.25}$ is linear (Fig. 1) confirming the above conclusion.

Thus, the kinetic measurements to determine the exponents in the rate law give

$$-dc_{S_2O_8^{2-}}/dt = k_1(S_2O_8^{2-})[\mathrm{Cu\ (II)}]^{0\cdot25}$$

TABLE 4

Rate dependence on copper (II)

$10^4[CuSO_4]_0$ M	$10^1[CuSO_4]_0^{0.25}$	10^5k_1 S^{-1}	10^7R moles $l^{-1}S^{-1}$	$\frac{10^4k_1}{[CuSO_4]^{0.25}}$	$\frac{10^5R}{[CuSO_4]^{0.25}}$
0.5	0.840	0.78	1.23	0.93	1.46
1.0	1.000	0.90	1.49	0.90	1.49
5.0	1.495	1.28	2.22	0.86	1.48
10.0	1.778	1.52	2.63	0.86	1.47
20.0	2.114	1.84	3.10	0.87	1.46
40.0	2.515	2.22	3.81	0.88	1.51

$[K_2S_2O_8]_0 = [\mathrm{Acetone}]_0 = 0.02M$, Temperature = 55°C

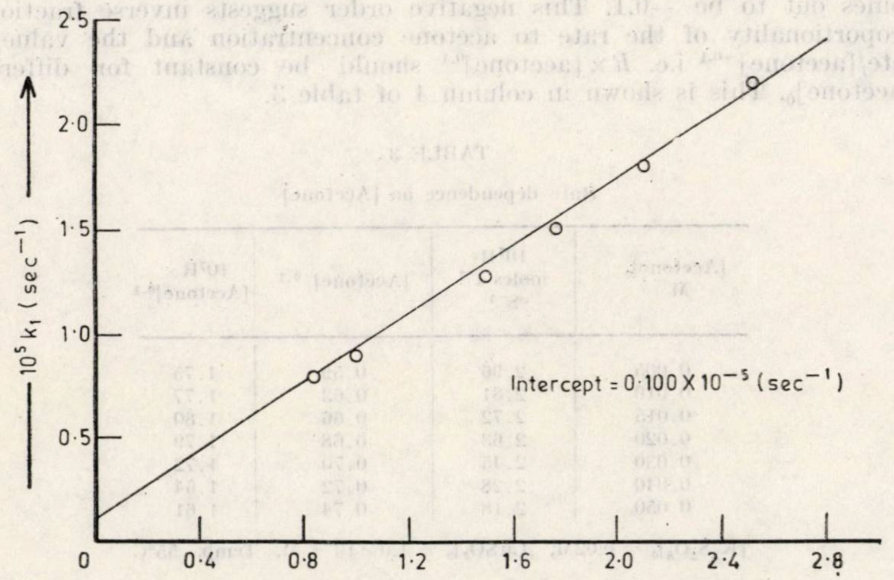

Fig. 1. Fractional dependence in $CuSO_4$ concentration.

The rate law

The rate law is therefore adequately expressed by

$$-d[S_2O_8^{2-}]/dt = k_1[S_2O_8^{2-}][\mathrm{acetone}]^{-0\cdot1}[\mathrm{Cu(II)}]^{0\cdot25}.$$

The total order of the reaction $(x+y+z)$ is then 1.15, which may be taken as unity since k_1 exhibits satisfactory consistency throughout the whole course of the reaction and therefore the velocity at any instant is dependent on $K_2S_2O_8$ concentration only.

Temperature dependence

The effect of temperature of k_1 was studied in the range of 45—60°C with the results shown in table 5.

TABLE 5

Temperature dependence

Temp. °C	45	50	55	60
$10^5 k_1(S^{-1})$	0.505	0.750	1.52	1.20

$[K_2S_2O_8]_0 = [\text{Acetone}]_0 = 0.02M$, $[CuSO_4]_0 = 1.00 \times 10^{-3}M$

The Arrhenius plot is linear and gives

$$k_1 = 4.95 \times 10^8 \text{ exp. } (-95.9/RT) S^{-1}$$

The entropy of activation and heat of activation are −10.8 e.u. mol^{-1} and 93.1 kJ mol^{-1} respectively.

Influence of acids, salts, surface and gases

Table 6 shows that the reaction is retarded by acids, K_2SO_4 and allyl acetate while glass beads accelerate it. Oxygen gas is observed to inhibit the reaction.

TABLE 6

Influence of acids, salts, surface and gases

	Nil	0.05M H_2SO_4	0.05M K_2SO_4	0.05M Allyl acetate	500 Glass beads	in O_2 Atmosphere
$10^5 k_1$ (S^{-1})	1.52	1.35	1.05	0.705	1.87	0.837

$[K_2S_2O_8]_0 = [\text{Acetone}]_0 = 0.02M$, $[CuSO_4]_0 = 1.00 \times 10^{-3}$ M, Temp. 55°C

DISCUSSION

For the interpretation of the kinetic data reported herein few points bear significance.

Cu (II) is known to exist in acetone as a weak complex [21-22] as is evidenced by the pH variation and conductivity studies.

Measurements reveal that the rate of peroxodisulphate disappearance is first order in $[S_2O_8^{2-}]_0$, while a -0.1 and 0.25 dependence in acetone and Cu (II) is observed respectively. The rate determining step therefore involves peroxodisulphate or some species produced therefrom. Since a bimolecular reaction between the oxidant and the catalyst is fuled out on kinetic grounds[23], a reasonable mechanism which accounts ror the faster oxidation rate in the presence of Cu (II) is shown in scheme 1.

Scheme 1

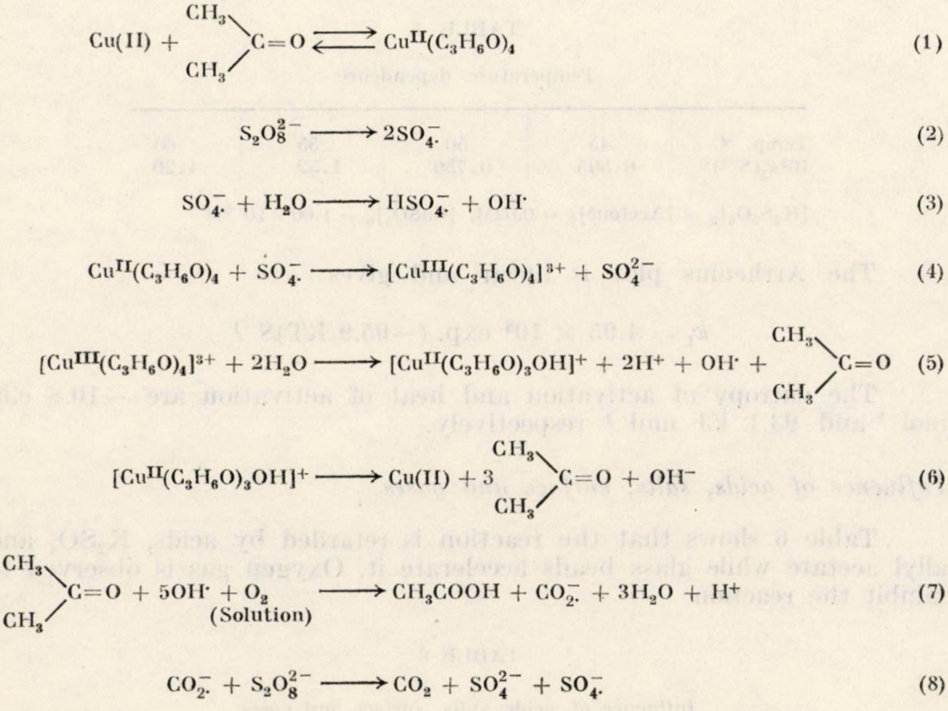

$$\mathrm{Cu(II)} + (CH_3)_2C{=}O \rightleftharpoons Cu^{II}(C_3H_6O)_4 \quad (1)$$

$$S_2O_8^{2-} \longrightarrow 2SO_4^{-\cdot} \quad (2)$$

$$SO_4^{-\cdot} + H_2O \longrightarrow HSO_4^{-\cdot} + OH^{\cdot} \quad (3)$$

$$Cu^{II}(C_3H_6O)_4 + \dot{S}O_4^{-\cdot} \longrightarrow [Cu^{III}(C_3H_6O)_4]^{3+} + SO_4^{2-} \quad (4)$$

$$[Cu^{III}(C_3H_6O)_4]^{3+} + 2H_2O \longrightarrow [Cu^{II}(C_3H_6O)_3OH]^{+} + 2H^{+} + OH^{\cdot} + (CH_3)_2C{=}O \quad (5)$$

$$[Cu^{II}(C_3H_6O)_3OH]^{+} \longrightarrow \mathrm{Cu(II)} + 3\,(CH_3)_2C{=}O + OH^{-} \quad (6)$$

$$(CH_3)_2C{=}O + 5OH^{\cdot} + \underset{\text{(Solution)}}{O_2} \longrightarrow CH_3COOH + CO_2^{-\cdot} + 3H_2O + H^{+} \quad (7)$$

$$CO_2^{-\cdot} + S_2O_8^{2-} \longrightarrow CO_2 + SO_4^{2-} + SO_4^{-\cdot} \quad (8)$$

$$SO_4^{-\cdot} + CO_2^{-\cdot} \longrightarrow CO_2 + SO_4^{2-} \quad (9)$$

It is postulated from scheme 1 that the Cu (II) acetone complex is oxidised to the Cu (III) oxidation state by the $SO_4^{-\cdot}$ radical (reaction 4) as observed by Kovats,[24] Allen[3] and Kimura.[25] It is generally known that the complex formation leads to favourable conditions for the oxidation of metal ion. This is presumably the reason why this causes $SO_4^{-\cdot}$ to oxidise Cu (II) acetone instead of acetone.[16-17]

Catalytic influence of surface such as glass beads may be due to the absorption of the reactants with the result that the concentration of the reactants will increase on the surface and cause enhancement in the velocity of the reaction. Decrease in rate by H_2SO_4 is due to the increasing ionic strength and common ion effect of $SO_4^{-\cdot}$ ions. The retarding effect of neutral salts such as K_2SO_4 is due to the interaction of oppositely charged ions in the rate determining step.

$$K^+ + SO_4^{-\cdot} = KSO_4$$

$$2KSO_4 = K_2S_2O_8$$

Allyl acetate, an effective radical scavenger for the sulphate ion,[28-30] inhibits the reaction considerably. Oxygen is known to inhibit certain chain reactions involving $CO_2^{-\cdot}$ radical[3]; $O_2 + CO_2^{-} = O_2CO_2^{-}$. That $CO_2^{-\cdot}$ is produced, is evident from the fact that the system reduces Hg(II) chloride.

Accordingly, the rate of peroxodisulphate disappearance is given by

$$-\mathrm{d}[S_2O_8^{2-}]/\mathrm{d}t = k_1[S_2O_8^{2-}] + k_7[CO_2^{-\cdot}][S_2O_8^{2-}] \ldots \qquad (1)$$

Applying steady state treatment to the various radicals in the above scheme of reactions, and assuming $k_9 \ll k_2$ in the initial stage, one can derive

$$CO_2^{-\cdot} = -\,k_1 + \sqrt{k_1^2 + 8k_1k_3k_7/k_8(\mathrm{Cu^{II}}[C_3H_6O)_4]}/4k_7$$

Substitution in equation (I) leads to the rate law

$$-\mathrm{d}[S_2O_8^{2-}]/\mathrm{d}t = \{k_1' + k''[\mathrm{Cu^{II}}(C_3H_6O)_4]^{\frac{1}{2}}\}[S_2O_8^{2-}] \qquad (2)$$

Where $k' = 3k_1/4$ and $k'' = (k_1k_3k_7/k_8)^{\frac{1}{2}}$

We can conclude by the rate law (2) that the experimentalresults cannot be entirely justified by the reaction mechanism.

EXPERIMENTAL

All chemicals used were either 'BDH' 'Analar' or E. Merck 'GR' samples. Reactants solutions were prepared in double distilled water. Kinetics were followed by estimating the residual peroxodisulphate iodometrically at different intervals of time.[18] The reaction vessel was fitted with a condenser by which the vapours of acetone could not escape outside.

The $S_2O_3^{2-}$ equivalents of Cu(II) (kept in any experiment) in terms of titre volume (of 0.04N) have been substracted from the observed titre values to obtain $(a - x)$. Table 1 shows how the rate (R) and first order rate constant (k_1) were calculated in a run. Data reported in different tables were similarly evaluated.

REFERENCES

[1] L. B. Morgan, *Trans Faraday Soc.*, **42**, 169 (1946).

[2] C. V. King and O. F. Steinbach, *J. Amer. Chem. Soc.*, **52**, 4779 (1931).

[3] E. Ben-Zvi and T. L. Allen, *J. Amer. Chem. Soc.*, **83**, 4352 (1961).

[4] Y. K. Gupta and S. Ghosh, *J. Inorg. Nuclear Chem.*, **11**, 62 (1959).

[5] A. P. Bhargava, Y. K. Gupta and K. S. Gupta, *J. Inorg. Nuclear Chem.*, **31**, 777 (1969).

[6] A. P. Bhargava, R. Swaroop and Y. K. Gupta, *J. Chem. Soc.*, 2183 (1970).

[7] H. S. Samant and S. P. Srivastava, *Proc. Nat. Acad. Sci.*, India, **27**, 282 (1958).

[8] D. L. Ball, M. M. Crutchfield and J. O. Edwards, *J. Org. Chem.*, **25**, 1599 (1960).

[9] J. O. Edwards and A. P. Gallopo, *J. Org. Chem.*, **36**, 4089 (1971).

[10] A. G. Khachatryan, N. M. Beileryan and D. A. Chaltykyan, *Doklady Akad. Nauk. Armyan S.S.R.*, **54**, 249 (1972).

[11] S. C. Agarwal and L. K. Saxena, *Indian J. Chem.*, **16A**, 602 (1978).

[12] S. C. Agarwal, G. Chandra and S. K. Jha, *J. Inorg. Nuclear Chem.*, **41**, 899 (1979).

[13] S. C. Agarwal and L. K. Saxena, *J. Inorg. Nuclear Chem.*, **42**, 932 (1980).

[14] S. C. Agarwal, R. S. Pal and V. B. Agarwal, *Bull. Soc. chim, France*, **1979**, 143.

[15] (i) W. K. Wilmarth and A. Haim, "Mechanism of Oxidation by Peroxodisulphate Ion" ("Peroxide Reaction Mechanism" by J. O. Edwards) Conference Rhode Island, 1960, p. 175 ; (ii) D. A. House, *Chem. Rev.*, **62**, 185 (1962).

[16] E. Bekier and S. W. Kijowski, *Roczniki Chem.*, **15**, 136 (1935).

[17] K. C. Khulbe and S. P. Srivastava, *Agra University Res. J. (Sci)*, **9**, 177 (1960).

[18] L. K. Saxena and C. P. Singhal, *Agra Univ. J. Res. (Sci)*, **6**, 43 (1957).

[19] F. Fiegl, "Spot Test in Organic Analysis", 6th ed., Elsevier publishing Co., New York, 1960, p. 353.

[20] (i) G. Chandra and S. N. Srivastava, *J. Inorg. Nuclear Chem.*, **34**, 197 (1972) ; (ii) R. L. Eagar and C. A. Winkler, *Canad. J. Res.*, **268**, 527 (1948) ; (iii) M. C. Agarwal and S. P. Mushran, *J. Ind. Chem. soc.*, **42**, 629 (1965) ; ibid, **43**, 343 (1966).

[21] A. E. Martell and M. Calvin, "Chemistry of the Metal Chelate Compounds", Prentice-Hall, Inc., Englewood Cliffs New York, 1952.

[22] T. Moelter, Inorganic Chemistry ; An Advanced Text Book", Asia Publishing House, Bombay, 1962.

[23] S. C. Agarwal and L. K. Saxena, *Agra Univ. J. Res (Sci)*, **23**, 53 (1974).

[24] Z. Kovats, *Magyar Kém. Fólyóirat*, **66**, 181 (1960).

[25] Misaru Kimura, *J. Phys. Chem.*, **77**, 1265 (1973).

[26] W. C. Vasudeva, M. F. Iaha and E. Wasif, *J. Inorg. Nuclear Chem.*, **34**, 3159 (1972) ; *Carbohydrate Res.*, *2*, 175 (1966).

[27] W. V. Vasudeva, Ph. D. Dissertation, Agra University, Agra (1971).

[28] H.G.S. Senger and Y. K. Gupta, *Indian J. Chem.*, **6**, 119 (1968).

[29] A. Sabesman, and N. Venkatasubramanian, *Indian J. Chem.*, **9**, 942, (1971).

[30] M. G. Ram Reddy, B. Sethuram and T. N. Rao, *Indian J. Chem.*, **16A**, 31 (1978).

Revue Roumaine de Chimie, 27, 2, 273–279 (1982)

CONTRIBUTION À L'ÉTUDE DE QUELQUES HÉTÉROCYCLES. LI *)

L'OBTENTION DE QUELQUES 2-PHÉNYL-5-R-THIAZOLO [3,2-*b*]-1,2,4-TRIAZOLES

I. SIMITI et AURELIA MĂRIE
Institut de Médecine et Pharmacie, Cluj-Napoca
Laboratoire de Chimie Organique
Str. V. Babeş 41, Romania

Reçu le 17 Mai 1979

Dans cet ouvrage on étudie l'obtention de quelques nouveaux thiazolo [3,2-*b*]-1,2,4-triazoles avec divers substituents dans la position 5 du système bicyclique comme : $-CH_3$; $-CH_2Cl$; $-CH_2OH$; $-CHO$.

The present paper deals with the preparation of some new thiazolo [3,2-*b*]-1,2,4-triazoles having various substituents in position 5 of the bicyclic system like : $-CH_3$; $-CH_2Cl$; $-CH_2-OH$; $-CHO$.

Puisque dans un travail antérieur on s'est occupé de la synthèse de quelques thiazolo [4,5-*d*]-pyridazines, [1] on a considéré nécessaire de poursuivre les recherches par l'obtention de quelques thiazolo [3,2-*b*]-1,2,4-triazoles, afin d'obtenir certaines substances potentiellement bioactives, d'autant plus que des substances à une structure semblable comme TETRAMISOL, LEVAMISOL, sont connues comme des substances ayant une action antihelmintique.

Pour obtenir ces composés, on a considéré que la meilleure voie serait la condensation du 5-mercapto-1,2,4-triazole avec des composés α-halocarbonyliques [2] du fait que les mercapto-triazoles renferment les deux hétéroatomes (S, N) de la composante nucléophile.

Essayant de condenser le 3-phényl-5-mercapto-1,2,4-triazole [4] (I) avec la mono et dichloroacétone (II) dans une solution acétonique, on a obtenu des composés du type III sous la forme de chlorhydrates.

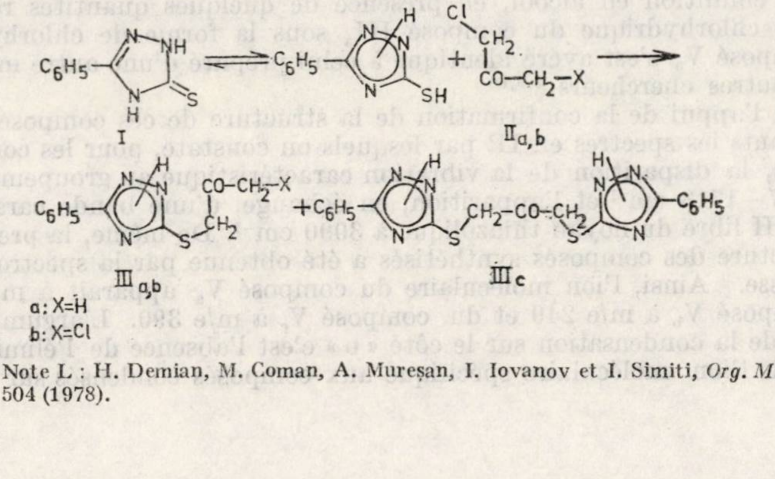

---

*) Note L : H. Demian, M. Coman, A. Mureşan, I. Iovanov et I. Simiti, *Org. Mass Spectrom.*, **9**, 504 (1978).

Le composé III_c a été obtenu en mélange avec le composé III_b uniquement dans le cas de la condensation avec de la dichloroacétone.

Contrairement à la N-arythio-urée[5] et aux benzaldéhyd-thiosemicarbazones[6] qui, avec la dichloroacétone forment directement, dans les mêmes conditions, des dérivés thiazoliques, tandis que les arylthioamides conduisent aux Δ_2-thiazolines correspondantes,[7] les composés obtenus par nous, dans ce cas-là, ne sont pas thiazoliques.

Les composés acycliques obtenus donnent des réactions caractéristiques au carbonyl et présentent en IR la bande caractéristique au groupement CO entre 1713–1727 cm^{-1}.

La séparation des composés III_b et III_c a été réalisée par des recristallisations répétées, de leur mélange du benzène. La meilleure séparation a été cependant obtenue par l'acétylation du mélange et la séparation des acétyldérivés, en raison de la différence de leur solubilité dans l'alcool.

Les composés III_{a-c} de même que les dérivés acétylés IV_{a-c} traités à l'acide sulfurique concentré[7,8] à froid conduisent aux thiazoles correspondants V_{a-c}. Le composé V_c s'est avéré identique à celui préparé par la condensation dans le milieu alcalin de I avec V_b.

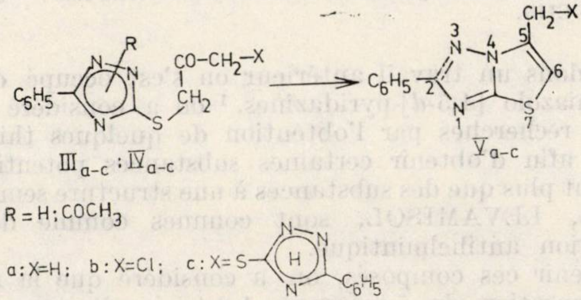

III_{a-c} ; IV_{a-c}

V_{a-c}

R = H; $COCH_3$

a: X=H; b: X=Cl; c: X=S–

Tenant compte de l'obtention des composés S-acétonyliques III_{a-c} et de leur cyclisation ultérieure, on peut supposer que la réaction de Hantzsch a lieu en deux étapes et, étant donné la différence de nucléophylicité entre N et S, la première attaque est celle du soufre.[7]

On doit mentionner que le composé V_a a été obtenu également par simple ébullition en alcool, en présence de quelques quantités réduites d'acide chlorhydrique du composé III_a sous la forme de chlorhydrate. Le composé V_a s'est avéré identique à celui préparé d'une autre manière, par d'autres chercheurs.[3,9,10]

A l'appui de la confirmation de la structure de ces composés, sont concluants les spectres en IR par lesquels on constate, pour les composés cyclisés, la disparition de la vibration caractéristique au groupement CO de 1727–1713 cm^{-1} et l'apparition, en échange, d'une bande caractéristique CH libre du noyau thiazolique à 3090 cm^{-1}. De même, la preuve de la structure des composés synthétisés a été obtenue par la spectrométrie de masse. Ainsi, l'ion moléculaire du composé V_a apparaît à m/e 215, du composé V_b à m/e 249 et du composé V_c à m/e 390. L'argument en faveur de la condensation sur le côté « b » c'est l'absence de l'élimination du N_2 de l'ion moléculaire spécifique aux composés condensés sur le côté

« c » du triazole, avec d'autres hétérocycles. Les spectres de masse de ces dérivés font l'objet d'étude d'un autre travail.[11]

Par l'hydrolyse, le composé V_b donne l'hydroxyméthyle dérivé VI qui, par oxydation avec du bichromate de sodium dans de l'acide acétique donne le formyl dérivé VIII obtenu à son tour par la réaction Sommelet, par l'intermédiaire du sel d'urotropine IX. Cependant, on doit mentionner que par réaction Sommelet le rendement est très réduit et la purification difficile. Le dérivé hydroxyméthyle, de même que l'aldéhyde ont été caractérisés par leurs dérivés fonctionnels correspondants. De même, on a réussi à réduire le composé V_b avec du zinc en acide acétique, pour le dérivé V_a.[12]

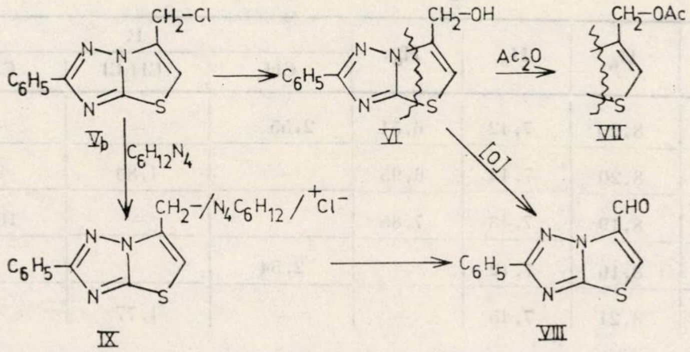

Les composés V_a et V_b par bromuration en acide acétique avec du Br_2 forment des bromodérivés correspondants dans la position 6 du système bicyclique. C'est à remarquer que la vitesse de bromuration du composé V_b est plus réduite que celle du composé V_a. La position du brome a été confirmée par la spectrométrie de masse. Le pic moléculaire des composés X et XI est en concordance avec le poids moléculaire des composés (m/e 293 respectivement m/e 327). L'apparition dans le cas des deux composés du pic m/e 123 ($Br-C\equiv S^+$) est la preuve de la présence du brome, dans la position 6 du système condensé.

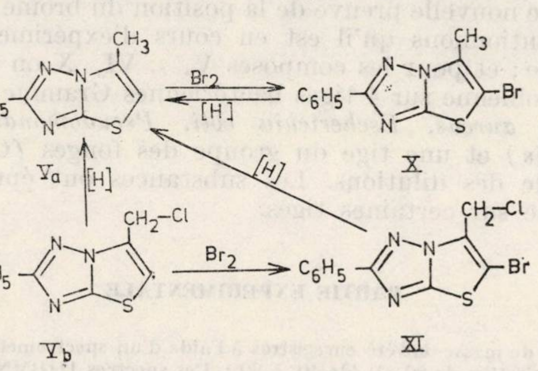

On a enregistré aussi les spectres RMN en $CDCl_3$ pour les composés V_a, V_b, VIII, X, XI (tableau 1).

Les protons phényliques, comme on peut observer dans le tableau, apparaissent dans tous les cas aux mêmes valeurs. Les deux protons de la position *ortho* par rapport au triazole (H_a) apparaissent comme un multiplet étroit, à peu près quartet, peu résolu, dû au déplacement provoqué par les autres 3 protons à peu près équivalents aux valeurs δ comprises entre 8,16–8,21.

TABLEAU 1

Les spectres RMN des composés V_a, V_b, VIII, X, XI exprimés en δ ppm

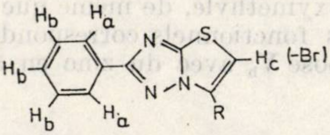

	H_a	H_b	H_c	R		
				CH_3	CH_2Cl	CHO
V_a	8,20	7,42	6,51	2,55	—	—
V_b	8,20	7,44	6,95	—	4,80	—
VIII	8,19	7,43	7,85	—	—	10,02
X	8,16	7,42	—	2,54	—	—
XI	8,21	7,45	—	—	4,77	—

Les trois protons de la position *méta* et *para* par rapport au triazole (H_b) donnent pratiquement un seul signal, multiplet étroit, à peu près triplet peu résolu dû au fendage provoqué par les deux protons équivalents aux valeurs comprises entre 7,42–7,45. Le proton de l'hétérocycle, fonction du voisinage des groupements $-CH_3$; $-CH_2-Cl$; $-CHO$; est de plus en plus désécrané (6,51 ; 6,95 respectivement 7,85).

Dans le cas des composés X et XI le signal du proton H_c disparaît constituant une nouvelle preuve de la position du brome dans la molécule.

Nous mentionnons qu'il est en cours d'expérimentation l'activité antihelmintique ; et pour les composés V_{a-c}, VI, X on a déterminé l'activité antimicrobienne sur 4 tiges bactériennes Gramme + et Gramme – *(Staphylococus aureus*, *Escherichia coli*, *Pseudomonas aeruginosa* et *Bacillus subtilis)* et une tige du groupe des fonges *(Candida albicans)* par la méthode des dilutions. Les substances ont éprouvé une action antimicrobienne sur certaines tiges.

PARTIE EXPÉRIMENTALE

Les spectres de masse ont été enregistrés à l'aide d'un spectromètre VARIAN MAT 111 à un potentiel d'ionisation de 80 eV (de 40° à 90°). Les spectres 1HRMN ont été enregistrés à l'aide d'un spectromètre TESLA BS 487C 80 MHz en utilisant $CDCl_3$ comme solvant et DMS comme solvant de référence. Les spectres IR ont été enregistrés en pastille de KBr à l'aide d'un spectromètre IR 27 G Shimadzu.

3-Phényl-5-S-acétonyl-1,2,4-triazole III_a

0,88 g (0,005 mol) I est dissous en 15 ml d'acétone, en y ajoutant 0,52 g (0,0055 mol) de monochloroacétone. Après un repos de 24 h III_a dépose sous forme de chlorhydrate. P.F. = 89–90°.

$C_{11}H_{11}N_3OS\ HCl$

N% calculé = 15,05 ; trouvé = 14,74.

Le chlorhydrate III_a se décompose en solution de carbonate de sodium, quand il dépose la base correspondante III_a.

L'obtention et la séparation des composés III_b *de* III_c. $C_{11}H_{10}ClN_3OS$ et $C_{19}H_{16}N_6OS_2$

0,88 g (0,005 mol) I est dissous en 15 ml d'acétone et ajouté ensuite à 0,68 g (0,0055 mol) de dichloroacétone dissous en 5 ml d'acétone. On le laisse au repos pendant 24 h. Il dépose le mélange III_b et III_c sous la forme de chlorhydrates qui sont traités par une solution de carbonate de sodium lorsqu'on obtient le mélange de III_b et III_c sous la forme de base.

a) Le mélange de bases III_b et III_c est séparé par ébullition avec du benzène. Le composé III_b est soluble en benzène à chaud, tandis que III_c moins soluble, reste, en grande partie, sur le filtre.

b) Le mélange III_b et III_c après une courte ébullition avec de l'anhydride acétique se transforme en acétyldérivés correspondants. L'acétyldérivé IV_b est soluble en alcool, tandis que l'acétyldérivé IV_c est insoluble.

TABLEAU 2

3-Phényl-5-SR-1,2,4-triazoles

Composé*)	Formule brute	P.F.°C	N%		IR cm^{-1}
			calculé	trouvé	C=O
III_a	$C_{11}H_{11}N_3OS$	147	18,01	17,79	1727
III_b	$C_{11}H_{10}ClN_3OS$	67–68	15,69	15,51	1727
III_c	$C_{19}H_{16}N_6OS_2$	210–211	20,57	20,52	1713

---

*) III_a—recristallisation de l'alcool aqueux ; III_b, III_c-recristallisation du benzène.

TABLEAU 3

3-Phényl-5-SR-N-acetyl-1,2,4-triazoles

Composé*)	Formule brute	P.F.°C	N%		IR cm^{-1}
			calculé	trouvé	C = O
IV_a	$C_{13}H_{13}N_3O_2S$	106	15,26	15,21	1723
IV_b	$C_{13}H_{12}ClN_3O_2S$	127–129	13,56	13,20	1723
IV_c	$C_{23}H_{20}N_6O_3S_2$	191–192	17,06	16,97	1723 1727

---

*) IV_a — recristallisation de l'alcool ; IV_b—recristallisation de l'alcool aqueux ; IV_c—recristallisation de l'acide acétique.

2-Phényl-5-méthyl-thiazolo[3,2–b]-1,2,4-triazole (V_a)

a) 0,23 g (0,001 mol) III_a sous forme de chlorhydrate est dissous dans 10 ml d'alcool absolu ; on y ajoute 0,1 ml d'acide chlorhydrique concentré et l'on porte à l'ébullition en réflux pendant une heure. On obtient le chlorhydrate de V_a qui fond à 154–155°.

$C_{11}H_9N_3S \cdot HCl$

N% calculé = 16,69 ; trouvé = 16,42.

Par la décomposition de ce clorhydrate d'une solution de carbonate de sodium on obtient V_a.

b) 0,23 g (0,001 mol) III_a est traité avec 1 ml d'acide sulfurique concentré, par refroidissement à glace, ensuite on agite, jusqu'à ce qu'il entre complètement en solution. Le mélange de réaction est laissé au repos à la température de la chambre pendant 1 h, ensuite il est versé sur de la glace et il dépose le dérivé thiazolique correspondant V_a.

On a obtenu, de manière similaire, les composés V_b et V_c présentés dans le tableau 4.

TABLEAU 4

2-Phényl-5-R-thiazole[3,2-*b*]-1,2,4-triazoles

Composé[*]	Formule brute	P.F.°C	Analyse {calculé trouvé				
			C	H	Cl	N	S
V_a	$C_{11}H_9N_3S$	126[1]	61,03 61,20	4,21 4,55	— —	19,51 19,29	14,88 14,98
V_b	$C_{11}H_8N_3SCl$	134–135	52,91 53,11	3,22 3,65	14,19 13,80	16,83 16,59	12,80 12,65
V_c	$C_{19}H_{14}N_6S_2$	113–114	— —	— —	— —	21,52 21,35	— —

---

[*] V_a, V_c—recristallisation de l'alcool aqueux ; V_b—recristallisation de l'alcool.

[1] Lit [3] : P.F. = 125–126° ; Lit [10] : P.F. = 123°.

2-Phényl-5-hydroxyméthyl-thiazolo[3,2–b]-1,2,4-triazole. (VI)

2,49 g (0,01 mol) V_b est maintenu en ébullition avec 200 ml d'eau pendant 20 h. Il est filtré à chaud et par refroidissement, il dépose le dérivé VI recristallisé de l'alcool aqueux. P.F = 162°.

$C_{11}H_9N_3OS$

Calculé % : C = 57,12 ; H = 3,94 ; N = 18,17 ; S = 13,86.

Trouvé % : C = 57,31 ; H = 4,29 ; N = 18,30 ; S = 13,78.

2-Phényl-5-hydroxyméthyl-thiazolo/3,2-b/-1,2,4-triazole (VI), par courts ébullition dans l'anhydride acétique a donné l'acétyldérivé VII qui après recristallisation de l'alcool fond à 93°. N% calculé = 15,41 ; trouvé = 15,24.

2-Phényl-5-formyl-thiazolo[3,2-b]-1,2,4-triazole. (VIII)

a) 0,23 g (0,001 mol) VI est dissous en 5 ml d'acide acétique glacial et ensuite on y ajoute une solution de 0,12 g bichromate de sodium légèrement réchauffée dans un bain d'eau pendant 10 minutes, on laisse au repos pendant 1 h, ensuite, versée sur de la glace, elle dépose une substance, VIII qui, après recristallisation de l'alcool aqueux fond à 174°.

$C_{11}H_7N_3OS$

Calculé % : C = 57,62 ; H = 3,07 ; N = 18,32 ; S = 13,98.

Trouvé % : C = 58,00 ; H = 3,35 ; N = 18,56 ; S = 14,10. IR cm^{-1} 1685 (C=O) ; *Oxime* : P.F. = 217–218° ; N% calculé = 22,94 ; trouvé = 22,88.

2,4-Dinitrophénylhydrazone : P.F. = 280—281° N% calculé = 23,96 ; trouvé = 14,14

b) 0,50 g (0,002 mol) V_b est dissous en 5 ml chloroforme, on y ajoute 0,40 g d'urotropine. Tout est maintenu en ébullition pendant 2 h, après quoi, par refroidissement on obtient du sel d'urotropine IX avec P.F. = 222—224°.

N% calculé = 25,14 ; trouvé = 25,19.

On dissout 0,60 g sel d'urotropine en 10 ml d'acide acétique 50% ; on y ajoute 0,20 g d'urotropine et on le maintient en ébullition pendant 45 minutes. La solution est versée en eau et on l'extrait avec de l'éther. La solution éthérique est neutralisée, quand elle dépose une substance visqueuse très difficile à purifier. C'est pour cela que le produit a été caractérisé sous la forme de 2,4-dinitrophénylhydrazone qui, après recristallisation de l'acide acétique, fond à 278—280°

N% calculé = 23,96 ; trouvé = 24,00.

2-Phényl-5-méthyl-6-bromo-thiazolo[3,2-b]-1,2,4-triazole (X)*)

1,1 g (0,005 mol) V_a est dissous en 10 ml d'acide acétique glacial et traité ensuite avec 1,13 g (0,0075 mol) Br_2. Après avoir laissé la solution au repos pendant 24 h, elle est versée dans l'eau, quand elle dépose le bromodérivé correspondant qui, après recristallisation de l'alcool, fond à 157—158°.

$C_{11}H_8BrN_3S$

Calculé % : C = 44,91 ; H = 2,74 ; Br = 27,16 ; N = 14,28 ; S = 10,89.

Trouvé % : C = 45,13 ; H = 3,24 ; Br = 26,90 ; N = 14,04 ; S = 11,22.

On a préparé de manière semblable le composé XI qui, après recristallisation de l'alcool, fond à 188—189°.

$C_{11}H_7BrClN_3S$

Calculé % : C = 40,19 ; H = 2,14 ; Br = 24,30 ; Cl = 10,77 ; N = 12,78 ; S = 9,75.

Trouvé % : C = 39,96 ; H = 2,49 ; Br = 24,25 ; Cl = 10,37 ; N = 12,55 ; S = 9,65.

BIBLIOGRAPHIE

[1] I. Simiti et M. Coman, *Arch. Pharm.*, **311**, 480 (1978).

[2] W. V. Dymek, B. Janik, A. Cygankiewicz et H. Gawron, *Acta Pol. Phärm.*, **24**, 97 (1967) ; *Chem. Abstr.*, **68**, 78208 (1968).

[3] K. T. Potts et S. Husain, *J. Org. Chem.*, **36**, 10 (1971).

[4] E. Hoggarth, *J. Chem. Soc.*, 1163 (1949).

[5] I. Simiti, M. Farkas et S. Silberg, *Chem. Ber.*, **95**, 2672 (1962).

[6] I. Simiti et M. Coman, *Bull. Soc. chim. France*, **9**, 3276 (1969).

[7] I. Simiti, M. Coman et I. Schwartz, *Rev. Roumaine Chim.*, **18**, 685 (1973).

[8] Al. Silberg, I. Simiti et H. Mantsch, *Chem. Ber.*, **94**, 2287 (1961).

[9] Y. Tamura, H. Hayashi, J. H. Kim et M. Ikeda, *J. Heterocyclic Chem.*, **10**, 947 (1973).

[10] U. V. Bramond, N. T. G. Surendra et V. R. Srinivasan, *Sythesis*, **4**, 288 (1978).

[11] I. Simiti, H. Demian, A. Marie et N. Palibroda, *Org. Mass Spectrom*, 15, **4**, 172 (1980).

[12] I. Simiti et H. Demian, *Ann. Chim. (France)*, **10**, 317 (1975).

[13] Y. Tamura, H. Hayashi, E. Saeki, J. H. Kim et M. Ikeda, *J. Heterocyclic Chem.*, **11**, 459 (1974).

---

*) Le composé X est connu dans la littérature [13] mais on l'a préparé d'une autre manière (P.F. = 155—156°).

Revue Roumaine de Chimie, **27**, *2*, 281 – 284 (1982)

REACTIONS OF SYDNONES*

BHARATI V. BADAMI and GURUBASAV S. PURANIK
Department of Chemistry, Karnatak University, Dharwad-580003
India

Received July 1, 1980

In a single step reaction 2-methyl-indole-3-acetic acid is prepared starting with 3-phenylsydnone and levulinic acid. A facile synthesis of the bromo-, chloro- and methoxy-substituted tetrahydrocarbazoles has been carried out from the corresponding substituted 3-phenylsydnones.

INTRODUCTION

Sydnones undergo hydrolysis with acids giving rise to the corresponding hydrazines or their N-substituted hydrazines. [1,2] This has been recommended as a general and convenient method of converting the primary amines in to the corresponding hydrazines, especially when the hydrazines are otherwise difficult to prepare. [3] These hydrazines could be converted into the tetrahydrocarbazoles *in situ*. [4]

Taking advantage of the above reaction, various substituted sydnones have been used to prepare the tetra-hydrocarbazoles without isolating the hydrazines or the corresponding hydrazones. Various bromo-, chloro-, methoxy- and nitro-substituted tetrahydrocarbazoles (I) have been synthesized where the hydrazone precursors are difficult to isolate by usual methods. This method offers an advantage over the earlier methods, [5,6] wherein the hydrazones were isolated and cyclized with the appropriate acidic reagents. Moreover, the formation of isomers or less pure compounds (as reported earlier) could be avoided.

Following the above method of utilizing the hydrazones *in situ*, for the first time 3-phenylsydnone has been converted into 2-methyl-indole-3-acetic acid through hydrolysis and reaction with levulinic acid.

The difficulty of preparing 5-halogenopyrazoles has been pointed out earlier. [7] Various substituted 3-phenyl sydnones have been subjected to bromination and chlorination (II) by literature methods [7,8] and these halogen derivatives are further subjected to 1,3-dipolar addition reaction with dimethyl acetylene dicarboxylate to give the corresponding 5-bromo- and 5-chloro substituted pyrazole dicarboxylates (III).

* This work has been partly financed by the Karnatak University under the scheme "Research in Karnatak University during the Five Year Plan Period".

EXPERIMENTAL

2-Methyl-indole-3-aceticacid

3-Phenylsydnone (3.24 g) was added to a mixture of hydrochloric acid, ethanol and water (10.0 ml each) and the reaction mixture was heated for 20 minutes on a water-bath. Levulinic acid (1.96 g) was added and heated for another 3 hours. Then the black slurry was dissolved in warm NaOH solution and acidified with acetic acid. The separated crystals of indolyl acetic acid were filtered and crystallized from benzene and petroleum ether; yield — 1.2 g; m.p. 190°C; literature [9] m.p. 195°C.

Tetrahydrocarbazoles

Sydnone (0.01 mole) was added to a mixture of hydrochloric acid, ethanol and water (10.0 ml each) and the reaction mixture was heated for 20 minutes on a water-bath. On addition of cyclohexanone (0.01 mole) the carbazole began to separate within few minutes. The solid was then crystallized from aqueous ethanol. The results are set out in Table 1. Yields are in the range of 50—55%. The physical constants and the spectral data are in agreement with the values reported in the literature (Campaigne et al. 1959 and Deorha et al. 1961).

TABLE 1

Tetrahydrocarbazoles

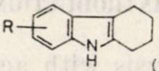

(I)

Compound R	Formula	m.p. °C	Analytical data			
			Req. %		Found %	
			C	H	C	H
H	$C_{12}H_{13}N$	146	84.21	7.60	84.10	7.54
8-Meo	$C_{13}H_{15}NO$	b.p. 205°/154	77.61	7.46	77.52	7.40
6-Meo	$C_{13}H_{15}NO$	92	77.61	7.46	77.50	7.30
6-Chloro	$C_{12}H_{12}NCl$	130	70.07	5.83	69.50	5.75
7-Bromo	$C_{12}H_{12}NBr$	150	57.60	4.80	57.50	4.75
8-Chloro	$C_{12}H_{12}NCl$	56	70.07	5.83	69.85	5.72
8-Nitro	$C_{12}H_{12}N_2O_2$	149	66.60	5.50	66.55	5.40
6-Nitro	$C_{12}H_{12}N_2O_2$	147	66.60	5.50	66.45	5.28
7-Nitro	$C_{12}H_{12}N_2O_2$	152	66.60	5.50	66.30	5.48
7-Chloro	$C_{12}H_{12}NCl$	181	70.07	5.83	69.80	5.70

Chlorination

A solution of sydnone (0.1 mole) and N-chlorosuccinimide (0.011 mole) in methanol (100 ml) was stirred for 5—10 minutes at room temperature. Evaporation of methanol furnished a slurry which was poured into water and then extracted with chloroform. Evaporation of the chloroform extracts gave a residue which was crystallized from alcohol. The 4-chloro-sydnones are listed in Table 2.

Pyrazoles

To a solution of sydnone (0.5 g) in dry xylene (20 ml) dimethyl acetylenedicarboxylate (1.0 ml) was added and the mixture was heated till the evolution of CO_2 ceased. Xylene was removed under pressure and the excess of dimethyl acetylenedicarboxylate was washed several

TABLE 2

4-Chlorosydnones

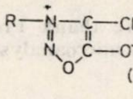
(II)

Compound R	Formula	m.p. °C	Analytical data			
			Calc. %		Found %	
			C	H	C	H
o-Meo-C_6H_4	$C_9H_7ClN_2O_3$	92	47.68	3.09	47.26	2.80
o-NO_2-C_6H_4	$C_8H_4ClN_3O_4$	128	39.76	1.63	39.11	2.00
m-NO_2-C_6H_4	$C_8H_4ClN_3O_4$	120	39.76	1.63	39.31	2.16
o-Cl-C_6H_4	$C_8H_4Cl_2N_2O_2$	115	41.60	1.80	41.02	2.10
m-Cl-C_6H_4	$C_8H_4Cl_2N_2O_2$	98	41.60	1.80	41.26	2.31

times with petroleum ether. The residue crystallized from petroleum ether (80—100°). The pyrazoles thus obtained are listed in Table 3.

TABLE 3

Pyrazoles

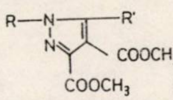
(III)

Compound		Formula	m.p. °C	Analytical data			
R =	R′			Calc. %		Found %	
				C	H	C	H
o-Meo-C_6H_4	H	$C_{14}H_{14}N_2O_5$	72	57.93	4.82	57.89	4.49
o-Meo-C_6H_4	Br	$C_{14}H_{13}BrN_2O_5$	115	45.56	3.52	46.20	3.85
o-Meo-C_6H_4	Cl	$C_{14}H_{13}ClN_2O_5$	75	51.71	4.00	50.85	3.80
o-NO_2-C_6H_4	H	$C_{13}H_{11}N_3O_6$	145	51.17	3.60	51.02	3.80
o-NO_2-C_6H_4	Br	$C_{13}H_{10}BrN_3O_6$	90	40.62	2.60	40.22	2.30
o-NO_2-C_6H_4	Cl	$C_{13}H_{10}ClN_3O_6$	105	45.95	2.94	46.22	2.63
m-NO_2-C_6H_4	H	$C_{13}H_{11}N_3O_6$	140	51.17	3.60	51.22	3.70
m-NO_2-C_6H_4	Br	$C_{13}H_{10}BrN_3O_6$	128	40.62	2.60	40.15	2.24
m-NO_2-C_6H_4	Cl	$C_{13}H_{10}ClN_3O_6$	125	45.95	2.94	45.27	2.65
o-Cl-C_6H_4	H	$C_{13}H_{11}ClN_2O_4$	75	53.01	3.73	52.61	3.60
o-Cl-C_6H_4	Br	$C_{13}H_{10}BrClN_2O_4$	105	41.77	2.67	41.20	2.30
o-Cl-C_6H_4	Cl	$C_{13}H_{10}Cl_2N_2O_4$	110	47.44	3.04	46.90	2.80
m-Cl-C_6H_4	H	$C_{13}H_{11}ClN_2O_4$	96	53.01	3.73	53.00	3.69
m-Cl-C_6H_4	Br	$C_{13}H_{10}BrClN_2O_4$	160	41.77	2.67	41.75	2.60
m-Cl-C_6H_4	Cl	$C_{13}H_{10}Cl_2N_2O_4$	75	47.44	3.04	47.40	3.00

Spectral data

The infrared spectrum of 4-halogenosydnones showed the absence of a band at *ca* 3100 cm^{-1}, which is very typical of sydnone C—H. The carbonyl absorption (usually at 1750—1790 cm^{-1}), however, showed some positional changes.

The infrared spectrum of dimethyl-(1-arylpyrazole)-3,4-dicarboxylates showed absorptions (nujol) at 1750 and 1740 cm^{-1} ($COOCH_3$).

The indolyl acetic acid showed two prominent bands; one at 3500 cm^{-1} (NH) and another at 1690 cm^{-1}(C=0).

The tetrahydrocarbazoles showed a prominent peak at *ca* 3330 cm^{-1}(NH).

ACKNOWLEDGEMENT. We thank Professor E. S. Jayadevappa for encouragement, Mr. V. A. Desai for microanalyses and the authorities of the University for financial assistance.

REFERENCES

[1] R. A. Eade and J. C. Earl, *J. Chem. Soc.*, **1946**, 591.
[2] J. Kenner and K. Mackay, *Nature*, **160**, 465 (1947).
[3] J. Fugger, J. M. Tien and I. M. Hunsberger, *J. Amer. Chem. Soc.*, **86**, 463 (1964).
[4] D. P. Ainsworth and H. Suschitzky, *J. Chem. Soc. (C)*, **1967**, 315.
[5] E. Campaigne and R. D. Lake, *J. Org. Chem.*, **24**, 478 (1959).
[6] D. S. Deorha and S. S. Joshi, *J. Org. Chem.*, **26**, 3527 (1961).
[7] B. V. Badami and G. S. Puranik, *Indian J. Chem.*, **12**, 671 (1974).
[8] G. S. Puranik and H. Suschitzky, *J. Chem. Soc. (C)*, **1967**, 1006.
[9] I. G. Farbenindustrie, A. G. Brit, 517, 692 Feb. 6 (1940); *Chem. Abstr.*, **35**, 7107 (1941).

Revue Roumaine de Chimie, 27, 2, 285–290 (1982)

CALCULOS CONFORMACIONALES DE ALGUNOS ISOMEROS AZO DE LA BILIRRUBINA II.[1]

DERIVADO 3'-METIL-4'-VINIL*

MANUEL RUBIO,* RAÚL CETINA y MANUEL SALMÓN
Instituto de Química, Universidad Nacional Autónoma de México, México 20, D.F.

Recibido junio 12, 1980

Se presenta el análisis conformacional por cálculo de un derivado azo de la bilirrubina en sus — configuraciones *Z y E*, utilizando el método PCILO. Los resultados muestran el predominio de la configuración *Z* en este tipo de compuestos. Se presenta — la conformación más estable de los grupos funcionales y la población electrónica del isómero *Z*. La barrera de energía (> 200 kcal/mol) para la conversión $Z \rightarrow E$ sugiere que no es posible un proceso térmico para tal transformación. El momento dipolar de la configuración E indica que esta forma es la más polar.

A theoretical conformational analysis of an azobilirubin isomer in both *E* and *Z* configurations was performed using the PCILO method. The results showed that the *Z* configuration is the predominant form of these compounds. The most stable functional groups conformation and *Z* electronic population are reported. The energy barrier (higher than 200 kcal/ mol) for the *Z*–*E* conversion suggests that thermal transformation is unlikely. The *E*-configuration is found to be more polar than *Z* one, as can be judged from the theoretical dipole moment obtained.

INTRODUCCIÓN

No obstante que la estructura de la bilirrubina ha sido elucidada y demostrado que tiene una configuración $Z-Z$ en el cristal, [2,3] existe un considerable interés en la configuración y conformación de sus isómeros geométricos $Z-E$, $E-Z$ y $E-E$, los cuales son generados por irradiación de la bilirrubina IX α con luz visible, de acuerdo con el estudio realizado por Lightner, Wooldridge y McDonagh. [4] Estos autores concluyen que dichos isómeros son más polares, menos lipofílicos y posiblemente más ácidos que el pigmento natural y que en consecuencia, el proceso de formación de la denominada fotobilirrubina es cuantitativamente el más importante y fundamental en la fototerapia de la ictericia en los recién nacidos.

Tales hechos y los resultados encontrados por nosotros en un estudio previo [1] motivan el presente trabajo, en el que efectuamos el análisis conformacional y cálculo de la estructura electrónica del ácido 4-metil-5-

---

* Contribución No. 564 del Instituto de Química, U.N.A.M.

[(3-metil-5-oxo-4-vinil-3-pirrolin-2-ilideno)metil]-2-(fenilazo)-pirrol-3-propiónico, el cual es un fragmento azo derivado de la bilirrubina que experimentalmente puede ser separado y caracterizado sin modificación de su configuración original.[5]

MÉTODO Y CÁLCULOS

Para nuestros propósitos hemos utilizado el método PCILO (Perturbative Configuration Interaction using Localized Orbitals).[6] Las longitudes de enlace y ángulos usados en todos los cálculos fueron tomados del primer trabajo de esta serie.[1]

El isómero azo de la bilirubina tiene, entre otros, seis grados de libertad de torsión importantes, definidos por medio de los ángulos diedros τ_1 (C4′ – C3′ – C13 – H13), τ_2 (C3′ – C4′ – C11 – C12), τ_3 (C2′ – C10 – C5 – C4), τ_4 (C3 – C8 – C7 – C6), τ_5 (C2 – C3 – C8 – C7) y τ_6 (C3 – C2 – N – N), fig. 1.

La posición óptima de los grupos en las configuraciones *E* y *Z* fue determinada usando como conformación inicial la correspondiente a $\tau_3 = 0°$. Para estas conformaciones, fueron determinadas las deformaciones fuera del plano N1 – H y N1′ – H. Posteriormente por variaciones sucesivas de τ_1, τ_2, τ_4, τ_5 y τ_6, fueron analizadas las posiciones relativas de los

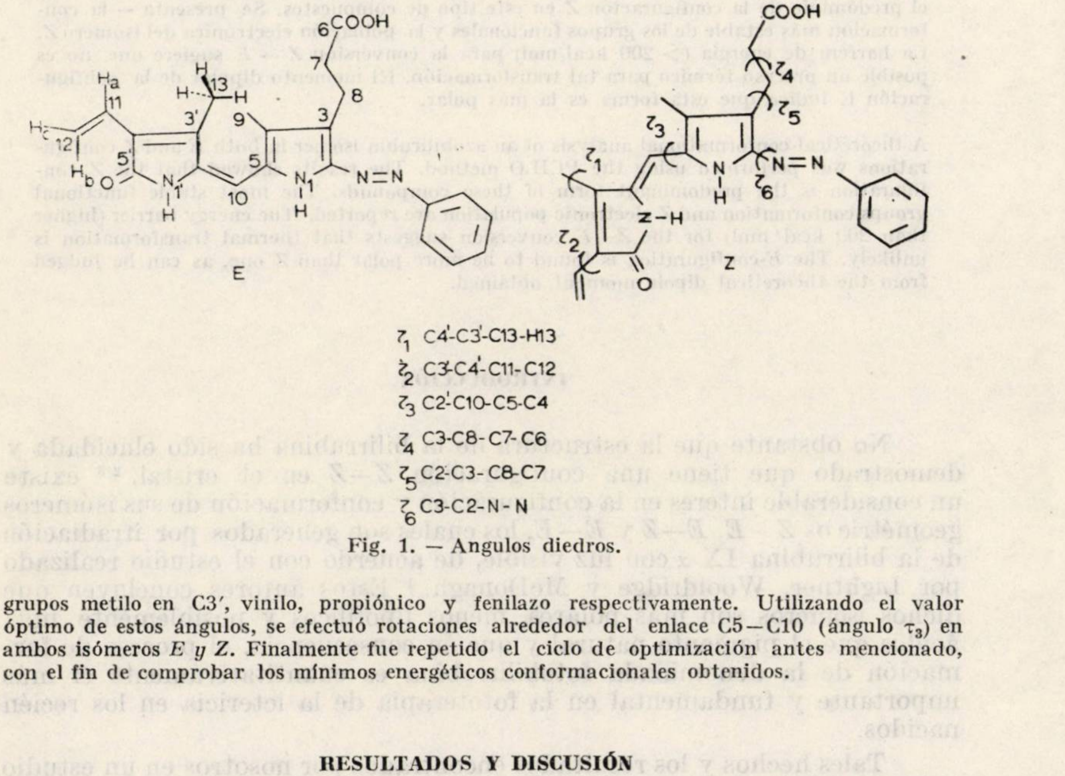

Fig. 1. — Angulos diedros.

grupos metilo en C3′, vinilo, propiónico y fenilazo respectivamente. Utilizando el valor óptimo de estos ángulos, se efectuó rotaciones alrededor del enlace C5 – C10 (ángulo τ_3) en ambos isómeros *E y Z*. Finalmente fue repetido el ciclo de optimización antes mencionado, con el fin de comprobar los mínimos energéticos conformacionales obtenidos.

RESULTADOS Y DISCUSIÓN

La conformación óptima para N1 – H, N1′ – H, grupo propiónico (ángulos τ_4 y τ_5) y grupo fenilazo (ángulo τ_6) son aproximadamente las mismas en las formas *E* y *Z* y bastante similares a las encontradas en el isómero 3′-vinilo, [1] ya que este último sólo difiere con el considerado aquí (4′-vinilo) en las posiciones relativas de los grupos metilo y vinilo. En consecuencia, por los resultados obtenidos, podemos suponer que tal diferencia no influye en las conformaciones preferentes de los grupos unidos al anillo pirrólico, en particular el propiónico y fenilazo, tal y como se manifiesta en el espectro de resonancia magnética de estos isómeros. [5]

Las desviaciones del protón N1′-H arriba del plano del anillo de la pirrolinona y el protón N1-H abajo del plano del anillo pirrólico fueron 0.66 y 0.72 Å respectivamente. La diferencia de energía entre esta conformación y la plana es -12.0 kcal/mol. Los ángulos óptimos para el grupo propiónico son $\tau_4 = 90°$ y $\tau_5 = 56°$.

La energía de rotación del grupo fenilazo alrededor de la unión C2—N16, es función de la orientación del grupo propiónico. La conformación de menor energía del grupo fenilazo es la inicial, $\tau_6 = 0°$, en la que dicho grupo es coplanar y anti anillo pirrólico.

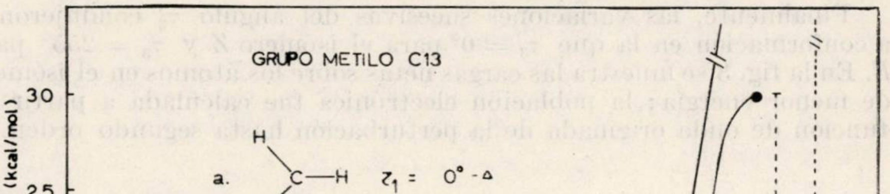

Fig. 2. — Rotación del grupo vinilo en el isómero Z.

De manera similar la rotación del grupo vinilo alrededor del enlace C4′-vinilo (ángulo τ_2) depende de las posiciones relativas de los hidrógenos unidos al C13 (grupo metilo). La fig. 2a, 2b, y 2c muestra el valor de la energía trazado ante el ángulo de rotación del vinilo τ_2 para cada una de las diferentes posiciones de los hidrógenos del grupo metilo C13, $\tau_1 =$ 0°, 30° y 180°, para la forma *Z*. Se observa en dicha figura que se obtiene el menor valor de energía cuando el grupo vinilo es coplanar con el resto de la molécula ($\tau_2 = 0°$), para cualquier valor de τ. Conforme se inicia la rotación la energía aumenta hasta llegar a un máximo en $\tau_2 = 90°$, la altura de la barrera en este punto es similar a la encontrada en la isomerización del trans butadieno. [7] Posteriormente la energía disminuye y después de cerca de $\tau_2 = 120°$ en donde tiene otro mínimo, crece debido a la interacción de los hidrógenos del vinilo con los del metilo C13, tal interacción es importante para $\tau_1 = 180°$ y $\tau_2 = 180°$ por la pequeña distancia internuclear de dichos hidrógenos. Para $\tau_2 = 180°$ y $\tau_2 = 0°$ y 30°, evidentemente la altura de la barrera es menor debido a las posiciones intrínsecas de los hidrógenos del metilo C13 con relación a los del grupo vinilo. Para los valores mayores de $\tau_2 = 180°$ la curva es aproximadamente la simétrica.

Los valores óptimos de τ_1 y τ_2 son los mismos en ambas configuraciones E y Z ($\tau_1 = 180°$ y $\tau_2 = 0°$).

Finalmente, las variaciones sucesivas del ángulo τ_3 condujeron a una conformación en la que $\tau_3 = 0°$ para el isómero *Z* y $\tau_3 = 255°$ para el *E*. En la fig. 3 se muestra las cargas netas sobre los átomos en el isómero *Z* de menor energía; la población electrónica fue calculada a partir de la función de onda originada de la perturbación hasta segundo orden. [8]

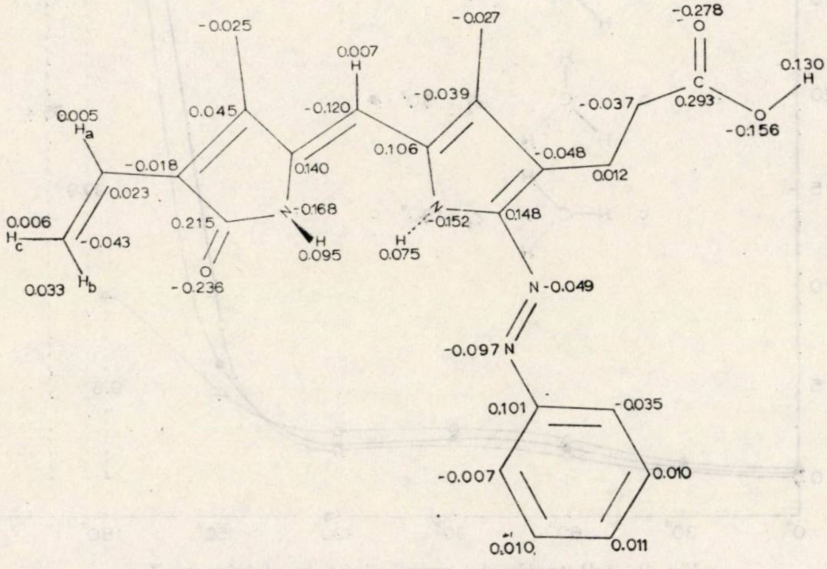

Fig. 3. — Cargas netas sobre los átomos en el isómero Z.

Los resultados obtenidos para los grupos vinilo y metilo (C13), sugieren que existe una rotación fácil de estos grupos en un intervalo de $\tau_2 = 0 - 150°$, en particular cuando $\tau_1 = 0°$, la barrera a la rotación del grupo vinilo es de 9.6 kcal/mol ($\tau_2 = 180°$). Aún más, la barrera de energía en el máximo, interacción con el metilo, $\tau_2 = 90°$, es apenas de 2.6 kcal/mol que puede vencerse con poco incremento de temperatura. Con respecto a los hidrógenos de este grupo, se observa una deficiencia electrónica en el H-b superior a la del H-c al y del H-a (fig. 3), provocada por la proximidad del primero al grupo carbonilo. Al existir la rotación del grupo vinilo en el intervalo $\tau_2 = 0 - 180°$, el protón *a* adquiere una posición y deficiencia electrónica similar a la inicial del *b*, no obstante el H-c conserva prácticamente sus características electrónicas.

Lo anterior explica los resultados experimentales de Salmón et. al.,[5] en los que se hace notar que el grupo vinilo con tres hidrógenos, tiene efectivamente dos en la misma posición en el espectro (H-a y H-b, 6.50 δ) y el tercero separado de ellos (H-c, 5.59 δ). Es decir se manifiesta una rotación poco restringida tal que sólo se distingue a uno de los protones. Al adicionar el reactivo de desplazamiento y formar el compuesto complejo, se hacen totalmente diferentes los tres debido a que, por una parte, las modificaciones de la población electrónica acentúa las diferencias y por otra, el volumen del reactivo de Europio restringe más la rotación, hasta casi anularla.

Al igual que en el isómero 3'-vinilo, en el derivado 4'-vinilo la diferencia de energía entre la forma *Z* y *E* es pequeña (3.8 kcal/mol.). Esto no quiere decir que uno puede convertirse fácilmente al otro. En efecto la barrera de energía necesaria para efectuar dicho proceso es desmesuradamente grande ($>$ 200 kcal/mol) debido a la localización de los enlaces, en particular la del C2'-C10. Este es esencialmente un doble enlace (1.37 Å, calc.), mientras que C5-C10 es un enlace simple (1.46 Å, calc.). Aún más la diferencia de energía de deslocalización[9] entre el isómero *Z* y *E* es 2.8 kcal/mol, diferencia sorprendentemente pequeña si consideramos que en la forma *Z* los anillos están en el mismo plano y en la *E* aproximadamente en planos perpendiculares. Esto sugiere que la deslocalización electrónica entre los anillos de la pirrolinona y del pirrol es mínima y que no es posible una conversión térmica $Z \rightarrow E$, por el gasto de energía que involucra la rotación alrededor del enlace C2'-C10, pero si fotoquímica por ruptura, rotación y formación sucesivas de enlaces covalentes.[4,10] Además la localización de los enlaces se hace evidente por la densidad electrónica de los átomos, que es prácticamente la misma en los dos isómeros, es decir no hay una diferencia apreciable en población electrónica de los átomos entre las formas *Z* y *E*. Sin embargo difieren notablemente sus momentos dipolares resultantes de estos cálculos, *Z*, $\mu = 2.86$ D y *E*, $\mu = 4.33$ D. Este último valor indica que la forma *E* es la más polar de acuerdo con la referencia 4.

CONCLUSIONES

De los isómeros estudiados el más estable es el Z en su conformación coplanar $\tau_3 = 0°$, con los grupos funcionales en la posición que se indica en la fig. 4. Tales resultados concuerdan con informes experimentales de moléculas similares[11,12] y evidentemente con la estructura de los anillos C y D de la bilirrubina.[3] Por otra parte este isómero 4'-vinilo es de menor energía que su homólogo 3'-vinilo, $\Delta E = 1.2$ kcal/mol.

La conformación más estable del grupo vinilo encontrada en este trabajo ($\tau_2 = 0°$) coincide con la obtenida por estudios de rayos X del éster dimetílico de la biliverdina[13] y de la bilirrubina.[2,3] La barrera de rotación que exhibe este grupo es congruente con el espectro de Resonancia Magnética Nuclear que manifiesta.[5]

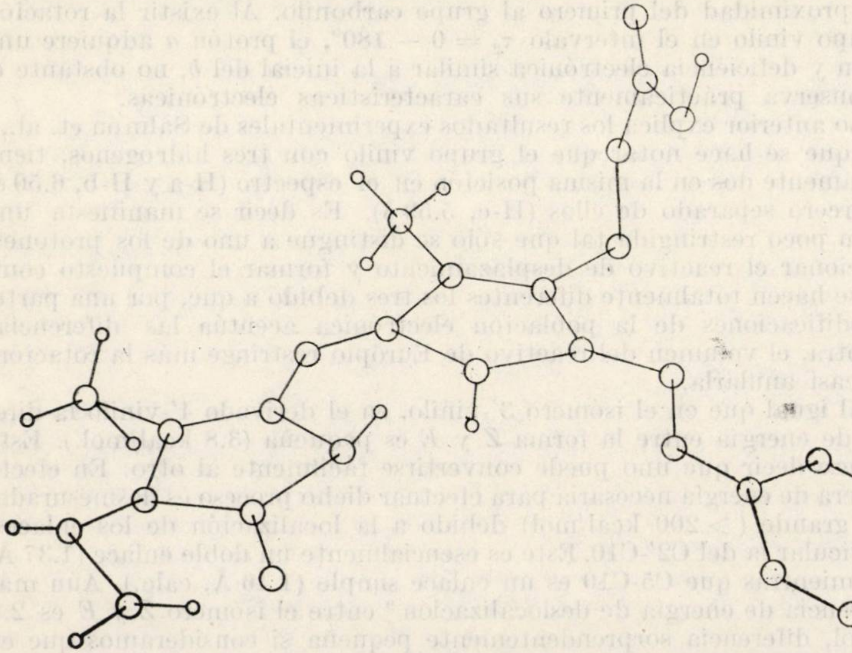

Fig. 4. — Estructura final del isómero azo de la bilirrubina.

Nuestros resultados predicen una conversión fotoquímica aunque no térmica de la forma *Z* a la *E* y que esta última es la más polar.

BIBLIOGRAFIA

[1] R. Cetina, M. Rubio, M. Salmón y J. Bernal, *Austral. J. Chem.*, **31**, 1911 (1978).

[2] R. Bonnett, J. E. Davies y M. B. Hursthouse, *Nature*, **262**, 326 (1976).

[3] R. Bonnett, J. E. Davies, M. B. Hursthouse y G. M. Sheldrick, *Proc. Roy. Soc. London*, **B. 202**, 249 (1978).

[4] D. A. Lightner, T. A. Wooldridge y A. F. McDonagh, *Biochem. Biophys. Res. Commun.*, **86**, 235 (1979).

[5] M. Salmón, E. Díaz, M. C. Rock y C. Fenselau, *Org. Magn. Resonance*, **8**, 126 (1976).

[6] R. Cetina, M. Rubio y M. A. Mora, *Rev. Latinoam. Quím.*, **10**, 50 (1979).

[7] K. Kuchitsu, T. Fukuyama y T. Morino, *J. Mol. Struct.*, **1**, 463 (1968).

[8] R. Cetina, M. Rubio y A. Sigrist, *Rev. Latinoam. Quím.*, **6**, 25 (1975).

[9] J. Langlet y J. P. Malrieu, *J. Amer. Chem. Soc.*, **94**, 7254 (1972) y referencias ahí citadas.

[10] H. Falk, K. Grubmayr, U. Herzig y O. Hofer, *Tetrahedron Letters*, **1975**, 559.

[11] D. L. Cullen, P. S. Black, E. F. Meyer Jr., D. A. Lightner, G. B. Quistad y C. S. Pak, *Tetrahedron*, **33**, 477 (1977).

[12] W. S. Sheldrick, A. Borkenstein, M. Blacha-Puller y A. Gossauer, *Acta. Cryst.*, **B. 33**, 3625 (1977).

[13] W. S. Sheldrick, *J. Chem. Soc., Perkin Trans.*, **2**, 1457 (1976).

Revue Roumaine de Chimie, 27, 2, 291–299 (1982)

L'ÉTUDE DU COMPORTEMENT À L'HYDROLYSE DE CERTAINS POLYESTERS ET POLYAMIDES CONTENANT DU PHOSPHORE DANS LA CHAÎNE

FLORIN POPESCU, LIDIA ROSESCU,
SIMONA PERCEC et OANA PETREUȘ
Institut de chimie macromoléculaire « Petru Poni »,
Aleea Gr. Ghica Vodă 41 A, Iași — 6600, România

Reçu le 15 Juillet 1980

On met en évidence des différences de comportement à l'hydrolyse dans des milieux neutres, acides ou alcalins, pour les cas des deux phosphopolyesters et d'un phospholyamide. Les données viscosimétriques sont corrélées par des études IR, UV et des analyses élémentaires. On tire des conclusions sur les limites d'utilisation de tels composés en qualité d'additifs ignifugeants.

The differences in hydrolysis behaviour of two phosphorus-containing polyesters and a phosphorus-containing polyamide in neutral, acid and basic media are reported. The viscosity measurements are correlated with IR, UV and elemental analysis. The limits of these compounds utilization as flameproofing additives are discussed.

Le nombre des phosphopolyamides et phosphopolyesters synthétisés croît continuellement. Une partie trouvent leurs applications en qualité d'ignifugeants et aussi de plastifiants des matières plastiques. L'industrie utilise les composés ignifugeants pour des traitements de surface ou pour additiver les polymères inflammables. [1–9]

L'attaque des composés macromoléculaires par les agents agressifs auxquels ils sont exposés peut conduire à la scission des liaisons estériques ou amidiques.

Pour les ignifugeants macromoléculaires utilisés en qualité d'additifs, présente le plus vif intérêt la modification des propriétés dues à l'hydrolyse, qui conduisent soit à une mauvaise compatibilité et à la lente exudation du mélange polymère inflammable—additif ignifugeant, des fractions de petit poids moléculaire, soit à la perte de l'adhérence pour les ignifugeants déposés en couches superficielles sur les matériaux inflammables. [10–12]

Dans le présent travail on compare le comportement à l'hydrolyse des trois phosphopolymères suivants :[5,13-15]

E :
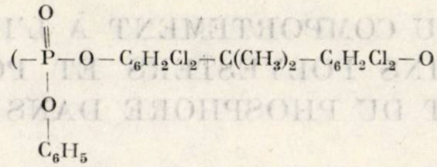
$$(-\overset{\overset{\displaystyle O}{\|}}{\underset{\underset{\displaystyle C_6H_5}{|}}{\underset{\underset{\displaystyle O}{|}}{P}}}-O-C_6H_2Cl_2-C(CH_3)_2-C_6H_2Cl_2-O-)_n \qquad n = 30-40$$

B :
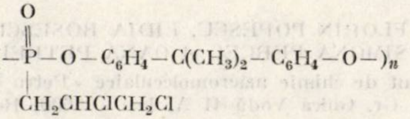
$$(-\overset{\overset{\displaystyle O}{\|}}{\underset{\underset{\displaystyle CH_2CHClCH_2Cl}{|}}{P}}-O-C_6H_4-C(CH_3)_2-C_6H_4-O-)_n \qquad n = 30-40$$

C :
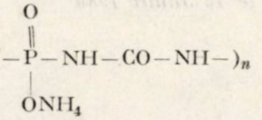
$$(-\overset{\overset{\displaystyle O}{\|}}{\underset{\underset{\displaystyle ONH_4}{|}}{P}}-NH-CO-NH-)_n \qquad n = 10-15$$

Les composés *E* et *B* sont des polyesters. En ce qui concerne l'atome de phosphore, le composé *E* contient seulement des liaisons estériques (P—O—C), tandis que le composé *B* contient aussi des liaisons P—C. Le composé *C* est le sel d'ammonium d'un phosphopolyamide.

Nous avons effectué des études hydrolytiques à diverses températures (20—100°) dans les milieux suivants :

Neutre : eau et mélange DMF avec 13—14 % eau.

Acide : solution aqueuse d'acide sulphurique 5 %.

Basique : NaOH 5—10 % solution aqueuse et mélange DMF et solution aqueuse d' hydroxyde de sodium.

On a déterminé la viscosité relative pour les produits soumis à l'hydrolyse. Les absorptions UV des solutions utilisées ont montré des modifications caractéristiques qui ont été interprétées.

Les résultats ont été corrélés avec les absorptions IR des résidus solides.

RÉSULTATS IR

Les absorptions IR déterminées à l'aide des données connues[16-18] concernant les composés du phosphore, le phénol, les chlorphénoles, le bisphénol A, sont indiquées dans le tableau 1.

Le polyester *E* peut être transformé par hydrolyse dans le bisphénol A tétrachloré et l'acide phénoxyphosphorique. A son tour l'acide phénoxyphosphorique peut hydrolyser en libérant l'acide phosphorique et le phénol. Il existe aussi la possibilité de la séparation du phénol de la chaîne polymérique, par l'hydrolyse.

Les modifications IR du polyester *E* chauffé dans une solution aqueuse de SO_4H_2 5 % à 100° sont insignifiantes : on constate la superposition de certaines bandes d'absorption de petite intensité, dans les domaines 1150–1200 cm^{-1}, 1000–1050 cm^{-1} et 800–840 cm^{-1}. Le spectre caractéristique pour le composé *E* n'est pas modifié (tab. 1.).

TABLEAU 1

Absorptions IR pour les polyesters *E*, *B*, *C* (cm^{-1})

E	B	C
3000 sν(= CH) 1600 mν (C = C)	3000 sν (= CH) 1600 mν (C = C)	3440 vs (N–H) 2600– –3300 vs ν (CH_2), (NH_8)
1550 s ?	1500 vs δas (CH_3) ν (C = C)	2200 m ? 1940 m ?
1440 vs δas (CH_3) ν (C = C)	1450 mδ s (CH'_2)	1680 s ?
1380– –1360 s δs (CH_3) ν (C = C)	1380– –1360 w δas(CH_3) ν (C = C)	1600 s ?
1300 m ? 1250 s P–O–C arom. 1240 s (P=O) 1153 mβ (= CH)	1250– –1240 vs (P–C) (P–O–C) 1140 vs β (= CH) 1100 m (P=O)	1450 vs ? 1400 s (P=0) 1070 vs (P–O+P=0)
		950 s ?
1070 mβ (=CH)	1060 mβ (=CH)	890 s P–N
1020–1040 mν (C–O) 990 s P–O–C arom	1020 s β (=CH) ν (C–O)	550 vs ?
910 mγ (=CH)		530 m
815 s ?	930– –980 vs (P–O–C)	
695 mδ (noyau) 775 m (C–Cl)	840 vs γ (=CH) 755– –765 w γ (=CH) 655 m (C–Cl) alif.	200– –260 s complexe

Le spectre IR du composé *E*, maintenu 3 heures à 100° dans NaOH solution aqueuse 5% et 9 heures à 100° dans Na_2CO_3 solution aqueuse 5% se modifie totalement. Les bandes d'absorption se réduisent en nombre et s'amplifient. On constate l'existence des groupes phosphoriques à 1000–1100 cm^{-1}.

Les absorptions sont plus intenses pour le polyester *E* chauffé dans la solution de NaOH 5% (1) et plus réduites dans le cas d'une solution de Na_2CO_3 5% (2) :

1. 1400–1500 s ; 1000–1100 vs ; 850 m ; 450 s ; 600 s (cm^{-1})
2. 1400–1500 s ; 1000–1100 w ; 850 s ; 600 w ; 470 s (cm^{-1})

Les résidus résultés par l'évaporation des solutions après l'hydrolyse présentent les absorptions IR suivantes :

3091 s ν(OH) ; ν(=CH) ; 3076 m ν(=CH) ; 1810 s, 1777 s (?) ; 1596 γ(C=C) 1344 m γ(C=C) ; 1267 s β(=CH) ; 1153 m β(=CH) ; 1000 m noyau ; 884 m γ(=CH) ; 762 s γ(CH) ; 688 s (CC).

Les absorptions indiquent la présence du phénol. Les absorptions pour le chlore (aromatique) et pour le $-CH_3$ du spectre IR concernant le bisphénol A tétrachloré ne sont pas visibles.

Le polyester *B* contient la liaison P—C aliphatique, au lieu de la liaison phénoxy du polyester *E*. Par l'hydrolyse on ne peut obtenir (théoriquement) que deux composés : le bisphénol A et l'acide 2,3-dichloropropyle phosphorique (ou son sel de sodium).

L'analyse IR montre que le polycondensé *B* n'est pas changé à la suite de l'action des solutions acides ou basiques. On ne trouve pas d'absorptions IR spécifiques pour les composés organiques dans les solutions d'hydrolyse.

Dans le cas du polyphosphonamide *C*, après chauffage dans des solutions de NaOH 10 %, nous retrouvons les absorptions caractéristiques initiales des spectres IR.

Les indications des spectres IR montrent que la résistance hydrolytique de la chaîne des phosphopolyesters aromatiques étudiés est bonne dans des milieux acides et basiques étudiés.

La comparaison des polyesters *E* et *B* montre que les liaisons phénoliques de la chaîne du polyester *E* sont sensibles à l'hydrolyse alcaline.

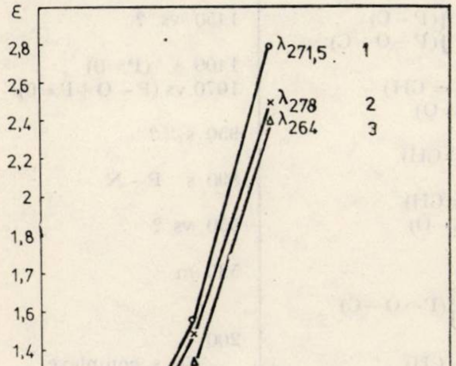

Fig. 1. — Absorptions UV du composé *E* après l'action de H_2SO_4 5 % jusqu'à trois heures ; t° = 100°, 1 — 4 absorptions distinctes.

RÉSULTATS UV

Les absorptions UV des solutions testées pendant l'hydrolyse présentent des croissances limitées dans le milieu alcalin pour le polycondensé *E*, des variations insignifiantes dans le cas du polycondensé *B* et nulles dans le cas du polyphosphonamide *C*.

Dans le milieu acide les absorptions UV des solutions présentent des croissances importantes pour les polycondensés *E* et *B*. (Fig. 1 et 2). L'absorption UV des solutions du polyphosphonamide *C* est petite dans le SO_4H_2 5 % et présente une période stationnaire comprise entre 30—120 minutes de chauffage à la température de 100° (fig. 3).

Dans le milieu alcalin est décelable une seule absorption UV à chacun des trois composés étudiés. Dans le milieu acide, pour les produits *E* et *B*, apparaissent aussi des absorptions spécifiques pour le bisphénol A et pour le bisphénol A tétrachloré (fig. 1 et 2 ; $\lambda = 278$). Ce fait conduit à l'hypothèse que dans le milieu acide a lieu la dissolution soit d'une

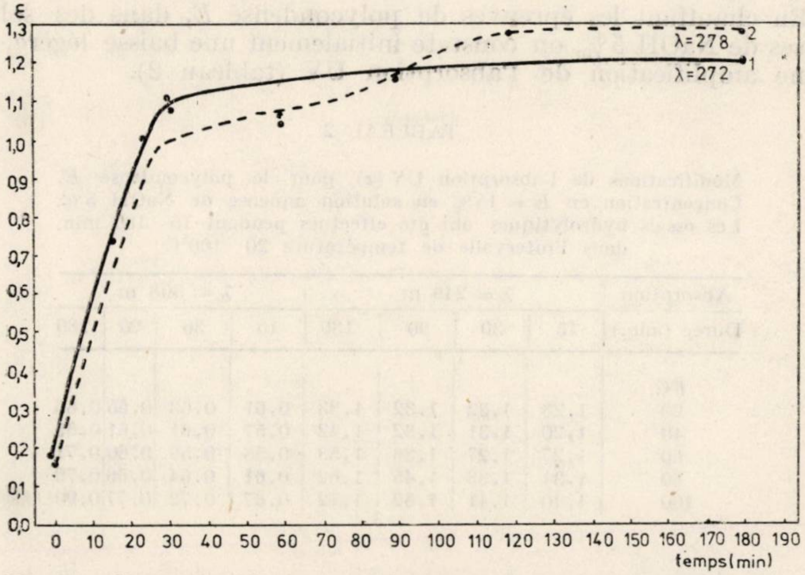

Fig. 2. — Absorptions UV du composé *B*, fraction solubilisée dans H_2SO_4 5 %, jusqu'à trois heures ; t° = 100°, 1 — 2 absorptions distinctes.

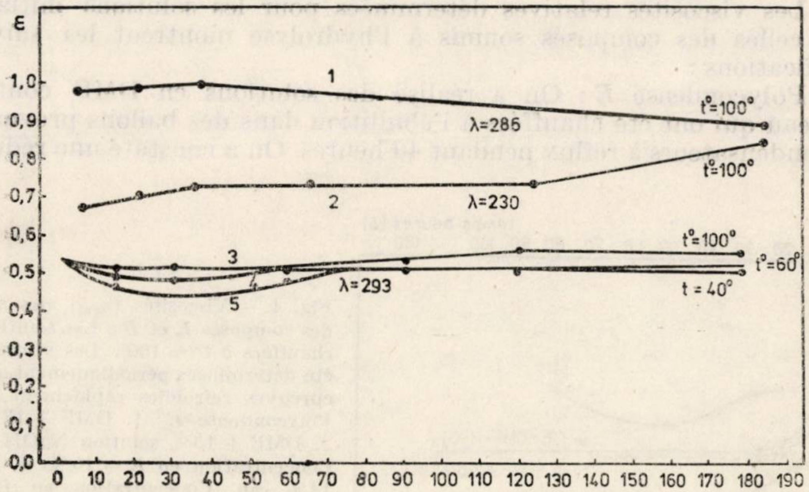

Fig. 3. — Absorptions UV du polycondensé *C* fractions solubilisées : 1. SO_4H_2 5 %. Température d'hydrolyse 100°. Absorptions UV du polycondensé B fraction solubilisée dans NaOH 5 % solution aqueuse. Températures d'hydrolyse : 2. 100° ; 3. 60° ; 4. 40°.

quantité de bisphénol A, soit de quelques fragments de chaîne contenant du bisphénol A aux extrémités.

L'hypothèse est appuyée par le fait que dans le cas du polyphosphonamide *C* (parfaitement soluble dans la solution de H_2SO_4 5 %) manque la croissance spectaculaire, de l'absorption UV.

En chauffant les épreuves de polycondensé *E*, dans des solutions aqueuses de NaOH 5 %, on constate initialement une baisse légère, suivie par une amplification de l'absorption UV (tableau 2).

TABLEAU 2

Modifications de l'absorption UV (ε) pour le polycondensé *E*. Concentration en $E = 15\,\%$ en solution aqueuse de NaOH 5 %. Les essais hydrolytiques ont été effectués pendant 15—180 min. dans l'intervalle de température 20—100°C

Absorption	λ = 249 m				λ = 308 m			
Durée (min.)	15	30	90	180	15	30	90	180
t°C								
20	1,28	1,32	1,32	1,33	0,61	0,63	0,65	0,66
40	1,20	1,31	1,32	1,42	0,57	0,61	0,61	0,65
60	1,27	1,27	1,36	1,53	0,58	0,59	0,60	0,71
80	1,31	1,33	1,45	1,62	0,61	0,64	0,66	0,79
100	1,40	1,41	1,52	1,72	0,67	0,72	0,77	0,90

VISCOSITÉS

Les viscosités relatives déterminées pour les solutions initiales et pour celles des composés soumis à l'hydrolyse montrent les suivantes modifications :

Polycondensé *E* : On a réalisé des solutions en DMF contenant 13 % eau qui ont été chauffées à l'ébullition dans des ballons prévus avec des condensateurs à reflux pendant 40 heures. On a constaté une réduction limitée de la viscosité pendant les premières 4 heures. Ensuite la viscosité reste constante. Le même phénomène a été observé dans des solutions alcalines homogènes du polycondensé *E* en DMF mélangé avec 13 % solution aqueuse NaOH concentration 5 % (Fig. 4). Une suspension du

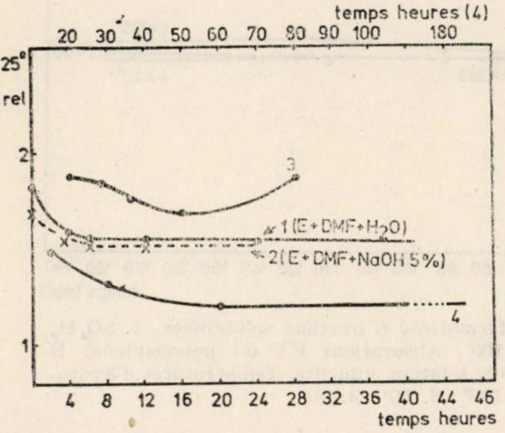

Fig. 4. — Viscosités (η_{rel}) des solutions des composés *E* et *B* : Les solutions sont chauffées à t° = 100°. Les viscosités ont été déterminées périodiquement avec des épreuves refroidies rapidement à 18°C. Polycondensé *E* : 1. DMF + 13 % eau ; 2. DMF + 13 % solution NaOH 5 %. 3. Concentration en $E = 15\,\%$. 4. DMF + 14 % eau. Concentration en $E = 6\,\%$. Polycondensé *B* : 4. Solution aqueuse de NaOH 5 %. Concentration en $B = 6\,\%$.

composé *E*, dans la solution aqueuse de NaOH 5% conduit au même résultat. La viscosité ne se modifie point, pour des épreuves du polycondensé *E* hydrolysé dans une solution de H_2SO_4 5%. Dans les deux derniers cas, après l'action de l'acide ou de l'alcali la suspension a été filtrée, lavée, séchée et dissoute dans le DMF.

Polycondensé *B* : les hydrolyses effectuées avec des solutions homogènes en DMF contenant 14% eau et chauffées à l'ébullition ont conduit à la réduction initiale de la viscosité suivie d'une croissance qui après 24 heures dépasse la valeur de la viscosité initiale (fig. 4). L'hydrolyse en NaOH 5% solution aqueuse conduit à une réduction de la viscosité dans les premières 60 minutes. Ensuite la viscosité reste stationnaire (fig. 4).

Polycondensé *C* : les solutions aqueuses neutres, alcalines ou acides ont présenté des modifications non significatives de la viscosité.

La viscosité (η_{rel}) varie dans l'intervalle de temps 0—3 heures de l'hydrolyse pour le composé *C* de la manière suivante :

— Solution neutre 1,31 → 1,52
— Sol. aqueuse de NaOH 5% 1,40 → 1,38
— Sol. aqueuse de H_2SO_4 5% 1,33 → 1,43

Le composé *C* chauffé à la température de 100° C dans une solution aqueuse de NaOH 10%, se décompose.

Les composés *E* et *B* suspendus dans une solution aqueuse d'acide sulphurique 5% à 100° perdent en poids jusqu'à 3%.

Dans des solutions aqueuses de NaOH 5—10% et à 100° ils se solubilisent en proportion de 98%.

On peut ajouter l'observation que les produits d'hydrolyse: le phénol, l'acide phosphorique, l'acide 2,3-dichloropropyle-phosphonique et son sel de sodium ne présentent pas d'absorptions mesurables dans les conditions des déterminations UV (dilution 1/100, spectrophotomètre UNICAM SP—800). Le bisphénol A et le bisphénol A tétrachloré présentent des absorptions mesurables dans les conditions indiquées.

L'analyse élémentaire des fractions restées insolubles après les essais hydrolytiques est presentée dans le tableau 3.

Les faibles variations constatées dans l'analyse élémentaire indiquent pourtant que dans le cas du composé *E* a lieu la perte du phénol (C% diminué et croissance en Cl%), qui explique la solubilisation partielle dans les milieux fortement alcalins, par la formation de groupes polaires

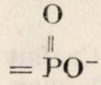

$= \overset{\overset{O}{\|}}{P}O^-NA^+$.

Dans le cas du composé *B*, on constate une perte en chlore alyphatique (de moyenne réactivité) fait qui nous permet d'expliquer la solubilisation partielle de ce composé dans des milieux fortement alcalins, aussi par la possible formation des groupes — C—OH.

Ces observations exposées plus haut conduisent aux suivantes conclusions :

1. Dans un milieu acide le spectre UV se modifie profondément, les absorptions croissant progressivement aux composés E et B.

Aussi le spectre présente plusieurs domaines d'absorption. L'absorption 278 nm est aussi rencontrée au bisphénol A et est visible aux deux produits soumis à l'hydrolyse alcaline. Les spectres IR montrent que

TABLEAU 3

L'analyse élémentaire des fractions restées insolubles après les essais hydrolytiques

Composé *E*

Initial	H_2SO_4 5 % – 3 heures à $t°$ = 100°	NaOH 10 %–3 heures à $t°$ = 100°
C % = 50,03	C % = 48,00	C % = 46,80
H % = 2,97	H % = 3,20	H % = 3,22
Cl % = 28,16	Cl % = 29,00	Cl % = 30,00
P % = 6,15	P % = 6,3	P % = 6,5

Composé *B*

Initial	H_2SO_4 5 % – 3 heures à $t°$ = 100°	NaOH 10 %–3 heures à $t°$ = 100°
C % = 56,11	C % = 56,08	C % = 58,15
H % = 4,94	H % = 4,94	H % = 5,05
Cl % = 18,42	Cl % = 18,40	Cl % = 16,25
P % = 8,00	P % = 8,06	P % = 8,18

Composé *C*

Totalement soluble.

les composés *E* et *B* insolubles ne sont pas changés dans le milieu acide, en ce qui concerne leur structure. En conséquence passent en solution, soit le bisphénol A soit des fractions de petit poids moléculaire contenant aux extrémités du bisphénol A.

2. Dans le milieu basique, le polycondensé E élimine du phénol, en se transformant dans un polyélectrolyte à cause de la formation des groupes à polarité phosphorique, sur la chaîne 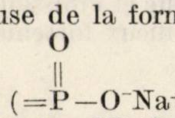 $(=\overset{\overset{\displaystyle O}{\|}}{P}-O^{-}Na^{+})$. Ce fait qui explique la solubilisation est illustré par le spectre IR (fig. 3), mais n'est pas décelable dans le spectre UV. Aussi en UV n'est pas visible le bisphénol A et le bisphénol A tétrachloré, fait qui montre que la solubilisation des produits a lieu avec la conservation du caractère macromoléculaire.

3. La viscosité présente des modifications initiales dans quelques cas, mais ne subit pas de diminutions progressives avec la durée de l'hydrolyse, indiquant ainsi que les trois substances étudiées gardent leur caractère macromoléculaire.

4. Le composé *C* se décompose dans la solution de NaOH 10 %.

5. Dans le carbonate de sodium 5 % on ne constate pas de transformations pour les composés étudiés.

6. On met en évidence le fait que les produits E et B ont tendance à se dissoudre à chaud dans des solutions fortement alcalines. En milieu légèrement alcalin ou acide les composés E et B sont résistants, étant ainsi utiles à des ignifugations à caractère permanent. Le composé C est aussi sensible à des solutions alcalines concentrées, étant modifié par des solutions d'hydroxyde de sodium 10%.

BIBLIOGRAPHIE

[1] D. W. van Krevelen, *Chem. Ing. Tehn.*, **47**, 783 (1975).

[2] A. Yehaskel, "Fire and Flame Retardant Polymers. Recent Developments", Noyes Data Corporation, London, 1979, p. 82, 182, 348, 410, 424, 462.

[3] M. Lewin, S. M. Atlas et Eli M. Pearce, "Flame Retardant Polymeric Materials" vol. 2, Plenum Press, New York, 1978, p. 103–128.

[4] A. Wiliams, "Flame Resistant Fabrics", Noyes Data Corporation, London, 1974, p. 65–295.

[5] El. S. Percec et Fl. Popescu, Pat. RSR, 64.155, 1978.

[6] V. V. Korshak, E. S. Kurgranz et A. M. Berlin, *Izvest. Akad. Nauk S.S.S.R., Otdel. khim. Nauk*, **1962**, 1412.

[7] D. M. Harrier, R. J. Jenkins et M. L. Nielsen, *J. Polymer Sci.*, **35**, 541 (1959).

[8] S. K. Brauman, *J. Fire Retard. Chem.*, **7** 61 (1980).

[9] R. Z. Greenley, M. L. Nielsen et L. Parts, *J. Org. Chem.* **29**, 1009 (1964).

[10] W. A. Reeves, G. L. Drake jr. et R. M. Perkins, "Fire Resistant Textiles Handbook", Technomik Publishing Co, Westport S.U.A., 1979, p.51–227.

[11] M. W. Ranney, "Fire Resistant and Flame Retardant Polymers", Noyes Data Corporation London, 1974, p. 3–100, 114–156.

[12] H. Hantge, *Textilveredlung*, **6**, 637 (1971).

[13] Fl. Popescu et El. S. Percec, Pat. RSR, 63.975, 1978.

[14] O. Petreuş, Fl. Popescu et El. S. Percec, Pat. RSR, 64.218, 1974.

[15] O. Petreuş et Fl. Popescu, Pat. RSR, 63.976, 1976.

[16] L. C. Thomas "The Identification of Functional Groups in Organophosphatous Compounds", Academic Press, London, 1974, p. 23–44, 60–67.

[17] H. A. Szymansky "Interpreted Infrared Spectra" Plenum Press New York 1964, vol. 1 et 2. Serial no 1910–2268.

[18] J. H. S. Green, *J. Chem. Soc.*, **1961**, 2236.

6. On met en évidence le fait que les produits F et K ont tendance à se dissoudre à chaud dans des solutions fortement alcalines. En milieu légèrement alcalin ou acide les composés E et H sont résistants, étant aussi utiles à des ignifugations à caractère permanent. Le composé C est aussi sensible à des solutions alcalines concentrées, étant modifié par des solutions d'hydroxyde de sodium 10%.

BIBLIOGRAPHIE

[1] D. W. van Krevelen, Chem. Ing. Tech., 47, 793 (1975).
[2] A. Yehaskel, "Fire and Flame Retardant Polymers, Recent Developments", Noyes Data Corporation, London, 1979, p. 89, 132, 348, 410, 424, 455.
[3] M. Lewin, S. M. Atlas et E. M. Pearce, "Flame-Retardant Polymeric Materials", vol. 2, Plenum Press, New York, 1978, p. 103–138.
[4] A. Williams, "Flame Resistant Fabrics", Noyes Data Corporation, London, 1974, p. 65–289.
[5] El. S. Petrer et Fl. Popescu, Pat. RSR, 64 136, 1978.
[6] V. V. Korshak, S. S. Kurmanaz et A. M. Bychk, Izvest. Akad. Nauk SSSR, Ser. Khim. Nauk, 1962, 112.
[7] G. H. Hardey, B. L. Jennings et H. E. Nielsen, J. Polymer Sci., 48, 411 (1959).
[8] S. K. Brauman, J. Fire Retard. Chem., 3, 117 (1980).
[9] S. Z. Gonzales, M. L. Nielsen et L. Yoris, J. Org. Chem., 29, 1060 (1964).
[10] M. N. Reeves, G. L. Drake jr. et R. M. Perkins, "Fire Resistant Textiles Handbook", Technomic Publishing Co., Westport, S.U.A., 1974, p. 31–227.
[11] R. W. Runney, "Fire Resistant and Flame Retardant Polymers", Noyes Data Corporation, London, 1974, p. 95–100, 141–155.
[12] H. Hanitgs, Textilveredlung, 8, 637 (1973).
[13] Fl. Popescu et El. S. Petrer, Pat. RSR, 66 976, 1978.
[14] G. Petrean, Fl. Popescu et El. S. Petrer, Pat. RSR, 61 318, 1974.
[15] G. Petrean et Fl. Popescu, Pat. RSR, 65 576, 1978.
[16] L. C. Thomas, "The Identification of Functional Groups in Organophosphorus Compounds", Academic Press, London, 1974, p. 28–44, 80–87.
[17] D. A. Szymanski, "Interpreted Infrared Spectra", Plenum Press, New York 1964, vol. 1, 2, Serial no 1910–2268.
[18] J. R. S. Loomis, J. Chem. Soc., 1961, 2291.

Revue Roumaine de Chimie, **27**, *2*, 301–304 (1982)

UTILIZATION OF CHROMOTROPIC ACID IN SEPARATION OF TITANIUM WITH ION EXCHANGE RESINS. I.

CATION EXCHANGE BEHAVIOUR

LUMINIŢA VLĂDESCU and ARIADNA HARLES
National Institute of Chemistry, Laboratory of Analytical Chemistry, Splaiul Independenţei 202, Bucharest, Romania

Received September 29, 1980

In order to establish the optimal working conditions which ensure the elimination of interferences in spectrophotometric determination of titanium with Chromotropic acid, the cation and the anion exchange behaviour of Ti(IV), U(VI), Cr(VI), Zr(IV), Ce(IV), Cr (III), Fe (III) in the presence of the mentioned reagent, was studied.

The Chromotropic acid (1,8-dihydroxy-3,6-naphtalendisulfonic acid) and its disodic salt react easily with titanium to yield, depending on pH, complex combinations of 1 : 1, 1 : 2, 1 : 3, 1 : 4 composition Ti: Reagent.[1,2]

This behaviour underlies a sensitive and accurate method for the spectrophotometric determination of titanium, which suffers from the interference of Fe (III), U (VI), and elements of the IV group.

The Chromotropic acid was also employed as complexing agent in separation of titanium from copper by means of an anion exchange resin.[3]

This contribution deals with the cation exchange behaviour of Ti (IV), U (VI), Cr (VI), Zr (IV), Ce (IV), Cr (III), Fe (III) in the presence of Chromotropic acid, in order to establish the optimal working conditions which ensure the elimination of interferences in spectrophotometric determination of titanium.

EXPERIMENTAL

Chemical and equipment

— Strongly acid cation exchange resin, type Amberlite IR–120.

— Strongly basic Amberlite IRA–400 anion exchange resin.

— Aqueous solution of known titrum of TiO^{2+}, Fe^{3+}, Cr^{3+}, Ce^{4+}, ZrO^{2+}, UO_2^{2+}, CrO_4^- ions.

— 5×10^{-4} M – 10^{-1} M aqueous solution of Chromotropic acid.

— 1 M — 4 M HCl, 0.5 M — 1 M H_2SO_4, 1 M Na_2SO_4, 0.5 M — 1 M $HClO_4$, 0.1 M — 1 M $NaClO_4$, 25 % NH_3 solutions.

— SPEKORD UV — VIS and SPEKOL spectrophotometers.

— MV — 11 pH-meter.

The quantitative determination of ions investigated was performed by spectrophotometric methods ; use has been made of organic reagents : the Chromotropic acid for titanium,[1] the Sulphosalycilic acid for uranium,[4] and cerium,[5] Pyrocatechine Violet for zirconium[6] and Diphenylcarbazide for chromium.[7]

The ion exchange took place in glass column, 15 cm long, 1 cm in diameter, provided with stopcocks at bottom and funnel with ground joint at top. 5 g of cation or anion exchanger were transferred into each column, purified, activated in H^+ or Cl^- ionic form, respectively and washed with distilled water up to negative Cl^- test.

RESULTS AND DISCUSSION

In order to establish the optimal working conditions, the influence of concentration and pH of Chromotropic acid solution upon the cation exchange behaviour of titanium have been studied firstly. Use has been made of strongly acid Amberlite IR — 120 cation exchange resin in ionic Na^+ form so that on passing through the resin the reagent remains as disodic salt.

Two procedures were applied : either the TiO^{2+} cations were fixed in the cationite and then eluted with Chromotropic acid solutions of various concentrations and pH's, or a sample containing the solution of reagent and titanium was passed through the resin and then eluted with reagent of the same concentration and pH.

Both procedures have evidenced the cation exchange behaviour shown in table 1. Examination of this table shows that titanium passes quantitatively into the effluent when the concentrations of Chromotropic acid solutions are higher than 10^{-2}M, no matter what the value of pH. Iron (III) also passes into the effluent when the pH of the solution is 3.5 but it is fixed into the cationite at a more acid pH.

TABLE 1

Influence of Chromotropic acid concentration and pH upon the cation exchange behaviour of titanium

Resin		Chromotropic acid		pH	Ti(IV)			Fe (III)		
						Determined			Determined	
Type	Ionic form	Conc. (M)	Volume (cm^3)		In sample (mg)	In resin (mg)	In solution (mg)	In sample (mg)	In resin (mg)	In solution (mg)
Amberlite IR-120	Na^+	10^{-1}	5	3.5	0.960	—	0.960	0.560	—	0.562
		10^{-2}	5	3.5	0.960	—	0.962	0.560	—	0.557
		10^{-1}	5	1.5	0.960	—	0.957	0.560	0.559	—
		5×10^{-2}	5	1.5	0.960	—	0.958	—	—	—
		10^{-2}	5	1.5	0.960	—	0.956	—	—	—
		10^{-2}	5	0.5	0.960	—	0.958	—	—	—

Further on, the cation exchange behaviour of Cr (VI), U (VI), Zr (IV), Ce (IV), Cr (III) in the presence of Chromotropic acid 10^{-1} M pH=1.5 was studied. For this purpose, known amounts of each mentioned element were fixed in turn on the resin. All cations, except Cr (VI) (which is excluded by cationite since it exists as CrO_4^- anions) are fixed in the resin. They are not eluted by a 10^{-1} M solution of Chromotropic acid of pH = 1.5. Finally, Cr (III) was eluted with 4 M HCl solution and the other elements with 0.5 N H_2SO_4 solution.

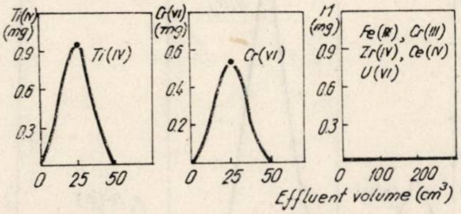

Fig. 1. — Cation exchange behaviour of Ti(IV), Cr(VI), U(VI), Zr(IV), Ce(IV), Fe(III) and Cr(III) in the presence of Chromotropic acid.

Thus, as Fig. 1 and table 2 show, titanium may be separated from the studied elements by means of a cation exchange resin in Na^+ ionic form and a 10^{-2} M solution of Chromotropic acid of pH = 1.5.

TABLE 2

Cation exchange behaviour of Cr(III), Zr(IV), Ce(IV), U(VI), Cr(VI) in the presence of 10^{-1} M Chromotropic acid at pH = 1.5

	Cr(III)	Zr(IV	Ce(IV)	U(VI)	Cr(VI)
In sample (mg)	0.520	0.900	1.400	2.380	0.520
Determined in resin (mg)	0.518	0.896	1.398	2.378	—
Determined in solution (mg)	—	—	—	—	0.519

The method was first applied for separation of some Ti (IV) — Cr(VI)—Fe (III) mixtures. The results are listed in table 3 and the elution curves shown in Fig. 2 prove the possibility of separating the three elements.

TABLE 3

Results of Ti(IV) — Cr(VI) — Fe(III) separation with cation exchange resins

Ti(IV)		Cr(VI)		Fe(III)	
In sample (mg)	Determined (mg)	In sample (mg)	Determined (mg)	In sample (mg)	Determined (mg)
0.043	0.042	0.520	0.517	0.056	0.055
0.960	0.958	0.520	0.521	0.056	0.058
9.600	9.578	0.520	0.518	0.112	0.110

The separation of titanium from mixtures where there were also Cr, Fe, Zr, Ce, U, was approached. The results given in table 4 show a good agreement between the amounts included in the sample and those determined after separation.

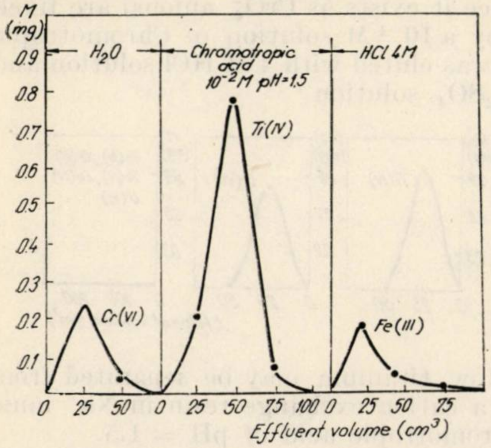

Fig. 2. — Elution curves for a cation exchange Ti(IV) — Cr(VI) — Fe(III) separation.

TABLE 4

Results of titanium separatiom from Cr, Fe, Zr, Ce and U with cation exchange resins

	In sample (mg)	0.043	0.960	4.340	9.600
Ti(IV)	Determined after separation (mg)	0.042	0.958	4.339	9.598
	Determined without separation (mg)	0.122	1.266	6.122	12.678

CONCLUSIONS

Utilization of a strongly acid cation exchange resin in Na^+ ionic form and of Chromotropic acid as complexing agent allows selective separation of titanium from UO_2^{2+}, ZrO^{2+}, Ce^{4+}, Fe^{3+} ions which interfere in its spectrophotometric determinations with the same reagent. The procedure is handy and rapid; it consists of simply passing the solution to be analyzed with Chromotropic acid added at $pH = 1.5$ through the column with resin. A measurement of absorbtion of effluent solution yields the amount of titanium in the sample.

REFERENCES

[1] L. Sommer, *Z. analyt. Chem.*, **163**, 412 (1963).
[2] W. W. Brand and A. E. Preiser., *Analyt. Chem.*, **25**, 567 (1953).
[3] K. Brayter, *J. Chromatog.*, **102**, 385 (1974).
[4] A. Muller, *Z. anorg. Chem.*, **109**, 235 (1920).
[5] K. A. Das, *J. Indian Chem. Soc.*, **10**, 306 (1972).
[6] J. P. Yung, J. R. French and J. C. White, *Analyt. Chem.*, **30**, 422 (1958).
[7] A. J. Blair and D. A. Pontony, *Analyt. Chem. Acta*, **14**, 545 (1956).

Revue Roumaine de Chimie, 27, 2, 305–309 (1982)

COMPTES RENDUS

OLEN L. RIGGS, Jr. and CARL E. LOCKE, Anodic Protection. Theory and Practice in the Prevention of Corrosion, Plenum Press, New York, 1981.

The objectives of this book are to give technical information about anodic protection, explain how economic analyses are made to determine whether or not it should be used, and describe some of the applications and equipment. Limitations of the anodic protection technique are also presented.

It is well known that the technological changes that have resulted in higher temperatures, pressures, and velocities increase corrosion rates and markedly influence materials selection on design decisions. New processes require more sophisticated equipment made of costlier metals which are often in short supply.

Some problems caused by these considerations can be solved, or solutions simplified, by the use of anodic protection.

This volume is the first truly comprehensive book on anodic protection, which discusses the scientific background, practical applications and industrial uses of this advanced technique for corrosion control. Basic electrochemical theory necessary for understanding anodic protection and polarization phenomena is provided. The volume then details the design, operation, installation, and maintenance of sophisticated anodic protection equipment, as well as economic analyses for determining the suitability of anodic protection in a given instance.

From the principles of anodic protection to the equipment for anodic protection, especially for protection of sulfuric acid equipment, from the laboratory equipment to the design, operation, maintenance of anodic protection systems and the economic evaluation of anodic protection, from the laboratory tests and procedures to the selected examples of anodic protection, this book presents a good technical and scientific information about anodic protection of metals — a technique whose time has come.

It is important to acknowledge that much of the information has been from the original work of authors and many of the applications come from developments pioneered by scientists in the USSR, whose innovative work involves corrosive solutions to which anodic protection has not been applied elsewhere.

Reflecting the authors' original research, as well as that of the other leading scientists in the US and USSR and throughout the world, the volume delineates specific laboratory tests and procedures of anodic protection. In addition, an incisive chapter, meant to stimulate expansion of this technique, covers the future of anodic protection.

These is every reason to believe that an increasing number of anodic protection installations will be made in environments where it has been successful in the past, as well as in others in which it is not commonly used now. Better understanding of reactions accumulated from actual working equipment and from laboratory and pilot plant experimentation will permit its use in systems where it has not been employed frequently so far.

Techniques and applications described in this book may encourage increased applications of anodic protection.

A comprehensive list of US patents for significant developments in this area, a historical summary, glossary of terms, a subject index and unusually extensive bibliography, with references dating back to the eighteenth century till now, are also included in this book.

This volume will be of particular interest for engineers, researchers, and students of corrosion science, electrochemistry, materials science, metallurgy, and chemical engineering, as well as plant corrosion control specialists.

M. V. Popa

ADVANCES IN POLYMER SCIENCE — 38, Polymerization Processes, Springer-Verlag, Berlin, Heidelberg, New York, 1981.

The 38th volume in the series Advances in Polymer Science contains five survey paper- dealing with some peculiarities of polymerization processes ; the authors, from Japan, Italy, USSR and USA, are well-known research-workers in the fields reviewed.

Thus, the first paper entitled "New condensation polymerizations by means of phosphorus compounds" describes new ways for producing polyamides, polypeptides, polyureas, polythioureas and polyesters, *via* polycondensation reactions. The basic idea of these syntheses is borrowed from biochemistry. It is known that adenosine triphosphate (ATP) represents a high-energy compound existing in living cells and playing an important role as an energy source in the production of lipids, proteins and carbohydrates ; ATP is consumed and subsequently regenerated by using energy obtained from reactions such as the oxidative breakdown of glucose.

In a similar manner, high-energy phosphonium compounds were prepared (either by the oxidation of phosphorous acids and their esters with mercuric salts in pyridines, or by the reaction of phosphorus halides with tertiary amines). These salts have been proved to be very reactive toward nucleophiles, activating carboxil-, amino- or hydroxil compounds, *via* the corresponding phosphonium salts. These reactions, especially the hydrolysis-dehidration reactions with phosphites, were extended to the direct polycondensation reactions of dicarboxylic acids with diamines and to other polycondensation reactions. It is remarkable that high molecular weight polyamides may be obtained by using this technique.

The second review is dedicated to the electrochemical production of initiators for polymerization processes. Electrochemical polymerizations may be carried out on one hand by a direct activation of monomer at the electrodes, and on the other hand the polymerization can be promoted by initiators (free radicals, ions, organo-metallic species), produced as a result of an electrochemical reaction. The paper surveys the work done in the field of polymerization initiator preparation by means of electrochemical methods ; there are presented electrochemical ways to produce coordination compounds, Ziegler-Natta type catalysts (a problem of the highest technological interest), ions from sacrificial anodes, anion-radicals, radical-cations, free radicals and ions from the solvent, etc.

The influence of solvent on free radical polymerization of vinyl compounds has been studied since long ; an impressive number of reports cover topics such as solvent effect on propagation and termination rate constants, interactions between propagating radical, monomer or polymer, on one hand and solvent, on the other. All these facts, concerning the abovementioned problem are presented and discussed in the third review ; moreover, separate chapters dealing with quantum chemical considerations on the radical complex and solvent effect on free radical copolymerization are included as well.

The next review bears the unpretentious name "Kinetics of polymerization processes" ; in fact, under this general title, three different aspects are discussed. The first chapter, dedicated to radical polymerization, includes the questions of the dependence of termination rate constant on the length of the macroradical chain, the possibility for continuous radical polymerization to be achieved through the complexing and stabilization of free radicals, and of catalytic chain transfer in radical polymerization. The second chapter presents some fundamental problems of ionic polymerization such as thermodynamic aspects of ionic heterogeneous polymerization kinetics, or polymerization kinetics of heterocycles. Perhaps the most interesting chapter is the third one, presenting major contributions in the field of modeling the kinetics of polymerization processes (applications of mathematical models for the verification of kinetic schemes and the values of kinetic constants, as well as in the design of industrial polymerization reactors). It is of interest to notice that the great majority of works reviewed were carried out by kinetic schools in the Soviet Union over the past five years.

The volume also contains a review due to J. P. Kennedy, a well-known research-worker in the field of cationic polymerization ; the paper concerns the synthesis of poly(butadiene-*g*-styrene) by cationic grafting of polystyrene cations onto polybutadiene, using alkyl halide/alkylaluminium initiating systems. An important emphasis is placed upon the effect of reaction conditions on grafting and mechanism studies with model reactions ; the characterization and morphology of poly(butadiene-*g*-styrene) are also presented.

Thus, the present work represents a precious aid, bringing up-to-date information to those interested in the fields reviewed and stimulating new research ways.

D. S. Vasilescu

HOUBEN-WEYL ,,METHODEN DER ORGANISCHEN CHEMIE, BAND XIII/5 g METALLORGANICHE VERBINDUNGEN SI" 4-Auflage, Georg Thieme Verlag, Stuttgart, New York, 1980, 502 S

In der von E. Müller und O. Bayer herausgegebene Reihe Houben-Weyl Methoden der organischen Chemie erschien vor kurzem der von dr. Stephan Pawlenko bearbeitete Band XIII/5 über organo-Silicium Verbindungen.

Im diesem Band werden die organischen Verbindungen des Siliciums beschrieben, die mindestens eine Silicium — Kohlenstoff-Bindung enthalten.

Die umfangreiche zitierte Literatur besonders nach 1965, beweist die stürmische Forschungsentwicklung des Fachgebietes.

Nach kurzem Eingang auf Struktur, Reaktivität, Toxizität der monomeren und polymeren organo-Silicium Verbindungen, technische Anwendung und Nomenklatur, folgen vier Abschnitte über die Herstellung, Umwandlung, organo-Silicium Verbindungen als Hilfsmittel in der organischen Chemie, Strukturaufklärung und Analyse.

Der Band enthält auch eine ausführliche Bibliographie.

In dem umfassenden Abschnitt A werden Herstellungsmethoden für alle organo-Silicium Verbindungen ausführlich besprochen, die nach Stoffklassen gruppiert werden : symetrische, unsymetrische, zyklische Tetraorganosilane und heterofunktionell substituierte Tetraorganosilane, Organo-H-silane, Deutero-organo-silane, Halogen-organo-silane, Organo-pseudohalogensilane, Organo-Silicium Verbindungen, die Sauerstoff, Schwefel, Selen, Tellur, Stickstoff, Phosphor, Arsen, Antimon und Wismut enthalten, Organo di- und polysilane und endlich makromolekulare organo-Silicium Verbindungen.

Die Herstellungsmethoden, mit einigen Ausnahmen betreffen : Direkte Synthese, Synthese aus Metallorganischen Verbindungen und Hydrolisierung von ungesättigten Kohlenwasserstoffen.

Im Abschnitt B werden die Reaktionsmöglichkeiten aller C—Si Bindungen Spaltung sehr kurz behandelt.

In den meisten Fällen werden die organo-Silicium Verbindungen in der präparativen organischen Chemie als Reduktions-oder Deoxidierungsmittel und als Hilfsmittel zur Einführung von gewünschten Alkyl, Aryl, Alken, Alkin, Azid, Alkoxi, oder Trimethylsilyl-Resten eingesetzt, wobei die leichte Abspaltungsreaktion der C—Si Bindung maßgebend ist. Weiterhin wird im Abschnitt C dieses Verhalten ausführlich und kritisch besprochen. Hiermit wird eine Einordnung nach Reaktionstypen geleistet, die für dieses Gebiet und hauptsächlich für die präparative organische Chemie einen sehr wichtigen Beitrag darstellt.

Auschließend werden Verfahrensmethoden für Strukturaufklärung und Analyse der organo-Silicium Verbindungen gegeben. Hierbei wird Schwingungsspektrometrie (IR, Raman) ^{29}Si-NMR-Spektrometrie, Elementaranalyse und Gruppenanalyse besprochen.

Es wurden auch chromatographische Verfahren für die Bestimmung der Einzelverbindungen in Substantzgemischen berücksichtigt.

Am Ende wird die berücksichtigte Literatur in Monographien und Handbücher, Themenspezifische Übersichtsabhandlungen und Autorenregister eingeteilt. Der Band enthält auch ein sehr nützliches Sachregister, eine Zeitschriftenliste und eine Abkürzungenliste.

Es kann eingeschätzt werden, daß der vorliegende Band einen bedeutenden Literaturbeitrag von hohem theoretischen und praktischen Wert darstellt und daß er sich durch eine kritische und methodische Behandlung eine zusammenfassende und übersichtliche Darstellung der auf diesem Gebiete veröffentlichen Arbeiten auszeichnet.

Aglaia Ciobanu

T. MURAYAMA, "Dynamic Mechanical Analysis of Polymeric Material", Elsevier, Amsterdam, 1979, 231 p.

The book represents the authoritative lead-off volume of a new and very interesting Elsevier series of monographs in materials science.

During the past decade polymeric materials and composites have gained increasing use, and as is well known the methods of investigating the dynamic mechanical properties of these materials have advanced greatly. However, unfortunately, widespread research work on these topics has often established diverse results and principles. Consequently, there has long been a vital need for a monograph to cover critically the field of the dynamic mechanical analysis of polymeric materials and especially to present the physical principles, the methods of identification and interpretation of the dynamic mechanical data as well as the rational application of these results to the very important question of the structure-property relationships

The dynamic mechanical analysis involves the determination of the dynamic mechanical properties — the dynamic modulus and internal friction — over a wide range of temperatures and frequencies, and as a result the relationships between the dynamic properties and the structural parameters (crystallinity, molecular orientation, molecular weight, crosslinking, copolymerization, plasticization, etc.) and external variables (temperature, pressure, time, frequency, type of deformation, surrounding atmosphere, humidity, etc.) can be explained. The dynamic parameters are used in this way to determine the glass region transition, relaxation spectra, degree of crystallinity, phase separation, structural and morphological changes resulting from processing ,as well as the chemical composition in polyblends, graft polymers and copolymers.

The book opens with a critical review of the physical principles and related concepts of dynamic mechanical analysis, the viscoelastic character of the mechanical response of polymeric materials being clearly presented. Moreover, the key variables — time, frequency and temperature — as well as the intimate connection of these to structure are thoroughly given.

Chapter II points to the development of different characterization techniques in the dynamic mechanical analysis (rheovibron, torsion pendulum, torsional braid analysis, vibrating reed, mechanical spectrometer, complex modulus apparatus and dynamic mechanical analyzer).

Although now it is well established that dynamic modulus and internal friction are the fundamental mechanical properties, the correlation between the molecular interpretation of such data and the viscoelastic character of the mechanical behaviour of polymer needs the careful presentation given by the author in chapter III.

Chapter IV is devoted to the analysis of different structural units, the greatest attention being paid to the effect of these structural assemblies on the end-use performances of polymeric materials.

Experimental relationships between dynamic properties and viscoelasticity are given in chapter V. The author presents in a natural and clear way the important question of the applicability of phenomenological theory, stress relaxation-creep-dynamic properties, and stress-strain behaviour in the light of the typical viscoelastic character of the mechanical response of polymers.

Given the anisotropic behaviour of many polymeric materials, in chapter VI the recent developments in the field of experimental techniques on dynamic shear, compression, and bending methods are discussed.

External variables which affect dynamic mechanical properties of polymers include not only various deformations, temperature and geometry of structural assemblies but also the environment (liquid or gas), and in the end chapter, the techniques of dynamic mechanical analysis in liquid and gas media are presented. The effects of humidity, relationships between dynamic loss modulus and diffusion as well as the special case of the biopolymers are carefuly presented.

This book, reflecting the significant experience in the field of one of the authoritative investigators of dynamic mechanical properties of polymeric materials, represents a valuable reference volume not only for physicists and chemists but also for chemical and mechanical engineers engaged in research and development programs. Moreover, the work is an up-to-date text for senior and undergraduate level courses in materials science and engineering.

Horia Paven

P. BENEDEK (Editor), "Steady-state flow-sheeting of chemical plants", Akadèmiai Kiadó, Budapest, 1980, 410 pages.

The book describes in detail the SIMUL system developed in Hungary for simulating complex operations (processes, plants), primarily major petro-chemical plants. Simulation is used in order to obtain by simple means and with low cost the informations necessary for taking economic-technical decisions, which could otherwise be available only by measurements on the original system.

The work is structured in twelve chapters : 0. Simulation. Fundamental principles, scope, realization ; 1. The process ; 2. Streams ; 3. Equipment ; 4. Network ; 5. Process simulation ; 6. Information feedback ; 7. Optimization ; 8. Organizing program ; 9. Flow-sheeting ; 10. Computer-aided process design ; 11. The state-of-the-art.

The first chapters provide the reader information on how to produce the operation-order flow-sheet by analysing, simplifying and elaborating all the stream-, equipment- and network-characteristics of a complex operation. The structure of these chapters is similar : the first part handles the subject based on an example, the second contain the terminology together with the strict rules of the SIMUL system, the third deals with conventions and the fourth outlines the results of developing the system, as boxes, procedures, etc.

A program package FISC allows the calculation of the physical and chemical properties of various mixtures in liquid or gaseous state of 214 chemical components which form the material streams. Using up to 40 basic properties for each of these components, this program may calculate : pseudo-constants of a mixture, pseudo-vapour-pressure and enthalpy of vaporization of a liquid mixture, molal density, viscosity, thermal-conductivity, surface-tension, enthalpy, molal heat capacity, pressure correction of enthalpy, temperature pertaining to the molal enthalpy, mean molecular weight, equilibrium vapour ratio, boiling- and dew-point of mixtures.

The equipment is simulated by equipment-type boxes which produce the output stream vectors as a function of the input stream vectors, taking the main dimensions and the parameters characterising the steady-state performance of the equipment. The equipment boxes produce models of : pressure drop and temperature change of a substance flowing in a pipe ; mixing homogeneous streams ; separation ; heat transfer ; distillation unit ; compression of gases ; chemical transformation ; absorption in plate towers ; gas absorption and desorption, etc.

The problem of material and informational network is solved with the connection indices which serve to identify the connecting points formed by the interconnection of two boxes and the stream passing through them.

The flow-sheet program and the input data system are processed by computation on a GIER computer ; the computation is governed by an organizing program written in ALGOL.

The general characteristics of the SIMUL system, which distinguish it from other simulating systems, considered by the authors, are : 1. The SIMUL language has its own syntactics and semantics. The user is not expected to possess experience in programming ; 2. In the SIMUL system more than one stream type may be declared and it is therefore possible to handle individually qualitatively different objects of work involved in complex operations ; 3. The SIMUL system is operation-oriented so it calculates automatically, where and when necessary, the property values of the objects of work. The user has only to stipulate the sequence of the calculations, the input streams and the main equipment dimensions for the calculation of the operations. 4. In the SIMUL system it is possible to formulate complex statements with the aid of some boxes (solving systems of equations or optimizing). 5. In the SIMUL system references are defined, so that with appropriate coding we may state that any parameter of a box or any element of a stream vector should be substituted by a value which has been already found from calculation. 6. In the SIMUL system references may be made to an arithmetic expression ; this allows for including functions of any variables in the place of a value. 7. The SIMUL system may be operated automatically or interactively. The automatic order of calculation may be interrupted at completion of the calculation of a box and it is possible to modify either the sequence of statements or the data system.

The planning and programming of calculation is exemplified for catalytic isomerization of butane (chap. 2—5), for simulation of the gas-separating section of a naphtha craker (chap. 9), for computer-aided process design of the manufacture of acetic anhydride (chap. 13).

The chapters 2—7 and 10 are ended by problems which serve readers to cover the use of SIMUL procedures and the develop of new procedures.

M. Chirca

REVUE ROUMAINE
DE
CHIMIE

ORSZÁGOS MŰSZAKI KÖNYVTÁR ÉS DOKUMENTÁCIÓS KÖZPONT
1883

Tome 27, N° 3 Mars, 1982

RODICA VÎLCU, A. CIOCHINĂ and GH. VASU, Absolute measurement of thermal conductivity and thermal diffusivity of gases by the classical procedure of the transient hot wire method . . . . 313—323 R

Ş. MOLDOVEANU and V. DAVID, An extended Hückel FORTRAN program for molecules including the elements from hydrogen to xenon except the transition metals . . . . 325—343 R

S. STERNBERG and T. VIŞAN, Electroreduction of nitrate ions in molten alkali nitrates . . . . 345—349 R

ORTANSA LANDAUER, CORNELIA MATEESCU and OLGA IULIAN, The influence of the solvent on the reaction rate. The alkaline hydrolysis of the n-butyl acetate, propionate and butyrate in the mixed solvent water-dimethylsulphoxide (in French) . . . . 351—355

FAYEZ Y. KHALIL and M. T. HANNA, Kinetic and thermodynamic parameters of the reversible acid hydrolysis of benzyl acetate in water—methanol mixtures . . . . 357—363 Bc

N. DOCA, F. KLEPP and E. SEGAL, Reactant — catalyst interaction parametrisation . . . . 365—380 C

F. DOMKA, W. ZMIERCZAK and J. MICIUKIEWICZ, Catalytic properties of iron chromite, activated by alkali oxides (in French) . . . . 381—384

N. CALU, EUGENIA SAVIUC, TEODORA POPOVICI, Study of the Fe(III)-3-hydroxypyridine N-oxide system . . . . 385—391

RAGHUNATH P. GUPTA and ASHUTOSH K. SRIVASTAVA, Thiosemicarbazones as ligands and evaluation of their virus inhibitory behaviour. I. Some transition metal complexes of substituted Isatin β-thiosemicarbazones . . . . 393—400 Bc

P. M. DEYA, A. COSTA, J. V. SINISTERRA and J. M. MARINAS, The $AlPO_4$ and related systems as catalysts in organic reactions. I. Tertbutylbenzene cracking . . . . 401—410

C. I. CHIRIAC, A new synthesis of hydrazides by a direct condensation reaction 411—414

A. ESSAWY, Synthesis and reactions of 2-furyl-3,1-benzothiazine-4(*H*)-thione, 2-furyl-4(3H)-quinazolinone and 2-furyl-3,1-benzoxazin-4(*H*)-one . . . . 415—421

A. C. RĂZUŞ, ZS. ARVAY and ALICE-MARIE GLATZ, Aluminium chloride catalyzed reactions of unsaturated acids with benzene. XIV. Reaction of *t*-butyl acrylic acid . . . . 423—428

A. I. HASHEM, Replacement of the nitro group in pentachloronitrobenzene by nucleophiles . . . . 429—431

Rev. Roumaine Chim. **27**, *3*, 311—468 (1982) Bucarest

GH. HUBCA, CR. OPRESCU, GH. DRĂGAN and M. DIMONIE, Synthesis and polymerization of polyethylene glycol dimethacrylates. IV. Study of the polymerization process of polyethylene glycol dimethacrylates . . . . . 433—442
LI QILONG, C. LUCA, A. CĂLUŞARU and F. G. BĂNICĂ, Catalytic hydrogen discharge by cycloserine in metal-ion containing ammonia buffer . . . . 443—451
LUMINIŢA VLĂDESCU and ARIADNA HARLES, Utilization of chromotropic acid in separation of titanium with ion exchange resins. II. Anion exchange behaviour . . . . 453—458
A. F. DĂNEŢ and ANCA MARIANA BERCARU, Extraction, complexing and determination of phenyl-mercuric ion with diazoaminobenzene . . . . . . 459—465

BOOK REVIEW . . . . 467—468

Revue Roumaine de Chimie, 27, *3*, 313–323 (1982)

ABSOLUTE MEASUREMENT OF THERMAL CONDUCTIVITY AND THERMAL DIFFUSIVITY OF GASES BY THE CLASSICAL PROCEDURE OF THE TRANSIENT HOT WIRE METHOD

RODICA VÎLCU*, A. CIOCHINĂ** and GH. VASU**
* Polytechnic Institute, Department of Physical Chemistry, Bd. Republicii 13, Bucharest, Romania
** ICECHIM, Centre of Physical Chemistry, Spl. Independenței 202, Bucharest, Romania

Recived June 15, 1981

The purpose of this work is to prove experimentally that the wire diameter represents the main difficulty of principle of the classical procedure of the transient hot wire method when it is used for gases. The paper describes briefly the theory of the method and the measuring principle of the apparatus using a platinum wire 0.015 mm in diameter as a transducer. The thermal conductivity and thermal diffusivity are determined by the classical procedure of the method. The experimental results on gaseous argon at 299.8 K and atmospheric pressure are given. The analysis of both measurement and phenomenological errors shows clearly that by the classical procedure, the thermal conductivity and thermal diffusivity of gases can be measured only if the wire diameter is of the order of microns.

1. INTRODUCTION

Accurate measurements of the transport properties of gases are important for both engineering calculations and experimental testing of the molecular theory of transport properties. The viscosity of many gases has been accurately measured over a large temperature range.[1] The values of experimentally determined viscosities and those theoretically calculated using different models, are well correlated. The results for the thermal conductivity of gases are less well correlated than the viscosity data and it is difficult to specify whether this is due to theoretical shortcomings or to experimental errors.[2]

Almost all experimental values for the thermal conductivity of gases, used in the comparison with the molecular theory of transport properties,[3] have been determined with steady state methods,[4–9] for which reaching the steady state thermal regime is a slow process.

Transient measurement methods allow for rapid determination of the thermal conductivity of fluids by applying a short-duration thermal pulse.[4] Among them, the transient hot wire method, intensively employed in thermal conductivity measurements of liquids,[10-16] encounters experimental difficulties when used for gases,[2,17] because *the classical procedure of the method* is valid only if the wire can be approximated as a linear source of heat. The transient hot wire method briefly consists in meaduring the temperature rise, $\theta(r_1, t)$ as a function of time, t for a metallic wire of radius r_1, heated with a step-pulse of constant power. The wire, vertically immersed in the fluid, acts as both electric heater and thermoresistance.

From the theory of the method,[18] as pointed out in a previous paper,[19] correct results are obtained only when the main following conditions are fulfilled: the wire diameter is as small as possible, the wire is long enough and the experiment duration is shorter than a critical value. The measurements have to be run at such times t as we might have $t_A \leqslant t \leqslant t_B$, where t_A is determined by the finite values for radius, density and heat capacity of the wire, and t_B by the natural convection onset, and/or wall cell effect and heat losses at the wire ends. Thus, following this classical procedure of the method, the measurement range towards the short times is decided by the wire diameter. For gases, if the wire diameter is not of the order of microns, a critical situation occurs, that is $t_A > t_B$, and the classical procedure of the method is no longer suitable.

This restrictive condition — the choice of the wire diameter — represents the main difficulty of principle of the classical procedure of the method, especially when it is used for gases.

In the present contribution, after a brief discussion of the theory of the transient hot wire method, of the experimental set and measurement principle of the apparatus, the experimental values are given for the thermal conductivity and thermal diffusivity of argon at 299.8K and atmospheric pressure, as obtained by the classical procedure of the method.

The difficulties of this procedure are exemplified by computing the (t_A, t_B) measuring range as a function of wire and fluid characteristics (as given in literature) and of the experimental parameters of the apparatus.

2. FUNDAMENTALS OF THE METHOD

The transient hot wire apparatus determines the thermal conductivity, λ, of the fluid by measuring the temperature rising rate as a function of time for a metallic wire vertically immersed in the fluid. The wire, electrically heated by a step-pulse of constant voltage, simulates a linear source of heat[18] with a constant heat flow per unit length, q, and develops within the fluid a temperature field which increases radially in time and is axially symmetrical.

The temperature rise, $\theta(r_1, t)$, for a wire of radius, r_1, at $r = r_1$ and time t counted from the heating turning on $t = 0^+$, against the initial temperature T_0 of the cell at $t = 0^-$, is given by the relation [14,17,18]:

$$\theta(r_1, t) = \frac{q}{4\pi\lambda}\left[\ln\frac{4\tau}{C} + \frac{1}{2\tau} + \frac{b-2}{2b\tau}\ln\frac{4\tau}{C} + \dots\right]$$
$$= \frac{q}{4\tau\lambda}\left[\left(1 - \frac{\rho_1 c_1 - \rho c_p}{2\lambda t}\, r_1^2\right)\ln\frac{4\tau}{C} + \frac{1}{2\tau} + \dots\right] \qquad (1)$$

where: ρ, c_p and $a = \lambda/(\rho c_p)$ are the density, heat capacity at constant pressure and, respectively, thermal diffusivity of the fluid; ρ_1 and c_1 are the density and specific heat of the wire material, respectively; $\tau = a\,t/r_1^2$; $b = 2\rho c_p/(\rho_1 c_1)$; $C = \exp\gamma = 1.781$ and $\gamma = 0.5772$ is Euler's constant.

After a certain time, t_A, from starting the step-pulse ($t = 0^+$), i.e. for $t \geqslant t_A$, the temperature rise $\theta(r_1, t)$ of the wire is described by the formula:

$$\theta(r_1, t) = \frac{q}{4\pi\lambda}\ln\frac{4\tau}{C} \qquad (2)$$

In plot $\theta(\ln t)$, equation (2) represents a straight line with a slope inversely proportional to the thermal conductivity. This linear logarithmic law is obeyed only for $t \geqslant t_A$, because it contains approximations for reducing the complete equation of the energy conservation and idealising the wire behaviour to a linear source of heat. [14] Therefore, equation (2) is valid only for high enough $\tau = a\,t/r_1^2$ values. This condition has to be fulfilled experimentally and it can be satisfied by increasing t (duration of the experimental run) and diminishing the wire diameter. But the experimentally measurable t values are limited towards long times at $t \leqslant t_B$ by the natural convection onset of the fluid within the cell, or/and by the radial limitation of the fluid, (cell wall effect) and heat losses at the wire ends. The natural convection onset is determined by the fluid physical properties and $\theta(r_1, t)$ values; the heat losses at the wire ends are determined by the length L, radius r_1 and thermal conductivity, λ_1, of the wire. Towards the short times, t values are limited at $t \geqslant t_A$ by the finite r_1, ρ_1 and c_1 values of the wire.

Thus, in order to obtain high enough τ values, but still having a (t_A, t_B) measuring range as large as possible (the validity range of the linear logarithmic law described by equation (2)), both r_1 and q values must be as small as possible (the former to diminish t_A, the latter to increase the critical time, t_B, of the natural convection onset).

The classical procedure of the method [19] is based on the validity of equation (2):

— thermal conductivity, $\lambda^{(0)}$, is calculated from the slope of straight line (Δ) fitted by the least square method to the experimental pairs $(\theta(r_1, t), \ln t)$, within the linear range of curve $\theta(\ln t)$, i.e. $t_A \leqslant t \leqslant t_B$;

— thermal diffusivity, $a^{(0)}$, is determined by extrapolating the straight line (Δ); the computation formula implies the r_1 and t_0 values, the latter being the intercept of straight line (Δ) to the axis ($\ln t$).

With individual experimental pairs, for example (Φ_1, t_1) and (Φ_2, t_2) with $t_2 > t_1$, one gets:

$$\lambda^{(0)} = \frac{\ln t_2 - \ln t_1}{\Phi_2 - \Phi_1} \tag{3}$$

$$\Phi_1 = \frac{4\pi}{q}\,\theta(r_1, t_1); \quad \Phi_2 = \frac{4\pi}{q}\,\theta(r_1, t_2)$$

$$a^{(0)} = r_1^2\, C/(4t_0) \tag{4}$$

$$\ln t_0 = \ln t_1 - \Phi_1 \lambda^{(0)}$$

$$a^{(0)} = \frac{r_1^2 C}{4\, t_1} \exp\,(\Phi_1\, \lambda^{(0)}) \tag{5}$$

The index $^{(0)}$ means that λ and a values were obtained by the classical procedure of the method.

The time t_A, determined by the finite r_1, ρ_1 and c_1 values of the wire, can be chosen by computing the relative error, e_1 in the slope of curve $\theta(\ln t)$, which is a function of τ and b values.[20,21]

$$\frac{d\,\theta(r_1, t)}{d(\ln t)} = \frac{q}{4\pi\lambda}\left\{1 - \frac{1}{2\tau}\left[1 + \left(1 - \frac{\rho_1 c_1}{\rho c_p}\right)\left(\ln\frac{4\tau}{C} - 1\right)\right] + \dots\right\} \tag{6}$$

$$e_1 = \frac{1}{2\tau}\left[1 + \chi\left(\ln\frac{4\tau}{C} - 1\right)\right] \tag{7}$$

where: $\chi = 1 - [(\rho_1 c_1)/(\rho c_p)]$.

The critical time, t_B, of the natural convection onset can be approximately evaluated from the equation[20,21]:

$$\frac{g\beta r_1^3}{\nu a}\;\frac{q}{4\pi\lambda}\;\ln\frac{4at}{r_1^2 C}\left(\sqrt{\frac{4at}{r_1^2 C}} - 1\right)^3 \leqslant 1000 \tag{8}$$

where $g = 9.81$ m/s^2 is the acceleration of gravity; β, $\nu = \eta/\rho$ and η are, respectively, the thermal expansion coefficient, kinematic viscosity and dynamic viscosity of the fluid. It results from equation (8) that:

$$t_B \leqslant 0.445\left[\left(\frac{1\,000\nu}{g\beta\theta(r_1, t)\sqrt{a}}\right)^{1/3} + \frac{r_1}{\sqrt{a}}\right]^2 \tag{9}$$

The wall cell effect is negligible if $r_2^2/(4at) > 6$, where r_2 is the inner radius of the cell.

The finite length, L, of the wire affects the ideal wire temperature rise ($L = \infty$, $\lambda_1 = \infty$) twofold. First, the discontinuity in heating along the wire axis distorts the temperature field near each end. The relative error, e_2, introduced in the slope $d\,\theta(r_1, t)/d(\ln t)$, averaged over the wire length, L, is given approximately by the relation[20,21]:

$$e_2 \simeq \frac{\sqrt{4at}}{L}\; ierfc\, \frac{L}{\sqrt{4at}} \tag{10}$$

NOTE POUR LES AUTEURS

La Revue Roumaine de Chimie publie des articles en anglais, français, russe, allemand ou espagnol. Les auteurs sont priés d'envoyer des articles et des comptes rendus inédits.

Les manuscrits seront dactylographiés à double interligne. La bibliographie, les tableaux et la légende des figures seront placés après le texte.

Si l'article fait partie d'une série numérotée, la partie précédente sera donnée comme première référence.

Chaque article sera précédé d'un résumé comprenant quinze lignes au maximum.

Les références bibliographiques dans le texte seront faites par des exposants sans parenthèses et paraîtront à la fin de l'ouvrage.

Les publications périodiques mentionnées dans la bibliographie seront présentées suivant les prescriptions internationales ; le nom de l'auteur précédé de l'initiale du prénom, le titre du périodique abrégé conformément à « Chemical Abstracts » et souligné par une ligne, le numéro du tome indiqué par des chiffres arabes et souligné par deux lignes, suivi de la première page de l'article : à la fin, l'année de la parution sera placée entré paranthèses. Le numéro de la revue ne sera pas indiqué si les pages du volume sont numérotées consécutivement.

Les textes des livres ou traités inclueront : le nom des auteurs, précédé de l'initiale du prénom, le titre du livre entre guillemets et sans être souligné, le numéro du tome précédé par l'abréviation « vol » (ou « Bd. »), le numéro de l'édition, les éditions (the publisher), la localité de la parution du livre, l'année de la parution et la page de la référence précédée(s) par l'abréviation « p » (ou « S »).

Les brevets seront indiqués comme suit : l'auteur ou la firme, le pays et le numéro du brevet, la date et la revue *(Chem. Abstr.)*. Par ex. : M. Jones (to Union Carbide Co.), Brit. Pat. 601 238, 2 Sept. 1959, *Chem. Abstr.*, **54**, 12808 (1960).

Si la référence n'a pas été lue en original, on indiquera aussi la revue de références consultée.

Les diagrammes seront tracés à l'encre de Chine sur papier calque. Les tableaux et les figures (en nombre strictement nécessaire) ainsi que les courbes dans les figures seront numérotés par des chiffres arabes. Leur explication sera donnée dans la légende des figures. Prière de ne pas inscrire les mêmes données dans les tableaux et les figures. Chaque tableau aura un titre. On indiquera dans le texte la place approximative des tableaux et des figures. Les formules chimiques seront incluses dans le texte : en outre, elle seront transcrites sur papier calque, à l'encre de Chine.

Les auteurs sont priés d'indiquer les caractères italiques (en soulignant les lettres au crayon), ainsi que tout autre caractère spécial : les préfixes *ortho*, *meta*, *para*, *cis*, *trans*, etc. seront soulignés pour indiquer leurs caractères italiques et ne seront jamais écrits avec des majuscules.

Aucune correction à la main ne sera admise sur le manuscrit. Les corrections seront tapées à la machine. Les lettres grecques ou autres symboles spéciaux seront insérés à la main à l'encre clairement.

Le manuscrit sera signé par l'auteur.

Le colonne-titre aura 50 lettres au maximum.

L'entière responsabilité du contenu des articles appartient aux auteurs.

Sur demande on peut obtenir une note plus complète.

PRINTED IN ROMANIA

1982 AOU 3

TRAVAUX PARUS AUX ÉDITIONS DE L'ACADÉMIE DE LA RÉPUBLIQUE SOCIALISTE DE ROUMANIE

ELENA CEAUŞESCU, **Noi cercetări în domeniul compuşilor macromoleculari** (Nouvelles recherches dans le domaine des composés macromoléculaires), 1981, 536 p.

I. G. MURGULESCU, TATIANA ONCESCU, E. SEGAL, **Introducere în chimia fizică. Vol. II. 2. Cinetică chimică şi cataliză** (Introduction à la chimie physique. Vol. II. 2. Cinétique chimique et catalyse), 1981, 1024 p.

T. GĂLĂŢEANU, **Procese şi metode radiochimice aplicate în energetica nucleară** (Processus et méthodes radiochimiques appliqués dans l'énergetique nucléaire), 1981, 234 p.

V. DRĂGUŢAN, A. T. BALABAN, M. DIMONIE, **Metateza olefinelor şi polimerizarea prin deschidere de inel a cicloolefinelor** (La métathèse des olefines et la polymérisation par ouverture annulaire des cyclooléfines), 1981, 254 p.

O. IORDACHE, **Procese polistocastice aplicate la fenomenele de transfer** (Processus polystochastiques appliqués aux phénomènes de transfert), 1981, 187 p.

C. SIMIONESCU, VALERIA GORDUZA, **Polimeri biocompatibili şi biologic activi** (Polymères biocompatibles et biologiquement actifs), 1980, 497 p.

ELENA CEAUŞESCU, **Polimerizarea stereospecifică a izoprenului** (La polymérisation stéréospecifique de l'isoprène), 1979, 307 p.

M. FLORESCU, **Metode ştiinţifice în dezvoltarea industriei chimice moderne** (Méthodes scientifiques dans le développement de l'industrie chimique moderne), 1979, 256 p.

A. T. BALABAN, I. GĂLĂŢEANU, G. GEORGESCU, LIGIA SIMIONESCU, **Compuşi marcaţi şi radiofarmaceutici cu aplicaţii în medicina nucleară** (Composés marqués et radiopharmaceutiques à application en médecine nucléaire), 1979, 495 p.

CONST. GH. MACAROVICI, **Analiza chimică cantitativă anorganică** (L'Analyse chimique quantitative inorganique), 1979, 457 p.

I. G. MURGULESCU, E. SEGAL, **Introducere în chimia fizică, vol. II.1. Teoria molecular cinetică a materiei** (Introduction à la chimie physique, vol. II. 1. La théorie moléculaire-cinétique de la matière), 1979, 1036 p.

I. E. TEODORESCU, MARIA FITI, **Iradierea tehnologică** (Irradiation technologique), 1979, 216 p.

S. STERNBERG, FL. DANEŞ, **Termodinamica chimică aplicată** (La thermodynamique chimique appliquée), 1978, 400 p.

I. G. MURGULESCU, V. EM. SAHINI, **Introducere în chimia fizică. Vol. I.2. Structura şi proprietăţile moleculelor** (Introduction à la chimie physique. Vol. I.2. La structure et les propriétés des molécules), 1978, 604 p.

C. DRĂGULESCU, E. PETROVICI, **Chimie structurală modernă. Chimia coordinanţei 8** (La chimie structurale moderne. La chimie de la coordinence 8), 1977, 947 p.

D. PURDELA (sous la direction de), **Nomenclatura chimiei anorganice** (La nomenclature de la chimie inorganique), 1977, 153 p.

I. ZUGRĂVESCU, MAGDA PETROVANU, **N-ylid chemistry**, coédition avec McGraw-Hill International Book Company, U.S.A., 1977, 396 p.

I. G. MURGULESCU, **Introducere în chimia fizică. Vol. I.1. Atomi, molecule, legătură chimică** (Introduction à la chimie physique. Vol. I.1. Atomes, molécules, liaison chimique), 1976, 560 p.

CONST. GH. MACAROVICI, D. MACAROVICI, **Chimia oxizilor dubli şi utilizările lor** (La chimie des oxydes doubles et leur utilisation), 1975, 195 p.

ELENA CEAUŞESCU, **Research work on synthesis and characterization of macromolecular compounds. Contributions**, 1974, 251 p.

CR. SIMIONESCU, VIORICA RUSAN, V. POPA, **Chimia algelor marine** (La chimie des algues marines), 1974, 212 p., 1 pl.

I. P. INFORMAŢIA c. 1667

43426

Lei 25

$ 55 (pour un abonnement annuel)

F 1103

ACADÉMIE DE LA RÉPUBLIQUE ~~SOCIALISTE~~ DE ROUMANIE

REFERÁLVA

R

REVUE ROUMAINE DE CHIMIE

TOME 27
N° 3
Mars 1982

EDITURA ACADEMIEI REPUBLICII SOCIALISTE ROMÂNIA

Rev. Roumaine Chim.

RRCHAX, **27**, *3*, p. 311–468 (1982), Bucarest

ACADÉMIE DE LA RÉPUBLIQUE SOCIALISTE DE ROUMANIE

COMITÉ DE RÉDACTION

Rédacteur en chef:

I. G. MURGULESCU, membre de l'Académie de la République Socialiste de Roumanie

Rédacteurs en chef adjoints:

A. T. BALABAN et V. EM. SAHINI, membres correspondants de l'Académie de la République Socialiste de Roumanie

Collège de rédaction:

EM. BRATU, ELENA CEAUȘESCU, ECATERINA CIORĂNESCU-NENITZESCU, CR. SIMIONESCU, membres de l'Académie de la République Socialiste de Roumanie; P. SPACU, membre correspondant de l'Académie de la République Socialiste de Roumanie; MARGARETA AVRAM, M. BANCIU, I. HAIDUC, D. I. MARCHIDAN, I. MOLDOVAN, G. NIAC et D. SĂNDULESCU

La Revue Roumaine de Chimie paraît 10 fois par an. Toute commande de l'étranger pour les travaux parus aux Editions de l'Académie de la République Socialiste de Roumanie sera adressée à ILEXIM, Departamentul Export-Import Carte (Livres)/Departamentul Export-Import Presă (Revues), P.O.B. 136—137, télex 11226, 3, str. 13 Decembrie, 79517 Bucarest, Roumanie

Les manuscrits, les livres et les revues proposés en échange ainsi que toute correspondance seront envoyés à la rédaction:

REVUE ROUMAINE DE CHIMIE

125, Calea Victoriei, 79717 Bucarest, Roumanie, téléphone 50 76 80

EDITURA ACADEMIEI REPUBLICII SOCIALISTE ROMÂNIA
125, Calea Victoriei 79717, Bucarest, Roumanie, téléphone 50 76 80

Secondly, the heat is lost by conduction along the wire towards the connecting leads. Due to this effect, the relative error, e_3, introduced in the slope $d\theta(r_1, t)/d(\ln t)$ is given approximately by the relation [20,21]:

$$e_3 \simeq \frac{3r_1}{2L}\sqrt{\frac{\lambda_1}{\lambda}}\sqrt{\ln\frac{4\tau}{C}} \tag{11}$$

3. EXPERIMENTAL SET

The experimental set consists of : measurement cell, thermostat, vacuum unit, thermal conductivimeter and electrical measurement apparatus. Details on the experimental set and working mode were given in a previous paper.[22]

3.1. MEASURING CELL

The measuring cell, made of Pyrex glass tube (60 mm i.d.), contains the investigated gas. The transducer consists of a pure platinum wire (Heraeus Degussa) 0.015 mm in diameter and 0.22 m in length, soldered at the ends to thick copper leads. The transducer is vertically immersed in the gas-filled cylindrical cell. The whole set is immersed in the thermostating vessel. [9]

3.2. MEASURING PRINCIPLE OF THE APPARATUS

The platinum wire is calibrated as a thermoresistance, that is the electrical resistance variation is a measure for the temperature rise, $\theta(r_1, t)$, and it is measured on a Wheatstone bridge. [22] At $t = 0^-$ and T_0, the bridge is either balanced or submitted to a known resistive unbalance, x_p : the heating current is nil. At $t = 0^+$, a step-pulse of D. C. constant voltage, E_p, is applied on the bridge input. The bridge is activated and, simultaneously, seven electronic timers are released. By Joule heating, the current in the bridge brings about a temperature rise, that is an increase in the wire electrical resistance. At the very moment when the bridge output signal (amplified) becomes successively equal to seven present voltage levels, x_i, of the comparators, each of the comparators triggers a stopping signal to the corresponding timer. Thus, the time intervals are measured from the $t = 0^+$ (START of the timers) till instants t_i $(i = 1, \ldots, 7)$ (successive STOP of the timers). The wire temperature rise, $\theta(r_1, t_i)$, between instants $t = 0^+$ and $t = t_i$ can be calculated from the bridge equation, $f(x_p, x_i)$, and temperature coefficient of the wire electrical resistance, α_{T_0}, at temperature T_0.

$$\theta(r_1, t_i) = \frac{2}{\alpha_{T_0}} \, \frac{f(x_p, x_i)}{1 - f(x_p, x_i)} \tag{12}$$

$$\Phi_i = \frac{4\pi}{q}\,\theta(r_1, t_i) \tag{13}$$

The amount of heat, q, produced in the wire unit length is calculated from the measurable E_p, L and R_1^0 values, the latter being the wire electrical resistance at $t = 0^-$ and T_0

$$q = E_p^2/(4LR_1^0). \tag{14}$$

4. EXPERIMENTAL RESULTS

The experimental results for argon (gas) at 299.8 K and atmospheric pressure are presented in Tables 1 and 2.

TABLE

The experimental time $t(s)$ values mea

$R(\Omega)\downarrow$ $x_i \rightarrow$	0.5000	0.8395	0.8880	0.9115
				$x_p =$
135.15	0.02638	0.20357	0.37262	0.52427
	0.02645	0.20401	0.37318	0.52546
	0.02642	0.20332	0.37467	0.52211
	0.02639	0.20376	0.36998	0.51675
	0.02636	0.20317	0.37161	0.51637
135.13	0.02640	0.20397	0.37156	0.51855
	0.02645	0.20285	0.37422	0.52123
	0.02645	0.20516	0.37408	0.51986
	0.02645	0.20510	0.37415	0.52356
	0.02629	0.21068	0.36798	0.51400
	0.02647	0.20337	0.37489	0.52244
135.09	0.02626	0.20373	0.37243	0.52381
		0.20364	0.37261	0.52069
		2.69×10^{-4}	5.99×10^{-4}	1.04×10^{-3}
		0.132	0.161	0.200
		1.82×10^{-4}	4.04×10^{-4}	7.02×10^{-4}
				$x_p =$
135.17	0.03087	0.31323	0.61484	0.88251
	0.03087	0.31280	0.61326	0.87901
	0.03086	0.31619	0.62219	0.88833
	0.03068	0.31172	0.60720	0.86770
	0.03072	0.31128	0.60727	0.87113
135.16	0.03085	0.31479	0.61324	0.88027
	0.03086	0.31392	0.61880	0.88454
	0.03087	0.31651	0.61487	0.88255
	0.03077	0.31319	0.61316	0.87947
	0.03082	0.31189	0.61250	0.87607
135.15	0.03084	0.31416	0.61572	0.88061
		0.31360	0.61390	0.87927
		5.20×10^{-4}	1.32×10^{-3}	1.77×10^{-3}
		0.166	0.214	0.201
		3.51×10^{-4}	8.87×10^{-4}	1.19×10^{-3}
				$x_p =$
135.21	0.03150	0.33752	0.66845	0.95798
	0.03152	0.33615	0.66725	0.95971
	0.03140	0.33572	0.66336	0.95306
135.21	0.03228	0.33886	0.67112	0.96516
	0.03162	0.33987	0.67118	0.96474
	0.03155	0.33763	0.66763	0.95458
135.19	0.03147	0.33558	0.66348	0.95387
	0.03154	0.33745	0.66781	0.96078
	0.03146	0.33626	0.66402	0.95001
135.18	0.03150	0.33603	0.66673	0.95490
		0.33710	0.66710	0.95747
		4.51×10^{-4}	8.95×10^{-4}	1.60×10^{-3}
		0.134	0.134	0.167
		3.04×10^{-4}	6.04×10^{-4}	1.08×10^{-3}

1

sured on gaseous argon at $T_0 = 299.8$ K

0.9362	0.9601	0.9843	
0.1000			
0.74733	1.07904	1.5858	
0.75011	1.08305	1.5851	
0.74655	1.07910	1.5833	
0.73978	1.07225	1.5698	
0.74023	1.07100	1.5694	
0.74243	1.06982	1.5755	
0.74579	1.07506	1.5828	
0.74300	1.07844	1.5780	
0.75264	1.08710	1.5900	
0.73456	1.05588	1.5430	
0.74691	1.07694	1.5837	
0.74694	1.07978	1.5721	
0.74467	1.07559	1.5765	$\bar{t}(s)$
1.43×10^{-3}	2.29×10^{-3}	3.61×10^{-3}	$S(s)$
0.192	0.213	0.229	100 $S/\bar{t}(\%)$
9.63×10^{-4}	1.55×10^{-3}	2.44×10^{-3}	$E(s)$
0.0650			
1.28763	1.90023	2.8626	
1.28699	1.89649	2.8599	
1.29635	1.90685	2.8773	
1.27119	1.87006	2.8171	
1.26297	1.86949	2.8204	
1.28168	1.89501	2.8516	
1.29024	1.90237	2.8706	
1.28416	1.89797	2.8651	
1.28673	1.89062	2.8574	
1.28275	1.89288	2.8564	
1.28585	1.89597	2.8630	
1.28329	1.89250	2.8546	$\bar{t}(s)$
2.75×10^{-3}	3.65×10^{-3}	5.75×10^{-3}	$S(s)$
0.214	0.193	0.202	100 $S/\bar{t}(\%)$
1.86×10^{-3}	2.46×10^{-3}	3.88×10^{-3}	$E(s)$
0.0600			
1.39762	2.06155	3.0851	
1.40006	2.07016	3.1140	
1.39220	2.06045	3.1078	
1.40764	2.07804	3.1499	
1.40629	2.07828	3.1419	
1.39789	2.06117	3.1142	
1.38594	2.05748	3.1179	
1.40556	2.07863	3.1553	
1.39037	2.05546	3.1110	
1.38869	2.06030	3.1216	
1.39721	2.06613	3.1218	$\bar{t}(s)$
2.45×10^{-3}	2.91×10^{-3}	6.76×10^{-3}	$S(s)$
0.176	0.141	0.216	100 $S/\bar{t}(\%)$
1.65×10^{-3}	1.96×10^{-3}	4.56×10^{-3}	$E(s)$

TABLE 2

Experimental results on gaseous argon at $T_0 = 299.8$ K

$$f(x_i,\ x_p) = C_1\left[\frac{2x_i - 1}{1 - C_2(2x_i - 1)^2} - \frac{2x_p - 1}{1 - C_2(2x_p - 1)^2}\right]$$

$C_1 = 1.9968 \times 10^{-3}$; $C_2 = 1.838565 \times 10^{-3}$; $\alpha_{T_0} = 3.507 \times 10^{-3}(\mathrm{K})^{-1}$; $\bar{R} = 135.15\Omega$; $L = 0.222\ m$; $E_p = 1.998\ V$; $r_1 = 7.76 \times 10^{-6}\ m$

Set	$\theta(r_1,\ t)$ (K) eq(12)	Φ (mK/W) eq. (13)	$\bar{t}$ (s)	$\lambda^{(0)}$ (W/(mK)) eq. (3)	$10^5 a^{(0)}$ (m^2/s) eq. (5)	e_1 (%) eq.(7)	e_3 (%) eq.(11)
I	1.69	638.8	0.2036	0.0144	0.127	−26.3	1.16
	1.80	680.9	0.3726	0.0163	0.463	−15.1	1.19
	1.86	701.4	0.521	0.0167	0.648	−11.2	1.20
	1.91	722.8	0.745	0.0177	1.29	− 8.0	1.22
	1.97	743.6	1.076	0.0181	1.79	− 5.7	1.24
	2.02	764.7	1.577			− 4.0	1.25
II	1.77	669.2	0.3136	0.0159	0.353	−17.7	1.18
	1.88	711.4	0.614	0.0177	1.26	− 9.6	1.21
	1.94	731.8	0.879	0.0176	1.19	− 6.9	1.23
	1.99	753.3	1.283	0.0187	2.69	− 4.9	1.25
	2.05	774.1	1.893	0.0195	5.03	− 3.4	1.26
	2.11	795.2	2.855			− 2.3	1.28
III	1.78	673.6	0.3371	0.0162	0.440	−16.6	1.18
	1.90	715.7	0.667	0.0177	1.27	− 8.9	1.22
	1.95	736.1	0.957	0.0176	1.18	− 6.4	1.23
	2.01	757.6	1.397	0.0188	2.97	− 4.5	1.25
	2.06	778.4	2.066	0.0196	5.28	− 3.1	1.27
	2.12	799.5	3.122			− 2.1	1.28

In table 1, the mean value, $\bar{t}$, the standard deviation of the mean, S, and the most probable error of the mean values, E, are calculated by the following equations:

$$\bar{t} = \exp\left[\frac{\overset{n}{\Sigma}\,(\ln t_i)}{n}\right]$$

$$S = \left[\frac{\Sigma(\bar{t} - t_i)^2}{n(n-1)}\right]^{1/2}$$

$$E = 0.6745\ S$$

In table 2, $\lambda^{(0)}$ and $a^{(0)}$ values are calculated from subsequent $(\Phi, \ln \bar{t})$ pairs. In the computation of errors e_1, e_2 and e_3 use has been made of the following values of physical properties of argon and platinum, at 300 K, as given in literature [23-25]: $\lambda = 0.0177$ W/(mK),

$\rho = 1.6023\ \mathrm{kg/m^3}$, $c_p = 522\ \mathrm{J/(kg\ K)}$, $a = 2.116 \times 10^{-5}\ \mathrm{m^2/s}$,

$\eta = 2.271 \times 10^{-5}\ \mathrm{N\ s/m^2}$, $\lambda_1 = 70.5\ \mathrm{W/(mK)}$, $\rho_1 = 21450\ \mathrm{kg/m^3}$,

$c_1 = 134\ \mathrm{J/(kg\ K)}$.

Assuming that the physical properties of the gas are temperature independent, the values of the critical time, t_B, of natural convection onset, computed by eq.(9), are $t_B \leqslant 6.1$ s for $\theta = 1.7$ K and $t_B \leqslant 5.3$ s for $\theta \doteq 2.1$ K.

From $r_2^2/(4\ at) > 6$ and $r_2 = 0.03$ m, the wall cell effect is negligible if $t < 1.7$ s.

The relative error e_2, computed from eq. (10), is less than 0.1% even for $t = 3$ s.

The results listed in Table 2 confirm both qualitatively and quantitatively the nonideal behavior of the wire, predicted by theory and evidence the difficulties of the classical procedure of determining the thermal conductivity and thermal diffusivity in gases.

In the short times range the thermal inertia of the wire affects strongly the time threshold above which the function $\theta(\ln t)$ follows a linear logarithmic law (eq. (2)). The measured temperature rise is lower than the ideal one (eq. (2)), the slope of curve $\theta(\ln t)$ at point t is lower than the slope of asymptotic zone; the measured λ values are lower than the ideal value and increases in time. The magnitude of the relative error, e_1, for a gas of given λ, ρ and c_p values is strongly influenced by the wire diameter.[16]

In the long time range, the determining effect is the radial limitation of the fluid rather than the natural convection which, however, can not be completely excluded. The radial limitation of the fluid yields $\theta(r_1, t)$ measured values that are lower than ideal i.e., the slope of curve $\theta(\ln t)$ at t is gradually lower than the asymptote slope; the measured λ is higher than ideal and rises with time. Both the heat losses at the wire ends and the natural convection act in the same way.

It turns out that in the case of gases and for $2r_1 \simeq 0.015$ mm, curve $\theta(\ln t)$ has no linear logarithmic region and calculation of quantities $\lambda^{(0)}$ and $a^{(0)}$ by the classical procedure becomes subjective.

Therefore the accuracy of runs may not be evaluated by comparison of $\lambda^{(0)}$ and $a^{(0)}$ values with data in literature but by estimation of measuring errors of Φ and t. Equations (12) — (14) and (3) — (5) yield:

$$\Phi_i = \frac{32\,\pi\, RL}{E_p^2}\ \frac{f(x_i, x_p)}{1 - f(x_i, x_p)}\ \frac{1}{\alpha_{T_0}} = A_i \frac{1}{\alpha_{T_0}} \tag{15}$$

$$\Phi_j = A_j \frac{1}{\alpha_{T_0}} \tag{16}$$

where $0 \leqslant x_p \leqslant 1.000$ and $0.500 \leqslant x_i \leqslant 1.000$.

$$\lambda_{ji}^{(0)} = \left(\frac{1}{A_j - A_i} \ln \frac{t_j}{t_i}\right)\alpha_{T_0} \tag{17}$$

$$a_i^{(0)} = \frac{1.781}{4}\ r_1^2 \exp\left[\frac{A_i}{A_j - A_i} \ln \frac{t_j}{t_i}\right] \tag{18}$$

The accuracy of quantities $\bar{t}$, E_p, R and L quantities is of 0.2 %, 0.1 %, 0.1 % and 1 % respectively. The precision of quantities x_p, x_i and α_{T_0} is of 0.1 %, 0.2 % and 1.5–3 % respectively. $A_{i,j}$ and $\Phi_{i,j}$ values are thus measured with an accuracy of 1.2 % and 1.7 – 3.5 % respectively. S and E values of $\bar{t}$ decrease with the number of averaged values.

The systematic errors which can interfere especially with x_i and α_{T_0} values have an outstanding importance. These errors might be traced if quantities (Φ, t) were within the linear logarithmic range and determinations were effected on a fluid of known λ and a. Thus, if $\lambda_{j,i}^{(0)}$ is different from the real value but $a_i^{(0)}$ is correct, $A_{i,j}$ does not carry any systematic errors due to x_i values, yet $\Phi_{i,j}$ values are affected by a systematic error that originates in α_{T_0}. Value $a_i^{(0)}$ senses the measuring error of the wire diameter and the error of the argument of the exponential; the diameter could not be measured optically with an accuracy higher than 3.33 % ($15 \pm 0.5\mu$); a systematic error stemming from grading standardisation should be added; an accuracy of 1.5 % of the argument of the exponential affects the accuracy of $a^{(0)}$ by 10 – 12 %, that is at best $a^{(0)}$ is determined within 10–15 %.

For measurements in liquids,[10,19] eq. (2) stands with an accuracy better than 1 % within a relatively wide time range (0.2 – 2 s) and the estimates above are confirmed.

5. CONCLUSIONS

In order that the classical procedure may still be used in gases the following conditions should be observed: — lowering of the wire diameter to the order of microns in order to decrease the minimum time above which the linear logarithmic law stands; — lowering of θ (r_1, t) values, i.e., q, in order to delay the onset of natural convection; this condition may be achieved by lowering E_p and rising L; — utilization of some cells of highest inner diameter 2 r_2 in order to eliminate the cell wall effect.

Observance of these conditions entails some drawbacks: — platinum wires whose diameter is of the order of microns (Wollaston) are very expensive; manufacturing of long transducers is difficult due to the fragility of wires; since chemical dissolution of silver coating is achieved with HNO_3 aq., the wire supporting leads have to be either of tantalum or of platinum; the high unevenness of Wollaston wire diameter entails systematic errors in λ values; the wire diameter included in the calculation of thermal diffusivity as r_1^2, may no longer be measured by optical microscope and the measured value is uncertain due to large nonuniformities of the diameter along the wire; — lowering of θ (r_1, t) values disfavours the accuracy of their measurement; — the relative errors e_2 and e_3 rise with time and are systematic; they may be lowered by increasing the wire length and decreasing time (which is unacceptable, as mentioned above); — utilization of some bulky cells, of large diameter and length, cause thermosetting to be difficult (the time required to reach the thermal equilibrium is longer; the vertical temperature gradients, which can induce natural convection in the cell even before the experiment has started are smoothed out).

All these observations point to the strongly contradictory action of various experimental parameters involved in the establishment of the time interval within which the linear logarithmic law (eq. (2)) stands. In the case of gases, the possibility of applying the classical procedure is disputable and depends first on the wire diameter.

The next contribution will present a new calculation method and a new experimental procedure which allow absolute and simultaneous determination of thermal conductivity, λ, of thermal diffusivity, a, and of volumic heat capacity, $\rho c_p = \lambda/a$, of gases and liquids, no matter the diameter of the wire employed.

REFERENCES

[1] J. Kestin, S. T. Ro and W. Wakeham, *J. Chem. Phys.*, **56**, 4119 (1972).

[2] J. W. Haarman, Dissertation, Technical University of Delft, 1969.

[3] A. G. Saskov, T. N. Abramenko, "Teploprovodnosti gazovyh smesei", Energhia, Moscow, 1970, p. 26–143.

[4] "Thermal Conductivity", ed. R. P.Tye, vol. II, Academic Press, London, 1969, p. 66–145.

[5] N. V. Tsederberg, "Thermal Conductivity of Gases and Liquids", Edward Arnold Ltd., London, 1965, p. 1 – 66.

[6] R. Vîlcu and A. Ciochină, *Rev. Roumaine Chim.*, **17**, 1679 (1972).

[7] R. Vîlcu and A. Ciochină, *Studii și Cercetări Chim. Acad. R.S.R.*, **21**, 571 (1973).

[8] R. Vîlcu and A. Ciochină, *Studii și Cercetări Chim. Acad. R.S.R.*, **21**, 643 (1973).

[9] R. Vîlcu and A. Ciochină, *Rev. Roumaine Chim.*, **26**, 161 (1981).

[10] R. Vîlcu, A. Ciochină and Gh. Vasu, *Rev. Roumaine Chim.*, **26**, 1355 (1981).

[11] P. Salé, Thèses, Univ. Paris, 1967.

[12] A. G. Turnbull, *J. Chem. Eng. Data*, **16**, 79 (1971).

[13] P. S. Davis, F. Theenwes, R. J. Bearman and R. P. Gordon, *J. Chem. Phys.*, **55**, 4776 (1971).

[14] E. McLaughlin and J. F. T. Pittman, *Phil. Trans. Roy. Soc. London*, **270**, 557 (1971).

[15] P. Anderson and G. Backstrom, *Rev. Sci. Instrum.*, **47**, 205 (1976).

[16] R. Vîlcu and A. Ciochină, *Rev. Roumaine Chim.*, **25**, 1113 (1980).

[17] J. J. de Groot, J. Kestin and H. Sookiazian, *Physica*, **75**, 454 (1974).

[18] H. S. Carslaw and J. C. Jaeger, "Conduction of Heat in Solids", Oxford Univ. Press, London, 1959, p. 261, 334, 345.

[19] R. Vîlcu and A. Ciochină, *Rev. Roumaine Chim.*, **26**, 527 (1981).

[20] A. F. O. Falcao, *Rev. Port. Quim.*, **7**, 65 (1965).

[21] A. F. O. Falcao, *Rev. Port. Quim.*, **9**, 139 (1967).

[22] D. Șerbănescu, Gh. Vasu, R. Vîlcu and A. Ciochină, *Rev. Roumaine Chim.*, **26**, 1047 (1981).

[23] N. B. Vargaftik, "Sravochnik po teplofizicheskim svoistvam gazov i zhidkostei", Nauka, Moscow, 1972, p. 543.

[24] Y. S. Touloukian, P. E. Liley and S. C. Saxena, "Thermophysical Properties of Matter", vol. 3, TPRC Data Series, Plenum Press, New York, 1970, p. 5.

[25] K. Raznjevic, "Tabele și diagrame termodinamice", Ed. tehnică, București, 1978, p. 264.

Revue Roumaine de Chimie, 27, 3, 325–343 (1982)

AN EXTENDED HÜCKEL FORTRAN PROGRAM FOR MOLECULES INCLUDING THE ELEMENTS FROM HYDROGEN TO XENON EXCEPT THE TRANSITION METALS

Ş. MOLDOVEANU and V. DAVID
I.P.B., Faculty of Chemical Technology, Spl. Independenţei 202, Bucharest, Romania

Received December 5, 1980

A FORTRAN program for the computation of the EHT type is given. The program allows to perform computations for closed shell molecules including atoms from hydrogen to xenon except the transition metals. The main advantages of the program are the relatively low memory (96 K) with modules not exceeding 64 K and the short running time requested, as well as the large variety of molecules accepted and the information given.

INTRODUCTION

Different FORTRAN programs for computations based on the extended Hückel theory [1] are given by specialised libraries for computer programs. [2,3]

The use of these programs may have several shortcomings. Some of these are related to the type of computer, while others – to the limitations in the type of molecules accepted and in the quantity of information given, i.e. the number of physical properties simulated by the program.

The present EHT program has been written and tested using a FELIX C256 computer. The memory requested is of 96 K for maximum 50 atoms having 110 orbitals.

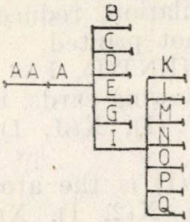

Fig. 1. – The description of the tree.

The program is broken into many modules (the tree is given in fig. 1) and uses disks such as the memory used by one module should not exceed 64 K. This fact offers the possibility to extend the program to 128 orbitals, using also the modules of 64 K but more total memory.

Different artifices have been used in order to reduce the time of the computation for a given molecule.

For example a molecule such as chloranil (48 orbitals) requires 7.5 minutes.

The subroutines for the solving of the eigen problem and for the printing of a matrix are not original. They are taken over from. [4] Some names of subroutines and variables given in the initial Hoffmann's EHT are maintained.

The program performs computations for closed shell molecules including the elements from hydrogen to xenon except the transition elements and has been widely used by the authors. [5–8]

In order to better simulate different properties, a parametrization as given in [9] has been adopted.

The results are:

— Orbital energies
— Energy for the ground state
— Energy for the first excited state
— Wave functions
— Mulliken overlap population
— Reduced Mulliken overlap population
— Complete charge matrix
— Orbital charges
— Net charge for each atom
— Dipole moment.

DESCRIPTION OF THE INPUT DATA

The input data consist of:

The first card, in FORMAT (3I2, 4X, 10A4) on which are punched the values for variables KOD, KONTA, ITI and KOMENT(I), I = 1, 10.

— KOD is an option; if KOD = 0 the program runs; if KOD > 0 the program is stopped.

— KONTA is the charge of the molecules.

— ITI is an option; if ITI $\leqslant 0$ all the mentioned information for the molecule are printed; if ITI = 1, the Mulliken overlap population is not printed; if ITI = 2, the Mulliken overlap population and the reduced overlap population are not printed; if ITI = 3, the Mulliken overlap population, reduced overlap population and Complete Charge matrix are not printed.

— KOMENT(I), I = 1, 10, contains a commentary or title.

The following cards, in FORMAT (I2, 8X, 3F10.5) which contain:

— NAT (I), X(J, I), J = 1, 3, for each atom in the molecule, on one card.

— NAT(I) is the atomic number of the element.

X(1, I), X(2, I), X(3, I) are the x, y, z Cartesian coordinates in Å of the atom.

There is no preferential order of atoms in the molecule.

The last card of the data set is a blank card.

A new data set follows.

A BRIEF DESCRIPTION OF THE SUBROUTINES

The main program calls the subroutine MAINN
— MAINN calls the other subroutines
— CITIRI reads the input data
— PREGAT furnishes initial data for the computation
— ACOPER and OVRLP, SUM, FACT, F1, A1, B1, CO3, S1 compute the overlap matrix based on the theory given for example in[10]
— HMAT computes the H matrix
— EIGEN and GIVENS solve the eigen problem
— MMULT, MUFRA, OOULT and MOFRA multiply matrices.
— IESIRI selects the output data
— ISHTAR computes the nonorthogonalised wave functions
— MOP computes the Mulliken overlap population
— ROP computes the reduced overlap population
— CCM computes the complete charge matrix
— SARC computes the orbital charges and the net charges
— DIPMOM computes the dipole moment.

REFERENCES

[1] R. Hoffmann, *J. Chem. Phys.*, **39**, 1397 (1963).

[2] QCPE 30.

[3] QCPE 64.

[4] QCPE 12.

[5] S. Moldoveanu, unpublished results.

[6] S. Moldoveanu, C. Mircioiu, V. Voicu and A. Medeșan, *Rev. Roumaine Biochim.* **18**, 119 (1981)

[7] I. Rusu, A. Medeșan, S. Grigoraș, S. Moldoveanu and E. Păușescu, *Rev. Roumaine Biochim.* **16**, 321 (1979).

[8] V. E. Sahini, S. Moldoveanu and C. Mihailciuc, *Rev. Roumaine Chim.*, **25**, 1055 (1980).

[9] A. Botrel and C. R. Guerillot, *J. Chim., phys.* **71**, 974 (1974).

[10] S. Moldoveanu and A. Savin, "Aplicații în chimie ale metodelor semiempirice de orbitali moleculari", Ed. Academiei, București, 1980.

THE LIST OF THE PROGRAM

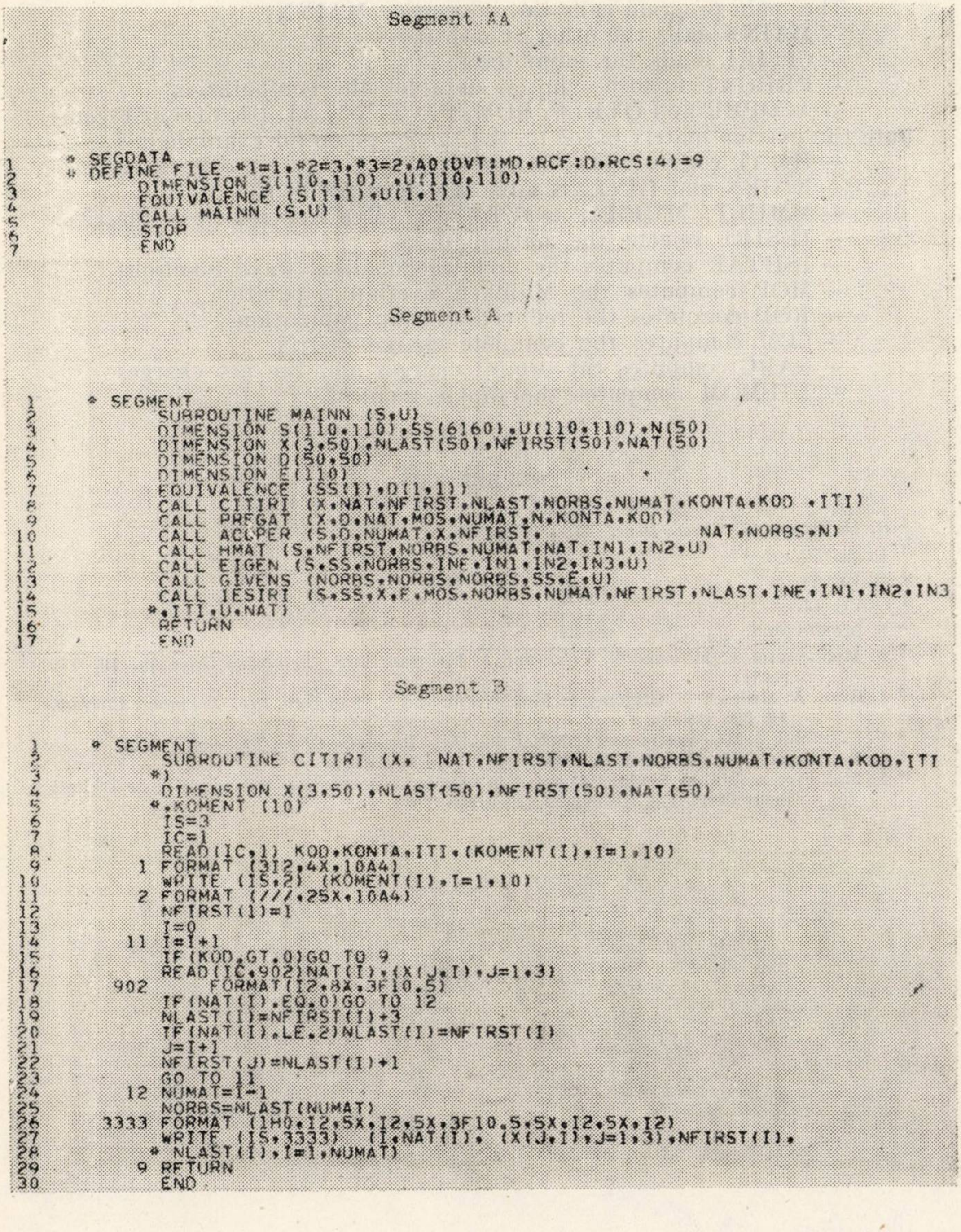

Segment AA

```
* SEGDATA
* DEFINE FILE *1=1,*2=3,*3=2,A0(DVT:MD,RCF:D,RCS:4)=9
      DIMENSION S(110,110) ,U(110,110)
      EQUIVALENCE (S(1,1),U(1,1) )
      CALL MAINN (S,U)
      STOP
      END
```

Segment A

```
* SEGMENT
      SUBROUTINE MAINN (S,U)
      DIMENSION S(110,110),SS(6160),U(110,110),N(50)
      DIMENSION X(3,50),NLAST(50),NFIRST(50),NAT(50)
      DIMENSION D(50,50)
      DIMENSION E(110)
      EQUIVALENCE (SS(1),D(1,1))
      CALL CITIRI (X,NAT,NFIRST,NLAST,NORBS,NUMAT,KONTA,KOD ,ITI)
      CALL PREGAT (X,D,NAT,MOS,NUMAT,N,KONTA,KOD)
      CALL ACCPER (S,D,NUMAT,X,NFIRST,             NAT,NORBS,N)
      CALL HMAT (S,NFIRST,NORBS,NUMAT,NAT,IN1,IN2,U)
      CALL EIGEN (S,SS,NORBS,INE,IN1,IN2,IN3,U)
      CALL GIVENS (NORBS,NORBS,NORBS,SS,E,U)
      CALL IESIRI (S,SS,X,E,MOS,NORBS,NUMAT,NFIRST,NLAST,INE,IN1,IN2,IN3
     *,ITI,U,NAT)
      RETURN
      END
```

Segment B

```
* SEGMENT
      SUBROUTINE CITIRI (X,  NAT,NFIRST,NLAST,NORBS,NUMAT,KONTA,KOD,ITI
     *)
      DIMENSION X(3,50),NLAST(50),NFIRST(50),NAT(50)
     *,KOMENT (10)
      IS=3
      IC=1
      READ(IC,1) KOD,KONTA,ITI,(KOMENT(I),I=1,10)
    1 FORMAT (3I2,4X,10A4)
      WRITE (IS,2) (KOMENT(I),I=1,10)
    2 FORMAT (///,25X,10A4)
      NFIRST(1)=1
      I=0
   11 I=I+1
      IF(KOD.GT.0)GO TO 9
      READ(IC,902)NAT(I),(X(J,I),J=1,3)
  902     FORMAT(I2,8X,3F10.5)
      IF(NAT(I).EQ.0)GO TO 12
      NLAST(I)=NFIRST(I)+3
      IF(NAT(I).LE.2)NLAST(I)=NFIRST(I)
      J=I+1
      NFIRST(J)=NLAST(I)+1
      GO TO 11
   12 NUMAT=I-1
      NORBS=NLAST(NUMAT)
 3333 FORMAT (1H0,I2,5X,I2,5X,3F10.5,5X,I2,5X,I2)
      WRITE (IS,3333)  (I,NAT(I), (X(J,I),J=1,3),NFIRST(I),
     * NLAST(I),I=1,NUMAT)
    9 RETURN
      END
```

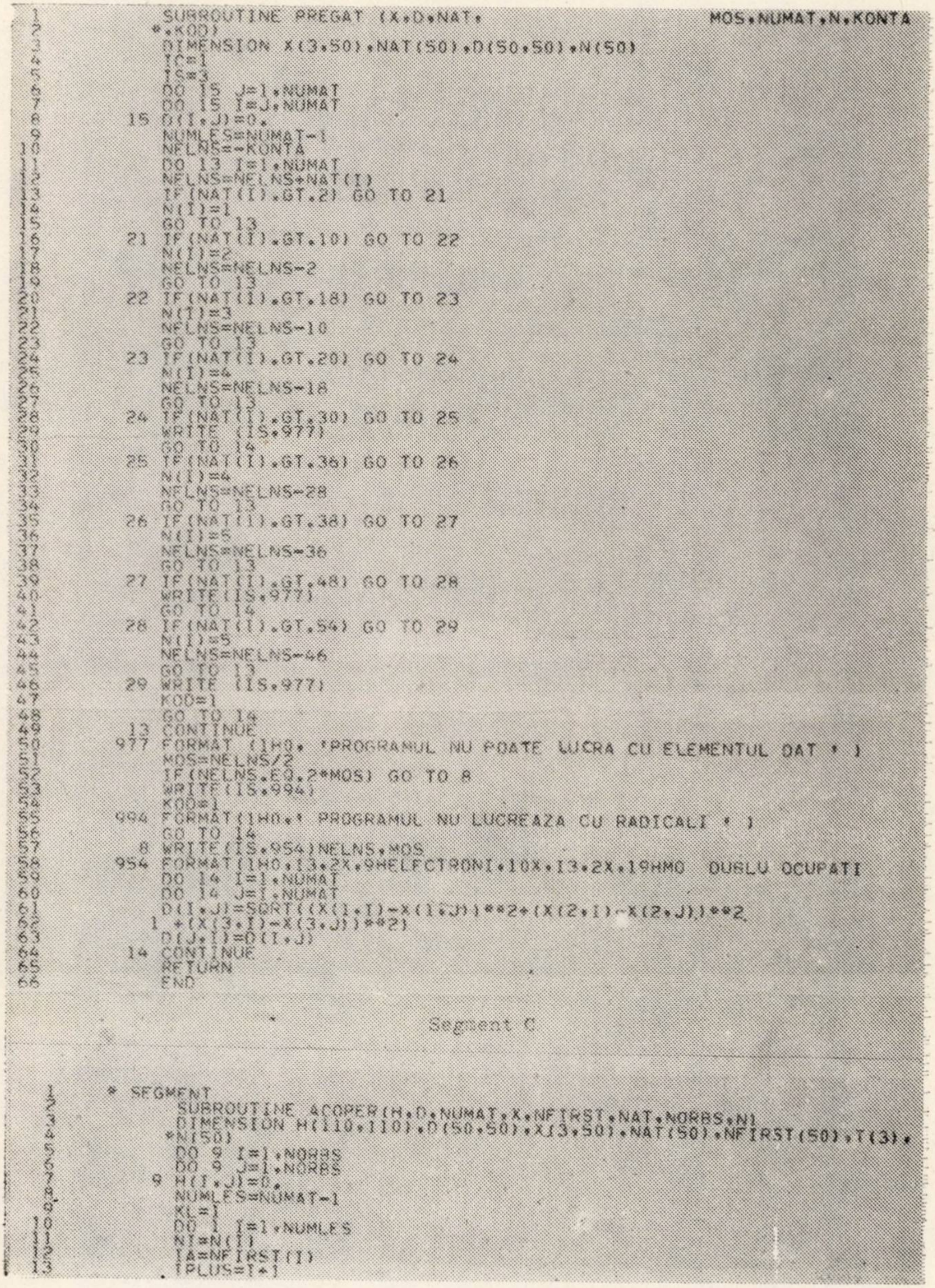

```
      SUBROUTINE PREGAT (X.D.NAT.                        MOS.NUMAT.N.KONTA
     *.KOD)
      DIMENSION X(3.50).NAT(50).D(50.50).N(50)
      IC=1
      IS=3
      DO 15 J=1.NUMAT
      DO 15 I=J.NUMAT
   15 D(I.J)=0.
      NUMLES=NUMAT-1
      NELNS=-KONTA
      DO 13 I=1.NUMAT
      NELNS=NELNS+NAT(I)
      IF(NAT(I).GT.2) GO TO 21
      N(I)=1
      GO TO 13
   21 IF(NAT(I).GT.10) GO TO 22
      N(I)=2
      NELNS=NELNS-2
      GO TO 13
   22 IF(NAT(I).GT.18) GO TO 23
      N(I)=3
      NELNS=NELNS-10
      GO TO 13
   23 IF(NAT(I).GT.20) GO TO 24
      N(I)=4
      NELNS=NELNS-18
      GO TO 13
   24 IF(NAT(I).GT.30) GO TO 25
      WRITE (IS.977)
      GO TO 14
   25 IF(NAT(I).GT.36) GO TO 26
      N(I)=4
      NELNS=NELNS-28
      GO TO 13
   26 IF(NAT(I).GT.38) GO TO 27
      N(I)=5
      NELNS=NELNS-36
      GO TO 13
   27 IF(NAT(I).GT.48) GO TO 28
      WRITE(IS.977)
      GO TO 14
   28 IF(NAT(I).GT.54) GO TO 29
      N(I)=5
      NELNS=NELNS-46
      GO TO 13
   29 WRITE (IS.977)
      KOD=1
      GO TO 14
   13 CONTINUE
  977 FORMAT (1H0. 'PROGRAMUL NU POATE LUCRA CU ELEMENTUL DAT ' )
      MOS=NELNS/2
      IF(NELNS.EQ.2*MOS) GO TO 8
      WRITE(IS.994)
      KOD=1
  994 FORMAT(1H0.' PROGRAMUL NU LUCREAZA CU RADICALI ' )
      GO TO 14
    8 WRITE(IS.954)NELNS.MOS
  954 FORMAT(1H0.I3.2X.9HELECTRONI.10X.I3.2X.19HMO  DUBLU OCUPATI
      DO 14 I=1.NUMAT
      DO 14 J=I.NUMAT
      D(I.J)=SQRT((X(1.I)-X(1.J))**2+(X(2.I)-X(2.J))**2
     1 +(X(3.I)-X(3.J))**2)
      D(J.I)=D(I.J)
   14 CONTINUE
      RETURN
      END
```

Segment C

```
* SEGMENT
      SUBROUTINE ACOPER(H.D.NUMAT.X.NFIRST.NAT.NORBS.N)
      DIMENSION H(110.110).D(50.50).X(3.50).NAT(50).NFIRST(50).T(3).
     *N(50)
      DO 9 I=1.NORBS
      DO 9 J=1.NORBS
    9 H(I.J)=0.
      NUMLES=NUMAT-1
      KL=1
      DO 1 I=1.NUMLES
      NI=N(I)
      IA=NFIRST(I)
      IPLUS=I+1
```

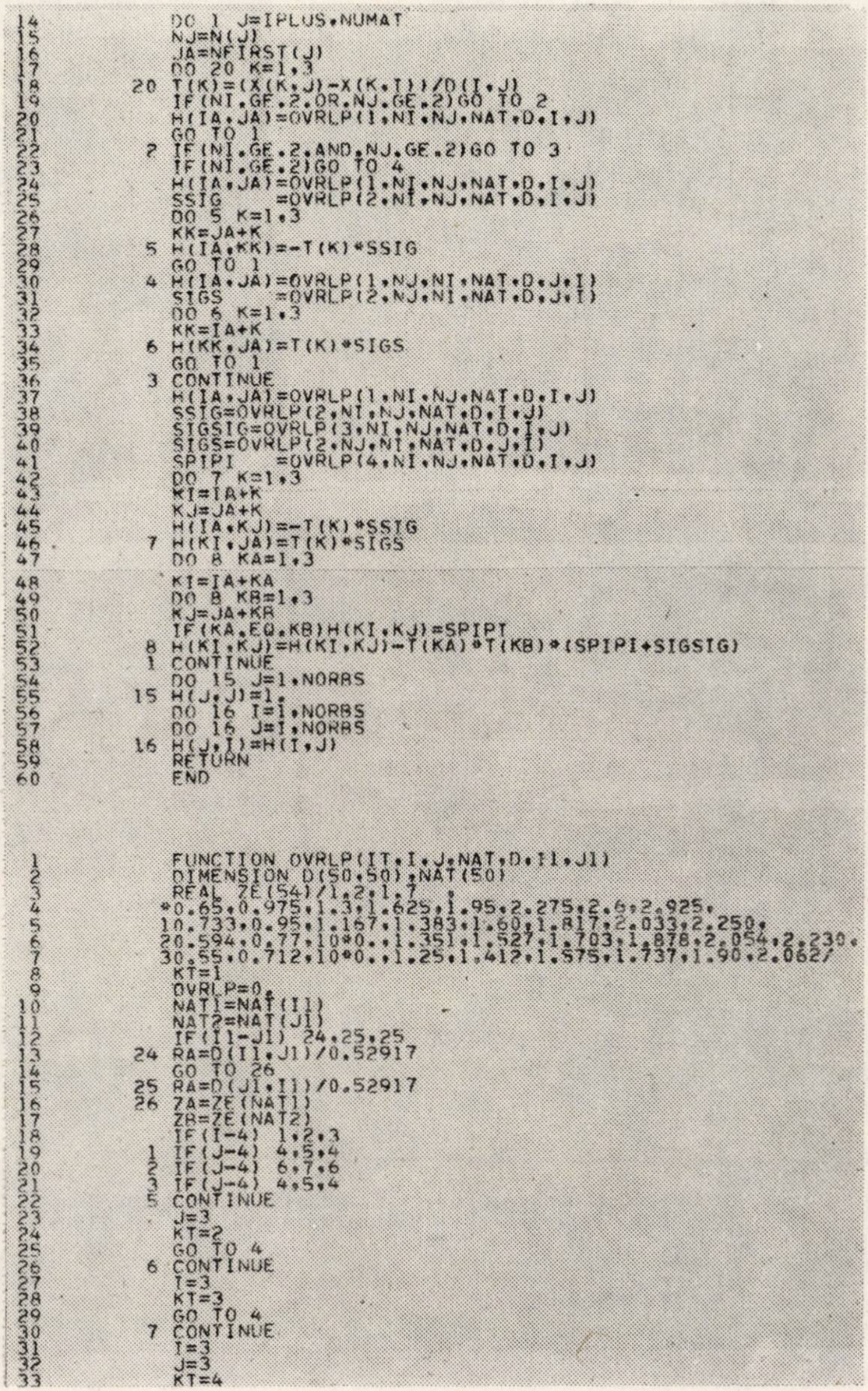

```
      DO 1 J=IPLUS,NUMAT
      NJ=N(J)
      JA=NFIRST(J)
      DO 20 K=1,3
   20 T(K)=(X(K,J)-X(K,I))/D(I,J)
      IF(NI.GF.2.OR.NJ.GE.2)GO TO 2
      H(IA,JA)=OVRLP(1,NI,NJ,NAT,D,I,J)
      GO TO 1
    2 IF(NI.GE.2.AND.NJ.GE.2)GO TO 3
      IF(NI.GE.2)GO TO 4
      H(IA,JA)=OVRLP(1,NI,NJ,NAT,D,I,J)
      SSIG    =OVRLP(2,NI,NJ,NAT,D,I,J)
      DO 5 K=1,3
      KK=JA+K
    5 H(IA,KK)=-T(K)*SSIG
      GO TO 1
    4 H(IA,JA)=OVRLP(1,NJ,NI,NAT,D,J,I)
      SIGS    =OVRLP(2,NJ,NI,NAT,D,J,I)
      DO 6 K=1,3
      KK=IA+K
    6 H(KK,JA)=T(K)*SIGS
      GO TO 1
    3 CONTINUE
      H(IA,JA)=OVRLP(1,NI,NJ,NAT,D,I,J)
      SSIG=OVRLP(2,NI,NJ,NAT,D,I,J)
      SIGSIG=OVRLP(3,NI,NJ,NAT,D,I,J)
      SIGS=OVRLP(2,NJ,NI,NAT,D,J,I)
      SPIPI   =OVRLP(4,NI,NJ,NAT,D,I,J)
      DO 7 K=1,3
      KI=IA+K
      KJ=JA+K
      H(IA,KJ)=-T(K)*SSIG
    7 H(KI,JA)=T(K)*SIGS
      DO 8 KA=1,3
      KI=IA+KA
      DO 8 KB=1,3
      KJ=JA+KB
      IF(KA.EQ.KB)H(KI,KJ)=SPIPT
    8 H(KI,KJ)=H(KI,KJ)-T(KA)*T(KB)*(SPIPI+SIGSIG)
    1 CONTINUE
      DO 15 J=1,NORBS
   15 H(J,J)=1.
      DO 16 I=1,NORBS
      DO 16 J=I,NORBS
   16 H(J,I)=H(I,J)
      RETURN
      END
```

```
      FUNCTION OVRLP(IT,I,J,NAT,D,I1,J1)
      DIMENSION D(50,50),NAT(50)
      REAL ZE(54)/1.2,1.7   ,
     *0.65,0.975,1.3,1.625,1.95,2.275,2.6,2.925,
     10.733,0.95,1.167,1.383,1.60,1.817,2.033,2.250,
     20.594,0.77,10*0.,1.351,1.527,1.703,1.878,2.054,2.230,
     30.55,0.712,10*0.,1.25,1.412,1.575,1.737,1.90,2.062/
      KT=1
      OVRLP=0.
      NAT1=NAT(I1)
      NAT2=NAT(J1)
      IF(I1-J1) 24,25,25
   24 RA=D(I1,J1)/0.52917
      GO TO 26
   25 RA=D(J1,I1)/0.52917
   26 ZA=ZE(NAT1)
      ZB=ZE(NAT2)
      IF(I-4) 1,2,3
    1 IF(J-4) 4,5,4
    2 IF(J-4) 6,7,6
    3 IF(J-4) 4,5,4
    5 CONTINUE
      J=3
      KT=2
      GO TO 4
    6 CONTINUE
      I=3
      KT=3
      GO TO 4
    7 CONTINUE
      I=3
      J=3
      KT=4
```

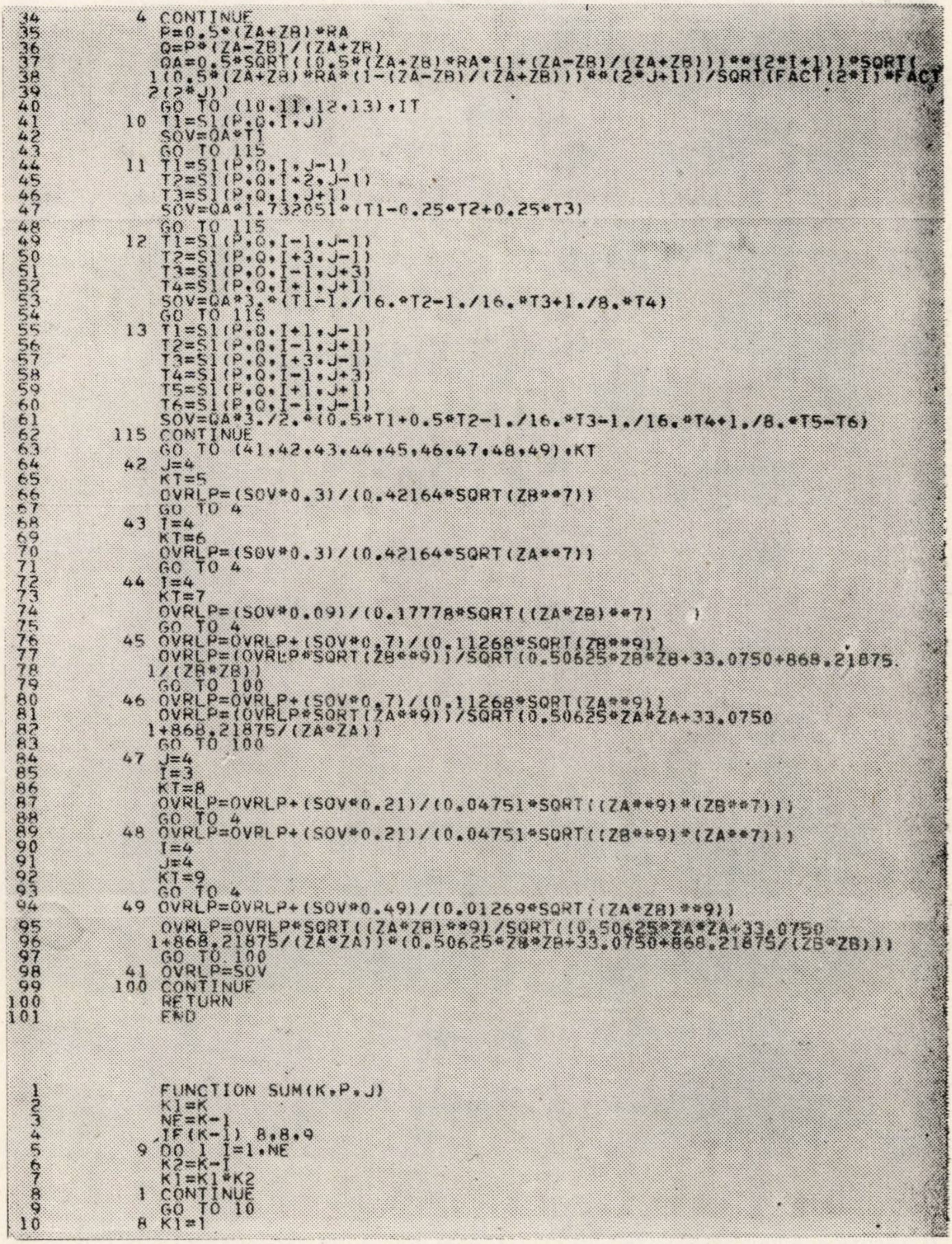

```
    4 CONTINUE
      P=0.5*(ZA+ZB)*RA
      Q=P*(ZA-ZB)/(ZA+ZB)
      QA=0.5*SQRT((0.5*(ZA+ZB)*RA*(1+(ZA-ZB)/(ZA+ZB)))**(2*I+1))*SQRT(
     1(0.5*(ZA+ZB)*RA*(1-(ZA-ZB)/(ZA+ZB)))**(2*J+1))/SQRT(FACT(2*I)*FACT
     2(2*J))
      GO TO (10.11.12.13).IT
   10 T1=S1(P.Q.I.J)
      SOV=QA*T1
      GO TO 115
   11 T1=S1(P.Q.I.J-1)
      T2=S1(P.Q.I+2.J-1)
      T3=S1(P.Q.I.J+1)
      SOV=QA*1.732051*(T1-0.25*T2+0.25*T3)
      GO TO 115
   12 T1=S1(P.Q.I-1.J-1)
      T2=S1(P.Q.I+3.J-1)
      T3=S1(P.Q.I-1.J+3)
      T4=S1(P.Q.I+1.J+1)
      SOV=QA*3.*(T1-1./16.*T2-1./16.*T3+1./8.*T4)
      GO TO 115
   13 T1=S1(P.Q.I+1.J-1)
      T2=S1(P.Q.I-1.J+1)
      T3=S1(P.Q.I+3.J-1)
      T4=S1(P.Q.I-1.J+3)
      T5=S1(P.Q.I+1.J+1)
      T6=S1(P.Q.I-1.J-1)
      SOV=QA*3./2.*(0.5*T1+0.5*T2-1./16.*T3-1./16.*T4+1./8.*T5-T6)
  115 CONTINUE
      GO TO (41.42.43.44.45,46.47.48.49).KT
   42 J=4
      KT=5
      OVRLP=(SOV*0.3)/(0.42164*SQRT(ZB**7))
      GO TO 4
   43 I=4
      KT=6
      OVRLP=(SOV*0.3)/(0.42164*SQRT(ZA**7))
      GO TO 4
   44 I=4
      KT=7
      OVRLP=(SOV*0.09)/(0.17778*SQRT((ZA*ZB)**7)    )
      GO TO 4
   45 OVRLP=OVRLP+(SOV*0.7)/(0.11268*SQRT(ZB**9))
      OVRLP=(OVRLP*SQRT(ZB**9))/SQRT(0.50625*ZB*ZB+33.0750+868.21875
     1/(ZB*ZB))
      GO TO 100
   46 OVRLP=OVRLP+(SOV*0.7)/(0.11268*SQRT(ZA**9))
      OVRLP=(OVRLP*SQRT(ZA**9))/SQRT(0.50625*ZA*ZA+33.0750
     1+868.21875/(ZA*ZA))
      GO TO 100
   47 J=4
      I=3
      KT=8
      OVRLP=OVRLP+(SOV*0.21)/(0.04751*SQRT((ZA**9)*(ZB**7)))
      GO TO 4
   48 OVRLP=OVRLP+(SOV*0.21)/(0.04751*SQRT((ZB**9)*(ZA**7)))
      I=4
      J=4
      KT=9
      GO TO 4
   49 OVRLP=OVRLP+(SOV*0.49)/(0.01269*SQRT((ZA*ZB)**9))
      OVRLP=OVRLP*SQRT((ZA*ZB)**9)/SQRT((0.50625*ZA*ZA+33.0750
     1+868.21875/(ZA*ZA))*(0.50625*ZB*ZB+33.0750+868.21875/(ZB*ZB)))
      GO TO 100
   41 OVRLP=SOV
  100 CONTINUE
      RETURN
      END


      FUNCTION SUM(K.P.J)
      K1=K
      NE=K-1
      IF(K-1) 8.8.9
    9 DO 1 I=1.NE
      K2=K-I
      K1=K1*K2
    1 CONTINUE
      GO TO 10
    8 K1=1
```

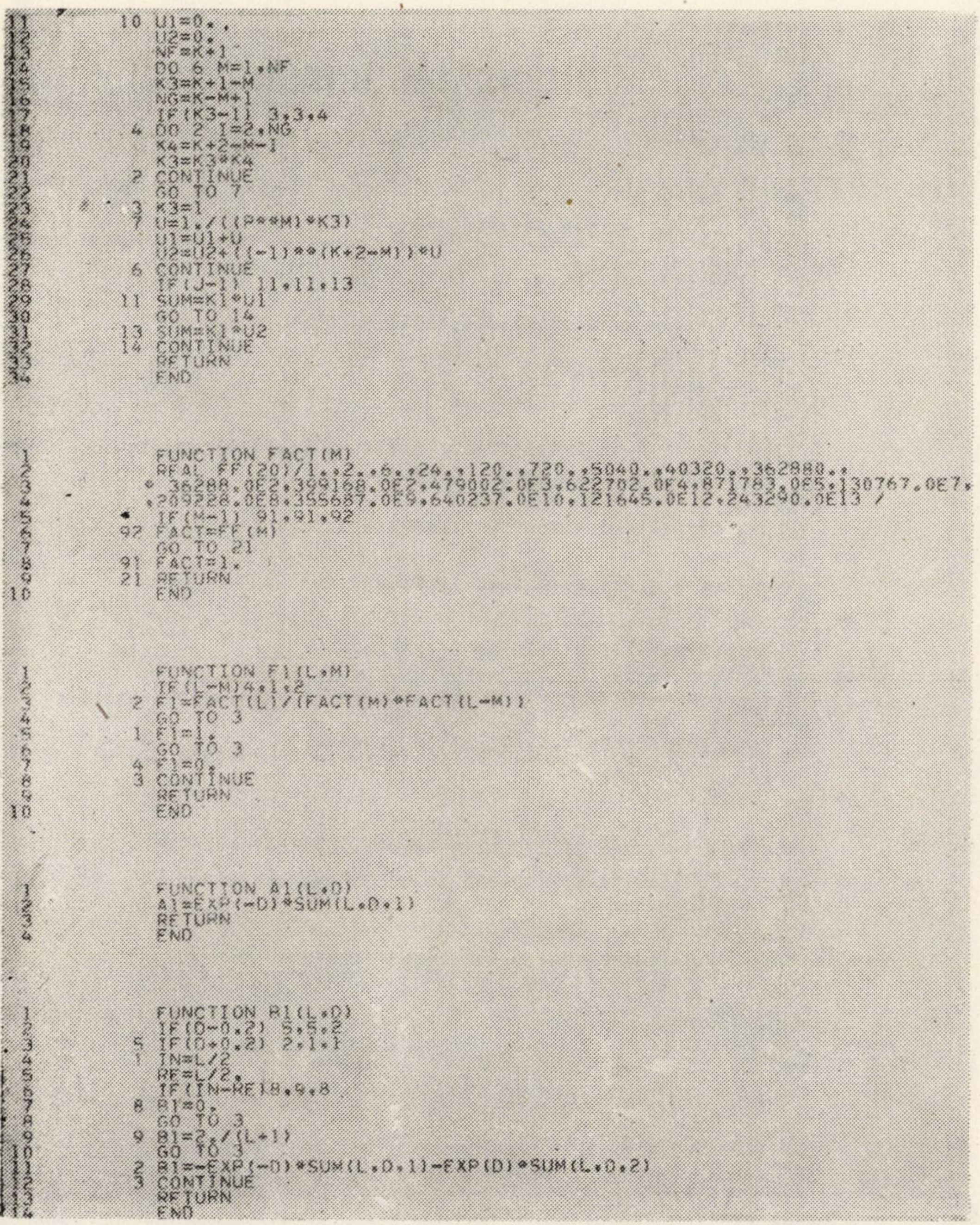

```
   10 U1=0.,
      U2=0.
      NF=K+1
      DO 6 M=1,NF
      K3=K+1-M
      NG=K-M+1
      IF(K3-1) 3,3,4
    4 DO 2 I=2,NG
      K4=K+2-M-I
      K3=K3*K4
    2 CONTINUE
      GO TO 7
    3 K3=1
    7 U=1./((P**M)*K3)
      U1=U1+U
      U2=U2+((-1)**(K+2-M))*U
    6 CONTINUE
      IF(J-1) 11,11,13
   11 SUM=K1*U1
      GO TO 14
   13 SUM=K1*U2
   14 CONTINUE
      RETURN
      END
```

```
      FUNCTION FACT(M)
      REAL FF(20)/1.,2.,6.,24.,120.,720.,5040.,40320.,362880.,
     * 36288.0E2,399168.0E2,479002.0E3,622702.0E4,871783.0E5,130767.0E7,
     ,209228.0E8,355687.0E9,640237.0E10,121645.0E12,243290.0E13 /
      IF(M-1) 91,91,92
   92 FACT=FF(M)
      GO TO 21
   91 FACT=1.
   21 RETURN
      END
```

```
      FUNCTION F1(L,M)
      IF(L-M)4,1,2
    2 F1=FACT(L)/(FACT(M)*FACT(L-M))
      GO TO 3
    1 F1=1.
      GO TO 3
    4 F1=0.
    3 CONTINUE
      RETURN
      END
```

```
      FUNCTION A1(L,D)
      A1=EXP(-D)*SUM(L,D,1)
      RETURN
      END
```

```
      FUNCTION B1(L,D)
      IF(D-0.2) 5,5,2
    5 IF(D+0.2) 2,1,1
    1 IN=L/2
      RE=L/2.
      IF(IN-RE)8,9,8
    8 B1=0.
      GO TO 3
    9 B1=2./(L+1)
      GO TO 3
    2 B1=-EXP(-D)*SUM(L,D,1)-EXP(D)*SUM(L,D,2)
    3 CONTINUE
      RETURN
      END
      FUNCTION CO3(L,M,N)
      IF(L)8,8,9
    8 C4=1.
      GO TO 10
    9 C4=0.
      L1=L+1
      DO 1 L2=1,L1
      L3=L2-1
      C1=F1(M,L3)
      L4=L-L3
      C2=F1(N,L4)
      C3=((-1)**L4)*C1*C2
      C4=C4+C3
    1 CONTINUE
   10 CO3=C4
      RETURN
      END
```

```
      FUNCTION S1(S,R,M,N)
      A2=0.
      MAB=M+N+1
      DO 4 L1=1,MAB
      L2=L1-1
      IX=M+N-L2
      A3=CO3(L2,M,N)*A1(IX,S)*B1(L2,R)
      A2=A2+A3
    4 CONTINUE
      S1=A2
      RETURN
      END
```

Segment D

```
* SEGMENT
      SUBROUTINE HMAT (S,NFIRST,NORBS,NUMAT,N,IN1,IN2,H)
      DIMENSION S(110,110),N(50),H(110,110),NFIRST(50)
      REAL CON /-0.875/
      REAL GS(54) /13.6,0.,
     * 5.39,9.92,        15.75,21.40,26.00,32.30,40.00,0.,
     * 5.14,8.95,        12.48,17.93,20.20, 20.08,30.00,0.,
     *4.35,7.09,10*0.,14.58,18.57,16.22,20.49,28.50,0.,
     *4.18,6.62,10*0.,12.60,16.34,18.80,20.78,18.00/
      REAL GP(54) /0.0,0.0,
     *3.54,5.86,8.30,11.40,13.40,14.80,18.10,0.,
     *3.04,4.52,6.41,8.99,12.78,13.32,14.50,0.,
     * 2.73,3.96,10*0.,6.75,9.43,12.16,11.68,14.50,0.,
     * 2.60,3.63,10*0.,6.19,8.51,8.75,11.04,12.68/
      INE=1
      WRITE (9'INE,INE) ((S(I,J),J=1,NORBS),I=1,NORBS)
      IN1=INE
      NUMLES=NUMAT-1
      KL=1
      DO 1 I=1,NUMLES
      NI=N(I)
      IA=NFIRST(I)
      IPLUS=I+1
      DO 1 J=IPLUS,NUMAT
      NJ=N(J)
      JA=NFIRST(J)
      IF(NI.GE.2.OR.NJ.GE.2) GO TO 2
      H (IA,JA)=CON*S(IA,JA)*(GS(1)+GS(1))
      GO TO 1
    2 IF(NI.GE.2.AND.NJ.GE.2) GO TO 3
      IF (NI.GE.2) GO TO 4
      H(IA,JA)=CON*S(IA,JA)*(GS(1)+GS(NJ))
      SSIG=CON*(GS(1)+GP(NJ))
      DO 5 K=1,3
      KK=JA+K
    5 H(IA,KK)=SSIG*S(IA,KK)
      GO TO 1
    4 H(IA,JA)=CON*S(IA,JA)*(GS(NI)+GS(1))
      SIGS=CON*(GP(NI)+GS(1))
      DO 6 K=1,3
      KK=IA+K
    6 H(KK,JA)=SIGS*S(KK,JA)
      GO TO 1
    3 CONTINUE
      H(IA,JA)=CON*S(IA,JA)*(GS(NI)+GS(NJ))
      SSIG=CON*(GS(NI)+GP(NJ))
      SGGSIG=CON*(GP(NI)+GP(NJ))
      SIGS=CON*(GP(NI)+GS(NJ))
      DO 7 K=1,3
```

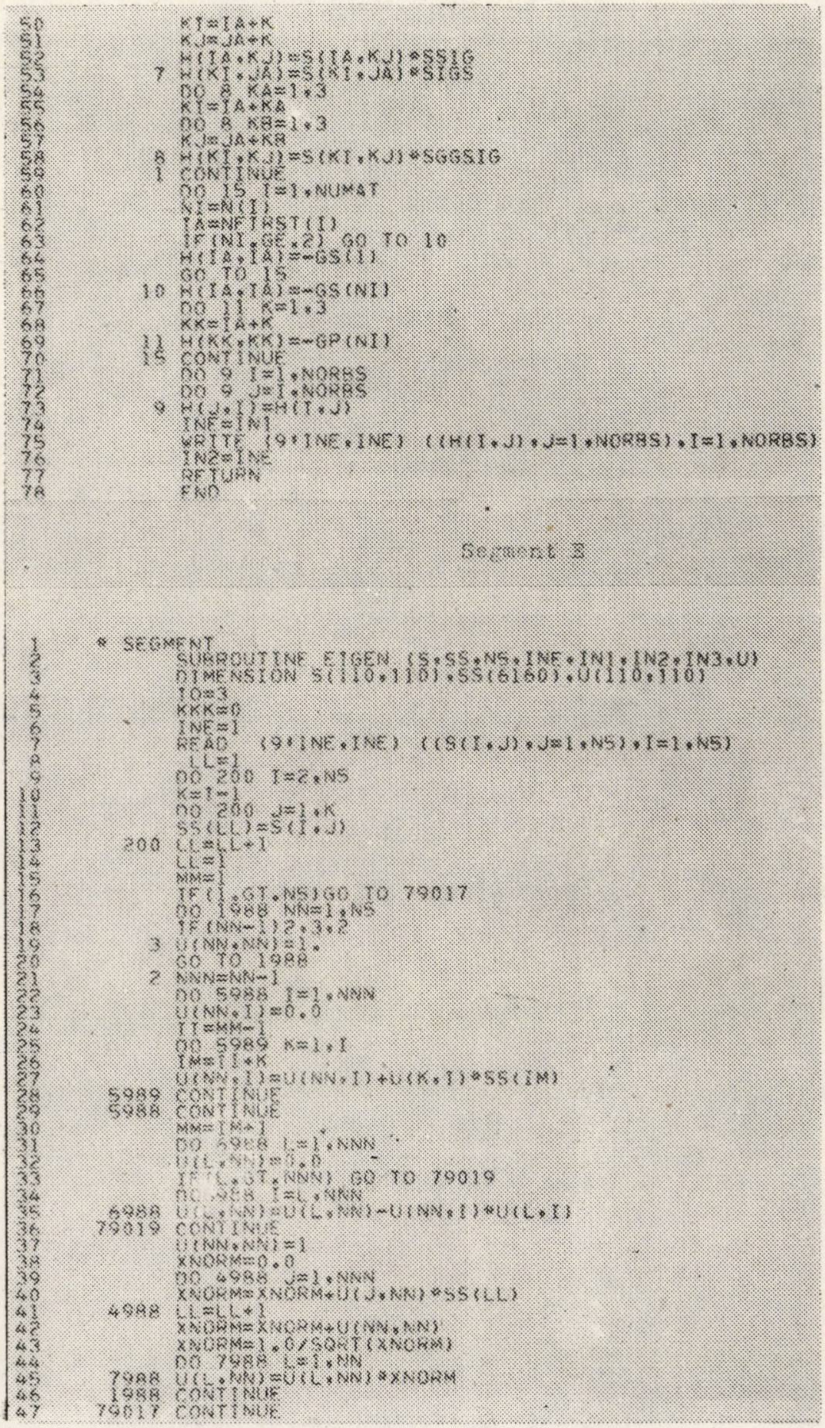

```
        KI=IA+K
        KJ=JA+K
        H(IA,KJ)=S(IA,KJ)*SSIG
      7 H(KI,JA)=S(KI,JA)*SIGS
        DO 8 KA=1,3
        KI=IA+KA
        DO 8 KB=1,3
        KJ=JA+KB
      8 H(KI,KJ)=S(KI,KJ)*SGGSIG
      1 CONTINUE
        DO 15 I=1,NUMAT
        NI=N(I)
        IA=NFIRST(I)
        IF(NI.GE.2) GO TO 10
        H(IA,IA)=-GS(1)
        GO TO 15
     10 H(IA,IA)=-GS(NI)
        DO 11 K=1,3
        KK=IA+K
     11 H(KK,KK)=-GP(NI)
     15 CONTINUE
        DO 9 I=1,NORBS
        DO 9 J=1,NORBS
      9 H(J,I)=H(I,J)
        INE=IN1
        WRITE (9'INE,INE) ((H(I,J),J=1,NORBS),I=1,NORBS)
        IN2=INE
        RETURN
        END
```

Segment 3

```
  * SEGMENT
        SUBROUTINE EIGEN (S,SS,NS,INE,IN1,IN2,IN3,U)
        DIMENSION S(110,110),SS(6160),U(110,110)
        IO=3
        KKK=0
        INE=1
        READ  (9'INE,INE) ((S(I,J),J=1,NS),I=1,NS)
         LL=1
        DO 200 I=2,NS
        K=I-1
        DO 200 J=1,K
        SS(LL)=S(I,J)
    200 LL=LL+1
        LL=1
        MM=1
        IF(1.GT.NS)GO TO 79017
        DO 1988 NN=1,NS
        IF(NN-1)2,3,2
      3 U(NN,NN)=1.
        GO TO 1988
      2 NNN=NN-1
        DO 5988 I=1,NNN
        U(NN,I)=0.0
        II=MM-1
        DO 5989 K=1,I
        IM=II+K
        U(NN,I)=U(NN,I)+U(K,I)*SS(IM)
   5989 CONTINUE
   5988 CONTINUE
        MM=IM+1
        DO 6988 L=1,NNN
        U(L,NN)=0.0
        IF(L.GT.NNN) GO TO 79019
        DO 6988 I=L,NNN
   6988 U(L,NN)=U(L,NN)-U(NN,I)*U(L,I)
  79019 CONTINUE
        U(NN,NN)=1
        XNORM=0.0
        DO 4988 J=1,NNN
        XNORM=XNORM+U(J,NN)*SS(LL)
   4988 LL=LL+1
        XNORM=XNORM+U(NN,NN)
        XNORM=1.0/SQRT(XNORM)
        DO 7988 L=1,NN
   7988 U(L,NN)=U(L,NN)*XNORM
   1988 CONTINUE
  79017 CONTINUE
```

```
      DO 3111 I=2,N5
      ING=I-1
      DO 3111 J=1,ING
 3111 U(I,J)=0.0
      INE=IN2
      WRITE (9'INE,INE) ((S(I,J),I=1,N5),J=1,N5)
      IN3=INE
      CALL MUFRA (S,SS,N5,IN1,IN2,IN3,ISCF)
      CALL MUFRA (S,SS,N5,IN2,IN3,ISCF,ISC2)
      LL=1
      DO 8 J=1,N5
      DO 8 I=1,J
      SS(LL)=S(I,J)
    8 LL=LL+1
      INE=ISCF
      RETURN
      END
```

```
      SUBROUTINE MMULT(A,B,N,M)
      DIMENSION A(110,110),B(6160),X(50)
      DO 1 I=1,N
      LL=1
      DO 2 J=1,M
      X(J)=0
      DO 2 K=1,N
      X(J)=X(J)+A(I,K)*B(LL)
    2 LL=LL+1
      DO 1 L=1,M
    1 A(I,L)=X(L)
      RETURN
      END
```

```
      SUBROUTINE MUFRA (S,SS,N5,INCA,INCB,ISCR,ISCF)
      DIMENSION S(110,110),SS(6160)
      INE=INCA
      READ  (9'INE,INE) ((S(I,J),J=1,N5),I=1,N5)
      NP5=N5*N5
      IF(N5-75) 1,1,2
    1 INE=INCB
      READ    (9'INE,INE)(SS(I),I=1,NP5)
      CALL  MMULT(S,SS,N5,N5)
      INE=ISCR
      WRITE (9'INE,INE) ((S(I,J),I=1,N5),J=1,N5)
      GO TO 3
    2 IN5=6050/N5
      IN6=IN5*N5
      INE=INCB
      READ(9'INE,INE)     (SS(I),I=1,IN6)
      ISFB=INE
      CALL MMULT(S,SS,N5,IN5)
      INE=ISCR
      WRITE (9'INE,INE) ((S(I,J),I=1,N5),J=1,IN5)
      ISFS=INE
      INE=INCA
      READ(9'INE,INE)((S(I,J),J=1,N5),I=1,N5)
      INE=ISFB
      IN7=NP5-IN6
      READ(9'INE,INE)(SS(I),I=1,IN7)
      IN8=N5-IN5
      CALL MMULT(S,SS,N5,IN8)
      INE=ISFS
      WRITE (9'INE,INE) ((S(I,J),I=1,N5),J=1,IN8)
      INE=ISCR
      READ(9'INE,INE)((S(I,J),I=1,N5),J=1,N5)
      INE=ISCR
      WRITE (9'INE,INE) ((S(I,J),I=1,N5),J=1,N5)
    3 ISCF=INE
      RETURN
      END
```

Segment G

```
 * SEGMENT
      SUBROUTINE GIVENS(NX,NROOTX,NJX,A,   ROOT,VECT)
      IMPLICIT REAL*4(A-H,O-Z)
      DIMENSION B(110,5),A(1),ROOT(NROOTX),VECT(NJX,NROOTX)
      ETA=1.E-7
```

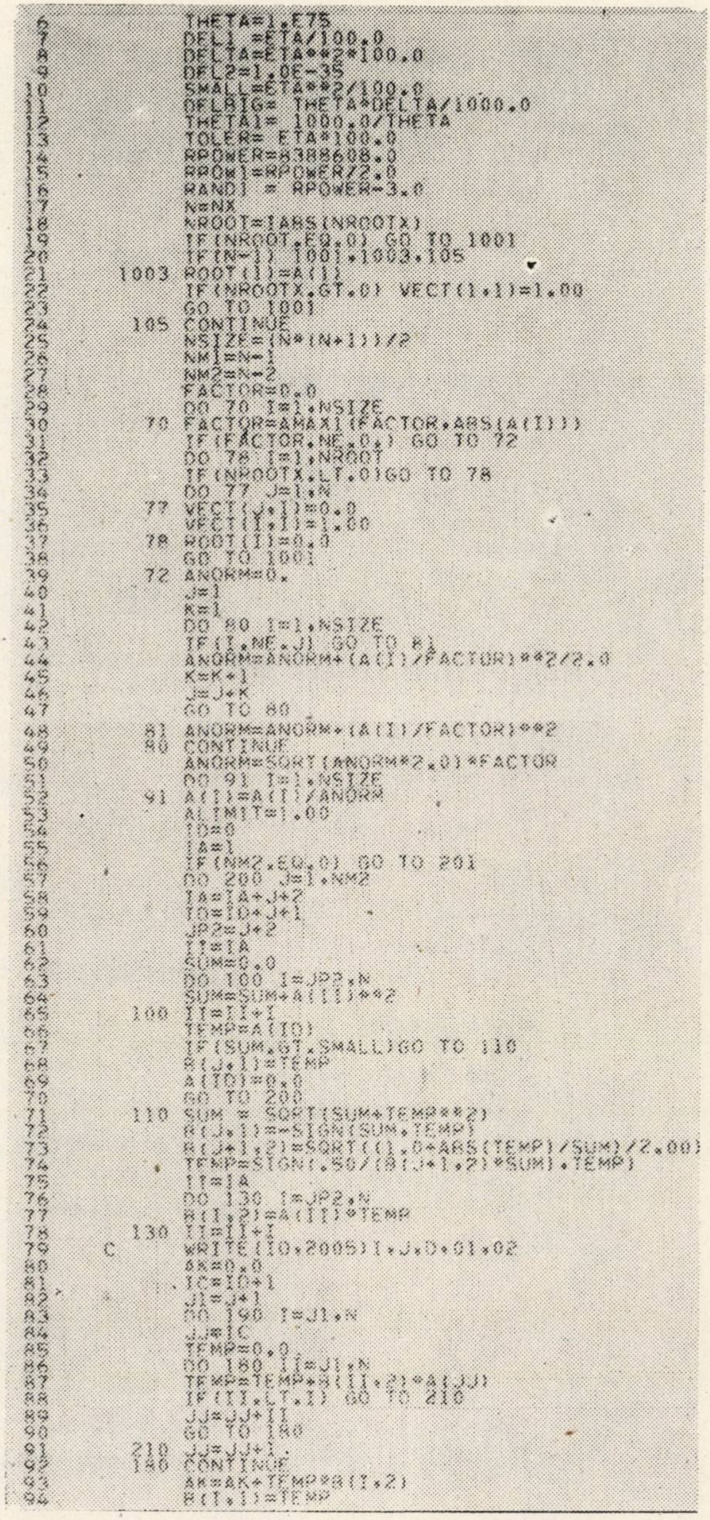

```
      THETA=1.E75
      DEL1 =ETA/100.0
      DELTA=ETA**2*100.0
      DEL2=1.0E-35
      SMALL=ETA**2/100.0
      DELBIG= THETA*DELTA/1000.0
      THETA1= 1000.0/THETA
      TOLER= ETA*100.0
      RPOWER=8388608.0
      RPOW1=RPOWER/2.0
      RAND1 = RPOWER-3.0
      N=NX
      NROOT=IABS(NROOTX)
      IF(NROOT.EQ.0) GO TO 1001
      IF(N-1) 1001,1003,105
 1003 ROOT(1)=A(1)
      IF(NROOTX.GT.0) VECT(1,1)=1.00
      GO TO 1001
  105 CONTINUE
      NSIZE=(N*(N+1))/2
      NM1=N-1
      NM2=N-2
      FACTOR=0.0
      DO 70 I=1,NSIZE
   70 FACTOR=AMAX1(FACTOR,ABS(A(I)))
      IF(FACTOR.NE.0.) GO TO 72
      DO 78 I=1,NROOT
      IF(NROOTX.LT.0)GO TO 78
      DO 77 J=1,N
   77 VECT(J,I)=0.0
      VECT(I,I)=1.00
   78 ROOT(I)=0.0
      GO TO 1001
   72 ANORM=0.
      J=1
      K=1
      DO 80 I=1,NSIZE
      IF(I.NE.J) GO TO 81
      ANORM=ANORM+(A(I)/FACTOR)**2/2.0
      K=K+1
      J=J+K
      GO TO 80
   81 ANORM=ANORM+(A(I)/FACTOR)**2
   80 CONTINUE
      ANORM=SQRT(ANORM*2.0)*FACTOR
      DO 91 I=1,NSIZE
   91 A(I)=A(I)/ANORM
      ALIMIT=1.00
      ID=0
      IA=1
      IF(NM2.EQ.0) GO TO 201
      DO 200 J=1,NM2
      IA=IA+J+2
      ID=ID+J+1
      JP2=J+2
      II=IA
      SUM=0.0
      DO 100 I=JP2,N
      SUM=SUM+A(II)**2
  100 II=II+I
      TEMP=A(ID)
      IF(SUM.GT.SMALL)GO TO 110
      B(J,1)=TEMP
      A(ID)=0.0
      GO TO 200
  110 SUM = SQRT(SUM+TEMP**2)
      B(J,1)=-SIGN(SUM,TEMP)
      B(J+1,2)=SQRT((1.0+ABS(TEMP)/SUM)/2.00)
      TEMP=SIGN(.50/(B(J+1,2)*SUM),TEMP)
      II=IA
      DO 130 I=JP2,N
      B(I,2)=A(II)*TEMP
  130 II=II+I
C     WRITE(10,2005)I,J,D,01,02
      AK=0.0
      IC=ID+1
      J1=J+1
      DO 190 I=J1,N
      JJ=IC
      TEMP=0.0
      DO 180 II=J1,N
      TEMP=TEMP+B(II,2)*A(JJ)
      IF(II.LT.I) GO TO 210
      JJ=JJ+II
      GO TO 180
  210 JJ=JJ+1
  180 CONTINUE
      AK=AK+TEMP*B(I,2)
      B(I,1)=TEMP
```

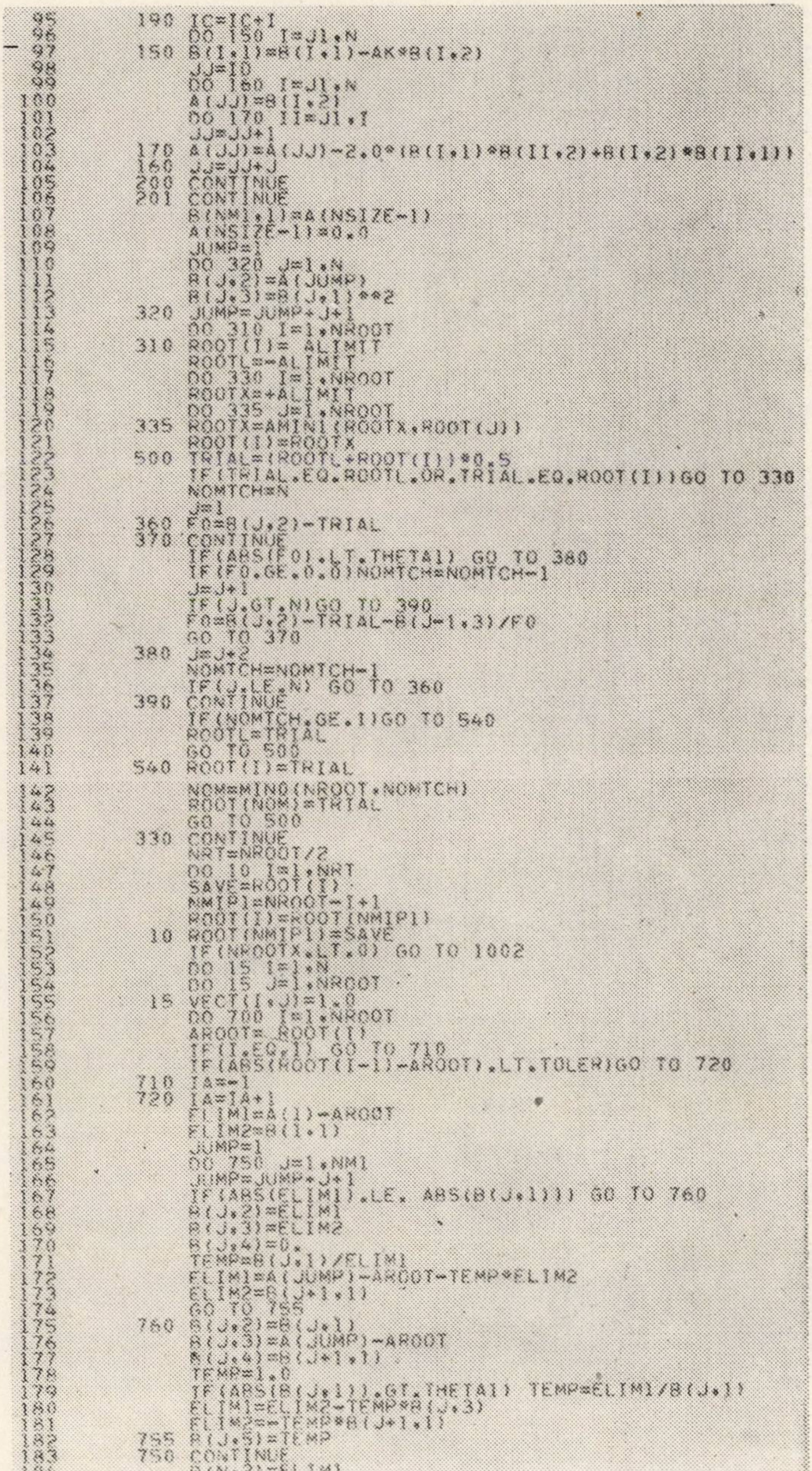

```
  190 IC=IC+I
      DO 150 I=J1,N
  150 B(I,1)=B(I,1)-AK*B(I,2)
      JJ=I0
      DO 160 I=J1,N
      A(JJ)=B(I,2)
      DO 170 II=J1,I
      JJ=JJ+1
  170 A(JJ)=A(JJ)-2.0*(B(I,1)*B(II,2)+B(I,2)*B(II,1))
  160 JJ=JJ+J
  200 CONTINUE
  201 CONTINUE
      B(NM1,1)=A(NSIZE-1)
      A(NSIZE-1)=0.0
      JUMP=1
      DO 320 J=1,N
      B(J,2)=A(JUMP)
      B(J,3)=B(J,1)**2
  320 JUMP=JUMP+J+1
      DO 310 I=1,NROOT
  310 ROOT(I)= ALIMIT
      ROOTL=-ALIMIT
      DO 330 I=1,NROOT
      ROOTX=+ALIMIT
      DO 335 J=1,NROOT
  335 ROOTX=AMIN1(ROOTX,ROOT(J))
      ROOT(I)=ROOTX
  500 TRIAL=(ROOTL+ROOT(I))*0.5
      IF(TRIAL.EQ.ROOTL.OR.TRIAL.EQ.ROOT(I))GO TO 330
      NOMTCH=N
      J=1
  360 F0=B(J,2)-TRIAL
  370 CONTINUE
      IF(ABS(F0).LT.THETA1) GO TO 380
      IF(F0.GE.0.0)NOMTCH=NOMTCH-1
      J=J+1
      IF(J.GT.N)GO TO 390
      F0=B(J,2)-TRIAL-B(J-1,3)/F0
      GO TO 370
  380 J=J+2
      NOMTCH=NOMTCH-1
      IF(J.LE.N) GO TO 360
  390 CONTINUE
      IF(NOMTCH.GE.1)GO TO 540
      ROOTL=TRIAL
      GO TO 500
  540 ROOT(I)=TRIAL
      NOM=MIN0(NROOT,NOMTCH)
      ROOT(NOM)=TRIAL
      GO TO 500
  330 CONTINUE
      NRT=NROOT/2
      DO 10 I=1,NRT
      SAVE=ROOT(I)
      NMIP1=NROOT-I+1
      ROOT(I)=ROOT(NMIP1)
   10 ROOT(NMIP1)=SAVE
      IF(NROOTX.LT.0) GO TO 1002
      DO 15 I=1,N
      DO 15 J=1,NROOT
   15 VECT(I,J)=1.0
      DO 700 I=1,NROOT
      AROOT= ROOT(I)
      IF(I.EQ.1) GO TO 710
      IF(ABS(ROOT(I-1)-AROOT).LT.TOLER)GO TO 720
  710 IA=-1
  720 IA=IA+1
      ELIM1=A(1)-AROOT
      ELIM2=B(1,1)
      JUMP=1
      DO 750 J=1,NM1
      JUMP=JUMP+J+1
      IF(ABS(ELIM1).LE. ABS(B(J,1))) GO TO 760
      B(J,2)=ELIM1
      B(J,3)=ELIM2
      B(J,4)=0.
      TEMP=B(J,1)/ELIM1
      ELIM1=A(JUMP)-AROOT-TEMP*ELIM2
      ELIM2=B(J+1,1)
      GO TO 755
  760 B(J,2)=B(J,1)
      B(J,3)=A(JUMP)-AROOT
      B(J,4)=B(J+1,1)
      TEMP=1.0
      IF(ABS(B(J,1)).GT.THETA1) TEMP=ELIM1/B(J,1)
      ELIM1=ELIM2-TEMP*B(J,3)
      ELIM2=-TEMP*B(J+1,1)
  755 B(J,5)=TEMP
  750 CONTINUE
      B(N,2)=ELIM1
      B(N,3)=0.
      B(N,4)=0.0
      B(NM1,4)=0.0
      ITER=1
      IF(IA.NE.0) GO TO 801
  790 L=N+1
      DO 780 J=1,N
      L=L-1
  786 CONTINUE
      ELIM1=VECT(L,I)-VECT(L+1,I)*B(L,3)-VECT(L+2,I)*B(L,4)
      IF(ABS(ELIM1).GT.DELBIG) GO TO 782
      TEMP=B(L,2)
      IF(ABS(B(L,2)).LT.DELTA) TEMP=DELTA
      VECT(L,I)=ELIM1/TEMP
      GO TO 780
  782 DO 784 K=1,N
  784 VECT(K,I)=VECT(K,I)/DELBIG
      GO TO 786
  780 CONTINUE
      GO TO (820,800), ITER
  820 ITER=ITER+1
  890 ELIM1=VECT(1,I)
      DO 830 J=1,NM1
      IF(B(J,2).EQ.B(J,1)) GO TO 840
      VECT(J,I)=ELIM1
      ELIM1=VECT(J+1,I)-ELIM1*B(J,5)
      GO TO 830
  840 VECT(J,I)=VECT(J+1,I)
      ELIM1=ELIM1-VECT(J+1,I)*TEMP
  830 CONTINUE
      VECT(N,I)=ELIM1
      GO TO 790
  801 CONTINUE
      DO 802 J=1,N
      RAND1=AMOD(4099.0*RAND1,RPOWER)
  802 VECT(J,I)=RAND1/RPOW1-1.
      GO TO 790
  800 IF(IA.EQ.0) GO TO 885
      DO 860 J1=1,IA
      K=I-J1
      TEMP=0.
      DO 870 J=1,N
  870 TEMP=TEMP+VECT(J,I)*VECT(J,K)
      DO 880 J=1,N
  880 VECT(J,I)=VECT(J,I)-TEMP*VECT(J,K)
  860 CONTINUE
  885 GO TO (890,900),ITER
  900 ELIM1=0.
      DO 904 J=1,N
  904 ELIM1=AMAX1(ABS(VECT(J,I)),ELIM1)
      TEMP=0.
      DO 910 J=1,N
      ELIM2=VECT(J,I)/ELIM1
      IF(ABS(ELIM2).LT.DEL2)GO TO 910
      TEMP=TEMP+ELIM2**2
  910 CONTINUE
      TEMP=1.0/(SQRT(TEMP)*ELIM1)
      DO 920 J=1,N
      VECT(J,I)=VECT(J,I)*TEMP
      IF(ABS(VECT(J,I)).LT.DEL1) VECT(J,I)=0.
  920 CONTINUE
  700 CONTINUE
      IF(NM2.EQ.0) GO TO 1002
      IM=NM1
      JUMP=NSIZE-(N+1)
      DO 950 I=1,NM2
      J1=JUMP
      DO 955 J=IM,N
      B(J,2)=A(J1)
  955 J1=J1+J
      DO 960 K=1,NROOT
      TEMP=0.
      DO 970 J=IM,N
  970 TEMP=TEMP+B(J,2)*VECT(J,K)
      TEMP=TEMP+TEMP
       DO 980 J=IM,N
  980 VECT(J,K)=VECT(J,K)-TEMP*B(J,2)
  960 CONTINUE
      JUMP=JUMP-IM
  950 IM=IM-1
 1002 CONTINUE
      DO 95 I=1,NROOT
   95 ROOT(I)=ROOT(I)*ANORM
 1001 RETURN
      END
```

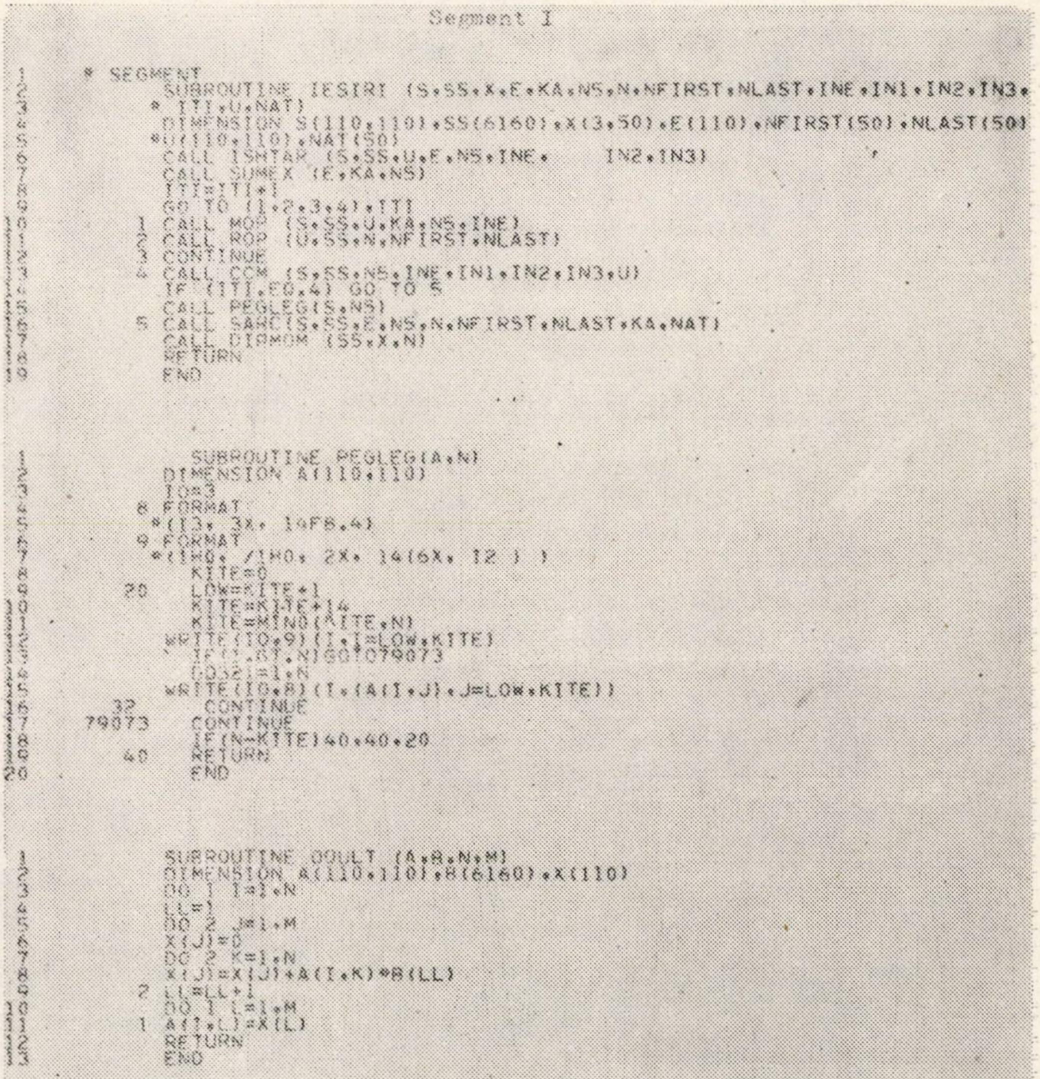

Segment I

```
* SEGMENT
      SUBROUTINE IESIRI (S,SS,X,E,KA,NS,N,NFIRST,NLAST,INE,IN1,IN2,IN3,
     * ITI,U,NAT)
      DIMENSION S(110,110),SS(6160),X(3,50),E(110),NFIRST(50),NLAST(50)
     *U(110,110),NAT(50)
      CALL ISHTAR (S,SS,U,E,NS,INE,     IN2,IN3)
      CALL SUMEX (E,KA,NS)
      ITI=ITI+1
      GO TO (1,2,3,4),ITI
    1 CALL MOP (S,SS,U,KA,NS,INE)
    2 CALL ROP (U,SS,N,NFIRST,NLAST)
    3 CONTINUE
    4 CALL CCM (S,SS,NS,INE,IN1,IN2,IN3,U)
      IF (ITI.EQ.4) GO TO 5
      CALL PEGLEG(S,NS)
    5 CALL SAHC(S,SS,E,NS,N,NFIRST,NLAST,KA,NAT)
      CALL DIPMOM (SS,X,N)
      RETURN
      END
```

```
        SUBROUTINE PEGLEG(A,N)
      DIMENSION A(110,110)
      IO=3
    8 FORMAT
     *(I3, 3X, 14F8.4)
    9 FORMAT
     *(1H0, /1H0, 2X, 14(6X, I2 ) )
        KITE=0
   20   LOW=KITE+1
        KITE=KITE+14
        KITE=MIN0(KITE,N)
      WRITE(IO,9)(I,I=LOW,KITE)
      ` IF(I.GT.N)GOTO79073
        DO32I=1,N
      WRITE(IO,8)(I,(A(I,J),J=LOW,KITE))
   32   CONTINUE
79073   CONTINUE
        IF(N-KITE)40,40,20
   40   RETURN
        END
```

```
      SUBROUTINE OOULT (A,B,N,M)
      DIMENSION A(110,110),B(6160),X(110)
      DO 1 I=1,N
      LL=1
      DO 2 J=1,M
      X(J)=0
      DO 2 K=1,N
      X(J)=X(J)+A(I,K)*B(LL)
    2 LL=LL+1
      DO 1 L=1,M
    1 A(I,L)=X(L)
      RETURN
      END
```

```
      SUBROUTINE MOFRA (S,SS,NS,INCA,INCB,ISCR,ISCF)
      DIMENSION S(110,110),SS(6160)
      INE=INCA
      READ  (9'INE,INE) ((S(I,J),J=1,NS),I=1,NS)
      NPS=NS*NS
      IF(NS-75) 1,1,2
    1 INE=INCB
      READ   (9'INE,INE)(SS(I),I=1,NPS)
      CALL  OOULT(S,SS,NS,NS)
      INE=ISCR
      WRITE (9'INE,INE) ((S(I,J),I=1,NS),J=1,NS)
      GO TO 3
    2 INS=6050/NS
      IN6=INS*NS
      INE=INCB
      READ(9'INE,INE)     (SS(I),I=1,IN6)
      ISFB=INE
      CALL OOULT(S,SS,NS,INS)
      INE=ISCR
      WRITE (9'INE,INE) ((S(I,J),I=1,NS),J=1,INS)
      ISFS=INE
```

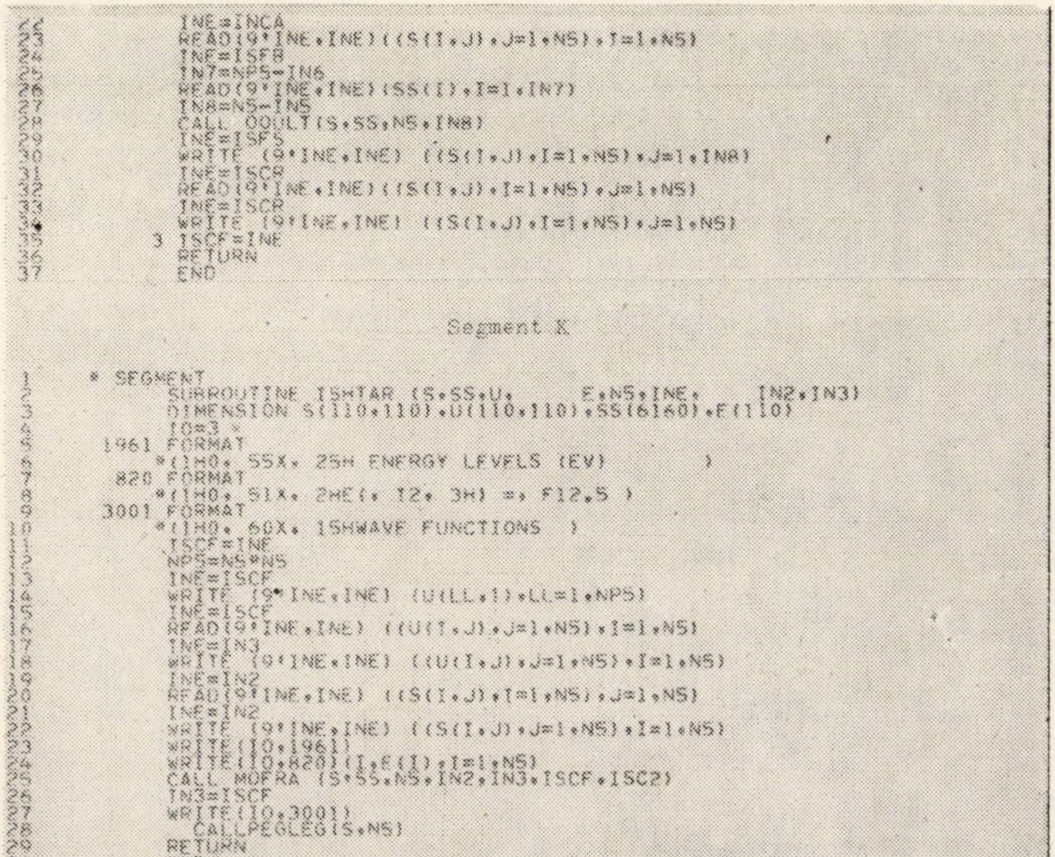

```
      INE=INCA
      READ(9'INE,INE)((S(I,J),J=1,NS),I=1,NS)
      INE=ISF8
      IN7=NPS-IN6
      READ(9'INE,INE)(SS(I),I=1,IN7)
      IN8=NS-INS
      CALL OOULT(S,SS,NS,IN8)
      INE=ISF5
      WRITE (9'INE,INE) ((S(I,J),I=1,NS),J=1,IN8)
      INE=ISCR
      READ(9'INE,INE)((S(I,J),I=1,NS),J=1,NS)
      INE=ISCR
      WRITE (9'INE,INE) ((S(I,J),I=1,NS),J=1,NS)
    3 ISCF=INE
      RETURN
      END
```

Segment K

```
* SEGMENT
      SUBROUTINE ISHTAR (S,SS,U,     E,NS,INE,     IN2,IN3)
      DIMENSION S(110,110),U(110,110),SS(6160),E(110)
      IO=3
 1961 FORMAT
     *(1H0, 55X, 25H ENERGY LEVELS (EV)          )
  820 FORMAT
     *(1H0, 51X, 2HE(, I2, 3H) =, F12.5 )
 3001 FORMAT
     *(1H0, 60X, 15HWAVE FUNCTIONS  )
      ISCF=INE
      NPS=NS*NS
      INE=ISCF
      WRITE (9*INE,INE) (U(LL,1),LL=1,NPS)
      INE=ISCF
      READ(9'INE,INE) ((U(I,J),J=1,NS),I=1,NS)
      INE=IN3
      WRITE (9'INE,INE) ((U(I,J),J=1,NS),I=1,NS)
      INE=IN2
      READ(9'INE,INE) ((S(I,J),I=1,NS),J=1,NS)
      INE=IN2
      WRITE (9'INE,INE) ((S(I,J),J=1,NS),I=1,NS)
      WRITE(IO,1961)
      WRITE(IO,820)(I,E(I),I=1,NS)
      CALL MOFRA (S,SS,NS,IN2,IN3,ISCF,ISC2)
      IN3=ISCF
      WRITE(IO,3001)
        CALLPEGLEG(S,NS)
      RETURN
      END
```

Segment L

```
* SEGMENT
      SUBROUTINE SUMEX (E,KA,NS)
      DIMENSION E(110)
  793 FORMAT
     *(1H0,10X,'GROUNDSTATE ENERGY=',F16.8,4H EV.,10X,'FIRST EXCITED STA
     *TE=',F16.8,4H EV.,///)
      IO=108
        KAK=NS-KA+1
        SUM=0.0
        IF(KAK.GT.NS)GOTO79061
        DO1I=KAK,NS
    1   SUM=SUM+E(I)
79061   CONTINUE
        SUM=SUM+SUM
      EX=SUM+E(KAK-1)-E(KAK)
      WRITE(IO,793)SUM,EX
      RETURN
      END
```

Segment M

```
* SEGMENT
      SUBROUTINE MOP (S,SS,U,KA,NS,INE)
      DIMENSION S(110,110),SS(6160),U(110,110)
      IO=3
   17 FORMAT
     *(1H0, 40X, 35H MULLIKEN OVERLAP POPULATIONS FOR  , I2, 30H FILLED
     *ORBITALS                )
```

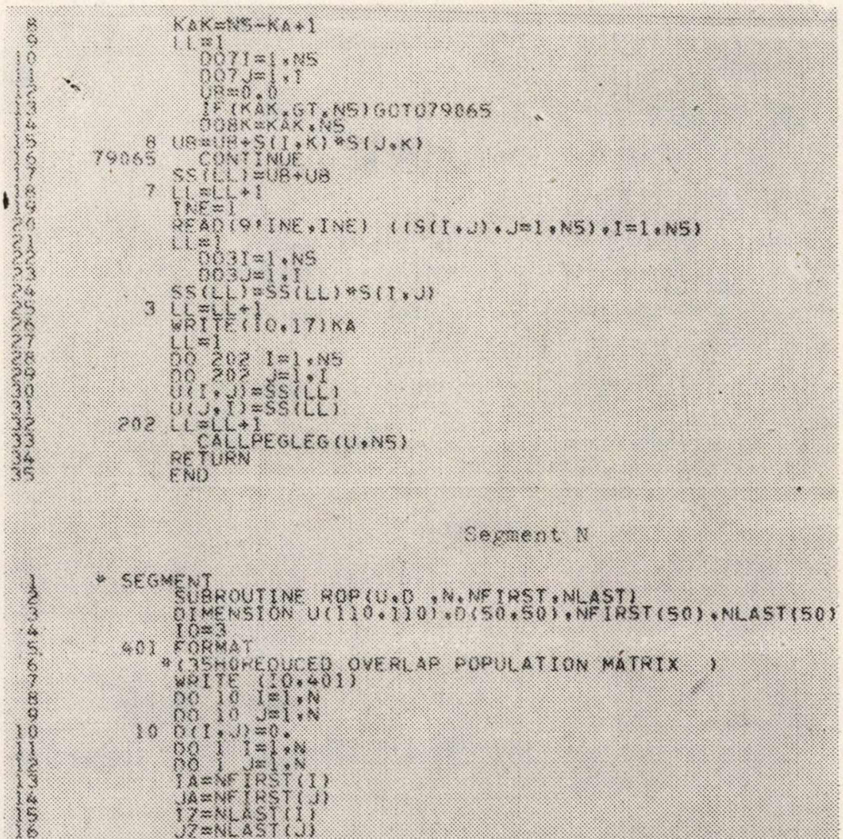

```
      KAK=NS-KA+1
      LL=1
        DO7I=1,NS
        DO7J=1,I
        UR=0.0
        IF(KAK.GT.NS)GOTO79865
        DO8K=KAK,NS
    8 UR=UR+S(I,K)*S(J,K)
79065   CONTINUE
      SS(LL)=UR+UR
    7 LL=LL+1
      INE=1
      READ(9'INE,INE) ((S(I,J),J=1,NS),I=1,NS)
      LL=1
        DO3I=1,NS
        DO3J=1,I
      SS(LL)=SS(LL)*S(I,J)
    3 LL=LL+1
      WRITE(IO,17)KA
      LL=1
      DO 202 I=1,NS
      DO 202 J=1,I
      U(I,J)=SS(LL)
      U(J,I)=SS(LL)
  202 LL=LL+1
        CALLPEGLEG(U,NS)
      RETURN
      END
```

Segment N

```
* SEGMENT
      SUBROUTINE ROP(U,D ,N,NFIRST,NLAST)
      DIMENSION U(110,110),D(50,50),NFIRST(50),NLAST(50)
      IO=3
  401 FORMAT
     *(35H0REDUCED OVERLAP POPULATION MATRIX  )
      WRITE (IO,401)
      DO 10 I=1,N
      DO 10 J=1,N
   10 D(I,J)=0.
      DO 1 I=1,N
      DO 1 J=1,N
      IA=NFIRST(I)
      JA=NFIRST(J)
      IZ=NLAST(I)
      JZ=NLAST(J)
      IF(IA.NE.IZ.OR.JA.NE.JZ)GO TO 2
      D(I,J)=U(IA,JA)
      GO TO 1
    2 IF(IA.EQ.IZ.AND.JA.NE.JZ) GO TO 3
      IF(IA.NE.IZ.AND.JA.NE.JZ) GO TO 4
      DO 5 K=1,4
      KK=IA+K-1
    5 D(I,J)=D(I,J)+U(KK,JA)
      GO TO 1
    3 DO 6 K=1,4
      KK=JA+K-1
    6 D(I,J)=D(I,J)+U(IA,KK)
      GO TO 1
    4 DO 7 K=1,4
      DO 7 L=1,4
      KK=IA+K-1
      LL=JA+L-1
    7 D(I,J)=D(I,J)+U(KK,LL)
    1 CONTINUE
      DO 11 I=1,N
      DO 11 J=1,N
   11 U(I,J)=D(I,J)
      CALL PEGLEG (U,N)
      RETURN
      END
```

Segment O

```
* SEGMENT
      SUBROUTINE CCM(S,SS,NS,INE,IN1,IN2,IN3,U)
      DIMENSION S(110,110),SS(6160),U(110,110)
 2005 FORMAT
     *(25H0COMPLETE CHARGE MATRIX   )
      CALL MOFRA (S,SS,NS,1,IN3,IN1,ISCF)
      IO=3
```

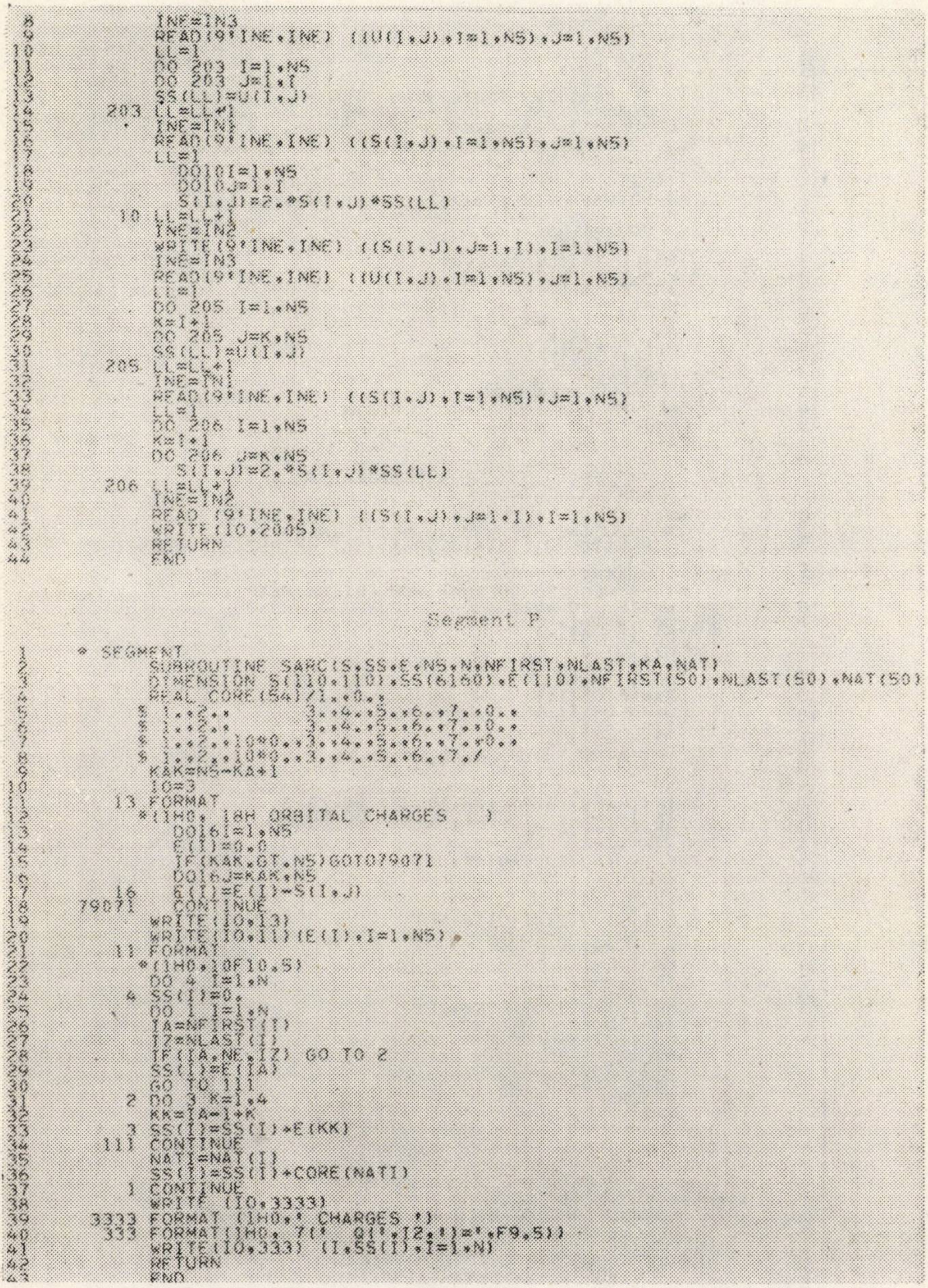

```
      INE=IN3
      READ(9'INE,INE) ((U(I,J),I=1,NS),J=1,NS)
      LL=1
      DO 203 I=1,NS
      DO 203 J=1,I
      SS(LL)=U(I,J)
  203 LL=LL+1
      INE=IN1
      READ(9'INE,INE) ((S(I,J),I=1,NS),J=1,NS)
      LL=1
         DO10I=1,NS
         DO10J=1,I
         S(I,J)=2.*S(I,J)*SS(LL)
   10 LL=LL+1
      INE=IN2
      WRITE(9'INE,INE) ((S(I,J),J=1,I),I=1,NS)
      INE=IN3
      READ(9'INE,INE) ((U(I,J),I=1,NS),J=1,NS)
      LL=1
      DO 205 I=1,NS
      K=I+1
      DO 205 J=K,NS
      SS(LL)=U(I,J)
  205 LL=LL+1
      INE=IN1
      READ(9'INE,INE) ((S(I,J),I=1,NS),J=1,NS)
      LL=1
      DO 206 I=1,NS
      K=I+1
      DO 206 J=K,NS
         S(I,J)=2.*S(I,J)*SS(LL)
  206 LL=LL+1
      INE=IN2
      READ (9'INE,INE) ((S(I,J),J=1,I),I=1,NS)
      WRITE(IO,2005)
      RETURN
      END
```

Segment P

```
* SEGMENT
      SUBROUTINE SARC(S,SS,E,NS,N,NFIRST,NLAST,KA,NAT)
      DIMENSION S(110,110),SS(6160),E(110),NFIRST(50),NLAST(50),NAT(50)
      REAL CORE(54)/1.,0.,
     $ 1.,2.,      3.,4.,5.,6.,7.,0.,
     $ 1.,2.,      3.,4.,5.,6.,7.,0.,
     $ 1.,2.,10*0.,3.,4.,5.,6.,7.,0.,
     $ 1.,2.,10*0.,3.,4.,5.,6.,7./
      KAK=NS-KA+1
      IO=3
   13 FORMAT
     *(1H0, 18H ORBITAL CHARGES    )
        DO16I=1,NS
        E(I)=0.0
        IF(KAK.GT.NS)GOTO79071
        DO16J=KAK,NS
   16   E(I)=E(I)-S(I,J)
79071   CONTINUE
      WRITE(IO,13)
      WRITE(IO,11)(E(I),I=1,NS)
   11 FORMAT
     *(1H0,10F10.5)
      DO 4 I=1,N
    4 SS(I)=0.
      DO 1 I=1,N
      IA=NFIRST(I)
      IZ=NLAST(I)
      IF(IA.NE.IZ) GO TO 2
      SS(I)=E(IA)
      GO TO 111
    2 DO 3 K=1,4
      KK=IA-1+K
    3 SS(I)=SS(I)+E(KK)
  111 CONTINUE
      NATI=NAT(I)
      SS(I)=SS(I)+CORE(NATI)
    1 CONTINUE
      WRITE (IO,3333)
 3333 FORMAT (1H0,' CHARGES ')
  333 FORMAT(1H0, 7('  Q(',I2,')=',F9.5))
      WRITE(IO,333) (I,SS(I),I=1,N)
      RETURN
      END
```

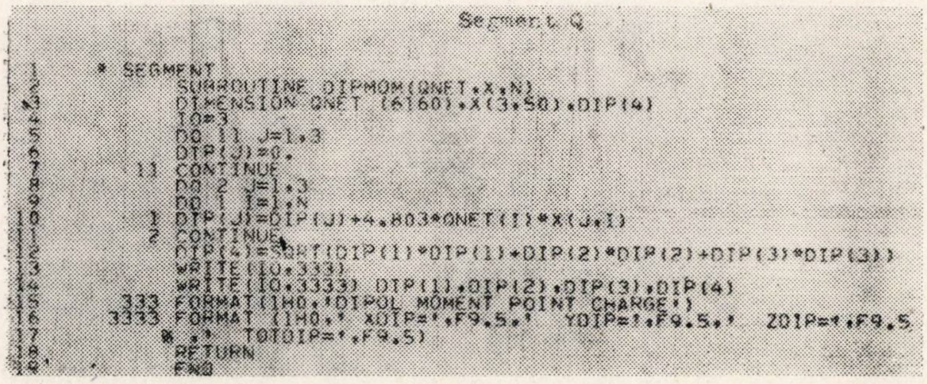

Segment Q

```
* SEGMENT
      SUBROUTINE DIPMOM(QNET,X,N)
      DIMENSION QNET (6160),X(3,50),DIP(4)
      IO=3
      DO 11 J=1,3
      DIP(J)=0.
   11 CONTINUE
      DO 2 J=1,3
      DO 1 I=1,N
    1 DIP(J)=DIP(J)+4.803*QNET(I)*X(J,I)
    2 CONTINUE
      DIP(4)=SQRT(DIP(1)*DIP(1)+DIP(2)*DIP(2)+DIP(3)*DIP(3))
      WRITE(IO,333)
      WRITE(IO,3333) DIP(1),DIP(2),DIP(3),DIP(4)
  333 FORMAT(1H0,'DIPOL MOMENT POINT CHARGE')
 3333 FORMAT (1H0,' XDIP=',F9.5,'  YDIP=',F9.5,'  ZDIP=',F9.5
     & ,'  TOTDIP=',F9.5)
      RETURN
      END
```

Revue Roumaine de Chimie, **27**, *3*, 345–349 (1982)

ELECTROREDUCTION OF NITRATE IONS IN MOLTEN ALKALI NITRATES

S. STERNBERG and T. VIŞAN
Dept. of Physical Chemistry and Electrochemical Technology, Cal. Griviţei 132, Polytechnic Institute, Bucharest

Received July 28, 1980

The electroreduction of nitrate ions in molten alkali nitrates as $LiNO_3$, $NaNO_3$ KNO_3 has been studied in the temperature range 350–370°C, in galvanostatic conditions by chronopotentiometric method. A "three-electrode system" glass cell has been used and current densities were of 10 – 10^4 mA/cm². The existence and position of transients on potential-time curves have been ascribed to different products formed on the cathode, during the high current density electrolysis. The experimental results are discussed in terms of various cathodic reactions involving O^{2-}, O_2^{2-}, O_2^- ions and of alkali metal deposition.

INTRODUCTION

During the past several years, the electroreduction of nitrate ions in molten alkali nitrates has been the subject of numerous investigations. [1-3] The primary products of nitrate reduction have been identified as nitrite and oxide according to the reaction

$$NO_3^- + 2e = NO_2^- + O^{2-} \qquad (1)$$

Recent studies [4,5] indicate that the oxide species is unstable in the melt and converts into peroxide and superoxide:

$$O^{2-} + NO_3^- = NO_2^- + O_2^{2-} \qquad (2)$$

$$O_2^{2-} + 2NO_3^- = 2NO_2^- + 2O_2^- \qquad (3)$$

In the same papers [4,5] the difference between anhydrous and hydrated melts was emphasized in relation to the chemistry of oxides; the formation of high oxidation state oxides (peroxide-superoxide) can be limited or precluded by the presence of acid species such as water, carbon dioxide, silica.

The electroreduction of nitrate ions in alkali nitrates has been investigated so far by potentiometric and potentiostatic techniques. In the present paper, the electroreduction processes on Pt cathode in molten alkali nitrates as $LiNO_3$, $NaNO_3$, and KNO_3, by chronopotentiometric method is discussed; sequential potential-time curves were obtained at high current densities up to the electrodeposition of alkali metal.

EXPERIMENTAL

Alkali nitrates as $NaNO_3$ and KNO_3 were reagent grade and $LiNO_3$ was Merck reagent. $NaNO_3$ and KNO_3 aqueous solutions were first filtered to eliminate small amounts of a brown precipitate probably due to the oxidation of organic substances. Alkali nitrates were twice or thrice recrystallised from distilled water, then dried at about 150°C for some days and melted twice; before runs, the salts were kept in a dessicator. Very careful dehydration of the solvent was indispensable. Water was eliminated from the melts by bubbling dry argon through the electrolysis cell before electrolysis for 1 — 2 hours; argon was dried by flowing it through traps stuffed with molecular sieves and oxygen traces were retained in a special catalyst-filled column.

The cell assembly consisted of a "three-electrode system": Pt microelectrode as cathode ($s = 0.09 - 0.12\ cm^2$), a large Pt electrode as anode ($s = 2 - 3\ cm^2$) and a $Ag/AgNO_3$ (0.01M) $+ AlkNO_3$ as reference electrode. The Pt cathode sheet was replaced with a Pt wire of 6 mm^2 ($\varnothing = 1$ mm) for electrolysis at high current densities. The working surface was delimited by protective Pyrex glass tubes. After cathodic polarisation in melt, the electrodes were immersed in dilute nitric acid solution until the product, adhering to the surface was dissolved completely. The electrolysis cell contained about 100 g molten salt.

A conventional set-up was used for galvanostatic measurements: it consisted of a d.c. power supply (100 — 300 V) and a variable resistor. The current was determined by measuring the voltage across a standard resistance with an electronic voltmeter. Potential-time curves were obtained on the X — Y recorder with time base. The current was reversed after each measurement for redissolution on the deposited cathodic product and a new measurement was started after 10 — 15 minutes waiting time.

Chronopotentiometric measurements were carried out in the temperature range 350 — 370°C; the temperature, as determined with a Pt—PtRh thermocouple was maintained within ± 1°C and controlled by a proportional thermoregulator.

Sequential potential-time curves were obtained starting from $t = 0$ at different current densities at the end of the electroreduction of NO_3^- by the deposition of alkali metal. The current densities were selected in the 10 — 4000 mA/cm^2 range.

RESULTS AND DISCUSSION

The chronopotentiometric method at very high current densities evidenced the transients on potential-time curves which point out the intricacy of cathodic processes in alkali nitrates.

Figs. 1 — 3 show the chronopotentiograms for $LiNO_3$, $NaNO_3$ and KNO_3 at various current densities. The shape of chronopotentiograms depends on the nature of melt and may be accounted for on the basis of cathode reactions.

In alkali nitrates, the electroreduction of nitrate ion with oxide formation was shown to be the main reaction (1) followed by reactions (2) and (3) which are favoured in Li-Na-K sequence established by the increasing degree of solubility of alkali oxide formed.

In KNO_3 there are O_2^- superoxide and O_2^{2-} peroxide, the former being predominant. The primary oxide O^{2-} is shown on chronopotentiograms by the plateau (A), while higher oxides by intermediate plateaus

(B) and (C) brought about by reduction of O_2^- and O_2^{2-} ions, according to the reactions

$$O_2^{2-} + 2e = 2O^{2-} \tag{4}$$

$$O_2^- + e = O_2^{2-} \tag{5}$$

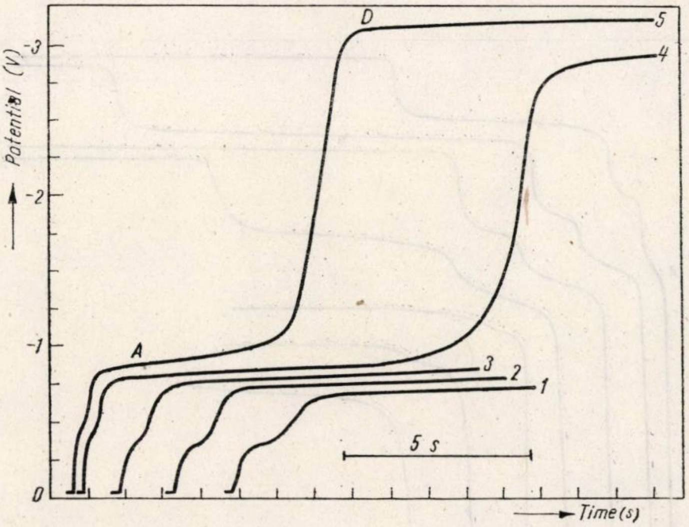

Fig. 1. — Chronopotentiograms for the cathodic reduction on Pt in LiNO$_3$ at 360°C : *1* — i = 390 mA/cm^2 ; *2* — i = 780 mA/cm^2 ; *3* — i = 1000 mA/cm^2 ; *4* — i = 1950 mA/cm^2 ; *5* — i = 3900 mA/cm^2.

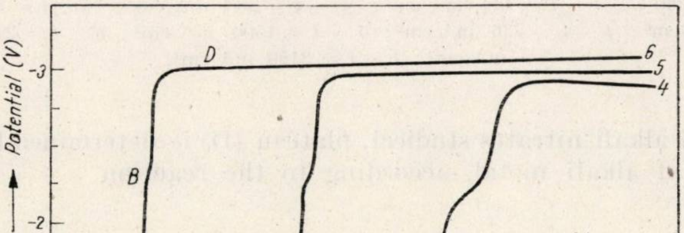

Fig. 2. — Chronopotentiograms for the cathodic reduction on Pt in NaNO$_3$ at 360°C : *1* — i = 16 mA/cm^2 ; *2* — i = 166 mA/cm^2 ; *3* — i = 330 mA/cm^2 ; *4* — i = 416 mA/cm^2 ; *5* — i = 725 mA/cm^2 ; *6* — i = 1660 mA/cm^2.

In $NaNO_3$, O_2^{2-} peroxide predominates; it is shown by an intermediate plateau (B), explained by reaction (4). In $LiNO_3$ the tendency of higher oxide formation is lower and two plateaus are distinct: **(A)** and (D).

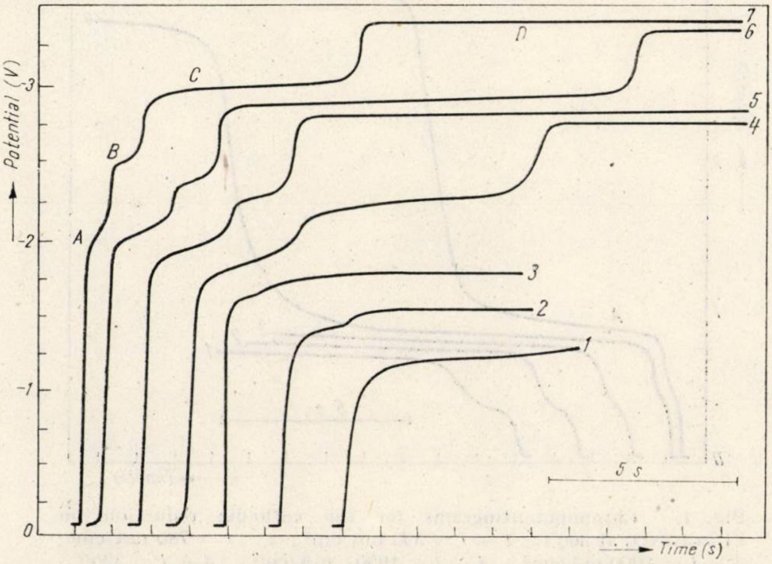

Fig. 3. — Chronopotentiograms for the cathodic reduction on Pt in KNO_3 at 360°C: *1* — i = 111 mA/cm²; *2* — i = 250 mA/cm²; *3* — i = 500 mA/cm²; *4* — i = 736 mA/cm²; *5* — i = 1500 mA/cm²; *6* — i = 2400 mA/cm²; *7* — i = 3150 mA/cm².

In all alkali nitrates studied, plateau (D) is determined by electrodeposition of alkali metal, according to the reaction

$$Me^+ + e = Me \qquad (6)$$

The transients are caused by formation of a diffusion layer, probably consisting of the oxide film which forms on cathode.

The dependence of "layer" properties of alkali oxide formed, on the degree of solubility and thickness of oxide film was studied by Shibata and Sumino. [6]

Thus Na_2O layer is adherent and compact, which explains the higher tendency of forming transients, i.e. lowest $i\tau^{1/2}$.

K_2O layer is not compact though it is thick. Although Li_2O is the least soluble it does not form an adherent film on the cathode surface, which is proved by the high value of the $i\tau^{1/2}$ product (Table 1).

TABLE 1

The values of the constant product $i\tau^{1/2}$ for alkali oxide formation in molten alkali nitrates (plateau A on chronopotentiograms)

Parameter	Alkali oxide		
	Li_2O	Na_2O	K_2O
i (plateau A) A/cm^2	1.3	0.25	1.0
$i\tau^1$ $(A.s^{1/2}.cm^{-2})$	8.0	1.3	2·1

REFERENCES

H. S. Swofford Jr. and H. A. Laitinen, *J. Electrochem. Soc.*, **110**, 814 (1963).
K. E. Johnson and P. S. Zacharias, *J. Electrochem. Soc.*, **124**, 448 (1977).
H. E. Bartlett and K. E. Johnson, *J. Electrochem. Soc.*, **111**, 64 (1967).
P. G. Zambonin and J. Jordan, *J. Amer. Chem. Soc.*, **89**, 6365 (1967); *ibid.*, **91**, 2225 (1969).
P. G, Zambonin, *J. Electroanal. Chem.*, **24**, 365 (1970); *ibid.*, **33**, 243 (1971); *J. Phys. Chem.*, **78**, 1294 (1974).
S. Shibata and M. P. Sumino, *Electrochim. Acta*, **20**, 871 (1975).

Revue Roumaine de Chimie, 27, 3, 351–355 (1982)

L'INFLUENCE DU SOLVANT SUR LA VITESSE DE RÉACTION. L'HYDROLYSE ALCALINE DE L'ACÉTATE, DU PROPIONATE ET DU BUTYRATE DE n-BUTYLE DANS LE SOLVANT MIXTE EAU—DYMÉTHYLSULFOXYDE

ORTANSA LANDAUER, CORNELIA MATEESCU et OLGA IULIAN
Laboratoire de Chimie Physique, Institut Polytechnique str. Polizu 1, Bucarest, Roumanie

Reçu le 5 Juin 1981

La cinétique chimique de l'hydrolyse alcaline de l'acétate, du propionate et du butyrate de n-butyle dans le solvant mixte, eau—dyméthylsulfoxide (DMSO) a été étudiée a 20°, 25°, 30°, 40°C. Les résultats obtenus sont mis en corrélation avec la constante diélectrique du solvant mixte. On attribue la variation de la constante de vitesse avec la teneur en DMSO, ainsi que la variation de l'énergie d'activation, au phénomène de solvatation.

The Chemical kinetics of the alkaline hydrolysis of the n-butyl acetate, propionate and butyrate in the mixed solvent water—dimethylsulphoxide (DMSO) has been studied at 20°, 25°, 30°, 40°C. The results that have been obtained are correlated with the dielectric constant of the mixed solvent. The variation of the coefficient of velocity with the DMSO content, as well as the variation of the activation energy is attributed to the solvation phenomenon.

En poursuivant nos recherches sur l'influence du solvant sur la vitesse de réaction, [1-6] nous avons étudié l'hydrolyse alcaline de l'acétate, du propionate et du butyrate de n-butyl dans le solvant mixte eau-dyméthylsulfoxyde (DMSO).

PARTIE EXPÉRIMENTALE

Les esters étudiés dans ce travail ont été préparés et purifiés par des méthodes données dans la littérature .[7] La pureté a été vérifiée par des méthodes chromatographiques. Le dyméthylsulfoxyde a été séché avec hydroxyde de calcium et puis purifié par distillation à pression réduite (10 mm Hg). Le produit final a le point de fusion $P_f = 18{,}52°C$ et $n_D^{20} = 1{,}3590$. L'hydroxyde de sodium est un produit Merck. La concentration initiale de l'ester, déterminée par saponification totale était approximativement de 0,01 M et celle de l'hydroxyde de sodium, constante dans tous les cas était de 0,015N.

Les données cinétiques ont été obtenues par titrage. Les valeurs obtenues pour les constantes de vitesse représentent la moyenne d'environ dix résultats cinétiques, calculés avec une erreur de ± 2%.

La réaction vérifie l'équation cinétique suivante :

$$k = \frac{1}{t(a-b)} \ln \frac{b(a-x)}{a(b-x)}.$$

où a — est la concentration de l'ester et
b — la concentration de l'hydroxyde de sodium.

L'hydrolyse de ces trois esters a été étudiée dans des solutions eau-dymethylsulfoxyde avec des compositions variables, aux températures de : 20, 25, 30 et 40°C.

RÉSULTATS EXPÉRIMENTAUX

Les constantes de vitesse de l'hydrolyse alcaline des trois esters aux températures mentionnées dans l'intervalle de concentration du solvant mixte : $x_{DMSO} = 0{,}05$ à $x_{DMSO} = 0{,}7$, sont réunies dans les tableaux 1, 2 et 3.

TABLEAU 1

Constantes de vitesse de l'hydrolyse alcaline de l'acétate de n-butyle

x_{DMSO}	$k.10^3$ (l mole^{-1}s^{-1})			
	20°C	25°C	30°C	40°C
0,058	7,34	10,09	12,83	20,68
0,098	7,69	10,63	13,57	21,17
0,145	8,63	11,33	14,02	24,17
0,202	9,29	12,24	15,18	28,46
0,276	11,54	14,71	17,87	31,79
0,372	14,52	18,91	23,30	42,01
0,504	26,20	32,93	39,66	69,86
0,695	58,10	73,36	88,61	150,00

On remarque que les valeurs des constantes de vitesse pour tous les esters étudiés présentent une croissance avec la croissance de la quantité de DMSO. Le même effet a été constaté par d'autres auteurs aussi, qui ont étudié l'hydrolyse de divers esters dans le même solvent.[8-10] La

TABLEAU 2

Constantes de vitesse de l'hydrolyse alcaline du propionate de n-butyle

x_{DMSO}	$k.10^3$ (l mole^{-1}s^{-1})			
	20°C	25°C	30°C	40°C
0,098	4,40	7,17	9,94	15,77
0,145	5,45	7,73	10,00	16,42
0,202	5,67	8,04	10,40	18,02
0,276	6,12	9,17	12,21	20,62
0,372	8,40	13,14	17,87	26,05
0,504	14,02	21,63	29,23	49,91
0,695	30,70	52,76	74,83	112,97

cause principale de la croissance des constantes de vitesse avec la quantité de DMSO est déterminée par l'équilibre suivant :

$$[HO^{-}nH_2O] + (n - n')DMSO \rightleftarrows [HO^{-}n'H_2O] + (n - n')[DMSO.H_2O]$$

TABLEAU 3

Constantes de vitesse de l'hydrolyse alcaline du butyrate de n-butyle

x_{DMSO}	$k.10^3(l\,mole^{-1}s^{-1})$			
	20°C	25°C	30°C	40°C
0,145	1,85	3,12	4,39	6,12
0,202	2,41	4,07	5,73	7,24
0,276	3,32	4,76	6,20	10,33
0,372	4,56	6,73	8,90	14,57
0,504	6,21	19,36	12,50	29,21
0,695	14,99	22,50	30,00	60,46

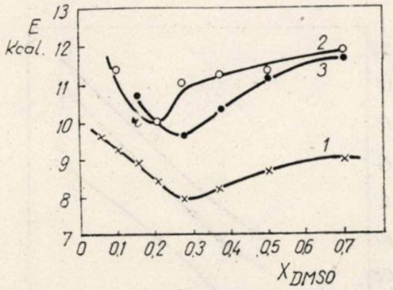

Fig. 1. — Variation de l'énergie d'activation de l'hydrolyse alcaline de *1.* acétate ; *2.* propionate, *3.* butyrate de n-butyle avec la teneur en DMSO du solvant mixte.

où n est le numéro maximal des molécules d'eau liées par l'ion d'hydroxyde. Avec la croissance du contenu en DMSO l'équilibre sera bien déplacé à droite en résultant un ion hydroxyde moins solvaté. La désolvatation de l'anion est la cause de l'augmentation de la vitesse de réaction avec x_{DMSO}.

La variation de l'énergie d'activation de l'hydrolyse alcaline de l'acétate, du propionate et du butyrate de n-butyle avec la teneur en DMSO du solvent mixte est représentée par la figure 1. On remarque que pour $x_{DMSO} \sim 0,3$ l'énergie d'activation passe par un minimum.

L'influence du solvant mixte sur la vitesse de réaction s'exprime par la dépendance log k—x_{DMSO}. Pour tous les esters aux températures mentionnées on obtient une variation linéaire, toujours positive, qui change de pentes à $x_{DMSO} \sim 0,3$. La dépendance est exprimée par l'égalité (1) :

$$\log k = m x_{DMSO} + a \qquad (1)$$

où *m* est « la sensibilité » du substrat à la teneur en DMSO.[8-11]

On peut diviser l'intervalle de concentration du solvant mixte en deux régions : I pour $x_{DMSO} < 0,3$ et II, pout $x_{DMSO} > 0,3$. Les valeurs des pentes calculées figurent dans le tableau 4.

TABLEAU 4

Variation de la constante de vitesse en fonction de la teneur en DMSO du solvant mixte

Ester	m_I	m_{II}
Acétate de n-butyle	1	1,75
Propionate de n-butyle	0,8	1,80
Butyrate de n-butyle	2,2	1,55

Pour $x_{DMSO} > 0{,}3$, m_{II} présente des valeurs similaires pendant que pour $x_{DMSO} < 0{,}3$, m_I est variable d'un ester à l'autre. Cette chose concorde avec l'idée que là se produit une désolvatation de l'anion hydroxyde avec la croissance du contenu en DMSO. À de petites concentrations du composant organique parce que l'anion hydraté de hydroxyde est l'unité cinétique qui réagit avec le substrat, on obtient des valeurs qui dépendent de la nature du substrat.

L'influence électrostatique du milieu de réaction sur la vitesse de réaction s'exprime par l'équation (2)

$$\frac{\mathrm{d}\ln k}{\mathrm{d}\left(\frac{1}{D}\right)} = \frac{\mathrm{d}x_{DMSO}}{\mathrm{d}\left(\frac{1}{D}\right)}\,\frac{\mathrm{d}\ln k}{\mathrm{d}x_{DMSO}} \qquad (2)$$

Suivant l'équation (2) en représentant graphiquement la variation de lg k en fonction de $\frac{1}{D}$ (fig. 2), on obtient pour les trois esters, une variation linéaire.

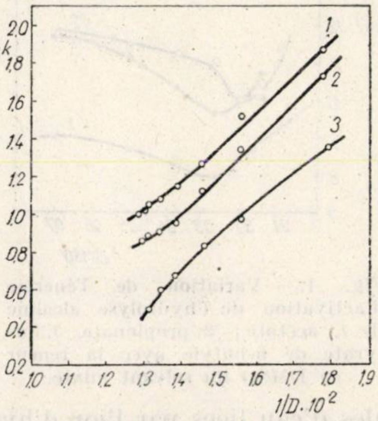

Fig. 2. — Variation de log k en fonction de 1/D pour *1.* acétate, *2.* propionate et *3.* butyrate de n-butyle à 25°.

Les valeurs des pentes calculées pour la dépendance lg $k - \frac{1}{D}$, le produit des pentes pour la dépendance $x_{DMSO} - \frac{1}{D}$ et lg $k - x_{DMSO}$ dans le domaine I et II figurent le tableau 5.

TABLEAU 5

Variation de la constante de viţesse en fonction de la constante diélectrique

	$\left[\frac{\mathrm{d}\lg k}{\mathrm{d}\left(\frac{1}{D}\right)}\right]_{I} 10^{-2}$	$\left[\frac{\mathrm{d}\lg k}{\mathrm{d}\left(\frac{1}{D}\right)}\right]_{II} 10^{-2}$	$\left[\frac{\mathrm{d}x_{DMSO}}{\mathrm{d}\left(-\frac{1}{D}\right)}{}^{*)}\,\frac{\mathrm{d}\lg k}{\mathrm{d}x_{DMSO}}\right]_{I} 10^{-2}$	$\left[\frac{\mathrm{d}x_{DMSO}}{\mathrm{d}\left(-\frac{1}{D}\right)}\,\frac{\mathrm{d}\ln k}{\mathrm{d}x_{DMSO}}\right]_{II} 10^{-2}$
Acétate de n-butyle	1,5	1,9	1,2	2,1
Propionate de n-butyle	1,6	2,0	0,96	2,2
Butyrate de n-butyle	2,2	1,6	2,6	1,9

*) $\frac{\mathrm{d}x_{DMSO}}{\mathrm{d}\left(\frac{1}{D}\right)} = 1{,}20^{8}$

On remarque que l'équation (2) ne se vérifie pas, en résultant que les forces électrostatiques n'ont une influence décisive, ni pour $x_{DMSO} > 0,3$, ni pour $x_{DMSO} < 0,3$.

On peut supposer que les effets de solvatation qui ont un rôle important se superposent aux effets électrostatiques.

L'existence du minimum de l'énergie d'activation du $x_{DMSO} \sim 0,3$ plaide pour une solvatation plus grande du complexe actif, par rapport à la solvatation des molécules réagissantes, à cette concentration.[11, 12]

Les valeurs pour la densité d'excès, la viscosité, l'indice de réfraction et les fonctions thermodynamiques d'excès,[13–15] montrent que dans le système H_2O — DMSO, à la concentration du solvant de $x_{DMSO} \sim 0,35$ se forme un groupement moléculaire, de formule $DMSO(H_2O)_2$, qui détermine une meilleure solvatation du complexe activé par rapport à la solvatation des molécules des réactants.

BIBLIOGRAPHIE

[1] G. Costeanu et C. Mateescu, *Rev. Roumaine Chim.*, **16**, 1083 (1971).
[2] G. Costeanu et C. Mateescu, *Rev. Roumaine Chim.*, **17**, 95 (1972).
[3] G. Costeanu et C. Mateescu, *Rev. Roumaine Chim.*, **17**, 1353 (1972).
[4] G. Costeanu et O. Landauer, *Rev. Roumaine Chim.*, **17**, 1331 (1972).
[5] G. Costeanu et O. Landauer, *Rev. Roumaine Chim.*, **17**, 1347 (1972).
[6] G. Costeanu et O. Landauer, *Rev. Roumaine Chim.*, **17**, 1339 (1972).
[7] A. I. Vogel, "A Text Book of Practical Organic Chemistry", vol. III, ed. III, Longmans-Green, London, 1956, p. 382.
[8] D. D. Roberts, *J. Org. Chem.*, **30**, 3517 (1965).
[9] D. D. Roberts, *J. Org. Chem.*, **31**, 4037 (1966).
[10] D. D. Roberts, *J. Org. Chem.*, **29**, 2039 (1964), ibid. 2714.
[11] B. J. Yager, Ch. B. Kay, J. D. Mastrovici et L. E. Whittington, *Texas J. Sci.*, **21**, 3 (1969).
[12] N. J. Cleve, *Suomen Kemistilehti B*, **46**, 385 (1972).
[13] J. J. Lindberg et J. Kenttämaa, *Suomen Kemistilehti B*, **33**, 104 (1960).
[14] J. M. G. Gowie et P. Toporowski, *Canad. J. Chem.*, **39**, 2240 (1961).
[15] M. R. Reynaud, *Compt. rend. B*, **266**, 489 (1968).

Revue Roumaine de Chimie, 27, 3, 357–363 (1982)

KINETIC AND THERMODYNAMIC PARAMETERS OF THE REVERSIBLE ACID HYDROLYSIS OF BENZYL ACETATE IN WATER–METHANOL MIXTURES

FAYEZ Y. KHALIL* and M. T. HANNA
Department of Chemistry, Faculty of Science, University of Alexandria, Alexandria, Egypt

Received July 9, 1980

A kinetic study of the acid-catalysed hydrolysis of benzyl acetate in a series of water-methanol mixtures containing up to 93% (w/w) of MeOH and at 25–50°C was made. In purely aqueous medium the reaction was found to proceed to completion, while in the presence of methanol it followed a reversible course in which the hydrolysis was opposed by an esterification process. The magnitude of the equilibrium constant decreased as the ionising power of the mixed solvent was decreased by addition of methanol. The isocomposition activation energies were found to be only poorly dependent on solvent composition. The role of electrostatic effects according to the different theories available was investigated. The thermodynamic activation terms were calculated and found to vary in a limited manner with composition of the binary mixed solvent.

INTRODUCTION

In view of the existing electrostatic theories of different interactions in solution, and based on a large crop of kinetic data, it was firmly established that medium changes represent the most efficient means for affecting rates and yields of many chemical reactions. Carboxylic esters in non-hydroxylic solvents are known to hydrolyse to completion, while in hydroxylic solvents a reverse reaction is initiated and an equilibrium is attained.[1] The present investigation is concerned with the influence of variation in solvent composition on the position and magnitude of this equilibrium. For this purpose, a kinetic study of the acid hydrolysis of benzyl acetate in binary mixtures of water and methanol at different temperatures was performed. The objective was to investigate the problem of correlating both rates and activation parameters with solvent composition, and to shed more light on the role of the dielectric constant of the medium in such an opposed reaction.

EXPERIMENTAL

Materials and Procedure

Benzyl acetate (Narden) was dried over anhydrous magnesium sulphate[2] then distilled twice. Methanol (Merck) was purified according to the method of Lund and Bjerrum.[3]

The kinetic experiments involved a direct analysis of the acid released during the reaction course.[4] The infinity (or equilibrium) values corresponding to complete (or maximum) reaction were independently obtained for each kinetic run by heating samples of the reaction mixture in sealed ampoules at 50°C for several days, then analysed until two concordant successive readings were obtained. The equilibrium values were found to decrease with increasing methanol content, as shown in Table 1.

---

* Present address : Department of Chemistry, Faculty of Science, University of Maiduguri, P.M.B. 1069 Maiduguri, Nigeria.

TABLE 1

Equilibrium values (mls of 0.0217 N NaOH equivalent to 4 ml aliquots of the reaction mixtures)

MeOH, wt %	0.00	12.19	24.93	43.06	63.19	74.27	86.84	92.92
V_e	8.91	8.61	8.14	7.73	7.43	7.23	6.92	6.62

RESULTS AND DISCUSSION

Kinetic data

The reaction was studied in the range 0 — 93 wt % water-methanol solvent mixture and at 25 — 50°C in steps of 5°C. A first-order kinetic law was followed by the reaction in all media studied. The plots shown in Fig. 1, based on an irreversible first order kinetic equation, gave straight line only in one case, namely, purely aqueous solution. However, in the presence of methanol as a cosolvent, departure from linearity was observ-

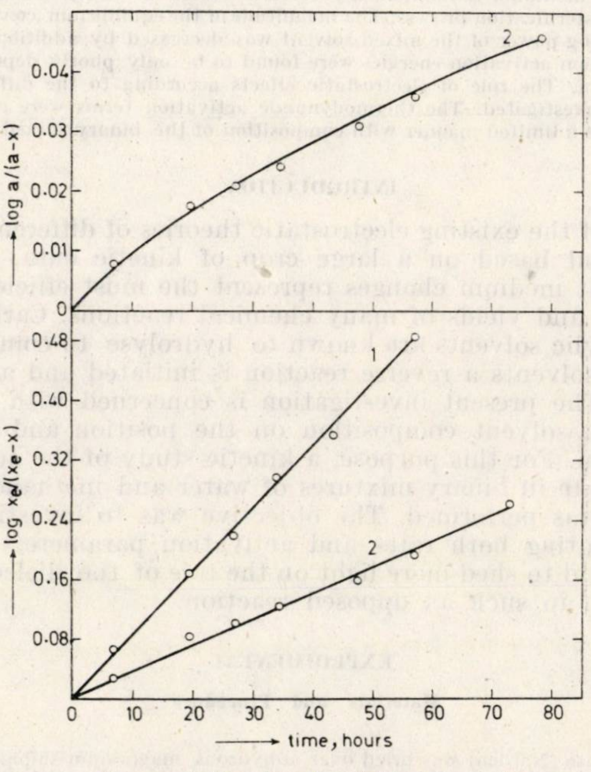

Fig. 1. — Representative kinetic plots of log $a/(a-x)$ and log $x_e/(x_e - x)$ for water (1) and 86.84 % (w/w) MeOH (2) at 30°C.

ed which increased as the amount of methanol was increased. On the other hand, the same plots based on the reversible first-order kinetic equation[1,5] gave good linearity throughout the whole range of solvent composition. This observation confirms that the forward hydrolysis reaction is opposed by a backward esterification one.[1] The rate constants for the forward and reverse reactions together with the equilibrium constants at different temperatures along the range of solvent composition are all set forth in Table 2. There is a possibility that in the presence of methanol, benzyl acetate undergoes an acid-catalysed ester-interchange reaction and thereby converting into methyl acetate. Such a reaction is, however, reported to be extremely slow[6,7] as compared to the hydrolysis reaction and thus can be neglected without any appreciable error. The forward isocomposition activation energies, E_{1c} and the corresponding E_{2C} values of the reverse reaction are almost independent of solvent composition (cf. Table 3), which indicates that in such a strongly hydrogen-bonded system solvation effects of the reactants relative to the transition complex do not change appreciably with change of solvent composition.[8-10] Similar experimental observations were reported previously for several hydrolysis reactions in different binary solvent systems including

TABLE 2

Rate constants ($k'.10^6 \text{min}^{-1}$) and equilibrium constant K for the acid hydrolysis of benzyl acetate in water-methanol mixtures. All measurements above 25°C were corrected for thermal expansion

t, °C	$k'.10^6$ min^{-1}	MeOH, wt %							
		0.00	12.19	24.93	43.06	63.19	74.27	86.84	92.94
25	k'_1	192	164	134	104	65	44	30	14
	k'_2	—	28	58	88	89	90	93	111
	K	—	5.76	2.33	1.18	0.73	0.49	0.32	0.13
30	k'_1	295	240	202	132	91	69	48	22
	k'_2	—	42	86	112	124	132	147	168
	K	—	5.77	2.34	1.18	0.73	0.52	0.33	0.13
35	k'_1	422	359	302	200	159	115	89	38
	k'_2	—	64	129	169	217	221	273	291
	K	—	5.65	2.33	1.18	0.73	0.52	0.33	0.13
40	k'_1	614	567	438	309	227	166	100	79
	k'_2	—	98	176	263	301	315	325	394
	K	—	6.02	2.49	1.18	0.75	0.53	0.31	0.20
45	k'_1	864	816	704	457	347	251	167	95
	k'_2	—	146	283	388	459	476	544	602
	K	—	5.58	2.49	1.18	0.76	0.53	0.31	0.16
50	k'_1	1408	1263	986	692	525	372	219	115
	k'_2	—	216	395	587	695	704	716	891
	K	—	5.84	2.49	1.18	0.76	0.53	0.31	0.12

TABLE 3

Isocomposition activation energies for the forward (E_1) and reverse (E_2) reactions

E, kcal/mole	MeOH, wt %							
	0.00	12.19	24.93	43.06	63.19	74.27	86.84	92.94
Forward, E_1	16.2	16.3	16.1	16.3	15.9	16.8	16.8	16.3
Reverse, E_2	—	16.5	16.5	16.5	16.1	16.4	16.1	16.5

alcohol—water mixtures.[1,11,15] The present activation energies depicted in Table 3 lie also within the range 14 — 20 kcal/mole assigned for esters hydrolysing via $A_{AC}2$ mechanism.[16]

Dependence of Rate on Water Concentration

The forward rate increases progressively with increase of the water concentration of the medium. The general rate expression will then be:

$$\frac{dx}{dt} = k[H_2O]^n(a - x)$$

in which the rate is assumed to be proportional to the nth power of the molar concentration of water, k is a proportionality constant and $(a - x)$ is the concentration of ester at any time. Since the concentration of water remains practically constant during the course of the reaction, $k[H_2O]^n$ will then be equal to the specific rate constant k_1' of the forward reaction

$$k_1' = k\ [H_2O]^n.$$

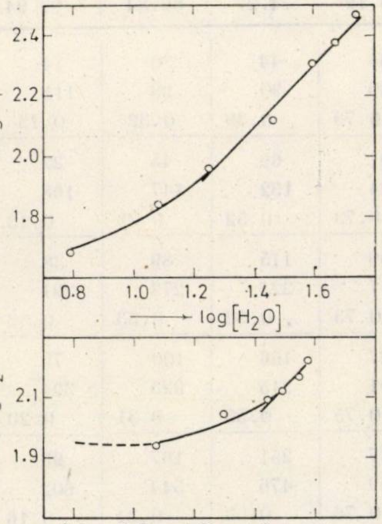

Fig. 2. — Dependence of the forward and reverse rate constants on water and methanol concentrations, respectively, at 30°C.

Hence, a plot of log k_1' against log $[H_2O]$ should be linear with a positive slope equal to n, the number of water molecules involved in the forward reaction. This plot is illustrated in Fig. 2. where straight line of unit slope was obtained in the range of high water content indicating that the forward reaction is first order with respect to water. On the other hand, the reverse reaction rate increases continuously with increase in the methanol concentration and it should be expected that a plot of log k_2' against log [MeOH] will also give a linear relationship with unit slope according to the expression:

$$k_2' = k[\mathrm{MeOH}]^n$$

Such a plot is given in Fig. 2 and the slope n was found to be 1 in the range of high methanol content, thus indicating that the reverse esterification is first order with respect to MeOH.

The Role of Electrostatic Effects

In many reactions the influence of solvents upon rates can be satisfactorily visualised in view of electrostatic effects expressing the rate constant as a function of the dielectric constant D of the solvent.[17–21]

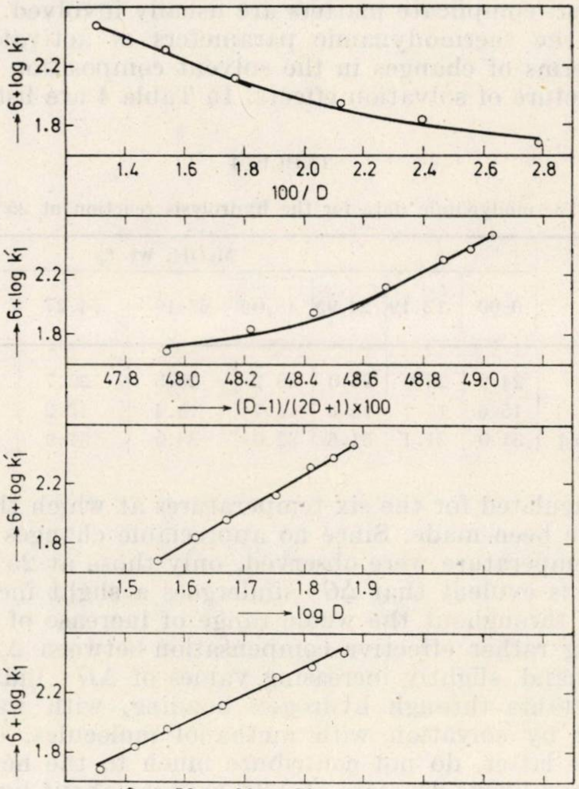

Fig. 3. — Variation of log k_1' at 30°C with the dielectric constant of the medium according to different electrostatic theories.

Fig. 3 illustrates the dependence of the forward reaction rate on the dielectric constant as formulated by the different electrostatic theories.[8,17,18,22–26] The data are seen to fit in best with the Laidler-Landskroener treatment based on an ion-dipole interaction. It should be borne in mind, however, that complications due to the reversibility of the reaction are expected to arise. In addition, one should not neglect the remarkable deviation of plots in Fig. 3, but they can well be interpreted as due to specific solvation effects [17] exhibited by the activated complex, being the more polar entity in solution, and described as short-range nonelectrostatic forces sensitive to steric bulk. [27]

Thermodynamic Data

Arnett and coworkers [28] stated that solvent effects when interpreted as functions of relative degrees of solvation of initial and activated states or of specific solvation effects giving special priority to water as an ion solvator, represents in many cases an oversimplification since other interactions that complicate matters are usually involved. However, consideration of the thermodynamic parameters of activation $\Delta G^{\neq}$, $\Delta H^{\neq}$ and $\Delta S^{\neq}$ in terms of changes in the solvent composition may provide a satisfactory picture of solvation effects. In Table 4 are listed these data, which were calculated for the six temperatures at which the kinetic measurements have been made. Since no appreciable changes in these parameters with temperature were observed, only those at 25°C are depicted in Table 4. It is evident that $\Delta G^{\neq}$ undergoes a slight increase of about 1.5 k cal/mole throughout the whole range of increase of methanol content, indicating rather effective compensation between $\Delta H^{\neq}$ and $T\Delta S^{\neq}$. On the other hand, slightly increasing values of $\Delta H^{\neq}$ indicate that solvation of reactants through hydrogen bonding, with water molecules. when replaced by solvation with methanol molecules, during gradual addition of the latter, do not contribute much to the net enthalpy of reaction. The non-linear decrease of $\Delta S^{\neq}$ brought about by the successive addition of methanol to the reaction medium is indicative of specific solvation effects [29] which result in an increase in the degree of order of the hydrogen bonded system thus causing the solvent molecules not to be randomly distributed. However, such small changes in $\Delta S^{\neq}$ reflect small changes also in the degree of solvation of the activated complex relative to the ground state as the solvent composition is changed. Much more entropy changes are known to occur for reactant molecules as a result of solvent molecules being "frozen" around the activated complex.

TABLE 4

Thermodynamic data for the hydrolysis reaction at 25°C

Parameter	MeOH, wt %							
	0.00	12.19	24.93	43.06	63.19	74.27	86.84	92.94
$\Delta G^{\neq}$, kcal/mole	24.9	25.0	25.0	25.2	25.5	25.7	25.9	26.4
$\Delta H^{\neq}$, kcal/mole	15.6	15.7	15.6	15.7	15.4	16.2	16.2	15.7
$-\Delta S^{\neq}$, cal/mole deg	31.0	31.1	31.6	32.0	34.0	31.9	32.8	35.8

REFERENCES

[1] L. Pekkarinen, *Ann. Acad. Sci. Fennicae, Ser. AII*, **1957**, 85.

[2] A. I. Vogel, "A Text Book of Practical Organic Chemistry Including Qualitative Organic Analysis", Third Edition, Longmans, Green, London, 1959, p. 783.

[3] H. Lund and J. Bjerrum, *Chem. Ber.*, **64B**, 210 (1931).

[4] Fayez Y. Khalil, H. Sadek and M. T. Hanna, *Monatsh.* **108**, 469 (1977).

[5] A. A. Frost and R. G. Pearson, "Kinetics and Mechanism", Second Edition, Wiley, New York, 1962.

[6] T. S. Rao and B. R. Gandhe, *Z. Naturforsch.*, **27a**, 1529 (1972).

[7] J. D. Roberts and M. C. Caserio. "Basic Principles of Organic Chemistry", W. A. Benjamin, Inc., New York, 1965, p. 532.

[8] S. Glasstone, K. J. Laidler and H. Eyring, "The Theory of Rate Processes", McGraw-Hill, New York, 1941.

[9] E. Tommila, A. Koivisto, J. P. Lyyra, K. Antell and S. Heimo, *Ann. Acad. Sci. Fennicae, Ser AII*, **1952**, 47.

[10] R. A. Ogg and O. K. Rice, *J. Chem., Phys.*, **5**, 140 (1937).

[11] H. S. Harned and A. M. Ross, Jr., *J. Amer. Chem. Soc.*, **63**, 1993 (1941).

[12] E. Tommila and A. Hella, *Ann Acad. Sci. Fenn. AII*, **1954**, 53.

[13] H. Sadek and F. Y. Khalil, *Suomen Kemistilehti, B*, **40**, 59 (1967).

[14] W. A. Waters, *J. Chem. Soc.*, **1936**, 1014.

[15] F. Y. Khalil and M. T. Hanna, *Z. Naturforsch.*, **33b**, 1479 (1978).

[16] K. R. Adam, I. Lauder and V. R. Stimson, *Austral. J. Chem.*, **15**, 467 (1962) and references cited therein.

[17] K. J. Laidler and H. Eyring, *Ann. New York Acad. Sci.*, **39**, 303 (1940).

[18] K. J. Laidler and C. A. Landskroener, *Trans. Faraday Soc.*, **52**, 200 (1956).

[19] E. A. Moelwyn-Hughes, "The Kinetics of Reactions in Solution", University Press, Oxford 1947.

[20] S. Kilpi and U. H. Puranen, *Z. phys. Chem. (Frankfurt)*, A **145**, 124 (1929).

[21] E. S. Amis and G. Jaffé, *J. Chem. Phys.*, **10**, 598 (1942).

[22] E. S. Amis, *J. Chem. Educ.*, **29**, 337 (1952).

[23] A. H. Fainberg and S. Winstein, *J. Amer. Chem. Soc.*, **78**, 2770 (1956).

[24] H. Böhme and W. Schurhoff, *Chem. Ber.*, **84**, 28 (1951).

[25] H. Böhme and H. J. Henning, *Z. Naturforsch.*, **1**, 850 (1946).

[26] E. Tommila, E. Paakkala, U. K. Virtanen, A. Erva, and S. Varila, *Ann. Acad. Sci. Fennicae, Ser. A II*, **1959**, 91.

[27] D. D. Roberts, *J. Org. Chem.*, **30**, 3516 (1965).

[28] E. M. Arnett, W. G. Bentrude, J. J. Burke and P. M. Duggleby, *J. Amer. Chem. Soc.*, **87**, 1541 (1965).

[29] R. F. Hudson and B. Saville, *J. Chem. Soc.*, **1955**, 4114.

REFERENCES

1 [illegible], Ann. [illegible], 1967, 83.
2 A. I. Vogel, "A Text Book of Practical Organic Chemistry Including Qualitative Organic Analysis", Third Edition, Longmans, Green, London, 1956, p. [illegible].
3 [illegible], Chem. Ber., [illegible] (1961).
4 [illegible], 108, 469 (1957).
5 A. A. Frost and R. G. Pearson, "Kinetics and Mechanism", Second Edition, Wiley, New York, 1961.
6 [illegible] (1965).
7 J. D. Roberts and M. C. Caserio, "Basic Principles of Organic Chemistry", W. A. Benjamin, Inc., New York, 1965, p. [illegible].
8 S. Glasstone, K. J. Laidler and H. Eyring, "The Theory of Rate Processes", McGraw-Hill, New York, 1941.
9 [illegible], 1962, [illegible].
10 [illegible] (1957).
11 [illegible], 63, [illegible] (1941).
12 [illegible], 1956, [illegible].
13 [illegible], B, 19, [illegible].
14 [illegible], 1958, [illegible].
15 [illegible] (1959).
16 [illegible], 15, [illegible] (1962) and references cited therein.
17 [illegible] (1950).
18 [illegible] (1959).
19 [illegible], University Press, Oxford, 1949.
20 [illegible], A, [illegible] (1930).
21 [illegible].
22 [illegible].
23 [illegible].
24 [illegible].
25 [illegible].
26 [illegible], 1959, [illegible].
27 D. D. Roberts, [illegible].
28 [illegible].
29 [illegible], 1958, [illegible].

Revue Roumaine de Chimie, 27, *3*, 365–380 (1982)

REACTANT – CATALYST INTERACTION PARAMETRISATION

N. DOCA *, F. KLEPP * and E. SEGAL**

* Chemical Research Center, Bd. Mihai Viteazul 24, Timişoara, Romania

** Chair of Physical Chemistry and Electrochemical Technology, National Institute of Chemistry, Bucharest, Romania

Received May 6, 1981

The surface species resulted from the interaction between a molecule and a catalytic surface is formalized as a graph. By attaching specific numerical values to the graph elements and introducing them into a matrix model, descriptive parameters (topologic and energetic) of the surface species were obtained. By these parameters a linear equation was generated, that models the catalytic answer of the system. The statistic quality and the descriptive ability of these equations were tested on three heterogeneously catalysed elimination reactions.

INTRODUCTION

Recent theoretical papers concerning reactant molecules — catalyst surface interactions, approach problems of interaction dynamics and surface states electronic structure by quantum-chemical proceedings. [1-13] The difficulties of "ab initio" calculations for more complicated molecule-catalysts ystems is not a real and significant impediment in understanding the interaction phenomenon. These difficulties constitute rather a disadvantage, that may be removed by adopting models that describe the total interaction as a sum of individual contributions. The descriptive ability will depend on the selected model (respectively the used mathematical formalism) and on the parameters used at the reactant and surface characterisation.

In the present paper, we intend to develop a mathematical formalism for a linear parametric model, that should describe the surface state (resulted from reactant-catalyst interaction) in a manner following the conception of Balandin, [14-16] of simultaneous energetic and geometric characterisation of molecules and catalyst surface. Our choice of a matrix representation is due to the results obtained by such models in solid state physics. [17-20] The model must include both catalyst and reactant parameters, and the characterisation must be made from an energetic, as well as from a topologic viewpoint.

THE SURFACE STATE PARAMETERS

Formally, the surface species is made up of the atom set A and the bond set L,

$$S = A \cup L \tag{1}$$

Set A includes two subsets, one arising from the reactant, A_R, and another from the catalyst surface, A_C,

$$A \supset A_R \cup A_C \tag{2}$$

Similarly

$$L \supset L_R \cup L_C \tag{3}$$

Equation (1) defines a graph having the following characteristics:

1. it contains only edges, as for the characterisation of bond $l_{ij} \in L$, it is of no consequence which of the two atoms $(a_i\ a_j) \in A$ is considered to be the initial peak;

2. it is spatial, except the simplest cases;

3. cases of isomorphism do not occur;

4. the graph vertices belong either exclusively to subset A_R or exclusively to subset A_C, i.e.

$$A_R \cap A_C = \Phi \tag{4}$$

5. in graph S, beside the initial bonds, belonging to the reactant and to the catalyst respectively, there appears the subset of the molecule-catalyst bonds, L_I, i.e.

$$L_I = L \cap (L_R \cup L_C) \tag{5}$$

As a rule, $\{a_i\} \subset A$, therefore A contains all the atoms (or ions) of the catalyst lattice and all reactant molecule atoms, indexed according to i. For the parametric description of the molecule and catalytic surface, it is not always necessary to take into account all these atoms. By the introduction of an optional variable v_i, so that $v_i = 1$ if the atom i is taken into account, and $v_i = 0$ in the opposite case, the parameter generating elements become:

$$\hat{a}_i = a_i \cdot v_i \tag{6}$$

In order to characterise numerically graph S, a form of the function f, must be found, so that

$$\forall\{\hat{a}_i \vee \hat{a}_j\} \Rightarrow \exists l_{ij}\, ;\ l_{ij} = f(\hat{a}_i, \hat{a}_j) \tag{7}$$

A simple form of f is defined by the product;

$$l_{ij} = \hat{a}_i \cdot \hat{a}_j \tag{8}$$

The numerical values of a_i vertices can be arbitrarily selected. In order to take into account the chemical specificity of the i atom, and considering that the hydrogen atoms bonded to it have no essential contribution to the structure definition, the following values were assigned to the graph peaks:

$$a_i = Z_i - \Sigma(H_i) \tag{9}$$

where Z_i represents the atomic number and $\Sigma\,(\mathrm{H}_i)$ the number of hydrogen atoms bonded on the i atom.

The topologic characterisation of the surface state can be carried out through $\Sigma\,(\mathrm{l}_{ij})$, but the obtained values are extended on a large space, making the correlation difficult. Therefore, another function is defined for description of the system topology, the connectivity

$$K_{ij} = (l_{ij})^{-1/2} = (\hat{a}_i \cdot \hat{a}_j)^{-1/2} \tag{10}$$

The energetic characterisation of each atom is carried out by ascribing a proper energy level. The surface lattice atoms are components of the solid state and the energy level distribution is given by the Fermi-Dirac statistics. The reactant molecule, bonded on the surface, keeps only its vibrational degrees of freedom, but the energy exchange with the catalytic surface is facilitated by the quantum carriers (excitons, phonons), with an energy distribution according to the Bose-Einstein statistics. Therefore, the proper energy level of the i atom will be defined according to the function

$$\varepsilon_i = \begin{cases} (\varepsilon_F)_i \text{ for } a_i \in A_C \\ (\varepsilon_B)_i \text{ for } a_i \in A_R \end{cases} \tag{11}$$

THE MATRIX MODEL

The common case

The most frequent surface states are the singlet (Σ) and the doublet (Δ). The L_I subset contains two bonds, formed between:

— two reactant atoms and one surface atom (Σ);

— two reactant atoms and two surface atoms (Δ).

In the common case, when one is interested only in the atoms and bonds directly involved in the reactant-catalyst interaction, the optional variable becomes:

$$v_i = \begin{cases} 1 \text{ for } a_i \subset l \in L_I \\ 0 \text{ for } \forall\, a_i,\ i = 1, 2, \ldots N \end{cases} \tag{12}$$

Diagrammatically, the situation is reproduced in figure 1.

The surface state model is set up by a square matrix, the elements of which

$$M = (b_{ij})_{(N\cdot N)};\ i, j = \overline{1, N} \tag{13}$$

are defined according to the function

$$b_{ij} = \begin{cases} \varepsilon_i & \text{for } i = j \\ k_{ij} & \text{for } i \neq j\,;\ i = \overline{1,\ N}\,;\ j = \overline{1,\ N} \end{cases} \tag{14}$$

but in the case of $N = 4$, $b_{13} = b_{31} = b_{24} = b_{42} = 0$. Obviously $k_{ij} \equiv k_{ji}$.

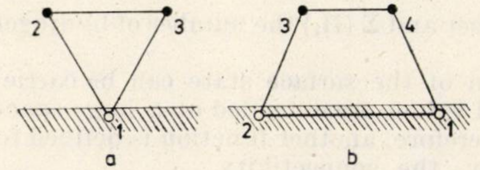

Fig. 1. — S_I graphs for the chemisorption on surface singlet (a), respectively doublet (b).

Therefore, according to equations (13) and (14),

$$M_\Sigma = \begin{pmatrix} \varepsilon_1 & K_{12} & K_{13} \\ K_{12} & \varepsilon_2 & K_{23} \\ K_{13} & K_{23} & \varepsilon_3 \end{pmatrix} \tag{15}$$

and

$$M_\Delta = \begin{pmatrix} \varepsilon_1 & K_{12} & 0 & K_{14} \\ K_{12} & \varepsilon_2 & K_{23} & 0 \\ 0 & K_{23} & \varepsilon_3 & K_{34} \\ K_{14} & 0 & K_{34} & \varepsilon_4 \end{pmatrix} \tag{16}$$

The following properties of these matrixes have to be noticed :

1. The matrixes are symmetrical, i.e.

$$M_{\Sigma,\Delta} = M^t_{\Sigma,\Delta} \tag{17}$$

(where M^t represents the transposed of matrix M), since the relation "atom i is bonded on atom j" is itself symmetrical.

2. The matrixes are not orthogonal. By direct computation it results that :

$$M_{\Sigma,\,\Delta} \times M^t_{\Sigma,\Delta} \neq I \tag{18}$$

3. The reverse of matrix M, denoted by M^{-1}, is a diagonal matrix. Because the products $K_{ij} \cdot K_{kl}$, with $i \neq k$ and $j \neq l$, have not a chemical significance, we considered them zero, so that :

$$M^{-1}_{\Sigma,\Delta} = \text{diag}\,(1/\varepsilon_i) \tag{19}$$

4. The traces of matrix M and M^{-1},

$$T_r(M) = \sum_i^N \varepsilon_i \tag{20}$$

respectively

$$T_r(M^{-1}) = \sum_{i}^{N} (1/\varepsilon_i) \tag{21}$$

represent functions of the sum of energy levels of the involved atoms being able to set up the energetic parameter of the surface species.

In order to obtain a topological parameter of the surface species, also as a matrix tracer, we multiplied the matrix $M_{\Sigma.\Delta}$ at left, with a matrix B obtained by a line or column permutation of the unit matrix I. Indeed, if $B = \text{Perm}_{(i,j)}\ I$, then

$$T_r(B \times M) = \Sigma K_{ij} \tag{22}$$

represents the connectivity of the surface species atoms, thus resulting a parameter similar to the Randić topologic index.[21]

The facility of small number correlations has determined us to select an energetic parameter defined according to equation (21). The homogeneous definition of the energetic and topologic parameters is possible by means of the following relationships

$$X_E = T_r(I \times M^{-1}) \tag{23}$$

respectively

$$X_K = T_r(\text{Perm}_{(i,\,j)}\, I \times M) \tag{24}$$

Model extension

If $v_i = 1$ also for the atoms neighbouring those directly involved in L_I, but $K_{ij} \neq 0$ only for the adjacent atoms, then one may write a (N, N) type matrix, similar to M_Σ and M_Δ. As an example, for the structure in figure 2, the (10, 10) type matrix is:

$$M_{STS} = \left(\begin{array}{ccc|ccc|cccc}
\varepsilon_1 & K_{12} & K_{13} & K_{14} & K_{15} & K_{16} & 0 & 0 & 0 & 0 \\
K_{12} & \varepsilon_2 & K_{23} & 0 & 0 & 0 & K_{27} & K_{28} & 0 & 0 \\
K_{13} & K_{23} & \varepsilon_3 & 0 & 0 & 0 & 0 & 0 & K_{39} & K_{310} \\
\hline
K_{14} & 0 & 0 & \varepsilon_4 & 0 & 0 & 0 & 0 & 0 & 0 \\
K_{15} & 0 & 0 & 0 & \varepsilon_5 & 0 & 0 & 0 & 0 & 0 \\
K_{16} & 0 & 0 & 0 & 0 & \varepsilon_6 & 0 & 0 & 0 & 0 \\
\hline
0 & K_{27} & 0 & 0 & 0 & 0 & \varepsilon_7 & 0 & 0 & 0 \\
0 & K_{28} & 0 & 0 & 0 & 0 & 0 & \varepsilon_8 & 0 & 0 \\
0 & 0 & K_{39} & 0 & 0 & 0 & 0 & 0 & \varepsilon_9 & 0 \\
0 & 0 & K_{310} & 0 & 0 & 0 & 0 & 0 & 0 & \varepsilon_{10}
\end{array}\right) \tag{25}$$

The surface state matrix M_{STS} may be divided into a table of matrixes:

$$M_{STS} = \begin{pmatrix} M_\Sigma & M^t_{KC} & M^t_{KR} \\ M_{KC} & M_{EC} & 0 \\ M_{KR} & 0 & M_{ER} \end{pmatrix} \tag{26}$$

where:

— the surface singlet matrix, M_Σ, is defined by equations (13) and (14), and detailed by (15);

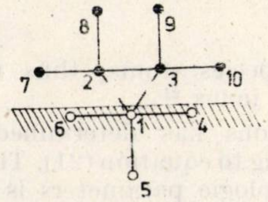

Fig. 2. — Representation of the extended surface state.

— the connectivity matrixes in the catalyst, and in the reactant molecule respectively, are given by:

$$M_{KC} = \begin{pmatrix} K_{14} & 0 & 0 \\ K_{15} & 0 & 0 \\ K_{16} & 0 & 0 \end{pmatrix} \text{ respectively } M_{KR} = \begin{pmatrix} 0 & K_{27} & 0 \\ 0 & K_{28} & 0 \\ 0 & 0 & K_{39} \\ 0 & 0 & K_{310} \end{pmatrix} \tag{27}$$

— the energetic matrixes of the catalyst and of the reactant respectively, defined by:

$$M_{EC} = \operatorname{diag}(\varepsilon_i), \quad a_i \in A_C, \text{ and } M_{ER} = \operatorname{diag}(\varepsilon_i), \quad a_i \in A_R \tag{28}$$

It turns out that:

$$\begin{aligned} M_{STS} = (M_{ij})_{(3,3)}, \text{ where: } \quad & M_{11} = M_\Sigma \\ & M_{21} = M_{KC} \\ & M_{31} = M_{KR} \\ & M_{12} = M^t_{21}\,; \; M_{13} = M^t_{31} \\ & M_{23} = M_{32} = \emptyset \\ & M_{22} = M_{EC} \\ & M_{33} = M_{ER} \end{aligned} \tag{29}$$

By means of matrix M_{STS} we defined the surface state parameters :

1. The energetic parameter, similar to equation (23), is defined by equation :

$$X_E = T_r(I \times M_{STS}^{-1}) \tag{30}$$

2. The topologic parameter. For the structure directly implied in L_I(see figure 1), the topologic parameter was defined by equation (24). For the rest of atoms $a_i \in (A_C \vee A_R)$ it may find a similar definition. Introducing the matrix :

$$J = (a_{ij})\,;\; a_{ij} = 1,\, i = \overline{1, n},\, j = \overline{1, n} \tag{31}$$

then

$$K_C = T_r(J \times M_{KC}) \text{ and } K_R = T_r(J \times M_{KR}), \tag{32}$$

and the connectivity of the entire surface species will be :

$$X_K = \sum_{i,j}^{N} K_{ij} = T_r(\text{Perm}\, I \times M_\Sigma) + T_r(J \times M_{KC}) + T_r(J \times M_{KR}) \tag{33}$$

The general case

When the surface state cannot be described (structurally, energetically, etc.) without some simplifying hypothesis, the generality of the model and parameter generating method become of major importance.

The component of the surface species atoms, taken into account as peaks of the S graph (equations 1, 2 and 3), are grouped in subsets according to the criterion of nearness to the structure directly implied in the interaction. We will distinguish peaks at the zero level :

$$a_i^0 \in S_I = A_I \cup L_I\,;\; A_I = A_{IC} \cup A_{I_R} \tag{34}$$

represented by atoms which take part directly in the singlet or doublet structure ; then, vertices of first level

$$(a_i^1)_C \in A_C^1 \text{ respectively } (a_i^1)_R \in A_R^1, \tag{35}$$

represented by atoms directly bound to the atoms from A_I vertices of the second level

$$(a_i^2)_C \in A_C^2,\; (a_i^2)_R \in A_R^2 \tag{36}$$

represented by atoms directly bound to A_C^1, respectively A_R^1, etc. The numbering of the $a_i \in S$ atoms is accomplished in a direction opposite to the trigonometrical direction, the order of the subsets being :

$$A_I,\; A_C^1,\; A_R^1,\; A_C^2,\; A_R^2, \text{ etc.} \tag{37}$$

An example of numbering is rendered in figure 3.

If the number of atoms (peaks) taken into discussion (for which $v_i = 1$) is N, one can get a square matrix similar to matrixes (15), (16) and (25), generally defined by equation:

$$M_{STS} = (b_{ij});\ b_{ij} = \begin{cases} \varepsilon_i \text{ for } i = j \\ K_{ij} \text{ for } i \neq j \text{ and } a_i \text{ adjacent to } a_j \\ 0 \text{ for any other } i \text{ and } j \end{cases} \tag{38}$$

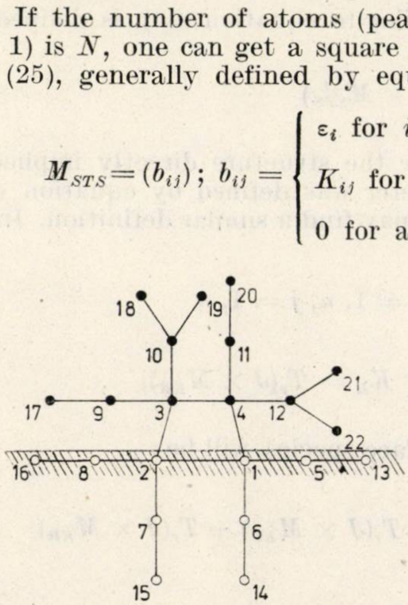

Fig. 3. — Numbering of the atoms in a general representation of the surface state.

Elements of the M_{STS} matrix may be grouped in some matrixes of inferior order:

— matrix of the interaction structure, M_I, defined according to equation (14), for $(a_i \vee a_j) \in A_I$;

— energy matrixes, defined on subsets A^1_U, A^1_R, etc. (generally annotated A_P or A_Q):

$$M_E(A_P) = \text{diag}\,(\varepsilon_i),\ a_i \in \forall\ A_P \neq A_I \tag{39}$$

— connectivity matrixes between the peaks of A_P and A_Q:

$$M_K(P,\ Q) = (b_{ij});\ b_{ij} = \begin{cases} K_{ij};\ a_i \in A_P;\ a_j \in A_Q \\ 0;\ a_i,\ a_j \text{ nonadjacent} \end{cases} \tag{40}$$

By means of M_I, M_E and M_K matrixes, a triangular inferior matrix may be defined.

$$M_\tau = (M_{ij}) = \begin{cases} M_I \text{ for } i = j = 1 \\ M_E(A_P) \text{ for } i = j = n \neq 1 \\ M_K(I,\ C_1) \text{ for } i = 2,\ j = 1 \\ M_K(I,\ R_1) \text{ for } i = 3,\ j = 1 \\ M_K(C_n,\ C_{n+1}) \text{ for } i = 2n,\ j = i - 2 \\ M_K(R_n,\ R_{n+1}) \text{ for } i = (2n+1),\ j = i - 2 \\ 0 \text{ for any other situation} \end{cases} \tag{41}$$

where $n = 1, 2, \ldots$, represents the level of the component peaks of the A_C or A_R subsets. Worth noting is that, starting from $n = 2$, connectivity matrixes are located on the second subdiagonal; on the lines with even indexes are those M_K that correspond to the atoms of the catalyst, while on the lines with uneven indexes are those corresponding to the atoms of the reactant molecule.

The transposed of the M_τ matrix will be a triangular superior square matrix, of the same n order. From direct computations, it turns out that:

$$M_{STS} = M_\tau + M_\tau^t \tag{42}$$

Since through equation (42) the general matrix model (equation 38) may be reproduced by means of matrixes M_I, M_E and M_K, the latter will be taken into account for the general definition of the parameters.

The optional variable from equation (12) will be generalized, in the sense that $V_n = 1$ if the n level of the A set is taken into account and $V_n = 0$ in the contrary case. The energetic parameter will then be:

$$X_E = T_r(I \times M_I^{-1}) + \sum_n T_r[V_n(I \times M_E^{-1}(n))], \tag{43}$$

while the topological one:

$$X_K = T_r\ (\mathrm{Perm}\ I \times M_I) + \sum_n T_r[V_n(J \times M_K(n))] \tag{44}$$

CATALYTIC ANSWER

In the following the column matrixes and the line matrixes that enter the analysis will be denoted by $\{\ \}$ and $\|\ \|$.

The parameters of the surface state (descriptor variables) define a column vector:

$$\{\mathbf{P}\} \equiv \begin{pmatrix} 1 \\ X_E \\ X_K \end{pmatrix} \tag{45}$$

where the first element generates the term which is independent of parameters.

The vector $\{\mathbf{P}\}$ may be associated with a susceptibility vector defined by the line matrix:

$$\|S\| \equiv (\alpha\ \ \beta_1\ \ \beta_2) \tag{46}$$

The catalytic answer of the system will then be:

$$\bar{Y} \equiv \|S\| \times \{\mathbf{P}\} = (\alpha + \beta_1 X_E + \beta_2 X_K) \tag{47}$$

that is a linear combination of the {**P**} vector elements. Obviously, these elements must be linearly independent.

Applications

The determination of the susceptibility values (coefficients α and β_i from linear model 47) was accomplished by the least squares method. The statistic quality of regressional equations was characterised by: r — correlation coefficient; s — standard deviation; F — Fisher statistics and EV — explained variance. In the following, some examples are presented:

1. *Dehydrogenation and dehydration of some alcohols*. The set of data is shown in table 1 and allows the testing of the significance of the reactant molecule topology.

TABLE 1

Experimental conditions and the corresponding Y figures

Reaction	Reactant	Y value	Reference
Alcohols dehydrogenation on equimol. $CaO-SiO_2$		Activation energy (kcal/mole)	[23]
	Ethanol	14	
	n-Propanol	19	
	n-Butanol	23	
	i-Propanol	17	
Alcohols dehydration on equimol. $CaO-SiO_2$		E_a(kcal/mole)	[23]
	Ethanol	35	
	n-Propanol	29	
	n-Butanol	26	
	i-Propanol	23	
	t-Butanol	33	
Alcohols dehydrogenation on Cu at 200°C		Activity (arbitrary units)	[24]
	Ethanol	5.50	
	n-Propanol	6.45	
	n-Butanol	7.45	
	i-Propanol	3.52	
	2-Butanol	7.10	

If:

$$v_i = 1 \text{ for } a_i \in A_R \tag{48}$$

then

$$X_K = \sum K_{ij} \equiv \sum (a_i a_j)^{-1/2} \tag{49}$$

and

$$\mathbf{P} = \begin{pmatrix} 1 \\ 0 \\ X_{\varkappa} \end{pmatrix} \qquad (50)$$

The topologic parameter according to equation (49) is identical with the connectivity index $\varkappa$. [21] The linear model becomes:

$$\log \hat{Y} = \alpha + \beta\varkappa \qquad (51)$$

where $\hat{Y}$ represents the estimation (according to the model) of the determined value Y. In table 2 are presented the connectivity index values for the discussed reactants, and in table 3, the regressional coefficients and the statistic quality of the equations.

TABLE 2

The Randić connectivity indexes for the molecules of some alcohols

Molecules	$\varkappa$ Value
Ethanol	1 0233
n-Propanol	1.5233
n-Butanol	2.0233
i-Propanol	1.4128
2-Butanol	1.8790
t-Butanol	1.7236

TABLE 3

The regressional coefficients and the statistic quality of equation (51)

Reaction	Reg. coeff.		Statistic quality			
	α	β	r	s	F	EV
$-H_2(CaO-SiO_2)$	0.93	0.22	0.991	0.012	26.2	0.972
$-H_2(Cu)$	3.52	1.93	0.995	0.417	38.2	0.983
$-H_2O(CuO-SiO_2)$	1.58	−0.08	0.380	0.069	0.168	−0.141

A dependence of the statistic quality on the type of the modelled catalytic reaction is noticed. Thus, for the dehydrogenation of alcohols both on the oxide and on the metal catalyst, the equation is satisfactory in relation with both r and F, attesting the importance of the reactant topology in the case of reactions involving surface doublets.

The lack of correlation in the case of alcohol dehydration confirms the low significance of the reactant topology when the reaction mechanism implies a single surface centre.

2. *Dehydrochlorination of some chloroethanes.* The set of data presented in table 4 allows a detailed analysis of the parameters generated by reactant and catalyst, respectively.

TABLE 4

The Y values (activity, in arbitrary units) for the dehydrochlorination of some chloroethanes on sulfates (ref. [25])

Reactant Catalyst	1, 1 dichloro-ethane	1, 2 dichloro-ethane	1, 1, 1, trichloro-ethane	1, 1, 2, trichloro-ethane	1, 1, 2, 2 tetrachloro-ethane
$NiSO_4$ on SiO_2	214	1.3	1910	48	2
$CuSO_4$ on SiO_2	198	0.5	2490	90	6.4
$Fe_2(SO_4)_3$ on SiO_2	237	2.7	2575	73	6.9
$CdSO_4$ on SiO_2	432	1.2	2870	45	3.5
Tl_2SO_4 on SiO_2	5.6	1.2	219	2.6	57
K_2SO_4 on SiO_2	9.3	7.5	139	7.9	100

In the vector of the descriptor variables, the variables may be grouped not only according to the numerically described property (see equation (45)), but also according to the described chemical species (reactant or catalyst). If the values that characterise numerically the property i of the reactant, j of the catalyst respectively, are denoted by R_i and C_j respectively, the vector of variables may be written :

$$\{\mathbf{P}\} = \begin{pmatrix} 1 \\ R_1 \\ \vdots \\ R_i \\ C_1 \\ \vdots \\ C_j \end{pmatrix} \tag{52}$$

and the linear model :

$$\log \hat{\mathbf{Y}} = \alpha + \sum_i \beta_i R_i + \sum_j \gamma_j C_j \tag{53}$$

The reactant topology may be described by :

$$R_1 = \varkappa \equiv (a_i a_j)^{-1/2}, \quad (a_i \vee a_j) \in A_R \tag{54}$$

It is very important for the discussed reaction to characterise the reactant under its entropic aspect as well, expressing the relative frequency of the favourable reactant-surface positions. Considering the inserted conformation as the most probable and projecting the spatial structure of the ethane molecule on a perpendicular plane on the $C - C$ axis, a rectangular (2, 3) matrix may be defined:

$$M = M_1 + M_2 \tag{55}$$

where the atoms bound on the first carbon define the matrix:

$$M_1 = \begin{pmatrix} 0 & a_{12} & 0 \\ a_{21} & 0 & a_{23} \end{pmatrix} \tag{56}$$

and the atoms bound on the second carbon define the matrix:

$$M_2 = \begin{pmatrix} b_{11} & 0 & b_{13} \\ 0 & b_{22} & 0 \end{pmatrix} \tag{57}$$

Thus

$$M = \begin{pmatrix} b_{11} & a_{12} & b_{13} \\ a_{21} & b_{22} & a_{23} \end{pmatrix} \tag{58}$$

If the elements a_{ij} and b_{ij} represent the chlorine atom, they are assigned the value 1 and if they represent the hydrogen atom they are given the value 0. The number of favourable cases of dehydrochlorination will be represented by the sum of oriented arcs for which the condition $(a_{ij} + b_{ij}) = 1$ is fulfilled, that is:

$$\Gamma_f = \sum \left[(a_{ij} + b_{ij}) = 1 \right] \tag{59}$$

The total number of atoms that may contact the surface is $\Gamma_t = 6$. If the entropic parameter is defined as relative frequency of favourable cases, then:

$$R_2 \equiv \Gamma = \Gamma_f / \Gamma_t \tag{60}$$

Table 5 presents the values ϰ and Γ for the discussed chloroethanes, and table 6 illustrates the regressional coefficients and the statistic quality of equation:

$$\log \hat{Y} = \alpha + \beta_1 \varkappa + \beta_2 \Gamma \tag{61}$$

It turns out that the reactivity of chloroethanes depends significantly on the parameters of the reactant molecule, among which the entropic parameter is outstanding.

For the topological characterisation of the catalyst surface, the constants of the elementary cell a_0, b_0 and c_0 are used (sulphates crystallise in the orthorhombic system). Due to the possibilities of a preferential interaction on different crystallographic planes, [22] the three diagonals d_1, d_2 and d_3 were also taken into account. Thus

TABLE 5

The values of $\varkappa$ and Γ parameters for some chloroethanes

Molecule	$\varkappa$	Γ
1, 1	1.0137	1.333
1, 2	1.0344	1.333
1, 1, 1	1.0667	2.000
1, 1, 2	1.1118	1.333
1, 1, 2, 2	1.2061	0.666

TABLE 6

The coefficients and the statistic quality characteristics of equation (61)

Catalyst	α	β_1	β_2	r	$r(\varkappa)$	$r(\Gamma)$	s	F	EV
$NiSO_4$	−5.52	3.33	2.58	0.796	−0.395	0.783	0.814	57.7	0.267
$CuSO_4$	−10.68	7.92	2.78	0.723	−0.169	0.646	0.985	36.5	0.045
$Fe_2(SO_4)_3$	−6.42	4.60	2.40	0.792	−0.317	0.759	0.728	56.0	0.254
$CdSO_4$	−5.30	3.32	2.53	0.745	−0.367	0.732	0.940	41.5	0.109
Tl_2SO_4	−13.55	11.45	1.63	0.738	0.398	0.218	0.640	39.8	0.088
K_2SO_4	−8.93	8.29	0.97	0.764	0.529	0.079	0.411	46.7	0.168

$$C_1 = \{a_0 \wedge b_0 \wedge c_0 \wedge d_1 \wedge d_2 \wedge d_3\} \tag{62}$$

In order to characterise the energetic aspects, the interaction between catalytic surface (metal ion → sulphate ion) and chlorine atom of the reactant is taken into account, for example in the form :

$$C_2 = 10^3/(\Delta H^0_{SO_4} - \Delta H^0_{Cl}) \tag{63}$$

Equations of the form :

$$\log \hat{Y} = \alpha + \gamma_1 C_1 \tag{64}$$

are completely unsignificant (see table 7).
Nevertheless, starting from the significant equation :

$$\log \hat{Y} = -0.373 + 1.377\,\Gamma \tag{65}$$

n	r	s	F	EV
30	0.535	0.940	4.41	0.255

and adding the parameter C_2, one obtains :

$$\log \hat{Y} = -1.236 + 2.072\ \Gamma - 0.020\ C_2 \qquad (66)$$

n	r	s	F	EV
30	0.724	0.853	5.89	0.470

TABLE 7

The regressional and correlational coefficients for equation (64)

Eq.no.	Parameter C_1	γ_1	$r(C_1)$
1	a^1_0	0.010	−0.047
2	b^1_0	−0.003	−0.180
3	c^1_0	0.005	−0.182
4	d^2_1	0.003	−0.159
5	d^2_2	−0.005	−0.186
6	d^2_3	0.002	−0.175

[1] According to ASTM No. 13—435 ; 15—775 ; 14—352 ; 7—188 ; 5—0613,

[2] Computed using the a_0, b_0, c_0 values.

The significance of parameters from equation (66) allows the following remarks :

1. log $\hat{Y}$ increases with Γ;

2. log $\hat{Y}$ decreases with the increase of $C_2 (C_2 < 0)$. If C_2 changes its sign, log $\hat{Y}$ decreases and the reaction is stopped when $C_2 \geqslant 0$ (there appear strongly chemisorbed surface species);

3. the reaction takes place on a single surface centre (topology of reactant and surface does not count), by the chlorine interaction with the surface cation.

CONCLUSIONS

1. A molecule bound on a catalytic surface represents formally a graph S. Beside the atoms and the bonds that existed initially and separately in the reactant molecule and in the catalyst, the catalytic interaction generates a subset of bonds L_I, between some atoms of the catalytic surface on the one side and of the reactant on the other side.

2. Graph S may acquire values specific to the peaks, thus resulting in a simple and realistic energetic and topologic characterisation.

3. Subgraph S_I derived from graph S is important and significant as it contains only the atoms directly implied in the interaction bond formation. Vertices of graph S_I are considered of zero level. Atoms that are adjacent to those from S_I are considered of first level, etc., resulting in a hierarchisation of subsets of molecule and catalyst atoms respectively.

4. The ordering of subsets A_p and the numbering of the included vertices allow the simple generation of the surface matrix. This matrix may be reconstructed by means of some matrixes of inferior order : interaction matrix, energetic matrixes and topologic matrixes.

5. The three categories of matrixes allow the simple definition of energetic and connectivity parameters, that constitute quantitative characteristics of graph S.

6. The analysis of the statistic quality of linear equations, generated by the descriptor variables, allow a realistic assessment of the influence of each parameter on the variation of experimental data.

REFERENCES

[1] A. G. Diebold and G. Wolken, *Surface Sci.*, **82**, 245 (1979).

[2] K. Binder, "Monte Carlo Methods in Statistic Physics", Springer, Berlin, 1979, p. 347.

[3] R. C. Kittler and K. H. Bennemann, *Solid State Commun.*, **32**, 403 (1979).

[4] H. F. Fink, K. Faulian and E. Bauer, *Phys. Rev. Lett.*, **44**, 1008 (1980).

[5] G. M. Sayers, *Surface Sci.*, **99**, 471 (1980).

[6] N. V. Richardson, *Surface Sci.*, **87**, 622 (1979).

[7] J. C. Tully, *J. Chem. Phys.*, **73**, 1975 (1980).

[8] E. Shustorovich and R. C. Baetzold, *J. Amer. Chem. Soc.*, **102**, 5989 (1980).

[9] A. C. Switendick, *Z. phys. Chem.* (Frankfurt), **117**, 89 (1979).

[10] H. Hjelmberg, *Surface Sci.*, **81**, 539 (1979).

[11] N. M. Popova and L. V. Babenkova, *React. Kinet. Catal. Lett.*, **11**, 187 (1979).

[12] L. B. Babenkova, N. M. Popova, and Yu. G. Kulevskaya, *React. Kinet. Catal. Lett.*, **11**, 325 (1979).

[13] B. Van Keulen, W. R. Wichers and V. Ponec, *React. Kinet. Catal. Lett.*, **12**, 125 (1979).

[14] A. A. Balandin, *Zhur. obshchei Khim.*, **17**, 793 (1946).

[15] A. A. Balandin, *Uspekhi Khim.*, **31**, 1265 (1962).

[16] A. A. Balandin, "Multipletnaia teoria kataliza", vol. I and II, Izd. MGU, Moskva, 1963—1964.

[17] J. A. Van Vechten, *Phys. Rev.*, **182**, 891 (1969) ; **187**, 1007 (1969).

[18] J. C. Phillips, *Rev. Mod. Phys.*, **42**, 317 (1970).

[19] V. A. Harrison, *Phys. Rev.*, *B*, **14**, 702 (1976).

[20] D. J. Newman, *Austral J. Phys.*, **31**, 489 (1978).

[21] M. Randić, *J. Amer. Chem. Soc.*, **97**, 6609 (1975).

[22] T. H. Rhodin, Jr., *J. Amer. Chem. Soc.*, **72**, 4343 ; 5691 (1950).

[23] H. Niiyama and E. Echigoya, *Bull. Chem. Soc. Japan*, **44**, 1739 (1971).

[24] N. Doca, unpublished data.

[25] I. Mochida, Y. Anju, H. Yamamoto, A. Kato and T. Seiyama, *Bull. Chem. Soc. Japan*, **44**, 3305 (1971).

Revue Roumaine de Chimie, **27**, *3*, 381–384 (1982)

LES PROPRIÉTÉS CATALYTIQUES DU CHROMITE DE FER ACTIVÉ PAR LES OXYDES ALCALINS

F. DOMKA, W. ZMIERCZAK et J. MICIUKIEWICZ
Laboratoire de Cinétique et de Catalyse, Institut de Chimie UAM 60–780 Poznań, Pologne

Reçu le 13 septembre 1980

On a étudié l'influence des oxydes alcalins (jusqu'a 5% en poids) sur les propriétés catalytiques du chromite de fer dans la réaction de conversion de CO par la vapeur d'eau. On a constaté que le promoteur de l'oxyde alcalin (surtout K_2O) influence l'accroissement de l'activité catalytique du chromite de fer.

Catalytic activity of iron chromite doped with alkaline oxides (up to 5 mol. %) for water gas shift reaction was studied. It was established that the presence of alkaline oxides (especially of K_2O) causes the rise in catalytic activity of iron chromite.

INTRODUCTION

Dans plusieurs réactions d'oxydation [1,5] et dans les processus où l'hydrogène participe [6–9] les chromites présentent une assez grande activité catalytique. Dans des conditions de la réaction catalytique la formation de la phase chromitique est souvent en relation avec une grande activité de catalyseurs ferro-chromiques. [10] Ces propriétés spécifiques du chromite de fer dépendent de sa synthèse, de sa formation et des promoteurs utilisés. En prenant en considération ces aspects nous avons étudié l'influence des oxydes alcalins sur les propriétés physiques et catalytiques du chromite de fer.

PARTIE EXPÉRIMENTALE

Le chromite de fer a été obtenu par l'activation des hydroxydes de chrome et de fer (II) coprécipités à 60°. Le précipité a été séché à 40° pendant 72 heures. Après, il a été broyé dans un mortier d'agate et ensuite on l'a fait passer au tamis (le diamètre de la maille = 0,102 mm). A la fin, le précipité a été imprégné par une solution de carbonate alcalin ayant le concentration comprise entre 0,2 et 5% de Me_2O. Après l'imprégnation les préparations ont été à nouveau séchées à 40°C pendant 72 heures), broyées dans un mortier et à la fin on les a fait passer au tamis. Le processus de la synthèse du chromite de fer se passait dans un four tubulaire à 600° pendant 5 heures en atmosphère d'hydrogène.[11] Le degré de réaction et la quantité des oxydes de fer et de chrome qui n'ont pas réagi ont été déterminés par la méthode de dissolution sélective dans une solution de HCl 5%.

La surface spécifique a été déterminée par la méthode de désorption thermique d'argon (par chromatographie). [12]

L'activité catalytique a été exprimée par le taux de conversion de CO par la vapeur d'eau. L'étude a été faite par la méthode continue [10] dans l'appareillage illustré sur la figure 1. Les mesurages de l'activité des préparations ont été faits à 350°C, le débit des corps réagissants a été fixé a 3,5 dm^3/h, le rapport CO : $H_2O = 1 : 2,5$. Dans le réacteur on mettait chaque fois 0,5 g de catalyseur mélangé à des brins de verre (le diamètre compris entre 0,06 et 0,102 mm). Le temps de la réaction a été 3 heures. Pour l'évaluation de l'activité catalytique on a introduit l'indice de l'activité spécifique.

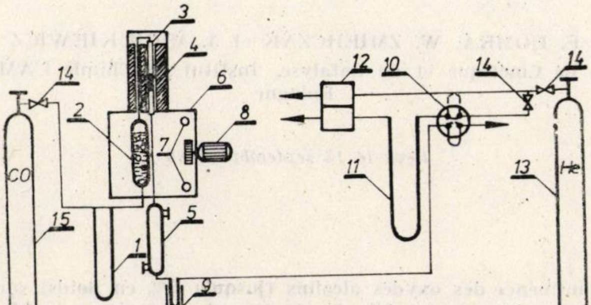

Fig. 1. — Schéma d'appareillage pour l'étude catalytique : *1*, débitmètre ; *2*, saturateur ; *3*, réacteur à catalyseur ; *4*, four ; *5*, refroidisseur ; *6*, thermostat ; *7*, élément chauffant ; *8*, ventilateur ; *9*, traiteur au froid ; *10*, soupape de dosage ; *11*, colonne chromatographique ; *12*, détecteur du chromatographe ; *13*, bouteille avec hélium ; *14*, robinet à aiguille ; *15*, bouteille avec CO.

RÉSULTATS EXPÉRIMENTAUX

Les hydroxydes alcalins introduits dans le chromite de fer modifient ses propriétés catalytiques et sa valeur de la surface spécifique. Dans certains cas on observe aussi les modifications de quantité (en %) de la phase spinelle. D'après les données du tableau 1 il apparaît que l'augmentation de la quantité du promoteur favorise l'accroissement de la surface spécifique. Dans le cas des composés contenant 5 % de l'oxyde alcalin cet accroissement de la surface spécifique semble dépendre du rayon ionique du promoteur. Ces modifications n'influencent pas toujours d'une façon univoque l'accroissement de l'activité catalytique. Le plus petit accroissement de cette activité est observé dans le cas des composés contenant le promoteur Li_2O et il est beaucoup plus grand (environ 6 fois) si les préparations contiennent 5 % de K_2O.

La plus grande valeur de l'activité spécifique a été obtenue en introduisant dans le chromite de fer 5 % de Li_2O ou de Na_2O ou bien 1 %

de K_2O, de Rb_2O ou de Cs_2O. Ces différentes valeurs de l'activité spécifique influencent le nombre de centres actifs présents à la surface accessible.

L'influence des oxydes alcalins sur les propriétés catalytiques du chromite de fer a été illustrée sur la figure 2. Il est intéressant de constater que la chromite de fer activé par les oxydes de potassium présente la plus grande activité. L'oxyde de lithium est le promoteur le moins effectif parmi les oxydes alcalins. Il faut noter également que le degré de changement des composés en chromite de fer diminue dans la limite de 10 % en présence de 5 % de l'oxyde alcalin. Le meilleur résultat est obtenu dans le cas de Li_2O (tableau 1).

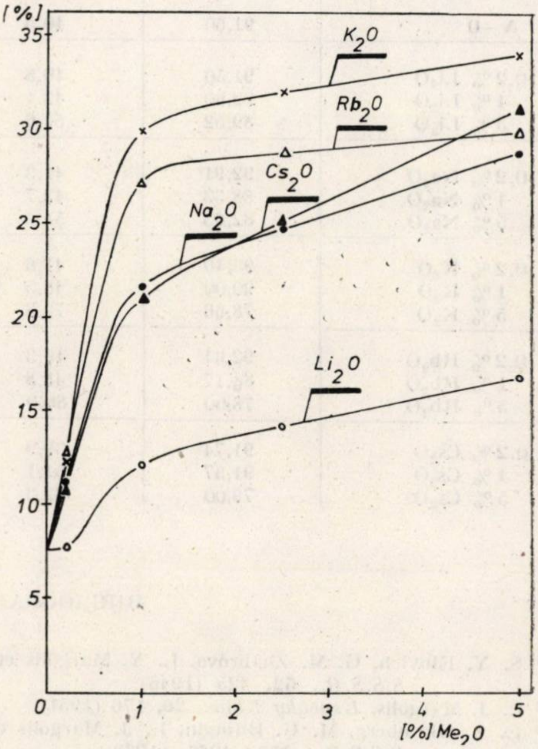

Fig. 2. — Influence des oxydes alcalins sur les propriétés catalytiques du chromite de fer.

L'influence des oxydes alcalins sur l'accroissement de la surface spécifique et sur l'activité catalytique est en relation avec l'échange ionique entre les groupes acides OH à la surface des composés et les cations du métal alcalin d'une part et d'autre part avec la teneur en oxydes de fer et de chrome qui n'ont pas réagi. D'après les données de l'analyse diffractométrique et chromatographique nous n'avons pas constaté la présence de nouvelles phases. Toutefois on ne peut pas exclure l'existence des combinaisons entre les oxydes .

TABLEAU 1

Certaines propriétés physiques et chimiques du chromite de fer activé par les oxydes alcalins

$FeCr_2O_4$ activé	Teneur de la phase $FeCrO_4$ (%)	Surface spécifique (m^2/g)	Taux de conversion dans la réaction $CO + H_2O$ (%)	Activité spécifique dans la réaction $CO + H_2O$ ($cm^3h^{-1}m^2$)
A–0	91,60	40,5	7,59	1312
0,2% Li_2O	91,50	40,8	7,61	1304
1% Li_2O	92,60	43,1	12,09	1961
5% Li_2O	89,52	51,6	16,76	2275
0,2% Na_2O	92,91	41,3	11,20	1900
1% Na_2O	88,33	43,7	21,56	3456
5% Na_2O	82,63	51,3	28,80	3931
0,2% K_2O	93,40	41,6	12,20	2051
1% K_2O	90,00	48,5	29,86	4306
5% K_2O	78,66	72,8	34,04	3270
0,2% Rb_2O	92,64	40,3	12,82	2227
1% Rb_2O	86,17	48,8	27,15	3890
5% Rb_2O	78,00	80,0	29,78	2604
0,2% Cs_2O	91,74	39,9	11,14	1953
1% Cs_2O	91,57	51,1	21,10	2889
5% Cs_2O	79,00	82,3	31,01	2636

BIBLIOGRAPHIE

[1] S. Y. Elovich, G. M. Zhabrova, L. Y. Margolis et S. Z. Roginskii, *Doklady Akad. Nauk S.S.S.R.*, **52**, 425 (1946).
[2] L. J. Margolis, *Uspekhy Khim.*, **20**, 176 (1951).
[3] E. A. Blumberg, M. G. Buługin, L. J. Margolis et N. M. Emanuel, *Doklady Akad. Nau S.S.S.R.*, **150**, 1066 (1963).
[4] B. Gillot, *Bull. Soc. Chim. France*, **6**, 2382 (1968).
[5] Yung-Fang Yu Yao, *J. Catalysis*, **39**, 104 (1975).
[6] W. M. Własenko, *Kataliz i Katalizatory*, **2**, 154 (1966).
[7] H. Adkins, E. Burgoyne et H. Schneider, *J. Amer. Chem. Soc.*, **72**, 2626 (1950).
[8] J. Stroupe, *J. Amer. Chem. Soc.*, **71**, 569 (1949).
[9] T. M. Yurieva, G. K. Boreskov, W. W. Popovskii, W. A. Chigrina et L. S. Yegorova, *Kinetika i Kataliz*, **12**, 140 (1971).
[10] F. Domka, M. Łaniecki et Z. Ruszkowski, *Reac. Kinet. Catal. Letters*, **3**, 261 (1975).
[11] F. Domka et W. Zmierczak, "Some Aspects of Physical Inorganic Chemistry", Proceeding of the First Regional Symposium, Polish Academy of Science, Poznań, 1976, p. 218.
[12] T. Paryjczak, « Les études d'adsorption et de catalyse par la chromatographie de gaz » PWN, Warszawa, 1975.

Revue Roumaine de Chimie, 27, 3, 385–391 (1982)

STUDY OF THE Fe(III)-3-HYDROXYPYRIDINE N-OXIDE SYSTEM

N. CALU, EUGENIA SAVIUC, TEODORA POPOVICI

Polytechnic Institute, Chair of Inorganic and Analytical Chemistry, Iași, Spl. Bahlui 71

Received June 12, 1980

The study performed on Fe(III)-3-hydroxypyridine N-oxide system emphasizes the stepwise formation of several complex species. The compositon, structure and stability of the complexes have been studied by potentiometric and spectrophotometricm ethods.

1. INTRODUCTION

Pyridine and its derivatives, such as 3-hydroxypyridine, pyridine N-oxide and 3-hydroxypyridine N-oxide are used as ligands. Their behaviour in this respect may be defined from the investigation of the UV and visible spectra, from the data of electrical dipole moments.

Sharpe and Walker [1,2] have studied the electric dipolemoments of pyridine and pyridine N-oxide. They have pointed out the great importance of hyperconjugation in the determination of the dipolemoment. The NO group of pyridine N-oxide is stabilized by resonance to the cycle. Pyridine N-oxide has a stronger mesomeric effect than pyridine and benzene for the electron-releasing substituents and a lower one for electron-attracting ones.

Grandberger, Faizova and Kost [3] made a comparative study of basicity and electronegativity in the series of substituted pyridines. They have established that 3-hydroxypyridine has mesomeric effects. The other hydroxypyridines, namely 2- and 4-hydroxypyridines, exhibit tautomers.

Lezina and co-workers [4] have investigated the structure of some hydroxypyridines by means of ^{1}H-NMR, and Seibold, Wagniere and Labhart [5] have interpreted the UV absorption bands of pyridine N-oxide (in electric field) as belonging to $\pi-\pi^*$ transitions.

The present work records a study of the Fe(III)-3-hydroxypyridine N-oxyde system which emphasized the stepwise formation of several complexes. The composition, structure and stability of these complexes have been studied by the potentiometric and spectrophotometric methods. The experimental data obtained by this system are a continuation of our previous investigations. [6]

2. EXPERIMENTAL

2.1. Apparatus and method

Spectrophotometric determination in the UV and visible range were performed with a Specord UV—VIS Carl Zeiss Jena spectrophotometer. Quartz cell 0.5 cm in length was used for measurements ; pH determinations were performed with a Radelkis — Budapest pH-meter.

2.2. Reagents

a. Ferric chloride "pro analysi" was used in aqueous solution, with concentrations between 4.10^{-3} and 2.10^{-2} M.

b. 3-Hydroxypyridine N-oxide "pro analysi" was used in aqueous solution, with concentrations of 1.10^{-1} and 2.10^{-5} M.

c. 3-Hydroxypyridine "pro analysi" was used in aqueous solution, with concentrations of 1.10^{-1} and 2.10^{-5} M.

d. Sodium hydroxide and hydrochloric acid were used in solution of 0.1 M and 2M respectively.

3. RESULTS AND DISCUSSION

3.1. Behaviour of 3-hydroxypyridine and 3-hydroxypyridine N-oxide in aqueous solution

The behaviour of 3-hydroxypyridine N-oxide (I) in solution was studied in comparison with 3-hydroxypyridine (II).

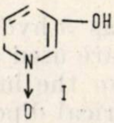

I

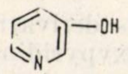

II

As a result of the molecular structure, 3-hydroxypyridine N-oxide is more acidic than 3-hydroxypyridine. This conclusion is corroborated by pH determinations. Thus, 3-hydroxypyridine N-oxide (0.1 M) has a pH of 2.97, while hydroxypyridine (0.1 M) has a pH of 6.84.

3-Hydroxypyridine has a basic centre at the nitrogen atom through which it forms complex compounds with Fe (III), possibly with a cyclic structure.

3-Hydroxypyridine N-oxide has a basic centre at the oxygen of the NO group, through which it forms a covalent-coordinative bond with Fe(III). A second (normal) bond of this ligand with Fe (III) is possible by substitution of the proton of the OH group. But this tendency of the ligand towards the second bond may be compensated by the instability resulting from the increase in the number of atoms in the cycle. The possibility to achieve this second bond has to be accepted since other structures than the cyclic ones can be achieved as well.

3.1.1. *Data on the acid-basic character of the two ligands*

The behaviour of 3-hydroxypyridine N-oxide when acids and bases are added, is shown in figures 1 and 2 by comparison with 3-hydroxypyridine.

Fig. 1. — pH-metric titration of 3-hydroxypyridine : N-oxide with NaOH in comparison with 3-hydroxypyridine : *1* and 1′ -3 hydroxypyridine N-oxide of 1.10^{-1} M ; *2* and *2′*-3 hydroxypyridine of 1.10^{-1}M ; *1′* and *2′* — —ΔpH/ΔV variant.

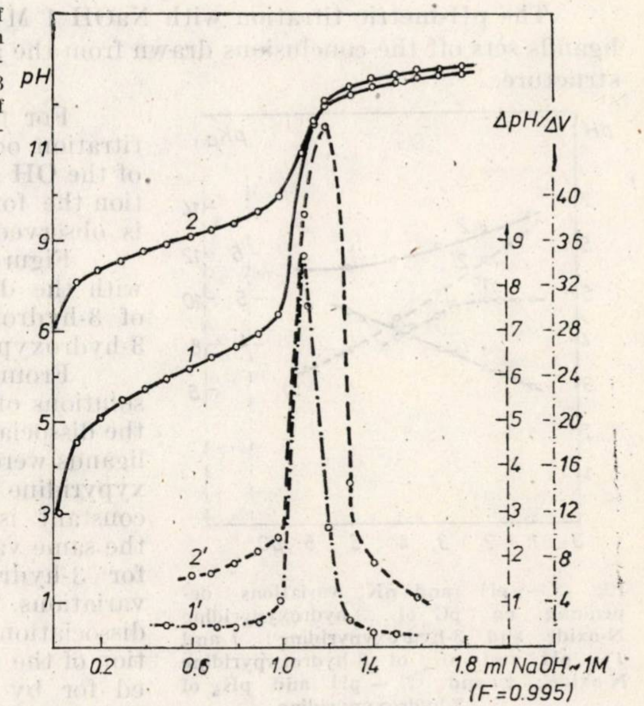

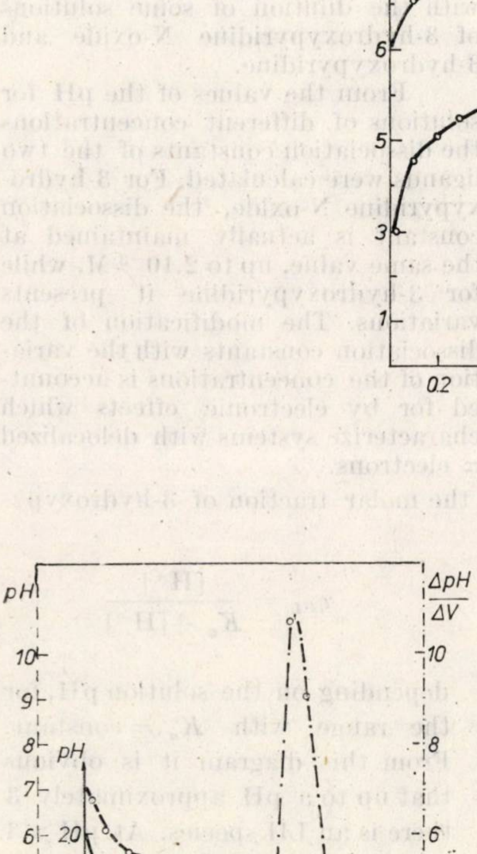

Fig. 2. — pH-metric titration of 3-hydroxypyridine N-oxide with HCl in comparison with 3-hydroxypyridine : *1* and *1′*-3-hydroxypyridine N-oxide of 3.10^{-1}M ; *2* and *2′*-3-hydroxypyridine of 3.10^{-1}M ; *1′* and *2′* — Δ pH/ΔV variant.

The pH-metric titration with NaOH 1 M and HCl 2 N of the two ligands sets off the conclusions drawn from the analysis of their electronic structure.

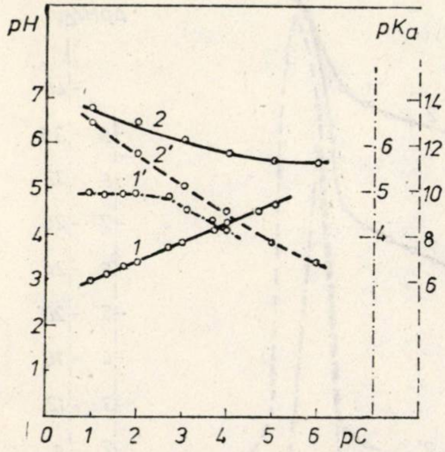

Fig. 3. — pH and pK_a variations depending on pC of 3-hydroxypyridine N-oxide and 3-hydroxypyridine : *1* and *1'* — pH and pK_a of 3-hydroxypyridine N-oxide ; *2* and *2'* — pH and pK_a of 3-hydroxypyridine.

For the two compounds, base titration occurs with neutralization of the OH group while for acid titration the formation of pyridinium ion is observed in 3-hydroxypyridine.

Figure 3 shows the pH variation with the dilution of some solutions of 3-hydroxypyridine N-oxide and 3-hydroxypyridine.

From the values of the pH for solutions of different concentrations the dissociation constants of the two ligands were calculated. For 3-hydroxypyridine N-oxide, the dissociation constant is actually maintained at the same value, up to 2.10^{-3} M, while for 3-hydroxypyridine it presents variations. The modification of the dissociation constants with the variation of the concentrations is accounted for by electronic effects which characterize systems with delocalized π electrons.

Figure 4 shows the variation of the molar fraction of 3-hydroxypyridine N-oxide :

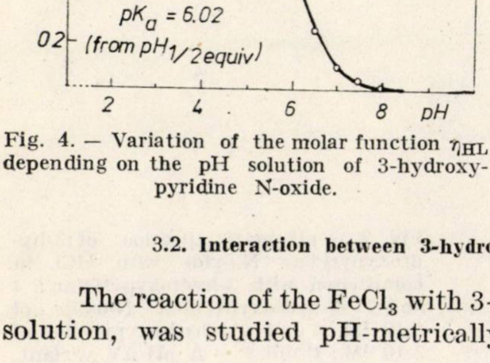

Fig. 4. — Variation of the molar function η_{HL} depending on the pH solution of 3-hydroxypyridine N-oxide.

$$\eta_{HL} = \frac{[H^+]}{K_a + [H^+]}$$

depending on the solution pH, for the range with K_a = constant. From this diagram it is obvious that up to a pH approximately 3 there is an LH species. At pH > 3 there begins the dissociation of the ligand L,

$$LH \rightleftharpoons L^- + H^+$$

3.2. Interaction between 3-hydroxypyridine N-oxide and $FeCl_3$

The reaction of the $FeCl_3$ with 3-hydroxypyridine N-oxide in aqueous solution, was studied pH-metrically and spectrophotometrically.

pH-metric determinations

The pH variation depending on the L/M ratio is shown in figure 5. When the reaction between 3-hydroxypyridine N-oxide (HL) and $FeCl_3$ proceeds with the substitution of the proton from OH group,

$$HL + FeCl_3 \rightleftharpoons LFeCl_2 + HCl$$

the solution pH should decrease since a strong acid-HCl results from it. Practically, the solution pH gradually rises with the addition of the ligand to the complex generator, which suggests that no HCl is produced in system and the M—L bond is not achieved by the OH group. Determinations were performed for pH < 3. For higher pH, the reaction was no longer followed as $Fe(OH)_3$ precipitates. The M—L interaction is probably achieved coordinatively by the oxygen of the NO group.

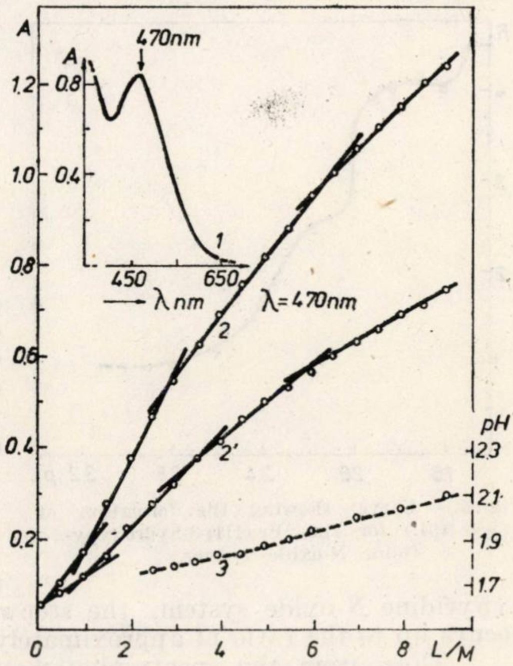

Fig. 5. — Data concerning Fe(III)-3-hydroxypyridine N-oxide : *1*—absorption band of the complex at the ratio [Fe(III) : 3-hydroxypyridine N-oxide] ; *2* and *2'* — graphic representation of A = f(L/M) for establishing the composition of complexes in the mentioned sytem ; A = absorbance ; M = Fe(III) ; L = 3-hydroxypyridine N-oxide ; $C_{Fe(III)} = 7.52 \cdot 10^{-3}$ M (*2*) ; $C_{Fe(III)} = 5 \cdot 10^{-3}$ M (*2'*) ; λ = 470 nm ; *3* — pH = f(L/M).

Spectrophotometric determinations

The complexes formed in the Fe(III)-3-hydroxypyridine N-oxide system have a characteristic absorption band at $\lambda_{max} = 470$ nm with $\varepsilon_{max} = 6.37 \times 10^2$ l/moles. cm. This band is accounted for by a charge transfer L → M.

The determination of the composition of complex combinations was performed by the molar ratios [7] and Bjerrum methods. [8] From the molar ratios method,

$$A = f(L/M),$$

results the formation of complexes with L/M ratios of 1:1, 1 : 3 and possibly 1 : 6 (Fig. 5).

According to the Bjerrum method, in the variant of corresponding solutions, [8] the average number of ligands $\bar{n}$ and the concentration of the ligand at equilibrium [L], were calculated by the relations

$$[\mathrm{L}] = \frac{C'_\mathrm{M} C''_\mathrm{L} - C''_\mathrm{M} C'_\mathrm{L}}{C'_\mathrm{M} - C''_\mathrm{M}};$$

$$\bar{n} = \frac{C'_\mathrm{L} - C''_\mathrm{L}}{C'_\mathrm{M} - C''_\mathrm{M}}$$

where :

C'_L and C''_L = total concentrations of the ligand ;

C'_M and C''_M = total concentrations of the complex generator.

With these data was plotted (Fig. 6),

$$\bar{n} = f(\mathrm{pL})$$

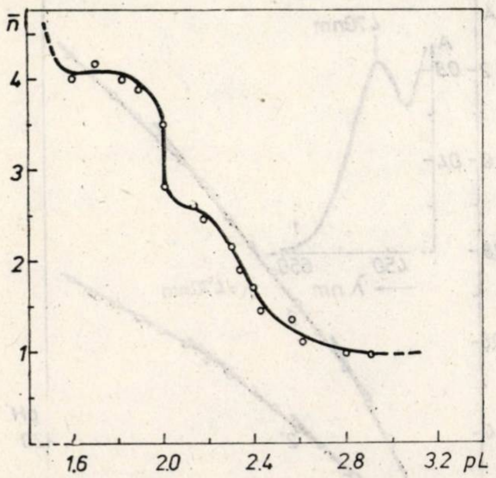

Fig. 6. — Curve showing the formation of $\bar{n}$= f(pL) for the Fe(III)-3-hydroxypyridine N-oxide system.

The Bjerrum method revealed that in the Fe(III) - 3-hydroxypyridine N-oxide system, the stepwise formation of the complexes occurs up to the ratio of approximately 1 : 4.

Thus, from the spectrophotometric measurements it results that Fe(III) ions form, in a stepwise manner, some complex species with 3-hydroxypyridine N-oxide (HOC_5H_4NO), namely $[Fe(HOC_5H_4NO)_n]^{3+}$, where $n_{\max}$ is 6.

3.3. Stability of the complex combinations $[Fe(HOC_5H_4NO)_n]^{3+}$

The global constant of formation of complexes in the Fe(III)-3-hydroxypiridine N-oxide system, in excess of ligand, was determined by the Edmonds-Birnbaum method. [9] The calculation of this constant was made on the basis of the relation

$$\mathrm{K} = \frac{C^n_{\mathrm{L}'} \cdot C^n_{\mathrm{L}''} (\mathrm{A}' - \mathrm{A}'')}{C^n_{\mathrm{L}'} \cdot \mathrm{A}'' - C^n_{\mathrm{L}''} \cdot \mathrm{A}'}$$

where :

$C_{L'}$ and $C_{L''}$ = concentrations of the ligand from the samples ; A′ and A″ = the absorbances of the corresponding solutions ; $n = 6$ the maximum coordonation number of the complex admitted for a great excess of the ligand ; K = dissociation constant.

Hence,

$$\beta_6 = \frac{1}{\mathrm{K}}$$

The value $\beta_6 = 8.28 \times 10^5 l^6 \text{mol}^{-6}$, practically determined, points out that these complexes are of medium stability.

CONCLUSIONS

The spectrophotometric and pH-metric study of the Fe(III)-3-hydroxypyridine N-oxide system leads to several conclusions concerning the formation and stability of the corresponding complexes.

— The spectrophotometric determinations revealed the stepwise formation of complexes, namely $[\text{Fe}(\text{HOC}_5\text{H}_4\text{NO})_n]^{3+}$ where n_{max} is **6.**

— The parameters calculated on the basis of these determinations are $K_a \simeq 1.30 \cdot 10^{-5}$ for 3-hydroxypyridine N-oxide and $\beta_6 = 8.28 . 10^5 . 1^6$ mol^{-6}, the global constant of stability of the complexes in the Fe(III)-3-hydroxypyridine N-oxide system.

— The value of the global constant of stability points out that in the Fe(III)-3-hydroxypyridine N-oxide system, complexes of medium stability are formed.

REFERENCES

[1] N. A. Sharpe and S. Walker, *J. Chem. Soc.*, **1961**, 2974.

[2] N. A. Sharpe and S. Walker, *J. Chem. Soc.*, **1961**, 4522.

[3] I. I. Grandberger, G. K. Faizova and A. N. Kost, *Khim. Geterosikl. Soedin.*, **4**, 561 (1966).

[4] V. P. Lezina, V. F. Bistrov, L. D. Smirnov and K. M. Dyumoev, *Teor. i Experim. Khim. A. N. Ukr. SSR*, **3**, 281 (1965).

[5] K. Seibold, G. Wagniere and H. Labhart, *Helv. Chim. Acta*, **52**, 789 (1969).

[6] N. Calu and A. Rang, *Rev. Roumaine Chim.*, (under print).

[7] G. Joe and A. Jones, *Ind. Eng. Chem. Analyt. Ed.*, **16**, 11 (1944).

[8] J. Bjerrum, *Kgl. Danske Videnskab. Selskab Mat-Phys. medd.*, **21**, 4, (1944); **22**, 18 (1946).

[9] S. E. Edmonds and N. Birnbaum, *J. Amer. Chem. Soc.*, **63**, 1471 (1941).

Revue Roumaine de Chimie, 27, *3*, 393—400 (1982)

THIOSEMICARBAZONES AS LIGANDS AND EVALUATION OF THEIR VIRUS INHIBITORY BEHAVIOUR. I

SOME TRANSITION METAL COMPLEXES OF SUBSTITUTED ISATIN β-THIOSEMICARBAZONES

RAGHUNATH P. GUPTA and ASHUTOSH K. SRIVASTAVA*
Department of Pharmaceutics, Institute of Technology, Banaras Hindu University, Varanasi — 221005, India

Received August 16, 1980

Complexes of 4-phenyl Isatin β-thiosemicarbazone; (*ortho*-methyl-4-phenyl) Isatin β-thiosemicarbazone; 4-phenyl, 5-chloro Isatin β-thiosemicarbazone; 4-phenyl, 6-chloro Isatin β-thiosemicarbazone; 4-phenyl, 5-methyl Isatin β-thiosemicarbazone and (*ortho*-methyl-4-phenyl), 5-methyl Isatin β-thiosemicarbazone have been isolated. The complexes are of the type $M[L_2]$ where M = cobalt (II), nickel (II) and copper (II), $M[(L)(H_2O)]$ where M = cobalt (II) and copper (II) and $M[(L_2)(H_2O)_2]$ where M = nickel (II). The compounds have been characterised by elemental analysis, IR, electronic spectral data and magnetic moments. All the bivalent metal ions form both 1 : 1 and 1 : 2 complexes. The IR spectra of the complexes indicate metal ligand bonding through sulphur, hydrazinic nitrogen and ketonic oxygen atoms of the ligands.

INTRODUCTION

A number of thiosemicarbazones are known to give stable complexes with transition metal ions.[1-4] Since Domagk et a l.'s original report [5] on the antitubercular activity of thiosemicarbazones, the number of works on the pharmacology of these compounds has been expanded. They have also been found to be active against influenza, protozoa, smallpox and certain kinds of tumour.[6-9] Their activity has frequently been thought to be due to their ability to chelate trace metals. Liebermeister [10] showed in his work that copper ion enhance the antitubercular activity of *para*-acetamidobenzaldehyde thiosemicarbazone.

Metal ions are known to have a considerable effect on many biological processes, and depending upon their concentration, may either contribute towards the health of the organism or cause toxicity.[11] This together with the fact that metal ions have been shown [12,13] to be associated with both DNA and RNA synthesis, has opened up new possibilities in the search for effective antiviral agents.

The recent reviews [14-15] dealing with metal complexes of thiosemicarbazides and thiosemicarbazones indicate that very little data are available on complexes of Isatin β-thiosemicarbazones and its derivatives.[16-18] As a part of our studies on chelation of substituted Isatin β-thiosemicarbazones vis-à-vis their virus inhibitory behaviour, we report here the synthesis and characterization of cobalt (II), nickel(II) and copper (II), complexes of 4-phenyl Isatin β-thiosemicarbazone (PITS) I ; (*ortho*-methyl 4-phenyl) Isatin β-thiosemicarbazone (OMPITS) II ; 4-phenyl, 5-chloro Isatin β-thiosemicarbazone (PCITS, III ; 4-phenyl; 6-chloro Isatin β-thiosemicarbazone (PC'ITS) IV ; 4-phenyl-5-methyl Isatin β-thiosemicarbazone (PMITS) V ; and (*ortho*-methyl-4-phenyl), 5-methyl Isatin β-thiosemicarbazone (OMPMITS) VI.

---

* To whom the correspondence should be addressed.

I ; X = X′ = H, R = H.
II ; X = X′ = H, R = CH$_3$.
III ; X = Cl, X′ = R = H.
IV ; X′ = Cl, X = R = H.

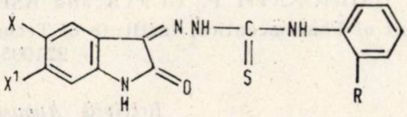

V ; X = R$_1$ = H, R = CH$_3$.
VI ; R = R$_1$ = CH$_3$, X = H.

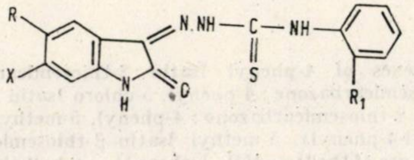

EXPERIMENTAL

Thiosemicarbazide (Merck), 4-phenyl thiosemicarbazide (Fluka) and Isatin (S. D. Chemical) were best purity products and were used as received. The ligands were synthesized by the methods given in the literature,[19] recrystallized and checked for purity by elemental analysis and melting point determination. Metal salts used were procured from E. Merck Chemicals limited, F. R. of Germany.

Preparation of Complexes. The complexes of cobalt (II) and nickel (II) were synthesized by the following general method. A solution of the ligand (0.02M) in ethanol was added to the metal chloride solution (0.01M) in ethanol. The coloured mixture so obtained was refluxed and concentrated to yield the precipitate of the complex. It was filtered then, washed successively with ethanol, ether and dried in vacuo.

The copper (II) complexes were obtained by refluxing mixture of the metal salt (0.01M) and the ligand (0.02M) solutions in ethanol on a water bath. The mixture was kept in a refrigerator overnight when dark brown crystals were obtained. The crystals were washed with ethanol and ether. Some of the copper (II) complexes were obtained by mixing cold solution of the metal chloride and the ligands.

All the complexes did not melt up to 200° and were found fairly soluble in common organic solvents e.g., dimethyl formamide and dimethyl sulphoxide.

Analysis. The metal and sulphur were determined by standard procedures.[20,21] Nitrogen analyses were carried out by Kjeldahl apparatus.[22] The microanalysis of carbon and hydrogen was obtained through the kind courtesy of microanalytical division, department of chemistry, B.H.U., Varanasi. The analytical data of the complexes are given in Table I.

Physicochemical studies. The magnetic susceptibility measurements were carried out using Gouy method and employing mercury tetracyanatocobaltate (II) as calibrant. The IR spectra were recorded in nujol on a Perkin Elmer 621. The electronic spectra were also recorded in nujol on a Cary model-14 spectrophotometer. Conductance was measured in M/1000 dimethyl formamide solution on Toshniwal conductivity bridge. Dimethyl formamide was dried over KOH and then distilled under reduced pressure.

TABLE 1

Analytical and magnetic data
(d = decomposed)

Compounds	M.P. °C	Colour	Found, %				Required, %				μ_m (mhos cm^{-1} $mole^{-1}$ in DMF	μ_{eff} (BM)
			Metal	Nitrogen	Sulphur	Water	Metal	Nitrogen	Sulphur	Water		
Co[(PITS-H)(H_2O)]	270^d	Dark pink	15.15	15.05	8.34	4.65	15.89	15.10	8.64	4.85	41	4.49
Co[(OMPITS-S)(H_2O)]	260	-do-	15.81	14.42	8.61	4.92	15.63	14.86	8.48	4.77	49	4.51
Co[(PCITS-H)(H_2O)]	307^d	light brown	19.40	18.11	10.71	5.98	19.25	18.29	10.47	5.88	45	4.52
Co[(PC'ITS-H)(H_2O)]	282^d	-do-	19.12	18.05	10.65	5.78	19.25	18.29	10.47	5.88	50	4.39
Co[(PMITS-H)$_2$]	285^d	-do-	8.92	8.12	4.54	—	8.71	8.28	4.74	—	25	4.61
Co[(OMPMITS-H)$_2$]	291^d	-do-	8.68	7.75	4.65	—	8.37	7.95	4.55	—	28	4.58
Ni[(PITS-H)$_2$]	300^d	Brown	9.28	8.49	4.76	—	9.08	8.66	4.96	—	15	3.51
Ni[(OMPITS-H)$_2$]	273^d	-do-	8.71	8.61	4.77	—	8.91	8.50	4.87	—	19	3.31
Ni[(PCITS-H)$_2$]	309^d	Violet green	11.55	10.69	6.11	—	11.35	10.83	6.20	—	29	3.05
Ni[(PC′ITS-H)$_2$]	260^d	-do-	11.25	10.73	6.30	—	11.35	10.83	6.20	—	24	3.29
Ni[(PMITS-H_2)(H_2O)$_2$]	275^d	Yellowish brown	8.51	8.17	4.52	5.21	8.46	8.07	4.62	5.19	34	2.99
Ni[(OMPMITS-H)$_2$(H_2O)$_2$]	283	-do-	8.31	7.64	4.31	4.83	8.13	7.76	4.44	4.98	39	3.20
Cu[(PITS−H)(H_2O)]	230	Dark brown	16.71	14.81	8.42	4.85	16.92	14.92	8.54	4.79	50	1.71
Cu[(OMPITS−H)(H_2O)]	203^d	-do-	16.81	14.79	8.49	4.65	16.65	14.68	8.40	4.72	49	1.69
Cu[(PCITS−H)(H_2O)]	305^d	Reddish brown	20.64	18.12	10.19	5.89	20.44	18.02	10.32	5.79	52	1.83
Cu[(PC′ITS−H)(H_2O)]	242^d	-do-	20.61	18.21	10.23	5.85	20.44	18.02	10.32	5.79	42	1.81
Cu[(PMITS−H)$_2$]	234	Light brown	9.49	8.17	4.62	—	9.33	8.22	4.71	—	31	1.73
Cu[(OMPMITS−H)$_2$]	254	-do-	8.81	7.79	4.41	—	8.96	7.90	4.52	—	28	1.74

RESULTS AND DISCUSSION

The conductance, magnetic, electronic and IR spectral data for the complexes discussed here indicate that (a) all the complexes are non-electrolyte in dimethyl formamide; (b) the ligand fields around cobalt complexes are tetrahedral, while the complexes of divalent nickel are octahedral in nature. The copper (II) complexes are square planar; and (c) the ligands (PITS, OMPITS, PCITS and PC'ITS) are tridentate, ketonic oxygen, hydrazinic nitrogen and sulphur atoms being involved in bonding with the metal ions. But in the case when PMITS and OMPMITS ligands behave as bidentate,[18] ketonic oxygen atom does not take part in the bonding. Complexes are probably polymeric in nature. Analysis reveals the metal to ligand ratio to be 1 : 2 and in few cases the ratio is 1 : 1 too.

Electronic spectra. The magnetic moment values of all the cobalt (II) complexes at room temperature have been found in the range of 4.39 – 4.61 BM, within the expected range of 4.2 – 4.8 BM for cobalt (II) ion in tetrahedral field.[23,24] The spectral results indicate tetrahedral geometry around cobalt (II) ion. The ν_2 and ν_3 bands correspond to the transitions $^4T_2 \rightarrow {}^4T_1(F)$ and $^4A_2 \rightarrow {}^4T_1(P)$ respectively, which are observed as a single frequency. High intensity bands (5460 –6550 cm^{-1}) and (14550 – 16560 cm^{-1}) are probably due to the mixing of metal "*d*" functions with ligand functions.[23] The observed bands for individual complexes are listed in Table 2.

The electronic spectra of all the divalent nickel complexes which show three absorption bands indicate octahedral geometry around nickel (II). These bands can be assigned to spin allowed *d*–*d* transitions, the first at (7576 – 9950 cm^{-1}) to $^3A_{2g}(F) \rightarrow {}^3T_{2g}(F)$, the second at (12738 – 17100 cm^{-1}) to $^3A_{2g}(F) \rightarrow {}^3T_{1g}(F)$ and the third at (23890 – 26000 cm^{-1}) to $^3A_{2g}(F) \rightarrow {}^3T_{1g}(P)$ transitions respectively. Few other bands are also observed but these are weak in intensity and are probably spin forbidden. The magnetic moment values of the nickel (II) complexes, 2.99 – 3.51 BM lie in the expected range of divalent nickel in octahedral field.[25]

No significant conclusion concerning the stereochemistry of copper(II) can be drawn from magnetic data. The copper (II) complexes under study have magnetic moment values in the range (1.69 – 1.83 BM). Of the three absorption bands observed in the electronic spectra of the complexes which correspond to square planar stereochemistry,[26] the first two at (17550 – 18970 cm^{-1}) and (15120 – 15640 cm^{-1}) have been assigned to transitions from $^2B_{1g}$ to ^2E_g and $^2A_{1g}$ respectively. The third absorption band (13000 – 13550 cm^{-1}) is probably the split component of the first transition. All the electronic spectral bands have been listed in Table 2.

Infrared spectra. Infrared spectra of the ligands as well as of their complexes with cobalt (II), nickel (II) and copper (II) have been recorded. Some of them are tabulated in Table 3, together with assignments for most of the major peaks. The assignments are based on the corresponding ones in thiosemicarbazide and thiocarbahydrazide[27] and the complexes derived from them.

TABLE 2

Electronic spectral data

Compounds	Observed bands (cm^{-1})	Assignments
Co[(PITS−H)(H_2O)]	5870	$^4A_2 \rightarrow {}^4T_1(F)$ (ν_2)
	15575	$^4A_2 \rightarrow {}^4T_1(P)$ (ν_3)
Co[(OMPITS−H)(H_2O)]	5950	$^4A_2 \rightarrow {}^4T_1(F)$ (ν_2)
	14550	$^4A_2 \rightarrow {}^4T_1(P)$ (ν_3)
Co[(PMITS−H)$_2$]	6050	$^4A_2 \rightarrow {}^4T_1(F)$ (ν_2)
	15725	$^4A_2 \rightarrow {}^4T_1(P)$ (ν_3)
Ni[(PITS−H)$_2$]	9850	$^3A_{2g}(F) \rightarrow {}^3T_{2g}(F)$
	13158	$\rightarrow {}^3T_{1g}(F)$
Ni[(PCITS−H)$_2$]	27040	$\rightarrow {}^3T_{1g}(P)$
	27050	
	9958	$^3A_{2g}(F) \rightarrow {}^3T_{2g}(F)$
	12738	$\rightarrow {}^3T_{1g}(F)$
	26135	$\rightarrow {}^3T_{1g}(P)$
Ni[(PC'ITS−H)$_2$]	8575	$^3A_{2g}(F) \rightarrow {}^3T_{2g}(F)$
	16738	$\rightarrow {}^3T_{1g}(F)$
	25156	$\rightarrow {}^3T_{1g}(P)$
Ni[(PMITS−H)$_2$]	7576	$^3A_{2g}(F) \rightarrow {}^3T_{2g}(F)$
	17100	$\rightarrow {}^3T_{1g}(F)$
	23890	$\rightarrow {}^3T_{1g}(P)$
Cu[(PITS−H)(H_2O)]	13510	$^2B_{1g} \rightarrow {}^2A_{1g}$
	15420	$\rightarrow {}^2E_g$
	18670	
Cu[(OMPITS−H)(H_2O)]	13345	$^2B_{1g} \rightarrow {}^2A_{1g}$
	15540	$\rightarrow {}^2E_g$
	17550	$\rightarrow {}^2E_g$
Cu[(PMITS−H)$_2$]	14490	$^2B_{1g} \rightarrow {}^2A_{1g}$
	15250	$\rightarrow {}^2E_g$
	18970	

PITS = $C_{15}H_{12}N_4OS$; OMPITS = $C_{16}H_{14}N_4OS$;
PCITS and PC'ITS = $C_{15}H_{11}N_4OSCl$; PMITS = $C_{16}H_{14}N_4OS$
OMPMITS = $C_{17}H_{16}N_4OS$

The absorption bands in the region 3300 − 3000 cm^{-1} in the free ligands and their complexes are assigned to the NH stretching frequencies.

The C=S stretching vibrations contributed to two bands at 1320 cm^{-1} and 750 cm^{-1} in the free ligand. But according to Randall et al. [28] the cyclic CS−NH−R groups give rise to absorption near 1550 cm^{-1}. However, other vibrations, particularly CN stretching also appear at these vibrations. The band at ~ 1320 cm^{-1} however, is much weakened on complex formation and is shifted to lower wave numbers. The νCN contribution in this region may thus be considered very small. The band at 750 cm^{-1} is not much lowered in intensity on complex formation perhaps due to the large contribution of νCN. However, the changes in the frequency and intensity of the observed C=S stretching vibrations may be taken as evidence [29] for sulphur coordination in all the complexes under investigation. The broad bands in the region ~ 3300 cm^{-1} − 3500 cm^{-1} and ~ 1600 cm^{-1} in the complexes are assigned to the OH group of water molecules. [30]

TABLE 3

Infrared spectral data and assignments

Ligand PC’ITS	$Cu[(L)(H_2O)]$	$Ni[(L)_2]$	$Co[(L)(H_2O)]$	Assignments
—	3305 (m)	—	3415 (s)	(OH) of H_2O
3100 (m)	3205 (b)	3190 (s)	3160 (s)	(NH)
1690 (s.sh)	1670 (m)	1675 (w)	1650 (w)	(C=O) stretching
1615 (m.sh)	1605 (m)	1622 (s)	1630 (s)	Amide I + NH bend
1550 (s.sh)	1530 (m)	1542 (w)	1528 (w)	NH bend and CN stretch (Amide II)
1510 (w)	1480 (w)	1495 (w)	1505 (s)	
1320 (s)	1310 (m)	1290 (w)	1295 (w)	CS stretch and
1270 (s)	1260 (m)	—	1265 (w)	CN stretch
1240 (s)	1225 (m)	—	1242 (m)	CN stretch and
—		—	1210 (m)	CS bend (Amide III)
1155 (s)	1170 (s)	1155 (m)	1165 (w)	NCS bend
1060 (m, sh)	1070 (m, sh)	1110 (m)	1050 (w)	
1030 (w, sh)	1028 (w)	—	—	
945 (w)	—	—	—	
850 (w, sh)	858 (w)	—	862 (w)	NN stretch
805 (w)	—	810 (w)	—	
750 (w, sh)	742 (w)	742 (w)	749 (w)	CS and CN stretch
700 (s, sh)	695 (w)	—	685 (m)	
640 (w, sh)	—	—	—	
—	3430 (sh)	—	3415 (w)	(OH) of H_2O
3205 (m)	3300(b)	3250 (s)	3275 (m)	(NH)
1740 (m.sh)	1700 (w)	1720 (m)	1710 (w)	(C=O) stretching
1680 (s.sh)	1660 (s)	1650 (m)	1675 (w)	
1615 (m.sh)	1600 (s)	1595 (m)	1590 (w)	Amide I + NH bend
1570 (m.sh)	1545 (m)	1550 (s)	1528 (w.sh)	NH bend and CN
1525 (m)	1890 (m)	1495 (s)	1480 (s)	stretch (Amide II)
—	1410 (s)	—	—	
1300 (s)	1290 (m)	1280 (w)	—	CS stretch and
1260 (w)	1255 (s)	—	1284 (w.sh)	CN stretch
1220 (w.b)	1230 (s)	1210 (w)	1190 (w.b)	CN stretch and CS
1200 (s)	—	—	1160 (s)	bend (Amide III)
1155 (s)	1170 (s)	1150 (m)	1155 (w)	NCS bend
1060 (m.sh)	1050 (s)	1045 (m)	1055 (w)	
1020 (w.b)	—	—	—	
940 (w.sh)	890 (s)	893 (m)	910 (s)	
850 (s)	868 (s)	—	858 (w)	NN stretch
805 (s.sh)	—	812 (m)	—	
750 (w.sh)	745 (s)	742 (m)	749 (s)	CS and CN stretch
710 (m.sh)	700 (m)	—	—	
680 (w)	670 (w)	—	675 (m)	

s.sh = strong sharp, w = weak, m = medium, b = broad.

The C = O stretching frequency has been observed at 1690 cm^{-1} in the free ligands. In the complexes it has been shifted to a lower wave number and lower intensity. It shows that oxygen has also taken part in coordination. But this shift has been observed in tridentate ligands and their complexes only. In bidentate ligands (PMITS and OMPMITS) it seems to be excluded.

The IR spectra thus suggest the coordination of the ligands to the metal through the thioketo sulphur and the hydrazinic nitrogen atoms; the ketonic oxygen (Isatin) is also involved in bond formation, thus making the ligand tridentate. The very low solubility of these complexes which have prevented us from determining the extinction coefficient, suggests a polymeric structure involving probably a bridging through bicovalent sulphur.

The metal ligand vibrations are difficult to assign on an empirical basis, since their frequencies are sensitive to both the metal and the ligand and often they compete with other low frequency modes in metal chelate compounds. A comparison between IR spectra of a free ligand and its metal complex fails to give a clear-cut assignment since some ligand vibrations activated by complex formation may appear in the same region as the metal ligand vibration. Of the several bands observed in the low energy IR region, some may be tentatively assigned to ν(M—S) and ν(M—N) vibrations.[31]

Virus inhibitory behaviour of the compound. The activity of antiviral drugs is dependent upon metal ion complexing. It is known that in some cases their efficiency is increased when co-ordinated. It may be that the metal complex is more liposoluble than the drug, and so the metal ions help to transport it across the cell membrane. Levy and Mrosczk [32] and Gupta et al.[33] have shown that the rate of transfer of several model drug compounds through an artificial lipoid barrier can be modified by complex formation. They have also reported complexes that are more lipid soluble than the drug itself, and penetrate the lipid barrier more rapidly than the uncomplexed drug.

The antiviral screening of the metal chelates and other physicochemical parameters, *viz.*, membrane permeability, charge distribution, shape and redox potentials are in progress with a view to allowing a better understanding of the mechanism of antiviral activity. The details will be reported in our next communication.

ACKNOWLEDGEMENT. The authors are grateful to university authorities for providing research facilities and financial assistance. Thanks are also due to Chemistry Department, B.H.U. for spectral measurements.

REFERENCES

[1] B. Beecroft, M. J. M. Compbell and R. Grzeskowiak, *Inorg. Nuclear Chem. Letters*, **8**, 1097 (1972).
[2] M. A. Malik and D. J. Phillips, *Austral. J. Chem.*, **28**, 305 (1975).
[3] A. V. Ablow and N. V. Gerbeler, *Zhur. neorg. Khim.*, **9**, 46 (1964).
[4] M. K. Akhmedli and L. F. Zhirova, *ibid.*, **5**, 2742 (1960).
[5] G. Domagk, R. Behmisch, F. Mietzsch and H. Schmidt, *Naturwiss*, **33**, 315 (1946).

[6] N. N. Orlova, V. A. Aksenova, D. A. Selidovkin, N. S. Bogdanova and G. N. Pershim, *Russ. Pharm. Toxic.*, 348 (1968).

[7] K. Butler, U. S. Patent No. 3, 382, 266 (1968).

[8] D. J. Baur, L. St. Vincet, C. H. Kempe and A. W. Downe, *Lancet*, **27**, 494 (1963).

[9] H. G. Petering, H. H. Buskirk and G. E. Underwood, *Cancer Res.*, **64**, 367(1967).

[10] K. Liebermeister, *Z. Naturforsch B*, **5**, 79 (1950).

[11] "Introduction to Bioinorganic Chemistry", Edited by D. R. Williams, Thomas, Illinois, 1976.

[12] J. P. Slater, A. S. Mildvan and L. A. Loeb, *Biochem. Biophys. Res. Comm.*, **44**, 37 (1971).

[13] M. C. Scrutton, C. W. Wu and D. A. Goldthwaik, *Proc. Nat. Acad. Sci., U.S.A.*, **68**, 7497. (1971).

[14] A. Ali and S. E. Livingstone, *Coord. Chem. Rev.*, **13**, 101 (1974).

[15] M. J. M. Campbell, *ibid.*, **15**, 279 (1975).

[16] I. Grecu and M. Neamţu, *Rev. Chim. miner.*, **6**, 625 (1969).

[17] Idem, *ibid.*, **5**, 813 (1968).

[18] P. Barz and P. H. Fritz, *Z. Naturforsch. B*, **25**, 199 (1970).

[19] A. A. Tsuskam, T. A. Chaban, *Fitokhim. Tzuch. Flory BSSR Biopharm. Issled. Leckprep.*, **144**, (1975).

[20] E. P. Treadwell and W. T. Hall, "Analytical Chemistry", Vol. II, Wiley, New York, 1958.

[21] A. I. Vogel, "A Text Book of Quantitative Inorganic Analysis", Longmans, London, 1969.

[22] A. I. Vogel, "Elementary Practical Organic Chemistry", part III, Longmans, London, 1969.

[23] A. B. P. Lever, "Inorganic Electronic Spectroscopy", Elsevier, Amsterdam, 1968, p. 254, 325, 337.

[24] S. F. A. Kettle, "Coordination Compounds", Thomas Nelson, London, 1969, p. 135.

[25] R. S. Nyholm, *Proc. Roy Soc.*, 273 (1961).

[26] B. N. Figgis, "Introduction to Ligand Fields", Interscience, New York, 1967 p. 223–27, 315.

[27] G. R. Burns, *Inorg. Chem.*, **7**, 227 (1968).

[28] H. M. Randall, R. G. Fowler, N. Fuson and R. Damyl, "Infrared Determination of Organic Structures", Van Nostrand, Reinhold, Princeton, New Jersey, 1949.

[29] A. Yamaguchi, R. B. Pendland, S. Mizushima, T. J. Lane, C. Curran and J. V. Quagliano, *J. Amer. Chem. Soc.*, **80**, 527 (1958).

[30] K. Nakamoto, "Infrared Spectra of Inorganic and Coordination Compounds" , Wiley, New York, 1963.

[31] A. B. P. Lever and E. Mantovani, *Inorg. Chem.*, **5**, 429 (1971).

[32] G. Levy and E. J. Mrosczk, *J. Pharm., Sci.*, **57**, 235 (1968).

[33] B. P. Gupta, B. N. Yadav, R. Gulati and A. K. Srivastava, *Acta Pharm. Jugoslavica*, **30**, 79 (1980).

Revue Roumaine de Chimie, 27, *3*, 401–410 (1982)

THE $AlPO_4$ AND RELATED SYSTEMS AS CATALYSTS IN ORGANIC REACTIONS. I

TERTBUTYLBENZENE CRACKING

P. M. DEYA, A. COSTA, J. V. SINISTERRA and J. M. MARINAS *
Department of Organic Chemistry of the Science Faculty of Palma de Mallorca, Spain
* Department of Organic Chemistry of the Science Faculty of Cordoba, Spain

Received May 6, 1980

In the present paper the tertbutylbenzene catalytic cracking on $AlPO_4$ and related systems is carried out. The process is studied by microcatalytic pulse technique. In the experimental conditions, the process may be described for all the catalysts tested by an equation of the $\ln (1/1 - X) = RTK_H\overrightarrow{k}W/F$ type. So, the catalytic cracking of this hydrocarbon on these catalysts may be described in our experimental conditions as a first-order catalytic reaction occurring in two steps. The first would be the exothermic adsorption of the aromatic ring on the active site. The second, the surface reaction, is the rate-controlling step according to the Habgood and Bassett postulate. The adsorption constants and the ΔH_{ads} are determined by a gas chromatographic method. The activation energy for the surface reaction is determined and it has been found to be the same for all the catalysts (30 – 33 kcal mole^{-1}). Thus it may be deduced that the surface process would be the same for all the catalysts tested by us.

I. INTRODUCTION

The catalytic cracking of monoalkylbenzenes on different $AlPO_4$ catalysts obtained in several media has been studied by the authors during the last several years. Improvement of this process [1] and the deactivation reaction [2,3] have been studied in previous papers.

The recent synthesis of several $AlPO_4$—SIO_2 systems has demonstrated that these substances are more active than $AlPO_4$ catalysts in the monoalkylbenzenes cracking reaction. [4]

In the present paper the process mechanism is studied in order to see whether the process may be the same for all the catalysts tested. The experiments were carried out by means of the microcatalytic pulse technique.

II. EXPERIMENTAL

II. 1. Materials

The synthesis procedure of the catalysts has been described in the literature (BD, PD and FD [5], F–72[6] and CF4 [7]). In every case the catalysts were calcined for 3 hours at 650 10°C at one atmosphere.

The catalysts that were used are listed in Table 1 together with their properties. The tertbutylbenzene used was a Merck analytical product.

TABLE 1

Catalysts

Symbol	Composition (% wt).	Surface area * (m^2/g)	ΣV^*_p (ml/g)	Surface acidity** (meq/g)
BD	100% $AlPO_4$	190	0.39	0.42
PD	100% $AlPO_4$	224	0.41	0.46
FD	100% $AlPO_4$	110	0.18	0.24
F−72	20%$AlPO_4$−80%SiO_2	357	0.55	0.19
CF4	75%$AlPO_4$−25%Al_2O_3	236	0.31	0.37

* Measured by the BET method with N_2.

** Measured by Johnson method using n-$BuNH_2$ as base and amine-p-dimethyl-azobenzene ($pK_a = +3.3$) as Hammett indicator.

II.2. Apparatus and procedure

The apparatus used in the study described here was a conventional pulse reactor, consisting of a gas chromatograph modified by the introduction of a small reactor between the sample inlet and the analytical column.

The gas chromatograph was a Hewlett-Packard 58 34 A model and the analytical column was 2 m. by 1/4″, packed with 5% polyphenylether on Chromosorb G AW−DMCS 80/100.

The catalytic reactor consisted of a stainless steel tube, 0.067 m. long and 1/4″ in diameter. The top section of the reactor was joined to another 0.067 m. stainless steel tube of 1/8″ diameter which functioned as a vaporizer and preheater.

Catalyst charges of 0.020 g. were used. They were stabilized by heating in a nitrogen atmosphere at 200°C for 12 hours. The temperature was measured with a NiCr−Ni DIN Thermocouple adjacent to the packed section of the reactor, connected to a Getrosist 96 Philips controller.

In order to maintain a low reactant pressure, the magnitude of the pulse used in the adsorption and the kinetics experiments was 0.5 μl.

Determination of the Henry adsorption constant (K_H) and the heat of adsorption was made by the gas chromatographic method described by Arita et al.[8] and recently modified by Atkinson and Curthoys.[9]

III. RESULTS AND DISCUSSION

Preliminary experiments were carried out to study the extension of the cracking of tertbutylbenzene at different temperatures with all of the catalysts. The results obtained are shown in Figure 1 for F−72, CF4 and BD catalysts. It was observed that the F−72 catalyst is the most active one. The activity order observed in this process is :

$$F - 72 > CF4 > BD > PD > FD$$

in agreement with their surface areas (see Table 1). This conclusion has also been reached working with integral reactors.[2,3]

The thermal cracking process begins to be noticed at 460°C. For this reason, temperatures never exceeded 460°C in order to avoid secondary reactions. In this way only one catalytic reaction was observed :

Tertbutylbenzene → Benzene + Isobutylene

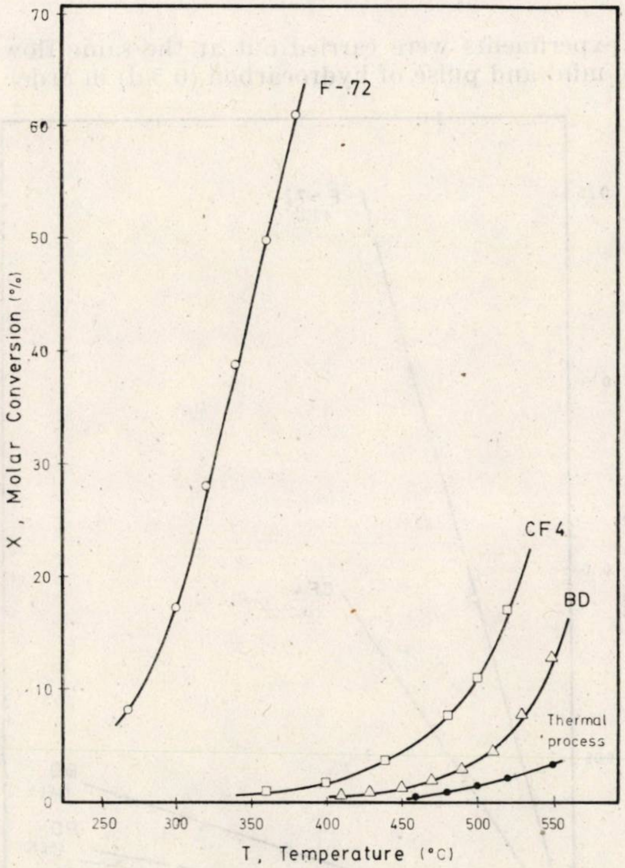

Fig. 1. — Effect of temperature on tertbutylbenzene conversion to benzene and isobutylene at $W = 50$ mg. of catalyst and pulse = 0.5 μl.

III.1. Kinetic experiments

The kinetic experiments were carried out by the gas chromatographic method. This technique only permits a simple quantitative study of first-order reactions. This is because the partial pressure of the reactant varies from point to point through the reactant pulse and it is only for first-order reactions that the fractional conversion of reactant to products is independent of pressure. In these cases equation (1) of Bassett and Habgood[10] may be used, according to the postulates of these authors. This equation describes the behaviour of a first-order catalytic reaction under gas chromatographic conditions if the partial pressure of the reactant is low and the adsorption process is rapid with respect to the rate of surface reaction. Results show good correlation to this equation (Fig. 2).

$$\ln \frac{1}{1 - X} = RTK_H\vec{k}W/F \qquad (1)$$

All the experiments were carried out at the same flow-rate of carrier gas (15 cc/min) and pulse of hydrocarbon (0.5μl) in order to maintain

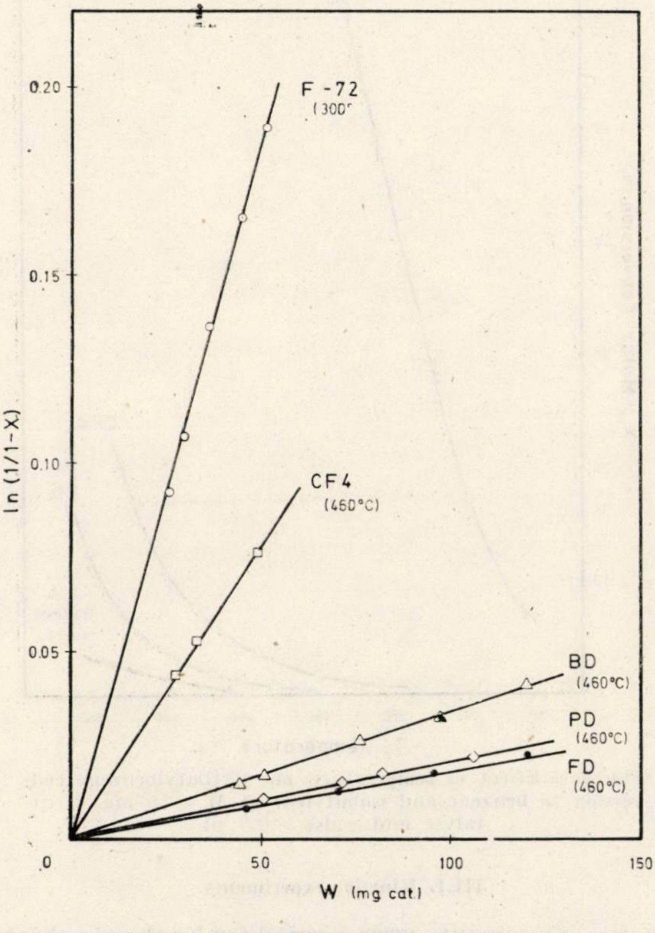

Fig. 2. — Test of first-order rate law for the tertbutylbenzene cracking on the tested $AlPO_4$, $AlPO_4-SiO_2$ and $AlPO_4-Al_2O_3$ catalysts.

a low pressure of tertbutylbenzene in the reactor. In order to avoid secondary reactions, the cracking temperature was kept at 460 ±2°C. With the F −72 catalyst, the most active one, the work proceeded at 300 ± 2°C, in order to get molar conversions lower than 12% by wt. and to avoid the back reaction and the catalyst poisoning.[11]

In Table 2, the slope and intercept of the straight lines of Fig. 2 are given, with their statistics-correlation and Student's "t" coefficients.

TABLE 2

Values of the slope, intercept and statistics of the Bassett and Habgood equation ($T = 460°C$)

Catalyst	Slope (g^{-1})	Intercept	t_{exp} (95%)	t_{theor}(95%)	r^2
F−72*	3.693	$-8.95\ 10^{-4}$	0.341	2.776	0.998
CF^4	1.551	$8.14\ 10^{-4}$	0.591	4.303	0.998
BD	0.339	$-1.49\ 10^{-4}$	0.346	2.776	0.999
PD	0.199	$3.24\ 10^{-4}$	0.619	3.182	0.996
FD	0.188	$5.03\ 10^{-4}$	0.948	3.182	0.996

* For F−72 catalyst, temperature was 300°C.

From the "t" values it can be deduced — with 95% confidence — that the intercepts are non-significant and so the process can be described, at low reactant pressure, by equation (1). Thus the catalytic cracking process over pure $AlPO_4$, $Al_2O_3-AlPO_4$ and SiO_2-AlPO_4 systems, is a first-order reaction. The rate-controlling step is the surface reaction for all catalysts. From the slope, we can deduce the kinetic constant, $\vec{k}$, if the adsorption constant, K_H, is known.

III.2. Adsorption constants determination

The Henry adsorption constants (K_H) needed for determination of kinetic constants ($\vec{k}$), were obtained by a gas chromatographic method from the net corrected retention volume (V'_R) of the compounds using equation (2):

$$K_H = \frac{V'_R}{RT} \qquad (2)$$

This experimental method is described in the literature.[12] The Langmuir adsorption constant (K_L) can be obtained from Henry's constant (K_H) by means of equation (3):

$$K_L = \frac{K_H \cdot N_A \cdot w_m}{S_{esp}} \qquad (3)$$

Experimental values of these constants for the catalysts at different temperatures are shown in Table 3. In this table we can see that the net retention volume (V'_R) and therefore the adsorption equilibrium constants, K_H and K_L, diminish with increasing temperature. Therefore, the adsorption of tertbutylbenzene over these catalysts is an exothermic phenomenon. Plotting the K_L values versus $1/T$, the ΔH_{ads} and ΔS_{ads} of this process may be obtained. These plots are given in Figure 3 and the values of these magnitudes are shown in Table 4. These results show that for $AlPO_4$ catalysts, the higher the acidity density, the greater the adsorption enthalpy (ΔH_{ads}) and the adsorption entropy (ΔS_{ads}).

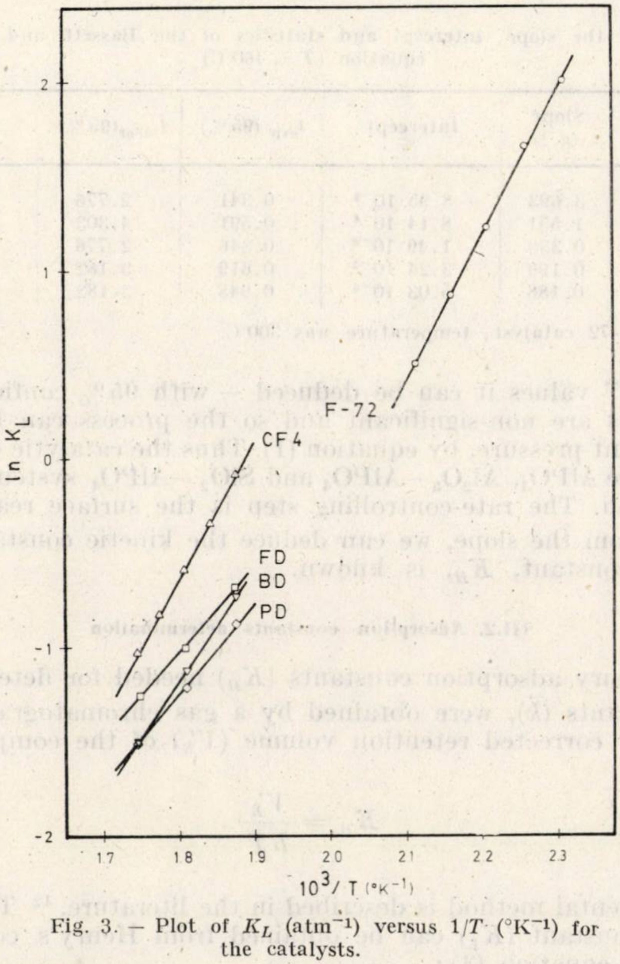

Fig. 3. — Plot of K_L (atm^{-1}) versus $1/T$ (°K^{-1}) for the catalysts.

When the values of ΔH_{ads} and ΔS_{ads} are compared for the catalysts FD, CF_4 and F —72, obtained in the same ammoniacal medium, it can be observed that the higher the surface area, the higher the values of ΔH_{ads} and ΔS_{ads}. This fact seems to indicate that the systems show greater affinity for the alkylaromatic hydrocarbons than the pure $AlPO_4$ catalysts. The values of ΔH_{ads} and ΔS_{ads} could explain the observation that when working with these catalysts in the continuous gas flow reactor the higher the surface area of the catalysts, the greater the yield obtained in the cracking process if all the catalysts are synthetized in the same way. [4,5,6]

TABLE 3

Adsorption constants

Catalyst	T (°C)	$V'_R \times 10^2$ (ml/g)	$K_H \times 10^2$ (mole/atm.g)	K_L (atm^{-1})	$K_H = A.\exp(-B/RT)$	
					A	B
F—72	160	21.84	61.48	8.08		
,,	170	14.59	40.16	5.28		
,,	180	9.74	26.21	3.45		
,,	190	6.89	18.16	2.39		
,,	200	4.94	12.74	1.68	5.15 10^{-11}	15.99
CF4	260	2.02	4.62	0.92		
,,	270	1.59	3.58	0.71		
,,	280	1.26	2.78	0.55		
,,	290	1.02	2.21	0.44		
,,	300	0.85	1.80	0.36	5.79 10^{-10}	14.39
BD	260	0.85	1.94	0.48		
,,	280	0.59	1.31	0.32		
,,	300	0.42	0.90	0.22	2.99 10^{-9}	11.74
PD	260	0.87	1.98	0.42		
,,	280	0.64	0.42	0.30		
,,	300	0.50	1.06	0.22	2.62 10^{-8}	9.46
FD	260	0.51	1.17	0.50		
,,	280	0.39	0.86	0.37		
,,	300	0.31	0.67	0.29	3.55 10^{-8}	8.58

TABLE 4

Thermodynamics of adsorption

Catalyst	ΔS_{ads} (u.e.)	ΔH_{ads} (kcal/mole)
F—72	−32.78	15.99 0.25
CF4	−27.17	14.39 0.23
BD	−23.46	11.73 0.16
PD	−19.48	9.45 0.59
FD	−17.46	8.57 0.81

III.3. Activation energy of surface reaction

The K_H values at reaction temperatures may be obtained by means of the expression K_H for tertbutylbenzene over the five catalysts (Table 3). With these values and the slopes of the straight lines of Figure 2, the $\vec{k}$ values versus $1/T$, the activation surface reaction energy and the *PZ* factor were obtained.

The values of the *PZ* factor and the activation enthalpy of tertbutylbenzene are shown in Table 5. In this table it can be observed that the activation energy is the same for the cracking reaction (30 — 33 kcal.mole^{-1}), that the surface process is probably the same for all the catalysts and, therefore, the catalytic active sites for the tertbutylbenzene cracking are the same for the AlPO$_4$, AlPO$_4$—SiO$_2$ and AlPO$_4$—Al$_2$O$_3$ catalytic systems. This fact is not singular for these catalysts only. It has also been observed by Cortés et al. [13] when studying several different catalysts. In the present case, this could be explained by the method of precipitation of the catalysts. The SiO_2-AlPO_4 system is made from deposition of $AlPO_4$ over a neutral silica gel. The SiO_2-AlPO_4 and the pure $AlPO_4$ obtained in the same medium could therefore have the same active centers since the active substance is $AlPO_4$. The three $AlPO_4$ catalysts

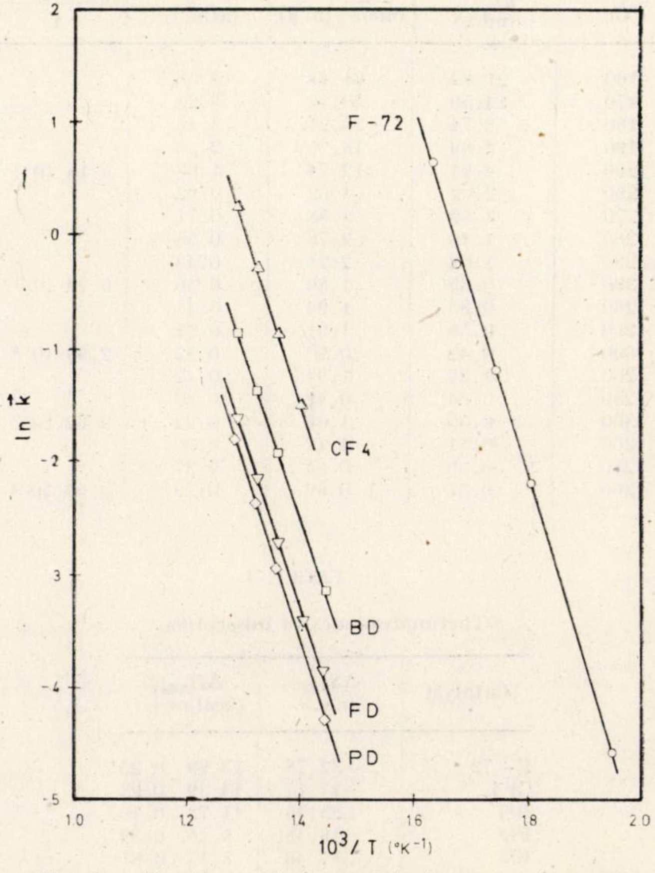

Fig. 4. — Reaction velocity constant versus temperature for the tested catalysts.

TABLE 5

Catalyst	K_L (atm^{-1})	$\overrightarrow{k}$ (mole/g.sec)	ln (PZ)	E_a (kcal/mole)
F-72	$3.994\ 10^{-3}$	$3.854\ 10^{-6}$	27.4	32.66
CF4	$2.241\ 10^{-2}$	$2.878\ 10^{-7}$	21.1	32.19
BD	$2.344\ 10^{-2}$	$6.018\ 10^{-8}$	18.8	30.22
PD	$3.842\ 10^{-2}$	$2.155\ 10^{-8}$	19.5	32.84
FD	$5.474\ 10^{-2}$	$1.430\ 10^{-8}$	18.2	30.69

obtained in different media (NH_4OH, ethylene oxide and propylene oxide) might have different textural properties because their methods of synthesis differ. They probably have the same active centers for the cracking reaction, however, because their structure is the same. For this reason all three show the same surface activation energy in the catalytic cracking of tertbutylbenzene. Due to the very similar structure of their components (tetrahedrons of AlO_4^- and PO^+), [14] the pure $AlPO_4$ and the Al_2O_3—$AlPO_4$ system will probably have the same structure and hence the same active centers since they are isomorphous.

The values obtained for the surface activation energy may seem very high if they are compared with those reported elsewhere (10—12 kcal mole^{-1}).[15] This is due to the fact that equation (1) used here allows for a distinction between the two elementary processes of the reaction: adsorption of the hydrocarbon over the active center, and the surface reaction. [10] The activation energy obtained from equation (1) is due to the transfer of the adsorbed molecule to the activated state.

Assuming that the $\Delta(PV)$ between the adsorbed molecule and activated state is $\simeq 0$, $\Delta H = \Delta E + \Delta(PV)$ becomes $\Delta H \simeq \Delta E$ and the $\Delta H_{\text{ads}} (< 0)$ and the $\Delta E (> 0)$ values may be added obtaining one "apparent activation energy of the process" whose value is in agreement with those reported in the literature for the activation energy of the process ($8 - 14$ kcal.mole^{-1}; see Table 5).

$$E_{\text{act. app.}} = E_{\text{act. sup.}} + (-\Delta H_{\text{ads}})$$

In sum, the catalytic cracking of tertbutylbenzene over $AlPO_4$ and related systems at low reactant pressures may be described as a two-step reaction. The first is the exothermic adsorption of the aromatic ring on the active center. The second is the rate controlling one: the reaction of the breakdown of the $C_{\text{alif}} - C_{\text{arom}}$ linkage of the adsorbed molecule to yield the reaction products.

NOMENCLATURE

E_a = activation energy of surface reaction
F = flow rate of carrier gas
ΔH_{ads} = adsorption enthalpy
$\vec{k}$ = reaction rate constant
K_H = Henry adsorption constant
K_L = Langmuir adsorption constant
N_A = Avogardo's number
r = correlation coefficient
R = gas constant
ΔS_{ads} = adsorption entropy
t = Student's coefficient
T = temperature
V'_R = net corrected retention volume
ΣV_p = accumulated pore volume

W = weight of catalyst
w_m = surface occupied by one hydrocarbon molecule
X = molar conversion
Z = collision number
P = probability or steric factor

REFERENCES

[1] J. V. Sinisterra, J. M. Marinas and C. Jimenez, *An. Quim.*, **72**, 254 (1976).
[2] J. V. Sinisterra, J. M. Marinas and C. Jimenez, *An. Quim.*, **70**, 860 (1974).
[3] J. V. Sinisterra, J. M. Marinas and C. Jimenez, *An. Quim.*, **72**, 185 (1976).
[4] J. V. Sinisterra, J. M. Marinas and C. Jimenez, "Abstracts of Vth Iberoamerican Symposium of Catalysis", Lisbon, 1976, p. 378.
[5] J. V. Sinisterra, J. M. Marinas and R. Perez-Ossorio, "Abstracts of IVth Iberoamerican Symposium of Catalysis", Mexico, 1974, p. 33.
[6] J. V. Sinisterra, J. M. Marinas and C. Jimenez, *An. Quim.*, **73**, 561 (1977).
[7] C. Campelo, Doctoral Thesis, Science Faculty of Madrid, 1977.
[8] K. Arita, Y. Kuge and Y. Koshikawa, *Bull. Chem. Soc. Japan*, **38**, 632 (1965).
[9] D. Atkinson and G. Curthoys, *J. Chem. Ed.*, **55**, 564 (1978).
[10] D. W. Bassett and H. W. Habgood, *J. Phys. Chem.*, **64**, 769 (1960).
[11] D. A. Best and B. W. Wojciechowski, *J. Catalysis*, **47**, 343 (1977).
[12] Y. A. Guerasimov, "Physical Chemistry Course", "Mir" Publishing House, Moscow, p. 572.
[13] A. Cortés, J. F. García de la Banda and E. Hermana, *An. Quim.*, **63**, 847 (1967).
[14] J. B. Peri, *Discuss Faraday Soc.*, **52**, 55 (1971).
[15] P. Andreu, G. Martin and H. Noller, *J. Catalysis*, **21**, 255 (1971).

Revue Roumaine de Chimie, 27, 3, 411–414 (1982)

A NEW SYNTHESIS OF HYDRAZIDES BY A DIRECT CONDENSATION REACTION

C. I. CHIRIAC
"P. Poni" Institute of Macromolecular Chemistry, Aleea Gr. Ghica Vodă no. 41 A, Iași, Romania

Received January 22, 1981

By a direct condensation reaction between diacylphenylphosphites prepared *in situ* and hydrazines, under mild conditions, hydrazides resulted with good yields.

In a previous paper,[1] we showed that diacylphenylphosphites prepared *in situ* from aromatic acids and phenyldichlorophosphite can react with amines (nucleophile reagents), affording the corresponding amides.

In this paper, we have investigated the reactivity of the diacylphenylphosphites versus other nucleophilic reagents such as hydrazines, in order to obtain the corresponding hydrazides.

A common method for preparing N-monosubstituted hydrazides, utilized the reaction of hydrazines with acyl chlorides. The latter compounds are often prepared by the reaction of a carboxylic acid with phosphorus trichloride or thionyl chloride. Various investigators [2,3] have found that the two steps could be combined successfully into a single operation. The preparation of hydrazides is one of the fundamental reactions in organic synthesis. However, a relatively little contribution has been reported on the successful preparation of hydrazides in comparison with amides or polypeptides.

As reagents for the synthesis of hydrazides, we mention : acylimidazoles [2], phosphonitrilic chloride [3] and 2,4,6-trichloro-s-triazine.[4]

RESULTS AND DISCUSSION

For the synthesis of hydrazides from diacylphenylphosphites and hydrazines, we used the described procedure [1] starting from diacylphenylphosphites prepared *in situ*. In this way, the method of synthesis becomes very simple.

The reactivity of diacylphenylphosphites with hydrazines has not been investigated. Our investigations have shown that these compounds manifest high reactivity with the hydrazines. To this end we prepared a number of diacylphenylphosphites (reactive compounds), in pyridine as solvent and acceptor for hydrochloric acid. These reactive compounds, prepared *in situ*, reacted with phenylhydrazine or hydrazine, affording hydrazides or diacylhydrazines, with good yields.

The reaction was checked up with pure dibenzoylphenylphosphite, prepared from phenyldichlorophosphite and sodium benzoate. [1] The pure dibenzoylphenylphosphite reacts with hydrazines in solution of pyridine under the same conditions as the compound prepared *in situ*. The purity and the yields of hydrazides obtained from dibenzoylphenylphosphite prepared *in situ* were similar to those obtained from pure dibenzoylphenylphosphite. Therefore, it is not necessary to isolate these reactive compounds, because pyridine hydrochloride does not affect the reaction like in other cases. [1,5] In this reaction, we tried many tertiary amines, but pyridine was found to be the most suitable base, which served also as reaction medium. The diacylphenylphosphites (1 mole) prepared *in situ* can react with phenylhydrazine (2 moles) affording acylphenylhydrazines (2 moles,) or with hydrazine (0.5 moles) affording diacylhydrazines (1 mole).

As a result of these investigations, we suggest the following mechanism of reaction :

$$\underset{(I)}{2\,\mathrm{Ar{-}COOH}} + \mathrm{C_6H_5OPCl_2} \xrightarrow[\mathrm{O-20^\circ}]{\mathrm{Py}} \underset{(II)}{(\mathrm{Ar{-}COO})_2\mathrm{POC_6H_5}} + 2\mathrm{PyH^+Cl^-}$$

$$\mathrm{II} + 2\,\mathrm{C_6H_5{-}NH{-}NH_2} \xrightarrow[\mathrm{reflux}]{\mathrm{Py}} \underset{(III)}{2\,\mathrm{Ar{-}CONH{-}NH{-}C_6H_5}} + \mathrm{C_6H_5OP(OH)_2}$$

$$(\mathrm{II}) + \frac{1}{2}\,\mathrm{NH_2{-}NH_2} \xrightarrow[\mathrm{reflux}]{\mathrm{Py}} \underset{(IV)}{\mathrm{Ar{-}CONH{-}NHCO{-}Ar}} + \mathrm{C_6H_5OP(OH)_2}$$

In this reaction, similar to other cases, [6,7] $C_6H_5OP(OH)_2$ and PyH^+Cl^- have resulted as by-products. We supposed, as in other cases, [7,8] hat this reaction involves a four-centre transition state (V) :

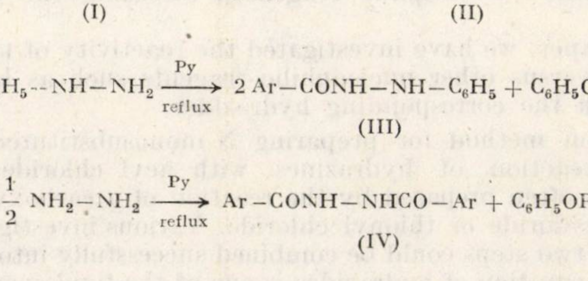

(V)

In a typical procedure, to a solution under stirring of 2 moles (I) in dried pyridine and cooled to 0°, 1 mole phenyldichlorophosphite was added very slowly (the reaction is very exothermic), and then 2 moles phenylhydrazine or 0.5 mole hydrazine were also added. After 4 hours at reflux (110 − 120°), the desired products resulted with good yield. At room temperature, the yield is low. In the case of phenylhydrazine, an excess of 5−10% is necessary in order to improve the yield. The yield of this method ranged from 55 to 85% (Table 1).

TABLE 1

Hydrazides from diacylphenylphosphites prepared *in situ*

Acid	Hydrazine	Hydrazides[a]		
		Yield[b] %	M.p.[c] °C	Reported m.p.[d] °C
Benzoic	Phenylhydrazine	66	166−168	167−168
—,,—	Hydrazine	85	237−239	238−239
p-Toluic	Phenylhydrazine	62	165−166	166−167
—,,—	Hydrazine	81	252−254	253−254
p-Chloro-benzoic	Phenylhydrazine	57	188−189	188−190
—,,—	Hydrazine	76	290−292	291−292
Anisic	Phenylhydrazine	58	178−180	178−180
—,,—	Hydrazine	79	223−225	224−225
m-Bromo-benzoic	Phenylhydrazine	55	151−153	151−153
—,,—	Hydrazine	72	263−265	264−266

[a] The products were identified by comparing m.p. and IR spectra with authentic samples.

[b] Yields calculated on acid employed.

[c] After recrystallisation from ethanol (compounds **6** and **10** from acetic acid.)

[d] From "Beilsteins Handbuch der organischen Chemie"

By this new direct synthesis, we obtained, with good yields hydrazides which are difficult to obtain by heating of aromatic acids with hydrazines.

EXPERIMENTAL

1. β-Benzoylphenylhydrazine

To 2.44 g (0.02 mole) of benzoic acid in 15 ml dried pyridine in a 50 ml 3-necked flask, 1.4 ml (0.01 mole) of phenyldichlorophosphite[9] dissolved in 5 ml dried benzen was added slowly under stirring and cooling. The rate of addition was regulated that the temperature of reaction mixture was kept in the interval of 0−10°. After stirring for 2 hours at room temperature, 2.37 g (0.0002 mole + 10% excess) phenylhydrazine was added. The solution was then heated and the solvent was distilled till the temperature of the mixture reached 115°C. The heating was continued under reflux (115−120°) for 4 hours. The obtained solution was poured into a large volume of water with ice (100−150 ml), under vigorous stirring. The product was collected by filtration, washed with 20−30 ml 7% Na_2CO_3 solution, 20−30 ml 7% HCl solution, for three times with 20−30 ml water and dried. After recrystallisation from ethanol, 2.8 g β-benzoylphenylhydrazine with m.p. 166–168°C were obtained (mixed m.p. with pure β-benzoylphenylhydrazine undepressed). Yield 66% (calculated on benzoic acid employed). Anal. Calculated for $C_{13}H_{12}N_2O$; C, 73.58 ; H, 5.66 ; N, 13.20%. Found : C, 73, 22 ; H, 5.41 ; N, 13.36%.

2. Dibenzoylhydrazine

By a similar procedure, using 1.04 g (0.01 mole) $NH_2-NH_2.2HCl$ for 2.44 g (0.02 mole of benzoic acid, 1.90 g (85%) dibenzoylhydrazine with m.p. 237–239° (ethanol) was obtained (mixed m.p. with pure dibenzoylhydrazine undepressed).
Anal. Calculated for $C_{14}H_{12}N_2O_2$; C, 70.00 ; H, 5.00 ; N, 11.66%. Found : C, 69.35 ; H, 4.91 ; N, 11.12%.

Under similar conditions, the other hydrazides (presented in Table 1) were prepared in good yields from the corresponding aromatic carboxylic acids and phenylhydrazine or hydrazine.

REFERENCES

[1] C. I. Chiriac *Rev. Roumaine Chim.*, (in press. 1980).
[2] H. Staab, *Chem. Ber.*, **95**, 1280 (1962).
[3] L. Cagliati and M. Peloni, *J. Org. Chem.*, **33**, 2979 (1968).
[4] G. Baccolini and G. Rosini, *Chimica & Industria (Milano)*, **51**, 287 (1969) ; Chem. Abstr., **72**, 3441 (1970).
[5] C. I. Chiriac and J. K. Stille, *Macromolecules*, **10**, 710 (1977).
[6] B. Iselin and W. Rittel, *Helv. Chim. Acta*, **40**, 373 (1957).
[7] N. Yamazaki, *Tetrahedron Letters*, **49**, 5047 (1972), *Polymer* Letters, **12**, 185 (1974).
[8] H. O. Becker and K. F. Funk, *J. prakt. Chem.*, **14**, 55 (1961).
[9] H. Tölkmith, *J. Org. Chem.*, **23**, 1682 (1958).

Revue Roumaine de Chimie, 27, 3, 415–421(1982)

SYNTHESIS AND REACTIONS OF 2-FURYL-3,1-BENZOTHIAZINE-4(*H*)-THIONE, 2FURYL-4(3H)-QUINAZOLINONE AND 2-FURYL-3,1- BENZOXAZIN-4(*H*)-ONE

A. ESSAWY
Chemistry Department, Faculty of Science, Zagazig University, AR Egypt

Received July 2, 1980

Reactions of 2-furyl-3,1 benzoxazin-4 (*H*)-one (**1**) with ethyl acetoacetate, malononitrile, hydrazines, morpholine, primary aliphatic amines, primary aromatic amines, Grignard reagents, sodium azide, formamide and phosphorous pentasulphide have been investigated. The 2-furyl-4 (3*H*)-quinazolinone **10** undergoes reaction with phosphorous oxychloride, dimethyl sulphate, ethyl chloroacetate, ethyl α-bromopropionate and with formaldehyde and piperidine or morpholine to give compounds **16a**–**d**, **17a** and **17b** respectively. 2-Furyl 3,1-benzothiazine-4(*H*) thione reacts with Grignard reagents, hydrazines, amines, hydroxylamine hydrochloride and copper bronze to give compounds **12a**, **12b**, **13a**–**d**, **14** and **15** respectively.

Earlier [1] we have described the synthesis and some reactions of 2-substituted 3,1-benzoxazin-4 (*H*)-one and related compounds. We now report an investigation on 2-furyl-3,1-benzoxazin-4(*H*)-one (**1**). The action of ethyl acetoacetate [2] on the benzoxazinone (**1**) in boiling dry pyridine has been found to give ethyl-2-furamido benzoyl acetate (**2**). On the other hand, the benzoxazinone **1** on reaction with malononitrile under the same conditions gave two products; the monocyano compound (**3**) and the dicyanocompound (**4**).

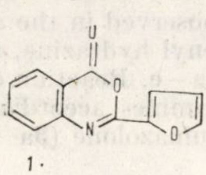

1·

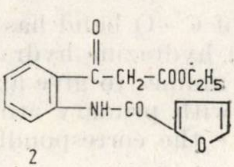

2

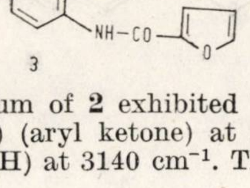

3

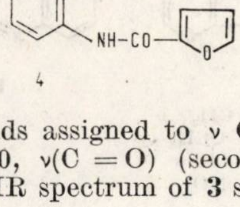

4

The IR spectrum of **2** exhibited bands assigned to ν C = O (ester) at 1725, ν(C = O) (aryl ketone) at 1680, ν(C = O) (secondary amide) at 1650 and ν (NH) at 3140 cm^{-1}. The IR spectrum of **3** showed bands attributable to ν (C = O) (carboxyl) at 1715, ν(C = 0) (aryl ketone) at 1680, ν(C = O) (secondary amide) at 1660, ν($C \equiv N$) 2210 and ν(NH) at 3100 cm^{-1}. However, the IR spectrum of **4** lack stretching frequency of carboxyl group. When the benzoxazinone **1** reacted with sodium azide in boiling acetic acid following the metod of Fahmy et al. [3] a mixture of the tetrazole **5** and the benzimidazolone **6** was obtained.

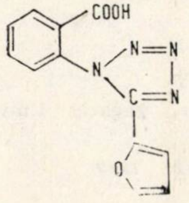

5

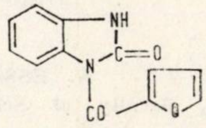

6

The behaviour of compound **1** towards the action of Grignard reagents, [4] namely methyl magnesium iodide and phenyl magnesium bromide has been investigated and found to give *O*-(furoyl aminophenyl)-di-(aryl or alkyl) carbinol (**7a, b**). The IR spectrum of **7a** exhibited bands at 1670 (>C O), 3250 (NH) and 3350 cm^{-1} (OH).

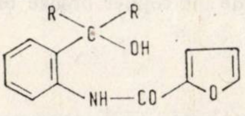

7

R

a, CH_3
b, C_2CH_5

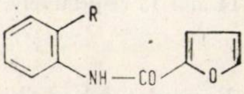

8

R

a, $-CONH-NH_2$
b, $-CO-NH-NH-Ph$
c, $-CO-N\langle\ \rangle O$
d, $-CO-NH-CH_3$
e, $-CO-NH-CH_2-Ph$

Similar cleavage of C—O bond has been observed in the reaction of benzoxazinone 1 with hydrazine hydrate, phenyl hydrazine, morpholine and primary aliphatic amines to give amides **8a—e**. Reaction of 2-substituted benzoxazinone **1** with primary aromatic amines according to Zentmyer and Wagner [5] gave the corresponding 4-quinazolone (**9a—d**).

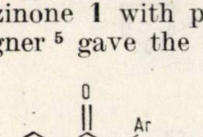

9 Ar

a, $-C_6H_4-CH_3-p$
b, $-C_6H_4-OCH_3-p$
c, $-C_6H_4-Cl-o$
d, $-C_6H_4-NO_2-m$

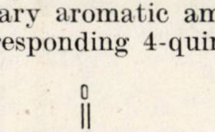

10

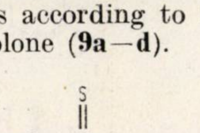

11

Compound **8c** has defined absorption bands attributable to $\nu C=O$ at 1660 and $\nu(NH)$ at 3290 cm^{-1} The IR spectrum of compound **9a** showed $\nu(C=N)$ at 1605 and $\nu(C=O)$ at 1700 cm^{-1}. On heating **1** with formamide at 170 C°, 2-furyl-4(3*H*)-quinazolinone (**10**) was obtained. The reaction of **1** with P_2S_5 in dry xylene [6] gave 2-furyl-3,1-benzothiazine-4(*H*)-thione (**11**).

The i.r. spectrum of compound **10** showed bands at 1690, $\nu(C=0)$; 1635, $\nu(C=N)$ and 3350 cm^{-1} $\nu(NH)$. Compound **11** had defined absorption bands at 1335, $\nu(C=S)$ and 1620 cm^{-1}, $\nu(C=N)$. By analogy with the recently reported reaction of thiones with Grignard reagents [7], the thione **11** reacted with ethyl magnesium iodide and phenyl magnesium bromide and gave the carbinols (**12a**) and (**12b**) respectively.

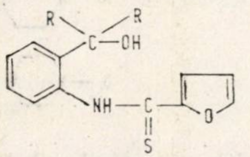

12

R

a, C_2H_5-
b, C_6H_5-

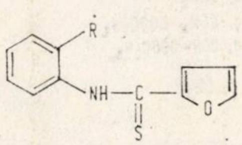

13

R

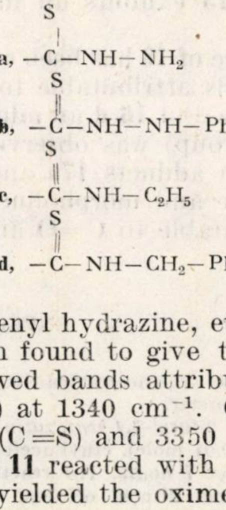

a, $-\overset{S}{\overset{\|}{C}}-NH-NH_2$

b, $-\overset{S}{\overset{\|}{C}}-NH-NH-Ph$

c, $-\overset{S}{\overset{\|}{C}}-NH-C_2H_5$

d, $-\overset{S}{\overset{\|}{C}}-NH-CH_2-Ph$

The action of hydrazine hydrate, phenyl hydrazine, ethylamine and benzyl amine on the thione **11** has been found to give thioamides **13 a–d.**

The IR spectrum of **12b** showed bands attributable to ν OH at 3500, ν (NH) at 3350 and $\nu(C=S)$ at 1340 cm^{-1}. Compound **13a** had defined absorption bands at 1346, $\nu(C=S)$ and 3350 cm^{-1} $\nu(NH)$.

On the other hand, the thione **11** reacted with hydroxylamine hydrochloride in boiling pyridine and yielded the oxime (**14**).

The IR spectrum of **14** shows the absence of $\nu(C=S)$ and reveals bands attributable to $\nu(C=N)$ in the region of 1610 – 1640 and $\nu(OH)$ at 3500 –3350 cm^{-1}.

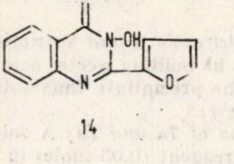

14

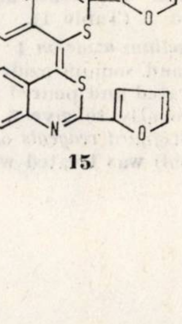

15

On heating thione **11** with copper bronze in xylene a coupling product [$\Delta^{4,4'}$-bi-3,1-benzothiazine]-2,2′-difuryl (15) was obtained. The reaction of quinazolinone **10** with $POCl_3$ gave 4-chloro-2-furyl quinazoline **(16a).**

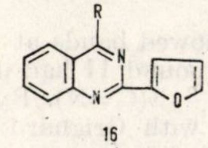

16

R
a, Cl
b, OCH_3
c, $OCH_2-COOC_2H_5$
d, $OCH(CH_3)-COOC_2H_5$

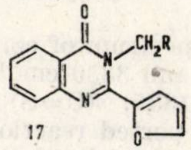

17

R

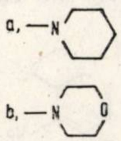

The quinazolinone **10** on reaction with dimethyl sulphate, ethyl chloroacetate or ethyl α-bromopropionate in the presence of anhydrous potassium carbonate afforded exclusively O-substituted products **16 b**–**d**. The IR spectrum of **15** exhibits an intense absorption band at 1645 cm^{-1} $\nu(C{=}N)$.

The structure of **16** has been established by studying its IR spectrum which shows bands attributable to C=N at 1620–1630 cm^{-1}; however in the case of **16 c** and **16 d** an additional band at 1735–1745 cm^{-1} due to C=O (ester group) was observed. As expected the quinazolinone **10** gave the Mannich adducts **17a** and **17b** with formaldehyde and amines such as piperidine and morpholine; **17a** showed IR bands at 1680 and 1640 cm^{-1} attributable to C=O and C=N groups respectively.

EXPERIMENTAL

The melting points are uncorrected. IR spectra in KBr (cm^{-1}) were recorded on a Unicam Sp 1200 spectrophotometer.

Condensation of 2-furyl-3,1-benzoxazin-4(H)-one **(1)** *with ethyl acetoacetate*; *formation of* **2** : A mixture of **1** (0.01 mole), ethyl acetoacetate (0.05 mole) in dry pyridine (50 ml) was heated under reflux for 7 hours. The reaction mixture was poured into ice-cold HCl. The solid that separated was filtered off and recrystallized from ethanol to give compound **2** (Table 1).

Condensation of **1** *with malononitrile*; *formation of* **3** *and* **4** : A mixture of **1** (0.01 mole), malononitrile (0.05 mole) in dry pyridine (50 ml) was heated under reflux for 6 hours. The reaction mixture was poured into ice-cold HCl. The solid that separated was filtered off and recrystallized from ethanol to give compound **4**. On the other hand, the aqueous solution was shaken with ether and the ethereal layer was left aside at room temperature to give compound **3** (Table 1).

Action of sodium azide on **1** ; *Formation of tetrazole* **5** *and benzimidazolone* **6** : A mixture of **1** (0.01 mole) and sodium azide (0.015 mole) in boilling acetic acid (40 ml) was refluxed for 3 hr, concentrated and poured into water. The precipitate thus obtained was filtered and crystallized fractionally to give **5** and **6** (Table 1).

Action of Grignard reagents on **1** ; *Formation of* **7a** *and* **7b** : A solution of **1** (0.01 mole) in dry ether (50 ml) was treated with Grignard reagent (0.03 mole) in dry ether (50 ml) for

TABLE 1

Characterisation of compounds **2**, **3**, **4**, **5**, **6**, **7a**, **7b**, **8a–e**, **9a–d**, **10**, **11**, **12a**, **12b**, **13a–d**, **14**, **15**, **16a–d**, **17a** and **17b**

Compound	m. pC°	solvent* yield (%)	Formula	Analysis (%)	
				Calculated	Found
2	152	E	$C_{16}H_{15}NO_5$	C 63.78	63.82
		50		H 4.98	5.01
				N 4.65	4.56
3	205	B	$C_{15}H_{10}N_2O_5$	C 60.40	60.35
		40		H 3.35	3.40
				N 9.39	9.42
4	215	E	$C_{15}H_9N_3O_3$	C 64.51	64.53
		35		H 3.22	3.31
				N 15.05	15.12
5	240	E	$C_{12}H_8N_4O_3$	C 56.25	56.22
		20		H 3.12	3.16
				N 21.87	21.91
6	230	A	$C_{12}H_8N_2O_3$	C 63.15	63.21
		50		H 3.50	3.48
				N 12.28	12.32
7a	90	B/P	$C_{14}H_{15}NO_3$	C 68.57	68.62
		40		H 6.12	6.11
				N 5.71	5.69
7b	195	E	$C_{24}H_{19}NO_3$	C 78.04	78.12
		55		H 5.14	5.09
				N 3.79	3.73
8a	165	B_4P	$C_{12}H_{11}N_3O_3$	C 58.77	58.82
		45		H 4.48	4.45
				N 17.14	17.12
8b	110	B	$C_{18}H_{15}N_3O_3$	C 67.28	67.24
		40		H 4.67	4.62
				N 13.08	13.12
8c	130	B/P	$C_{16}H_{16}N_2O_4$	C 64.00	64.10
		40		H 5.33	5.31
				N 9.33	9.40
8d	138	B	$C_{13}H_{12}N_2O_3$	C 63.93	64.00
		35		H 4.91	4.87
				N 11.47	11.43
8e	150	E	$C_{19}H_{16}N_2O_3$	C 71.25	71.32
		70		H 5.00	5.10
				N 8.75	8.69
9a	120	B/P	$C_{19}H_{14}N_2O_2$	C 75.49	75.51
		50		H 4.63	4.62
				N 9.27	9.30
9b	170	E	$C_{19}H_{14}N_2O_3$	C 71.69	71.70
		60		H 4.40	4.41
				N 8.80	8.75
9c	130	E	$C_{18}H_{11}N_2O_2Cl$	C 66.97	66.93
		65		H 3.41	3.32
				N 8.68	8.73
9d	176	E	$C_{18}H_{11}N_3O_4$	C 64.86	64.91
		60		H 3.30	3.28
				N 12.61	12.58
10	250	E	$C_{12}H_8N_2O_2$	C 67.92	68.00
		40		H 3.77	3.72
				N 13.20	13.18
11	140	E	$C_{12}H_7NOS_2$	C 58.77	58.69
		70		H 2.85	2.82
				N 5.71	5.69

TABLE 1 (*continued*)

Compound	m. pC°	solvent* yield (%)	Formula	Analysis (%)	
				Calculated	Found
12a	150	B	$C_{16}H_{19}NO_2S$	C 66.43	66.38
		50		H 6.57	6.49
				N 4.84	4.81
12b	160	B/P	$C_{24}H_{19}NO_2S$	C 74.80	74.78
		40		H 4.93	4.91
				N 3.63	3.66
13a	170	E	$C_{12}H_{11}N_3OS_2$	C 58.77	58.82
		60		H 4.48	4.43
				N 17.14	17.12
13b	150	B/P	$C_{18}H_{15}N_3OS_2$	C 67.28	67.31
		50		H 4.67	4.59
				N 13.08	13.11
13c	172	E	$C_{14}H_{14}N_2OS_2$	C 65.11	65.14
		40		H 5.42	5.39
				N 10.85	10.82
13d	180	E	$C_{19}H_{16}N_2OS_2$	C 71.25	71.31
		55		H 5.00	5.01
				N 8.75	8.69
14	145	E	$C_{12}H_9N_3O_3$	C 59.25	59.18
		35		H 3.70	3.67
				N 17.28	17.31
15	128	E	$C_{24}H_{14}N_2O_2S_2$	C 73.09	73.13
		50		H 3.55	3.52
				N 7.10	7.06
16a	160	E	$C_{12}H_7N_2OCl$	C 62.47	62.42
		55		H 3.03	3.13
				N 12.41	12.36
16b	120	B/P	$C_{13}H_{10}N_2O_2$	C 69.02	69.15
		40		H 4.42	4.39
				N 12.38	12.34
16c	80	E	$C_{16}H_{14}N_2O_4$	C 64.42	64.37
		45		H 4.69	4.72
				N 9.39	9.41
16d	110	B/P	$C_{17}H_{16}N_2O_4$	C 65.38	65.41
		50		H 5.12	5.11
				N 8.97	8.95
17a	160	E	$C_{18}H_{19}N_3O_2$	C 69.90	69.87
		60		H 6.14	6.21
				N 13.59	13.54
17b	180	B/P	$C_{17}H_{17}N_3O_3$	C 65.59	65.62
		50		H 5.46	5.42
				N 13.50	13.48

* A = acetic acid ; B = benzene ; B/P = benzene/light petrol (40—60°) and E = ethanol.

30 min. The reaction mixture was then heated under reflux for 4 hr, left overnight at room temperature and decomposed the usual way. The oil obtained was triturated with light petrol to give compounds **7a** and **7b** (Table 1).

Action of hydrazine hydrate, phenyl hydrazine, morpholine and primary aliphatic amines on **1** ; *Formation of* **8a—e** : A solution of **1** (0.01 mole) and hydrazine hydrate, phenyl hydrazine, morpholine or primary aliphatic amine (0.05 mole) in ethanol (50 ml) was refluxed for 6 hr. The solid that separated out on cooling was recrystallized from a proper solvent to give **8a—e**. (Table 1).

Reaction of **1** *with primary aromatic amines* ; *Formation of* **9a—d** : A mixture of **1** (0.01 mole), the appropriate amine (0.01 mole) and zinc chloride (0.5 g) was heated in an oil bath at 180° for 5 hr. The solid product was washed with hot water and recrystallized from a proper solvent to give **9a**—**d** (Table 1).

Reaction of **1** *with formamide; Formation of 2-furyl-4(3H) quinazolinone* **10** : A mixture of **1** (0.01 mole) and formamide (0.01 mole) was heated in an oil-bath at 180° for 5 hr. The resulting solid product was cooled, filtered and crystallized from ethanol to give **10** (Table 1).

Action of phosphorous pentasulphide on **1** ; *Formation of thione* **11** : A solution of **1** (0.01 mole), P_2S_5(0.02 mole) and dry xylene (100 ml) was boiled under reflux for 6 hr. The reaction mixture was filtered hot and concentrated. The product that separated on cooling was recrystallized from ethanol to give **11** (Table 1).

Action of Grignard reagents on thione **11** ; *Formation of carbinols* **12a** *and* **12b** : A solution of thione **11** (0.01 mole) in dry ether (50 ml) was treated with Grignard reagent (0.03 mole) in dry ether (50 ml) for 30 min. The reaction mixture was heated under reflux for 4 hr, left overnight at room temperature and decomposed in the usual way. The oil obtained was triturated with light petrol to give carbinols **12a** and **12b** (Table 1).

Reaction of thione **11** *with hydrazine hydrate and phenyl hydrazine; Formation of* **13a** *and* **13b** : A solution of thione **11** (0.01 mole) and hydrazine hydrate or phenyl hydrazine (0.05 mole) in ethanol (50 ml) was refluxed for 5 hr. The solid that separated on cooling was recrystallized from a proper solvent to give **13a** and **13b** (Table 1).

Action of amines on thione **11** ; *Formation of* **13c** *and* **13d** : The thione **11** (0.01 mole) was heated with appropriate amines (0.015 mole) in an oil bath at 180° for 4 hr. and the resulting solid substance recrystallized from the proper solvent to give **13c** and **13d** (Table 1).

Condensation of thione **11** *with hydroxylamine hydrochloride; Formation of the oxime* **14** : A mixture of **11** (0.01 mole), hydroxylamine hydrochloride (0.03 mole), sodium acetate (0.5 mole) and dry pyridine (40 ml) was heated under reflux for 3 hours. The reaction mixture was poured into cold dilute hydrochloric acid to give a solid product **14** (Table 1).

Action of copper bronze on thione **11** ; *Formation of* **15** : A mixture of **11** (0.01 mole) and copper bronze (0.005 g-atoms) in 20 ml dry xylene was heated for 5 hr, filtered while hot to make free from copper bronze, cooled and the solid thus product was crystallized from ethanol to give **15** (Table 1).

Action of phosphorousoxychloride on **10** ; *Formation of* **16a** : A suspension of **10** (0.01 mole) and phosphorous oxychloride (0.06 mole) was heated on a water bath for 2 hr and then poured slowly into crushed ice. The solid thus separated was filtered and crystallized from ethanol to give **16a** (Table 1).

Reaction of **10** *with dimethyl sulphate, ethyl chloroacetate and ethyl α-bromopropionate; Formation of* **16b**—**d** : A mixture of **10** (0.01 mole), dimethyl sulphate, ethyl chloroacetate or α-bromoethyl propionate (0.04 mole), anhyd. potassium carbonate (0.04 mole) and acetone (20 ml per 1 g. of **10**) was refluxed for 30 hr on a water bath, the solvent evaporated and water added. The organic material was extracted with ether and removal of ether gave the desired products **16b**—**d** (Table 1).

Formation of the Mannich bases **17a** *and* **17b** : A mixture of quinazolinone **10** (0.01 mole), formaldehyde (0.02 mole) and piperidine or morpholine (0.012 mole) in 20% (w/v) hydrochloric acid was dissolved in 50 ml ethanol. The reaction mixture was heated under reflux on a steambath for 6 hr and left to stand overnight. The solution was diluted with water and dilute sodium hydroxide was added till the solution becomes alkaline. After extraction with ether and acidifying with acetic acid, the solid product that separated out was crystallized from the proper solvent to give **17a** and **17b** (Table 1).

REFERENCES

[1] A. Essawy, M. A. El-Hashash and M. M. Mohamed, *Indian. J. Chem.*, (accepted for publication).

[2] A. Sammour, A. F. M. Fahmy and M. Mahmoud, *Indian. J. Chem.*, **11**, 222 (1973).

[3] A. F. M. Fahmy, M. A. El-Hashash, M. M. Habashy and S. A. Elwannise, *Rev. Roumaine Chim.*, **23**, 1567 (1978).

[4] A. Sammour, M. I. B. Slim, M. El. Kasaby and M. Abdalla, *Acta. Chim. Acad. Sci. Hung.*, **78**, 293 (1973).

[5] D. T. Zentmyer and E. C. Wagner, *J. Org. Chem.*, **14**, 967 (1949).

[6] L. Ligrand, *Bull. Soc. chim. France*, **74**, 337 (1960).

[7] A. Sammour, M. I. B. Selim, A. F. M. Fahmy and K. Elewa, *Indian. J. Chem.*, **2**, 437 (1973).

Revue Roumaine de Chimie, **27**, *3*, 423–428 (1982)

ALUMINIUM CHLORIDE CATALYZED REACTIONS OF UNSATURATED ACIDS WITH BENZENE. XIV*

REACTION OF *t*-BUTYL-ACRYLIC ACID

A. C. RĂZUŞ, ZS. ARVAY and ALICE MARIE GLATZ
Centre of Organic Chemistry, Spl. Independenţei 202 B, R–78100 Bucharest,
Romania

Received April 23, 1981

In the course of the reaction between *t*-butylacrylic acid and benzene in the presence of aluminium chloride a skeletal isomerisation with formation of lactones and phenylated acids is reported. A reaction mechanism is proposed for the interpretation of the results.

In previous papers on the Friedel-Crafts reactions of α, β-unsaturated acids with benzene [1] we have shown that the nature and the ratio of the products can be explained by a mechanism involving carbocation formation (due to the protonation of the double bond or to a hydride ion extraction from a favourable position). This reaction involves the electrophilic replacement of benzene by these carbocations or by those resulted therefrom through various hydride or alkyl migrations.

In this respect we considered of interest to study the behaviour of 4,4-dimethylpenten-2-oic acid in the conditions described in the above mentioned papers. This acid has two remarkable particularities, namely the steric hindrance of the β-position of the carboxyl group due to the bulky *t*-butyl group, and the absence in the γ-position of hydrogen atoms which could migrate intramolecularly in the β-position or could be extracted by acceptors from the reaction medium. As a result we could expect that the conversion of the unsaturated acid (starting material) will follow at a smaller rate than in the case of unsaturated acids with no steric hindrance. One can also anticipate that the nature and the relative amounts of the reaction products will suffer dramatic modifications as a consequence of the structure of the studied acid.

RESULTS

In the course of our experiments we used the same conditions as in our previous works in this field. The relative amounts of the three reactants were : acid : $AlCl_3$: benzene $= 1 : 1.5 : 20$. The reaction temperature was 45°. The reaction times ranged from 15 to 240 minutes. The reaction products were analysed by v.p.c. as methyl esters.

---

* For part XIII see : A. M. Glatz, A. C. Răzuş, V. Drăguţan, Zs. Arvay and F. Badea, *Rev. Roumaine Chim.*, **24**, 1013 (1979).

To compare the reaction rates of acid **1** and of penten-2-oic acid (**2**) in the Friedel-Crafts reaction, we worked in the same conditions with both acids. The results are given in table 1.

TABLE 1

The conversion of 4,4-dimethylpenten-2-oic acid and penten-2-oic acid in the Friedel-Crafts reaction with benzene, in different reaction times

Acids	Reaction time, minutes			
	15	30	120	240
	Amounts of acid %transformed into products*			
4,4-Dimethyl-penten-2-oic (**1**)	4.7	20.4	40.8	67.3
Penten-2-oic (**2**)	19.9	51.2	82.0	—

* The nature of the reaction products of acid **1** will be discussed later. From acid **2** a mixture of 3- and 4-phenylvaleric acids were obtained.

As we expected, the steric hindrance from the reaction centre reduced the reaction rate, as shown by the different amounts of acid **1** and acid **2** transformed into products during the same period (for the latter acid this quantity was at least twice as great as for the former).

We further studied the reaction mixture (after treatment with an ethereal solution of diazomethane) by v.p.c. and we observed the presence of five components and different amounts of starting material.* Three of these components were methyl esters of the following acids (identified by v.c.p. in comparison with authentic samples): 4-phenyl-3,4-dimethylvaleric acid (**3**), 4-phenyl-3,3-dimethylvaleric acid (**4**) and 3-phenyl-4,4-dimethylvaleric acid (**5**). After alkali washing of the initial mixture two components disappeared on the chromatogram; one of the two unesterifiable components was the lactone of 4-hydroxy-3,4-dimethylvaleric acid (**6**) identified by v.p.c. in comparison with an authentic sample. We assigned to the fifth component the structure of the lactone of the 4-hydroxy-3,3-dimethylvaleric acid (**7**) because its retention time on v.p.c. was very close to that of lactone **6**, and also from reaction mechanism considerations. The evolution in time of the components ratio is presented in table 2.

---

* In some samples, especially at longer reaction time, in addition to these components, small amounts of 3,4-dimethylvaleric acid were observed.

TABLE 2

The variation in time of the component ratio from the reaction mixture of acid **1** with benzene and $AlCl_3$

Components % / Time	**6**	**7**	**5**	**4**	**3**
30	29.5	traces	1.3	4.7	64.5
60	22.7	0.4	3.3	4.5	69.1
120	24.1	0.5	2.6	8.8	64.0
240	13.5	0.9	2.6	20.0	63.1

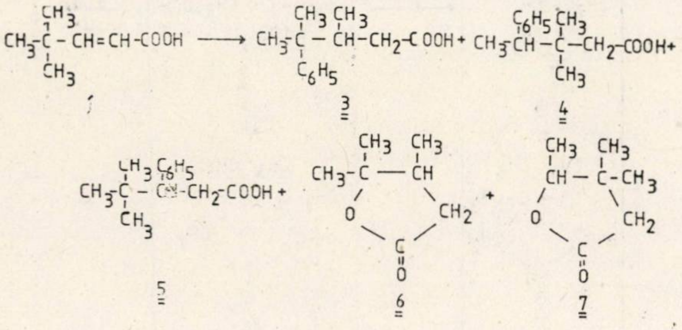

Scheme 1

DISCUSSION

As we supposed, the special structure of acid **1** leads to some mechanism particularities unobserved till now in the series of α, β-unsaturated acids. It is known that the faster stage in the Friedel-Crafts reaction of these acids is the protonation of the double bond with formation of a carbocation centre in β-position to the carboxyl group, in this case the formation of carbocation **8** (Scheme 2).

The reaction of the carbocation with benzene takes place only in a very small proportion due to the neighbourhood of the *t*-butyl group. The amount of acid **5** obtained by the phenylation of carbocation **8** is low from the start of the reaction and remains low even after eight hours. However this cation rearranges by a methyl group migration giving two equilibrating cations: **9** (acyclic) and **10** (protonated lactone). Carbocation **9** is a tertiary one (less reactive) and its cyclisation to the protonated lactone also contributes to the blocking of the cationic intermediate. Therefore the electrophilic substitution of benzene is relatively slow. From this it follows: (1) the small conversion in time of acid **1** in comparison with that of the nonmethylated acid **2**, and (2) the unexpected nature of some reaction products whose mode of formation will be discussed later. The formation of the key equilibrating cations **9** ⇌ **10** explains the obtaining of both the phenylated acid **3** and of lactone **6**. The latter consti tutes (at least at the beginning of the reaction) a reserve of equilibrating cations **9** ⇌ **10**. The transformation of lactone **6** into a mixture of acids **3** and **4** in the course of a Friedel-Crafts reaction is known. [2] The formation

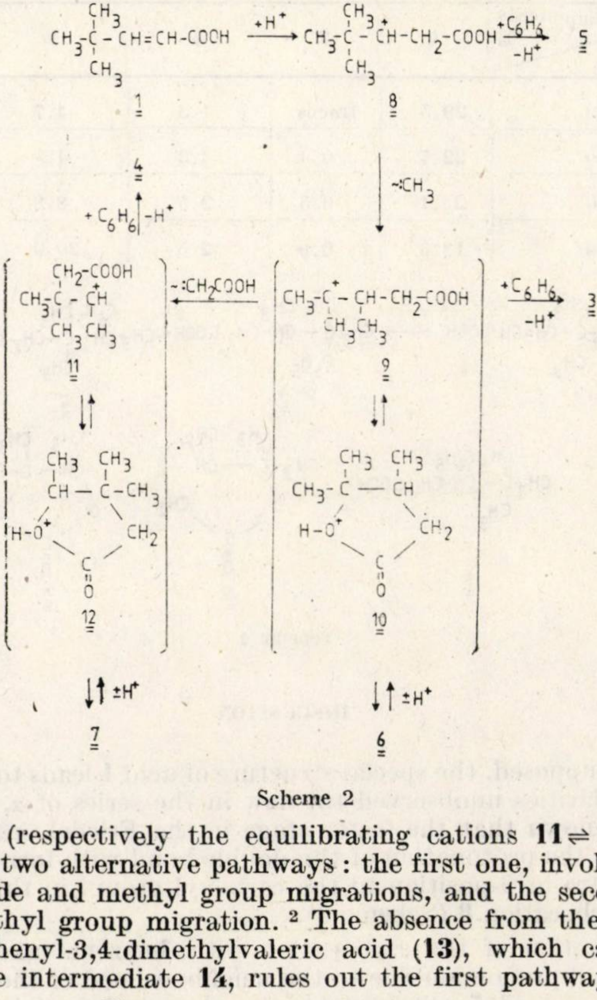

Scheme 2

of cation **11** (respectively the equilibrating cations **11** ⇌ **12**) could be explained by two alternative pathways: the first one, involving a succession of hydride and methyl group migrations, and the second, involving a carboxymethyl group migration. [2] The absence from the reaction products of 3-phenyl-3,4-dimethylvaleric acid (**13**), which can be formed only from the intermediate **14**, rules out the first pathway (Scheme 3).

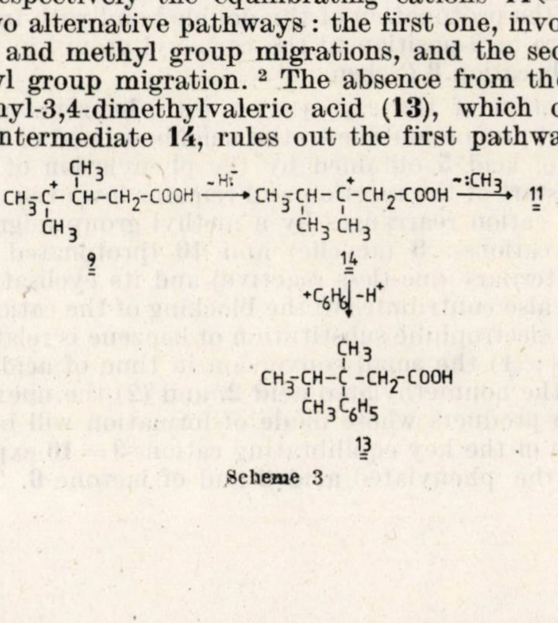

Scheme 3

In fact the transformation of carbocation **9** into **14** involves an ion hydride migration in an opposite sense to that imposed by the strong —I effect of the carboxyl group. It follows that the migration of the carboxymethyl group remains the only possible alternative for the formation of carbocation **11.** Therefore the formation of the equilibrating cations $\mathbf{11} \rightleftharpoons \mathbf{12}$ explains the appearance of the phenylated acid **4** and of lactone **7**.

We also studied, in the course of this work, the isomerisation of acid **5** in order to see whether it can be converted into the other acids. The results ruled out this suposition. The reaction of lactone **6** with benzene in the presence of aluminium chloride in our conditions gave the same products as acid **1**. This fact is in good agreement with our proposed mechanism.

EXPERIMENTAL

All melting points are uncorrected. ^{1}H—NMR spectra were recorded on a Varian A 60—A spectrometer, using TMS as internal standard. The v.p.c. analyses and separations were carried out on a Willy Giede model 18—3 gas-chromatograph using a 3 m × 4 mm column packed with 15% ethyleneglycol succinate + 5% ClF 1 on Chromosorb W (60 — 80 mesh); column temperature = 180°. IR spectra recorded on a UR—20 Carl Zeiss-Jena 20 spectrophotometer.

A. Syntheses of the starting materials and authentic samples

The structure and purity of the starting materials and authentic samples were checked by v.p.c. ^{1}H—NMR and IR spectra.

trans-t-Butylacrylic acid (**1**) was prepared starting from pivalic aldehyde and diethyl malonate using Cope and Hancock method modified by Foreman and McElvain.[3] We obtained an oily mixture of *cis* and *trans* isomers from which, on standing, crystals of pure *trans* isomer appeared. These crystals after digestion with petroleum ether are acid **1** m.p. 63° (lit. m.p. 62 — 63°).

Lactone of the 4-hydroxy-3,4-dimethylpentanoic acid (**6**) was obtained from the ester of α-acetylpropionic acid by Reformatsky's method followed by saponification and decarboxylation [1] leading to β-methyllevulinic acid, which with methyl-magnesium bromide gave lactone **6**, b.p.$_{1.0}$ 95 — 100° (lit.[2,4] b.p.$_{0.8}$ 89 — 92°).

IR Spectrum (CCl$_4$, cm^{-1}) : 1778 v.s.

^{1}H—NMR Spectrum (CCl$_4$, δ, ppm) : 1.05 (d, 3H, CH$_3$ group on C—3 ; J = 7.0 Hz), 1.25 and 1.40 (2s, 6H, two CH$_3$ sequence$>$CH—CH$_2$—).

3-Phenyl-4,4-dimethylvaleric acid (**5**) was prepared from dibenzylideneacetone and *t*-butylmagnesium bromide followed by the oxidative degradation [2] of the resulted compound, m.p. 147 — 148° (acetic acid ; lit. [2] m.p. 146 — 148°). Methyl ester was obtained by treating the acid with a solution of ethereal diazomethane. This ester has the same retention time in v.p.c. and the same ^{1}H—NMR spectrum as that obtained from the Friedel-Crafts reaction.

^{1}H—NMR Spectrum (CDCl$_3$, δ, ppm) : 0.88 (s, 9H *t*-butyl group), 2.55 — 3.30 (m, 3H the sequence $>$CH—CH$_2$ —), 7.21 (s, 5H aromatics), 10.55 (s, 1H—COOH).

4-Phenyl-3,3-dimethylvaleric acid (**4**.). Its methyl ester was separated by v.p.c. from the methyl ester mixture of the reaction products in the same way as above and identified by : ^{1}H—NMR *spectrum* (CCl$_4$, δ, ppm) : 0.96 and 1.05 (2s, 2H from CH$_2$ from α position), 2.90 (q, 1H from the benzyl group, J = 7.5 Hz), 3.64 (s, 3H from CH$_3$ ester) and 7.28 (s, 5H aromatics).

4-Phenyl-3,4,-dimethylvaleric acid (**3**). Its methyl ester was separated in the same manner as above from the reaction products and it was identified by :

^1H-NMR spectrum (CCl_4, δ, ppm), 0.84 (d, 3H from C—3, J = 7.0 Hz), 1.30, (s, 6H from two methyl groups on C—4), 1.58—2.63 (m, 3H sequence $> CH-CH_2-$), 3.58 (s, 3H, $COOCH_3$) and 7.10 — 7.51 (m, 5H aromatics).

3,4-Dimethylvaleric acid ester was separated in the same manner as above and was identified by :

^1H—NMR spectrum (CCl_4, δ, ppm) : 0.87 (d, 6H from two CH_3 groups of isopropyl, J = 6.5 Hz), 90 (d, 3H of the methyl group, J = 6.5 Hz), 1.48 — 2.68 (m, 3H sequence $> CH-CH_2-$) an 3.66 (s, 3H from the methyl ester group).

B. General method for the Friedel-Crafts reaction

To a stirred suspension of 15 mmoles aluminium chloride in 100 mmoles of benzene, at 45°, a solution of 10 moles of acid or lactone in 100 mmoles of benzene was added dropwise. After a definite time the reaction mixture was poured into diluted hydrochloric acid and broken ice. The organic layer was treated with an ethereal solution of diazomethane and then washed in a funnel with a solution of 5% KOH. The components were identified described above.

Initially, from the reaction products three phenylated acids (methyl esters), two lactones and part of the starting material (methyl ester) were observed by v.p.c. After washing with aqueous alkali, two components disappeared (the two lactones) on the chromatogram.

REFERENCES

1 A. M. Glatz, A. C. Răzuş and C. D. Nenitzescu, *Rev. Roumaine Chim.*, **11**, 555 (1966) ; A. C. Răzuş, Zs. Arvay and A. M. Glatz, *ibid.*, **23**, 753 (1978).

2 J. W. Huffman and T. W. Bethea, *J. Org. Chem.*, **30**, 2956 (1965).

3 A. C. Cope, E. M. Hancock, *J. Amer. Chem. Soc.*, **60**, 2901 (1938) ; E. L. Foreman, S. M. McElvain, *ibid.*, **62**, 1438 (1940).

4 J. N. Schumacher and D. L. Roberts, U. S. 3, 251, 366 ; *Chem. Abstr.*, **65**, 12113 (1966).

Revue Roumaine de Chimie, 27, *3*, 429–431 (1982)

REPLACEMENT OF THE NITRO GROUP IN PENTACHLORONITROBENZENE BY NUCLEOPHILES

A. I. HASHEM
Chemistry Department, Faculty of Science, Ain Shams University, Abbassia, Cairo

Received August 20, 1980

Pentachloronitrobenzene reacts with sodium hydroxide, sodium hydrogen sulphide, sodium methoxide and ammonia with replacement of the nitro group by $-OH$, $-SH$, $-OCH_3$ and $-NH_2$ groups respectively. Attempted replacement of the nitro group by $-CN$ group failed.

It was reported[1,2] that the replacement of chlorine by fluorine in 2,4-dinitrochlorobenzene is effected by treatment with anhydrous potassium fluoride. The reaction proceeded quite smoothly in polar solvents. The authors[1,2] observed brown fumes and traces of lower boiling point products suggesting the possibility of nitro group replacement. In this investigation, replacement of the nitro group of pentachloronitrobenzene I by some nucleophiles is studied.

Pentachloronitrobenzene I reacts with sodium hydroxide, sodium hydrogen sulphide, sodium methoxide, and ammonia with the formation of pentachlorophenol IIa, pentachlorothiophenol IIb, pentachloroanisole IIc and pentachloroaniline IId respectively.

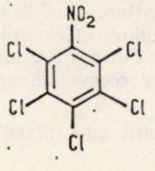

I

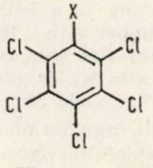

IIa, $X = OH$
IIb, $X = SH$
IIc, $X = OCH_3$
IId, $X = NH_2$

Evidence for the structures of the products IIa-d was obtained from :

(i) Comparison of the melting points of these products with those reported in the literature.

(ii) Authentic samples of pentachlorophenol, pentachlorothiophenol, pentachloroanisole and pentachloroaniline were prepared and shown by mixed melting point experiments (cf. experimental part) to be identical with the products IIa-d.

Potassium cyanide failed to effect replacement of the nitro group by — CN group under the reaction conditions employed (cf. experimental part). A plausible explanation for the above substitution reactions is obtained by considering the electronic factors in I. The chlorine atoms exerting their full inductive effect, as well as the strong electron-withdrawing effect of the nitro group, make the carbon the atom carrying the latter group more susceptible to attack by nucleophiles.

The failure of the cyanide ion to replace the nitro group is not unexpected since it is considered as a weak nucleophile for aromatic systems.

EXPERIMENTAL

a. Preparation of pentachloronitrobenzene I

In a conical flask, pentachlorobenzene[3] (2.0 g) was treated with concentrated sulphuric acid (20 ml), and then fuming nitric acid (20 ml) was added dropwise with shaking until the solid disappeared completely. The reaction mixture was then heated on a steam-bath for one hour. On cooling, colorless crystals separated out, were filtered off and washed thoroughly with water. The product obtained was recrystallised from ethanol in colorless needles, m.p. 144—5°C; yield 72%.

This product was shown from its melting point and mixed melting point with an authentic sample[4] to be pentachloronitrobenzene.

b. Action of sodium hydroxide on I

A mixture of I (0.5 g) and 30% sodium hydroxide (50 ml) was heated under reflux for two hours during which brown fumes were observed. Heating was continued for additional one hour after which the solution was acidified while hot with conc. HCl. On cooling, colorless crystals separated out, filtered off and then recrystallised from benzene in colorless needles, m.p. 188—190°C; Yield 50%. This product was shown from its melting point and mixed melting point with an authentic sample[5] to be pentachlorophenol IIa.

c. Action of sodium hydrogen sulphite on I

A warm solution of sodium hydroxide in methanol (50 ml) was saturated with hydrogen sulphide and added with stirring to a boiling solution of I (0.5 g) in 50 ml pyridine. The reaction mixture was heated under reflux for two hours after which the solution was cooled, diluted with water and then acidified with concentrated hydrochloric acid. The product obtained was filtered off, washed with water and finally recrystallised from benzene-n-hexane in colorless crystals, m.p. 240—2°C; Yield 55%.

This product was shown from its melting point and mixed melting point with an authentic sample[6] to be pentachlorothiophenol IIb.

d. Action of sodium methoxide on I

A mixture of I (0.5 g) and sodium methoxide solution (prepared by dissolving 1.0 g sodium metal in 50 ml absolute methanol) was heated under reflux for three hours. The reaction mixture was then cooled, diluted with water. The solid so obtained was filtered off and finally recrystallised from ethanol in colorless needles, m.p. 106—7°C; Yield 55%. This product was shown from its melting point and mixed melting point with an authentic sample[7] to be pentachloroanisole IIc.

e. Action of ammonia on I

A solution of I (0.5 g) in 50 ml ethanol was saturated with ammonia gas. The reaction mixture was heated in a sealed tube at 200°C for three hours. The solid obtained was filtered off and washed thoroughly with water, and finally recrystallised from toluene in pale yellow crystals, m.p. 230—1°C; Yield 45%.

The product was shown from its melting point and mixed melting point with an authentic sample[6] to be pentachloroaniline II d.

f. Action of potassium cyanide on I

The reaction was carried out as described in experiment (e) using KCN (2.0 g) instead of ammonia.

The product obtained was shown from its melting point and mixed melting point experiment to be unchanged pentachloronitrobenzene I.

REFERENCES

[1] H. B. Gottlieb, *J. Amer. Chem. Soc.*, **58**, 532 (1936).
[2] H. G. Cook and B. C. Saunders, *Biochem., J.*, **41**, 558 (1947).
[3] O. Silberrad, *J. Chem. Soc.*, **1922**, 1020.
[4] L. I. Nicodemus, *J. prakt. Chem.*, **83**, 319 (1911).
[5] W. C. Stoesser (to Dow Chem. Co.), U. S. 2, 131, 259, Sept. 27, 1938; *Chem. Abstr.*, **32**, 9102 (1938).
[6] A. L. Rocklin, *J. Org. Chem.*, **21**, 1480 (1956).
[7] D. Matheson and M. McCombie, *J. Chem. Soc.*, **1931**, 1103.

Revue Roumaine de Chimie, 27, 3, 433—442 (1982)

SYNTHESIS AND POLYMERIZATION OF POLYETHYLENE GLYCOL DIMETHACRYLATES. IV[1]

STUDY OF THE POLYMERIZATION PROCESS OF POLYETHYLENE GLYCOL DIMETHACRYLATES

GH. HUBCA*, CR. OPRESCU *, GH. DRĂGAN ** and M. DIMONIE *

* The Polytechnic, Bucharest, Laboratory of Macromolecular Technology, 149, Calea Victoriei, Bucharest, Romania

** Institute of Chemical Research. ICECHIM, 202, Spl. Independenţei, Bucharest, Romania

Received March 18, 1981

The process of bulk and solvent polymerization of ethylene dimethacrylate (EGDMA), diethylene glycol dimethacrylate (DEGDMA), triethylene glycol dimethacrylate (TEGDMA) and tetraethylene glycoldimethacrylate (TTEGDMA) has been studied. The investigations show that the kinetics of bulk polymerization process depends on the system geometry. The thin layer polymerization takes place by auto-acceleration and in the case of thick layer polymerization, the maximum rate is obtained at the beginning of the process. The performed investigations point out the influence of the main parameters upon polymerization process (solvent nature, temperature, monomer, initiator and oxygen concentration) and show that the rate of polymerization reaction increases with the length of oligomeric chain.

INTRODUCTION

Polyethylene glycol dimethacrylates are tetrafunctional monomers and lead to tridimensional products by polymerization. They can be considered as bicomponent systems made up of oligomeric and polymeric chains.

It is obvious that the process for obtaining these polymers and their properties will be determined by monomer structure as well as by the nature and length of oligomeric group. On the one hand, the polymerization process of these monomers has been studied in order to establish the best compositions for anaerobic adhesive resins and, on the other hand, in order to point out the peculiarities that characterize tridimensional polymerization of dimethacrylate esters.

The great majority of reports in the specialized literature study the polymerization process by thermometry [2,3] method and deal with the problem of tridimensional polymerization mechanism, determination of the rate constants of elementary reactions for different stages of the process, [4–7] influence of monomer nature [8–10] and oxygen concentration [11–12] upon the polymerization reaction.

This paper deals with the kinetic study of polymerization process of polyethylene glycol dimethacrylates using high vacuum method which assured a good reproductibility of the results.

EXPERIMENTAL

The monomers: ethylene dimethacrylate, diethylene glycol dimethacrylate, triethylene glycol dimethacrylate and tetraethylene glycol dimethacrylate were purified by distillation in high vacuum, and their purity was checked by double bond analysis and IR spectrum.

The solvents: dimethylformamide, tetrahydrofuran, ethyl cellosolve, dichloroethane, toluene, benzene, methylene chloride and hexane were carefully fractionated on a distillation column, of high efficacity, under argon.

Reductants: N,N'-dimethyl—1,3—diamino—2—hydroxy propane, dimethylaminopropionitrile and triethylamine were distilled at reduced pressure.

Methyl ethyl ketone peroxide (MEKP), a commercial pure grade reagent, was used without further purification and the content of peroxide by active oxygen was determined using iodometric method.[13]

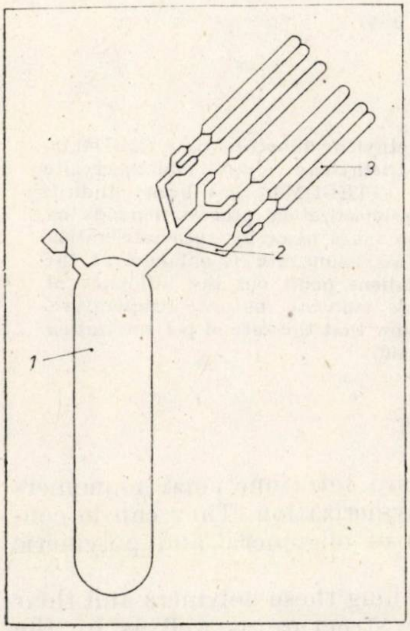

Fig. 1. — Polymerization device. 1 — Blending phial, 2 — Distribution device of reaction mixture, 3 — Polymerization phial.

The dosage of reactants and the polymerizations were carried out in a device welded to the high vacuum installation (Fig. 1).

The monomer, solvent and initiator, in perfectly determined quantities, were introduced in a phial (1).

The removal of oxygen dissolved in medium took place under vacuum by successive freezings and thawings of the reactions mixture composition; during the thawing, the connection with vacuum was interrupted.

The device was detached from the vacuum installation and by turning the phial (1), the mixture composition was distributed to the eight calibrated phials (3). The calibrated phials were sealed off to flame, separated from phial (1) and introduced in a thermostatic bath at wished temperature.

From time to time a phial was taken out and quickly cooled in liquid nitrogen for stopping the polymerization reaction. Finally, the phial was opened and the polymer was precipitated by pouring the reaction mixture into diethyl ether. The amount of the obtained polymer was gravimetrically determined, after benzene extraction for removal of unreacted monomer and drying in vacuum at constant weight.

The thin layer polymerizations were carried out in a special dilatomer whose bulb was filled with powdered glass of 100—200 μ size.

The polymerization process took place in the monomer layer comprised between glass particles of 10 and 40 μ thickness.

RESULTS AND DISCUSSIONS

Bulk polymerization of polyethylene glycol dimethacrylates in the presence of methyl ethyl ketone peroxide was studied in comparison with bulk polymerization of methyl methacrylate. The conducting of the polymerization process in a large quantity of monomer (thick layer) pointed out that the polymerization of dimethacrylic esters and of methyl methacrylate took place differently.

As it may be noticed from figure 2 the polymerization of methyl methacrylate is accompanied by auto-acceleration and conversion reaches high values. At the polymerization of ethylene dimethacrylate under the same conditions the reaction rate reaches the maximum value at the beginning, but the process is limited to low conversions, this fact being in agreement with the literature data. [14]

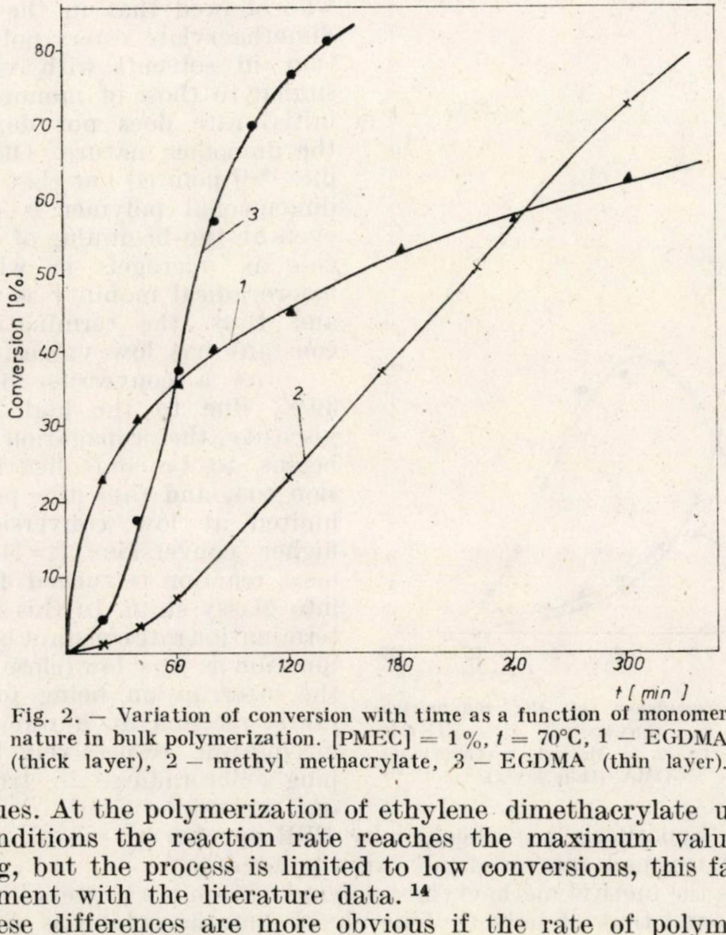

Fig. 2. — Variation of conversion with time as a function of monomer nature in bulk polymerization. [PMEC] = 1 %, t = 70°C, 1 — EGDMA (thick layer), 2 — methyl methacrylate, 3 — EGDMA (thin layer).

These differences are more obvious if the rate of polymerization is plotted against conversion (figure 3).

The registered differences may be explained as follows. As it is known, [15] in the case of methyl methacrylate the viscosity of the medium increases with conversion, and the viscosity is responsible for auto-acceleration by reducing the rate constant of termination.

For ethylene dimethacrylate bulk polymerization, due to formation of tridimensional polymer, the reaction mass is turned into gel at small conversion (~ 3 %). This aspect correlated with a greater viscosity of initial monomer leads to the conclusion that the termination reaction is controlled by diffusion from the beginning of the process, fact that explains the high rate of reaction.

The influence of diffusion upon the initial polymerization rate should become more important as the length of oligomeric chain and viscosity of monomer are greater (Table 1).

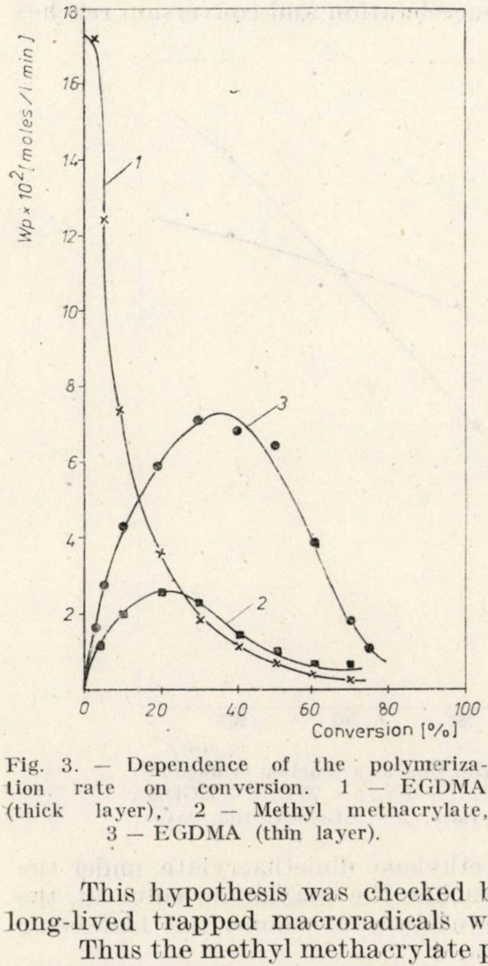

Fig. 3. — Dependence of the polymerization rate on conversion. 1 — EGDMA (thick layer), 2 — Methyl methacrylate, 3 — EGDMA (thin layer).

This explanation is also supported by the investigations made by Berlin and Korolev,[4] who showed that in the case of dimethacrylate esters polymerization in solvents with viscosities similar to those of monomers, the initial rate does not depend on the monomer nature. Other studies[16,17] pointed out that the tridimensional polymer is obtained even at the beginning of the process as microgels in which the macroradical mobility is very low and thus, the termination rate constant has low values.

At a conversion of about 30%, due to the high medium viscosity, the propagation reaction begins to be controlled by diffusion too, and thus the process is limited at low conversions. At higher conversions (> 50%) the mass reaction is turned from gel into glassy state. In this state, the termination rate constant by recombination is very low (close to zero), the interruption being preponderantly realized by a unimolecular mechanism, respectively by trapping macroradicals in tridimensional network.

This hypothesis was checked by ESR spectra by means of which long-lived trapped macroradicals were pointed out.

Thus the methyl methacrylate polymerization is a process kinetically controlled and that of polyethylene glycol dimethacrylates is diffusively controlled.

By conducting the thin layer polymerization, the reaction takes place in a different manner, being accompanied by a strong auto-acceleration effect and reaching much higher conversions (figure 2, curve 4). This may be explained by the decrease of diffusion influence upon the process.

The conducting of polymerization process in solvent showed that the reaction takes place with slower rate and higher limited conversions are reached than in the case of bulk polymerization. This may be explained, on the one side, by reaching later the conditions where the constant rate of termination is controlled by diffusion, and on the other side, by swelling the tridimensional network, that facilitates the monomer diffusion towards the increasing macroradicals.

An important influence of the nature of solvent upon the reaction rate has also been found (table 2), fact due to the different power of swelling of tridimensional network.

TABLE 1

Dependence of the polymerization rate and the initial viscosity of monomer on the length of oligomeric chain ; $t = 60°C$, $[PMEC] = 9.8 \times 10^{-3}$ (moles/mole of monomer)

Monomer	Viscosity, [cps/20°C]	Polymerization rate $\times 10^2$, [moles.l^{-1}. min^{-1}]
EGDMA	4.25	1.2417
DEGDMA	7.92	2.2145
TEGDMA	12.08	3.3668
TTEGDMA	18.18	6.2843

TABLE 2

Dependence of the polymerization rate on the nature of solvent. Monomer = ethylene dimethacrylate, $[EGDMA] = 2.65$ moles/l, $[PMEC] = 0.5\%$, $t = 70°C$

Solvent	Polymerization rate $\times 10^2$ [moles.l^{-1}. min^{-1}]
Dimethyl formamide	4.1957
Tetrahydrofurane	3.6438
Ethyl cellosolve	3.0918
Dichloroethane	1.4196
Toluene	1.3118
Benzene	1.2720
Methylene chloride	1.0931
Hexane	0.8502

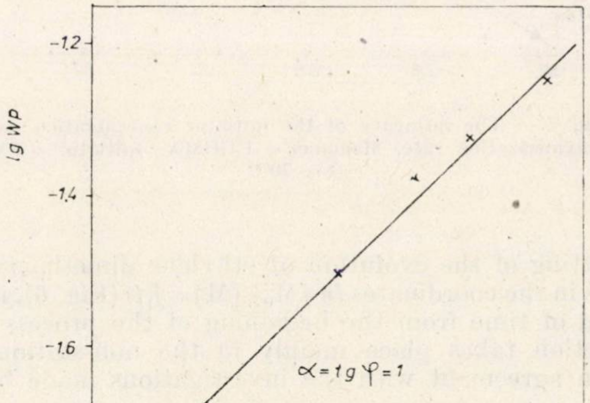

Fig. 4. — The influence of monomer concentration of the polymerization rate. Monomer — EGDMA 50%, Solvent = DMF, $[PMEC] = 1\%$, $t = 70°C$.

Studying the influence of monomer concentration (Fig. 4) and initiator (Fig. 5) upon the initial rate reaction it has been found that this is proportional to the first power of monomer concentration and 0.5 confronted with initiator concentration. This means that in the initial stage, the process is ruled by the same laws as in the case of methyl methacrylate polymerization, respectively:

$$w_p = k[\mathrm{M}][\mathrm{I}]^{1/2}$$

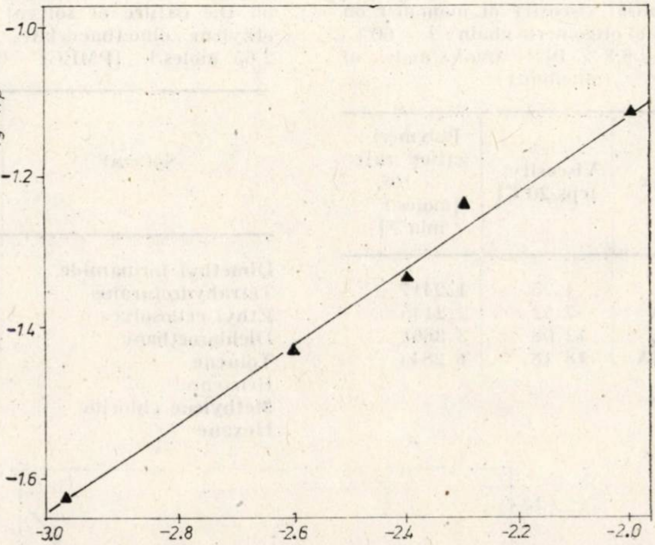

Fig. 5. — The influence of the initiator concentration on the polymerization rate. Monomer — EGDMA, Initiator = PMEC, t = 70°C.

The plotting of the evolution of ethylene dimethacrylate polymerization process in the coordinates $ln\ [M_0]/[M]=f(t)$ (Fig. 6), is liniar only for a short period of time from the beginning of the process; this suggests that the reaction takes place mainly in the non-stationary condition. This fact is in agreement with the investigations made by Tvorogov. [18]

It is also noticed that the period of the process in stationary condition decreases with the increase of monomer concentration.

The study of EGDMA, DEGDMA, TEGDMA and TTEGDMA polymerization process at different temperatures pointed out the strong dependence of the reaction rate on temperature (Fig. 7) and allowed the determination of activation energies of the respective process.

Table 3, shows that tetraethylene glycol dimethacrylate has the lowest activation energy, and this fact proves that the reactivity of these monomers increases with the length of oligomeric chain.

The use of redox systems allowed the conducting of polymerization process at low temperatures. N,N′-dimethyl-1,3-diamino-2-hydroxy-pro-

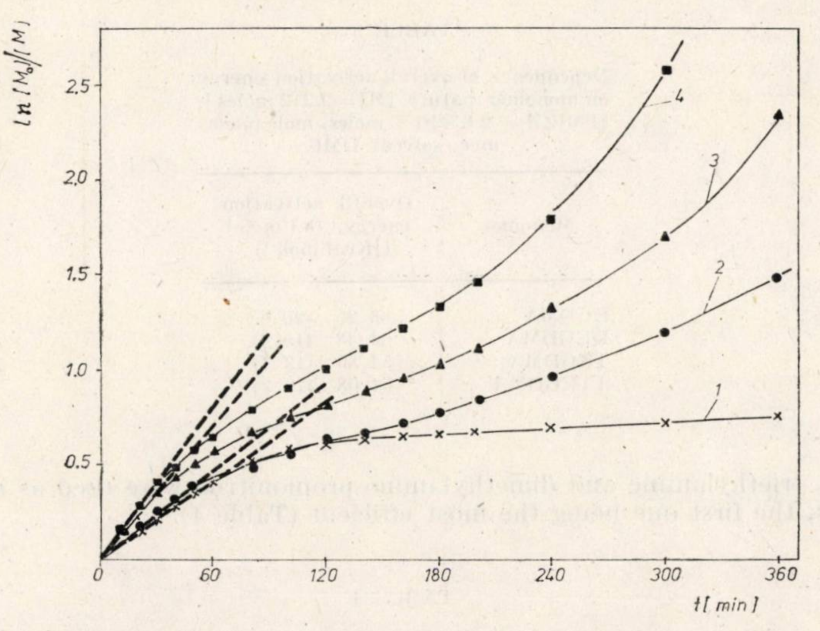

Fig. 6. — Dependence of *ln* $[M_0]/[M]$ with time in EGDMA polymerization, $t = 70°C$, $[PMEC] = 1\%$, Solvent — dimethyl formamide. 1 — $[M_0] =$ 1.3245 moles/l, 2 — $[M_0] = 2.1191$ moles/l, 3 — $[M_0] = 2.6489$ moles/l, 4 — $[M_0] = 3.1787$ moles/l.

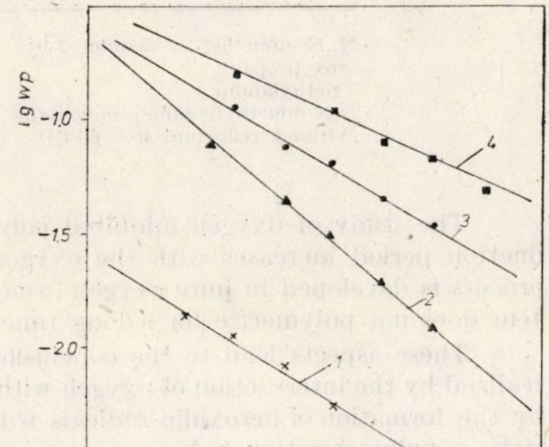

Fig. 7. — Dependence of polymerization rate of polyethylene glycol dimethacrylates on temperature. $[M] = 2.212$ moles/l, $[PMEC] = 9.8 \times 10^{-3}$ moles/mole of monomer, Solvent = dimethyl formamide. 1 — EGDMA, 2 — DEGDMA, 3 — TEGDMA, 4 — TTEGDMA.

TABLE 3

Dependence of overall activation energy on monomer nature. [M] = 2.212 moles/l, [PMEC] = 9.8×10^{-3} moles/ mole monomer, solvent DMF

Monomer	Overall activation energy, [kJ/mole] ([Kcal/mole])
EGDMA	86.25 (20.6)
DEGDMA	64.48 (15.4)
TEGDMA	54.85 (13.1)
TTEGDMA	51.08 (12.2)

pane, triethylamine and dimethylamino-propionitrile were used as reductants, the first one being the most efficient (Table 4).

TABLE 4

Dependence of polymerization rate on the nature of reductants of redox system. [PMEC] = 2 %, t = 40°C, [Reductant] = 5.414 moles/l monomer, Monomer = TEGDMA

Reductant	Polymerization rate × 10^2 [moles.l^{-1}. min^{-1}]
N, N′-dimethyl-1,3-diamino-2-hydroxypropane	2.0413
Triethylamine	1.6267
N,N-dimethyl-amino-propionitrile	1.2860
Without reductant (t = 60°C)	3.3668

The study of oxygen inhibited polymerization showed that the induction period increases with the oxygen concentration (Fig. 8). If the process is developed in pure oxygen atmosphere we can see that the system does not polymerize for a long time.

These aspects lead to the conclusion that the inhibition process is realized by the interraction of oxygen with free radicals, a process followed by the formation of peroxidic radicals with low reactivity, unable to initiate a polymerization act.

As the oxygen addition rate to the growing radical is higher than the monomer addition rate, the polymerization process will begin after the entire amount of the oxygen present in the system has been consumed. IR spectra made on the monomer that has not polymerized in oxygen atmosphere pointed out the existence of peroxidic groups.

The results presented are also in agreement with the kinetic study of inhibited polymerization process made by Korolev[10,11] using the thermometry method.

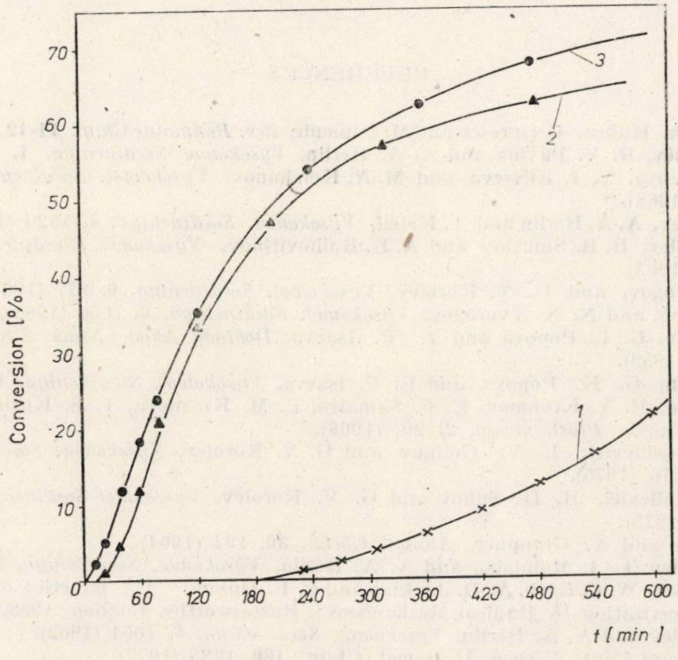

Fig. 8. — The influence of oxygen concentration in the polymerization process of EGDMA. Solvent — dimethyl formamide, [EGDMA] = 2.65 moles/l, [PMEC] = 4.336 × 10^{-2} moles/ l monomer, t = 70°C. 1 — P_{air} = 760 torr, 2 — $P_{\text{air}} = 10^{-1}$ torr, 3 — $P_{\text{air}} = 10^{-2}$ torr.

CONCLUSIONS

1. The study of EGDMA, DEGDMA, TEGDMA and TTEGDMA polymerization process showed that the kinetics of bulk polymerization process depends on the system geometry, in thin layer, the polymerization process taking place after a kinetics similar to methyl methacrylate bulk polymerization and, in thick layer, after a quite different kinetics. These differences are determined by the physical properties of the medium, in thin layer, the polymerization process being kinetically controlled, and in thick layer being diffusive.

2. The initial reaction rate depends on the monomer nature, increasing with the oligomeric chain length.

3. The overall activation energy decreases with the increase of the oligomeric chain length, and this fact demonstrates that the monomer reactivity increases in the same way.

4. In the initial stage, the reaction rate is proportional to the first power of monomer concentration and 0.5 confronted with the initiator concentration and this proves that the process nature is the same and is ruled by the same laws as in methyl methacrylate radical polymerization.

REFERENCES

[1] Part III, Gh. Hubca, C. Oprescu and M. Dimonie, *Rev. Roumaine Chim.* **11-12**, 1493 (1981).

[2] G. V. Korolev, B. V. Pavlov and A. A. Berlin, *Vysokomol Soedineniya*, **1**, 1396 (1959).

[3] E. M. Morozova, V. I. Eliseeva and M. A. Korshunov, *Vysokomol. Soedineniya*, **10**, 2354 (1968).

[4] E. V. Korolev, A. A. Berlin and T. Kefeli, *Vysokomol. Soedineniya*, **4**, 1520 (1962).

[5] G. V. Korolev, B. R. Smirnov and A. B. Bolhovitinov, *Vysokomol. Soedineniya*, **4**, 1660 (1962).

[6] N. N. Tvorogov, and G. V. Korolev, *Vysokomol. Soedineniya*, **6**, 877 (1964).

[7] G. V. Korolev and N. N. Tvorogov, *Vysokomol. Soedineniya*, **6**, 1006 (1964).

[8] A. A. Berlin, G. L. Popova and E. F. Isaeva, *Doklady Akad. Nauk S.S.S.R.* **126**, 83 (1959).

[9] A. A. Berlin, G. K. Popova, and E. F. Isaeva, *Vysokomol. Soedineniya*, **1**, 957 (1959).

[10] A. A. Berlin, R. V. Kronman, E. F. Samarin, L. M. Krasnova, T. S. Kozlova and I. G. Sumin, *Plast. massy*, **2**, 29 (1968).

[11] M. M. Moghilevici, I. V. Golikov and G. V. Korolev, *Vysokomol. Soedineniya*. **A17**, 776 (1975).

[12] M. M. Moghilevici, B. D. Suhov and G. V. Korolev, *Vysokomol Soedineniya*, **A17**, 782 (1975).

[13] R. D. Mair and A. Graupner, *Analyt. Chem.*, **36**, 194 (1964).

[14] G. V. Korolev, L. I. Mahonina and A. A. Berlin, *Vysokomol. Soedineniya*, **3**, 198 (1961).

[15] C. H. Bamford, W. C. Barb, A. D. Jenkins and P. F. Onyon, "The Kinetics of Vinyl Polymerization by Radical Mechanisms", Butterworths, London, 1958, p. 249.

[16] G. V. Korolev and A. A. Berlin, *Vysokomol. Soedineniya*, **4**, 1654 (1962).

[17] Kast Hans and Funk Werner, *Macromol. Chem.*, **180**, 1335 (1979).

[18] N. N. Tvorogov, *Vysokomol. Soedineniya*, **A10**, 2290 (1968).

Revue Roumaine de Chimie, 27, *3*, 443–451 (1982)

CATALYTIC HYDROGEN DISCHARGE BY CYCLOSERINE IN METAL-ION CONTAINING AMMONIA BUFFER

Li QILONG, C. LUCA, A. CĂLUȘARU and F. G. BĂNICĂ,
National Institute of Chemistry, Spl. Independenței No 202, 77208—Bucharest, Romania

Received September 16, 1981

Catalytic hydrogen discharge was studied in ammonia buffer containing cycloserine and Ni^{2+},Zn^{2+}, Cd^{2+} and Cu^{2+} ions. It has been found that the catalytic wave is enhanced in the presence of these ions. There is no essential difference on the species of metal ion, but the half-wave potential of the catalytic wave increases in the above-mentioned order of cations. The effect of the characteristic parameters was studied and it has been concluded that the catalytic wave is very similar to a wave of pre-sodium type. The enhancement of the wave can be explained by the convective transport of the metal ion due to electrolyte streaming as in the case of maxima of the first kind. Cycloserine transport toward the electrode in ligand form also plays an important role.

The heterocyclic compound D-4-amino-3-isoxazolidone is an important substance from the standpoint of its use as an antibiotic. It is called also cycloserine, oxamycine, seromycine or orientomycine. Among these commercial names the first is the widest used.

In a previous work the polarographic properties of the cycloserine in the presence of cobalt ions was studied.[1] Although this compound has a formally simple structure, in the presence of cobalt it shows complex properties in polarography.

In buffer solutions, cycloserine alone forms a catalytic hydrogen wave of the pre-sodium type. In cobalt-containing solution the behaviour of this substance depends strongly on cobalt concentration. At 10^{-5} MCo^{2+} the hydrogen wave produced by cobalt-cycloserine complex is diffusion-controlled and separated from the pre-sodium wave. Within the cobalt concentration range $10^{-5} - 2.5 \times 10^{-5}$ M, the pre-sodium wave is progressively displaced towards more positive potentials and over these concentrations only one wave can be found, which is identical with the so-called Brdička wave. This process was called the "superposition effect of catalytic hydrogen waves";[1] its particular importance for the mechanism of the catalytic hydrogen discharge consists especially in explaining the independence of the Brdička wave of the mercury reservoir height. This apparent independence is due to the composite character of the Brdička wave, which contains a diffusion-controlled and a pre-sodium component. Therefore the invariance of the Brdička wave cannot be ascertained to the kinetic character of the discharge, although the chemical reaction occurs at the same time with, or before the discharge of the proton proper.

The aim of the present work is to study the catalytic hydrogen discharge in ammonia buffer containing cycloserine and metal ions: Ni^{2+}, Cd^{2+}, Zn^{2+} and Cu^{2+}. It has been found that there is no essential difference in the presence of one or another of the above-mentioned ions. In contrast to the Co-containing system, no catalytic hydrogen wave due to metal ion-cycloserine complex forms; as a consequence, the effect of metal ions on the presodium wave can be studied without any interference.

EXPERIMENTAL PART

The purity of cycloserine, determined potentiometrically, was found to be 98 %. The melting point of 154°C and the dissociation constants $pK_{a,1} = 4.45$ and $pK_{a,2} = 7.45$ correspond to the values given in the literature.[2-4] The other substances were of analytical grade.

The polarograms were recorded under nitrogen atmosphere with a LP 7 e polarograph using a cell with a saturated calomel electrode as anode. The constants of the capillary were: $t_1 = 4.60$ s and $m = 2.44$ mg s^{-1} in 0.1 M ammonia buffer, open circuit at $h = 50$ cm.

EXPERIMENTAL RESULTS

1. Effect of metal ion concentration on catalytic hydrogen wave

In 0.1 M NH_3-NH_4Cl solution containing 2×10^{-3} M cycloserine and 10^{-3} M Me^{2+} (Me is Ni, Cd, Zn and Cu), two polarographic waves are formed: (1) a diffusion wave of Me^{2+} reduction and (2) a catalytic hydrogen wave. The half-wave potential of the catalytic wave depends on the nature of Me^{2+} as follows: $E_{1/2,\mathrm{Co}} = -1.72$ V[1]; $E_{1/2,\mathrm{Ni}^{2+}} = -1.87$ V; $E_{1/2,\mathrm{Cd}^{2+}} = -1.91$ V; $E_{1/2,\mathrm{Zn}^{2+}} = -1.92$ V and $E_{1/2,\mathrm{Cu}^{2+}} = -1.96$ V.

In Fig. 1 the polarographic wave of catalytic hydrogen discharge of cycloserine both in the absence and presence of nickel ions is shown. In the absence of nickel (Fig. 1, Curve 1), the catalytic wave is not defined well enough. When the nickel ion concentration increases, the height of the catalytic wave also increases and the corresponding limiting current becomes more clearly defined (Fig. 1, Curve 4). A similar behaviour is observed in the presence of Cd^{2+}, Zn^{2+} and Cu^{2+} ions.

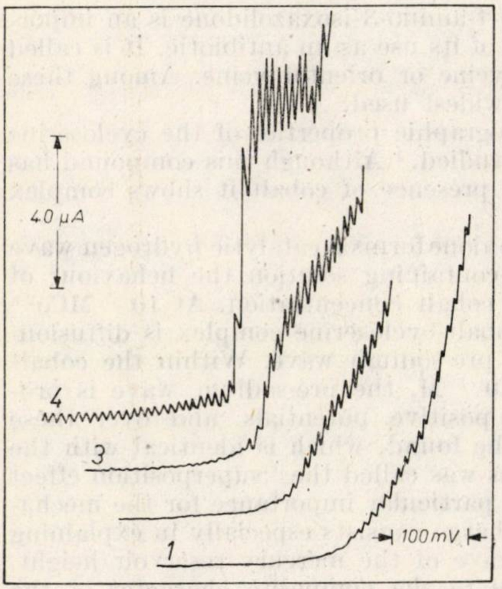

Fig. 1. — Effect of nickel ion concentration on catalytic hydrogen wave of 2×10^{-3} M cycloserine in 0.1 M NH_3-NH_4Cl buffer. Ni^{2+} concentration: *1* — 0; *2* — 8×10^{-5}; *3* — 3×10^{-4}; *4* — 10^{-3} M. Start potential, —1.60 V.

The variation of the catalytic current with nickel ion concentration is shown in Fig. 2. At higher nickel ion concentration, the catalytic current tends towards a limiting value, as in the case of other systems, where this kind of discharge was studied. [5]

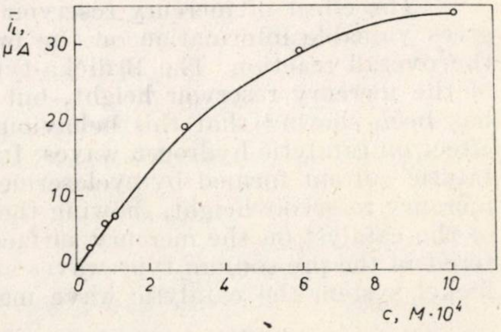

Fig. 2. — Variation of catalytic curren with nickel ion concentration in 0.1 M NH_3-NH_4Cl and 2×10^{-3} M cycloserine.

The catalytic current is enhanced not only by metal ions but also by several non-metallic depolarisers like oxygen, quinone and phenolphthaleine. As in the works of Březina and Kůtova, [6,7] this fact proves the lack of specific effects of complex formation.

2. Effect of cycloserine concentration

One of the most characteristic behaviours of the catalytic currents is that the relationship between the limiting current and the catalyst concentration is not linear. This kind of variation was found also in the present case. In Fig. 3 the variation of the catalytic hydrogen wave with

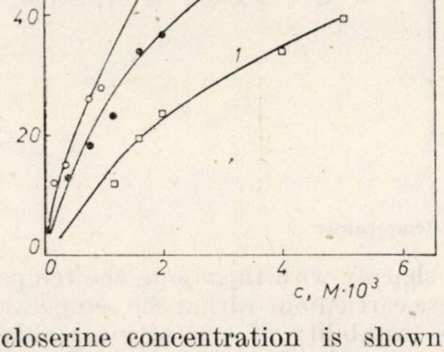

Fig. 3. — Variation of catalytic hydrogen current with cycloserine concentration in 0.1 M $NH_3 - NH_4Cl$ buffer. Ni^{2+} concentration : 1 — 5×10^{-4} ; 2 — 1×10^{-3} ; 3 — 2×10^{-3} M.

cycloserine concentration is shown in 0.1 M $NH_3 - NH_4Cl$ solution at three nickel ion concentrations : (1) 5×10^{-4}M ; (2) 1×10^{-3}M and (3) 2×10^{-3} M. In all cases the height of the catalytic wave increases with the catalyst concentration, but only at higher cycloserine concentrations the current does not vary linearly with this parameter.

3. Effect of mercury reservoir height

The effect of mercury reservoir height on the polarographic waves gives valuable information on the process which is rate determining in the overall reaction. The Brdička-type catalytic waves are independent of the mercury reservoir height, but in the cycloserine-cobalt system it has been shown[1] that this behaviour is produced by the superposition effect on catalytic hydrogen waves. In the presence of nickel ions the catalytic current formed by cycloserine decreases with the increase of the mercury reservoir height, showing the influence of the adsorption process of the catalyst on the mercury surface. This behaviour is always encountered in the pre-sodium type waves and therefore also in the cycloserine-nickel system the catalytic wave may be of this type.

4. Effect of buffer capacity

Since the catalytic wave is formed by the discharge of the proton, the increase of the buffer capacity produces in general a visible increase of this wave height. This behaviour is considered to be one of the most peculiar concerning the catalytic hydrogen discharge. In the case of the cycloserine-nickel system, the variation of the catalytic current with the buffer capacity is given in Fig. 4. The increase of the limiting current with the increase of the buffer capacity shows the determining role of the protonation reaction. The same behaviour was found in cycloserine-cobalt system.[1]

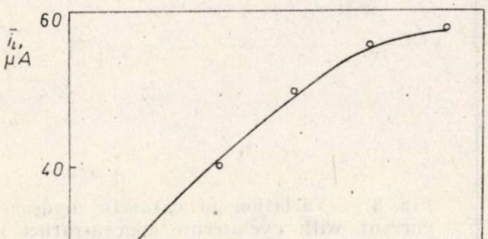

Fig. 4. — Effect of buffer capacity on catalytic wave. $NH_4Cl/NH_3 = 1$; 10^{-3} M Ni^{2+}; 2×10^{-3} M cycloserine.

5. Effect of temperature

The catalytic current increases sharply with the rise in the temperature. Experimental measurements were carried out within the temperature range 25 – 35°C only, owing to the instability of cycloserine at higher temperatures. For this temperature range the temperature coefficient is 10.4 %/°C. This high value is characteristic to the currents where the chemical reaction is the rate-determining step. In the present case the most probable chemical reaction is the protonation of the catalyst. It has been found, the same as in other systems, that the rate of protonation reaction is faster as compared with the catalyst adsorption.[8] However the effect of temperature depends on the cation present in solution. In the same conditions in the presence of Cd^{2+} the height of the catalytic wave reaches a maximum value at 27°C; for the higher temperatures, the wave height decreases. This complex behaviour can be explained by the concurrence of the reaction rate and the rate of adsorption. The latter becomes rate determining over 27°C.

6. Effect of ammonia concentration

In solution of ammonia buffer the increase of NH_3 concentration produces also an increase of the pH. This is why the height of the catalytic wave decreases with the increase of NH_3 concentration. This variations is of a general character in the case of catalytic hydrogen currents.

In Fig. 5 the variation of the limiting current is given as a function of NH_3 concentration. The polarographic catalytic wave decreases sharply in the initial part of the curve and then reaches a low limiting value.

7. Effect of ammonium chloride concentration

The increase of the ammonium chloride concentration results in two effects: (1) the decrease of pH; (2) the increase of the proton donor concentration. Both these effects contribute to increase the height of the catalytic wave. The variation of the catalytic wave in the presence of nickel ions as a function of ammonium chloride concentration is given in Fig. 6. The catalytic current increases with the increase of NH_4Cl concentration and tends to a limiting value for higher concentrations.

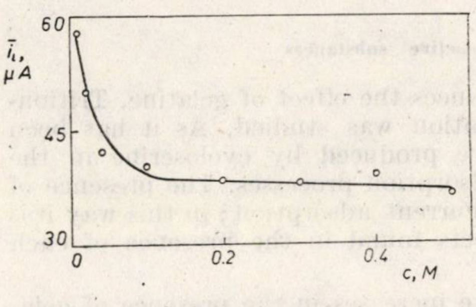

Fig. 5. — Variation of catalytic current with ammonium concentration. Solution: 10^{-3} M Ni^{2+}; 2×10^{-3} M cycloserine; 10^{-1} M NH_4Cl.

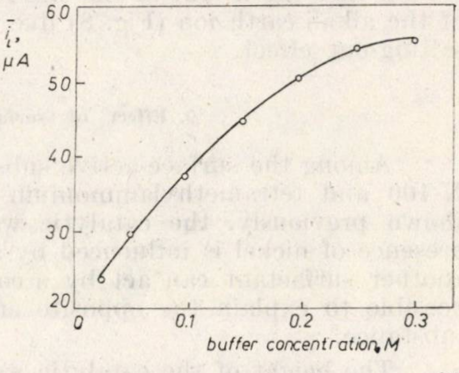

Fig. 6. — Variation of catalytic wave with ammonium chloride concentration. Solution: 10^{-3} M Ni^{2+}; 2×10^{-3} M cycloserine; 10^{-1} M NH_3.

8. Effect of ionic strength

The ionic strength modifies the structure and the pH of the electrical double layer. Therefore the discharge process is influenced by the variation of ionic strength, especially when the catalyst is adsorbed on electrode surface, as it occurs in the case of cycloserine containing system. The variation of the catalytic wave as a function of concentration of several alkali chlorides is shown in Fig. 7. The same variation is shown in Fig. 8 for the alkali-earth chlorides. In the first case (Fig. 7) the character of variation is influenced by the cation species in a rather complex manner. A similar variation has been found in other systems.[1,5] In the second case the height of the wave is increased at higher concentrations of the alkali-earth ion (Fig. 8) due to the increase of adsorption via the salting-out effect.

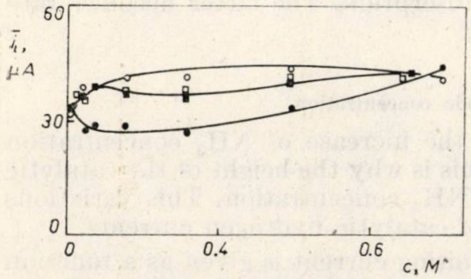

Fig. 7. — Effect of ionic strength on the catalytic wave in the presence of alkali chlorides. Solution : 0.1 M $NH_3 - NH_4Cl$; 10^{-3} M Ni^{2+} ; 2 × 10^{-3} M cycloserine.
○ LiCl ; □ KCl ; ■ NaCl ● CsCl.

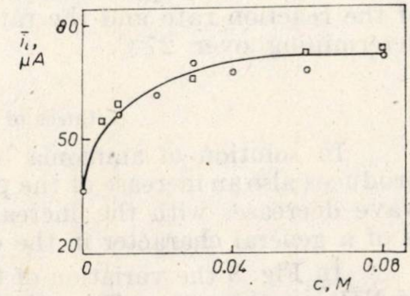

Fig. 8. — Effect of ionic strength on catalytic hydrogen wave in the presence of alkali earth chlorides. Solution : 10^{-1} M NH_3-NH_4Cl ; 10^{-3} M Ni^{2+} ; 2 × 10^{-3} M cycloserine ; ○ $BaCl_2$; □ $CaCl_2$.

9. Effect of surface-active substances

Among the surface-active substances the effect of gelatine, Trition-X-100 and tetramethylammonium cation was studied. As it has been shown previously, the catalytic wave produced by cycloserine in the presence of nickel is influenced by adsorption processes. The presence of another surfactant can act by a concurrent adsorption ; in this way it is possible to explain the opposite effects found in the presence of each substance.

The height of the catalytic wave increases in the presence of gelatine. This means that the cycloserine molecules may be bound by the gelatine which is stronger absorbed at the electrode surface. By this process a higher cycloserine concentration participates in the hydrogen discharge. Unlike the gelatine influence, both Triton and tetramethylammonium ion produce a decrease of the wave height. This effect can be explained by the partial coverage of the electrode surface by the added substance and no binding with the cycloserine molecules. In the presence of tetramethylammonium cation the half-wave potential of the catalytic wave is displaced towards more positive values. It is possible in this case that the character of the current changes by transition from surface into bulk catalytic current.[9]

10. Electrolyte streaming

Electrolyte streaming around the mercurry drop is a salient feature of the pre-sodium wave.[6,7 10,11] As shown by Březina and Kûtova[6,7] the presodium wave is enhanced in the presence of several depolarisers due to convective transport.

In the case of cycloserine electrolyte streaming occurs also, as it was found by microscopical observation in solution containing fine carbon powder. The streaming is directed towards the neck of the drop, like in the case of maxima of first kind. Beside the regular flow, some circular streams were also observed, especially in the equatorial region of the drop. These irregular movements can be due to hydrogen bubbling near the electrode.

DISCUSSION

In aqueous solution the cycloserine behaves as a polyacid[4,12] having the following forms in equilibrium:

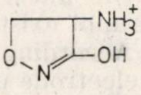

I

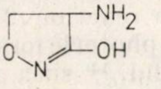

II

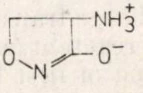

III

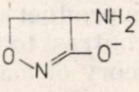

IV

cationic form $CycH_2^+$

amphoteric forms CycH

anionic form Cyc^-

Using the macroscopic dissociation constants the ratio of these forms at pH = 9.4 was found to be:

$$[CycH_2^+] : [CycH] : [Cyc^-] = 1 : 10^5 : 10^7$$

CycH denotes the sum of the forms II and III; their individual concentrations cannot be calculated as the values of the microscopic dissociation constants are not known.

The last two species form the catalytic acid–base couple. The amphoteric form III can be adsorbed on the negatively charged surface and the proton bound to the amino group acts as electron acceptor. Since the equilibrium is strongly displaced to the anionic form, the catalytic wave appears at relatively high cycloserine concentration.

The catalytic hydrogen wave produced by cycloserine in the presence of Ni^{2+}, Zn^{2+}, Cd^{2+}, and Cu^{2+} appears to be of pre-sodium type owing to two reasons: (1) it is located in the very negative potential region; (2) the effect of mercury reservoir height showed the surface character of this wave, as in the case of catalytic hydrogen discharge of pre-sodium type. It has been shown that these waves have also a bulk component [9]; so we can consider both components of such type of wave.

The reaction mechanism can be described by the following reactions, where the subscripts *b* and *s* refer to solution bulk and electrode surface, respectively :

1) The adsorption of amphoteric form III of cycloserine :

$$(\mathrm{CycH})_b \rightarrow (\mathrm{CycH})_s \tag{1}$$

2) Electron transfer and hydrogen evolution :

$$(\mathrm{CycH})_s + e \rightarrow (\mathrm{Cyc}^-)_s + 1/2\ \mathrm{H}_2 \tag{2}$$

3) Desorption of anion form :

$$(\mathrm{Cyc}^-)_s \rightarrow (\mathrm{Cyc}^-)_b \tag{3}$$

4) Protonation of anion form in the bulk of the solution :

$$(\mathrm{Cyc}^-)_b + \mathrm{NH}_4^+ \rightleftarrows (\mathrm{CycH})_b + \mathrm{NH}_3 \tag{4}$$

Now the anphoteric form III can enter again the first step.

As it can be seen in the above mechanism, the anion form which results as a product of charge transfer reaction (2) cannot exist in adsorbed state, in contrast to the reactant (amphoteric form). According to Guidelli's unified theory of maxima of first kind, [14] such an electrode process gives rise to a negative maxima. However, although the electrolyte streaming occurs in agreement with the theory, no maximum can be observed due to the interference of ammonium discharge. Other conclusions of Guidelli's theory are also verified in this case; for instance the decrease of current at higher indifferent electrolyte concentrations and the depressing effect of some surfactants.

In the range of the catalytic wave the total current $\bar{i}_t$ is given in a first approximation by the following expression :

$$\bar{i}_t = \bar{i}_{pw} + \bar{i}_c \tag{5}$$

where $\bar{i}_{pw}$ is the proper catalytic hydrogen current and $\bar{i}_c$ corresponds to convective transport of the depolariser. In the absence of any depolariser the second term vanishes. At constant tangential velocity of the electrolyte, linear increase of i_t with the depolariser concentration must be observed, if the first term does not change. Such a dependence was observed for the catalytic wave of quinine, α-picoline and proteins. [6]

The non-linear dependence observed in the present case can be explained taking into account another effect, namely the transport of the catalyst towards the electrode due to complex formation. Indeed, no concentration gradient of the catalyst is to be expected outside the electrical double layer in the absence of metal ions. If the catalyst is partly bound in a reducible complex, at more negative potentials than the metal ion half-wave potential, the diffusion of this complex increases the catalyst concentration near the electrode as compared with the bulk concentration. In this connection it is interesting to underline that to an increase of the stability of complexes in the series[13]:

$$Cu^{2+} > Zn^{2+} \text{ and } Cd^{2+} > Co^{2+} \text{ and } Ni^{2+}$$

there corresponds the following sequence of half-wave potentials of catalytic wave (absolute values):

$$Co^{2+} < Ni^{2+} < Cd^{2+} \text{ and } Zn^{2+} < Cu^{2+}$$

As it has been previously mentioned for Co^{2+}, [1] the structure of the complexes in the case of Ni^{2+} ion may be of the type:

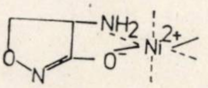

Obviously one or two molecules of cycloserine can be bound in the complex, depending on the pH and ligand concentration.[13]

Taking into account the present results and those previously given,[1] we can infer that the enhancement of the pre-sodium wave in the presence of the metal ions or of other depolarisers is a rather general phenomenon. If the metal ion forms complexes with catalytic properties (for instance cobalt or nickel), the superposition effect can occur. It is necessary to take into account this effect in order to avoid serious errors in the interpretation of the so-called Brdička wave.

REFERENCES

[1] A. Călușaru, *Electrochim. Acta*, **17**, 213 (1972).

[2] C. H. Stammer, A. N. Wilson, F. W. Holly and K. Folkers, *J. Amer. Chem. Soc.*, **77**, 2346 (1955).

[3] L. F. Yakhontova B. P. Bruns, V. D. Kartseva, S. N. Kobzieva and N. A. Perevozokaya, *Antibiotiki*, **14**, 205 (1969).

[4] J. B. Neilands, *Arch. Biochem. Biophys.*, **62**, 151 (1956).

[5] A. Călușaru, *J. Electroanalyt. Chem.*, **151**, 269 (1967); A. Călușaru and V. Voicu, *ibid.*, **43**, 257 (1973).

[6] M. Březina and M. Kůtova, *Coll. Czech. Chem. Comm.*, **30**, 4307 (1965).

[7] M. Březina and M. Kůtova, *Naturwiss.*, **52**, 640 (1965).

[8] M. Korolczuk and J. Matysik, *J. Electroanalyt. Chem.*, **113**, 265 (1980).

[9] S. G. Mairanovskii, "Kataliticeskie i kineticeskie volny v poliarografii", Nauka, Moscow, 1966.

[10] M. von Stackelberg, W. Hans and W. Jensch, *Z. Elektrochem.*, **62**, 839 (1958).

[11] V. Chmelař, M. Březina and V. Kalous, *Coll. Czech. Chem. Comm.*, **28**, 197 (1963).

[12] A. P. Kondrateva, B. P. Bruns and G. S. Libinson, *Khim. Farm. Zhur.*, **5**, 38 (1971).

[13] E. Neusil and J. C. Breton, *Bull. Med. A.O.F.*, **3**, 149 (1958).

[14] R. Guidelli, *J. Electroanalyt. Chem.*, **100**, 711 (1979).

Revue Roumaine de Chimie, **27**, *3*, 453–458 (1982)

UTILIZATION OF CHROMOTROPIC ACID IN SEPARATION OF TITANIUM WITH ION EXCHANGE RESINS. II

ANION EXCHANGE BEHAVIOUR

LUMINIŢA VLĂDESCU and ARIADNA HARLES

National Institute of Chemistry, Laboratory of Analytical Chemistry, Splaiul Independenţei 202, Bucharest, Romania

Received September 29,1980

The experiments of anionic exchange presented in this paper have set the foundation of a new method for the separation of titanium from various elements, and of titanium concentration in dilute solutions in order to perform its quantitative determination.

The cation exchange behaviour of titanium in the presence of Chromotropic acid, discussed in the first part of this contribution,[1] has evidenced the possibility of utilizing cation exchange resins to separate titanium from a series of ions which interfere in its spectrophotometric determination with reagent under study.

Since the complex combinations titanium – Chromotropic acid are anionic, it is relevant to find out how they behave in the presence of an anion echange resin.

The experiments of anionic exchange presented here have set the foundation of a new method for separation of titanium from various elements and of titanium concentration in dilute solutions in order to perform its quantitative determination.

RESULTS AND DISCUSSION

To establish the optimal working conditions, a study has been undertaken of het influence exerted by Chromotropic acid concentration, by the pH and by the ionic form of the resin on the anionic exchange behaviour of titanium.

Thus small volumes of solution containing known constant amounts of TiO^{2+} and variable amounts of Chromotropic acid at $pH = 1.5$ were passed through the column with Amberlite IRA – 400 anion exchange resin in Cl^- or Chromotropic acid ionic form. After washing the resin with solution of Chromotropic acid of the same concentration as that in the solution to be analyzed and $pH = 1.5$, the amount of titanium not retained by the anion exchange resin was determined.

TABLE 1

Influence of Chromotropic acid concentration and pH upon the anion exchange behaviour of titanium, iron and chromium

Resin		Chromotropic acid		pH	Ti(IV)			Fe(III)			Cr(IV)		
Type	Ionic form	Conc. M	Volume (cm^3)		In sample (mg)	Determined		In sample (mg)	Determined		In sample (mg)	Determined	
						in R (gm)	in S (mg)		in R (mg)	in S (mg)		in R (mg)	in S (mg)
Amberlite IRA-400	Cl^-	10^{-2}	10	1.5	0.288	0.286	—	0.112	—	0.110	0.520	—	0.518
		10^{-3}	10	1.5	0.288	0.290	—	—	—	—	—	—	—
	Chr.$^{2-}$	5×10^{-4}	10	1.5	0.288	0.256	0.030	—	—	—	—	—	—
		10^{-2}	30	1.5	0.288	0.286	—	0.112	—	0.113	—	—	—

Note: R = resin ; S = solution

Examination of table 1 shows that titanium is quantitatively retained by anionite no matter what the ionic form of the resin and the concentration of reagent on condition that it is present in amounts that ensure the quantitative formation of anionic complex combination of titanium with Chromotropic acid.

Fig. 1. — Anion exchange behaviour of Ti(IV), Cr(VI) and Fe(III).

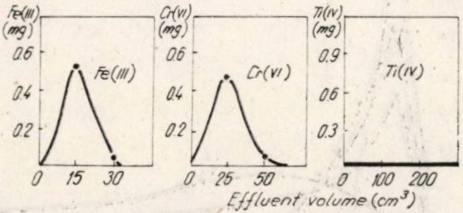

The anion exchange behaviour of iron and chromium was studied under the same working conditions. Data presented in table 1 and Fig. 1 show that these elements pass into the effluent when titanium is retained in the column.

To establish the conditions of elution of titanium from anionite, solutions of various concentrations of H_2SO_4, Na_2SO_4, $HClO_4$, $NaClO_4$ and HCl were employed. Table 2 and Fig. 2 show that besides H_2SO_4 and Na_2SO_4 which could not elute titanium, all the other eluants are equally suitable. From among them the most efficient are 1 M $HClO_4$ and 4 M HCl. Utilization of more dilute solutions requires large eluent volumes which yields dilute titanium solutions.

TABLE 2

Establishment of elution conditions for titanium retained by anionite in the presence of Chromotropic acid

Amount of titanium in sample (mg)	Eluent			Amount of titanium eluated (mg)
		conc. M	volume cm³	
0.288	$NaClO_4$	0.1	325	0.289
	$NaClO_4$	0.2	200	0.287
	$NaClO_4$	1.0	120	0.286
	$HClO_4$	0.5	80	0.286
	$HClO_4$	1.0	50	0.287
	HCl	1.0	100	0.289
	HCl	4.0	75	0.286
	H_2SO_4	1.0	175	—
	Na_2SO_4	1.0	200	—

Molecular absorption spectra in Fig. 3 evidence elution of titanium from anionite as a Chromotropic acid complex with $HClO_4$; this is a proof of the high stability of the complex formed.

Thus, the anion exchangers may also be used in separation of titanium from other elements in the presence of Chromotropic acid.

The method of ionic exchange was applied at first on binary mixtures Ti(IV) – Fe(III) and Ti(IV) – Cr(VI) (Fig. 4) and then on complex mixtures.

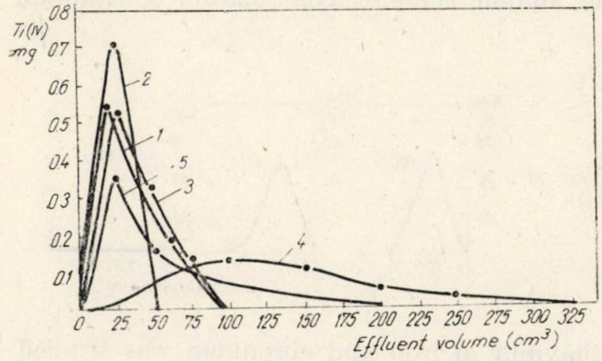

Fig. 2. – Elution of titanium retained in an anion exchange resin, with some eluent agents: 1. $HClO_4$ 0.5M; 2. $HClO_4$ 1M; 3. HCl 4M; 4. $NaClO_4$ 0,1M; 5. $NaClO_4$ 0.2M.

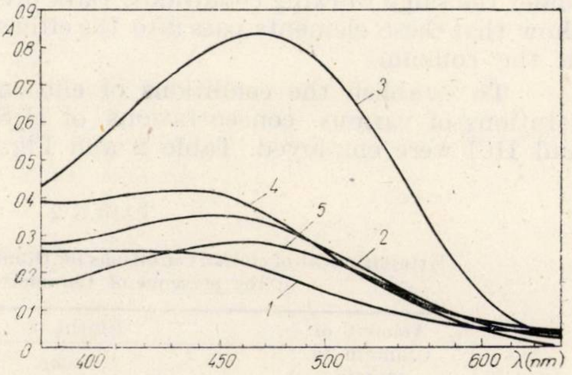

Fig. 3. – Molecular absorption spectra. 1. Standard solution Chromotropic acid + $HClO_4$
2. Standard solution Ti + Chromotropic acid + $HClO_4$
4. Effluent solution: Chromotropic acid.
3,5. Effluent solutions: Ti - Chromotropic acid complex + $HClO_4$

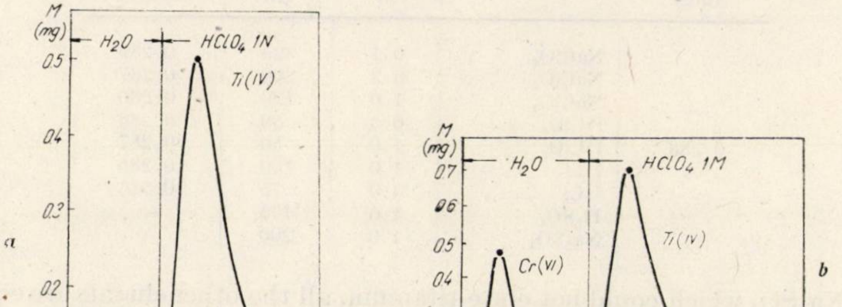

Fig. 4. – Elution curves: *a*) Ti(IV) – Fe(III) separation; *b*) Ti(IV)–Cr(VI) separation.

The results of titanium determination with Chromotropic acid after Cr(VI) and Fe(III) separation with anion exchanger are presented in table 3. A good agreement between titanium amounts taken in the sample and determined after separation is observed.

TABLE 3

Results of titanium separation from iron (III) and chrcmium (VI) with anion exchange resins

	In sample (mg)	0.043	0.960	4.340	9.600
Ti (IV)	Determined after separation (mg)	0.040	0.957	4.336	9.598
	Determined without separation (mg)	0.120	1.265	6.119	12.678

Finally, the two procedures with cation and anion exchangers were applied to determine quantitatively titanium in solutions obtained by desintegration with potassium pyrosulphate of some synthetic rutile samples. The results are listed in table 4 and agree to those yielded by classical analysis.

TABLE 4

Results of titanium separation and determination in synthetic rutile samples

Rutile sample		Titanium content			
		Cationic exchange procedure		Anionic exchange procedure	
No.	Amount (g)	Ti (%)	TiO_2 %	Ti %	TiO_2 %
1	0.5243	51.0 50.8	85.0 84.6	50.9 51.1	84.7 85.1
2	0.5002	49.8 49.6	83.0 82.6	49.9 50.0	83.2 83.3

CONCLUSIONS

Utilization of ion exchange resins and Chromotropic acid allows quantitative determination of titanium in samples in which it coexists with Fe (III), Cr (III), Zr (IV), Ce(IV), U(VI) and Cr (VI).

The cationic exchange procedure is suitable for samples of high titanium and low interfering elements content, while the anionic exchange procedure for samples of low titanium content in which case its separation and concentration are allowed.

The Chromotropic acid serves both as complexing agent allowing separation of titanium from interfering elements and as colour reagent making possible the spectrophotometric determination of titanium by measurements of absorbance of solution after it was passed through the column with resin.

REFERENCES

[1] L. Vlădescu and A. Harles, *Rev. Roumaine Chim.*, **27**, 305 (1982).

Revue Roumaine de Chimie, **27**, *3*, 459–465 (1982)

EXTRACTION, COMPLEXING AND DETERMINATION OF PHENYL-MERCURIC ION WITH DIAZOAMINOBENZENE

A. F. DĂNEŢ and ANCA MARIANA BERCARU

Department of Analytical Chemistry, Faculty of Chemical Technology, Polytechnic Institute, Splaiul Independenţei, 202, Bucharest, Romania

Received July 31, 1980

The phenyl-mercuric ion forms with diazoaminobenzene a complex with a 1/1 combination ratio and a stability constant of 5.5×10^{12}. The partition constants of the reagent and mercury complex in the benzene – 0.2 M sodium acetate aqueous solution system are 2.7×10^5 and 3.6×10^4, respectively. The extraction constant of the complex in benzene is 0.6. The complex molar absorbance is 1.54×10^4 l mol^{-1} cm^{-1} at 410 nm. The Lambert-Beer law is obeyed within the 1 – 35 μg $C_6H_5-Hg^+$/ml range. Ag(I), Hg(II), Hg_2(II), Mn(II), Cl^-, Br^-, I^-, MnO_4^-,EDTA, CN^- and SCN^- interfere on determining phenyl-mercury with diazoaminobenzene.

Mercury in the biosphere is a pollutant with peculiar properties. Due to the high volatility of most of its compounds it can easily disperse into the environment. During a series of biochemical processes, mercury can also be turned from inorganic products into organo-mercuric ones, the latter being much more toxic. [1,2] So far, only a few analytical methods are known to allow the quantitative determination of the mercury content in its different inorganic or organic forms. Most of the analytical methods proposed for determining this element indicate the overall mercury content in the studied sample. [3–5] The analytical methods permitting a discrimination among different forms in which mercury is found are especially the chromatographic ones, [6–9] but there are also other methods that may be used for this purpose. [10,11] As the diazoamino compounds react quite selectively with mercury (II), a series of determination methods using this type of reagents have been proposed. [12–14] In order to elaborate a method for phenyl-mercuric ion determination, its reaction with diazoaminobenzene has been studied.

EXPERIMENTAL PART

Reagents and apparatus

Phenyl-mercuric acetate (Merck) solution with titre 68 μg phenyl-mercury/ml in distilled water. Solution of 0.1 % diazoaminobenzene in benzene and alcohol.

2 M sodium acetate solution in distilled water.

The absorption spectra were carried out on a Specord UV—VIS Carl Zeiss Jena spectrophotometer and the absorbance determinations at a fixed wavelength were carried out on a VSU-2G Carl Zeiss Jena spectrophotometer.

The pH determinations were made with a Radelkis OP—208 apparatus.

Procedure

In 50 ml graduated cylinders, each provided with a groundglass stopper, the following quantities are introduced: 1 ml sodium acetate solution, different amounts from the solution containing the phenyl-mercuric ion and 3 ml of 0.1% reagent in alcohol solution. The volume is brought to 10 ml with distilled water, the solution thus obtained being then homogenized. After a reaction time of 5 minutes, the formed complex is extracted in 10 ml benzene, by shaking the phases for 1 minute. After a complete separation of the phases (10 minutes), a portion is taken with a dry pipette from the organic phase and is introduced into the measurement cell of the spectrophotometer. Similar results are obtained when, after introducing into the graduated cylinders 1 ml sodium acetate solution and the solution containing the phenyl-mercuric ion and bringing to 10 ml with distilled water, the extraction is done with 10 ml of 0.03% reagent solution in benzene, by shaking the phases for two minutes.

Determination of reagent and mercury complex solubilities both inorganic and aqueous phases

A 0.2 M sodium acetate aqueous solution was stirred mechanically for 2 hours with benzene and diazoaminobenzene, or its complex with the phenyl-mercuric ion, in excess in the solid state. The phases were separated and filtered. Since the molar absorbances of the reagent and of its complex with the phenyl-mercuric ion can be different in the two phases the absorbance measurements were carried out only in the organic phase, the reagent or the phenyl-mercuric complex, dissolved in the aqueous phase, being reextracted in benzene. Taking into account the absorbances measured at wavelengths corresponding to the absorption maxima and the molar absorbances of the reagent and of its complex with the phenyl-mercuric ion, their solubilities in the two phases were determined.

Determination of the NH group formation constant in the reagent molecule

A saturated reagent solution was prepared in a 0.2 M sodium acetate solution containing 8% alcohol (in volume). The reagent had an absorption maximum at 363 nm and the resulting anion at 394 nm. From the obtained values, the NH group formation constant was determined, being found equal to the pH value at which the anion concentration is the same with the non-dissociated reagent concentration.

RESULTS AND DISCUSSION

In Figure 1, the absorption spectra are presented for a 1.5×10^{-4} M solution of reagent extracted in benzene (curve 1) and for some solutions containing the same reagent amount and increasing quantities of phenyl-mercuric ion: 2.2×10^{-5} M(2), $3,7 \times 10^{-5}$ M (3), 7.4×10^{-5} M (4), 1.1×10^{-4}M (5), $1,5 \times 10^{-4}$ M (6). As it can be seen, the reagent has an absorption maximum at 357 nm and the mercury complex at 395 nm. The subsequent absorbance determinations were carried out at 410 nm, a wavelength at which the reagent has a low absorbance. On examining these spectra, it comes out that a single isosbestic point appears, this fact suggesting the formation of a single complex between the reagent and the phenyl-mercuric ion, extracted in the organic phase. The thick curve presents the absorbance variation at a 395 nm wavelength as a function of the phenyl-mercury/reagent ratio. The formation of a 1/1 combination ratio compound is observed.

The phenyl-mercury compound is quantitatively extracted within a pH domain of 6 — 9. At a pH value lower than 6, a decrease of the complex extractability takes place. At the same time a partial decomposition of the reagent occurs, leading to the formation of coloured compounds which are extracted in benzene and disturb the determinations.

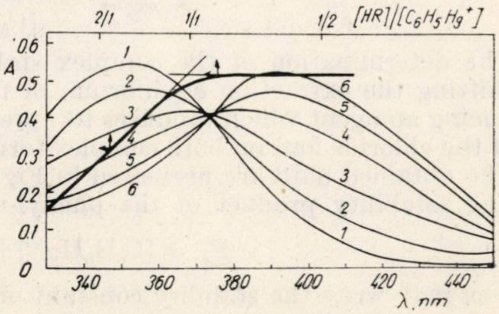

Fig. 1. — Spectra of some benzene extracts containing 1.5×10^{-4} M reagent and the following quantities of phenyl-mercuric ion : *1* — 0 ; *2* — 2.2×10^{-5} M ; *3* — $3,7 \times 10^{-5}$ M ; *4* — 7.4×10^{-5} M ; *5* — 1.1×10^{-4} M ; *6* — 1.5×10^{-4} M. The thick curve represents the absorption variation at 395 nm as a function of $C_6H_5Hg^+$/reagent ratio.

The stability in time of the complex solution in benzene is good, only insignificant variations of the absorbance being recorded over an interval of several tens of hours.

In order to express quantitatively the equilibria occurring on phenyl-mercuric ion extraction with diazoaminobenzene, we start from the following theoretical considerations. We denote the reagent molecule by HR, the formation constant of the NH group in reagent molecule being given by :

$$K_{HR} = \frac{[HR]}{[H^+]\,[R^-]}$$

and the partition constant of the reagent by :

$$P_{HR} = \frac{[HR]_0}{[HR]}$$

We consider that the complex extraction takes place according to the following reaction (the compounds in the organic phase have an index "0") :

$$C_6H_5Hg^+ + (HR)_0 \rightleftharpoons (C_6H_5HgR)_0 + H^+ \tag{1}$$

The extraction constant of the complex is expressed as :

$$K_{ext} = \frac{[C_6H_5HgR]_0[H^+]}{[C_6H_5Hg^+]\,[HR]_0} \tag{2}$$

We consider that the complex compound formation in an aqueous medium takes place according to the equilibrium :

$$C_6H_5Hg^+ + R^- \rightleftharpoons C_6H_5HgR \tag{3}$$

with the stability constant:

$$\beta = \frac{[C_6H_5HgR]}{[C_6H_5Hg^+][R^-]} \tag{4}$$

and the partition constant:

$$P_{complex} = \frac{[C_6H_5HgR]_0}{[C_6H_5HgR]} \tag{5}$$

The determination of the complex stability constant was performed by shifting the extraction equilibrium of the phenyl-mercuric ion, on introducing an agent which produces its precipitation. To do so, the influence of the chloride ions on both complex formation and extraction was pursued (the obtained data are presented in Figure 2).

The solubility product of the phenyl-mercury chloride is [15]:

$$P_s = [C_6H_5Hg^+]\,[Cl^-] = 10^{9,3} \tag{6}$$

One may write the stability constant of the mercury complex as:

$$\beta = \frac{[C_6H_5HgR]_0\,[H^+]\,K_{HR}}{P_{complex}\,[HR]\,[C_6H_5Hg^+]} = \frac{P_{HR}\,K_{HR}[H^+]\,[C_6H_5HgR]_0}{P_{complex}\,P_s\,[HR]_0}\,[Cl^-] \tag{7}$$

We denote by "A" the above constant values:

$$A = \frac{P_{HR}\;K_{HR}\;[H]^+}{P_{complex}\;P_s} \tag{8}$$

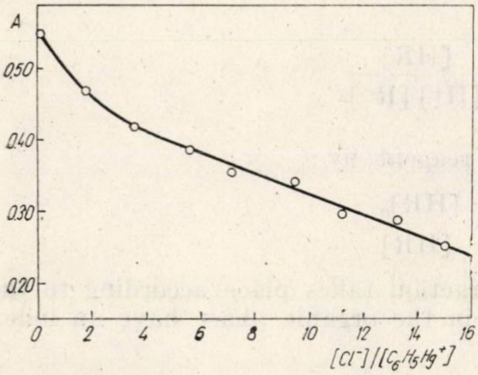

Fig. 2. – Absorbance variation of the complex of phenyl-mercury with diazoaminobenzene, extracted in benzene as a function of $[Cl^-]/[C_6H_5Hg^+]$ ratio.

and subsequently:

$$\frac{[HR]_0}{[C_6H_5HgR]_0} = \frac{A}{\beta}\,[Cl^-] \tag{9}$$

Plotting $[HR]_0/[C_6H_5HgR]_0$ as a function of chloride ion concentration, we obtain a straight line whose slope is the A/β ration (Fig. 3).

To obtain the stability constant, β, a determination of the partition constant values of both reagent and complex was necessary, as they enter in the "A" value given by relation (8). They were calculated from the ratio between the reagent and mercury complex solubilities in the two phases, taking into account that, for low solubilities of a compound, the partition constant is given by the ratio of the compound solubilities in the two phases.

In Table 1, the solubilities and partition constants of both reagent and mercury complex are listed.

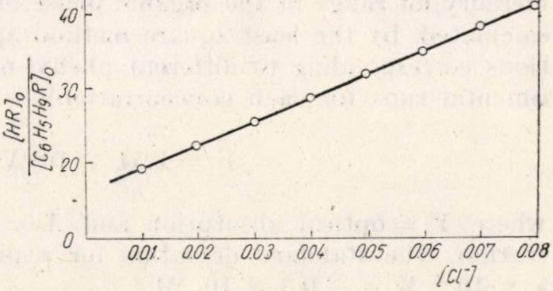

Fig. 3. — Variation of $[HR]_0/[C_6H_5HgR]_0$ ratio as a function of Cl^- ion concentration.

TABLE 1

Solubility and partition constants of diazoaminobenzene and of its complex with the phenyl-mercuric ion in benzene — 0.2 M sodium acetate system

Compound	Solubility in aqueous phase M	Solubility in organic phase M	Partition constant
Diazoaminobenzene	2.0×10^{-6}	5.4×10^{-1}	2.7×10^{5}
Complex with phenyl-mercury	3.0×10^{-8}	1.1×10^{-3}	3.6×10^{4}

The formation constant of the NH group in the reagent molecule has a value of $K_{HR} = 10^{12.1}$. The experiments were carried out at $pH = 7$ in the aqueous phase. From these data, the value of the complex stability constant, $\beta = 5.5 \times 10^{12}$, and extraction constant, $K_{ext} = 0.6$, were calculated.

Kuzmina et al.[16] synthetized the compound formed by the phenyl-mercuric ion with 2-chloro-diazoaminobenzene and determined by X-ray diffraction the elementary cell parameters. We consider that the phenyl-mercuric ion forms with diazoaminobenzene a similar compound, which can be represented as:

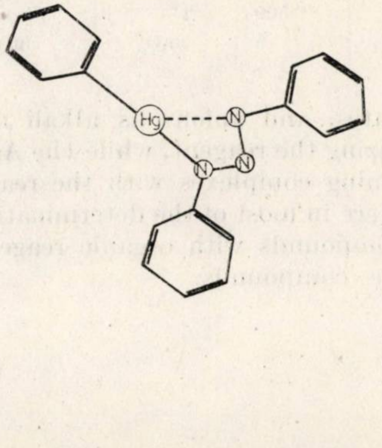

We have proposed a method for determining the phenyl-mercuric ion by studying the extraction equilibria and its complexing with diazoaminobenzene. The experiments were carried out according to the given procedure. A linear dependence was obtained for the absorbance as a function of phenyl-mercury concentration within the 1 – 36 μg phenyl-mercury/ml range in the organic phase. The calibration curve equation, calculated by the least square method applied to 5 series of determinations corresponding to different phenyl-mercury concentrations (9 experimental runs for each concentration), is :

$$Y = 1.54 \times 10^4 X - 0.042$$

where Y = optical absorption and X = phenyl-mercury molar concentration. The standard deviation for a phenyl-mercury concentration of 5×10^{-5} M is $\pm 0.3 \times 10^{-2}$M.

The influence of several ions on phenyl-mercuric ion determination with diazoaminobenzene was studied. It was considered that an ion does not interfere when, at a maximum admitted ion/$C_6H_5Hg^+$ ratio, it causes an error lower than 5% on determining mercury concentration. The influence of some anions and cations on phenyl-mercuric ion determination with the studied reagent is presented in Table 2. The cations were used as nitrates or sulphates, and anions as alkali metal salts. The MnO_4^- ion interferes by oxidizing the reagent, while the Ag(I) Hg(II) and Hg_2(II) ions interfere by forming complexes with the reagent. The CN^-, SCN^- and EDTA ions interfere in most of the determination methods of mercury or organomercuric compounds with organic reagents, by forming either precipitates or stable compounds.

TABLE 2

Influence of some ions on phenyl-mercuric ion determination with diazoaminobenzene

Ion	Maximum admitted ion/$C_6H_5Hg^+$ ratio	Ion	Maximum admitted ion/$C_6H_5Hg^+$ ratio
Cu(II)	500	Co(II)	500
Be(II)	1000	Ni(II)	500
Mg(II)	1000	Hg(II)	interfere
Ca(II)	1000	Hg_2(II)	interfere
Sr(II)	1000	Mn(II)	interfere
Ba(II)	1000	Ag(I)	interfere
Zn(II)	500	Cl^-	interfere
Cd(II)	500	Br^-	interfere
Pb(II)	500	I^-	interfere
Fe(II)	5	MnO_4^-	interfere

CONCLUSIONS

The phenyl-mercuric ion forms with diazoaminobenzene a stable complex with a 1/1 combination ratio and a 5.5×10^{12} stability constant as determined from the influence of the chloride ions on the complex extraction. A value of 2.7×10^5 was determined for the reagent partition constant and a value of 3.6×10^4 for that of the phenyl-mercuric complex, in the benzene —0.2M sodium acetate solution system. Diazoaminobenzene allows the phenyl-mercuric ion determination with a good sensibility and selectivity. The molar absorbance of the complexe is 1.54×10^4 l mol^{-1} cm^{-1} at 410 nm. Among the studied ions, only Ag(I), Hg(II) and Hg_2(II) ions form stable complexes with diazoaminobenzene under the given procedure. The interference of other ions is due to either reagent decomposition, or precipitation by turning the phenyl-mercuric ion into stable complexes. The method can be applied for phenyl-mercuric ion determination in waste waters.

REFERENCES

[1] P. A. D'Itri and F. M. D'Iitri, "Mercury Contamination", Wiley, New York 1977, p. 227.
[2] J. M. Wood, F. S. Kennedy and C. G. Rosen, *Nature*, **220**, 173 (1968).
[3] H. Ayemian and A. S. Y. Chan, *Analyt. Chem.*, **50**, (1978).
[4] C. Luca, A. F. Dăneţ and M. Tărăbîc, *Rev. Chim. (Bucureşti)*, **30**, 260 (1979).
[5] R. A. Nicholson, *Analyst*, **102**, 399 (1977).
[6] Westoö, *Acta Chem. Scand.*, **22**, 2277 (1968).
[7] C. A. Bache and D. J. Lisk, *Analyt. Chem.*, **43**, 950 (1971).
[8] I.O.G. Tatton and P. J. Wagstaffe, *J. Chromatog.*, **44**, 284 (1969).
[9] P. Zarnegar and P. Mushak, *Analyt. Chim. Acta*, **69**, 389 (1974).
[10] R. J. Baltisberger and C. I. Knudson, *Analyt. Chim. Acta*, **73**, 265 (1974).
[11] J. C. Gage, *Analyt.* **86**, 457 (1961).
[12] Gr. Popa, A. F. Dăneţ and M. Popescu, *Talanta*, **25**, 546 (1978).
[13] A. F. Dăneţ and M. Tiron, *Rev. Chim. (Bucureşti)*, **30**, 376 (1979).
[14] A. F. Dăneţ, R. Dreptu and Gh. Nicolae, *Rev. Roumaine Chim.*, **24**, 1229 (1979).
[15] T. D. Vaugh, H. F. Walton and J. A. Laswick, *J. Phys. Chem.*, **59**, 395 (1955).
[16] L. G. Kuzmina, Y. U. T. Struktov and D. N. Kravtsov, *Zhur. strukt. Khim.*, **20**, 522 (1979).

Revue Roumaine de Chimie, 27, 3, 467 –468 (1982)

COMPTES RENDUS

ELENA CEAUȘESCU, *"Noi cercetări în domeniul compușilor macromoleculari"*. (Recent Research, in the Field of Macromolecular Compounds), Editura Academiei, Bucharest, 1981, 535 pages.

The collection in one volume of the scientific research papers carried out during the 1976–1981 period under the direction and guidance of Doctor Engineer Elena Ceaușescu, member of the Academy of the Socialist Republic of Romania, in the field of macromolecular compounds, is an editorial event of particular interest. This book is a sequel to the studies published by the Academy Publishing House in 1974 ("Research Workon the Synthesis and Characterization of Macromolecular Compounds. Contributions") and in 1979 ("Stereospecific Polymerization of Isoprene") by the same author.

The forty-two papers in the present volume are grouped into 6 chapters:

Chapter I – Polymers synthesized in solution with complex catalysts (12 papers)
Chapter II – Polymers synthesized in solution with lithium-based catalysts (7 papers)
Chapter III– Polymers synthesized by polycondensation (3 papers)
Chapter IV – Modified polymers (6 papers)
Chapter V – Relationships between structure and properties (9 papers)
Chapter VI – The characterization of polymers (5 papers)

Abstracts in English and Russian complete the volume.

The papers concern classical polymers having elastomer properties (polyisoprene, polybutadiene and ethene-propene-diene copolymers) and also modern elastomers (polypentenamer obtained by ring-opening polymerization of cyclopentene).

The first chapter includes investigations having in view the improvement of technologies for obtaining classical elastomers and the development of original technologies for modern elastomers. Modern physical methods (paramagnetic electronic resonance, electrical conductibility) were applied for the characterization and optimization of Ziegler-Natta catalysts used in the syntheses. In order to reduce the experimental effort and optimize the results, the procedure consisted of experiments planned on the basis of a factorial programme.

Chapter II contains papers describing the polymerization and copolymerization of butadiene and isoprene with lithium-based catalysts, having an anionic mechanism.

Sensitive experimental methods (kinetic studies, isothermal calorimetry, viscometry) and also refined theoretical methods (mathematical modelling with mono- and diparametric models based on computer programs) are used.

The structures of the elastomers discussed in chapter 3, obtained by polycondensation, differ from those of the previous chapters. They belong to the class of thiocols with special utilization, and polyesters for polyurethanes.

Chapter 4 describes the behaviour of polyisoprene elastomers under the action of Lewis acids, leading to the formation of cyclised rubber, and also the degradation and substitution reactions of ethene-propene copolymers under the action of the same agents.

Since these researches have a practical aim, that of obtaining elastomers with properties consistent with their utilization, the study of the relationships between the chemical structure of polymers and their elastomer properties is of foremost importance. Chapter V dwells on the relationships between the properties of polymers and the way of obtaining them as reflected in the polymer structure. The rheological, physico-mechanical, optical etc. properties of the polyisoprene, polybutadiene and ethylene-propylene rubber are discussed as well as those of other polymers (antishock grafted polystyrene, thermoplastic butadiene-styrene block-copolymers, rigid polyurethane foams) in terms of the kinetics and reaction mechanisms applied for obtaining them.

The last chapter deals with the methods for the analysis and characterization of copolymers. Determination of the molecular mass by viscosimetry, light diffusion and ultracentrifugation are discussed. The conclusions that can be drawn from the roentgenographical study of polypentenamer are considered, together with a method and an apparatus for the study of the stability of polymers with regard to the action of oxygen in the air.

In conclusion, the grouping into one volume of the works of Acad. Dr. Eng. Elena Ceaușescu carried out in the course of five years and presented at scientific meetings or published in the scientific literature reveals the amplitude and importance attributed to scientific research in Romania and the way in which scientific research merges with the implementation of results. This collection successfully presents the intensity of Romanian scientific research in the field of macromolecular chemistry.

Alexandru T. Balaban

GH. LUPUȘOR, E. MERICĂ and C. GOREA, *Ingineria sintezei intermediarilor aromatici. Procese fundamentale.* 2 (Engineering of the synthesis of aromatic intermediates. Basic processes), Ed. Tehnică, București, 1981, 419 pages.

This is a welcome addition to the chemical engineering literature covering the most important aspects in the synthesis of aromatic intermediates as reagents in organic industry. The book presents new and current concepts in the mentioned field and it can be used by technologists, organic chemists or workers in related areas of aromatic intermediates research without requiring extensive supplementary reading.

The book is based on a very rich bibliography; the authors have selected about a thousand articles and patents published in the field. All the collected data were excellently organized in a comprehensive manner in 8 chapters – halogenation, nitration, sulfonation, alkylation, amination by reduction, acylation of aromatic amines, oxidation and esterification.

The complex aspects of the synthesis of aromatic intermediates are approached by joining the elements of chemical reaction engineering and technological problems. Thus, each chapter contains data concerning the catalysts and agents used for the mentioned unitary chemical processes. Particular attention is paid to the thermodynamic and kinetic features, while factors influencing the process development are treated in detail. The numerous thermodynamic and kinetic data given are of real use for process design and development. Some new aspects in aromatic intermediates synthesis like dealkylation, electrolytic reduction or ammonolytic oxidation are treated on the basis of the most up-to-date information in the field.

The book is also completed with a subject index.

This work is highly recommended for chemists involved in the chemistry and technology of aromatic intermediates and it is of real interest and use for students whose major field is organic technology.

Victor Bulacovschi

NOTE POUR LES AUTEURS

La Revue Roumaine de Chimie publie des articles en anglais, français, russe, allemand ou espagnol. Les auteurs sont priés d'envoyer des articles et des comptes rendus inédits.

Les manuscrits seront dactylographiés à double interligne. La bibliographie, les tableaux et la légende des figures seront placés après le texte.

Si l'article fait partie d'une série numérotée, la partie précédente sera donnée comme première référence.

Chaque article sera précédé d'un résumé comprenant quinze lignes au maximum.

Les références bibliographiques dans le texte seront faites par des exposants sans parenthèses et paraîtront à la fin de l'ouvrage.

Les publications périodiques mentionnées dans la bibliographie seront présentées suivant les prescriptions internationales ; le nom de l'auteur précédé de l'initiale du prénom, le titre du périodique abrégé conformément à « Chemical Abstracts » et souligné par une ligne, le numéro du tome indiqué par des chiffres arabes et souligné par deux lignes, suivi de la première page de l'article : à la fin, l'année de la parution sera placée entre parenthèses. Le numéro de la revue ne sera pas indiqué si les pages du volume sont numérotés consécutivement.

Les textes des livres ou traités inclueront : les noms des auteurs, précédés de l'initiale du prénom, le titre du livre entre guillemets et sans être souligné, le numéro du tome précédé par l'abréviation « vol » (ou « Bd. »), le numéro de l'édition, les éditions (the publisher), la localité de la parution du livre, l'année de la parution et la page de la référence précédée(s) par l'abréviation « p » (ou « S »).

Les brevets seront indiqués comme suit : L'auteur ou la firme, le pays et le numéro du brevet, la date et la revue (*Chem. Abstr.*). Par ex. : M. Jones (to Union Carbide Co.), *Brit. Pat.* 601 238, 2 Sept. 1959, *Chem. Abstr.*, 54, 12808 (1960).

Si la référence n'a pas été lue en original, on indiquera aussi la revue de références consultée.

Les diagrammes seront tracés à l'encre du Chine sur papier calque. Les tableaux et les figures (en nombre strictement nécessaire) ainsi que les courbes dans les figures seront numérotés par des chiffres arabes. Leur explication sera donnée dans la légende des figures. Prière de ne pas inscrire les mêmes données dans les tableaux et les figures. Chaque tableau aura un titre. On indiquera dans le texte la place approximative des tableaux et des figures. Les formules chimiques seront incluses dans le texte : en outre, elle seront transcrites sur papier calque, à l'encre de Chine.

Les auteurs sont priés d'indiquer les caractères italiques (en soulignant les lettres au crayon), ainsi que tout autre caractère spécial; les préfixes *ortho*, *meta*, *para*, *cis*, *trans*, etc. seront soulignés pour indiquer leurs caractères italiques et ne seront jamais écrits avec des majuscules.

Aucune correction à la main ne sera admise sur le manuscrit. Les corrections seront frappées à la machine. Les lettres grecques ou d'autres symboles spéciaux seront insérés à la main à l'encre clairement.

Le manuscrit sera signé par l'auteur.

Le colonne-titre aura 50 lettres au maximum.

L'entière responsabilité du contenu des articles appartient aux auteurs.

Sur demande on peut obtenir un note plus complète.

MŰSZAKI KÖNYVTÁR ÉS DOKUMENTÁCIÓS KÖZPONT 1883

PRINTED IN ROMANIA

1982 AUG 12

TRAVAUX PARUS AUX ÉDITIONS DE L'ACADÉMIE DE LA RÉPUBLIQUE SOCIALISTE DE ROUMANIE

ELENA CEAUŞESCU, **Noi cercetări în domeniul compuşilor macromoleculari** (Nouvelles recherches dans le domaine des composés macromoléculaires) 1981, 536 p.

I. G. MURGULESCU, TATIANA ONCESCU, E. SEGAL, **Introducere în chimia fizică. Vol. II.2. Cinetică chimică şi cataliză** (Introduction à la chimie physique. Vol. II.2. Cinétique chimique et catalyse), 1981 1024 p.

V. DRĂGUŢAN, A. T. BALABAN, M. DIMONIE, **Metateza olefinelor şi polimerizarea prin deschidere de inel a cicloolefinelor** (La métathèse des oléfines et la polymérisation par ouverture annulaire des cyclooléfines) 1981, 254 p.

LYDIA-MARIA VAICUM, **Epurarea apelor uzate cu nămol activ. Bazele biochimice,** (L'épuration des eaux résiduelles à boue active. Les bases biochimiques), 1981, 218 p.

I. GĂLĂŢEANU, **Procese şi metode radiochimice în energetica nucleară** (Processus et méthodes radiochimiques dans l'energétique nucléaire), 1981, 234 p.

O. IORDACHE, **Procese polistocastice aplicate la fenomenele de transfer** (Processus polystochastiques appliqués aux phénomènes de transfert), 1981, 187 p.

CR. SIMIONESCU, VALERIA GORDUZA, **Polimeri biocompatibili şi biologic activi** (Polymères biocompatibles et biologiquement actifs), 1980, 497 p.

ELENA CEAUŞESCU, **Polimerizarea stereospecifică a izoprenului** (La polymérisation stéréospécifique de l'isoprène), 1979, 307 p.

M. FLORESCU, **Metode ştiinţifice în dezvoltarea industriei chimice moderne** (Méthodes scientifiques dans le développement de l'industrie chimique moderne), 1979, 256 p.

A. T. BALABAN, I. GĂLĂŢEANU, G. GEORGESCU, LIGIA SIMIONESCU, **Compuşi marcaţi şi radiofarmaceutici cu aplicaţii în medicina nucleară** (Composés marqués et radiopharmaceutiques à application en médecine nucléaire), 1979, 495 p.

CONST. GH. MACAROVICI, **Analiza chimică cantitativă anorganică** (L'analyse chimique quantitative inorganique), 1979, 457 p.

I. G. MURGULESCU, E. SEGAL, **Introducere în chimia fizică**, vol. II.1. **Teoria molecular cinetică a materiei** (Introduction à la chimie physique, vol. II.1. La théorie moléculaire-cinétique de la matière), 1979, 1036 p.

S. STERNBERG, FL. DANEŞ, **Termodinamica chimică aplicată** (La thermodynamique chimique appliquée), 1978, 400 p.

I. G. MURGULESCU, V. EM. SAHINI, **Introducere în chimia fizică. Vol. I.2. Structura şi proprietăţile moleculelor** (Introduction à la chimie physique. Vol. I.2. La structure et les propriétés des molécules), 1978, 604 p.

C. DRĂGULESCU, E. PETROVICI, **Chimie structurală modernă. Chimia coordinanţei 8** (La chimie structurale moderne. La chimie de la coordinence 8), 1977, 947 p.

I. ZUGRĂVESCU, MAGDA PETROVANU, **N-ylid chemistry**, coédition avec McGraw-Hill International Book Company, U.S.A., 1977, 396 p.

I. G. MURGULESCU, **Introducere în chimia fizică. Vol. I.1. Atomi, molecule, legătură chimică** (Introduction à la chimie physique. Vol. I.1. Atomes, molécules, liaison chimique), 1976, 560 p.

ELENA CEAUŞESCU, **Research work on synthesis and characterization of macromolecular compounds. Contributions**, 1974, 251 p.

CR. SIMIONESCU, VIORICA RUSAN, V. POPA, **Chimia algelor marine** (La chimie des algues marines), 1974, 212 p., 1 pl.

I. P. Informaţia c. 1755

43 426

Lei 25

$ 55 (pour un abonnement annuel)

F 1103

ACADÉMIE DE LA RÉPUBLIQUE SOCIALISTE DE ROUMANIE

R

REVUE ROUMAINE DE CHIMIE

REFERÁLVA

TOME 27

N° 4

Avril 1982

EDITURA ACADEMIEI REPUBLICII SOCIALISTE ROMÂNIA

Rev. Roumaine Chim.

RRCHAX, **27**, *4*, p. 469–594 (1982), Bucarest

ACADÉMIE DE LA RÉPUBLIQUE SOCIALISTE DE ROUMANIE

COMITÉ DE RÉDACTION

Rédacteur en chef:

I. G. MURGULESCU, membre de l'Académie de la République Socialiste de Roumanie

Rédacteurs en chef adjoints:

A. T. BALABAN et V. EM. SAHINI, membres correspondants de l'Académie de la République Socialiste de Roumanie

Collège de rédaction:

EM. BRATU, ELENA CEAUȘESCU, ECATERINA CIORĂNESCU-NENITZESCU, CR. SIMIONESCU, membres de l'Académie de la République Socialiste de Roumanie ; P. SPACU, membre correspondant de l'Académie de la République Socialiste de Roumanie ; MARGARETA AVRAM, M. BANCIU, I. HAIDUC, D. I. MARCHIDAN, I. MOLDOVAN, G. NIAC et D. SĂNDULESCU

La Revue Roumaine de Chimie paraît 10 fois par an. Toute commande de l'étranger pour les travaux parus aux Editions de l'Académie de la République Socialiste de Roumanie sera adressée à ILEXIM, Departamentul Export-Import Carte (Livres)/ Departamentul Export-Import Presă (Revues). P.O.B. 136 — 137, télex 11226, 3, str. 13 Decembrie, 79517 Bucarest, Roumanie

Les manuscrits, les livres et les revues proposés en échange, ainsi que toute correspondance seront envoyée à la rédaction :

REVUE ROUMAINE DE CHIMIE

125, Calea Victoriei, 79717 Bucarest, Roumanie, téléphone 50 76 80

EDITURA ACADEMIEI REPUBLICII SOCIALISTE ROMÂNIA

125, Calea Victoriei, 79717 Bucarest, Roumanie, téléphone 50 76 80

REVUE ROUMAINE DE CHIMIE

Tome 27, N° 4 Avril, 1982

ȘERBAN MOLDOVEANU and VICTOR DAVID, The generalization of Beveridge-Schnuelle solvating model 471–474

KASEM K. KASEM and MOHAMED T. ISMAIL, Additional physical properties for butyrate and isobutyrate anions 475–479

N. I. IONESCU and DOMNINA POPESCU, Oxidation of methanol on copper phthalocyanine . . . . 481–484 R

P. BAHADUR and K. SINGH, Solubilization of alkanols in the presence of alkaline earth metal soaps 485–490

J. HERNANDEZ MENDEZ, G. LOPEZ CUETO, A. ALONSO MATEOS and C. SANCHEZ BURON, Kinetics of the reaction between oxygen and tin (II): stabilization of Sn(II) solutions and their utilization in reductimetry (in Spanish) 491–501

A. KALYUZHNYI, V. MILYUTIN, J. FAZAKAS and MARIA NEGOIU, On the extraction of palladium (II) and gold(III) from solution on inorganic electron exchangers (in Russian) 503–508

S. A. K. LODHI and A. RASHEED KHAN, Vinyl monomer complexes. I. The complexes of acrylonitrile with some inorganic salts 509–512

ALEXANDRU T. BALABAN and MARIA PARASCHIV, Molecular complexes with aromatic cations as electron acceptors. V. Inter- and intramolecular charge transfer of amino-substituted pyridinium salts evidenced by electronic absorption spectra 513–521

S. C. PATI and B. R. DEV, Kinetics and mechanism of Ru (III) catalysed oxidation of aliphatic diols and cyclanols by phenyliodoso acetate 523–532

C. I. CHIRIAC, Aromatic esters by a new direct condensation reaction using triaryl borates . . . . 533–536 R

S. R. El-EZBAWY, A. A. ABDEL-WAHAB and A. A. KHALAF, Synthesis of some new biologically active 2-aminopyridine derivatives . . . . 537–544 BC

LIDIA POP and F. HODOȘAN, Synthesis of (Z)-9-tricosene (Muscalure) . . . 545–547

G. E. M. MOUSSA, M. N. BASYOUNI, M. E. SHABAN, A. F. El-KAFRAWY and N. K. Al-AASAR, Synthesis and some reactions of 1-arylisoindoles 549–555

Revue Roumaine Chim.

27, *4*, p. 469— 594 (1982), Bucarest

SHERIF El-BASIL, On the cyclization of 3-α-naphthyl-propenoyl carbonium ion (An intramolecular perturbation) 557–560

A. CHIRIAC, VERONICA CHIRIAC, S. HOLBAN, I. MOTOC and Z. SIMON, Quantitative structure — activity relations with the MTD-procedure for plant growth regulating optically active acetic acid derivatives 561–568

LUMINIȚA VLĂDESCU and STELUȚA GHINEA, Utilization of Tiron in the separation and concentration of titanium with ion exchange resins . . 569–574

DAN SORIN VASILESCU, Alternating tendency in copolymerization. IV. Simultaneous cationic polymerization and radical terpolymerization 575–583

GH. DRĂGAN, GH. HUBCA, CR. OPRESCU and M. DIMONIE, Synthesis and polymerization of polyethylene glycol dimethacrylates. V. Analysis of kinetic data obtained at polymerization based on topoenergetic principles 585–590

BOOK REVIEWS 591–593

Revue Roumaine de Chimie, 27, 4, 471–474 (1982)

THE GENERALIZATION OF BEVERIDGE-SCHNUELLE SOLVATING MODEL

ŞERBAN MOLDOVEANU and VICTOR DAVID
The Polytechnic, Faculty of Chemical Technology, Splaiul Independenţei 202, 77208,
Bucharest, Romania

Received June 8, 1981

The Beveridge-Schnuelle solvating model is generalized for a finite number s of continuous and polarizable layers of different dielectric constants.

In this generalized model the solute molecule is considered as a charge collection and the solvating medium is divided into s number of solvent layers of dielectric constants ε_s(Fig. 1). Any layer is polarizable in accordance with Kirkwood model[1–3] so that to each one a reaction field is assigned.

The potentials Φ_i in each layer i are :

$$\Phi_0 = \frac{1}{\varepsilon_0}\sum_{m=0}^{n}\sum_{n=-\infty}^{+\infty}\left(A^1_{nm}r^n + A^2_{nm}r^n + \ldots + A^s_{nm}r^n + \frac{B^0_{nm}}{r^{n+1}}\right)P^m_n(\cos\theta)e^{im\varphi} \qquad (1)$$

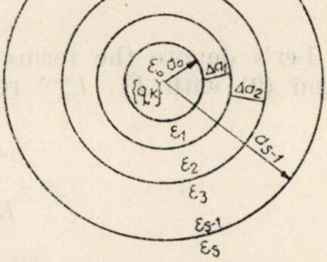

Fig. 1. — Concentric spheres of the generalised Beveridge-Schnuelle model.

$$\Phi_1 = \frac{1}{\varepsilon_1}\sum_{m=0}^{n}\sum_{n=-\infty}^{+\infty}\left(A^2_{nm}r^n + A^3_{nm}r^n + \ldots + A^s_{nm}r^n + \frac{B^1_{nm}}{r^{n+1}}\right)P^m_n(\cos\theta)e^{im\varphi} \qquad (2)$$

. . . .

$$\Phi_{s-1} = \frac{1}{\varepsilon_{s-1}} \sum_{m=0}^{n} \sum_{n=-\infty}^{+\infty} \left(A^{s}_{nm} r^{n} + \frac{B^{s-1}_{nm}}{r^{n+1}} \right) P^{m}_{n} (\cos \theta) e^{im\varphi} \tag{3}$$

$$\Phi_{s} = \frac{1}{\varepsilon_{s}} \sum_{m=0}^{n} \sum_{n=-\infty}^{+\infty} \frac{B^{s}_{nm}}{r^{n+1}} P^{m}_{n} (\cos \theta) e^{im\varphi} \tag{4}$$

The radii of the cavities taken spherically are:

$$\begin{aligned} a_1 &= a_0 \times \Delta a \\ a_2 &= a_0 + \Delta a_1 + \Delta a_2 \\ &\ldots\ldots\ldots\ldots\ldots \\ a_{s-1} &= a_0 + \sum_{i=1}^{s-1} \Delta a_i \end{aligned} \tag{5}$$

The boundary conditions for the cavities are:

$$\Phi_{l-1} = \Phi_{l}, r = a_{l-1} \tag{6}$$

$$\varepsilon_{l-1} \frac{\partial \Phi_{l-1}}{\partial r} = \varepsilon_{l} \frac{\partial \Phi_{l}}{\partial r}, r = a_{l-1} \tag{7}$$

These conditions for the last boundary between the layers $s - 1$ and s give:

$$A^{s}_{nm} = \frac{(n+1)}{(2n+1) a^{2n+1}_{s-1}} \left(\frac{\varepsilon_{s-1}}{\varepsilon_{s}} - 1 \right) B^{s}_{nm} \tag{8}$$

$$B^{s-1}_{nm} = \frac{n\left(\frac{\varepsilon_{s-1}}{\varepsilon_{s}} + 1 \right) + 1}{(2n+1)} B^{s}_{nm} \tag{9}$$

Let's denote the terms which multiply B^{s}_{nm} from the expressions (8) and (9) with F^{s}_{n}, L^{s-1}_{n} respectively:

$$A^{s}_{nm} = F^{s}_{n} B^{s}_{nm} \tag{10}$$

$$B^{s-1}_{nm} = L^{s-1}_{n} B^{s}_{nm} \tag{11}$$

Then the same conditions give all $A^{l}_{nm} (l = 1, 2, \ldots, s)$ and $B^{j}_{nm} (j = 2, 3, \ldots s - 1)$ as functions of B^{s}_{nm} thus:

$$A^{l}_{nm} = F^{l}_{n} B^{s}_{nm} \tag{12}$$

$$B^{j}_{nm} = L^{j}_{n} B^{s}_{nm} \tag{13}$$

It can be proved that:

$$F^l_n = F^l_n(F^{l+1}_n, F^{l+2}_n, \ldots, F^s_n) \tag{14}$$

We obtain:

$$\Phi_0 = \frac{1}{\varepsilon_0}\sum_m \sum_n \left(\sum_{l=1}^{s} F^l_n r^n B^s_{nm} + \frac{B^0_{nm}}{r^{n+1}} \right) P^m_n(\cos\theta) e^{im\varphi} \tag{15}$$

$$\Phi_1 = \frac{1}{\varepsilon_1}\sum_m \sum_n \left(\sum_{l=2}^{s} F^l_n r^n B^s_{nm} + \frac{B^0_{nm}}{r^{n+1}} \right) P^m_n(\cos\theta) e^{im\varphi} \tag{16}$$

The conditions (6) and (7) for the potentials Φ_0 and Φ_1 give B^s_{nm} and B^1_{nm} as functions of B^0_{nm}:

$$B^s_{nm} = B^0_{nm} \frac{(n+1)}{a_0^{2n+1}} \left(1 - \frac{\varepsilon_1}{\varepsilon_0}\right) \Bigg[nF^1_n + (n+1)\left(\frac{\varepsilon_1}{\varepsilon_0} \sum_{l=1}^{s} F^l_n - \sum_{l=2}^{s} F^l_n \right) \Bigg]^{-1} \tag{17}$$

$$B_{nm} = B^0_{nm} \Bigg\{ 1 - nF^1_n \left(1 - \frac{\varepsilon_1}{\varepsilon_0}\right) \Bigg[nF^1_n + (n+1)\left(\frac{\varepsilon_1}{\varepsilon_0} \sum_{l=1}^{s} F^l_n - \sum_{l=2}^{s} F^l_n \right) \Bigg]^{-1} \Bigg\} \tag{18}$$

Where B^0_{nm} is[3]:

$$B^0_{nm} = \frac{(n-|m|)!}{(n+|m|)!} \sum_{k=1}^{M} q_k r_k P^m_n(\cos\theta_k) e^{-im\varphi_k} \tag{19}$$

M being the number of components of the collection.

The reaction field is given by the formula:

$$\Phi_R = \frac{1}{\varepsilon_0} \sum_m \sum_n (A^1_{nm} r^n + A^2_{nm} r^n + \ldots + A^s_{nm} r^n) P^m_n(\cos\theta) e^{im\varphi} \tag{20}$$

The polarization energy becomes:

$$F_{\text{pol}} = \frac{1}{2\varepsilon_0} \sum_{k=1}^{M} \sum_{m=-n}^{+n} \sum_{n=0}^{\infty} \sum_{l=1}^{s} A^l_{nm} r^n q_k P^m_n(\cos\theta) e^{im\varphi} \tag{21}$$

ε_0 is always taken 1. For $s = 2$, the Beveridge-Schnuelle model is obtained which is aplicable to the dilute solutions.

We can choose different formulas of variation of a. Thus, one of these can be the following:

$$\Delta a_n = n\delta a \tag{22}$$

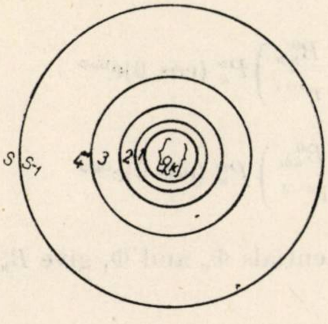

Fig. 2. — The choice of the radius in the generalised Beveridge-Schnuelle model.

where $n = 2, \ldots, s$, and if we put $\delta a \to 0$, then $s \to \infty$ and $\varepsilon_s \to \varepsilon_{\text{bulk}}$ and thus we shall obtain a continuum model with gradient (Fig. 2).

REFERENCES

[1] J. G. Kirkwood, *J. Chem. Phys.*, **1**, 351 (1934).
[2] L. Onsager, *J. Amer. Chem. Soc.*, **58**, 1486 (1936).
[3] D. L. Beveridge and G. W. Schnuelle, *J. Phys. Chem.*, **79**, 2562 (1972).

Revue Roumaine de Chimie, **27**, *4*. 475–479 (1982)

ADDITIONAL PHYSICAL PROPERTIES FOR BUTYRATE AND ISOBUTYRATE ANIONS

STANDARD POTENTIALS AND THERMODYNAMIC PARAMETERS AT DIFFERENT TEMPERATURES

KASEM K. KASEM and MOHAMED T. ISMAIL
Chemistry Department, Faculty of Science, Assiut University, Assiut, Egypt

Received November 14, 1980

The standard molal potential (E_m^0) of the $HgHg_2(OBu)_2/BuO^-$ electrode in 10% by volume dioxane–water mixture was determined at 20, 25, 30, 35 and 40°C. These potentials were found to be lower than that of $Hg/Hg_2(iBuO)_2/iBuO^-$ electrode determined under the same conditions. The changes in standard free energy (ΔG°), entropy (ΔS°), and enthalpy (ΔH) were calculated for the appropriate cell reaction.

INTRODUCTION

Earlier reviews [1–3] and papers [4, 6] discussed the nature of acetate electrode concerning its standard potentials [3] in the temperature range between 5 and 37°C. The effect of dioxane-water ratio at different temperatures on the standard potential of this electrode has been investigated.[5, 6] Aditya et al. [7] reported the values of the standard potentials of propionate electrode and related thermodynamic parameters in the temperature range between 15 and 35°C. In the present paper, a comparison between the values of the standard molal potentials E_m^0 and related thermodynamic parameters has been recorded for both butyrate and iso-butyrate electrodes in 10% by volume of dioxane–water mixture at 20, 25, 30, 35 and 40°C.

EXPERIMENTAL

The preparation of the electrode techniques described by Nath[8] has been adopted in this present study. The measurements of the e.m.f. of the cell were carried out using a H. Tinsley & Co. Ltd potentiometer, type 3387 B. All the cell e.m.f. values were corrected to 1 atm. of hydrogen pressure. The working temperatures were 20, 25, 30, 35 and 40°C. To avoid any solubility of the mercurous salt, the lowest concentration of the acid was 0.4 molal. All chemicals used were of the analytical grade.

RESULTS AND DISCUSSION

For the cell consisting of the electrode under investigation and H_2 electrode as a reference, the cell reaction is

$$1/2\,H_2 + 1/2\,Hg_2(OBu)_2(s) \rightarrow H^+ + Hg(I) + BuO^-$$

The e.m.f. of the cell is given by

$$E = E^0_m - (RT/F)\ln a_{H^+} \cdot a_{BuO^-} \tag{1}$$

where R — gas constant; T — absolute temperature; F — Faraday's constant; a — activity. The previous formulae are also applied for isobutyrate electrode.

It is well known that for m moles of weak acid HA we have

$$\underset{(1-\alpha)m}{HA} \rightleftharpoons \underset{\alpha m}{H^+} + \underset{\alpha m}{A^-}$$

Since $K = \dfrac{a_{H^+} \cdot a_{A^-}}{a_{HA}} = \dfrac{a_{H^+} \cdot a_{A^-}}{(1-\alpha)m\,\nu_u}$

hence

$$a_{H^+} \cdot a_{A^-} = Km(1-\alpha)\,\nu_u$$

$$A^- = BuO^- \text{ or } iBuO^-$$

where K — the dissociation constant, α — the degree of dissociation, ν_u the activity coefficient of undissociated acid. Equation (1) therefore becomes:

$$E = E^0_m - k\log Km(1-\alpha) - k\log \nu_u \tag{2}$$

where, $k = (RT/F)\ln 10$. Equation (2) could be written as follows:

$$E^{0\prime} = E^0_m - k\log \nu_u \tag{3}$$

as

$$E^{0\prime} = E + k\log Km(1-\alpha) \tag{4}$$

According to Covington et al. [9] $\log \nu_u = S.I.$ where, S — constant, I — ionic strength.

hence

$$E^{0\prime} = E^0_m - k.S.I. \tag{5}$$

In order to determine $E^{0\prime}$ according to (4), α is taken equal to $\left(\dfrac{K}{m}\right)^{1/2}$ and I in our case equal to m (molality).

The e.m.f. of the cell (E/V) corrected to one atmosphere of hydrogen were recorded in tables 1 and 2 for both butyrate and isobutyrate electrodes, respectively.

TABLE 1

E.m. f of the cell (E/V) corrected to 1 atm. of H_2 for butyrate electrode

m/mol.kg^{-1}	E/V				
	20°C	25°C	30°C	35°C	40°C
2.0010	0.7391	0.7578	0.7595	0.7603	0.7610
1.5000	0.7631	0.7618	0.7625	0.7618	0.7620
0.9980	0.7651	0.7658	0.7680	0.7683	0.7690
0.6007	0.7851	0.7848	0.7840	0.7835	0.7830
0.4009	0.7791	0.7838	0.7805	0.7838	0.7820

TABLE 2

E.m.f of the cell (E/V) corrected to 1 atm. of H_2 for isobutyrate electrode

m/mol.kg^{-1}	E/V				
	20°C	25°C	30°C	35°C	40°C
1.9981	0.7821	0.7863	0.7870	0.7873	0.7865
1.4925	0.8056	0.8043	0.8030	0.8108	0.8100
1.0000	0.7961	0.7988	0.7985	0.7973	0.7965
0.6008	0.8176	0.8143	0.8140	0.8138	0.8130
0.3990	0.8136	0.8173	0.8205	0.8206	0.8205

E^0_m was obtained by the extrapolation of the linear plot [5] of $E^{0\prime}$ against I as in equation (5).

The standard Gibbs energy change ΔG^0, standard entropy ΔS^0 and (standard enthalpy) ΔH^0 were calculated according to the following relationship.

$$\Delta G^0 = -FE^0_m$$

$$\Delta S^0 = -\,\partial(\Delta G^0)/\partial T$$

$$\Delta H^0 = \Delta G^0 + T\,\Delta S^0$$

E^0_m and thermodynamic parameters (ΔG^0, ΔS^0, ΔH^0) for both electrodes were listed in tables 3 and 4.

TABLE 3

$E°$ and standard molal potential and derived thermodynamic parameters at different temperatures for butyrate electrode

m/mol.kg^{-1}	$E^{0\prime}/V$				
	20	25	30	35	40
2.0010	0.4970	0.4907	0.4873	0.4828	0.4781
1.5000	0.4937	0.4873	0.4828	0.4771	0.4713
0.9980	0.4854	0.4811	0.4777	0.4724	0.4674
0.6007	0.4925	0.4867	0.4804	0.4740	0.4676
0.4009	0.4765	0.4703	0.4662	0.4638	0.4556

TABLE 3 (continued)

m/mol.kg^{-1}	$E^{0\prime}/V$				
	20	25	30	35	40
E_m^0	0.4730	0.4720	0.4695	0.4595	0.4506
$-\Delta G^0/\mathrm{Jmol}^{-1}$	45642	45545	45304	44339	43422
$-\Delta S^0/\mathrm{JK}^{-1}\mathrm{mol}^{-1}$	28.9	36.0	120.6	188.2	189.6
$-\Delta H^0/\mathrm{Jmol}^{-1}$	45109.7	56273.0	81845.8	102308.6	102766.8

TABLE 4

$E^{0\prime}$ and standard molal potential and derived thermodynamic parameters at different temperatures for isobutyrate electrode

m/mol.kg^{-1}	$E^{0\prime}/V$				
	20°C	25°C	30°C	35°C	40°C
1.9981	0.5425	0.5375	0.5290	0.5350	0.4290
1.4925	0.5338	0.5282	0.5218	0.5244	0.5184
1.0000	0.5150	0.4970	0.5062	0.5002	0.4940
0.6008	0.5235	0.5147	0.5088	0.5031	0.4967
0.3990	0.5092	0.5067	0.5047	0.4981	0.4922
E_m^0	0.5045	0.5015	0.4981	0.4900	0.4830
$-\Delta G^\circ/\mathrm{Jmol}^{-1}$	48681.0	48391.7	48063.6	47282	46606.6
$-\Delta S^\circ/\mathrm{JK}^{-1}\mathrm{mol}^{-1}$	58.2	52.0	110.9	165.4	170.9
$-\Delta H^\circ/\mathrm{Jmol}^{-1}$	65733.6	63887.3	81666.3	98225.2	100098.3

The correlation of these values with the corresponding temperature shows a parabola of the form:

$$Y = a_0 + b_0 Z + C_0 Z^2$$

where $Y = E_m^0/V$ and $Z = (t/C^\circ - 30)$ and $Z^2 = (t/^\circ C - 30)^2$. Using the least squares method for solving such equations we have:

$$E_m^0/V = 0.4683 - 11.7 \times 10^{-4}\,(t/^\circ\mathrm{C} - 30) - 7 \times 10^{-5}\,(t/^\circ\mathrm{C} - 30)^2$$

for butyrate electrode

and

$$E_m^0/V = 0.4958 - 10.9 \times 10^{-4}(t/^\circ\mathrm{C} - 30) - 36.3 \times 10^{-6}\,(t/^\circ\mathrm{C} - 30)^2$$

for isobutyrate electrode.

It could be seen that E_m^0 for butyrate electrode is lower than that of isobutyrate electrode under the same conditions. This behaviour may be explained on the basis of structural role, as the cross section of isobutyric acid is larger than that of *n*-butyric acid. Hence, this difference could affect the solvation energy, hydrophobic properties, lattice energy and the dielectric constant [10, 11] of the medium, which consequently results in the changes obtained in the values of E_m^0.

REFERENCES

[1] W. D. Larson and F. H. McDaugal, *J. Phys. Chem.*, **41**, 493 (1937).
[2] W. D. Larson and W. J. Tomisicek, *J. Amer. Chem. Soc.*, **61**, 65 (1939).
[3] W. D. Larson *J. Phys. Chem.*. **67**, 937 (1963).
[4] A. K. Covington, P. K. Talukdar and H. R. Thirsk, *Trans. Faraday Soc.*, **60**, 412 (1964).
[5] A. K. Basu and S. Aditya, *J. Ind. Chem. Soc.*, **48**, 129 (1971).
[6] A. K. Basu and S. Aditya, *ibid.*, **48**, 155 (1971).
[7] A. K. Basu and S. Aditya, *Electrochim. Acta*, **23**, 1341 (1979).
[8] S. Nath, S. Aditya and B. Prasad, *J. Ind. Chem. Soc.*, **28**, 683 (1951).
[9] A. K. Covington, J. V. Dobson and Lord Wynne-Jones, *Trans. Faraday Soc.*, **61**, 2050 (1965).
[10] I. T. Oiwa, *J. Phys. Chem.*, **60**, 754 (1956).
[11] S. K. Banerjee, K. K. Kundu and M. N. Das, *J. Chem. Soc., A.*, **1967**, 161.

could affect the solvation energy, hydrophobic properties, lattice energy and the dielectric constant[11] of the medium, which consequently results in the change obtained in the values of E^0_m.

REFERENCES

[1] W. D. Larson and F. H. MacDougall, J. Phys. Chem., 41, 493 (1937).
[2] W. D. Larson and W. J. Tomsicek, J. Amer. Chem. Soc., 61, 65 (1939).
[3] W. D. Larson J. Phys. Chem. 67, 967 (1963).
[4] A. K. Covington, P. K. Talukdar and H. B. Thirsk, Trans. Faraday Soc., 60, 412 (1964).
[5] A. K. Basu and S. Aditya, J. Ind. Chem. Soc., 48, 135 (1971).
[6] A. K. Basu and S. Aditya, ibid., 48, 155 (1971).
[7] A. K. Basu and S. Aditya, Electrochim. Acta, 23, 1311 (1978).
[8] S. Nath, S. Aditya and B. Prasad, J. Ind. Chem. Soc., 28, 683 (1951).
[9] A. K. Covington, J. V. Dobson and Lord Wynne-Jones, Trans. Faraday Soc., 61, 2050 (1965).
[10] T. Olwe, J. Phys. Chem., 60, 737 (1956).
[11] S. K. Banerjee, K. K. Kundu and M. N. Das, J. Chem. Soc., A, 1967, 161.

Revue Roumaine de Chimie, 27, *4*, 481–484 (1982)

OXIDATION OF METHANOL ON COPPER PHTHALOCYANINE

N. I. IONESCU and DOMNINA POPESCU
Center of Physical Chemistry, Bucharest, 77208, Spl. Independenţei 202, Romania

Received June 18, 1981

The catalytic activity of copper phthalocyanine changes during the vapour-phase oxidation of methanol. This fact is due to the thermal decomposition of copper phthalocyanine in oxygen atmosphere, which leads to a more active catalyst than the initial one.

Gas phase oxidation of alcohols on catalysts of the first transition period metal phthalocyanines (MePc) reveals contradictory aspects, which raise the problem of the nature of catalytically active centers. Particularly, in the oxidation of 2-propanol or 2-propanethiol, the catalytic activity of MePc is assigned to the central metal[1–5], as a good correlation was found between the activation energies of oxidation and the energies of molecular orbitals of predominantly metallic character (metal orbitals) in MePc. The lack of catalytic effect when using H_2Pc in the oxidation of methanol[6], 2-propanol[2, 5] or 2-propanethiol[7] indicates that the pseudoaromatic system cannot realise a good activation of reactants (although oxygen adsorption on CuPc and H_2Pc is very similar).[8,9] On the other side, a change of the chemical structure of MePc subsequent to the contact with oxygen at high temperatures was observed.[10] This effect of thermal treatment of the MePc catalyst seems to account for the catalytic activity, which increases as the degree of conversion of MePc increases.[6] It was concluded that not only the central metallic ion is important for catalytic oxidation, but also the pseudoaromatic part of the complex. In this respect, the study of the influence of thermal treatment of CuPc in oxygen on its catalytic activity could provide new information concerning the nature of the active centers.

EXPERIMENTAL

The catalytic activity of CuPc for methanol oxidation was measured using a steady-state flow reactor (12 mm i.d. ; 8.5 g CuPc), at atmospheric pressure. The catalyst was conditioned *in situ* : it was heated and cooled for 5 times between 260 and 360°C, in a nitrogen flow. During each complete cycle, several activity measurements were performed, at different temperatures, by switching the nitrogen flow to a constant flow of methanol—air (at a constant ratio). The catalyst was kept for 45 min in contact with the methanol—air mixture, at constant temperature : in the last 15 min the liquid reaction product was collected in a cold trap

(–10°C) and analysed. The thermal treatment of the catalyst lasted for 80 h, but CuPc was kept in reagent flow for only 18 h, at different temperatures in the above-mentioned range.

The analysis of reaction products was carried out using a Carlo Erba gas Chromatograph, a 2307 model, with hot wire detector, on a 3 m × 4 mm column with 10% Ethofat on Polytrifluorethylene 30/60 mesh and H_2 as carrier gas (45 cm^3/min).

Elementary analyses of CuPc samples were performed in oxygen atmosphere, in a quartz tube, according to Korschun.

Reagents : CuPc and H_2Pc (techn., Th. Schuchardt) were purified by vacuum sublimation, at 10^{-4} – 10^{-5} mm Hg. The powder was pelletised and the pellets were crushed and sieved to 1.0 – 1.5 mm.

Methanol was dried by refluxing with magnesium and iodine and then distilled.

Air and nitrogen were dried by means of several columns filled with $CaCl_2$(anh) and molecular sieves.

RESULTS AND DISCUSSION

The measurements performed with copper phthalocyanine at temperatures between 260 and 300°C show a very low catalytic activity of CuPc in methanol oxidation to formaldehyde, as long as the catalyst is freshly purified and kept in a nitrogen flow before each activity test. After starting the thermal treatment of copper phthalocyanine, by its alternative heating in nitrogen and in a mixture of reagents flow, at temperatures higher than 300°C, a steady rise of the catalytic activity is observed as CuPc is kept for a longer time in contact with air. This effect is shown in figure 1 by the variation of the mole fraction of formal-

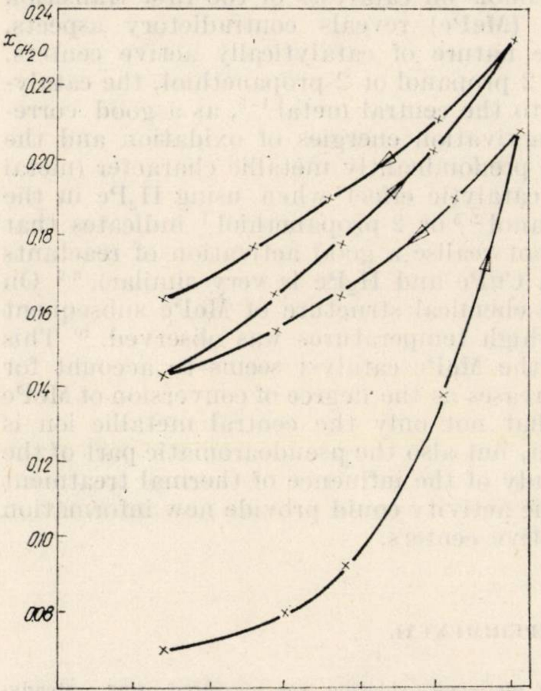

Fig. 1. – The influence of reaction temperature on the catalytic activity of CuPc, in methanol oxidation to formaldehyde.

dehyde in the liquid reaction product: x_{CH_2O} (assuming that $x_{CH_2O} = x_{H_2O}$ and the excess amount of water appears from phthalocyanine oxidation) versus reaction temperature.

Only the first two activation cycles have been drawn in figure 1; it can be seen that, for some constant temperature in the range 260 – 360°C the catalytic activity of CuPc increases steadily. This is in good agreement with the previous observations concerning the increase of the degree of conversion in 2-propanol oxidation on several MePc [2] or 2-propanethiol oxidation on CuPc [5] after the pre-treatment of phthalocyanine by oxygen. Moreover, these experiments [2, 5] have been performed in a microcatalytic pulse reactor, where the amount of oxygen available for phthalocyanine degradation is much less than in the flow system.

In the following conditioning cycles of our experiments, the activity of CuPc was expected to reach a steady value, constant for each temperature; this fact was not observed.

It appears as a strong evidence that simultaneously with methanol oxidation catalysed by CuPc, the oxidation of CuPc itself takes place; this process explains the formation of extra amounts of water (found in the liquid collected from the reactor) and of phthalic acid, which could be collected from the cooler part of the reactor. The substance which remains in the catalyst bed exhibits a larger activity for methanol oxidation at 340 – 360°C and a smaller activity at 250 – 260°C, as compared to CuPc working in the first two thermal conditioning cycles.

Elementary analyses of different samples of CuPc kept in an oxygen flow at 350°C show that the extent of CuPc degradation is a function of the time of contact between phthalocyanine and oxygen (table 1).

TABLE 1

Composition and catalytic activity of copper phthalocyanine, after heating in oxygen, at 10 cm^3/min and 350°C

Sample	Composition (%)			x_{CH_2O}
	C	H	Cu	
CuPc (initial)	66.60	2.76	11.03	0.01
CuPc, after 40 h heating	56.40	2.69	13.76	0.12
CuPc, after 100 h heating	48.21	2.48	20.97	0.31

The results in table 1 indicate that the increase of catalytic activity cannot be correlated only with the increase of copper content in the sample, but also with the changes taking place in the nature of the chemical bonds between the central metallic ion and the organic ligand. This idea is supported by the comparison between the activity tests using CuPc heated in oxygen for 100 hours and respectively 40 hours, with the initial CuPc catalyst (non-treated). A change in the copper percent by a factor of 2 leads to a raise of the catalytic activity by a factor of 30.

As to the reaction itself, one can suppose that oxygen can be adsorbed and activated by the central metallic ion. At the same time, it could be also adsorbed on the nitrogen atoms of the phthalocyanine ligand, as in the case of H_2Pc. If this is true, the surface of CuPc cannot be considered any more as an homogenous adsorptive surface, but as a heterogenous one. Indeed, the adsorption of oxygen on CuPc and H_2Pc is described by the kinetic law of Bangham-Burt,[9] which is typical for adsorption on non-homogenous surfaces.

The other component of the system, methanol, can be weakly adsorbed either by copper or by the nitrogen atoms of the phthalocyanine ring, in the same way as water.[11] An evidence for a weak adsorption of methanol on CuPc is the adsorption heat of –6.0 kcal/mol, determined from gaschromatographic data.[12] The adsorption heat of –5.4 kcal/mol for methanol on H_2Pc,[12] suggests a similar type of bond for both phthalocyanines.

The thermal treatment of CuPc in oxygen atmosphere can equally influence all these interactions and creates a greater heterogeneity of the active surface. At the same time, during the activation, the structure and catalytic properties of CuPc change to a great extent. This fact suggests that later studies concerning these oxidation processes should use kinetic methods for the study of catalysts with variable activity.

In conclusion, the investigation of methanol oxidation on copper phthalocyanine activated by heating in an oxygen atmosphere reveals a steady rise of the catalytic activity, during the first two conditioning cycles. However, the catalyst does not reach a constant activity and therefore, its use in oxidation reactions is restricted.

REFERENCES

[1] F. Steinbach and K. Hiltner, *Ber. Bunsenges. physik. Chemie*, **76**, 1119 (1972).

[2] F. Steinbach and K. Hiltner, *Z. phys. Chem. (Frankfurt)*, **83**, 126 (1973).

[3] F. Steinbach and K. Hiltner, in "Katalyse an Phthalocyaninen", Eds. H. Kropf and F. Steinbach, G. Thieme Verlag, Stuttgart, 1973, p. 122.

[4] F. Steinbach, H. Schmidt and M. Zobel, in "Catalysis : Heterogenous and Homogenous", Proc. of the Intern. Symposium on Catalytic Phenomena, Brussells 1974 ; Elsevier, Amsterdam, 1975, p. 417.

[5] F. Steinbach and H. Schmidt, *J. Catalysis*, **39**, 190 (1975).

[6] N. I. Ionescu, R. H. Schuster, D. Trestianu and A. Mihăilescu, *Z. Chem.*, **15**, 496 (1975).

[7] F. Steinbach and H. Schmidt, *J. Catalysis*, **52**, 302 (1978).

[8] N. I. Ionescu and P. Banyai, *Rev. Roumaine Chim.*, **23**, 1023 (1978).

[9] N. I. Ionescu and P. Banyai, *Rev. Roumaine Chim.*, **24**, 267 (1979).

[10] F. Steinbach and H. Joswig, *J. Chem. Soc., Faraday Trans. I*, **75**, 2594 (1979).

[11] S. A. Borisenkova, A. A. Skliankin, O. Maltseva and V. A. Novikov, *Khim. Kinet. Katal.*, **1979**, 162.

[12] N. I. Ionescu, D. Popescu and R. H. Schuster, *Rev. Chim., (București)* **29**, 117 (1978).

Revue Roumaine de Chimie **27, *4*** 485–490 (1982)

SOLUBILIZATION OF ALKANOLS IN THE PRESENCE OF ALKALINE EARTH METAL SOAPS

P. BAHADUR and K. SINGH
Chemical Laboratories, D.A.V. College, Muzaffarnagar,
251001, India

Received June 26, 1980

Solubilization of 1-butanol and 2-methyl-1-propanol within the micelles of aqueous alkaline earth metal soaps has been studied at 40°C. The solubilization as observed even below the critical micelle concentration (CMC) of the respective soap solutions has been satisfactorily explained in terms of limiting association concentration (LAC). The influence of electrolytes and temperature on the extent of solubilization has also been observed.

INTRODUCTION

Lawrence [1] correlated the increased solubility of solubilizate with colloidal properties of surfactants. Several techniques [2] e.g. conductivity, light scattering, viscosity, sedimentation, X-ray diffraction, spectroscopy, NMR etc. were followed to study the solubilization.

Shinoda [3] concluded that the addition of solubilizate may cause a lowering in the critical micelle concentration so that the solubilization takes place below CMC of normal surfactant solvent system. Ekwall [4] also pointed out that solubilization may take place at a surfactant concentration i.e. limiting association concentration (LAC) which is lower than the CMC of surfactant.

The influence of electrolytes and nonelectrolytes on solubilization and surfactant solutions has many important consequences not only of academic interest but also in their industrial applications. Addition of salt decreases the concentration of monomers present, thereby increases the concentration of surfactant present as micelles, with a concomitant increase in the solubilization power. [2] CMC of the alkaline earth metal soaps in aqueous [5–7] electrolytic solutions [8,9] has already been reported in our earlier communications.

The present paper deals with the solubilizing action of alkaline earth metal soaps in aqueous solution as well as with the influence of electrolytes on the solubilizing power of soaps at 40°C.

EXPERIMENTAL

Aqueous soap solutions of laboratory prepared strontium, calcium and magnesium valerates and strontium caprylates were prepared by weighing calculated amounts of soaps in a measuring flask and then making up to the mark with water or the aqueous salt solution as the case may be. The soap solutions of varying concentrations were hanged in a thermostat at 40°C and the respective alcohols were added dropwise from microburette with continuous shaking. The solubilization of 1-butanol and 2-methyl -1-propanol was observed in terms of the first excess of respective alcohols at which the turbidity appeared in soap solutions. The visually noticed solubilization results were then confirmed by measuring the conductivities of soap solution for a wide concentration range and with addition of varying amounts of solubilizates (added dropwise from a microburette).

RESULTS AND DISCUSION

The specific conductance, K of respective soap solutions is plotted against the amount of alcohols in ml/10 ml of aqueous soap solutions (a representative set of curves is shown in Fig. 1). Initially the K values decrease linearly with the increasing amounts of added alcohols for all the soap concentrations studied and afterwards they attain constancy for amounts of alcohols added. The decrease in the values of the specific conductances on the addition of 1-butanol and 2-methyl-1-propanol is probably due to the solubility of these alkanols in water, forming thus a less conducting medium. This predominates over the increasing effects of conductances by the orientation of polar solubilizates in the micelle water interface keeping the surfactant ions farther apart and thus allowing some of the bound counterions to escape. The extent of solubilization was determined from the plot (Fig. 1) where the trend in conductance values changes. The data showing the extent of solubilization with increasing soap concentrations for aqueous calcium valerate solution are recorded in table 1. These results obtained by solubility and conductivity method are in close agreement with each other. Figure 2 shows the extent of solubilization of alkanols against the concentration of calcium valerate in water. It may be concluded that the solubility of alkanols does not change at lower soap concentrations. The solubilization is noticed in between the soap concentrations ranging from 7 MM to 15 MM and again the amount of alkanols solubilized becomes constant above 15 MM. It

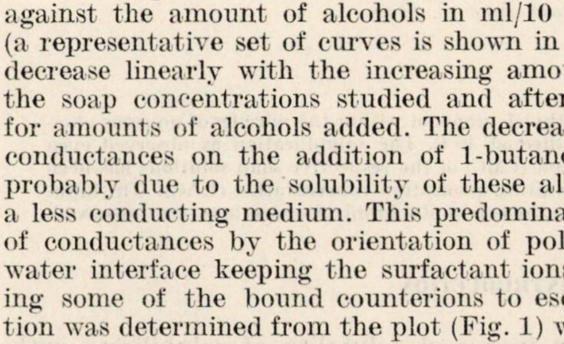

Fig. 1. — Plot of specific conductance vs. amount of 1-butanol added for aqueous calcium valerate solution at 40°C.

TABLE 1

Solubility of alcohols (moles litre^{-1}) in aqueous solution of calcium valerate at 40°C

Conc. of soap in moles litre^{-1}	Amount of alcohol solubilized			
	By conductivity method		By solubility method	
	1-Butanol	2-Methyl-1-propanol	1-Butanol	2-Methyl-1-propanol
0.000	1.08	1.18	1.08	1.18
0.003	1.08	1.18	1.08	1.18
0.005	1.08	1.18	1.10	1.20
0.006	1.08	1.18	1.10	1.20
0.008	1.04	1.41	1.32	1.39
0.010	1.48	1.53	1.45	1.51
0.015	1.69	1.72	1.67	1.72
0.020	1.69	1.72	1.67	1.72
0.030	1.69	1.72	1.67	1.70
0.040	1.69	1.72	1.67	1.72
0.050	1.69	1.72	1.67	1.72

is to be pointed out here that the CMC of calcium valerate in water is 15 MM. The constant values of solubilization for alkanols in soap solutions above the CMC of normal soap solution are taken as the maximum amount of alcohols solubilized in the presence of soap. The solubilization below CMC may be attributed, due to the shifting of CMC of calcium valerate, to some lower concentration i.e. limiting association concentration by the addition of solubilizates. Thus it may be concluded that the solubilization of alcohols in the presence of alkaline earth metal soaps occurs only between LAC and CMC of soaps.

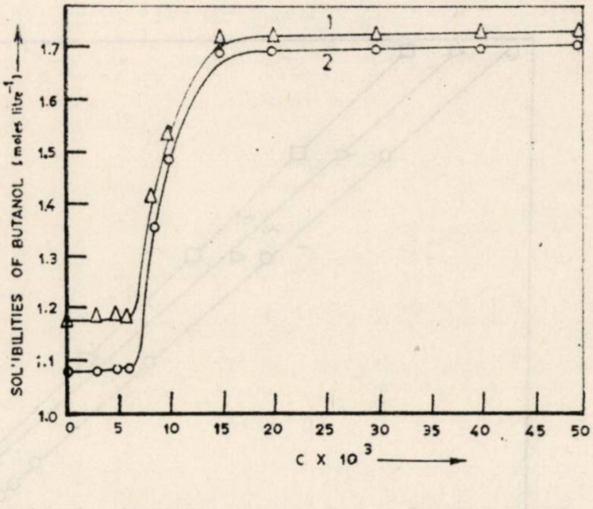

Fig. 2. — Plots of solubilities of alkanols vs. concentration of calcium valerate in water : *1.* 2-Methyl-1-propanol ; *2.* 1-Butanol.

The variation of CMC for calcium valerate in the presence of varying amounts of 1-butanol (Fig. 3) is independent of the amount of butanol solubilized. Figure 4 represents the CMC of alkaline earth metal valerates

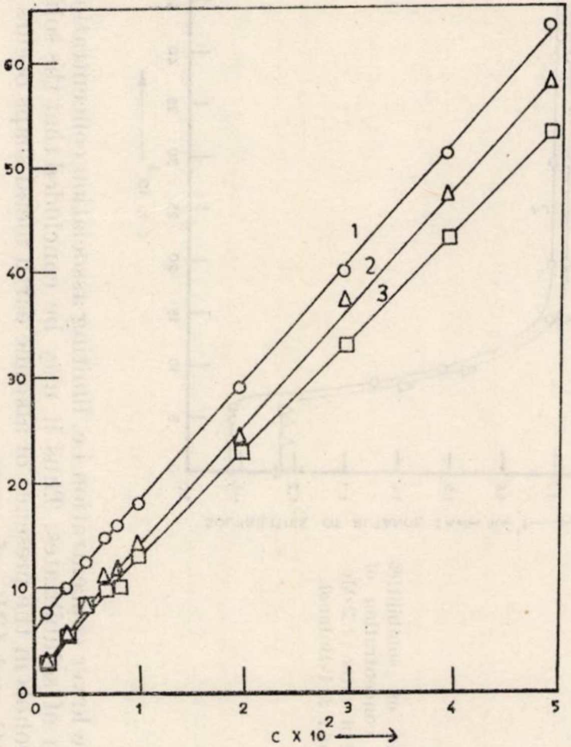

Fig. 3. — Plots of specific conductance vs. concentration of calcium valerate in the presence of varying amounts of 1-butanol : *1.* 0.135 M ; *2.* 0.68 M ; *3.* 1.35 M.

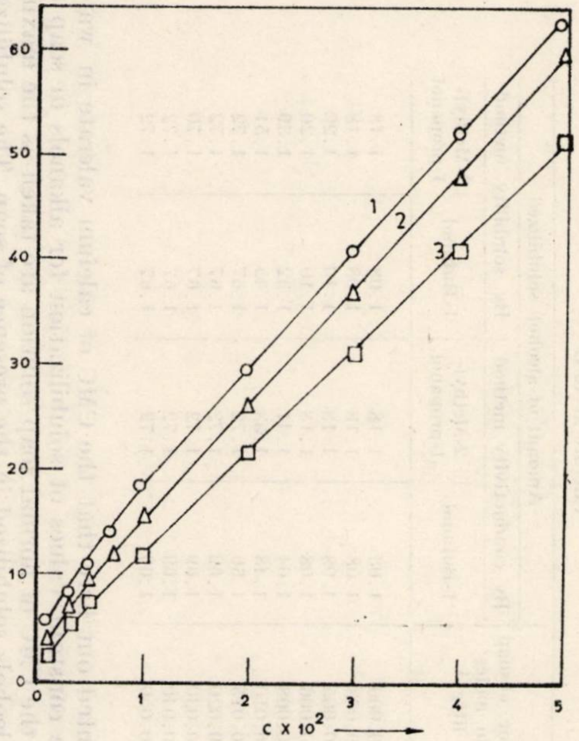

Fig. 4. — Plots of specific conductance vs. concentration of alkaline earth metal valerate in the presence of 0.68 M 1-butanol : *1.* Sr Valerate ; *2.* Ca Valerate ; *3.* Mg Valerate.

in the presence of 0.68 M 1-butanol solubilized which are 5MM, 7 MM and 10 MM respectively for magnesium, calcium and strontium valerates.

Figures 5 and 6 show the influence of electrolytes (KNO_3 and $Mg(NO_3)_2$ on the variation of specific conductances with the amounts of 1-butanol added as well as on the extent of solubilization. The maximum amounts of alcohols solubilized for alkaline earth metal soaps in the presence of 0.002 N KNO_3, 0.002 N $Mg(NO_3)_2$ as obtained from Figs 5 and 6 are recorded in table 2. Table 2 shows that the amount of solubilizates

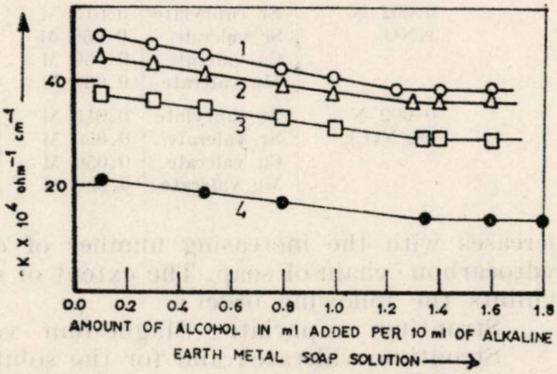

Fig. 5. — Plots of specific conductance vs. amount of 1-butanol added for alkaline earth metal soap in the presence of 0.002 N KNO_3: *1.* 0.03 M Sr Valerate; *2.* 0.03 M Ca Valerate; *3.* 0.03 M Mg Valerate; *4.* 0.01 M Sr Caprylate.

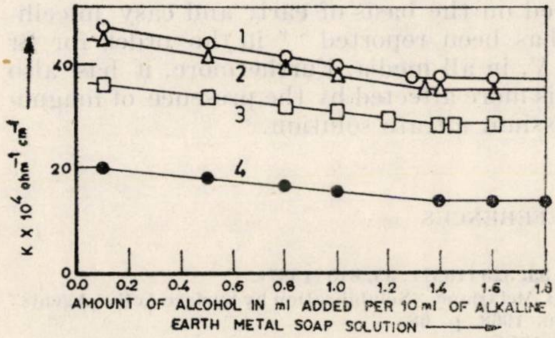

Fig. 6. — Plots of specific conductance vs. amount of 1-butanol added for alkaline earth metal soap in the presence of 0.002 N $Mg(NO_3)_2$: *1.* 0.03 M Sr Valerate; *2.* 0.03 M Ca Valerate *3.* 0.03 M Mg Valerate; *4.* 0.01 M Sr Caprylate.

TABLE 2

Maximum solubility of alcohols (moles litre^{-1}) in alkaline earth metal soaps at 40°C

Solvent	Soap	Soap conc. in moles litre^{-1}	Conductivity method	
			1-Butanol	2-Methyl--1-propanol
Water	Sr caprylate	0.015 M	1.76	1.82
	Sr valerate	0.050 M	1.62	1.66
	Ca valerate	0.050 M	1.69	1.72
	Mg valerate	0.050 M	1.76	1.78

TABLE 2 (continued)

Solvent	Soap	Soap conc. in moles litre^{-1}	Conductivity method	
			1-Butanol	2-Methy--1-propanol
0.002 N KNO_3	Sr caprylate	0.015 M	1.82	1.88
	Sr valerate	0.050 M	1.69	1.73
	Ca valerate	0.050 M	1.76	1.80
	Mg valerate	0.050 M	1.82	1.86
0.002 N $Mg(NO_3)_2$	Sr caprylate	0.015 M	1.89	1.93
	Sr valerate	0.050 M	1.73	1.77
	Ca valerate	0.050 M	1.81	1.85
	Mg valerate	0.050 M	1.86	1.91

increases with the increasing number of carbon atoms present in the hydrocarbon chain of soap. The extent of solubilization in all the media exhibits the following order:

Strontium caprylate > Magnesium valerate > Calcium valerate > Strontium valerate; and for the solutions:

0.002 N $Mg(NO_3)_2 >$ 0.002 N $KNO_3 >$ water.

The trend may be explained on the basis of early and easy micellization. An early micellization has been reported [8, 9] in the order for Sr caprylate > Mg V > Ca V > Sr V, in all media. Furthermore, it has also been seen that the micellization is more affected by the presence of magnesium nitrate solution than potassium nitrate solution. [8]

REFERENCES

[1] A. S. C. Lawrence, *Trans. Faraday Soc.*, **33**, 325 (1937); **33**, 815 (1937).

[2] P. H. Elsworthy, A. T. Florence and C. B. Mcfarlane, "Solubilization by Surface Active Agents" Chapman and Hall, London, 1968, p. 68.

[3] K. Shinoda, *J. Phys. Chem.*, **58**, 1136 (1954).

[4] P. Ekwall, *Finska, Kemastam fundlets Medd.*, **72**, 59 (1963).

[5] R. P. Varma and P. Bahadur, *J. Amer. Oil Chemists' Soc.*, **51**, 545 (1974).

[6] R. P. Varma and P. Bahadur, *Indian J. Chem.*, **10**, 1189 (1972).

[7] R. P. Varma and P. Bahadur, *Cellulose Chem. Technol.*, **8**, 27 (1976).

[8] P. Bahadur, K. Singh and P. Bahadur, *Ann. Chim. (Ital.)*, **69**, 417 (1979).

[9] K. Singh, S. Deepak and P. Bahadur, *Colloid and Polymer Sci.*, **257**, 57 (1979).

Revue Roumaine de Chimie, 27, 4, 491—501 (1982)

CINÉTICA DE LA REACCIÓN ENTRE EL OXÍGENO Y EL Sn(II): ESTABILIZACIÓN DE SUS DISOLUCIONES Y SU UTILIZACIÓN EN REDUCTIMETRÍA

J. HERNANDEZ MENDEZ, G. LOPEZ CUETO, A. ALONSO MATEOS y
C. SANCHEZ BURON

Departamento de Química Analítica, Facultad de Química, Universidad de Salamanca,
España

Recibido el 27 de noviembre de 1980

Se ha estudiado la cinética de la oxidación del Sn(II) por el oxígeno en medio ácido con el fin de encontrar las condiciones experimentales en las que se consiga la máxima estabilización de sus disoluciones. La velocidad de la reacción aumenta al aumentar la acidez y la temperatura, mientras que el Sn(IV), los iones Cl^- y las especies captadoras de radicales libres, como la glicerina y la N,N-dimetilformamida, ejercen un efecto negativo. A partir de estos datos se proponen dos métodos para aumentar la estabilidad de las disoluciones de Sn(II) : Aumentar las concentraciones de Cl^- y de Sn(IV), y trabajar en medio dimetilformamida. Por último, se comprueba la validez de las soluciones de Sn(II) estabilizadas por uno y otro método para la determinación volumétrica de diferentes oxidantes en medio ácido (cloramina T, dicromato, hierro (III), vanadio (V) y ferricianuro).

The kinetics of the oxidation of Sn(II) by oxygen in hydrochloric acid is studied in order to find the experimental conditions in which the maximum stabilization of these solutions is attained. The reaction rate increases as acidity and temperature increase. Sn(IV), Cl^- acceptors of free radicals (glycerol, N,N-dimethylformamide) exert a negative effect. From the results obtained two methods are proposed to stabilize the Sn(II) solutions in hydrochloric acid: to increase the Cl^- and Sn(IV) concentration and to work in N, N-dimethylformamide medium.
The availability of these solutions for titrimetric determinations of oxidants (chloramine T, dichromate, iron (III), vanadium (V) and hexacyanoferrate (III)) in acidic medium is tested and the obtained results are satisfactory.

INTRODUCCIÓN

El potencial formal del sistema redox Sn(IV)/Sn(II) en medio clorhídrico es relativamente bajo, lo que confiere a las disoluciones de cloruro de estaño (II) capacidad para reducir a numerosas sustancias. Las disoluciones clorhídricas de Sn(II) presenten, sin embargo, el notable inconveniente de su inestabilidad frente al oxígeno atmosférico. Este hecho supone un serio inconveniente para la utilización del Sn(II) como agente valorante en reductimetrías; por una parte, porque obliga a una frecuente normalización de sus disoluciones y por otra porque la presencia de oxígeno disuelto provoca errores por exceso. Estos inconvenientes se pueden subsanar conservando las disoluciones de Sn(II) en atmósfera inerte y realizando las valoraciones en las mismas condiciones, lo que requiere el montaje de dispositivos especiales.

Existen algunos antecedentes sobre el estudio de la cinética de la reacción de oxidación de las disoluciones clorhídricas de Sn(II) por el oxígeno atmosférico [1,2] y la influencia de algunas variables sobre la velocidad del proceso, [3,4] pero los resultados aportados no son muy concordantes.

Los únicos trabajos sistemáticos encaminados a estabilizar las disoluciones de Sn(II) son los realizados por Arribas y col., [5] quienes comprueban la mayor estabilidad de las disoluciones de Cl_2Sn en presencia de glicerina y las utilizan con éxito en valoraciones reductimétricas, principalmente en medio CO_3Na_2. Sin embargo, en medio ácido, la glicerina presenta el inconveniente de su poder reductor, lo que limite su utilización.

En este trabajo se realiza en primer lugar un estudio cinérico de la reacción entre el Sn(II) y el oxígeno en medio ácido comprobando la influencia de aquellas variables que afectan a la velocidad de dicha reacción. Por otra parte, se estudian y proponen nuevos procedimientos de estabilización de sus disoluciones que permitan trabajar en medios ácidos. Finalmente, se comprueba la utilidad de las disoluciones de Sn(II) así estabilizadas, aplicándolas a la determinación volumétrica de diversos oxidantes en medio ácido.

EXPERIMENTAL

REACTIVOS

$Cl_2Sn \cdot 2H_2O$, $Cl_4Sn \cdot 5H_2O$, ClNa sólidos en calidad R. A. ClH en calidad reactivo análisis. Disoluciones de I_2 preparadas a partir de IO_3K y de IK de calidad R.A. en agua previamente deaireada. Estas disoluciones se almacenan en recipiente topacio y se valoran periódicamente frente a As_2O_3. Solución indicadora de almidón, preparada por el procedimiento descrito por Kolthoff. [6] Glicerina bidestilada del 98 % y densidad 1.255 – 1.260. N,N-dimetilformamida del 98 % y densidad 0.948.

MATERIAL Y APARATOS

Caudalómetro „de burbuja" de 10 ml de capacidad. Termostato Selecta. Espectrofotómetro Perkin-Elmer, Coleman 55

PREPARACIÓN Y VALORACIÓN DE LAS DISOLUCIONES DE Sn(II)

Las soluciones de Sn(II), con o sin glicerina, se preparan en ClH 0.1 M (concentración que se mantiene constante excepto cuando se estudia la influencia de la acidez), evitando agitar para no introducir burbujas de aire.

La valoración de Sn(II), tanto en ausencia como en presencia de glicerina, se lleva a cabo con disolución valorada de I_2, utilizando a Imidón como indicador del punto final, siguiendo el procedimiento utilizado por Berenguer Navarro y Hernández Méndez [7] en la determinación de estaño en aleaciones. Se han efectuado 14 determinaciones sobre volúmenes diferentes conteniendo la misma cantidad de Sn(II) en presencia de glicerina a I 30 % en volumen, obteniéndose resultados satisfactorios.

PROCEDIMIENTO DE ESTUDIO DE LA CINÉTICA DE LA REACCIÓN

En estudios previos se encontró que la luz y el caudal de oxígeno (Figura 1) influyen notablemente sobre la cinética de la reacción ; por ello todas las experiencias se efectuaron manteniendo la solución de Sn(II) en recipientes de color topacio. Para comprobar la posible influencia del aporte de oxígeno exterior se efectuaron en todos los casos dos experimento paralelos, dejando oxidar la disolución libremente por oxígeno atmosférico en uno de ellos y haciendo burbujear un caudal de aire equivalente a 90 mg de oxígeno por minuto.

Para calcular la velocidad de la reacción se prepara una solución de Sn(II) de concentración conocida, se toman alicuotas de 5 ml a diferentes tiempos y se determina iodométricamente el Sn(II) que permanece sin oxidar.

RESULTADOS Y DISCUSIÓN

INFLUENCIA DE LA CONCENTRACIÓN DE ESTAÑO (II)

Con relación a la influencia de estaño (II), pudo comprobarse que la velocidad inicial, v_0, permanece prácticamente constante para las distintas concentraciones de estaño (II), lo que indica que la reacción sigue inicialmente una dependencia de orden cero con relación a la concentración de estaño (II) :

$$v_0 = k_0 \quad y v'_0 = k'_0 \tag{1}$$

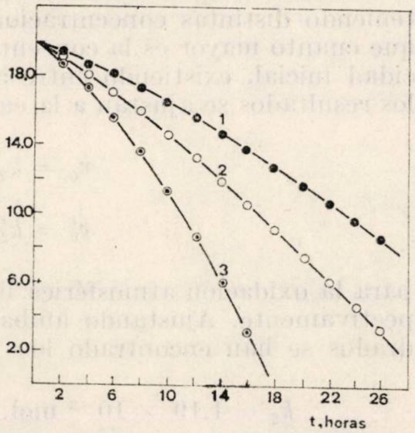

Fig. 1. — Influencia de la luz. Oxidación atmosférica libre : *1.* — Disolución en frasco topacio ; *2.* — Disolución en frasco incoloro ; *3.* — Disolución en frasco incoloro e irradiación UV.

Los valores encontrados para k_0 (oxidación atmosférica libre) y k'_0 (oxidación con corriente de aire) son 0.20×10^{-3} mol. 1^{-1}. hr^{-1} y $0.58 \times \times 10^{-3}$ $mol.l^{-1}.min^{-1}$, respectivamente, para las siguientes condiciones experimentales : $[H^+]$, 0.6M ; $[Cl^-]$, 1.7 M ; fuerza iónica, 1.8 y T, 24°C.

Por otra parte, las velocidades medidas en cualquier momento aumentan linealmente con la concentración de estaño (II) reaccionado, ajustándose los resultados a líneas rectas cuyas ecuaciones son del tipo

$$v_t = k_0 + k_1 \{[\mathrm{Sn(II)}]_0 - [\mathrm{Sn(II)}]\} \tag{2}$$

y

$$v'_t = k'_0 + k'_1 \{[\mathrm{Sn(II)}]_0 - [\mathrm{Sn(II)}]\} \tag{3}$$

Ajustando ambas rectas por el método de mínimos cuadrados, se encuentran para k_1 y k'_1 valores de $40.8 \times 10^{-3}\,hr^{-1}$ y $14.0 \times 10^{-3}\,min^{-1}$ respectivamente.

El hecho de que la expresión de la velocidad conste de dos términos parece indicar que el Sn(II) participa simultaneamente en dos reacciones paralelas siendo la velocidad de la primera de ellas independiente de la concentración de Sn(II) y aumentando la de la segunda proprocionalmente a la concentración de Sn(II) que ha reaccionado. Este efecto puede atribuirse, bien al producto de la oxidación del Sn(II), es decir, el Sn(IV), lo que supondría un proceso autocatalítico, o a un producto intermedio de reducción del oxígeno (un peroxocompuesto) que actúe de iniciador de una reacción en cadena. El hecho de que la reacción esté favorecida por la luz está de acuerdo con esta segunda pisibilidad.

INFLUENCIA DE LA CONCENTRACIÓN DE ESTAÑO (IV)

Para comprobar si el responsable del proceso de autoaceleración es el estaño (IV) se estudió la cinética de la reacción en disoluciones conteniendo distintas concentraciones iniciales de estaño (IV) y se observó que cuanto mayor es la concentración de Sn(IV) inicial, menor es la velocidad inicial, existiendo entre ambas variables una relación lineal, pues los resultados se ajustan a la ecuación de sendas líneas rectas :

$$v_0 = k_2 - k_3\,[\mathrm{Sn(IV)}]_0 \tag{4}$$

$$v'_0 = k'_2 - k'_3\,[\mathrm{Sn(IV)}]_0 \tag{5}$$

para la oxidación atmosférica libre y provocada con caudal de aire, respectivamente. Ajustando ambas rectas por el método de mínimos cuadrados se han encontrado los siguientes valores para las constantes :

$$k_2 = 1.19 \times 10^{-3}\ \mathrm{mol.l^{-1}\ hr^{-1}}\ ;\ k_3 = 35.9 \times 10^{-3}\ \mathrm{hr^{-1}}$$

$$k'_2 = 0.45 \times 10^{-3}\ \mathrm{mol.l^{-1}\ hr^{-1}}\ ;\ k'_3 = 9.4 \times 10^{-3}\ \mathrm{min^{-1}}$$

y para las siguientes condiciones experimentales : [H^+], 1.0M ; [Cl^-], 1.7M ; fuerza iónica, 1.8 y T, 24°C.

Para hallar la posible influencia de la concentración de estaño (IV) en la reacción paralela, se calcula la velocidad de la misma en todo momento, restando a la velocidad experimental v_t (total) el valor conocido de la velocidad inicial v_0.

A partir de los resultados obtenidos se comprobó que la concentración de estaño (IV) no afecta a la valocidad de la segunda reacción, por lo que cabe destacar la posibilidad de una autocatálisis por parte de dicha especie. Si se representa la velocidad de reacción frente a $[\mathrm{Sn(II)}]_0 - [\mathrm{Sn(II)}]$, se obtienen haces de rectas paralelas cuya ordenada en el origen es tanto menor cuanto mayor es la concentración de Sn(IV) y que responden a las ecuaciones :

$$v_t = k_2 - k_3\,[\mathrm{Sn(IV)}]_0 + k_4\,\{[\mathrm{Sn(II)}]_0 - [\mathrm{Sn(II)}]\} \tag{6}$$

$$v'_t = k'_2 - k'_3\,[\mathrm{Sn(IV)}]_0 + k'_4\,\{[\mathrm{Sn(II)}]_0 - [\mathrm{Sn(II)}]\} \tag{7}$$

Los valores obtenidos en estas conditiones para k_4 y k^1_4 son 53.8 × × 10^{-3} $\mathrm{hr^{-1}}$ y 25.9 × 10^{-3} $\mathrm{min^{-1}}$ respectivamente.

INFLUENCIA DE LA CONCENTRACIÓN DE ION HIDRÓGENO

De los valores obtenidos a partir de las experiencias realizadas para estudiar la influencia de la concentración de ion hidrógeno se ha podido comprobar que la velocidad incial v_0 depende linealmente de la concentración de ion hidrógeno hasta una concentración 1.2 M, dependencia que puede expresarse por las ecuaciones:

$$[H^+] \leqslant 1.2M \qquad \begin{aligned} v_0 &= k_5 + k_6[H^+] \\ v'_0 &= k'_5 + k'_6[H^+] \end{aligned}$$

Los valores encontrados para las distintas constantes a partir de las ordenadas en el origen y de las pendientes de las rectas antes mencionadas son:

$$k_5 = 0.08 \times 10^{-3} \text{ mol. l}^{-1}\text{ hr}^{-1}; \quad k_6 = 0.37 \times 10^{-3}\text{ hr}^{-1}$$

$$k'_5 = 0.22 \times 10^{-3} \text{ mol. l}^{-1}\text{ min}^{-1}; \quad k'_6 = 0.82 \times 10^{-3}\text{ min}^{-1}$$

y para las siguientes condiciones experimentales: Sn(II) inicial, 20.0 × × 10^{-3}M; [Cl^-], 0.6 M; fuerza iónica 1.8 y T, 24°C.

Por otra parte, la velocidad de la reacción paralela resulta ser directamente proporcional a la concentración de iones hidrógeno para una concentración constante de Sn(II):

$$\begin{aligned} v = v_t - v_0 &= k_7 \{[H^+]([Sn(II)]_0 - [Sn(II)])\} \\ v' = v'_t - v'_0 &= k'_7 \{[H^+]([Sn(II)]_0 - [Sn(II)])\} \end{aligned} \qquad (9)$$

Representando el valor de las pendientes de las rectas así obtenidas frente a la diferencia $[Sn(II)]_0 - [Sn(II)]$ se obtienen rectas a partir del valor de cuyas pendientes se calculan las constantes k_7 y k'_7 resultando los valores 56.3×10^{-3} mol^{-1} l.hr^{-1} y 24.7×10^{-3} mol. l. min^{-1}, respectivamente.

INFLUENCIA DE LA CONCENTRACIÓN DE CLORURO

En cuanto a la influencia del ion cloruro, se ha comprobado que existe una proporcionalidad entre la velocidad inicial y el inverso de la concentración de dicho ion. Dicha proporcionalidad puede expresarse mediante ecuaciones del tipo:

$$\begin{aligned} v_0 &= k_0 [Cl^-]^{-1} \\ v'_0 &= k'_0 [Cl^-]^{-1} \end{aligned} \qquad (10)$$

Los valores encontrados para k_8 y k'_8 a partir de las pendientes de las rectas mencionadas son 0.46×10^{-3} y 1.20×10^{-3} hr^{-1} y min^{-1} respectivamente. Y para las siguientes condiciones experimentales: [H^+] 0.6 M, fuerza iónica 1.8 y T, 24°C.

Por otra parte, el segundo término de la ecuación de la velocidad resulta ser directamente proporcional a $Cl^{-1/2}$.

$$\begin{aligned} v = v_t - v_0 &= k_{10}\,[\mathrm{Cl}^-]^{1/2}\,\{[\mathrm{Sn(II)}]_0 - [\mathrm{Sn(II)}]\} \\ v' = v'_t - v'_0 &= k'_{10}\,[\mathrm{Cl}^-]^{1/2}\,\{[\mathrm{Sn(II)}]_0 - [\mathrm{Sn(II)}]\} \end{aligned} \tag{11}$$

Representando los valores de las pendientes de las rectas obtenidas frente a $[\mathrm{Sn(II)}]_0 - [\mathrm{Sn(II)}]$ se obtienen líneas rectas a partir de cuyas pendientes se calculan las constantes k_{10} y k'_{10} los valores de 25.2×10^{-3} mol$^{-1/2}$ l$^{1/2}$ hr$^{-1/2}$ y 11.3×10^{-3} mol $^{-1/2}$ l$^{1/2}$ min$^{-1/2}$ respectivamente.

INFLUENCIA DE LA FUERZA IÓNICA

Con respecto al efecto de la fuerza iónica puede comprobarse a partir de los datos obtenidos que no afecta prácticamente a la cinética de la reacción, si bien puede apreciarse, para valores de fuerza iónica, un ligero efecto iónico salino negativo.

INFLUENCIA DE LA TEMPERATURA

Las energias de activación encontradas aplicando la ecuación de Arrhenius fueron las siguientes :

$$E\ a = 14.04 \text{ y } E'\ a = 9.73 \text{ kcal. mol}^{-1}$$

No obstande, estos valores deben considerarse como energias de activación ,,aparentes"; por una parte porque son varias las reacciones que tienen lugar simultáneamente y por otra, porque la solubilidad del oxígeno varía con la temperatura, lo que afectaría indirectamente a la velocidad de la reacción.

CÁLCULO DE LAS CONSTANTES

A partir de las ecuaciones parciales obtenidas para la dependencia de la velocidad de la reacción con respecto a la concentración de las especies Sn(II), Sn(IV), H^+ y Cl^-, puede deducirse la siguiente ecuación global :

$$\begin{aligned} v_t = k_a[\mathrm{Cl}^-] + k_b\,[\mathrm{H}^+]/[\mathrm{Cl}^-] - k_c[\mathrm{Sn(IV)}]_0 \,+ \\ + \,k_d\,[\mathrm{H}^+][\mathrm{Cl}^-]^{1/2}\,\{[\mathrm{Sn(II)}]_0 - [\mathrm{Sn(II)}]\} \end{aligned} \tag{12}$$

Sustituyendo en esta ecuación los valores de las concentraciones que se mantuvieron constantes durante el estudio de la influencia del Sn(IV) y H^+ y comparando las ecuaciones obtenidas con las ecuaciones (6),

(7) y (9) respectivamente, se puede calcular el valor de las constantes de la ecuación (12)

$$k_a = k_5/0.59 = 1.4 \times 10^{-4}\,\mathrm{mol.}^2\,\mathrm{l}^{-2}.\,\mathrm{hr}^{-1}$$

$$k_b = k_6/0.59 = 6.3 \times 10^{-4}\,\mathrm{mol.}\,\mathrm{l}^{-1}.\,\mathrm{hr}^{-1}$$

$$k_c = k_3 = 2.6 \times 10^{-2}\,\mathrm{hr}^{-1}$$

$$k_d = k_7/1.30 = 4.3 \times 10^{-3/2}\,\mathrm{l}^{3/2}\,\mathrm{hr}^{-1}$$

Operando de forma similar, se obtienen los siguientes valores para las constantes de la reacción de oxidación con corriente de aire:

$$k_a' = k_5'/0.59 = 3.7 \times 10^{-4}\,\mathrm{mol}^2.\mathrm{l}^2.\mathrm{min}^{-1}$$

$$k_b' = k_6'/0.59 = 1.4 \times 10^{-3}\,\mathrm{mol.}\,\mathrm{l}^{-1}\,\mathrm{min}^{-1}$$

$$k_c' = k_3' = 9.4 \times 10^{-3}\,\mathrm{min}^{-1}$$

$$k_d' = k_7'/1.30 = 1.9 \times 10^{-2}\,\mathrm{mol}^{-3/2}\ \mathrm{l}^{3/2}.\ \mathrm{min}^{-1}$$

Para comprobar si la ecuación (12) es correcta así como el valor de las constantes deducidas, se obtiene por integración de la misma, la ecuación que relaciona la concentración de Sn(II) con el tiempo

$$[\mathrm{Sn(II)}] = [\mathrm{Sn(II)}]_0 - n/m\,(e^{mt} - 1),\ \text{siendo} \tag{13}$$

$$n = k_a\,[\mathrm{Cl}^-] + k_0\,[\mathrm{H}^+]/\mathrm{Cl}^- - k_c[\mathrm{Sn(IV)}]_0 \tag{14}$$

$$m = k_d\,\mathrm{H}^+\,\mathrm{Cl}^{-1/2}$$

En esta expresión se introduce valores experimentales de las variables que incluye, deduciendose un valor teórico para la concentración de Sn(II); este valor se encontró coincidente con el experimental.

A la vista de dicha ecuación cabe deducir que le mecanismo de la reacción es complejo. Los cuatro términos de que consta, independientes entre sí, parecen indicar que la oxidación del Sn(II) se produce a través de cuatro reacciones paralelas e independientes y siendo, por otra parte, todas ellas de orden cero respecto a la concentración de Sn(II).

A partir de las curvas cinéticas obtenidas de los datos experimentales cabe admitir un proceso de autoinducción por parte de algún producto intermedio de reducción del oxígeno, probablemenete un peróxido.

Mediante la adición de Ti(IV) se ha observado visual y espectrofotométricamente el color amarillo caráterístico de los peroxocomplejos de Ti(IV) en los últimos instantes de la reacción.

EFECTO DE LA GLICERINA

Para comprobar el efecto de la glicerina sobre la estabilidad de las disoluciones de Sn(II) frente a la acción del oxígeno atmosférico, se estudió la cinética de la oxidación en soluciones de aguaglicerina en relación variable.

Se observa que la velocidad inicial se hace menor cuanto mayor es la concentración de glicerina en disolución, existiendo entre ambas variables una relación lineal cuya ecuación es del tipo :

$$v_0 = k_{10} - k_{11}\,[\mathrm{Glic}] \qquad (15)$$

El valor de las constantes obtenido a partir de la ordenada en el origen y de la pendiente de dicha recta es respectivamente :

$$2.03 \times 10^{-3}\ \mathrm{mol.l^{-1}\ min^{-1}}\ \text{y}\ 0.33 \times 10^{-3}\ \mathrm{min^{-1}}.$$

Se ha comprobado posteriormente que el resto de las variables que afectaban a la velocidad de la reacción en ausencia de glicerina, ejercen en presencia de la misma un efecto cualitativamente similar, observándose tan sólo diferencias cuantitativas.

De este hecho parece deducirse que la presencia de glicerina no modifica sustancialmente el mecanismo de la oxidación atmosférica, sino que su efecto consiste unicamente en disminuir la velocidad de la reacción.

Este efecto puede ser debido a una reacción con las sustancias reactivas intermedias responsables de la reacción en cadena. En efecto, realizado el ensayo de peróxidos con Ti(IV) resultó negativo en todo momento, lo cual parece confirmar que los radicales libres intermedios reaccionan con la glicerina antes de poder unirse entre sí para formar el peróxido.

EFECTO DE LA N,N-DIMETILFORMAMIDA

Según Haring y Walton [4] algunas aminas y también la urea ejercen un efeco catalítico negativo sobre la velocidad de oxidación del Sn(II) por el oxígeno. Ante la possibilidad de que otras amidas, además de la urea, ejerzan un efecto similar, se ensayó el efecto de la N, N-dimetilformamida sobre la cinética de la reacción.

Como la determinación del Sn(II) en presencia de N, N-dimetilformamida no puede llevarse a cabo con I_2, ya que este oxida a los productos de hidrólisis de la dimetilformamida, se utilizó en este caso disolución de $Cr_2O_7K_2$ y difenilaminosulfonato de bario como indicador.

De los datos obtenidos se comprobó que la dimetilformamida no modifica sustancialemente el mecanismo de la oxidación atmosférica ; su efecto consiste, al igual que en el caso de la glicerina, en disminuir la valocidad de la reacción.

La N,N-dimetilformamida ejerce un notable efecto inhibidor si bien inferior al de la glicerina. Una disolución de Sn(II) 0.1 N en N, N-dimetilformamida se mantiene practicamente invariable unicamente durante 8 horas, si bien frente a las disoluciones en glicerina presentan dos ventajas apreciables : Su pequeña viscosidad y que en los ensayos realizados parece ser que no reacciona con los oxidantes utilizados.

UTILIZACIÓN DE LAS DISOLUCIONES DE Sn(II) EN PRESENCIA DE INHIBIDORES

A la vista de los resultados obtenidos a partir del estudio cinético se deduce que el Sn(IV), los iones Cl^-, la glicerina y la N-N-dimetilformamida presenta un evidente carácter inhibidor sobre la reacción de oxidación del Sn(II).

Dado que las disoluciones de Sn(II) en glicerina han sido ampliamente utilizadas, se han estudiado las posibles aplicaciones de las disoluciones de Sn(II) estabilizadas por una parte en presencia de Sn(IV) y Cl^- y por otra parte en presencia de N, N-dimetilformamida como reactivos reductimétricos en medio ácido. Las disoluciones utilizadas han sido:

A : Disolución 0.1 N de Sn(II) en ClH 0.5 M y Sn(IV) 0.2 M
B : Disolución de Sn(II) en N, N-dimetilformamida.

NORMALIZACIÓN DE DISOLUCIÓN DE CLORAMINA T

Se prepara una disolución aproximadamente 0.1 N de cloramina T disolviendo el producto sólido en agua destilada. Esta disolución se normaliza por el método de Noll[8] y frente a soluciones de Sn(II) estabilizado por los dos métodos propuestos utilizando como indicator IK y almidón. Los resultados obtenidos son satisfactorios presentando un valor para la desviación standard relativa del orden de 0.4 %.

DETERMINACIÓN DE DICROMATO

Se determinó en medio ClH 3—4M y utilizando difenilaminosulfonato de bario como indicador. Los resultados obtenidos con las dos disoluciones de Sn (II) propuestas son satisfactorios, como se aprecia en la Tabla 1. Se ha utilizado también cacotelina como indicador observandose un buen viraje y resultados semejantes a los obtenidos con difenilaminosulfonato.

TABLA 1
Determinación de dicromato
Disolución A : Disolución de Sn(II) estabilizada en presencia de Sn(IV)
Disolución B : Disolución de Sn(II) estabilizada en N,N-dimetilformamida

$Cr_2O_7^{2-}$ mg puestos	$Cr_2O_7^{2-}$, mg encontrados	
	Disol. : A	Disol. : B
25.5	25.5	25.6
36.1	36.4	36.4
38.5	38.4	38.4
43.2	43.4	43.5
46.4	46.5	46.6
53.2	53.3	53.3
54.3	54.1	54.5
66.5	66.1	66.7
70.2	69.9	69.8
76.4	76.7	76.0
80.1	80.8	80.6
82.2	82.0	81.9

DETERMINACIÓN DE HIERRO (III)

Se prepara una disolución de hierro (III) y se normaliza frente a Sn(II) previamente valorado por el método de Szabo y Sugar. [9, 10] Se toman cantidades variables de la solución de Fe(III) y se valoran con las soluciones de Sn(II) propuestas, operando en medio ClH 0.8 — 1.0 M y utilizando como indicador tanto cacotelina como tiocianato. La valoración con Sn(II) estabilizado con Sn(IV) y Cl^- es preciso realizarla a 65°C; no así cuando se opera en dimetilformamida, ya que la mezcla de este solvente con agua es exotermica y el calor liberado es suficiente para que la reacción transcurra rápida y cuantitativamente. Los resultados, que se expresan en la Tabla 2, son satisfactorios.

TABLA 2

Determinación de hierro (III)

Disolución A : Disolución de Sn(II) estabilizada en presencia de Sn(IV)
Disolución B : Disolución de Sn(II) estabilizada en N,N-dimetilformamida

Fe(III) mg puestos	Fe(III), mg encontrados	
	Disol : A	Disol : B
38.9	38.8	39.0
42.1	41.9	42.4
44.4	44.2	44.0
48.4	48.4	48.2
52.2	52.4	52.0
56.3	56.0	56.3
58.3	58.3	58.6
60.1	60.4	60.0
65.3	65.1	65.0
70.4	70.0	70.2

DETERMINACIÓN DE VANADIO (V)

La valoración de vanadio (V) (previamente normalizada frente a sal de Mohr) se realiza en medio ClH aproximadamente 6 M, utilizando difenilamina como indicator. En la Tabla 3 se muestran los resultados obtenidos.

DETERMINACIÓN DE FERRICIANURO

El $Fe(CN)_6^{3-}$, previamente normalizado por iodometría, se valora en medio ClH 0.85 M y actuando el sistema $Fe(CN)_6^{3-}/Fe(CN)_6^{4-}$ como autoindicador. La solución amarilla inicial evoluciona a verde durante la valoración para virar a azul en el punto final, aproximadamente unos 15 minutos después del punto final se forma un precipitado gelatinoso azulado, que según Wallace [11] está constituido por ferrocianuro estánico que contiene azul de Prusia adsorbido en la superficie. El viraje es neto y los resultados satisfactorios (Tabla 4).

TABLA 3

Determinación de vanadio (V)

Disolución A : Disolución de Sn(II) estabilizada en presencia de Sn(IV)

Disolución B : Disolución de Sn(II) estabilizada en N,N-dimetilformamida

V(V) mg puestos	V(V), mg encontrados	
	Disol : A	Disol : B
215.2	215.0	215.6
206.4	206.0	206.3
160.6	160.0	160·9
130.9	131.0	130.4
99.8	99.9	99.2
85.4	85.7	85.7
73.2	72.9	73.0
66.1	66.5	66.0
57.4	57.3	57.6
53.1	53.4	53.0
50.2	50.0	50.4
48.4	48.1	48.2

TABLA 4

Determinación de ferricianuro

Disolución A : Disolución de Sn(II) estabilizada en presencia de Sn(IV)

Disolución B : Disolución de Sn(II) estabilizada en N,N-dimetilformamida

$Fe(CN)_6^{3-}$ mg puestos	$Fe(CN)_6^{3-}$, mg encontrados	
	Disol : A	Disol : B
198.3	198.5	199.0
201.3	201.0	199.3
230.4	230.0	231.2
234.3	234.9	234.9
242.6	243.1	241.9
257.2	256.9	256.9
262.2	261.7	262.9
277.3	278.9	278.4
279.2	280.0	280.7
281.3	282.0	282.2

BIBLIOGRAFIA

[1] Lachman y Tompkis, *Trans. Faraday. Soc.*, **40**, 130 (1944).
[2] Miyamoto, *Bull. Chem. Soc. Japan*, **2**, 155 (1927).
[3] G. W. Filson y J. H. Walton, *J. Phys. Chem.*, **36**, 740 (1932).
[4] R. C. Haring y J. H. Walton, *J. Phys. Chem.*, **37**, 133 (1933).
[5] S. Arribas Jimeno, R. Rincón, R. Moro y M. L. Alvarez, *Analyt. Chim. Acta*, **33**, 205 (1965).
[6] S. Arribas Jimeno, R. Moro, M. L. Alvarez y G. García, *Inf. Quim. Anal.*, **21**, 85 (1967).
[7] J. Hernández Méndez y V. Berenguer, *Ion*, **37**, 265 (1977).
[8] A. Noll, *Chem. Ztg.*, **48**, 162 (1924) ; **64**, 308 (1940) ; *Chem. Abstr.*, 57, 77757.
[9] E. Sugar y K. M. Kovack, *Magyar Kém. Lapjá.*, **17**, 428 (1962) ; *Chem. Abstr.*, **58**, 2835.
[10] Z. G. Szabo y E. Sugar, *Analyt. Chim., Acta*, **6**, 292 (1952).
[11] W. Wallace, *J. Chem. Soc.*, **7**, 77 (1855).

Revue Roumaine de Chimie, 27, 4, 503–508 (1982)

ОБ ИЗВЛЕЧЕНИИ ПАЛЛАДИЯ (II) И ЗОЛОТА (III) ИЗ РАСТВОРОВ НА НЕОРГАНИЧЕСКИХ ЭЛЕКТРОНООБМЕННИКАХ

А. КАЛЮЖНЫЙ, В. МИЛЮТИН, Я. ФАЗАКАШ и МАРИЯ НЕГОЙЮ
Бухарестский политехнический институт, кафедра неорганической химии, Сплаюл-Индепенденцей 202 А, район 6, Бухарест.

Получена 13 июля 1981 г.

Неорганические электроннообменники (ЭО) на основе смешанного ферроцианида никеля и гидразония и ЭО на основе мелкодиспергированной металлической меди испытаны в процессе извлечения микроколичеств палладия (II) и золота (III) из растворов, содержащих макроколичества никеля и меди. Достигнуто количественное извлечение благородных металлов из растворов. Сорбция палладия и золота на ЭО протекает за счет восстановления их до металлического состояния и закрепления на поверхности и в порах ЭО за счет адгезии.

The inorganic electronic changers (E.S.) based on a mixture of nickel ferrocyanide, and hydrazine, and E.S. based on fine dispersed metallic copper have been tested in the extraction of microquantities of Pd(II) and Au(III) from solutions containing microquantities of nickel and copper.
The quantitative extraction of noble metals has been fulfilled.
Palladium and gold sorption on E.S. is due to their reduction to the metallic state and, their strengthening on the E.S. surface and pores to the adherent forces.

Одним вариантом сорбционных процессов на неорганических электронообменниках (ЭО) является ред — окс — взаимодействие сорбтива с компонентами ЭО, сопровождающееся выделением восстановленной формы сорбтива в свободном состоянии[1]. При этом выделившейся в свободном состоянии элемент удерживается на поверхности и в порах гранул ЭО за счет сил адгезии. Конкретным примером такого сорбционного процесса является взаимодействие палладия (II) с ЭО на основе смешанных ферроцианидов никеля — калия и никеля — гидразония.[1–4] Ред—окс—сорбционные процессы с участием этих ЭО протекают в соответствии с уравнениями реакции:

$$K_{1.22}Ni_{1.39}Fe^{II}(CN)_6 + Pd^{2+} \rightarrow K_{0.22}Ni_{1.39}Fe^{III}(CN)_6 \cdot Pd^0 + K^+ \qquad (1)$$

$$(N_2H_5)_{1.40}Ni_{1.30}Fe^{II}(CN)_6 + 2{,}5\,Pd^{2+} \rightarrow$$
$$(N_2H_5)_{0.40}Ni_{1.30}Fe^{III}(CN)_6 \cdot 2{,}5\,Pd^0 + N_2 + 5\,H^+ \qquad (2)$$

В[4] приведены данные по извлечению Pd (II) из нейтральных растворов, содержащих Ni (II). Извлечение Au (III) из растворов содержащих Ni (II), и извлечение Au(III) и Pd(II) из сильно кислых растворов, содержащих Cu(II) на ЭО ранее не проводилось. В связи с этим в настоящей работе поставлена задача — осуществить подбор ЭО, которые могут быть использованы в качестве эффективных сорбентов для извлечения Pd(II) и Au(III) из указанных типов растворов. Кроме того представлялось интересным добиться количественного извлечения благородных металлов из растворов, что ранее не было достигнуто.

В качестве сорбентов для извлечения Pd(II) и Au(III) из растворов были опробованы ЭО с общей формулой:

$$(N_2H_5)_m Ni_n Fe^{II}(CN)_6 \cdot pN_2H_5Cl(a)$$

$$\text{где } m = 1{,}20 - 1{,}60, \ n = 1{,}20 - 1{,}40 \ \text{и} \ p = 0 - 0{,}10$$

и ЭО, включающие 80—90 вес. % мелкодиспергированной металлической меди и 10 — 20 вес. % связующего вещества (б). Сорбцию проводили в динамическом режиме колоночной хроматографии из растворов составов, г/л: Ni—40, Cu—0,4, H_2SO_4—1, Pd(Au)—5·10^{-3} (1) и Cu—25, H_2SO_4—150, Pd(Au)—5·10^{-3} (2). Растворы готовили на основе сульфатов никеля, меди и хлоридных комплексов палладия и золота. Скорость фильтрации растворов при сорбции варьировали в пределах 5—10 уд. об/час.

Проведенные эксперименты показали, что ЭО (а) обеспечивает практически количественное извлечение Pd(II) и Au(III) из раствора 1. Остаточные концентрации благородных металлов в фильтратах после сорбции составили 0,1—1 мкг/л. Однако ЭО (а) оказался недостаточно эффективным при извлечении Pd(II) и Au(III) из раствора 2. Так в этом случае остаточные концентрации Pd(II) и Au(III) составили соответственно 50 и 100 мкг/л. Несколько более высокая степень извлечения Pd(II) по сравнению с Au(III) из раствора 2 на ЭО (а) обусловлена вероятно, лучшей кинетикой процесса сорбции Pd(II). В целом уменьшение степени извлечения благородных металлов из раствора 2 по сравнению с раствором 1 на ЭО(а) связано, по-видимому, с уменьшением движущей силы ред—окс—сорбционного процесса в сильно кислой среде. Рассмотрим этот вопрос более подробно.

Как известно,[5] движущая силь ред—окс— сорбционного процесса определяется разностью потенциалов $\varphi_{0.5}$ и φ^0_p, где $\varphi_{0.5}$ — ред— окс — потенциал ЭО, соответствующий $\theta = 0{,}5$ (θ доля окисленной или восстановленной формы ЭО) и φ^0_p — нормальный потенциал растворимой ред—окс—системы, взаимодействующей с ЭО. С этих позиции движущая сила ред — окс— процесса в системе ЭО(а) — Pd(II) — Au(III) достаточна для полного его протекания $\varphi_{0.5} = 0{,}42$ в^3, $\varphi^0_{PdCl_4^{2-}/Pd} = 0{,}64$ в^6, $\varphi^0_{AuCl_4^-/Au} = 0{,}99$ в.

В литературе отсутствуют данные о ред—окс—потенциалах Pd(II)/Pd и Au(III)/Au в сульфатных растворах. Поэтому следует иметь в виду, что данные[6] можно использовать лишь для приблизительной оценки полноты протекания ред—окс—процессов в сульфатно-хлоридных растворах, содержащих преобладающие количества сульфат — ионов.

Однако при оценке движущей силы ред—окс — процесса необходимо учитывать влияние на текущие значения ред—окс — потенциала ЭО ($\varphi_{ЭО}$) ряда факторов,[7, 8] в том числе и активности в растворе тех ионов, которые участвуют в процессе массопередачи, сопровождающей ред—окс — процесс. Увеличение активности этих ионов в растворе может привести к увеличению значений $\varphi_{ЭО}$ и соответственно к уменьшению э. д. с процесса в случае взаимодействия ЭО с окислителем. Рассмотрим это положение на примере ЭО (а).

Для ЭО(а) электронообменный процесс складывается из двух одновременно протекающих полуреакций:

$$(N_2H_5)_{1.40}Ni_{1.30}Fe^{II}(CN)_6 - e^- \rightarrow (N_2H_5)_{0.40}Ni_{1,30}Fe^{III}(CN)_6 + N_2H_5^+ \qquad (3)$$

$$N_2H_5^+ - 4e^- \rightarrow N_2 + 5\,H^+ \qquad (4)$$

Полуреакция (3) протекает в твердой фазе, и полуреакция (4) в жидкой фазе системы (1). В соответствии с данными работы[8] уравнение, описывающее зависимость φ от ряда факторов для полуреакции типа (3) имеет вид:

$$\varphi = \varphi^0 + 0{,}059\,\lg \frac{\theta \cdot V_{N_2H_5^+} \cdot a_{N_2H_5^+}}{(1-\theta)\,E_{N_2H_5^+}} \qquad (5)$$

где θ — доля окисленной формы ЭО;

$V_{N_2H_5^+}$ — концентрация вакансий в позициях ионов $N_2H_5^+$ участвующих в процессе массопередачи между твердой фазой и раствором;

$E_{N_2H_5^+}$ — текущее значение обменной емкости ЭО по ионам $N_2H_5^+$

$a_{N_2H_5^+}$ — активность ионов $N_2H_5^+$ в растворе.

Уравнение (5) учитывает два равновесия: между окисленной и восстановленной формами ЭО в твердой фазе;

между обменными в растворе и соответствующими вакансиями в позициях этих ионов в твердой фазе. Уравнение, описывающее φ для полуреакции (4), имеют вид:

$$\varphi = \varphi^0 + \frac{0{,}059}{4}\,\lg \frac{p_{N_2} \cdot a^5_{H^+}}{a_{N_2H_5^+}} \qquad (6)$$

где p_{N_2} — парциальное давление азота в системе.

Суммируя уравнения (5) и (6) получаем уравнение, описывающее зависимость φ от ряда факторов для ЭО (а):

$$\varphi = \varphi^0 + \frac{0{,}059}{5}\,\lg \frac{\theta \cdot V_{N_2H_5^+}\, p_{N_2}}{(1-\theta)\,E_{N_2H_5^+}} - 0{,}059\ pH \qquad (7)$$

Как видно из уравнения (7) увеличение кислотности сорбтива приводит к повышению значений $\varphi_{ЭО}$ и соответственно к уменьшению движущей силы ред—окс—процесса при взаимодействии ЭО(а) с Pd(II) и Au(III). Это и является, вероятно, причиной неколичественного извлечения благородных металлов на ЭО(а) из сильно кислых растворов.

С целью повышения степени извлечения Pd(II) и Au(III) из сильно кислых растворов, содержащих макроколичества Cu(II), было предложено использовать в процессе сорбции ЭО на основе мелкодиспергированной металлической меди — ЭО(б). В этом случае $\varphi_{ЭО}$ зависит лишь от активности ионов Cu^{2+} в растворе в соответствии с уравнением:

$$\varphi = \varphi^0 + 0{,}029 \lg a_{Cu^{2+}}. \qquad (8)$$

Ионы H^+ не принимают участия в процессе массопередачи при взаимодействии ЭО(б) с Pd (II) или А (III) и, таким образом, изменение значений pH сорбтива не может привести в данном случае к изменению значений $\varphi_{ЭО}$. Кроме того судя по значению величины $\varphi^0_{Cu^{2+}/Cu} = 0{,}36$ в, движущая сила ред—окс— процесса в данном случае должна быть вполне достаточной для полного его протекания. Проведенные сорбционные эксперименты подтвердили эти соображения. Так концентрации благородных металлов в фильтратах после сорбции на ЭО(б) оказались значительно ниже чем в случае ЭО(а) и составили 0,1—1 мкг/л.

Следует отметить, что для ЭО(а) предусмотрена регенерация, вследствие чего он может быть использован в ряде циклов сорбция — регенерация, то есть в режиме накопления благородных металлов в сорбционной колонне. Процесс регенерации проводится путем пропускания через слой окисленной формы ЭО в колонне раствора N_2H_5Cl. При этом протекает процесс восстановления ионов $Fe(CN)_6^{3-}$ до $Fe(CN)_6^{4-}$ в твердой фазе и сопровождающий его процесс внедрения ионов $N_2H_5^+$ из растворов в кристаллическую решетку образующегося ферроцианида. Процесс регенерации ЭО (например, после сорбции на нем палладия) описывается следующим уравнением реакции:

$$(N_2H_5)_{0.40}Ni_{1.30}Fe^{III}(CN)_6 \cdot 2{,}5\ Pd^0 + 1{,}25\ N_2H_5^+ \rightarrow$$
$$\rightarrow (N_2H_5)_{1.40}Ni_{1.30}Fe^{II}(CN)_6 \cdot 2{,}5\ Pd^0 + 0{,}25\ N_2 + 1{,}25\ H^+ \qquad (9)$$

Регенерированный ЭО(а) готов к следующему циклу сорбции Pd(Au).

Для ЭО(б) регенерация не предусмотрена, поскольку ред—окс—сорбционный процесс в этом случае сопровождается постепенным растворением ЭО в соответствии с уравнением реакции

$$A.Cu^0 + Pd^{2+}\left(\frac{2}{3}Au^{3+}\right) \rightarrow A.Pd^0\left(\frac{2}{3}Au^0\right) + Cu^{2+} \qquad (10)$$

где А — связующий материал.

Оба ЭО обладают значительными величинами сорбционной емкости, однако емкость ЭО(а) больше чем ЭО(б). Так, например, при извлечении палладия из раствора 1 емкости до проскока палладия в фильтрат для ЭО(а) и ЭО(б) составили 200 и 100 мг Pd/г ЭО соответственно. За проскок палладия было условно принято его содержание в фильтрате на уровне 100 мкг/л.

Для выделения сорбированных благородных металлов из состава твердой фазы в раствор продукт сорбции разлагали путем обработки при нагревании царской водкой (в случае ЭО(а) дополнительно проводили обработку концентрированной H_2SO_4). Оставшийся сухой остаток растворяли в горячей воде. При этом в полученном растворе достигается концентрирование Pd(II) и Au(III) (по сравнению с раствором из которого проводилось извлечение) в $10^2 - 10^3$ раз.

В целом осуществлен выбор неорганических ЭО, обеспечивающих практически количественное извлечение палладия и золота из нейтральных и кислых растворов, содержащих макроколичества никеля и меди. Эти ЭО рекомендуются для концентрирования Pd(II) и Au(III), что является полезным при количественном определении малых содержаний этих элементов в сложных по составу объектах.

ПОЛУЧЕНИЕ ЭЛЕКТРОНООБМЕННИКОВ

Электронообменник (ЭО) на основе смешанного феррицианида никеля и гидразония получали путем осаждения ферроцианида никеля — $Ni_{1,5}Fe^{III}(CN)_6$ и последующего восстановления коагулата феррицианида раствором N_2H_5Cl. В общем случае состав полученного ЭО выражается формулой:

$$(N_2H_5)_mNi_nFe^{II}(CN)_6\cdot pN_2H_5Cl, \text{ где } m = 1{,}20 - 1{,}60,\ n = 1{,}20 - 1{,}40$$

$$\text{и } p = 0 - 0{,}10$$

Процесс получения ЭО (например, $m=1{,}40$, $n=1{,}30$ и $p=0$) описывается следующими уравнениями реакций:

$$K_3Fe^{III}(CH)_6 + 1{,}50\ NiSO_4 \rightarrow Ni_{1,50}Fe^{III}(CH)_6 + 1{,}50\ K_2SO_4 \qquad (11)$$

$$Ni_{1,50}Fe^{III}(CH)_6 + 1{,}65\ N_2H_5Cl \rightarrow (N_3H_5)_{1,40}Ni_{1,30}\ Fe^{II}(CH)_6 +$$

$$+ 0{,}20\ NiCl_2 + 0{,}25\ N_2 + 1{,}25\ HCl \qquad (12)$$

Для получения ЭО сливали при перемешивании 0,1 М раствор $K_3Fe^{III}(CN)_6$ (33 г соли в 1 л H_2O) и 0,1 М раствор $NiSO_4\cdot 7H_2O$ (56 г соли в 2 л H_2O). К образовавшемуся коагуляту феррицианида никеля добавляли при перемешивании раствор N_2H_5Cl (10 мл 70% раствора $N_2H_4\cdot H_2O$ разбавляли водой до 0,5 л и нейтрализовали 20% раствором HCl до pH=7—8), после чего реакционную смесь выдерживали в течение 30 мин. для полного протекания реакции по уравнению (12). Полученный коагулят ферроцианида никеля и гидразония, трижды промывали дистиллированной водой методом последовательных декантаций (расход воды — 15—20 л на одну декантацию) и гранулировали замораживанием в воздушном криостате при t=—5°С. Выход готового продукта обычно составляет около 50 г в расчете на массу воздушно сухого вещества.

ЭО, включающий мелкодиспергированную металлическую медь, получали по следующей методике. 16—18 г мелкодисперсного порошка меди и 2—4 г связующего вещества (например, жидкого стекла) перемешивали до получения однородной массы. Полученную пасту высушивали на воздухе и подвергали декриптации.

Для проведении сорбционных экспериментов использовали фракции электронообменников с размером гранул 0,5—1 мм.

АНАЛИТИЧЕСКИЙ КОНТРОЛЬ

Для аналитического контроля в ходе сорбционных экспериментов использовали атомно — абсорбционный спектрофотометр Р—Е—5000 с электротермическим атомизатором HGA—500.

ЛИТЕРАТУРА

1. В. В. Вольхин и А. В. Калюжный, *ЖПХ*, **53**, 78 (1980).
2. С. А. Колесова, В. В. Тетенов и В. В. Вольхин. «Химия и химическая технология» (материалы IV областной научно-технической конференции,) ч. II, 113. Пермь, 1973.
3. А. В. Калюжный, В кн.: «Химия и технология неорганических сорбентов» (межвузовский сборник научных трудов), 44. Пермь, 1979.
4. А. В. Калюжный, С. А. Колесова и В. В. Милютин. В кн.: « Химия и технология неорганических сорбентов» (межвузовский сборник научных трудов), 108. Пермь, 1980.
5. В. В. Вольхин, *ЖПХ*, **49**, 1728 (1976).
6. В. Латимер, «Окислительные состояния элементов и их потенциалы в водных растворах» Москва, Издатинлит, 1952.
7. М. В. Зильберман, *ЖФХ*, **52**, 1815 (1978). Деп. ВИНИТИ *АН СССР*, №77—78 деп. (1978).
8. В. В. Вольхин и А. В. Калюжный, *ЖПХ*, **53**, 1216 (1980).

Revue Roumaine de Chimie, 27, 4, 509–512 (1982)

VINYL MONOMER COMPLEXES. I.

THE COMPLEXES OF ACRYLONITRILE WITH SOME INORGANIC SALTS

S.A.K. LODHI* and A. RASHEED KHAN
Polymer Research Division, Pakistan Council of Scientific and Industrial Research Laboratories, Karachi

Received November 7, 1980

The complexes of acrylonitrile with some inorganic salts like $CuCl_2$, $CoCl_2$, $HgCl_2$, $ZnCl_2$, $H_2Pt.Cl_6$ and $CrCl_3$ were prepared. Acrylonitrile forms complexes ($AN \rightarrow MX_n$) with inorganic salts through nitrile group in the 1 : 1 (AN ; salt) molar ratio. These complexes are hygroscopic and soluble in polar solvents.

INTRODUCTION

It has been reported by several authors[1–4] that vinyl monomers containing carbonyl or nitrile group form complexes with inorganic salts like $ZnCl_2$, $AlCl_3$ etc. The complexes of the monomers with inorganic salts undergo polymerization easier than the uncomplexed monomers. The accelerating or inhibiting effect of these complexes on the homopolymerization and copolymerization of vinyl and allyl monomers has been discussed by several workers. [5–10, 11]

This paper deals with the preparation of acrylonitrile complexes with inorganic salts like copper chloride, cobalt chloride, mercury chloride, zinc chloride, platinum chloride and chromium chloride.

EXPERIMENTAL

MATERIALS

1. Acrylonitrile (BDH) was dried over sodium sulphate and distilled at 76°C. Laboratory grade acetone and dimethylformamide were purified according to known methods.

2. All metal salts shown below were used without further purification. Extra pure copper chloride ($CuCl_2 . 2H_2O$), cobalt chloride ($CoCl_2 . 6H_2O$) and anhydrous zinc chloride ($ZnCl_2$) of E. Merck ; fine crystals of mercury chloride ($HgCl_2$) of E. Merk, Laboratory reagent grade chloroplatinic acid ($H_2PtCl_6 .6H_2O$) and Analar grade chromium chloride ($CrCl_3 . 6H_2O$) were used.

---

* Present address : Department of Chemistry, University of Baluchistan, Quetta, Pakistan.

TABLE 1

The composition of complexes of acrylonitrile (AN) with metal halides

Name of salt	Amount of salt (moles)	Amount of AN consumed (moles)	Composition of complex (AN/Mx_n) (mole ratio)	IR Spectra	Physical properties
$CuCl_2 \cdot 2H_2O$	5.87×10^{-3}	0.602×10^{-3}	1.125	$-C\equiv N$ 2 325 cm^{-1} $-CH=CH_2$ 1 600 cm^{-1}	Hygroscopic, green crystalline substance, soluble in acetone and DMF.
$CoCl_2 \cdot 6H_2O$	4.204×10^{-3}	4.460×10^{-3}	1.061	$-C\equiv N$ 2 325 cm^{-1} $-CH=CH_2$ 1 590 cm^{-1}	Hygroscopic, pink crystalline substance soluble in acetone and DMF.
$HgCl_2$	1.8×10^{-3}	1.76×10^{-3}	0.954	$-C\equiv N$ 2 325 cm^{-1} $-CH=CH_2$ 1 590 cm^{-1}	Hygroscopic, green powder substance soluble in acetone and DMF.
$ZnCl_2$	7.34×10^{-3}	7.43×10^{-3}	1.013	$-C\equiv N$ 2 300 cm^{-1} $-CH=CH_2$ 1 600 cm^{-1}	Highly hygroscopic colour less crystalline substance, soluble in acetone and DMF.
$H_2 \cdot PtCl_6 \cdot H_2O$	0.42×10^{-3}	0.42×10^{-3}	0.998	$-C\equiv N$ 2 325 cm^{-1} $-CH=CH_2$ 1 600 cm^{-1}	Highly hygroscopic, yellow substance soluble in acetone and DMF.
$CrCl_3 \cdot 6H_2O$	3.75×10^{-3}	3.79×10^{-3}	1.010	$-C\equiv N$ 2 300 cm^{-1} $-CH=CH_2$ 1 590 cm^{-1}	Hygroscopic, dark green, crystalline substance, soluble in acetone and DMF.

PROCEDURE FOR PREPARATION OF COMPLEXES

A known amount of each salt was added to a ground glass neck tube already containing pure acrylonitrile in excess. The salt was dissolved [2] by shaking at 50 — 60°C. Excess of monomer was distilled off under reduced pressure. The resulting complexes were further kept for 50 hours in a vacuum desiccator. The composition of a complex was determined from the weight of each salt initially used and of the resulting complexes. [1,2]

RESULTS AND DISCUSSION

The results obtained from the preparation of complexes of acrylonitrile with different inorganic salts are summarized in the table which shows that acrylonitrile forms complexes with copper chloride, cobalt chloride, mercury chloride, zinc chloride, platinic chloride and chromium chloride in 1 : 1 (AN : salt) molar ratio. Although polyacrylonitrile is not soluble in acetone yet all these complexes are hygroscopic and soluble in polar solvents like acetone, dimethylformamide, ethyl ether etc.

The IR spectral studies of these complexes show nitrile absorption band at 2 300 — 2 325 cm^{-1} frequency whereas vinyl band appears at 1570 — 1600 cm^{-1} frequency. The absorption band at a frequency 3 500 cm^{-1} indicates the attachment of water molecules to the complexes. The shift of the nitrile band from 2220 cm^{-1} to 2 300 — 2 325 cm^{-1} in the spectra shows that the nitrile group of monomer takes part in complex formation. [2, 12, 13] However the appearance of the absorption band at 2 300 — 2325 cm^{-1} frequency shows that vinyl group does not take part in complexation. [13-14] Yabumoto et al. [5] and others [13-17] prepared AN — $\mathrm{ZnCl_2}$ complex in 1 : 1 ratio. The complex was a white hygroscopic, crystalline substance. The IR spectra of the complex showed a shift of the nitrile absorption band towards higher frequency and no change in vinyl group absorption.

The UV spectral studies were also carried out. The maxmium absorption was due to the complexes like AN → $\mathrm{CuCl_2}$, AN→$\mathrm{CoCl_2}$ and AN→$\mathrm{ZnCl_2}$, 750 nm, 590 nm and 280 nm respectively whereas the maximum absorption due to the complexes AN → $\mathrm{PtCl_6}$ and AN → $\mathrm{CrCl_2}$ was found respectively to be 370 nm and 580 nm. The complex AN → $\mathrm{HgCl_2}$ does not show any absorption maxima. It gives a continuous absorption. The maxima of $\mathrm{CuCl_2}$, $\mathrm{CoCl_2}$, $\mathrm{PtCl_6}$, $\mathrm{CrCl_2}$ and $\mathrm{ZnCl_2}$ are changed certainly [18-19] due to the formation of complex with acrylonitrile.

The complexation between metal salts (MXm) and AN takes place due to the delocalization of the π electrons in the double bond of monomers. This polarity of AN gets increased as a result of complexation of AN with inorganic salts. The electron accepting character of complexed AN as compared with acrylonitrile monomer also gets enhanced. The suggested structure of the complex is the following :

$$\mathrm{H_2C{=}CH{-}C{\equiv}N{\rightarrow}MX_{\mathit{n}}{\rightarrow}MX_{\mathit{n}}}(\mathrm{MX}_n = \text{metal salt}).$$

REFERENCES

[1] M. Imoto, T. Otsu and Y. Harads, *Makromol. Chem.*, **65**, 180 (1963).

[2] M. Imoto, T. Otsu and M. Nakabayashi, *Makromol. Chem.*, **65**, 194, (1963).

[3] W. Kuran, S. Pasynkiewicz, Z. Florjanczyk and E. Lusztyk, *Makromol. Chem.*, **177**, 2627 (1976).

[4] W. Kuran, S. Pasynkiewicz, R. Nadir and Z. Florjanczyk, *Makromol. Chem.*, **178**, 1881 (1977).
[5] Shigeru Yabumoto, K. Ishi and K. Arita, *J. Polymer Sci. A-1*, **7**, 1577 (1969).
[6] M. Imoto, T. Otsu and K. Murata, *Kogyo Kagaku Zasshi*, **66**, 1900 (1963).
[7] H. C. Hass, *Makromol. Chem.*, **80**, 232 (1964).
[8] M. Imoto, T. Otsu and T. Ito, *Bull. Chem. Soc. Japan*, **36**, 310 (1963).
[9] M. B. Lachinov, B. M. El-Hair, V. P. Zubov, V. A. Kabanov, *Vysckomol. Soedinniya Ser. A*, **15**, 504 (1973).
[10] M. B. Lachinov, V. P. Zubov, V. A. Kabanov, *Vysokomol. Soedinniya Ser. B*, **12**, 4 (1970).
[11] H. J. Coerver and C. Curren., *J. Amer. Chem. Soc.*, **80**, 3522 (1958).
[12] M. P. Coakledy and C. Curren, "Abstract of the 129 meeting of Amer. Chem. Soc.", Atlantic City P-53-R (September 1956).
[13] M. Imoto and Kujehiro, *Kobanshi Kagaku Kyotei*, Asakura Tokyo, (1965) p. 43.
[14] G. N. Shrauzer, *J. Amer. Chem. Soc.*, **81**, 5310 (1959).
[15] S. F. A. Kettle and L. E. Orgel, *Chemistry and Industry*, **No. 2**, 49 (1960).
[16] I. Tadeshi and H. Hidefumi, *J. Polymer Sci. Part A*, **18**, 195 (1970).
[17] M. Imoto, T. Otsu and S. Shimizu, *Makromol. Chem.*, **65**, 174 (1963).
[18] A thesis entitled "Spectrophotometric and potentiometric studies of Chromium of Amino acid" by Mashood Ahmed submitted to Aligarh University on 1960—1961.
[19] International Critical Table, National Press Council, McGraw Hill Book Company Inc., New York, **5**, p. 326.
[20] S. Tazuke, K. Tsuji, T. Yonezenw, *J. Phys. Chem.*, **71**, 2957 (1967).
[21] J. Furakawa, E. Kobayashi, S. Nagata and T. Moritani, *J. Polymer, Sci., Polymer Chem.Ed.*, **12**, 1799 (1974).

Revue Roumaine de Chimie, 27, 4, 513–521 (1982)

MOLECULAR COMPLEXES WITH AROMATIC CATIONS AS ELECTRON ACCEPTORS. V.[1]

INTER- AND INTRAMOLECULAR CHARGE TRANSFER OF AMINO-SUBSTITUTED PYRIDINIUM SALTS EVIDENCED BY ELECTRONIC ABSORPTION SPECTRA

ALEXANDRU T. BALABAN[a] and MARIA PARASCHIV[b]

[a] Polytehnic Institute, Department of Organic Chemistry, Bucharest, Romania
[b] Institute of Nuclear and Engineering Physics, Bucharest, Romania

Received September 30, 1981

Electronic and vibrational spectra are reported for pyridinium salts III, IV, VI, VIII—XI, possessing either N-diphenylamino groups, or *p*-(dimethyl- or diphenylaminophenyl) groups bonded to the nitrogen heteroatom in 2,4,6-trisubstituted pyridinium salts. The electronic absorption spectra indicate that in pyridinium iodides, as known, interionic charge transfer bands appear, while when a donor dialkyl- or diarylamino group is present (either bonded directly or through a *p*-phenylene group with the nitrogen heteroatom), strong intramolecular charge transfer bands appear, which vanish on protonating the lone electron pair of VIII or XI to form IX and X, respectively. The N-aminopyridinium salts IV — VII cannot be protonated at the exocyclic nitrogen in the usual conditions. The solvatochromy of the intramolecular charge transfer band is discussed, and predictions are made for cases with stronger solvatochromy than the compounds already known.

INTRODUCTION

From a study of the ^1H—NMR spectra of N-alkyl-2,4,6-trimethylpyridinium salts *versus* N-aryl-2,4,6-trimethylpyrydinium salts,[2] it became evident that the magnetic shielding exerted by the N-aryl group on the methyl groups in positions 2 and 6 (α-positions) indicated that the aryl and pyridinium rings were not coplanar. The dihedral angle of twist between these rings was found for N-phenyl-2,4,6-trimethylpyridinium perchlorate (I) to amount to 85° in the single crystal. [3] Such a large angle was expected owing to the steric hindrance exerted by the α-methyl groups and the hydrogens in *ortho*-positions to the interannular bond. This steric hindrance is responsible for the existence of atropisomers in *ortho*-substituted N-arylpyridinium salts with different α-groups, [4] analogously to the known atropisomers in the biphenyl series. The magnetic shielding of α-standing 2,6-dimethyl substituents in I and related compounds (actually, the difference in chemical shifts relatively to the 4-methyl group) was used to provide a qualitative and quantitative indication for the aromaticity of the N-bonded group in the compounds analogous to I.[5]

On the other hand, it is known that the two rings of biphenyl are twisted in vapour phase or in solution,[6] but coplanar in the single crystal,[7] therefore it appeared interesting to study the N-phenylpyridinium isosteric and isoelectronic analogue (whose only difference relative to biphenyl is the electrical charge). The X-ray diffraction analysis[8] afforded the crystal and molecular structure of N-phenylpyridinium chloride hydrate. In the single crystal, the phenyl and pyridinium rings form a dihedral angle of 47°, and an interesting intermolecular pairwise association of cations is observed, as indicated by formula II: two cations lie

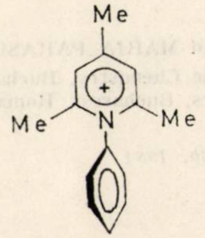

I

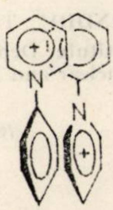

II

with their rings in antiparallel orientation; such a pairwise association of cations sugests an intermolecular charge transfer (CT) in which each pyridinium ring acts as electron acceptor, and each phenyl ring as donor. The shortest interatomic distance between ring planes is 3.447Å. Thus, electron donor—acceptor interactions should manifest themselves in such compounds: actually, the single crystals II are pale yellow.

Such donor—acceptor interactions should be reflected in electronic absorption spectra by the appearance of CT bands, especially in non-polar solvents. It is known[9-12] that CT bands arise both by intermolecular (or, in the present case, interionic) and by intramolecular interactions. The present study was undertaken in order to evidence if such inter- and intramolecular CT bands appear in solutions of substituted pyridinium salts with structure II or possessing strongly donor substituents like tertiary amino groups.

EXPERIMENTAL PART

Infrared spectra were recorded with a Jena UR-10 instrument in potasium bromide pellets. Electronic absorption spectra were recorded at various dilutions with an Optica (Milan) CF-4 instrument.

N-Substituted pyridinium salts were prepared from the corresponding pyrylium salts and primary amines (either N,N-disubstituted hydrazines, or N,N-disubstituted *p*-phenylenediamines), with one exception only:

N-Phenylpyridinium salts (II, III) were prepared as described earlier.[3] We studied both the *chloride hydrate* (used in the X-ray diffraction experiments) and the corresponding *iodide*, prepared from the former by anion exchange.

2,4,6-Trimethyl-N-diphenylamino-pyridinium perchlorate (IV) was obtained by refluxing stoichiometric amounts of 2,4-6-trimethylpyrylium perchlorate and 1,1-diphenylhydrazine in ethanol for one hour. Yellowish needles, m.p. 185° C (from water ; despite the low solubility, the purity thus obtained is better than from ethanol) Found : C, 62.4 ; H, 5.5 ; N, 7.3 %. $C_{20}H_{21}N_2^+ ClO_4^-$ requires : C, 61.8 ; H, 5.4 ; N, 7.2 %.

2,4,6-Triphenyl-N-diphenylamino-pyridinium perchlorate (VI) was obtained by stirring in ethanol 2,4,6-triphenylpyrylium perchlorate with N,N-diphenylhydrazine for two hours at room temperature, filtering the unreacted triphenylpyrylium perchlorate, and adding to the dilute ethanolic solution ethyl ether for precipitating the reaction product. Yellowish crystals with m.p. 150°C (from ethanol with mild heating, in order to avoid the formation of 2,4,6-triphenylpiridine by a reaction of bond fission analogous to that discovered by Susan and Balaban,[13] and intensely used recently for various syntheses by Katritzky).[14]

2,4,6-Triphenyl-N-(p-dimethylaminophenyl)-pyridinium mono- and *diperchlorates* (VIII and IX, respectively) were obtained as described by Dimroth et al.[15] The yellow monoperchlorate VIII has m.p. 291°C and the colourless diperchlorate IX has m.p. 275°C.

2,4,6-Trimethyl-N-(p-dimethylaminophenyl)-pyrydinium mono- and *diperchlorates* (XI and X, respectively), were obtained analogously.

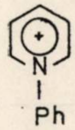

III

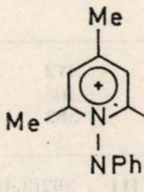

IV

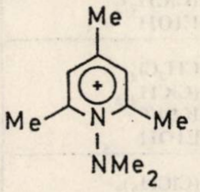

V

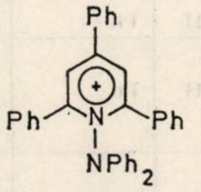

VI

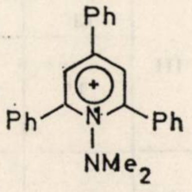

VII

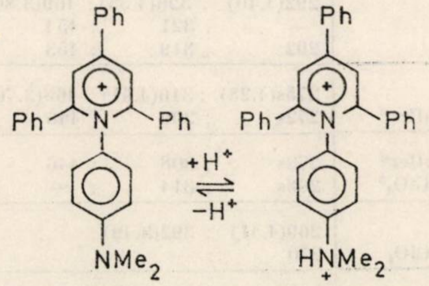

VIII IX

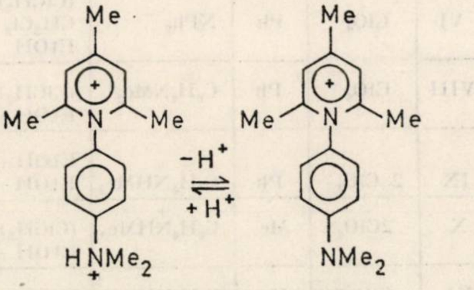

X XI

We also describe the preparation of two related pyridinium salts (i) and (ii) whose spectra were not investigated in detail, and which will not be discussed in the next section of this paper :

(i) *2,4,6-Triphenyl-N-(p-diphenylaminophenyl)-pyridinium perchlorate* was prepared from 2,4,6-triphenylpyrylium perchlorate and *p*-amino-triphenylamine in equimolar amounts, by refluxation for two hours in ethanol. Orange-coloured needles, m.p. 290° (from acetic acid, yielding blue-green fluorescent solutions). Found : C, 75.37 ; H, 5.38 %. $C_{41}H_{31}N_2^+ ClO_4^-$ requires : C, 75.62, H, 4.80 %

(ii) *2,4,6-Trimethyl-N-(p-diphenylaminophenyl)-pyridinium perchlorate* was prepared by refluxing equimolar amounts of 2,4,6-trimethylpyrylium perchlorate and *p-amino-triphenylamine*. Needles m. p. 273°C (from acetic acid). Found : C, 66.63 ; H, 5.63 %. $C_{26}H_{25}N_2^+ ClO_4^-$ requires : C, 67.16 ; H, 5.42 %.

1-Dimethylamino-2,4,6-trimethylpyridinium perchlorate (V) was prepared from, 2,4,6-trimethylpyrylium perchlorate and 1,1-dimethylhydrazine in aqueous ethanol. M. p. 155°C from aqueous ethanol, tan-coloured needles. Found : N, 10.85 ; Cl, 13.77 %. $C_{10}H_{17}N_2^+ ClO_4^-$ requires : N, 10.56 ; Cl, 13.40 %.

RESULTS AND DISCUSSIONS

Results of ultraviolet and visible spectrophotometric determinations are presented in Table 1, where pyridinium cations and anions, solvents, and pH values were varied (all determinations were carried out at room temperature).

TABLE 1

Electronic absorption spectra of N-substituted 2,4,6-tri-R-substituted pyridinium salts (s denotes shoulder)

No.	Anion	R	N-Substituent	Solvent	Absorption maxima, in nm (lg ε)
III	Cl^-	H	Ph	$(ClCH_2)_2$	270
				EtOH	265
	I^-	H	Ph	CH_2Cl_2	245 ; 412
				$(ClCH_2)_2$	266s ; 405
				KBr [a]	— ; 382
				EtOH	265
IV	ClO_4^-	Me	NPh_2	$(ClCH_2)_2$	269(4.41) ; 392(3.48)
				$EtOH+HClO_4$ [b]	268 ; 378
				70 % $HClO_4$	269 ; 384
VI	ClO_4^-	Ph	NPh_2	$(ClCH_2)_2$	292(4.40) ; 326(4.53) ; 469(3.86)
				CH_2Cl_2	— ; 321 ; 454
				EtOH	292 ; 319 ; 453
VIII	ClO_4^-	Ph	$C_6H_4NMe_2$ [c]	$(ClCH_2)_2$	275s(4.28) ; 316(4.61) ; 468(3.76)
				EtOH+buffer [d]	272s ; 309 ; 446
IX	2 ClO_4^-	Ph	$C_6H_4\overset{+}{N}HMe_2$	EtOH+buffer [d]	273s ; 308 ; 446
				$EtOH+HClO_4$ [b]	268s ; 314 ; —
X	$2ClO_4^-$	Me	$C_6H_4\overset{+}{N}HMe_2$	$(ClCH_2)_2$	269(4.41) ; 392(3.49)
				$EtOH+HClO_4$	270 ; —
XI	ClO_4^-	Me	$C_6H_4NMe_2$	EtOH+buffer [d]	266 ; 308s ; 360s

[a] Potassium bromide pellet ;
[b] Mixture 1 : 1 by volume of ethanol and 70 % perchloric acid ;
[c] Literature values (in MeOH) : 307(4.63), and 438 nm (3.44) ;[15]
[d] Ethanol with aqueous sodium acetate buffer for pH = 5.5

Table 2 presents the vibrational spectra, and these will not be discussed in more detail here, except for noting that the IR spectra confirm the strucure of the compounds (no absorption band in the carbonyl region, and distinction between diperchlorates which present NH stretching bands between 2500 and 3000 cm^{-1}, like all ammonium ions with N—H bond(s), and between monoperchlorates which have no bands in this range).

The N-phenylpyridinium chloride III does not evidence any absorption (either in polar solvents such as ethanol, or in non-polar ones such

TABLE 2

Main IR bands of N-substituted 2,4,6-tri-R-pyridinium-salts

No.	Anion	R	N-Substituent	IR Bands in KBr pellets (in cm^{-1})[a]
IV	ClO_4^-	Me	NPh_2	1640s, 1590s, 1498vs, 1465w, 1440w, 1410vw, 1382m, 1348ms, 1330ms, 1302s, 1280s, 1260ms, 1190m, 1160m, 1035ms, 862m, 760vs, 730m, 694s
VI	ClO_4^-	Ph	NPh_2	1625vs, 1600s, 1564m, 1556m, 1500s, 1470m, 1450w, 1420m, 1342m, 1328w, 1305m, 1285m, 1250ms, 1190w, 1170w, 1035w, 1008w, 896ms, 765ms, 754s, 698vs
VIII	ClO_4^-	Ph	$C_6H_4NMe_2$	1630vs, 1610m, 1585w, 1555ms, 1530s, 1500m, 1452m, 1420m, 1370ms, 1240ms, 1200ms, 1035w, 1000w, 950m, 895ms, 822ms, 780s, 760s, 698vs
IX	$2ClO_4^-$	Ph	$C_6H_4\overset{+}{N}HMe$[b]	1628vs, 1600s, 1560s, 1510s, 1478m, 1450m, 1415m, 1408m, 1370ms, 1300w, 1250w, 1240s, 1200w, 1190w, 1170m, 1000w, 935w, 908m, 865ms, 840w, 790s, 760s, 705vs
X	$2ClO_4^-$	Me	$C_6H_4\overset{+}{N}HMe$[b]	1650vs, 1620w, 1575m, 1570m, 1522s, 1485s, 1475m, 1450m, 1425m, 1405w, 1385w, 1320ms, 1305m, 1270m, 1250m, 1000m, 930m, 902m, 872s, 858ms

[a] Abbreviations for intensities : *s* = strong ; m = medium ; w = weak ; v = very.

[b] Several bands (NH stretching) appear in the 2500 − 3000 cm^{-1} range.

as 1,2-dichloroethane) which would indicate intermolecular charge transfer in solution, as observed in the crystal (II). This can be explained by the fact that in the crystal molecules occupy fixed positions with CT minimizing the energy, while in solution where the molecules tumble freely the energy is minimized by ion-pair association involving ions of opposite electrical charges (unlike the crystal, where the electric repulsions between the two cations in I are counterbalanced by packing forces).

The iodide III, however, does present in non-polar solvents an additional band (CT band) at 404 − 412 nm, similar to that evidenced by Kosower for pyridinium iodides, [16] and by Balaban et al. [17] for pyrylium iodides. In potassium bromide pellet, the CT absorption maximum of the iodide undergoes a hypsochromic shift, and in polar solvents such as ethanol, where the iodide anion can no longer act as an electron donor in an intimate ion pair because of strong solvation, the CT band vanishes completely.

N-Diphenylamino-pyridinium salts IV and VI absorb at much higher wavelengths, and this may be considered to be due to intramolecular charge transfer (CT). As seen from Table 1, the exocyclic nitrogen cannot be protonated in aqueous or ethanolic acids. The ^1H-NMR spectra of the analogous N-dimethylamino-2,4,6-trimethylpyridinium perchlorate (V) indicate that in deuterochloroform ($\delta = 2.55$, 3 H, γ-Me ; 2.83, 6H, α-Me; 3.18, 6H, NMe_2; 7.59, 2H, β-H) or in trifluoroacetic acid (δ = = 2.60, 3H, γ-Me; 2.89, 6H, α-Me; 3.23, 6H, NMe_2; 7.56, 2H, β-H) the exocyclic nitrogen cannot be protonated. The ^{1}H-NMR spectrum in trifluoromethanesulfonic acid or in sulfuric acid could be interpreted to involve protonation to some extent, because all peaks move slightly to higher fields with 0.2 – 0.4 ppm except the dimethylamino peak which is slightly deshielded, moving with about 0.35 ppm to lower field (in H_2SO_4, δ = 2.20, 3H, γ-Me; 2.67, 6H, α-Me; 3.55, 6H, NMe_2; 7.31, 2H, β-H). However, the UV absorption spectra of the same salt in CH_2Cl_2 and in conc. sulfuric acid do not differ markedly in the positions of the absorption bands (274 and 234 nm in CH_2Cl_2, ε for the former, stronger band being 7800); in H_2SO_4 $\lambda_{max} = 276$ and 235 nm. We conclude, therefore, that under these conditions protonation, if it occurs, is slight, and that the ^{1}H-NMR observations are to be explained as solvent effects involving hydrogen bonding rather than protonation.

An interesting conclusion can be drawn when comparing the ^{1}H-NMR spectra of V in (1) trifluoroacetic acid (TFA); (2) trifluoroacetic acid to which trifluoromethanesulfonic (triflic) acid had been added; and (3) in triflic acid as solvent, as seen in Table 3. It can be seen from this Table that a practically constant difference of 0.47 ± 0.02 ppm exists between lines (1) and (2), which can be explained as a general solvent effect. On the other hand, the differences between lines (2) and (3) indicate upfield shifts for all protons: 0.1 ppm for γ-Me, 0.3 ppm for α-Me and β-H, but 0.9 ppm for NMe_2. This means that on adding into the solution of a very weak base (cation V) in the very strong triflic acid another weak base, namely TFA (which indeed acts as base in triflic acid), one loses the hydrogen bonding effect (which is markedly felt on the NMe_2 group, and decreases as the distance from this group increases).

TABLE 3

Chemical shifts (δ—values in ppm) for perchlorate V

Row (line)	Solvent	γ-Me	α-Me_2	NMe_2	β-H
1	TFA	2.51	2.80	3.15	7.43
2	TFA+triflic acid	2.05	2.31	2.66	6.98
3	Triflic acid	2.13	2.62	3.57	7.27

The fact that ^{1}H-NMR spectra indicate protonation or strong hydrogen bonding of V in H_2SO_4 or in F_3CSO_3H, while the electronic absorption spectra are much less affected, can be reconciled. Indeed, protonation of pyridine-N-oxides to N-hydroxypyridinium salts has little influence on the electronic absorption spectra. Only in longer conjugated systems is the intramolecular CT band strongly affected by protonation of the lone electron pairs.

Unlike compounds IV and VI, the 2,4,6-triphenyl-N-(*p*-dimethylaminophenyl)-pyridinium salt can be obtained both as a colourless dication IX and as a yellow monocation VIII. The disppearance of the visible absorption band observed on protonating the lone pair of VIII to form IX is conclusive proof for the existence of intramolecular charge transfer. Thus the band at 446 nm (in ethanol) or 468 nm (in 1,2-dichloroethane) is the intramolecular CT band. The same spectrum is obtained from both VIII or IX on dissolution in buffer-containing ethanol.

As in the preceding case, the spectrum of the non-protonated species, XI, with 2,4,6-trimethyl substituents, with an intramolecular CT band at 360 nm, is obtained from the dication X in buffer-containing ethanol.

An analogous case of intramolecular CT band appearing at even longer wavelengths (lower energies) is encountered in tropylium salts: the blue monocation XII ($\lambda_{max} = 570$ nm in ethanol) becomes colourless on protonation to the dication XIII.[18]

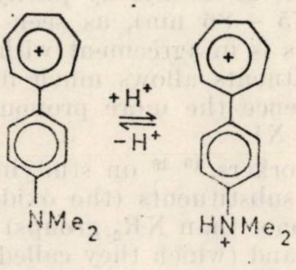

XII XIII

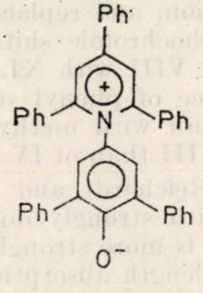

XIV

The solvatochromy of the intramolecular CT bands in IV, VI, and VIII, is similar, as observed from Table 4 for only two solvents. One observes a negative solvatochromy, i.e. on increasing the solvent polarity,

TABLE 4

Solvatochromy of CT bands

Solvent	E_T (kcal mol)	Interionic CT band in III (nm)	Intramolecular charge transfer bands in		
			IV (nm)	VI (nm)	VIII (nm)
CH_2Cl_2	41.1	412	—	—	—
$(ClCH_2)_2$	41.9	405	392	469	468
EtOH	51.9	—	378	453	446

the λ_{max} values decrease: on replacing ethylene dichloride as solvent by ethanol, hypsochromic shifts of 14 − 22 nm are observed for the intramolecular CT band at longest wavelengths in IV, VI and VIII. A similar, but more pronounced solvatochromy was observed by Dimroth, Reichardt et al.[15, 19] for the pyridinium betaine XIV which will be discussed in more detail below. Such a negative solvatochromy is normal in compounds whose ground state possesses pronounced charge separation, and whose electronically excited state has a lower charge separation; the excited state is similarly solvated by both polar and non-polar solvents, but the ground state is better solvated by polar solvents which lower its energy, hence the transition energy will be higher (and the wavelength of the CT band will be lower) in polar solvents. The same effect is observed from Table 4 for the interionic CT band in the iodide III, but in this case only halogenated solvents such as methylene and ethylene dichlorides can be employed as solvents (ethanol is too polar for allowing an interionic CT band to appear).

By comparing the values of λ_{max} in Table 1, it may be seen that the presence or absence of a *p*-phenylene ring, and the nature of substituents in the dimethyl- or diphenylamino groups, have little influence on the energy of the intramolecular CT band, therefore λ_{max} differs little (7 — 18 nm) between VI and VIII, or between IV and XI. On the other hand, the nature of substituents in positions 2, 4, 6 of the pyridinium ring has a considerable influence on the energy of the intramolecular CT transition, and replacement of methyl by phenyl substituents causes large bathochromic shifts (75 — 86 nm), as seen on comparing IV with VI, and VIII with XI. This is in agreement with expectations, since the presence of phenyl substituents allows much more electronic delocalization than with methyl, hence the more pronounced conjugation of VI and VIII than of IV and XI.

Dimroth, Reichardt and coworkers,[15, 19] on studying pyridinium betaines XIV with strongly donor substituents (the oxide group of the phenoxide anion is more strongly donor than NR_2 groups) observed that the longest-wavelength absorption band (which they called the "solvatochromic band" and which corresponds to the intramolecular CT band) presented an extremely strong negative solvatochromy. On the basis of this observation, they developed the E_T scale of an empirical parameter for the solvent polarity. The E_T parameter is similar to Kosower's Z-values[16] (both being based on electronic absorption maxima), but differs from it because E_T values are intramolecular CT band energies (in kcal/mole), while Kosower's Z-values are the corresponding interionic CT band energies of the pyridinium iodide XVII in the respective solvent (also in kcal/mole).[19, 21]

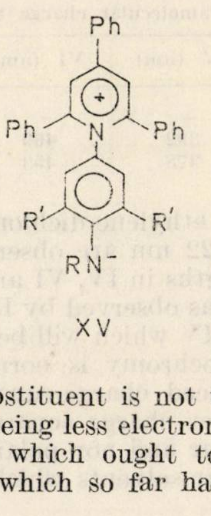

XV

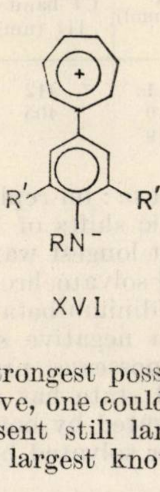

XVI

The oxide substituent is not the strongest possible donor; indeed, the nitrogen atom being less electronegative, one could imagine structures like XV and XVI which ought to present still larger solvatochromic effects than XIV (which so far has the largest known solvatochromy).

Of course, it is to be expected that protic solvents will be able to protonate the strongly basic betaines XV and XVI, but for a comparable range of solvent polarities, one could expect XV to have a larger solvatochromy than XIV, while XVI (which unlike the cation XII is a neutral betaine) will probably absorb at very long wavelengths and its solvatochromy will span the visible range even more spectacularly than XIV.

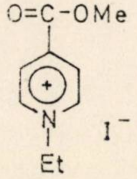

XVII

REFERENCES

[1] Part V, S. Bădilescu, L. Manu and A. T. Balaban, *Rev. Roumaine Chim.*, **24**, 947(1979).

[2] C. Toma and A. T. Balaban, *Tetrahedron*, Suppl. 7, **22**, 9 (1966).

[3] A. Camerman, L. H. Jensen and A. T. Balaban, *Acta Cryst.*, **25 B**, 2623 (1969).

[4] C. Uncuţa and A. T. Balaban, *Rev. Roumaine Chim.*, **21**, 251 (1976).

[5] A. T. Balaban, A. Dinculescu, H. N. Koutrakis and F. Chiraleu, *Tetrahedron Letters*, 437 (1979); A. T. Balaban, *Pure Appl. Chem.*, **52**, 1409 (1980); A. Dinculescu, H. N. Koutrakis and A. T. Balaban, *Rev. Roumaine Chim.*, **24**, 439 (1979); A. T. Balaban, A. Dinculescu, F. Iordache, F. Chiraleu, and D. Pătrăşcoiu, *Chem. Scripta*, **18**, 230(1981).

[6] O. Bastiansen, *Acta Chem. Scand.*, **3**, 408 (1949).

[7] J. M. Robertson, "Organic Crystals and Molecules", Cornell University Press, Ithaca, N.Y., 1953.

[8] L. H. Jensen and A. T. Balaban, unpublished; see also A. T. Balaban and M. D. Gheorghiu, *Rev. Roumaine Chim.*, **23**, 1065 (1978) for the molecular structure of II.

[9] G. Briegleb, "Elektronen Donator-Acceptor Komplexe", Springer, Berlin, 1961.

[10] R. Foster, "Organic Charge-Transfer Complexes", Academic Press, London, 1969.

[11] J. Rose, "Molecular Complexes", Pergamon Press, Oxford, 1967.

[12] R. S. Mulliken and W. B. Pearson, "Molecular Complexes", Wiley-Interscience, New York, 1969.

[13] A. B. Susan and A. T. Balaban, *Rev. Roumaine Chim.*, **14**, 111 (1969).

[14] A. R. Katritzky, *Tetrahedron*, **36**, 679 (1980).

[15] K. Dimroth, C. Reichardt, T. Siepmann and F. Bohlmann, *Liebigs Ann. Chem.*, **661**, 1 (1963).

[16] E. M. Kosower, *J. Amer. Chem. Soc.*, **80**, 3253 (1958); *J. Chem. Phys.*, **61**, 230 (1964); "Molecular Biochemistry" McGraw-Hill, New York, 1962, p. 180; "An Introduction to Physical Organic Chemistry", Wiley, New York, 1968, p. 293.

[17] A. T. Balaban, M. Mocanu and Z. Simon, *Tetrahedron*, **20**, 119 (1964); S. Bădilescu and A. T. Balaban, *Spectrochem. Acta*, **32 A**, 1311 (1976).

[18] C. Jutz and D. Voitenleitner, *Chem. Ber.*, **97**, 29 (1963); J. J. Looker, *J. Org. Chem.*, **30**, 4180 (1965).

[19] C. Reichardt and K. Dimroth, *Fortschr. Chem. Forsch.*, **11**, 1 (1958); C. Reichardt, "Solvent Effects in Organic Chemistry", Monographs in Modern Organic Chemistry, No. 3, Verlag Chemie, Weinheim, 1979.

[20] V. Gutmann, "The Donor-Acceptor Approach to Molecular Interactions", Plenum Press, New York, 1978.

[21] M. Răileanu, "Influenţa mediului asupra reactivităţii chimice", Scrisul Românesc, Craiova, 1981.

Revue Roumaine de Chimie, **27**, *4*, 523–532 (1982)

KINETICS AND MECHANISM OF Ru(III) CATALYSED OXIDATION OF ALIPHATIC DIOLS AND CYCLANOLS BY PHENYLIODOSO ACETATE

S. C. PATI* and B. R. DEV

Department of Chemistry, Berhampur University, Berhampur 760007,
Ganjam (Orissa), India

Received December 5, 1980

Kinetics of Ru(III) catalysed oxidation of aliphatic diols like ethyleneglycol, 1,2-propanediol and 1,4-butanediol and some cyclanols viz. cyclopentanol, cyclohexanol, cycloheptanol and cyclooctanol by phenyliodosoacetate (PIA) in aqueous acetic acid—perchloric acid medium has been found to be zeroth order in oxidant, first order in substrate and first order in the catalyst Ru(III). The effect of acidity is marginal. The order of reactivity among the cyclanols is $C_7 \geq C_8 > C_5 > C_6$. Activation parameters are evaluated. The reaction mechanism is discussed.

INTRODUCTION

Ru(III) catalysed oxidation of diols by hexacyanoferrate (III) was reported earlier. [1] Very recently Singh et al. [2,3] have reported the kinetic studies on the oxidation of diols and cyclanols by hexacyanoferrate (III) in the presence of Ru(III) as the homogeneous catalyst in alkaline medium, where the active species of the catalyst were invoked to be $[Ru(OH)_x(H_2O)_{6-x}]^{3-x}$ $(x < 6)$. We have now studied the catalytic activity of Ru(III) in the oxidation of some diols viz. ethyleneglycol, 1,2-propanediol and 1,4-butanediol and cyclanols like cyclopentanol, cyclohexanol, cycloheptanol and cyclooctanol by phenyliodosoacetate (PIA) in acid medium.

EXPERIMENTAL

MATERIALS AND METHOD

All the diols used for the purpose were of BDH(AR) grade and were used after redistillation. All the cyclanols used were Fluka products.

Phenyliodosoacetate (PIA) was prepared by the modified method of Boesken and Schneider.[4] Hydrogen peroxide (70 ml, 30 %) and acetic anhydride (305 ml) were stirred together for four hours at 40°C. Iodobenzene (50 gms) was added to the solution, which was kept overnight. Some PIA crystallized out and was filtered off and the filtrate was concentrated to a small volume under reduced pressure, when a second crop of crystals was obtained. The crystals were washed with ether and dried; m.p. 158°C. Ru(III) chloride was John Mathey (London) sample and its aqueous solution was standardised by the method of Horiuchi et al.[5]

---

* For correspondence.

The progress of the reaction was monitored by estimating iodometrically PIA at regular intervals of time. The experiments were also conducted under nitrogen atmosphere and no difference in rates was observed in the presence and absence of nitrogen. An electrically operated thermostatic water bath was used. The temperature fluctuation was not more than ± 0.02°C. The experiments were carried out in duplicate to ensure reproducibility.

STOICHIOMETRY AND PRODUCT ANALYSIS

The stoichiometry of the reaction was studied by mixing reactants containing excess of PIA over that of substrate at a fixed Ru(III) concentration. The rate of the reaction was found to be enormously reduced after one mole of PIA was consumed per mole of the substrate.

TABLE 1

Effect of varying the [oxidant]/[substrate] on the reaction rate
$[HClO_4] = 0.01$ M; HOAc = 10 % (V/V),
$[Ru(III)] = 8.87 \times 10^{-7}$ M; $^*17.74 \times 10^{-7}$M; Temp. = 35°C

Substrate	10^3[Oxidant] M	10^4[Substrate] M	$10^5 k_0$ moles litre^{-1} min^{-1}	$10^2 k_1$ min^{-1}
Ethyleneglycol	0.383	10.04	0.79	0.79
	0.470	10.04	0.78	0.78
	0.863	10.04	0.78	0.78
	0.470	5.002	0.39	0.78
	0.470	20.008	1.52	0.76
1,4-butanediol	0.250	10.04	1.25	1.25
	0.445	10.04	1.27	1.27
	0.900	10.04	1.28	1.28
	0.454	5.002	0.74	1.44
	0.454	15.006	1.82	1.21
	0.454	20.008	2.73	1.33
Cyclopentanol*	0.231	25.09	1.17	0.46
	0.465	26.30	1.10	0.42
	0.890	25.09	1.11	0.44
	1.407	25.09	1.08	0.43
	0.465	13.12	0.55	0.42
	0.465	50.05	2.10	0.42
Cyclohexanol*	0.313	25.09	0.94	0.38
	0.473	25.09	0.95	0.38
	0.947	25.09	0.95	0.38
	1.352	25.09	0.97	0.38
	0.4890	12.0	0.49	0.37
	0.4890	52.28	1.96	0.37
	0.4890	102.00	3.76	0.37
Cycloheptanol*	0.477	26.48	2.27	0.86
	0.971	25.93	2.20	0.85
	1.423	25.93	2.25	0.86
	0.4767	13.18	1.13	0.86
	0.5141	50.08	4.28	0.86

The products in the case of 1,2-propanediol and 1,4-butanediol are identified to be 2-hydroxypropanal and 4-hydroxybutanal respectively, confirmed by their hydrazone derivatives.[6] The hydrazone derivatives of the carbonyl compounds obtained have been estimated gravimetrically and found to be approximately 70 %.

Stoichiometry in the case of cyclanols was found to be 1 : 4 (substrate : oxidant). The products were identified to be corresponding dicarboxylic acids, confirmed by characteristic spot test.[7]

RESULTS AND DISCUSSION

Kinetics of oxidation of some aliphatic diols viz. ethylene glycol, 1,2-propanediol and 1,4-butanediol and cyclanols like cyclopentanol, cyclohexanol, cycloheptanol and cyclooctanol have been studied in aqueous acetic acid—perchloric acid medium.

I. EFFECT OF VARYING THE OXIDANT CONCENTRATION ON THE REACTION RATE

The effect of varying the oxidant concentration on the reaction kinetics has been observed at different initial oxidant concentrations. The reactions have been found to be zeroth order in oxidant. The plot of percentage of reaction versus time is linear up to 75 % reaction in an individual run. The zeroth order rate constants k_0 moles $l.^{-1}$ $\min^{-1}$ as calculated from x/t (where x is the concentration of oxidant (PIA) reacted at time t) is found to be constant in an individual run and also at varying concentrations of oxidant (PIA) (Table 1).

II. EFFECT OF VARYING THE SUBSTRATE CONCENTRATION ON THE REACTION RATE

The zeroth order rate constants are found to increase with an increase in the concentration of the substrate. The plots of log k_0 *versus* $\log[S]$ are linear with unit slopes (Fig. 1), and the first order rate constant $k_1 = k_0/[S]$ (where 'S' stands for substrate) is constant over a wide range of the [substrate], thus showing unit dependence of the [substrate] (Table 1).

III. EFFECT OF CATALYST

The effect of catalyst, Ru(III) chloride on the reaction kinetics has been studied. The k_1 values increase linearly with an increase in the concentration of Ru(III). The plots of log k_1 versus log[Ru(III)] are linear with unit slope (Fig. 2). The rate constants are recorded in Table 2.

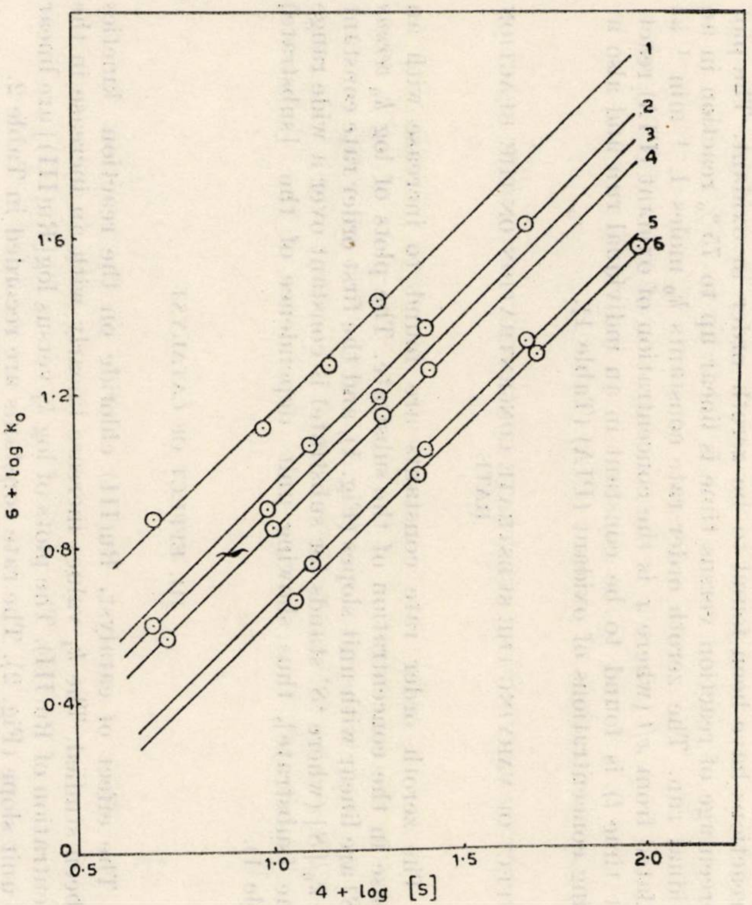

Fig. 1. — *Plot of log k_0 vs log[S]*.[PIA] = 0.0005M ; [[Ru(III)] = 8.87 × × 10^{-7} ; 17.74 × 10^{-7}M ; [$HClO_4$] = 0.01M ; HOAc = 10 % (V/V) ; Temp. = 35°C. 1. 1,4-butanediol ; 2. Cycloheptanol ; 3. Ethylene glycol ; 4. Cyclooctanol ; 5. Cyclopentanol ; 6. Cyclohexanol.

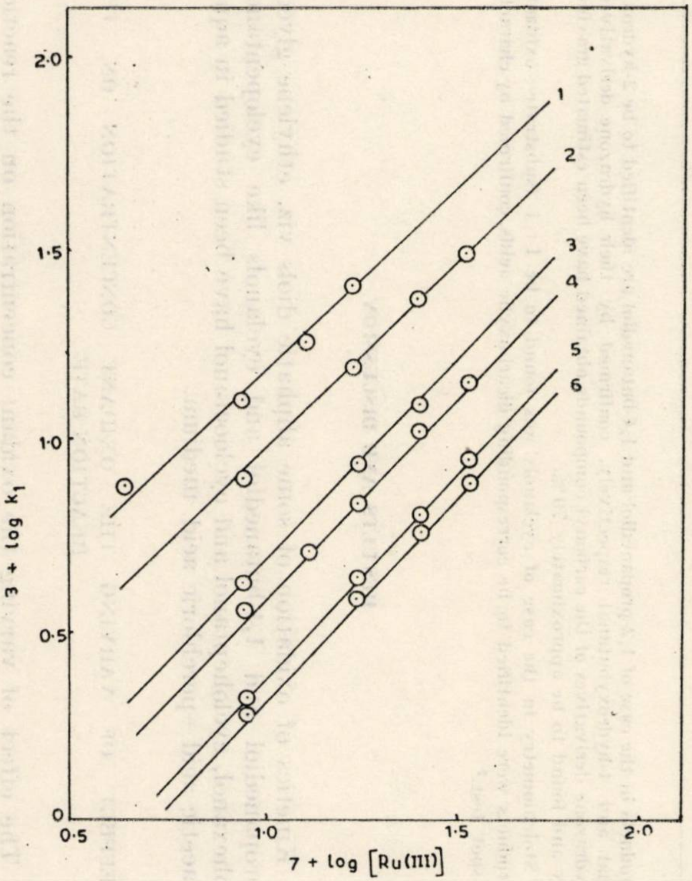

Fig. 2. — Plot of log k_1 vs log [Ru(III)]. [PIA] = 0.0005 M ; [S] = 0.001M ; 0.0025M ; [$HClO_4$] = 0.01M ; HOAc = 10 %(V/V) ; Temp = 25°C. 1. 1,4-butanediol ; 2. Ethylene glycol ; 3. Cycloheptanol ; 4. Cyclooctanol ; 5. Cyclopentanol ; 6. Cyclohexanol.

TABLE 2

Effect of varying the [Ru(III)] on the reaction rate

[PIA] = 0.0005M ; [Substrate] = 0.001 M ; [HClO$_4$] = = 0.01M ; Temp. = 35°C HOAc = 10% (V/V)

Substrate	10^7[Ru(III)]$_M$	10^5 k_0 moles litre^{-1} min^{-1}	10^2 k_1 min^{-1}
Ethyleneglycol	8.87	0.78	0.78
	17.74	1.52	1.51
	26.61	2.29	2.28
	35.48	3.05	3.04
1,2-Propanediol	4.43	0.73	0.73
	8.87	1.39	1.29
	13.30	1.97	1.96
	17.74	2.61	2.60
1,4-Butanediol	4.43	0.76	0.76
	8.87	1.27	1.27
	13.30	1.80	1.79
	17.74	2.54	2.54
Cyclopentanol*	8.87	0.55	0.21
	17.74	1.10	0.42
	26.61	1.62	0.62
	35.48	2.24	0.85
Cyclohexanol*	8.87	0.47	0.19
	17.74	0.95	0.38
	26.61	1.37	0.54
	35.48	1.85	0.74
Cycloheptanol*	8.87	1.12	0.42
	17.74	2.27	0.86
	26.61	3.10	1.200
Cyclooctanol*	8.87	0.90	0.36
	13.30	1.25	0.48
	17.74	1.78	0.66
	26.61	2.67	1.03
	35.48	3.56	1.38

*[Substrate] = 0.0025M

IV. EFFECT OF ACIDITY

The effect of acid concentration (HClO$_4$) on the reaction rate has been studied by carrying out the kinetic runs at different perchloric acid concentrations. There is a marginal effect on the rate on increasing [H$^+$]. The rate constants obtained at various acidities of different substrates are given in Table 3.

V. EFFECT OF SOLVENT COMPOSITION

An increase in the proportion of acetic acid (solvent) i.e. a decrease in the dielectric constant increases the rate (Table 3). The plots of log k_1 versus 1/D are found to be linear with positive slopes. Hence the reaction is a positive ion dipole type.

TABLE 3

Effect of varying $[HClO_4]$ / Percentage of acetic acid (solvent) on the reaction rate

$[PIA] = 0.0005M$, $[Ru(III)] = 8.87 \times 10^{-7}M$, $* 17.74 \times 10^{-7}$ M,
$[Substrate] = 0.001M$; $*0.0025M$, Temp. = 35C°

Substrate	% HOAc	$[HClO_4]$M	$10^5 k_0$ moles litre $^{-1}$ min $^{-1}$	$10^2 k_1$ min $^{-1}$
Ethyleneglycol	10	0.005	0.67	0.66
	10	0.01	0.78	0.78
	10	0.02	1.20	1.19
	10	0.04	1.74	1.73
	20	0.01	1.32	1.31
	30	0.01	1.62	1.62
	40	0.01	1.89	1.88
1,4-Butanediol	10	0.005	1.33	1.22
	10	0.01	1.27	1.27
	10	0.02	1.43	1.43
	20	0.01	2.03	2.02
	40	0.01	2.31	2.30
Cyclopentanol*	10	0.005	1.04	0.41
	10	0.01	1.10	0.42
	10	0.02	1.13	0.45
	10	0.05	1.30	0.51
	20	0.01	1.36	0.53
	30	0.01	1.52	0.56
	40	0.01	1.61	0.64
	50	0.01	1.66	0.69
Cyclohexanol*	10	0.005	0.88	0.35
	10	0.01	0.95	0.38
	10	0.015	0.98	0.39
	10	0.02	0.99	0.40
	20	0.01	1.08	0.41
	40	0.01	1.13	0.44
	60	0.01	1.22	0.49
Cycloheptanol*	10	0.005	2.11	0.84
	10	0.01	2.27	0.86
	10	0.015	2.30	0.91
	10	0.02	2.51	0.99
	20	0.01	2.71	1.06
	30	0.01	3.50	1.29
Cyclooctanol*	10	0.005	1.64	0.62
	10	0.01	1.78	0.66
	10	0.02	1.93	0.73
	10	0.03	2.11	0.80
	20	0.01	2.06	0.82
	30	0.01	2.84	1.06

VI. EFFECT OF SODIUM ACETATE AND SODIUM PERCHLORATE

In order to investigate the effect of pH and of neutral salts the reaction rate measurements were caried out at various concentrations of NaOAc and $NaClO_4$ in aqueous acetic acid medium. There is no appreciable effect on the rate. Hence it can be inferred that there is no acid catalysis.

VII. EFFECT OF TEMPERATURE

The reaction has been studied at different temperatures i.e. 308 K, 313 K and 318 K for diols and at 303 K, 308 K and 313 K for cyclanols. The rate constants are recorded in Table 4. The different thermodynamic parameters are evaluated and given in Table 5.

TABLE 4

Effect of varying the temperature on the reaction rate

[PIA] = 0.0005M ; [HClO$_4$] = 0.01M ; [Ru(III)] = 8.87×10^{-7} M ;
[Substrate] = 0.001 M ; HOAc = 10 %(V/V)

Substrate	$10^2 k_1$ min^{-1} at			
	303 K	308 K	313 K	318 K
Ethyleneglycol	—	0.780	1.27	2.18
1,2-Propanediol	—	1.29	1.57	2.33
Cyclopentanol*	0.35	0.42	0.56	—
Cyclohexanol*	0.29	0.38	0.46	—
Cycloheptanol*	0.66	0.86	1.23	—
Cyclooctanol*	0.60	0.66	0.99	—

*[Substrate] = 0.0025M ; *[Ru(III)] = 17.74×10^{-7}M

TABLE 5

Arrhenius activation parameters for aliphatic diols and cyclanols at 308 K

Substrate	$\Delta E^{\neq}$ K.cal/mole	$\Delta H^{\neq}$ K.cal/mole	$\log_{10}A$	$\Delta S^{\neq}$ e.u.
Ethyleneglycol	11.70	11.08	4.63	−39.45
1,2-Propanediol	13.40	12.79	5.92	−33.19
Cyclopentanol	17.56	16.95	8.30	−22.61
Cyclohexanol	17.56	16.95	8.26	−22.93
Cycloheptanol	10.40	7.79	3.53	−44.81
Cyclooctanol	12.04	11.43	4.59	−39.63

STRUCTURE AND REACTIVITY

The order of reactivity among the diols is : 1,4-butandiol $\simeq$ 1,2-propandiol $>$ ethylene glycol. This is quite in consonance with the inductive effect of the alkyl groups. However, among the cyclanols the reactivity order is : $C_7 \geqslant C_8 > C_5 > C_6$. The reactivity order among the cyclanols has to be explained. In cyclic systems, changes in bond hybridisation may produce concomitant changes in angle strain (Bayer's strain), bond opposition strain (torsional or Pitzer strain) or transannular strain. When the hybridisation is changed from sp^3 to sp^2 the four bond oppositions are relieved. This favours the $sp^3 - sp^2$ transitions and correspondingly the displacement reactions in cyclopentane system are relatively rapid. Similar arguments also apply for seven-membered rings which are also mobile and beset with bond oppositions (eclipsation) of adjacent C−H bonds. In the six membered ring the rigid form is free of bond opposition and change in the hybridisation from sp^3 to sp^2 engenders bond opposition and is therefore resisted. A similar variation in kinetic rate with ring size was reported by Roček and Mareš[8] in the chromic acid oxidation of cycloparaffins. The authors suggested that the reactivity of bicyclic compounds should be directly related to the thermochemical strain in the molecules. Consequently the reactivity order should be a linear function of the strain energy.

A plot of the logarithm of the rates of oxidation versus the strain energy shows that the plot is linear up to cycloheptanol and is then levelled off at cyclooctanol. This behaviour is different from earlier observations in V^{+5} oxidation[9] where cyclooctanol was found to react faster than cycloheptanol. Although the I-strain[10] concept requires a higher rate of oxidation for cyclooctanol, the Bayer's strain theory requires that six, seven and eight membered rings should be more or less equally stable. Thus the levelling off the rate at seven and eight membered rings must be due to the predominance of Bayer's strain over the I-strain.

MECHANISM AND RATE LAW

In the oxidation of diols Singh et al.[2] have invoked an acyclic mechanism. The formation of an outersphere complex was substantiated by the decrease in the $k_0/[S]$ value with the increase in concentration of substrate and a finite intercept on the inverse rate axis when $1/k_0$ was plotted against $1/[S]$. In the present investigation, the double reciprocal plots of $1/k_0$ versus $1/[S]$ pass through origin (Fig. 3). Moreover the $k_0/[S]$

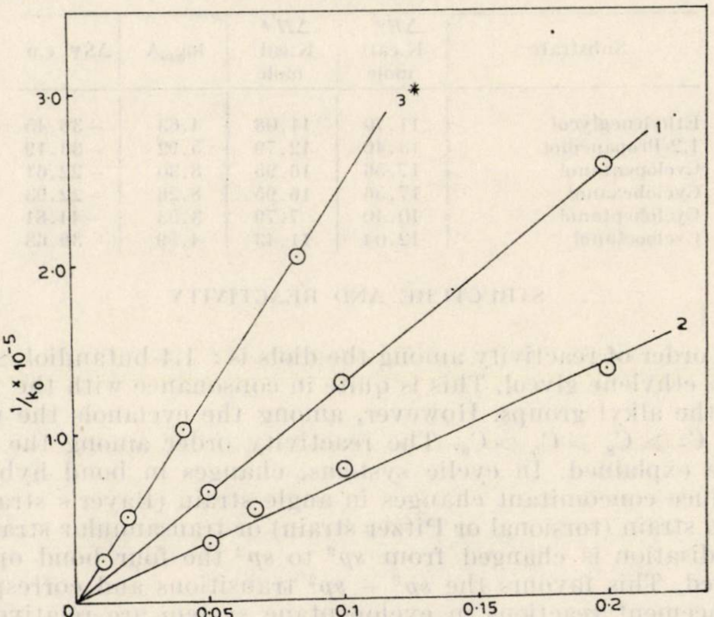

Fig. 3. — Plot of $1/k_0$ vs $1/[S]$.[PIA] = 0.0005 M ; [Ru(III)] = = 8.87×10^{-7}, 17.74×10^{-7} M* ; [$HClO_4$] = 0.01 M ; HOAc = = 10 %(V/V) ; Temp. = 35°C. 1. Ethylene glycol ; 2. 1,4-butane diol ; *3. Cyclohexanol.

is constant and does not show a decreasing trend. This makes us believe that the hydride ion abstraction from the diols occurs by a direct bimolecular path rather than through an outersphere complex. Further evidence for the acyclic mechanism can be obtained from the reactivity of diols, which shows that the larger the separation of hydroxyl groups in the molecule, the more reactive is the diol. Such an argument was reported earlier by Radhakrishnamurti et al.[11] in their work on oxidation of glycols by CrO_3 in aqueous medium.

Thus the following mechanism is proposed (Scheme 1). The proposed mechanism involves the abstraction of hydride ion from the diol by Ru(III) in a slow step. Such hydride ion abstraction by transition metal ions was reported by earlier workers. [12] The carbonium ion formed in the slow step gives rise to a carbonyl compound with the loss of a proton in a fast step. The ruthenium hydride is oxidised in a fast step by a mole of PIA to regenerate Ru(III).

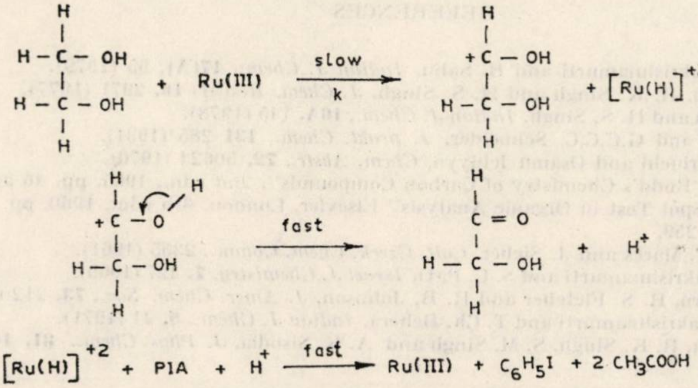

The Ru(III) species does not suffer a change in the oxidation state in the above mechanism.

The analogous mechanism for cyclanols may be depicted as in Scheme II.

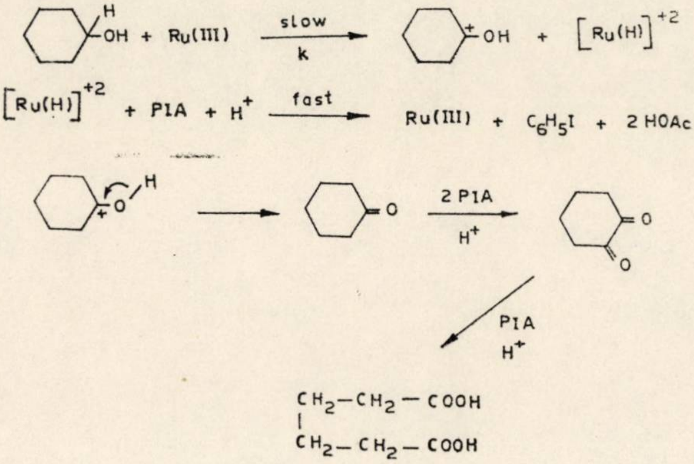

The rate for both sequences is given by

$$V = k[\mathrm{Ru(III)}]\ [\mathrm{Substrate}]$$

ACKNOWLEDGEMENT. Our thanks are due to Prof. P. S. Radhakrishnamurti, Professor and Head of the Department of Chemistry, Berhampur University for his keen interest and suggestions throughout the work. One of us (BRD) thanks UGC New Delhi for a fellowship and Godavaris Mohavidyalaya, Banpur for sanctioning study leave.

REFERENCES

[1] P. S. Radhakrishnamurti and B. Sahu, *Indian J. Chem.*, **17(A)**, 95 (1979).
[2] R. N. Singh, R. K. Singh and H. S. Singh, *J. Chem. Res(M)* **10**, 2971 (1977).
[3] R. N. Singh and H. S. Singh, *Indian J. Chem.*, **16A**, 145 (1978).
[4] J. Boesken and G.C.C.C. Schneider, *J. prakt. Chem.*, **131** 285 (1931).
[5] Yoshizo Horiuchi and Osamu Ichiyyo, *Chem. Abstr.*, **72**, 50624 (1970).
[6] S. Coffey, "Rodd's Chemistry of Carbon Compounds", 2nd edn., 1965, pp. 46 and 49.
[7] F. Feigl, "Spot Test in Organic Analysis" Elsevier, London, 6th edn., 1960, pp. 145, 146 and 259.
[8] J. Rocek, F. Mares and J. Sicher, *Coll. Czeck. Chem. Comm.*, 2355 (1961).
[9] P. S. Radhakrishnamurti and S. C. Pati, *Israel J. Chemistry*, **7**, 427 (1969).
[10] H. C. Brown, R. S. Fletcher and R. B. Johnson, *J. Amer. Chem. Soc.*, **73**, 212 (1951).
[11] P. S. Radhakrishnamurti and T. Ch. Behera, *Indian J. Chem.*, **9**, 41 (1971).
[12] H. S. Singh, R. K. Singh, S. M. Singh and A. K. Sisodia, *J. Phys. Chem.*, **81**, 1044 (1977).

Revue Roumaine de Chimie, 27, 4, 533–536 (1982)

AROMATIC ESTERS BY A NEW DIRECT CONDENSATION REACTION USING TRIARYL BORATES

C. I. CHIRIAC
"P. Poni" Institute of Macromolecular Chemistry, Aleea Gr. Ghica Vodă 41 A,
Iași, Romania

Received June 18, 1981

By a direct condensation reaction between triaryl borates and aromatic acids in xylene at 200 – 210°C, aromatic esters resulted in high yield. The yield was improved by removing the water by azeotropic distillation.

The preparation of esters is one of the most fundamental reactions in organic chemistry. The classical method of preparing aromatic esters utilizes the reaction of phenols with acyl chlorides or anhydrides. The reaction of aromatic acids with phenols proceeds with difficulty. For the synthesis of aromatic esters by direct condensation reactions, several methods are known. As reagents used in synthesis of this type, we mention: polyphosphoric acid,[1] polyphosphate ester,[2,3] triarylphosphite,[4,5] *p*-toluensulfonyl chloride,[6] mixed sulfonic-carboxylic anhydrides[7] and diarysulfites.[5]

RESULTS AND DISCUSSION

In this paper we present a new method for the synthesis of aromatic esters using the reaction between aromatic acids and triaryl borates. Reactive compounds containing boron have been used for the synthesis of aliphatic amides,[8,9] but not for aromatic esters. We have investigated triaryl borates by analogy with triaryl phosphites and diphenyl sulfites.[5] Thus, by heating a mixture of triphenyl borates (1 mole) and benzoic acid (3 moles) at 200 – 210°C, phenyl benzoate resulted in 50 – 55 % yield. The yield increased to 60 – 63 %, when a 20 % excess of triphenyl borate was used. For 30 % excess of triphenyl borate, the yield remained the same. When the reaction took place in small quantities of xylene at 200 – 210°C using a Dean-Stark trap for the recirculation of the solvent, the yield rose to 85 – 90 %. This increase of the yield is explained by removing the water which resulted by the dehydration of boric acid by heating.[10]

A similar situation occurred in the synthesis of amides using boron trifluoride etherate as reagent, when the water formed was removed by azeotropic distillation.[11] The removal of the water is necessary because the triaryl borates are readily hydrolyzed.[12,13]

As a result of the present investigation and similar to other cases,[5] we propose the following mechanism of reaction:

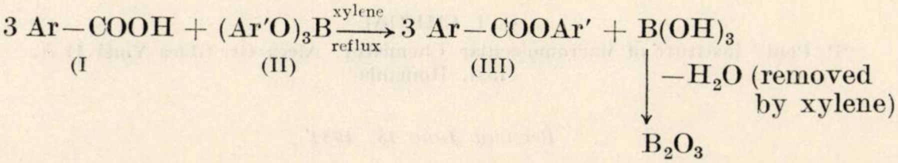

$$\underset{(I}{3\,\mathrm{Ar{-}COOH}} + \underset{(II)}{(\mathrm{Ar'O})_3\mathrm{B}} \xrightarrow[\text{reflux}]{\text{xylene}} \underset{(III)}{3\,\mathrm{Ar{-}COOAr'}} + \mathrm{B(OH)_3} \xrightarrow{-\mathrm{H_2O}\ \text{(removed by xylene)}} \mathrm{B_2O_3}$$

The presence of the water was proved by identification with anhydrous $CuSO_4$.

We supposed, similar to other cases,[5,8,11] that this reaction involves a transition state (IV):

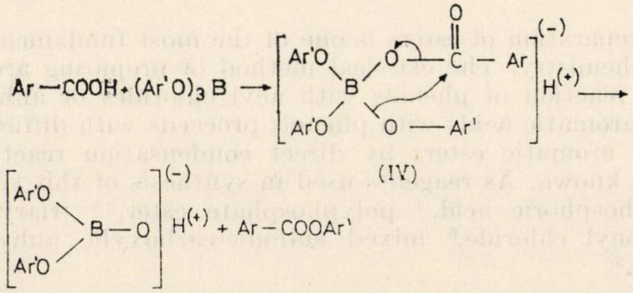

The formation of a transition state (IV) or $(\mathrm{Ar'O})_2\mathrm{B{-}OOC{-}Ar}$ (by elimination of phenol) is demonstrated by the reaction between tribenzoyl borate[14] and phenol, under the same condition, when phenyl benzoate results.

The general method for obtaining aromatic esters (III) consists in refluxing for 4—5 hours, a very concentrated solution of aromatic acid (3 moles) and triaryl borate (1.2 moles) in xylene as solvent using a Dean-Stark trap for water removing. The temperature of the solution is 200 — 210°C using very little xylene, which strongly refluxes during the reaction (at lower temperatures the yield decreases). Using lower boiling solvents as toluene or benzene the yield decreases.

The yields obtained by this method ranged from 76 to 94 % (Table 1).

By this new direct synthesis we obtained aromatic esters, which are difficult to obtain by heating aromatic acids with phenols. By this simple method we avoid the acyl halides or anhydrides used as reagents in the classical methods for synthesis of aromatic esters.

TABLE 1

Aromatic esters obtained from triaryl borates

Acid	Borate	Esters a)		
		Yield b) %	M.p. c) °C	Literat.m.p. d) °C
C_6H_5-COOH	$(C_6H_5O)_3B$	84	68–70	69–71
p-$CH_3-C_6H_4-COOH$	,,	86	75–77	76–77[17]
p-$CH_3O-C_6H_4-COOH$	,,	87	73–75	73–74[17]
m-$Cl-C_6H_4-COOH$	,,	94	52–54	53–55
m-$Br-C_6H_4-COOH$	,,	91	64–66	65–66
o-$Cl-C_6H_4-COOH$	,,	81	35–37	36–38
C_6H_5-COOH	$(p\text{-}CH_3-C_6H_4O)_3B$	89	67–69	68–70
p-$CH_3-C_6H_4-COOH$	,,	82	90–92	90–91[17]
$p-CH_3O-C_6H_4-COOH$	,,	85	65–67	66–67
o-$Cl-C_6H_4-COOH$	,,	79	67–69	68–69[18]
C_6H_5-COOH	$(p\text{-}Cl-C_6H_4O)_3B$	76	85–87	85–87

a) The products were identified by comparison of m.p. IR spectra with authentic samples.

b) Yields calculated on acid employed.

c) Before recrystallization.

d) From "Beilsteins Handbuch der organischen Chemie".

EXPERIMENTAL

1. PHENYL BENZOATE

A solution of triphenyl borate[15] 3.48 g (1.2 moles) and benzoic acid 3.66 g (3 moles) in 20 ml anh. xylene was refluxed for 4 – 5 hours in a 50 ml flasks a Dean-Stark trap for removing the water by azeotropic distillation. During the reaction, only 2 – 4 ml of xylene remained in the flask at permanent reflux and the rest of 16 – 18 ml condensed in trap after the first 10 – 15 minutes and remained in the trap all the time of the reaction (the temperature of salts bath is 210 – 220°). Under these conditions the boiling temperature of the solution increased very much (200 – 210°) because it contained very little solvent, which was sufficient for removing the water (the reaction needs a heating at temperature as high as 200–210°). At the end of the reaction, the solvent was completely removed by heating under vacuum. The resulted melted ester was poured still hot into a large volume of water with ice (80 – 100 ml) under stirring. The product was collected by filtration, washed well with 20–40 ml 5% NaOH solution, 20 – 40 ml 5% HCl solution, then three times with 30 – 50 ml water. After drying under vacuum at 40 – 50°, 4.98 g phenyl benzoate with m.p. 68 – 70° were obtained (mixed m.p. with pure phenyl benzoate undepressed). Yield 84% (calculated on benzoic acid employed).

Anal. Calculated for $C_{13}H_{10}O_2$; C, 78.75 ; H, 5.08%. Found : C, 78.13 ; H, 4.97%.

Under similar conditions, other aromatic esters (presented in Table 1), were prepared in good yields from p-tolylborate or p-chlorophenyl borate[16] and the corresponding aromatic acids.

REFERENCES

[1] A. R. Bader and A. D. Kontowicz, *J. Amer. Chem. Soc.*, **75**, 5416 (1953).
[2] Y. Kanaoka and K. Matsuzaki, *Chem. and Ind. (London)*, **1964**, 2102.
[3] H. J. Adams and J. R. Lewis, *Synthesis*, **1979**, 430.
[4] J. Lorentz, *Angew. Chem.*, **77**, 1031 (1965).
[5] B. Iselin and W. Rittel, *Helv. Chim. Acta*, **40**, 373 (1957).
[6] J. H. Brewster and C. J. Ciotti jr., *J. Amer. Chem. Soc.*, **77**, 6214 (1955).
[7] G. Overberger and E. Sarlo, *J. Amer. Chem. Soc.*, **85**, 2446 (1963).
[8] A. Pelter, T. E. Levitt and P. Nelson, *Tetrahedron*, **26**, 1539 (1970).
[9] D. B. Collum and B. Ganem, *J. Org. Chem.*, **43**, 4393 (1978).
[10] M. F. Lapert, *Chem. Rev.*, **56**, 971 (1956).
[11] J. Tani, I. Oine and I. Inoue, *Synthesis*, **1975**, 714.
[12] W. H. Miller and A. Scattergood, *J. Amer. Chem. Soc.*, **67**, 2150 (1945).
[13] A. G. Cook, J. D. Saunders and G. J. Stacy, *J. Chem. Soc.*, **1950**, 3125.
[14] A. Pictet, *Chem. Ber.*, **36**, 2219 (1903).
[15] T. Colclough and W. Gerrard, *J. Chem. Soc.*, **1955**, 905.
[16] L. H. Thomas, *J. Chem. Soc.*, **1942**, 822.
[17] H. Rheinboldt, *Quimica*, **1951**, 52; *Chem. Abstr.*, **45**, 7552 (1952).
[18] K. R. Robinson, *J. Amer. Chem. Soc.*, **73**, 2483 (1951).

Revue Roumaine de Chimie, **27**, *4*, 537–544 (1982)

SYNTHESIS OF SOME NEW BIOLOGICALLY ACTIVE 2-AMINOPYRIDINE DERIVATIVES

S. R. El-EZBAWY, A. A. ABDEL-WAHAB and A. A. KHALAF*
Chemistry Department, Faculty of Science, Assiut University, Assiut, Egypt

Received November 27, 1980

This work describes the conversion of 2-amino-pyridine into derivatives with anticipated biological activity. Derivatives with sulphide and sulphone functions were obtained *via* acylation of 2-aminopyridine with chloroacetyl and/or γ-chlorobutyryl chlorides to give chloroacylaminopyridines (I). Reaction of I with RSNa or ArSNa gave the corresponding sulphides (II) which upon treatment with H_2O_2 underwent oxidation at both sulphur and ring nitrogen yielding the respective sulphone N-oxides (III). The biologically important aminoacylamide derivatives (IV and VI) containing the $-NHCO(CH_2)_n-N\langle$ group were obtained by the reaction of I and chloroacyl – sulphapyridine with secondary amines. The structures of the new compounds were proved using modern analytical methods. Biological testing of the prepared compounds against some strains of bacteria and fungi, showed strong antimicrobial activities in most cases.

Over the years, experimental results obtained by various investigators have illustrated that certain structural moieties are characterized by specific biological effects. For example, 2-aminopyridines have been shown to have local anesthetic activity[1,2] and pyridine N-oxides were reported to have effects on bacteria and fungi.[3] Many diaryl sulphides and sulphones were found to have antituberculous activity.[4] Also, diaryl sulphones closely related to the sulphonamide antibiotics proved to be effective against leprosy.[5,6] Compounds containing the aminoacylamide grouping $\rangle NCO(CH_2)_nN\langle$ have been shown to have very interesting medical properties especially as local anesthetics.[7–10]

RESULTS AND DISCUSSION

The above indicated biological potency associated with pyridine, pyridine-N-oxide, sulphide, sulphone and aminoacylamide functions prompted us to prepare some model compounds in which two or more of these functions are present together in the same molecule. As a first step in this direction, we report here the biological testing and the chemistry involved in the preparation of certain stuctures including the 2-pyridinyl or 2-pyridinyl-N-oxide moiety together with sulphur containing acylamide and/or aminoacylamide grouping (II – V). The steps followed to convert 2-aminopyridine into compounds II and III are outlined in Scheme 1 and the properties of the resulting compounds are summarised in Table 1.

---

* To whom correspondence should be addressed.

Scheme 1

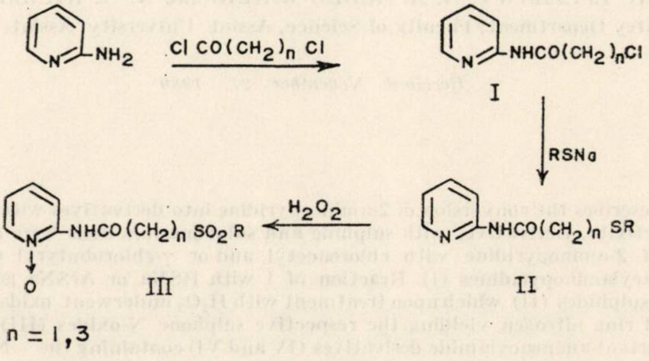

TABLE 1

Characteristics of sulphides and sulphones (II and III)

Compound No.	n ; R	M.p. (°C)	Yield (%)	Molecular formula	Analytical data* (%) Calculated N	Calculated S	Observed N	Observed S
IIa	1 ; C_6H_5—	67.5–68.5	62	$C_{13}H_{12}N_2OS$	11.48	13.11	11.55	13.26
IIb	1 ; *o*-$NH_2C_6H_4$—	178–9	69	$C_{13}H_{13}N_3OS$	16.21	12.36	16.35	12.48
IIc	1 ; *p*-$CH_3C_6H_4$—	72–74	49	$C_{14}H_{14}N_2OS$	10.85	12.40	10.89	12.51
IId	1 ; $HOOCCH_2$—	52–3	36	$C_9H_{10}N_2O_3S$	12.39	14.16	12.48	14.26
IIe	1 ; $HOOCCH_2$—	170–2	41	$C_{11}H_{14}N_2O_3S$	11.02	12.59	11.15	12.63
IIf	3 ; C_6H_5—	35–7	38	$C_{15}H_{16}N_2OS$	10.29	10.29	10.34	11.83
IIg	3 ; *o*-$NH_2C_6H_4$—	170–1	62	$C_{15}H_{17}N_3OS$	14.63	11.15	14.71	11.28
IIh	3 ; *p*-$NH_2C_6H_4$—	74–5	42	$C_{15}H_{17}N_3OS$	14.63	11.15	14.68	11.21
IIi	3 ; $EtOOCCH_2$—	40–2	39	$C_{13}H_{18}N_2O_3S$	9.93	11.35	9.98	11.39
IIIa	1 ; *p*-$NH_2C_6H_4$	201–3	83	$C_{13}H_{13}N_3O_4S$	13.68	10.42	13.72	10.51
IIIb	1 ; C_6H_5—	205–6	75	$C_{13}H_{12}N_2O_4S$	9.59	10.95	9.65	10.91
IIIc	1 ; *p*-$CH_3C_6H_4$—	215–6	57	$C_{14}H_{14}N_2O_4S$	9.15	10.46	9.22	10.52
IIId	3 ; *p*-$NH_2C_6H_4$—	206–7	48	$C_{15}H_{17}N_3O_4S$	12.54	9.55	12.61	9.63

* Satisfactory elemental analyses were obtained for C and H.

It can be seen from the above scheme and from the data presented in Table 1 that treatment of II with hydrogen peroxide in acetic acid led to oxidation at both the sulphur and the ring nitrogen atoms. This fact was confirmed in all cases by the infrared analysis[11] which showed the N →O band at 1200 – 1300 cm^{-1}, —SO_2—band at 1320 – 1350 cm^{-1}

and the —CONH—bands at ~ 1700 cm^{-1} ν(C = O) and ~ 3400 cm^{-1} ν(N—H) as well as by the elemental analyses indicated in Table 1. Further confirmation of structure II came from mass spectrometric analysis which will be discussed later in some detail.

In this work, beside preparing the above described 2-acylaminopyridine sulphides and sulphones, II and III respectively, we prepared also some related aminoacyl derivatives of 2-aminopyridine and sulphapyridine. These derivatives comprised the anesthetically active aminoacylamide moiety $\left(-NHCO(CH_2)_2N\langle\right)$ together with the biologically active 2-aminopyridine[1,2] as in compounds IV and with sulphapyridine[12] as in compounds V. Compounds IV and V were successfully prepared through the steps outlined in Scheme 2. Some of their properties are summarised in Table 2.

TABLE 2

Characteristics of aminoacyl derivatives (IV)*

Compound No.	n ; 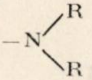 $-N\langle^{R}_{R}$	M.p/or B.p. (°C)	Yield (%)	Molecular formula	Analytical data * (%)					
					Calculated			Observed		
					N	S	Cl	N	S	Cl
IV-a	1; 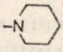	67—8	81	$C_{12}H_{17}N_3O$	19.17	—	—	19.29	—	—
IV-b	1; 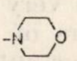	65—6	87	$C_{11}H_{15}N_3O_2$	19.00	—	—	19.13	—	—
IV-c	1 ; 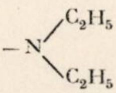 $-N(C_2H_5)_2$	136°/2.5 mm Hg	66	$C_{11}H_{17}N_3O$	20.29	—	—	20.32	—	—
IV-d	3; 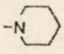	78—9	59	$C_{14}H_{21}N_3O$	17.00	—	—	17.09	—	—
IV-e	3; 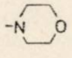	74—5	89	$C_{13}H_{19}N_3O_2$	16.86	—	—	17.01	—	—
IV-f	3 ; 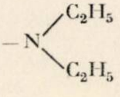 $-N(C_2H_5)_2$	145—8°/2.5 mm Hg	76	$C_{13}H_{21}N_3O$	17.87	—	—	17.89	—	—
V	—	192—93	96	$C_{13}H_{12}ClN_3O_3S$	12.90	9.53	10.80	13.02	9.71	10.97
VI-a	1; 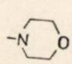	233	70	$C_{18}H_{22}N_4O_3S$	14.97	8.55	—	14.92	8.61	—
VI-b	1; 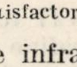	228—30	61	$C_{17}H_{20}N_4O_4S$	14.89	8.51	—	14.85	8.58	—

* Satisfactory elemental analyses for C and H were obtained.

The infrared spectra[11] of IV revealed bands at ~1700 cm^{-1} ν(C = O) and ~3400 cm^{-1} ν(N—H) characteristic of —CONH— and at ~1350 cm^{-1} characteristic of —SO_2NH.

Scheme 2 (For R see Table 2)

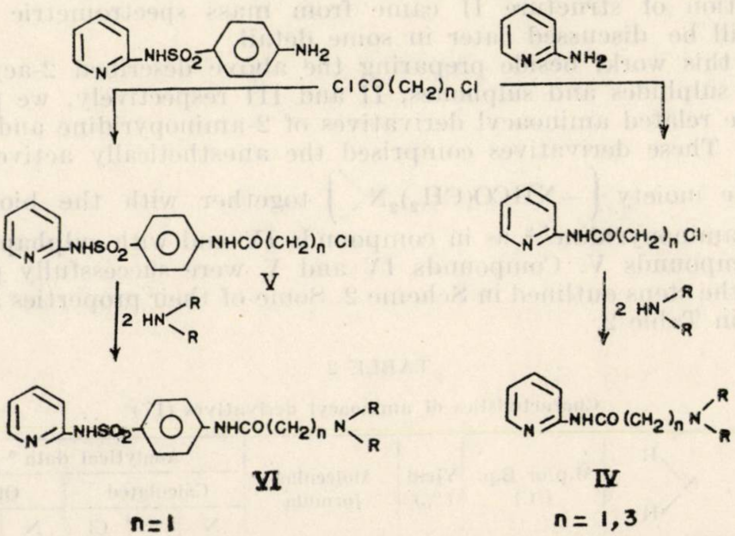
NHSO2
NH2
ClCO(CH2)n Cl
NH2
NHSO2
NHCO(CH2)n Cl
V
NHCO(CH2)n Cl
2 HN R R
2 HN R R
NHSO2
NHCO(CH2)n N R R
NHCO (CH2)n N R R
VI
IV
n = 1
n = 1,3

Our interest in the mass spectra of sulphones[13] has been extended to involve sulphones containing pyridine N-oxide- and acylamido groups as in compound IIIa. The mass spectrum of IIIa showed a very interesting fragmentation pattern as revealed by the characters of N-oxide, pyridine, sulphone and amide functions. The most important ions in the spectrum are given in Table 3.

TABLE 3

Partial mass spectrum of III a

Ion		m/e	% Abundance
$C_{13}H_{12}N_2O_4S$	[M]	292	4
$C_{13}H_{11}N_2O_4S$	[M−H]	291	20
$C_{13}H_{12}N_2O_3S$	[M−O]	276	2
$C_{13}H_{11}N_2O_3S$	[M−OH]	275	4
$C_7H_7N_2O_2$		151	8
$C_6H_5SO_2$		141	25
$C_6H_5N_2O_2$		137	75
$C_6H_4N_2O_2$		136	13
C_6H_5SO		125	2
$C_6H_5N_2O$		121	34
$C_5H_6N_2O$		110	15
$C_5H_5N_2O$		109	100
C_6H_5O		93	44

The base peak at *m/e* 109 may be attributed to ion VII formed by simple β-cleavage of the N−C bond as suggested for pyridine derivatives.[14] The appearance of M-109 ion, though in low abundance (4 %), confirms this type of β-cleavage (Scheme 3-a).

In line with Spiteller[15] who pointed out that a γ-cleavage is especially favoured in pyridines bearing substituents in the 2-position, the abundant peak at *m/e* 137 may be attributed to ion VIII resulting from γ-cleavage. The M-137 ion may lose a methylene group leading to a fragment ion at *m/e* 141. Also, the ions at *m/e* 121 and 136 may originate from ion VIII via loss of oxygen or hydrogen atom, respectively (see Scheme 3—b).

Scheme 3

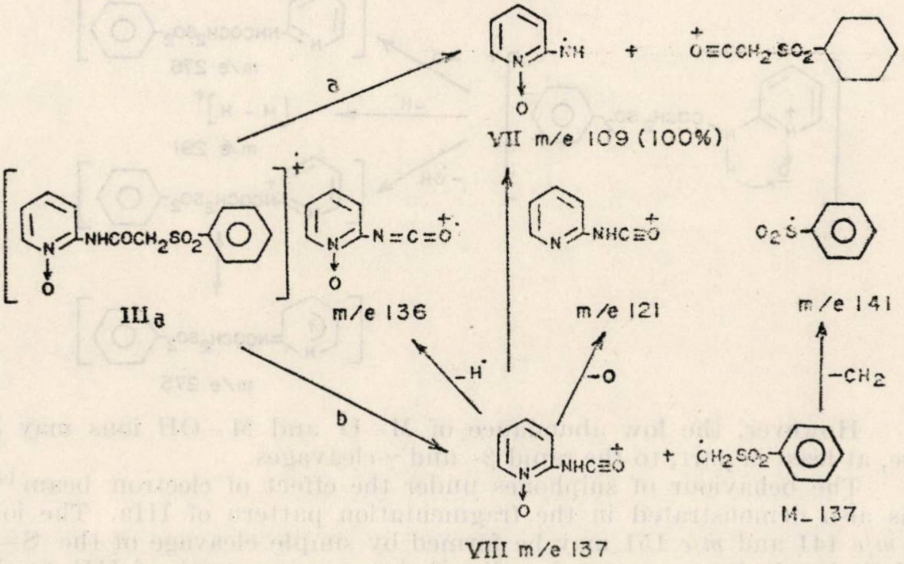
a
VII m/e 109 (100%)
IIIa
m/e 136
m/e 121
m/e 141
−H˙
−O
−CH₂
b
M− 137
VIII m/e 137

The McLafferty type rearrangement[16,17] (Scheme 4) is expected to be responsible for ion IX at *m/e* 110 (Scheme 4).

Scheme 4

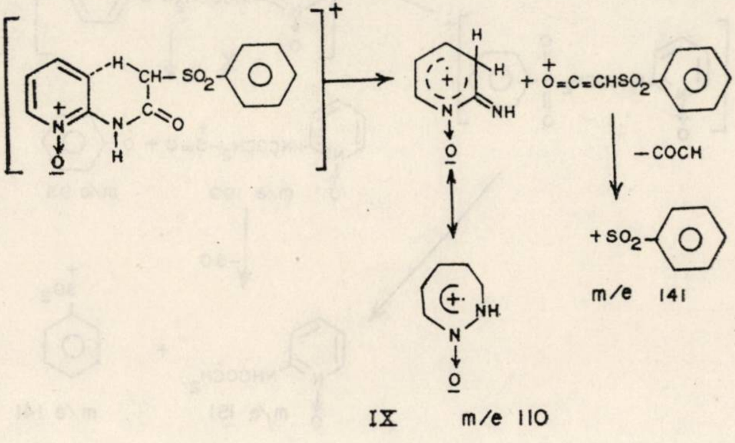
−COCH
m/e 141
IX m/e 110

As a typical N-oxide, IIIa gave a molecular ion at *m/e* 292 and a group of ions at m/e 291 (M-1), 276 (M-16) and at 275 (M-17). The latter ion may be due to the loss of OH from III a, as reported for *ortho*-substituted pyridine N-oxides [18] (see Scheme 5).

Scheme 5

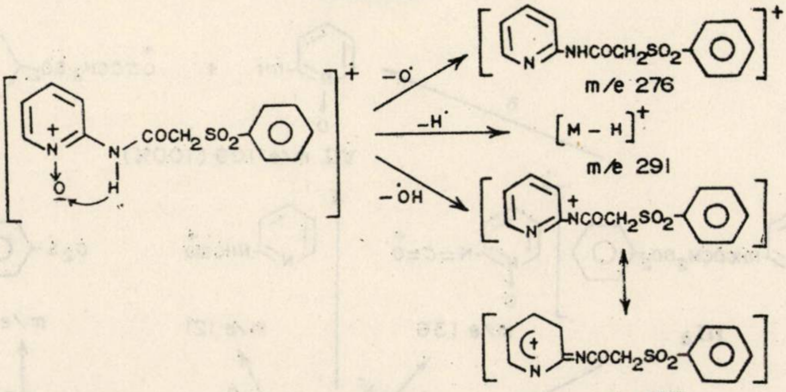
COCH₂SO₂
N
H
O
+
−O˙
−H˙
−˙OH
NHCOCH₂SO₂
m/e 276
[M − H]⁺
m/e 291
NCOCH₂SO₂
=NCOCH₂SO₂
m/e 275

However, the low abundance of M—O and M—OH ions may be due, at least in part, to the rapid β- and γ-cleavages.

The behaviour of sulphones under the effect of electron beam [19,20] was also demonstrated in the fragmentation pattern of IIIa. The ions at *m/e* 141 and *m/e* 151 may be formed by simple cleavage of the S—C (alkyl) bond. As we reported earlier,[13] the rearrangement of IIIa to the corresponding sulphinate (X) took place through migration of phenyl rather than of alkyl group. This is confirmed by the appearance of an abundant ion at *m/e* 93 (PhO) and of a weak ion at *m/e* 125, PhSO, (see Scheme 6) :

Scheme 6

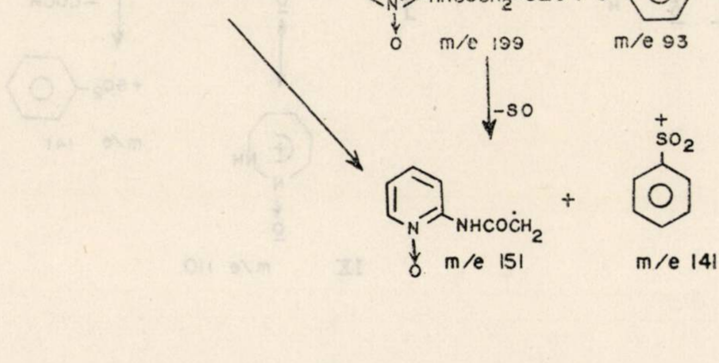
NHCOCH₂
S
O
O
NHCOCH₂S-O
X
HNCOCH₂—S=O + Ȯ
m/e 199
m/e 93
−SO
SO₂
NHCOĊH₂
+
m/e 151
m/e 141

ANTIMICROBIAL ACTIVITIES

The antimicrobial activities of the prepared compounds were determined against a variety of microbes. This included *Gram-positive* and *Gram-negative* bacteria as well as fungi. The bacteria used were : *Bacillus megalherium*, *Staphylococcus albus*, *Proteus vulgare* and *Escherichia coli.* The fungi used were *Aspergillus flavus*, *Penicilium nigricans*, *Myrothecium sp.* and *Fusarium oxysporum.*

The results showed that most of these compounds are active at a concentration of 50 μg/ml in ethylene glycol using the paper disc technique.[21] Noteworthy, the oxidised derivatives (III) exhibited stronger activities than the corresponding sulphides (II).

Compounds IIIa, IIIb, IIIc, IIId, IVd, VIa and VIb exhibited moderate to strong activities against *Bacillus megatherium*, *Staphylococcus albus* and *Escherichia coli.* Compounds IIa, IIb, IIIb, IIIc, IVd and VIb exhibited moderate to strong activities against *Aspergillus flavus*, *Penicilium nigricans* and *Fusarium oxysporum.*

EXPERIMENTAL

All melting points are uncorrected and were measured using a Kofler melting point apparatus. Infrared spectra were recorded on a Pye-Unicam spectrophotometer model SP 200G. Mass spectra were obtained using a Varian MAT/12 mass spectrophotometer at 70 eV.

PREPARATION OF 2-(CHLOROACYLAMINO)PYRIDINES (I)

2-(2-Chloroacetamido)pyridine was prepared by the method of Hach and Protiva.[2]

2-(γ-CHLOROBUTYRAMIDO)PYRIDINE

To a well stirred mixture of 2-aminopyridine (47 g) in dry benzene (200 ml), a solution of γ-chlorobutyryl chloride (50 ml) in dry benzene (100 ml) was added dropwise during a period of two hours. The reaction mixture was refluxed for 1.5 hrs on a water bath and then cooled. The precipitated HCl salt was filtered, washed with ethanol and disolved in Na_2CO_3 solution. On cooling the carbonate solution, the desired product was precipitated, filtered and recrystallised from ethanol to give 26.5 g. (50.6 % yield) of the title compound : m.p. 71°C.

Anal. Calcd. for $C_9H_{11}ClN_2O$: Cl, 17.88 % ; Found : Cl, 17.79 %.

2-(ACYLAMINO)PYRIDINYL ARYL AND ALKYL SULPHIDES (II)

Reaction of the alkyl or the aryl mercaptan (0.01 mole) with alcoholic NaOH (0.01 mole) gave the corresponding sodium salt. This was added to 2-(chloroacylamino) pyridine (0.01 mole) in ethanol (20 ml) and the mixture was refluxed for 0.5–2 hrs. The solvent was removed by distillation and the remaining product was crystallised from the proper solvent. In certain cases, the reaction mixture was poured on water and the product was filtered off and recrystalised. The data are given in Table 1.

2-(ACYLAMINO)PYRIDINYL N-OXIDE ARYL SULPHONES (III)

A solution of II (0.001 mole) in acetic acid (30 ml) was treated with excess 30 %H_2O_2 and the mixture was refluxed for 0.5–2 hours then concentrated. The precipitated solid was filtered and recrystallised from the proper solvent. The data are collected in Table 1.

AMINOACYL α-AMINOPYRIDINES (IV)

The haloacyl-α-aminopyridine (0.1 mole) was dissolved in benzene (40 ml) and heated under reflux with excess of the appropriate amine (0.26 mole). The amine hydrochloride was separated and the bezene solution was evaporated leaving the product which was purified by distillation under vacuum or crystallization from the proper solvent. Results are found in Table 2.

2-(N^4-CHLOROACETYLSULPHANILAMIDO)PYRIDINES (V)[21]

To a suspension of sulphapyridine (1.15 g) in a mixture of chloroform (10 ml) and dry pyridine (0.5 ml) 1.5 ml of chloroacetyl chloride was added dropwisely with stirring. The crude product (1.39 g, 96 % yield) was separated and recrystallized from dioxane ; m.p. 192 – 93°C.

Analysis : Calculated for $C_{13}H_{12}ClN_3O_3S$: Cl, 10.8 ; N, 12.9 Found : Cl, 10.97 ; N, 13.02 %

2-(N^4-AMINOACETYLSULPHANILAMIDO)PYRIDINE (VI)[22]

The intermediate V (1.3 g, 0.004 mole) was dissolved in benzene–toluene mixture (40 ml, 1 : 1 ratio) then refluxed for 10–15 hrs with heterocyclic amines. The precipitated amine hydrochloride was filtered and the filtrate was extracted with dilute hydrochloric acid. The acid extract was neutralised with sodium carbonate solution and the produced precipitate was filtered and purified.

Interaction of V with piperidine gave VIa in 70 % yield : m.p. 223°C. Analysis :
Calculated for $C_{18}H_{22}N_4O_3S$: S 8.55 ; N, 14.97 ;
Found : S, 8.61 ; N, 14.92 %
Reaction of V with morpholine gave VIb in 61.0 % yield :
m.p. 228 – 30°C Analysis: Calculated for $C_{17}H_{20}N_4O_4S$: S, 8.51 ; N, 14.89 ;
Found : S, 8.58 ; N, 14.85 %.

REFERENCES

[1] E. Dingemanse and J. P. Wibaut, *Arch. Exptl. Path. Pharmakol.*, **132**, 365 (1928).
[2] V. Hach and M. Protiva, *Chem Listy*, **57**, 729 (1953) ; *Chem. Abstr.* ; **49**, 205, 3048 (1955).
[3] F. E. Anderson and D. M. Green, *Antibiotics and Chemotherapy*, **6**, 261 (1956).
[4] H. Gilman and H. S. Broadbent, *J. Amer. Chem. Soc.*, **69**, 2053 (1947).
[5] H. Bauer, *J. Amer. Chem. Soc.*, **61**, 617 (1939).
[6] B. Siegfiled, *Swiss Patent* 234, 108 (1944) ; *Chem. Abstr.*, **43**, 4297 (1949).
[7] N. Lofgren, *Ark. Kemi Uineral Geol.*, **22A**, 1 (1946).
[8] I. Lalezri, A. Shafiee, M. A. Khoyi, F. Abtahi, *J. Med. Chem.*, **15**, 113 (1972).
[9] P. B. Patel, J. J. Trivedi, *J. Indian Chem. Soc.*, **50**, 287 (1973).
[10] Adchi, Kikuo, Terakado, Yasuo, *Japan Kokai*, **73**, 48, 441 (1973).
[11] L. J. Bellamy, "The Infrared Spectra of Complex Molecules", John Wiley, New York, 1954.
[12] E. Winterbottom, *J. Amer Chem. Soc.*, **62**, 160 (1940).
[13] A. I. Khodair, A. A. Swelim and A. A. Abdel-Wahab, *J. Phosphorous and Sulfur*, **2**, 173, (1976).
[14] K. Biemann, "Mass Spectrometry", Mc Graw-Hill, New York, 1962 p. 130.
[15] G. Spiteller, "Mass Spectrometry of Heterocyclic Compounds", in (A. R. Katritzky, ed.) Advances of Heterocyclic Chemistry, vol. 7, Academic Press, New York, 1967.
[16] J. H. Beynon, "Mass Spectrometry and its Application to Organic Chemistry", Elsevier Amsterdam, 1960 p. 403.
[17] J. L. Cotter, *J. Chem. Soc.*, 1964, 5477 ; 1965, 5742.
[18] R. Grigg and B. G. Odell, *J. Chem. Soc.* (*B*), 1966, 218.
[19] H. Budzikiewicz, C. Djerassi and D. H. Williams, "Mass Spectrometry of Organic Compounds", Holden-Day, Inc., San Francisco, California, 1967, p. 556.
[20] A. I. Khodair and A. A. Swelim, *J. Phosphorous and Sulfur*, **4**, 49 (1969).
[21] K. A. Oster and M. J. Golden, J. *Amer. Pharm. Assoc. Sci. Ed.*, **36**, 283 (1947).
[22] J. Finkelstein, *J. Amer. Chem. Soc.*, **66**, 407 (1944).

Revue Roumaine de Chimie, 27, 4, 545–547 (1982)

SYNTHESIS OF (Z)-9-TRICOSENE (MUSCALURE)*

LIDIA POP and F. HODOŞAN
Institute of Chemistry, Str. Donath 65, 3400 Cluj-Napoca,
Romania

Received February 19, 1981

Condensation of erucoyl chloride with diethyl ethoxymagnesium malonate followed by hydrolysis and decarboxylation of the reaction product led to 22-oxo-(Z)-9-tricosene. Huang-Minlon reduction of the latter gave the title compound in an overall yield of 45 %.

(Z)-9-Tricosene (I), the sex pheromone of the house fly (*Musca domestica*), was isolated and synthetized about ten years ago by Carlson et al.[1] Since then a relatively large number of preparation methods involving Wittig reaction,[1,2] acetylenic route,[3,4] olefin cross methatesis,[5,6] were reported. In addition, procedures starting with two easily available fatty acids, oleic and erucic, were developed. Thus the latter was transformed in six steps through the intermediary of tricosenenitril into muscalure.[7] Electrolysis of sodium salts of the acid pairs oleic – hexanoic[8] and erucic – propionic[9] gave also the pheromone I. The same fatty acids were converted under the action of lithium organic reagents into ketones which by Huang-Minlon reduction led also to compound I. Thus oleic acid with pentyl lithium afforded 18-oxo-(Z)-9-tricosene,[10] while erucic acid (II) and methyl lithium gave 22-oxo-(Z)-9-tricosene (III).[11,12]

We carried out a conversion of erucic acid (II) into ketone III following a different and very convenient route. A Romanian patent containing this method was already applied in 1977.[13] Two years later Cormier et al.[14] reported a synthesis based on the same scheme. This fact prompted us to publish herein our former results in all details.

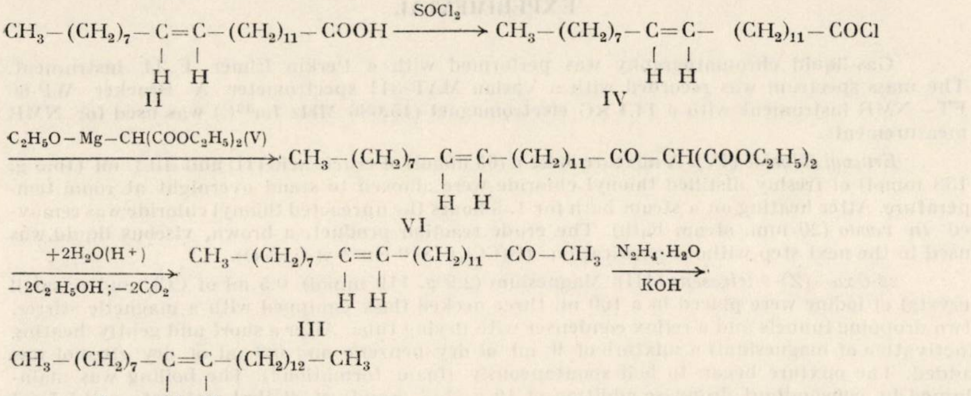

$$\underset{\text{II}}{CH_3-(CH_2)_7-\underset{H}{C}=\underset{H}{C}-(CH_2)_{11}-COOH} \xrightarrow{SOCl_2} \underset{\text{IV}}{CH_3-(CH_2)_7-\underset{H}{C}=\underset{H}{C}-(CH_2)_{11}-COCl}$$

$$\xrightarrow{C_2H_5O-Mg-CH(COOC_2H_5)_2(V)} \underset{\text{VI}}{CH_3-(CH_2)_7-\underset{H}{C}=\underset{H}{C}-(CH_2)_{11}-CO-CH(COOC_2H_5)_2}$$

$$\xrightarrow[-2C_2H_5OH;\,-2CO_2]{+2H_2O(H^+)} \underset{\text{III}}{CH_3-(CH_2)_7-\underset{H}{C}=\underset{H}{C}-(CH_2)_{11}-CO-CH_3} \xrightarrow[KOH]{N_2H_4\cdot H_2O}$$

$$\underset{\text{I}}{CH_3-(CH_2)_7-\underset{H}{C}=\underset{H}{C}-(CH_2)_{12}-CH_3}$$

---

* Exo- and endohormones. IV. Previous paper : A. Gocan and F. Hodoşan, *Rev. Roumaine Chim.*, **21**, 627 (1976).

Erucic acid (II) was obtained from rapeseed oil by alkaline hydrolysis [15] and converted under the action of thionyl chloride into erucoyl chloride (IV).[16] The reaction was monitored observing the disappearance in the IR spectrum of the band at 1720 cm^{-1} and the appearance of a new band at 1810 cm^{-1}. The transformation occurred nearly quantitatively and the reaction product IV could be utilized in the next step without purification.

TABLE

$^{13}C-NMR$ spectrum of (Z) -9-tricosene (40% in $CDCl_3$)

Signal no.	Chemical shift δ(ppm)	Carbon no.
1	14.3	1, 23
2	23.05	2, 22
3	27.7	8, 11
4	29.9	4, 5, 6, 7, 18, 19, 20
5	30	12, 13, 14, 15
6	30.2	16, 17
7	32.5	3, 21
8	130.5	9, 10

Erucoyl chloride (IV) was then condensed with diethyl ethoxymagnesium malonate (V) and the reaction product VI was subjected without previous purification to an acidic hydrolysis with concomitant decarboxylation. 22-Oxo-(Z)-9-tricosene (III) thus formed was purified by treatment of the petroleum ether solution with active alumina (yield 75% from II; purity 90% determined by g.l.c.). Purification by vacuum distillation (0.1 mm), or repeated crystallizations of the semicarbazone from ethanol, resulted in considerable loss of material.

Huang-Minlon reduction of compound III gave finally the expected (Z)-9-tricosene (I) in a yield of 67%; the crude product has a purity of 92% (g.l.c.). No E isomer could be detected either on $AgNO_3$ impregnated silica gel plates or by gas–liquid chromatography. The spectral data were in perfect agreement with the structure ascribed. Thus mass spectrometry showed a molecular peak of *m/e* 322 and a fragmentation pattern characteristic of mono-unsaturated hydrocarbons. The $^{13}C-NMR$ data are given in the table.

EXPERIMENTAL

Gas-liquid chromatography was performed with a Perkin Elmer F 11 instrument. The mass spectrum was recorded with a Varian MAT 311 spectrometer. A Brucker WP-60 FT–NMR instrument with a 14.1 kG electromagnet (15.086 MHz for ^{13}C) was used for NMR measurements.

Erucoyl chloride (IV). A mixture of 22 g (65 mmol) of erucic acid (II) and 10.1 ml (16.5 g, 138 mmol) of freshly distilled thionyl chloride were allowed to stand overnight at room temperature. After heating on a steam bath for 1. 5 hours the unreacted thionyl chloride was removed *in vacuo* (20 mm, steam bath). The crude reaction product, a brown, viscous liquid, was used in the next step without purification. IR(CCl_4) 1810 cm^{-1} ν(C = O).

22-Oxo–(Z)-9-tricosene (III). Magnesium (2.9 g, 119 mmol), 0.5 ml of CCl_4 and a small crystal of iodine were placed in a 100 ml three necked flask equipped with a magnetic stirrer, two dropping funnels and a reflux condenser with drying tube. After a short and gently heating (activation of magnesium) a mixture of 9 ml of dry benzene and 0.9 ml of dry ethanol was added. The mixture began to boil spontaneously (foam formation !). The boiling was maintained by concomitant dropwise addition of 19 g (148 mmol) of diethyl malonate and 5.5 ml of dry ethanol in 24 ml of dry benzene. The mixture was then refluxed on a steam bath under stirring over a period of 2 hours. The unreacted alcohol was removed by distillation. To the remained benzene solution 24 g (67 mmol) of erucoyl chloride (IV) and 15 ml of benzene were added. The addition was carried out under stirring at room temperature and lasted about 30 minutes. When the mixture became too viscous a gently heating was necessary. The mixture was then refluxed for 1 hour and allowed to stand at ambient temperature overnight. It was finally poured onto 25 g of ice acidulated with 60 ml of 2N sulfuric acid, the organic layer was separated, washed twice with diluted sulfuric acid, and twice with water. The benzene solution was dried on magnesium sulfate and the solvent completely removed by distillation *in vacuo*. Diethyl erucoyl malonate (VI) was thus obtained in the form of a brownish oil, in a yield of 24 g (50.6 mmol) ; $n_D^{24} = 1.4671-1.4689$.

The compound VI was treated with a mixture of 8.6 ml of conc. sulfuric acid, 34.4 ml of acetic acid and 22.8 ml of water. The mixture was refluxed for 5 hours under stirring. After cooling at room temperature it was poured onto 100 g of ice. It was neutralized with a 10% sodium hydroxide solution and extracted with ether. The organic layer was washed successively with water, diluted hydrochloric acid and water. After drying on magnesium sulfate the solvent was removed *in vacuo*. The orange oil thus obtained was dissolved in 150 ml of petroleum ether and treated with 25 g of alumina (activity II). After shaking for 20 minutes at ambient temperature the mixture was filtered and the solvent removed *in vacuo*. A light yellow oil was thus obtained (15 g ; 44.5 mmol) ; purity 90% (g.l.c. SE 30, 2m × 4 mm, 245°, Ar 0.45 at, t_R 7.2 min.). IR (film) : 1720 cm^{-1} ν(C = O), 3100 sh, 760 cm^{-1} (δ cis = C—H).

(Z)-9-tricosene (I). To a solution of 9.6 g of KOH (85%) in 95 ml of diethylene glycol 14.8 g (44 mmol) of ketone III and 6.2 ml of hydrazine hydrate (85%) were added. The water was removed by distillation (external temperature 140°C). The mixture was then heated at 190 — 195°C for 4 — 5 hours. After cooling to ambient temperature the mixture was poured onto 300 g of ice, neutralized with 6N hydrochloric acid and extracted five times with hexane. The combined extracts were dried and the solvent removed *in vacuo*. Muscalure (I) was thus obtained in the form of a yellow oil (9.5 g, 29 mmol) ; $n_D^{24.5} = 1.4589$; purity (2%(g.l.c. SE 30,2 m × 4 mm, 245°C, Ar 0.45 at, t_R 10 min.). IR (CCl_4) : 3100, 760 cm^{-1} δ cis= C—H). ^1H—NMR ($CDCl_3$) : δ 0.88 ppm (6H, *t*, $-C\mathbf{H}_3$), 1.27 ppm (32H, *m*, $-C\mathbf{H}_2-$), 1.99 ppm (4H, *m*, $-C\mathbf{H}_2-CH=CH-C\mathbf{H}_2-$), 5.28 ppm (2H, t, $-C\mathbf{H}=C\mathbf{H}-$).

ACKNOWLEDGEMENT. Thanks are expressed to Dr. A. Barabás (Institute of Chemistry Cluj-Napoca) for interpretation of the NMR spectra.

REFERENCES

[1] D. A. Carlson, M. S. Mayer D. L. Silhacek and M. Beroza, *Science* **174**, 76 (1971).
[2] H. E. Bestmann, O. Vostrowsky and H. Platz, *Chem. Ztg.*, **98**, 161 (1974).
[3] K. Eiter, *Naturwiss.*, **59**, 468 (1972).
[4] K. Eiter (Bayer A.—G.) Ger. offen, 2 249 679 ; *Chem. Abstr.*, **81**, 13088 (1974).
[5] L. Di Nunno and S. Florio, *Chimica e Industria*, **57**, 242 (1975).
[6] R. Rossi, *Chimica e Industria*, **57**, 242 (1975).
[7] I. Richter and H. K. Mangold, *Chem. Phys., Lipids*, 210 (1973).
[8] G. W. Griblle and J. K. Sanstead, *J.C.S.Chem.comm.*, 733 (1973).
[9] O. Merész and C. Mozsgai, *Ger. offen.*, 2 331 657 ; *Chem. Abstr.*, **80**,26699 (1974).
[10] Tse-Lok Ho and Chiu Ming Wong, *Canad. J. Chem.*, **52**, 1923 (1974).
[11] L. R. Cargill, U. S. patent 3798273 ; *Chem. Abstr.*, **80**, 120275 (1974).
[12] L. R. Cargill and M. G. Rosenblum, *J. Org. Chem.*, **37**, 3971 (1972).
[13] L. Pop and F. Hodoșan, Rom. Patent 70999/1979 (Appl. 12 May 1977).
[14] R. A. Cormier, M. Duc Phan, T. Graddis and R. Singer, *J. Chem. Educ.*, **56**, 345 (1979).
[15] C. R. Noller and R. H. Talbot, *Organic Syntheses*, Collect. vol. II, Willeys, New York, 1943, p. 258.
[16] L. F. Fieser and E. M. Chamberlin, *J. Amer. Chem. Soc.*, **70**, 74 (1948).

Revue Roumaine de Chimie, **27**, *4*, 549–555 (1982)

SYNTHESIS AND SOME REACTIONS OF 1-ARYLISOINDOLES

G. E. M. MOUSSA, M. N. BASYOUNI, M. E. SHABAN, A. F. El-KAFRAWY and N.K.Al-AASAR

Chemistry Department, Faculty of Science, Ain Shams University, Abassia, Cairo, Egypt

Received December 29, 1980

The synthesis of 1-arylisoindoles **2b** and **2c** (or isoindolenines **2′**) and their dimerisation, under different conditions, are described. Nitrous acid converted **2a-c** into the corresponding *o*-aroylbenzoic acids **4a-c**. Maleic anhydride reacted with **2b** and **2c** to give the corresponding substitution products **5b** and **5c** which yielded the corresponding pyrrolo[2, 3a] isoindoles **6b** and **6c** upon heating. Whereas aromatic aldehydes condensed with **2b** and **2c** in the presence of alkali to give the corresponding 1-aryl-3-arylideneisoindolenines **7a** and **7b**, **2a** gave the corresponding dimer **3a**. A mechanism is given for this discrepancy in behaviour.

Although the synthesis of N-substituted arylisoindoles and their reactions have been extensively investigated,[1] few reports have dealt with the synthesis and reactions of N-unsubstituted arylisoindoles.[1–4] The present work was aimed, therefore, to synthesise some N-unsubstituted 1-arylisoindoles and to study their dimerisation, under different conditions as well as their reactions with nitrous acid, maleic anhydride and aromatic aldehydes.

The method adopted by Veber and Lwowski [2] for the synthesis of 1-phenylisoindole was applied to the synthesis of 1-(4-methyl phenyl)- and 1-(2,5-dimethyl phenyl)-isoindoles, **2b** and **2c** (or isoindolenines **2′b** and **2′c**). Thus, treatment of the hitherto unknown 2-phthalimidomethyl-4′-methyl- and 2-phthalimidomethyl-2′, 5′-dimethylbenzophenones (**1a** and **1b**), which were prepared from α-phthalimido-*o*-toluic chloride and the corresponding aromatic hydrocarbon in the presence of anhydrous aluminium chloride (cf. Experimental), with hydrazine hydrate gave the corresponding 1-arylisoindoles **2b** and **2c** (or **2′**). Although these could not be purified for analysis either by recrystallisation or by sublimation under reduced pressure, they were identified by conversion into the corresponding dimers **3b** and **3c** by refluxing in benzene for a long time. This reaction was developed earlier [2] for the conversion of 1-phenylisoindole into its dimer.

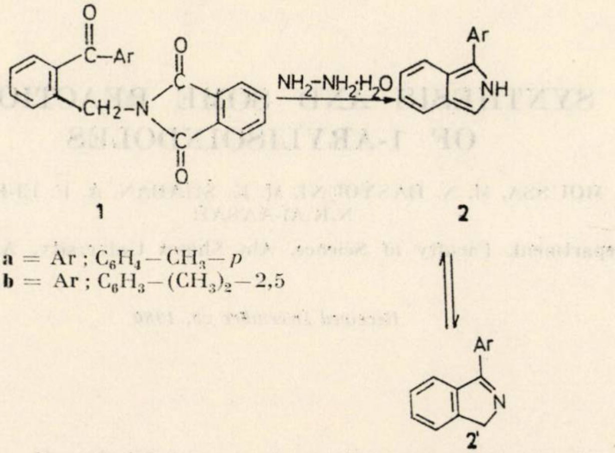

a = Ar ; $C_6H_4-CH_3-p$
b = Ar ; $C_6H_3-(CH_3)_2-2,5$

b = Ar : $C_6H_4-CH_3$-p
c = Ar ; $C_6H_3-(CH_3)_2-2,5$

However, the same dimers **3b** and **3c** and also **3a** (Ar = C_6H_5) were obtained by dimerisation of the isoindoles **2** or isoindolenines **2′** in the presence of aqueous sodium hydroxide (cf. Experimental). The mechanism of the dimerisation in this case seems to involve addition of the carbanion of the isoindolenine tautomer **2′** ; generated *in situ* in the presence of alkali, to the isoindole tautomer followed by loss of hydride ion and a real oxidation :

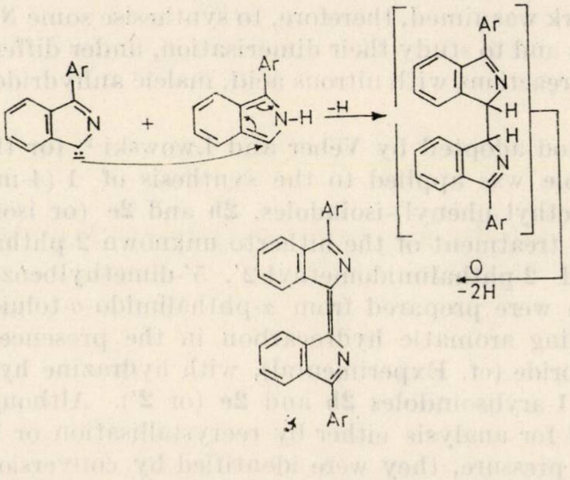

Treatment of the 1-arylisoindoles **2**(or **2′**) with nitrous acid at 0°C gave the corresponding *o*-aroylbenzoic acids **4a-c** which were identical with authentic specimens (cf. Experimental).

The reaction seems to involve formation of the intermediate (A) which can yield the final product either by route *a* (solid arrow) or by route *b* (dotted arrow) as follows :

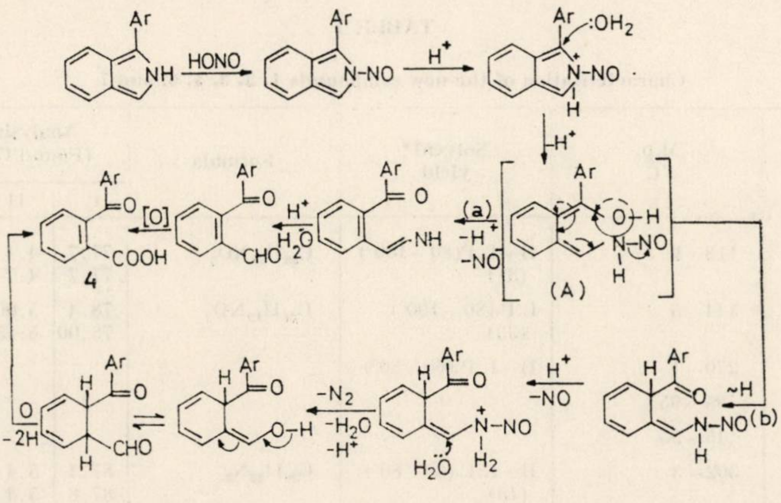

The reaction of maleic anhydride with 1-phenylisoindole has been reported[2] to give 1-carboxy-1, 2-dihydro-3-oxo-5-phenyl-3H-pyrrolo[2,3a] isoindole (**6a**), *via* the addition product **5a** rather than the normal Diels-Alder adduct (B). A similar result is now obtained from the other 1-arylisoindoles **2b** and **2c** (or **2′**). Thus, treatment of **2b** and **2c** with maleic

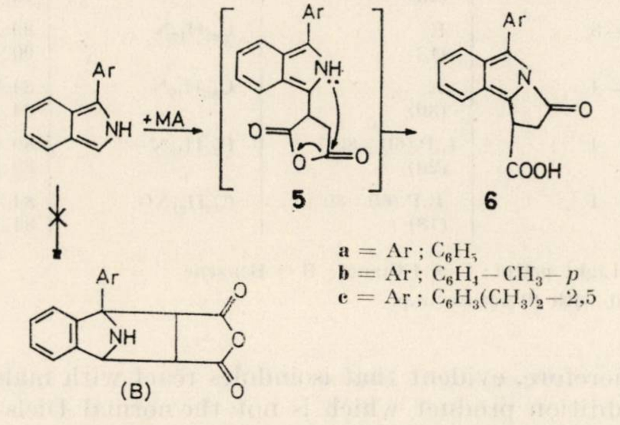

a = Ar ; C_6H_5
b = Ar ; $C_6H_4-CH_3-p$
c = Ar ; $C_6H_3(CH_3)_2-2,5$

anhydride in an ethereal solution gave an immediate precipitate, presumably of the corresponding 1-arylisoindole-3-succinic anhydride, **5b** and **5c** which upon recrystallisation yielded the corresponding 1-carboxy-1,2-dihydro-3-oxo-5-aryl-3H-pyrrolo [2, 3a] isoindoles (**6b** and **6c**) (cf. Experimental).

The structures of **6b** and **6c** were substantiated from analytical data and infrared spectra (cf. Table 1). Moreover, the ^{1}H-NMR spectrum of **6c** is consistent with the structure assigned to it.

TABLE 1

Characterisation of the new compounds **1**, **2**, **3**, **4**, **6**, and **7**

Compound	M.p. °C	Solvent* yield	Formula	Analysis % (Found/Calcd.)		
				C	H	N
1a	118–9	B–L.P(80–100°) (31)	$C_{23}H_{17}NO_3$	77.7 77.7	4.4 4.7	3.7 3.9
1b	144–5	L.P.(80–100°) (33)	$C_{24}H_{19}NO_3$	78.4 78.00	5.00 5.15	3.8 3.7
2a**	270–1	B–L.P.(60–80°)				
2b**	85–95					
2c**	45–55					
3b	302–3	B–L.P.(60–80°) (15)	$C_{30}H_{22}N_2$	87.4 87.8	5.4 5.4	
3c	206–7	B–L.P.(60–80°) (10)	$C_{32}H_{26}N_2$	88.2 87.9	5.6 5.8	
4a**	126–7					
4b**	138–9					
4c**	147–8					
6b	174–5	B–L.P.(60–80°) (25)	$C_{19}H_{15}NO$	75.2 74.9	5.3 5.5	3.4 3.6
7a	117–8	E (13)	$C_{22}H_{17}N$	89.50 90.40	5.8 5.9	4.7 4.8
7b	143–4	E (30)	$C_{23}H_{19}N$	84.90 84.50	5.8 5.95	4.3 3.9
7c	213–4	L.P.(60–80°) (20)	$C_{23}H_{19}N$	89.30 89.80	6.2 6.6	4.5 4.7
7d	223–4	L.P.(60–80°) (18)	$C_{24}H_{21}NO$	84.95 84.70	6.2 5.9	4.1 4.9

* L.P. = Light petrol ; E = Ethanol ; B = Benzene

** Identical with literature m.p.

It is, therefore, evident that isoindoles react with maleic anhydride to give an addition product which is not the normal Diels-Alder adduct and that this product can cyclise to give the pyrrolo [2, 3a] isoindole derivatives.

When the 1-arylisoindoles **2** (or **2′**) were treated with benzaldehyde or *p*-methoxybenzaldehyde in the presence of aqueous sodium hydroxide, they gave rise to dehydrobisisoindolenine, **3a** (Ar = C_6H_5) in the case of **2a**(Ar = C_6H_5) and to the corresponding 1-aryl-3-arylidene isoindolenines, **7a-d**, in the case of **2b** and **2c** (or **2'b** and **2'c**).

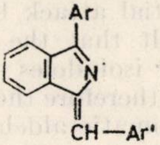

7

a ; Ar = $C_6H_4-CH_3$-*p*, Ar' = C_6H_5
b ; Ar = $C_6H_4-CH_3$-*p*, Ar' = $C_6H_4-OCH_3$-*p*
c ; Ar = $C_6H_3(CH_3)_2$—2,5 Ar = C_6H_5
d ; Ar = $C_6H_3(CH_3)_2$—2,5 Ar' = $C_6H_4-OCH_3$-*p*

The structures of the 1-aryl-3-arylidene isoindolenines **7** were established by the following evidences : (1) analytical data and (ii) the ^{1}H-NMR spectrum of **7b** which shows the following signals : δ 6.8 — 8.4 (aromatic and olefinic protons, 13 H), δ 3.8 (OCH_3, 3H) and δ 2.45 (CH_3, 3H).

TABLE 2

Spectral data for compounds **1**, **2**, **3**, **6** and **7**

Compound	Infrared Spectra cm^{-1} ν(C = O)	ν(NH)	Electronic spectra λ_{max}, nm		^{1}H-NMR
1a	1655 1718 1770				
1b	1660 1715 1775				
2b		3400 ($CHCl_3$)			
2c		3400 ($CHCl_3$)			
3b					Aromatic proton signals
3c					Aromatic proton signals
6b	1800 (γ-lactone) 1710 (carboxylic) 3340 ν(OH)				δ 6.8—7.6 (aromatic, 7 protons), δ 6.2 (CH, one proton), δ 3.85 (CH_2, 2 protons) δ 2.3 (CH_3, 3 protons) and δ 2.2 (CH_3, 3 protons)
7a			258 382	2180 3820	
7b			294 376	2230 2180	

The discrepancy in behaviour between **2a** (Ar = C_6H_5) and **2b** and **2c** towards the reaction under investigation may be explained as follows : the carbanion of the isoindolenine tautomer **2'a** can attack either the isoindole tautomer or the C = O group of the aromatic aldehyde.

The factor that determines which attack occurs seems to depend on the isoindole-isoindolenine tautomer ratio.

Thus, since 1-phenyl isoindole is known [2] to exist exclusively in the isoindole tautomer, a preferential attack by the carbanion on isoindole system occurred with the result that the dimer **3a** (Ar = C_6H_5) was obtained (see above). The other isoindoles seem to exist predominantly in the isoindolenine tautomer and therefore the preferential attack took place on the C = O group of the aromatic aldehyde to give the 1-aryl-3-arylidene isoindolenine **7**.

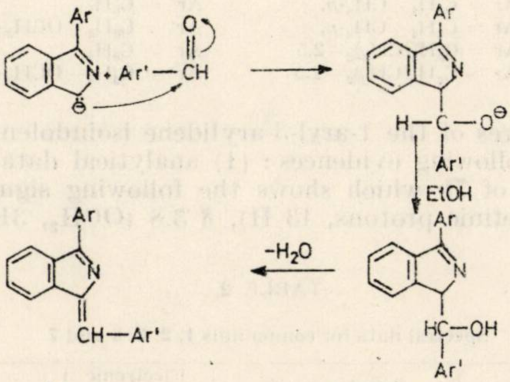

7

EXPERIMENTAL

All melting points are not corrected. Infrared spectra (KBr discs) and electronic spectra (in ethanol) were determined on a Unicam SP 1200 and respectively Varian 664 'Spectrophotometers, ^{1}H-NMR spectra (in $CDCl_3$) were determined on a Varian T60 spectrometer using TMS as internal reference.

Synthesis of 2-phthalimidomethyl-4'-methyl and 2-phthalimidomethyl-2', 5'-dimethylbenzophenones (1a and 1b)

The title compounds were prepared by applying the same procedure used earlier for 2-phthalimidomethyl benzophenone.[2] The interaction of α-phthalimido-*o*-toluic chloride[5] (0.017 mole), anhydrous aluminium chloride (0.05 mole) and toluene or *p*-xylene (0 ; 017 mole) in dry CS_2 (100 ml) under reflux for 2—5 hours gave **1a** or **1b**, respectively. The product obtained was crystallised from the suitable solvent (Table 1).

Action of hydrazine hydrate on 1a *and* 1b ; *Formation of* 2b—e, 3b and 3e

The compounds **2b**, **e** and **3b**, **e** were prepared according to the method outlined earlier[2] for the synthesis of 1-phenylisoindole. Thus, refluxing the phthalimidobenzophenone **1a** or **1b** (0.002 mole) in ethanol (20 ml) with excess of hydrazine hydrate (0.008 mole) for 30 min., followed by the normal work-up procedure[2] gave the title compounds which gave a positive Ehrlich test with *p*-dimethylaminobenzaldehyde in acidic medium.[2]

Refluxing a stirred solution of **2b** or **2e** (0.005 mole) in benzene (50 ml) for 48 hours followed by concentration of the resulting orange solution gave the corresponding dimers, dehydrobis(1,1'-di(4-methylphenyl) isoindolenine (**3b**) and dehydrobis(1, 1'-di(2,5-dimethylphenyl) isoindolenine (**3e**), respectively. The products obtained were crystallised from a suitable solvent (Table 1).

Dimerisation of **2a-c** *by action of aqueous sodium hydroxide* ; *Formation of* **3a-c**

Aqueous sodium hydroxide (10%, 2ml) was added to a solution of the 1-arylisoindole (**2a-c**) (0.005 mole) in ethanol (30 ml) and the reaction mixture was stirred for 6 hours at room temperature. The precipitated solid was filtered off, washed with water and dried. The m.p. of the compound **3a** was undepressed upon admixture with an authentic specimen,[2] the m.p. of **3b** and **3c** were undepressed upon admixture with the products from the dimerization in benzene (Table 1).

Action of nitrous acid on **2a-c** ; *Formation of o-aroylbenzoic acids* **4a-c**

An aqueous solution of sodium nitrite (5g ; 0.07 mole) in 20 ml H_2O was added dropwise with constant stirring to an ice-cold solution of the **2a-c** (0.005 mole) in a mixture of glacial acetic acid (20 ml) and concentrated hydrochloric acid (10 ml). After the addition had been completed, stirring was continued for other 2 hours and the reaction mixture was diluted with water and kept in a refrigerator overnight. The precipitated solid was then filtered off, washed several times with water until the washings were free from acid and the dried solid was recrystallised from an appropriate solvent (Table 1). The compounds **4a-c** gave the m.p. and mixed m.p. with authentic specimens.[6-8]

Addition of **2b** *and* **2c** *to maleic anhydride* : *Formation of 1-carboxy-1,2-dihydro-3-oxo-5-aryl-3H-pyrrolo* [2,3 a] *isoindole* (**6b** *and* **6c**)

An ethereal solution of maleic anhydride (0.004 mole in 50 ml ether) was added to a solution of the **2b** or **2c** (0.004 mole) in ether (20 ml). An immediate precipitate (presumably 1-aryl-isoindole-3-succinic-anhydride) was formed ; after 20 min., the reaction mixture which acquired a purple colour was filtered off and the product was washed with ether and crystallised from an appropriate solvent (Table 1).

Condensation of **2** (*or* **2′**) *with aromatic aldehydes* ; *Formation of 1-aryl-3-arylidene isoindolenines* (**7a-d**)

To a cold stirred solution of sodium hydroxide (0.2 g ; 0.005 mole) in water (2 ml) and ethanol (30 ml) the compound **2** (0.7 g ; 0.003 mole) was added and the temperature of the reaction mixture was not allowed to rise above 25°C. After 6 hours of stirring the reaction mixture was filtered off and the precipitate was crystallised from a suitable solvent to give **7a-d** (Table 1) as orange crystals in the case of **2b** and **2c**.

However, 1-phenylisoindole gave in all cases dehydrobis(1,1′-diphenyl isoindolenine) (**3a**).

REFERENCES

[1] R. M. Acheson, "An Introduction to the Chemistry of Heterocyclic Compounds", Interscience Publishers, 1964.

[2] D. F. Veber and W. L. Lwowski, *J. Amer. Chem. Soc.*, **86**, 4152 (1964).

[3] H. Fletcher, *Tetrahedron*, **22**, 2481 (1966).

[4] R. I. Fryer, B. Bruest, J. V. Earley and L. H. Sternbach, *J. Chem. Soc.*, (*C*), **1976**, 366.

[5] J. Bornstein, S. F. Bedell, P. E. Drummond and C. L. Kosloski, *J. Amer. Chem. Soc.*, **78**, 85 (1956).

[6] C. R. Rubidage and N. C. Qua, *J. Amer. Chem. Soc.*, **36**, 732 (1914).

[7] M. E. Smith, *J. Amer. Chem. Soc.*, **43**, 1920 (1921).

[8] F. Meyer, *Ber. dtsch. chem. Ges.*, **15**, 638 (1882).

Revue Roumaine de Chimie, 27, 4, 557–560 (1982)

ON THE CYCLIZATION OF 3-α-NAPHTHYL-PROPENOYL CARBONIUM ION

AN INTRAMOLECULAR PERTURBATION

SHERIF El-BASIL
Organic Chemistry Dept., Faculty of Pharmacy, Kasr El-Aini, Cairo, Egypt

Received June 12, 1980

Self-consistent intramolecular perturbation calculation is carried out for both transition states involved in the ring closure of 3-α-naphthyl propenoyl carbonium ion. It is shown that consideration of frontier orbitals only might lead to wrong conclusions. The results of the calculations including all interactions within π approximations indicate that transition state leading to perinaphthenone is more favored over the five-membered analog, as it is observed experimentally.

3-α-Naphthylpropenoyl carbonium ion, (I), is an intermediate in the synthesis of perinaphthene,[1] the cyclization of which might follow two possible routes : viz.,

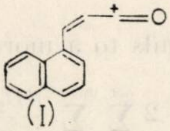

(I)

(a) An attack at the β-carbon of naphthalene to give a 5-membered ketone, or

(b) An attack at the α-carbon in the *peri*-position to give the corresponding 6-membered ketone.

One can write five resonance structures for each transition state, yet experimentally route (b) predominates. In a related development,[2] treatment of the anhydride (II) with $AlCl_3$, leads to the formation of the six-membered acid, (III), rather than the five-membered analog, (IV) :

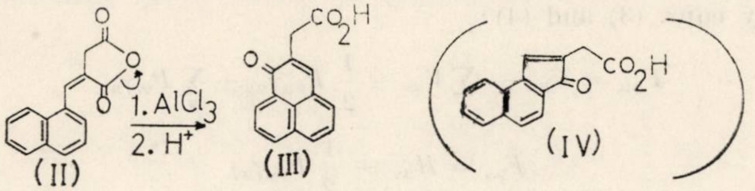

(II) (III) (IV)

It seemed therefore, interesting to carry out an intramolecular perturbation calculation on the ring closure of the two possible conformers of carbocation (I), viz., (A) and (B) : (an arbitrary numbering system is used).

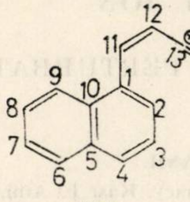

(A)

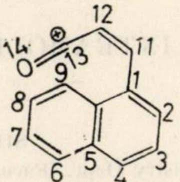

(B)

METHOD OF CALCULATION

Perturbation energy, ΔE, is given by eqn. (1),

$$E = 2 \sum_{i}^{\text{occ}} \langle \psi_i | \mathbf{P} | \psi_i \rangle + 2 \sum_{i}^{\text{occ}} \sum_{j}^{\text{unocc}} (\langle \psi_i | \mathbf{P} | \psi_j \rangle)^2 / (\epsilon_i - \epsilon_j)$$

$$i = 1, \ldots, 7 ; \quad j = 8, \ldots, 14 \tag{1}$$

in which $\mathbf{P}$ is matrix, the elements of which, P_{nm} are given by :

$$P_{nm} = \begin{cases} \beta \text{ if } n(\text{or } m) = 2(\text{structure A}) \text{ or } 9 \text{ (structure B)} \\ \quad m(\text{or } n) = 13 \text{ (both A and B).} \\ 0, \text{ otherwise.} \end{cases}$$

Expansion of eqn. (1) leads to a more explicit form for ΔE, viz.,

$$\Delta E = \underbrace{2 \sum_{i}^{\text{occ}} C_{2(9)i} \, C_{13i} \beta}_{\text{First-order term}} + \underbrace{2 \sum_{i}^{\text{occ}} \sum_{j}^{\text{unocc}} \frac{(C_{2(9)i} C_{13j} \beta + C_{13i} C_{2(9)j} \beta)^2}{\epsilon_i - \epsilon_j}}_{\text{Second-order term}} \tag{2}$$

in which $C_{2(9)i}$ means the coefficient of the second atom (structure A) or 9th atom (structure B) of the ith MO. In general subscripts i and j denote occupied and unoccupied MOs respectively. The ϵ's are eigenvalues. β is a σ-resonance integral, for which a value of -6.97 ev, obtained by Houk [3] using CNDO/2 approximation, is adopted.

Values of C's and ϵ's are obtained using the SCF-PPP method.[4] The elements of the Fock Hamiltonian matrix to be diagonalized are given by eqns. (3) and (4) :

$$F_{\mu\mu} = U_{\mu\mu} - \sum V_{\mu\nu} + \frac{1}{2} P_{\mu\mu} \gamma_{\mu\mu} + \sum_{\nu} P_{\nu\nu} \gamma_{\mu\nu} \tag{3}$$

$$F_{\mu\nu} = H_{\mu\nu} - \frac{1}{2} P_{\mu\nu} \gamma_{\mu\nu} \tag{4}$$

The symbols have their conventional meanings[4] and the summation in eqn. (3) is taken over all pi electrons within the ZDO approximation. The quantity $U_{\mu\mu}$ is the energy of an orbital, $\O_{\mu}$, in the bare field of its own atom and V_{μ} represents electrostatic interaction of an electron in $\O_{\mu}$ and the cores of other atoms. One-electron, two-center off-diagonal terms, $H_{\mu\nu}$, were computed using an expression due to Flurry.[5]

Two-center electron repulsion integrals, $\gamma_{\mu\nu}$, were computed using an equation due to Nishimoto and Mataga,[6] Throughout the work valence-state data compiled by Flurry are used.[4] Bond-lengths are those adopted by Dewar.[7]

RESULTS AND DISCUSSION

Table 1 lists values of C's for the two carbocations A and B. Table 2 outlines the values of the first and second-order perturbations, prevailing in the two cyclizations which show that B is more favored than A as observed experimentally.

TABLE 1

SCF C's of the relevant atoms in carbocations A and B

i (or j)	A		B	
	C_2	C_{13}	C_9	C_{13}
1	.2325	.1475	.2283	.2401
2	.0291	−.5354	.1399	−.5033
3	.3624	−.1375	−.1688	−.1289
4	−.2391	−.0786	.2708	−.0607
5	.1416	.0195	.3705	.0157
6	.4001	−.0033	.0422	.0053
7*	.2416	−.0327	−.4350	−.0316
8**	−.2913	−.3609	−.2405	−.3654
9	−.0707	.5364	−.3085	.5624
10	.4050	.0450	.0427	−.0132
11	−.2917	.3837	.3737	.3234
12	.1592	−.1990	.2409	−.2913
13	−.2877	−.2393	−.2097	−.1649
14	−.2663	−.0307	.3189	−.0270

* HOMO
** LUMO

The following points are worth observing:

(1) One could have reached proper conclusions considering only first-order terms. The author[8] has shown this to be true by considering just the sign of the first-order term for a series of intramolecular transformations.

(2) The largest contribution to the total first-order term does not necessarily come from HOMO or even MO's right before this level. For the case at hand one observes that for structure A, the lowest level, $(i=1)$, contributes the largest stabilizing part of the first-order term, while the third MO, the largest destabilizing, the net effect being destabilizing.

For case B the second MO destabilizes the transition state most, while the lowest level offers the largest stabilizing effect. The net effect is stabilizing. It is rather unexpected that the higher levels (HOMO and the ones right before it) offer very little, almost negligible contributions to E! These observations are reproduced for the interconversions of prismane — benzene and related intramolecular cycloadditions.[8]

TABLE 2

First and second-order intramolecular perturbations, (ev.) prevailing in A and B

i	A		B	
	1st-order	2nd-order	1st-order	2nd-order
1	−0.4779606	−0.43492	−0.7640878	−0.45482
2	0.2175562	−1.0858	0.9814958	−1.0111
3	0.694712	−0.8056	−0.3034298	−0.2292
4	−0.2621442	−0.3860	0.2291896	−0.4695
5	−0.0384828	−0.13532	−0.0810912	−0.925434
6	0.0184044	−1.1258	−0.0031178	−0.0132
7*	0.1100338	−0.48706	−0.191671	−1.58406
	Total : 0.2621188	Total : −4.4605	Total : −0.1327112	Total : −4.687314
	$\Delta E_{\text{Tot(A)}} = -4.19838$ Exptl. Not observed		$\Delta E_{\text{Tot(B)}} = -4.820025$ Observed	

* HOMO

(3) Similar conclusions might be stated regarding contributions to second-order terms. For both transition states almost one fourth of the stabilization comes from the level just next to ground ($i = 2$). It would seem, therefore, rather faulty to depend on conclusions based on considerations of the higher levels only.

(4) Overlap effects are quite important and not energetic differences alone. The coefficients of C_{13} in the HOMO of both cases are vanishingly small (table 1) thus lowering contributions from these levels.

Because of the summation in the squared brackets in the second order terms the sign of the coefficient is just as important as its magnitude.

REFERENCES

[1] E. H. Rodd, "Chemistry of Carbon Compounds", Vol. 3B, D. Van Nostrand Company, London. 1956, p. 1349.

[2] W. I. Awad, Private communication.

[3] K. N. Houk, J. Sims, R. E. Duke, R. W. Strozier and J. K. Jeorge, *J. Amer. Chem. Soc.*, **95**, 7287 (1973).

[4] R. L. Flurry, Jr., "Molecular Orbital Theories of Bonding in Organic Molecules", Marcel Dekker, New York, 1968, Chapter 8.

[5] R. L. Flurry, Jr., E. W. Stout and J. J. Bell, *Theor. Chim. Acta.*, **8**, 203 (1967).

[6] K. Nishimoto and N. Mataga, *Z. phys. Chem. (Frankfurt)*, **12**, 335 (1957).

[7] M.J.S. Dewar, "The Molecular Orbital Theory of Organic Chemistry", McGraw Hill, New York, 1969, p. 381.

[8] S. El-Basil and R. Hilal, *Bull. Chem. Soc. Japan*, **51**, 2749 (1978).

Revue Roumaine de Chimie, **27**, *4*, 561–568 (1982)

QUANTITATIVE STRUCTURE – ACTIVITY RELATIONS WITH THE MTD-PROCEDURE FOR PLANT GROWTH REGULATING OPTICALLY ACTIVE ACETIC ACID DERIVATIVES

A. CHIRIAC *, VERONICA CHIRIAC **, S. HOLBAN **, I. MOTOC *** and Z. SIMON ****

* – University of Timişoara, Department of Natural Sciences

** – Polytechnical Institute of Timişoara "Traian Vuia", Department of Inorganic Chemistry

*** – Chemical Research Centre, Timişoara

**** – Medical High School of Timişoara, Department of Biophysics, Piaţa 23 August 2, Timişoara 1900, Romania

Received June 1, 1981

Quantitative structure—activity relations are established for a series of 31 aryloxy-alkyl-acetic acid derivatives with plant growth inhibiting activity. Correlations with group hydrophobicities, eudismic correlations and receptor site mapping with the MTD-procedure are performed. The regressional equations and receptor map are tested on another series of 24 α-phenoxy-propionic acid derivatives. Only the MTD-procedure combined with group hydrophobicities gives satisfactory results: correlation coefficient $r = 0.93$ for the series of 31 aryloxy-alkyl-acetic acid derivatives and $r = 0.84$ for the test series.

INTRODUCTION

The first quantitative structure – activity relation (QSAR) for large series of enantiomers was published in 1976 by Lien, Rodriguez de Miranda and Ariens.[1] For 56 aryloxy-alkyl-acetic acid derivatives (Table 1 and Table 2), with 5 structural parameters, they obtained a correlational coefficient $r = 0.802$, but only $r = 0.617$ if their regressional equation (1) is applied only to the more active R-enantiomers, and they cannot explain the much reduced activity differences between the enantiomers of aryl-methyl-acetic acid derivatives (Table 3). *

In this paper we study the same series of compounds with our minimal steric (topological) difference procedure, the MTD-procedure, described in detail elsewhere.[2,3] Our aim is to map the receptor for these plant growth inhibitors and to test the real predictability of the MTD-procedure, in comparison with other QSAR-methods.

---

* For uniformity of table headings, we shall employ the term "methyl-acetic" instead of the correct name, propionic acid.

We apply here our MTD-procedure to the 31 compounds of Table 1, to obtain the receptor map and regressional equation which will be used to calculate biological activities, $\hat{A}_T$, for the test series of Table 2. The regressio nal coefficient $r(A_T, \hat{A}_T)$ for the correlation of $\hat{A}_T$ with the experimental activities, A_T, for the test series, will give the real predictive power of the MTD and other QSAR procedures. The activity of α-aryl propionic acids (Table 3) will be also discussed.

CALCULATIONS WITH CLASSICAL QSAR METHODS

The 31 aryloxy-alkyl-acetic acid derivatives are listed in Table 1. The experimental activities, $A = -\log C_{50}$, the molar concentration of the derivative which reduces the growth to 50% of control in the flax root test, are those quoted by Lien et al. [1] The C_{50} values for Table 1 are

TABLE 1

Series for optimisation : aryloxy-alkyl-acetic acids*

i	Configuration	Substituents R_1, R_2	A	MTD_A	MTD_B
1	R(+)	2-NaphO, CH_3	7.70	6	0
2	R(+)	4-Cl, 2-CH_3-PhO, CH_3	7.68	6	0
3	R(+)	3,4-di-Cl-PhO, CH_3	7.55	6	0
4	R(+)	2,4-di-Cl-PhO, C_2H_5	7.55	7	0
5	R(+)	2,4,5-tri-Cl-PhO, CH_3	7.49	5	0
6	R(+)	2,4-di-Cl-PhO, CH_3	7.48	6	0
7	R(+)	2-NaphO, C_2H_5	7.00	7	0
8	R(+)	2-NaphS, CH_3	6.74	6	0
9	R(+)	PhO, CH_3	5.89	8	0
10	R(+)	PhO, C_2H_5	5.85	9	0
11	R(+)	PhNH, CH_3	5.66	8	0
12	R(+)	2-NaphO, n-C_4H_9	5.55	9	1
13	S(−)	CH_3, 3,4-di-Cl-PhO	5.46	7	2
14	S(−)	CH_3, 2,4,5-tri-Cl-PhO	5.00	8	2
15	R(+)	1-Cl-2-NaphO, CH_3	4.92	12	2
16	S(−)	CH_3, 2,4-di-CL-PhO	4.89	8	2
17	S(−)	C_2H_5, 2,4-di-Cl-PhO	4.85	9	2
18	R(+)	1-NaphO, CH_3	4.84	10	2
19	S(−)	CH_3, 4-Cl-2-CH_3-PhO	4.74	8	2
20	S(−)	CH_3, 1-NaphO	4.64	9	2
21	S(−)	n-C_4H_9, 2-NaphO	4.30	12	3
22	S(−)	CH_3, 2-NaphS	4.30	9	2
23	S(−)	C_2H_5, 1-NaphO	4.33	11	2
24	S(−)	CH_3, 1-Cl-2-NaphO	4.21	10	2
25	S(−)	C_2H_5, 2-NaphO	4.14	10	2
26	S(−)	CH_3, 2-NaphO	4.09	10	2
27	S(−)	C_2H_5, PhO	4.05	10	2
28	S(−)	CH_3, PhO	3.96	9	2
29	R(+)	PhO, n-C_4H_9	3.52	11	1
30	S(−)	n-C_4H_9, PhO	3.52	12	3
31	S(−)	CH_3, PhNH	3.52	9	2

* We denote by Ph a benzene ring and by Naph a naphthalene system ;
A = biological activities ; MTD_A, MTD_B= minimal steric differences calculated with the optimised receptor maps S_A and respectively S_B.

taken from the compilation of Jonsson.[4] The 24 phenoxy-methyl-acetic acid derivatives are listed in Table 2. The source of experimental activities is the same, but the C_{50} values are taken from the compilation of Aberg.[5] The aryl-methyl-acetic acids are listed in Table 3; the C_{50} values are taken from the compilation of Jonsson.[4]

In the QSAR study of Lien et al.,[1] the 56 compounds of Table 1 and Table 2 are considered as a single series. The carboxyl group and the hydrogen atom of the acetic acid moiety were considered by Lien in fixed positions, the aryloxy and alkyl groups interchange positions in the *R* and *S* enantiomer. The R_1-group is "at right" (aryloxy in *R*-enantiomers), the R_2-group "at left" (alkyl in *R*-enantiomers); the orientations are those of Fig. 1. We remind the regressional equation of Lien et al[1]:

TABLE 2

Test series. Substituted phenoxy-methyl-acetic acids*

i	Configuration	Substituents R_1, R_2	A	$\hat{A}(3)$	$\hat{A}(4)$	MTD_B	$\hat{A}(5)$
32	R(+)	3-I-PhO, CH_3	7.4	6.27	6.70	0	6.92
33	R(+)	2,5-di-Cl-PhO, CH_3	7.3	6.54	7.35	0	7.12
34	R(+)	4-Br-PhO, CH_3	6.6	6.18	6.64	0	6.86
35	R(+)	4-Cl-PhO, CH_3	6.5	5.95	6.49	0	6.67
36	R(+)	2,3-di-Cl-PhO, CH_3	6.5	6.54	6.41	0	7.12
37	R(+)	4-I-PhO, CH_3	6.2	6.35	6.75	0	6.99
38	R(+)	4-F-PhO, CH_3	6.0	5.55	6.22	0	6.31
39	R(+)	2-I-PhO, CH_3	6.0	6.11	6.59	0	6.80
40	R(+)	4-CH_3-PhO, CH_3	5.9	5.82	6.40	0	6.56
41	R(+)	2,6-di-Cl-PhO, CH_3	5.6	6.54	5.46	2	4.84
42	R(+)	3,5-di-Cl-PhO, CH_3	5.4	6.54	6.40	0	7.12
43	S(−)	CH_3, 2,6-di-Cl-PhO	5.4	4.24	3.93	2	4.84
44	S(−)	CH_3, 3-I-PhO	5.1	4.31	4.92	2	4.64
45	R(+)	2,4,6-tri-Cl-PhO, CH_3	5.1	7.04	6.26	2	5.14
46	S(−)	CH_3, 2,5-di-Cl-PhO	5.0	4.24	4.40	2	4.87
47	S(−)	CH_3, 2,3-di-Cl-PhO	5.0	4.24	4.88	2	4.84
48	S(−)	CH_3, 2-I-PhO	5.0	4.36	4.48	2	4.51
49	S(−)	CH_3, 3,5-di-Cl-PhO	4.8	4.24	4.88	2	4.84
50	R(+)	2,4,5,6-tetra-Cl-PhO, CH_3	4.7	7.59	6.16	2	5.40
51	S(−)	CH_3, 2,4,6-tri-Cl-PhO	4.6	4.12	4.80	2	5.14
52	S(−)	CH_3,2,4,5,6-tetra-Cl-PhO	4.6	3.97	4.70	2	5.40
53	S(−)	CH_3, 4-Br-PhO	4.5	4.34	4.94	2	4.64
54	S(−)	CH_3, 4-Cl-PhO	4.4	4.40	4.94	2	4.39
55	S(−)	CH_3, 4-F-PhO	4.0	4.50	5.05	2	4.04
56	R(+)	2-iC_3H_7-4-Cl-5-CH_3-PhO, CH_3	4.3	—	—	—	—

* — $\hat{A}(3)$, $\hat{A}(4)$ and $\hat{A}(5)$ are calculated activities according to eqs. (3), (4) and respectively (5). The derivative $i = 56$ was not considered in the test series, because the isopropyl group occupies vertices which are not occupied by the molecules of Table 1.

$$\hat{A}(1) = -\,0.57\,\pi_1^2 + 3.22\,\pi_1 - 4.26\log V_1 + 0.58\,\sigma - 0.29\,\pi_2^2 + \qquad (1)$$

$$+\,2.19\,\pi_2 - 6.86\log V_2 + 16.36$$

$$N = 56,\ r = 0.802,\ s = 0.767$$

The parameters π_1 and π_2 are Hansch-hydrophobicities for R_1 and R_2 respectively, V_1 and V_2 the corresponding molar group volumes, σ — the sum of aromatic σ — Hammett constants for the substituents in the aryloxy-group. The π_1 and π_2 hydrophobicities are listed in the paper of Lien et al [1]; they are taken from the review of Leo, Hansch and Elkins, [6] or calculated according to the aditivity rules given there. Some partial correlation coefficients for these 56 compounds:

$$r(A,\ \pi_1) = 0.506;\ r(A, \pi_2) = -0.568;\ r(A, I_1) = 0.646;$$
$$r(A, I_2) = -0.533$$

I_1 and I_2 are 1 if R_1 and respectively R_2 are bound to the -C_α - atom by an oxygen atom and zero if bound by other atoms (-S, -NH-, -CH_2-). Possibly, there is a hydrogen donating X—H group at the "right"-side in the receptor site, (see Fig. 1 and Fig. 2) binding the oxygen atom of aryloxy-groups.

The importance of steric fit for series of enantiomers can be assessed, according to Lehman, [7] by the eudismic correlation. For the $N = 24$ pairs of enantiomers of Table 1 and Table 2, this correlation is:

$$\log \mathrm{EI} = -3.152 + 0.786 \log \mathrm{EU}, \quad r = 0.910 \tag{2}$$

Here EI is the "eudismic ratio"-the quotient of activities (C_{50}) for the more active and the less active enantiomer. EU is the activity (C_{50}) of the more active, R, enantiomer (eutomer). The rather high $r = 0.91$ value indicates an important contribution of steric fit in this case of receptor — effector interaction. This eudismic correlation fails with the arylalkyl-acetic derivatives of Table 3 with S-enantiomers usually of similar or even somewhat higher activity than the R-enantiomers.

TABLE 3

Aryl-methyl-acetic acids

i	Configuration	Substituents R_1, R_2	A
57	S(−)	CH_3, 3-Indolyl	8.00
58	R(+)	3-Indolyl, CH_3	7.70
59	R(+)	3-Thianaphthyl, CH_3	7.30
60	S(−)	CH_3, 1-Naphthyl	7.00
61	R(+)	1-Naphthyl, CH_3	6.82
62	S(−)	CH_3, 2-Naphthyl	6.10
63	S(−)	CH_3, 4-CH_3-1-Naphthyl	6.00
64	R(+)	Phenyl, CH_3	5.52
65	R(+)	4-CH_3-1-Naphthyl, CH_3	5.40
66	R(+)	2-Naphthyl, CH_3	5.30
67	S(−)	CH_3, Phenyl	4.16

R(+) stands for the D(+) notation of configurations of Jonsson, [4] S(−) for L(−).

The activity — hydrophobicity correlation for the Table 1 compounds is:

$$\hat{A}(3) = 4.412 + 0.722\ \pi_1 - 0.185\ \pi_2$$
$$r = 0.716,\ s = 0.910,\ r(A_T, \hat{A}_T) = 0.581 \tag{3}$$

Equation (3) suggests a cavity accomodating R_1, while R_2 protrudes into a region of low rigidity of the receptor walls. Its real predictive power, as indicated by the $r(A_T, \hat{A}_T)$-correlation for the test series, is low, corresponding to an explained variance, EV = 34%.

CALCULATIONS WITH THE MTD-PROCEDURE

The first step in the MTD-procedure is the construction of the hypermolecule. As the aryloxy and alkyl groups of Table 1 — molecules have a rather high conformational flexibility, there exist several ways to superpose these molecules in order to obtain a hypermolecule. Some information, concerning the conformations of the R_1 and R_2 groups of these molecules in the receptor site, results from the fact that eq. (3) gives too high $\hat{A}(3)$ values for compounds $i = 18$ with R_1 : 1-NaphO- and for $i = 15$ with R_1 : 1-Cl-2-NaphO-. This suggests that the receptor cavity is a narrow pocket oriented perpendicular to the plane of the H-C$_\alpha$-COOH moiety of the acetic acid derivative. If the 1-NaphO- and 1-Cl, 2-NaphO- groups are fixed into this cavity, a steric repulsion appears between the 8-H-atom or 1-Cl-atom at the naphthalenic cycle and the CH$_3$-group, the R_2-substituent of the acetic acid derivative. The naphthalenic cycle is distorted around the O-C-bond and forced into the walls of this cavity. If we consider the COOH group and the H$_\alpha$-atom of the acetic acid derivative in fixed position, as in the paper of Lien, [1] the hypermolecule H_A, depicted in Fig. 1, results.

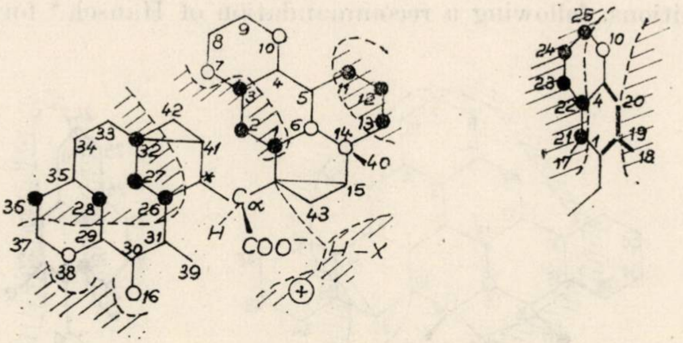

Fig. 1. — Hypermolecule $\hat{H}_A$ — The receptor model of Lien with separate sites for R_1(right) and R_2(left). The plane of the R_1-site is perpendicular to the plane of the H-C$_\alpha$-COOH moiety. For the R(+)-α-1-NaphO-propionic acid and the R(+)-α-1-Cl, 2-NaphO-propionic acid the 8-CH-group and respectively the 1-Cl-atom of the naphthalene nucleus would occupy the $j = 41$-vertex and a strong steric repulsion with the CH$_3$ group (in the starred *vertex) would appear; the aryloxy-group is therefore distorted along the C$_1$-O bond occupying the vertex j = 1, 4, 10, 17 — 25 as depicted in the figure at right. The "cavity" ($\varepsilon_j = -1$) vertices are marked by open circles (○) the "wall" ($\varepsilon_j = +1$) vertices by full circles (●). H — X is a receptor site group forming hydrogen bond with the phenolic O-atom of the compounds.

The optimised receptor map, S_A, obtained by the MTD-procedure, the regressional equation and the regressional coefficient for the test with the Table 2-compounds are:

$$S_A \begin{cases} j(\varepsilon = -1) : 6,\ 7,\ 10,\ 14,\ 16,\ 38 \\ j(\varepsilon = 0) : 4,\ 5,\ 9,\ 15,\ 17 - 19,\ 29 - 31,\ 33 \quad 35,\ 37,\ 39 \\ j(\varepsilon = +1) : 1 - 3,\ 11 - 13,\ 20 - 28\ \ 32,\ 36 \end{cases}$$

$$\hat{A}(4) = 8.781 + 0.480\pi_1 - 0.123\ \pi_2 - 0.474\,\mathrm{MTD_A} \qquad (4)$$

$$r = 0.946,\ s = 0.440,\ F = 48.5$$

$$r(A_T,\ \hat{A}_T) = 0.766,\quad F_{\mathrm{test}} = 15.8$$

The receptor cavity vertices are marked by $j(\varepsilon = -1)$; the wall vertices by $j(\varepsilon = +1)$; the exterior, irrelevant vertices by $j(\varepsilon = 0)$. $\mathrm{MTD_A}$ are the minimal steric differences calculated with the optimised map, S_A, according to the MTD-procedure.[2,3]

Another hypermolecule, $\hat{H}_B$ (Fig. 2) results, if we consider in both R and S enantiomers, the carboxyl and the bulkier aryloxy-group in fixed positions, following a recommandation of Hansch[8] for orientation

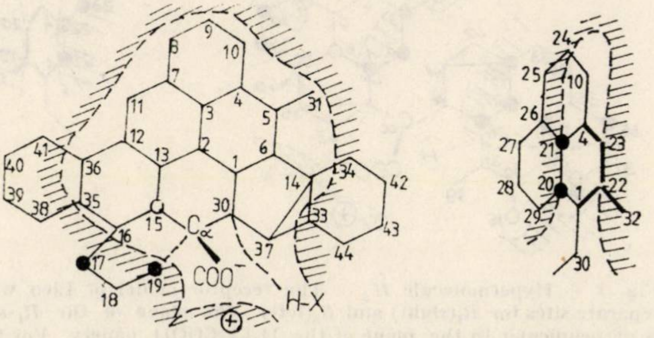

Fig. 2. — Hypermolecule $\hat{H}_B$ — The Hansch-type receptor model; the large aryloxy-group occupies always the same site (approximately vertices 1 — 14). In the R-isomers, the CH_3-group of the propionic acid moiety occupies the $j = 15$ vertex, in the S-isomer the $j = 19$ vertex. For other details, see the caption of Fig. 1. The MTD-mapping procedure, applied upon the Table 3 — compounds, concerns only the $j = 1 - 30$ vertices; the hypermolecule is completed with vertices occupied by the molecules of Tables 2 and 3. The receptor walls are marked by the dotted line and by dashes.

of substituents at chiral centres. The optimised map, S_B, regressional equation and test-values for this hypermolecule are :

$$S_B \begin{cases} j(\varepsilon = -1) : 15 \\ j(\varepsilon = 0) : 1 - 14, 16, 18, 22 - 30 \\ j(\varepsilon = +1) : 17, 19 - 21 \end{cases}$$

$$\hat{A}(5) = 6.024 + 0.928\,\pi - 0.071\,\pi^2 - 1.125\ \mathrm{MTD_B} \qquad (5)$$

$$r = 0.932, \quad s = 0.580, \quad F = 33.6$$

$$r(A_T, \hat{A}_T) = 0.846, \quad F_{\text{test}} = 28.3$$

$\mathrm{MTD_B}$ are the minimal steric differences calculated with the optimised map, S_B, while π are always the hydrophobicities of the aryloxy-groups. The correlation coefficients for other possible combinations of parameters are (for Table 1 compounds) : $r(A\,;\ \mathrm{MTD_B}) = 0.850$,

$$r(A\,;\pi) = 0.342, \quad r(A\,;\pi\,;\mathrm{MTD_B}) = 0.930, \quad r(A\,;\pi\,;\pi^2) = 0.350$$

DISCUSSION AND CONCLUSION

The best correlation of calculated and experimental activities for the test series of Table 2 is given by the optimised map, S_B, and the regressional equation $\hat{A}(5)$, corresponding to an explained variance of about EV = 73%. Therefore, the shape of the receptor site for plant growth inhibition by aromatic derivatives of carboxylic acids corresponds, probably, to the shape depicted in Fig. 2. The carboxyl group should be fixed to the receptor site by electrostatic interaction, the aryloxy-group into a rather narrow hydrophobic pocket, with an orientation perpendicular to the $H-C_\alpha-COOH-$ plane, with the phenolic oxygen atom bonded to a group (XH) of the receptor site (Fig. 2).

For the aryloxy-alkyl-acetic acid derivatives, the CH_3-group in the active R-enantiomers occupies the $j = 15$ cavity vertex, while for the S-enantiomers with low activity, this CH_3-group occupies the $j = 19$ wall vertex, producing steric repulsion. For the aryl-methyl-acetic derivatives of Table 3, the aryl group should fit into the hydrophobic pocket, the C_α-atom should occupy the vertex of the phenolic O-atom, while the CH_3-group should occupy an irrelevant vertex in both the *R* and the *S* enantiomer. This would explain the low activity differences between *R*- and *S*-enantiomers for most of the Table 3 compounds.

REFERENCES

[1] E. J. Lien, J. F. Rodriguez de Miranda and E. J. Ariens, *Molec. Pharmacol.*, **12**, 599 (1976).

[2] A. T. Balaban, A. Chiriac, I. Motoc and Z. Simon "Steric Fit in Quantitative Structure—Activity Relations", Lecture Notes in Chemistry, vol. 15, Springer Verlag, Berlin—Heidelberg—New York, 1980.

[3] Z. Simon, N. Dragomir, M. G. Plauchitiu, S. Holban, H. Glatt and F. Kerek, *Eur. J. Med. Chem.*, **15**, 521 (1980).

[4] A. Jonsson, in "Handbuch der Pflanzenphysiologie", W. Ruhland editor, vol. 14, Springer, Heidelberg, 1971, p. 959.

[5] B. Aberg, in "4-th International Conference on Plant Growth Regulation", Ames Yowa University Press, Yonkers, New York, 1961, p. 219.

[6] A. Leo, C. Hansch and D. Elkins, *Chem. Revs.*, **71**, 525 (1971).

[7] P. A. Lehman, in "Receptor and Recognition", P. Cuadre Casas editor, vol. 5, Chapman and Hall, London, 1979.

[8] C. Hansch, C. Grieco, C. Silipo and A. Vittoria, *J. Med. Chem.*, **20**, 1420 (1977).

Revue Roumaine de Chimie, 27, *4*, 569–574 (1982)

UTILIZATION OF TIRON IN THE SEPARATION AND CONCENTRATION OF TITANIUM WITH ION EXCHANGE RESINS

LUMINIŢA VLĂDESCU and STELUŢA GHINEA
National Institute of Chemistry, Laboratory of Analytical Chemistry, Splaiul Independenţei 202,
Bucharest, Romania

Received September 14, 1981

With the view to using ion exchange resins for the separation of titanium from the ions interfering in its spectrophotometric determination with Tiron, the influence of reagent and of the working conditions on the ion exchange behaviour of several elements was studied in this paper.

Disodium salt of 4,5-dihydroxybenzene-1,3-disulfonic acid, known as Tiron, is a widely recognized reagent studied in analytical chemistry owing to the readiness with which it forms stable and dyed complex compounds with a great number of cations.

Tiron forms with titanium, in the pH range 4.3 – 9.6, a water-soluble intense yellow complex which is utilised for the photometric determination of Ti.[1-8]

When Tiron is used for determining Ti in various materials, the main interfering ion is Fe(III). The methods suggested in the literature for the reduction or masking of iron increase the difficulty of the process and sometimes introduce errors in the analysis.

With the view to using ion exchange resins for the separation of titanium from the ions interfering in its spectrophotometric determination with Tiron, the influence of this reagent and of working conditions on the ion exchange behaviour of several elements, was studied in this paper.

EXPERIMENTAL

CHEMICALS AND EQUIPMENT

- Strongly acid cation exchange resin Amberlite IR–120 ;
- Strongly basic anion exchange resin Vionit AT–1 ;
- known titrum aqueous solutions of Ti(IV), Zr (IV), Cr(III), Fe(III), Mg(II) ions ;
- 10^{-3} M – 10^{-1} M Tiron aqueous solutions ;
- 1M–2M $NaClO_4$, 0.5M–3M $HClO_4$, 0.5M–4M HCl, 0.05 M H_2SO_4 – 3 % H_2O_2, 10 % Ascorbic acid, NH_3, NH_4Cl aqueous solutions ;

- 5 % Pyrocatechine Violet, 5 % Diphenylcarbazide, 1 % Eriochrome black T solutions ;
- SPECOL Carl-Zeiss Jena spectrophotometer ;
- MV-84 pH-meter.

The quantitative determination of investigated ions was performed by spectrophotometric methods in the presence of Tiron for Ti[3] and Fe,[9] Pyrocatechine Violet for Zr, [10] Diphenylcarbazide for Cr[11] and Eriochrome black T for Mg. [12]

Use has been made, for ion exchange experiments, of glass columns 20 cm long, 1 cm in diameter, provided with a stopcock at the bottom and with a dropping funnel with ground glass joint at the top. Known amounts of ion exchanger swolen in water, purified and activated in H^+ or Cl^- ionic form were packed in the columns.

RESULTS AND DISCUSSION

The influence of the type and ionic form of the ion exchange resin, of the pH and Tiron concentration on the ion exchange behaviour of titanium and iron were studied with a view to establish the best working conditions.

To this end, solutions containing known quantities of the ion to be studied were passed through a column with ion exchange resin in the presence of varied concentrations of Tiron and pH values. After separation the resin was washed with the working solution. The quantity of metal ion retained in the resin was determined by measuring the absorbency of the effluent solutions. The quantity of cation fixed in the resin was determined after elution with a corresponding eluant.

The results in table 1 show that when a cation exchange resin is used in H^+ ionic form, both titanium and iron are retained by the cationite from solutions at pH 3—4.7 and partially at pH 7 and pass quantitatively in the effluent at pH 10.

When resin in the Na^+ ionic form is used, titanium and iron pass through the resin without being retained, irrespective of pH and concentration of the reagent, and can be determined quantitatively by measuring the absorbency of the effluent solution.

When a strongly basic anion exchange resin is used in Cl^- ionic form, titanium and iron have a similar behaviour, being retained in the anionite as an anionic complex compound.

Tiron concentration can be reduced to the limit that ensures the formation of these complex compounds without requiring additional reagent.

Furthermore, the ion exchange behaviour of other cations : ZrO^{2+}, Cr^{3+}, and Mg^{2+} was studied in the presence of Tiron 10^{-2} M at $pH = 3$. As shown in table 2, under these conditions, ZnO^{2+}, and Cr^{3+} ions behave similarly to titanium and iron, being retained quantitatively in an ion exchange resin and excluded by cationites whereas magnesium exhibits a contrary behaviour.

For establishing the elution conditions of the ions fixed in anion exchange resin in the presence of Tiron, a series of eluents : HCl, H_2SO_4, $HClO_4$, $H_2SO_4—H_2O_2$, was tested.

Table 3 shows that titanium is strongly retained in the resin and can only be eluted by destruction of the complex compounds formed with Tiron and transition into a complex cation, excluded by the anionite, under the action of a H_2SO_4 0.05 M—H_2O_2 3 % mixture. The other cations fixed in the anionite can be eluted with various HCl concentrations .

TABLE 1

Influence of Tiron concentration and pH upon the ion exchange behavior of Ti(IV) and Fe(III)

Resin		pH	Tiron conc. M	Ti(IV)			Fe(III)		
					Determined in			Determined in	
Type	Ionic form			In sample mg	resin mg	solution mg	In sample mg	resin mg	solution mg
Amberlite IR 120	H^+	3.0	10^{-1}	0.1197	0.1195	—	0.1112	0.1104	—
	H^+	4.7	10^{-1}	0.1197	0.1190	—	0.1112	0.1110	—
	Na^+	4.7	10^{-1}	0.1197	—	0.1190	—	—	—
	Na^+	3.0	10^{-1}	0.1197	—	0.1200	0.1112	—	0.1118
	Na^+	4.7	10^{-2}	0.1197	—	0.1195	—	—	—
	Na^+	4.7	10^{-3}	0.1197	—	0.1193	0.1112	—	0.1108
	H^+	7.0	10^{-2}	0.1197	0.0050	0.1135	—	—	—
	H^+	10.0	10^{-2}	0.1197	—	0.1190	—	—	—
Vionit AT-1	Cl^-	3.0	10^{-1}	0.1197	0.1200	—	0.1112	0.1114	—
	Cl^-	3.0	10^{-2}	0.1197	0.1192	—	0.1112	0.1109	—
	Cl^-	3.0	10^{-3}	0.1197	0.1190	—	0.1112	0.1110	—
	Tiron	—	—	0.1197	0.1180	0.0010	0.1112	0.1090	0.0020

TABLE 2

Ion exchange behaviour of Zr (IV), Ce(III), and Mg(II) in the presence of 10^{-2}M Tiron

Resine		Element	Quantities of elements		
				Determined	
Type	Ionic form		In sample mg	resin mg	solution mg
Amberlite IR 120	Na^+	Zr (IV)	0.253	—	0.249
		Cr (III)	0.130	—	0.135
		Mg (II)	0.486	0.483	—
Vionit AT—1	Cl^-	Zr (IV)	0.253	0.250	—
		Cr (III)	0.130	0.128	—
		Mg (II)	0.486	—	0.489

TABLE 3

Eluents tested for establishing the elution conditions of the ions fixed in anionite in the presence of Tiron

Element	Fixed in anionite (mg)	Eluent								
		HCl			$NaClO_4$		$HClO_4$			$H_2SO_4+H_2O_2$
		0.5M	1M	4M	1M	2M	0.5	1M	3M	0.05M 3%
		Quantities of elements determined in effluent (mg)								
Ti(IV)	0.119	—	—	—	—	—	—	—	0.100	0.118
Zr(IV)	0.253	0.250								
Cr(III)	0.130	—		0.129						
Fe(III)	0.111	0.113								

APPLICATIONS

Analysis of the results obtained shows that when an anion exchange resin is used, titanium can be separated, in the presence of Tiron, from a series of ions whose presence in solution prevents spectrophometric determination with this reagent.

The working method was checked by applying it to the separation and determination of titanium in solutions in which it is to be found in the presence of other ions. To this end, solution containing known quantities of the ions to be separated in the presence of Tiron at pH 3, were prepared and then passed through a column with a strongly basic anions exchange resin. After washing the column with a 10^{-3} M Tiron solution, the accompanying elements were eluted with a corresponding eluent, after which titanium was eluted with a mixture of $H_2SO_4-H_2O_2$. The effluent collected in a calibrated flask was used for the spectrophotometric determination of titanium.

The results in table 4 show good agreement between the quantities of titanium taken in the sample and those determined after separation. The elution curves were plotted for one of the separations performed (Fig. 1.).

TABLE 4

Results of titanium separation from synthetic mixtures

Ti(IV)		Other elements in mixture mg
In sample mg	Determined after separation mg	
0.476	0.469	Fe(III)
0.476	0.470	Zr(IV)
0.476	0.479	Cr(III)
0.476	0.472	Fe(III), Zr(IV), Cr(III)
0.714	0.716	Fe(III), Zr(IV), Cr(III), Mg(II)
1.728	1.731	Fe(III), Zr(IV), Cr(III), Mg(II)

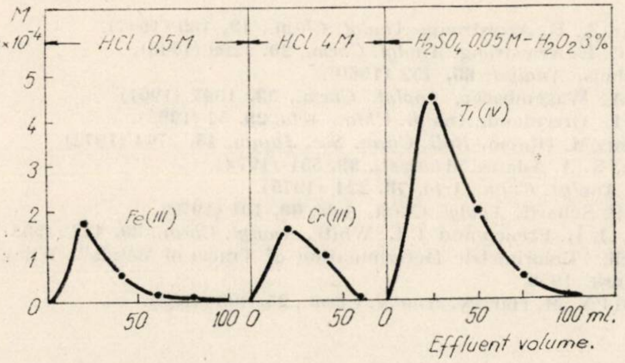

Fig. 1. — Elution curves.

The separation method described was applied for titanium and iron determination in the solution obtained by disintegration of some synthetic rutile samples. The data in table 5 show good agreement between the results obtained by this method and those obtained by other procedures.

TABLE 5

Results of titanium and iron separation from synthetic rutile samples

Rutile		Ion exchange procedure		Other methods	
Type	g	Fe_2O_3 %	TiO_2 %	Fe_2O_3 %	TiO_2 %
R_2	0.4875	5.0	94.5	4.2	95.0
R_3	0.4953	9.4	90.0	8.0	91.0

CONCLUSIONS

Although Tiron readily forms complex anions with many ions whose presence in the solution prevents the spectrophotometric determination of titanium with this reagent, study of ion exchange behaviour furnished evidence of important differences in the elution of ions from an anion exchange resin.

Titanium proved to be strongly retained in anion exchange resin and could only be eluted by the complete break down of the complex compound, whereas the other elements leave the resin under the action of hydrochloric acid in various concentrations. This different behaviour stands at the basis of the method, for the separation and concentration of titanium from the solutions in which other cations that react with Tiron also exist.

The separation method was applied on synthetic mixtures and for quantitative analysis of several synthetic rutile samples.

REFERENCES

[1] J. H. Yoe and A. R. Armstrong, *Analyt. Chem.*, **19,** 100 (1947).
[2] C. V. Potter, C. E. Armstrong, *Analyt. Chem.*, **20,** 1208 (1948).
[3] P. N. R. Nichols, *Analyst*, **85,** 452 (1960).
[4] T. Rigg, H. A. Wagembauer, *Analyt. Chem.*, **33,** 1347 (1961).
[5] A. J. Easton, L. Greenland, *Analyt. Chim. Acta*, **29,** 52 (1963).
[6] Y Wakamatsu, M. Otomo, *Bull. Chem. Soc. Japan*, **45,** 2764 (1972).
[7] W. J. French, S. J. Adams, *Analyst.*, **99,** 551 (1974).
[8] A. J. Eaton, *Analyt. Chim. Acta*, **78,** 224 (1975).
[9] M. Morin, J. P. Scharff, *Analyt. Chim. Acta*, **60,** 101 (1972).
[10] J. P. Young, J. R. French and J. C. White, *Analyt. Chem.*, **30,** 422 (1958).
[11] E. B. Sandell, "Colorimetric Determination of Traces of Metals", Wiley-Interscience, New York, 1959.
[12] E. Aubary and Y. M. Harvey, *Analyt. Chem.*, **25,** 493 (1953).

Revue Roumaine de Chimie, 27, 4, 575–583 (1982)

ALTERNATING TENDENCY IN COPOLYMERIZATION. IV[1]

SIMULTANEOUS CATIONIC POLYMERIZATION AND RADICAL TERPOLYMERIZATION

DAN SORIN VASILESCU
Laboratory of Macromolecular Chemistry, Polytechnical Institute, Calea Victoriei 149,
Bucharest, Romania

Received February 5, 1980
Revised September 5, 1981

In a previous paper [1] we have reported the cationic homopolymerization of isobutyl vinyl ether in the presence of the complex acrylonitrile-$ZnCl_2$. On the other hand, it is known that in the system acrylonitrile — $ZnCl_2$ — styrene, only the alternating copolymerization of acrylonitrile and styrene takes place. In order to gather evidence for a common initiation mechanism, we have studied the system acrylonitrile — $ZnCl_2$ — styrene — isobutyl vinyl ether. Two processes, namely the cationic polymerization of vinyl ether and radical regulated terpolymerization take place simultaneously. An appropriate experimental technique was developed; that allowed us to put into evidence the kinetics of the two processes. Consequently, a suitable mechanism regarding the initiation step was suggested.

1. INTRODUCTION

In a previous paper [1] we have presented the homopolymerization of various vinyl ethers in the presence of the complex acrylonitrile — $ZnCl_2$.

Yabumoto and his co-workers [2] reported the formation of a strictly alternating copolymer when acrylonitrile (AN) and styrene (S) are copolymerized in the presence of $ZnCl_2$. Both reactivity ratios decrease as the ratio $[ZnCl_2]/[AN]$ increases, the tendency towards alternation being very noteworthy. Yabumoto et al.[2] calculated the apparent "Q" and "e" values for the acrylonitrile — zinc chloride complex (24 and 2.53 respectively). This high "e" value compared to that of pure AN ($e = 1.2$) shows the intense electron withdrawal from the double bond of AN, produced by complexation. Nine different propagation reactions are taken into account in the kinetic scheme proposed by the above quoted authors. The alternation is due to the augmentation in the cross-propagation coefficients, as a result of the change in the polarity of AN. This conclusion was backed by Zubov et. al.,[3] who developed this idea. Zubov, Kabanov and Kargin [3] consider that the alternating copolymerization may be understood, in terms of a normal chain reaction, but the monomers and the corresponding derived radicals have modified reactivities as a consequence of complexation with metal salts.

Many alternating copolymerizations start in a "spontaneous" way ; it is likely that this is the main reason which made a lot of research-workers[4-9] propose mechanisms involving charge-transfer complexes. Gaylord[7,8] pointed out that the alternating copolymerization in the system AN $-$ ZnCl$_2$ $-$ S is the result of the homopolymerization of the charge transfer complex.

In the terpolymerization of S $-$ AN $-$ MMA (methyl methacrylate) in the presence of ethyl aluminium sesquichloride (EASC) the resulting copolymer contains 50% styrene units.[10] The formation of terpolymers with a constant composition, independent of temperature, irradiation etc. is considered by Gaylord[10] to be a proof for the fact that the S $-$ MMA $-$ EASC and S $-$ AN $-$ EASC complexes are aligned in the same array or matrix of complexes, preventing the conversion to uncomplexed monomers. Attempts to use terpolymerization in order to elucidate the mechanism did not throw more light on the assumed autopropagation of the charge transfer complexes.[11]

In our previous paper, we have shown that isobutyl vinyl ether (IBVE) undergoes cationic polymerization in the presence of the complex AN $-$ ZnCl$_2$.[1] The investigation of the system AN $-$ S $-$ IBVE $-$ ZnCl$_2$ offers an intermediate situation between a system which copolymerizes in a regulated manner (AN $-$ S $-$ ZnCl$_2$) and one in which only the cationic homopolymerization takes place (AN $-$ IBVE $-$ ZnCl$_2$).

2. EXPERIMENTAL

Styrene was purified according to the usual methods and dried over calcium hydride ; the pure monomer was stored over calcium hydride in vacuum. The purifications of AN, IBVE, benzene (B), ZnCl$_2$ as well as the appropriate technique used for preparing "in situ" the complex AN $-$ ZnCl$_2$, were previously described.[1]

The polymerization procedure used in this work was the same as for the study of the system AN $-$ IBVE $-$ ZnCl$_2$;[1] the only difference consisted in the fact that IBVE and S were mixed with B, prior to the final mixing with the AN $-$ ZnCl$_2$ $-$ B solution.

Under these conditions, two processes, namely the homopolymerization of IBVE and copolymer formation, take place. A typical separation technique is given below.

The copolymer is insoluble in the reaction mixture and precipitated at the bottom of the dilatometer, while the poly-vinyl ether is present in solution. The dilatometer (previously described[1]) was opened and the homogeneous mass was sucked with a syringe ; the solution was poured with vigorous stirring into a small preweighed beaker containing a dilute ammonia solution. The precipitate remained at the bottom of the dilatometer was twice washed with benzene and the solution also poured into the ammonia $-$ water mixture. As a result of the stirring, an emulsion was formed. In time, this emulsion easily separated into two layers ; the upper layer contained benzene, poly-vinyl ether and residual monomers, while the bottom layer consisted mainly in water, ammonia and zinc chloride. The beaker was left for several days at room temperature ; a quite consistent film may be obtained in this way from the upper layer after the evaporation of volatiles. By making holes in the film, the aqueous layer could be removed. After drying, the quantity of homopolymer may be calculated by weighing the beaker again.

The copolymer remained at the bottom of the bulb of the dilatometer ; its isolation does not present any special problems. Dimethylformamide was introduced into the bulb by using a syringe and the copolymer was consequently dissolved ; the solution obtained was taken out in the same manner and precipitated in methanol. The copolymer was subsequently filtered, dried and weighed.

3. RESULTS AND DISCUSSION

If the charge transfer complex between $AN-ZnCl_2$ and S is indeed formed, then in the system $AN-S-IBVE-ZnCl_2$, a higher initiation rate of IBVE is to be expected, as a result of a greater number of hypothetical radical-cations, possible initiators.

The direct kinetic observation of the process presents some experimental difficulties, which arise from the fact that the dilatometrically followed contraction is due to two different causes :

— The homopolymerization of IBVE, resulting in a polymer soluble in the reaction medium.

— The formation of a tertiary copolymer containing approximately 50% AN, which precipitates in the bulb of the dilatometer.

For this reason we have represented the total contraction (recalculated for a standard dilatometer, with a volume of 2 cm^3 and the diameter of the capillary 1 mm.), as a function of time (see figures 1 and 2). We have maintained constant the ratio $[AN]/[ZnCl_2]$, the concentration of acrylonitrile and $[S]+[IBVE]$; the experiments represented by curves 1 — 10 differ in $[S]/[IBVE]$ ratio. Under these conditions it was noticed that as the initial [IBVE] increases, the value of the contraction rate decreases, reaches a minimum, and afterwards increases again : at the end of every kinetic experiment we have got, in addition to these con-

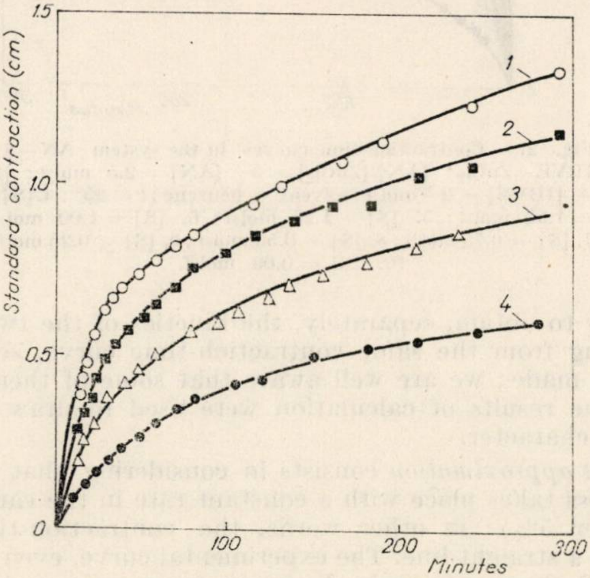

Fig. 1. — Observed contractions due to the IBVE homopolymerization superimposed onto the tertiary copolymerization of AN, S and IBVE ; $[AN]/[ZnCl_2] = 5$; $[AN] = 2.5$ mol/l ; $[IBVE] + [S] = 2.5$ mol/l ; solvent — benzene ; $t = 25°$: 1. $[S] = 2.25$ mol/l ; 2. $[S] = 2.00$ mol/l ; 3. $[S] = 1.75$ mol/l ; 4. $[S] = 1.50$ mol/l.

traction-time data, the final conversions (for the copolymer containing acrylonitrile and for the hompolymer, respectively). These conversions were obtained according to the procedure previously described.

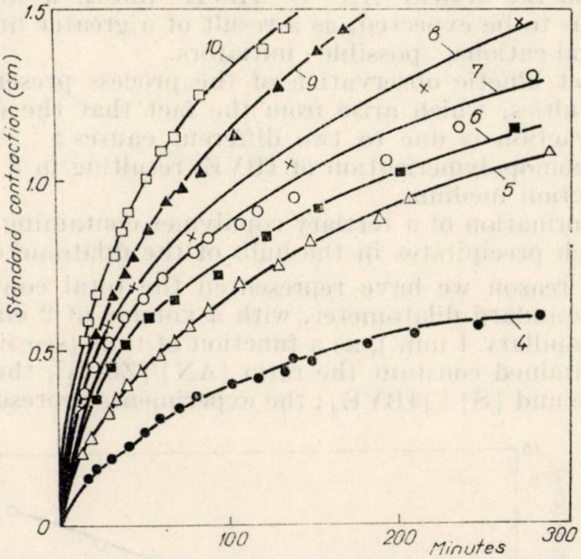

Fig. 2. — Contraction-time curves in the system AN—S—IBVE—$ZnCl_2$; $[AN]/[ZnCl_2] = 5$; $[AN] = 2.5$ mol/l; $[S] + [IBVE] = 2.5$ mol/l; solvent — benzene; $t = 25°$: 4. $[S] = 1.50$ mol/l; 5. $[S] = 1.25$ mol/l; 6. $[S] = 1.00$ mol/l; 7. $[S] = 0.75$ mol/l; 8. $[S] = 0.50$ mol/l; 9. $[S] = 0.25$ mol/l; 10. $[S] = 0.00$ mol/l.

In order to obtain, separately, the kinetics of the two distinct processes, starting from the same contraction-time curve, several approximations were made; we are well aware that some of them may involve errors, but the results of calculation were used to draw conclusions of a qualitative character.

The *first approximation* consists in considering that the copolymerization process takes place with a constant rate in the early stages (conversions under 5%): in other words, the contraction-time curve was thought to be a straight line. The experimental curve, even for the system AN—$ZnCl_2$—S shows a certain deviation from such an ideal behaviour (see figure 3). Nevertheless, we supposed a constant rate for the copolymerization reaction in its first stage: consequently, the copolymerization rates could be obtained by dividing the experimentally-established conversions to time. We have plotted the rate for the copolymer formation against monomer feed composition; the results are presented in figure 4.

As $[S] + [IBVE]$ was kept constant, the only variable being the ratio $[S]/[IBVE]$, we have noticed that as $[IBVE]$ increased, the rate of copolymerization decreased sharply. This recalls the similar behaviour of vinyl ethers in the radical copolymerization.[12] This fact strengthens our belief in a radical mechanism for this copolymerization process. The

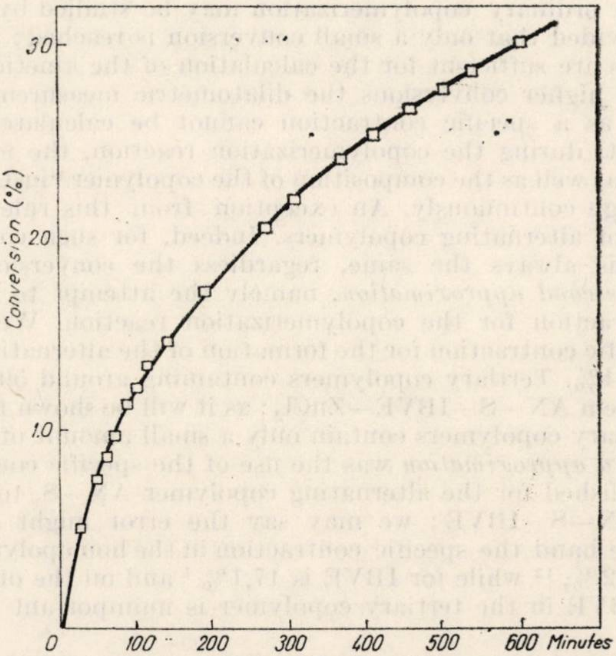

Fig. 3. — Copolymerization of acrylonitrile and styrene at 25° in the presence of $ZnCl_2$; $[AN]/[ZnCl_2] = 5$; $[AN] = [S] = 2.5$ mol/l ; solvent — benzene.

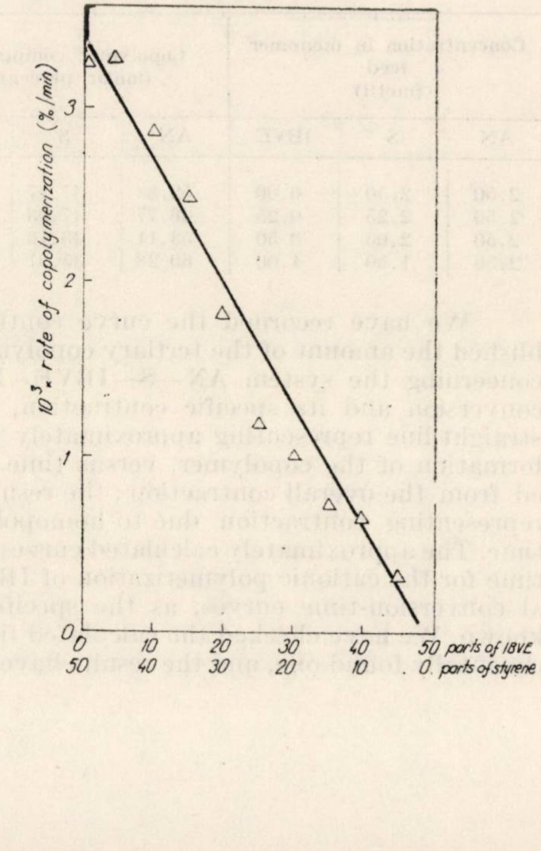

Fig. 4. — Copolymerization rate against composition of monomer feed ; $[AN]/[ZnCl_2] = 5$; $[AN] = 2.5$ mol/l ; $[S] + [IBVE] = 2.5$ mol/l ; solvent — benzene ; $t = 25°$.

kinetics of an ordinary copolymerization may be studied by dilatometric methods, provided that only a small conversion is reached; usually, such measurements are sufficient for the calculation of the kinetic parameters. However, for higher conversions the dilatometric measurements become meaningless, as a specific contraction cannot be calculated. The main reason is that, during the copolymerization reaction, the monomer feed composition, as well as the composition of the copolymer "instantaneously" formed, change continuously. An exception from this rule is presented by the case of alternating copolymers. Indeed, for such copolymers, the composition is always the same, regardless the conversion; this fact justifies our *second approximation*, namely the attempt to calculate the specific contraction for the copolymerization reaction. We have found that the specific contraction for the formation of the alternating copolymer AN—S is 23.4%. Tertiary copolymers containing around 50% AN result from the system AN—S—IBVE—$ZnCl_2$; as it will be shown farther (Table 1), these tertiary copolymers contain only a small amount of IBVE units.

Our *third approximation* was the use of the specific contraction previously established for the alternating copolymer AN—S, to the tertiary copolymer AN—S—IBVE; we may say the error might be neglected as on the one hand the specific contraction in the homopolymerization of styrene is 13.2%, [13] while for IBVE is 17.1% [1] and on the other hand the content of IBVE in the tertiary copolymer is unimportant (see table 1).

TABLE 1

Copolymer composition for the tertiary copolymers obtained simultaneously with poly-IBVE; $t = 25°$; solvent — benzene; the ratio $[AN]/[ZnCl_2] = 5.0$

Concentration in monomer feed (mol/l)			Copolymer composition (molar percents)			[IBVE]/[S] ratio in copolymer		
						Theoretically		Experimentally
AN	S	IBVE	AN	S	IBVE	Cationic	Radical	Found
2.50	2.50	0.00	52.83	47.17	0.00		0.000	0.0000
2.50	2.25	0.25	46.77	47.93	5.30	3.43	0.002	0.1106
2.50	2.00	0.50	53.11	45.16	1.73	7.97	0.005	0.0383
2.50	1.50	1.00	60.28	35.91	3.85	21.70	0.013	0.1072

We have recorded the curve contraction-time and we have established the amount of the tertiary copolymer formed for every experiment concerning the system AN—S—IBVE—$ZnCl_2$. Knowing the copolymer conversion and its specific contraction, it becomes possible to draw a straight line representing approximately the contraction arising from the formation of the copolymer, versus time. This contraction was substracted from the overall contraction; the result of this operation was a curve representing contraction due to homopolymerization of IBVE, against time. The approximately calculated curves representing contraction against time for the cationic polymerization of IBVE may be transformed in usual conversion-time curves, as the specific contraction of IBVE is now known. We have checked the calculated final conversion against the experimentally found one, and the results have been in a reasonable agreement.

The initial homopolymerization rates may be easily deduced graphically from the curves conversion against time; however, we have to remember that due to the experimental conditions, the dependence for the initial period has been obtained by extrapolation,[1] of the recorded curve representing overall contraction as a function of time.

A comparison between the initial homopolymerization rates of IBVE in the presence of styrene (curve 1) and in its absence is given in figure 5; the homopolymerization rates in the presence of styrene have been calculated according to the approximate methods described, while the homopolymerization rates in the absence of styrene were obtained from the experimental data presented in our previous work.[1]

The dependence of the initial homopolymerization rate of IBVE on [IBVE] may be considered as linear, in the absence of styrene (curve 2, figure 5). Since the AN concentration and the [AN]/[$ZnCl_2$] ratio were kept constant, a first order dependence on [IBVE] may be deduced, at least for the initial stage. The curve 1 (figure 5) shows the results obtained in the presence of styrene; [S] depends upon [IBVE], obeying the condition [S] + [IBVE] = 2.5 mol/l. The left side of the curve 1 indicates a great discrepancy between the initial homopolymerization rate of IBVE in the presence of styrene and in its absence (Figure 5); this seems to be caused by a greater rate of initiation in the presence of styrene. In our opinion the only possible explanation is the formation of the charge-transfer complex: the derived radical-cation from styrene could be an initiator for the cationic polymerization of IBVE, besides the oxonium ion (derived from IBVE). As IBVE reaches a concentration of 1 mole/l or more, the homopolymerization rate for the vinyl ether is practically the same with that measured in the absence of styrene. Even if the concentration of the charge-transfer complexes cannot be measured

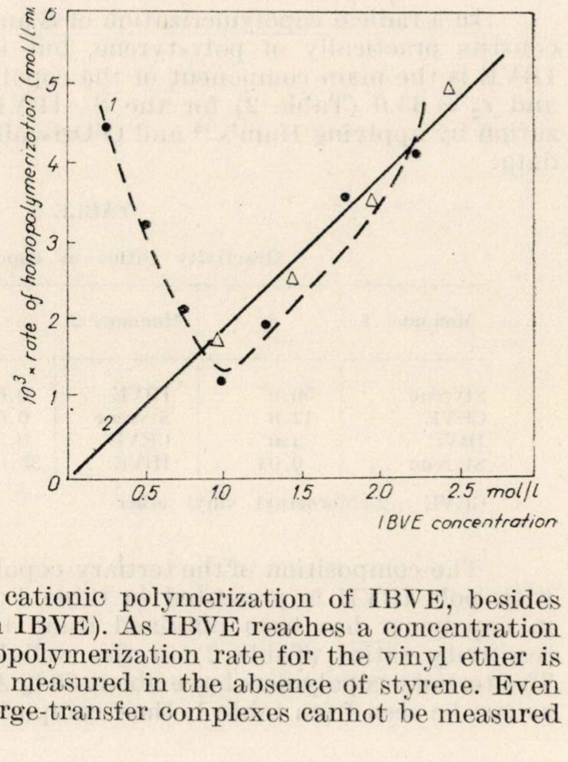

Fig. 5. — Homopolymerization of IBVE in the presence of styrene (1) and in its absence (2); [AN]/[$ZnCl_2$] = 5; [AN] = 2.5 mol/l; solvent — benzene; t = 25°: 1. [S] + [IBVE] = 2.5 mol/l; 2. [IBVE] = variable.

(the initiation efficiencies either for the oxonium ion, or the radical-cation derived from styrene are unknown) we may however appreciate that this is very small indeed.

Our proposal raises the question why in the radical copolymerization of maleic anhydride with IBVE,[14,15] although the equilibrium constant for the charge-transfer complex between the monomers was established as K = 1.11 $l.mol^{-1}$,[14] no cationic polymerization of IBVE was noticed and the 1 : 1 copolymer was the only product of the reaction; it is important to notice that in this work[14] tetrahydrofuran, a strong electron-donor, was used as solvent, while in our experiments, a nonpolar solvent (benzene) was used.

We partially agree with the mechanism proposed by Hirai [4] regarding the possibility of charge-transfer complex formation, but we stress again that the concentration of the complex should be very small; its role consists only in initiating the process, which may be either the radical copolymerization, or the cationic homopolymerization for the donor monomers, such as vinyl ethers, which exhibit a great tendency towards cationic polymerization.

In the system AN$-$$ZnCl_2$$-$IBVE copolymer formation has not been noticed.[1] Introduction of styrene causes the formation of tertiary copolymers, but at monomer feeds rich in IBVE, the copolymerization rate is exceedingly small (Figure 4), in agreement with the behaviour of vinyl ethers in radical copolymerization. Moreover, the composition of the copolymers formed is close to that which would be expected in a radical copolymerization (See tables 1 and 2).

In a radical copolymerization of S and IBVE the polymeric product consists practically of polystyrene, but in a cationic copolymerization IBVE is the main component of the copolymer; we found that $r_1 = 0.04$ and $r_2 = 33.0$ (Table 2) for the S$-$IBVE pair in cationic copolymerization by applying Ham's [15] and O'Driscoll's [16] equations to the literature data.

TABLE 2

Reactivity ratios in copolymerization

Monomer 1	r_1	Monomer 2	r_2	Mechanism	Reference
Styrene	50.0	IBVE	0.01	Radical	13
CEVE	12.0	Styrene	0.06	Cationic	13
IBVE	2.0	CEVE	0.5	Cationic	13
Styrene	0.04	IBVE	33.0	Cationic	Calculated

CEVE = 2-chloroethyl vinyl ether

The composition of the tertiary copolymers obtained simultaneously with poly-IBVE is presented in table 1; the theoretical IBVE/S ratio in copolymer has been obtained using the appropriate values for the reactivity ratios (Table 2) in the well known composition equation.[17] The tertiary copolymers have about 50% AN and a low content of IBVE; as can be seen from table 1, their composition is in the neighbourhood of those expected in a radical copolymerization. The presence of IBVE and S units in the tertiary copolymer was also confirmed by analysing the corresponding IR spectra. This experimental evidence suggests that the radical terpolymerization takes place likely by a radical mechanism controlled by polar factors, as Zubov and Golubev[3] have proposed.

4. CONCLUSION

The literature concerning regulated copolymerization is exceedingly rich, but unfortunately few kinetic data are available ; the great majority of papers report only final conversions in polymer and the corresponding compositions. In the present work a kinetic approach of the problem has been attempted. A charge transfer complex, present in a very low concentration and which does not autopropagate, may initiate either the cationic polymeritation of some vinyl monomers, or the regulated copolymerization, or both ; the copolymerization reaction remains a radical process controlled by polar factors.

In literature, the main objection against the mechanism in which the copolymerization occurs by radical chains and the cross-propagation is favoured, has been that the copolymerization rate ought to be far higher than experimentally observed. However, if we take into account that the charge transfer complex (initiator) is present only at a very low concentration, a reduced initiation rate correlated with a high propagation rate coefficient would lead to an average value for the overall reaction velocity. This interpretation is also consistent with the fact that a great number of research-workers have reported high molecular weights for the alternating copolymers.

We do not consider our mechanism as being a very general one, but we believe many previously described systems might fit it and they deserve a further kinetic investigation.

REFERENCES

[1] Part. III. D. S. Vasilescu, *Rev. Roumaine Chim.*, **25**, 1101 (1980).

[2] S. Yabumoto, K. Ishii and K. Arita, *J. Polymer. Sci., A-1*, **7**, 1577 (1969) ; **8**, 295 (1970).

[3] V. P. Zubov, L. I. Valuev, V. A. Kabanov and V. A. Kargin, *J. Polymer Sci., A-1*, **9**, 833 (1971).

[4] H. Hirai and M. Komiyama, *J. Polymer Sci., A-1*, **13**, 2419 (1975).

[5] S. Pasynkiewicz, T. Diem, W. Kuran and K. Kolbrecka, *Makromol. Chem.*, **156**, 251 (1972).

[6] N. G. Gaylord and A. Takahashi, *J. Polymer Sci., B*, **7**, 443 (1969)

[7] N. G. Gaylord and H. Antropiusova, *J. Polymer Sci., B*, **8**, 183 (1970).

[8] N. G. Gaylord and A. Takahashi, *J. Polymer Sci., B*, **7**, 443 (1969).

[9] B. L. Funt and J. Rybicky, *J. Polymer Sci.. A-1*, **9**, 1441 (1971).

[10] N. G. Gaylord and B. Patnaik, *J. Polymer Sci., B*, **10**, 653 (1972).

[11] N. G. Gaylord and B. Patnaik, *J. Polymer Sci., B*, **8**, 411 (1970).

[12] D. S. Vasilescu, *Rev. Roumaine Chim.*, **10**, 1393 (1974).

[13] M. L. Hallensleben and I. Lumme, *Makromol Chem.*, **144**, 267 (1971).

[14] R. Endo, H. Iimura and M. Takeda, *Kobunski Kagaku*, **29**, 44 (1972) ; *Chem. Abstr.*, **76**, 141390 (1972).

[15] G. E. Ham, *J. Polymer. Sci., A*, **2**, 4169 (1964).

[16] K. F. O'Driscoll, T. Higashimura and S. Okamura, *Makromol. Chem.*, **85**, 178 (1965).

[17] F. R Mayo and F. M. Lewis, *J. Amer. Chem. Soc.*, **66**, 1594 (1944).

those expected in a radical copolymerization. The presence of DVN and [illegible] nitrile in the tertiary copolymer was also confirmed by analysing the corresponding IR spectra. This experimental evidence suggests that the radical terpolymerization takes place likely by a radical mechanism controlled by polar factors, as Zubov and Gaylord [illegible] have proposed.

8. CONCLUSION

The literature concerning regulated copolymerization is exceedingly rich, but unfortunately few kinetic data are available: the great majority of papers report only final conversions in polymer and the corresponding compositions. In the present work a kinetic approach of the problem has been attempted. A charge transfer complex, present in a very low concentration and which does not homopropagate, may initiate either the radical polymerization of some vinyl monomers, or the regulated copolymerization, or both: the copolymerization reaction remains a radical process controlled by polar factors.

In literature, the main objection against the mechanism in which the copolymerization occurs by radical chains and the cross propagation is favoured has been that the copolymerization rate ought to be far higher than experimentally observed. However, if we take into account that the charge transfer complex (initiator) is present only at a very low concentration, a reduced initiation rate correlated with a high propagation rate coefficient would lead to an average value for the overall reaction velocity. This interpretation is also consistent with the fact that a great number of research workers have reported high molecular weights for the alternating copolymers.

We do not consider our mechanism as being a very general one, but we believe many previously described systems might fit it and they deserve a further kinetic investigation.

REFERENCES

[illegible] S. Vasilescu, Rev. Roumaine Chim., [illegible] (1960).
[illegible] J. Polymer Sci., A-1, 7, [illegible] (1969); 8, [illegible] (1970).
V. P. Zubov, L. I. Valuev, V. A. Kabanov and V. A. Kargin, J. Polymer Sci., A-1, 9, [illegible] (1971).
[illegible] J. Polymer Sci., A-1, [illegible]
[illegible]
[illegible] J. Polymer Sci., [illegible]
[illegible]
[illegible]
[illegible]
[illegible]
[illegible]
[illegible]
[illegible]
[illegible]
[illegible] J. Polymer Sci., [illegible]
[illegible]
[illegible] J. Am. Chem. Soc., 66, 1594 (1944).

Revue Roumaine de Chimie, 27, 4, 585—590 (1982)

SYNTHESIS AND POLYMERIZATION OF POLYETHYLENE GLYCOL DIMETHACRYLATES. V[1]

ANALYSIS OF KINETIC DATA OBTAINED AT POLYMERIZATION BASED ON TOPOENERGETIC PRINCIPLES

GH. DRĂGAN*, GH. HUBCA **, CR. OPRESCU ** and M. DIMONIE **

* Institute of Chemical Research, ICECHIM, Spl. Independenţei 202, Bucharest, Romania

** Polytechnic Institute of Bucharest, Laboratory of Macromolecular Technology, Calea Victoriei no. 149, Bucharest, Romania

Received June 9, 1981

Kinetic data regarding polyethylene glycol dimethacrylate polymerization are interpreted using a kinetic model associated with the direct measuring system recently established on the basis of topoenergetic principles. Analysis of results showed that within the limit of experimental errors, the nature of polymerization process is the same within the monomer series studied, and the amplitude decreases by increasing the oligomeric chain length. Thus, it has been noticed that the kinetic term defining the extent of the process may be used as a measure of kinetic entity mass.

INTRODUCTION

Development of topological thermodynamics principles [2-4] has recently led to establishing the significance of parameters associated with kinetic equation thus found. In the case of composite systems which develop with temperature as thermodynamic pontential, it has been considered that the basic law ruling the capacitive accumulations of components under transforming is of Arrhenius type.[4]

For this category of systems the conversion of transforming processes can be visualized in two types of measuring systems, i.e. direct and differential systems, respectively. Any transforming process is accompanied by thermal effects, so that the calorimetric systems may be used as measuring systems for the study of any composite system progress.

In fact, these systems represented the first measuring systems whose energetic circuits were modelled on the basis of topoenergetic principles.[2,4] Recently, it has been observed that the power circuits associated to composite systems, driven by temperature, can be generalized to any other measuring system.[5]

For example, this series of papers[1] covers the kinetic data obtained by gravimetric conversion of polymerization process as a function of the response defining the measuring system considered. Similar kinetic data could be obtained by considering any other measuring system such as calorimetric or thermometric (previously mentioned)[1] viscometric, spectroscopic systems, etc, all these being subjected to the latest interpretation way.[3] It is important to notice that for the same composite system which represents only the internal energetic circuit of the measuring system, the overall energetic circuit can be represented as depending on either direct or differential functions of response. Thus we draw the attention that the temporary reference system called *laboratory*, where temporary dependence of the function of response is observed, differs from the local temporary reference system where capacitive accumulation of component under transformation is obtained.[2] This relativistic principle explains the energetic effects noticed at various measuring systems.[6]

This paper reconsiders the previously indicated kinetic data[1] obtained by gravimetric measuring system at the polymerization of polyethylene glycol dimethacrylate; ethylene dimethacrylate (EGDMA), diethylene glycol dimethacrylate (DEGDMA), triethylene glycol dimethacrylate (TEGDMA) and tetraethylene glycol dimethacrylate (TTEGDMA). The conversion of this function of response is covered in this case by the category of direct measuring systems and enables a relative identification of the nature and extent of transforming processes within the studied series of monomers based on the recently determined significance of resulting kinetic parameters.[7]

DISCUSSION

Although the experimental conditions were detailed previously,[1] some aspects should be noticed which are important in interpreting the results on topoenergetic bases.[7]

It has been thus pointed out that the "geometry" of composite system is determined in the form of conversion curve so that for thin layer polymerization achieved by reaction mixture settling on glass beads, conversion occurs as a self-accelerated process and in thick layer (mass polymerization of reaction mixture) conversion has its maximum rate at the initial moment of process start. The two cases correspond to the measuring system types, differential and direct, respectively, recently defined on topological bases.[3] This is a typical case when the measuring system changes by the modification of the inside circuit of the composite system so that, in the case of differential system the inert component represented by glass beads prevails whereas in the case of direct conversion the transforming component prevails.

We shall further on consider the kinetic data obtained from the direct conversions for the polymerization process of mentioned polyethylene glycol dimethacrylates. In order that these results may be comparable in point of total transforming process nature and extent, for each four types of polymerization corresponding to the four monomers, have been considered the conversions at various temperatures obtained on the same reaction geometry. In this case, by the "geometry" of the measuring system we defined both the shape and dimensions and the reaction system analysis. Thus, the differences in the nature and extent of polymerization process are due only to nature and extent at the molecular level of a monomeric entity which forms the transforming components. On the other hand we have to mention that the static deviations of kinetic parameters resulting after static processing of kinetic data depend on the one hand, on the deviations from these values which define the system geometry and, on the other hand, on the thermo-control and measuring accuracy of response function.

Under these conditions we mention that polymerizations were carried out in glass bottles of 5 ± 0.5 mm in diameter and 100 ± 2 mm in length and reaction mixture column of 50 ± 5 mm in height. The reaction mixtures considered in this study had the following composition: monomer 50% in weight, dimethylformamide as solvent 50% in weight and methylethyl ketone peroxide 0.0098 mol/l (monomer).

For each polymerization system corresponding to a monomer type, 4 — 5 conversion curves have been considered as determined at temperatures ranging between 50 and 85°C.

The response function is expressed in percentage corresponding to the case of normalized conversion curves.[3] Relaxation periods τ can be estimated from these curves as the inverse of the reaction rate at the initial moment.[3]

From the Arrhenius relation for these values:

$$\tau = \tau_0 \cdot \exp(-E/RT) \tag{1}$$

it results that:

$$\ln \tau = -E/RT + K \tag{2}$$

where $\tau_0 = RC_{\text{inert}}$, R — being the dissipative element value which couples the internal circuit on boundary condition.[2,3] Thus K becomes a function directly proportional to the inert component value expressed logarithmically.

Table 1 shows the activation energy values, E, and the extent term value K, resulting from the linear regression of τ values according to equation (2). Coefficient R^2 represents the correlation factor associated

TABLE 1

Values of primary kinetic parameters resulting from statistic processing of conversion data

Monomer	$-E$ KJ/mol	$-K$ ln(min/%)	R^2 —	R_{id} —
EGDMA	74 ± 4	21.0 ± 1.0	0.9964	1.000
DEGDMA	67 ± 2	17.3 ± 0.6	0.9989	0.899
TEGDMA	57 ± 7	16.5 ± 2.0	0.9838	0.998
TTEGDMA	42 ± 5	12.0 ± 1.0	0.9853	0.964

to the linear regression and by means of which standard deviations have been established according to the relation :

$$\sigma_a \simeq a\sqrt{1-R^2} \tag{3}$$

A good agreement of experimental values in relation (2) is noticed although just from the beginning we could see important deviations from system geometry. Based on E/K ratio we can identify the relative nature of polymerization process for each reaction system, considering the EGDMA system as standard.[7] Thus, Table 1 gives the values of R_{id} coefficient which represents the probability normalized to unity, as, one of the reaction systems should have the nature of polymerization process identical to the one of reference system. Taking into account the deviations of E and K values we can conclude that the nature of polymerization processes is the same for all the four systems considered.

The second important aspect of composite system behaviour, in general, is the extent of total transforming process. In this case, the primary value, determined experimentally, expressing this aspect in absolute units, is K. From the above mentioned significance it will result that the bigger the K, the smaller the transforming process extent . On the other hand, the considered monomer series which forms the transforming component in the reaction system has as active element or effective transforming component double bonds, two per molecule. We remind the structure of the molecule

$$CH_2 = C(CH_3)-COO-(CH_2-CH_2-O)_n-OC-C(CH_3) = CH_2 \tag{4}$$

Thus, the molecular contribution to inert component is proportional to monomer mass, M_{monomer}.

Figure 1 shows E and K values depending on $\ln M_{\text{monomer}}$ and we notice a permissible linearity within the experimental deviation limit. The positive slope expresses that the extent decreases with K increase and E decreases in absolute value. By means of these two values we can relatively express the extent of transforming process as against the system considered standard,[7] namely :

$$\Delta E \equiv 1 - E/E_{\text{standard}} \text{ and } \Delta K \equiv 1 - K/K_{\text{standard}} \tag{5}$$

The two values in Figure 1 are practically equal for the same reaction system as against the standard system (EGDMA) but show an exponential variation with $\ln M_{\text{monomer}}$.

We can also notice that in the case of the four monomer polymerization systems, the extent of processes identical in nature, can be quantitatively expressed by kinetic values which define the behaviour of the whole system on the one hand and by values which define the kinetic entity extent on the other hand. Proportionality relation between them is expressed by *affine relation* recently defined as : [3]

$$\theta_2 = N\theta_1 + M \tag{6}$$

where θ_1 and θ_2 correspond to the values of the two categories mentioned above.

Table 2 gives the values for N, M and correlation coefficient for affine relations of extent values $\theta_1 = \ln M_{\text{monomer}}$ and $\theta_2 = E, K, \ln n, \ln \Delta E$ and $\ln \Delta K$. A good correlation is noticed between these pairs with $N > 0$.

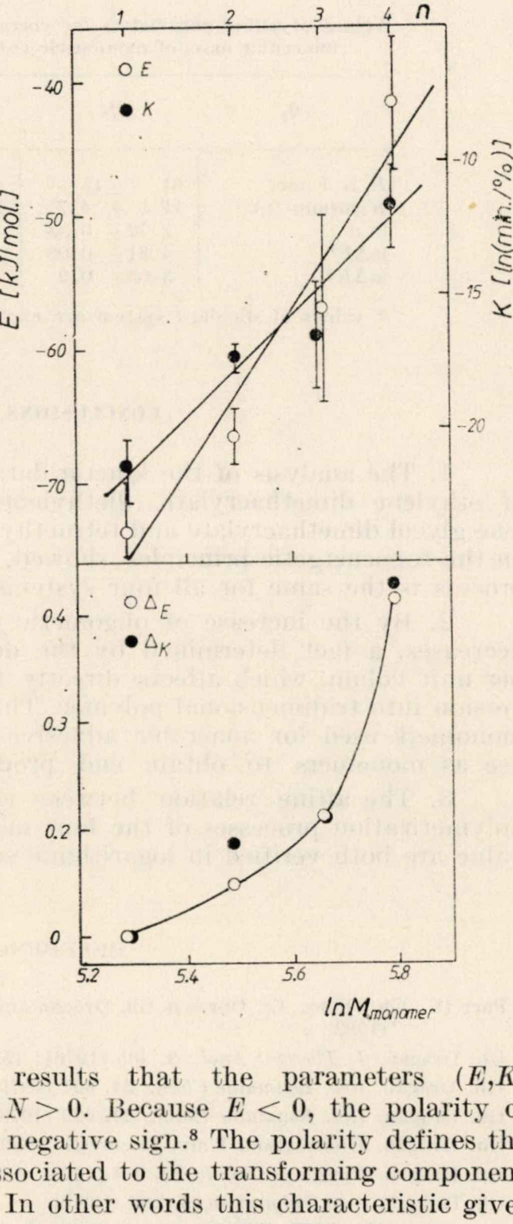

Fig. 1. — The plot of E and K primary kinetic parameter dependence and of ΔE and ΔK relative parameters on the molecular mass of monomeric units (n-number of ethylenic units in polyethylenic chain).

As an immediate consequence it results that the parameters (E,K) are also in affine relation with $N > 0$. Because $E < 0$, the polarity of the polymerization process has a negative sign.[8] The polarity defines the direction of the energetic flux associated to the transforming component relative to the inert component. In other words this characteristic gives the relative sense of time between LocRS and LabRS. This direction can be directly observed in calorimetric measuring systems in which the transforming caloric flux is exothermic and the inert one is endothermic. The relative correlation between (E, K) shows the nature identity of the polymerization processes for the four monomers.[8]

TABLE 2

Values of affine parameters for correlation of extent values with molecular mass of monomeric entities $\theta_1 = \ln M_{\text{monomer}}$

θ_2	N	$-M$	R^2
E, K J /mol	61 ±15	400 ±99	0.9384
K, ln(min/%)	17.5 ± 4.7	114 ±31	0.9284
ln n	2.72± 0.33	14.3± 1.8	0.9851
lnΔE*	4.81± 0.09	28.7± 0.6	0.9996
lnΔK*	3.03± 0.9	18.5± 0.2	0.9083

* values of standard system are excluded

CONCLUSIONS

1. The analysis of the kinetic data obtained at the polymerization of ethylene dimethacrylate, diethylene glycol dimethacrylate, triethylene glycol dimethacrylate and tetraethylene glycol dimethacrylate based on the topoenergetic principles showed, evidently, that the nature of the process is the same for all four systems studied.

2. By the increase of oligomeric chain length, the process extent decreases, a fact determined by the decrease of double bonds number per unit volum, which affects directly the contraction at monomer conversion into tridimensional polymer. This is important not only for the monomers used for anaerobic adhesive compositions, but also for their use as monomers to obtain end products by shape polymerization.

3. The affine relation between the values defining the extent of polymerization processes of the four monomers studied and kinetic unit value are both verified in logarithmic scale.

REFERENCES

[1] Part IV : Gh. Hubca, Cr. Oprescu, Gh. Drăgan and M. Dimonie, *Rev. Roumaine Chim.*, **27**, 433 (1982).

[2] Gh. Drăgan, *J. Thermal Anal.*, **9**, 405 (1976) ; 15, 297 (1979).

[3] Gh. Drăgan, *Rev. Roumaine Chim.*, **24**, 627 (1979).

[4] Gh. Drăgan, *Rev. Roumaine Chim.*, **23**, 629 (1978).

[5] Gh. Drăgan, Dissertation, Univ. București, 1980.

[6] Gh. Drăgan, *Revista de Chimie*, **29**, 214 (1978).

[7] Gh. Drăgan, *Acta Polymerica*, **5**, 293 (1980).

[8] Gh. Drăgan, *J. Thermal Anal.*, in print (1982).

Revue Roumaine de Chimie, 27, 4, 591—593 (1982)

COMPTES RENDUS

M. RĂILEANU, ***Influence of the Medium on Chemical Reactivity*** **(Influenţa mediului asupra reactivităţii chimice), Scrisul Românesc, Craiova, 1981 (420 pages).**

The book, written in Romanian (with the table of contents presented in English and Russian) is a systematic and up-to-date discussion of various physical and chemical phenomena depending on the nature of the solvent.

After a historical introductory chapter the intermolecular forces in liquid phase are reviewed. The third chapter presents the various classifications of solvents (including those after Pearson, Parker, and Gutmann). The next chapter presents the influence of solvents on IR and electronic absorption spectra, as well as on ESR and NMR spectra. On the basis of electronic absorption spectra several empirical parameters of solvent polarity have been defined by Dimroth and Reichardt, Brooker, Kosower, and they are discussed in this chapter.

The next chapters discuss the influence of solvents on

— the synthesis of inorganic complexes (stressing the role of solvent donicity)
— the redox potentials and half-wave polarographic potentials
— the formation, structuration and dissociation of ion pairs
— the ionization of covalent bonds
— chemical equilibria (emphasizing tautomeric equilibria)
— reaction mechanisms and stereochemistry
— reaction rates for homogeneous reactions (discussing in detail the Hughes-Ingold theory for SN1, SN2 and SE1 substitutions, cage effects, etc.)
— reactivities of bidentate anions
— electronic structures in mesomeric systems
— conformations of proteins and nucleic acids

The last (16th) chapter presents the use of solvents in various fields like chromatography, spectroscopy, non-aqueous titration, extraction processes, recrystallization, and as reaction media. A subject index is appended.

Each chapter has its own bibliography running into hundreds of quotations and amounting to a total of over 1500 literature references.

Owing to its wide coverage, the book had to be selective and to discuss certain aspects in more depth than other ones. The reviewer would have greeted more space to be devoted to the ionization of covalent bonds, especially the problem of superacids which is treated on three pages only.

The abundant illustration of the book with chemical formulas, figures and many tables provides both easy reading and a wealth of reference material. The graphical conditions and the clarity of the exposition are of high quality.

The book constitutes an excellent review of an important field for chemistry and chemical physics.

A. T. Balaban

CANDIN LITEANU, SIMION GOCAN and ANIŞOARA BOLD : *Analytical Separatology* *
(Separatologie analitică), Ed. Dacia, Cluj-Napoca, 1981, 438 p.

The work approaches a theme of a particular interest, due to the unprecedented development of analytical methods, imposed by the requirement of a rigorous control on the quality of many products and modern technologies in continuous diversification. The increased exigency, regarding the exactness degree of the determinations led to high parameters of sensitivity and efficiency for the separating methods. In the book "Analytical Separatology" the most modern and efficient separating methods are described, well selected from the present available literature.

---

* A term advanced by the authors.

The structure of the book is conceived in three parts and 18 chapters, judiciously organized, granting adequate extended space for the discussed subjects.

In the first part, some generalities concerning the separating methods are presented. After an introduction where the necessity and the characters of these methods are presented, interphase equilibrium and mass transfer — very important phenomena by their implications in all separating processes — are treated.

The second part of the book is the largest one justified by the fact that the main separating methods, based on interphase equilibrium are included, namely : gas-chromatography and liquid chromatography with different stationary phases, field flow fractionation, solvent extraction, ionic flotation, the formation of inclusion compounds and supported thermal capillary extraction.

The third part of the book deals with separating methods based on transport rate, including the electrophoresis and other methods.

At the beginning of each chapter a presentation of the main theoretical aspects, necessary for understanding the practical implication of approached methods is given. After that, a detailed description of the most modern instrumentation, techniques, node of data collection, interpretation of results follow. At the end of each chapter, well selected practical examples are included. This is a way to prove a good opportunity of the possibility and performance of the methods. By some significant examples the reader is given the possibility to understand the utilisation area and the particular features of the described methods. Some of them, such as the chromatographic ones, lead to the best results in the analysis of samples, where other techniques failed. It is also to be noticed that the examples are oriented to the actual scientific research and industrial practice.

The book encloses many and well systematized data, which emphasize the authors' long experience in this difficult and great important field. The largest part is dedicated to chromatographic methods (18 chapters) and this seems justified by their special involvement in separating and analysis for the largest area of analytical applicability. At the some time, has to be pointed out the actualization of the contents, with recent methods having verified perspectives. For example in chapter 12 the field flow fractionation method is described, which although very new, has a rapid evolution due to its success in difficult analysis fields.

The book includes many figures, diagrams and tables, which are useful for understanding the interpretation of the presented phenomena and estimation of the quality of separations. In each chapter extensive specific references are included, which will be of great benefit for those interested in the different approached fields.

Considering the rigorous and modern way of presentation of the most important and newest separating methods with deep scientific and technological involvment, we consider the book very useful for researchers and chemists who are working in different fields : biology, pharmacy, metallurgy, food chemistry etc.

Elena Jercan

Advances in Polymer Science, Volume 39, *Polymer Products*, Springer-Verlag, Berlin, Heidelberg, New York, 1981, 214 pages

The book contains three contributions on new data in the synthesis and characterization of polymer materials.

The first chapter "Foamed polymers based on reactive oligomers" (64 pages, 128 references) is written by F. A. Shutov. The author presents the theoretical problems which must be resolved for foamed polymers. The new data on morphology of oligomeric foams (quantitative concept of uniformity, microcellular structure, the mechanism of microcell formation, specific surface, degree of dispersion and open porosity) are discussed. The promising oligomeric foams (oligoesters based on fumarates and maleates or methacrylates, products of aliphatic ketones, mixtures of resol phenolic and carbamide oligomers, resol and novolac oligomers) are reviewed. The most notable properties of oligomeric foams (moisture and water absorption and electrical properties) are investigated. The foamed polymers always contain a liquid phase, due to the condensation of water vapor in the air, which affects all physical-mechanical properties and sharply reduces the heat and electrical insulation properties of materials. Electroconductivity is one of the most important characteristic of foams. It determines the reliability of a foam and it serves as a technological parameter. Studies on the increase of the dielectric strength and the reduction of the static electrization of foamed polymers are presented.

At present, the foamed plastics are used in all branches of industry, replacing traditional natural materials (wood, glass, metals). The special importance of the foamed polymers is explained by a favorable combination of lightness with unique properties (buoyancy, high strength, excellent heat, electrical and acoustic insulation), a variety of techniques of preparation and a smaller consumption of polymers. The use of reactive oligomers permits the combination of the process of formation of the polymer with those of the article. By the use of polymer-oligomeric compositions it is possible to obtain articles direct at the place of utilization with a considerable reduction of energy consumption as compared to traditional processing methods. The perspectives of development in this field of polymer science and technology (superlight foams and foamed articles instead of foamed materials) are pointed out.

The second chapter "Applications of soluble polymeric supports" (30 pages, 174 references) is written by K. Geckeler, V. N. R. Pillai and M. Mutter. This article is a critical survey of the literature in relation to the use of soluble polymers as supports for organic synthesis, chromatography, and as carriers of organic reagents, catalysts, enzymes and pharmacologically active compounds.

Polyethylene glycol, linear polystyrene, partially hydrolyzed poly(vinyl pyrrolidone) and its copolymers with vinyl acetate have been functionalized for use in sequential type organic synthesis. The intrinsic problems of the heterogeneous solid-phase peptide synthesis are not solved satisfactorily by using non-crosslinked polystyrenes as support. The use of linear polyethers as soluble supports was found to be effective. The liquid-solid-phase technique which combines the features of the liquid-and solid-phase synthesis and the polymer reagent technique is a new method for stepwise peptide synthesis. The use of linear soluble polymers for reagents in organic synthesis and for preparation of soluble polymeric catalysts is of growing interest. The reagents based on polystyrene and analogous linear polymers, the reagents attached to polyamides, poly(ethylene glycol)-bound reagents for peptide synthesis are reviewed. The soluble polymer attached to homogeneous transition metal catalysts exhibit higher substrate selectivity, better reproductibility and reactivity under mild conditions than the heterogeneous catalysts. The separation of the polymer-bound catalyst is achieved by membrane filtration or selective precipitation.

The studies about the metal-chelation of some soluble polymers with chelating groups and some charge transfer polymer-iodine complexes are concerned.

The main advantages of polymeric drugs are their delayed action, sustained release. lower toxicity, choice of delivery and potentation of activity. The polymeric antimicrobial agents, polymeric and polymer-bound antibiotics, polymeric anti-cancer agents, polymeric radioprotecting agents have been reported.

A number of articles have been published on the application of soluble polymers supports for the immobilization of enzymes. The synthesis of polymers with catalytic activity mimicing that of enzymes (synzymes) has been achieved very recently.

The third chapter "Flow and electric birefrigence in rigid-chain polymers solution" is written by Victor N. Tsvetkov and Larisa N. Andreeva. The article contains 112 pages and 256 references.

Flow birefrigence (FB) is a widely used method for the study of optical, conformational and hydrodynamic properties of flexible-chain polymers. Relatively few papers on the FB for rigid-chain polymers have been reported. The analysis of experimental data and the use of some theoretical concepts allows conclusion that FB method is effective for studying the structure of rigid-chain polymers. The experimental data for ladder polysiloxanes, cellulose esters and ethers, aromatic polyamides, aromatic copolymers, poly(cyclohexane amide)s, comb-like polymers, poly(alkyl acrylate)s and poly(alkyl methacrylate)s, graft copolymers are reviewed. FB permits the determination of both the anisotropy and the equilibrium rigidity of the polymer chain using molecular weight dependence of the shear optical coefficient.

The application of the electrical birefrigence (EB) to rigid-chain polymers is more effective than to flexible chains. The combination of FB and EB methods, or the use of electrodynamic birefrigence (EDB) provides complete information on a number of characteristic properties of rigid-chain polymers.

Kristiana Goșa

IUPAC NEWS RELEASE

Commission II.1 on Atomic Weights and Isotopic Abundances

At the 31st IUPAC General Assembly held in Leuven, 26 – 29 August 1981, the following changes in the recommended values for atomic weights were approved:

Hydrogen	from	1.0079±1	to	1.00794±7
Silver	from	107.868±1	to	107.8682±3
Lutetium	from	174.967±3	to	174.967 ±1

A discussion of the reasons for these changes and the detailed Table of Standard Atomic Weights will appear in the Commission's full report to be published in the Journal of Pure and Applied Chemistry. The Commission's Table on Isotopic Abundances of the Elements will accompany this report.

GOS MŰSZAKI INFORMÁCIÓS KÖZPONT KÖNYVTÁR 1983

NOTE POUR LES AUTEURS

La Revue Roumaine de Chimie publie des articles en anglais, français, russe, allemand ou espagnol. Les auteurs sont priés d'envoyer des articles et des comptes rendus inédits.

Les manuscrits seront dactylographiés à deux intervalles. La bibliographie, les tableaux et la légende des figures seront placés après le texte.

Si l'article fait partie d'une série numérotée, la partie précédente sera donnée comme première référence.

Chaque article sera précédé d'un résumé comprenant quinze lignes au maximum.

Les références bibliographiques dans le texte seront faites par des exposants sans parenthèses et paraîtront à la fin de l'ouvrage.

Les publications périodiques mentionnées dans la bibliographie seront présentées suivant les prescriptions internationale : le nom de l'auteur précédé de l'initiale du prénom, le titre du périodique abrégé conformément à «Chemical Abstracts» et souligné par une ligne, le numéro du tome indiqué par des chiffres arabes et souligné par deux lignes, suivi de la première page de l'article : à la fin, l'année de la parution sera placée entre parenthèses. Le numéro de la revue ne sera pas indiqué, si les pages du volume sont numérotées consécutivement.

Les textes des livres ou traités inclueront : le nom des auteurs, précédés de l'initiale du prénom, le titre du livre entre guillements et sans être souligné, le numéro du tome précédé par l'abréviation «vol» (ou «Bd.»), le numéro de l'édition, les éditions (the publisher), la localité de la parution du livre, l'année de la parution et la page de la référence précédées(s) par l'abréviation «p» (ou «S»).

Les brevets seront indiqués comme suit : l'auteur ou la firme, le pays et le numéro du brevet, la date et la revue (*Chem. Abstr.*). Par ex. : M. Jones (to Union Carbide Co.) Brit. Pat. 601 238, 2 Sept. 1959 ; cf. *Chem. Abstr.*, **54**, 12808 (1960).

Si la référence n'a pas été lue en original, on indiquera aussi la revue de références consultée.

Les diagrammes seront tracés à l'encre de Chine sur papier calque. Les tableaux et les figures (en nombre strictement nécessaire), ainsi que les courbes dans la figures seront numérotés par des chiffres arabes. Leur explication sera donnée dans la légende des figures. Prière de ne pas inscrire les mêmes données dans les tableaux et les figures. Chaque tableau aura un titre. On indiquera dans le texte la place approximative des tableaux et des figures. Les formules chimiques seront incluses dans la texte : en outre, elle seront transcrites sur papier calque, à l'encre de Chine.

Les auteurs sont priés d'indiquer les caractères italiques (en soulignant les lettres au crayon), ainsi que tout autre caractère spécial : les préfixes *ortho, meta, para, cis, trans,* etc., seront soulignés pour indiquer leurs caractères italiques, et ne seront jamais écrits avec des majuscules.

Aucune correction à la main ne sera admise sur le manuscrit. Les corrections seront frappées à la machine. Les lettres grecques ou autres symboles spéciaux seront insérés à la main à l'encre clairement.

Le manuscrit sera signé par l'auteur.

Le colonne-titre aura 50 lettres au maximum.

L'entière responsabilité du contenu des articles appartient aux auteurs.

Sur demande on peut obtenir une note plus complète.

PRINTED IN ROMANIA

TRAVAUX PARUS AUX ÉDITIONS DE L'ACADÉMIE DE LA RÉPUBLIQUE SOCIALISTE DE ROUMANIE

ELENA CEAUŞESCU, **Noi cercetări în domeniul compuşilor macromoleculari** (Nouvelles recherches dans le domaine des composés macromoléculaires) 1981, 536 p.

I. G. MURGULESCU, TATIANA ONCESCU, E. SEGAL, **Introducere în chimia fizică. Vol. II. 2. Cinetică chimică şi cataliză** (Introduction à la chimie physique. Vol. II.2. Cinétique chimique et catalyse), 1981, 1024 p.

V. DRĂGUŢAN, A. T. BALABAN, M. DIMONIE, **Metateza olefinelor şi polimerizarea prin deschidere de inel a cicloolefinelor** (La métathèse des oléfines et la polymérisation par ouverture annulaire des cyclooléfines), 1981, 254 p.

LYDIA-MARIA VAICUM, **Epurarea apelor uzate cu nămol activ. Bazele biochimice** (L'épuration des eaux résiduelles à boue active. Les bases biochimiques), 1981, 218 p.

I. GĂLĂŢEANU, **Procese şi metode radiochimice în energetica nucleară** (Processus et méthodes radiochimiques dans l'énergétique nucléaire), 1981, 234 p.

I. IORDACHE, **Procese polistocastice aplicate la fenomenele de transfer** (Processus polystochastique appliqués aux phénomènes de transfert), 1981, 187 p.

CR. SIMIONESCU, VALERIA GORDUZA, **Polimeri biocompatibili şi biologic activi** (Polymères biocompatibles et biologiquement actifs), 1980, 497 p.

ELENA CEAUŞESCU, **Polimerizarea stereospecifică a izoprenului** (La polymérisation stéréospécifique de l'isoprène), 1979, 307 p.

M. FLORESCU, **Metode ştiinţifice în dezvoltarea industriei chimice moderne** (Méthodes scientifiques dans le développement de l'industrie chimique moderne), 1979, 256 p.

A. T. BALABAN, I. GĂLĂŢEANU, G. GEORGESCU, LIGIA SIMIONESCU, **Compuşi marcaţi şi radiofarmaceutici cu aplicaţii în medicina nucleară** (Composés marqués et radiopharmaceutiques à application en médecine nucléaire), 1979, 495 p.

CONST. GH. MACAROVICI, **Analiza chimică cantitativă anorganică** (L'Analyse chimique quantitative inorganique), 1979, 457 p.

I. G. MURGULESCU, E. SEGAL, **Introducere în chimia fizică, vol. II. I. Teoria molecular cinetică a materiei** (Introduction à la chimie physique, vol. II. 1. La théorie moléculaire-cinétique de la matière), 1979, 1036 p.

S. STERNBERG, FL. DANEŞ, **Termodinamica chimică aplicată** (La thermodynamique chimique appliquée), 1978, 400 p.

I. G. MURGULESCU, V. EM. SAHINI, **Introducere în chimia fizică Vol. I.2. Structura şi proprietăţile moleculelor** (Introduction à la chimie physique. Vol. I.2. La structure et les propriétés des molécules), 1978, 604 p.

C. DRĂGULESCU, E. PETROVICI, **Chimie structurală modernă. Chimia coordinaţiei 8** (La Chimie structurale moderne. La Chimie de la coordination 8), 1977, 947 p.

I. ZUGRĂVESCU, MAGDA PETROVANU, **N-ylid chemistry**, coédition avec McGraw-Hill International Book Company, U.S.A., 1977, 396 p.

I. G. MURGULESCU, **Introducere în chimia fizică Vol. I. 1 Atomi molecule, legătură chimică** (Introduction à la chimie physique. Vol. I. 1. Atomes, molécules, liaison chimiques), 1976, 560 p.

ELENA CEAUŞESCU, **Research work on synthesis and characterization of macromolecular compounds. Contributions**, 1974, 251 p.

CR. SIMIONESCU, VIORICA RUSAN, V. POPA, **Chimia algelor marine** (La chimie des algues marines), 1974, 212 p., 1 pl.

I. P. INFORMAŢIA cd. 1816

43 426

Lei 40

$ 70 (pour un abonnement annuel)

F 1103

ACADÉMIE DE LA RÉPUBLIQUE SOCIALISTE DE ROUMANIE

R

REVUE ROUMAINE DE CHIMIE

REFERÁLVA

TOME 27
N° 5
Mai 1982

EDITURA ACADEMIEI REPUBLICII SOCIALISTE ROMÂNIA

Rev. Roumaine Chim.

RRCHAX, 27, 5, p. 595–692 (1982), Bucarest

ACADÉMIE DE LA RÉPUBLIQUE SOCIALISTE DE ROUMANIE

COMITÉ DE RÉDACTION

Rédacteur en chef:

I. G. MURGULESCU, membre de l'Académie de la République Socialiste de Roumanie

Rédacteurs en chef adjoints:

A. T. BALABAN et V. EM. SAHINI, membres correspondants de l'Académie de la République Socialiste de Roumanie

Collège de rédaction:

EM. BRATU, ELENA CEAUŞESCU, ECATERINA CIORĂNESCU-NENITZESCU, CR. SIMIONESCU, membres de l'Académie de la République Socialiste de Roumanie; P. SPACU, membre correspondant de l'Académie de la République Socialiste de Roumanie; MARGARETA AVRAM, M. BANCIU, I. HAIDUC, D. I. MARCHIDAN, I. MOLDOVAN, G. NIAC et D. SĂNDULESCU

La Revue Roumaine de Chimie paraît 10 fois par an. Toute commande de l'étranger pour les travaux parus aux Editions de l'Académie de la République Socialiste de Roumanie sera adressée à ILEXIM, — Departamentul Export-Import Carte (Livres)/Departamentul Export-Import Presă (Revues) P.O.B. 136—137, télex 11226; 3, str. 13 Decembrie, 79517 Bucarest, Roumanie

Les manuscrits, les livres et les revues proposés en échange, ainsi que toute correspondance seront envoyés à la rédaction :

REVUE ROUMAINE DE CHIMIE

Calea Victoriei, 125, 79717 Bucarest, Roumanie, téléphone 50 76 80

EDITURA ACADEMIEI REPUBLICII SOCIALISTE ROMÂNIA
125, Calea Victoriei, 79717 Bucarest, Roumanie, téléphone 50 76 80

REVUE ROUMAINE
DE
CHIMIE

1983

Tome 27, N° 5 Mai, 1982

I. G. MURGULESCU and MARILENA ŞERBAN, Viscosity of liquids with quasispherical molecules. Checking Eyring's equation 597–602

ORTANSA LANDAUER, CORNELIA MATEESCU, OLGA IULIAN and G. COSTEANU, On the viscosity of the mixed system tetrahydrofuran-water (in French) 603–607

RODICA ENE, I. BICĂ and D. SĂNDULESCU, Determination of hydrogen solubility in liquid hydrocarbons at atmospheric pressure . . . . 609–613 Bc

LI QILONG, C. LUCA, A. CĂLUŞARU and F. G. BĂNICĂ, Catalytic hydrogen discharge by cycloserine in nickel ion containing phosphate buffer. . . . 615–619 Bc

D. K. BANERJEE, V. MATEI and V. VANTU, Kinetic studies of the pyrolysis of some alkylbenzenes 621–628

M. IOVU and ELIZA-MANUELA VASILESCU, New vibration modes made evident in the IR spectra of a class of alkyl aryl ethers 629–633

FLORENTINA GEORGESCU, E. I. GEORGESCU, F. CHIRALEU and I. ZUGRĂVESCU, Pyrimidinium-ylids. III. Synthesis of carbanion-disubstituted pyrimidinium-ylids (in French) 635–643

C. I. CHIRIAC. A new method for the preparation of triaryl-*s*-triazoles from diaroylhydrazines . . . . 645–649 R

SPIRIDON OPREA and EMIL DUMITRIU, Reactivity of acrylic monomers. XI. Synthesis and copolymerization of 3-chloro-2-hydroxypropyl acrylate 651–658

GH. HUBCA, C. OPRESCU, AGNETA CARAGHEORGHEOPOL, H. CĂLDĂRARU, D. RACOŢI and M. DIMONIE, Synthesis and polymerization of polyethylene glycol dimethacrylates. VI. Study of copolymerization process of polyethylene glycol dimethacrylates with styrene 659–666

CLEOPATRA CALU and EUGENIA DONIGA, Amperometric determination of thiamine . . . . 667–671 R

LUMINIŢA VLĂDESCU and ANA ISUF, Ion exchange procedure for the elimination of interferences in the spectrophotometric determination of magnesium with Eriochrome black T 673–679

LUIGI CAMPANELLA, TOMMASO FERRI, MARA GABRIELLI, Liquid membrane electrodes for benzoic acid determination 681–683

JÁNOS FAZAKAŞ, Determination of gold by graphite furnace — Atomic absorption spectrometry with atomization under pressure . . . . 685–689 R

BOOK REVIEWS 691–692

Rev. Roumaine Chim. **27**, *5*, 595–692 (1982) Bucarest

Revue Roumaine de Chimie, 27, *5*, 597–602 (1982)

VISCOSITY OF LIQUIDS WITH QUASISPHERICAL MOLECULES. CHECKING *EYRING'S* EQUATION

I. G. MURGULESCU and MARILENA ŞERBAN
Chemistry Institute, Department of Physical Chemistry, Bd. Republicii 13, Bucharest, Romania

Received June 1, 1981

An equation of viscosities for liquids with low melting temperatures was developed starting from Eyring's equation. This equation was applied for tetrahalides, mercury, and noble gases. The vibration partition function was used in its general form. The tetrahalide molecules were considered as spherical ensembles vibrating according to Lindemann law ; the vibration frequency was not changed to a noticeable extent during the melting process. In order to estimate the activation energy, the rotational energy of the molecules was also taken into account.

In the present paper we are carrying on the application of the viscosity equations, previously developed,[1–4] for some tetrahalides, Hg and noble gases in the liquid state.

In a previous paper,[5] we pointed out that Batschinski's equation and corpuscular significance of the limiting molar volume [1] hold also for the tetrahalides.

In another earlier paper,[2] starting from an equation advanced by Eyring, we developed the relationship :

$$\eta = \frac{Nh}{\gamma M} \frac{\rho \exp(h\nu/kT)}{\exp(h\nu/kT) - 1} e^{E/RT} \tag{1}$$

where : η and ρ are the viscosity and density, respectively, at a given temperature T ; M is the molecular weight, γ and ν are the packing coefficient and vibration frequency of the particles in liquid state, respectively, and E is the activation energy of the viscous flow. The other symbols have the known significance. This equation was developed supposing that close to the melting temperature the particles in the liquid state are arranged as a close packed lattice with holes. Each particle has only harmonic vibratory motion around its equilibrium position with a constant, temperature independent frequency, smaller than the corresponding frequency in the solid state.

In order to calculate the liquid viscosity using eq. (1) it is necessary to know the vibration frequency and activation energy. In two previous papers,[2,3] we gave the necessary relationships for the calculation of these two magnitudes in the case of molten metals having high melting temperatures. The two different relationships obtained for viscosity are specific for normal metals and abnormal metals. The agreement between theoretical and experimental activation energies is very good for the both groups. For the preexponential constant the agreement is very good only for normal metals.

These calculations have been carried out supposing that while for the normal metal melts only the atoms are implied in the flow process, for the abnormal metal melts the dimers are also involved, near the melting temperature.

In contrast with the liquid metals (except Hg), the tetrahalides CCl_4, $SiCl_4$, $SiBr_4$, $TiCl_4$, $GeCl_4$, $SnCl_4$, $SnBr_4$, as well as the liquid noble gases, have low melting temperature ; except for $SiBr_4$ and $SnBr_4$ they are below 273 K.

While the atoms of the tetrahalide molecules are linked by covalent forces, between the molecules as well as between noble gases atoms van der Waals forces operate.

X ray studies [6–10] showed that the liquid state near the melting temperature is characterized by a compact packing of the spherical molecules. The change of the macroscopic density when the temperature increases can be essentially explained (for CH_4), by the holes formation. There are no molecular associations in the liquid SnI_4. In the solid state the tetrahalides are characterized by a compact structure.

On the basis of the above mentioned data we can also use eq. (1) for these molecular liquids. Consequently, we consider the molecules as spherical ensembles vibrating with the characteristic frequency. As these molecules are heavy it is reasonable to suppose that the vibration frequency does not change to a noticeable extent during the melting process. ν can be estimated using Lindemann's relationship :

$$\nu = 2.8 \times 10^{12} \sqrt{\frac{T_m}{M V_m^{2/3}}} \tag{2}$$

where V_m is the solid state molar volume at the melting temperature T_m.

The preexponential constant in eq. (1) :

$$A = \frac{Nh}{\gamma M} \tag{3}$$

can be easily evaluated containing only mass as molar quantity.

Assuming that the vibration energy of the molecules at temperatures close to the melting temperature can be taken as the harmonic oscillator energy, the vibration energy for N oscillators is :

$$E_v = 3R \frac{h\nu/k}{\exp(h\nu/kT_m) - 1} \tag{4}$$

In order to estimate the activation energy of the viscous flow it is necessary to take into account the rotational energy :

$$E = 3R\frac{h\nu/k}{\exp(h\nu/kT_m)-1} + 3\,\frac{RT_m}{2} \tag{5}$$

giving the minimum energy necessary for the molecules to participate in the flowing process. It can be calculated from the known vibration frequency and melting temperature.

RESULTS AND DISCUSSIONS

Both the preexponential constant A and activation energy E can be estimated from viscosity and density data, using the plot : $\log \eta[\exp(h\nu/kT) - 1]/\rho \exp(h\nu/kT)$ vs. $1/T$. It can be seen from the plots in Figure 1 that there is a slight curvature toward higher temperatures for $SiBr_4$, $SnCl_4$ and $SnBr_4$, as well as for some metals with normal and abnormal behaviour. For $SiCl_4$ and $TiCl_4$ the curvature is in the opposite direction.

The experimental values of A and E, given in table 1, refers to the temperature range around the melting temperature.

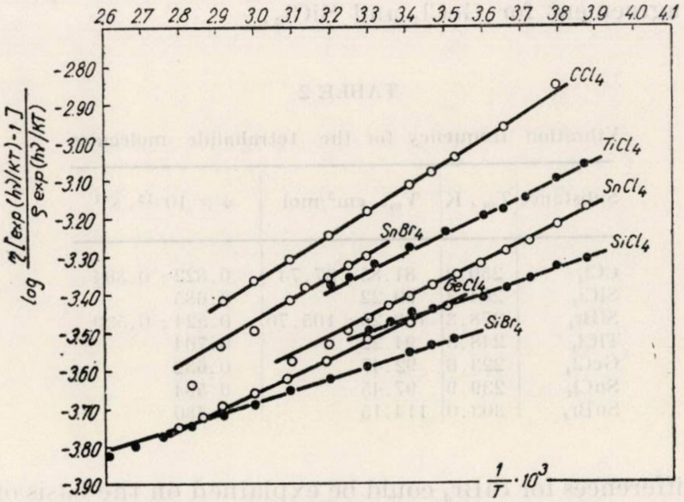

Fig. 1. — Plot of log η [exp $(h\nu/kT)$ — 1)]/ρ exp $(h\nu/kT)$ vs.$1/T$. for the liquid tetrahalides.

Table 1 also shows the theoretical values of these parameters, A and E, estimated from eqs. (3) and (5). Table 2 gives the data necessary for calculation.

The experimental data have been taken from the literature indicated in a previous paper.[5]

TABLE 1

Preexponential constant and activation energ y of some liq uid tetrahalides

Substance	$A \times 10^5$, cm^2 s^{-1}		E, cal/mol		Valability range. K
	Experim.	Calcd.	Experim.	Calcd.	
CCl_4	0.577 ; 0.567	1.834	2845	2115 ; 2120	ΔT
$SiCl_4$	1.905	1.660	1670	1730	258–278
$SiBr_4$	2.320 ; 2.339	0.811	1450	2405 ; 2405	283–333
$TiCl_4$	1.415	1.487	2090	2110	258–285
$GeCl_4$	1.073	1.316	1995	1905	ΔT
	0.928		2180		258–298
$SnCl_4$	0.356	1.083	2730	2060	ΔT
	0.671		2310		ΔT
$SnBr_4$	0.623	0.644	2640	2630	303–323

An analysis of the figures in table 1 indicates a very good agreement between the experimental and theoretical values for $TiCl_4$, $SnCl_4$, $SnBr_4$ and a fair agreement for $GeCl_4$ and $SiCl_4$.

TABLE 2

Vibration frequency for the tetrahalide molecules

Substance	T_m, K	V_m, cm^3/mol	$\nu \times 10^{-12}$, s^{-1}
CCl_4	250.2	81.85 ; 87.74	0.822 ; 0.804
$SiCl_4$	204.4	90.22	0.685
$SiBr_4$	278.3	109.25 ; 105.70	0.524 ; 0.530
$TiCl_4$	248.3	94.22	0.704
$GeCl_4$	223.6	92.47	0.632
$SnCl_4$	239.9	97.45	0.584
$SnBr_4$	303.0	114.15	0.480

The differences for $SiBr_4$ could be explained on the basis of the molecular association in liquid state, at the melting point, suggested in the literature, although our previous results[5] showed that there was not such an association. If we consider that besides monomers there exists a fraction x of dimers, then the activation energy becomes :

$$E = (1 - x)E_v + \frac{x}{2}E_v + 3(1 - x)\frac{RT_m}{2} + 2\frac{x}{2}\frac{RT_m}{2} \qquad (6)$$

It is composed of the vibration energy of $(1-x)$ monomers and of $x/2$ dimers, of the rotational energy of monomers having 3 freedom degrees and the rotational energy of dimers having 2 freedom degrees. The association degree x can be calculated as follows:

$$x = \frac{E_{\text{calcd}} - E_{\text{experim}}}{\frac{1}{2}E_v + RT_m} \qquad (7)$$

giving $x = 0.71$. The vibration energy for dimers was considered similar to that of monomers, without a significant change of the activation energy. The lack of experimental data referring to $SiBr_4$ does not allow a final conclusion.

The results for CCl_4 regarding A parameter are similar to those for Sb and Bi having a negative volume change during the melting process. Among different tetrahalides only for CCl_4 the Mott relationship leads to the ratio $\nu_S/\nu = 1.497$ similar to the corresponding ratio of metals.

The behaviour of Hg, previously considered similar to the other[2,3] metals, can be explained on the basis of eq. (1). The preexponential constant is calculated with eq.(3) and the vibration energy with eq. (4). For the activation energy the following relationship is proposed:

$$E = (1-x)E_v + \frac{x}{2}E_v + 2\frac{x}{2}\frac{RT_m}{2} \qquad (8)$$

where, besides the vibration energy of $(1-x)$ monomers, the vibration and rotation energies of $x/2$ dimers are also considered. The vibration energy of dimers was also supposed to be similar to that of monomers. The vibration frequency of monomers in liquid state was calculated from the vibration frequency in solid state, resulted from eq.(2), and using Mott's equation[2]: $\nu_S = 1.231 \times 10^{12}\ s^{-1}$ and $\nu = 0.840 \times 10^{12}\ s^{-1}$. The association degree, $x = 0.208$, was taken from a previous paper.[1]

TABLE 3

Preexponential constant and activation energy of the liquid Hg

Element	$A \times 10^5$, $cm^2\ s^{-1}$		E, cal/g atom	
	Experim.	Calcd.	Experim.	Calcd.
Hg	1.982	1.406	1170	1190

The experimental values of A and E were evaluated from the plot $\log \eta[\exp(h\nu/kT) - 1]/\rho \exp(h\nu/kT) = f(1/T)$, where ν was supposed to be the vibration frequency of monomers in liquid state. Table 3 gives the values obtained for the range 253 – 373 K.

The agreement between the calculated and experimental values is very good.

The results obtained for the liquid noble gases using the same procedure as that for Hg are given in table 5. The data needed in calculation, missing in our previous papers, are given in table 4.

TABLE 4

Vibration frequency for the noble gas atoms

Element	M	L, cal/g atom	$e^{L/3RT_m}$ (average)	$\nu_S \times 10^{-12}$, s^{-1}	$\nu \times 10^{-12}$, s^{-1}
Ar	39.948	274	1.754	1.385	0.790
Kr	83.80	391		1.079	0.615
Xe	131.30	549		0.923	0.526

TABLE 5

Preexponential constant and activation energy of the liquid noble gases

Element	$A \times 10^5$, cm^{2}s^{-1}		E, cal/g atom	
	Experim.	Calcd.	Experim.	Calcd.
Ar	3.241	7.062	520	390
Kr	2.083	3.367	680	605
Xe	0.655	2.147	1185	890

The agreement between experimental and calculated values is less satisfactory than in the other cases.

REFERENCES

[1] I. G. Murgulescu and M. Şerban, *Rev. Roumaine Chim.*, **17**, 431(1972).
[2] I. G. Murgulescu and M. Şerban, , *Rev. Roumaine Chim.*, **19**. 1417(1974).
[3] I. G. Murgulescu and M. Şerban, *Rev. Roumaine Chim.*, **20**, 591(1975).
[4] I. G. Murgulescu and M. Şerban, *Rev. Roumaine Chim.*, **22**, 807(1977).
[5] I. G. Murgulescu and M. Şerban, *Rev. Roumaine Chim.*, **24**, 1417(1979).
[6] S. D. Ravicovich, *Dopovidi Akad. Nauk Ukrain. S.S.R.*, nr. 4, 328(1957).
[7] J. I. Petz, *J. Chem. Phys.*, **43**, 2238 (1965),.
[8] R. W. Harris and G. T. Clayton, *J. Chem. Phys.*, **45**, 2681 (1966).
[9] R. E. Wood and H. L. Ritter, *J.Amer.Chem.Soc.*, **74**, 1763 (1952).
[10] A. Einstein, *Phys. Rev.*, **63**, 304(1943)

Revue Roumaine de Chimie, 27, 5, 603–607 (1982)

SUR LA VISCOSITÉ DU SYSTÈME MIXTE TÉTRAHYDROFURANNE-EAU

ORTANSA LANDAUER, CORNELIA MATEESCU, OLGA IULIAN et G. COSTEANU

Chaire de Chimie Physique et de Technologie Electrochimique, Institut Polytechnique,
Bucarest, 132, Calea Griviței, Roumanie

Reçu le 14 août 1981

Les auteurs ont étudié la viscosité du système mixte tétrahydofuranne-eau à différentes concentrations et aux températures de 25, 30, 40 et 45°. D'après les valeurs de η^E et de V^E on a tiré des conclusions sur les interactions des molécules du système.

The authors have studied the viscosity of the mixed tetrahydrofuran-water system at different concentrations and at temperatures of 25, 30, 40 and 45°. On the basis of η^E and V^E values, conclusions were drawn concerning the interactions between the molecules of the mixed system.

La viscosité des systèmes mixtes permet de tirer certaines conclusions sur les interactions des molécules présentes et aussi sur l'existence des associations moléculaires.

Pour l'étude de notre système nous avons utilisé du tétrahydrofuranne (THF), bien purifié au préalable, d'après les méthodes indiquées par la littérature,[1] et de l'eau bidistillée.

La viscosité des liquides purs et des solutions de différentes concentrations du système mixte a été déterminée avec un viscosimètre Ubbelohde aux températures de 25, 30, 40 et 45°.

Les valeurs obtenues, exprimées en cP, sont réunies dans le tableau 1.

TABLEAU 1

Valeurs des viscosités, en *cP*, et des énergies d'activation, en cal. mole $^{-1}$

X_{THF}	η 25°	η 30°	η 40°	η 45°	$E_{cal.\,mole^{-1}}$
0,000	0,9040	0,8007	0,6560	0,6198	3522
0,024	1,1686	1,0367	0,8301	0,7488	4221
0,052	1,4129	1,2563	0,9714	0,8599	4720
0,086	1,6535	1,4369	1,1053	0,9842	4906
0,129	1,7579	1,5216	1,1984	1,0485	4856
0,181	1,7425	1,5123	1,1854	1,0765	4559
0,249	1,6398	1,4058	1,1191	1,0174	4481
0,340	1,3708	1,2100	0,9884	0,9134	3833
0,469	1,0638	0,9533	0,8056	0,7453	3317
0,665	0,7330	0,6828	0,5933	0,5644	2504
0,826	0,6233	0,5647	0,5813	0,4889	2227
0,924	0,5527	0,5093	0,4663	0,4436	1988
1,000	0,4900	0,4688	0,4324	0,4109	1630

La viscosité passe par un maximum, d'autant plus marqué que la température est plus basse.

Il faut remarquer que la valeur maxima de la viscosité se situe dans le domaine de concentration de $0{,}1 \leqslant X_{THF} \leqslant 0{,}2$, en fraction molaire, aux températures de 25−45°C.

Pour mieux illustrer ces résultats, nous les avons représentés graphiquement, à deux températures, dans la figure 1.

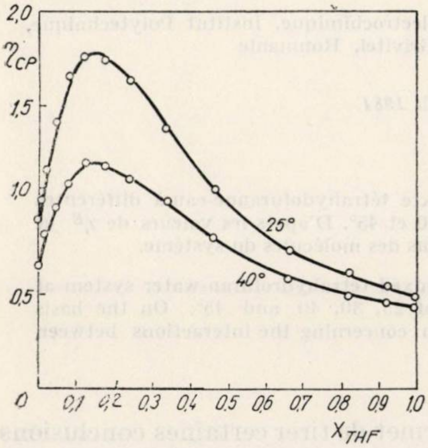

Fig. 1. Variation de la viscosité avec la fraction molaire.

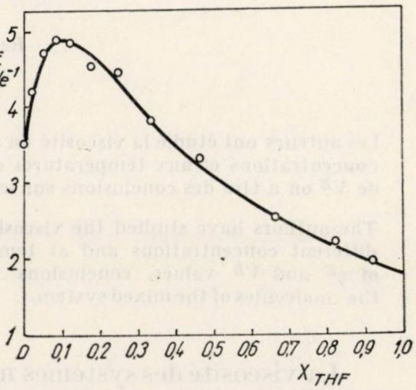

Fig. 2. Variation de l'énergie d'activation avec la fraction molaire.

Le maximum des courbes est attribué aux interactions assez fortes entre les molécules de l'eau et du tétrahydrofuranne.

On attribue également à ces interactions le maximum de la courbe de l'énergie d'activation de l'écoulement visqueux en fonction de la fraction molaire (Fig. 2).

Il est bien évident que les liaisons hydrogène doivent jouer un rôle très important dans ces interactions.

Nous avons obtenu une courbe $E - f(X_{DMSO})$, presque identique à la précedente, en étudiant la viscosité du système diméthylesulfoxyde-eau.[2]

La variation de la viscosité des mélanges liquides est en rapport principalement avec le changement de volume au moment du mélange. Donc, il nous a semblé intéressant de connaître aussi les volumes molaires. Pour cela, nous avons déterminé d'abord les densités des mêmes solutions indiquées plus haut, et aux mêmes températures, avec un picnomètre à paroi double vidée.

Les résultats obtenus sont réunis dans le tableau 2.

On ne voit aucun parallélisme entre les viscosités et les densités des solutions. Donc, la variation de la viscosité avec la concentration des solutions doit être soumise à des influences qui sont prépondérantes.

Nous avons calculé ensuite, en partant de densités, les volumes molaires moyens des mélanges étudiés, et dont les valeurs sont réunies dans le tableau 3.

On a calculé aussi les viscosités d'excès et les volumes molaires d'excès, en utilisant les formules données dans un travail antérieur. [3]

TABLEAU 2

Valeurs des densités, en gcm^{-3}

X_{THF}	d 25°	d 30°	d 40°	d 45°
0,000	0,9970	0,9957	0,9922	0,9903
0,024	0,9932	0,9906	0,9871	0,9845
0,052	0,9895	0,9859	0,9816	0,9781
0,086	0,9835	0,9792	0,9727	0,9692
0,129	0,9759	0,9711	0,9635	0,9591
0,181	0,9653	0,9598	0,9525	0,9479
0,249	0,9533	0,9469	9,9375	0,9320
0,340	0,9396	0,9333	0,9252	0,9206
0,469	0,9241	0,9179	0,9067	0,9013
0,665	0,9046	0,8991	0,8878	0,8828
0,826	0,8910	0,8851	0,8739	0,8689
0,924	0,8880	0,8824	0,8731	0,8667
1,000	0,8810	0,8750	0,8630	0,8580

TABLEAU 3

Valeurs des volumes molaire, en cm^3

X_{THF}	$\bar{V}$ 25°	$\bar{V}$ 30°	$\bar{V}$ 40°	$\bar{V}$ 45°
0,000	18,0524	18,0777	18,1415	18,1763
0,024	19,4251	19,4815	19,5506	19,5967
0,052	21,0450	21,1364	21,2253	21,2903
0,086	23,0491	23,1615	23,3162	23,3892
0,129	25,5500	25,6945	25,8971	25,9990
0,181	28,7744	28,9618	29,1837	29,3026
0,249	32,9899	33,2414	33,5747	33,7439
0,340	38,7163	39,0123	39,3539	39,5153
0,469	46,9178	47,2751	47,8539	48,1046
0,665	59,6669	60,0641	60,8286	61,1403
0,826	70,3493	70,8182	71,7258	72,1386
0,924	76,6285	77,1148	77,9362	78,5117
1,000	81,8388	82,4000	83,5458	84,0326

Les valeurs obtenues dans les deux cas ont été réunies dans les tableaux 4 et 5.

Nous avons représenté aussi graphiquement les valeurs des ln η^E et des V^E en fonction de la concentration du système, à deux températures. Voir les figures 3 et 4.

On voit que les ln η^E présentent une valeur maxima à la concentration de $X_{THF} = 0{,}181$, à toutes les températures, alors que les V^E ont des valeurs négatives, dont le minimum se situe dans le domaine de concentrations de $0{,}340 \leqslant X_{THF} \leqslant 0{,}469$.

TABLEAU 4

Valeurs des ln ηE

X_{THF}	ln η 25°	ln η 30°	ln η 40°	ln η 45°
0,000	0,0000	0,0000	0,0000	0,0000
0,024	0,2714	0,2712	0,2454	0,1998
0,052	0,4783	0,4767	0,4143	0,3502
0,086	0,6569	0,6313	0,5580	0,4997
0,129	0,7437	0,7111	0,6564	0,5811
0,181	0,7718	0,7328	0,6671	0,6274
0,249	0,7541	0,6962	0,6379	0,6002
0,340	0,6236	0,5949	0,5516	0,5264
0,469	0,4487	0,4255	0,4009	0,3788
0,665	0,1963	0,1973	0,1771	0,1776
0,826	0,1334	0,0922	0,0903	0,1014
0,924	0,0741	0,0421	0,0437	0,0449
1,000	0,0000	0,0000	0,0000	0,0000

TABLEAU 5

Valeurs des volumes d'excès, V^E, en cm³ mole⁻¹

X_{THF}	V^E 25°	V^E 30°	V^E 40°	V^E 45°
0,000	0,0000	0,0000	0,0000	0,0000
0,024	−0,1599	−0,1399	−0,1606	−0,1602
0,052	−0,3040	−0,2861	−0,3172	−0,3105
0,086	−0,4906	−0,4480	−0,4501	−0,4508
0,129	−0,7505	−0,6989	−0,6997	−0,6910
0,181	−0,8248	−0,7582	−0,7960	−0,7937
0,249	−0,9467	−0,8526	−0,8525	−0,8306
0,340	−1,0247	−0,9350	−1,0251	−1,0521
0,469	−1,0514	−0,9698	−0,9622	−0,9583
0,665	−0,7860	−0,7699	−0,7886	−0,8305
0,826	−0,3910	−0,3897	−0,4396	−0,4284
0,924	−0,3627	−0,3967	−0,6388	−0,5422
1,000	0,0000	0,0000	0,0000	0,0000

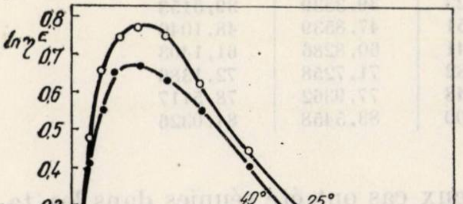

Fig. 3. Ln des viscosités d'excès, η^E, en fonction de la fraction molaire.

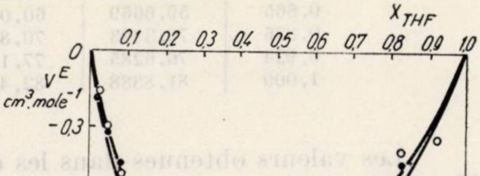

Fig. 4. Volumes d'excès en fonction de la fraction molaire.

Les résultats obtenus plus haut nous conduisent à admettre l'aptitude du système THF-eau à former des associations moléculaires à une certaine concentration.

L'existence des interactions assez fortes entre les molécules des deux constituants du système THF-eau a été aussi mise en évidence par d'autres méthodes physiques, à savoir, la résonance magnétique nucléaire, [4] et les spectres d'absorption dans l'infrarouge. [5]

Dans nos travaux antérieurs [6,7] sur l'hydrolyse acide et alcaline de certains esters aliphatiques, dans THF-eau, nous avons constaté, d'après les données cinétiques, des interactions moléculaires assez fortes à la concentration de $X_{THF} = 0,175$ du solvant mixte. Ceci est en très bon accord avec les résultats donnés plus haut.

Nous admettons donc, d'après les résultats obtenus par nous, que le système THF-eau est susceptible de donner une association moléculaire de composition 1 THF : 4 H_2O, à une certaine concentration.

BIBLIOGRAPHIE

[1] M. Erondon, M. Tamers et S. Scott Jr., *J. Amer.Chem.Soc.*, **82**, 2121 (1960).
[2] O. Landauer, G. Costeanu et C. Mateescu, *Rev.Roumaine Chim.*, **19**, 1420 (1974).
[3] O. Landauer, G. Costeanu et G. Mateescu, *Rev. Roumaine Chim.*, **24**, 1024 (1979).
[4] W. Khöler et L. Neuheiser, *Z. Chem. B.*, **11**, 425 (1968).
[5] M. Claude Quinvoron et J. Néel, *Compt. rend.*, **259**, 1845 (1964).
[6] G. Costeanu et C. Mateescu, *Rev. Roumaine Chim.*, **17**, 1353 (1972).
[7] G. Costeanu, C. Mateescu et O. Landauer, *Bul. Inst. Politeh. Iaşi*, **18**, 1(1972).

Revue Roumaine de Chimie, 27, 5, 609–613 (1982)

DETERMINATION OF HYDROGEN SOLUBILITY IN LIQUID HYDROCARBONS AT ATMOSPHERIC PRESSURE

RODICA ENE*, I. BICĂ* and D. SĂNDULESCU **
* Centre of Physical Chemistry, Splaiul Independenței 202, Bucharest, 77208, Romania
** Institute of Petroleum and Gases, Ploiești, 2000, Romania

Received November 5, 1981

The solubility of a gas in a liquid at atmospheric pressure was measured by saturation method. The solubility of hydrogen in the homologous series of liquid *n*-paraffins nC_7—nC_{10} and in isooctane was measured and the temperature coefficient of gas solubility over a temperature range between 25 and 50°C was determined.

The determination of solubility equilibrium in a gas—liquid system is important from practical point of view in designing all gas—liquid absorbers with or without chemical reaction; on the other hand, since the absorption of gases in liquids is related to the nature of molecular interactions and structures in solutions the study of solubility of gases in liquids presents a theoretical importance.

EXPERIMENTAL

A device was built up based on saturation method; [1,2] it ensured the accuracy required by the nature of the problem and the reaching of the equilibrium of the gas-liquid system in question.

In dynamic systems the solubilities at several flow rates were determined in order to check if equilibrium was reached.

The device consisted of two parts: one for degasing the solvent and another one that includes the cell employed in determination of solubility. The degasing of solvent was achieved by boiling followed by cooling in vacuum.[3] The criterion of the complete degasing was the reproductibility of measurements. In the device used the liquid film flowed through the gas. The solvent flowed in drops in thin films through an absorption spiral and from there through a burette that contained the gas to be dissolved. The saturated solvent flowed from the absorption burette at such a rate that the level of the liquid remained constant during a run *i.e.* the flow rates into and out of the burette were equal. Fairly large variations at solvent flow rates had no appreciable effect on solubilities.

Hydrogen was 99 % pure; the solvents employed were Fluka A.G., Chemische Fabrik CH—9470 Buchs, of purity higer than 99 % determined by gas chromatography.

The solvent flow rate was between 0.08 and 0.15 cm^3/min and that of hydrogen between 0.16 and 0.25 cm^3/min. The determinations were carried out at atmospheric pressure (760 mm Hg) and at 25°, 40° and 50°C.

The results obtained with this device, for solubilities of H_2 in some normal-paraffine hydrocarbons $C_7 - C_{10}$ at normal pressure and 25°C, agree fairly well with the data in the literature [6].

RESULTS AND DISCUSSION

The solubility of hydrogen at partial pressure equal to atmospheric pressure was determined in the homologous series of liquid *n*-paraffins from *n*-heptane to *n*-decane and in isooctane (2,2,4-trimethylpentane).

The solubility of the gas in liquids was expressed by the relation:

a – the Ostwald coefficient, L

$$L = \frac{V_g}{V_s} \tag{1}$$

where V_g stands for the volume of absorbed gas, V_s for the volume of solvent, both of them measured at the same temperature.

b – the Bunsen coefficient, α, calculated for normal conditions of pressure and temperature:

$$\alpha = \frac{V_g}{V_s} \cdot \frac{T_0}{T} \tag{2}$$

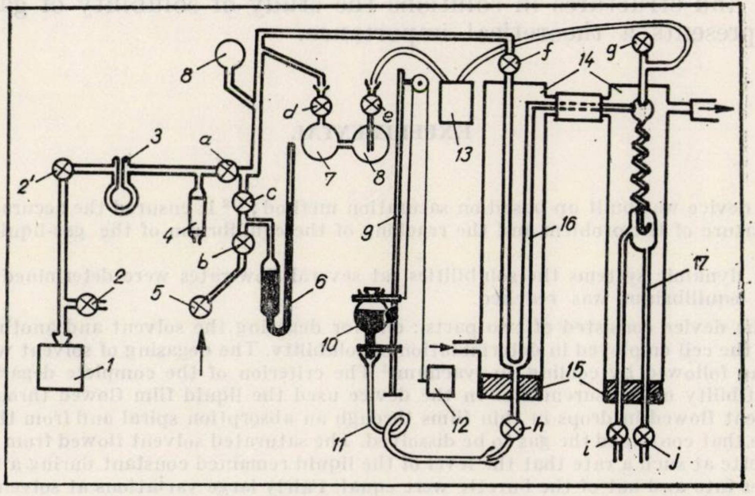

Fig. 1. – Setup for determination of gas solubility in liquids: 1 – vacuum pump; 2,2', 5 and a – j – stopcock; 3 – trap; 4 – vacuum transducer; 6 – mercury manometer; 7,8 – solvent vessels; 9 – support; 10 – mercury reservoire; 11 – rubber tube; 12 – motor; 13 – micropump; 14 – water thermostat; 15 – rubber stoppers. 16, 17 – liquid and gas burettes.

where T is the working temperature (in K)

c — the mole fraction of dissolved gas, x_2 was calculated by relation :

$$x_2 = \frac{LV_l^0}{RT} \tag{3}$$

TABLE 1

Variations of hydrogen solubility with temperature at atmospheric pressure

	t°C	L	α	$x_2 \times 10^4$
n-heptane	25	0.110 ±0.010	0.097 ±0.010	6.650 ±0.64
	40	0.126 ±0.016	0.100 ±0.006	7.400 ±0.39
	50	0.135 ±0.010	0.114 ±0.010	7.740 ±0.56
n-octane	25	0.098 ±0.003	0.090 ±0.003	6.524 ±0.21
	41.5	0.110 ±0.004	0.095 ±0.004	7.064 ±0.26
	51.5	0.121 ±0.016	0.102 ±0.013	7.581 ±0.37
n-nonane	25	0.095 ±0.003	0.086 ±0.008	6.925 ±0.65
	41.5	0.106 ±0.009	0.092 ±0.008	7.500 ±0.62
	52.5	0.113 ±0.003	0.095 ±0.002	7.850 ±0.19
n-decane	25	0.082 ±0.004	0.075 ±0.004	6.660 ±0.34
	41	0.091 ±0.008	0.079 ±0.007	7.040 ±0.66
	50	0.097 ±0.005	0.081 ±0.004	7.500 ±0.37
isooctane	26,5	0.112 ±0.010	0.102 ±0.010	7.602 ±0.20
	41.5	0.127 ±0.002	0.110 ±0.002	8.315 ±0.10
	50	0.134 ±0.010	0.113 ±0.010	8.610 ±0.20

where V_l^0 is the mole volume of pure solvent and R the constant of ideal gas $\left(\frac{\mathrm{l \cdot at}}{\mathrm{mole \cdot K}}\right)$ and T the absolute temperature (K).

To calculate the molar volume V_l^0 of pure solvent, the densities available in references [4,5] were employed.

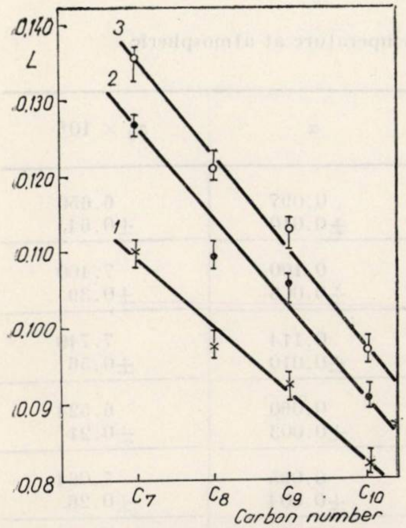

Fig. 2. — Variation of hydrogen solubility with the number of carbon atoms in the solvent, at 101.325 kPa (1 atm). 1—t = 25°C ; 2 — t = 40°C ; 3—t = 50°C.

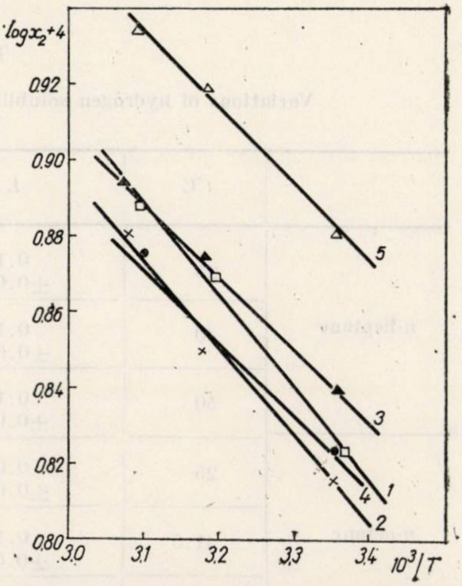

Fig. 3. — Logarithm of hydrogen solubility *versus* reciprocal of absolute temperature in *n*-heptane — *n*-decane series and isooctane : 1 — *n*-heptane ; 2 — *n*-octane ; 3 — *n*-nonane ; 4 — *n*-decane ; 5 — isooctane.

The results are listed in table 1. They were utilized to plot the variation of the hydrogen solubility with the number of carbon atoms in the solvent (Fig. 2) and the variation of the logarithm of hydrogen solubility *versus* the reciprocal of temperature (Fig. 3). The partial molar heats of solution of hydrogen in solvents were determined from the slopes of the least squares plots of log x_2 *versus* $1/T \cdot 10^3$.

TABLE 2

Partial molar heats of the hydrogen solution in solvents

Solvent	ΔH_s (cal/mol)
n-heptane	1170
n-octane	1068
n-nonane	883
n-decane	884
isooctane	950

One can conclude that:

– the solubility of hydrogen in *n*-paraffinic hydrocarbons decreases with the increase of the number of carbon atoms in the solvent molecule;

– the solubility of hydrogen in *n*-paraffinic hydrocarbons increases with temperature, which proves that the dissolution of hydrogen is an endothermal process;

– the solubility is higher in isoparaffinic hydrocarbons than in the corresponding *n*-paraffinic ones;

– the variation of the logarithm of hydrogen solubility with the reciprocal of thermodynamic temperature is linear and allows the calculation of enthalpies of dissolution.

REFERENCES

[1] T. J. Morrison and F. Billett, *J. Chem. Soc.*, **1948**, 2033.
[2] W. Hayduk and S. C. Cheng, *Canad. J. Chem. Eng.*, **48**, 93 (1970).
[3] D. A. Armitage, R. G. Linford and D. T. Thornhill, *Ind. Eng. Chem. Fundam.*, **17**, 362 (1978).
[4] J. Timmermans, "Physico-chemical Constants of Pure Organic Compounds" Elsevier Publishing Company, New York, 1950, p. 60—90.
[5] * * * Technical Data Book, Petroleum Refining, Second Edition 1970, American Petroleum Institute, Washington, D.C., 20006.
[6] I.U.P.A.C., "Solubility data series. vol. 5/6. Hydrogen and deuterium" — Pergamon Press, 1981.

Revue Roumaine de Chimie, 27, *5*, 615–619 (1982)

CATALYTIC HYDROGEN DISCHARGE BY CYCLOSERINE IN NICKEL ION CONTAINING PHOSPHATE BUFFER

LI QILONG*, C. LUCA, A. CĂLUȘARU and F. G. BĂNICĂ

National Institute of Chemistry, Spl. Independenței, No 202, 77208 Bucharest, Romania

Received September 16, 1981

The catalytic hydrogen discharge produced by cycloserine in the presence of Ni^{2+} and phosphate buffer was studied. In this media the amphoteric form of the cycloserine is predominant. The catalytic wave is of pre-sodium type in the both presence and absence of nickel ions, but in the last case it is considerably enhanced and better defined. The effect of several parameters on the wave height was studied. The results were interpreted considering the effect of electrolyte streaming on nickel ion transport in the range of pre-sodium wave.

Although the heterocyclic compound D-4-amino-3-isoxazolidone (cycloserine) is not a depolariser, it has an interesting polarographic behaviour, acting in simple or ligand form as catalyst for hydrogen discharge.[1,2] The most complex processes were found in cobalt containing solutions where a diffusion controlled and pre-sodium type catalytic waves are superimposed, forming a wave of Brdička type. This process was termed as "the superposition effect on catalytic hydrogen waves" since it is of particular importance in understanding the mechanism of the catalytic hydrogen discharge and especially the independence of the Brdička limiting current of the mercury reservoir height. This behaviour cannot be attributed to the kinetic character of the discharge, but to the composite character of the wave, although a protonation–deprotonation reaction occurs in the case of the catalytic hydrogen discharge. Indeed the diffusion component is increased at higher mercury reservoir height, while the pre-sodium component with a predominant surface character decreases in the same conditions.

In the presence of other ions such as Ni^{2+}, Cd^{2+}, Zn^{2+} and Cu^{2+} only a catalytic wave of pre-sodium type is formed. In a previous work [2] the properties of this polarographic wave were studied in ammonia buffer. The cycloserine is an amphoteric substance, and therefore in alkaline media such as ammonia buffer, the anionic form is predominant. In order to study the properties as catalyst of the cationic form it is necessary to use another buffer system.

The aim of the present work is to investigate the polarographic behaviour of the cycloserine in phosphate buffer containing Ni^{2+} ions.

EXPERIMENTAL PART

The cycloserine was of pure grade (about 98 %). The other substances were of analytical grade. A polarograph LP 7 e was used for recording the polarograms under nitrogen atmosphere. The polarographic cell has a calomel electrode as anodic compartment.

The capillary constants were : $t_1 = 4.60$ s and $m = 2.44$ mg s^{-1} in 0.025 M buffer, open circuit at $h = 50$ cm.

---

* On leave from Beijing Normal University, Dep. of Chemistry, China

EXPERIMENTAL RESULTS

1. Catalytic wave in phosphate buffer

In phosphate buffer containing cycloserine only, at pH = 6.8 a pre-sodium wave having $E_{1/2} = -1.79$ V is formed, which corresponds to the data published previously.[1] If a divalent ion such as Ni^{2+} or Cu^{2+} is present in the solution the wave height increases and becomes better defined (Fig. 1). This behaviour is similar with those found in ammonia buffer.[2] In the presence of metal cations only a small change of the half-wave potential can be observed. In Fig. 1 the effect of Ni^{2+} ions on the catalytic hydrogen wave of cycloserine is shown.

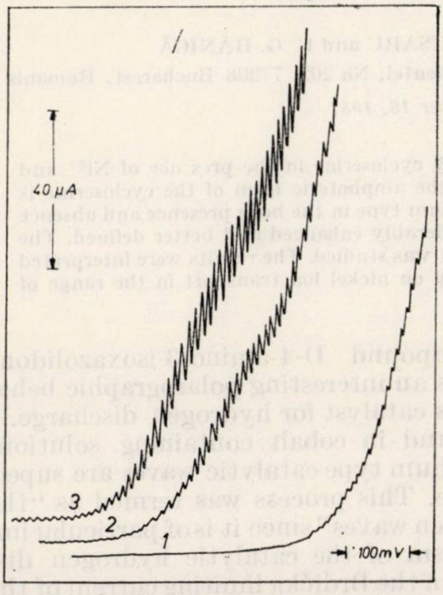

Fig. 1. — Catalytic hydrogen waves of cycloserine in phosphate buffer. 1 — 0.025 M $KH_2PO_4 - Na_2HPO_4$; 2 — as 1, + 10^{-3} M cycloserine ; 3 — as 2, + 10^{-3} M Ni^{2+}. Start potential, −1.50 V.

2. Effect of cycloserine concentration

The variation of the hydrogen catalytic wave as a function of the cycloserine concentration is shown in Fig. 2 in both the absence (1) and presence (2) of nickel ions (10^{-3}M). We can see that there is no linear relationship between the limiting current and the catalyst concentration, as in the general case of the catalytic current.[3] For higher concentrations of the catalyst the current tends toward a limiting value. Even at low Ni^{2+} ion concentration (10^{-3} M, Fig. 1, Curve 2) the catalytic current is considerable higher than in the case of the cycloserine alone (Fig. 1, Curve 1).

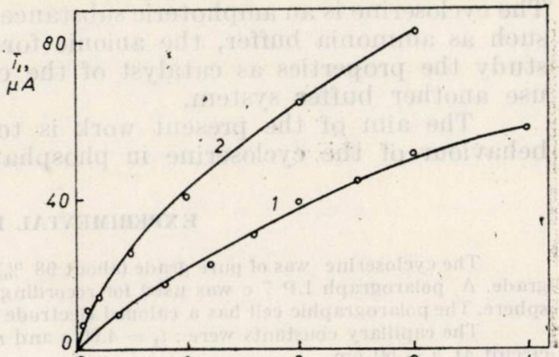

Fig. 2. — Variation of catalytic current as a function of cycloserine concentration. 1 — 0.025 M $KH_2PO_4 - Na_2HPO_4$; 2 — as 1, + 10^{-3} M Ni^{2+}.

3. Effect of nickel concentration

The general relationship between the catalytic currents and complexing metal concentration is a parabolic one.[1-3] However in the present case a linear relationship has been found for two cycloserine concentrations, a is shown in Fig. 3. Both lines have the same slope. Such a dependence has been previously observed by Březina and Kůtova for the pre-sodium wave of quinine, α-picoline and proteins.[4]

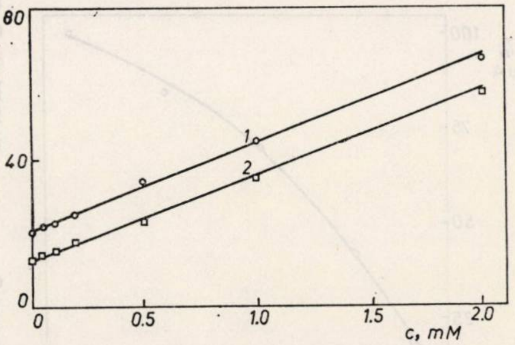

Fig. 3. — Influence of Ni^{2+} ion concentration on the catalytic wave height in 0.025 M KH_2PO_4—Na_2HPO_4. Cycloserine : 1—10^{-3}M; 2—5×10^{-4}M.

4. Effect of mercury reservoir height

The variation of the catalytic hydrogen wave produced by cycloserine in both the absence and presence of nickel ions as a function of the mercury reservoir height is shown in Fig. 4. In both cases a decrease of the wave height was found, which shows the influence of the adsorption as rate determining step in the overall process. This variation shows that the catalytic wave is of pre-sodium type.

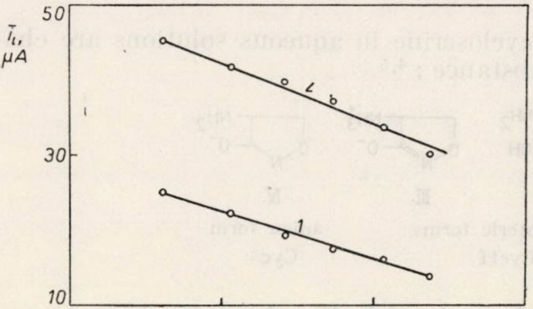

Fig. 4. — Variation of the catalytic current as a function of the square root of the mercury reservoir height in 0.025 M KH_2PO_4 — Na_2HPO_4 · Ni^{2+} concentration : 1 — 0 ; 2 — 10^{-3} M.

5. Effect of temperature

In the temperature range of 22—34°C the catalytic current displays a small increase, with a temperature coefficient of 2.9 %/°C. Compared with the alkaline media[2] this increase is much smaller. This behaviour is rather surprising since in both cases a protonation—deprotonation reaction occurs and the rate constant of this reaction varies visibly with temperature. In alkaline media it has been found that the effect of temperature depends on the cation present in solution.[2] Taking into account the results obtained here we can conclude that the effect of temperature depends also on the pH of the solution which modifies the complexation equilibria and is therefore rather complicated to be interpreted.

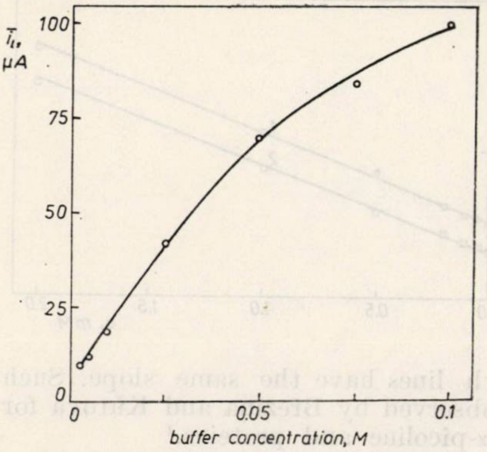

Fig. 5. — Influence of buffer capacity on the catalytic wave of cycloserine (10^{-3} M) in presence of Ni^{2+} (10^{-3} M).

6. Effect of buffer capacity

The effect of buffer capacity on the catalytic wave is shown in Fig. 5. The visible increase of the limiting current with the increase of the buffer capacity shows the important role played by the protonation reaction. This behaviour is very specific to catalytic hydrogen waves and has been found in other systems concerning cycloserine catalysis.

DISCUSSION

The equilibrium states of cycloserine in aqueous solutions are characteristic of an amphoteric substance: [4,5]

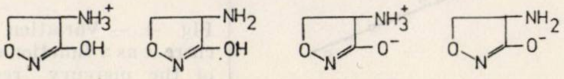

I II III IV

cation form $CycH_2^+$ amphoteric forms CycH anion form Cyc^-

We have shown[2] that in ammoniacal buffer the anion form is predominant. In the case of phosphate solution of pH = 6.8 the ratio of these forms is: [6,7]

$$[CycH_2^+] : [CycH] : [Cyc^-] = 1 : 230 : 52$$

Therefore the amphoteric form is the predominant one. Obviously the form III is easier adsorbable as compared with the anion form, since in the range of the catalytic wave the electrode surface is negatively charged. At the same time the amino-group is protonated and the proton excess can be neutralised within the catalytic wave.

The mechanism of catalytic hydrogen discharge in phosphate buffer containing cycloserine does not differ in an appreciable manner from the mechanism found in ammonia-buffer.[2] The adsorbtion of amphoteric molecules III on the electrode surface is followed by the electron transfer toward the proton bound to the amino-group. After this process the anion form appears and is readily desorbed. The proton transfer from $H_2PO_4^-$ HPO_4^{2-} ions to the anion form is produced afterwards in the bulk of the solution. The different surface activity of the reactant (amphoteric form) and product (anion form) owing to the charge-transfer reaction gives rise to electrolyte streaming as in the case of the maxima of first kind.[8]

If the solution contains some depolariser with half-wave potential less negative than the pres-sodium wave, the current produced by depolariser reduction is higher in the range of the catalytic wave due to addition of the convective to the diffusion component. Consequently, the current measured in the range of the pre-sodium wave increases with the increase of depolariser concentration, although the current corresponding to catalytic hydrogen discharge may remain constant.

In alkaline media cycloserine can be bound to metal ions giving complex compounds. Since cycloserine molecules in ligand form are transported to the electrode, the catalytic hydrogen current increases in the presence of metal ions. Therefore, a nonlinear dependence of total current on the metal ion concentration was observed.[2]

The principal peculiarity of the process occurring in phosphate buffer at $pH = 6.8$ is the linear dependence of catalytic wave height on the nickel ion concentration. This behaviour can be explained taking into account the low complex concentration in neutral medium. Therefore, no cycloserine transport proceeds toward the electrode and the catalytic hydrogen current proper does not change with the increase of nickel concentration.

At constant cycloserine concentration the tangential electrolyte velocity near the electrode surface is constant. Consequently the convective component of nickel reduction increases linearly if the nickel concentration is increased, giving, the dependence shown in Fig. 3.

The data above presented allow us to conclude that two effects are to be expected if some depolariser is added to systems showing pre-sodium wave : (1) enhancement of discharge current of depolariser due to convective transport in the range of catalytic wave ; (2) increase of proper catalytic hydrogen current produced by cycloserine transport in ligand form. Unlike the first effect which seems to be rather general, the second one is observed only if the complexation is possible.

REFERENCES

[1] A. Călușaru, *Electrochim. Acta*, **17**, 213 (1972).

[2] Li Qilong, C Luca, A. Călușaru and F. G. Bănică, *Rev. Roumaine Chim.*, **27**, (1982).

[3] A. Călușaru, *J. Electroanalyt. Chem.*, **15**, 269 (1967).

[4] M. Březina and M. Kůtova, *Coll. Czech. Chem. Comm.*, **30**, 4307 (1965).

[5] J. B. Neilands, *Arch. Biochem. Biophys.*, **62**, 151 (1956).

[6] A. P. Kondrateva, B. P. Bruns and G. S. Libinson, *Khim. Farm. Zhur.*, **5**, 38 (1971).

[7] E. Neusil and J. C. Breton, *Bull. Med. A.O.F.*, **3**, 149 (1958).

[8] R. Guidelli, *J. Electroanalyt. Chem.*, **100**, 711 (1979).

Revue Roumaine de Chimie, 27, 5, 621–628 (1982)

KINETIC STUDIES OF THE PYROLYSIS OF SOME ALKYLBENZENES

D. K. BANERJEE*, V. MATEI and V. VANTU
Faculty of Petroleum Technology and Petrochemistry,
Institute of Petroleum and Gases, Ploiești, Romania

Received September 21, 1981

Kinetic studies of the pyrolysis of some alkyl-benzenes and benzene have been made in a dynamic system. Their purpose is to obtain information about the behaviour of the thermal decomposition of the aromatics which can be useful for the petrochemical industries. The kinetic data are correlated with the structure of the hydrocarbons. The self-inhibition effect of the reactions is also discussed. The real global order of the reaction is calculated and found to be different from the widely accepted order of unity.

INTRODUCTION

The kinetic studies of the pyrolysis of aromatic hydrocarbons are of a great interest for the petrochemical industries, especially for determination of the behaviour of the thermal decomposition of petroleum fractions containing different amounts of aromatics. The quantity of aromatic hydrocarbons, may it be more or less, has technological implications that can be more and more important with the increase of the capacity of industrial installations.

A large volume of work has been devoted to studies of the thermal decompositions of paraffins and cycloparaffins.[1–7] Among the aromatics the pyrolysis of benzene [8–12] and toluene [13–18] has been extensively investigated whereas the higher members of the series have been less studied.[19] Among the earliest works on the pyrolysis of alkylbenzenes mention should be made of those of Szwarc [20] who used the toluene carrier technique. The procedure was later modified to aniline carrier technique by Kerr.[21] However, both approaches were aimed at obtaining bond-dissociation energies of the C—C character in higher alkylbenzenes.

In the present paper, we report our experimental results on the pyrolysis of some aromatics. An attempt has been made to correlate kinetic parameters with the structure of the alkylbenzenes chosen for study. The retardation effect of the reactions is also discussed. The mechanisms of different reactions are discussed on the basis of the formation rate of the main products, such as: ethylene, styrene and polycyclic aromatics, in the original work.[22]

---

* Present Address: Department of Chemistry, University of Ottawa, Ottawa, Ontario, Canada KIN 9B4

EXPERIMENTAL

Benzene, toluene, *o*-xylene and ethylbenzene were obtained from Merck Chemical Co. (W. Germany). The chemicals were used without further purification. n-Butylbenzene and t-butylbenzene were synthesized in the laboratory and the purification (99.2 %) was checked by IR spectroscopy and gaschromatography.

Experiments were carried out in a flow type apparatus, in gaseous phase. The tubular reactor was made of transparent quartz tube. The 22 cm long tube was divided into two parts by narrowing 1 cm of the length inbetween. The upper part was used as preheater and the lower part as the reaction zone, having a volume of 7.7 cm³. The temperature was recorded at different points of the reactor axis with a cromel-alumel thermocouple.

Experiments were performed within 600—700°C, at atmospheric pressure, in inert medium, at residence times ranging from 0.01 to 12 seconds. Oxygen free nitrogen was used as inert diluent in the molar ratio 1 : 1.

The gaseous and liquid products were collected separately and analysed by gaschromatographic method.

RESULTS

The distribution of products from the pyrolysis of aromatics varies as a function of reaction conditions and the structure of reactants. The gaseous products observed were : methane, ethane, propane, ethylene, propylene, butanes, butenes and butadienes. The major liquid components were : benzene, toluene and styrene. Some of the minor components observed were : methylstyrene, phenylbutenes, phenylbutadienes, tetraline, naphtalene, diphenyl, dibenzyl, stilbene and anthracene.

Kinetic calculations were done assuming that the reaction is homogeneous and of the first order as considered by several authors.[1–7] In the present work we have calculated the global rate constant for the disappearance of the aromatics, using a relation of the type given by Hougen and Watson :[23]

$$k = \frac{RT}{P(V/F)}\left(-x_A + (n_0 + n_{A0})\ln\frac{n_{A0}}{n_{A0} - x_A}\right) \qquad (1)$$

where,

k = the first order rate constant, (s^{-1})
R = gas constant, (atm/mol K)
T = temperature of the reactor, (K)
P = pressure, (atm)
V = volume of the reactor, (l)
F = flow rate of the total feed, (gm/s)
x_A = number of mole of reactant, A, converted per gram of feed, (mol/gm)
n_0 = total number of moles entered the reactor per gram of feed, (mol/gm)
n_{A0} = total number of moles of reactant A, entered the reactor per gram of feed, (mol/gm).

The calculated kinetic data for the pyrolyses of ethylbenzene and n-butylbenzene are presented in table 1. Figure 1 shows a plot based on eqn.(1) for benzene, toluene and *o*-xylene.

TABLE 1

First order rate constant values for the pyrolytic reactions of alkylbenzene at different temperatures

Temp. (°)	V/F (l·s/g)	n_0 (mol/g)	n_{A0} (mol/g)	conv. (/wt %)	x_T (mol/g)	k_1 (s^{-1})
A) 600	1.190	13.15	5.747	23.88	1.776	0.3294
600	3.298	13.85	5.511	48.89	2.713	0.2618
600	5.838	13.57	5.846	57.60	3.906	0.2147
600	10.823	13.23	5.937	75.10	4.883	0.1866
650	1.252	12.03	5.724	42.07	2.675	0.5904
650	3.298	12.58	5.811	66.89	3.986	0.4596
650	5.993	13.85	5.853	79.78	5.463	0.4514
650	11.675	13.53	5.891	94.95	5.720	0.4060
700	0.396	12.29	5.658	52.21	3.358	2.9138
700	0.585	12.64	5.495	63.65	3.924	2.8632
700	0.806	12.10	5.665	75.44	4.713	2.7996
700	1.571	13.49	5.864	93.59	5.566	2.6160
B) 600	1.46	14.12	8.71	21.19	1.845	0.1897
600	3.92	14.91	8.64	32.36	2.536	0.1003
600	11.50	13.21	7.59	50.84	4.116	0.0513
650	0.64	14.10	8.39	35.17	2.347	0.6165
650	1.11	14.20	8.69	43.27	3.759	0.5216
650	2.38	14.31	8.72	49.70	4.990	0.4012
650	5.60	14.24	8.48	67.31	5.034	0.2851
700	1.39	14.24	8.74	69.76	6.102	1.3256
700	3.31	14.32	8.84	85.53	7.561	0.8665
700	6.40	14.91	8.66	95.97	7.654	0.8410

A) n-Butylbenzene
B) Ethylbenzene

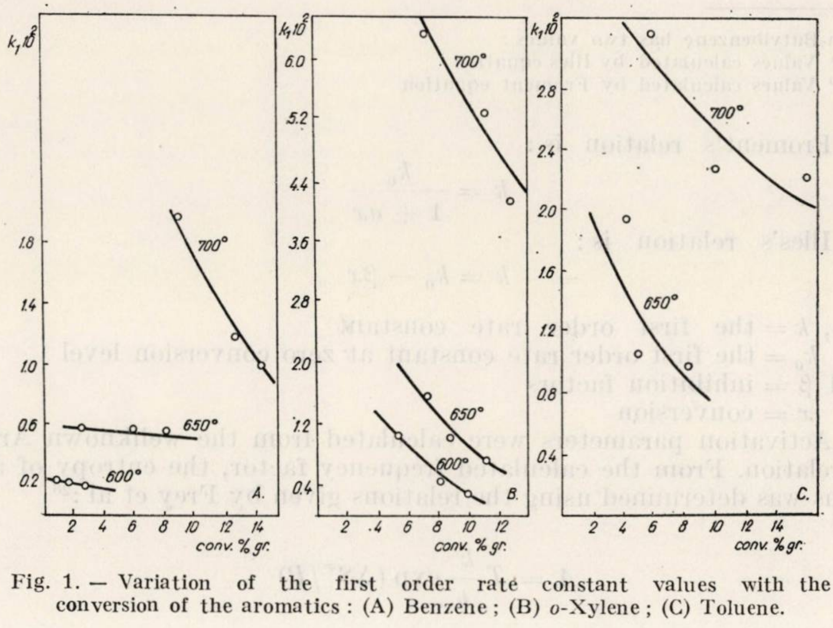

Fig. 1. — Variation of the first order rate constant values with the conversion of the aromatics : (A) Benzene ; (B) *o*-Xylene ; (C) Toluene.

The retardation effect of the pyrolytic reactions was determined by calculating the inhibition factor with the relations given by Buekens and Froment [24] and Illes. [25] The results are presented in table 2.

TABLE 2

Inhibition factor and the k_0 values for the pyrolysis of alkylbenzene

Compound	Temp. (°)	x	k (s^{-1})	k_0	Inhibition factor
Ethylbenzene	600	0.22	0.160		
		0.31	0.105	0.233[a]	0.373[a]
		0.51	0.045		
	650	0.35	0.58		
		0.44	0.51	0.890[a]	0.912[a]
		0.48	0.41		
	700	0.69	1.31		
		0.87	0.86	2.545[a]	1.839[a]
		0.96	0.83		
n-Butylbenzene	600	0.24	0.31		
		0.49	0.26	0.3932[a]	0.3097[a]
		0.57	0.21	0.3903[b]	0.9583[b]
		0.76	0.18		
	650	0.43	0.58		
		0.66	0.43	0.7667[a]	0.4281[a]
		0.78	0.45	0.9240[b]	1.4030[b]
		0.92	0.40		
	700	0.52	2.92		
		0.63	2.86	3.327[a]	0.7577[a]
		0.75	2.77		

---

n-Butylbenzene has two values :

[a] Values calculated by Illes equation

[b] Values calculated by Froment equation

Froment's relation is :

$$k = \frac{k_0}{1 + ax} \tag{2}$$

Illes's relation is :

$$k = k_0 - \beta x \tag{3}$$

where, k = the first order rate constant
k_0 = the first order rate constant at zero conversion level
a and β = inhibition factors
x = conversion

Activation parameters were calculated from the wellknown Arrhenius relation. From the calculated frequency factor, the entropy of activations was determined using the relations given by Frey et al :[26]

$$A = T\frac{k'}{h}\exp\left(\Delta S^{\neq}/R\right) \tag{4}$$

or,

$$\Delta S^{\neq} = 2.303R(\log A - (10 + \log 2.084\ T)) \qquad (5)$$

where,

$k'/h = 2.084 \times 10^{10}$ (universal frequency factor for unimolecular reactions)

$\Delta S^{\neq}$ = entropy of activation (e.u)

The calculated entropy values are presented in table 3.

TABLE 3

Activation parameters for pyrolytic reactions of alkylbenzenes

Alkylbenzenes	conv. (wt %)	E (kcal/mole)	log A	$\Delta S^{\neq}$ (e.u.)
Benzene	8.0	48.41	9.184	−18.75
Toluene	12.0	44.55	8.567	−21.57
o-Xylene	12.0	48.46	9.735	−16.24
Ethylbenzene	60.0	43.22	9.525	−17.19
n-Butylbenzene	60.0	43.14	10.292	−13.68
t-Butylbenzene	60.0	35.97	8.910	−22.50

An attempt has been made to calculate the global order of reaction for the pyrolytic reactions of the aromatics studied. The following Froment's relation was used on a computer programme to find the real order :[27]

$$k = \frac{1}{\tau C_0^{n-1}} \int_0^{x_A} \left(\frac{1 + \delta + \varepsilon_A x_A}{1 - x_A} \right)^n \mathrm{d}x \qquad (6)$$

where,

k = integral rate constant of order 'n'

C_0 = initial concentration, (mol/l)

τ = reaction time (sec)

δ = dilution factor (mole of diluent/mole or aromatics)

ε_A = expansion factor (total number of moles produced/total mole injected)

x_A = total convertion

n = global order of reaction.

The calculated global order of reaction is presented in table 4.

TABLE 4

Global reaction order for the pyrolytic reactions of aromatic hydrocarbons

Compound	Temp. (°C)	n	k $((\text{mol/l})^{1-n} \cdot \text{s}^{-1})$	% error
n-Butylbenzene	600	1.55	0.070	±5.3
	650	1.10	0.330	±8.5
	700	0.75	7.467	±4.8
Ethylbenzene	650	2.15	1.68×10^{-4}	±3.6
	700	1.55	0.1031	±5.2
t-Butylbenzene	600	1.30	0.0658	±5.5
Benzene	650	2.15	2.64×10^{-6}	±5.6

DISCUSSION

The kinetic data obtained from relation 1, presented in table 1 and Fig. 1, indicate that n-butylbenzene has the highest first order rate constant values (k_1), whereas benzene has the smallest ones under the same experimental conditions. Toluene and xylene have k_1 values only 2 or 3 times higher than benzene, whereas those of ethylbenzene and n-butylbenzene are more than 200 and 300 times respectively. The order of reactivity can be explained taking into consideration the rate determining step of the reactions, which is also the initiating reaction. The initiating reaction for benzene is due to the cleavage of $C_{aryl}-H$ bond, for toluene and cylene to C—H bond of the methyl group and for ethylbenzene and n-butylbenzene is due to βC—C bond from the alkyl group. This clearly indicates that the rate of β C—C bond-breaking is much faster than the C—H bond of the alkyl group.

The rate constant values of the aromatics increase with the increase of the length of the alkyl group, whereas they decrease in the case of branching the alkyl group from normal to tertiary butyl benzene. It has been observed that the k_1 value decreases by the substitution of the alkyl group in the aromatic nucleus from toluene to xylene and also from t-butylbenzene to *p*-ethyl t-butylbenzene.[22] It has also been observed that the reactivity of the xylene is lower than toluene at 650°C but higher at 700°C.

Figure 1 shows the variation of the first order rate constant with the conversion of aromatics. This clearly indicates that the rates of reactions are retarded with the increase of conversion. Such an effect was suggested by others [24,25] as a self-inhibition phenomenon in the case of the pyrolysis of aliphatic hydrocarbons. This is probably caused by the formation of olefins styrene and some polycyclics obtained in a large quantity (about 10—15 %). They are known to be good inhibitors of free radical reactions (3). The inhibition effect was studied by using the mathematical models proposed by Froment and Illes (the models suggested by authors for the pyrolysis of some paraffinic hydrocarbons) for the data of ethylbenzene and n-butylbenzene pyrolysis. The data presented in table 2 show on the whole, that the Illes equation is better fitted for both alkylbenzenes than that of Froment. In each of these methods, we concluded that the degree of inhibition is more prominent for ethylbenzene as compared to n-butylbenzene. The calculated values (β or a) show that the degree of inhibition increases with the increase of the reaction temperature.

Due to variation of k_1 values with conversion, the activation parameters were calculated at the same conversion level (table 3) for all the aromatics. The Arrhenius plots for the three aromatics are parallel

(Fig. 2) as observed by Szwarc under different conditions.[20b]

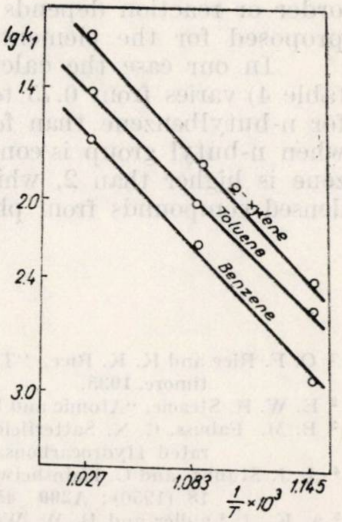

Fig. 2. — Arrhenius plot for the pyrolytic reactions of aromatics.

The activation energy values vary from 43 to 49 kcal/mole, for all the aromatics except t-butylbenzene (36 kcal/mole). The values reported here are lower than those in the literature, which may be due to the different experimental conditions and calculation methods used. For example, in this work the rate of the feed disappearance has been taken into consideration, but Szwarc (with toluene diluent) and Kerr (with aniline diluent) calculated the kinetic data from the rate of formation of the products, considering a stoichiometric relation. Our data show that this may not be true for all the conditions. Otherwise stated the results can also differ due to the different degrees of inhibition. However, we have obtained the value of activation energy for benzene (48.41 kcal/mole) quite close to the value reported by Mead[8] (50 kcal/mole), under different conditions.

As far as steric efects is concerned, as expected, the values of activation energy decrease with the increase of alkyl groups and also in the case of branching the group. A similar result was observed due to the substitution of the alkyl group in the aromatic nucleus. Owing to the variation of the k_1 values with the conversion it was observed that the E values also vary. A similar observation was made by Froment for lower hydrocarbons.

The calculated frequency factor (A) values for the alkylbenzenes vary between 10^8 and 10^{10} s^{-1}. These are smaller than the reported values.[20,21] Szwarc has calculated bond dissociation energies considering A factor 10^{13} s^{-1}.

The references in the literature concerning the correlation of the activation entropy values of hydrocarbon pyrolysis with the transtion state variations are rather scarce. Taking the Fery considerations into account, the low and negative values of the activition entropy are due to the less efficient recombination of the inactive benzyl radicals formed in the case of all the alkylbenzenes studied. This can be verified by our data, where benzene has a higher entropy value than toluene, because phenyl radical is more active than benzyl.

The entropy value increases with the increase of alkyl group length. This is in accordance with the Setser theory: [28] the entropy of activation increases as the moment of inertia of the alkyl group on the $C_{arm}-C_{alk}$ bond increases. Thus n-butylbenzene with a bulky butyl group has a higher entropy value as compared to the others. Similarly, *o*-xylene with two alkyl groups has a higher entropy value than its isomer, ethylbenzene.

In general, a first order relation is used for the pyrolytic reactions of hydrocarbons, but it can vary, as mentioned in the literature, from 0.5 to 2.0 depending on the reaction conditions.[6] Otherwise, the plausible order or reaction depends on the hypothesis of the reaction mechanism proposed for the elementary steps.[1]

In our case the calculated global order of reaction (presented in table 4) varies from 0.75 to 2 for alkylbenzenes. The *n* values are lower for n-butylbenzene than for ethylbenezne. The value is further lowered when n-butyl group is converted into t-butyl group. The *n* value for benzene is higher than 2, which may be due to the formation of polycondensed compounds from phenyl radicals.

REFERENCES

[1] O. F. Rice and K. K. Rice, "The Aliphatic Free Radicals", The Johns Hopkins Press, Baltimore, 1935.

[2] E. W. R. Steacie, "Atomic and Free Radical Reactions", Reinhold, New York, 1954.

[3] B. M. Fabuss, C. N. Satterfield and J. O. Smith, "Thermal Cracking of Pure and Saturated Hydrocarbons, Wilesy, 1964, Ch. IV.

[4] J. J. Stubbs and C. Hainshelwood, *Proc. Roy. Soc. Soc. (London)*, **A214** 20 (1952) ; **A201** 18 (1950) ; **A200** 458 (1950).

[5] a. K. J. Laidler and B. W. Wojciechowski, *Proc. Roy. Soc. (London)*, **A260** 103 (1961) ; **A270** 254 (1962) ; b. M. H. Back and K. J. Laidler, *Canad. J. Chem.* **44** 215 (1966).

[5] V. Vantu, R. Mihail, V. Măcriș and G. Ivănuș, "Pyrolysis of Hydrocarbons" (in Romanian Ed. Tehnică, Bucharest, 1980.

[7] G. C. Suciu, "Progress in Process and Principles of Hydrocarbons" (in Romanian), Ed. Technică, Bucharest, 1977.

[8] F. C. Mead and R. E. Burk, *Ind. Eng. Chem.* **27,** 299 (1935).

[9] S. Tomoya, W. Seiro and K. Taiseki, *Ing. Eng. Chem. Proc. Des. Dev.*, **10**, 305 (1971).

[10] R. N. Pease and J. M. Morton, *J. Amer. Chem. Soc.*, **55** 3190 (1933).

[11] S. H. Bauer and C. H. Aten, *J. Chem. Phys.*, **39** 1253 (1963).

[12] K. C. Hou and H. B. Palmer, *J. Phys. Chem.* **69** 863 (1965).

[13] T. Toyosaburo, S. Masakazu and T. Yoshiu, *Bull. Chem Soc. Japan,* **39** 1437 (1966).

[14] J. Takenaka, E. Harumi, M. Hitoshi and T. Makota, *Bull. Chem. Soc. Japan.* **40** 1613 (1967).

[15] D. Brackman, C. Delaunois and C. Nguyen, *Fuel. Proc. Tech,* **1** 57 (1977).

[16] A. L. Shapiro, V. A. Kuznetsov and D. N. Grinberg, *Naft.*, **17** 537 (1977).

[17] S. J. Price, *Canad. J. Chem.*, **40** 1310 (1962).

[18] J. R. Kershaw, *S. Afric. J. Chem.* **31** 15 (1978).

[19] G. M. Badger and T. M. Spotswood, *J. Chem. Soc.*, **1960**, 4420 ; 4427 **1960** ; 4437 **1960**.

[20] a. M. Szwarc, *J. Chem. Phys*, **16**, 128 (1948) ; **17** 431 (1949) ; **20** 403 (1952) ; b. M. Szwarc, *Chem. Rev.*, **47** 75 (1950).

[21] J. A. Kerr, *Chem. Rev.*, **66** 465 (1966).

[22] D. K. Benerjee. D. Sc. Thesis, Institute of Oil and Gas, Romania, 1980.

[23] O. A. Hougen and K. M. Watson, "Chemical Process Principles", Part III, Willey, New York, 1947.

[24] A. G. Bulkens and G. F. Froment, *Ind. Eng. Chem. Proc. Des. Dev.*, **7** 435 (1968).

[25] V. Illes, *Acta. Chim. ASH.*, 59 1229 (1969).

[26] H. M. Frey and R. Walsh, *Chem. Rev.*, **1968,** 103.

[27] G. F. Froment and Van de Steen, *A. I. Ch. E.I.*, **23** 93 (1977).

[28] D. W. Setser, *J. Chem. Soc.*, **1964,** 2477.

Revue Roumaine de Chimie, 27, 5, 629–633 (1982)

NEW VIBRATION MODES MADE EVIDENT IN THE IR SPECTRA OF A CLASS OF ALKYL ARYL ETHERS

M. IOVU [a] and ELIZA-MANUELA VASILESCU [b]

a) The Faculty of Pharmacy, Bucharest, Str. Traian Vuia nr. 6

b) The Petroleum and Gas Institute, Ploiești, Str. București, no. 39

Received July 2, 1980

Starting with the fact that C(Ar)–O and C(Alk)–O bonds have different force constants, we evidenced the duplication of the bands assigned to the antisymmetric and symmetric vibrations and consequently the appearance of four bands in the KBr pellets spectra of the non-symmetric ethers, instead of two as given in the IR literature.

In the IR literature most of the authors assign two bands to the C–O stretching vibration of the asymmetric ethers, coresponding to the symmetric and antisymmetric stretching vibrations. The strength of the C–O bonds from aromatic ethers being greater than that of the aliphatic ones, because of the p-π conjugation, the two bands are situated at different values of frequency, namely at 1285–1200 cm^{-1} for antisymmetric vibration and at 1075–1000 cm^{-1} for symmetric vibration of aromatic ethers, respectively at 1150 – 1070 cm^{-1} and at 940 cm^{-1} for aliphatic ethers.

Although in the case of non-symmetric ethers, especially in arylalkyl ethers, Ar–O–(Alk), where the two C–O bonds have different force constants, one should expect that the number of bands could be greater, corresponding to the stretching vibrations νC(Ar)–O and νC(Alk)–O In the IR literature there is only one band mentioned in the range 1275–1200 cm^{-1} for the antisymmetric vibration and another one in the range 1050–1000 cm^{-1} for the symmetric vibration of the etheric band (see for instance Flett, [1] Avram, [2] Rao [3]). At the same time, Scott [4] assigned for compounds such as dibenzylether only one band at 1099 cm^{-1} (νC–O bond) and for 1,2-diphenoxyethane two bands (1250 cm^{-1} for antisymmetric vibration and 1093 cm^{-1} for symmetric band); also Nakanishi [5] assigned for 2-methoxynaphtalene the band from 1255 cm^{-1} for antisymmetric vibration and that from 1020 cm^{-1} for symmetric vibration of etheric bond. Let us mention the following exception: Thachalmer and Leutner [6] assigned for compounds such as α-diphenoxy-alkanes one band to νC(Alk)–O.

RESULTS AND DISCUSSION

In order to verify the hypothesis of the existence of several bands for the C—O stretching vibrations of asymmetric ethers, we have synthesized a great number of aryl alkyl ethers, using an original method [7]. For these ethers we have recorded the IR spectra (as KBr pellets). The non-symmetric ethers which have been studied belong to the following three groups:

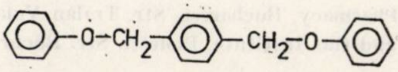

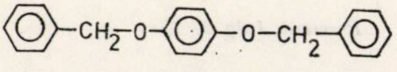

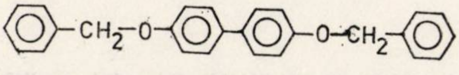

where the benzene rings may be or may not be substituted by methyl radicals. We have recorded also the spectra of some symmetric ethers, either alyphatic or aromatic (Table 1, entries 14—17) and we have made comparisons with the spectra of some similar compounds given by Szimanski. [8] The influence of the number and position of the substituents from the aromatic ring, on the position of the ν_{as} C—O—C in the IR spectra as well as ^{1}H—RMN spectra of these alkyl-aryl ethers has been previously studied by us. [9]

The range 1300—900 cm^{-1} from IR spectra, is given in Table 1 in detail for some of the studied ethers and is compared with the spectra of similar models in order to remove the bands assigned to the C—H or C—C bonds; at the same time, we have given the bands for symmetric ethers (aromatic and aliphatic). In Table 1 the height of segments is proportional with the intensity of the bands. The intensity of the etheric band, which is larger than other bands of spectrum in the same range (C—C bond and C—H bond) has facilitated its assignment.

All the ethers from Table 1 have three bands between 1300—1200 cm^{-1}, two of them (between 1210—1240 cm^{-1}) being very strong; the band from 1284—1264 cm^{-1} with a medium intensity can also be found in the non-etheric models, being assigned by Szimanski [8] to a deformation vibration mode of the C—H bond (β = C—H).

We assume that the first two bands are antisymmetric etheric bands. According to the force constants, we have assigned the band of higher frequency to the C(Ar)—O bond and the other one to the C(Alk)—O bond.

The C(Ar)—O bond is stronger in the compounds with two central benzene rings (entries 6—9, table 1) than in the ethers with only one central benzene ring (entries 1—3). This implies the shift of the C—O band to the higher frequencies (from 1239 cm^{-1} to 1230 cm^{-1}). One can see that in the sixth compound the oxygen is bound, for example, to the

TABLE 1

The bands in the range 1300–900 cm^{-1} from the IR spectra of the studied compounds*)

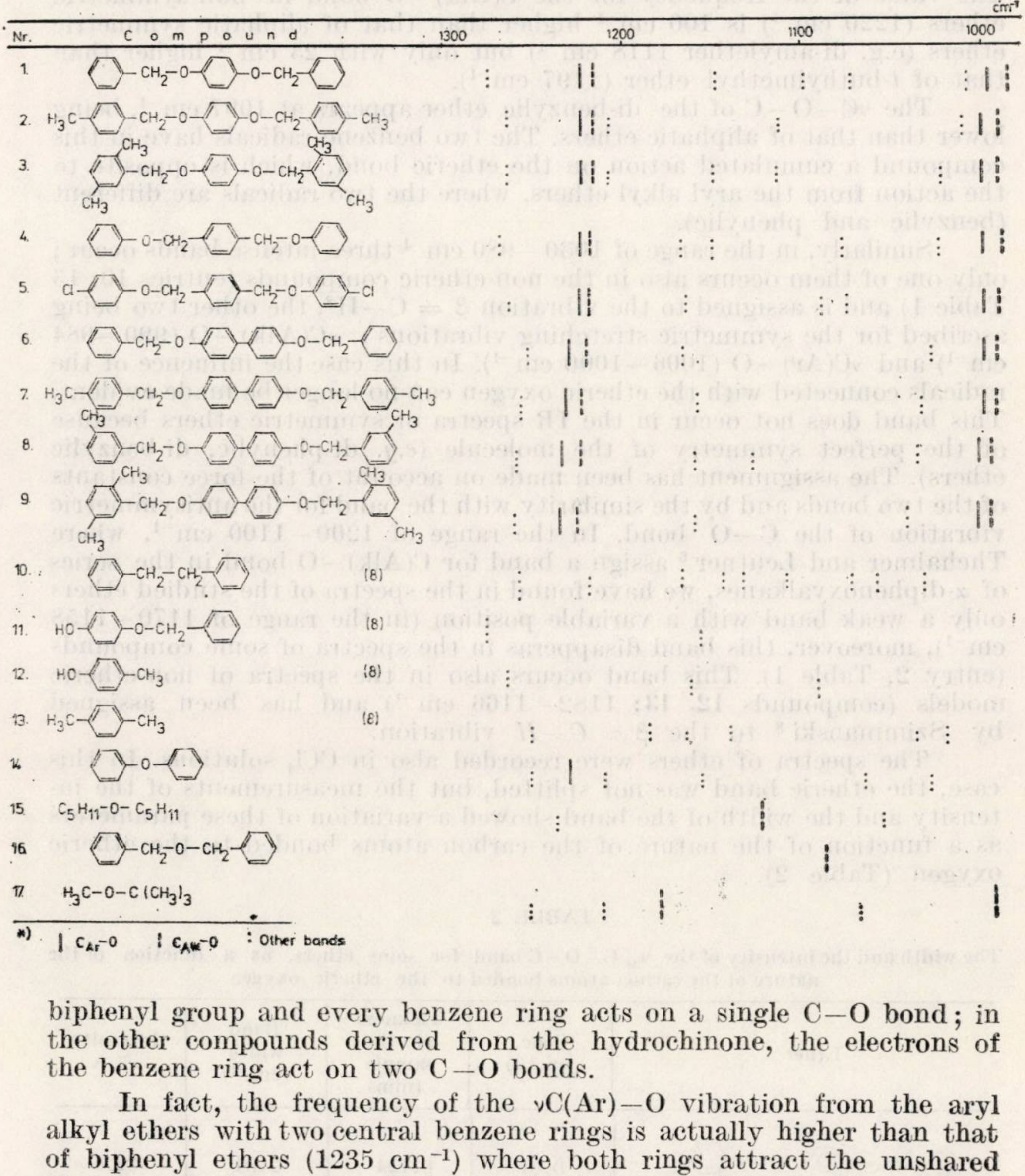

biphenyl group and every benzene ring acts on a single C—O bond; in the other compounds derived from the hydrochinone, the electrons of the benzene ring act on two C—O bonds.

In fact, the frequency of the νC(Ar)—O vibration from the aryl alkyl ethers with two central benzene rings is actually higher than that of biphenyl ethers (1235 cm^{-1}) where both rings attract the unshared electrons of the oxygen, their activity being annihilated. We conclude that the C(Ar)—O bond in non-symmetric ethers with two central benzene rings is stronger than that of biphenyl ether.

While the higher frequency band which has been assigned to the C(Ar)—O bond moves under the influence of the substituents of the aromatic ring, the value of the frequency C(Alk)—O remains constant. This is in accordance with the assignment of the antisymmetric vibration band to the C(Alk)—O bond, as in the case of lower frequency band. The value of the frequency for the C(Alk)—O bond in non-symmetric ethers (1220 cm^{-1}) is 100 cm^{-1} higher than that of aliphatic symmetric ethers (e.g. di-amylether 1118 cm^{-1}) but only with 23 cm^{-1} higher than that of *t*-buthylmethyl ether (1197 cm^{-1}).

The νC—O—C of the di-benzylic ether appears at 1097 cm^{-1}, being lower than that of aliphatic ethers. The two benzene radicals have in this compound a cumulated action on the etheric bond, which is opposite to the action from the aryl alkyl ethers, where the two radicals are different (benzylic and phenylic).

Similarly, in the range of 1030—980 cm^{-1} three intense bands occur; only one of them occurs also in the non-etheric compounds (entries 10, 13 Table 1) and is assigned to the vibration β = C—H[8], the other two being ascribed for the symmetric stretching vibrations: νC(Alk)—O (990—984 cm^{-1}) and νC(Ar)—O (1006—1000 cm^{-1}). In this case the influence of the radicals connected with the etheric oxygen can no longer be made evident. This band does not occur in the IR spectra of symmetric ethers because of the perfect symmetry of the molecule (*e.g.* di-phenylic, di-benzylic ethers). The assignment has been made on account of the force constants of the two bonds and by the similarity with the band for the antisymmetric vibration of the C—O bond. In the range of 1200—1100 cm^{-1}, where Thchalmer and Leutner [6] assign a band for C(Alk)—O bond in the series of α-diphenoxyalkanes, we have found in the spectra of the studied ethers only a weak band with a variable position (in the range of 1170—1158 cm^{-1}), moreover, this band disapperas in the spectra of some compounds (entry 2, Table 1). This band occurs also in the spectra of non-etheric models (compounds **12, 13**; 1182—1166 cm^{-1}) and has been assigned by Szimmanski [8] to the β = *C—H* vibration.

The spectra of ethers were recorded also in CCl_4 solutions. In this case, the etheric band was not splitted, but the measurements of the intensity and the width of the band showed a variation of these parameters as a function of the nature of the carbon atoms bonded to the etheric oxygen (Table 2).

TABLE 2

The width and the intensity of the ν_{as} C—O—C band for some ethers, as a function of the nature of the carbon atoms bonded to the etheric oxygen

Ether	Conc. (mol/l)	Tickness of the sample (mm)	Band width (cm^{-1})	Intensity % A
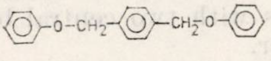	0.01	0.124	2.04	32.5
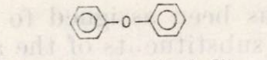	0.01	0.124	2.07	32.1
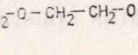	0.02	0.124	1.31	24.1
$CH_2-O-CH_2-CH_2-O-CH_3$	0.01	0.124	1.24	16.3

In this way, for two aliphatic carbon atoms bonded to the etheric oxygen, the width of the band is 1.24 cm^{-1} and increases to 1.31 for two aromatic carbon atoms. For the non-symmetric ethers the width of the band is unpredictably great, at almost a double value of 2.04–2.07 cm^{-1}.

The intensity of the band changes in the same direction 16.35 % A for aliphatic carbon; 24.1 for aromatic carbon and almost 32 % A for aryl alkyl ethers (table 2).

CONCLUSIONS

We have made evident for the aryl-alkyl ethers studied in this paper, the existence of four bands for etheric bond in the IR spectra of these substances in solid state; on the other hand we have noticed the broadening of the etheric band in the spectra recorded in liquid state. The duplication of the band in solid state might not be explained by special effects occurred as an alteration due to the technique of KBr pelleting; in the spectra of symmetric ethers, also in solid state, only one band can be observed.

The frequencies of the bands from some models (Table 1) prove that the second band of symmetric and antisymmetric vibration of C–O–C bond is not due to a substitution in the benzene ring. The rise of the two additional bands with a great intensity and in a constant position for the thirty examined ethers is another proof for the assignement of the four bands for the C–O–C bands in the IR spectra of aryl alkyl ethers.

Consequently, we have pointed out for the first time for non-symmetric ethers, the existence of four bands in the IR spectra, corresponding to the antisymmetric and symmetric stretching modes, which is similar to the case of the non-symmetric secondary amines (aryl alkyl amines [10]).

EXPERIMENTAL

The IR spectra have been recorded with a SPECORD 75–IR Carl-Zeiss Jena spectrometer in CCl_4 solution, pathlength 0.1 mm, concentration 0.1 % and in solid state as KBr pellets, concentration 0.1 %.

REFERENCES

[1] M. S. Flett, "Characteristic Frequencies of Chemical Groups in the Infrared", Elsevir, Amsterdam, 1963, p. 226.

[2] M. Avram and C. Mateescu, "Spectroscopia in I.R. Aplicații în chimia organică", Editura tehnică, București, 1966, p. 345.

[3] C. W. R. Rao, "Chemical Applications of IR Spectroscopy", Academic Press, New York, 1963, p. 193.

[4] I. R. Scott "Encyclopedic IR Spectra", Holden Day, San Francisco 1961, p. 276.

[5] K. Nakanishi, "Infrared Absorption Spectroscopy", Holden Day, San Francisco, 1962, p. 56.

[6] A. Thchalmer and F. Leutner, *Monatsh.* **29**, 630 (1952).

[7] M. Iovu, *Rev. Roumaine Chim.*, **16**, 1223 (1971).

[8] H. A. Szimaski, "Infrared Band Handbook", Plenum Press, New York, 1963, p. 89.

[9] M. Iovu, F. Chiraleu and E. M. Vasilescu, *Rev. Roumaine Chim.*, **25**, 1383 (1980).

[10] H. W. Thomppson, *Discuss. Faraday Soc.*, **9**, 222 (1950).

Revue Roumaine de Chimie, 27, 5, p. 635–643 (1982)

PYRIMIDINIUM-YLURES. III*

LES SYNTHÈSES DE QUELQUES PYRIMIDINIUM-YLURES CARBANION-DISUBSTITUÉS

FLORENTINA GEORGESCU[a], E. I. GEORGESCU[a], F. CHIRALEU[b]
et I. ZUGRĂVESCU[c]

a) Centre de Recherche. Rm. Vîlcea, 1, str. Uzinei, Roumanie
b) Centre de Chimie Organique, Bucarest, Spl. Independenței 202 A
c) Institut Polytechnique, Jassy, Roumanie

Reçu le 21 mars 1981

On a étudié les possibilités de synthèse des 4-phénylpyrimidinium-ylures carbanion-disubstitués et on a mis en évidence le caractère dipolaire de ces produits par la réaction de cycloaddition [3 + 2] dipolaire avec le diméthylacétylènedicarboxylate.

The possibilities for the synthesis of 4-phenyl-pyrimidinium-ylides with disubstituted carbanion are investigated. The dipolar structure of these compounds is proved by the [3 + 2] dipolar cycloaddition reactions with dimethylacetylenedicarboxylate.

La stabilité des ylures carbone-azote (**1**) dépend de deux facteurs importants : la structure de la composante cationique et la structure de la composante anionique.

Par rapport à d'autres ylures carbone-azote [1] les cycloimmonium-ylures, dont l'atome d'azote appartient à un cycle hétéroaromatique, présentent une augmentation de la stabilité moléculaire à la possibilité de délocalisation de la charge cationique sur le cycle hétéroaromatique.

Dans la série de 4-phénylpyrimidinium-ylures étudiés par nous [2], la possibilité de stabilisation de la charge cationique est agrandie par l'extension du système résonnant sur l'ensemble : le cycle hétéroaromatique et le cycle phénylique de la position 4.

Pourtant, on a constaté [2] que ce facteur est insuffisant pour assurer la stabilité de ces composés. La composante anionique a le rôle prédominant, la stabilité des 4-phénylpyrimidinium-ylures étant dépendant de la possibilité de délocalisation de la charge anionique. Ainsi, dans la série de 4-phénylpyrimidinium-1-phénacylures *p*-substitués, **2a – 2d**, le plus stable s'est révélé le 4-phénylpyrimidinium-1-(*p*-nitrobenzoyle)-

---

* Deuxième partie – voir réf. 7.

-méthylure (**2b**) par suite du puissant effet a électronattraction du groupement *p*-nitro-benzoyle.

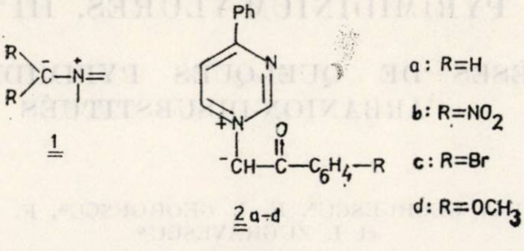

Schéma 1

Pour obtenir de nouveaux ylures stables en cette série, on a étudié les possibilités de synthèse des 4-phénylpyrimidinium-ylures avec deux substituants électronattractifs à l'atome de carbone ylurique.

Dans ce but on a essayé d'obtenir les 4-phénylpyrimidinium-ylures carbanion-disubstitués par le déhydrohalogénation des sels quaternaires en milieu alcalin,[3] méthode utilisée par nous [2] pour la synthèse des 4-phénylpyrimidinium-ylures carbanion-monosubstitués **2a** — **2d**. On peut obtenir les sels quaternaires disubstitués par traitement de la 4-phénylpyrimidine aux dérivés α-halogénés substitués par deux groupements électronattractifs, à l'atome de carbone.

Ainsi, par la réaction de 4-phénylpyrimidine **3** avec le bromomalonate d'éthyle on a obtenu le bromure de 1-dicarbéthoxy-4-phénylpyrimidinium (**4**) qui, par déhydrobromuration en milieu alcalin, a conduit à 4-phénylpyrimidinium-1-dicarbéthoxyméthylure (**5**).

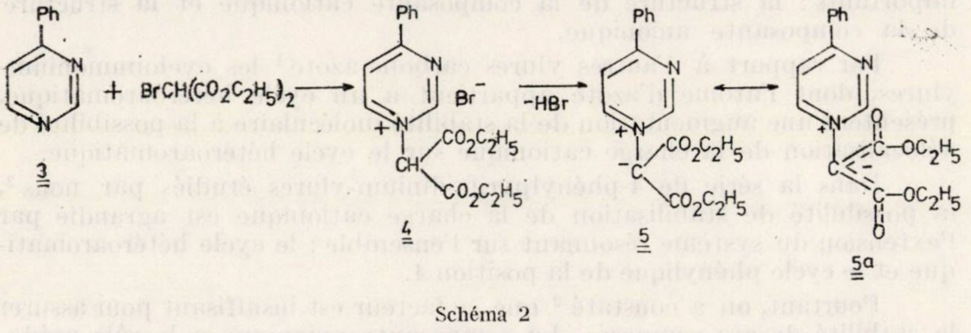

Schéma 2

La réaction de la 4-phénylpyrimidine (**3**), avec d'autres dérivés α-halogénés disubstitués comme le bromocyanoacétate d'éthyle et le bromomalonodinitrile a conduit au bromhydrate de 4-phénylpyrimidine (**6**). Dans la réaction de la 4-phénylpyrimidine (**3**) avec le bromocyanoacétate d'éthyle on a obtenu le bromhydrate de 4-phénylpyrimidine (**6**) et le 1,2-dicyano-1,2-dicarbéthoxyéthylène (**8**). L'apparition du composé

8 est dûe probablement à la formation du cyanocarbéthoxycarbéne **7** qui se stabilise par dimérisation.

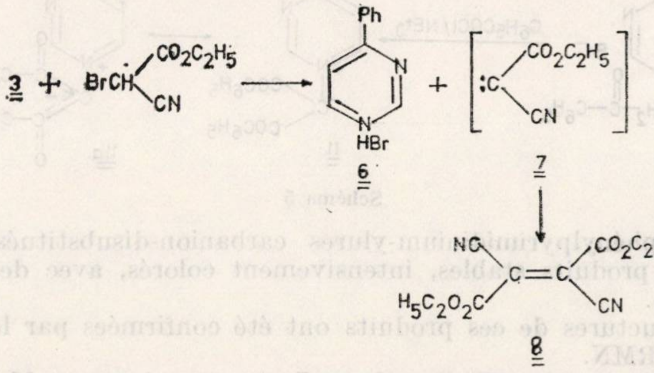

Schéma 3

Les difficultés rencontrés dans la quaternisation de la 4-phénylpyrimidine (**3**) avec des dérivés α-halogénés disubstitués nous ont déterminé à recourir à d'autres méthodes pour la synthèse de ces ylures.

Ainsi, le 4-phénylpyrimidinium-1-dicyanméthylure (**9**) a été obtenu par la réaction de 4-phénylpyrimidine (**3**) avec le tétracyanoéthylèneoxyde, méthode utilisée par Rieche [4] et Linn [5] pour la synthèse du pyridinium-dicyanméthylure.

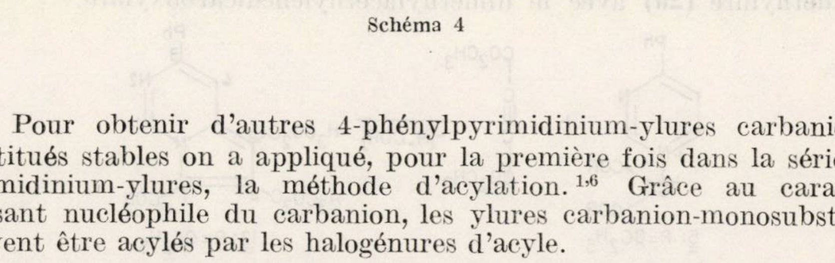

Schéma 4

Pour obtenir d'autres 4-phénylpyrimidinium-ylures carbaniondisubstitués stables on a appliqué, pour la première fois dans la série des pyrimidinium-ylures, la méthode d'acylation. [1,6] Grâce au caractère puissant nucléophile du carbanion, les ylures carbanion-monosubstitués peuvent être acylés par les halogénures d'acyle.

Par la réaction du chlorure de benzoyle avec le 4-phényl-pyrimidinium-1-benzoyle-méthylure (**2a**), obtenu «in situ» dans du bromure de 1-phénacyle-4-phénylpyrimidinium (**10**) en présence de triéthylamine, on a obtenu le 4-phénylpyrimidinium-1-dibénzoylméthylure (**11**).

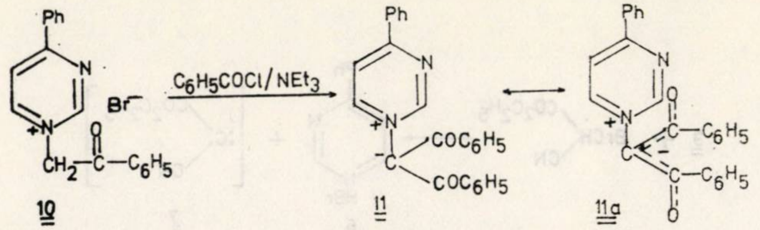

Schéma 5

Les 4-phénylpyrimidinium-ylures carbanion-disubstitués **5**, **9** et **11** sont des produits stables, intensivement colorés, avec des points de fusion élevés.

Les structures de ces produits ont été confirmées par les spectres IR et ^1H-RMN.

Ainsi, les spectres IR des ylures **5** et respectivement **11** présentent les bandes d'absorption correspondant aux groupements carbonyle à 1590 cm^{-1} et respectivement 1620 cm^{-1}.

Dans le spectre IR du 4-phénylpyrimidinium-1-dicyan-méthylure (**9**) on remarque les deux bandes d'absorption correspondant aux groupements cyan à 2190 cm^{-1} et 2145 cm^{-1}.

Les spectres IR mettent en évidence le déplacement des bandes d'absorption des groupements carbonyle, resp. cyano, aux fréquences plus basses que leurs valeurs normales. Ces déplacements pourraient indiquer l'extension de la charge anionique conformément aux structures **5a**, **9a** et **11a** qui pourraient expliquer les stabilités de ces composés.

Les spectres ^1H-RMN des produits **5**, **9** et **11** confirment les structures des ylures carbanion-disubstitués.

Le caractère dipolaire de ces produits a été démontré par la participation directe des ylures **5**, **9** et **11** réactions de cycloaddition [3 + 2] dipolaires.

Par la réaction des ylures **5** et **11** avec le diméthylacéthylènedicarboxylate, on a obtenu les dérivés pyrrolo [1,2–c] pyrimidiniques **12** et **13**. Ces produits sont identiques avec les produits obtenus par la réaction de cycloaddition [3 + 2] dipolaire des 4-phénylpyrimidinium-1-carbéthoxyméthylure ($\mathbf{2}: R = OC_2H_5$) et 4-phénylpyrimidinium-1-dibénzoylméthylure (**2a**) avec le diméthylacéthylènedicarboxylate. [7]

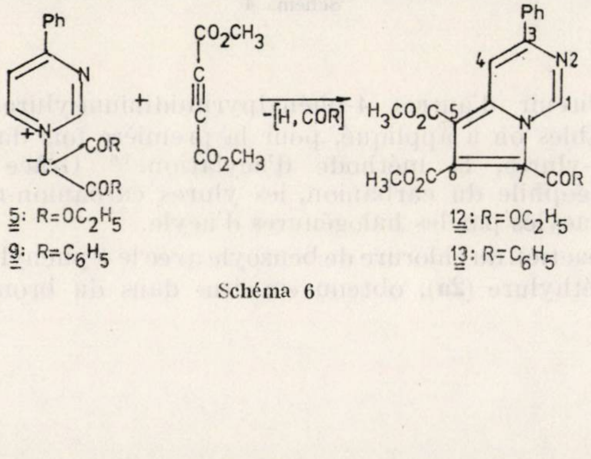

Schéma 6

Les réactions de cycloaddition des ylures **5** et **11** se produisent par élimination d'un substituant du carbanion, comme dans le cas d'autres cycloimmonium-ylures carbanilon-disubstitués.[5,6,8]

La réaction du 4-phénylpyrimidinium-1-dicyanométhylure (**9**) avec le diméthylacéthylènedicarboxylate a conduit au 2-phényl-6-cyano-7,8-dicarbométhoxypyrrolo [1, 2-a] pyrimidine (**14**). L'adduct **14** a une structure similaire au structure d'adduct obtenu[9] par la réaction du 4-méthoxypyrimidinium-1-dicyanméthylure avec le diméthylacétylènedicarboxylate. La réaction se produit dans ce cas aussi par élimination d'un groupement cyano.

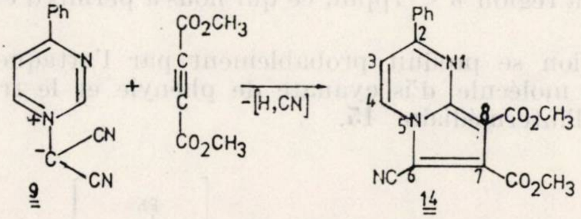

Schéma 7

La structure du cycloaduct **14** a été prouvée par les analyses chimiques et par les spectres IR et ^1H-RMN.

Le spectre IR présente une bande d'absorption forte à 2220 cm^{-1} caractéristique au groupement cyano et deux bandes d'absorption à 1710cm^{-1} et à 1730 cm^{-1} correspondant aux deux groupements carbonyle.

Le spectre ^1H-RMN présente deux signaux sous forme de singulets aux déplacements chimiques très rapprochés ($\delta = 4{,}21$ ppm et $\delta = 4{,}28$ ppm) correspondant aux groupements carbométhoxyliques. Le signal du proton H—4 apparaît sous forme d'un doublet avec la constante de couplage $J_{3,4} = 7{,}0$ Hz, caractéristique à un couplage vicinal des protons H—3 et H—4.

Le comportement différent de l'ylure **9** vis-à-vis des ylures **5** et **11** dans la réaction avec le diméthylacéthylènedicarboxylate n'a pas pu être encore expliqué. L'accumulation des données contribuera à l'élucidation de ce problème.

Pour obtenir de nouveaux ylures carbanion-disubstitués stables nous avons étudié la réaction des 4-phénylpyrimidinium-ylures carbanion-monosubstitués, **2a** —**2d**, avec l'isocyanate de phényle.

L'isocyanate de phényle réagit avec les cycloimmoniumylures de deux manières. Dans certains cas [10,11] on a isolé les produits de cycloaddition de l'ylure à double liaison $>C=N-$ de l'isocyanate de phényle et en d'autres cas [12,13] on a obtenu de nouveaux ylures carbanion-disubstitués.

Les 4-phénylpyrimidinium-ylures **2a** — **2d** réagissent avec l'isocyanate de phényle conduisant aux produits jaunes, très stables **16a** — **16d**.

En tenant compte des analyses chimiques et des spectres IR, ^1H-RMN et UV, on a attribué les structures **16a** — **16d** à ces produits et on a exclu les structures **17a** — **17d**.

Ainsi, les spectres IR des produits **16a — d** présentent entre 2910—3100 cm^{-1} les bandes d'absorption correspondant aux groupements NH amidiques et deux bandes à 1690—1705 cm^{-1} et 1605—1625 cm^{-1}, correspondant aux vibrations des groupements $C=O$ amidiques et respectivement cétoniques. L'une des bandes amidiques est superposée à la bande du groupement cétonique. Le déplacement de ces bandes vers des longueurs d'onde plus élevées que leur valeur normale nous indique un amoindrissement de la constante de force de la liaison sous l'influence de la charge anionique.

Les spectres ^1H-RMN des produits obtenus ne présentent pas de signaux dans la région $\delta < 7$ppm, ce qui nous a permis d'exclure la structure **17**.

La réaction se produit probablement par l'attaque du carbanion d'ylure sur la molécule d'isocyanate de phényle et le transfert 1,3 de proton dans l'intermédiaire **15**.

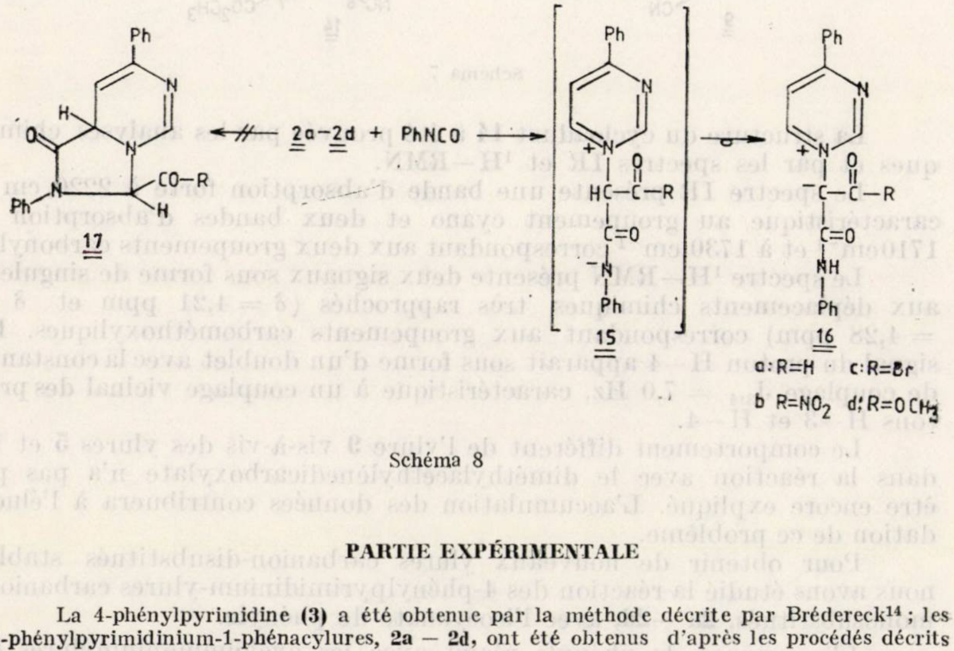

Schéma 8

PARTIE EXPÉRIMENTALE

La 4-phénylpyrimidine **(3)** a été obtenue par la méthode décrite par Brédereck[14] ; les 4-phénylpyrimidinium-1-phénacylures, **2a — 2d**, ont été obtenus d'après les procédés décrits dans un travail antérieur. [2]

Les points de fusion ne sont pas corrigés. Les spectres ^1H-RMN ont été enregistrés sur un spectromètre VARIAN A—60A et les spectres IR sur un spectromètre Perkin-Elmer 621.

Le bromure de 1-méthyldicarbéthoxy-4-phényl-pyrimidinium (4)

A une solution de 3,12 g (20 mmoles) 4-phénylpyrimidine **(3)** dans 25 ml d'acétonitrile ou benzène, on ajoute 3,35 ml (20 moles) bromomalonate d'éthyle. On laisse le mélange pendant 7 jours à le température ambiante, en agitant de temps en temps. On filtre et on recristallise le produit obtenu dans du méthanol ; p.f. = 139—142°C (rend. 60 %). Analyse $C_{17}H_{19}N_2O_4Br$: *calculé* : C 51,64 ; H 4,55, N 7,08 % ; *trouvé* : C 51,9, H 4,44, N 7,02 %.

Spectre IR (KBr) : 1740 cm^{-1} et 1725 cm^{-1} ($\nu_{C=O}$ estèrique)

Spectre ^1H-RMN (CF_3COOH, δ, ppm) ; 1,40 et 1,46, 2 tr., 6 H, 2 CH_3 des groupements carbéthoxy ; 4,40 et 4,48, 2 q, 4 H, 2 CH_2 des groupements carbéthoxy ; 5,80, s, 1 H, CH lié de l'atome d'azote ; 7,70−8,70, m, 6 H, les protons du groupement phényl + H−5 ; 9,10,d, 1 H, H−6 ($J_{5,6}$ = 7,0 Hz) ; 9,60, s, 1 H, H−2.

4-Phénylpyrimidinium-1-dicarbéthoxymèthylure (5)

A une solution de 3,95 g (10 mmoles) de bromure de 1-méthyldicarbétoxy-4-phénylpyrimidinium **(4)** dans 50 ml d'éthanol-eau (1 :1) on ajoute, sous agitation et refroidissement, 1,5 ml de solution de NaOH 1 N dans l'eau. On continue l'agitation pendant 30 minuits et on filtre le produit. On obtient 2,6 g de produit rouge ; p.f. = 173−175°C. *Analysé* : $C_{17}H_{18}N_2O_4$: *calculé:* C 64,96, H 5,73, N 8,92% ; trouvé : C 64,9, H 5,68, N 9,05 %.

Spectre IR (KBr) : 1590 cm^{-1} ($\nu_{C=O}$ estérique).

Spectre ^1H-RMN ($CDCl_3$, δ, ppm) ; 1,30, tr, 6 H, 2 CH_3 des groupements carbéthoxy ; 4,25, q, 4 H, 2 CH_2 des groupements carbéthoxy ; 7,50−7,75, m, 3 H, H−3′, H−4′ et H−5′ du groupement phényle de la position 4 ; 8,05−8,36, m, 3 H, H−2′, H−6′ du groupement phényle de la position 4 + H−5 ; 8,90, d.d., 1 H, H−6 ($J_{5,6}$= 7,0 Hz ; $J_{2.6}$ = 1,5 Hz) ; 9,26, d., 1 H, H−2.

La réaction de la 4-phénylpyrimidine (3) avec le bromocyanoacétate d'éthyle

A une solution de 3,12 g (20 mmoles) 4-phénylpyrimidine **(3)** dans 20 ml benzène on ajoute 2,4 ml (20 mmoles) de bromocyanoacétate d'éthyle. On agite 6−8 heures. On laisse 8−10 jours à la température ambiante, sous agitation occasionnelle pendant qu'une précipitatation d'un produit jaune se produit. On obtient 1,5 g de bromohydrate de 4-phébylpyrimidine **6** ; p. f. = 171−173°C. Analyse $C_{10}H_9N_2Br$: *calculé* : 50,63 ; H 3,80, N 11,81, Bn. 33,71 %, trouvè : C 51,02, H 3,53, N 11,95, Br 34,2 %.

Le traitement de la suspension de **6** dans l'eau avec une solution aqueuse de K_2CO_3 10 % produit une effervescence ; dans la solution précipite la 4-phénylpyrimidine **(3)**.

1, 2, Dicyano-1,2-dicarbéthoxyéthylène **(8)**. Après la séparation du bromohydrate de 4-phénylpyrimidine **6** on a chassé sous vide le benzène jusqu'à ce qu'on arrive à un volume de 5 ml. Pendant le refroidissement précipitent des cristaux aciculaires. Après recristalisation en éthanol on obtient 1,3 g de 1,2-dicyano-1,2-dicarbéthoxythylène **(8)** ; p.f.= 118−120,5°C[15]. Le mélange avec un échantillon original de 1,2-dicyano-1,2-dicarbéthoxyéthylène[15] présente le même point de fusion. Analyse $C_{10}H_{10}N_2O_4$ *calculé* : C 54,05, H 4,50, N 12,61 % ; *trouvé* : C 54,25, H 4,6 6,N 12,70 %.

Spectre IR (KBr) : 2270 cm^{-1}($\nu_{C\equiv N}$) ; 1770 cm^{-1} ($\nu_{C=O}$) ; 1600^{-1}($\nu_{C=C}$)

Spectre ^1H-RMN ($CDCl_3$, δ, ppm) : 1,44 et 1,48, 2 tr., 6 H, 2 CH_3 des groupements carbéthoxy ; 4,52 et 4,59, 2 q, 4 H, 2 CH_3 des deux groupements carbéthoxy.

4-Phénylpyridinium-1-dicynaométhylure (9)

A une solution de 7,8 g (50 mmoles) 4-phènylpyrimidine dans 20 ml tétrahydrofuranne on ajoute, goutte à goutte sous agitation et refroidissement (glace), une solution de 3,6 (25 mmoles) tétracyanoéthylèneoxyde[5], fraîchement préparée, dans 10 ml tétrahydrofuranne. On continue l'agitation pendant 2 heures à la température ambiante et on laisse en repos durant la nuit. On filtre le produit formé et on recristallise dans l'acétonitrile. On obtient 8, 8 g de produit jaune ; p.f. = 285 − 287°C. Analyse $C_{13}H_8N_4$, *calculé* : C 70,9 ; H 3,6, N 25,4 % ; *trouvé* : C 71,0, H 3,8, N 25,34 %.

Spectre IR (KBr) : 2145 cm^{-1}, 2190 cm^{-1} ($\nu_{C\equiv N}$).

Spectre ^1H-RMN (DMSO d_6, δ, ppm) : 7,51−7,80, m, 3 H, H−3′, H−4′ et H−5′ du groupement phényle de la position 4, 8m16−8,50, m, 3 H, H−2′, H−6′ du groupement phényle de la position 4 + H−5 ; 8,80, d.d., 1 H. H−6 ($J_{5.6}$ = 7,0 Hz, $J_{2.6}$ = 1,5 Hz) ; 9,26, d, 1 H, H−2.

4-Phénylpyrimidinium-1-dibenzoylméthylure (11)

A une solution de 3,55 g (10 mmoles) de bromure de 1-phénacyle-4-phénylpyrimidinium **(10)** dans 20 ml de chloroforme on ajoute 1,2 ml (10 mmoles) de chlorure de benzoyle et sous agitation et refroidissement on ajoute 3 ml (22 mmoles) de triéthylamine. On laisse le mélange pendant 5 jours à la température ambianté, après, on le porte à reflux pendant 16 heures. On chasse une partie du solvant et on filtre le précipité formé. On lave sur la filtre à l'eau pour éliminer le mélange de chlorhydrate et bromohydrate de triéthylamine. On obtient 2,5 g de produit orange au p.f. = 238–240°C (benzène) ; rend. 66 %. Analyse $C_{25}H_{18}N_2O_2$ *calculé* : C 79,36, H 4,76, N 7,40 ; *trouvé* : *C* 79,45, H 4,70, N 7,56 %.

Spectre IR (KBr) : 1620 cm^{-1} ; 1595 cm^{-1}

Spectre ^{1}H–RMN ($CDCl_3$, δ, ppm) : 6,95 – 7,80, m, 13 H, les protons aromatiques ; 8,05 – 8,43, m, 3 H, H–2′, H–6′ du groupement phényle de la position 4 + H–5 ; 9,02, d.d., 1 H, H–6 ($J_{5,6}$ = 7, 0 Hz, $J_{2,6}$ = 1,0 Hz) : 9,48, s.1., .1 H, H–2.

Les réactions des ylures 5, 9 et 11 avec diméthylacétylènedicarboxylate ; procédé général

A une suspension de 10 mmoles ylure **5**, respectivement **11**, dans 50 ml d'acétonitrile, on ajoute 11 mmoles (1,35 ml) diméthylacétylènedicarboxylate. On agite le mélange pendant 8–10 heures à la température ambiante, après, on le porte à reflux pendant 15–16 heures. On chasse la pluspart du solvant, on reprend avec un peu d'éthanol, on laisse au réfrigérateur pour 2–3 heures et on filtre le produit obtenu.

3-Phényl-5,6-dicarbométhoxy-7-carbéthoxypyrrolo[1,2-c]-pyrimidine **(12)** : cristaux blancs avec p.f. = 175 – 176°C (dans du méthanol) ; rend. 36 %. Analyse $C_{20}H_{20}N_2O_6$, *calculé* : C 62,82, H 4,71, N 7,32 % ; *trouvé* ; C 62,76, H 4,69, N 7,41 %.

Spectre IR (KBr) : 1735 cm^{-1}, 1715 cm^{-1}, 1705 cm^{-1} ($\nu_{C=O}$).

Spectre ^{1}H-RMN (CF_3COOH, δ, ppm) : 1,41, tr., 3 H, CH_3 du groupement carbéthoxy ; 4,00 et 4,08, 2 s, 6 H, 2 CH_3 des groupements carbométhoxyliques ; 4,46, q, 4 H, CH_2 du groupement carbéthoxy ; 7,46–7,68, m, 3 H, H–3′, H–4′ et H–5′ du groupement phényle de la position 3 ; 8,11–8,33, m, 2 H, H–2′ et H–6′ du groupement phényle de la position 3 ; 8,59, d, 1 H, H–4 ; 10, 28, d, 1 H, H–1 ($J_{1,4}$ = 1,2 Hz).

3-Phényl-5,6-dicarbométhoxy-7-bénzoyloyrrolo[1,2-c]-pyrimidine **(13)** : cristaux blancs au p. f. = 259–261°C (dans du chloroforme) ; rend. 33 %. Analyse : $C_{24}H_{18}N_2O_5$ *calculé* : C 69,56, H 4,34, N 6,76 ; *trouvé* : C 69,03, H 4,12, N 6,51 %.

Spectre IR (KBr) : 1730 cm^{-1} et 1700 cm^{-1}($\nu_{C=O}$ estérique), 1620 cm^{-1}($\nu_{C=O}$ cétonique).

Spectre ^{1}H–RMN (CF_3COOH, δ, ppm) : 3,62 et 4,18, 2 s, 6 H, 2 CH_3 des deux groupements carbométhoxylique ; 7,60–8.16, m, 10 H, les protons aromatiques ; 9,00, s.l., 1 H, H–4 ; 11, 39, s. l., 1 H, H–1.

2-phényl-6-cyan-7,8, dicarbométhoxpyrrolo [1,2-a]-pyrimidine **(14)** : cristaux blancs, au p.f. = 207–208°C (dans du méthanol) ; rend. 46 %. Analyse $C_{18}H_{13}N_3O_4$: *calculé* : C 64,48, H 3,88, N 12,54 % ; *trouvé* : C 64,21, H 4,10 ; N 12,66 %.

Spectre IR (KBr) : 2220 cm^{-1}($\nu_{C\equiv N}$), 1710 cm^{-1} et
1730 cm^{-1} ($\nu_{C=O}$ estérique)

Spectre ^{1}H–RMN (GF_3COOH, δ, ppm) : 4,21 et 4,27, 2 s, 6 H, 2 CH_3 des groupements carbométhoxyliqués, 7,76–8.41, m, 6 H, les protons du groupement phényle + H–3 ; 9,45, d, 1 H, H–4 ($J_{3,4}$ = 7,5 Hz).

La réaction des 4-phénylpyrimidinium-1-phénacylures 2a–2d avec isocyanate de phényl ; procédé général

A une suspension de 10 mmoles 4-phénylpyrimidinium-1-phénacylure, **2a** – **2d**, obtenu « in situ » par le traitement des sels quaternaires respectifs avec le triéthylamine [2], dans 25 ml d'acétonitrile, on ajoute 1,3 ml (12 mmoles) isocyanate de phényle. On agite le mélange pendant 4 –5 heures à la température ambiante puis on le porte à reflux pendant 8 heurs. On chasse sous vide le solvant et on laisse en repos durant la nuit au réfrigérateur. On filtre le produit formé et on lave sur le filtre à beaucoup d'eau.

4-Phénylpyrimidinium-benzoyl-(N-phénylcarbamyl)méthylure **(16 s)** : produit jaune ; p.f. = 306–308°C (dans éthanol) rend. 79,4 % . Analyse $C_{25}H_{19}N_3O_3$ *calculé* : C 76,33, H 4,83, N 10,64, *trouvé* : C 76,14, H 4,85, N 10,7 % .

Spectre IR (BKr) : 3060 cm^{-1}, 2910 cm^{-1}, 1702 cm^{-1} ;
1695 cm^{-1} et 1620 cm^{-1}

Spectre ^{1}H–RMN (CF_3COOD, δ, ppm) : 7,58–7,95 et 8,13–8,41, 2 m, 18 H, les protons aromatiques ; 9,75, m, 1 H, le 18 H, les protons aromatiques ; 9,75 m, 1 H, le proton du groupement NH.

Spectre UV (EtOH) : λ_{max} = 404 nm (E = 38).

4-Phénylpyrimidinium-1-(p-nitrobenzoyl)-(N-phénylcarbamyl) méthylure **(16 b)** : produit jaune ; *p.f.* = 305—306,5°C (dans éthanol) ; rend. 79,9 %. Analyse $C_{25}H_{18}N_4O_4$ *calculé* : C 68,49, H 4,10, N 12,79 % *trouvé* : C 68,72, H 4,11, N 12,56 %.

Spectre IR (KBr) : 3115 cm^{-1}, 3060 cm^{-1}, 2910 cm^{-1}, 1705 cm^{-1}, 1625 cm^{-1}.

Spectre ^1H-RMN (CF_3COOD, δ, pp) : 7,55—7,83 et 7,93—8,61, 2m, 17 H, les protons aromatiques ; 10,14, m, 1 H, le proton du groupement NH.

Spectre UV (EtOH) : λ_{max} = 405 nm (E = 34).

4-Phénylpyrimidinium-1-(p-brombénzoyl)-(N-phénylcarbamyl) méthylure **(16 c)** : produit jaune au p.f. = 319—321°C (dans l'éthanol) ; rend. 75,3 %. Analyse $C_{25}H_{18}N_3O_2$ Br calculé : C % 63,57, H 3,81, N 8,90, Br. 16,93 % ; trouvé : C 63,55, H 3,88, N 9,05, Br 17,20 %.

Spectre IR (KBr) : 3110 cm^{-1} ; 3065 cm^{-} 1, 2910 cm^{-1} V, 1690 cm^{-1}, 1605 cm^{-1}.

Spectre ^1H-RMN (CF_3COOH, δ, ppm) : 7,56—7,86 et 8,10—8,36, 2m, 17 H, les protons aromatiques ; 9,80 m, 1 H, le proton du groupement NH.

Spectre UV (EtOH) : λ_{max}= 402 nm (E = 33, 5).

4-Phénylpyrimidinium-1-(p-méthoxybenzoyl)-(N-phénylcarbamyl) méthylure **(16 d)** : produit jaune au p.f. = 235—237°C (dans éthanol) ; rend. 67,4 %. Analyse $C_{26}H_2N_2O_3$: *calculé* : C 73,75, H 4,96, N 9,93 % ; *trouvé* : C 73,86, H ,4,83, N 10,04 %.

Spectre IR(KBr) : 3110 cm^{-1}, 3068 cm^{-1} 1700 cm^{-1}, 1610 cm^{-1}.

Spectre ^1H-RMN (CF_3COOD, δ, ppm) : 4,10, s, 3 H, CH_3 du groupement OCH_3 ; 7,20, d, 2 H, H—3′ et H—5′ du groupement benzoyle ; 7,60 — 7,98 et 8,18—8,50, 2 m, 15 H, les protons aromatiques ; 9,63, m, 1 H, le proton du groupement NH.

Spectre UV (EtOH) : λ_{max} = 405 nm (*E* = 32,5).

RÉFÉRENCES

[1] I. Zugrăvescu et M. Petroveanu, « Chimia N-ilidelor », Ed. Academiei, București, 1974.

[2] I. Zugrăvescu, F. Georgescu, F. Chiraleu, P. Filip et E. I. Georgescu, *Rev. Chim. (București)*, **31**, 11 (1980).

[3] F. Kröhnke, *Chem. Ber.*, **68**, 1177 (1935).

[4] A. Reiche et P. Dietrich, *Chem.Ber.*, **96**, 3047 (1963).

[5] W. J. Linn, Q. W. Webster et R. E. Benson, *J. Amer. Chem. Soc.*, **87**, 3651 (1965).

[6] C. A. Henrick, R. Ritchie et W. C. Taylor, *Austral. J. Chem.*, **20**, 2467 (1967).

[7] F. Georgescu, F. Chiraleu, E. I. Georgescu et I. Zugrăvescu, *Rev. Roumaine Chim.*, **26**, 879 (1981),

[8] G. Leonte et I. Zugrăvescu, *Tetrahedron Letters*, **20**, 2029 (1972).

[9] Y. Kobayashi, T. Kutsuma et K. Murinaga, *Chem. Pharm.Bull.*, **19** 2106 (1971).

[10] R. Huisgen, M. Morikawa, K. Herbig et E. Brunn., *Chem.Ber.*, **100**, 1094 (1967).

[11] M. Caproșu, M. Petroveanu et I. Zugrăvescu, *Rev. Roumaine Chim.*, **15**, 619 (1970).

[12] I. Zugrăvescu, E. Rucinschi et G. Surpățeanu, *Tetrahedron Letters*, **12**, 941, (1970).

[13] I. Zugrăvescu, J. M. Herdan et I. Druță, *Rev. Roumaine Chim.*, **19**, 659 (1974).

[14] H. Bredereck, R. Compper. H. Rempfer, K. Klemm et H. Keck, *Chem. Ber.*, **92**, 329 (1959).

[15] D. G. I. Felton, *J. Chem. Soc.*, **1955**, 515.

Revue Roumaine de Chimie; 27, *5*, 645–649 (1982)

A NEW METHOD FOR THE PREPARATION OF TRIARYL-*s*-TRIAZOLES FROM DIAROYLHYDRAZINES

C. I. CHIRIAC
"P. Poni" Institute of Macromolecular Chemistry,
Aleea Gr. Ghica Vodă 41 A – Iași – Romania

Received June 18, 1981

By a direct condensation reaction between diamides of phenylphosphorous acid prepared *in situ* and diaroylhydrazines, 3,4,5-triaryl-*s*-triazoles resulted in high yield.

In two previous papers,[1, 2] we showed that diacylphenyl-phosphites (reactive compounds), prepared from aromatic acids and phenyldichlorophosphite, can be used for the synthesis of amides and hydrazides.

In this paper we have investigated other reactive compounds prepared from phenyldichlorophosphite for the syntesis of the triaryl-*s*-triazoles.

RESULTS AND DISCUSSION

The synthesis of 3,4,5-triaryl-*s*-triazoles from diaroylhydrazines and primary amines is a well-known reaction, but few contributions have been reported in this field.

The following reagents were used in this synthesis: phosphorus pentoxide,[3] phenylphosphoazoanilide [4] and zinc chloride.[5]

By the reaction between phenyldichlorophosphite and amine, diamides of phenylphosphorous acid [6] result, which contain two reactive groups. The reactivity of these compounds with diaroylhydrazines has not been investigated. Our investigations have shown that these compounds can react with diaroyl-hydrazines affording the corresponding triazoles in high yield.

In order to simplify this synthesis method, we prepared diamides of phenylphosphorous acid *in situ*.

In this way, we have prepared a series of diamides of phenylphosphorus acid (1 mole) from an aromatic primary amine (4 moles) and phenyldichlorophosphite (1 mole) in *o*-dichlorobenzene, which react with diaroylhydrazines (1 mole) in the same solvent at reflux (175–185°). From the four moles of amine, two are necessary for the formation of diamides of phenyl-phosphorous acid and two as acceptors for the hydrochloric acid (other acceptors for HCl, for example pyridine or other tertiary amines afford impure final products). In the case of 3,4,5-triphenyl-1,2,4-triazole, the yield is 92 – 94 % when we used 1 mole of phenyldichlorophosphite for 1 mole of dibenzoylhydrazine and only 45–48 % in the case of 0.5 mole of phenyldichlorophosphite. This shows that the two reactive amide groups are necessary in the reaction of cyclisation with dibenzoylhydrazine.

The yield increases with the temperatures of reaction. At temperatures under 170 – 180°C, the yield decreases very much (at 100 – 120°C being only of 30 – 40 %).

We have chosen *o*-dichlorobenzene as solvent because it has a high boiling point and is an inert solvent for this reaction. In addition, *o*-dichlorobenzene is a good solvent for the final products (at reflux), which precipitate on cooling at room temperature.

The reaction of dibenzoylhydrazine with pure dianilide of phenylphosphorous acid [6] takes place under similar conditions with those used at the product prepared *in situ*.

As a result of these investigations, we propose the following mechanism of reaction :

$$4Ar^1-NH_2 + C_6H_5OPCl_2 \xrightarrow[0-20^\circ]{o-\text{dichlorobenzene}} (Ar^1-NH)_2P-OC_6H_5 + 2Ar^1-NH_3^+Cl^-$$

(I) (II)

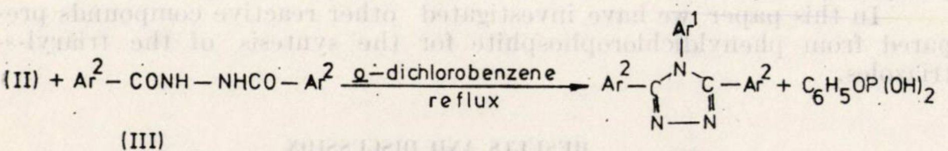

(III)

(IV)

In this reaction, similar to other cases,[1, 2, 7, 8] $C_6H_5OP(OH)_2$ and $Ar^1-NH_3^+Cl^-$ result as by-products.

We supposed, similar to other cases,[7, 9, 10] that this reaction involves a mechanism with two transition states, A and B :

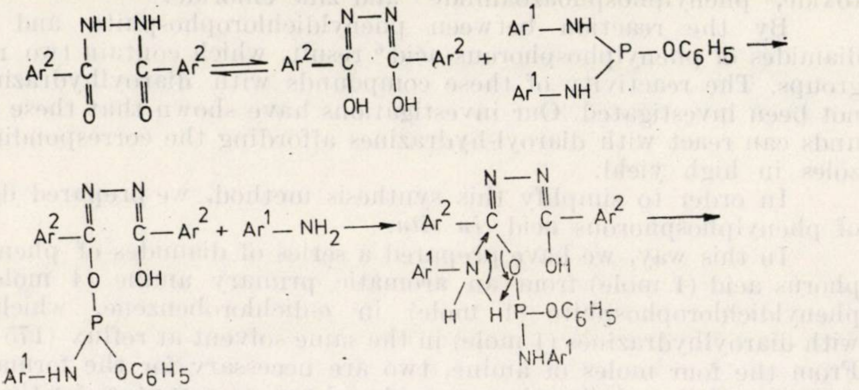

(A)

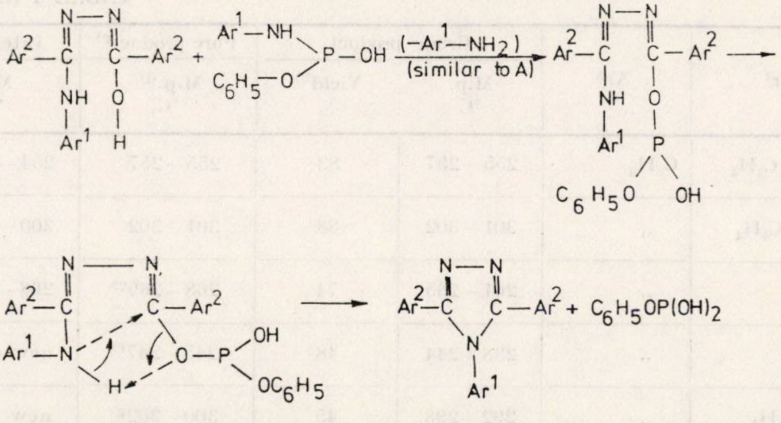

(B)

In a typical procedure, to a solution of 4 moles I in dried o-dichlorobenzene cooled to 0°C, 1 mole phenyldichlorophosphite was added very slowly, under stirring (the reaction is very exothermic), when (II) and $Ar-NH_3^+Cl^-$ precipitate. After 1 – 2 hours at room temperature, 1 mole III was added and the stirring was continued for 4 – 5 hours at reflux (175 – 185°C). Then by cooling, the final poducts IV precipitate.

Table 1 shows the triazoles IV obtained by this procedure.

TABLE 1

Triaryl-*s*-triazoles obtained from diamides of phenylphosphorous acid prepared *in situ*

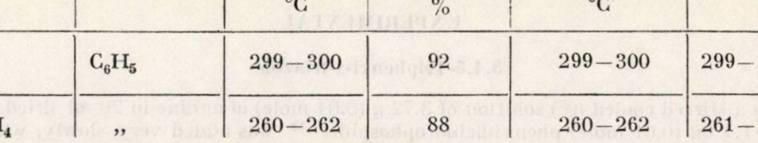

Ar^1	Ar^2	Crude product		Pure product[c)]	Literature
		M.p. °C	Yield[b)] %	M.p.[d)] °C	M.p. °C
C_6H_5	C_6H_5	299–300	92	299–300	299–300[3, 4, 11]
p-$Cl-C_6H_4$	,,	260–262	88	260–262	261–262[5]

a) Amides of phenylphosphorous acid were prepared *in situ* from phenyldichlorophosphite and the corresponding amines.
b) Yields calculated on diaroylhydrazine employed, before recrystallisation, and for some triazoles (entries 5–8) after recrystallisation.
c) The products were identified by comparing the m.p. and IR spectra with those of authentic samples.
d) Before recrystallisation.

TABLE 1 (*Continued*)

Ar^1	Ar^2	Crude product		Pure product[c]	Literature
		M.p. °C	Yield[b] %	M.p.[d] °C	M.p. °C
m-$CH_3-C_6H_4$	C_6H_5	255–257	83	255–257	254–256 [5]
p-$CH_3-C_6H_4$	,,	301–302	88	301–302	300–302 [5]
2-$C_{10}H_7$	,,	261–265	74	268–269[e]	268–269 [4]
1-$C_{10}H_7$	,,	238–244	48	245–247[f]	new comp. [h]
o-$Br-C_6H_4$	,,	292–298	45	300–302[g]	new comp. [i]
m-$Br-C_6H_4$	,,	249–254	69	257–259[g]	new comp. [j]
C_6H_4	p-$CH_3OC_6H_4$	249–251	89	250–252	250–252 [k]

e) Crystallized from dil.acetic acid.

f) Crystallized from ethanol.

g) Crystallized from acetic acid.

h) Anal. Found : C, 82, 33 ; H, 4.16 ; N, 11.51. Calculated for $C_{24}H_{17}N_3$; C, 82.96 ; H, 4.93 ; N, 12.09 %.

i) Anal. Found : C, 63.54 ; H, 3.71 ; N. 11.12. Calculated for $C_{20}H_{14}BrN_3$; C, 63,88 ; H, 3.80 ; N, 11.16 %

j) Anal. Found : C, 63.68 ; H, 3.62 ; N, 10.87. Calculated for : $C_{20}H_{14}BrN_3$; C, 63.88 ; H, 3.80 ; N, 11.16 %.

k) From "Beilsteins Handbuch der Organischen Chemie", Verlag von Julius Springer, Berlin, **26**, 125 (1937).

The large majority of the final products IV had correct melting points before recrystallization and the yields ranged from 45 to 92 % (Table 1).

In conclusion, by this new direct synthesis we obtained, in high yield, triaryl-*s*-triazoles from diaroylhydrazines.

EXPERIMENTAL

3,4,5-Triphenyl-*s*-triazole

To a stirred cooled (0°) solution of 3.72 g (0.04 mole) of aniline in 20 ml dried *o*-dichlorobenzene, 1.4 ml (0.01 mole) phenyldichlorophosphite [12] was added very slowly, when phenylphosphorous dianilide and $C_6H_5-NH_2 \cdot ClH$ precipitate. The mixture was stirred for 1–2 hrs at room temperature. After the addition of 2.4 g (0.01 mole) of dibenzoylhydrazine, the final mixture was stirred and refluxed (175–185°C) for 4 hrs in an oil (or molten salts) bath at 190–200°C (maximum 200°C). Efficient stirring is desirable. By colling, the product precipitated. The white 3,4,5-triphenyl-*s*-triazole was collected by filtration, washed well with 30–50 ml ethylic ether and dried. Then it was stirred and heated at 70–90°C with 80–100 ml H_2O and NaOH solution till the pH=9 – 10. After filtration, the same operation was repeated with solution of hydrochloric acid till the pH = 1–2. After filtration, the precipitate was washed for

2–3 times with 40–50 ml water. After drying 2.8g crude product, at 100–150°C, in vacuum, yield 92 % was obtained. M.p. 299–300°C (m.p of the mixture with an authentic sample of 3,4,5-triphenyl-*s*-triazole undepressed).
Anal. Found : C, 80.23 ; H, 4.94 ; N, 14.06. Calculated for $C_{20}H_{15}N_3$; C, 80.77 ; H, 5.12 ; N, 14.13 %.

Under similar conditions, the other triazoles presented in table 1 were obtained (for the triazoles 2 and 5, we used 25 ml *o*-dichlorobenzene).

REFERENCES

[1] C. I. Chiriac, *Rev. Roumaine Chim.*, **26**, 1001 (1981).
[2] C. I. Chiriac, *Rev. Roumaine Chim.*, (in press).
[3] M. Bush, *J. prakt. Chem.* , **89**, 552 (1914).
[4] E. Klinsberg, *J. Org. Chem.*, **23**, 1086 (1958).
[5] K. L. Bhagot and J. N. Ray, *J. Chem. Soc.*, **1930**, 2357.
[6] S. Goldschmidt, *Liebigs Ann. Chem.*, **588**, 24 (1954).
[7] B. Iselin and W. Rittel, *Helv. Chim. Acta*, **40**, 376 (1957).
[8] N. Yamazaki, *Tetrahedron Letters*, **49**, 5047 (1972).
[9] W. Gerrard and J. A. Cade, *J. Chem. Soc.*, **1954**, 2034.
[11] H. O. Becker and K. F. Funk, *J. prakt. Chem.*, **286**, 55 (1961).
[11] R. Stollé, *J. prakt. Chem.*, **73**, 288 (1906).
[12] H. Tolkmith, *J. Org. Chem.*, **23**, 1682 (1958).

Revue Roumaine de Chimie, 27, 5, 651–658 (1982)

REACTIVITY OF ACRYLIC MONOMERS. XI[1]

SYNTHESIS AND COPOLYMERIZATION OF 3-CHLORO-2-HYDROXYPROPYL ACRYLATE

SPIRIDON OPREA and EMIL DUMITRIU
Department of Organic Chemical Technology, Faculty of Chemical Technology, Polytechnic Institute of Jassy, Bahlui Stînga 71, Jassy 6600, Romania

Received November 17, 1980

The esterification of epichlorohydrin with acrylic acid on anionic exchangers was investigated. The reaction order of the first order for each component was determined. The behaviour of the system N,N-dimethylaminoethyl methacrylate and 3-chloro-2-hydroxypropyl acrylate in the copolymerization process was also studied. The reactivity ratios $r_1 = 0.38$ and respectively $r_2 = 0.67$ were evaluated.

A very important group of vinylic monomers characterized by a great diversity of applications is formed by the acrylic derivatives. Certainly, in the frame of this group there are preoccupations both to increase the number of acrylic monomers and to find new applications, usually materialized by new polymers (here the copolymerization has an important role) for already accepted monomers.

Among the acrylic monomers whose recent applications have determined an increased interest, 3-chloro-2-hydroxypropyl acrylate can be mentioned. This interest is caused by two factors : (a) the 3-chloro-2-hydroxypropyl acrylate constitutes the starting product in the glicydil acrylate synthesis and (b) the 3-chloro-2-hydroxypropyl acrylate can constitute a valuable monomer. Thus, the copolymers of 3-chloro-2-hydroxypropyl acrylate with styrene, acrylates, acrylonitrile, acrylamides etc, can be used as stabilizers for plastisols,[2,3] adhesive coatings,[4,7] antiflame composites,[8,9] synthetic leather,[10,11] photosensitive polymers for xerox,[12–15] coloured resins for textile printing,[16–20] etc.

The aim of this paper is to study the synthesis of 3-chloro-2-hydroxypropyl acrylate on anionic exchangers and the copolymerization of this monomer with N,N-dimethylaminoethyl methacrylate.

EXPERIMENTAL

Esterification

Acrylic acid, commercial product, was first dried then distilled under vacuum ; the middle fraction was collected, b.p. = 69°C/50 mm Hg, $n^{20} = 1{,}4212$.

Epichlorohydrin was distilled under vacuum before use, b.p. = 116°C, $n^{20} = 1{,}4375$. A macroporous anionic exchanger[21] (with quaternary ammonium groups) was used as catalyst. The exchanger was brought in Cl^- form, washed with deionised water and then

dried under vacuum at constant weight. The esterification reactions were carried out in a glass reactor with jacket, connected to a thermostat, and fitted up with stirrer, condenser and thermometer. The reagents were introduced in the thermostated reactor and the proceeding of reaction was controlled by the determination of acrylic acid content.

Copolymerization

3-Chloro-2-hydroxypropyl acrylate (CHPA) was synthesised at 80°C by the reaction between acrylic acid and epichlorohydrin, 1.1 :1 molar ratio, using the same anionic exchanger as catalyst. Hydrochinone was also introduced as a polymerization inhibitor. When the reaction has been finished ethyl ether was added and the unreacted acrylic acid was extracted with distilled water into a separatory funnel. The lower layer was separated, dried on anhydrous K_2SO_4, then fractionated. The fraction with b.p. = 130°/4 mm Hg was collected. The purity of the monomer was checked by thin layer chromatography.

N,N-Dimethylaminoethyl methacrylate (DMAEM) was distilled under vacuum and nitrogen to remove the inhibitor, b.p. = 110°/10 mm Hg.

2,2′-Azobis(isobutironitrile) (AIBN) was purified by recrystalization from ethanol.

Dioxane used as solvent in the polymerization process was refluxed 8 hrs on sodium wire then distilled and the middle fraction collected. The copolymerization was carried out in dioxane solution at 60°C in the same manner as previously reported. [22] The copolymers were precipitated in the ethyl ether-light petroleum mixture (1 : 1 v/v). The composition of copolymers was determined by their nitrogen content by micro Kjeldhal method. The result and reaction conditions are summarised in Table 1.

TABLE 1

Copolymerization of N,N-dimethylaminoethyl methacrylate with 3-chloro-2-hydroxypropyl acrylate in dioxane at 60°C

No.	Mole fraction of DMAEM in monomer feed	Mole fraction DMAEM in copolymer	N_2 %	Conversion %
1	0.1	0.134	1.15	4.74
2	0.2	0.229	1.98	5.11
3	0.3	0.306	2.65	3.93
4	0.4	0.385	3.34	4.14
5	0.5	0.451	3.92	3.32
6	0.6	0.519	4.52	2.24
7	0.7	0.592	5.08	2.21
8	0.8	0.693	6.22	4.77
9	0.9	0.809	7.15	4.00

RESULTS AND DISCUSSION

In the studies regarding the mechanism of the esterification of epichlorohydrin with organic acids it was observed that the nature of the catalyst determines the mechanism and kinetics. Thus, in the esterification of caproic acid with various oxiranes (including epichlorohydrin), without catalyst, the reaction takes place according to a second order kinetics (first order in acid and first order in oxirane, respectively)[23]. For the same reaction in the presence of a tertiary amine as catalyst it was observed that the reaction order for the organic acid is zero and first order for both oxirane and catalyst. In this case the authors[23] have suggested that the reaction proceed by a six membered cyclic complex. The kinetic law which describes the process is :

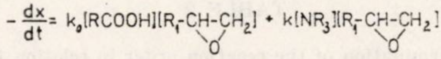

$$-\frac{dx}{dt} = k_0[RCOOH][R_1-\underset{\diagdown O \diagup}{CH-CH_2}] + k[NR_3][R_1-\underset{\diagdown O \diagup}{CH-CH_2}]$$

Scheme 1

The first term of the right member describes the uncatalysed reaction which proceeds in parallel with the catalytic reaction. If one uses the hydroxydes as catalysts the reaction is of first order for each component of the system and therefore the kinetic law has the following form :[23]

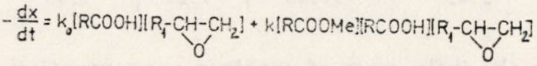

$$-\frac{dx}{dt} = k_0[RCOOH][R_1-\underset{\diagdown O \diagup}{CH-CH_2}] + k[RCOOMe][RCOOH][R_1-\underset{\diagdown O \diagup}{CH-CH_2}]$$

Scheme 2

where : RCOOM — the salt of organic acid formed by the reaction with the alcaline hydroxyde.

In the present study taking into account the above mentioned observations and those previously reported[21,24,25] about the catalysis of the process by synthetic polymers having quaternary ammonium groups we have tried to establish the kinetic model corresponding to the process catalysed by anionic exchangers (having quaternary ammonium groups). This catalyst has been chosen for technologycal reasons also due to the advantages of the ions exchangers which are easily removable and possess a good selectivity.[21,26] It can be remembered from the previous studies[21,24,25] the observation that the reaction between the acrylic acid and epichlorohydrin proceeds with a small rate even at higher temperature (the reaction rate being negligible at ambient temperature). It was also observed that the reaction rate can be influenced by the amount of catalyst, temperature and reagent ratio. For the latest factor it was observed that the effect of epichlorohydrin is not similar to those of the acrylic component.

For the kinetic study the procedure previously described[23] was used ; modifying the initial concentrations of the reacting substances one determines the partial order for each component. The reaction order for epichlorohydrin was determined in excess of acrylic acid (Table 2).

As it can be observed from this table the reaction is of the first order indicating a monomolecular reaction catalysed by the anionic exchanger against epichlorohydrin.

The determination of the reaction order for acrylic acid in the epichlorohydrin excess and in the presence of catalyst gives the same first order (Table 3).

From Table 3 it can be observed that the rate constant rises with the increasing of the epichlorohydrin excess. The fact indicated some influence of epichlorohydrin both as reagent and solvent.

TABLE 2

Determination of the reaction order in relation to epichlorohydrin ; catalyst concentration 10 g/100 g reaction mixture, reaction temperature 70°C

Initial concentration of epichlorohydrin mol/1000 g	Initial concentration of acrylic acid mol/1000g	Reaction order	Rate constant $k \cdot 10^3$ min^{-1}
4.67	9.32	1.25	1.40
3.54	10.67	1.13	1.42
2.42	11.93	1.21	1.48

As concerns the influences of catalyst concentration on the reaction rate at 70°C it can be observed from Figure 1 that the reaction rate increases proportionally with the amount of catalyst (the interception being equal to the rate constant without catalyst and the slope of the line giving the rate constant of the catalysed reaction).

From the data given above it may be concluded that the process catalysed by anionic exchanger shows similitudes with the base catalysed process, but more important seems to be the observation that the nature of organic acids and oxiranes can be essential for the manner in which the reaction proceeds. This assumes some peculiarity of the mechanisms and kinetics for each reaction system.

TABLE 3

Determination of the reaction order in relation to acrylic acid ; catalyst concentration 10 g/100 g reaction mixture, reaction temperature 70°C

Initial concentration of acrylic acid mol/1000 g	Initial concentration of epichlorohydrin mol/1000g	Reaction rate	Rate constant $k \cdot 10^3$ min^{-1}
4.41	7.37	1.16	2.69
3.36	8.19	1.14	4.37
2.27	10.13	0.95	11.2

Further, the behaviour of 3-chloro-2-hydroxypropyl acrylate in the copolymerization process with N,N-dimethylaminoethyl methacrylate was studied. Figure 2 is a plot of the variation of the copolymer composition against the monomer feed on the basis of the data listed in Table 1.

As it can be observed from Figure 2 the behaviour of the N,N-dimethylaminoethyl methacrylate -3-chloro-2-hydroxypropyl acrylate system has the feature specific to the systems for which the reactivity ratios, r_1 and r_2, are smaller than the unity. This behaviour reflects some affinity of the monomers for the opposite macroradicals. The extent of this affinity is given by the r_1 and r_2 values.

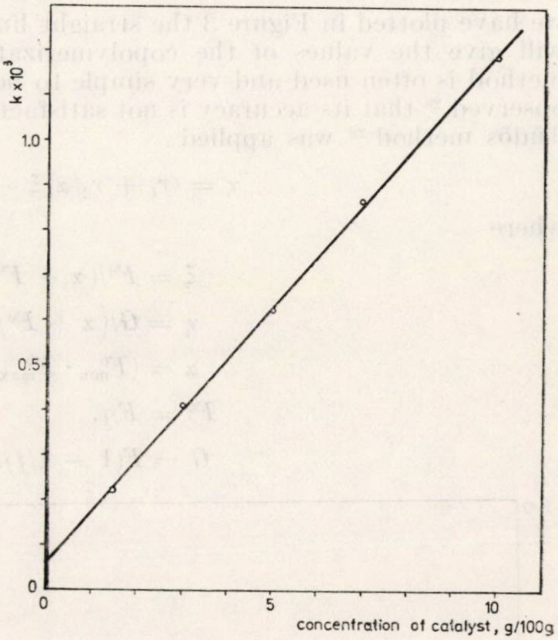

Fig. 1. — The influence of the catalyst concentration on the reaction rate at 70°C.

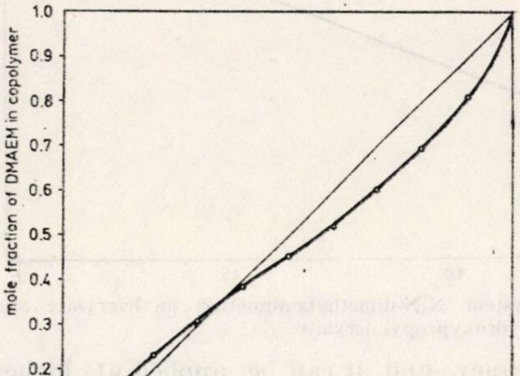

Fig. 2. — The composition diagram for the copolymerization of N,N-dimethylaminoethyl methacrylate with 3-chloro-2-hydroxypropyl acrylate at 60°C in dioxane solution.

Two methods based on the differential equation of composition were applied for the estimations of the values of copolymerization parameters. Applying the Fineman-Ross equation [27]

$$F(1 - 1/f) = -r_2 + (F^2/f)r_1,$$

where $F = [M_1]/[M_2]$,

$$f = d[M_1]/d[M_2],$$

we have plotted in Figure 3 the straight line whose intersection and slope will give the values of the copolymerization parameters. Though this method is often used and very simple to be rapidly applied, it has been observed [28] that its accuracy is not satisfactory. Consequently, the Kelen-Tüdös method [29] was applied

$$\eta = (r_1 + r_2/\alpha)\xi - r_2/\alpha$$

where

$$\xi = F^0/(\alpha + F^0),$$
$$\eta = G/(\alpha + F^0),$$
$$\alpha = (F^0_{\min} \cdot F^0_{\max})^{1/2},$$
$$F^0 = F/f,$$
$$G = F(1 - 1/f).$$

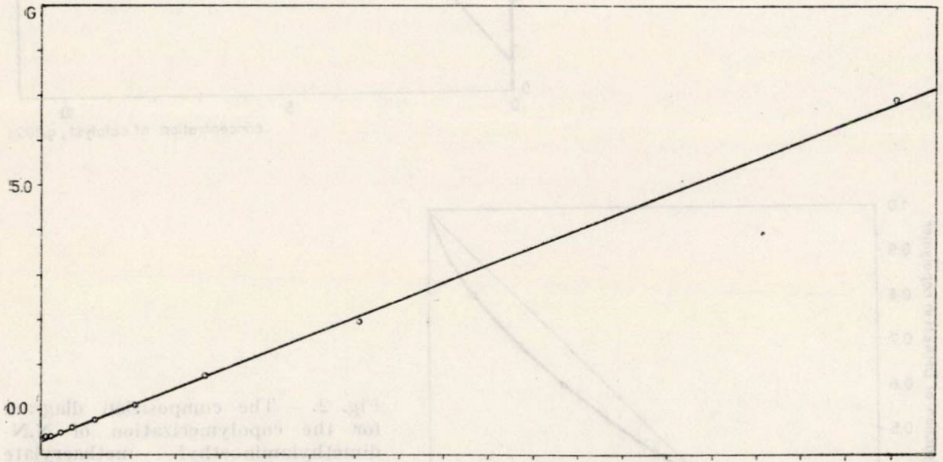

Fig. 3. — Fineman-Ross plott for the system N,N-dimethylaminoethyl methacrylate and 3-chloro-2-hydroxypropyl acrylate.

This method has a better accuracy and it can be applied at higher conversions;[30] moreover it allows the checking of the kinetic model of the copolymerization.

From Figure 4 it can be observed that the copolymerization of N,N-dimethylaminoethyl methacrylate with 3-chloro-2-hydroxypropyl acrylate takes place according to the terminal model. The line was plotted by the least square method and from its parameters the reactivity ratios were determined.

On the basis of the data shown in Table 4 one observes that the reactivity ratios determined by the two methods are close as values.

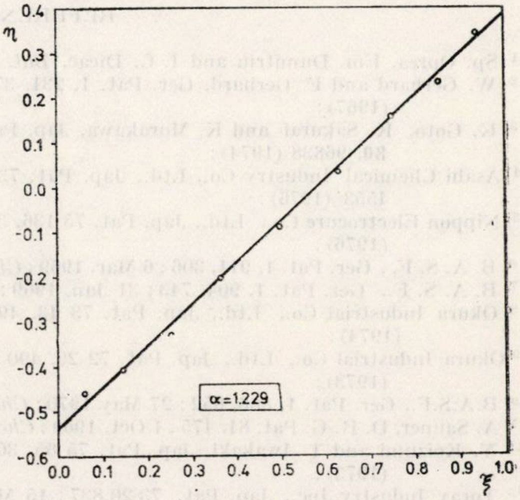

Fig. 4. Kelen-Tüdös plott for the system N,N-dimethylaminoethyl methacrylate and 3-chloro-2-hydroxypropyl acrylate.

The obtained values for the reactivity ratios confirm the initial observation based on the pattern of the curve from the composition diagram. Regarding the composition diagram (Figure 2) one also observes that the azeotropic point is found at the low concentration of N,N-dimethylaminoethyl methacrylate, a fact which can be, to some extent, an advantage for certain technical applications where the concentration of the aminoester must be low.

TABLE 4

Copolymerization parameters

Monomer	Reactivity ratio	Method of evaluation	
		Fineman-Ross	Kelen-Tüdös
N,N-dimethylaminoethyl methacrylate	r_1	0.39	0.38
3-Chloro-2-hydroxypropyl acrylate	r_2	0.69	0.67

Another observation is related to the homogeneity of the copolymer, this having a peculiar interest because the homogeneity of copolymer influences the physical and chemical properties of polymers. In the case when the concentration of N,N-dimethylaminoethyl methacrylate is greater than azeotropic concentration if the copolymerization process is carried out at high conversions the progressive diminution of the 3-chloro-2-hydroxypropyl acrylate concentration takes place (this monomer being more reactive), until complete consumption of this, after which the homopolymerization of N,N-dimethylaminoethyl methacrylate follows.

REFERENCES

[1] Sp. Oprea, Em. Dumitriu and I. C. Dieac, *Bul. Inst. Pol., Iași,* (in press);

[2] W. Gerhard and F. Gerhard, Ger. Pat. 1, 231, 372, 27 Nov. 1963; *Chem. Abstr.,* **66**, 95364 (1967);

[3] K. Goto, K. Sakurai and K. Murakawa, Jap. Pat. 73 49, 863; 27 Oct. 1971; *Chem. Abstr.* **80**, 96838 (1974);

[4] Asahi Chemical Industry Co., Ltd., Jap. Pat. 73 16, 431; 12 Feb. 1973; *Chem. Abstr.,* **84,** 4553 (1976);

[5] Nippon Electrocure Co., Ltd., Jap. Pat. 75 136, 325; 29 Oct. 1975; *Chem. Abstr.,* **84.** 61340 (1976);

[6] B. A. S. F., Ger. Pat. 1, 911, 306; 6 Mar. 1969; *Chem . Abstr.,* **73**, 99769 (1970);

[7] B. A. S. F., Ger. Pat. 1. 904, 743; 31 Jan. 1969; *Chem. Abstr.,* **73**, 99733 (1970);

[8] Okura Industrial Co., Ltd., Jap. Pat. 73 43, 491; 23 Jun. 1973; *Chem. Abstr.,* **80**. 48692 (1974);

[9] Okura Industrial Co., Ltd., Jap. Pat. 72 29, 490; 2 Aug. 1972; *Chem. Abstr.,* **78**, 128906 (1973);

[10] B.A.S.F., Ger. Pat. 1, 806, 652; 27 May 1970; *Chem. Abstr.,* **73**, 99801 (1970);

[11] A. Sauner, D. R. G. Pat. 81, 475; 1 Oct. 1969; *Chem. Abstr.,* **76**, 160928 (1927);

[12] Y. Koizumi and T. Iwakaki, Jap. Pat. 75 65, 305; 3 Jun. 1975; *Chem. Abstr.,* **84,** 143064 (1973);

[13] Toray Industry Inc., Jap. Pat. 73 20,837; 15 May 1973; *Chem. Abstr.,* **79**, 67531 (1974);

[14] Toray Industries Inc., Jap. Pat. 75 18,913; 2 Jul. 1975); *Chem Abstr.,* **85**, 27366 (1976);

[15] Toray Industries Inc., Jap. Pat. 73 22,345; 5 Jul. 1973; *Chem. Abstr.,* **81**, 31877 (1974);

[16] Shiurochi Co., Ltd., Jap. Pat. 73 58,038; 15 Aug. 1973; *Chem, Abstr.,* **81**, 31878 (1974);

[17] B. A. S. F., Brit. Pat. 1, 185, 861; 25 Mar. 1970; *Chem. Abstr.,* **76**, 160841 (1972);

[18] B. A. S. F., Ger. Pat. 1, 513, 899; 16 Feb. 1968; *Chem. Abstr.,* **70**, 72346 (1969);

[19] B.A.S.F., Ger. Pat., 2, 147, 972; 29 Mar. 1973; *Chem. Abstr.,* **78**, 56732 (1973);

[20] B. A.S.F., U.S. Pat. 3, 313, 649; 11 April 1967; *Chem. Abstr.,* **67**, 90347 (1967);

[21] Em. Dumitriu. Sp. Oprea, M. Dima and S. Avramescu, *Rev. Chim. (București),* **32**, 224 (1981);

[22] M. Dima. Sp. Oprea and Em. Dumitriu, *Rev. Roumaine Chim.,* **26**, 131 (1981);

[23] M. F. Sorokin and E. L. Gershanova, *Kinetika i Kataliz,* **8**, 512 (1967);

[24] Sp. Oprea, Em. Dumitriu and L. Ștefănel, *Rev. Roumaine Chim,* **25**, 1039 (1980);

[25] Sp. Oprea, Em. Dumitriu, L. Ștefănel and V. Hulea, *Bul. Inst. Pol. Iași,* (in press);

[26] V. A. Podgorova, N. A. Speht and E. V. Vohmiania, *Zhur. priklad. Kim.,* **50**, 878 (1977);

[27] M. Fineman and S. A. Ross, *J. Polymer Sci.,* **5**, 259 (1950);

[28] P. W. Tidwell and G. A. Mortimer, *J. Macromol. Sci. — Revs. Macromol. Chem.,* **C4**, 281 (1970);

[29] T. Kelen and F. Tüdös, *J. Macromol. Sci. — Chem.,* **A9**, 1 (1975);

[30] S. P. Rao, S. Ponratnam, S. L. Kapur and P. K. Iyer, *Polym. Letters Ed.,* **14**, 513 (1976).

Revue Roumaine de Chimie, 27, 5, 659–666 (1982)

SYNTHESIS AND POLYMERIZATION OF POLYETHYLENE GLYCOL DIMETHACRYLATES. VI.[1]

STUDY OF COPOLYMERIZATION PROCESS OF POLYETHYLENE GLYCOL DIMETHACRYLATES WITH STYRENE

GH. HUBCA*, C. OPRESCU*, AGNETA CARAGHEORGHEOPOL**, H. CĂLDĂRARU**, D. RACOȚI* and M. DIMONIE*

* Polytechnical Institute of Bucharest, Laboratory of Macromolecular Technology, Calea Victoriei 149, Bucharest, Romania

** Center of Physical Chemistry, ICECHIM, Splaiul Independenței, 202 Bucharest, Romania

Received April 29, 1981

The bulk copolymerization process of ethylene dimethacrylate, diethylene glycol dimethacrylate, triethylene glycol dimethacrylate and tetraethylene glycol dimethacrylate with styrene against methylethyl ketone peroxide, as initiator, has been studied. Researches carried out have shown that the process develops according to a kinetics similar to homopolymerization of polyethylene glycol dimethacrylates. The calculation of copolymerization constants permitted a comparison of monomers reactivity studied *versus* the same comonomer and the determination of copolymer composition variation as a function of conversion.

INTRODUCTION

Copolymerization of polyethylene glycol-dimethacrylates with other monomers favours greatly both modification of adhesive properties of anaerobic adhesive resins and modification of other polymers. In this way addition of some vinyl monomers (styrene, methyl methacrylate etc.), to anaerobic adhesive resins permits modification of link strength within required limits. At the same time, certain monomers such as ethylene dimethacrylate, diethylene glycol dimethacrylate, triethylene glycol dimethacrylate and tetraethylene glycol dimethacrylate are used to modify the chemical fibers[1], the plastic[2–7] and the synthetic rubber[8–10] and to produce some macroporous copolymers for the ion exchange[11–14] manufacturing; production of certain hydrophilic materials used in gel-chromatography[15,16]; acceleration of copolymerization radiochemically[17–19] initiated; manufacturing of plastics used in dental technique and as artificial bones as well as of some hydrophilic polymers used in medical therapeutics for absorption of some vitamins[20–23], etc.

In this paper the study of copolymerization process of the above mentioned monomers with styrene aimed at determining copolymerization constant values in order to compare their reactivity *versus* the same comonomer, as well as determination of styrene effect upon copolymerization reaction kinetics, composition and thermal properties of copolymers obtained.

The copolymerization process was carried out in block, under high vacuum, the apparata used and working method being identical with those used in the study of homopolymerization process.[24]

RESULTS AND DISCUSSIONS

The study of copolymerization reaction has outlined the identity between this process kinetics and the homopolymerization process, conversion curves having the same slope (Fig. 1).

The same figure (1) shows that the process reveals conversions higher than in the ethylene dimethacrylate block homopolymerization, due to a looser tridimensional network and to the fact that the styrene diffuses easier towards growing macroradicals.

The copolymerization reaction develops faster than the styrene homopolymerization under the same conditions but slowlier than the ethylene dimethacrylate homopolymerization. By analysing the influence of diester content upon copolymerization process rate, one finds out that thus the rate grows simultaneously with the diester concentration growth (Fig. 2).

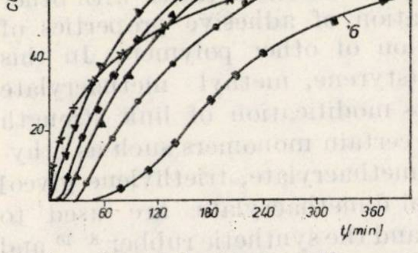

Fig. 1. — Conversion time-variation on copolymerization of ethylene glycol dimethacrylate (EGDMA) with styrene (ST). Initiator — 1 % methyl-ethyl ketone peroxide; $t = 60°C$. 1 — Block EGDMA ; 2 — EGDMA : ST = 60 : 40 ; 3 — EGDMA : ST = 50.50 ; 4 — EGDMA : ST = 40 :60 ; 5 — EGDMA : ST = 20 :80 (volume ratios) ; 6 — Block ST.

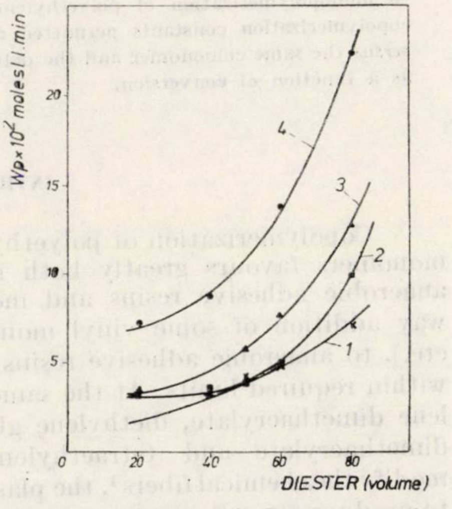

Fig. 2. — Influence of diester concentration on copolymerization rate. 1 — Ethylene dimethacrylate styrene ; 2 — Diethylene glycol dimethacrylate-styrene ; 3 — Triethylene glycol dimethacrylate styrene ; 4 — Tetraethylene glycol dimethacrylate styrene.

Interruption of copolymerization reaction at lower conversions (3–5 %) and elementary analysis of products obtained permitted calculation of copolymerization constants.

The graphical method devised by Kelen and Tüdos [25] has been used to determine the copolymerization constants. According to this method, function $\eta = f(\xi)$ is represented graphically, defined by relation (1):

$$\eta = r_1 \xi - \frac{r_2}{\alpha}(1 - \xi) \qquad (1)$$

where:

$$\eta = \frac{G}{\alpha + F}\,; \quad \xi = \frac{F}{\alpha + F}\,;$$

$$\alpha = \sqrt{F_{\max} \cdot F_{\min}}\,; \quad G = x(y - 1)/y,$$

$$F = x^2/y\,; \quad x = [\mathrm{M}_1]/[\mathrm{M}_2] \text{ and } y = \mathrm{d}[\mathrm{M}_1]/\mathrm{d}[M_2].$$

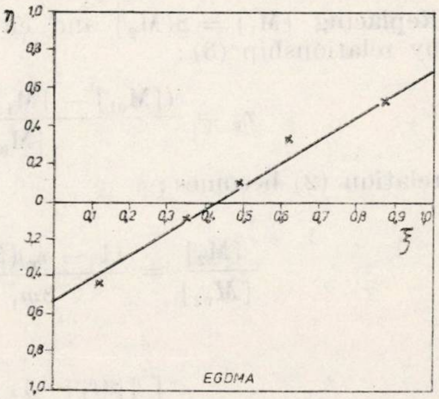

Fig. 3. — Dependence $\eta = f(\xi)$ for EGDMA — ST system.

The graphical representation of the above mentioned function is a straight line which extrapolated to $\xi = 0$ and $\xi = 1$ yields the values r_2/α and r_1, both as ordinates. For the ethylene-dimethacrylate system, he graphical representation is shown in Fig. 3, and the results obtained for the four systems examined are enlisted in table 1.

TABLE 1

Values of copolymerization constants of diesters (M_1) with styrene (M_2)

Diester	r_1	α	r_2/α	r_2
Ethylene dimethacrylate	0.70	0.3371	0.53	0.1787
Diethylene glycol dimethacrylate	0.72	0.2362	0.73	0.1724
Triethylene glycol dimethacrylate	0.74	0.1703	0.84	0.1430
Tetraethylene glycol dimethacrylate	0.76	0.1525	0.88	0.1342

Determination of copolymerization constants has permitted calculation of sublayer and copolymer composition variations depending on conversion, by application of mathematical model drawn up by Dimonie and Vasilescu. [26]

According to the model, one starts from the copolymer momentary equation under differential form (2):

$$\frac{d[M_1]}{d[M_2]} = \frac{[M_1]}{[M_2]} \cdot \frac{r_1[M_1] + [M_2]}{r_2[M_2] + [M_1]} \tag{2}$$

Replacing $[M_1] = \beta[M_2]$ and entering gravimetrical efficiency defined by relationship (3):

$$\eta_g = \frac{([M_{01}] - [M_1])m_1 + ([M_{02}] - [M_2])m_2}{[M_{01}]m_1 + [M_{02}]m_2} \tag{3}$$

relation (2) becomes:

$$\frac{[M_2]}{[M_{02}]} = \frac{(1-\eta_g)(\beta_0 m_1 + m_2)}{\beta m_1 + m_2} = \left(\frac{\beta}{\beta_0}\right)^{\frac{r_2}{1-r_2}} \cdot \left[\frac{\beta(r_1 - 1) + 1 - r_2}{\beta_0(r_1 - 1) + (1 - r_2)}\right]^{\frac{1-r_1r_2}{(r_1-1)(1-r_2)}} \tag{4}$$

where: $[M_{01}]$, $[M_1]$ — initial and momentary concentration of M_1 monomer; $[M_{02}]$, $[M_2]$ — initial and momentary concentration of monomer M_2; r_1, r_2 — copolymerization constants; m_1, m_2 — monomer gram-molecular weights; $\beta = [M_1]/[M_2]$ and $\beta_0 = [M_{01}]/[M_{02}]$.

Instantaneous composition of copolymer results from the following equation (5):

$$\gamma = \beta\,\frac{r_1 + 1}{r_2 + \beta} = \frac{\varphi_1}{\varphi_2} \tag{5}$$

Equation (4) was solved by computer programming. In this way, introducing both terms of the equation in the same member and entering the symbols:

$$C_1 = (1 - \eta_g)(\beta_0\, m_1 + m_2); \quad r_{11} = r_1 - 1; \quad r_{21} = 1 - r_2;$$

$$e_1 = \frac{r_2}{1 - r_2}; \; e_2 = \frac{1 - r_1 r_2}{(r_1 - 1)(1 - r_2)}; \; C_2 = \left(\frac{1}{\beta_0}\right)^{e_1};$$

$C_3 = \left[\dfrac{1}{\beta_0(r_1 - 1) + (1 - r_2)}\right]^{e_2}$; $C_{23} = C_2 \cdot C_3$, we obtain:

$$f(\beta) = \frac{C_1}{m_1 + m_2} - C_{23}\beta^{e_1}[\beta \cdot r_{11} + r_{21}]^{e_2} \tag{6}$$

where: C_1, C_{23}, m_1, m_2, e_1, e_2, r_{11} and r_{21} are constants. For solving equation (6) we proceed in the following way;

a) Define the interval where f(β) changes sign;
  1) — Given β_1 (initially $\beta_1 = 0$).
  2) — Calculate $f(\beta_1)$.
  3) — Calculate $\beta_2 = \beta_1 + \Delta\beta$; $\Delta\beta = 0.1$
  4) — Calculate $f(\beta_2)$
  5) — Evaluate $f(\beta_1) \cdot f(\beta_2)$ and
    if $f(\beta_1) \cdot f(\beta_2) < 0$ pass on to point b, retaining interval (β_1, β_2).
    — if $f(\beta_1) \cdot f(\beta_2) > 0$ replace β_1 by β_2 and resume calculation under point 2.

b) Given interval $[\beta_1, \beta_2]$, $f(\beta_1) \cdot f(\beta_2) < 0$ solution of equation (6), $f(\beta) = 0$ is found by the method of interval halving (Muller algorithm), by using standard procedure RTMI.[27]

This mathematical model permitted the determinations of sublayer and copolymer compositions as a function of conversion (Figs 4—7).

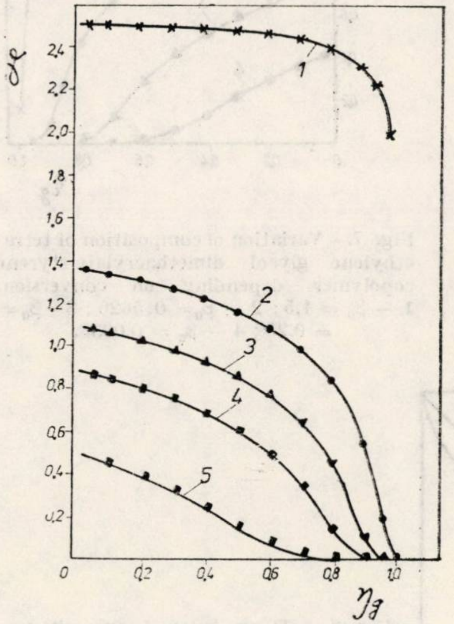

Fig. 4. — Variation of composition of ethylene dimethacrylate styrene copolymer depending on conversion. 1 — $\beta_0 = 2.4246$; 2 — $\beta_0 = 0.9092$; 3 — $\beta_0 = 0.6062$; 4 — $\beta_0 = 0.4041$; 5 — $\beta_0 = 0.1515$.

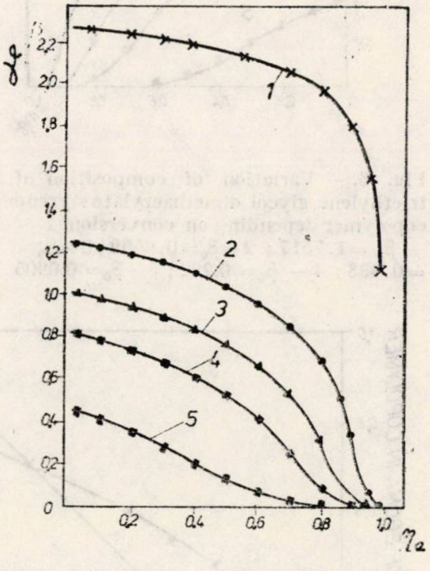

Fig. 5. — Variation of composition of diethylene glycol dimethacrylate styrene copolymer depending on conversion. 1 — $\beta_0 = 2.025$; 2 — $\beta_0 = 0.7594$; 3 — $\beta_0 = 0.5063$; 4 — $\beta_0 = 0.3375$; 5 — $\beta_0 = 0.1266$.

All these figures show a significant modification of copolymers composition depending on conversion for all systems studied previously. As known, copolymer composition depends on molar ratio of comonomers in the sublayer. As concerns ethylene dimethacrylate styrene, this dependence is represented in Fig. 8.

Mention should be made that the copolymerization process of diesters with styrene has the same peculiarities as the homopolymerization of the respective monomers. In this case, physical properties of the medium (growth of medium viscosity and formation of tridimensional polymer)

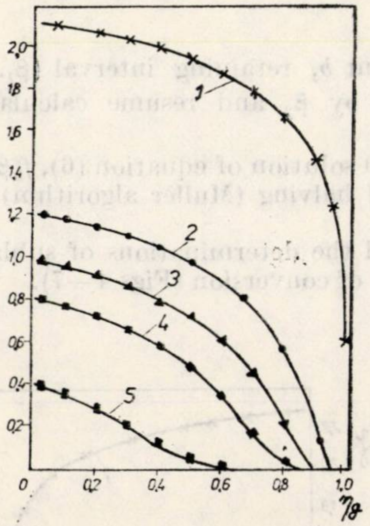

Fig. 6. — Variation of composition of triethylene glycol dimethacrylate styrene copolymer depending on conversion· 1 — — $\beta_0 = 1.7517$; 2 — $\beta_0 = 0.6569$; 3 — $\beta_0 = 0.438$; 4 — $\beta_0 = 0.292$; 5 — $\beta_0 = 0.0905$

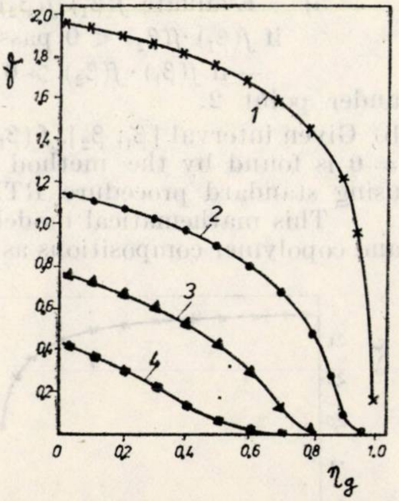

Fig. 7. — Variation of composition of tetraethylene glycol dimethacrylate styrene copolymer depending on conversion. 1 — $\beta_0 = 1.5$; 2 — $\beta_0 = 0.5626$; 3 — $\beta_0 = 0.25$; 4 — $\beta_0 = 0.0938$.

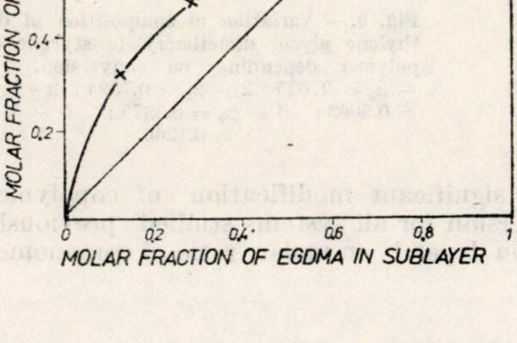

Fig. 8. — Dependence of composition of EGDMA-styrene copolymer depending on comonomer initial ratio.

will influence not only the process kinetics but also the instantaneous composition of copolymers.

It is quite conspicuous that the dependence of composition upon conversion, calculated on the basis of copolymerization constants, as well as the influence of the comonomer molar ratio on the copolymers formed, will be observed only in the first part of the process until the limiting conversion has been reached. When limiting conversion has been reached, the termination reaction takes place preeminently by a unimolecular mechanism, respectively by macroradical trapping in the tridimensional network. This allows the study of the copolymerization process of the ethylene dimethacrylate with styrene by ESR spectra, and will be treated in another paper.

CONCLUSIONS

1) The study of copolymerization process of ethylene dimethacrylate, diethylene glycol dimethacrylate, triethylene glycol-dimethacrylate and of tetraethylene glycol dimethacrylate with styrene has proven that the copolymerization process develops according to a kinetics similar to homopolymerization, the reaction rate depending on the diester content, growing simultaneously with the latter, while the limiting conversion is much higher.

2) The copolymerization constants grow from ethylene dimethacrylate to tetraethylene glycol dimethacrylate, proving that the reactivity of these monomers grows accordingly.

3) The copolymer compositions depend on the molar ratio of sublayer comonomers and are strongly modified depending on conversion.

REFERENCES

1 Part. V. Gh. Drăgan, Gh. Hubca, C. Oprescu and M. Dimonie, *Rev. Roumaine Chim.*, **27**, 585(1982).

[2] Tsuneo Kodama and Ide Fumio, *Kobunshi Kagaku*, **27**, 65 (1970); *Chem. Abstr.* **72** (26), 23 (1970).

[3] M. A. Askarov, Z. Stratu, T. Azizkhanov and S. D. Savranskaya, *Uzb. Khim. Zhur.*, **12** (5), 46 (1968); *Chem. Abstr.*, **70** (16), 18 (1969).

[4] M. S. Zlotnikov, *Ref. Zhur. Chem*, **1972**, 1179; *Chem Abstr.* **78** (4), 16833 (1973).

[5] J. Janacek and J. D. Ferry, *Reol. Acta.* **9**, 208 (1970).

[5] Ide Fumio and Kodama Tsuneo, Jap. Pat. 6.927.901 (1969); *Chem. Abstr.*, **74** (14), 33 (1971).

[7] Kawakara Tetsuya and Uno Hikatomo, Jap. Pat. 71. 38. 345 (1971); *Chem. Abstr.*, **77**, (14), 44 (1972).

[8] Ide Fumio and Deguchi Seiji, Jap. Pat. **71**. 11. 0 30 (1971); *Chem. Abstr.*, **75** (2), 56 (1971).

[9] L. H. Sperling. H. Volker and D. A. Thomas "Polymer Networks, Stuctt. Mech. Prop. Proc., ACS Symp", 1970; *Chem. Abstr.*, **77** (14), 33 (1972).

[10] Kadowaki Takaski, Itoyama Kenji and Kushida Yuichiro. Jap. Pat. 72. 35. 773 (1972); *Chem. Abstr.*, **78** (16), 57 (1973).

[11] R. Charomecek, I. Gavrilova and V. Satava, *Makromol. Chem.*, **135**, 35 (1970).

[12] Field Nathan D. and Williams Earl Pieree, Fr. Pat. 2.010.746 (1976); *Chem. Abstr.*, **73** (10), 31 (1970).

[13] A. B. Davankov, B. N. Trushin, SSSR Pat. 246.052 (1969); *Chem. Abstr.*, **71** (26), 69) (1969).

[14] A. B. Davancov, B. N. Trushin and Yu. E. Doroshenko, S.S.S.R. Pat. 246.049 (1969); *Chem. Abstr.* **71** (26), 56 (1969).

[15] Lim Drahoslav, Coupek Jiri, Pokorny Svatopluk and Krivakova Miroslava, German Pat. 2.157.627 (1972); *Chem. Abstr.*, **78** (12), 33 (1973).

[16] Pfitzner K. and F. Fraffczyk, German Pat. 1.816.380 (1970); *Chem. Abstr.*, **74** (14), 54 (1971).

[17] C. C. Allen, W. Oraby, D. R. Squire, E. P. Stahel and V. T. Stannett, *J. Macromol. Sci. Chem.*, **8**, 965 (1974).

[18] M. M. Micko and L. Paszner; *J. Radiat. Curing*, **1** (3), 3 (1974).

[19] M. M. Micko and L. Paszner; *J. Radiat. Curing*, **1** (4), 2 (1974).

[20] B. P. Pashinin, M. M. Gerner, I. Ya, Poyurovskaya, V. N. Batovskii, L. N. Mats and N. K. Vlasova; S.S.S.R. Pat. 303.067 (1971); *Chem. Abstr.*, **75** (26), 33 (1971).

[21] T. H. Shepherd and F. E. Gould; U.S. Pat. 3. 574.826 (1971); *Chem. Abstr.*, **75** (2), 69 (1971).

[22] T. H. Shepherd and F. E. Gould; U.S.Pat. 3.520.949 (1970); *Chem. Abstr.*, **73** (16), 39 (1970).

[23] Atsuda Mitsuru, Nakabayaski Nobuo and Masuhara Eüchi; *J. Biomed. Mater. Res.*, **5** (3), 183 (1971).

[24] Gh. Hubca, C. Oprescu, Gh. Drăgan and M. Dimonie; *Rev. Roumaine Chim.*, **27**, 433(1982).

[25] T. Kellen and F. Tüdos, *J. Macromol. Sci. Chem.*, **A9** (1), 1 (1975).

[26] D. S. Vasilescu and M. Dimonie, *Mat. Plastice*, **9**, 11 (1972).

[27] G.S.P./360, IBM, Gh. 20 — 0205 — 4.

Revue Roumaine de Chimie, 27, 5, 667–671(1982)

AMPEROMETRIC DETERMINATION OF THIAMINE

CLEOPATRA CALU and EUGENIA DONIGA
Department of Analytical Chemistry, Polytechnical Institute of Iassy, 71
Splai Bahlui 6600 Iassy, Romania

Received July 1, 1981

Thiamine (vitamin B_1) forms with metawolframic acid a sparingly soluble compound of a clearly defined composition. That is why this reagent has been used for separating and determining thiamine in the B vitamin complex. For determinations, the amperometric method with mercury dropping electrode was used.

1. INTRODUCTION

The large class of iso- and heteropolycombinations, the metawolframic acid belongs to attracted firstly the investigators' attention only from a theoretical point of view, owing to their structural peculiarities, obtaining ways, properties, high water content. Later, these combinations found wider and wider applications in numerous fields of the chemistry, under various aspects. Their ability to take part in hardly soluble or coloured combinations made them interesting for the analytical chemists.[1]

Known among the iso- and heteropolywolframates as one of the most stable compounds[2], the metawolframic acid $H_6[H_2W_{12}O_{40}]$ was scarcely used owing especially to the difficulties encountered in its synthesis and the low yields. The development of a new route of synthesis,[3] based on the ionic exchange between the sodium wolframate and a strongly acid resin added accessibility to the good analytical qualities of the metawolframic acid.

2. EXPERIMENTAL

2.1. Metawolframic acid as precipitating reagent

The metawolframic acid forms hardly soluble salts with a series of heavy metal ions such as Pb^{2+}, Hg_2^{2+}, Ag^+, Tl^+, as well as with many organic substances such as alcaloids, dyes, drugs.

As a compound with a large molecular weight (2854.24 g/mole), stable all over the concentration range and over a large pH range (its decomposition under the action of ions OH starts only after adding six moles of a basis per mole of acid), the metawolframic acid meets all the requirements for a good precipitating reagent.

Its use as a reagent for thiamine (B_1 vitamin):

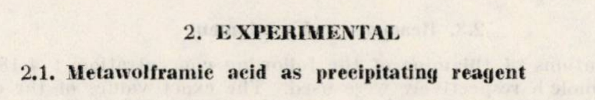

Fig. 1. — Thiamine.

has also the advantage of a particularly good selectivity in all media and in the presence of other substances which frequently accompany thiamine such as B_2, B_6, and B_{12} vitamins and phosphobion. The fact can be also mentioned that in dosing the B_1 vitamin in biological liquids the previous removal of proteins is required.

By reaction between the metawolframic acid and thiamine a white, amorphous precipitate is formed characterized by a combination ratio of 1/2 (1/2 metawolframic acid to thiamine mole ratio). The reaction can be used as a gravimetrical mode of thiamine dosing. In this case the obtained precipitate washed and filtered on a filter with small pores is brought to the WO_3 stable form by calcinating at 650°C.

2.2. Amperometric method of thiamine dosing

The range of metawolframic acid uses has been greately extended since the elucidation of its behavior in the presence of polarizable electrodes. The polarogram recorded in the presence of a 1M Na_2SO_4 solution, $s = 1/100$, using Hg dropping electrode, as indicator electrode and saturated calomel electrode as reference electrode (Fig. 2) has three clear polarographical steps with well defined and constant half-wave potentials ($E'_{1/2}=0.57$ V, $E''_{1/2}= -0.78$ V, $E'''_{1/2}= -0.99$ V. Both the polarographical behavior and the ability of precipitating quantitatively and selectively thiamine justify the use of metawolframic acid as a reagent in the amperometric titration of the B_1 vitamin.

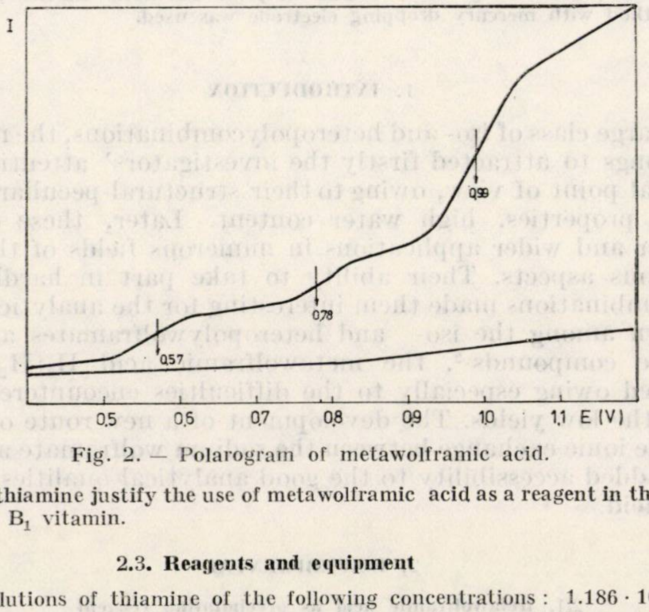

Fig. 2. — Polarogram of metawolframic acid.

2.3. Reagents and equipment

Three solutions of thiamine of the following concentrations : $1.186 \cdot 10^{-2}$, $2.96 \cdot 10^{-3}$ and $5.92 \cdot 10^{-4}$ mole/l, respectively were used. The exact values of the concentrations were determined using the volumetric method, according to the Romanian Pharmacopeea. [4]

The solutions of metawolframic acid used for titration had the following concentrations $1.138 \cdot 10^{-2}$, $2.276 \cdot 10^{-3}$ and $4.552 \cdot 10^{-4}$ mole/l, respectively. In order to determine the concentrations exactly measured, the volumes of the acid solutions were calcinated at 600°C, the amount of WO_3 being then measured.

The samples submitted to the amperometric analyses were obtained by adding variable volumes of thiamine solutions in 20 ml Na_2SO_4 solution 1M. The measurements were taken on a Heyrovsky LP 55A type apparatus with optical recording system at a constant potential value of -0.65 V.

3. RESULTS AND DISCUSSION

The experimental data evidenced the accuracy of the method. The obtained results are perfectly reproducible, clear and easily workable up to a thiamine concentration of $1.44 \cdot 10^{-5}$ mole/l in the analysed solu-

TABLE 1

Amperometric determination of thiamine with metawolframic acid

Nr.	Thiamine concentration (in the titrated sample) mole/l	Concentration of metawolframic acid mole/l	Amount of thiamine		Relative accuracy of the run
			Introduced g	Found experimentally g	
1_1	$1.07.10^{-3}$	$1.13\cdot10^{-2}$	$8.00\cdot10^{-3}$	$7.98\cdot10^{-3}$	99.79
1_2	$9.88\cdot10^{-4}$	$1.13\cdot10^{-2}$	$8.00\cdot10^{-3}$	$8.01\cdot10^{-3}$	100.17
1_3	$8.45\cdot10^{-4}$	$1.13\cdot10^{-2}$	$7.98\cdot10^{-3}$	$7.99\cdot10^{-3}$	99.985
2	$4.92\cdot10^{-4}$	$1.13.10^{-2}$	$3.99\cdot10^{-3}$	$3.91\cdot10^{-3}$	98.05
3	$2.19\cdot10^{-4}$	$2.27\cdot10^{-3}$	$1.89\cdot10^{-3}$	$1.85\cdot10^{-3}$	97.52
4	$7.20\cdot10^{-5}$	$2.27\cdot10^{-3}$	$4.99\cdot10^{-4}$	$4.91\cdot10^{-4}$	98.415
5_1	$1.44\cdot10^{-5}$	$4.55\cdot10^{-4}$	$9.98\cdot10^{-5}$	$9.82\cdot10^{-5}$	98.42
5_2	$1.44\cdot10^{-5}$	$4.55\cdot10^{-4}$	$9.98\cdot10^{-5}$	$1.04\cdot10^{-5}$	104.60
5_3	$1.44\cdot10^{-5}$	$4.55\cdot10^{-4}$	$9.98\cdot10^{-5}$	$1.02\cdot10^{-5}$	103.00

tion, which corresponds to a minimum thiamine content in the sample of $9.98\cdot10^{-5}$g (Table 1, Fig. 3).

As it can be seen in table 1 and Fig. 3 the obtained data evidence both the accuracy of the method and the reproducibility of results at the upper and down limits, respectively, of the concentration range investigated by us (10^{-3} – 10^{-5} mole/l thiamine in the solution submitted to the amperometric analysis). The fact can be emphasized that the maximum error value of the run does not exceed 5 %.

In table 2 a comparison of the sensitivity of the amperometric method with that of other methods used in analysing the B_1 vitamin is given.

The method developed by us proves to be more sensitive than all the other methods used in thiamine determination, including the colorimetric method, the mostly used method at present.

TABLE 2

Sensitivity limits of the method used in thiamine determination

Determination method	Minimum amount of substance for which the determination is possible
Gravimetric	$2.4\cdot10^{-2}$*
Volumetric	$1.0\cdot10^{-1}$ 4
Colorimetric	$3.0\cdot10^{-4}$ 5
Amperometric	$9.98\cdot10^{-5}$

* Determination as thiaminemetawolframate.

Another question that had to be solved was connected with the behavior of other substances accompanying usually the B_1 vitamin in the presence of metawolframic acid. With this aim in view, in three solutions containing B_1 vitamin with a concentration of $4.92\cdot10^{-4}$ mole/l, the following were added: 0.05 g B_6 vitamin (pyridoxine chloride) and 0.001 g B_{12} vitamin (cyancobalamine) in the first, 0.01 g phosphobion in the second and 0.01 g B_2 vitamin (riboflavine) in the third solution, respectively. The curves of amperometric titration were recorded in the three cases and compared to those obtained in the presence of thiamine alone.

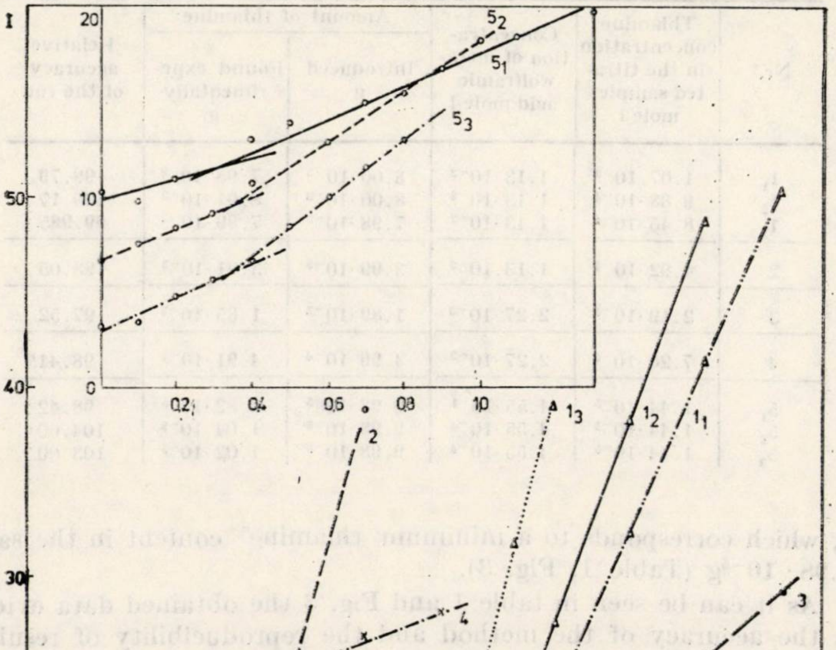

Fig. 3. — Amperometric determination of thiamine. 1_1 — 2 ml thiamine $1.186 \cdot 10^{-2}$ mole/l; $s = 1/500$; 1_2 — 4 ml thiamine $5.930 \cdot 10^{-3}$ mole/l; $s = 1/500$; 1_3 — 8ml thiamine $2.960 \cdot 10^{-3}$ mole/l; $s = 1/300$; 2 — 4 ml thiamine $2.960 \cdot 10^{-3}$ mole/l; $s = 1/300$; 3 — 1.6ml thiamine $2.96 \cdot 10^{-3}$ mole/l; $s = 1/200$; 4 — 0.5ml thiamine $2.96 \cdot 10^{-3}$ mole/l; $s = 1/200$; 5_1 — 0.5ml thiamine $5.92 \cdot 10^{-4}$ mole/l; $s = 1/30$; 5_2 — 0.5ml thiamine $5.29 \cdot 10^{-4}$ mole/l; $s = 1/30$, 5_3 — 0.5 ml thiamine $5.92 \cdot 10^{-4}$ mole/l; $s = 1/30$.

As it can be seen, the presence of the mentioned compounds does not influence either the thiamine behavior or the process stoichiometry.

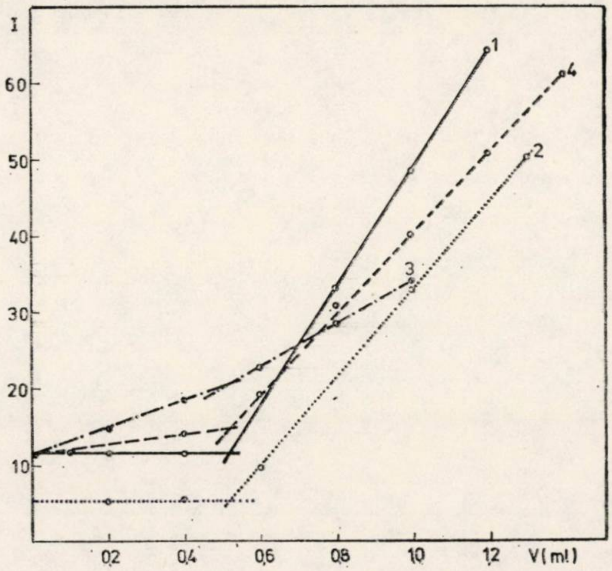

Fig. 4. Influence of the components of B complex on the amperometric titration of thiamine. 1 — thiamine solution $4.92 \cdot 10^{-4}$ mole/l ; 2 — thiamine solution $4.92 \cdot 10^{-4}$ mole/l+ +0.05 g pyridoxine chloride + 0.001 g cyancobalamine ; 3 — thiamine solution $4.92 \cdot 10^{-4}$ mole/l + 0.01 g phosphobion ; 4 — thiamine solution $4.92 \cdot 10^{-4}$ mole/l + 0.01 g riboflavine. In all cases $s = 1/300$.

4. CONCLUSIONS

1. Using the remarkable qualities of the metawolframic acid as precipitating reagent an amperometric method for thiamine determination was developed.

2. The accuracy of thiamine determination within the 10^{-3} — 10^{-5} mole/l concentration range and the sensitivity of the method were determined.

3. The behavior of the compounds accompanying frequently the thiamine in B complex towards the metawolframic acid was investigated.

REFERENCES

[1] E. A. Nikitina, "Kheteropolicombinatsii", Ed. Khimiia, Moscow 1962, p. 393—413.
[2] Cl. Calu, Ph. D. Thesis, Biblioteca I. P. Iași, 1971.
[3] Cl. Calu and N. Calu, *Bul. Inst. Politeh. Iași*, in press.
[4] "Farmacopeea Română", ed. IX, Ed. medicală, București, 1976.
[5] Gh. Nuță and C. Bușneag, "Investigații biochimice", Ed. didactică și pedagogică, București, 1977, p. 284.

Revue Roumaine de Chimie, 27, 5, 673–679 (1982)

ION EXCHANGE PROCEDURE FOR THE ELIMINATION OF INTERFERENCES IN THE SPECTROPHOTOMETRIC DETERMINATION OF MAGNESIUM WITH ERIOCHROME BLACK T.

LUMINIȚA VLĂDESCU and ANA ISUF

National Institute of Chemistry, Laboratory of Analytical Chemistry,
Splaiul Independenței 202, Bucharest, Romania

Received September 14, 1981

The present investigation is designed to study the influence of the complexing agent Eriochrome black T on the ion exchange behaviour of Mg, Ca and Fe under various working conditions. Evidence is furnished of the possibility of coupling spectrophotometric determination of Mg, using the mentioned reagent, with an ion exchange procedure leading to elimination of the interferences produced by Ca^{2+} and Fe^{3+} present in the products in which Mg is determined.

The use of Eriochrome black T for quantitative determination of magnesium is well known, either as indicator in titration with Complexon IIII, [1] or as dye reagent for spectrophotometric determination.[2]

In alkaline solution (pH ~ 10) Eriochrome black T [2-Hydroxy-1-(1-hydroxy-2-naphthylazo)-6-nitronaphthalene-4-sulfonic acid sodium salt] form with magnesium ions a red, water-soluble complex. At pH 10.6 the absorption maximum of the colour complex is at 560 nm.

Spectrophotometric determination of magnesium with Eriochrome blak T is a sensitive, reproducible method but a series of elements interfere, the most common being Ca and Fe. Na and K interfere at a concentration greater than 0.01 M as the result of a salt effect. [2–6]

The procedures proposed in the literature for eliminating these interferences are arduous and their use could bring about a number of errors, as reported in various publications.[2]

The present investigation is designed to study the influence of the complexing agent Eriochrome black T on the ion exchange behaviour of Mg, Ca and Fe under various working conditions. Evidence is furnished on the possibility of coupling spectrophotometric determination of Mg, using the mentioned reagent with an ion exchange procedure leading to elimination of the interferences produced by Ca^{2+} and Fe^{3+} present in the products in which Mg is determined.

EXPERIMENTAL

Chemicals and equipment

— Strongly acid cation exchange resin Amberlyte IR — 120 ;
— strongly basic anion exchange resin Vionit AT—1
— known titrum aqueous solutions of Mg^{2+}, Ca^{2+} and Fe^{3+} ions ;
— $5 \cdot 10^{-3}$ M — 10^{-2} M Eriochrome black T aqueous and methanolic (50—90 % v/v) solutions ;
— NH_3, NH_4Cl, KSCN, α,α′-dipyridyl solutions ;
— methyl alcohol, acetone ;
— SPECOL spectrophotometer Karl Zeiss-Jena ;
— mechanical stirrer.

The quantitative determination of investigated ions was performed by spectrophotometric methods, in the presence of Eriochrome black T for Mg and Ca[2], and KSCN[7] or α,α′-dipyridyl [8] for Fe.

Use has been made for ion exchange experiments of glass columns, 20 cm long, 1 cm in diameter, provided with a stopcock at the bottom and with a dropping funnel with ground glass joint at the top.

Known amounts of ion exchanger swolen in water, purified and activated in H^+ or Cl^- ionic form were packed in the columns, or were used in stirring experiments.

RESULTS AND DISCUSSION

With a view to establishing the best working conditions the influence of the ionic form of the resin and pH on Mg, Ca and Fe ion exchange behaviour, in the presence of Eriochrome black T, was studied.

To this end, 50 ml of a solution containing known quantities of metal ion and reagent, at different pH, were passed through a column with strongly acid cation exchange resin Amberlite IR—120 in the H^+ or NH_4^+ ionic form. The column was washed with a reagent solution in the concentration and pH of the sample. The effluent was collected in calibrated flasks and the absorbance was measured thus determining the quantity of metal ion not retained within the resin. The quantity of ion fixed in the cationite was determined after elution with 2M HCl.

TABLE 1

Influence of the ionic form of the resin and of pH upon the cation exchange behaviour of Mg(II), Ca(II) and Fe (III) in the presence of 10^{-2}M Eriochrome black T

Ionic form of the resin	pH	Mg(II)			Ca(II)			Fe(III)		
		In sample mg	Determined		In sample mg	Determined		In sample mg	Determined	
			R mg	S mg		R mg	S mg		R mg	S mg
H^+	10	0.0486	0.0480	—						
NH_4^+	10	0.0486	0.0470	0.0020	0.0800	0.0792	—	0.0540	0.0536	—
NH_4^+	9	0.0486	0,0496	—						

The results in table 1 show that all the elements studied have the same behaviour, i.e. irrespective of the ionic form of the resin and pH, they are retained in resin.

Furthermore, the effects of substituting water by methyl alcohol and of increasing NH_3 concentration in the system, were also studied.

Optical absorption spectra showed that with increase in methanol and NH_3 concentration in the reaction system, absorbance increases but remains proportional to concentration.

The influence of methyl alcohol and ammonia concentration on the ion exchange behaviour of Mg, Ca and Fe was established by two procedures.

a) under the working conditions chosen the sample containing the complex was passed through the column with resin in NH_4^+ ionic form, pre-treated with reagent solutions in methanol and ammonia concentrations corresponding to those in the sample (working solution); the effluent solutions resulting after passing the sample through the resin column and washing it with the working solution, were collected in calibrated flasks and then used for establishing the quantity of metal ion in the effluent by measuring its absorbance;

b) the cation was fixed in the resin in NH_4^+ ionic form, then eluted with the reagent solution of a given concentration and pH. In this case both separation through the column and stirring method were used.

Table 2 shows that, irrespective of the working method, Mg prefers the resin phase at low NH_3 concentration but remains in solution in the form of a complex compound with Eriochrome black T when NH_3 concentration is increased and water is substituted with methanol.

Under similar working conditions iron presents an analogous behaviour whereas calcium is always retained in the cationite.

Therefore, Mg can be determined spectrophotometrically with Eriochrome black T in the presence of Ca^{2+} by measuring the absorbance of analyzed solution in the presence of reagent, 90% methanol, 0.76 M NH_3, after passing the latter through a column with cation exchange resin in NH_4^+ ionic form, that retains Ca^{2+} ions.

For eliminating the interferences produced by iron ions, one of the procedures presented in schemes A and B can be used.

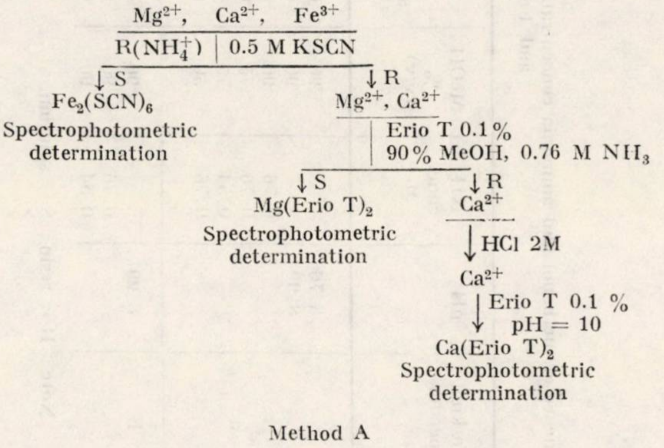

Method A

Note: R = resin; S = solution

TABLE 2

Influence of methanol and ammonia concentrations, of working procedure and of pH upon the cation exchange behaviour of Mg(II), Ca (II) and Fe(III), in the presence of 10^{-2} M Eriochrome black T

Working procedure	pH*	NH_3 conc. M	MeOH % (v/v)	Mg(II)			Ca(II)			Fe(III)		
				In sample mg	Determined		In sample mg	Determined		In sample mg	Determined	
					R mg	S mg		R mg	S mg		R mg	S mg
a	8.70	—	90	0.0486	0.0480	—	—	—	—	—	—	—
	8.99	—	90	0.0486	0.0478	—	—	—	—	—	—	—
		0.76	90	0.0486	—	0.0482	0.0800	0.0796	—	0.0540	—	0.0546
		0.76	75	0.0486	—	0.0479	0.0800	0.0796	—	0.0540	—	0.0533
		0.54	75	0.0486	0.0120	0.0358	—	—	—	—	—	—
		0.76	50	0.0486	0.0477	—	—	—	—	—	—	—
b	8.99	—	90	0.0486	0.0186	0.0305	—	—	—	—	—	—
		0.76	90	0.0486	—	0.0490	0.0800	0.0792	—	0.0540	—	0.0535
		0.54	90	0.0486	0.0360	0.0118	—	—	—	—	—	—

Note : R = resin ; S = solution.

In the case of procedure A, the sample is passed through a cation exchange resin that fixes all the cations from the solution. Iron can be eluted selectively with a KSCN solution in acetone, and the effluent collected in a calibrated flask is used directly for its spectrophotometric determination.

Following introduction of the resin in a flask, repeatedly shaken with 50 ml Eriochrome black T solution in 90% methanol, 0.76 M NH_3, Mg is extracted and determined by measuring the extract absorbance.

Calcium is then eluted with 2M HCl and determined quantitatively.

In the case of procedure B the solution is treated with KSCN and the complex anion formed by Fe(III) with this reagent is fixed in an anion exchange resin.

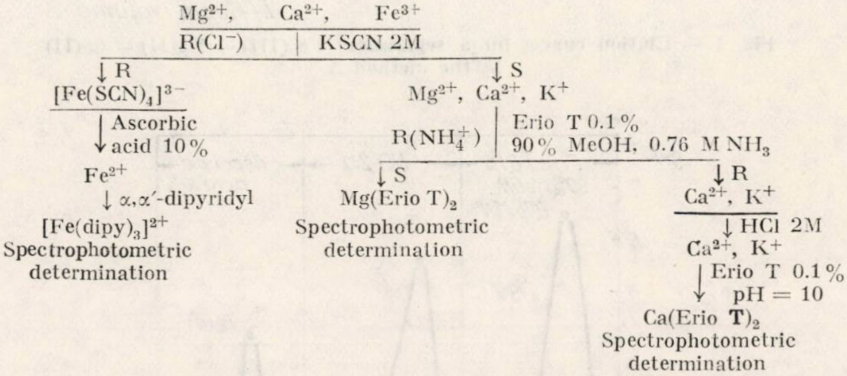
Mg^{2+}, Ca^{2+}, Fe^{3+}
$R(Cl^-)$ | KSCN 2M
R
S
$[Fe(SCN)_4]^{3-}$
Mg^{2+}, Ca^{2+}, K^+
Ascorbic acid 10%
$R(NH_4^+)$
Erio T 0.1%
90% MeOH, 0.76 M NH_3
Fe^{2+}
S
R
α,α′-dipyridyl
$Mg(Erio\ T)_2$
Ca^{2+}, K^+
$[Fe(dipy)_3]^{2+}$
Spectrophotometric determination
Spectrophotometric determination
HCl 2M
Ca^{2+}, K^+
Erio T 0.1%
pH = 10
$Ca(Erio\ T)_2$
Spectrophotometric determination

Method B

Note : R = resin ; S = solution.

By adding to the iron-free solution, Eriochrome black T under the established conditions and measuring the absorbance of the effluent collected after passing through a cation exchange resin column, the quantity of magnesium in the analyzed sample can be determined.

Calcium can be eluted from cationite with 2M HCl and iron is separated from the cation exchange resin by elution with α,α-dipyridyl solution after reduction with 10% ascorbic acid.

The A and B procedures were applied on synthetic mixtures containing known quantities of Mg, Ca and Fe. Figures 1 and 2 show the elution curves obtained in two cases.

Table 3 gives the results obtained by the two procedures applied for the determination of magnesium in samples containing various quantities of calcium and iron. Good agreement is observed between the Mg quantities in the samples and those determined after separation.

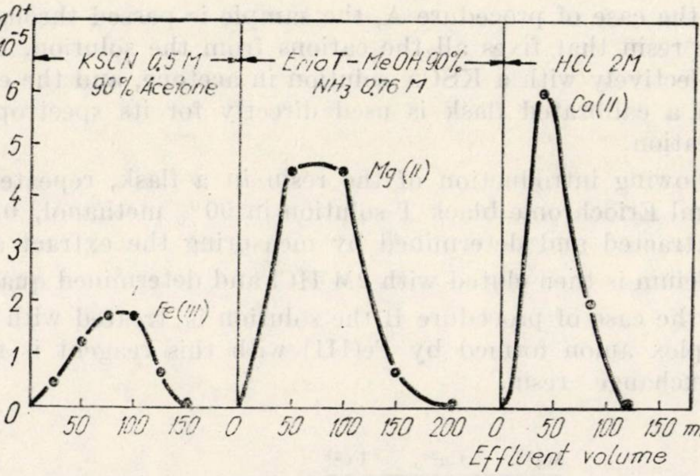

Fig. 1. — Elution curves for a separation Fe (III) — Mg(II) — Ca(II) by the method A.

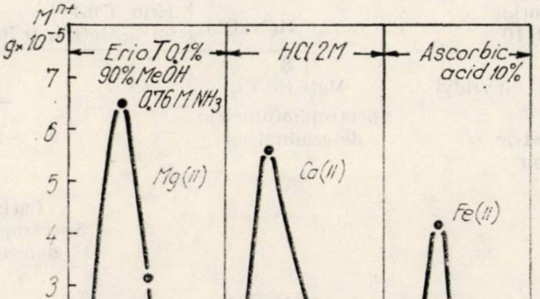

Fig. 2. — Elution curves for a separation Mg(II) — Ca(II) — Fe(III) by the method B.

TABLE 3

Results of magnesium determination from syntetic mixtures with Ca(II) and Fe(III) content

Mg(II)		Method			
	In sample mg		0.0486	0.0972	0.486
	Determined after separation mg	A	0.0478		
		B	0.0480	0.0769	0.5855

Note : A and B = working procedure

CONCLUSIONS

Magnesium can be determined by the method using the organic reagent Eriochrome black T in samples containing Ca and Fe, by coupling the spectrophotometric method with an ion exchange procedure that permits elimination of the interfering elements.

Eriochrome black T is used both as complexing agent, permitting separation with cation exchange resins and as dye reagent for spectrophotometric determination.

REFERENCES

[1] C. Liteanu and E. Hopîrtean, "Chimie analitică cantitativă. Volumetria", Ed. didactică şi pedagogică, Bucureşti, 1972.

[2] E. Aubary and Y. M. Harvey, *Analyt. Chem.*, **25**, 493 (1953).

[3] H. Pohl. *Z. analyt. Chem.*, **155**, 263 (1957).

[4] W. Dirscherl and H. Breuer, *Mikrochim. Acta*, **40**, 322 (1953).

[5] J. K. R. Gasser, *Analyst*, **80**, 482 (1955).

[6] F. H. Pollard and J. V. Martin, *Analyst*, **81**, 348 (1956).

[7] M. Zimmermann, "Photometric Metal and Water Analysis", W. V. C, Stuttgart, 1962, section B—b 6/1 (61).

[8] S. T. Woods and M. G. Mellon, *Ind. Eng. Chem., Anal. Ed.*, **13**, 551 (1941).

Revue Roumaine de Chimie, 27, 5 681–683 (1982)

LIQUID MEMBRANE ELECTRODES FOR BENZOIC ACID DETERMINATION

LUIGI CAMPANELLA, TOMMASO FERRI, MARA GABRIELLI
Institute of Analytical Chemistry, University, Rome, Italy

Two liquid membrane electrodes, based on quaternary ammonium exchangers, are prepared and characterized for the analytical problems of determining benzoic acid. Their behaviour is comparatively investigated and discussed.

In previous papers [1–6] we described the preparation, characteristics and application of liquid membrane electrodes for the determination of organic anions, such as benzoate, oxalate, acetate. The liquid membrane is constituted by a solution in 1-decanol of a quaternary ammonium corresponding salt, the nature of the ammonium cation being always the same (trimethylcetylammonium).

We thought of some interest to study the influence of the nature of the alkyl groups bound to nitrogen atom on the electrode characteristics. So, in this paper two other liquid membrane electrodes selective to benzoate are prepared and characterized, based respectively on dimethyldicetylammonium and benzyldimethylcetylammonium-benzoate (DMDCAB and BDMCAB).

EXPERIMENTAL

Reagents : to prepare DMDCAB firstly DMDCABr was prepared by the reaction between dimethylamine and cetylbromide in ethanol/water mixture ($v/v = 2:1$)

$$\mathrm{Me_2NH + C_{16}H_{33}Br \longrightarrow HBr + Me_2NC_{16}H_{33} \xrightarrow[\text{(NaOH)}]{\mathrm{C_{16}H_{33}Br}} Me_2N(C_{16}H_{33})_{22}\,Br^-}$$

DMDCABr was made to react with silver benzoate at room temperature and in the absence of light. A quantitative yield of DMDCAB is ensured by the great difference between the solubilities of AgBr (5.9×10^{-7}M) and Ag benzoate (1.1×10^{-2} M). For the obtained product recrystallized from acetone elemental and thermal analysis, u.v and NMR spectra guaranteed the postulated nature and indicated the presence of two crystallization water molecules.

BDMCAB was prepared by reaction between BDMCACl commercially available and silver benzoate, in this case too the ratio between the solubilities of AgCl and Agbenzoate (about 10^{-3}) being sufficient to ensure the completness of the reaction, even if at a lower degree than in the preceeding case. The prepared compound was checked by thermal and elemental analysis and by U.V and NMR spectra ; its formula can be assumed as $\mathrm{BDMCAB \cdot H_2O}$.

Apparatus and membrane electrodes : as described in previous papers [1,2,5] with the only difference of the employment of the new sensors. Cell : Ag—AgCl 0.01 M NaCl, 0.1 M Na benzoate—membrane—DMDCAB (or BDMCAB) 0.01 M in 1-decanol—membrane solution under test//S.C.E.

RESULTS AND DISCUSSION

The characteristics of the two electrodes are summarized below :

Response time	DMDCAB electrode from few seconds to one minute according to concentration to be determined ; critical functions of stirring conditions	BDMCAB electrode the same as for DMDCAB electrode
Linearity response concentration range	$5 \times 10^{-4} - 10^{0}$M	,,
Slope as a function of the membrane solution concentration	ranging from -59.5 mV/concn decade to -54 mV/concn decade for concn ranging from 5×10^{-4} to 5×10^{-4} M (-57 mV/concn decade for 5×10^{-3} M)	ranging from -59.5 to -55.0 mV/concn decade for concn ranging from 5×10^{-2} M to 5×10^{-4} M (-57 mV/concn dec for 5×10^{-3} M)
Reproducibility	± 5%	± 5%

The selectivity constants determined by the Moody and Thomas method [7] resulted to be :

Selectivity constants of the three liquid membrane electrodes sensitive to benzoate

X^{n-}	DMDCAB	BDMCAB	TMCAB[5]
F^-	8.5×10^{-3}	7.5×10^{-3}	6.2×10^{-3}
Cl^-	9.6×10^{-2}	9.0×10^{-2}	4.6×10^{-2}
Br^-	2.4×10^{-1}	1.5×10^{-1}	9.4×10^{-2}
I^-	1.1	1.4	4.0×10^{-1}
NO_3^-	2.9×10^{-1}	3.5×10^{-1}	1.3×10^{-1}
NO_2^-	1.3×10^{-1}	1.5×10^{-1}	5.0×10^{-2}
HPO_4^{2-}	3.2×10^{-3}	1.1×10^{-3}	no interference
PO_4^{3-}	5.5×10^{-3}	3.0×10^{-3}	no interference
CO_3^{2-}	6.9×10^{-3}	5.2×10^{-3}	no interference
OH^-	8.3×10^{-3}	1.4×10^{-1}	3.0×10^{-2}
ClO_4^-	2.7	3.1	6.1×10^{-1}
CH_3COO^-	2.6×10^{-2}	2.9×10^{-2}	1.4×10^{-1}
oxalate	4.7×10^{-3}	6.7×10^{-3}	no interference
nicotinate	1.8×10^{-1}	4.7×10^{-1}	1.3×10^{-1}
SO_4^{2-}	1.0×10^{-3}	9.0×10^{-4}	no interference
SO_3^{2-}	9.0×10^{-4}	1.4×10^{-2}	

By comparing the two new electrodes selective to benzoate prepared by us and the already described one [5] it can be concluded that the reproducibility, response time, slope are almost the same or, in any case, very near. The linearity concentration ranges are characterized by some differences of the upper limit value and exactly by the same value of the lower limit one. This value seems to be established by the nature of the solvent in the membrane solution ; really if 1-undecanol is employed in the place of decanol such a limit results to be shifted down to 5×10^{-5} M.

The values of the selectivity constants show that only little differences are observed : anyway TMCAB electrode is generally a little bit more selective than the other ones, even if BDMCAB looks to be preferred if employed in the presence of acetate and sulphate. The observed differences and the comparison between the behaviour of DMDCAB electrode and of BDMCAB one, favourable to the latter, seem to advise the opportunity of employing, for the membrane, ion exchangers which are not too heavy and characterized by not too much hindering counter ions.

Applications : the two electrodes can be advantageously employed for determining benzoic acid and its salts in commercial products of different nature, such as medicinal syrups and biological liquids.

Work carried out with the aid of Italian National Researches Council (CNR).

REFERENCES

[1] L. Campanella T. Ferri and D. Gozzi, *Rev. Roumaine Chim.*, **23**, 281 (1978).
[2] L. Campanella, G. De Angelis, T. Ferri and D. Gozzi, *Analyst*, **102**, 723 (1977).
[3] L. Campanella and D. Gozzi, *Ann. Chim. (Ital.)*, **67**, 345 (1977).
[4] D. Gozzi, L. Campanella and T. Ferri, *Electrochim. Acta*, **24**, 817 (1979).
[5] M. T. Benignetti, L. Campanella and T. Ferri, *Z. analyt. Chem.*, **296**, 412 (1979).
[6] L. Campanella and T. Ferri, *Z. analyt. Chem.*, **302**, 304 (1980).
[7] G. J. Moody and D. R. Thomas, "Selective Ion Electrodes", Merrow Techn. Library, Watford, 1971.

Revue Roumaine de Chimie; *27, 5,* 685–689 (1982)

DETERMINATION OF GOLD BY GRAPHITE FURNACE —ATOMIC ABSORPTION SPECTROMETRY WITH ATOMIZATION UNDER PRESSURE

JÁNOS FAZAKAS
Center of Analytical Spectrochemistry,
Bd. Marasti 61, R—71331 Bucharest, Romania

Received September 1981

Atomization under pressure decreases the peak height but enhances slightly the peak area sensitivity of gold. The improvement in the peak area sensitivity is probably explained by the prolonged residence time of atoms with pressurized atomization. Peak characterization times are altered considerably with atomization under pressure. The linearity of the calibration curves is considerably improved in both peak area and peak height modes. This is probably explained by the Lorentz broadening of the absorption profile, and the improvement of the relative time resolution of the detection system.

1. INTRODUCTION

Atomization under pressure formed the subject of several recent investigations in this laboratory. Thus it was found that for palladium [1] the sensitivity of resonance lines is worsened while that of the nonresonance lines improves with increasing atomization pressure. In the case of manganese [2] only peak areas are enhanced for the resonance lines while peak height is diminished. In the case of the nonresonance lines of manganese however [2] both peak area and height are enhanced with increassing atomization pressure. Aluminium [3] and silver [4] were found to have only improved peak area with pressurized atomization. For all elements and wavelengths investigated so far, the linearity of the calibration curves was extended with increasing atomization pressure.

In an interesting investigation Donega and Burgess [5] found better sensitivity with atomization below atmospheric pressure. Chakrabarti et al. [6] found a decrease of peak and integrated absorption for all elements investigated (cadmium, lead, copper and molybdenum). Using a graphite furnace of a different design Hoenig et al. [7] found improved sensitivity for copper lead and cadmium. Chakrabarti et al. [6] and Hoenig et al. [7] also noted an improved linearity of calibration curves with atomization under pressure.

The purpose of the present communication is to investigate the behaviour of gold with atomization under pressure. To the author's knowledge no such report was as yet published in the literature.

2. EXPERIMENTAL

The graphite furnace used was an IL 555B CTF. Single piece pyrocoated graphite tubes were used as supplied by the manufacturer. 99.997% argon was used as purge gas. Atomization pressure was as read on the manometer of the furnace power supply. When not pressurized the purges gas flow rate was ca. 4.7 l. min^{-1} (10 SCFH). Ashing was made at 550° C and atomization at 1750°C as recommended [8] by the manufacturer.

Samples were deposited as a spray in the furnaces heated to ca. 150°C, using a FASTAC 254 autosampler. Calibration curves were constructed using different deposition times[1-4]. Under the conditions used a 1 second deposition time corresponded to approximately 1 microliter of sample.

Absorbance measurements were performed with an IL 551 Video spectrometer used in the single beam mode. Peak shapes and parameters were studied from the video display of the instrument. The numerical values quoted for the peak characterization times represent the mean of several hundred determinations obtained with different graphite tubes during a period of ca. 6 months.

The primary radiation source was a Varian hollow cathode lamp operated at 5 mA. The 242.8 nm line was used with a slit size of 1.0 nm.

The stock solution was prepared by dissolving 0.1 g of gold in 100 ml aqua regia. Dilute standards were prepared by serial dilutions, and were made 0.05 % in HNO_3 to prevent hydrolysis.

Other experimental details were described elsewhere. [1-4]

3. RESULTS AND DISCUSSIONS

Figure 1 shows the variation of the response of gold as a function of atomization pressure. It may be seen from Figure 1 that while the peak area is slightly enhanced as pressure is increased, peak height shows a steady decrease. The decrease in peak height is probably due to the Lorentz broadening of the absorption profile. [1-4,6]. Since with increasing atomization pressure the mean residence time of atoms is also increased, the Lorentz broadening is compensated for when considering peak area. In order to check the validity of the above statement the peak shapes

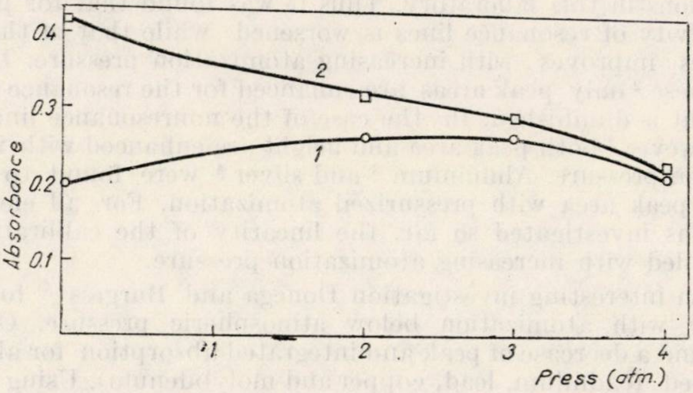

Fig. 1. Variation of gold sensitivity in PA and PH as a function of atomization pressure. Argon used as purge gas. Atomization at 1750°C. For other conditions see Experimental. 1 — PA, 2 — PH.

and parameters were studied. Figure 2 shows the peak shapes of gold with normal and pressurized atomization, and Table 1 shows the variation of peak parameters as a function of atomization pressure. It may be seen from Table 1 that indeed as expected t_{res} increases significantly with pressure. The longer residence time of atoms in the furnace means also a higher atom vapor temperature. As a consequence vapor phase interferences should be diminished with atomization under pressure.

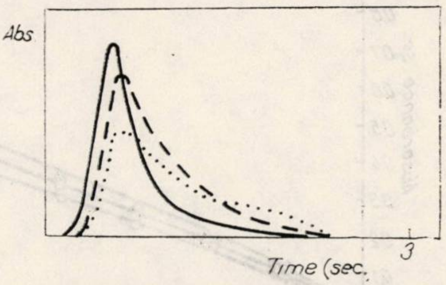

Fig. 2. Peak shapes of gold at various atomization pressures. Conditions as for Figure 1. Solid line — normal atomization, dashed line — 2 atm., dotted line — 4 atm.

Previous works from this laboratory[1-4] and elsewhere[6,7] already noted the increased linearity of calibration curves with increasing atomization pressure. Figures 3a and 3b shows the calibration curves of gold in the peak area and peak height modes respectively. It is obvious from Figures 3a and 3b that the linearity of the calibration curves improved considerably with pressure in both peak area and peak height, as was to be expected. The explanation is probably[1-4,6] that with increassing pressure the relative monochromacity of the source radiation improves as compared to the with of the absorption line.

TABLE 1

Influence of pressure on peak characterization times of gold

Press. (atm)	t_{app}	t_{pk}	t_{at}	t_{res}	t_{end}	t_{displ}	t_{hfw}
Norm.	0.15	0.54	0.39	0.19	2.20	2.05	0.36
2 atm.	0.22	0.62	0.40	0.40	2.27	2.05	0.58
3 atm.	0.26	0.66	0.40	0.66	2.38	2.12	0.73

For operating conditions see Experimental section of the paper. Peak times are defined in Ref.[6]

However, as it was mentioned previously[2,9] the insufficient time resolution of the detection system employed may contribute significantly to the premature bending of calibration curves. With increasing pressure the evolution of sample vapor is slowed down, so that the instrument has a better chance to "catch" the peak accurately. Therefore it can be assumed that the improvement of linearity of calibration curves with increasing pressure has two explanations;

a. the Lorentz broadening of the absorption profile ;
b. the relative time resolution of the instrument improves with increasing pressure, because of the slower evolution of the atomic vapor.

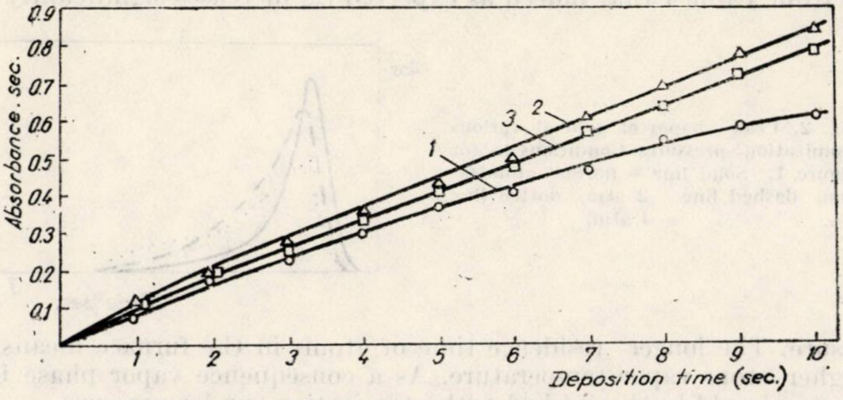

Fig. 3a. Peak area calibration curves for gold. For working conditions see Experimental. 1 — Norm., 2 — 2 atm., 3 — 3 atm.

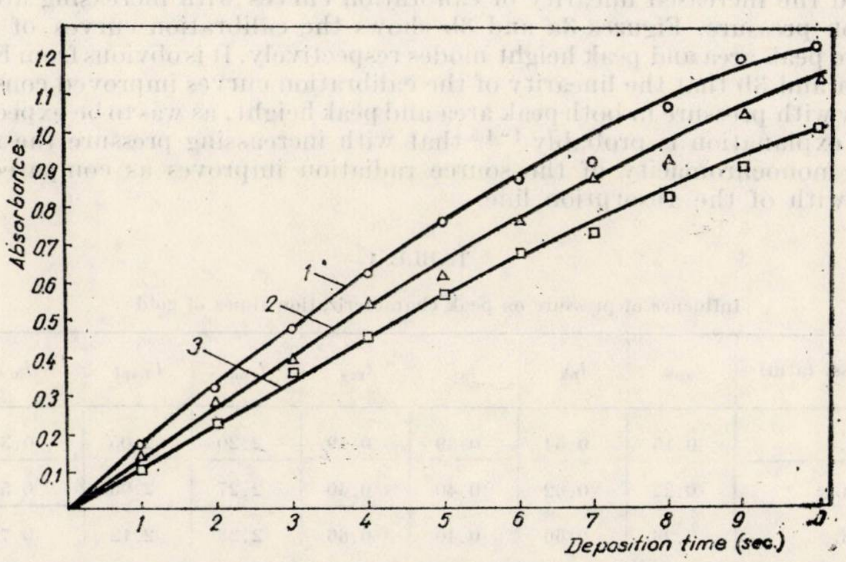

Fig. 3b. Peak height calibration curves for gold. For working conditions see Experimental. 1 — Norm., 2 — 2 atm., 3 — 3 atm.

4. CONCLUSIONS

The peak height sensitivity of gold is worsened with atomization under pressure probably because of the Lorentz broadening of the absorption lines. However, since residence time of atoms increases with pressure, this more than compensated for the Lorentz broadening when peak area is measured. Atomization under pressure actually increases slightly peak area sensitivity.

Because of the large residence time of atoms in the furnace with pressurized atomization it is to be expected that vapor phase interferences be diminished.

The linearity of the peak area and height calibration curves is improved with increasing atomization pressure. Some of the improvements may certainly be ascribed to the relative improvement of time resolution of the detection system used, with atomization under pressure.

REFERENCES

[1] J. Fazakaş, *Spectrochim. Acta,* Submitted.
[2] J. Fazakas, *Analyt. Chim. Acta.,* Submitted.
[3] J. Fazakas. *Talanta,* Submitted.
[4] J. Fazakaş. *Mikrochim. Acta,* Submitted.
[5] N. M. Donega and T. E. Burgess, *Analyt. Chem.,* **42**, 1521 (1970).
[6] R. E. Sturgeon and C. L. Chakrabarti, *Progr. Analyt. At. Spectr.,* **1**, 5 (1978).
[7] M. Hoening, R. Vanderstappen and P. Van Noeyuegnen, *Analusis,* **6**, 433 (1978).
[8] Operators Manual, vol. 2 Flameless Operations. Ed. Instrumentation Laboratory, Lexington Mass., 1976.
[9] D. D. Siemer and J. M. Baldwin, *Analyt. Chem.,* **52**, 295 (1980).

Revue Roumaine de Chimie, 27, 5, 691–692 (1982)

COMPTES RENDUS

W. E. MORF, "Studies in Analytical Chemistry", Volume 2, "The Principles of Ion-Selective Electrodes and of Membrane Transport", Akadémiai Kiadó, Budapest, 1981, 433 p.

This book is second in the serie "Studies in Analytical Chemistry" of Akadémiai Kiadó, dedicated to the needs to keep up the progress of research in field on ion-selective electrodes and on membrane transport.

The aim at the present work is to provide a unified, selfconsistent approach to the theory and principles of ion-selective membrane and membrane electrodes. Because of the complexity of the subject, the text has been subdivided into two parts.

Part A aims at a more general discussion of membrane potentials and membrane transport. Formulations of the interfacial potential contribution due to phase boundaries are given in Chapter 3. Chapter 4 contains a nearly encyclopedic treatment of the diffusion potential, taking into account the nonideality of diffusion layers or membrane phases. The extended Nernst, Planck, Teorell, and Schlögl solutions are derived in a new and simple way. Chapter 5 deals with the liquid-junction potentials arising in conventional potentiometric measuring cells. A comparison is given between different calculation procedures and experimental results. In Chapter 6 practical solutions for the membrane potential are derived and catalogued. Chapter 7 is meant to give a detailed analysis of the ion-transport and the electrical properties of bulk membranes. The discussions are based on the Nernst-Planck flux equation. The implications of Schlögl's theory and those of a simplified membrane model that leads to equivalent results are emphasized. A generalized theory of ion transport is set forth in Chapter 8 ; the treatment goes beyond the earlier models offered by Läuger's and Eisenman's groups. To account for the observed characteristics of lipid bilayer membranes, different shapes of the membrane-internal free energy profiles are considered. The given analysis permite rationalization of the free and carrier-mediated ion transport across membranes. For convenience, the key results of Part A are summarized in Chapter 9.

Part B deals in great detail with the fundamentals of ion-selective electrodes. Chapter 10 covers the principles of solid-state membrane electrodes. The response behavior, the ion selectivity, and the detection limits of such systems are discussed for the example of silver compound membranes. Special attention is paid to the role of dissolution and leaching processes, on the one hand, and of surface coverings, on the other. In Chapter 11 several important extensions and modifications of the Sandblom- Eisenman-Walker theory are presented. The new results contribute to a full understanding of the response phenomena observed for liquid ion-exchange membrane electrodes, so much the more since the chapter also includes an interpretation of the apparent selectivity of such sensors. Chapter 12 is considered to extensively cover the field of neutral carrier membrane electrodes. The theory of these systems has been revised in the light of new information concerning their response mechanism, and many practical examples are given to illustrate the results. The molecular basis of ion selectively and the design features of electrically neutral ionophores are also briefly discussed. Chapter 13 contains two unified approaches to the theory of glass electrodes. The first of these is based on solid-state principles and encompasses the earlier ion-exchange theories and *n*-type descriptions of glass membrane potentials. The second one, based on liquid-membrane concepts, is of like import. Both treatments bridge the gaps that heretofore existed between the earlier, more specific theories. In Chapter 14 the electrical, chemical, and diffusional processes contributing to the time response of ion-selective electrodes are reviewed. Finally, Chapter 15 gives a short introduction into the principles of gas-sensing probes and enzyme electrodes. A simple model is presented that is successful in reconstructing the observed response of enzyme electrodes. This chapter gives a more detailed study on ion selectivity and electrode mechanisms, as well as extensive practical applications of ion sensors, especially in clinical and envrionmental chemistry.

Both the qualities of contents and the graphic presentations make the book entitled ; "The Principles of Ion-Selective Electrodes and of Membrane Transport", by W. E. Morf, a very valuable reference source for researchers who are working in fields where measuring techniques with ion-selective electrodes are involved.

Iuliana Varlires

"ULTRASHORT LIGHT PULSES", Picosecond Techniques and Applications, Edited by S. L. Shapiro, Springer — Verlag, Berlin, Heidelberg, New York, 1977

The book is part of the series "Topics in Applied Physics" and is intended to those interested in the study of ultrafast processes that occur in physics, chemistry and biology.

Discovery of lasers as sources of ultrashort light pulses has elicited the development of a new field of research i.e. the study of ultrafast relaxation processes by removal of atoms or molecules from equlibrium with picosecond intense pulses followed by measurement of the time of return to equilibrium (picosecond techniques). This book reviews the sophisticated tools including the modelocked picosecond-pulse-emitting lasers, the picosecond detection technique, and picosecond devices.

The chapters of the book are contributed by various authors.

Chapter I, "Introduction — A Historical Overview" by S. L. Shapiro, presents a historical outline of techniques of measurement of short time intervals up to the very modern picosecond techniques.

In Chapter 2 "Methods of Generation" D. J. Bradley introduces the subject of picosecond pulses and describes how to produce them. He outlines the basic concepts that underlie the generation of picosecond pulses by modelocked lasers. The different kinds of modelocked lasers are described, and important measurements on the passive element responsible for modelocking i.e. the saturable absorber, are analysed in terms of laser operation. He describes the standard techniques for producing pulses at other frequences by harmonic generation and discusses techniques for producing pulses that are tunable in wavelength in the visible, for the production of infrared and x-ray pulses, and for producing ultrashort pulses by nonlinear optical, and the cw modelocked dye lasser techniques. Finally, he discusses some limitations of the detection techniques.

In Chapter 3 "Techniques for Measurements" E. P. Ippen and C. V. Shank describe picosecond detection techniques in detail. They also describe new cw techniques they have developed for use with cw modelocked dye lasers, and how they have applied them to study such phenomena as vibrational relaxation in dye molecules.

The intent of Chapter 4 "Picosecond Nonlinear Optics" by D. H. Auston, is to reviews the topic of nonlinear optics with particular emphasis on the utilization of picosecond pulses. The author also describes the electronic switches he recently invented, which use picosecond technology.

In Chapter 5, "Picosecond Interactions in Liquids and Solids", D. von der Linde gives an account of rapid relaxation measurements in liquids, solids, and plasmas. These explorations lie near the heart of picosecond activities, because many measurements of fundamental importance are becoming possible for the first time and many relaxation phenomena can now be studied and extended in some depth.

In Chapter 6, "Picosecond Relaxation Proceses in Chemistry", K. B. Eisenthal includes intermolecular energy transfer, molecular orientational relaxation in liquids, photodissociation and the cage effect in liquids, electron transfer phenomena and internal conversion and intersystem crossing in molecules.

Chapter 7, "Picosecond Relaxation Measurements in Biology" by A. J. Campillo and S. I. Shapiro, is divided into four parts. The first section deals with rapid photosynthetic processes, the area of biology which has received the greatest attention from picosecond experimentalists; the second section describes a measurement in hemoglobin made with the powerful, new, cw modelocked dye-laser techniques; the third section discusses measurements on molecules which play an important role in the visual process; and the fourth describes measurements in DNA.

The book is interesting since it deals with modern techniques of research and supplies a rich bibliography.

Marilena Vasilescu

NOTE POUR LES AUTEURS

La Revue Roumaine de Chimie publie des articles en anglais, francais, russe, allemand ou espagnol. Les auteurs sont priés d'envoyer des articles et des comptes rendus inédits.

Les manuscrits seront dactylographiés à double interligne. La bibliographie, les tableaux et la légende des figures seront placés après le texte.

Si l'article fait partie d'une série numéroté la partie précédente sera donnée comme première référence.

Chaque article sera précédé d'un résumé compremant quinze lignes au maximum.

Les références bibliographiques dans le texte seront faites par des exposants sans parenthèses et paraitront à la fin de l'ouvrage.

Les publications périodiques mentionnées dans la bibliographie seront présentées suivant les prescriptions internationales : le nom de l'auteur précedé de l'initiale du prénom, le titre du périodique abregé conformément à «Chemical Abstracts » et souligné par une ligne, le numéro du tome indiqué par des chiffres arabes et souligné par deux lignes, suivi de la première page de l'article : à la fin, l'année de la parution sera placée entre parenthèses. Le numéro de la revue ne sera pas indiqué si les pages du volume sont numérotées consécutivement.

Les textes des livres ou traités inclueront : le nom des auteurs, précédé de l'initiale du prénom, le titre du livre entre guillements et sans être souligné, le numéro du tome précédé par l'abréviation «vol.« (ou «Bd. »), Le numéro de l'édition, les éditions (the publisher), la localité de la parution du livre, l'année de la parution et la page de la référence précédée(s) par l'abréviation «p. » (ou «S. »).

Les brevets seront indiqués comme suit : l'auteur ou la firme, le pays et le numéro du brevet, la date et la revue (Chem. Abstr.). Par ex. : M. Jones (to Union Carbide Co.), *Brit. Pat.* 601 238, 2 Sept. 1959, *Chem, Abstr.*, 54, 12808 (1960).

Si la référence n'a pas été lue en original, on indiquera aussi la revue de références consultée.

Les diagrammes seront tracés à l'encre de Chine sur papier calque. Les tableaux et les figures (en nombre strictement nécessaire) ainsi que les courbes dans les figures seront numérotés par des chiffres arabes, Leur explication sera donnée dans la légende des figures. Prière de ne pas inscrire les mêmes données dans les tableaux et les figures. Chaque tableau aura un titre. On indiquera dans le texte la place approximative des tableaux et des figures. Les formules chimiques seront incluses dans le texte ; en outre, elles seront transcrites sur papier calque, à l'encre de Chine.

Les auteurs sont priés d'indiquer les caractères italiques (en soulignant les lettres au crayon), ainsi que tout autre caractère spécial : les préfixes *ortho*, *meta*, *para*, *cis*, *trans*, etc. seront soulignés pour indiquer leurs caractères italiques et ne seront jamais écrits avec des majuscules.

Aucune correction à la main ne sera admise sur le manuscrit. Les corrections seront frappèes à la machine. Les lettres grecques ou d'autres symboles spéciaux seront insérés à la main à l'encre clairement.

Le manuscrit sera signé par l'auteur.

Le colonne-titre aura 50 lettres au maximum.

L'entière responsabilité du contenu des articles appartient aux auteurs.

Sur demande on peut obtenir une note plus complète.

PRINTED IN ROMANIA

NOTE POUR LES AUTEURS

La Revue Roumaine de Chimie publie des articles en anglais, français, russe, allemand ou espagnol. Les auteurs sont priés d'envoyer des articles et des comptes rendus inédits.

Les manuscrits seront dactylographiés à double interligne. La bibliographie, les tableaux et la légende des figures seront placés après le texte.

Si l'article fait partie d'une série antérieure, la partie précédente sera donnée comme première référence.

Chaque article sera précédé d'un résumé comprenant [illegible] lignes au maximum.

Les références bibliographiques dans le texte seront faites par des exposants sans parenthèses et paraîtront à la fin de l'ouvrage.

Les publications périodiques mentionnées dans la bibliographie seront présentées suivant les prescriptions internationales : le nom de l'auteur précédé de l'initiale du prénom, le titre du périodique abrégé conformément à «Chemical Abstracts» et souligné par une ligne, le numéro du tome indiqué par des chiffres arabes et souligné par deux lignes, suivi de la première page de l'article ; à la fin, l'année de la parution sera placée entre parenthèses. Le numéro de la revue ne sera pas indiqué si les pages du volume sont numérotées consécutivement.

Les textes des livres ou traités incluront : le nom des auteurs, précédé de l'initiale du prénom, le titre du livre entre guillemets et sans être souligné, le numéro du tome précédé par l'abréviation vol. (ou Bd.), le numéro de l'édition, les éditions (the publishers), la localité de la parution du livre, l'année de la parution et la page de la référence précédée par l'abréviation «p.» (ou «S.»).

Les brevets seront indiqués comme suit : l'auteur ou la firme, le pays et le numéro du brevet, la date et la revue (Chem. Abstr.) : par ex. : a) Jones (to Union Carbide Co.), Brit. Pat. 601 258, 2 Sept. 1959; Chem. Abstr., 54, 12976 (1960).

Si la référence n'a pas été lue en original, on indiquera aussi la revue de références consultée.

Les diagrammes seront tracés à l'encre de Chine sur papier calque. Les tableaux et les figures (en nombre strictement nécessaire, ainsi que les courbes dans les figures) seront numérotés par des chiffres arabes. Leur explication sera donnée dans la légende des figures. Prière de ne pas inscrire les mêmes données dans les tableaux et les figures. Chaque tableau aura un titre. On indiquera dans le texte la place approximative des tableaux et des figures. Les formules chimiques seront inclues dans le texte ; en outre elles seront transcrites sur papier calque, à l'encre de Chine.

Les auteurs sont priés d'indiquer les caractères italiques (en soulignant les lettres au crayon), ainsi que tout autre caractère spécial. Les préfixes ortho, méta, para, cis, trans, etc., sont soulignés pour indiquer leurs caractères italiques et ne seront jamais écrits avec des majuscules.

Aucune correction à la main ne sera admise sur le manuscrit. Les corrections seront frappées à la machine. Les lettres grecques et d'autres symboles spéciaux seront insérés à la main à l'encre, clairement.

Le manuscrit sera signé par l'auteur.

Le colonne-titre aura 50 lettres au maximum.

L'entière responsabilité du contenu des articles appartient aux auteurs.

Sur demande on peut obtenir une note plus complète.

TRAVAUX PARUS AUX ÉDITIONS DE L'ACADÉMIE DE LA RÉPUBLIQUE SOCIALISTE DE ROUMANIE

ELENA CEAUŞESCU, **Noi cercetări în domeniul compuşilor macromoleculari** (Nouvelles recherches dans le domaine des composés macromoléculaires). 1981, 536 p.

I. G. MURGULESCU, TATIANA ONCESCU, E. SEGAL, **Introducere în chimia fizică. Vol. II.2. Cinetică chimică şi cataliză** (Introduction à la chimie physique. Vol. II. 2. Cinétique chimique et catalyse), 1981, 1024 p.

V. DRĂGUŢAN, A. T. BALABAN, N. DIMONIE, **Metateza olefinelor şi polimerizarea prin deschidere de inel a cicloolefinelor** (La métathèse des oléfines et la polymérisation par ouverture annulaire des cyclooléfines), 1981, 254 p.

LYDIA-MARIA VAICUM, **Epurarea apelor uzate cu nămol activ. Bazele biochimice.** (L'épuration des eaux résiduelles à boue active. Les bases biochimique), 1981, 218 p.

I. GĂLĂŢEANU, **Procese şi metode radiochimice în energetica nucleară** (Processus et méthodes radiochimique dans l'énergétique nucléaire), 1981, 234 p.

O. IORDACHE, **Procese polistocastice aplicate la fenomenele de transfer** (Processus polystochastiques appliqués aux phénomènes de transfert), 1981, 187 p.

CR. SIMIONESCU, VALERIA GORDUZA, **Polimeri biocompatibili şi biologic activi** (Polymères biocompatibles et biologiquement actifs), 1980, 497 p.

ELENA CEAUŞESCU, **Polimerizarea stereospecifică a izoprenului** (La polymérisation stéréospécifique de l'isoprène), 1979, 307 p.

M. FLORESCU, **Metode ştiinţifice în dezvoltarea industriei chimice moderne** (Méthodes scientifiques dans le développement de l'industrie chimique moderne), 1979, 256 p.

A. T. BALABAN, I. GĂLĂŢEANU, G. GEORGESCU, LIGIA SIMIONESCU, **Compuşi marcaţi şi radiofarmaceutici cu aplicaţii în medicina nucleară** (Composés marqués et radiopharmaceutiques à application en médecine nucléaire), 1979, 495 p.

CONST. GH. MACAROVICI, **Analiza chimică cantitativă anorganică** (L'Analyse chimique quantitative inorganique), 1979, 457 p.

I. G. MURGULESCU, E. SEGAL, **Introducere în chimia fizică, vol. II. 1. Teoria molecular cinetică a materiei** (Introduction à la chimie physique, vol. II. 1. La théorie moléculaire-cinétique de la matière) 1979, 1036 p.

S. STERNBERG, FL. DANEŞ, **Termodinamica chimică aplicată** (La thermodynamique chimique appliquée), 1978, 400 p.

I. G. MURGULESCU, V. EM. SAHINI, **Introducere în chimia fizică, Vol. I. 2.Structura şi proprietăţile moleculelor** (Introduction à la chimie physique. Vol. I.2. La structure et les propriétés des molécules), 1978, 604 p.

C. DRĂGULESCU, E. PETROVICI, **Chimie structurală modernă. Chimia coordinanţei 8** (La chimie structurale moderne. La chimie de la coordinence 8), 1977, 947 p.

I. ZUGRĂVESCU, MAGDA PETROVANU, **N-ylid chemistry,** coédition avec McGraw-Hill International Book Company, U.S.A., 1977, 396 p.

I. G. MURGULESCU, **Introducere în chimia fizică. Vol. I. 1. Atomi, molecule, legătură chimică** (Introduction à la chimie physique. Vol. I. 1. Atomes, molécules, liaison chimique), 1976, 560 p.

ELENA CEAUŞESCU, **Research work on synthesis and characterization of macromolecular compounds. Contributions,** 1974, 251 p.

CR. SIMIONESCU, VIORICA RUSAN, V. POPA, **Chimia algelor marine** (La chimie des algues marines), 1974, 212 p., 1 pl.

I. P. INFORMAŢIA cd. 2047

43 426

Lei 40

$ 70 (pour un abonnement annuel)

F 1103

ACADÉMIE DE LA RÉPUBLIQUE SOCIALISTE DE ROUMANIE

R

REVUE ROUMAINE DE CHIMIE

P.LIPERÁLVA

TOME 27
Nº 6
Juin 1982

EDITURA ACADEMIEI REPUBLICII SOCIALISTE ROMÂNIA

Rev. Roumaine Chim.

RRCHAX. 27, 6, p. 693–788 (1982), Bucarest

ACADÉMIE DE LA RÉPUBLIQUE SOCIALISTE DE ROUMANIE

COMITÉ DE RÉDACTION

Rédacteur en chef:

I. G. MURGULESCU, membre de l'Académie de la République Socialiste de Roumanie

Rédacteurs en chef adjoints:

A. T. BALABAN et V. EM. SAHINI, membres correspondants de l'Académie de la République Socialiste de Roumanie

Collège de rédaction:

EM. BRATU, ELENA CEAUŞESCU, ECATERINA CIORĂNESCU-NENITZESCU, CR. SIMIONESCU, membres de l'Académie de la République Socialiste de Roumanie; P. SPACU, membre correspondant de l'Académie de la République Socialiste de Roumanie; MARGARETA AVRAM, M. BANCIU, I. HAIDUC, D. I. MARCHIDAN, I. MOLDOVAN, G. NIAC et D. SĂNDULESCU

La Revue Roumaine de Chimie paraît 10 fois par an. Toute commande de l'étranger pour les travaux parus aux Editions de l'Académie de la République Socialiste de Roumanie sera adressée à ILEXIM, — Departamentul Export-Import Carte (Livres)/Departamentul Export-Import Presă (Revues) P.O.B. 136—137, télex 11226; 3, str. 13 Decembrie, 79517 Bucarest, Roumanie

Les manuscrits, les livres et les revues proposés en échange, ainsi que toute correspondance seront envoyés à la rédaction :

REVUE ROUMAINE DE CHIMIE

Calea Victoriei, 125, 79717 Bucarest, Roumanie, téléphone 50 76 80

EDITURA ACADEMIEI REPUBLICII SOCIALISTE ROMÂNIA
125, Calea Victoriei, 79717 Bucarest, Roumanie, téléphone 50 76 80

REVUE ROUMAINE
DE
CHIMIE

1983

Tome 27, N° 6 Juin, 1982

I. G. MURGULESCU, EUGENIA IVANA and E. POPA, Absorption spectrum and composition of SnI_2 vapour . . . . 695 – 702

EMIL CHIFU and IOAN STAN, Surface mobility of surfactant solutions. X. *Marangoni* flow against gravity forces . . . . 703 – 711

SURENDER K. JAIN, Surface properties of solutions of lithium nitrate in some molten hydrates. . . . . 713 – 717 R

RODICA VÎLCU and ELENA DIMITRIU, Microstructure of electroless deposited nickel in an ultrasonic field . . . . 719 – 726 R

G. MUNTEANU, C. I. LEPĂDATU, LUMINIȚA PATRON and MARIA BREZEANU, Electronic spectra, magnetic properties and structure of polynuclear complexes $[Fe_2^{III}M^{II}Cl_{12}]^{4-}$ of manganese (II) and cobalt(II). 727 – 734

IOAN MOȚOC and ALEXANDRU T. BALABAN, Testing the geometrical meaning of *Taft* type steric constants . . . . 735 – 739

S. K. SENGUPTA and SHYAM KUMAR, Five- and six-coordinated complexes of hafnium (IV) with triazoline thione . . . . 741 – 746

C. I. CHIRIAC, A new method for the synthesis of aromatic amides directly from acids . . . . 747 – 750 R

J. P. SHUKLA, Vanadium (V) chelates of N-substitued phenylhydroxylamines. A spectrophotometric study 751–759

ROYSTON M. ROBERTS and LOUIS W. ERLOD, *Friedel-Crafts* dealkylations of secondary heptylbenzenes . . . . 761 – 767

M. BANCIU, Photochemical ring contraction of 3-diazo-dibenzo [*f, i*]bicyclo[3.2.2] nona-6,8-dien-2-one . . . . 769 – 774

SIMONA PERCEC, ALMERIA NATANSOHN and FLORIN POPESCU, ^{1}H-NMR spectra of some flame-retardant polymers . . . . 775 – 780

A. E. ABDEL-RAHMAN, A. M. MAHMOUD, H. A. El-SHERIEF, and A. G. GHATTAS, Synthesis of some 1,3,4-thiadiazole derivatives with antibacterial activity . . . . 781 – 785

BOOK REVIEWS . . . . 787 – 788

Rev. Roumaine Chim. **27**, *6*, 693–788 (1982) Bucarest

Revue Roumaine de Chime, 27, 6, 695–702 (1982)

ABSORPTION SPECTRUM AND COMPOSITION OF SnI_2 VAPOUR

I. G. MURGULESCU, EUGENIA IVANA and E. POPA
Center of Physical Chemistry, Spl. Independenţei, 202 Bucharest, Romania

Received June 15, 1981

The absorption spectrum of the gaseous stannous iodide was studied in the temperature range 593 K – 920 K. A value of 22.59 kcal/mole was found for the vaporisation heat in the domain of saturated vapours. At 723 K and for liquid-vapour equilibrium, the degree of dimerization was estimated at 4.5%.

INTRODUCTION

The absorption spectrum of vapour SnI_2 continues our study on the composition of the molten salt vapour.

The interest for the knowledge of SnI_2 vapour composition has been stimulated among others by the practical implications concerning the use of the Sn^{2+} halides in manufactoring high intensity discharge lamps. The data available in the literature on SnI_2 are concerned mainly with the physical properties [1–3] and crystalline structure [4,5] and less with its optical properties. Karpenko [6] measured the vapour pressure of liquid SnI_2 and evidenced the presence of dimers in vapour by determining their molecular weight. Zollweg and Frost [7,8] studied the absorption spectrum of SnI_2 and tried to build up a model for the electronic states of the vapour SnI_2 molecule. They did not detect the presence of dimers in the vapour of liquid SnI_2. Maya [9] measured the absorption cross sections in the UV spectrum of SnI_2.

In the present contribution the UV and VIS absorption spectra of SnI_2 in vapour phase were studied over the 593 – 921 K temperature range, in order to determine the vapour composition of liquid SnI_2.

EXPERIMENTAL

SnI_2 used in the experiments was prepared from elements by a reaction in gaseous phase, according to the method des cribed in a previous paper.[10] This method gives a very pure SnI_2 free of SnI_4 as compared to the methods of synthesis in solution where the risk of oxidizing Sn^{2+} to Sn^{4+} is important. Metallic tin granules (p.a. grade) and iodine sublimed twice were used for the reaction. SnI_2 thus obtained is stable enough in contact with air and has the melting point at 320°C. The UV radiation source was a 30 W deuterium lamp.

In the visible range an incandescence lamp was used. The light beam was focused on the SnI_2 containing a cell placed in a furnace. The radiation transmitted through the cell was analysed with a VSU-1 type monochromator, using a P21 RCA photomultiplier as al

detector and recording the signals on a GIBI Chart-recorder. The cylindrical silica cell was 3–4.3 cm in length. The experimental details were presented in a previous paper. [11]

In order to measure the UV absorption of SnI_2 vapours, two sets of experiments were carried out. In the first set, the vapour was in equilibrium with liquid SnI_2 over the whole working temperature range ; in the second set, the amounts of solid SnI_2 poured into the cells were so chosen that only a section of the temperature range provided for the vapour-liquid coexistence (equilibrium). For the remainder of the temperature range, the whole quantity of SnI_2 introduced into the cell was in the vapour state ; for the latter set of experiments, amounts of SnI_2 were used, which by total evaporation, gave concentrations of 1.37×10^{-4} mol/l and 1.87×10^{-4} mol/l.

The VIS absorption of vapour SnI_2 was measured under the conditions of occurrence of the vapour-melt equilibrium.

We considered that SnI_2 vapour behaves as an ideal gas.

RESULTS AND DISCUSSIONS

The absorption spectra of both saturated and unsaturated SnI_2 vapours were recorded over 593–921 K temperature range.

In UV and VIS ranges of the SnI_2 absorption spectra, the vapour SnI_2 presents three unresolved absorption peaks, located at 358, 458 and 550 nm. They were attributed by Zollweg and Frost [7] to vapour SnI_2 molecular species. The UV absorption band is intense and has its maximum at 358 nm.

At lower temperatures, where the concentration of absorbing species is smaller, the absorption peak at 458 nm looks like a shoulder, due to the UV band overlapping ; only at high tempetatures (~ 150° above SnI_2 melting point) the absorption maximum becomes well marked. The absorption band with the peak at 550 nm is a weak one. For the temperature interval in which the vapour is in equilibrium with molten SnI_2, the saturated vapour absorption varies linearly with the concentration, according to the Beer's law.

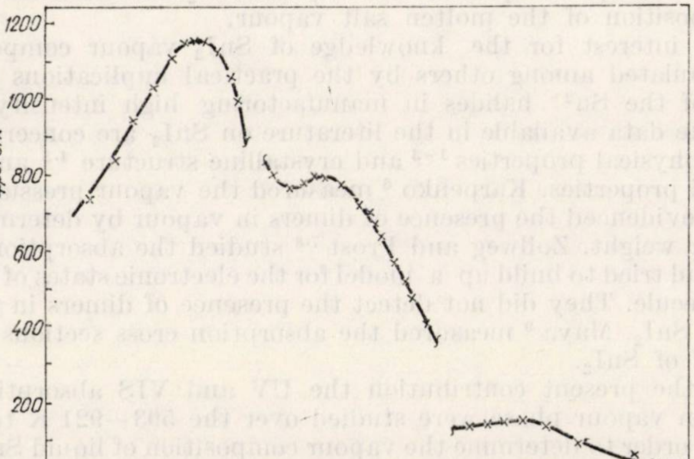

Fig. 1. — Absorption spectrum of SnI_2 vapour.

The concentration dependence of the absorption of the saturated vapour is presented in Fig. 2 for the maximum at $\lambda = 358$ nm.

The straight line equation was fitted by the least square method. The temperature variation of the absorption is shown in Fig. 3 for the UV maximum and for both saturated and unsaturated vapours.

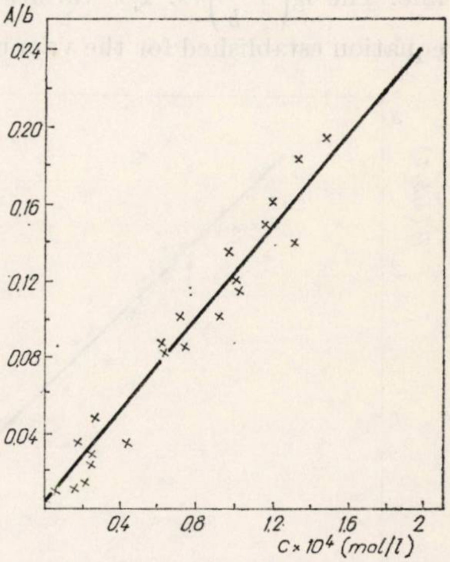

Fig. 2. — Concentration dependence of SnI_2 saturated vapour absorption for $\lambda_{max} =$ 358 nm, $Y = 1221.7 + 0.0028\ X$.

A similar curve was obtained by studying the temperature dependence of the pressure of the saturated and unsaturated SnI_2 vapours.[6]

In Fig. 4, $\lg\left(T \cdot \frac{A}{b}\right)$ vs. $1/T$ is presented for $\lambda = 358$ nm.

The straight line equation was fitted by the least square method over the temperature range for saturated vapours.

An increase in absorption was found experimentally when the temperature was higher than that corresponding to the complete vaporisation of SnI_2 in the cell. Under the conditions of a vapour-liquid unequilibrium, the absorption increases with temperature over a narrow interval, up to a constant value; the subsequent increase of about 200°C (Fig. 3) leads to a small change in the absorption of vapour SnI_2. The absorption increase over the temperature range where the vapour-liquid non-equilibrium conditions are

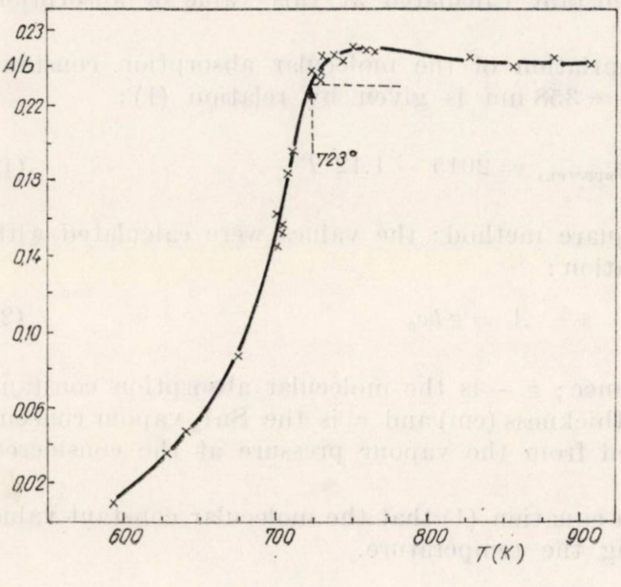

Fig. 3. — Temperature dependence of SnI_2 (saturated and unsaturated) vapour for $\lambda_{max} =$ 358 nm, $C = 1.8710^{-4}$ mol/l.

fulfilled pleads for another process than vaporization; this finding is illustrated by the data in Figs 3 and 4.

Thus, the absorption values in Fig. 4 do not lay on a straight line. The lg$\left(T\frac{A}{b}\right)$vs. $1/T$ variation can no longer be expressed by the equation established for the vapour-liquid equilibrium conditions.

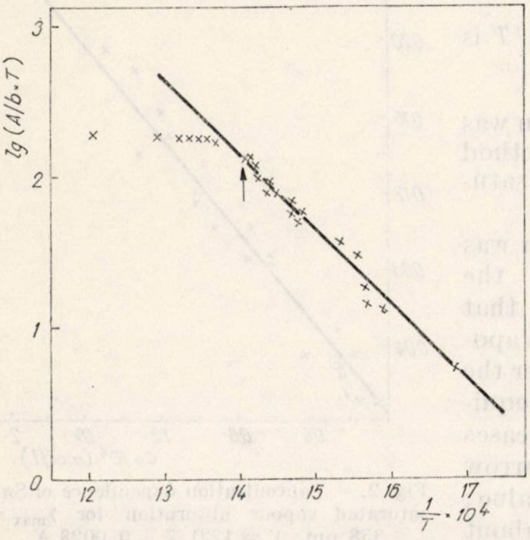

Fig. 4. — lg$\left(T\frac{A}{b}\right)$ *versus* $1/T$ for saturated vapour at $\lambda_{max} = 358$ nm, $Y = 9.128-0.49810^4X$.

We suppose that within the temperature range where unsaturated vapours exist, a dissociation process of the dimer takes place and the increase in absorption is due to an increase in SnI_2 monomer concentration. The maximum absorption value in the temperature range where unsaturated vapours exist is considered to be the real absorption, corresponding to the solid SnI_2 introduced into the cell. For the concentrations of 1.37×10^{-4} mol/l and 1.87×10^{-4} mol/l, the range of the unsaturated vapour, the maximum absorptions, respectively A/b — were 0.184 and 0.250. The molecular absorption constant calculated at this value of absorption is 1343 $l.mol^{-1}.cm^{-1}$.

The temperature variation of the molecular absorption constant for the maximum at $\lambda = 358$ nm is given by relation (1):

$$\epsilon_{apparent} = 2015 - 1.12\,T \tag{1}$$

obtained by the least square method; the values were calculated with the Lambert-Beer's equation:

$$A = \epsilon b c_0 \tag{2}$$

where: A is the absorbance; ϵ — is the molecular absorption constant (in mol/l), b — is the cell thickness (cm) and c_0 is the SnI_2 vapour concentration (mol/l), calculated from the vapour pressure at the considered temperatures.[6]

It can be seen from equation (1) that the molecular constant value decreases with increasing the temperature.

The decrease in the molecular absorption constant of the vapours of liquid SnI_2 can be the result of a change in the vapour composition due to the temperature rise. This composition change is attributted to the increase in the dimer proportion with the pressure increase, as well as to the photo- or thermal dissociation of the vapour SnI_2, the last two phenomena being characteristic for halides of the group IV metals. In both cases, the real concentration (c_1) of the vapor SnI_2 species at a given temperature is lower than the concentration (c_0) calculated from the vapour pressure at the considered temperature. Vapour pressure measurements[6] showed that the dimer/monomer ratio increases with increasing temperature. If we consider the $(SnI_2)_2$ dimer as the only species beside the monomer, then the experimentally measured vapour absorption corresponds to smaller SnI_2 concentration than that calculated from vapour pressure. Therefore, the apparent molecular constants of the absorption, calculated according to equation (1), are smaller than the real ones. If we suppose that, at the melting point, the dimer concentration is negligible compared to the monomer concentration (Brewer's law), by extrapolating ϵ apparent to the melting point (equation 1), a value of 1350 $l \cdot mol^{-1} cm^{-1}$ of the molecular absorption constant is found at the UV maximum. The molecular constant value at the UV maximum found by extrapolation is almost identical with the one-calculated (1343) when considering that the maximum value of the absorption is obtained when the dimer is totally dissociated (unsaturated vapours). Knowing the molecular absorption constant and the absorption increase in the range of the unsaturated vapours the concentration can be estimated for the SnI_2 monomers resulted by dissociation of the dimers in vapour state within the cell; the dimer concentration can be implicitly calculated.

Let us consider the case when, at a given temperature, respectively vapour pressure, the vapour concentration is 1.37×10^{-4} mol/l. This concentration corresponds to the moment when the whole amount of SnI_2 in the cell turns into the vapour state. The 1.37×10^{-4} mol/l concentration corresponds to the vapour pressure at 435°C.

From the A/b *vs.* concentration plot (Fig.2) it results that at a vapour concentration of 1.37×10^{-4} mol/l, A/b is 0.167.

We assume that the difference between the maximum A/b value (0.184) found experimentally in the unsaturated vapour and the A/b value taken from the plot is due to the absorption of the monomer resulting by dimer dissociation. Hence, it was found out that 0.12×10^{-4} mol/l monomer is formed by dimer dissociation.

At a temperature of 435°C and a concentration of 0.12×10^{-4} mol/l, the pressure of the monomer formed by dimer dissociation is 0.638×10^{-3} at. The partial pressure of the dimer existing in SnI_2 vapour at 435°C is 0.319×10^{-3} at. At this temperature, the dimer pressure/total pressure ratio is 0.04; therefore, the dimerization degree at 435°C is 4%.

The same treatment was applied to estimating the dimerization degree for a concentration of 1.87×10^{-4} mol/l. In this way, a dimerization degree of 4.5% was found at 450°C.

We have shown earlier that photo and thermal dissociation processes of vapour SnI_2 can also contribute to the molar absorbance variation;

these processes as already mentioned can lead to a decrease in the vapour SnI_2 species concentration, increasing at the same time the complexity of the SnI_2 vapours composition.

The species resulting from these processes can be SnI, I and Sn. They can appear according to the reactions :

$$SnI_2(g) \rightleftarrows SnI(g) + I \qquad (a)$$

$$SnI_2(g) \rightleftarrows Sn + I_2 \qquad (b)$$

Maya[9] assumed that absorption at $\lambda = 358$ nm can lead to a SnI_2 photodissociation according to the reaction (a), which is an equilibrium process. Measurements[9] of UV absorption cross section did not show a decrease in $SnI_2(g)$ concentration, respectively with increase in SnI (g) concentration, following the irradiation. SnI species can also appear by an (a) type reaction as a result of thermal dissociation. Our experimental measurements pointed out that no significant decrease in absorption took place when temperature increased by 200° over the temperature for which the unsaturated vapour absorption reached maximum value. Yet, the SnI species contribution to the absorption spectrum is negligible. They only exist in extremely small proportions, on the one hand, and they absorb at wavelengths shorter than 300 nm, [13] on the other hand. As much as reaction (b) is concerned, the rate constant of the reaction between tin and iodine is very large, so that their concentrations are negligible.

The iodine vapour participation in the absorption is not significant because of the extremely low concentration and of the very small molar absorbance in VIS [14] and UV [15]. However, the dissociation of even a very small amount of SnI_2 (reactions a and b), alters the molar absorbance values. Therefore, the value of 1350 l/mol.cm found for the molar absorbance at the UV maximum ($\lambda = 358$ nm) could be somewhat higher.

In Figs. 4 and 5, the $\lg\left(T\frac{A}{b}\right)$ *vs.* $1/T$ dependence is plotted at $\lambda = 358$ nm and $\lambda = 458$ nm, respectively. The equations of these straight lines were fitted by the least square method. The slopes are $\Delta Hv/2{,}303\,R$, where ΔHv is the vaporization heat and R is the gas constant.

The vaporization heat of liquid SnI_2 was calculated with the above slopes by assuming that, within the considered temperature range, this quantity is approximately constant.

At the UV maximum (Fig. 4), a value of 22.78 kcal/mol was found and at the VIS one (Fig. 5), a value of 22.41 kcal/mol. The mean value, 22.59 kcal/mol, for the vaporization heat is quite close to the one found by other methods.[6,16]

Dimer heat of dissociation. In Fig. 6, the $\lg\left(T\frac{A}{b}\right)$ *vs.* $1/T$ variation is given for the temperature range where the unsaturated vapour absorption increases up to a constant value. The straight line equation was fitted by the least square method at UV maximum having an unsaturated vapour concentration of 1.87×10^{-4} mol/l. The slope of this straight line in smaller (0.115 instead of 0.5) than that for the straight lines in Figs. 4 and 5. Therefore, the process leading to the concentration increase, respectively absorption, is other than the vaporization of the liquid SnI_2. As we have already shown, the absorption increases as a consequence of the increase of the vapour SnI_2 concentration, due to $(SnI_2)_2$ dimer dissociation.

The dimer heat of dissociation, calculated by means of the slope of the straight line in Fig. 6 is 5.274 kcal/mol. This value is lower than that obtained from vapour pressure measurements.[6]

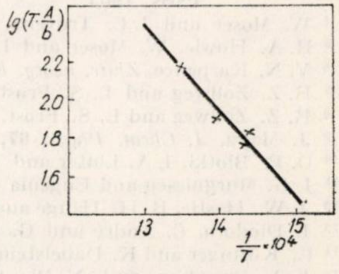

Fig. 5. — $\lg\left(T\frac{A}{b}\right)$ *versus* $1/T$ for saturated vapour at $\lambda_{max} = 458$ nm, $Y = 8.82 - 0.491 \cdot 10^4 X$

CONCLUSIONS

The vapours of liquid SnI_2 have a complex composition including the following species:

— SnI_2 monomer — predominant species;

— $(SnI_2)_2$ dimer — whose partial pressure increases with the temperature;

— SnI, I and Sn — species whose concentrations are negligible.

The absorption maxima observed in the vapour spectrum of the liquid SnI_2 were attributted to the vapour SnI_2 molecule, by taking into account the following reasons;

— The heat of vaporization calculated from the $\lg\left(\frac{AT}{b}\right)$ *vs.* $1/T$ dependence, for both UV and VIS maxima is the same;

— Also for saturated vapours, the slopes of the straight lines giving the absorption variation as a function of concentration is the same for both UV and VIS maxima;

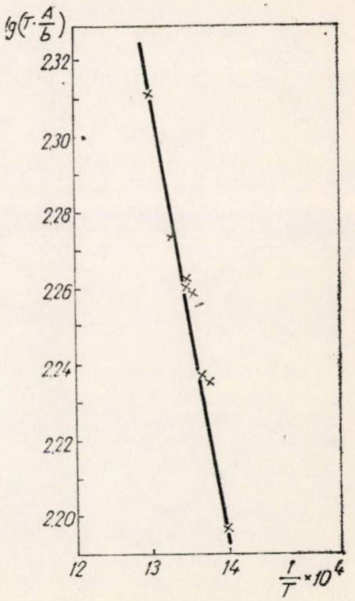

Fig. 6. — $\lg\left(T\frac{A}{b}\right)$ *versus* $1/T$ for unsaturated vapour at $\lambda = 358$ nm, $Y = 3.806 - 0.115 \cdot 10^4 X$, $C = 1{,}87 \cdot 10^4$ mol/l.

— The UV absorption spectrum of vapours of the liquid SnI_2 is similar to the spectrum for vapour halides of the group IV elements, that is the ones having 18 valence electrons and belonging to the $\mathbf{C_{2v}}$ symmetry group.[12,18]

REFERENCES

[1] W. Fischer and T. Petzel, *Z. anorg. Chem.*, **333**, 226 (1964).
[2] N. I. Muraci, "Metalurghia olova", Khimiya, Moskva, 1964, p. 53.
[3] Kubaschewski and E. Evans, "La thermochimie en métalurgie", Gauthier-Villars Ed., Paris, 1964.
[4] W. Moser and I. C. Trevena, *Chem. Comm.*, **1**, 25 (1969).
[5] R. A. Howie, W. Moser and I. C. Trevena, *Acta Cryst.*, B, **28**, 2965 (1972).
[6] V. N. Karpenco, *Zhur. neorg. Khim.*, **12**, 3248 (1967).
[7] R. Z. Zollweg and L. S. Frost, *J. Chem. Phys.*, **50**, 3280 (1969).
[8] R. Z. Zollweg and L. S. Frost, *Bull. Amer. Phys. Soc.*, **11**, 745 (1966).
[9] J. Maya, *J. Chem. Phys.*, **67**, 4976 (1977).
[10] D. P. Blotki, I. A. Linter and T. N. Sushkevich, *Ukrain. khim. Zhur.*, **40**, 989 (1974).
[11] I. G. Murgulescu and Eugenia Ivana, *Rev. Roumaine Chim.*, **18**, 1677 (1973).
[12] J. W. Hastie, R. H. Hauge and J. L. Margrave, *J. Mol. Spectroscopy*, **29**, 152 (1969).
[13] I. Diodora, C. André and G. Pannatier, *Compt. rend.*, **274**, 1892 (1972).
[14] E. Közinger and K. Dabelstein, Beckman Raport 1 + 2/74, p. 1.
[15] A. A. Parschier and N. W. Gregory, *J. Phys. Chem.*, **72**, 2697 (1968).
[16] L. P. Voporova, V. A. Voronin and L. A. Firsanova, *Izvest. V.U.Z.M.V.O. S.S.S.R., Khim. i khim. Tekhnol.*, **16**, 128 (1973).
[17] A. Buchler, J. L. Stauffer and W. Klemperer, *J. Amer. Chem. Soc.*, **86**, 4544 (1964).
[18] J. W. Hastie and J. L. Margrave, *J. Phys. Chem.*, **73**, 1105 (1069).

Revue Roumaine de Chimie, 27, 6, 703–711 (1982)

SURFACE MOBILITY OF SURFACTANT SOLUTIONS. X[1]

MARANGONI FLOW AGAINST GRAVITY FORCES

EMIL CHIFU * and IOAN STAN **

Departments of *Physical Chemistry and **Differential Equations and Mechanics, Babeş-Bolyai University, Cluj-Napoca, Romania

Received August 14, 1981

A model is presented for a thin liquid layer set on an inclined solid plane. The liquid/gas interface of this layer is acted by a surface tension gradient which determines an ascending Marangoni flux, accompanied by a simultaneously descending flux caused by the gravity forces. The conditions under which this "antiparallel" flow occurs through the thin liquid layer and the governing equations are discussed. They forecast the persistence of the Marangoni flow at zero gravity. The fact may be interesting mainly for sufficiently thin layers.

The mobility of liquid interfaces under the action of surface tension gradients – the so-called Marangoni effect[2] – has become again, in recent times, a subject of scientific interest. This phenomenon influences the behaviour of liquids at zero gravity,[3] occurs in mass transfer processes through fluid interfaces,[4] is interesting to the modelling of deformation processes at the biological membrane level,[5] etc.

Previously we have studied[6] some surface flow processes, using the model of a thin liquid layer, of thickness δ, found on an inclined solid plane (Fig. 1). The Ox axis is directed towards the maximum slope of the plane, Oz is perpendicular to the plane, and Oy links the points situated at the same level. The surface tension σ, at the liquid/gas interface, varies following the Ox axis. It has the constant values σ_0 (for $x = 0$) and σ_1 (for $x = H$) at the extremities of the liquid layer, so that $\sigma_1 < \sigma_0$. Such a model can be experimentally performed by means of certain liquid-reservoirs, which contain a surfactant solution at the distance $x = H$ and the pure solvent (or a more diluted solution) at $x = 0$. The level difference between the surfactant solution and the pure solvent is h (Fig. 1). In principle, the surface tension difference $\sigma_0 - \sigma_1$ can also arise as a result of temperature – or electric charge variations occurring at the interface.

In these circumstances, the liquid/gas interface moves towards negative values of the Ox axis (Fig. 1), due to the surface tension difference; is also drags, by viscosity forces, adjacent strates of liquid (Marangoni flow). But, simultaneously, the liquid in the thin layer is stressed towards the positive direction of the Ox axis, due to the inclination of the plane.

A competitive flow appears in this way within the thin liquid layer as a consequence of the simultaneous action of both surface and gravity forces.

Van den Bogaert and Joos [7] have recently studied a similar case in which a surfactant solution is forced to flow through a canal and, simultaneously, by means of the barriers situated at the ends of the canal, a surface tension gradient is created.

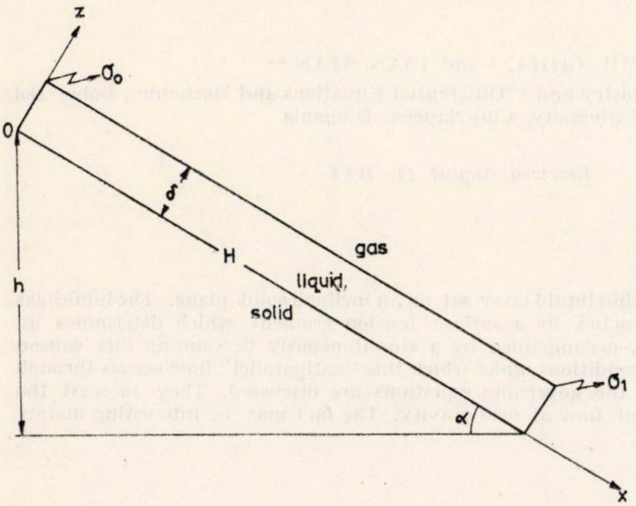

Fig. 1. — The thin liquid layer acted by a surface tension gradient on an inclined plane.

In the following we reconsider in a more general form than that previously reported [6] the equations which govern the "double" — surface and gravity — flow on the model of the thin liquid layer in Fig. 1.

MARANGONI FLOW VELOCITY WITHIN A SEMI-INFINITE THIN LIQUID LAYER FOUND ON AN INCLINED PLANE

It will be admitted that the liquid is viscous and incompressible. The continuity equation:

$$\operatorname{div} \vec{v} = 0 \tag{1}$$

and the Navier-Stokes equation:

$$\rho \frac{d\vec{v}}{dt} = \rho \vec{F} - \operatorname{grad} p + \mu \Delta \vec{v} \tag{2}$$

will be considered, where $\vec{v}$ is the velocity, $\vec{F}$ the external volume force, p the pressure, ρ the density, μ the viscosity of the liquid and t the time.

According to Fig. 1, the inclined plane is chosen as the xy plane, to which the Oz axis is perpendicular, so that equations (1) and (2) become, in the projection :

$$\frac{\partial v_x}{\partial x} + \frac{\partial v_y}{\partial y} + \frac{\partial v_z}{\partial z} = 0 \tag{3}$$

respectively

$$\rho\left(\frac{\partial v_x}{\partial t} + v_x\frac{\partial v_x}{\partial x} + v_y\frac{\partial v_x}{\partial y} + v_z\frac{\partial v_x}{\partial z}\right) = \\ = \rho F_x - \frac{\partial p}{\partial x} + \mu\left(\frac{\partial^2 v_x}{\partial x^2} + \frac{\partial^2 v_x}{\partial y^2} + \frac{\partial^2 v_x}{\partial z^2}\right) \tag{4}$$

$$\rho\left(\frac{\partial v_y}{\partial t} + v_x\frac{\partial v_y}{\partial x} + v_y\frac{\partial v_y}{\partial y} + v_z\frac{\partial v_y}{\partial z}\right) = \\ = \rho F_y - \frac{\partial p}{\partial y} + \mu\left(\frac{\partial^2 v_y}{\partial x^2} + \frac{\partial^2 v_y}{\partial y^2} + \frac{\partial^2 v_y}{\partial z^2}\right) \tag{5}$$

$$\rho\left(\frac{\partial v_z}{\partial t} + v_x\frac{\partial v_z}{\partial x} + v_y\frac{\partial v_z}{\partial y} + v_z\frac{\partial v_z}{\partial z}\right) = \\ = \rho F_z - \frac{\partial p}{\partial z} + \mu\left(\frac{\partial^2 v_z}{\partial x^2} + \frac{\partial^2 v_z}{\partial y^2} + \frac{\partial^2 v_z}{\partial z^2}\right). \tag{6}$$

Due to the symmetry of the problem, v_y and v_z equal zero and it results from Eq. (3) that

$$\frac{\partial v_x}{\partial x} = 0,$$

therefore, v_x is not a function of x. Supposing that the thin liquid layer has an indefinite width, y, – *i.e.* it is semi-infinite –, v_x is neither a function of y, whence $v_x = v_x(z)$. If the pressure, p, is taken as constant in the fluid layer, and if one sees in Fig. 1 that $F(g \sin \alpha, 0, -g \cos \alpha)$, equations (4), (5) and (6) for the steady flow become :

$$\mu\frac{d^2 v_x}{dz^2} + \rho g\frac{h}{H} = 0 \tag{7}$$

where $\sin \alpha = h/H$ and g is the acceleration of gravity.

A first limiting condition will be :

$$v_x(z) = 0 \text{ for } z = 0 \tag{8}$$

namely the velocity of the liquid equals zero at the solid plane surface.

The conditions at the free liquid surface ($z = \delta$) are derived from the equation describing the flow of the interface. The liquid/gas interface is considered as a two-dimensional fluid characterized by a surface density Γ (ML^{-2}), a shear surface viscosity coefficient, ε, and a dilatational surface viscosity coefficient $\varkappa$; $\varepsilon + \varkappa = \mu_s(MT^{-1})$.

On a fluid plane surface, in the case of an irotational velocity, the two-dimensional Navier-Stokes equation becomes [8]

$$\Gamma \frac{d\vec{w}}{dt} = \vec{F}_s + \text{grad}\ \sigma + (\varepsilon + \varkappa)\, \Delta \vec{w} \tag{9}$$

where $\vec{w} = (\vec{v})_{z=\delta}$.

The external force $\vec{F}_s$ applied on the surface unit of the liquid/gas interface is the resultant of two components: the first one originates in a field of external forces — in the studied case the gravity field acting upon the interface ($\Gamma\vec{g}$) — ; the second is the traction exercised by the two phases, — in our case the liquid ($\vec{T}_1$) and the gas ($\vec{T}_g$) — on both sides of the interface. Thus,

$$\vec{F}_s = \Gamma\vec{g} + \vec{T}_1 - \vec{T}_g$$

and, considering that the traction of the gas $\vec{T}_g$ is negligible, equation (9) becomes

$$\Gamma \frac{d\vec{w}}{dt} = \Gamma\vec{g} + \vec{T}_1 + \text{grad}\ \sigma + (\varepsilon + \varkappa)\, \Delta\vec{w} \tag{10}$$

where $\vec{T}_1 = -\mu \left(\frac{\partial \vec{v}}{\partial z} \right)_{z=\delta}$.

In projection, Eq. (10) takes the following form:

$$\Gamma \left(\frac{\partial w_x}{\partial t} + w_x \frac{\partial w_x}{\partial x} + w_y \frac{\partial w_x}{\partial y} \right) = \\ = \Gamma g \sin \alpha - \mu \left(\frac{\partial v_x}{\partial z} \right)_{z=\delta} + \frac{\partial \sigma}{\partial x} + \mu_s \left(\frac{\partial^2 w_x}{\partial x^2} + \frac{\partial^2 w_x}{\partial y^2} \right) \tag{11}$$

$$\Gamma \left(\frac{\partial w_y}{\partial t} + w_x \frac{\partial w_y}{\partial x} + w_y \frac{\partial w_y}{\partial y} \right) = \mu_s \left(\frac{\partial^2 w_y}{\partial x^2} + \frac{\partial^2 w_y}{\partial y^2} \right) \tag{12}$$

As the symmetry of the problem indicates $w_y = 0$, and w_x (like v_x) is neither a function of x nor of y, it results from Eqs (11) and (12) that, in the case of a steady flow:

$$\Gamma g \sin \alpha - \mu \left(\frac{\partial v_x}{\partial z} \right)_{z=\delta} + \frac{\partial \sigma}{\partial x} = 0 \tag{13}$$

Supposing that the surface tension gradient is constant (Fig. 1),

$$-\frac{\mathrm{d}\sigma}{\mathrm{d}x}=\frac{\sigma_0-\sigma_1}{H}$$

and taking into account that $\sin\alpha = h/H$, it results from Eq. (13) that :

$$\Gamma g\frac{h}{H}-\mu\left(\frac{\partial v_x}{\partial z}\right)_{z=\delta}+\frac{\sigma_0-\sigma_1}{H}=0 \tag{14}$$

which represents the limiting condition for $z = \delta$.

The solution of equation (7) is :

$$v_x=-\frac{\rho g h}{2\mu H}z^2+C_1 z+C_2. \tag{15}$$

The integration constants are determined from the conditions (8) and (14), resulting in :

$$C_1=\frac{\sigma_1-\sigma_0}{\mu H}+\frac{\Gamma g h}{\mu H}+\frac{\rho h g\delta}{\mu H}$$

$$C_2=0,$$

which leads by substitution in (15) to :

$$v_x=\frac{1}{\mu H}(\sigma_1-\sigma_0+\Gamma h g+\rho g h\delta)z-\frac{\rho g h}{2\mu H}z^2 \tag{16}$$

Adequately, the total flux of liquid through the thin layer section of area $1\times\delta$ will be :

$$Q=\int_0^\delta v_x\,\mathrm{d}z=-\frac{\sigma_0-\sigma_1}{2\mu H}\delta^2+\frac{1}{2\mu H}\Gamma g h\delta^2+\frac{1}{3\mu H}\rho g h\delta^3 \tag{17}$$

By writing out Eq. (16) under the following form :

$$v_x=\left(-\frac{\sigma_0-\sigma_1}{\delta h g}+\frac{\Gamma}{\delta}+\rho\right)\frac{\delta h g}{\mu H}z-\frac{\rho g h}{2\mu H}z^2 \tag{18}$$

it is realized that if the thickness δ of the liquid layer found on the inclined plane is large, so that $(\sigma_0-\sigma_1)/\delta h g\approx 0$ and $\Gamma/\delta\approx 0$, the surface Marangoni flow phenomena can be neglected and the flow velocity in the given fluid layer is

$$v_x=\frac{\rho g h}{2\mu H}z(2\delta-z) \tag{19}$$

Eventually, it is to be noticed that Eqs (16–18) do not contain any terms corresponding to the shear and/or the dilatational surface viscosity, what results from the symmetry of our problem.

DISCUSSION

The discussion of Eq. (16) leads to the following results.

The velocity $w_x = (v_x)_{z=\delta}$ of the liquid/gas interface is given by the expression

$$w_x = \frac{1}{\mu H}\left[-(\sigma_0 - \sigma_1) + \Gamma g h\right]\delta + \frac{1}{2\mu H}\rho g h \delta^2 \tag{20}$$

The velocity profile in the thin fluid layer will be thus dependent on the value of the interface velocity – according to Eq. (20) – and on the fact that at the surface ($z = 0$) of the inclined solid plane $v_x = 0$. The problem is analogous to the flow of a viscous fluid between two planes, one of which being fixed ($z = 0$) and the other mobile ($z = \delta$).

Three cases of flow can be distinguished depending on the value of the interface velocity:

- the interface undergoes an ascending movement ($w_x < 0$);
- the interface is at rest ($w_x = 0$);
- the interface undergoes a descending movement ($w_x > 0$).

From Eq. (16) it can be noticed that, if $h = 0$, that is the liquid flow occurs on the horizontal plane, the liquid/gas interface moves in the negative direction of the Ox axis (Fig. 1), respectively towards the higher values of the surface tension. The interface drags by viscosity forces subjacent strates of liquid and the flow velocity linearly varies with z:

$$v_x = -\frac{\sigma_0 - \sigma_1}{\mu H} z. \tag{21}$$

The corresponding velocity profile is given in Fig. 2 a.

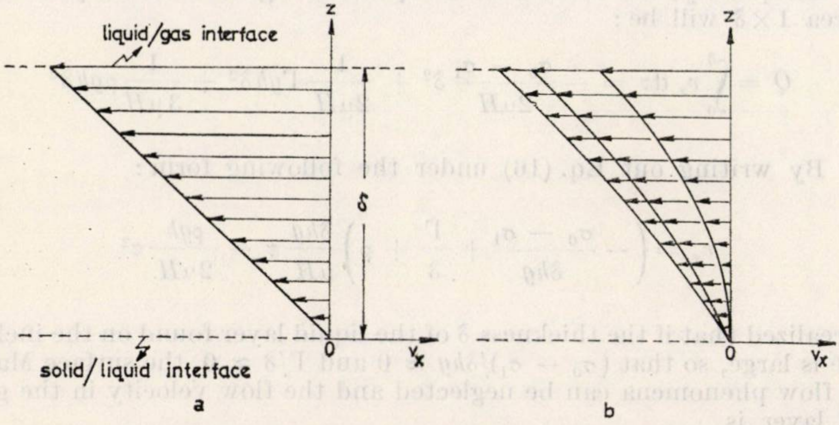

Fig. 2. — The velocity profile in the thin liquid layer. a) for the level difference $h = 0$; b) for $h \leqslant \dfrac{\sigma_0 - \sigma_1}{g(\rho\delta + \Gamma)}$.

As soon as a level difference arises ($h > 0$), a velocity component caused by the gravity forces opposes the Marangoni flow. However, from Eq. (18) it can be seen that, as long as

$$h \leqslant \frac{\sigma_0 - \sigma_1}{g(\rho\delta + \Gamma)} \tag{22}$$

the interface goes on dragging the entire subjacent liquid towards negative values on the Ox axis (Fig. 1) and the velocity profile in the thin liquid layer is that given in Fig. 2 b.

Only at the moment when

$$h > \frac{\sigma_0 - \sigma_1}{g(\rho\delta + \Gamma)}, \tag{23}$$

two streams of liquid appear; an ascending one, caused by the surface tension gradient, and a descending one, determined by the level difference — properly by the gravity forces. The separating plane between the two liquid fluxes inversely oriented to one another is obtained with the condition

$$(v_x)_{z = z_0} = 0 \tag{24}$$

introduced in Eq. (16), namely supposing that there is an immobile surface at the level $z = z_0$ between the two liquid fluxes. In this way the thickness of the descending liquid strate is obtained:

$$z_0 = \frac{2(\sigma_1 - \sigma_0)}{\rho g h} + \frac{2\Gamma}{\rho} + 2\delta, \tag{25}$$

as well as that of the ascending strate:

$$\Delta = \delta - z_0 = \frac{2(\sigma_0 - \sigma_1)}{\rho g h} - \frac{2\Gamma}{\rho} - \delta \tag{26}$$

The situation is illustrated by the profile of velocities given in Fig. 3.

Further on, by increasing the level difference h, the thickness Δ of the ascending liquid strate equals zero at a given moment, and so does the velocity of the liquid/gas interface. Thus, from the condition $\Delta = 0$ in Eq. (26) or, alternatively, $w_x = 0$ in Eq. (20), one obtains:

$$h = \frac{\sigma_0 - \sigma_1}{g\left(\rho\frac{\delta}{2} + \Gamma\right)} \tag{27}$$

The respective velocity profile is given in Fig. 4, being analogous to the flow of a liquid between two fixed planes.

Finally, for the level difference

$$h > \frac{\sigma_0 - \sigma_1}{g\left(\rho\frac{\delta}{2} + \Gamma\right)} \tag{28}$$

the interface is dragged by the liquid in the thin layer towards the positive direction of the Ox axis, that is inversely to the above-described case, $(w_x > 0)$.

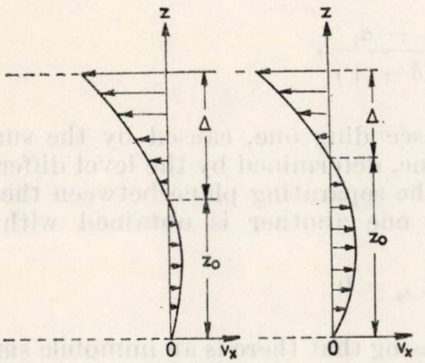

Fig. 3. — The velocity profile for the level difference interval

$$\frac{\sigma_0 - \sigma_1}{g(\rho\delta + \Gamma)} < h < \frac{\sigma_0 - \sigma_1}{g\left(\rho\frac{\delta}{2} + \Gamma\right)}$$

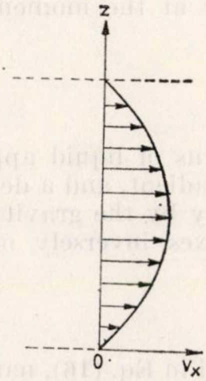

Fig. 4. — The velocity profile in the thin liquid layer for the cancelled out velocity of the liquid/gas interface, at the level difference $h = \dfrac{\sigma_0 - \sigma_1}{g\left(\rho\frac{\delta}{2} + \Gamma\right)}$.

It results that in the following range of the level differences:

$$\frac{\sigma_0 - \sigma_1}{g(\rho\delta + \Gamma)} < h < \frac{\sigma_0 - \sigma_1}{g\left(\rho\frac{\delta}{2} + \Gamma\right)} \tag{29}$$

an "antiparallel" flow arises in the thin liquid layer found on the inclined plane, due to the competition between the surface and gravity forces: the strate of thickness Δ goes upward, while that of thickness z_0 downward the inclined plane (Fig. 3).

In conclusion, in the theoretic model presented — a semi-infinite thin layer of liquid found on an inclined solid plane — , the competition between the Marangoni flow caused by interfacial tension gradients and the inversely oriented flow caused by the external gravity forces is discussed.

This situation, namely the existence of the two inversely oriented liquid streams in a thin layer, had been experimentally revealed by us in a previous work.[9] Those experiments had been performed with thin liquid layers having a thickness, δ, of the order of 10^{-2} cm; the studied thin layers were bordered by two solid walls, that is they had a triangular section. The profile of the thin layers was consequently different from that of the model studied in the present work. The problem will be treated again in some future papers.

Further on, from equation (16) it follows that in zero gravity conditions only the Marangoni flow will persist. The fact may present a practical interest concerning the transport of liquids through sufficiently thin liquid layers.

REFERENCES

[1] Part IX : E. Chifu, Z. Finta, M. Sălăjan and E. Gavrilă, *Rev. Roumaine Chim.*, **26,** 1345 (1981).

[2] C. G. M. Marangoni, *Ann. Phys. (Poggendorf)*, **142,** 337 (1871) ; *Nuovo Cimento*, Ser. **2,** **5–6,** 239 (1872) ; J. A. F. Plateau, *Phil. Mag. Ser.* 4, **38,**4 45 (1869) ; J. W. Gibbs, *Trans. Connecticut Acad.*, **3,** 343 (1878).

[3] Ref. 1 ; E. Chifu, I. Stan, Z. Finta, E. Gavrilă and H. Drotloff, "Astronomy and Astrophysics", Symposium, Cluj-Napoca, 26 – 27 Nov. 1977 ; I. Stan and E. Chifu, "Colloquy on the Fluid Mechanics and its Technical Application", Galatzi, 12–13 Oct., 1979, p. 88 ; E. Chifu, I. Stan, Z. Finta and E. Gavrilă, *Rev. Chim. (București)*, **31,** 765 (1980) ; E. Chifu and I. Stan, *Rev. Roumaine Chim.*, **25,** 1149 (1980) ; R. Pabst and H. Oertel, *Acta Astronautica*, **5,** 671 (1978) ; C. H. Chun and W. Wuest, *Acta Astronautica*, **5,** 681 (1978) ; **6,** 1073(1979).

[4] M. Hennenberg, P. M. Bisch, M. Vignes-Adler and A. Sanfeld, *J. Colloid Interface Sci.*, **69,** 128 (1979) ; **74,** 495 (1980).

[5] M. Dupeyrat and E. Nakache, *Bioelect. Bioenerg.*, **5,** 134 (1978).

[6] E. Chifu et al., *Studia Univ. Babeș-Bolyai Chem.*, **6,**(2), 19 (1961) ; **8,** (1), 49 (1963) ; **9,** (1), 95(1964) ; **9,** (1), 101 (1964) ; **10,** (2), 85 (1965) : **10,** (2), 91 (1965) ; **10,** (2), 99 (1965) ; *Rev. Roumaine Chim.*, **11,** 873 (1966).

[7] R. van den Bogaert and P. Joos, *J. Colloid Interface Sci.*, **69,** 301 (1979).

[8] L. E. Scriven, *Chem. Eng. Sci.*, **12,** 98 (1960) ; R. Aris, "Vectors, Tensors and the Basic Equations of the Fluid Mechanics", Prentice Hall, New Jersey, **1962,** Chap. X.

[9] E. Chifu and I. Albu, *Studia Univ. Babeș-Bolyai, Chem.*, **13,** (1), 99 (1968).

Revue Roumaine de Chimie, 27, 6, 713 – 717(1982)

SURFACE PROPERTIES OF SOLUTIONS OF LITHIUM NITRATE IN SOME MOLTEN HYDRATES

SURENDER K. JAIN
Hindu College, University of Delhi, Delhi – 110007

Received January 13, 1981

Surface tensions of fused $Cd(NO_3)_2 \cdot 4H_2O$, $Mn(NO_3)_2 \cdot 6H_2O$, $Cr(NO_3)_3 \cdot 9H_2O$ and their solutions containing $LiNO_3$ have been measured as a function of temperature and $LiNO_3$ content. Surface tension values show negative deviations from ideal behavior values and are observed to be linear as a function of surface layer mole fractions of $LiNO_3$ ($x^{\sigma}_{LiNO_3}$). The surface enrichment factor, *s*, for each system has been computed employing Eberhart's equation ; the order is $Cr(NO_3)_3 \cdot 9H_2O + LiNO_3 > Mn(NO_3)_2 \cdot 6H_2O + LiNO_3 > Cd(NO_3)_2 \cdot 4H_2O + LiNO_3$.

INTRODUCTION

Extensive supercooling, glass-forming tendencies and the high acidities associated with the hydrates of metals belonging to the 3d series of transitional elements make them of considerable intrinsic chemical and possibly of future applied interest. These liquids appear to promise some interesting solutions in chemistry. In the effort[1-8] to investigate the physicochemical properties of molten hydrates in pure and mixed state, some of the observations regarding the surface characteristics of the $Cd(NO_3)_2 \cdot 4H_2O + LiNO_3$; $Mn(NO_3)_2 \cdot 6H_2O + LiNO_3$ and $Cr(NO_3)_3 \cdot 9H_2O + LiNO_3$ systems are presented in this paper.

EXPERIMENTAL

The quality grade, source of material and the other related details *e.g.*, cross check[5] for the water content of hydrates, have already been described.[2,5] Lithium nitrate (Carlo Erba, Italy) was dried by heating at about 120–140°C under vacuum. Mixtures of varying compositions were prepared by melting the requisite amounts of the salts in hard glass flasks (c 100 cm^3) fitted with airtight ground glass joints and filtered through sintered glass filters (porosity G–3). The filtered melts were then maintined at about 60°C for about 2 h to mature. The surface tensions were measured by the differential capillary rise method, described in detail earlier.[5] The temperature of the constant temperature bath (c 15 liters) was controlled and measured with a precision of ± 0.1°C.

RESULTS AND DISCUSSION

The measured surface tension (σ) values for all the three system investigated in this study are presented in table 1 in the form of the least-square equations of the type

$$\sigma(\mathrm{mN\ m^{-1}}) = a - b(T - 273.16) \qquad (1)$$

TABLE 1

Surface tension — temperature equations for the solutions of $LiNO_3$ in some molten hydrates

Mole fraction, $LiNO_3$		Temp. range, K	$\sigma(\mathrm{mH\ m^{-1}}) = a - b\,(T - 273.16)$		
Bulk (x)	Surface (x^{σ})		a	$10^2\,b$	SE
		$Cr(NO_3)_3 \cdot 9H_2O + LiNO_3$			
0.00	0.0	308–351	94.50	21.42	0.01
0.10	0.020	308–351	95.20	21.16	0.02
0.20	0.043	308–351	96.60	21.83	0.09
0.30	0.072	308–351	97.39	20.66	0.07
0.40	0.108	308–351	98.96	20.30	0.11
0.50	0.154	308–351	102.58	22.55	0.36
0.60	0.214	308–351	103.84	19.70	0.11
		$Mn(NO_3)_2 \cdot 6H_2O + LiNO_3$			
0.00	0.0	304–350	98.09	10.34	0.21
0.10	0.028	304–350	98.77	10.25	0.20
0.20	0.061	304–350	100.02	10.19	0.14
0.30	0.100	304–350	101.19	10.02	0.15
0.40	0.148	304–350	103.07	10.25	0.20
0.50	0.206	304–350	105.37	10.41	0.24
0.60	0.280	304–350	107.81	10.26	0.20
		$Cd(NO_3)_2 \cdot 4H_2O + LiNO_3$			
0.0	0.0	315–346	111.66	24.47	0.03
0.10	0.035	315–346	112.12	23.97	0.09
0.20	0.076	315–346	113.72	23.97	0.09
0.30	0.123	315–346	115.65	24.57	0.05
0.40	0.179	315–346	118.29	25.13	0.28
0.50	0.247	315–346	120.13	23.82	0.22

a and b being the constants characteristic of the melt composition. The variation of surface tension at a typical temperature 348.16 K, for all the three systems, with mole fraction of $LiNO_3(x_{LiNO_3})$ in the mixture, is shown in Fig. 1. The extrapolation of the data to pure $LiNO_3$ was facilitated by adopting the value of σ_{LiNO_3}, obtained by extrapolating the results of Addison and Coldrey [9] to 348.16 K. In all the cases the surface tension showed the negative deviations from the additive values. Such a behavior is usually explained qualitatively by the fact that the surface layer of a solution is *enriched* in the component of the lower surface tension. If it is so, Eberhart[10] found it advantageous to describe the surface tensions in terms of surface-layer mole fraction (x_i^{σ}) of the components through the expression

$$\sigma = x_A^{\sigma}\,\sigma_A + x_B^{\sigma}\,\sigma_B = (s x_A\,\sigma_A + x_B\,\sigma_B)/(s x_A + x_B) \qquad (2)$$

where x_A and x_B are the bulk mole fractions of the two components of the binary mixture; σ_A and σ_B being the surface tensions of component A(hydrated salt) and of B ($LiNO_3$). Factor s, called ***surface enrichment factor***, is described as

$$s = \frac{(x_A^\sigma / x_B^\sigma)}{(x_A / x_B)} \tag{3}$$

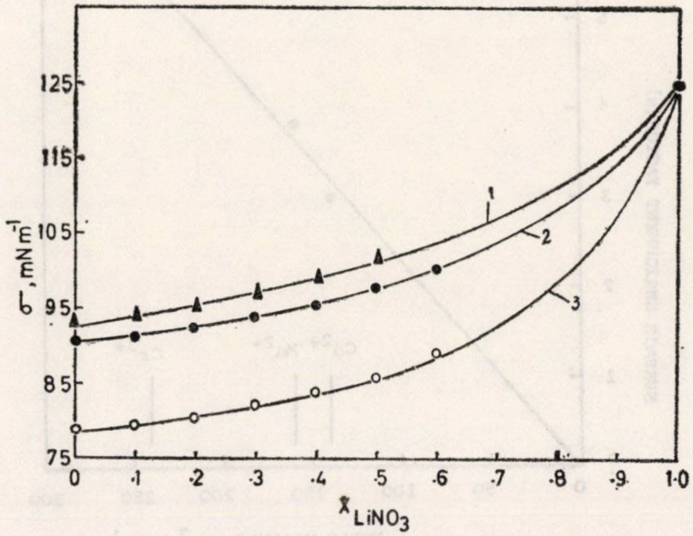

Fig. 1.—Surface tension (σ) of the solutions of $LiNO_3$ in molten : *1.* $Cd(NO_3)_2 \cdot 4H_2O$; *2.* $Mn(NO_3)_2 \cdot 6H_2O$; and *3.* $Cr(NO_3)_3 \cdot 9H_2O$ at 348.16 K, shown as a function of bulk mole fraction of $LiNO_3$.

where x_A^σ and x_B^σ are the mole fractions of the two components in the surface layer. The values of s (at 348.16 K) were determined by the method suggested by Eberhart,[10] in which the surface tension data are fitted into the equation $\xi = -s(\xi/r) + 1$; where

$$\xi = (\sigma - \sigma_A)/(\sigma_B - \sigma_A) \text{ and } r = x_B/x_A \tag{4}$$

ξ is thus the surface tension on a dimensionless scale varying from zero for pure A to unity for pure B. The analysis of the present data yields values of 3.0, 3.8 and 5.5. for the surface enrichment factor for systems containing $Cd(NO_3)_2 \cdot 4H_2O$, $Mn(NO_3)_2 \cdot 6H_2O$ and $Cr(NO_3)_3 \cdot 9H_2O$ respectively; it is interesting to note that the s value increases in the direction of the molar volume for the molten hydrates (Fig. 2). Sternberg and Terzi,[11] from their surface tension measurements on the molten mixtures containing silver chloride and alkali metal chlorides, have reported the sequence Na $<$ K $<$ Rb $<$ Cs for the s value, which appears to support the present findings regarding the molar volume dependence of the s values. Using these values of s, the surface tensions for the mixtures of different compositions were calculated and shown as a solid curve in Fig. 1. There is a striking agreement between the curve drawn and the experimental points. Employing these values of *s*, the mole fractions of lithium nitrate in the surface layer ($x^{\sigma}_{LiNO_3}$) were calculated; they are included in table 1. In Figure 3, the measured surface tensions are shown

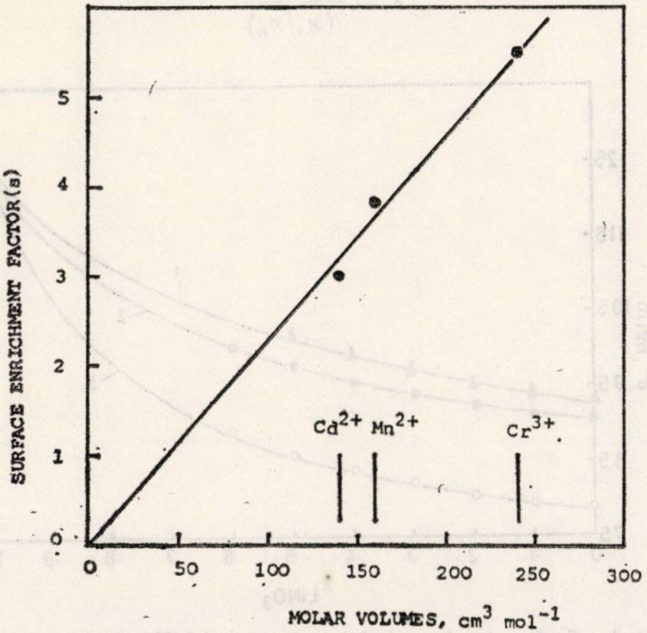

Fig. 2. — The surface enrichment factor, *s*, shown as a function of the molar volume (at 348.16 K) for the systems investigated in the present study.

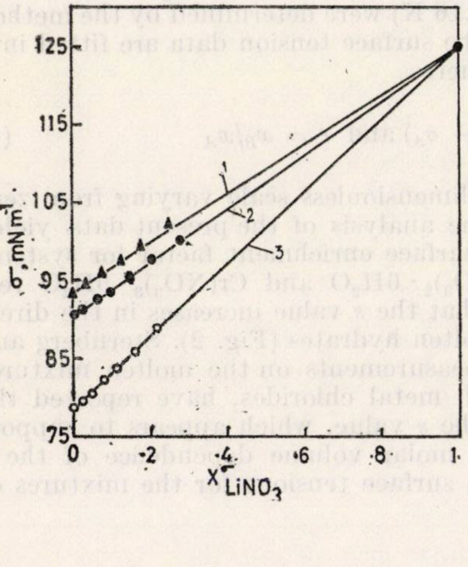

Fig. 3. — Surface tensions (348.16 K) shown as a function of surface layer mole fraction of lithium nitrate ($x^{\sigma}_{LiNO_3}$) for the solutions of lithium nitrate in : *1.* $Cd(NO_3)_2 \cdot 4H_2O$; *2.* $Mn(NO_3)_2 \cdot 6H_2O$; and *3.* $Cr(NO_3)_3 \cdot 9H_2O$.

as a function of surface layer mole fraction of $LiNO_3$. The linearity of these plots clearly shows that the surface tension is a linear function of the surface layer mole fraction and not of bulk concentration.

REFERENCES

[1] S. K. Jain, *J. Chem. Eng. Data*, **18**, 397 (1973).
[2] S. K. Jain, *J. Chem. Eng. Data*, **22**, 383 (1977).
[3] S. K. Jain, *J. Chem. Eng. Data*, **23**, 170 (1978).
[4] S. K. Jain, H. L. Jindal, and N. P. Kulshrestha, *J. Chem. Eng. Data*, **23**, 36 (1978).
[5] S. K. Jain, *J. Chem. Eng. Data*, **23**, 216 (1978).
[6] S. K. Jain, *J. Chem. Eng. Data*, **23**, 266 (1978).
[7] S. K. Jain, *J. Phys. Chem.*, **82**, 1272 (1978).
[8] S. K. Jain, *J. Chem. Eng. Data*, **25**, 36 (1980).
[9] C. C. Addison and J. M. Coldrey, *J. Chem. Soc.*, **86**, 468 (1961).
[10] J. G. Eberhart, *J.Phys. Chem.*, **70**, 1183 (1966).
[11] S. Stenberg and M. Terzi, *J. Chem. Therm.*, **3**, 259 (1971).

Revue Roumaine de Chimie, 27, 6, 719–726 (1982)

MICROSTRUCTURE OF ELECTROLESS DEPOSITED NICKEL IN AN ULTRASONIC FIELD

RODICA VÎLCU * and ELENA DIMITRIU **

* The National Institute of Chemistry, Chair of Physical Chemistry and Electrochemical Technology, 13, Bd. Republicii, Bucharest, Romania

** ICEFIZ, Institute of Physics and Technology of Materials, Măgurele – Bucharest, Romania

Received November 23, 1981

By reducing the nickel chloride with sodium hypophosphite on a ceramic substraten activated with an aluminium film, one obtains amorphous nickel with crystalline nickel traces. If an ultrasonic field (frequency = 25 kHz, transducer supply power = 50 W) is present during the reduction, the amorphous character of the deposit and the layer phosphorus content increase. The nickel layers deposited in an ultrasonic field in the best deposition conditions are harder, more adherent and present a greater stability to some chemical agent action. The thermal stability of the nickel layers is poor, since after annealing Ni and Ni_5P_2 crystallize.

INTRODUCTION

The chemical deposition of Ni on dielectrical substrates may be achieved by vacuum decomposition of $Ni(CO)_4$ at 316 K, or by reducing a solution that contains nickel salts with a suitable reducer (sodium hypophosphite, formaldehyde, borane) on a substrate previously made sensitive with stanium chloride and activated with palladium chloride,[1–5] or only activated by vacuum deposition of an aluminium film.[6–7]

The purpose of this paper is the comparative study of the nickel layers structure deposited in optimum conditions on ceramic substrates, activated with an aluminium film, in the absence and presence of an ultrasonic field by reducing the nickel chloride with sodium hypophosphite. The microstructure, the dependence of microstructure and of some properties with the layer phosphorus content have been studied.

NICKEL LAYERS DEPOSITION

The ceramic substrates (α-alumina 99 %, Al_2O_3 sintered at 1923 K, and barium titanate sintered at 1673 K) washed and dried, were activated by depositing an aluminium film in a V.E.B. Hochvacuum Dresden B 3 0.2 vacuum evaporation device. The outgassing of substrate surfaces was required as a preliminary stage before the aluminium activation, since these presented a 2.5–3.0 μm rugosity. The height of the source (tungsten filament) is 0.1 m, its length 0.075 m, the temperature of the substrate is the temperature of the environment,

the pressure during aluminium deposition is 2.10^{-5} Torr. Having been activated, the substrates were introduced in a nickel plating solution containing nickel chloride, ammonium chloride and ammonium citrate. The value of pH is 8–8.5 and the deposition temperature 368–373 K. The sodium hypophosphite is the reducing agent of nickel ions. The influence of the solution reducer amount over the chemical structure of the deposit has been pointed out depositing the nickel from two solutions with the compositions shown in table 1. (The quantities are given for a 100 ml solution). The nickel deposition was also carried out in an ultrasonic field supplied by a Ultramet® III Sonic Cleaner, from Buehler Ltd. Co. (frequency = 25 kHz, transducer supply power = 50 W). The optimum time of irradiation is of three minutes, from a total time of eight minutes. In order to get the best adherence, the activated substrate must be parallel with the propagation direction of the ultrasonic waves.

TABLE 1

The composition of nickel plating solutions

Substance	Nickel plating solution	
	I	II
$NiCl_2 \cdot 5H_2O$	1.5 g	1.5 g
NaH_2PO_2	0.5 g	1.5 g
NH_4Cl	2.5 g	2.5 g
30% ammonium citrate solution	10.8 ml	10.8 ml

EXPERIMENTAL METHODS

The microstructure has been investigated by means of the ISM-20 scanning electronmicroscope and X-ray diffraction method. The phosphorum spread on the layers has been investigated by means of JEOL electron microprobe. The nickel layers prepared from the two solutions both in the absence and the presence of an ultrasonic field have been annealed, in hydrogene medium, during one hour at the temperatures of 473, 673, 973 K.

RESULTS AND DISCUSSIONS

From the electron photomicrograph it has been ascertained that the nickel layers deposited in an ultrasonic field are made up of five times more particles with small diameters (between 0.1 and 0.5 μm) than those deposited in the absence of an ultrasonic field. For this reason the layers deposited in an ultrasonic field are more compact, harder and more adherent.[6] By examining the X-ray diffraction patterns one notes that deposits made up both in the absence and presence of the ultrasonic field are amorphous (Fig. 1). The amorphous character of the layer deposited in an ultrasonic field is more marked (the X-ray diffraction maximum is more diffused). The nickel layers deposited in an ultrasonic field are better arranged, the agglomeration of the particles is stronger, as was also observed by means of the scanning microscope.[6] Besides the amorphous nickel there are in both depositions traces of crystalline nickel, with preferred orientation in the ⟨111⟩ direction. The thermal stability of the nickel layers is poor since during the annealing the amorphous phase gradually crystallizes with the temperature increase. As a result of the thermal treatment besides the crystalline nickel the Ni_5P_2 phase crystallizes ; its crystallization is improved with the temperature increase. Figure 2 shows the X-ray diffraction patterns of the nickel layers after thermal treatment during one hour at 673 and 973 K.

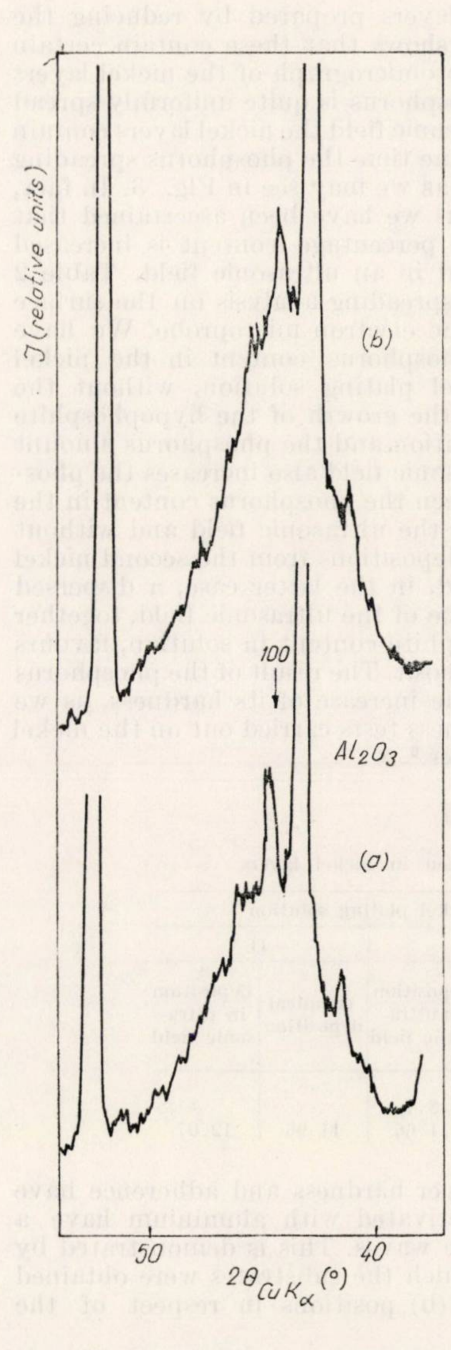

Fig. 1. — X-ray diffraction pattern of nickel layers deposited a) in the absence —, b) in the presence of the ultrasonic field.

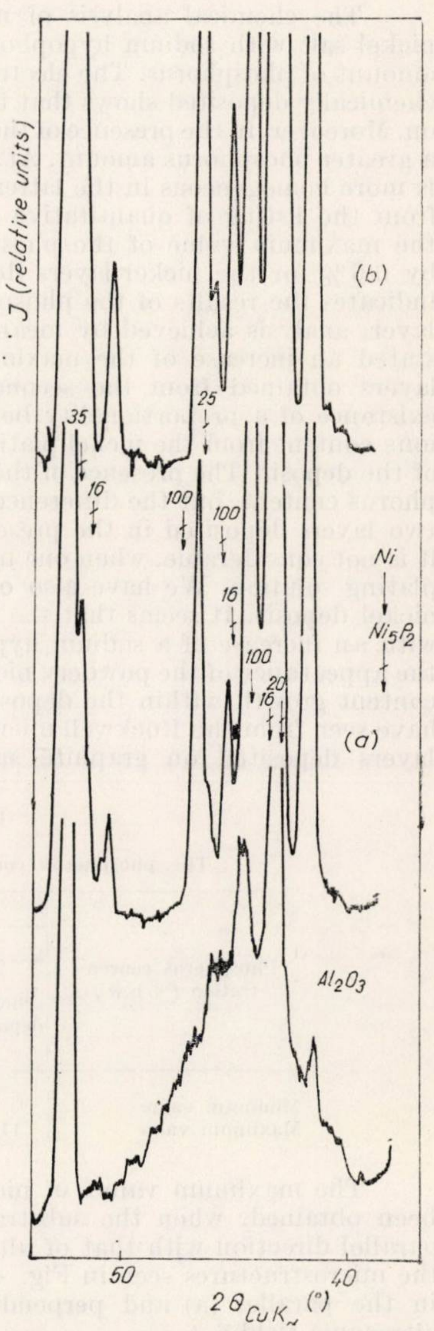

Fig. 2. — X-ray diffraction pattern of nickel layers annealed during one hour at a) 673 K, b) 973 K.

The chemical analysis of nickel layers prepared by reducing the nickel salt with sodium hypophosphite shows that these contain certain amount of phosphorus. The electron photomicrograph of the nickel layers chemically deposited shows that the phosphorus is quite uniformly spread on. Moreover, in the presence of the ultrasonic field the nickel layers contain a greater phosphorus amount. At the same time the phosphorus spreading is more homogeneous in the latter case, as we may see in Fig. 3. In fact, from the listing of quantitative analysis we have been ascertained that the maximum value of the phosphorus percentage content is increased by 0.6% for the nickel layers deposited in an ultrasonic field. Table 2 indicates the results of the phosphorus spreading analysis on the surface layer, analysis achieved by means of the electron microprobe. We have stated an increase of the maximum phosphorus content in the nickel layers obtained from the second nickel plating solution, without the existence of a proportionality between the growth of the hypophosphite ions content from the nickel plating solution and the phosphorus amount of the deposit. The presence of the ultrasonic field also increases the phosphorus content, but the difference between the phosphorus content in the two layers deposited in the presence of the ultrasonic field and without it is not considerable, when one makes depositions from the second nickel plating solution. We have also observed, in the latter case, a dispersed nickel deposit. It seems that the presence of the ultrasonic field, together with an increase of a sodium hypophosphite content in solution, favours the appearance of the powdery nickel deposit. The result of the phosphorus content growth within the deposit is the increase of its hardness, as we have seen from the Rockwell microhardness tests carried out on the nickel layers deposited on graphite substrates.[6]

TABLE 2

The phosphorus concentration in nickel layers

Phosphorus concentration (% b.w.)	Nickel plating solution			
	I		II	
	chemical deposition	deposition in ultrasonic field	chemical deposition	deposition in ultrasonic field
Minimum value	—	3.7	—	—
Maximum value	11.06	11.66	11.96	12.07

The maximum values of nickel layer hardness and adherence have been obtained, when the substrates activated with aluminium have a parallel direction with that of ultrasonic waves. This is demonstrated by the microstructures seen in Fig. 4 in which the substrates were obtained in the parallel (a) and perpendicular (b) positions in respect of the ultrasonic field.

The nickel deposition on ceramic substrate may be achieved only in the presence of a catalytic agent (Pd, Rh, Al), which decreases the activation energy of the reducing reaction.

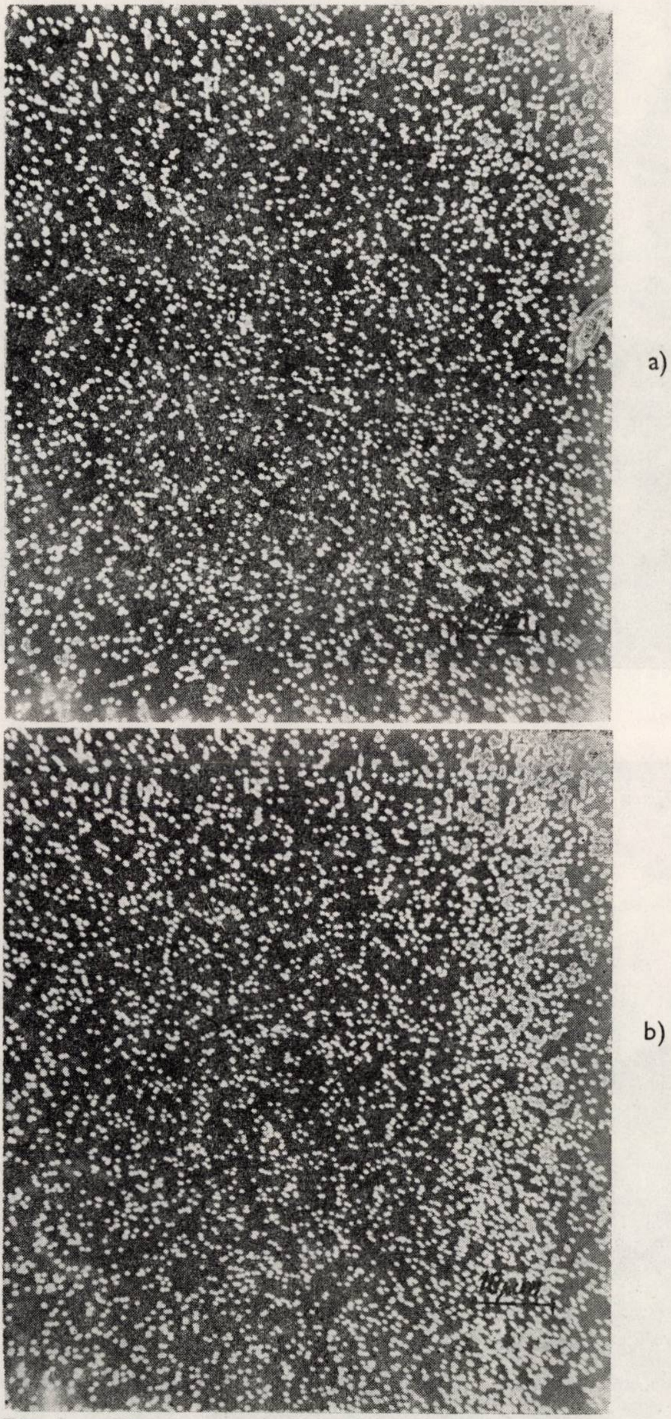

Fig. 3. — Phosphorus spreading on the nickel layers deposited a) in the absence — , b) in the presence of the ultrasonic field.

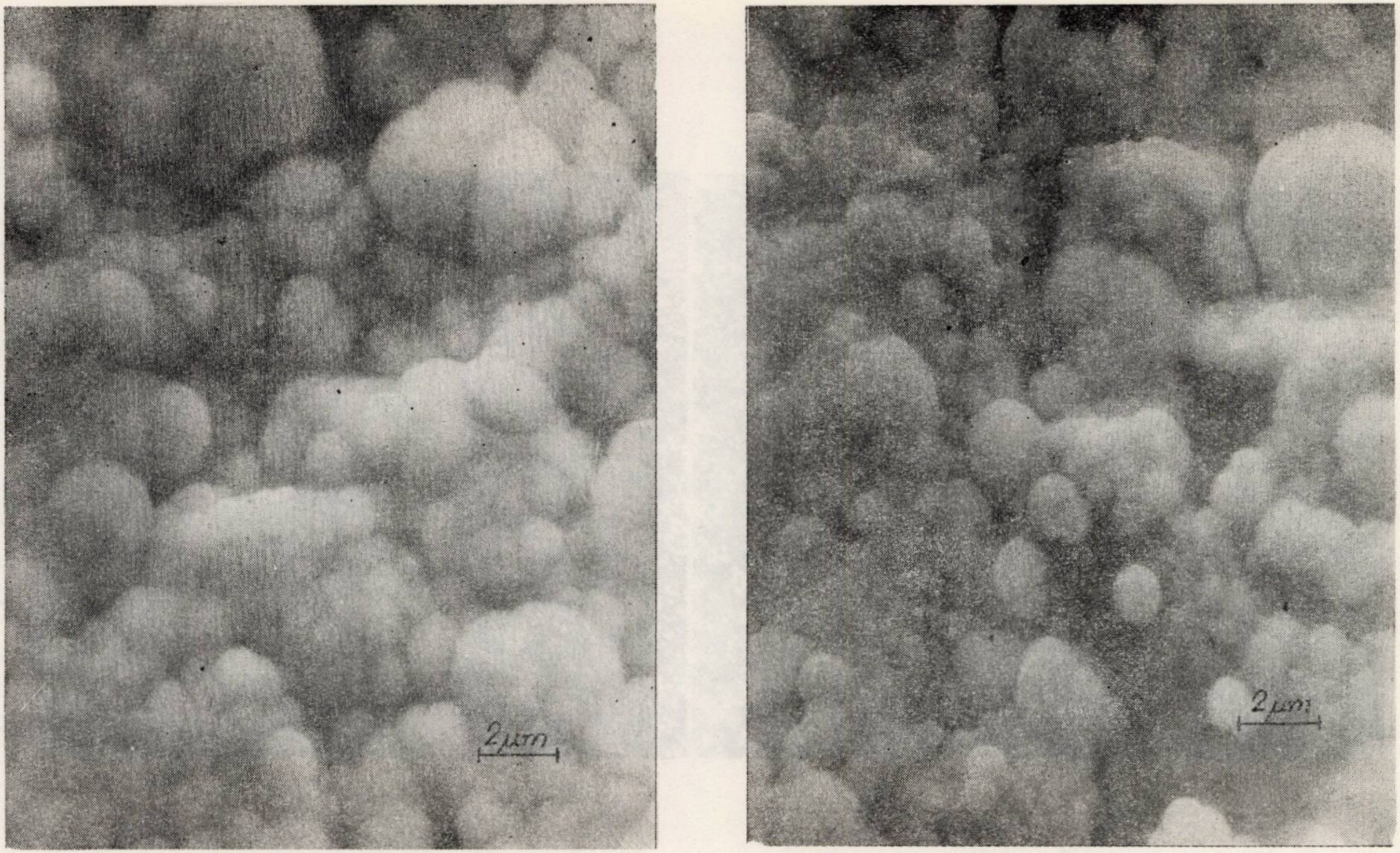

a) b)

Fig. 4. — Microstructures of nickel layers deposited on substrates with a) parallel- and b) perpendicular direction on the propagation direction of ultrasonic waves.

The chemical reducing of the nickel chloride with sodium hypophosphite takes place as follows:

$$NiCl_2 + NaH_2PO_2 + H_2O = Ni + NaCl + HCl + H_3PO_3$$

Because of the less electronegativity of the aluminium compared with that of the nickel, the following reaction may also take place:

$$3NiCl_{2(sol.)} + 2Al_{(substrate)} = 3Ni_{(substrate)} + 2AlCl_{3(sol.)}$$

In fact, it has been observed that the nickel weight deposited on the surface unity of the substrate increases both with the aluminium weight existent on the surface substrate and with the deposition time.

Since the amount of the sodium hypophosphite existent in the two nickel plating solutions is 3 to 9 times higher than that stoichiometric necessary, we may state that the hypophosphite ion is adsorbed in nickel deposits. Because of the conditions upon the substrate activated with aluminium, the hypophosphite ion is reduced and then reacts with the nickel forming the Ni_5P_2 compound, also observed in the X-ray diffraction patterns. The increase of the phosphorus amount in deposit as a result of the solution sodium hypophosphite concentration growth, or of the ultrasonic waves irradiation may be explained by the increase of the ions flow density impinging upon the surface substrate. It was shown [8] that the nickel chemical deposition takes place by the coalescence of the islands deposited on the substrate. This mechanism seems to be confirmed by the microstructure presented in Fig. 5, in which nickel islands deposited on a copper substrate activated with aluminium may be seen.

Fig. 5. — Nickel island formed on a copper substrate.

CONCLUSIONS

We have noted some of the advantages of the dielectrical substrates activation with an aluminium film :

— the nickel deposition takes place only upon the surface activated with aluminium ;

— the nickel deposition becomes possible both on ceramic surfaces and metallic ones ;

— the surface substrate outgassing carried out before the vacuum depositions, brings about the aluminium deposition upon the physical surface, not upon the geometrical one.[9] The bounds between the aluminium atoms and the surface substrate will be stronger, so that the activator layer will be more adherent to the surface ; the nickel layer deposited will be also more adherent ;

— the nickel layers are not attacked by hydrochloric acid or by ferric chloride, as it happens with the nickel strates deposited by activating the substrate surface with palladium chloride.

The presence of the ultrasonic field during the chemical deposition (frequency = 25 kHz, transducer power supply = 50 W, ultrasonic waves irradiation time = 3 minutes, from the deposition time of 8 minutes) increases the hardness and the adherence of the deposits, since a decrease of nickel particles diameters and a deposit outgassing have been produced.

REFERENCES

[1] A. Călușaru, "Depunerea electrolitică a metalelor în formă dispersă", Editura Academiei, București, 1962.

[2] Ch. R. Brumett and R. N. Shaak, *Official Gazette of the United States, Patents and Trademark Office*, **941**, 1901 (1975).

[3] A. Cziràky, B. Fagarassy, I. Bakonyi, K. Tompa, T. Bagi and Z. Hegedüs, *J. Physique, Colloque C8*, **41**, C8-141 (1980).

[4] H. Edward, *Official Gazette of the United States, Patents and Trademark Office*, **911**, 609 (1973).

[5] E. J. Fagden and E. B. Saubestre, *Official Gazette of the United States, Patents and Trademark Office*, **915**, 1421 (1973).

[6] R. Vîlcu and E. Dimitriu, *Rev. Roumaine Chim.* (to be published).

[7] R. Vîlcu, R. Mănăilă, E. Dimitriu and I. Nazarenco, Communication at the II-nd National Congress of Chemistry, Bucharest, 7—10 sept. 1981.

[8] "Handbook of Thin Film Technology", Edited by L. I. Maissel and R. Glang, Mc Graw-Hill, New York, 1970.

[9] A. Roth, "Vacuum Technology", North-Holland Publishing Company, Amsterdam, 1976.

Revue Roumaine de Chimie, 27, *6*, 727–734 (1982)

ELECTRONIC SPECTRA, MAGNETIC PROPERTIES AND STRUCTURE OF POLYNUCLEAR COMPLEXES $[Fe_2^{III}M^{II}Cl_{12}]^{4-}$ OF MANGANESE (II) AND COBALT (II)

*G. MUNTEANU, *C. I. LEPĂDATU, *LUMINIŢA PATRON
and **MARIA BREZEANU

* ICECHIM — Center of Physical Chemistry
** Polytechnical Institute, Splaiul Independenţei no. 202, Bucharest, Romania

Received September 21, 1981

The electronic spectra and magnetic properties of the polynulcear complexes $[Fe_2^{III}M^{II}Cl_{12}]^{4-}$, where $M^{II} = M^{II}$, Co^{II}, were interpreted. The “d-d” transitions and the charge transfer between coordinated metal ions occurring in the spectra were analyzed and accordingly assigned. The antiferromagnetism of the polynuclear complex containing the Co^{II} ion was also proved. Our study shows that the Fe^{III} ions possess an octahedral coordination. The spatial arrangement of the three metal ions in polynuclear complexes are most likely “in line”, with the M^{II} ion at the end of the chain.

INTRODUCTION

In the present paper we report the synthesis and the chemical characterization of some polynuclear complexes of general formula $(NH_4)_4[Fe_2^{III}M^{II}Cl_{12}]$, where M^{II} is Co^{II} or Mn^{II}. The aim of the present paper is also to obtain information on the chemical bonding and the coordination geometry of these complexes. The study will be mainly based on the electronic spectra and magnetic measurements.

We ascribe to these complexes two possible “in line” arrangements of the three ions (Fig. 1). The two spatial arrangements would better correspond to the chemical formula resulted from chemical analysis.

We assume also an octahedral coordination for the two Fe^{III} ions and a tetrahedral one for the M^{II} ion, with four chlorine bridges between metal ions.

EXPERIMENTAL

The synthesis of these polynuclear complexes was performed in strongly acidic medium, for molar ratios $FeCl_3 : MCl_2$ varying from 1 : 1 to 1 : 10. It should be mentioned that these polynuclear complexes are the only species which can be obtained in this medium, even with an excess of ferric chloride. To a solution obtained by dissolving 0.4 g $FeCl_3$ in 2.5 ml ethanol and 1.5 ml 36.5% HCl, one adds 0.3 g $CoCl_2 \cdot 6H_2O$ or 0.25 $MnCl_2 \cdot 4H_2O$, respectively, corresponding to the ratio $FeCl_3 : MCl_2 = 2 : 1$. Then ammonia is added dropwise, until pH = 2.5—3.0. The solid deposited is filtered after 24 hrs and washed with ethanol.

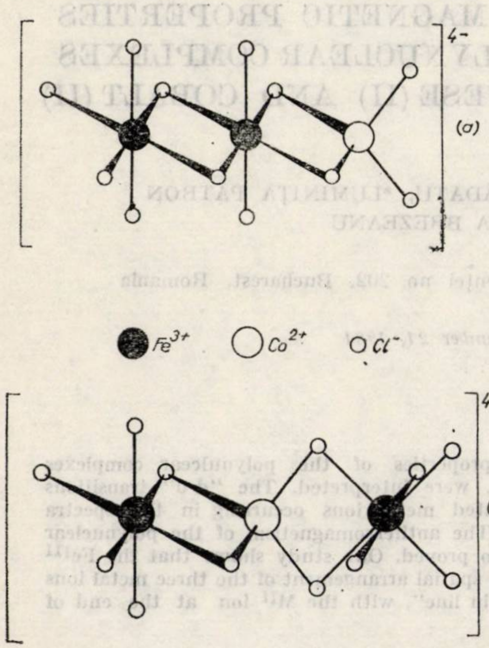

Fig. 1.—The two possible spatial arrangements of the metal ions in the polynuclear complex with cobalt. (a) — the Co^{2+} ion is at the end of chain ; (b) — the Co^{2+} ion is between the two Fe^{3+} ions.

According to the results of chemical analysis, the two polynuclear complexes are formulated as $(NH_4)_4[Fe_2^{III}M^{II}Cl_{12}]$. Electrical conductivity measurements agree with the chemical formulas :

$$(NH_4)_4[Fe_2CoCl_{12}] - 310 \text{ ohm}^{-1}\text{cm}^2\text{mol}^{-1}$$

$$(NH_4)_4[Fe_2MnCl_{12}] - 236 \text{ ohm}^{-1}\text{cm}^2\text{mol}^{-1}$$

The electronic spectra were recorded with a DK-2 Beckman spectrophotometer.

The magnetic susceptibility measurements were performed using the Faraday method. The magnetic susceptibilities were measured on samples of 0.1—1.0 g.

RESULTS AND DISCUSSION

(I) Electronic spectra

The interpretation of the electronic spectra is essentially based on the assumption that each polynuclear complex is formed from mononuclear species (that is a metal ion directly coordinated by the ligands) with weak metal-metal interactions. These mononuclear entities are mainly responsible for the absorption bands appearing in the electronic spectra. This assumption is partly justified by the weak interactions between metal ions in polynuclear complexes. Table 1 shows the overlap integrals between "d" metal orbitals in complexes. The overlap integrals were estimated using the Slater orbitals [1] and the interatomic distances Fe—Fe (2.35 Å), Fe—Mn (2.97 Å), Fe—Co (2.98 Å) as resulting from the geometry of the complexes (Fig. 1) and the interatomic distances Fe^{III}—Cl (2.30 Å),[2] Co^{II}—Cl (2.34 Å) and Mn^{II}—Cl (2.33 Å).[3]

TABLE 1

The overlap integrals between "d" metal orbitals in complexes

Overlap integral	Fe—Fe	Fe—Mn	Fe—Co
$S_\sigma(d_A, d_B)$	0.0043	0.0049	0.0203
$S_\pi(d_A, d_B)$	0.0026	0.0014	0.0076
$S_\delta(d_A, d_B)$	0.0001	0.0001	0.0008

As can be seen in table 1, the overlapping between "d" metal orbitals is not significant and justifies the partition of the polynuclear complexes into mononuclear entities.

Because the mononuclear species $[Fe^{III}Cl_6]^{3-}$ is not known, its electronic spectrum was "synthesized" using the spectral data of $[Fe^{III}Cl_4]^-$. We made use of the well established fact that the orbital energies are generally transferable from one complex to another, in which the same metal-ligand bond is present.[4] The orbital energies were parametrized according to the Angular Overlap Model [5] (AOM), the interelectronic repulsion matrices being the same as in the Ligand Field Theory with a strong coupling.[6]

The Racah parameters B and C were taken from the electronic spectrum of $[Fe^{III}Cl_4]^-$ ($B = 625$ cm^{-1}, $C = 4B$).[7] The AOM parameters $e_{\sigma,\pi}$ for Fe^{III}—Cl bonds were obtained from those of Cr^{III}—Cl bonds using a factorization rule [8] ($e_\sigma = 5500$ cm^{-1}, $e_\pi = 1380$ cm^{-1}).

The following sequence of "d-d" transitions should occur in the electronic spectrum of $[Fe^{III}Cl_6]^{3-}$:

$^6A_1 \rightarrow {}^4T_1(a)$	9705 cm^{-1}
$\rightarrow {}^4T_2(a)$	13703 cm^{-1}
$\rightarrow {}^4A_1, {}^4E(a)$	18750 cm^{-1}
$\rightarrow {}^4T_2(b)$	21029 cm^{-1}
$\rightarrow {}^4E(b)$	23124 cm^{-1}
$\rightarrow {}^4T_1(b)$	27842 cm^{-1}
etc.	. . . .

The absorption band occurring at 8470 cm^{-1} in the electronic spectra of both polynuclear complexes (Fig. 2) could be assigned to the first spin forbidden "d-d" transition of $[Fe^{III}Cl_6]^{3-}$, $^6A_1 \rightarrow {}^4T_1(a)$.

The most intense and characteristic absorption bands at 15380 cm^{-1} are undoubtedly[9] due to the transition $^4A_2 \rightarrow {}^4T_1(^4P)$ of the tetrahedral species $[Co^{II}Cl_4]^{2-}$.

The spin forbidden "d-d" transitions of $[Mn^{II}Cl_4]^{2-}$ are not observed in the spectrum of the corresponding polynuclear complex.

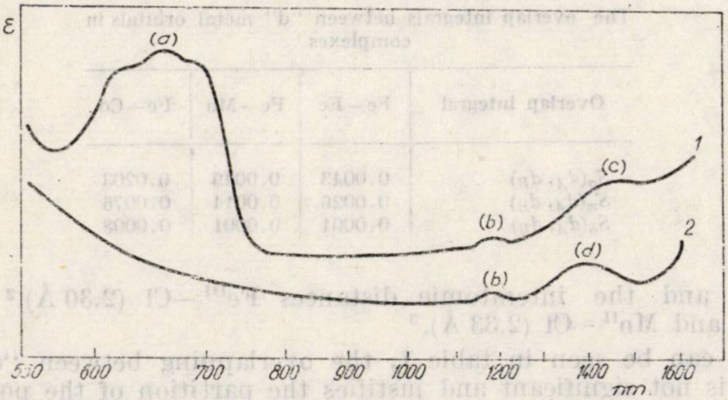

Fig. 2. — The electronic spectra of the polynuclear complexes : (1) — for the complex with Co^{2+} ; (2) — for the complex with Mn^{2+} ; (a) — $^4A_2 \rightarrow {}^4T_1(^4P)$ "d-d" transition in $CoCl_4^{2-}$; (b) — $^6A_1 \rightarrow {}^4T_1$ "d-d" transition in $FeCl_6^{3-}$; c) — $T_2(Co) \rightarrow T_{2g}(Fe)$ charge transfer transition ; (d) — $E(Mn) \rightarrow E_g(Fe)$ charge transfer transition.

As can be seen from Fig. 2, there are two supplementary absorption maxima in the electronic spectra : at 6700 cm^{-1} for the Co^{II} polynuclear complex and at 7140 cm^{-1} for that containing the Mn^{II} ion. These absorption maxima could be described to an electron transfer mechanism between two neighbour species from the polynuclear complexes $[Mn^{II}Cl_4]^{2-} \rightarrow [Fe^{III}Cl_6]^{3-}$. To prove that, one must evaluate the molecular levels in the mononuclear species. This can be done using the AOM approach.

$[Fe^{III}Cl_6]^{3-}$ (Octahedral) :

$$E(E_g) = E_0 + 3e_\sigma$$

$$E(T_{2g}) = E_0 + 4e_\pi$$

$$\Delta_{oct} = E(E_g) - E(T_{2g}) = 3e_\sigma - 4e_\pi$$

$[Mn^{II}Cl_4]^{2-}$ (Tetrahedral) :

$$E(T_2) = E_0 + 8/9\ e_\pi + 4/3\ e_\sigma$$

$$E(E) = E_0 + 8/3\ e_\pi$$

$$\Delta_{tetr} = E(T_2) - E(E) = -4/9\Delta_{oct}$$

The $e_{\sigma,\pi}$ parameters for the M^{II}—Cl and Fe^{III}—Cl bonds were calculated from those of the Cr^{III}—Cl bonds using a procedure reported elsewhere.[8] The ionization potentials for the neutral transition metals were taken[10] as the zeroth order energies E_0. We assumed therefore, that the formal charge on the coordinated transition metal ions is close to zero. The calculated "d" molecular levels are given in table 2. The two supplementary absorption maxima appearing in the electronic spectra of the polynuclear complexes (Fig. 2) could be attributed to a charge transfer between the mononuclear species, as follows :

TABLE 2

The calculated "d" molecular levels. The experimental values are from Jørgensen [7]

Complex	"d" molecular levels (cm^{-1})	Parameter Δ (cm^{-1})
$[Fe^{III}Cl_6]^{3-}$	$E(E)_g = -53500$ $E(T_{2g}) = -64480$	$\Delta_{tetr} = 4880$ (exp. 5000) $\Delta_{oct} = 10980$
$[Mn^{II}Cl_4]^{2-}$	$E(T) = -58666$ $E(F) = -61712$	$\Delta_{tetr} = 3046$ (exp. 3500)
$[Co^{II}Cl_4]^{2-}$	$E(T_2) = -70842$ $E(E) = -73786$	$\Delta_{tetr} = 2944$ (exp. 3100)

$E(Mn)_{tetr} \rightarrow E_g(Fe)_{oct}$ 8212 cm^{-1}(exp. 7140 cm^{-1})

$T_2(Co)_{tetr} \rightarrow T_{2g}(Fe)_{oct}$ 6362 cm^{-1}(exp. 6700 cm^{-1})

This assignment is only tentative in an attempt to explain the presence of the two absorption bands in the electronic spectra of the complexes.

(ii) Magnetic Properties

The measurements of the magnetic susceptibility carried out at room temperature are given in table 3, where :

$$\mu_{calc}(BM) = g \cdot \left[\sum_{i=1}^{3} S_i(S_i + 1) \right]^{1/2}$$

S_i being the total spin of each coordinated metal ion in its ground state.

As can be seen from table 3, a pronounced antiferromagnetism occurs for the polynuclear complex containing the Co^{II} ion. We shall try in what follows to study the antiferromagnetism of this polynuclear complex, using the Heisenberg phenomenological approach.

TABLE 3

The spin only and experimental magnetic moments (in Bohr magnetons)

$[Fe_2^{III}M^{II}Cl_{12}]^{4-}$	μ_{exp}^{298}	μ_{calc}
Mn^{II}	9.03	10.25
Co^{II}	2.65	9.22

The interaction Hamiltonian for the three interacting spins has been expressed in terms of operator equivalents:

$$\hat{H}_{\text{int}} = -2 \sum_{j>i=1}^{3} J_{ij}[1/2\, \hat{S}_{i+} \hat{S}_{j-} + 1/2\, \hat{S}_{i-} \hat{S}_{j+} + \hat{S}_{iz} \hat{S}_{jz}]$$

where J_{ij} are the coupling constants and $\hat{S}_{\pm}$ the shift spin operators.

The wavefunctions of the three spins were obtained by successive couplings:

$$|j'm'\rangle = \sum_{m_1 m_2} C^{j'm'}_{j_1 m_1, j_2 m_2} |j_1 m_1\rangle |j_2 m_2\rangle$$

$$|j\, m\rangle = \sum_{m' m_3} C^{jm}_{j'm', j_3 m_3} |j'm'\rangle |j_3 m_3\rangle$$

where C's are the Clebsch-Gordan coefficients.

We have estimated only the diagonal elements (see Appendix):

$$\langle j\, m | \hat{H}_{\text{int}} | j\, m\rangle = \sum_{i>j=1}^{3} C_{ij} J_{ij}$$

The effective magnetic moment is given by the formula[11]:

$$\mu_{ef}(BM) = g \cdot [\sum_{S} S(S+1)(2S+1) \exp(-E_S/kT)]^{1/2} \cdot$$

$$\cdot [\sum_{S} (2S+1) \exp(-E_S/kT)]^{-1/2}$$

where g is the Landé factor and E_S are the energies summarized in the Appendix.

We calculated the effective magnetic moment for the two possible spatial arrangements of the complex (Fig. 1):

(1) Fe – Fe – Co $\quad J_{23} = 0,\ J_{12} = J^{\text{Fe-Co}},\ J_{13} = J^{\text{Fe-Fe}}$

(2) Fe – Co – Fe $\quad J_{13} = 0,\ J_{12} = J_{23} = J^{\text{Fe-Co}}$

For the arrangement (1) the coupling constants were fitted for $T = 294$ K, as shown in Fig. 3. They remain almost constant for other temperatures ($J^{\text{Fe-Fe}} = -400\ \text{cm}^{-1}$, $J^{\text{Fe-Co}} = -80\ \text{cm}^{-1}$). For the arrangement (2) the coupling constant is equal to $J^{\text{Fe-Co}} = -50\ \text{cm}^{-1}$.

Table 4 contains the temperature variation of the effective magnetic moments for the two solutions, (1) and (2), compared with that experi-

TABLE 4

The temperature dependence of the effective magnetic moments (in Bohr magnetons). (1) — for the arrangement Fe — Fe — Co ; (2) — for the arrangement Fe — Co — Fe.

T(K)	μ_{exp}	$\mu_{calc}(1)$	$\mu_{calc}(2)$
95	3.12	3.44	7.88
100	3.11	3.43	7.87
109	3.09	3.42	7.85
135	3.06	3.40	7.75
153	3.02	3.38	7.68
170	2.99	3.37	7.61
215	2.97	3.36	7.47
254	2.95	3.35	7.39
276	2.90	3.35	7.37
294	2.70	3.35	7.37

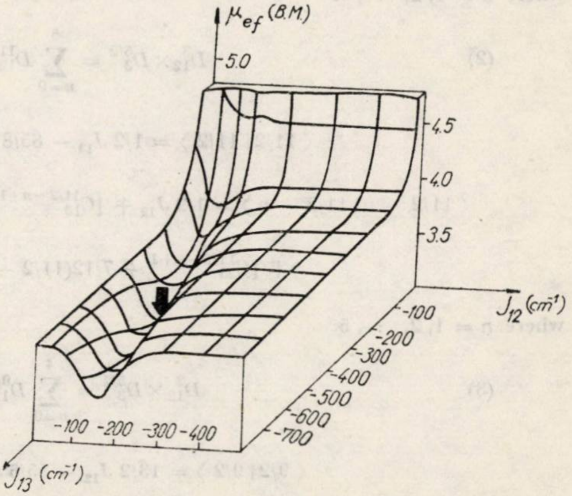

Fig. 3. — The variation of the effective magnetic moment *versus* the two coupling constants J_{12} and J_{13}. The arrow indicates the minimum of the function.

mentally found. As can be seen from table 4, the magnetic moment and the slope of its temperature variation corresponding to the Fe—Fe—Co arrangement are closer to those experimentally obtained. We have thus found supplementary information concerning the magnetic coupling type between the three transition metal ions, as well as the spatial arrangement of these ions and their coordination geometries in the polynuclear complex.

ACKNOWLEDGEMENT We thank Mr. V. Mincu of Physical Chemistry Chair (Polytech. Inst. — Bucharest) for the magnetic measurements.

APPENDIX

Coupling scheme ($S_1 = 5/2,\ S_2 = 3/2,\ S_3 = 5/2$) :

$$D_1^{5/2} \times D_2^{3/2} \times D_3^{5/2} = (D_{12}^4 + D_{12}^3 + D_{12}^2 + D_{12}^1) \times D_3^{5/2}$$

Energy matrix elements : $\langle S | S \rangle = C_{12}^S J_{12} + C_{13}^S J_{13} + C_{23}^S J_{23}$

$$D_{12}^4 \times D_3^{5/2} = \sum_{n=0}^{5} D_{123}^{13/2-n} \quad (1)$$

$$\langle 13/2 | 13/2 \rangle = -15/2 J_{12} - 25/2\, J_{13} - 15/2\, J_{23}$$

$$\langle 13/2 - n | 13/2 - n \rangle = -15/2\, J_{12} + [C_{13}^{13/2-n+1} + 4/5(13/2 - n + 1)]\, J_{13} + \\ + [C_{23}^{13/2-n+1} + 3/4(13/2 - n + 1)]\, J_{23}$$

where $n = 1, 2, \ldots, 5.$

$$D_{12}^{3} \times D_{3}^{5/2} = \sum_{n=0}^{5} D_{123}^{11/2-n} \tag{2}$$

$$\langle 11/2 | 11/2 \rangle = 1/2\, J_{12} - 85/8\, J_{13} - 35/8\, J_{23}$$

$$\langle 11/2 - n | 11/2 - n \rangle = 1/2\, J_{12} + [C_{13}^{11/2-n+1} + 17/12(11/2 - n + 1)]\, J_{13} +$$

$$+ [C_{23}^{11/2-n+1} + 7/12(11/2 - n + 1)]\, J_{23}$$

where $n = 1, 2, \ldots, 5.$

$$D_{12}^{2} \times D_{3}^{5/2} = \sum_{n=0}^{4} D_{123}^{9/2-n} \tag{3}$$

$$\langle 9/2 | 9/2 \rangle = 13/2\, J_{12} - 55/6\, J_{13} - 5/6\, J_{23}$$

$$\langle 9/2 - n | 9/2 - n \rangle = 13/2\, J_{12} + [C_{13}^{9/2-n+1} + 11/6(9/2 - n + 1)]\, J_{13} +$$

$$+ [C_{23}^{9/2-n+1} + 1/6(9/2 - n + 1)]\, J_{23}$$

where $n = 1, 2, 3, 4.$

$$D_{12}^{1} \times D_{3}^{5/2} = \sum_{n=0}^{2} D_{123}^{7/2-n} \tag{4}$$

$$\langle 7/2 | 7/2 \rangle = 21/2\, J_{12} - 35/4\, J_{13} + 15/4\, J_{23}$$

$$\langle 7/2 - n | 7/2 - n \rangle = 21/2\, J_{12} + [C_{13}^{7/2-n+1} + 7/2(7/2 - n + 1)]\, J_{13} +$$

$$+ [C_{23}^{7/2-n+1} - 3/2(7/2 - n + 1)]\, J_{23}$$

where $n = 1, 2.$

REFERENCES

[1] W. F. Cooper, G. A. Clarke and C. R. Hare, *J. Phys. Chem.*, **76**, 2268 (1972).

[2] "Interatomic Distances in Molecules and Ions", Chemical Society, Special Publication No. 21, London, 1958.

[3] I. H. Hillier, *J. Chem. Soc. A*, **1969**, 878.

[4] P. Spacu and C. I. Lepădatu, *Z. phys. Chem. (Frankfurt)*, **63**, 15 (1969).

[5] C. I. Lepădatu, *Z. phys. Chem. (Frankfurt)*, **60**, 202 (1968).

[6] J. S. Griffith, "The Theory of Transition-Metal Ions", University Press, Cambridge, 1961.

[7] C. K. Jørgensen, *Structure and Bonding*, **1**, 3 (1966).

[8] C. I. Lepădatu, *Z. phys. Chem. (Frankfurt)*, **57**, 28 (1968).

[9] A. B. P. Lever, "Inorganic Electronic Spectroscopy", Elsevier Publishing Company, Amsterdam, 1968.

[10] H. Gray, "Electrons and Chemical Bonding", W. A. Benjamin, New York, 1972.

[11] E. Sinn, *Coord. Chem. Rev.*, **5**, 313 (1970).

Revue Roumaine de Chimie 27, 6, 735–739 (1982)

TESTING THE GEOMETRICAL MEANING OF *TAFT*-TYPE STERIC CONSTANTS

IOAN MOȚOC [a] and ALEXANDRU T. BALABAN [b]

[a] Chemical Research Centre, B-dul M. Viteazul 24,1900 Timișoara, Romania
[b] The Polytehnic, Organic Chemistry Department, Bucharest, Romania

Received December 23, 1981

Using as predictor variables Verloop's STERIMOL parameters (i.e. L, B_1, B_2, B_3 and B_4, in Å) the geometrical meaning of Taft-type steric constants for a set of 14 alkyl, cycloalkyl and aralkyl groups (namely, E_S, E'_S and ν), as well as of the molecular refraction (MR) was investigated. The resulting equations indicate that in general there exist no significant correlations between the E_S, E'_S or ν values and the geometrical parameters L, B_1, B_2, B_3 and B_4 (the only correlation which could be evidenced was between E_S, E'_S or ν and B_3, with $r = 0.76 \div 0.73$, $F = 7.6 \div 6.2$ for the $n = 14$ groups). For MR a significant correlation was found with the arithmetic average $\bar{B}$ of the $B_1 - B_4$ values ($r = 0.90$, $F = 22.71$, $n = 14$). These results justify the effort to develop new steric constants with a clearer physical, geometrical or topological meaning, and with an obvious usefulness for quantitative structure – activity relationship (QSAR) studies.

1. INTRODUCTION

Taft's steric constant E_S for a substituent X is calculated as the average of log (k_X/k_H) values from four series of kinetic data in hydrolysis of ethyl esters in 79 % v/v aqueous acetone at 25°C ; esterification of carboxylic acids in methanol at 25°C ; esterification of carboxylic acids in ethanol at 25°C ; and hydrolysis of ethyl esters in 69 % v/v aqueous acetone.[1] The derivation of Taft constants is based on the Taft-Ingold hypothesis,[2] *i.e.*, the assumption that acid hydrolysis of esters is controlled by steric effects and that the other substituent effects are negligible. In all four cases above, the acid XCH_2COOH and the ester XCH_2COOR have the same skeleton. According to the definition, $E_S = 0$ for X = H, *i.e.*, for the case when the group attached to the acid or ester function is CH_3 as in acetic acid or ester. The E_S value for H on this scale is determined from reactions of formic acid or ester, and is 1.24.

A rescaled set of parameters, E''_S, may be derived from E_S by subtracting 1.24 from Taft's values and in this case one would consider X–COOR as the skeleton, and one could write

$$E_S = \log (k_X/k_{CH_3})\,; \quad E''_S = \log(k_X/k_H)$$

for the series X–COOR.

A corrected set of steric parameters E^c_S was developed[3,4] by Hancock *et al.* taking into account the N hydrogens at the α-carbon which introduce hyperconjugative electronic effects:

$$E^c_S = E_S + 0.306(N-3)$$

The averaging of $\log (k_X/k_{CH_3})$ values involved in calculating E_S constants implies also the assumption that the above four series of reactions have the same susceptibility. Since this hypothesis is not rigorously valid, it constitutes a source of errors. Arguing that a correct procedure would involve the use of a single series of standard reactions, McPhee *et al.* opted[5] for the acid esterification of carboxylic acids in methanol at 40°C and derived therefrom a revised Taft constant, $E'_S = \log (k_X/k_{CH_3})$, where the k values are rate constants for the reaction $X-COOH + CH_3OH$.

Charton defined[6] another steric constant ν_X according to the relationship:

$$\nu_X = r_X - r_H = r_X - 1.20$$

where r's indicate van der Waals radii (in Å); they are determined by calculation for monoatomic or symmetric substituents, and by an extension of the McPhee procedure for the remaining ones.

The three constants E_S, E'_S and ν are related to one another as shown by the following equations, calculated using the data presented in table 1.

$$-E_S = 0.005(\pm 0.015) + 1.108(\pm 0.021)(-E'_S) \qquad (1)$$

$$(r = 0.995,\ s = 0.055,\ F = 532.134,\ EV = 0.989)$$

$$-E_S = 1.135(\pm 0.018) + 2.212(\pm 0.021)\nu \qquad (2)$$

$$(r = 9.993,\ s = 0.063,\ F = 396.255,\ EV = 9.985)$$

$$-E'_S = -1.031(\pm 0.006) + 1.998(\pm 0.007)\nu \qquad (3)$$

$$(r = 0.999,\ s = 0.021,\ F = 2981.316,\ EV = 0.998)$$

Equation (3) indicates that E'_S and ν differ only (i) by the origin of the scale:

$$-E_{S,CH_3} = 0.00; \qquad -E_{S,H} = -1.12$$

$$\nu_{CH_3} = 0.52; \qquad \nu_H = 0.00$$

and (ii) by a scaling factor. This equation (3) represents an excelllent correlation so that it can be used for interconverting the McPhee and Charton steric constants E'_S and ν.

The molar refraction, defined as:

$$MR = \frac{n^2 - 2}{n^2 + 1}\,\frac{MW}{d}$$

where n is the refraction index (usually n_D^{20}), MW is the molecular weight and d is the density, is used [7] as a measure of the van der Waals volume (WV). In the preceding papers [8,9] it was shown that the WV component accounts for about 90 % of the MR, while the remaining 10 % can be ascribed to the electronic component.

The STERIMOL parameters (L, B_1, B_2, B_3 and B_4, expressed in Å) were introduced [10] by Verloop *et al.* and constitute convenient predictor variables for testing the geometrical significance of Taft-type steric constants : L represents the length of the substituent X, and B_1 – B_4 represent its width measured along two orthogonal directions. Ratios L/B_4 and B_4/B_1 indicate deviations of the substituent shape from the spherical shape. The relationship between these five parameters is : L is the length of the substituent along the direction of attachment to the remainder of the molecule ; B_1 is the smallest width on a perpendicular direction to the L_{axis} and B_4 is the largest width. The magnitudes of the B_1 – B_4 widths are determined by the maximum distances from the van der Waals envelope to the L_{axis}. The two mutually orthogonal planes on which the molecule is projected to find the four widths B_1 – B_4 intersect along the L_{axis}.

The B_1 parameter is known[11] to show some correlation with E_S ($r^2 = 0.719$).

2. RESULTS

Linear correlations of type (4) were investigated using the data collected in table 1 and a computer least square program :

$$(SP)_1 = a + b(SP)_2 \tag{4}$$

TABLE 1

The values of the steric parameters used in calculations

Substituent	$-E_S$	$-E'_S$	ν	MR	L	B_1	B_2	B_3	B_4	L/B_4	B_4/B_1	$\overline{B}$
Methyl	0.00	0.00	0.52	5.7	3.00	1.52	1.90	1.90	2.04	1.47	1.07	1.84
Ethyl	0.07	0.08	0.56	10.3	4.11	1.52	1.90	1.90	2.97	1.38	1.56	2.07
n-Propyl	0.36	0.31	0.68	15.0	5.05	1.52	1.90	1.90	3.49	1.45	1.84	2.20
n-Butyl	0.39	0.31	0.68	19·6	6.17	1.52	1.90	1.90	4.42	1.40	2.33	2.44
Isopropyl	0.47	0.48	0.76	15.0	4.11	2.04	2.76	3.16	3.16	1.30	1.00	2.78
s-Butyl	1.13	1.00	1.02	19.6	5.05	1.90	2.76	3.16	3.49	1.45	1.10	2.83
i-Butyl	0.93	0.93	0.98	19.6	5.05	1.52	1.90	3.16	4.21	1.20	1.33	2.70
t-Butyl	1.54	1.43	1.24	19.7	4.11	2.59	2.86	2.86	2.97	1.38	1.04	2.82
n-Pentyl	0.40	0.31	0.68	24.3	7.11	1.52	1.90	1.90	4.94	1.44	2.60	2.57
Cyclobutyl	0.06	0.03	0.51	17.9	4.69	1.95	2.64	2.64	3.83	1.22	1.45	2.76
Cxclopentyl	0.51	0.41	0.71	22.0	4.97	2.04	2.86	2.86	3.98	1.25	1.39	2.93
Cyclohexyl	0.79	0.69	0.87	26.7	6.17	2.04	3.16	3.16	3.49	1.77	1.10	2.96
Benzyl	0.38	0.39	0.70	30.0	3.63	1.52	3.11	3.11	6.02	0.60	1.94	3.44
Benzhydryl	1.76	1.50	1.25	54.3	5.15	2.01	4.99	5.28	5.82	0.88	1.10	4.39

where the steric parameters are :

$$(SP)_1 = E_S, E'_S, \nu \text{ or } MR$$

$$(SP)_2 = L, B_1, B_2, B_3, B_4, \overline{B}, L/B_1, L/B_4, B_4/B_1 \text{ or } B_4/L$$

The results of calculations are presented in tables 2 and 3. On testing biparametric equations, no statistically significant improvements over the equations grouped in tables 2 or 3 were obtained.

TABLE 2

Results of correlations : Taft-type constants *vs* STERIMOL parameters

Eq. no.	$(SP)_1$	$(SP)_2$	a	b	r	F
1	E_S	L	0.238	0.080	0.16	0.15
2	E_S	B_1	−1.168	0.997	0.61	3.27
3	E_S	B_2	−0.493	0.429	0.68	4.64
4	E_S	B_3	−0.625	0.451	0.76	7.63
5	E_S	$\underline{B}_4$	0.190	0.113	0.22	0.27
6	E_S	B	−1.035	0.601	0.69	4.95
7	Es	L/B_1	0.831	−0.074	0.12	0.08
8	Es	L/B_4	1.014	−0.297	0.15	0.13
9	Es	B_4/B_1	1.280	−0.438	0.41	1.14
10	Es	B_4/L	0.462	0.202	0.10	0.06
11	E'_S	L	0.324	0.049	0.11	0.07
12	E'_S	B_1	−1.046	0.893	0.61	3.25
13	E'_S	B_2	−0.395	0.367	0.64	3.88
14	E'_S	B_3	−0.547	0.399	0.75	7.14
15	E'_S	$\underline{B}_4$	0.206	0.092	0.20	0.22
16	E'_S	B	−0.878	0.521	0.66	4.34
17	E'_S	L/B_1	0.800	−0.087	0.15	0.13
18	E'_S	L/B_4	0.934	−0.291	0.17	0.16
19	E'_S	B_4/B_1	1.185	−0.418	0.44	1.32
20	E'_S	B_4/L	0.390	0.210	0.12	0.08
21	ν	L	0.666	0.027	0.12	0.08
22	ν	B_1	−0.001	0.443	0.60	3.16
23	ν	B_2	0.336	0.177	0.62	3.43
24	ν	B_3	0.260	0.194	0.73	6.23
25	ν	$\underline{B}_4$	0.636	0.042	0.18	0.18
26	ν	B	0.104	0.251	0.64	3.80
27	ν	L/B_1	0.906	−0.040	0.14	0.11
28	ν	L/B_4	0.952	−0.119	0.14	0.11
29	ν	B_4/B_1	1.104	−0.206	0.43	1.27
30	ν	B_4/L	0.729	0.082	0.09	0.05

TABLE 3

Results of correlations : MR *vs* STERIMOL parameters

Eq. no.	$(SP)_1$	$(SP)_2$	a	b	r	F
31	MR	L	0.780	0.102	0.50	1.81
32	MR	B_1	0.914	0.203	0.30	0.54
33	MR	B_2	0.778	0.192	0.73	6.30
34	MR	B_3	0.787	0.177	0.72	6.03
35	MR	$\underline{B}_4$	0.609	0.173	0.80	10.07
36	MR	B	0.381	0.325	0.90	22.71
37	MR	L/B_1	1.080	0.072	0.28	0.46
38	MR	B_4/B_1	1.200	0.053	0.12	0.08
39	MR	L/B	1.440	−0.088	0.19	0.21
40	MR	L/B_4	1.749	−0.361	0.45	1.42

3. CONCLUSIONS

(i) The correlations obtained in tables 2 and 3 are either insignificant or modest. For E_S, E'_S and ν one can observe some dependence on B_3 (it should be borne in mind that regressions having correlation coefficient $r^2 < 0.4$ are statistically insignificant, they do not indicate a cause–effect relationship, and may be due to chance [12]). Hence, one can consider that the geometric significance of Taft-type steric parameters is ambiguous.

(ii) The Charton equations, *i.e.*, E_S *vs.* $r_{\min}$ and E_S *vs.* $r_{\max}$ (ref. [6]), E_S *vs.* $r_{\text{av.}}$ (ref. [13]), E'_S *vs* $r_{\min}$ and E'_S *vs* $r_{\max}$ (ref. [5]), can be applied only to symmetrical substituents X, like halogen, and CR_3. Qualitatively, one can claim on this basis that Taft-type steric constants are proportional to the "magnitude" of the substituent. The modest correlations obtained with the STERIMOL parameters are an argument for the directional character of steric effects. However this aspect is irrelevant to Taft-type steric parameters because the E_S, E'_S or ν values are calculated independently of the geometry of the transition state.

(iii) Since the Taft-type steric constants cannot be correlated to geometrically significant data, their usefulness in QSAR is limited. Consequently, it is highly desirable to develop new approaches to steric interactions in biological systems.[14]

REFERENCES

[1] R. W. Taft, in "Steric Effects in Organic Chemistry", M. S. Newman ed., Wiley, New York, 1956.

[2] C. K. Ingold, *J. Chem. Soc.*, **1932**, 1032.

[3] C. K. Hancock, B. J. Yager, C. P. Falls and J. O. Schrenck, *J. Amer. Chem. Soc.*, **85**, 1297 (1963).

[4] J. P. Idoux, P. T. R. Huang and C. K. Hancock, *J. Org. Chem.*, **38**, 4239 (1973).

[5] J. A. McPhee, A. Panaye and J.-E. Dubois, *Tetrahedron*, **34**, 3553 (1978).

[6] M. Charton, *J. Amer. Chem. Soc.*, **91**, 615 (1969).

[7] C. Hansch and D. F. Calef, *J. Org. Chem.*, **41**, 124 (1976).

[8] I. Motoc, *Arzneim. Forsch.*, **31**, 290 (1981); I. Motoc, O. Dragomir-Filimonescu and R. Vâlceanu, *Math. Chem.*, **11**, 185 (1981).

[9] I. Motoc and A. T. Balaban, *Rev. Roumaine Chim.*, **26**, 593 (1981).

[10] A. Verloop, W. Hoogenstraaten and J. Tipker, in "Drug Design", ed. E. J. Ariens, vol. 7, Academic Press, New York, 1976.

[11] C. Hansch and A. J. Leo, "Substituent Constants for Correlation Analysis in Chemistry and Biology", Wiley, New York, 1979, p. 11.

[12] J. G. Topliss and R. J. Costello, *J. Med. Chem.*, **15**, 1066 (1972).

[13] E. Kutter and C. Hansch, *J. Med. Chem.*, **12**, 647 (1969).

[14] A. T. Balaban, A. Chiriac, I. Motoc and Z. Simon, "Steric Fit in QSAR", Lecture Notes in Chemistry, vol. 15, Springer, Berlin, 1980.

Revue Roumaine de Chimie, 27, 6, 741–746 (1982)

FIVE- AND SIX-COORDINATED COMPLEXES OF HAFNIUM(IV) WITH TRIAZOLINE THIONE

S. K. SENGUPTA * and SHYAM KUMAR **

* Department of Chemistry, University of Gorakhpur, Gorakhpur 273001, U. P., India
** Department of Chemistry, University of Delhi, Delhi–110007, India

Received September 30, 1980

The reactions of bis(cyclopentadienyl)hafnium(IV) dichloride with triazoline thiones have been studied in anhydrous dichloromethane. The reaction products, five-coordinated complexes of the types $[(C_5H_5)_2Hf(L)Cl]$, $[(C_5H_5)_2Hf(L')]$ and six-coordinated complexes of the type $[(C_5H_5)_2Hf(L)_2]$ (where HL = 3-trifluoromethyl-4-amino-1-2,4-triazoline-5-thione (HFAT), 3-trifluoromethyl-4-benzylidene-1, 2, 4-triazoline-5-thione (HFBT) and 3-trifluoromethyl-4-furylidene-1,2,4-triazoline-5-thione (HFFT) and H_2L' = 3-trifluoromethyl-4-salicylidene-1,2,4-triazoline-5-thione (H_2FST)), have been characterized on the basis of elemental analyses, electrical conductance, magnetic susceptibility and spectral (infrared and electronic) data. The ligands HFAT, HFBT and HFFT act as NS^- bidentate chelating agent whereas the ligand H_2SFT behaves as NS^-O^- tridentate chelating agent.

INTRODUCTION

The chemistry of transition metal complexes with heterocyclic thiones continues to be of unabated interest on account of the striking structural features presented by this class of compounds and also due to their biological importance.[1–4] These ligands, capable of undergoing thione thiol ($HN-C=S \rightleftharpoons N=C-SH$) tautomerism can coordinate to a metal atom through nitrogen or only through sulphur or simultaneously through nitrogen and sulphur. The ligand, triazoline thione, reflects the current interest in the coordination chemistry of thione derivatives of various heterocyclic molecules.[5–7] However, there is hardly any known example of such derivatives of hafnium (IV). We report here the synthesis and characterization of complexes of hafnium (IV) with different substituted triazoline thiones. The structures of the ligands are depicted below :

---

* Address for correspondence : Sumer Sagar, Behind Vijai Cinema, Golghar, Gorakhpur-273001 (U.P.), India.

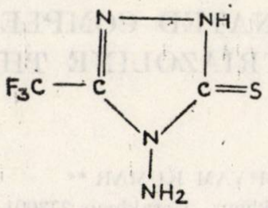

(HFAT)

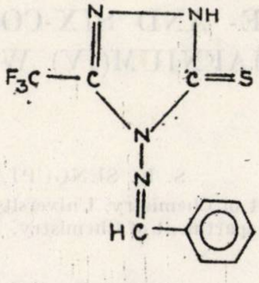

(HFBT)

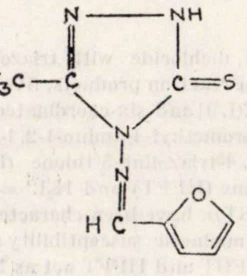

(HFFT)

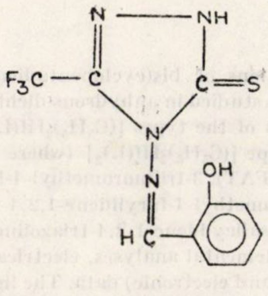

(H_2FST)

EXPERIMENTAL

All glass apparatus with interchangeable quick fit joints were used throughout. All operations were carried out under strictly anhydrous conditions. Dichloromethane was dried by refluxing it for 24 hrs over calcium hydride. Bis(cyclopentadienyl) hafnium (IV) dichloride was prepared as reported in the literature.[8] The ligands were prepared by the reported method.[9]

Preparation of complexes

All the complexes were prepared by a general procedure briefly described below.

The appropriate triazoline thione (1 mole or 2 mole except in H_2FST where only 1 mole was used) was added to a solution of bis(cyclopentadienyl) hafnium (IV) dichloride (1 mole) in anhydrous dichloromethane (60 ml) and the reaction mixture was refluxed. Evolution of hydrogen chloride began about after half an hour. The refluxing was continued until the evolution of hydrogen chloride ceased (8 – 12 hrs). The resulting mixture was then evaporated to dryness under reduced pressure. The complexes were thoroughly washed with ethanol and ether to remove the traces of the ligand and the metal salt.

Analyses : Hafnium was estimated gravimetrically as oxide, chloride as AgCl and sulphur as $BaSO_4$. Nitrogen was estimated by Kjeldahl's method.

Physico-chemical studies : Magnetic measurements were carried out by Gouy's method using copper sulphate as calibrant. Electrical conductance measurements were carried out in nitrobenzene on a Beckmann conductivity Bridge Model Nr. RC–18A. The infrared spectra were recorded on Perkin Elmer–621 instrument in KBr phase in the 4000–200 cm^{-1} ranges. The electronic spectra of the complexes were run on a visible range CΦ 10 spectrophotometers in dimethylformamide.

RESULTS AND DISCUSSION

The analytical data of the complexes are given in table 1. The complexes are soluble in dimethylformamide, dimethylsulfoxide, nitrobenzene and partially soluble in benzene, dichloromethane and tetrahydrofuran. The electrical conductance of the complexes in nitrobenzene indicates the non-electrolytic nature of the complexes.

TABLE 1

Analytical data of the complexes *

Complex	Found (Calcd.) %			
	N	S	Hf	Cl
$[(C_5H_5)_2Hf(FAT)Cl]$	10.4 (10.6)	5.9 (6.0)	33.5 (33.8)	6.5 (6.7)
$[(C_5H_5)_2Hf(FAT)_2]$	16.5 (16.6)	9.2 (9.4)	26.1 (26.4)	—
$[(C_5H_5)_2Hf(FBT)Cl]$	9.0 (9.1)	5.1 (5.2)	28.7 (29.0)	5.6 (5.7)
$[(C_5H_5)_2Hf(FBT)_2]$	13.0 (13.1)	7.2 (7.5)	20.7 (20.9)	—
$[(C_5H_5)_2Hf(FFT)Cl]$	9.3 (9.4)	5.2 (5.3)	30.0 (30.1)	5.8 (5.9)
$[(C_5H_5)_2Hf(FFT)_2]$	13.6 (13.8)	7.6 (7.9)	21.8 (22.1)	—
$[(C_5H_5)_2Hf(FST)]$	9.3 (9.4)	5.3 (5.3)	29.5 (30.0)	—

---

* where HFAT = $C_3H_3N_4F_3S$, HFBT = $C_{10}H_7N_4F_3S$, HFFT = $C_7H_5N_4F_3OS$, H_2FST = $C_{10}H_7N_4F_3OS$.

Magnetic and electronic spectral studies

The room temperature magnetic susceptibility measurements indicate the diamagnetic nature of the complexes. The electronic spectra of all the complexes show a single band in the 24600—24200 cm^{-1} region which can be assigned [10] to the charge transfer band and is in accord with their $(n-1)d^0$, ns^0 electronic configuration.

Infrared Spectral studies

The assignments of infrared spectral bands of the ligands and the complexes are based on an earlier study of similar ligands.[11] The important IR bands and their tentative assignments are given in table 2. Organic compounds having a thioamide group $(H-N-C=S)$ give rise to four thioamide bands in the IR spectra.[12] These are thioamide -I at about 1500 cm^{-1}, band-II at about 1300 — 1400 cm^{-1}, band-III at about 1000 cm^{-1} and band-IV at about 700—850 cm^{-1}. These bands have contributions from $\delta(C-H) + \delta(N-H)$, $\nu(C=S) + \nu(C=N) + \delta(C-H)$, $\nu(C-N) + \nu(C-S)$ and $\nu(C-S)$ modes of vibrations, respectively. In our ligands,

TABLE 2

Important infrared spectral bands (cm^{-1})

Complex	ν(NH)	ν(C=N)	Thioamide bands				ν(Hf−N)	ν(Hf−S)	ν(Hf−O) phenolic
			I	II	III	IV			
$[(C_5H_5)_2Hf(FAT)Cl]$	3160 s	—	1540 m	1260 m	1060 m	740 m	450 m	370 w	—
$[(C_5H_5)_2Hf(FAT)_2]$	3150 s	—	1535 m	1260 m	1055 m	745 m	420 m	360 w	—
$[(C_5H_5)_2Hf(FBT)Cl]$	—	1610 s	1550 m	1265 m	1070 m	745 m	445 m	365 w	—
$[(C_5H_5)_2Hf(FBT)_2]$	—	1600 s	1545 m	1260 m	1060 m	750 m	440 m	360 w	—
$[(C_5H_5)_2Hf(FFT)Cl]$	—	1605 s	1540 m	1270 m	1065 m	740 m	435 m	360 w	—
$[(C_5H_5)_2Hf(FFT)_2]$	—	1600 s	1540 m	1255 m	1060 m	735 m	430 m	365 w	—
$[(C_5H_5)_2Hf(FST)]$	—	1610 s	1550 m	1250 m	1060 m	745 m	440 m	370 w	490 m

s = strong, m = medium, w = weak

these bands appear at *ca* 1560 – 1550, 1250, 1090 – 1080 and 790 – 780 cm^{-1}. These bands are expected to be affected differently by different modes of coordination after complexation with the metal ions.[11,13,14] It has been suggested that the M – N coordination in thioamide system is accompanied by a small positive shift in the thioamide-I band; no such shift occurs in the spectra of our complexes. On the contrary it appears to be the band with the largest C – S contribution, thioamide-IV, which is the most affected. In the complexes, this bands shifts towards lower frequency ($\sim 50 - 40$ cm^{-1}) suggesting the coordination of the sulphur atom to the metal. A weak band at *ca.* 2550 – 2480 cm^{-1} in the spectra of the ligands due to the – SH group vibration, suggests the thione $\rightleftharpoons$ thiol ($HN-C=S \rightleftharpoons N=C-SH$) tautomerism. However, in the spectra of complexes, this band disappears indicating the coordination through suplhur after deprotonation. This is further confirmed by the appearance of the new band in the far IR region at *ca.* 370 – 360 cm^{-1} which can be assigned to the ν(Hf – S) vibration.

The bands observed around 3250 – 3150 (in HFAT), 1630 (in HFBT, HFFT and H_2FST), 1580 – 1565 and 1500 cm^{-1} in the spectra of the ligands may be assigned[11] to ν(N – H), ν(C = N) (N – N = C –), ν(C = N) (ring) and ν(C = C) (phenyl) vibrations, respectively. Strong vibrations in the region 1600 – 1550 cm^{-1} are usually associated with phenyl and C = N groups and it is not usually possible to identify such bands with particular C = C or C = N linkage. However, a stringent assignment of the C = N group can be made by comparing the spectrum of the ligand HFAT containing $N-NH_2$ group with that of the ligands HFBT, HFFT and H_2FST in which it is replaced by the N – N = CH group. Following this method, the strong band observed around 1630 cm^{-1} is assigned to the ν(C = N) vibration. However, the spectra of complexes show the shifting of this band to lower frequency (~ 25 cm^{-1}) indicating the coordination of the azomethine nitrogen to metal atom. The IR band in the region 3250 – 3200 cm^{-1} in the ligand HFAT due to ν(N – H) of the primary amino group is shifted towards the lower wave number (– 50 cm^{-1}) in its complexes which indicate the coordination of the amino nitrogen to the metal atom. The bands observed at *ca.* 450 – 420 cm^{-1} may be assigned to ν(Hf – N).

The ligand H_2FST shows one band at *ca.* 3400 – 3350 cm^{-1} which may be assigned to ν(CH) of phenolic group. However, in its complex, this band disappears indicating the coordination of the phenolic oxygen to the metal atom through deprotonation. The bands at 490 cm^{-1} region in the complex can be assigned to ν(Hf – O).

The absorption bands, indicating[15] the presence of the cyclopentadienyl group in all these complexes, are at *ca.* 3000 cm^{-1} ν(C – H), *ca.* 1440 cm^{-1} ν(C – C), *ca.* 1010 cm^{-1} δ(– CH) and a band at *ca.* 810 cm^{-1} δ(– CH). The persistence of the bands of cyclopentadienyl ring in the complexes indicate that this group remains delocalized and π-bonded to the metal and retains their aromatic character.

Thus, on the basis of elemental analyses, magnetic moments, electrical conductance, infrared and electronic spectra, the following structures are assigned for the complexes where 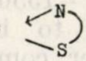 in the first two formulas represents the anion of HFAT, HFBT and HFFT, and 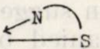 in the last formula represents the anion of H_2FST.

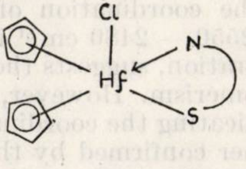

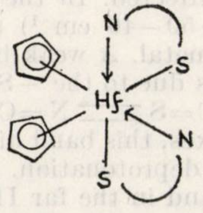

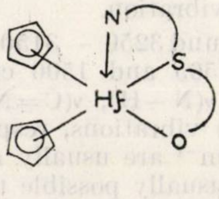

REFERENCES

[1] C. Preti and G. Tosi, *Austral. J. Chem.*, **29**, 543 (1976) ; *Canad. J. Chem.*, **54**, 1558 (1976).
[2] J. Reedijk, *J. Inorg. Nuclear Chem.*, **35**, 239 (1973).
[3] M. R. Gajendragad and U. Agarwala, *Austral. J. Chem.*, **28**, 763 (1975).
[4] J. C. Chudy and J. A. W. Dalziel, *J. Inorg. Nuclear Chem.*, **37**, 245 (1975).
[5] B. K. Gupta, D. S. Gupta and U. Agarwala, *Bull. Chem. Soc. Japan*, **51**, 2724 (1978).
[6] B. K. Sinha, R. Singh, J. P. Srivastava and L. K. Mishra, *J. Inorg. Nuclear Chem.*, **39**, 1797 (1977).
[7] S. K. Sengupta, S. K. Sahni and R. N. Kapoor, *Synth. React. Inorg. Met-Org. Chem.*, **10**, 269 (1980).
[8] P. M. Druce, B. M. Kingston, M. F. Lapport, T. R. Spalding and R. C. Srivastava, *J. Chem. Soc.*, **A**, **1969**, 2106.
[9] T. George, R. Tahilramani and D. A. Dobholkar, *Indian J. Chem.*, **7**, 959 (1969).
[10] P. B. Dorain, H. H. Patterson and P. C. Jordon, *J. Chem. Phys.*, **49**, 3845 (1968).
[11] B. Singh, Lakshmi and U. Agarwala, *Inorg. Chem.*, **8**, 2341 (1969) ;
B. Singh and U. Agarwala, *J. Inorg. Nuclear Chem.*, **31**, 2575 (1969).
[12] C. N. R. Rao, "Chemical Applications of Infrared Spectroscopy", Academic Press, London, 1963, p. 300.
[13] J. S. Dwivedi and U. Agarwala, *Indian J. Chem.*, **10**, 652 (1972).
[14] B. Singh and K. P. Thakur, *J. Inorg. Nuclear Chem.*, **36**, 1735 (1974).
[15] H. P. Fritz, *Adv. Organomet. Chem.*, **1**, 262 (1964).

Revue Roumaine de Chimie, 27, 6, 747–750 (1982)

A NEW METHOD FOR THE SYNTHESIS OF AROMATIC AMIDES DIRECTLY FROM ACIDS

C. I. CHIRIAC
"P. Poni" Institute of Macromolecular Chemistry Aleea Gh. Ghica Vodă 41 A, Iaşi, Romania

Received June 18, 1981

By a direct condensation reaction between triacylphosphates prepared *in situ* and aromatic amines, aromatic amides are formed in high yields, avoiding the synthesis of the acid chlorides or acid anhydrides as intermediary phases.

In a previous paper,[1] we showed that triacylphosphites prepared *in situ* from acids and phosphorus trichloride in the presence of pyridine are good reactives for the synthesis of amides.

Because only two acyl groups from the triacylphosphites can react under the conditions of this reaction, we investigated other reactive compounds, which avoid this disadvantage.

RESULTS AND DISCUSSION

It is known [2] that triacylphosphates (reactive compounds) can be employed for the electrophilic acylation of aromatic compounds.

We have investigated if this reactive compounds can be used in nucleophilic substitutions with amines and especially if all the three acyl groups can participate in the reaction. We have observed that this is possible only at high temperature (135 –145°C) in concentrated solution, using the pyridine as solvent. At lower temperatures (100 –115°C) two acyl groups reacted whereas at room temperature only one.

The triacylphosphates can be considered as mixed anhydrides of phosphoric acid with carboxylic acids, and from this reason, they can manifest high reactivity.

At the beginning, we used pure triacylphosphates,[2] but in order to simplify the procedure, we prepared triacylphosphates *in situ* from the corresponding aromatic acids and phosphorus oxychloride in pyridine as solvent and acceptor for hydrochloric acid. By the subsequent addition of an aromatic amine and heating at reflux, aromatic amides resulted in high yield.

For example, in the isolation of pure tribenzoylphosphate we used benzene as solvent and pyridine as acceptor for hydrochloric acid. The pyridine hydrochloride precipitated and the tribenzoylphosphate remained in solution and was easy isolated. By the reaction between pure tribenzoylphosphate and aniline, benzanilide resulted in high yield and good purity. The reaction between *in situ* prepared tribenzoylphosphate and aniline takes place under the same conditions. From this reason in all our further syntheses, we used triacylphosphates prepared *in situ*.

The pyridine was found to be the most suitable base, which acts also as a solvent. In this reaction, similar to other cases,[3,4] PyH^+Cl^- and H_3PO_4 result as by-products, which did not affect the reaction. The presence of H_3PO_4 was proved by identification with $AgNO_3$.[5]

The mechanism of this synthesis, similar to other reactions,[6,7] is the following :

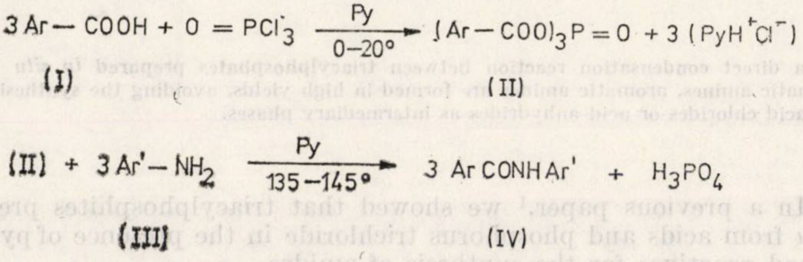

$$\underset{(I)}{3\,Ar-COOH} + O=PCl_3 \xrightarrow[0-20^\circ]{Py} \underset{(II)}{(Ar-COO)_3P=O} + 3\,(PyH^+Cl^-)$$

$$(II) + \underset{(III)}{3\,Ar'-NH_2} \xrightarrow[135-145^\circ]{Py} \underset{(IV)}{3\,ArCONHAr'} + H_3PO_4$$

We supposed, similar as in other cases,[3,6] that this reaction involves a four centre transition state (V):

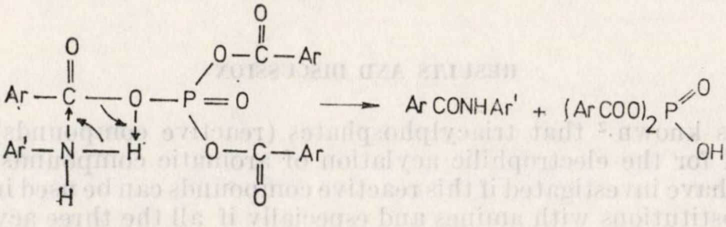

(V)

(A similar transition state, for the second and third stage).

The general method for obtaining aromatic amides (IV) consists thus in dissolving of 3 moles of acid (I) in dried pyridine, followed by the addition of 1 mole phosphorus oxychloride under stirring and cooling to 0°C (the reaction is very exothermal). The solution thus obtained is treated with 3 moles + 10% excess amine (III) *). After heating, the desired product was obtained.

The large majority of the obtained amides had correct melting points and the yields ranged from 61 to 91% (Table 1). The best results have been obtained in the reaction of benzoic acid with *p*-toluidine, when the yield was 91%.

---

*) The yield was improved when we used a small excess of amine (5–10%).

In conclusion, by this new direct synthesis we obtaiend in high yields aromatic amides, which are difficult to obtain by heating of aromatic amines with aromatic acids.

TABLE 1

Aromatic amides obtained from triacylphosphates prepared *in situ*

Acid	Amine	Yield [b)] %	Amides [a)] M.p. °C	Reported m.p. [c)] °C
Benzoic	Aniline	84	161–163	162–163
—,,—	*p*-Toluidine	91	157–158	157–158
—,,—	*p*-Chloroaniline	63	185–187[d)]	185–187
—,,—	2-Naphthylamine	90	156–158	156–158
p-Toluic	Aniline	82	143–145	144–145
—,,—	*p*-Toluidine	89	158–160	159–160
—,,—	2-Naphthylamine	81	172–174[d)]	172–174
Anisic	*p*-Toluidine	85	152–154	153–154
—,,—	Aniline	74	168–169[d)]	168–169
p-Chlorobenzoic	*p*-Toluidine	61	214–216[d)]	215–216
—,,—	Aniline	58	193–195[d)]	193–194

[a)] The products were identified by comparison of m.p. and IR spectra with those of authentic samples.

[b)] Yields calculated on acid employed before recrystallisation and for some amides (entries 3, 7, 9, 10 and 11) after recrystallization.

[c)] From „Belstein Handbuch Organischen Chemie"

[d)] Melting points after recrystallization.

EXPERIMENTAL

Benzanilide

To a stirred solution of benzoic acid (7.32 g, 0.06 moles) in dried pyridine (25 ml) cooled to 0°C, phosphorus oxychloride (1.8 ml, 0.02 moles) in 20 ml dried benzene was added very slowly, when PyH^+Cl^- (m.p. 80–82°C) precipitates. The mixture was stirred 1–2 hours at room temperature. Then, aniline (6.14 g, 0.06 mole + excess 10%) was added under stirring and was heated concomitantly with distillation of solvent till the temperature of the mixture rised to 135°C. The heating was continued at reflux (135–145°) for 4–5 hours. The obtained solution was poured into a large volume of water with ice (150–200 ml), under stirring. The precipitated product was collected by filtration, washed well with 7% NaOH (30–50 ml), 7% HCl (30–50 ml), then three times with 50–70 ml water. After drying at 80–100°C, then in vacuum, 9.93 g benzanilide with m.p. 161–163°C was obtained (m.p. of the mixture with pure benzanilide underpressed). Yield 84 % (calculated on benzoic acid employed). Anal. Found : C,78.25 ; H, 5.51 ; N, 6.93. Calcd. for : $C_{13}H_{11}ON$; C, 78.13 ; H, 5.62 ; N, 7.10 %.

Under similar conditions, the other amides presented in table 1, were obtained.

REFERENCES

[1] C. I. Chiriac, *Rev. Roumaine Chim.*, **24**, 609 (1979).
[2] C. J. Schoot and K. H. Klaassens, *Rec. Trav. chim.*, **80**, 1084 (1961).
[3] B. Iselin and W. Rittel, *Helv. Chim. Acta*, **40**, 373 (1957).
[4] N. Yamazaki, *Tetrahedron Letters*, **49**, 5047 (1972).
[5] M. Halmann, "Analytical Chemistry of Phosphorus Compounds", Wiley-Interscience, London, 1972, p. 29.
[6] H. O. Becker and K. F. Funk, *J. prakt. Chem.*, **14**, 55 (1961).
[7] R. N. Ring and D. Davidson, *J. Org. Chem.*, **27**, 2428 (1962).

Revue Roumaine de Chimie, 27, 6,751–759 (1982)

VANADIUM(V) CHELATES OF N-SUBSTITUTED PHENYLHYDROXYLAMINES. A SPECTROPHOTOMETRIC STUDY

J. P. SHUKLA
Radiochemistry Division, Bhabha Atomic Research Centre, Trombay, Bombay 400 085, India

Received January 29, 1981

The formation of violet chelates between vanadium (V) and several N-substituted phenylhydroxylamines was investigated spectrophotometrically. All the reagents reacted with V(V) and yielded chloroform extractable complexes of varying colours. Job's method of continuous variations as well as molar ratio method, as applied to two phase systems, were employed to establish the stoichiometry of metal hydroxamates extracted with chloroform from different hydrochloric acid concentrations. The metal to ligand ratio was found close to 1 : 2 in all the instances and the apparent stability constants were of the order of 10^8 to 10^9. The colours of the complexes varied from reddish-violet to bluish-violet, the wavelength of the maximum absorption from 505 to 570 nm and the molar absorptivity from 4008 to 7560 $l \cdot mole^{-1} \cdot cm^{-1}$. The ligational free energy of formation, $\Delta G°$ lies between − 11.1 and − 13.3 kcal/mole at 25°C. Attempts were also made to confirm the composition of these complexes both by isolating and analysing the hydroxamates in solid state.

INTRODUCTION

The potential analytical applications of N-substituted phenylhydroxylamines (HA) (I), especially of N-benzoylphenylhydroxylamine (BPHA) (II), and its analogues (R = alkyl or aryl) have been reviewed

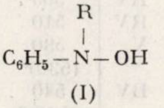

$$\begin{array}{c} R \\ | \\ C_6H_5-N-OH \end{array}$$

(I)

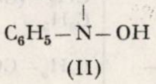

$$\begin{array}{l} C_6H_5-C{=}O \\ \qquad\quad | \\ C_6H_5-N-OH \end{array}$$

(II)

recently.[1,2] The remarkable versatility of phenylhydroxylamines as excellent reagents for the detection and quantification of even trace amounts of vanadium (V) has now been unequivocally established.[3-6] This has led to systematic searches for improved reagents in the family of these compounds as their selectivity and sensitivity can be suitably altered by changing the substituent groups attached to the functional group. The C-substitution of II has been found to have a strong bearing on its effectiveness as an analytical reagent. Compared to voluminous work primarily on their varied uses, little attention seems to have been paid to the study of their metal complexes, *e.g.* composition, stability, structure etc.

except for a few instances.[7-9] Needless to emphasize that an exact knowledge of these parameters, apart from being of basic interest, is imperative for the proper evaluation of analytical technique involving an organic ligand. Furthermore, a systematic study of their colour reactions can often lead to a better understanding of the cause of sensitivity and selectivity of the relevant analytical reaction.

The present communication deals with the spectrophotometric study of the formation of deep coloured chelates between vanadate ions and thirteen N-substituted phenylhydroxylamines and throws light on their empirical composition, structure, stability etc. 'Apparent' stability constants of the vanadate complexes have been computed from their respective absorption data. Investigations have also been carried out to substantiate their composition by isolating and subsequently analysing them in solid state. This work forms a part of our extensive studies on stoichiometry and stability of various metal hydroxamates.

EXPERIMENTAL

Apparatus: A Unicam SP 500 quartz spectrophotometer, with two matched 10 mm Corex cells, was used for all absorptiometric measurements.

Reagents and solutions: N-substituted phenylhydroxylamines (Table 1) were either available as gifts from the co-workers or were synthesized by the method of Priyadarshini et al.[10]

TABLE 1

Spectral characteristics of coloured vanadium (V) complexes of N-substituted phenylhydroxylamines in chloroform

Aqueous phase : ~ 4 M HCl

Compound number	Phenylhydroxylamines (HA)	*R*	Colour of $CHCl_3$ extract	Molar absorptivity		
				λ_{max} (nm)	(in terms of V)	(in terms of HA)
1	*N*-Acetoyl –	CH_3-	RV	505	4008	2033
2	*N*-Butyroyl –	$CH_3-(CH_2)_2-$	RV	510	4445	2116
3	*N*-Valeroyl –	$CH_3-(CH_2)_3-$	RV	505	4052	2097
4	*N*-Caproyl –	$CH_3-(CH_2)_4-$	RV	510	4611	2115
5	*N*-Capryl –	$CH_3-(CH_2)_6-$	RV	505	4017	2130
6	*N*-Capriyl –	$CH_3-(CH_2)_8-$	RV	505	4041	2125
7	*N*-Myristoyl –	$CH_3-(CH_2)_{12}-$	RV	510	4334	2210
8	*N*-Benzoyl –	C_6H_5-	V	530 (530)^{a}	4700 (4650)^{a}	2350
9	*N*-Cinnamoyl –	$C_6H_5-CO=CH$	BV	540 (540)^{a}	6379 (6300)^{a}	3179
10	*N*-*p*-Methoxy-cinnamoyl-	$N-CO-C_6H_4-CH=CH-$	BV	570 (570)^{b}	7560 (7500)^{b}	–
11	*N*-2-Furoyl –	C_4H_3O-	V	530 (530)^{c}	5167 (4650)^{c}	2286
12	*N*-2-Naphthoyl –	$C_{10}H_7-$	BV	545 (545)^{d}	7115 (7100)^{d}	–
13	*N*-2-Thenoyl –	C_4H_3S-	V	530 (530)^{c}	5465 (5450)^{c}	2697

a : ref. [3] *b* : ref. [4] *c* : ref. [2] *d* : ref. [5]

( ), Reported values V, Violet, BV, Bluish-violet RV, Reddish-violet

* Mean of at least 3 determinations at the corresponding λ_{max} and the values are believed to be within ± 50 l./mole.cm.

Standard vanadium solution was prepared from A. R. ammonium metavanadate and standardised titrimetrically with potassium permanganate. Solutions (0.1 % W/V) of I in alcohol-free chloroform were used for all extraction work. Commercial chloroform was washed free of alcohol with distilled water and distilled after drying over fused calcium chloride.

Procedure: Transfer an aliquot of vanadium solution to a separatory funnel and add dilute $KMnO_4$ solution dropwise until a faint pink colour persists to ensure complete oxidation of vanadium to + 5 state. Adjust the acidity to about 4M in a final volume of 25 ml with conc. HCl and distilled water and extract with 8—10 ml of reagent solution. Shake vigorously for 2—3 min and allow the phases to separate. Dry the chloroform extract over anhydrous sodium sulphate and transfer it to a 25 ml standard flask. Repeat the extraction twice to ensure complete recovery of vanadium. Dilute the extracts to 25 ml with chloroform and measure the absorbance against the corresponding reagent blank prepared in the same way. Compute the amount of vanadium extracted into the organic phase from a calibration curve.

Colour Reaction

Chloroform solution of compds. (**1**—**13**) reacted with vanadate ions yielding extracts the colour of which depended on HCl concentration of the aqueous phase. Between pH 1 and 6.5 mahogany red extracts were usually obtained ; when the aqueous acidity was more than 2MHCl, the extracts were reddish violet, violet or bluish violet. However, if the aqueous phase contained 0.1 to 2M HCl then the colour of the extracts was amethyst. All the hydroxylamines examined here reacted almost similarly.

The position of the absorption band of the chloroform extracts remained unaltered when the aqueous solutions were 2 — 10 M in HCl, but the maximum colour intensity was obtained when the acid concentration lay between 2.5 and 8 M. Fig. 1 gives some typical spectra recorded from different molarities. It may be noted that the hydrochloric acid concentrations here should not be higher than about 5M since the reduction of VO_2^+ to VO^{2+} by chloride ion occurs to an increasing extent with increase in the acid concentration[8] and only V(V) gives stable violet coloured complexes of a definite stoichiometry. An increase in acidity beyond 8M HCl, however, destroyed this complex. Only HCl was found suitable for adjusting the acidity but other acids such as H_2SO_4, HNO_3 and $HClO_4$, could be tolerated when their concentration in the aqueous phase was less than 1M. In practice, the measurements were performed with solutions which were about 4M in HCl. Colour formation was observed to be instantaneous and it was found that even up to 72 hrs, there was no change in absorbance readings at room temperature. Temperature change had little effect on the colour formation when the ligand was present in excess.

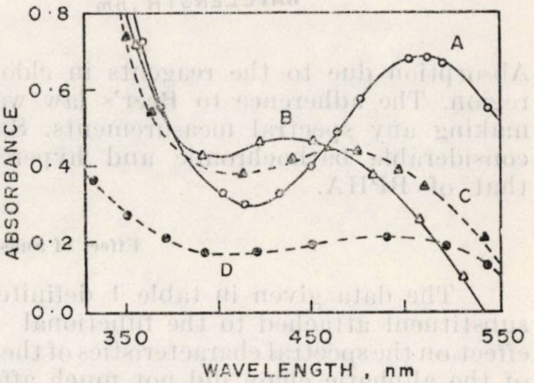

Fig. 1. — Effect of hydrochloric acid concentration on absorption spectra of vanadium(V) — BPHA complex ; A — 3.6 M HCl ; B — 1.8 M HCl ; C — 1.0 M HCl ; D — 0.01 M HCl. Organic phase : $CHCl_3$.

RESULTS AND DISCUSSION

Spectral Properties

The spectral characteristics of the vanadium (V) complexes of the various N-substituted phenylhydroxylamines studied are recorded in table 1. Their visible absorption bands are generally broad and symmetrical at the sides and the maxima, λ_{max}, occur between 505 and 570 nm (Fig. 2).

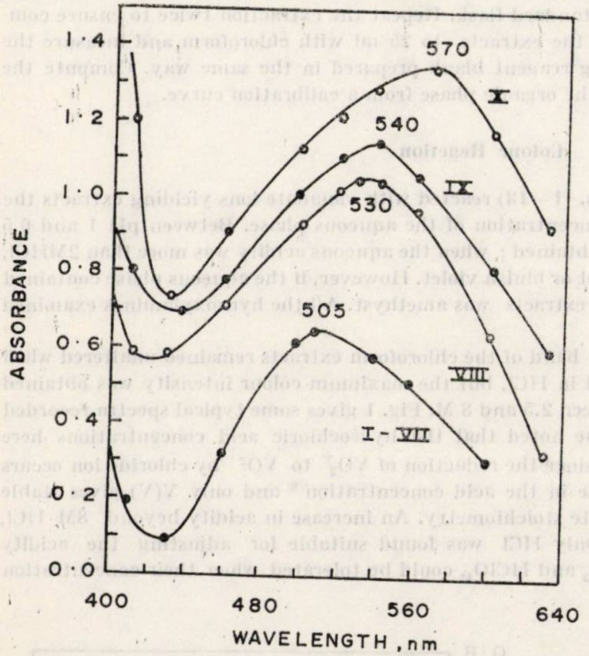

Fig. 2. — Absorption spectra of vanadium (V) complexes of some *N*-substituted phenylhydroxylamines in chloroform. Aqueous phase : 4 M HCl.

Absorption due to the reagents in chloroform was insignificant in this region. The adherence to Beer's law was tested for each system before making any spectral measurements. Spectra of these reagents showed considerable bathochromic and hyperchromic effects with respect to that of BPHA.

Effect of Substituent

The data given in table 1 definitely indicate that the type of the substituent attached to the functional carbonyl group had a marked effect on the spectral characteristics of the violet extracts. Firstly, the length of the aliphatic chain did not much affect the position and intensity of the absorption band (compds **1**–**7**). Secondly, when the alkyl group was replaced by an aryl group here, the absorption band shifted towards longer wavelengths and the molar absorption also increased. The intensity, as exemplified by molar absorptivity, is naturally dependent on the kind of the attached grouping and increases with an increase in the extent of π system. As was expected, compd. **8** possessed a higher value as compared to compds (**1**–**7**). This intensity was further enhanced by the introduction of side chain bonds in conjugation with the $-C=O$ group, as is seen in the case of compd. **9.** It appears therefore that this class of compounds should be more sensitive and/or selective in their colour reactions with metal ions. However, there is a limit to increase the effects of $\pi \longrightarrow \pi$ and $n \longrightarrow \pi$ systems present in conjugation with $-C=O$ group in the ligand molecules. Contrary to expectations, the reagents with triple bond have been observed to possess nearly the same or even less sensitivity to the vanadium (V) reaction on comparing with compounds containing double bonds in the side chain.[11] Lastly, the compounds having a heterocyclic group in the R position (**11**, **13**) show no better improvement over the one possessing a phenyl [8] or other aryl grouping (**9**, **12**) etc.

Choice of Extracting Agent

Several organic solvents such as chloroform, carbon tetrachloride, benzene, o-dichlorobenzene, diethyl ether and ethylacetate extracted the vanadium (V) – hydroxamates from the aqueous phase. Of these, chloroform was found to be the most suitable because of its high distribution ratio in addition to being convenient to handle and the extracts showed maximum sensitivity in it. Also, the reagent solution had no absorption at the wavelength region of interest and hence absorbance readings can be directly plotted without making any allowance for the selfabsorption of the reagent solution. Oxygenated solvents were not suitable as the colour intensity and stability of these systems were low. Small amounts of ethanol added to chloroform as a preservative cause a hypsochromic shift of λ_{max}. This shift has been attributed to the formation of different complexes of the types VOA_2Cl and $V_2O_3A_4$ (AH is the hydroxylamine derivative) as established by the isolation of these complexes in the solid state.[12] Other alcohols such as methanol, propanols, butanols, amyl alcohol, n-hexanol etc. when added to the chloroform extracts also exhibited similar behaviour.

Stoichiometry of the Complex in Solution

Job's method of continuous variations as modified by Vosburgh and Copper [13, 14] was used to elucidate the molar composition of vanadate complexes in solution. For this purpose, solutions were mixed in different proportions keeping the total molarity constant and their absorbances measured at 450, 490, 530 and 610 nm after adjusting the acidity to ~ 4M HCl. The curves obtained by plotting absorbance *vs.* mole fraction of vanadium show sharp peaks at a molar ratio of 1 : 2 : : metal : ligand. Similar conclusions have been drawn by Ryan [7] and Priyadarshini [8] in their studies with BPHA and Majumdar and Das [15] with N-o-tolybenzohydroxamic acid. Further, Job's curves obtained at different acidities *i.e.* from 2 to 8 M HCl and at different wavelengths conclusively indicate that only one complex species is present in these acidic solutions. Likewise, studies performed with different equimolar solutions of the reagents and vanadate ions add further support to this finding.

In the determination of the empirical formula of the vanadium (V) complexes employing the molar ratio method of Yoe and Jones [16], a series of solutions was prepared from 3.6×10^{-4}M and 1.8×10^{-4} M of the metal ion and equimolar solutions of the reagent in such a way that the molar ratio of the metal ion to the reagent varied from 1 : 0.5 to 1 : 30. The results when plotted showed no sharp breaks at 2 mol of ligand per mol of vanadium but results obtained on extrapolation point towards a 2 : 1 ligand — vanadium (V) complex. Representative data for only compds **2**, **8** are given in the form of a graph (Fig. 3).

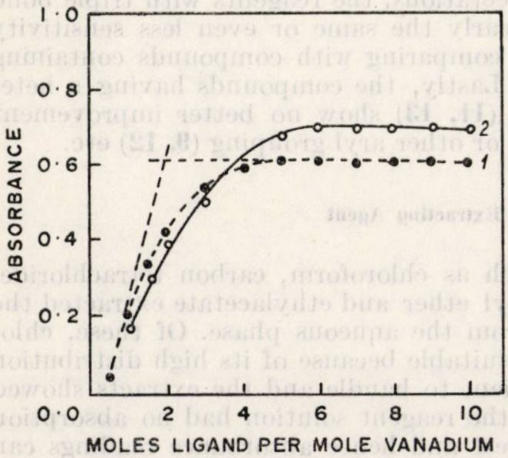

Fig. 3. — Molar ratio plots of extractions of vanadium (V) — N-substituted phenylhydroxylamine systems from 4M HCl. 1, Compd. **2** ; 2, Compd. **8**.

These spectral studies thus point towards the existence of a complex with vanadium and hydroxylamines in a molar ratio of 1 : 2. Since V(V) exists as unipositive ion VO_2^+ in acidic solutions, it is likely that a metal 1 : 1 complex (III) is formed

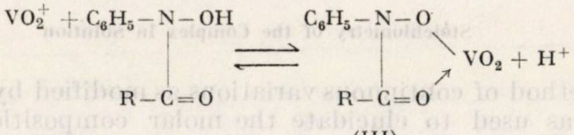

$$VO_2^+ + C_6H_5-N(OH)-C(=O)-R \rightleftharpoons [C_6H_5-N(O)-C(=O)-R]VO_2 + H^+$$

(III)

by the coordination of one molecule of the ligand with vanadate ions. The aqueous or chloride ions are omitted for brevity.

The 1 : 1 complex then adds another molecule of the ligand to give the species (IV) which gets extracted.

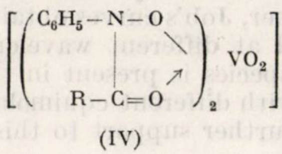

$$H\left[\left(C_6H_5-N(O)-C(=O)-R\right)_2 VO_2\right]$$

(IV)

These inner complexes, non-ionic in nature, thus can be extracted from aqueous solutions with water — immiscible organic solvents, forming the basis of separation by solvent extraction.

Evaluation of Stability Constant

With a view to determining the stability constants of the complexes, calculations were made from the absorbancy data by the method of Banerji and Dey[17] as well as by the molar ratio method.

The apparent stability constant, K, for the system in which the ratio of reactants is 1 : 2, is given by

$$K = x/(a - x)(b - 2x)^2 \tag{1}$$

where x denotes the concentration of the complex at equilibrium and a and b are the initial concentrations of metal ion and the ligand, respectively. Taking two concentrations with the same absorbance, *i.e.*, the same value of x, we have :

$$K = \frac{x}{(a - x)(b - 2x)^2} = \frac{x}{(a' - x)(b' - 2x)^2} \tag{2}$$

Thus from the knowledge of the initial concentrations of a and b, the value of x can be calculated from eqn. 2. By substituting the value of x in eqn. 1, K could be easily evaluated.

Values of K were calculated from the molar ratio plots also through the calculation of degree of dissociation. These were obtained following Harvey and Manning's [18] equation :

$$K = (1 - \alpha)/4\alpha^3 C^2$$

Here α and C stand for the degree of dissociation and the total concentration of the complex in moles/l assuming no dissociation, respectively. α is computed by the equation, $\alpha = (E_m - E_s)/E_m$ where E_m is the absorbance of the complex when excess of the reagent is present and E_s represents the absorbance of the complex at equivalent point.

The results obtained by both methods are summarised in table 2. The free energy of formation, ΔG°, for each chelate calculated according to Van't Hoff isotherm $\Delta G^\circ = -RT \ln k$ is also compiled in table 2.

Composition of Vanadium (V) Complex

Attemps were made to establish the composition of solid vanadium (V) hydroxamates. These could be isolated from the aqueous acidic media following two ways : (a) precipitation of the complex by adding a saturated aqueous solution of I to a V(V) solution containing HCl ; (b) extraction with $CHCl_3$ followed by evaporation of the solvent at room temperature and low pressure. Vanadium content of the complex was determined by igniting a weighed amount of the complex in a silica crucible and weighing the vanadium pentaoxide.

TABLE 2

Stability constants of vanadium(V) — N-substituted phenylhydroxylamine complexes

Organic phase : $CHCl_3$
Aqueous phase : 4 M HCl
Temp : 25 ± 1°C

Compound number	Ionization constant (pK_a)*	Stability Constant, K ($\times 10^8$)		$\Delta G°$ (Kcal/mole)	
		Job's method	Mole ratio method	Job's method	MR method
1	11.03^a	13.2	17.4	−12.5	−12.6
2	11.45^a	44.8	51.2	−13.2	−13.3
3	11.42^a	3.3	4.6	−11.6	−11.8
4	11.40^a	7.8	3.5	−12.1	−11.7
5	11.36^a	4.2	3.7	−11.8	−11.6
6	11.41^a	12.9	11.4	−11.1	−12.4
7	11.35^a	3.6	5.9	−11.7	−12.0
8	11.04^a	7.1	4.3	−12.1	−11.8
9	10.87^b	6.5	8.2	−12.0	−12.2
11	9.72^a	9.9	7.4	−12.3	−12.1
13	9.46^a	17.5	13.8	−12.6	−12.5

a, J. P. Shukla and S. G. Tandon, *J. Inorg, Nuclear Chem.*, **33**, 1681 (1971) ; *Indian J. Chem* ; **9**, 279 (1971).
b, D.C. Bhura and S. G. Tandon, *Indian J. Chem.*, **8**, 466 (1970).
* pK_a determined in 50% (V/V) aqueous dioxane at 25°.

Solid violet complexes obtained from strongly acidic media by both techniques were unstable and turned green after a few months. Elemental analyses of even freshly prepared complexes did not settle their empirical formula unambiguously. Similar difficulties have been encountered by other workers.[19−23] The red complexes, formed in weakly acidic solutions, were unstable too. Montenqui [24] isolated the solid complex of BPHA and vanadium (V) and assigned the formula $(C_{13}H_{10}O_2N)_2VO_2H.\ HCl$ to it. Majumdar et al.[25] obtained two solid complexes of vanadium (V) and BPHA, and assigned to them the formulae $(C_{13}H_{10}O_2N)_2 \cdot VOCl$ and $(C_{13}H_{10}O_2N)_4 \cdot V_2O_3$. It is thus quite evident that there is no agreement in the findings of different workers.

CONCLUSIONS

The present study has revealed the formation of 1 : 2 (metal : ligand) complex at the acidity range of 2−5 N HCl. Higher acidity than 8M HCl adversely affects this complex formation. The existence of complexes having such composition has been confirmed from the data obtained from measurements of absorbances of intense violet coloured complexes at different wavelengths, by Job's and molar ratio methods. These coloured, readily chloroform − extractable inner complexes, are formed instantaneously and the stability of the systems is adequate for any analytical application.

REFERENCES

[1] A. K. Majumdar, "N-Benzoyl Phenylhydroxylamine and its Analogues", Int. Series of Monographs in Anal. Chem ; Vol 50, Pergamon, Oxford, 1972.

[2] D. C. Bhura, "N-Phenylbenzohydroxamic Acid and Analogues as Analytical Reagents", Part I, II, Vol. V Technical News Service, Sarabhai M Chemicals, 1973.

[3] S. G. Tandon and S. C. Bhattachryya, *J. Indian Chem. Soc.*, **47**, 583 (1970).

[4] D. C. Bhura and S. G. Tandon, *Analyt. Chim. Acta*, **53**, 379 (1971).

[5] Y. K. Agrawal, *Analyt. Chem.* **47**, 940 (1975).

[6] S. A. Abbasi, *Analyt. Chem.* **48** 714 (1976).

[7] D. E. Ryan. *Analyst.* **85**, 569 (1960).

[8] U. Priyadarshini, Ph. D. Thesis, Jabalpur University, 1965.

[9] J. P. Shukla, Ph. D. Thesis, Jabalpur University, 1968.

[10] U. Priyadarshini and S. G. Tandon. *J. Chem. Eng. Data* **12**, 143 (1967).

[11] B. S. Chandravanshi and V. K. Gupta, *Croatica Chemica Acta.*, **51**, 107 (1978).

[12] A. K. Majumdar, B. C. Bhattacharyya and G. Das, *J. Indian. Chem. Soc.*, **45**, 964 (1968).

[13] W. C. Vosburgh and G. R. Copper, *J. Amer. Chem. Soc.* **63**, 437 (1941).

[14] H. Irving and T. B. Pierce, *J. Chem. Soc.*, **1959**, 2565.

[15] A. K. Majumdar and G. Das, *Analyt. Chem Acta,* **31**, 147 (1964).

[16] J. H. Yoe and A. L. Jones, *Ind. Eng. Chem. Anal. Edn.* **16**, 111 (1944).

[17] S. K. Banerji and A. K. Dey, *Z. analyt. Chem.*, **30**, 179 (1961).

[18] A. E. Harvey and D. L. Manning, *J. Amer. Chem. Soc.*, **72**, 4488 (1950).

[19] J. E. Land and W. M. McMahan, Jr., *J. Less Common Metals*, **7**, 458 (1964).

[20] A. R. Fields, B. B. Daye and R. Christian, Jr, *Talanta*, **13**, 929 (1966)'.

[21] R. L. Dutta and B. Chatterjee, *J. Indian. Chem. Soc.*, **46**, 268 (1969).

[22] N. N. Ghosh and G. Siddhanta, *J. Indian Chem. Soc*, **45**, 1049 (1968) ; **46**, 488 (1969).

[23] A. K. Majumdar and B. C. Bhattacharyya, *J. Indian. Chem. Soc.*, **45**, 964 (1968).

[24] R. Montenqui, *Anales real Soc. españ. Fis. Quím.*, **60**, 325 (1964) ; C. A. **62**, 4894 C (1965).

[25] A. K. Majumdar, B. C. Bhattachryya and G. Das, *J. Indian Chem. Soc.*, **45**, 465 (1968).

Revue Roumaine de Chimie, 27, 6, 761–767 (1982)

FRIEDEL-CRAFTS DEALKYLATIONS OF SECONDARY HEPTYLBENZENES

ROYSTON M. ROBERTS* and LOUIS W. ELROD
Department of Chemistry, The University of Texas at Austin
Austin, Texas 78712

Received February 16, 1981

The secondary heptylbenzenes, 2-, 3-, and 4-phenylheptane, were dealkylated with aluminium bromide/hydrogen bromide or fluoroantimonic acid to yield a mixture of isomeric heptanes and benzene. With Al_2Br_6/HBr catalyst at 35° the aliphatic product mixture was composed mostly of 2- and 3-methylhexane, with smaller amounts of 2,3- and 2,4-dimethylpentane, heptane, ethylpentane, and trimethylbutane. Addition of 1,4-dimethylcyclohexane as a hydride donor increased the amount of heptane relative to the branched isomers. No heptane was found when benzene or 1, 2, 4-trichlorobenzene were present as solvents. Results from reactions induced by HF/SbF_5 were similar, but 2,2- and 3,3-dimethylpentane were also identified among the products. Although 2-, 3-, or 4-phenylheptane was isomerized to a mixture containing all three linear phenylheptanes, no branched-chain phenylheptanes were found. Mechanisms for the dealkylations, including rearrangement of the alkyl group, are described.

In a previous paper we reported a study of the dealkylation of secondary butyl-, pentyl-, and hexylbenzenes by Friedel-Crafts catalysts.[1a] We now report results from a similar study of the reactions of the secondary heptylbenzenes, 2-, 3-, and 4-phenylheptane.

RESULTS AND DISCUSSION

As in the case of the pentyl- and hexylbenzenes, the major dealkylation products from the heptylbenzenes were branched heptanes. Seven of the nine isomeric heptanes were produced by treatment with Al_2Br_6/HBr (Table 1) and all nine were identified as products of the reaction with HF/SbF_5 (Table 2).

Al_2Br_6/HBr catalyzed reactions. The major isomers in all cases were 2- and 3-methylhexane, which appeared to be produced in approximately equal amounts.[2] The next most abundant branched heptanes were 2, 3- and 2,4-dimethylpentane, with the former isomer predominating. The amount of unbranched heptane found depended on the availability of a hydride donor in the reaction mixture, as in the case of the *sec*-butyl, pentyl-, and hexylbenzenes as reported previously.[1a] When the reaction was carried out with 2-phenylheptane and Al_2Br_6/HBr in the absence of inert solvent and added hydride donor (runs 1, 2, 9, 10), the proportion of unbranched heptane produced was 3—6%. When 1,4-dimethylcyclohexane (an effective hydride donor) was added (runs 4, 5, 11), the proportion of heptane was increased to 17—24%. The ratio of singly-branched to doubly-branched heptanes was not changed appreciably. 1, 3, 5-Cycloheptatriene was tested as a hydride donor (run 6), but although it appeared to prevent the formation of any doubly- and triply-branched heptane isomers, little dealkylation was effected and the reaction was complicated by the formation of tar from polymerization of the cycloheptatriene.

TABLE 1

Dealkylation of *sec*-heptylbenzenes by aluminium bromide/hydrogen bromide[a]

Run #	Solvent or H-donor[b]	Dealklyn, mole %[c]	Distribution of heptane isomers, %[d]							
			H	3MH	2MH and 23DMP			24DMP	EP	TMB
1		23	5	30	(30)	52[e]	(22)	11	1	1
2		69	6	32	(32)	53	(21)	8	1	
3	TCB(29)	62		37	(37)	51	(14)	10	2	
4	DMCH(1.2)	64	20	25	(25)	43	(18)	10	2	
5	DMCH(10)	84	24	25	(25)	40	(15)	9	1	1
6	CHT(1.1)	6	12	44	(44)	44				
7		56	7	28	(28)	53	(25)	11	1	
8		60	6	25	(25)	53	(28)	14	2	
9[f]		9	3	42	(42)	53	(11)	2		
10[g]		59	6	31	(31)	46	(15)	15	1	1
11[g]	DMCH(0.95)	77	17	25	(25)	44	(19)	11	2	1

[a] The PhC_7H_{15} was 2-phenylheptane in runs 1—6 and 9—11, 3-phenylheptane in run 7, and 4-phenylheptane in run 8. The mole ratio of $PhC_7H_{15} : Al_2Br_6$ was 1 : 0.3 ; HBr was added to saturate the solution in runs 1—8 except in run 1, in which the ratio of $PhC_7H_{15} : Al_2Br_6 :$ HBr was 1.0 : 0.3 : 0.2. Reaction conditions : 35°C for 3 h except in runs 9, 10 and 11.

[b] Abbreviations used are : TCB = 1,2,4-trichlorobenzene ; DMCH = 1,4-dimethylcyclohexane ; CHT = 1,3,5-cycloheptatriene ; the numbers in parentheses are the mole ratios, normalized to 1.0 mole of PhC_7H_{15}.

[c] Yield of all heptane isomers by GC, based on PhC_7H_{15}.

[d] Relative distribution of the heptane isomers by GC. Abbreviations used are : H = heptane, 3MH = 3-methylhexane, 2MH = 2-methylhexane, 23DMP = 2,3-dimethylpentane, 24DMP = 2,4-dimethylpentane, EP = 3-ethylpentane, TMB = 2,2,3-trimethylbutane.

[e] The sum of the amounts of these two isomers, which were not separated by GC. The values in parentheses are the amounts estimated on the basis of the assumption that 2MH% = 3MH%.

[f] Reaction temperature 2°C for 3 h.

[g] Reaction temperature 80°C for 1 h.

TABLE 2

Dealkylation of 2-phenylheptane by fluoroantimonic acid [a]

Run #	Solvent or H-donor[b]	Dealkyl., mole %[c]	Distribution of heptane isomers, %[d]							
			H	3MH	2MH and 23DMP	24DMP	22DMP	33DMP	EP	TBM
12		16	4	29	(29) 53[e] (24)	10			2	3
13		28	2	29	(29) 50 (21)	14			1	4
14	DMCH(1.1)	30	5	30	(30) 49 (19)	11	1	1	1	2
15	DMCH(10)	30	6	35	(35) 49 (14)	8	trace	trace	1	1
16	TCB(28)	30	1	27	(27) 58 (31)	12			2	

[a] The mole ratio of PhC_7H_{15} : HF/SbF_5 was 1 : 0.6 ; the reaction conditions were 2°C in run 12 and 25°C in all other runs, with a reaction time of 0.5 h in all runs.

[b] Abbreviations used are : DMCH = 1,4-dimethyicyclohexane ; TCB = 1,2,4-trichlorobenzene. The numbers in parentheses are the mole ratios, normalized to 1.0 mole of PhC_7H_{15}.

[c] Yield of all heptane isomers byGC, based on PhC_7H_{15}.

[d] Relative distribution of the heptane isomers by GC. Abbreviations are the same as in Table I with the additions of 22DMP = 2,2-dimethylpentane and 33DMP = 3,3-dimethylpentane.

[e] See this footnote in table 1.

Dealkylation of 3-phenylheptane (run 7) and 4-phenylheptane (run 8) gave results which were little different from those from 2-phenylheptane. This was not surprising since the rate of isomerization of each of the three phenylheptanes to an equilibrium mixture containing all three is probably of the same order of magnitude as the dealkylation reaction.

In the previous paper we rationalized the surprising difference in the proportion of branched alkanes to unbranched alkanes produced by dealkylation of *sec*-butylbenzene and *sec*-pentylbenzenes in terms of a mechanism in which protonated cyclopropane derivatives function as reactive intermediates.[1a, 3] We believe that the same type of mechanism is operative in the dealkylation of the secondary heptylbenzenes, and that Scheme I may be helpful in rationalizing the distribution of the isomeric heptanes produced.

The alkyl side chain is removed from the ring as a secondary heptyl cation **(1)**, which may be converted to unbranched heptane (H) by reaction with a hydride donor. In the absence of an added donor, the heptylbenzene itself can serve this function, as we have reported in a much earlier paper,[4] so that some unbranched heptane is produced (Runs 1, 2, 7 –10). In the presence of a solvent such as benzene [1a] or 1, 2, 4-trichlorobenzene, the ipso hydride donor will be diluted, and rearrangement of the unbranched secondary heptyl cation may compete more effectively with its capture by the hydride donor, so that little or no unbranched heptane is observed (run 3). If a high concentration of a good hydride donor is provided by the addition of a compound such as 1,4-dimethylcyclohexane, which has two tertiary hydrogens, the unbranched secondary heptyl cation is more likely to be trapped before rearrangement, leading to more unbranched heptane (runs 5, 6, 11).

The rearrangement of the unbranched secondary heptyl cation to branched cations via the protonated cyclopropane **2** is a lower energy pathway than one involving a primary carbocation.[3] The secondary carbocations **4** and **5**, produced by ring-opening of **2**, may undergo rapid isomerizations by 1, 2,-hydride and methide shifts to produce the tertiary carbocations **3** and **6**, which upon hydride capture give 2- and 3-methylhexane.[5]

The formation of doubly-branched heptanes requires the intermediacy of a set of protonated cyclopropane derivatives such as **8**–**11**. The opening of both **8** and **11** at *a* will produce tertiary carbocations (**7** and **12**) which lead to 23DMP upon hydride capture. Opening of **9** and **10** can give only secondary carbocations (**14** and **15**), which may lead to EP and 24DMP, respectively; these isomers were found in much smaller proportions than 23DMP. The opening of **8** and **11** at *b* is unfavored, compared to *a*, since it gives secondary carbocations rather than the tertiary ones, which may explain why no 33DMP or 22DMP were detected among the products from the Al_2Br_6/HBr catalyzed reactions.

The production of the triply-branched isomer, TMB, requires the intermediate formation of the protonated tetramethyl cyclopropane **19**, which may be produced from **16** if it is not trapped by a hydride donor. TMB was detected in very small amounts from the Al_2Br_6/HBr reactions.

It was interesting to note that the reaction carried out at 2°C (run 9) gave mostly 2- and 3-methylhexane, indicating that rearrangement from the unbranched secondary carbocation (**1**) to the singly branched carbocations (**3**–**6**) is facile, but the rearrangement from singly-branched to doubly-branched carbocations is much slower, judging from the small amounts of doubly-branched heptanes produced. This suggests that the activation energy for the rearrangement from unbranched to singly-

SCHEME I

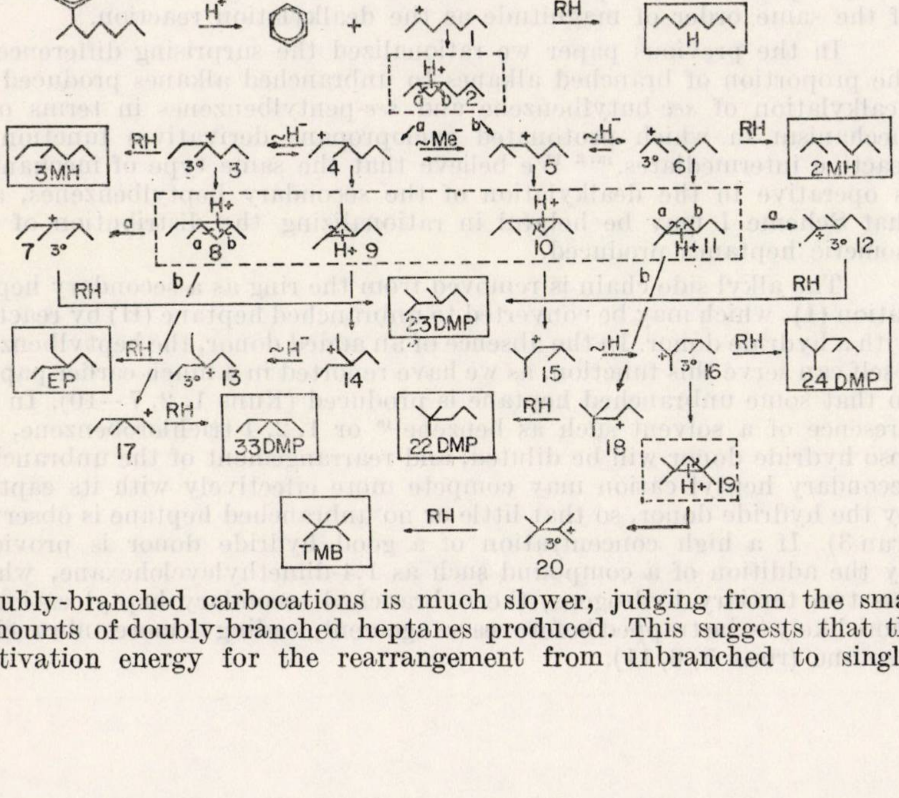

branched carbocations is significantly lower than the activation energy for the rearrangement of singly-branched to doubly-branched carbocations. An explanation for this situation may be found in the relative stabilities of the two types of cationic intermediates. Open chain tertiary carbocations such as **3** and **6** should be about 15 kcal/mol more stable than secondary carbocations such as **1**, whereas the trisubstituted protonated cyclopropanes **8** and **11** should be no more than 10 kcal/mol more stable than the disubstituted protonated cyclopropane **2**.[7] Thus, since the stability of the protonated cyclopropane intermediates should give an indication of the activation energies required to reach them, the rearrangement from singly-branched heptane isomers to doubly-branched isomers should have an activation energy of about five kcal/mol greater than the activation energy for the rearrangement from an unbranched to a singly-branched isomer.

Another experimental result that can be rationalized in terms of intermediate carbocations is the large effect that addition of the hydride donor 1,4-dimethylcyclohexane produced on the ratio of unbranched (ub) : singly-branched (sb) heptanes and the negligible effect it had on the ratio of singly-branched : doubly-branched heptanes : *e.g.*, in run 2 the ub : sb ratio was 6 : 64 (1 : 11) and the sb : db ratio was 64 : 29 (1 : 0.45), whereas in run 5 the ub : sb ratio was 24 : 50 (1 : 2.1) and the sb : db ratio was 50 : 24 (1 : 0.48). Although 1,4-dimethylcyclohexane can be expected to be effective in donating its hydride to a secondary carbocation such as **1**, and in so doing to become a tertiary carbocation, it cannot be expected to be as effective in exchanging its hydrogen with a tertiary carbocation such as **3** or **6**.

HF/SbF_5 catalyzed reactions. Dealkylations of 2-phenylheptane with fluoroantimonic acid were carried out and the products were analyzed in much the same way as with Al_2Br_6/HBr catalyst (Table 2). At 2°C for 0.5 h (run 12) the yield of heptanes was higher than with Al_2Br_6/HBr at 2°C for 3 h, and the distribution of isomeric heptanes was appreciably different; EP and TMB were produced by HF/SbF_5 but not by Al_2Br_6/HBr. At 35°C the yields of heptanes were lower than with Al_2Br_6/HBr catalyst, presumably because of more effective competition from side reactions.

The effects of adding 1,4-dimethylcyclohexane and 1,2,4-trichlorobenzene were qualitatively similar to those observed with the other catalyst; that is, DMCH increased the proportion of unbranched heptane and TCB decreased it, but the effects were much smaller. Perhaps the most interesting result from the use of HF/SbF_5 catalyst was the detection, albeit in very small concentrations, of the last two isomeric heptanes, 22DMP and 33DMP, which were not detected in the Al_2Br_6/HBr reactions. This finding recalls a similar result from the dealkylations of 2-phenylhexane with Al_2Br_6/HBr and HF/SbF_5.[1a] 2,2- and 3,3-Dimethylbutane were produced by the latter catalyst but not the former, and the proportion of 22DMB increased when the hydride donor methylcyclohexane was added. Increased proportion of the geminal dimethylalkane isomers by the presence of higher concentrations of a good hydride donor may be attributed to trapping of secondary carbocations such as **18** by a hydride donation which is essentially irreversible, because the geminal dimethylalkane does not have any tertiary hydrogens. (All of the other branched hexanes and heptanes do have tertiary hydrogens which may be exchanged and thus lead to other isomeric alkanes.)

Higher-boiling products. A mixture of 2-, 3-, and 4-phenylheptane in an approximate ratio of 1 : 0.6 : 0.2, respectively, was produced regardless of which of the phenylheptanes was treated with Al_2Br_6/HBr or HF/SbF_5. No other isomeric phenylheptanes with branched chains were observed, in spite of a careful check for the presence of 2-methyl-1-phenylhexane, specifically. This compound was sought especially because of the known rearrangement of 2-phenylbutane (*sec*-butylbenzene) to 2-methyl-1-phenylpropane (isobutylbenzene),[1a,8,9] of 2-phenylpentane to 2-methyl-1-phenylbutane,[1a,9] and of 2-phenylhexane to 2-methyl-1-phenylpentane.[1a] There is an interesting decline in the yields of the isomers produced from the 2-phenylalkanes in going from 2-phenylbutane to-2phenylheptane. Whereas 2-phenylbutane is isomerized extensively to 2-methyl-1-phenylpropane, only traces of 2-methyl-1-phenylpentane are produced from 2-phenylhexane, and no 2-methyl-1-phenylhexane could be detected as a product from 2-phenylheptane. This result is very likely attributable to the conversion of the initially-formed 2-methyl-1-phenylalkanes to cyclialkylation products when the side chain is longer than four carbon atoms, so that substituted indans and tetralins can be formed without the necessity of primary carbocation intermediates. Indan, tetralin, and naphthalene derivatives were identified among the reaction products from the secondary hexylbenzenes.[1a] In the present case of the heptylbenzenes, although tetralins were not detected, the molecular ions and the cracking patterns of the higher-boiling products were indicative of naphthalene derivatives. These naphthalenes may arise from tetralins by aromatization through hydride donation and proton elimination.

EXPERIMENTAL SECTION

Materials and instrumentation. 2-, 3-, and 4-Phenylheptane and 2-methyl-1-phenylhexane were synthesized by standard procedures from the appropriate Grignard reagents and ketones, followed by dehydration of the alcohols, and low-pressure hydrogenation of the alkenes, as described previously.[1a] Authentic samples of the nine heptane isomers were checked for purity and/or purified by GC. Aluminium bromide was prepared by the addition of bromide to aluminium powder and was distilled before use.[10] Fluoroantimonic acid, "Spectrograde", was purchased from Cationics, Inc. and was used as received.

Qualitative and quantitative analyses of product mixtures were carried out with a Varian Model 2440 chromatograph equipped with a linear temperature programmer, using a 50 ft. × 0.125 in. 10% SE-30 column and/or a 50 ft. × 0.125 in. 550 HiPak silicone oil column. Yields were determined by the addition of a known weight of octane or nonane as an internal standard. Qualitative and preparative work was done with a Varian Autoprep A-700 instrument using a 10 ft. × 0.25 in. 30% SE-30 column.

Six of the nine heptane isomers could be identified and analyzed quantitatively by GC, but 3,3-dimethylpentane and benzene had the same retention time, as did 2-methylhexane and 2,3-dimethylpentane. The presence of these three heptane isomers was established by GC-MS (Finnigan 4023 GC-MS interfaced with a Finnigan/INCOS data system, using a 100 ft. capillary column coated with SP-1200) and by ^{13}C-NMR spectroscopy (Brucker WH-90 or Varian FT-80A instruments). Identification of some of the GC-MS peaks was confirmed by computerized comparison of the spectrum with the National Bureau of Standards library.

Dealkylation of *sec*-heptylbenzenes with aluminium bromide/hydrogen bromide. Aluminium bromide (3—6 g) was distilled into a tared three-necked flask and weighted. The flask was fitted with a teflon-covered magnetic stirring bar, a reflux condenser, a rubber serum cap, and a gas-delivery tube reaching to the botton of the flask. Weighed amount of 2-, 3-, or 4-phenylheptane (3—6 g) and, in some runs, a hydride donor (see Table 1 for identity and amount) were added by syringe through the serum cap. Stirring was begun and hydrogen bromide was passed into the reaction mixture until it was detected at the open end of the reflux condenser. The reaction flask was then immersed in an electrically heated oil bath maintained at the desired temperature, ± 2°C. After a reaction time of 3 h, except in one run at 80° for 1 hr, the flask was cooled in an ice-water bath and the reaction mixture was decomposed by the slow addition of water by syringe. The two-phase mixture was separated, and the aqueous layer was extracted four times with ether, the combined organic phase was washed twice with saturated $NaHCO_3$ solution, once with water, and once with saturated NaCl solution. The organic solution was dried over $MgSO_4$ and analyzed without further purification.

When 1, 2, 4-trichlorobenzene was employed as a solvent, it was added by syringe after the Al_2Br_6 and before the phenylheptane.

Dealkylation of 2-phenylheptane with fluoroantimonic acid. These experiments were carried out essentially as those with Al_2Br_6/HBr except that they were conducted with the exclusion of air by means of a blanket of argon.

REFERENCES AND NOTES

[1] (a) Paper 36 in the New Friedel-Crafts Chemistry series. Part 35 : R. M. Roberts and H. H. Chen, *Rev. Roumaine Chim.*, **25**, 687 (1980).
(b) Generous support of this research by the Robert A. Welch Foundation is greatly acknowledged.

[2] 2-Methylhexane was not separated from 2,3-dimethylpentane on any of the GC columns available to us. Although the presence of both isomers was confirmed by GC-MS and ^{13}C-NMR (cf. Experimental Section), we could not get a quantitative measure of the proportion of these two isomers. In Tables 1 and 2 we give, in the center column, the value for the sum of the two isomers, based on the GC peak area. The numbers in parentheses on each side of this value represent the proportion of the two isomers estimated using the assumption that 2- and 3-methylhexane are produced in equal amounts. The basis of this assumption is described in footnote 5.

[3] (a) D. M. Brouwer and J. M. Oelderik, *Rec. Trav. Chim.*, **87**, 721 (1968).
(b) G. M. Kramer, *J. Amer. Chem. Soc.*, **91**, 4819 (1969).

[4] R. M. Roberts, E. K. Baylis, and G. J. Fonken, *J. Amer. Chem. Soc.*, **85**, 3454 (1963).

[5] If 2- and 3 methylhexane were to reach a thermodynamic equilibrium, they should be present in a proportion of 3MH : 2MH = 36 : 64.[6] The ratio of 3MH : (2MH + 23DMP) from all of the dealkylations of 2-phenylheptane was > 36/64 (in Run 6 it was 1/1), so that even if there were *no* 23DMH present, there would not be an equilibrium proportion of 3MH : 2MH. The proportion of these isomers must be kinetic controlled, and it appears reasonable that they are produced at approximately equal rates.

[6] D. R. Stull, E. F. Westrum, Jr., and G. C. Sinke, "The Chemical Thermodynamics of Organic Compounds", Wiley, New York, 1969, pp. 249—252.

[7] (a) N. Bodor, M. J. S. Dewar, and D. H. Lo, *J. Amer. Chem. Soc.*, **94**, 5303 (1972).
(b) M. J. S. Dewar, private communication.

[8] R. M. Roberts, Y. W. Han, C. H. Schmid, and D. A. Davis, *J. Amer. Chem. Soc.*, **81**, 640 (1959).

[9] R. M. Roberts and Y. W. Han, *J. Amer. Chem. Soc.*, **85**, 1168 (1963).

[10] (a) P. K. Winter and P. L. Cramer, *Ind. Eng. Chem.*, **32**, 856 (1940).
(b) D. G. Nicholson, P. K. Winter, and H. Fineberg, *Inorg. Syn.*, **3**, 30 (1950).

Revue Roumaine de Chimie, 27, *6*, 769–774 (1982)

PHOTOCHEMICAL RING CONTRACTION OF 3-DIAZO-DIBENZO [*f*, *i*]BICYCLO[3.2.2]NONA-6,8-DIEN-2-ONE

M. BANCIU
Laboratory of Organic Chemistry – TCH; Polytechnic Institute; 76206, Bucharest 16, Romania

Received December 23, 1981

The hydroxymethylene derivative 4b of the known ketone 3 was converted to the title diazoketone 5 by usual reactions. Illumination of 5 in dioxane-water or in methanol afforded 9,10-ethano-9,10-dihydroanthracene-11-carboxylic acid (9) respectively the corresponding methyl ester 10.

INTRODUCTION

In a study concerning the solvolytic behaviour of dibenzocycloalkanic systems, we described some years ago[1] the formation of the dibenzobicyclic alcohol **2** during the unbuffered acetolysis of the 5(2′-tosyloxyethyl)-5H-dibenzo[*a*, *d*]cycloheptene (**1**). Oxidation of the alcohol **2** afforded the corresponding ketone **3**.[1]

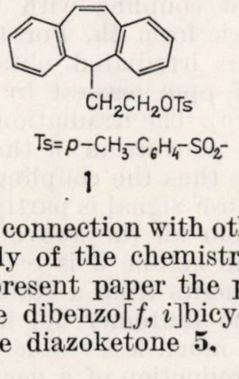

1

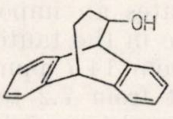

2

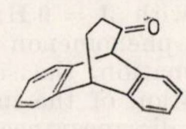

3

In connection with other recent works from this laboratory [2] pursuing the study of the chemistry of this dibenzobicyclic system, we describe in the present paper the photochemical ring contraction of a derivative with the dibenzo[*f*, *i*]bicyclo[3.2.2]nona-6,8-dien-2-one (**3**) skeleton, namely the diazoketone **5**.

RESULTS AND DISCUSSION

The diazoketone **5** was obtained in two steps starting with the ketone **3**, and passing through the corresponding formyl-derivative **4**.

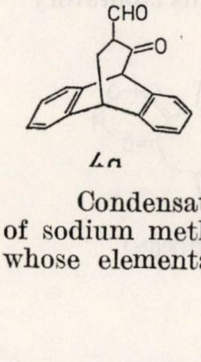

4a

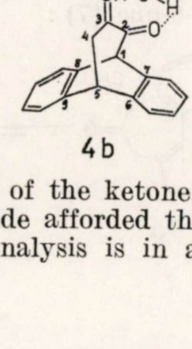

4b

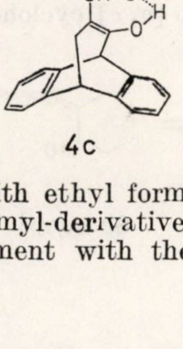

4c

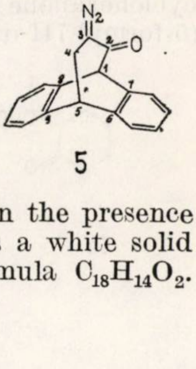

5

Condensation of the ketone **3** with ethyl formate in the presence of sodium methoxide afforded the formyl-derivative **4** as a white solid whose elemental analysis is in agreement with the formula $C_{18}H_{14}O_2$.

From the three possible tautomeric forms **4a**–**4c** the IR- and ^{1}H-NMR data — discussed below — are in agreement only with the hydroxymethylenic formula **4b**. Thus, in the IR spectrum a strong band at 1633 cm^{-1} and a medium one at 1605 cm^{-1} could be attributed to $\nu(C=O)$ respectively $\nu(C=C)$ vibrations from an unsaturated conjugated system $C=C-C=O$. Moreover, a large band from 2700 to 3300 cm^{-1} could be attributed to $\nu_{OH}^{assoc.}$ frequency. The lack of any band between 2680–2800 cm^{-1} is an indication that the compound does not possess the aldehydic group (as in formulas **4a** and **4c**).

The ^{1}H-NMR spectrum (in $CDCl_3$) presents the following signals (δ values) : 2.81, doubet (J = 4 Hz ; two protons) ; 4.29, triplet (J = 4 Hz ; one proton) ; 4.76, singlet ; (one proton) ; 7.2 –7.7, multiplet (nine protons) and 14.7 ppm, doublet, J = 9 Hz (one proton) which disappears by deuteration. The first three signals are characteristic for the dibenzobicyclo[3.2.2]nonadienic system [1] : the doublet for H^4 and $H^{4'}$, the triplet for H^5 and the singlet for H^1. In a double resonance experiment through irradiation of the signal from 2.81 ppm the triplet from 4.29 ppm was converted into a singlet whereas the irradiation of this triplet caused a conversion of the doublet from 2.81 ppm into a singlet. The inexistence of any signal between 9 and 10 ppm strongly indicates the absence of aldehydic tautomeric forms **4a** and **4c**. The signal from 14.7 ppm which disappears on deuteration, is characteristic for a chelated enolic OH groups [3] as in structures **4b** and **4c**. The splitting of this signal into a doublet with J = 9 Hz indicates an important coupling with another proton, a phenomenon possible in the tautomeric form **4b**. For the sake of confirmation, the signal from 14.7 ppm was irradiated obtaining a simplification of the multiplet from 7.2 to 7.7 ppm (easiest to remark being the dissapearance of a signal from 7.6 ppm). The irradiation of this multiplet in the region of 7.6 ppm causes the conversion of the signal from 14.7 ppm into a singlet and demonstrates thus the coupling of the hydroxyl proton with the vinylic proton H^{10} whose signal is partly superposed over the aromatic proton multiplet. From all the above data it follows that the product of formylation of the ketone **3** is exclusively the hydroxymethylene derivative **4b** which benefits from a stabilisation through intramolecular hydrogen bonding. The tautomer **4c**, in which similar hydrogen bonds may appear, would be much less stable than **4b** due to the important strain brought by the introduction of a new double bond into the bicyclic median ring.

The complete enolisation of the formyl-derivative **4a** (in $CDCl_3$; CCl_4) is in agreement with earlier literature data [4] (see for example 2-formylcyclohexanone **(6)** as well as with more recent results from this laboratory [5] (5-formyl-7H-dibenzo [*a*, *c*] cyclohepten-6-one **(7)** :

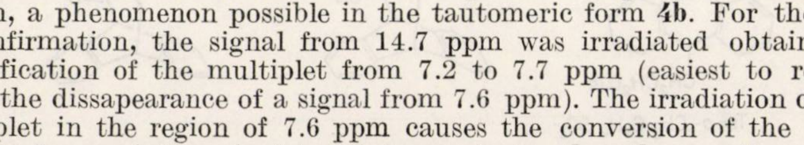

6a 6b (100%) 7a 7b (100%)

The hydroxymethylenederivative **4b** was then converted into the diazoketone **5** using a slightly modified [6] general method of Rosenberger *et. al.*[7] Treatment of **4b** with *p*-toluenesulfonylazide and triethylamine, afforded a yellow solid **5**. This structure was confirmed on the basis of its IR- and ^{1}H-NMR data: $\nu(C{=}O) = 1640\ cm^{-1}$; $\nu(N_2) = 2095\ cm^{-1}$ and $\delta = 3.05$, doublet ($J = 4$ Hz; $2H^4$); 4.28, triplet ($J = 4$ Hz; H^5); 4.78, singlet (H^1) and 7.2 – 7.5 ppm, multiplet ($H_{arom.}$).

The formation of the diazoketone **5** from **4** could be explained by a cyclic intermediate **8**, in agreement with the proposed mechanism:[7,6]

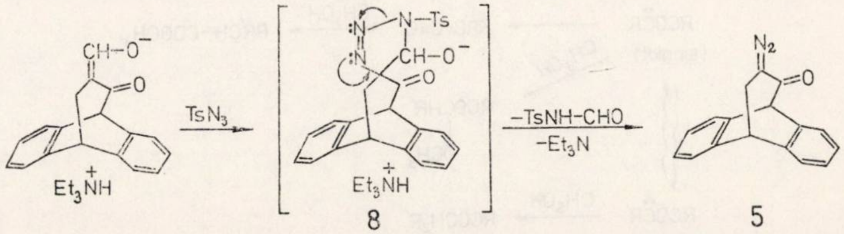

Illumination of the diazoketone **5** with a medium pressure Hg – UV lamp in dioxane/water solution afforded in good yield the 9,10-ethano-9,10-dihydroanthracene-11-carboxylic acid **(9)** and irradiation in methanol gave the corresponding methyl ester **10**. The melting points as well as the IR and ^{1}H-NMR data of **9** and **10** are in perfect agreement with the reported ones.[8]

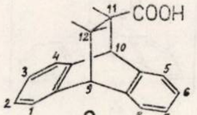

9

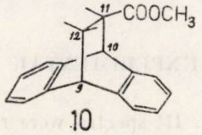

10

The illumination of diazoketones is a known alternative procedure of the Wolff rearrangement.[9] Recent studies [10] of the mechanism of this reaction underlined the importance of conformation in the determination of the product distribution (scheme 1): in the direct irradiations the *s*-E diazoketones eliminate nitrogen affording singlet carbonyl carbenes (which, in turn could give ketenes or different characteristic carbenic reactions *e.g.* insertions, 1,2-hydrogen migrations etc.) whereas *s*-Z diazoketones afford ketenes directly from their singlet excited state (the final products resulting usually from the reaction between these ketenes and the solvent).

Scheme 1

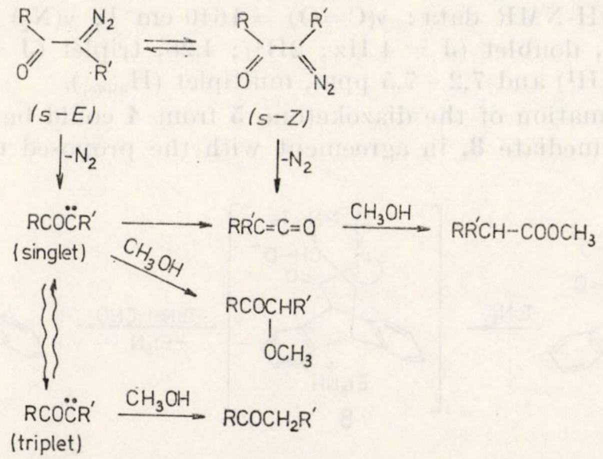

In the present case the diazoketone **5** being cyclic is locked in the *s*-Z conformation (no interconversion with *s*-E conformer being possible). The reaction product is, similarly to other cyclic diazoketones,[5,6,9,10] the ring contracted acid, namely the acid **9** (or its ester **10**).

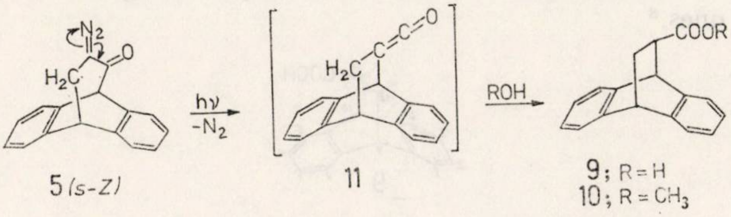

EXPERIMENTAL

Melting points are uncorrected. IR spectra were recorded with a double beam UR 20 Carl Zeiss Jena spectrometer. ^{1}H-NMR spectra were obtained on a VARIAN A 60-A spectrometer using TMS as internal standard.

3-Hydroxymethylene-dibenzo [f, i] *bicyclo*[3.2.2]*nona-6,8-dien-2-one* **(4b)**

In a 250 ml three-necked flask, sodium methoxide was prepared from 1 g (44.5 g-atoms) sodium and 30 ml methanol. The excess methanol was evaporated *in vacuo* then 40 ml anhydrous benzene were added. The mixture was cooled in ice and a solution of ketone 3[1] (6.5 g ; 27.6 mmoles) and freshly distilled ethyl formate (4.5 g ; 61 mmoles) in 70 ml anhydrous benzene was dropped with stirring during 1 hr. After 3 hrs of additional stirring at room temp. the reaction was left overnight. The reaction mixture was thoroughly extracted with 1N — sodium hydroxide solution (5 × 30 ml) then the cooled combined alkaline solutions were acidified with dil. HCl. The thick oily product was ether extracted, the combined ethereal solutions were washed with water, dried and evaporated affording a solid product (5.75 g ; 79 %).

The *hydroxymethylenederivative* **4b**, m.p. 163–4° (from ethanol). Found : C, 82.26 ; H, 5.51 ; Calc. for $C_{18}H_{14}O_2$ C, 82.42 ; H, 5.38 %.

IR spectrum (CS_2 ; CCl_4 ; cm^{-1}) : 560m, 735s, 745m, 775m, 1110m, 1205m, 1250m, 1400m, 1605s, 1633vs, 2850w, 2920w, 3030w, 3080w and 2700–3300 (large).

^{1}H-NMR spectrum ($CDCl_3$; δ ppm) : 2.81 (d ; 2H ; H^4 ; $J = 4$ Hz) ; 4.29 (t ; 1H, H^5 ; $J = 4$ Hz) ; 4.76 (s, 1H, H^1) ; 7.2 – 7.7 (m ; 9H ; 8 H_{arom} and = CH–O) ; 14.7 (d ; 1H, HO– ; $J = 9$ Hz).

3-Diazo-dibenzo[f, i]*bicyclo*[3.2.2]*nona-6,8-dien-2-one* **(5)**.

In a 250 ml three-necked flask a solution of **4b** (4 g ; 15.2 mmoles) in 100 ml anhydrous ethyl ether was prepared, then 3.2 g (15.6 mmoles) *p*-toluensulfonyl azide[11] were added with stirring and cooling in an ice bath. Maintaining the stirring and cooling triethylamine (3 g ; 30 mmoles) was dropped in three hours (a dark yellow precipitate was formed) then the reaction mixture was left overnight. The reaction was decomposed by dropping 50 ml water, the ethereal layer was separated and the aqueous one was ether extracted (3 × 30 ml). The combined organic layers were washed with water (10 × 10 ml) dried and evaporated *in vacuo* affording an orange oil which soon crystallised. The solid was washed with ethyl ether (2–3 ml) affording the diazoketone **5** (2.3 g ; 56 %) as yellow crystals with m.p. 125–128° (dec.). (From the filtrate small quantities of impure **5** could be obtained).

IR spectrum (CCl_4 ; cm^{-1}) : 1190s, 1315m, 1350s, 1640s, 2095vs, 2850w, 2923w, 3023w and 3037w.

^{1}H-NMR spectrum ($CDCl_3$; δ ppm) : 3.05 (d ; 2H ; H^4 ; $J = 4$ Hz) ; 4.28 (t ; 1H ; H^5 ; $J = 4$ Hz) ; 4.78 (s ; 1H ; H^1) ; 7.2–7.5 (m ; 8H ; H_{arom}).

Photochemical ring contraction of diazoketone **5**.

a) *In dioxane-water*. A solution of diazoketone **5** (0.5 g ; 1.92 mmoles) in 45 ml dioxane and 10 ml distilled water was irradiated for about 10 hrs with a medium pressure UV-Hg lamp (150 watt ; Pyrex filter) until the evolution of nitrogen ceased. The pale yellow solution was concentrated *in vacuo* up to 5 ml and the residue was diluted with 50 ml ethyl ether. The ethereal solution was extracted with 15% Na_2CO_3 solution (4 × 30 ml). The combined cooled alkaline solutions were acidified with dil. HCl and the solid organic acid formed was ether extracted. The ethereal extract was washed with water, dried and evaporated affording the *9,10-ethano-9,10-dihydroanthracene-11-carboxylic acid* **(9)** (0.35 g ; 73%) m.p. 188–90° (from ethanol) lit. m.p. 187–8°[8e] ; 186–9°[8g] ; 187°[8b].

IR spectrum (CCl_4 ; cm^{-1}) : 1230m, 1255m, 1416m, 1472m, 1715vs, 2883m, 2950s, 3023s, 3043m, 3073m and 2400–3400 (large).

^{1}H-NMR spectrum (CCl_4 ; δ ppm) : 1.85–2.2 (m ; 2H ; H^{12}) ; 2.7–3.1 (m ; 1H ; H^{11}) ; 4.32(t ; 1H ; H^9 ; $J = 2.5$ Hz) ; 4.68 (d ; 1H ; H^{10} ; $J = 2.5$ Hz) ; 7–7.5 (m ; 8H ; H_{arom}) ; 9.76 (large s ; 1H ; COOH).

b) *In methanol*. A solution of diazoketone **5** (0.5 g ; 1.92 mmoles) in 110 ml methanol was irradiated in the same conditions as described for a) (after 7 hours the evolution of nitrogen ceased). The solvent was evaporated *in vacuo*, affording the crude ester **8** as an oily solid (0.4 g ; 78 %). *9,10-Ethano-9,10-dihydroanthracene-11-methylcarboxylate* **(10)**, m.p. 117–119° (from ethanol) lit. m.p. 117–118°[8d] ; 117°[8b] ; 117–118°[8c].

IR spectrum (CCl_4 ; cm^{-1}) : 1180vs, 1197vs, 1210vs, 1438m, 1470m, 1744vs, 2953s, 3023m and 3073m.

^{1}H-NMR spectrum (CCl_4 ; δ ppm) : 1.8–2.15 (m ; 2H ; H^{12}) ; 2.6–2.95 (m ; 1H ; H^{11}) ; 3.5 (s ; 3H ; $COOCH_3$) ; 4.28 (t ; 1H ; H^9 ; $J = 2.5$ Hz) ; 4.61 (d ; 1H ; H^{10} ; $J = 2.5$ Hz) ; 6.9–7.4 (m ; 8H ; H_{arom}).

The ^{1}H-NMR spectrum agrees well with the described spectrum[8d] with the exception of coupling constants for H^9 and H^{10} which were indicated – probably erroneously – as being 5 Hz[8d] instead of 2.5 Hz.

Acknowledgment. The ^{1}H-NMR spectra were performed by Drs C. Drăghici and M. Gheorghiu to whom our thanks are due.

REFERENCES

[1] E. Ciorănescu, M. Banciu, R. Jelescu, M. Rentzea, M. Elian and C. D. Nenitzescu, *Tetrahedron Letters*, **1969**, 1871 ; *Rev. Roumaine Chim.*, **14**, 911 (1969).

[2] M. Banciu, A. T. Balaban, C. Drăghici and E. Ciorănescu, *Rev. Roumaine Chim.*, under press.

[3] L. M. Jackman and S. Sternhell, "Applications of NMR Spectroscopy in Organic Chemistry", Pergamon Press, Oxford, 2 Edition, 1969, p. 216.

[4] K. v. Auwers and H. Jacobsen, *Liebigs Ann. Chem.*, **426**, 161, 182, 224 (1922) ; *Chem. Zentr.*, **1922**, I, 635.

[5] M. Banciu, Phan Le Thuy and L. Stănescu, *Rev. Roumaine Chim.*, **24**, 957 (1979).

[6] L. Enescu and M. Avram, *Rev. Roumaine Chim.*, **22**, 1061 (1977).

[7] M. Rosenberger, P. Yates, J. B. Hendrickson and W. Wolf, *Tetrahedron Letters*, **1964**, 2285.

[8] a. E. de Barry Barnett, N. F. Goodway and E. V. Weekes, *J. Chem. Soc.*, **1935**, 1102 ; b) P. D. Bartlett and F. A. Tate, *J. Amer. Chem. Soc.*, **75**, 91 (1953) ; c) S. Wawzonek and J. V. Hallum, *J. Org. Chem.*, **18**, 288 (1953) ; d) R. K. Hill and G. R. Newcome *J. Org. Chem.*, **34**, 740 (1969) ; e) A. Ya. Berlin, *Zhur. obshchei Khim.*, **22**, 1656 (1952) ; f) A. E. Kretov and A. E. Okhramovich, *Zhur. priklad. Khim.*, **33**, 744 (1960) ; g) T. Shono, S. Kodama and R. Oda, *J. Chem. Soc. Japan*, **58**, 582 (1955).

[9] See for example : W. Kirmse, "Carbene Chemistry", Academic Press, New York, 1964, p. 120 and literature cited therein.

[10] H. Tomioka, H. Okuno and Y. Izawa, *J. Org. Chem.*, **45**, 5278 (1980).
F. Kaplan and M. L. Mitchell, *Tetrahedron Letters*, **1979**, 759.

[11] W. v. E. Doering and C. H. de Puy, *J. Amer. Chem. Soc.*, **75**, 5955 (1953).

Revue Roumaine de Chimie, 27, 6, 775–780 (1982)

^{1}H-NMR SPECTRA OF SOME FLAME-RETARDANT POLYMERS

SIMONA PERCEC, ALMERIA NATANSOHN and FLORIN POPESCU
Institute of Macromolecular Chemistry "P. Poni", Aleea Gr. Ghica Vodă 41 A, Jassy, Romania

Received March 14, 1981

By polycondensation of diols : bisphenol A or tetrachlorobisphenol A with phosphorus halides as : chloromethylphosphonic dichloride and bis(2,3-dichloropropyl) phosphorochloridite or with phosphonic acid derivatives as diethyl-N,N-bis(diethyl) aminomethyl phosphate, some polyphosphonates with flame-retardant properties were obtained. Structures of monomers and polymers were determined by ^{1}H-NMR spectroscopy.

INTRODUCTION

Flame-retardant additives influence the combustion of solid substances in three ways :

a. by shielding the contact zone
b. by modifying the pyrolysis
c. by modifying the burning mechanism

The first one is essentially a physical process, whereas the second and the third ones have chemical mechanisms. The main elements which can modify processes b and c are phosphorus and halogens.

For phosphorous additives, the main reaction is the formation of phosphorus pentoxide and its hydrates which strongly affect the formation [1] of the pyrolytic residues.

Halogens also influence the combustion, their efficacy growing with the decrease of carbon-halogen dissociation energy. It is obvious that phosphorus- and halogen-containing additives can offer a better flame-retardancy. Other elements, like nitrogen, can have a synergetic action in the presence of phosphorus, inducing the high-thermostable carbon formation in the hydrocarbon-decomposition phase.[2]

Phosphorus containing polymers with flame-retardant properties are obtained by different methods. Amongst them, the polycondensation is a convenient one.

In the previous papers we studied the mechanism and kinetic polycondensation of phosphorus acid chlorides with diols.[3,4,5,6]

In this paper the ^{1}H-NMR spectra of initial compounds and polymers are presented in order to determine the structures which were obtained.

EXPERIMENTAL

By melt polycondensation in the 80–200°C temperature range, under inert atmosphere (nitrogen) and without catalysts, some flame-retardant polymers have been synthesized. The ^{1}H-NMR spectra of monomers, reaction mixtures and polymers were obtained on a JEOL C-60HL spectrometer, operating at 60 MHz, in $CDCl_3$ or in $DMSOd_6$ solutions or in melt

.

RESULTS AND DISCUSSION

I. *Phosphorus- and halogen-containing polymers*

a. *Bisphenol A* has a ^{1}H-NMR spectrum assigned as follows:

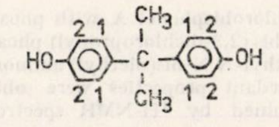

δ_{H_1}=7.06 ppm δ_{OH} = variable

δ_{H_2}=6.82 ppm

δ_{CH_3}=1.58 ppm J_{12}= 9 Hz

The polycondensation with chloromethylphosphonic dichloride takes place according [3] to the scheme:

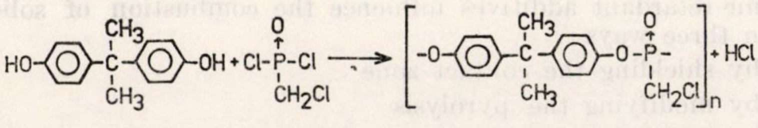

The ^{1}H-NMR spectrum of the obtained polymer is represented in Fig. 1.

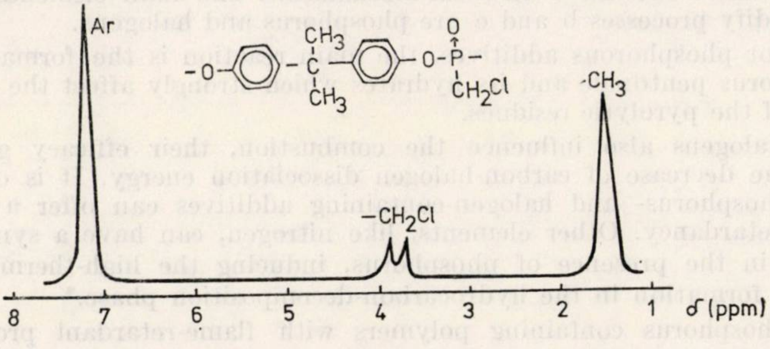

Fig. 1. — The ^{1}H-NMR spectrum of the polymer obtained by chloromethylphosphonic dichloride and bisphenol A.

As shown in the figure, all aromatic protons become equivalent by polycondensation, giving a singlet at 7.16 ppm. The CH_2Cl group has the spectral parameters: $\delta = 3.75$ ppm and $J_{PH} = 10$ Hz, *versus*

$\delta = 3.92$ ppm and $J_{PH} = 6$ Hz in chloromethylphosphonic dichloride. The polycondensation kinetics can be studied following the instantaneous concentrations of components.[3]

Polycondensation of bisphenol A with bis(2,3 dichloropropyl)phosphorochloridite follows a more complicated scheme[7]:

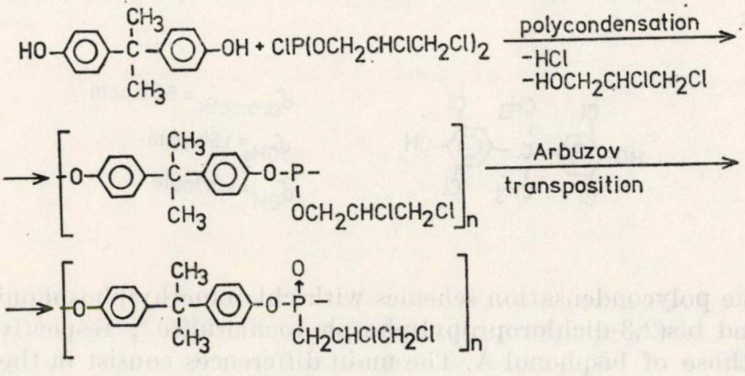

The spectral arguments for the above scheme are illustrated in Fig. 2.

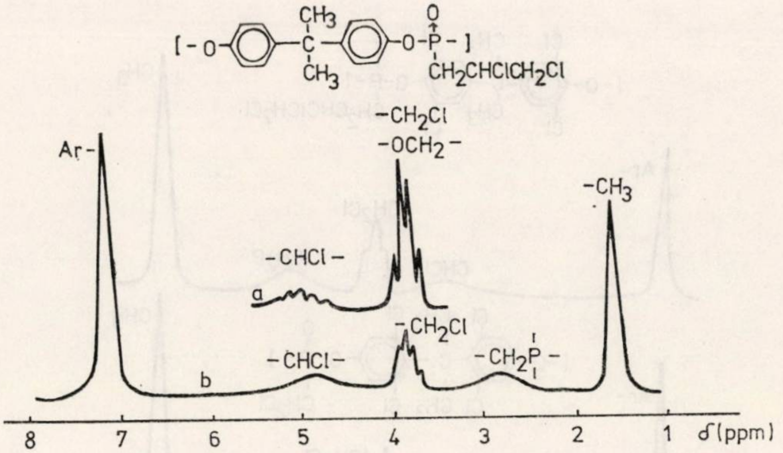

Fig. 2. — The ^{1}H-NMR spectrum of bis (2,3-dichloropropyl) phosphorochloridite (a) and its polymer with bisphenol A (b).

In comparison with the bis (2,3 dichloropropyl phosphorochloridite) spectrum (Fig. 2 a) which presents separate signals for CHCl group ($\delta = 4.82$ ppm) and CH_2 groups ($\delta = 3.78$ ppm), the polymer spectrum (figure 2 b) has signals at 7.16 ppm (8 aromatic protons); 4.82 ppm

(1 proton; CHCl groups); 3.78 ppm (2 protons; CH_2Cl group); 2.71 ppm (2 protons; CH_2P group); 1.58 ppm (6 protons; CH_3 group). The relative intensities of signals demonstrate the halogenated alcohol elimination whereas the presence of the 2.71 ppm signal is the proof for Arbuzov transposition. Also, following the reaction in time, the reaction rate can be determined.[4]

b. *Tetrachlorobisphenol A* has a ^{1}H-NMR spectrum assignable as follows:

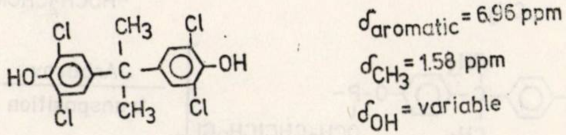

The polycondensation schemes with chloromethylphosphonic dichloride [5] and bis(2,3-dichloropropyl)phosphorochloridite [6], respectively, resemble those of bisphenol A. The main differences consist in the reaction conditions, which are harder for tetrachlorobisphenol A, owing to the inactivation introduced by the electronegative chlorine atoms. The ^{1}H-NMR spectra of the polymers together with the assignments are given in Fig. 3.

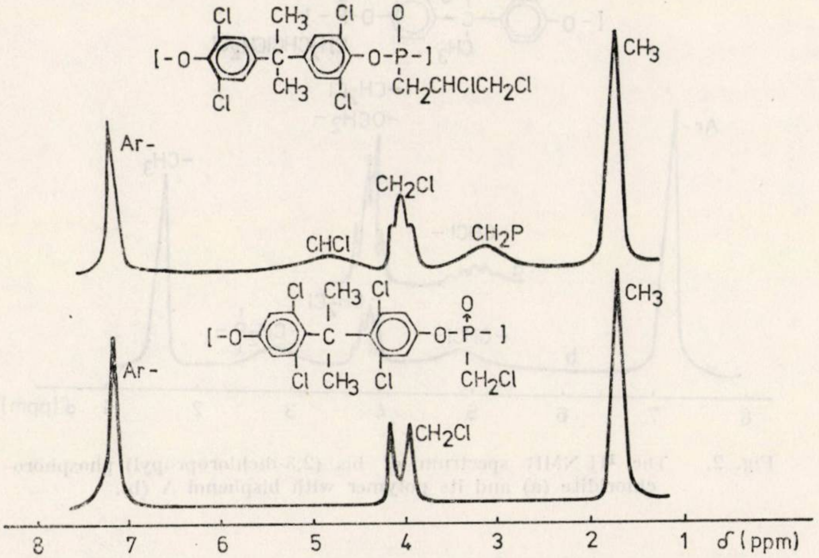

Fig. 3. — The ^{1}H-NMR spectra of polymers obtained by tetrachlorobisphenol A and bis(2,3 dichloropropyl)phosphorochloridite (a) and chloromethylphosphonic dichloride (b).

II. *Phosphorus- and nitrogen-containing polymers*

Diethyl-N,N-bis (diethyl)aminomethyl phosphate reacts with bisphenol A according to the scheme [8]:

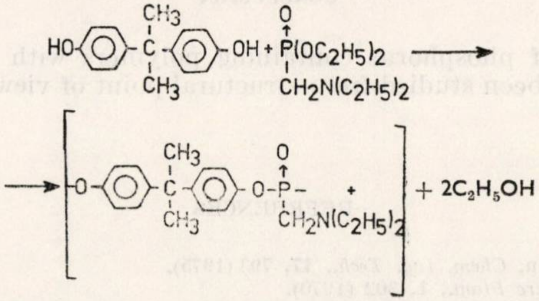

The ^{1}H-NMR spectrum of the polycondensation product is presented in Fig. 4.

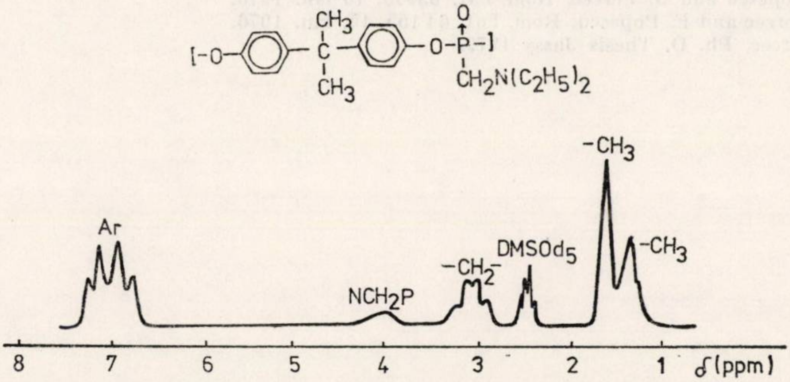

Fig. 4. — The ^{1}H-NMR spectrum of the polymer obtained by bisphenol A and diethyl-N,N-bis (diethyl)aminomethyl phosphate.

As it can be seen, in DMSOd$_6$, the aromatic protons are non-equivalent, giving an AB quartet. The ethyl group bound to nitrogen resonates at 1.42 ppm (CH_3) and 3.05 ppm (CH_2) as a triplet and quartet, respectively. The phosphorus- and nitrogen-bound CH_2 group resonates at approximately 4 ppm as a broad signal owing to heteroatoms coupling.

The proof for the inclusion of the phosphorus residue in the polymer chain is the disappearance of the 3.92 ppm quartet assigned to CH_2 protons in $-P(OCH_2CH_3)_2$ group, which exists in phosphonate monomer ^{1}H-NMR spectrum.

III. *Phosphorus, nitrogen and halogen containing polymers*

Similarly, the polycondensation of tetrachlorobisphenol A with diethyl-N,N-bis(diethyl)aminomethyl phosphate was described.[8] The spectral differences consist mainly in the singlet at 7.20 ppm of the aromatic zone, owing to the four aromatic equivalent protons.

CONCLUSION

A series of phosphorus containing polymers with flame-retardant properties [8] has been studied from structural point of view using ^{1}H-NMR spectroscopy.

REFERENCES

[1] D. W. Van Krevelen, *Chem. Ing. Tech.*, **47**, 793 (1975).
[2] J. W. Lyons, *J. Fire Flam.*, **1**, 302 (1970).
[3] S. Parcec, A. Natansohn, D. Gâlea and M. Dima, *Angew. Makromol. Chem.*, **72**, 1 (1978).
[4] S. Percec, F. Popescu and A. Natansohn, *Phosphorus and Sulphur*, **7**, 149 (1979).
[5] S. Percec, A. Natansohn and M. Dima, *Angew. Makromol. Chem.*, **80**, 143 (1979).
[6] S. Percec, F. Popescu and I. Natansohn, *Polymer*, **21**, 89 (1980).
[7] F. Popescu and S. Percec, Rom. Pat. 63975, 15 ian. 1976.
[8] S. Percec and F. Popescu, Rom. Pat. 64 155, 15. ian. 1976.
[9] S. Percec, Ph. D. Thesis Jassy 1979.

Revue Roumaine de Chimie, 27, 6, 781–785(1982)

SYNTHESIS OF SOME 1,3,4-THIADIAZOLE DERIVATIVES WITH ANTIBACTERIAL ACTIVITY

A. E. ABDEL–RAHMAN, A. M. MAHMOUD, H. A. El–SHERIEF
and A. G. GHATTAS
Chemistry Department, Faculty of Science, Assiut University, Assiut,
Egypt, A.R.E.

Received January 13, 1981

Some new 2(N-aryl and/or heterocyclocarboxamidomethyl thio)-5-(*p*-chlorophenyl)-1,3,4-thiadiazoles (I and II) were prepared through the reaction of 2-mercapto-5-(*p*-chlorophenyl)-1,3,4-thiadiazole with different N-aryl and/or heterocyclo-2-chloroacetamides in the presence of a basic catalyst. 3-Chloromethyl-5-(*p*-chlorophenyl)-2-thiono-1-3,4-thiadiazole interacted with various heterocyclic mercaptans and some heterocyclic bases to form IIIa-h and IVa-e respectively. The structural configurations of synthesised compounds were confirmed by elemental and spectroscopic analysis. Some of the above mentioned products have been bacteriologically screened.

In view of the fact that several substituted thiadiazole derivatives possess useful antibacterial properties,[1] it was of interest to incorporate this molecule into the well-known antimicrobial nucleus (thiadiazole) in order to evaluate the resulting compounds for pharmacological activity. Recently, considerable study has been directed in our laboratory towards the synthesis of some new 1,3,4-thiadiazole derivatives.

RESULTS AND DISCUSSION

The present investigation describes the reaction of 2-mercapto-5 (*p*-chlorophenyl)-1,3,4-thiadiazole[2] with different N-aryl and/or heterocyclo-2-chloroacetamides of substituted aniline, 3-amino-pyridine, 4,5-disubstituted 2-aminothiazole, 2-aminobenzthiazole and 4-aminophenazone, in the presence of alcoholic potassium hydroxide solution to give 2-(N-phenyl-, N-pyridyl-3′, N-benzthiazolyl-2′, N-thiazolyl-2′ and N-phenaz-5′-onyl-4′-carboxamidomethyl thio)-5-(*p*-chlorophenyl)-1,3,4-thiadiazole respectively (Ia-n and IIa-e).

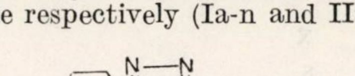

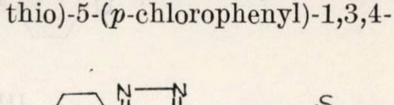

Ar
Ia ; = Phenyl
b ;= *p*-Chlorophenyl
c ;= *p*-Bromophenyl
d := *p*-Hydroxyphenyl
e ;= *p*-Anisyl
f ; = *p*-Tolyl
g ; = *p*-Acetylphenyl
h ;= *p*-Carboxyphenyl
i ; = *p*-Nitrophenyl
j ;= Benzyl
k ;= β-Naphthyl
l ;= 3-Pyridyl
m ;= 2-Benzthiazolyl
n ;= 4-Phenaz-5-onyl

	R	R′
IIa ;=	H	H
b ;=	H	Phenyl
c ;=	H	*p*-Anisyl
d ;=	H	*p*-Tolyl
e ;=	Carboethoxy	Methyl

The IR absorption spectra of the newly synthesised compounds (Ia-n and IIa-e) showed an absorption band at 3430 – 3350 cm^{-1} and 1660 cm^{-1} assigned to (NH amide) and (C = O amide), respectively.[3] Moreover, the structures of I and II were confirmed by UV spectra which showed the main absorption band at λ_{max} 300 nm which is characteristic of 2-S-alkylated products.[4]

On the other hand, 2-(N-aryl and/or heterocyclocarboxamidomethyl thio)-5-(*p*-chlorophenyl)-1,3,4-thiadiazoles (Ia-n and IIa-e) could also be obtained through another synthesising route, namely by condensation of 2-carboxymethylthio-5-(*p*-chlorophenyl)-1,3,4-thiadiazole[5, 6] with different aromatic amines and/or with heterocyclic amines in the presence of N-ethoxy-carbonyl-2-ethoxy-1,2-dihydroquinoline (EEDQ)[7] as condensing agent and DMF as a solvent. The identity of compounds Ia-n and IIa-e obtained by the two mentioned methods were established by their m.p. and mixed m.p., T.L.C. and I.R. absorption spectra.

Furthermore, 3-chloromethyl-5-(*p*-chlorophenyl)-1,3,4-thiadiazole reacted with various heterocyclic mercaptans, such as: benzoxazole-2-thiol, benzimidazole-2-thiol, benzthiazole-2-thiol, naphth [1,2,-*d*] oxazole-2-thiol, naphth [1,2-*d*] oxazole-2-thiol-5-sulphonic acid, 5-phenyl-2-thiono-1,3,4-thiadiazole, 5-(*p*-chlorophenyl)-2-thiono-1,3,4-oxadiazole and 5-phenyl-2-thiono-1,3,4-thiadiazole in the presence of alcoholic potassium hydroxide giving the corresponding 3-S-substituted mercaptomethyl-5-(*p*-chlorophenyl)-2-thiono-1,3,4-thiadiazole derivatives (IIIa-h).

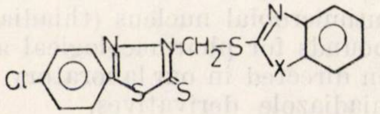

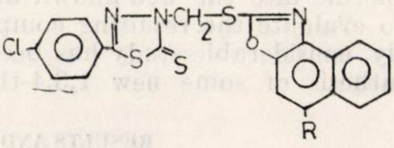

X
IIIa ; = O
b ; = NH
c ; = S

R
IIId ;= H
e ;= SO_3H

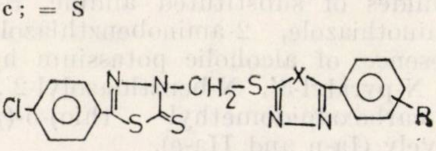

R X
IIIf ; = H S
g ; = Cl O
h ; = H O

The compounds IIIa-h have been identified by a combination of their elemental analysis and spectral data. The IR spectra, showed an absorption band at 1290 – 1280 cm^{-1} which characterized the C=S group.[8]

The above compounds showed the principal u.v. absorption band at 336 – 344 nm characteristic of 1,3,4-thiadiazole in the thiono-form.[9]

Also, 3-chloromethyl-5-(*p*-chlorophenyl)-2-thiono-1,3,4-thiadiazole interacted with some heterocyclic bases, such as : pyridine, α-picoline, quinoline, isoquinoline and quinaldine to afford the corresponding salts of IVa-e in high yields.

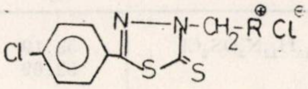

R R

IVa ; = N-pyridine
b ; = N-α-picoline
c ; = N-quinoline
d ; = N-isoquinoline
e ; = N-quinaldine

The IR spectra of IVa-e showed characteristic bands at 1290—1280 cm^{-1} and 1080 cm^{-1} assigned to $-C=S$[8] and $Cl-Ph$[3], respectively. The UV absorption spectra of compounds IVa-e showed the principal band at 336 — 344 nm corresponding to the absorption of substituted 2-thiono-1,3,4-thiadiazole system present in the thiono-form similar to 3-alkyl-5-(*p*-chloro-phenyl-2-thiono-1,3,4-thiadiazole.[9]

Antimicrobial Activities:

The antimicrobial activities of compounds IIIa, b, c, e and h were tested in vitro against a variety of microbes.[10] These microorganisms include Gram-positive, such as, *Staph. aureus* and Pyogenes and Gram-negative, such as, *E. coli* and *Proteus morganii.*

The results of the screening show no inhibitions on *Pyogenes* and a little too strong activity on the other microorganisms at a concentration of 10^{-4} M. The most strongly active compounds (more than 60 % inhibition) against *Staph. aureus* were IIIb and h, and against *E. coli* and *Proteus morganii* were IIIa, b and c.

EXPERIMENTAL

Melting points are uncorrected. IR spectra (KBr discs) were recorded on a Pye-Unicam SP 200 G spectrophotometer. UV spectra in spec. pure ethanol were taken on a Pye-Unicam SP 8000 Ultraviolet spectrophotometer.

Synthesis of 2-(N-aryl and/or heterocyclocarboxamidomethyl thio)-5-(p-chlorophenyl)-1,3,4-thiadiazole (Ia-n and IIa—e).

2-Mercapto-5-(*p*-chlorophenyl)-1,3,4-thiadiazole [2] (0.001 mole) was dissolved in the presence of an equivalent amount of KOH and the appropriate N-aryl and/or heterocyclo-2-chloroacetamide (0.001 mole) (N-(phenyl, *p*-chlorophenyl, *p*-bromophenyl, *p*-tolyl, *p*-anisyl, *p*-nitrophenyl, benzyl, *p*-acetophenyl, *p*-carboxyphenyl, *p*-hydroxyphenyl, β-naphthyl, 3-pyridyl and 4-phenaz-5-onyl) was added to it. The reaction mixture was refluxed for about half an hour, then concentrated and cooled, when a mixture of the crude aryl and/or heterocyclocarboxamidomethyl thio)-5-(*p*-chlorophenyl)-1,3,4-thiadiazole and potassium chloride was precipitated. It was acidified with acetic acid, filtered, washed with water to remove potassium chloride and recrystallised from ethanol to give Ia-n and IIa-e (Table 1).

TABLE 1

Physical Data of Compounds I, II, III and IV

Compound* No.	m.p. (°C)	Molecular formula	Analysis (Calc./found) %			
			C	H	N	S
Ia	207–8	$C_{16}H_{12}N_3OS_2Cl$	53.19 52.69	3.24 3.54	11.63 11.73	17.72 17.82
b	245–46	$C_{16}H_{11}N_3OS_2Cl_2$	48.61 47.91	2.78 3.58	10.63 9.73	16.21 16.61
c	191–92	$C_{16}H_{11}N_3OS_2ClBr$	43.64 44.50	2.50 2.40	9.54 10.20	14.55 15.30
d	225–27	$C_{16}H_{12}N_3O_2S_2Cl$	50.93 50.90	3.18 3.20	11.41 11.31	16.98 17.20
e	194–95	$C_{17}H_{14}N_3O_2S_2Cl$	52.17 52.20	3.58 3.49	10.74 10.70	16.37 16.27
f	218–20	$C_{17}H_{14}N_3OS_2Cl$	54.40 53.80	3.73 3.70	11.20 12.10	17.07 17.46
g	260–61	$C_{18}H_{14}N_3O_2S_2Cl$	53.60 54.40	3.47 3.27	10.42 9.81	15.88 15.42
h	259–60	$C_{17}H_{12}N_3O_3S_2Cl$	50.37 50.40	2.96 3.46	10.37 9.27	15.80 15.37
i	215–16	$C_{16}H_{11}N_4O_3S_2Cl$	47.29 48.01	2.71 2.61	13.79 12.91	15.76 15.91
j	168–69	$C_{17}H_{14}N_3OS_2Cl$	54.40 55.20	3.73 2.93	11.10 11.00	17.10 17.45
k	251–52	$C_{20}H_{14}N_3OS_2Cl$	58.39 59.19	3.41 3.21	10.22 9.42	15.57 15.77
l	202–3	$C_{15}H_{11}N_4OS_2Cl$	49.72 50.12	3.10 2.90	15.50 15.70	17.50 17.26
m	242–43	$C_{17}H_{11}N_4OS_3Cl$	48.80 48.80	2.63 2.62	13.40 13.20	22.97 23.10
n	199–200	$C_{21}H_{18}N_5O_2S_2Cl$	53.50 54.10	3.82 2.92	14.86 14.91	13.59 13.26
IIa	278–79	$C_{15}H_9N_4OS_3Cl$	45.92 46.52	2.30 1.90	14.29 14.39	24.49 24.68
b	208–9	$C_{21}H_{13}N_4OS_3Cl$	53.85 53.80	2.78 2.80	11.97 12.01	20.51 20.02
c	205–6	$C_{22}H_{15}N_4O_2S_3Cl$	53.01 53.00	3.01 2.90	11.24 11.30	19.28 19.00
d	231–32	$C_{22}H_{15}N_4OS_3Cl$	54.77 55.67	3.11 2.51	11.61 11.61	19.92 19.62
e	229–30	$C_{17}H_{15}N_4O_3S_3Cl$	44.93 44.92	3.30 3.20	12.33 12.33	21.14 21.53
IIIa	182–83	$C_{16}H_{10}N_3OS_3Cl$	49.10 49.6	2.56 3.16	10.74 10.74	24.55 24.84
b	212–13	$C_{16}H_{11}N_4S_3Cl$	49.23 49.2	2.82 2.81	14.36 14.40	24.62 24.31
c	149–50	$C_{16}H_{10}N_3S_4Cl$	47.17 48.00	2.46 2.10	10.32 9.60	31.45 31.04

TABLE 1. *(Continued)*

Compound* No.	m.p. (°C)	Molecular formula	Analysis (Calc./found) %			
			C	H	N	S
d	132–33	$C_{20}H_{12}N_3OS_3Cl$	54.42 55·22	2.72 1.92	9.52 9.42	21.77 21.83
e	164–65	$C_{20}H_{12}N_3O_4S_4Cl$	46.07 46.17	2.30 2.30	8.06 8.16	24.57 24.70
f	159–60	$C_{17}H_{11}N_4S_4Cl$	47.01 47.00	2.53 2.51	12.90 13.00	29.50 30.11
g	132–33	$C_{17}H_{10}N_4OS_3Cl_2$	45.13 45.10	2.21 2.20	12.39 12.20	21.24 21.03
h	130–32	$C_{17}H_{11}N_4OS_3Cl$	44.06 44.00	2.38 2.40	12.10 12.10	20.73 20.42
IVa	231–32	$C_{14}H_{11}N_3S_2Cl_2$	47.32 48.02	3.10 2.70	11.83 11.43	18.03 18.24
b	132–33	$C_{15}H_{13}N_3S_2Cl_2$	48.78 49.48	3.52 3.32	11.38 11.28	17.34 17.44
c	194–95	$C_{18}H_{13}N_3S_2Cl_2$	51.91 51.81	3.31 3.41	10.69 10.72	16.28 16.30
d	275–76	$C_{18}H_{13}N_3S_2Cl_2$	51.90 51.80	3.30 3.21	10.70 11.40	16.30 15.81
e	197–98	$C_{19}H_{15}N_3S_2Cl_2$	54.41 55.01	3.58 3.38	10.02 10.00	15.27 15.07

* Compounds Ia-n, IIa-e, IIIa-h and IVa-e were obtained in 75–80, 62–74, 60–70 and 90–95 % yields, respectively.

Synthesis of 3-S-substituted mercaptomethyl-5-(p-chlorophenyl)-2-thiono-1,3,4-thiadiazole (IIIa-h).

3-Chloromethyl-5-(*p*-chlorophenyl-2-thiono-1,3,4-thiadiazole (0.001 mole) was added to an equivalent amount of benzimidazole-2-thiol, benzthiazole-2-thiol, benzoxazole-2-thiol, naphth [1,2-*d*] oxazole-2-thiol, naphth[1,2-*d*]oxazole-2-thiol-5-sulphonic acid, 5-phenyl-2-thiono-1,3,4-thiadiazole, 5-phenyl-2-thiono-1,3,4-oxadiazole and 5-(*p*-chlorophenyl)-2-thiono-1,3,4-thiadiazole (0.001 mole) in the presence of KOH to give 3-S-substituted mercaptomethyl-5-(*p*-chlorophenyl)-2-thiono-1,3,4-thiodiazole derivatives IIIa-h, crystallised from ethanol (Table 1).

Salt formation of 3-chloromethyl-5-(p-chlorophenyl)-2-thiono-1,3,4-thiadiazole.

3-Chloromethyl-5-(*p*-chlorophenyl)-2-thiono-1,3,4-thiadiazole (0.001 mole) was refluxed with excess of some heterocyclic bases, such as : pyridine, α-picoline, quinoline, isoquinoline, and quinaldine giving precipitate (needles) crystallised from benzene (Table 1).

REFERENCES

[1] W. R. Sherman, *J. Org. Chem.*, **26**, 88 (1961).
[2] M. Baron, and C. V. Wilson, *J. Org. Chem.*, **23**, 1021 (1958).
[3] L. J. Bellamy, "The Infrared Spectra of Complex Molecules", 2*nd* edn, Methuen, London, 1958.
[4] J. Sandstrom, and I. Wemerbeck, *Acta. Chem. Scand.*, **20**, 57 (1966).
[5] H. Ohta, and M. Ohta, *Nippon Kagaku Zasshi,* **78**, 700 (1957).
[6] J. Sandstrom, *Arkiv. Kemi.*, **4**, 297 (1952).
[7] B. Belleav and G. Malek, *J. Amer. Chem. Soc.*, **90**, 1651 (1968).
[8] N. B. Colthup, L. H. Daly, and S. E. Wiberly, "Introduction to Infrared and Raman Spectroscopy", Academic Press, New York, 409, 1964.
[9] C. Ainsworth, *J. Amer. Chem. Soc.*, **77**, 1148 (1955).
Ibid., **78**, 1636 (1956) ; *Ibid.*, **87**, 5800 (1965).
[10] J. G. Vicent, and H. W. Vincent, *Pract. Exptl. Biol. Med.*, **55**, 162 (1944).

Revue Roumaine de Chimie, 27, *6*, 787, (1982)

COMPTES RENDUS

Advances in Polymer Science. Volume 40. "Luminiscence". Springer Verlag, Berlin, Heidelberg, New York, 1981, 174 pages

The volume contains two contributions and the author index for volumes 1—40.

The first paper "Investigation of Polymers in Solution by Polarized Luminiscence" (68 pages) is written by E. V. Anufrieva and Yu. Ya. Gotlib from Institute of High Molecular Compounds, Academy of Sciences of the USSR — Leningrad.

The method of polarized luminiscence — which has become one of the most valuable methods for investigation of macromolecules — is based on the study of polarization of light emitted by some "luminiscent groups" (*e.g.* anthracene structures) covalenty bonded to macromolecules.

The five main chapters are : 1) Introduction ; 2) Polarized luminiscence of macromolecules with conjugated luminiscent markers ; 3) Methods for the preparation of polymers with covalently attached luminiscent markers of the anthracene structure ; 4) Investigation of polymer solutions by polarized luminiscence and 5) Dynamic theory of the motions of macromolecules and polarized luminiscence.

Different interesting methods of preparation *e.g.* preparation of polymers with luminiscent markers at the chain ends, in side groups of macromolecules or in the main chain are developed in chapter 3.

From different interesting topics presented in chapter 4 we mention : application of polarized luminiscence for the study of mobility of various parts of the polymer chain, influence of the chemical structure of the polymer on the intramolecular mobility of macromolecules in solution, influence of intramolecular hydrogen bonds on the mobility of macromolecules, intramolecular mobility etc.

The reference list comprises 231 quotations.

The second paper : "Time resolved fluorescence techniques in polymer and biopolymer studies" (98 pages) is written by K. P. Ghiggino, A. J. Roberts and D. Phillips from Department of Phshical Chemistry, University of Melbourne and Davy-Faraday Research Laboratory, London.

The main chapters are : 1) Introduction (fluorescence spectral characteristics, polarization of electronic transitions, fluorescence decay times, time-resolved studies using fluorescent probes) ; 2) Experimental techniques (steady-state luminiscence instrumentation ; time-resolved techniques e.g. pulse sampling methods, phase modulation techniques, single photon counting methods, time resolved polarization measurements) ; 3) Fluorescence from synthetic polymers (e.g. polystyrene, polyvinylnaphtalene, polynaphthylmethacrylates, polyacenaphthylene and polyvinylcarbazole) ; 4) Time-resolved studies on biopolymers and 5) Time-resolved fluorescence depolarization in macromolecules.

The authors outlined experimental methods used recently for the study of the decay of fluorescence on a nanosecond (or less) time scale, which corresponds with the time of different motions or processes in macromolecular systems. Numerous interesting applications are developed but at the same time the difficulties in interpretation of the results are underlined.

The reference list comprises 237 quotations.

The book is recommended to macromolecular chemists and to physical chemists with interest in luminiscence field.

M. Banciu

NOTE POUR LES AUTEURS

La Revue Roumaine de Chimie publie des articles en anglais, français, russe, allemand ou espagnol. Les auteurs sont priés d'envoyer des articles et des comptes rendus inédits.

Les manuscrits seront dactylographiés à deux intervalles. La bibliographie, les tableaux et la légende des figures seront placés après le texte.

Si l'article fait partie d'une série numérotée, la partie précédente sera donnée comme première référence.

Chaque article sera précédé d'une résumé comprenant quinze lignes au maximum.

Les références bibliographiques dans le texte seront faites par des exposants sans parenthèses et paraîtront à la fin de l'ouvrage.

Les publications périodiques mentionnées dans la bibliographie seront présentées suivant les prescriptions internationales : le nom de l'auteur précédé de l'initiale du prénom, le titre du périodique abrégé conformément à « Chemical Abstracts » et souligné par une ligne, le numero du tome indiqué par des chiffres arabes et souligné par deux lignes, suivi de la première page de l'article ; à la fin, l'année de la parution sera placée entre parenthèses. Le numéro de la revue ne sera pas indiqué si les pages du volume sont numérotées consécutivement.

Les textes des livres ou traités incluront : le nom des auteurs, précédé de l'initiale du prénom, le titre du livre entre guillemets et sans être souligné, le numéro du tome précédé par l'abréviation « vol. » (ou « Bd. »), le numéro de l'édition, les éditions (the publisher), la localité de la parution du livre, l'année de la parution et la page de la référence précédée par l'abréviation « p. » (ou « S. »).

Les brevets seront indiqués comme suit : l'auteur ou la firme, le pays et le numéro du brevet, la date et la revue (Chem. Abstr.). Par ex. : M. Jones (to Union Carbide Co.), *Brit. Pat.* 601—238, 2 Sept. 1959 ; cf. *Chem Abstr.*, **54**, 12808 (1960).

Si la référence n'a pas été lue en original, on indiquera aussi la revue de références consultée.

Les diagrammes seront tracés à l'encre de Chine sur papier calque. Les tableaux et les figures (en nombre strictement nécessaire) ainsi que les courbes dans les figures seront numérotées par des chiffres arabes. Leur explication sera donnée dans la légende des figures. Prière de ne pas inscrire les mêmes données dans les tableaux et dans les figures. Chaque tableau aura un titre. On indiquera dans le texte la place approximative des tableaux et des figures. Les formules chimiques seront incluses dans le texte ; en outre, elles seront transcrites sur papier calque, à l'encre de Chine.

Les auteurs sont priés d'indiquer les caractères italiques (en soulignant les lettres au crayon), ainsi que tout autre caractère spécial ; les préfixes *ortho, meta, para, cis, trans*, etc. seront soulignés pour indiquer leurs caractères italiques et ne seront jamais écrits avec des majuscules.

Aucune correction à la main ne sera admise sur le manuscrit. Les corrections seront tapées à la machine. Les lettres grecques ou autres symboles spéciaux seront insérés à la main à l'encre clairement.

Le manuscrit sera signé par l'auteur.

Le titre courant aura 50 lettres au maximum.

L'entière responsabilité du contenu des articles appartient aux auteurs.

Sur demande on peut obtenir des indications plus complètes.

PRINTED IN ROMANIA

TRAVAUX PARUS AUX ÉDITIONS DE L'ACADÉMIE DE LA RÉPUBLIQUE SOCIALISTE DE ROUMANIE

ELENA CEAUŞESCU, **Noi cercetări în domeniul compuşilor macromoleculari** (Nouvelles recherches dans le domaine des composés macromoléculaires), 1981, 536 p.

I. G. MURGULESCU, J. PĂUN, **Introducere în chimia fizică. Vol. I.3. Nucleul atomic, reacţii nucleare, particule elementare** (Introduction à la chimie physique. Vol. I. 3. Noyau atomique, réactions nucléaires, particules élémentaires), 1982, 606 p.

ELENA JERCAN, **Analiza cromatografică** (Analyse chromatographique), 1982, 286 p.

I. G. MURGULESCU, TATIANA ONCESCU, E. SEGAL, **Introducere în chimia fizică. Vol. II.2. Cinetică chimică şi cataliză** (Introduction à la chimie physique. Vol. II.2. Cinétique chimique et catalyse), 1981, 1024 p.

V. DRĂGUŢAN, A. T. BALABAN, M. DIMONIE, **Metateza olefinelor şi polimerizarea prin deschidere de inel a cicloolefinelor** (La métathèse des oléfines et la polymérisation par ouverture annulaire des cyclooléfines), 1981, 254 p.

LYDIA-MARIA VAICUM, **Epurarea apelor uzate cu nămol activ. Bazele biochimice** (L'épuration des eaux résiduelles à boue active. Les bases biochimique), 1981, 218 p.

I. GĂLĂŢEANU, **Procese şi metode radiochimice în energetica nucleară** (Processus et methodes radiochimiques dans l'énergétique nucléaire), 1981, 234 p.

O. IORDACHE, **Procese polistocastice aplicate în fenomenele de transfer** (Processus polystochastiques appliqués aux phénomènes de transfert), 1981, 187 p.

CR. SIMIONESCU, VALERIA GORDUZA, **Polimeri biocompatibili şi biologic activi** (Polymères biocompatibles et biologiquement actifs), 1980, 497 p.

ELENA CEAUŞESCU, **Polimerizarea stereospecifică a izoprenului** (La polymérisation stéréospecifique de l'isoprène), 1979, 307 p.

M. FLORESCU, **Metode ştiinţifice în dezvoltarea industriei chimice moderne** (Méthodes scientifiques dans le développement de l'industrie chimique moderne), 1979, 256 p.

A. T. BALABAN, I. GĂLĂŢEANU, G. GEORGESCU, LIGIA SIMIONESCU, **Compuşi marcaţi şi radiofarmaceutici cu aplicaţii în medicina nucleară** (Composés marqués et radiopharmaceutiques à application en médecine nucléaire), 1979, 495 p.

CONST. GH. MACAROVICI, **Analiza chimică cantitativă anorganică** (L'analyse chimique quantitative inorganique), 1979, 457 p.

I. G. MURGULESCU, E. SEGAL, **Introducere în chimia fizică, (Vol. II.1. Teoria molecular cinetică a materiei** (Introduction à la chimie physique. Vol. II.1. La théorie moléculaire-cinétique de la matière), 1979, 1036 p.

S. STERNBERG, FL. DANEŞ, **Termodinamica chimică aplicată** (La thermodynamique chimique appliquée), 1978, 400 p.

I. G. MURGULESCU, V. EM. SAHINI, **Introducere în chimia fizică. Vol. I.2. Structura şi proprietăţile moleculelor** (Introduction à la chimie physique. Vol. I.2. La structure et les propriétés des molécules), 1978, 604 p.

I. ZUGRĂVESCU, MAGDA PETROVANU, **N-ylid chemistry**, coédition avec McGraw-Hill International Book Company, U.S.A., 1977, 396 p.

I. G. MURGULESCU, **Introducere în chimia fizică. Vol. I.1. Atomi, molecule, legătură chimică** (Introduction à la chimie physique. Vol. I.1. Atomes, molécules, liaison chimique), 1976, 560 p.

ELENA CEAUŞESCU, **Research work on synthesis and characterization of macromolecular compounds. Contributions**, 1974, 251 p.

CR. SIMIONESCU, VIORICA RUSAN, V. POPA, **Chimia algelor marine** (La chimie des algues marines), 1974, 212 p., 1 pl.

I. P. „Informaţia c. 2116

43 426

Lei 40

$ 70 (pour un abonnement annuel

F 1103

ACADÉMIE DE LA RÉPUBLIQUE SOCIALISTE DE ROUMANIE

R

REVUE ROUMAINE DE CHIMIE

REFERÁLVA

TOME 27
N° 7
Juillet 1982

EDITURA ACADEMIEI REPUBLICII SOCIALISTE ROMÂNIA

Rev. Roumaine Chim.

RRCHAX, **27**, 7, p. 789–894 (1982), Bucarest

ACADÉMIE DE LA RÉPUBLIQUE SOCIALISTE DE ROUMANIE

COMITÉ DE RÉDACTION

Rédacteur en chef :

I. G. MURGULESCU, membre de l'Académie de la République Socialiste de Roumanie

Rédacteurs en chef adjoints :

A. T. BALABAN et V. EM. SAHINI, membres correspondants de l'Académie de la République Socialiste de Roumanie

Collège de rédaction :

EM. BRATU, ELENA CEAUŞESCU, ECATERINA CIORĂNESCU-NENITZESCU, CR. SIMIONESCU, membres de l'Académie de la République Socialiste de Roumanie ; P. SPACU, membre correspondant de l'Académie de la République Socialiste de Roumanie ; MARGARETA AVRAM, M. BANCIU, I. HAIDUC, D. I. MARCHIDAN, I. MOLDOVAN, G. NIAC et D. SĂNDULESCU

La Revue Roumaine de Chimie paraît 10 fois par an. Toute commande de l'étranger pour les travaux parus aux Editions de l'Académie de la République Socialiste de Roumanie sera adressée à ILEXIM — Departamentul Export-Import Carte (Livres)/Departamentul Export-Import Presă (Revues), P.O.B. 136—137, télex 11226, 3, str. 13 Decembrie, 79517 Bucarest, Roumanie

Les manuscrits, les livres et les revues proposés en échange, ainsi que toute correspondance seront envoyés à la rédaction :

REVUE ROUMAINE DE CHIMIE

125, Calea Victoriei, 79717 Bucarest, Roumanie, téléphone 50 76 80

EDITURA ACADEMIEI REPUBLICII SOCIALISTE ROMÂNIA

125, Calea Victoriei, 79717 Bucarest, Roumanie, téléphone 50 76 80

REVUE ROUMAINE
DE
CHIMIE

ORSZÁGOS MŰSZAKI INFORMÁCIÓS KÖZPONT ÉS KÖNYVTÁR 1883

Tome 27, N° 7 Juillet 1982

SCIENTISTS AND PEACE . . . . 791—792

MESSAGE TO THE PARTICIPANTS IN THE INTERNATIONAL SYMPOSIUM "SCIENTISTS AND PEACE" FROM THE PRESIDENT OF THE SOCIALIST REPUBLIC OF ROMANIA, NICOLAE CEAUŞESCU 793—795

APPEAL BY THE PARTICIPANTS IN THE INTERNATIONAL SYMPOSIUM "SCIENTISTS AND PEACE" . . . . 796—798

I. G. MURGULESCU, E. POPA and EUGENIA IVANA, Optical properties of molten SnI_2 . . . . 799—802 R

S. P. SINGH, MISS MADHURI and P. BAHADUR, Stabilization of emulsions by surface active agents . . . . 803—814

J. ZSAKÓ, GH. MARCU and MARIA VÁRHELYI, Kinetic analysis of thermogravimetric data. XV. Thermal decomposition of $[Co(en)_2(pyridine)Br]X_2$ type complexes . . . . 815—821

BERNARD VIDAL, Influence on the UV spectrum of analiphatic chain included between a benzenic chromophore and an electron-withdrawing auxochrome (in Franch) . . . . 823—830

C. I. CHIRIAC, Aromatic esters by a new direct condensation reaction . . . . . 831—834 R

A. I. HASHEM, M. E. SHABAN and A. F. El-KAFRAWY, Reactions of some 5-oxo-2-pyrrolines . . . . 835—838

M. ANWAR, F.I. ABDEL-HAY and A.F. HASHEM, Action of hydrazines, hydroxylamine and urea on 5-aryl-3-chloromethyl-2-thiono-1, 3, 4-oxadiazoles 839—846

I. PETKOV and P. MARKOV, Influence of substituents on the photoketonization of some enolizable β-ketoesters in solution . . . . 847—852

M.A. ARAMENDIA, V. BORAU, C. JIMENEZ and J.M. MARINAS Pd/SiO_2—$AlPO_4$ catalyzed reduction of nitrobenzenes by hydrogen. Transfer from cyclohexene . . . . 853—857 Bc

A.N. OSMAN, M. KHALIFA, M.A. ISMAIL, A.E. OSSMAN and M.G. IBRAHIM, Synthesis and biological activity of certain derivatives of 2,4-dioxo-1, 2, 3, 4-tetrahydroquinazoline. I. . . . . 859—864

M.M. MOHAMED, M.A. EL-HASHASH, I. ISLAM and O.A. ABO-BAKER, 1,4-Arylation of β-(4-chloro-3-methylbenzoyl)-acrylic acid with activated hydrocarbons under Friedel-Crafts conditions and some studies on the products . . . . 865—877

J.L. BURGUERA, MARCELA BURGUERA and A. TOWNSHEND, The principles, applications and trends of flow injection analysis for monitoring chemiluminescent reactions . . . . 879—883

SHAMSHAD AHMAD KHAN and MURICE STONE, Spectrophotometric determination of fluorine in silicate rocks and minerals using zirconium-cyanine R. System . . . . 885—893 Bc

Rev. Roumaine Chim. **27**, 7, 789–894(1982), Bucarest

SCIENTISTS AND PEACE

On 4—5 September 1981 the international symposium "Scientists and peace" developed its proceedings in Bucharest, under the high patronage of the President of the Socialist Republic of Romania, Nicolae Ceaușescu.

The symposium was attended by 68 scientists from 32 countries among whom Nobel Prize winners, presidents of some academies of science, other prestigious scientific personalities, as well as general directors of international organizations.

In the opening session, they read the message of Nicolae Ceaușescu, President of the Socialist Republic of Romania, to the participants in the Symposium.

Expressive of the lofty conception of the Secretary-General of the Romanian Communist Party, the President of the Socialist Republic of Romania, concerning the problems of peace and international security, détente and disarmament, cooperation and understanding among peoples in their efforts to build a new economic order in the world, as well as the scientists' responsibility for the solution of national and international issues by placing the most advanced achievements of the contemporary scientific and technical revolution exclusively in the service of the peoples' peaceful development, President Nicolae Ceaușescu's message made an appeal to scientists all over the world to close their ranks in order to fight the hazards which crises, confrontations and war pose to the future of mankind. The President's message was a guideline for the proceedings of the Symposium.

The participants expressed their support for the leading ideas contained in the message of the President of Romania.

The proceedings closed with an Appeal by the participants addressed to the scientists worldwide. Reflecting the basic ideas contained in President Ceaușescu's message, the appeal suggested the establishing of an Action Committee for the organization of the World Congress "Scientists and Peace".

As an extension of this prestigious international reunion was founded the National Romanian Committee "Scientists and Peace" that unanimously elected as president of the Committee and of the Executive Bureau Academician Elena Ceaușescu, D. Chem. Eng., first vice-prime minister of the Government of the Socialist Republic of Romania, President of the National Council for Science and Technology, illustrious political personality and internationally reputed scientist.

The Romanian National Committee "Scientists and Peace" adopted a comprehensive programme of scientific manifestations, meant to illustrate the contribution of Romanian scientists to the efforts of the Romanian people, alongside all peoples, for safeguarding peace.

The National Romanian Committee "Scientists and Peace" takes action on the international plane for the preparation of the World Congress "Scientists and Peace". The Committee is also represented at the Special Session of the General Assembly of the United Nations Organization devoted to disarmament.

MESSAGE
TO THE PARTICIPANTS IN THE INTERNATIONAL SYMPOSIUM "SCIENTISTS AND PEACE" FROM THE PRESIDENT OF THE SOCIALIST REPUBLIC OF ROMANIA, NICOLAE CEAUȘESCU

It gives me particular pleasure to send to you, the participants in the Symposium "Scientists and Peace" which opens today in Bucharest — distinguished figures in contemporary science and technology — cordial greetings and best wishes for the success of the meeting, so that it may give an impetus to the struggle of progressive forces throughout the world for world progress and peace.

The Socialist Republic of Romanian attaches the greatest importance to scientific activities ; it gives the achievements of science and culture a place among the very foundations of its efforts to construct the new socialist system, in the belief that they are vital factors for progress and civilization.

We are living in the era of the greatest advances in scientific thought that mankind has ever experienced throughout the ages, in the midst of the most awesome technical and scientific revolution, marked by extraordinary discoveries which are constantly changing man's ideas about nature, society and the universe and influencing all aspects of human existence. We see science directly influencing the never-ending change in the conditions of material production, the discovery of the secrets of matter and the increasingly efficient exploitation of our natural wealth and the development of the creative capacity of peoples.

The development of a nation — both in terms of enhancement of the productive forces of society and as regards thinking and mental crea- the productive forces of society and as regards thinking and mental creativity — is inconceivable without the input of advanced science and technology. One cannot even envisage the future of mankind without the major accomplishments of scientific thought.

However, we must candidly admit that a great many of the major discoveries of scientific research and technological innovation are currently used for the production of highly sophisticated weapons of mass destruction, from atomic weapons down. We are witnessing a particularly alarming emphasis on the arms race, and a major build-up of military arsenals capable of annihilating the entire planet and endangering the very existence of mankind.

We see tension growing, world-wide, as a result of the imperialist policies of domination, force and *diktat*. A strong tendency to consolidate and divide up spheres of influence is evident, and conflicts between States and groups of States are becoming more and more bitter.

At the same time, peoples throughout the world are asserting with increasing vigour their will to live in freedom, to develop in complete independence, to put an end for ever to colonialism, neo-colonialism and all forms of oppression, to secure the democratic and progressive renewal of society, to ensure the welfare of the great working masses and to introduce a genuinely new set of relationships on the world scene involving full equality between countries, détente, collaboration and peace.

Socialist Romania is doing all in its power to develop its relations with all States irrespective of their social system. We base our relations with all countries on the principles of full equality of rights, profound respect for national independence and sovereignty, non-interference in internal affairs and non-use of force or threat of force. We believe that every effort must be made to stop the deterioration in the world situation, to ensure that all problems arising between States are settled exclusively by negotiation and to revive and pursue policies of détente and peace.

In the serious international situation which now obtains, scientists bear a tremendous responsibility for the present and future of mankind. No one knows better than the scientist or researcher the destructive power of modern weapons and the danger which the continuing arms race poses to civilization, to the security of peoples and to the very survival of humanity.

The choice between a policy of intensifying the arms race and manufacturing new nuclear weapons of mass destruction and a policy of disarmament, détente and peace is today a question of conscience.

There is no middle course !

It is obvious that scientists, who are very well aware of the destructive power of weapons, especially nuclear weapons, cannot but side with the policy of disarmament and peace. They therefore have a greater duty than ever to speak out and do all they can to ensure that the amazing attainments of the human spirit are no longer used in the manufacture of weapons of mass destruction, in preparing for war or to serve the policies of aggression, force and domination. The noblest task of scientists and researchers, in all fields and throughout the world, is to see to it that the entire potential of modern science and technology is devoted to the progress, welfare, freedom and independence of peoples and to the preservation of the supreme human right to life and to peace.

We must work with great determination and resolve for an end to the arms race, for disarmament, especially nuclear disarmament, for a cessation of the deployment and development of medium-range missiles in Europe, against the production of the neutron bomb, for a reduction in military budgets and armed forces, for the final abandonment of the use or threat of force in international life and for the creation of a world without weapons and without wars.

Under-development affects most of the population of the earth; nearly half a billion people suffer from chronic malnutrition. We must therefore establish a new international economic order guaranteeing free access by all peoples, particularly the least advanced, to the amazing achievements of the human spirit — a new international economic order which will guarantee the free flow of knowledge and discoveries and turn science into something that belongs to all mankind.

As the world economic crisis grows worse, science can play a particularly important role in the discovery and development of new sources of energy and raw materials to be placed at the disposal of people everywhere, making the earth more fertile, increasing its output and solving the great food problem. It has an obligation to contribute to protecting the health of people throughout the world, combating pollution, improving the environment, protecting natural resources and transforming the earth into a verdant garden which can sustain a decent existence for all peoples.

Scientists and specialists in Romania, being profoundly dedicate to the interests of the people, devote all their energies to Romania's economic and social prosperity while at the same time co-operating actively with scientists of other countries in campaigning for progress, for disarmament and for the basic right of all nations to existence, peace and freedom.

Nowadays, the peoples, the masses, throughout the world play an essential role in determining the course of history.

Scientists, vitally involved in the cause of progress and peace, must fight side by side with the peoples for the right to live and work in peace, freely to build their own future without external interference or pressure, to devote their resources and energies to their material and spiritual well-being. Scientists, whatever their philosophical, political and religious views, must close ranks and, together with the peace-loving and anti-imperialistic forces throughout the world, take a stand against the imperialist policy of domination, against war, and for a world of justice, equality and peace.

It is more important than ever to organize a world-wide front of scientists to act and convey their authoritative views to the United Nations, the Committee on Disarmament and other international bodies, concerning disarmament and the establishment of lasting peace on earth.

We are firmly convinced that united action by the men of science and culture, the workers and the progressive forces of all peoples can end the arms race and bring about a move to general disarmament, and in particular nuclear disarmament.

Let us do all we can to ensure for our children and grandchildren, for our generation and future generations, pace, freedom and happiness in a world without war, a more humane, more just and better world!

In keeping with these sentiments, I am convinced that this important meeting in Bucharest will have a great impact on researchers and scientists throughout the world, and I send you most cordial wishes for for much success and satisfaction in your noble work for the advancement of science and for the cause of collaboration, peace and the independence of peoples.

NICOLAE CEAUŞESCU
President of the Socialist Republic
of Romania

Bucharest, 3 September 1981

APPEAL
[illegible] THE PARTICIPANTS IN THE INTERNATIONAL SYMPOSIUM “SCIENTISTS AND PEACE”

Meeting in Bucharest on 4 and 5 September 1981 for the Symposium “Scientists and Peace” in order to discuss, in a wide-ranging and fruitful dialogue, the fundamental issue of the present day — peace, to which all mankind nobly aspires — we, the scientists from many countries of the world and from all continents, aware of the serious hazards which science and its servants may pose to the halting of the arms race, to continuing progress and to the future of the whole world, urgently appeal to scientists, researchers and intellectuals everywhere, and to all peoples, to join forces and co-operate ever more closely in defence of peace the supreme good of mankind.

The world today is witnessing not only the giant strides of science and technology, as evidenced by awesome discoveries affecting all areas of human existence, but also anachronistic actions which go against the interests of mankind, applying the products of science and technology to destructive ends injurious to the peace and freedom of peoples. Our age is one in which mankind is confronted by highly complex problems, with a new, frenzied arms race, unprecedented growth of military budgets, and the manufacture and development of new means of mass destruction, all of which severely aggravate the international situation, weighing more and more heavily on peoples and increasing the danger of conflagrations which may destroy life everywhere on earth and civilization itself, as it has evolved over the millenia.

Let us, in full awareness of the fact that scientists, faced with the alternative of peace or war, have a duty to defend peace, say a firm NO to war and armaments, this being not only our moral responsibility but essential to the continued existence of all mankind. We call on all scientists, whatever their political, philosophical, religious or other beliefs, to work side by side with the peoples of their countries to halt the deterioration in the international situation, the arms policy, so that we may resume and tirelessly pursue the course towards détente, peace and wide-ranging international collaboration !

Let us act now, before it is too late, now, when we have so great a responsibility for the fate of mankind, to end the arms race, to bring about disarmament, especially nuclear disarmament, to create a world without weapons and without wars and to defend the basic right of individuals and peoples — the right to life and to peace.

Let us, as scientists more aware than anyone of the destructive power of modern weapons and the tremendous danger they present to the security of peoples and to the very survival of humanity, join forces more closely and act resolutely against the use of atomic energy for other than peaceful purposes ! Let us do all we can to ensure that the immense potential of scientific and technical research is not used for weapons production but contributes exclusively to economic development and progress in every country, to the preservation of the finest that the human spirit has accomplished and to the creation of new and important values !

In present circumstances, when there exist numerous economic social and political problems at the world level, it is our special duty as scientists constantly to increase our contribution to the solution of these problems for the well-being of all nations. Let us use our discoveries to close the great gaps between the rich and poor countries of the world, to eradicate the malnutrition and under-development affecting two thirds of the world population, to eliminate the diseases which continue to claim millions of human lives, and to protect the environment and conserve it for the benefit of future generations ! Let us exert every effort to discover new sources of energy and raw materials, to solve the problems of food, water supply, health, and so forth, on which depend the progress and the future of all mankind ! Let us resolutely oppose any obstacle to the movement of the world's scientific and cultural assets, so that all peoples can derive extensive benefit from the awesome accomplishments of science and technology, so that science may truly become the property of all mankind !

Today, international peace and security provide the most favourable conditions for economic and social progress and for the application of what the human spirit has achieved, the daunting modern technical and scientific revolution, to the benefit of all mankind. Consequently, every effort, every action by scientific and cultural associations, civic organizations and private individuals, or by politicians, Governments and parliaments, that will help to defend and consolidate peace, to promote the cause of peaceful international collaboration based on respect for national independence and sovereignty, equal rights, non-interference in internal affairs and mutual advantage must be appreciated and given determined support, so that the legitimate aspirations of the peoples, of all who are aware of their responsibility for the fate of civilization, may be realized.

We call on scientists, and on their national and international associations, to establish suitable forms of co-operation transcending national, ideological or political differences, to the end that science may be used exclusively in accordance with its humanistic calling.

With this in mind, we have established an International Action Committee to organize scientific activities, to expose the dangers created by the frenzied arms race, particularly the nuclear arms race, to inform public opinion about these dangers and formulate concrete measures to avoid them, and to prepare for a world congress of scientists in the service of peace. We appeal to scientists and intellectuals throughout the world to join the Committee in this noble initiative for peace, to do all in their power to make our views known in the United Nations, in the Committee on Disarmament at Geneva and in all international forums where disarmament, peace and international security and co-operation are discussed.

Let us, in realization of our responsibility to science and to mankind and of the fact that we cannot create an acceptable future without a peaceful present, muster our strength of persuasion and the force of our arguments in order to induce the arms enthusiasts to change their approach, in order to influence Governments, parliaments and politicians to promote policies of peace, understanding and collaboration and to abandon entirely the use or threat of force, ensuring that all disputes are settled solely by peaceful means, through negotiation.

Let us do all in our power to ensure that the funds spent on armaments, the enormous military budgets, are used for socio-economic development programmes in each country, for helping the peoples of the developing countries in their struggle for progress, and for creating a more just and better world free from the threat of war !

Let us dedicate ourselves to the noble ideals of peace : let us do our duty to our own consciences, to our contemporaries, to the supreme commandments of mankind ! Let us show mankind a future commensurate to its most cherished aspirations and its creative abilities, let us prove worthy of all the most precious accomplishments of human civilization down through the centuries !

We are firmly convinced that, if we join forces and intensify our co-operation, science will truly become a weapon for living, enabling all peoples to increase their contributions to the heritage of universal knowledge, so that peace, security and collaboration may triumph on earth !

The participants in the
International Sympoium
"Scientists and Peace"

Bucharest, 5 September 1981

Revue Roumaine de Chimie 27, 7, 799–802 (1982)

OPTICAL PROPERTIES OF MOLTEN SnI_2

I. G. MURGULESCU, E. POPA and EUGENIA IVANA
Center of Physical Chemistry, Spl. Independenței, 202 Bucharest, Romania

Received June 15, 1981

The absorption spectrum of solid and molten SnI_2 was investigated in the wave number range 30,000 – 12,500 cm^{-1} and in the temperature range 428–648 K. The 0.084 ev energy jump at melting point is in agreement with the crystalline structure of stannous iodide.

The study of the SnI_2 absorption spectrum at high temperatures continues our concern with the structural transformations of halides on melting.

The information on SnI_2 available in the literature is concerned mainly with the physical properties [1–3] and crystalline structure [4–5] and less with its optical properties.[6–8]

In this work, the absorption spectrum of both solid and molten SnI_2 was studied within the spectral range of 30,000 – 12,500 cm^{-1} and over the 428 – 648 K temperature range.

EXPERIMENTAL

SnI_2 used for experiments was synthesized from elements by reaction in gaseous phase, according to the method described by Blotki et al.[9] This method allows preparation of a very pure SnI_2, free of SnI_4, as compared to the methods of synthesis in solution, [10] where the risk of oxidizing Sn^{2+} to Sn^{4+} is great.

Metallic tin granules employed were p.a. reagent grade and the iodine was purified by sublimation. SnI_2 thus obtained is stable when in contact with air and has the melting point at 320°C. The absorption spectra of both solid and molten SnI_2 were recorded on a Carl Zeiss Jena Specord UV–VIS spectrophotometer. Working temperatures were obtained by means of a furnace adjusted to the dimensions of the spectrophotometer sample compartment.

Measurements were carried out in silica cells of 8 to 10 μ thickness, sealed under vacuum.

Neither void formation nor crystallization along various directions within the obtained solid films could be entirely prevented in spite of all precautions taken, that is an as slow as possible cooling of the melt in the cell. Experimental details were presented in a previous paper. [11]

RESULTS AND DISCUSSION

The absorption spectra of both solid and molten SnI_2 are presented in Fig. 1.

The spectrum solid SnI_2 represents the absorption of a polycrystalline film obtained by cooling the molten SnI_2. The absorption values for solid films are affected by errors due to the voids as well as radiation scattering on the facets of the polycrystals.

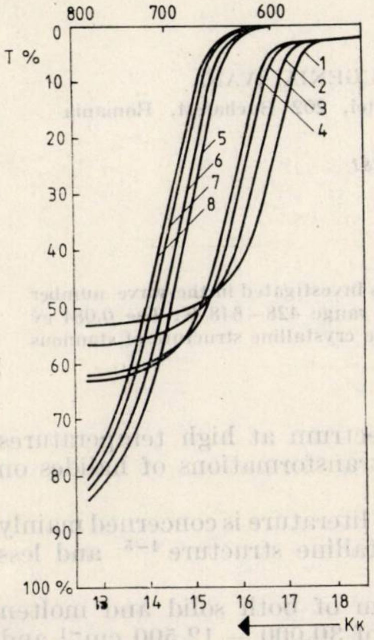

Fig. 1. — Absorption spectrum of SnI_2: 1 — 155°C; 2 — 212°C; 3—272°C; 4—300°C; 5—322°C; 6—337°C; 7—360°C; 8—375°C.

The background in the solid spectrum reaches high values as a consequence of radiation scattering. The radiation is completely absorbed in the range 30,000—17,000 cm^{-1}, for the solid and in the range 30,000—16,000 cm^{-1} for the melt, although the absorbant layer thickness was of the order of 8 — 10 μ.

Because of the total absorption of the radiation in the range 17,000–30,000 cm^{-1}, possible absorption maxima of SnI_2 could not be noticed.

Temperature variation of SnI_2 absorption was also studied at $\nu = 14{,}000\ cm^{-1}$ (Fig. 2a,b).

The experiments were carried out on the same sample in two ways:

a) either in passing from solid to melt, by increasing the temperature from 150 up to 325° at a rate of 3°/min;

b) or in passing from melt to solid, by cooling at a rate of 4.5°/min.

A slow temperature variation of transmittance is observed for both solid and melt; near the melting point (320°C) a steep variation of transmittance occurs in the a-type experiment. During the b-type experiment, this steep variation occurs at about 306°C.

This non-concordance between the two transmittance vs. temperature curves obtained as above indicates the occurrence of supercooling in the SnI_2 melt. The supercooling phenomenon in melts has been noticed for most alkali halides.[12]

Ubbelohde calculated the T_M/T_g ratio for a series of alkali halides, where T_M is the limiting critical supercooling temperature and T_g is the melting temperature. This ratio ranges between 0.76 and 0.86.

For SnI_2, the T_M/T_g ratio is 0.97.

The study of the temperature influence on the SnI_2 absorption in visible domain, both in solid and in molten state, evidenced a shift of the absorption band edge towards low energies with the temperature rise.

In Fig. 3, the temperature variation of the absorption band edge is drawn for $T = 40\%$.

The shift of the absorption edge is monotonous for both solid and melt, with slopes of 6.19×10^{-4} eV/dg and 11.77×10^{-4} eV/dg, respecti-

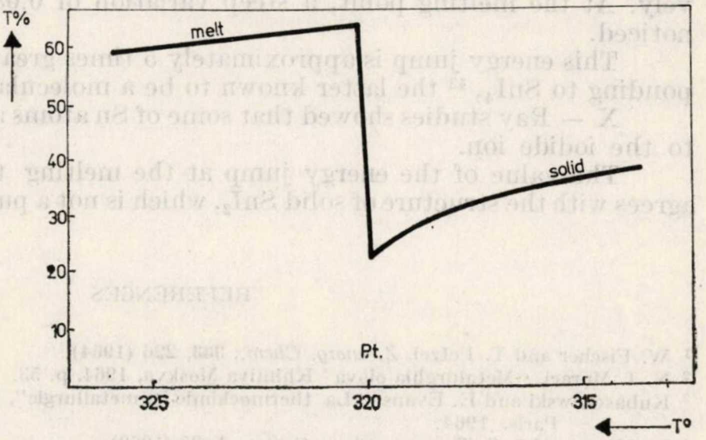

Fig. 2.a. — The variation of SnI_2 absorption at $\nu = 14\ 000\ cm^{-1}$ on increasing the temperature.

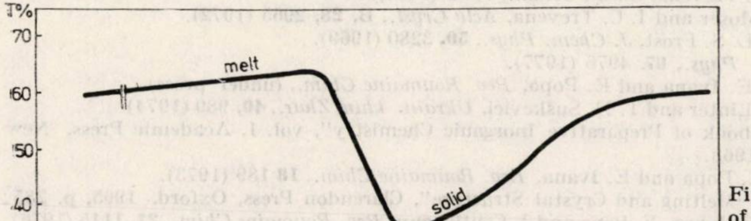

Fig. 2b — The variation of SnI_2 absorption at $\nu = 14\ 000\ cm^{-1}$ on the temperature decreasing.

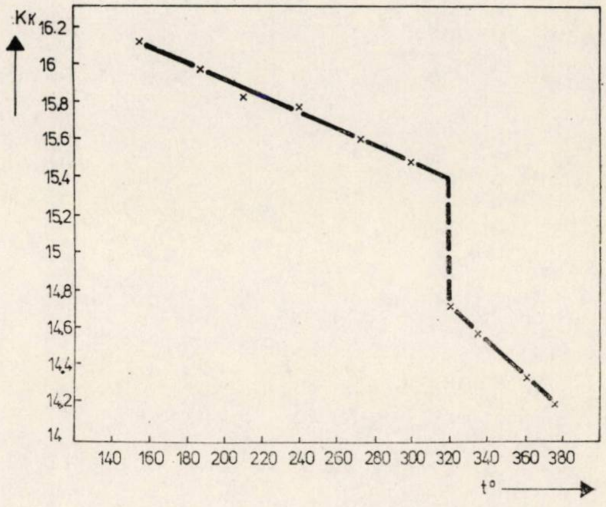

Fig.3. — The temperature dependence on SnI_2 absorption band edge for $T = 40\%$, $\Delta = 680\ cm^{-1}$.

vely. At the melting point, a steep variation of 0.084 eV (680 cm^{-1}) is noticed.

This energy jump is approximately 5 times greater than that corresponding to SnI_4, [13] the latter known to be a molecular crystal. [14]

X — Ray studies showed that some of Sn atoms are covalently bound to the iodide ion.

The value of the energy jump at the melting temperature (Fig. 3) agrees with the structure of solid SnI_2, which is not a purely ionic compound

REFERENCES

[1] W. Fischer and T. Petzel, *Z. anorg. Chem.*, **333**, 226 (1964).

[2] N. I. Muraci, "Metalurghia olova" Khimiya Moskva, 1964, p. 53.

[3] Kubaschewski and E. Evans, "La thermochimie en metallurgie", Gauthier — Villars, Edit., Paris, 1964.

[4] W. Moser and I. C. Trevena, *Chem. Comm.*, **1**, 25 (1969).

[5] R. A. Howie, W. Moser and I. C. Trevena, *Acta Cryst.*, B, **28**, 2965 (1972).

[6] R. Z. Zollweg and L. S. Frost, *J. Chem. Phys.*, **50,** 3280 (1969).

[7] J. Maya, *J. Chem. Phys.*, **67**, 4976 (1977).

[8] I. G. Murgulescu. E. Ivana and E. Popa, *Rev. Roumaine Chim.*, (under press).

[9] D. P. Blotki, I. A. Linter and T. N. Suskevici, *Ukrain. khim Zhur.*, **40**, 989 (1974).

[10] G. Brauer, "Handbook of Preparative Inorganic Chemistry", vol. 1, Academic Press, New York, 1963.

[11] I.G. Murgulescu, E. Popa and E. Ivana, *Rev. Roumaine Chim.*, **18** 189 (1973).

[12] A. R. Ubbelohde, "Melting and Crystal Structure", Clarendon Press, Oxford, 1965, p. 285.

[13] I. G. Murgulescu, E. Ivana, E. Popa and I. Contineanu, *Rev. Roumaine Chim.*, **21**, 1115 (1976).

[14] R. E. Wood and H. L. Ritter, *J. Amer. Chem. Soc.*, **74**, 1763 (1952).

Revue Roumaine de Chimie, 27, 7, 803—814 (1982)

STABILIZATION OF EMULSIONS BY SURFACE ACTIVE AGENTS

S. P. SINGH,[a] MISS MADHURI,[a] and P. BAHADUR[b] *

a Department of Chemistry, Agra College, Agra, India
b Department of Chemistry, South Gujarat University, Surat, India

Received November 29, 1979
Revised December 19, 1981

Surface active agents (anionic, cationic and non-ionic) were used as emulsifiers for xylene-in-water emulsions. Anionic and non-ionic emulsifiers produced negatively charged O/W type emulsions where as cationic surfactant stabilized emulsion droplets were positively charged. The influence of inorganic counter-ions with varying valency was examined on the coagulation of each emulsion. Electrophoretic and microscopic investigations were carried out. Energy calculations prove the validity of DLVO theory, and the flocculation in all cases was found reversible, which happens to occur in the secondary minimum region where the emulsion droplets are loosely trapped. Several adsorption parameters, flocculation and coalescence rate constants, free energy of adsorption etc. were calculated.

1. INTRODUCTION

The emulsifiers are known to be adsorbed around the oil globules in any oil-in-water (o/w) system where they keep the droplets sufficiently apart either by electric repulsion or by slowing down drainage of liquids from the thin film between the approaching globules or by purely mechanical means.

Surface active agents are of immense importance for emulsification. Several workers have attempted the stability and unstability of various hydrosols [1-4] and emulsions [5-7] in the presence of surfactants. In this paper attempts have been made to discuss the emulsion stability in the light of modern theories of colloid stability. Three surfactants belonging to each category have been chosen as emulsifying agents for the o/w type emulsions.

The coagulation of surfactant-stabilized systems is carried out by different inorganic ions and the stability of emulsions has been dealt with (i) by observing particle number with time and (ii) by electrophoretic measurements.

---

* Mailing address : Dr. P. BAHADUR, Reader in Chemistry Dept., South Gujarat University, Surat 395007 India

THEORETICAL

(a) The interaction energy

The interactions between the colloidal particles of lyophobic systems have been quantitatively treated by Derjaguin and Landau [8] and Verwey and Overbeek [9] on the basis of the free energy of the double layer and the London-van der Waals dispersion forces. According to their theory commonly known as DLVO theory, interaction energy on mutual approach of two particles is given by

$$V_{\text{total}} = V_R + V_A \tag{1}$$

where V_R is the repulsive energy and V_A is the attractive energy.

The repulsive energy calculations, between two spherical particles, were carried out by an approximate expression by Derjaguin and Kussakov.[10]

$$V_R = \frac{\varepsilon a \psi^2}{2} \text{In} \left[1 + \exp(-KH)\right] \tag{2}$$

where ψ is the surface potential (assumed to be equal to the zeta potential), ε is the dielectric constant in the double layer, 'a' is the particle radius, H the inter-particle distance and K is the Debye-Huckel parameter.

The attractive energies were calculated, keeping in view the retardation correction, by using the approximate equation due to Schenkel and Kitchener.[11] Two expressions are required for two different ranges of H. The equation

$$V_A = -\frac{Aa}{12H}\left[\frac{\lambda}{\lambda + 3.54\pi H}\right] \tag{3}$$

is valid for $H < 150$ Å
while the equation

$$V_A = -\frac{Aa}{\pi}\left[\frac{2.45\,\lambda}{120H^2} - \frac{\lambda^2}{1045H^3} + \frac{\lambda^3}{5.62 \times 10^4 H^4}\right] \tag{4}$$

is valid for $H > 150$ Å.
where λ is the wavelength of the London frequency, taken as 1000 Å and A is the van der Waals constant of the particle, π being 3.14.

Thus the interaction energy V could be evaluated and an energy profile could be drawn.

(b) The binding parameters at isoelectric point

The flocculating concentration (*i.e.*, the concentration of flocculating agent just required to bring the system at isoelectric point) has been determined from the point at which zeta potential-log C curves intersect x-axis (concentration axis).

The binding constants and free energy of adsorption of cations at zero point of charge can be calculated by the following treatment given by Wilkins and Ottewill.[12] On adding a small quantity of foreign ions (which in effect will not change the ionic strength), capable of being adsorbed or bound to the surfactants covering the emulsion droplets, the charge density will change and will be given by the Stern equation.[13]

$$\sigma s = \frac{N_1 \mathrm{ez}}{1 + (55.6/c)\exp(\Delta \mathrm{G}/kT)} \tag{5}$$

where N_1 is the number of the binding sites available per cm^2, ΔG is the free energy of adsorption per molecule and c is the molar concentration of the added electrolyte. This can be put in the form :

$$\sigma s = \frac{K_{1c}}{1 + K_{2c}} \tag{6}$$

where K_1 and K_2 are the adsorption constants and are given by

$$K_1 = N_1\, K_2 \mathrm{ez}. \tag{7}$$

$$K_2 = \exp(-\,\Delta G/kT)/55.6 \tag{8}$$

At the isoelectric point N_1 and constant K_2 can be evaluated by the following equations :

$$\frac{1}{c} = \frac{4\pi\, \mathrm{ez}\, N_1 N_2}{K\, \varepsilon\, \psi_0 \mathrm{s}} - K_2 \tag{9}$$

$$\left(\frac{\mathrm{d}\psi_\delta}{\mathrm{d}\ln C}\right)_{\psi_0\delta=0} = \left[\frac{\mathrm{e}\, \psi_0 \delta K}{4\pi\, \mathrm{ez}\, N_1} - 1\right]_{\psi_0\delta} \tag{10}$$

where z is the valency of counter-ions. C is the flocculating concentration of the electrolyte and $(\mathrm{d}\psi_\delta/\mathrm{d}\ln C)_{\psi_0\delta} = 0$ is the slope of the zeta potential $-\log C$ curve (assuming $\zeta = \psi)_0$. From the knowledge of N_1 and K_2, constant K_1 and the free energy of adsorption, ΔG, can be evaluated.

(c) The coagulation rate constants

The coagulation of an emulsion comprises two stages : flocculation and coalescence. Kinetically, flocculation is a bimolecular reaction and is represented by the equation :

$$-\frac{\mathrm{d}n}{\mathrm{d}t} = k_1 n^2 \text{ or } \frac{1}{n_1} - \frac{1}{n_0} = k_1 t \tag{11}$$

where n_0 is the number of oil droplets present initially and n_1 is the total number of droplets present at any time t. k_1 is the flocculation rate constant (Smoluchowski's rate constant) and denotes the frequency of collisions between two oil globules and is governed by the repulsive force between them.

Coalescence on the other hand is unimolecular and is shown as :

$$-\frac{dn}{dt} = k_2 n \quad \text{or} \quad \ln\frac{n_2}{n_0} = -k_2 t$$

$$\text{or} \quad n_2 = n_0\, e^{-k_2 t} \tag{12}$$

where n_2 is the number of individual droplets at any time t and k_2 is the coalescence constant which depends upon the lateral adhesion properties of the stabilizer film at the interface. From equations (11) and (12), $t_{\frac{1}{2}}$ the half-time of flocculation and coalescence is $k_1 n_0$ and $1/k_2$ respectively. The relative rates of flocculation and coalescence are thus evaluated by the ratio $\frac{k_1 n_0}{k_2}$ which if is $\gg 1$, the flocculation is very rapid and the coagulation of the system is determined entirely by the coalescence and vice-versa.

EXPERIMENTAL

(a) Materials

Extra pure samples of surfactants sodium cholate (Sigma), decyltrimethylammonium bromide (Eastman Kodak) and Triton X-100 (BDH) were purified and the purity was checked by observing no minima in surface tension curves. AnalaR (BDH) xylene was used as the oil phase. Double distilled water from all pyrex glass apparatus was used throughout the measurements. The flocculating salts used were metal nitrates *viz.* potassium, lead, chromium, lanthanum and thorium for negatively charged emulsions and bromide, sulphate, ferricyanide and ferrocyanide of potassium for positively charged emulsions. All these reagents were AR grade (BDN or E. Merck). Freshly prepared solutions of surfactants and electrolytes were used throughout the experiment.

(b) The emulsion

The xylene-in-water emulsions were prepared by suspending 1% by volume of the oil (xylene) in 0.01% aqueous surfacrant solution in 0.01 M KCl. The o/w mixture was hand shaken for fifteen minutes and finally homogenized twice through a stainless steel homogenizer (Schaar Scientific Co., Chicago). In all estimations, emulsions were prepared and sampled under similar conditions.

(c) The techniques

The particle concentration as well as flocculation studies of the emulsions with different electrolytes at their varying concentrations were carried out by counting the number of oil droplets present in a sample of an emulsion on a German double Neubaurer model haemocytometer at various intervals of time. Counts were taken in 50 squares of a calibrated graticule fitted in the eye piece (each square corresponding to a volume 5.397×10^{-8} ml) with a hand tally counter (Erma, Tokyo, Japan) under an Olympus microscope using 15×62 times magnification. A duplicate couting was always taken to determine the droplet number.

The particle size of the emulsions was determined from microphotographs, where the overall magnification amounted to 2400x. For each emulsion the diameter of 400 droplets was measured, thus allowing a size frequency curve to be drawn.

The electrophoretic mobility of emulsion droplets has been determined using Zeta-Meter. The emulsion droplets were tracked under a microscope as they migrated a distance *d* micron under an applied potential gradient, *v* volt, between two electrodes 1 cm apart; and the average migration time *t* second was measured by means of an electric timer.

The absolute electrophoretic mobility *U* could then be calculated from the equation:

$$U = \mathrm{d}.t/\mathbf{v}.t \tag{13}$$

The zeta potential in millivolt was obtained by the equation:

$$\zeta = 113000 \frac{\eta}{\varepsilon} U \tag{14}$$

where η and ε are the viscosity in poise and the dielectric constant of the suspended liquid respectively. The values of the conversion factor were obtained by interpolation from a large scale plot as a function of temperature.

RESULTS AND DISCUSSION

The zeta potential, particle size, initial number of droplets of the fresh diluted emulsions are recorded in table 1. The zeta potential values of emulsion have been plotted against concentration of flocculating salts for all the three emulsions in Figs 1—3. In general a decrease in the zeta potential has been observed with increasing salt concentration till the system reaches the isoelectric point. Further addition of electrolyte reverses the charge of the system and an increase in zeta potential was observed. However, the charge reversal could be seen for emulsions stabilized by ionic surfactants in the presence of tri- and tetravalent counterions. The decrease in the zeta potential of emulsion stabilized by non-ionic

TABLE 1

Zeta potential, size and number concentration of emulsions

Emulsifier	Zeta Potential (mV)	Average particle size (micron)	Initial number of droplets (per ml)
Sodium cholate	− 120.55	1.05	1.83×10^8
Decyltrimethylammonium bromide	+ 97.53	1.15	1.32×10^8
Triton X-100	− 43.20	1.15	1.23×10^8

Triton X-100 was slower and the charge reversal could not be observed here. The initial decrease in the zeta potential is due to the specific adsorption of counterions on the Stern layer. The flocculating concentrations of

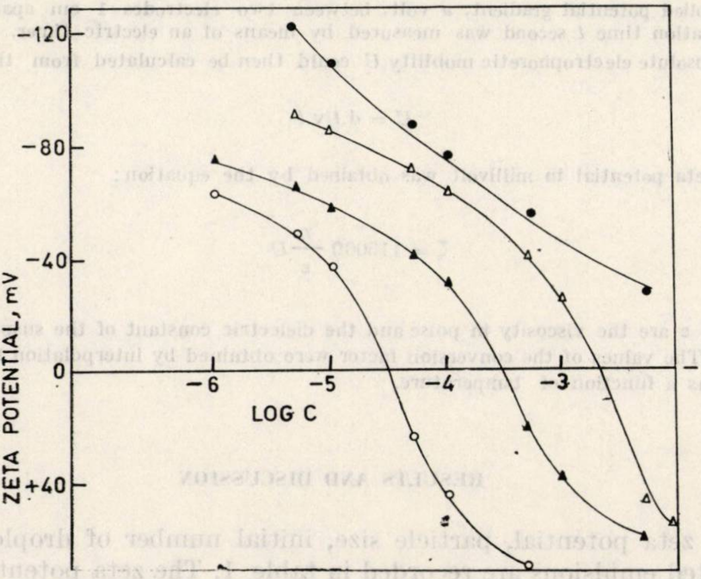

Fig. 1.— Plots of zeta potential against log molar concentration of electrolytes for sodium cholate stabilized emulsions.
● KNO_3, △ $Pb(NO_3)_2$, ▲ $La(NO_3)_3$, ○ $Th(NO_3)_4$.

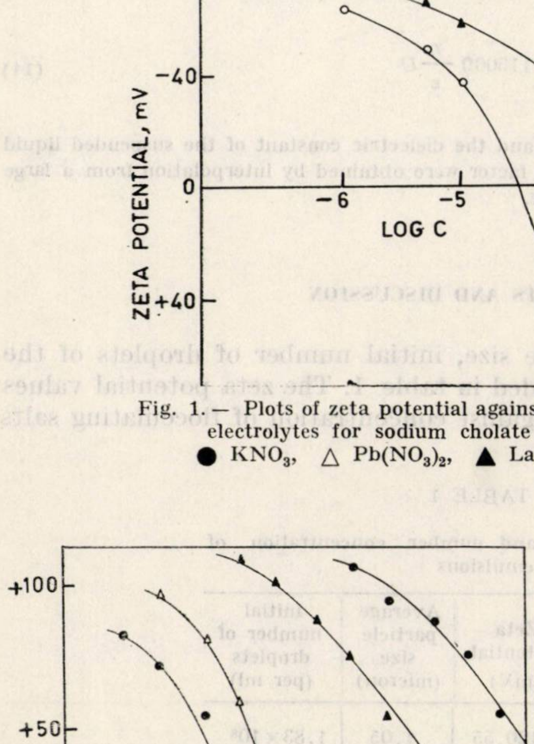

Fig. 2. Zeta potential against log molar concentration of electrolytes for decyltrimethylammonium bromide stabilized emulsion.
● KBr, ▲ K_2SO_4, △ $K_3[Fe(CN)_6]$, ● $K_4[Fe(CN)_6]$

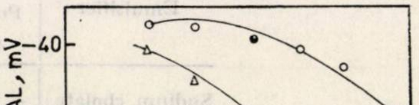

Fig. 3. — Plots of zeta potential against log molar concentration of electrolytes for triton X-100 stabilized emulsion.
○ $UO_2(NO_3)_2$, △ $La(NO_3)_3$, ● $Th(NO_3)_4$.

electrolytes have been recorded in Table 2. Obviously, the concentration values are dependent on the valency of counterions in the electrolytes used as flocculants.

The flocculation was examined by analysing the number concentration data obtained microscopically. Firstly, the number concentration n was plotted against time as denoted in Fig. 4 where the curves show an eventual levelling off owing to the temporary equilibrium state between monomeric and dimeric particles. Such an equilibrium implies the occurrence of the reversible flocculation which was further checked by gently shaking a flocculated emulsion where the aggregates were redispersed and the equilibrium was once more disturbed.

TABLE 2

Flocculating concentrations of electrolytes

Emulsion stabilized by	Flocculating agent	Flocculating concentration (mol/litre)
Sodium cholate	$Pb(NO_3)_2$	3.37×10^{-3}
	$La(NO_3)_3$	3.16×10^{-4}
	$Th(NO_3)_4$	3.55×10^{-5}
Decyltrimethylammonium bromide	$K_3(Fe(CN)^6]$	6.65×10^{-5}
	$K_4[Fe(CN)^6]$	1.30×10^{-5}

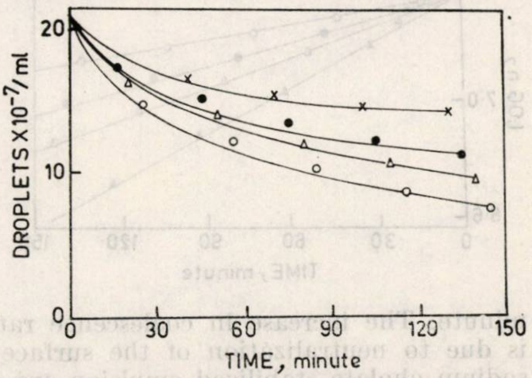

Fig. 4.— Plots of individual droplets against time for sodium cholate stabilized emulsion flocculated by $Pb(NO_3)_2$
× 1×10^{-5}M, ● 5×10^{-5}M, △ 1×10^{-4}M, ○ 5×10^{-4}M.

The plots of $\frac{1}{n_1}$ against t (Fig. 5) were linear and show the extent of flocculation in the presence of electrolytes. It is evident that the rate of flocculation increases with the increasing concentration of electrolytes and consequently the Smoluchowski rate constant K_1 increases. Increase in rate constant can be attributed to the partial neutralization of the surface charge rather than destruction in the surface elasticity.

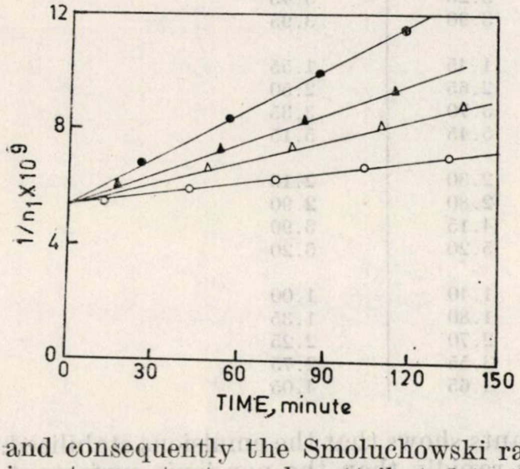

Fig. 5.— Plots of reciprocal number of droplets against time for sodium cholate stabilized emulsion flocculated by $Pb(NO_3)_2$
○ 1×10^{-5}M, △ 5×10^{-5}M, ▲ 1×10^{-4}M, ● 5×10^{-4}M.

The coalescence rates in the system are shown in Fig. 6 where the values of log n_2 are plotted against time. The value of coalescence rate constant is of the order of 10^{-3} min^{-1} which show that out of every thousand oil droplets contained in aggregates two will coalescence per minute. The increase in coalescence rate with electrolyte concentration is due to neutralization of the surface charge. The rate constants for sodium cholate stabilized emulsion are given in Table 3.

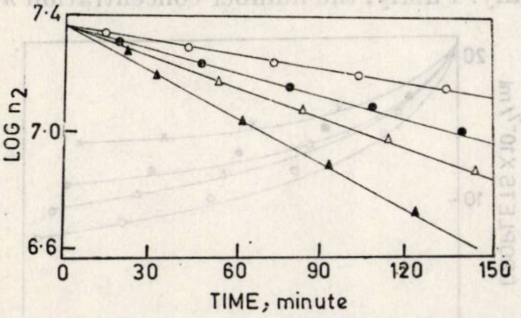

Fig. 6. — Plots of logarithm of number of droplets against time for sodium cholate stabilized emulsion flocculated by $Pb(NO_3)_2$
○ 1×10^{-5}M, ● 5×10^{-5}M, △ 1×10^{-4}M, ▲ 5×10^{-4}M.

TABLE 3

Rate constants for flocculation and coalescence of sodium cholate stabilized emulsion

Electrolyte concentration (mol/litre)	Flocculation rate constant $K_1\times10^9$ (cm^3 min^{-1})	Coalescence rate constant $K_2\times10^3$ (min^{-1})
KNO_3		
1×10^{-5}	1.10	1.60
5×10^{-5}	2.05	2.70
1×10^{-4}	2.65	3.00
5×10^{-4}	3.25	3.45
1×10^{-3}	3.90	3.95
$Pb(NO_3)_2$		
1×10^{-5}	1.45	1.55
5×10^{-5}	2.65	2.50
1×10^{-4}	3.70	3.35
5×10^{-4}	5.45	5.15
$La(NO_3)_3$		
1×10^{-6}	2.30	2.10
5×10^{-6}	2.80	2.90
1×10^{-5}	4.15	3.90
5×10^{-5}	5.20	5.20
$Th(NO_3)_4$		
1×10^{-6}	1.40	1.00
5×10^{-6}	1.80	1.35
1×10^{-5}	2.70	2.25
1×10^{-4}	3.55	2.75
5×10^{-4}	4.65	4.05

An examination of rate constants shows that the emulsions stabilized by ionic surfactants flocculate less rapidly than the non-ionic surfactant stabilized emulsions which may be due to the charge on the droplets in the former case. Non-ionic stabilized emulsions are characterised by showing low degree of coalescence because of the stabilization due to steric hinderance which is a result of bulkyness of the non-ionic surfactants. The steric stabilization induced by such surfactants has been explained by the theory of entropy stabilization.[14]

The interaction energies of the double layer around the particle for different electrolyte concentrations were calculated by taking the algebraic sum of potential energy of repulsion and attraction using equations 1—4. The van der Waals constant was taken equal to 3.16×10^{-13} erg (a value for pure xylene dispersed in water calculated using some theoretical equations).[15] The interaction energies have been plotted as a function of distance in the presence of different electrolytes, as represented in Figs 7—10 for sodium cholate emulsion only. The nature of the curves was the same for other two emulsions also.

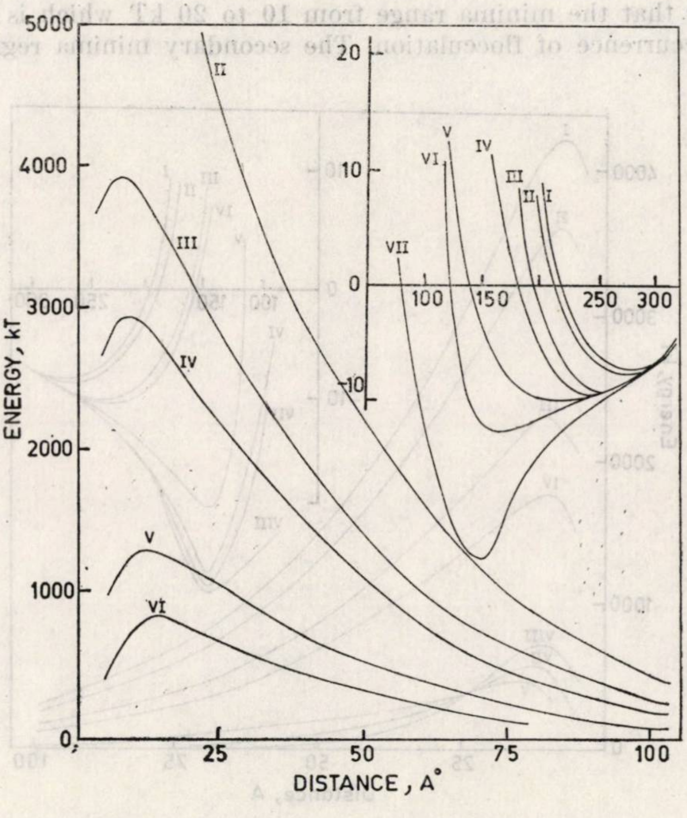

Fig. 7 — Plots of interaction energy *vs* interparticle distance for sodium cholate system flocculated by KNO_3
I 5×10^{-6}M, II 1×10^{-5}M, III 5×10^{-5}M,
IV 1×10^{-4}M, V 5×10^{-4}M, VI 1×10^{-3}M,
VII 5×10^{-3}M.

For emulsions stabilized by ionic detergents the interaction energies possess very high energy barrier ≫ 25 kT and thus the systems are highly stable and the possibility of occurrence of flocculation in the primary minima is completely excluded. The magnitude of energy barrier depends on zeta potential and double layer thickness which vary with the electrolyte content and valency. The addition of electrolyte causes a compression of the diffused layer around the particles and may, in addition, exert a specific effect through ionic adsorption into the Stern layer leading to a decrease in zeta-potential; this behaviour increases with the increasing valency.

From the plots of elaborated secondary minima shown in Figs. 7—10 it is clear that the minima range from 10 to 20 kT which is reasonable for the occurrence of flocculation. The secondary minima region mainly depends on attraction term which varies with particle size and the van der Waals constant. Significant secondary minima in the system exist because of the larger particle size as shown in the suspensions by earlier workers.[16-18]

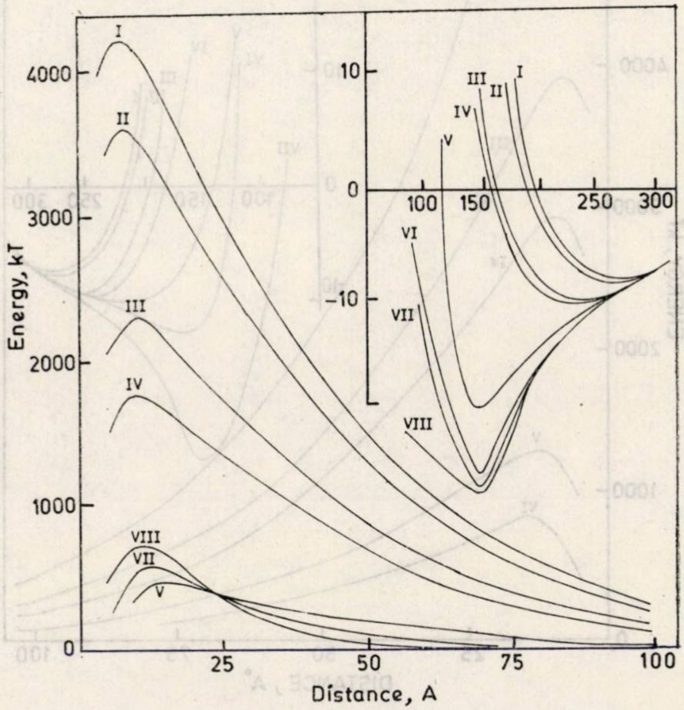

Fig. 8. — Plots of interaction energy *vs.* interparticle distance for sodium cholate system flocculated by $Pb(NO_3)_2$
I 5×10^{-6}M, II 1×10^{-5}M, III 5×10^{-5}M,
IV 1×10^{-4}M, V 5×10^{-4}M, VI 1×10^{-3}M,
VII 5×10^{-3}M, VIII 1×10^{-2}M.

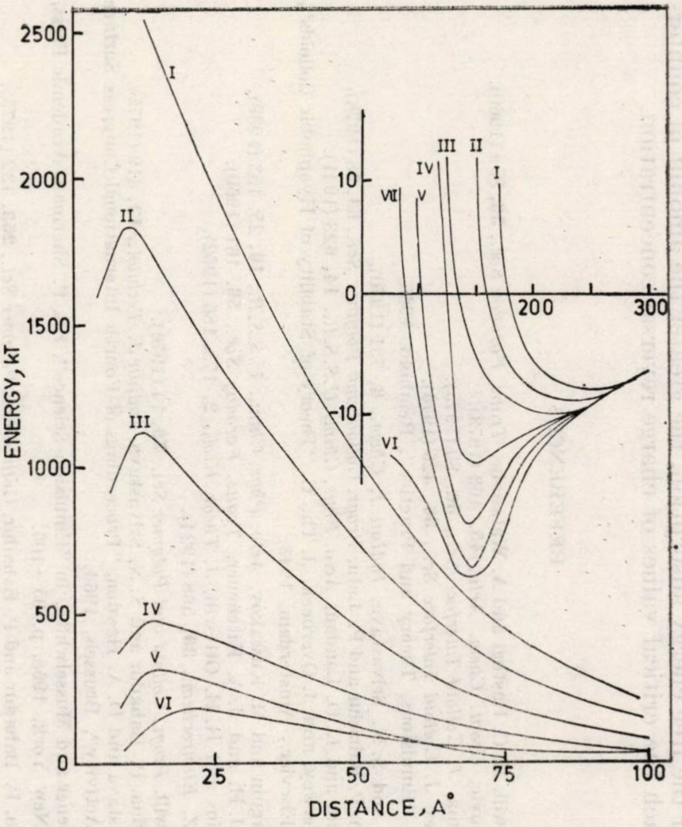

Fig. 9.— Plots of interaction energy *vs.* interparticle distance for sodium cholate system flocculated by $La(NO_3)_3$
I 1×10^{-6}M, II 5×10^{-6}M, III 1×10^{-5}M,
IV 5×10^{-5}M, V 1×10^{-4}M, VI 5×10^{-4}M,
VII 1×10^{-3}M.

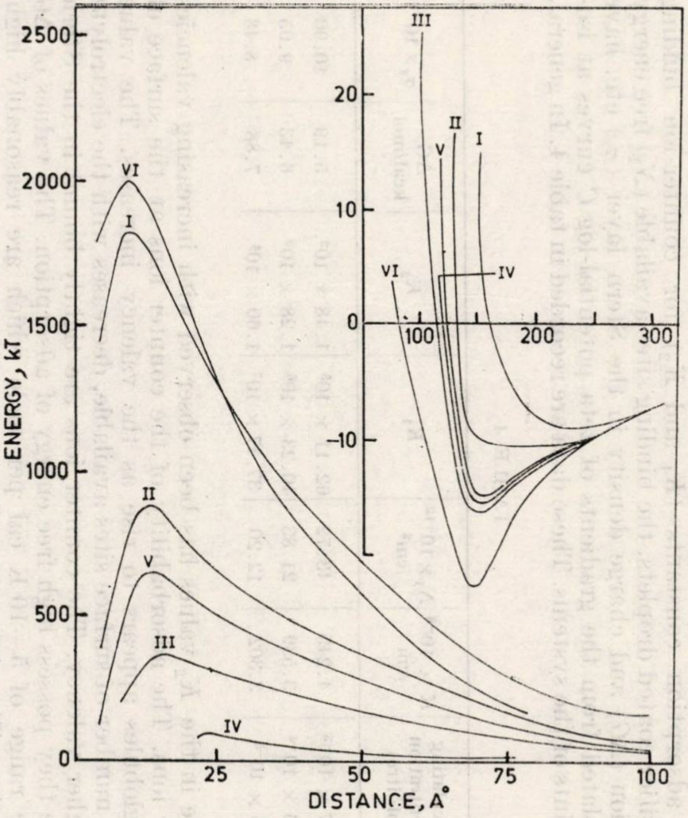

Fig. 10.— Plots of interaction energy *vs.* interparticle distance for sodium cholate system flocculated by $Th(NO_3)_4$
I 1×10^{-6}M, II 5×10^{-6}M, III 1×10^{-5}M,
IV 5×10^{-5}M, V 1×10^{-4}M, VI 5×10^{-4}M.

The adsorption constants (K_1 and K_2) for counter-ion binding with emulsifier coated droplets, the binding sites available (N_1) free energy of adsorption (ΔG) and charge density in the Stern layer (σ_s) etc. have been calculated from the gradients of zeta potential-log C curves at isoelectric points of the systems. These data are recorded in table 4. In general, an increase in the K_2 values has been observed with increasing valencies of counter ions. The adsorbability of the counter ions at the surface of emulsion globules appears to rise as the valency increases. The value of N_1, the number of surface sites available, decreases with the electrolyte having higher valency. The counter ions are tightly bound in the Stern layer since they possess high free energy of adsorption. The values of ΔG are in the range of 5—10 K cal per mole which are reasonably high for adsorption. The ΔG values increase with the counter-ion valency which indicates the influence of valency of the flocculated power because the smaller the free energy adsorption, the greater the amount of counter-ions to reach the critical values of charge reversal concentration.

TABLE 4

Cation	Flocculating concentration (mol/litre)	$K \times 10^{-6}$ /cm	$N_1 \times 10^{-12}$ /cm^2	K_1	K_2	ΔG kcal/mol	$\sigma_s \times 10^{-3}$
Pb^{+2}	3.37×10^{-3}	4.245	43.72	62.11×10^5	1.48×10^2	5.19	10.90
La^{+3}	3.16×10^{-4}	3.539	21.83	40.23×10^6	1.28×10^3	6.43	9.05
Tn^{+4}	3.55×10^{-5}	3.302	12.20	37.47×10^7	1.60×10^4	7.88	8.48

REFERENCES

[1] R. H. Ottewill, M. C. Rastogi and A. Watanabe, *Trans. Faraday Soc.*, **56**, 854 (1960).

[2] R. Despotovic, *Croat. Chem. Acta*, **45**, 163 (1973).

[3] N. Moriyama, *J. Colloid Interface Sci.*, **50**, 80 (1975).

[4] J. B. Kayes, *J. Colloid Interface Sci.*, **56**, 426 (1976).

[5] P. Becher, "Emulsions, Theory and Practice". Reinhold, 1965.

[6] S. P. Jain and S. N. Srivastava, *Indian J. Chem.*, **8**, 731 (1970).

[7] L. R. Singh, P. Bahadur and P. Lata, *Progr. Colloid and Polymer Sci.*, **63**, 68 (1978).

[8] B. Derjaguin and L. D. Landau, *Acta. Phys. Chim. U.S.S.R.*, **14**, 623 (1941).

[9] E. J. W. Verwey, and J. Overbeek, J. Th. G. "Theory of Stability of Hyophobic Colloids", Elsevier., Amsterdam, 1948.

[10] B. V. Derjaguin and M. Kussakov, *Acta. Phys. Chim., U.S.S.R.*, **10**, 25, 153 (1939).

[11] Schenkel, J. H. and J. A. Kitchener, *Trans. Faraday Soc.*, **56**, 161 (1960).

[12] D. J. Wilkins and R. H. Ottewill, *J. Theor. Biol.*, **2**, 173, 186 (1962).

[13] O. Stern, *Z. Electrochem.*, **30**, 568 (1924).

[14] R. H. Ottewill, *Progr. Colloid and Polymer Sci.*, **59**, 14 (1976).

[15] M. K. Sharma, P. Bahadur and S. N. Srivastava, *Indian J. Technol.*, **13**, 419 (1975).

[16] S. N. Srivastava and D. A. Haydon, "Proceedings of Fourth International Congress Surface Activity", Brussels, 1964.

[17] J. A. Kitchener and Musselwhite. In "Emulsion Science", Ed. P. Sherman, Academic Press, New York, 1968, p. 95—106.

[18] R. P. Verma, P. Bahadur and P. Bahadur, *Colloid and Polymer Sci.*, **253**, 132 (1975).

Revue Roumaine de Chimie, 27, 7, 815–821 (1982)

KINETIC ANALYSIS OF THERMOGRAVIMETRIC DATA. XV[1]

THERMAL DECOMPOSITION OF $[Co(en)_2(pyridine)\,Br]\,X_2$ TYPE COMPLEXES

J. ZSAKÓ, GH. MARCU and MARIA VÁRHELYI
Faculty of Chemical Technology, "Babeş-Bolyai" University, str. Arany János 11, 3400 – Cluj-Napoca, Romania

Received July 22, 1980

Kinetic parameters of the pyridine substitution by the outer sphere anion have been derived from the TG curves of $[Co(en)_2(pyridine)Br]Br_2$ and $[Co(en)_2(pyridine)Br]I_2$, by using the author's nomogram method and the Coats-Redfern method. The influence of sample weight and of heating rate have been studied. Statistical analysis of the results shows the apparent activation energy E to decrease in the order Br > I, while both E and pre-exponential factor values show a tendency to decrease with increasing sample weight and increasing heating rate. The kinetic compensation effect is discussed.

The first stage of the thermal decomposition of the $[Co(en)_2(amine)X]Y_2$ type complexes is a deamination reaction consisting presumably of the substitution of the amine molecule by an outer sphere anion :

$$[Co(en)_2(amine)X]Y_2 \rightarrow [Co(en)_2XY]Y + amine$$

Our TG study performed with complexes of this type, having amine = pyridine, X = Cl, Y = Cl, Br, I, showed a weight loss stop on the TG curves corresponding to the loss of a pyridine molecule.[2]

In the present paper a similar study has been made, by using analogous complexes with amine = pyridine, X = Br and Y = Br, I.

TG curves were recorded by using different heating rates (q) and different sample weights (G_0).

A typical TG curves of each compound studied is given in Fig. 1. The horizontal dashed line indicates the sample weight corresponding to the total loss of the pyridine. As seen, no well defined weight loss stop can be observed at the presumed $[Co(en)_2XY]Y$ intermediate, only a change of slope of the TG curves appears and even this at higher sample weight values than expected.

In Fig. 1 this change of slope is marked by an arrow. The mean value of the conversion of the initial complex into the presumed intermediate is of 0.93 in the case of the bromide and of only 0.81 with the iodide.

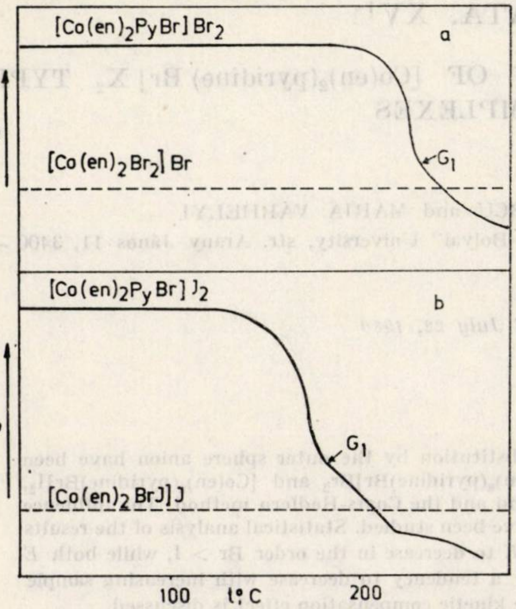

Fig. 1. – Typical TG curves of the complexes studied. a – $G_0 = 25$ mg, $q = 5$K/min ; b – $G_0 = 75$ mg, $q = 10$ K/min.

Although this deamination reaction is not complete, an attempt has been made to derive kinetic parameters, by presuming the first stage of the thermal decomposition to be finished at the above mentioned change of the slope.

DERIVATION OF KINETIC PARAMETERS

In order to characterize the TG curves obtained, the following kinetic parameters were derived: apparent reaction order n, activation energy E and pre-exponential factor Z.

Two methods were used, the nomogram method proposed in our previous paper [3] and the Coats- Redfern method, modified as described earlier.[2]

By using the experimentally obtained time-weight pairs, the TG curves were constructed for the first thermal decomposition stage, by plotting the fraction of the compound not transformed, $1-\alpha$, versus temperature (α is the transformation degree or conversion). The conversion was calculated by means of the formula

$$\alpha = \frac{G_0 - G}{G_0 - G_1}$$

where G_0, G and G_1 stand for the initial weight, actual weight and for the weight corresponding to the change of slope mentioned above.

In the case of the nomogram method, the quantities $\vartheta_{0.1}$, $\vartheta_{0.5}$ and $\vartheta_{0.9}$ (the reciprocal absolute temperature values corresponding to the conversion values $\alpha = 0.1, 0.5$ and 0.9 respectively) were determined graphically, by using the cited TG curves. The shape and position parameters

$$\nabla = \frac{\vartheta_{0.5} - \vartheta_{0.9}}{\vartheta_{0.1} - \vartheta_{0.9}}, \quad \Delta = 10^6(\vartheta_{0.1} - \vartheta_{0.5})$$

and

$$\tau = 10^3\ \vartheta_{0.1}$$

were calculated and used for the determination of kinetic parameters as described earlier.[3] Since the heating rates were very close (or even identical) to the value 10 K min^{-1}, taken as standard in the construction of the nomogram, two iteration cycles were sufficient; *i.e.*the second approximations could be taken as final values. Interpretations were performed by using the interpolation curve given in our previous paper.[2]

In our nomogram method the determination of the apparent reaction order n is based on an empirical formula expressing the correlation between n and the shape parameter ∇. This formula has been derived by considering the maximum possible value of n to be of about $n = 2$. Since in our previous paper [2] much higher n values were obtained and in these cases our formula gave lower n values than those obtained by using the Coats-Redfern method, a modification of this formula seemed to be necessary.

By calculating the shape parameter of the theoretical TG curves corresponding to n values comprised between 2 and 4, we could establish the following empirical formula, which gives a good approximation if $0 < n < 4$:

$$\nabla = 0.268 + 0.136\,\text{n} - 0.011\,\text{n}^2$$

Byfusing this formula, the nomogram method and the Coats-Redfern method gives practically the same results.

In the case of the Coats-Redfern method the same TG curves (plot of $(1 - \alpha)$ *vs.* T) were used as in the nomogram method and 9 temperature values were graphically derived, corresponding to $\alpha = 0.1, 0.2, 0.3 \ldots 0.8$ and 0.9. Kinetic parameters were derived as described earlier.[2]

RESULTS AND DISCUSSIONS

The kinetic parameters derived by means of both methods are presented in tables 1 and 2. The values obtained by means of the Coats-Redfern method are denoted as n_{CR}, E_{CR} and log Z_{CR}. Z and Z_{CR} values are calculated in s^{-1}. The same tables contain also the reduced position parameter τ^*.

TABLE 1

Kinetic parameters of thermal deamination of *cis*-[Co(en)$_2$(pyridine)Br] Br$_2$

Heating rate, K min^{-1}	Sample weight, mg	n	n_{CR}	E kJ mol^{-1}	E_{CR} kJ mol^{-1}	log Z	log Z_{CR}	τ^*
5	25	1.07	1.08	373	386	37.2	38.6	2.034
	50	0.65	0.62	280	279	26.6	26.5	2.002
	75	0.86	0.80	322	322	31.6	31.7	2.035
	100	1.69	1.73	335	313	32.9	30.4	2.026
10	25	3.49	3.44	605	604	60.0	61.0	2.006
	50	0.97	1.03	318	310	31.0	30.3	2.033
	75	0.99	0.89	334	329	32.5	32.0	2.010
	100	0.71	0.75	280	282	26.9	27.2	2.022
15	25	0.56	0.61	308	308	29.8	29.8	2.015
	50	2.43	2.48	352	357	34.7	35.7	2.050
	75	2.71	2.84	431	436	42.8	43.1	2.001
	100	1.73	1.70	291	296	28.3	28.7	2.029

TABLE 2

Kinetic parameters of thermal deamination of *cis*-[Co(en)$_2$(pyridine)Br] I$_2$

Heating rate, K min^{-1}	Sample weight, mg	n	n_{CR}	E kJ mol^{-1}	E_{CR} kJ mol^{-1}	log Z	log Z_{CR}	τ *
5	25	1.88	1.89	275	255	31.3	28.8	2.358
	50	1.19	1.31	224	223	25.0	24.8	2.352
	75	0.83	0.91	214	207	23.6	22.6	2.347
	100	1.62	1.73	418	434	48.8	50.6	2.338
10	25	2.30	2.25	243	220	27.0	24.0	2.325
	50	1.23	1.33	171	165	18.2	17.6	2.350
	75	1.29	1.29	172	171	18.5	18.4	2.357
	100	2.11	2.03	252	236	28.0	25.9	2.323
15	25	1.17	1.16	100	96	9.5	9.1	2.404
	50	0.64	0.72	144	147	15.1	15.5	2.382
	75	1.35	1.37	178	184	19.3	19.5	2.306
	100	1.41	1.37	171	166	18.3	17.7	2.353

As seen from these tables, both methods give nearly the same values for all kinetic parameters. As regards the influences of the sample weight and heating rate, no systematic variation of the kinetic parameters can be observed. Generally, the values obtained are rather scattered. Only the reduced position parameter τ^* has a practically constant value.

In order to obtain a clearer picture, a statistical analysis of the data obtained has been performed. For this purpose, the mean values of the kinetic parameters have been calculated separately for each compound, for sample weights and heating rates used. These mean values are presented in tables 3 and 4.

TABLE 3

Mean values of the kinetic parameters of *cis*-[Co(en)$_2$(pyridine) Br] Br$_2$

	n	n_{CR}	E kJ mol^{-1}	E_{CR} kJ mol^{-1}	$\log Z$	$\log Z_{CR}$	τ^*
25 mg sample	1.71	1.71	429	433	42.3	43.1	2.018
50 mg sample	1.35	1.38	317	316	30.8	30.8	2.028
75 mg sample	1.52	1.51	362	362	35.6	35.6	2.015
100 mg sample	1.38	1.39	302	297	29.4	28.8	2.029
$q = 5$ K/min	1.07	1.06	327	325	32.1	31.8	2.024
$q = 10$ K/min	1.54	1.53	384	381	37.6	37.6	2.020
$q = 15$ K/min	1.86	1.91	345	349	33.9	34.3	2.024
general mean	1.49	1.50	352	352	34.5	34.6	2.023

TABLE 4

Mean values of the kinetic parameters of *cis*-[Co(en)$_2$(pyridine) Br] I$_2$

	n	n_{CR}	E kJ mol^{-1}	E_{CR} kJ mol^{-1}	$\log Z$	$\log Z_{CR}$	τ^*
25 mg sample	1.78	1.77	205	190	22.6	20.6	2.362
50 mg sample	1.02	1.12	180	179	19.4	19.3	2.361
75 mg sample	1.16	1.19	190	187	20.5	20.2	2.337
100 mg sample	1.71	1.71	280	278	31.7	31.4	2.338
$q = 5$ K/min	1.38	1.46	283	280	32.2	31.7	2.349
$q = 10$ K/min	1.73	1.72	210	198	22.9	21.5	2.339
$q = 15$ K/min	1.14	1.15	149	148	15.6	15.4	2.361
general mean	1.42	1.45	214	209	23.5	22.9	2.350

This statistical analysis reveals no systematic variation of the apparent reaction order n with the sample weight, but it shows the increase of n with increasing heating rate q, which is very significant in the case of the bromide, but even not relevant with the iodide.

The apparent activation energy E and pre-exponential factor Z show a decreasing tendency with increasing sample weight, more clearly in the case of the bromide and a decreasing tendency with increasing heating rate, very obviously with the iodide.

As far as the physical meaning of these effects is concerned, if n increases with increasing heating rate, or E decreases both with increasing sample weight and with increasing heating rate, this means simply, that the temperature interval corresponding to the thermal decomposition increases with increasing sample weight and heating rate. The explanation of these effects, also observed in our previous papers,could be the limitation of the heat transfer or of the diffusion rate of the gaseous product evolved.

The general mean values obtained by means of both methods used are practically the same, which shows their equivalency with respect to the values of the kinetic parameters derived.

As seen from tables 1 and 2, E and $\log Z$ vary in parallel. The validity of a linear kinetic compensation law of the type

$$\log Z = aE + b$$

has been tested, by using all $E - \log Z$ and $E_{CR} - \log Z_{CR}$ pairs, *i.e.* 24 points for each compound. By means of the least square method the compensation parameters a and b, given in table 5, have been derived. The same table contains Jaffé's correlation coefficient ρ and its very high values indicate a practically perfect linearity.[4]

TABLE 5

Kinetic compensation parameters of the deamination reaction

Compound	a	b	ρ
$[Co(en)_2(pyridine)Br]Br_2$	0.104	−1.962	0.999
$[Co(en)_2(pyridine)Br]I_2$	0.124	−2.748	1.000

The mean values of E calculated for the 2 complexes studied are rather different and they decrease in the order Br $>$ I. This result shows that the kinetic parameter E does have some real physical significance, related to the chemical reaction occurring. It is true that the individual values of the kinetic parameters are affected very much by the working conditions (controlled and uncontrolled ones) and this is why the data presented in tables 1 and 2 are scattered. Nevertheless, the mean values for several runs performed under the same conditions for the two complexes are rather different. The decrease of the mean activation energy in the above order means the decrease of the real activation energy of the deamination reaction in the same order.

The general picture obtained is very similar to that found with the analogous chloro-complexes.[2] In order to compare the behaviour of the chloro and bromo complexes we present in table 6 the mean value of the kinetic parameter E calculated from both E and E_{CR} values, as well as the compensation parameter a.

TABLE 6

Comparison of activation and compensation parameters of analogous bromo- and chloro complexes

Compound	E, k J/mol	a mol/kJ	a' mol/kJ
$[Co(en)_2(pyridine)Cl]Br_2$	375	0.105	0.105
$[Co(en)_2(pyridine)Cl]I_2$	127	1.123	0.124
$[Co(en)_2(pyridine)Br]Br_2$	352	0.104	0.106
$[Co(en)_2(pyridine)Br]I_2$	212	0.124	0.123

As seen from this table, E values of the bromides are much higher than those of iodides. One can presume the Co-pyridine bond to be weakened by a polarization effect,which is more important with the iodides. On the other hand, this difference is much less in the case of the bromo complexes as compared to the chloro ones.

As far as the interpretation of the kinetic compensation effect is concerned, we presumed earlier that the weaker the chemical bond to be broken, the higher the compensation parameter a.[5] Data presented in table 6 are in perfect agreement with this hypothesis.

On the other hand, Garn [6] presumes this parameter a to represent simply $\log e/RT_c$, where T_c stands for a certain decomposition temperature. By taking for $1/T_c$ the reduced position parameter τ^* multiplied by 10^{-3}, one obtains

$$a' = \frac{\tau^* . 10^{-3} \log e}{R}$$

The a' values calculated from the mean values of τ^* (by introducing the value of R in kJ/mol.K) are presented in the same table 6. As seen, the a' values are practically identical with the a values derived by linear regression from the experimental $\log Z - E$ pairs. This means, that Garn's hypothesis seems to be correct and the compensation parameter a might be related to a standard decomposition temperature represented to a first approximation by the relation $T_c = 10^3/\tau^*$.

EXPERIMENTAL

Synthesis of *cis*-$[Co(en)_2Br(pyridine)]X_2$ complex salts. 0.1 mole *trans*-$[Co(en)_2Br_2]Br$ is dissolved in 150 ml water and 9.0 g (0.11 mole) of pyridine is added drop by drop. The green solution gradually becomes violet-red. After standing about 5–6 hours the solution is diluted to 200 ml and the *cis*-$[Co(en)_2Br(pyridine)]Br_2$ and *cis*-$[Co(en)_2Br(pyridine)]I_2$ are obtained from 100–100 ml solutions by double decomposition reactions with 40 g NaBr in conc. aqueous soln and with 20–25 g KI in 100 ml water. The crystalline products were filtered off, washed with a little ice water and dried in air.

The purities of the complex salts were controlled by determination of the cobalt (complexometrically) and of the halide (potentiometrically with $AgNO_3$ solution) contents.

For assignement of the geometrical configuration, we used the IR absorption band of the cobalt – ethylenediamine ring system (the splitting of the CH_2 rocking band in the 870–890 cm^{-1} region).[7]

Thermogravimetric measurements were performed by means of a thermobalance [8] by using a linear temperature program with the constant heating rates $q = 5$, 10 and 15 K min^{-1}. As sample holder a platinum crucible was used.

REFERENCES

[1] Previous part : J. Zsakó and J. Zsakó jr., *J. Thermal Anal.* **19**, 333 (1980).
[2] J. Zsakó, Maria Várhelyi and Cs. Várhelyi, *J. Thermal Anal.*, **17**, 123 (1979).
[3] J. Zsakó, *J. Thermal Anal.*, **15**, 369 (1979).
[4] H. H. Jaffé, *Chem. Rev.*, **53**, 191 (1953).
[5] J. Zsakó, Cs. Várhelyi, G. Lipaty and K. Szilágyi, *J. Thermal Anal.*, **7**, 41 (1975).
[6] P. D. Garn, *J. Thermal Anal.*, **7**, 475 (1975) ; **10**, 99 (1976).
[7] M. E. Baldwin, *J. Chem. Soc.*, **1960**, 4369.
[8] L. Erdey and F. Paulik, *Magy. Tud. Akad. Kém. Oszt. Közl.*, **5**, 461 (1955) ; L. Kékedy, P. Kröbl, Á. Szurkos and E. Kékedy, *Stud. Univ. Babeş-Bolyai, Chem.*, **3** 99 (1958).

Revue Roumaine de Chimie, 27, 7, 823—830 (1982)

RÔLE DE LA CHAÎNE ALIPHATIQUE DANS LA TRANSMISSION DES EFFETS D'UN AUXOCHROME ÉLECTRO-ATTRACTEUR SUR LE CHROMOPHORE DES N-PHÉNYL-ALCOYLAMINES

BERNARD VIDAL

Laboratoire de Physicochimie C2, UER de Chimie, Université des Sciences et Techniques de Lille 59655 — Villeneuve d'Ascq cédex, France

Recu: 13 Janvier 1981

Un auxochrome électroattracteur situé en ω par rapport au chromophore benzénique d'une chaîne aliphatique, bien qu'il exerce son influence à une distance d'autant plus grande qu'il est électroattracteur, voit cette influence subir une loi de décroissance d'autant plus rapide qu'il est précisément plus électroattracteur. Nous interprétons ce phénomène, observé en étudiant dans le proche ultra-violet le spectre des n-phénylalcoylamines dans divers solvants, sur la base d'un effet inductif variable de la fraction aliphatique de la chaîne.

The near UV spectra of n-phenylakylamines in various solvents show that for the aliphatic chain included between the chromophore and the electron-withdrawing auxochrome inductive effects are far from being a constant for a given length.

Dans l'étude spectroscopique UV des interactions lointaines la participation de la chaîne aliphatique, reliant le chromophore à l'auxochrome qui lui impose une perturbation, est, si l'on excepte les effets à travers l'espace,[1] mal connue. Nous proposons ici une première approche pour cerner le rôle de celle-ci. Notre étude sera basée sur la transmission, dans le cas des n-phénylalcoylamines, des effets électroniques de l'azote au niveau du chromophore pour des chaînes de longueur variable dans des milieux différents.

On sait qu'en première approximation le méthylène α, par ses effets donneurs, perturbe la symétrie hexagonale du nuage π du benzène provoquant ainsi l'apparition du système B, et de la bande 00, dans la „bande secondaire". L'intensité de ce système croît ou décroît selon qu'un substituant fixé sur le méthylène α, exalte l'effet donneur de celui-ci, donc la perturbation de symétrie, ou le diminue.[2,3]

PHÉNOMÈNES EXPÉRIMENTAUX

La diminution d'efficacité de l'auxochrome, si l'on excepte le cas du benzylammonium dont nous parlerons plus loin, avec l'accroissement du nombre de chainons conduit à une augmentation de la perturbation du chromophore par le méthylène α, donc à une augmentation de ε_{00} au moyen duquel on évalue l'intensité de *B*.[4] Hormis toujours le benzylammonium, les homologues de la série protonée ont des valeurs ε_{00} inférieures à celles correspondant aux fonctions non protonées. Les variations des courbes $\varepsilon_{00} = f(\mathrm{pH})$ sont moins marquées quand la chaîne s'allonge, bien que les pK ne devraient pas entre les derniers termes évoluer de façon prononcée (Fig. 1).

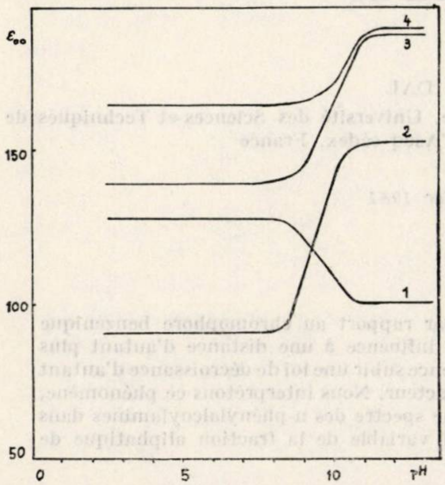

Fig. 1. — Evolution de ε_{00} en fonction du pH. Le chiffre à droite des courbes correspond au nombre de carbones de la chaîne ($\Phi-(CH_2)_nNH_2$)

On peut attribuer la décroissance très importante, sauf en ce qui concerne la benzylamine, de ε_{00} lors de la protonation, à ce que NH_3^+ étant beaucoup plus électroattracteur que NH_2 est plus efficace pour diminuer l'effet donneur de la chaîne, et en particulier du méthylène α, donc la perturbation qu'elle exerce sur le benzène. La symétrie du système π se restaure, la transition devient plus interdite et ε_{00} diminue. D'ailleurs dans les solvants hydroxylés les intensités sont en général plus faibles que dans le cyclohexane, car du fait des liaisons que le solvant peut exercer avec le doublet libre, celui-ci s'éloigne de l'azote qui se trouve alors déficient en électron. Cet atome compense le déficit en accroissant son pouvoir attracteur, ce qui provoque la diminution observée.

Si, contrairement aux autres termes de la série, le premier voit la valeur de ε_{00} croître par protonation c'est que le centre attracteur, étant directement fixé sur le méthylène α, est susceptible d'avoir une grande efficacité. La fonction NH_3^+ peut annuler l'effet donneur du méthylène. Il lui reste encore suffisamment de pouvoir attracteur pour exercer une perturbation, attractrice, sur le chromophore, perturbation plus importante que celle que le méthylène pouvait exercer lorsqu'il était substitué par NH_2. La valeur de ε_{00} croît donc. La protonation de NH_2 établit dans ce cas une perturbation en sens inverse de celle qu'il exerce dans la molécule neutre. La fonction NH_3^+ est d'ailleurs très efficace dans ses effets puisque la protonation fait encore décroître pour la n-phénylbutylamine de plus de 10 % l'intensité de la bande 00. On peut en déduire, à la vue de l'évolution de cette différence d'intensité entre formes protonées et non protonées, que la fonction NH_3^+ n'exercera pratiquement plus d'effet seulement si la chaîne est supérieure à cinq ou six carbones. Il s'agit là on le voit d'une interaction lointaine peu commune.

INTERVENTION DE LA CHAÎNE DANS LE COMPORTEMENT SPECTROSCOPIQUE

Il serait peu exact de penser que l'essentiel des variations d'intensité observées provient des groupes NH_2 et NH_3^+ dont les effets s'amenuiseraient progressivement au fur et à mesure que l'éloignement augmente. Ce serait réduire la chaîne à un simple rôle passif qui consisterait à assurer une sorte de séparation mécanique entre chromophore et auxochrome. Il est plus logique de considérer, dans une hypothèse simplificatrice de travail, que la contribution du groupe terminal est une constante dans une série donnée. Nous verrons plus loin s'il est nécessaire d'apporter des nuances à cette hypothèse. Il y a alors diminution, au niveau du chromophore, de l'influence de la fonction azotée avec l'éloignement parce qu'un nombre croissant de méthylènes vient s'intercaler entre le benzène et l'azote et que chacun d'eux diminue de son caractère donneur un peu plus de la contribution attractrice constante de la fonction. La variable du système est donc pour une série donnée la participation électronique de la chaîne aliphatique. Puisque l'auxochrome introduit un paramètre constant dans une série il devrait donc provoquer seulement un décalage d'abscisse d'une série à une autre. Aussi nous nous contenterons, dans un premier de la partie aliphatique du substituant. Nous pourrons alors examiner les problèmes qui se posent.

La courbe relative à ε_{00} en fonction des effets électroniques du substituant, c'est-à-dire de l'ensemble chaîne plus auxochrome, doit passer par un minimum. Celui-ci intervient lorsque s'annulent, du fait du caractère attracteur de l'auxochrome, les effets donneurs de la chaîne sur le chromophore et qu'en conséquence la perturbation disparaît. La valeur de ε_{00} augmentera d'autant plus à partir de ce minimum que la distribution hexagonale du nuage π sera modifiée soit par effet donneur croissant, soit par effet attracteur croissant.

On sait que l'influence inductive d'une chaîne suit une loi hyperbolique[5,6] en fonction du nombre n de chaînons : $\sigma = 0{,}0686\ n/(0{,}5 + n)$. Nous compterons dans ce travail comme positif l'effet donneur d'électrons et assimilerons l'effet inductif d'une chaîne en $-(CH_2)_n-$ à celui de $-(CH_2)_{n-1}-CH_3$.

On s'aperçoit à l'examen des courbes expérimentales de la figure 2 que la variation de ε_{00} en fonction de σ est linéaire, dans les limites de notre précision et dans le domaine considéré. En ce qui concerne les courbes relatives à NH_3^+ on doit se rappeler que le point correspondant au premier terme de la série ne peut figurer sur la même branche de la courbe que les autres points. Il faut donc que par le point relatif à l'ion benzylammonium passe une droite de même pente en valeur absolue que celle déterminée à partir des autres corps de la série, mais changée de signe. Les deux droites se recoupent pour une valeur $\varepsilon_{00} = 50-55$. Ceci correspond au minimum de la courbe $\varepsilon_{00} = f(\sigma)$. La valeur de ce minimum est celle de l'intensité sous-jacente à la bande 00, due au recouvrement avec les autre bandes de la transition. Il est difficile de chiffrer expérimentalement cette intensité de façon précise, mais si l'on considère le spectre de l'acide phénylacétique (dans eau + acide) dans lequel la bande 00 a pratiquement disparu, et que l'on corrige de l'absorption résiduelle de cette bande, le fond sous-jacent a un ε de 63 pour une valeur sans correction de 72. Selon les molécules que nous avons examinées il varie de 58 à 65. Il s'agit d'un point de rebroussement, or les données expérimentales respectent rarement les parties anguleuses des courbes. Nous avons donc ,,arrondi'' le minimum pour tenir compte de son évaluation approchée.

Nous avons jusqu'ici porté ε_{00} en fonction du σ de la partie aliphatique de la chaîne. Ceci entraine que les courbes relatives aux différents auxochromes sont décalées. Il est intéressant d'annuler ce décalage en fixant l'origine des σ à l'abscise du minimum. Celui-ci se produit en effet, quel que soit l'auxochrome, pour une annulation de tous les effets électroniques sur le chromophore. Toutes les courbes doivent donc passer par le même point minimum si on fixe l'origine des effets électroniques à son abscisse. Ceci entraine de décaler la courbe relative à NH_2 dans le cyclohexane de 0,035, celles dans le méthanol ou l'eau de 0,038, celles relatives à NH_3^+ de 0,052 en unités de σ. On pourrait avoir ainsi une évolution

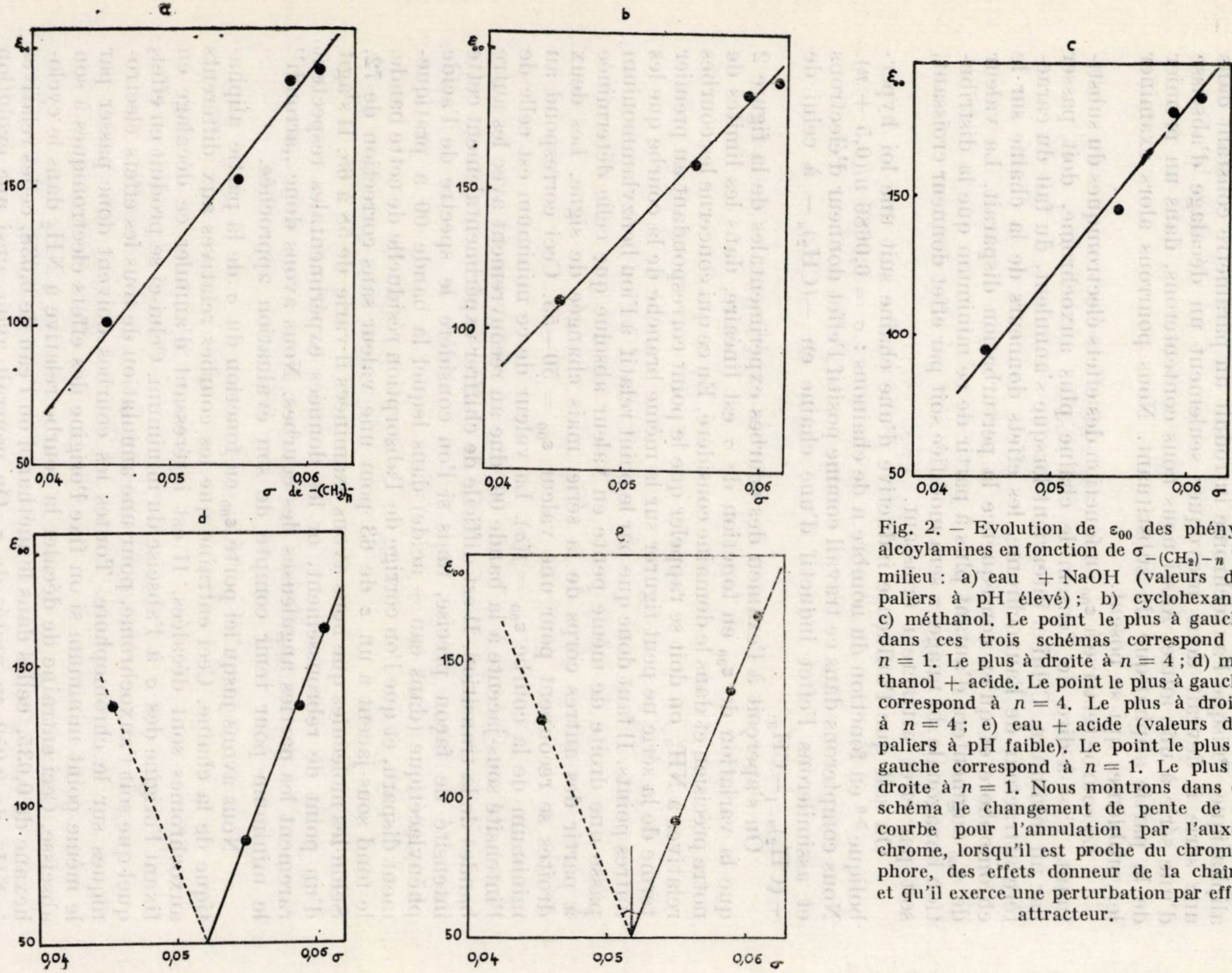

Fig. 2. — Evolution de ε_{00} des phénylalcoylamines en fonction de $\sigma_{-(CH_2)-n}$ en milieu : a) eau + NaOH (valeurs des paliers à pH élevé) ; b) cyclohexane ; c) méthanol. Le point le plus à gauche dans ces trois schémas correspond à $n = 1$. Le plus à droite à $n = 4$; d) méthanol + acide. Le point le plus à gauche correspond à $n = 4$. Le plus à droite à $n = 4$; e) eau + acide (valeurs des paliers à pH faible). Le point le plus à gauche correspond à $n = 1$. Le plus à droite à $n = 1$. Nous montrons dans ce schéma le changement de pente de la courbe pour l'annulation par l'auxochrome, lorsqu'il est proche du chromophore, des effets donneur de la chaîne et qu'il exerce une perturbation par effet attracteur.

du caractère électroattracteur (spectroscopiquement efficace) de l'auxochrome solvaté, et les valeurs de σ correspondraient désormais à l'effet inductif global du substituant, effet donneur pour les abscisses positives, attracteur pour la partie négative. Cependant les différentes courbes devraient se superposer, ce qui n'est pas le cas. En effet, quelle que soit la composition de substituant, à un σ donné, qui mesure ici la capacité de perturber, doit correspondre une perturbation donnée, donc une intensité donnée. Or cette intensité change selon l'auxochrome puisque les pentes des droites ne sont pas les mêmes. La simple addition des effets électroniques de la chaîne et de l'auxochrome ne permet donc pas l'évaluation du caractère inductif du substituant. Un paramètre supplémentaire intervient.

Remarquons que la pente k des droites augmente avec le caractère électroattracteur de la fonction terminale : 5500 dans le cyclohexane, 6200—6300 dans méthanol ou eau, 12500—13000 pour NH_3^+. Il existe donc une interaction chaîne-auxochrome différente d'un auxochrome à l'autre.

Il est intéressant de regrouper l'ensemble des points expérimentaux sur une même courbe car on peut ainsi faire correspondre à une perturbation donnée une intensité donnée. Ceci s'obtient par une modulation des pentes en mesurant l'effet inductif global par $\Sigma = k\sigma$ (Fig. 3) et en fixant logiquement l'origine au minimum puisque pour le minimum il y a annulation des effets électroniques au niveau du chromophore.

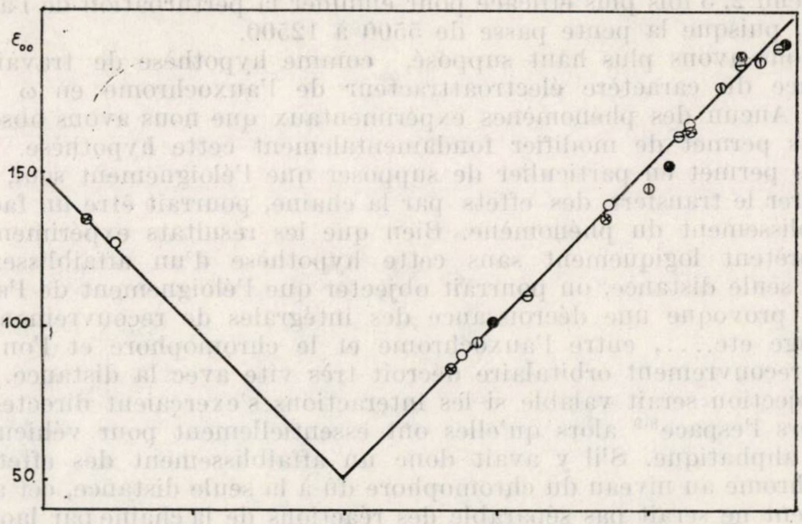

Fig. 3. — Evolution de ε_{00} en fonction de Σ, caractère électronique du substituant (pouvoir inducteur de la chaîne aliphatique isolée, corrigé du pouvoir attracteur de l'auxochrome en ω et des interactions réciproques). Le minimum correspond à l'origine : annulation des effets électroniques antagonistes de la chaîne aliphatique et de l'auxochrome. Le point le plus à gauche de chaque série correspond à une chaîne de 1 carbone. Le plus à droite à une chaîne de 4 carbones. ⊗) méthanol + acide ; ○) eau + acide ; ⦶) méthanol ; ●) eau + NaOH ; ⊖) cyclohexane.

La différence de pente k implique, avons nous dit, une réaction différente chaîne-auxochrome d'un auxochrome à l'autre. Cette différence de pente ne nous donne aucun renseignement sur un éventuel „affaiblissement" du caractère attracteur d'un auxochrome donné du seul fait de son éloignement, éloignement considéré hors de toute interaction avec la chaîne. Confronter les pentes en effet permet seulement d'étudier le comportement de substituants à longueur de chaîne donnée, ou si l'on préfère comparer l'évolution des phénomènes dans les différentes séries homologues dus à l'allongement. Les modifications de pente ont alors la signification suivante. La diminution d'efficacité de l'auxochrome dans son influence sur le chromophore, lorsque le nombre de méthylènes de la chaîne croît, est d'autant plus rapide que l'auxochrome est attracteur : NH_3^+ voit son influence subir une loi de décroissance plus rapide que celles relatives aux groupes moins attracteurs que lui. La résistance de la part de la chaîne aliphatique à la propagation de l'effet attracteur croît donc quand celui-ci croît. La chaîne tend ainsi à limiter spontanément l'influence de l'auxochrome. Son effet donneur est sollicité par le caractère électroattracteur de la fonction. Il n'est pas constant d'un auxochrome à l'autre. On peut ainsi déterminer que, en passant des phénylalcoylamines dans le cyclohexane aux phénylalcoylammoniums (eau + acide), un chaînon donné est devenu 2, 3 fois plus efficace pour éliminer la perturbation de l'auxochrome, puisque la pente passe de 5500 à 12500.

Nous avons plus haut supposé, comme hypothèse de travail, la constance du caractère électroattracteur de l'auxochrome en ω de la chaîne. Aucun des phénomènes expérimentaux que nous avons observés ne nous permet de modifier fondamentalement cette hypothèse. Rien ne nous permet en particulier de supposer que l'éloignement seul, sans considérer le transfert des effets par la chaîne, pourrait être un facteur d'affaiblissement du phénomène. Bien que les résultats expérimentaux s'interprètent logiquement sans cette hypothèse d'un affaiblissement avec la seule distance, on pourrait objecter que l'éloignement de l'auxochrome provoque une décroissance des intégrales de recouvrement, et d'échange etc. . . ., entre l'auxochrome et le chromophore et l'on sait que le recouvrement orbitalaire décroît très vite avec la distance. Une telle objection serait valable si les interactions s'exerçaient directement à travers l'espace[8,9] alors qu'elles ont essentiellement pour véhicule la chaîne aliphatique. S'il y avait donc un affaiblissement des effets de l'auxochrome au niveau du chromophore dû à la seule distance, cet affaiblissement ne serait pas séparable des réactions de la chaîne par laquelle cette distance se matérialise, et nous ne pourrions le voir. D'ailleurs la notion même de distance pure en ce qui concerne deux fonctions séparées par une chaîne aliphatique est caduque puisque, du fait de conformations statistiquement privilégiées, deux groupes qui sont séparés par une longue chaîne peuvent être spatialement très proches, plus parfois que deux groupes séparés par peu de chaînons.[1,10]

En conséquence on peut toujours supposer une constance des effets de l'auxochrome, la permanence de son identité dans son domaine spatial, et si ceci est perçu différemment au niveau du chromophore, seule la chaîne qui véhicule l'information et interagit avec l'auxochrome peut être considérée comme responsable de toute modification éventuelle.

Dans ce qui précède nous ne nous sommes pas préoccupés de la variation éventuelle d'hyperconjugaison avec le changement d'auxochrome, avec l'allongement de la chaîne et la variation d'effet inductif. Le fait que tous les phénomènes paraissent s'interpréter en termes d'effets inductifs ne veut pas dire que l'intervention de l'effet hyperconjugatif soit négligeable. On sait au contraire qu'il est spectroscopiquement prépondérant.[2,7] Cela vient simplement de ce que les variations d'effet hyperconjugatif proviennent des variations des effets électroniques, donneurs ou attracteurs, de la chaîne. La perturbation de symétrie qu'apporte l'hyperconjugaison au noyau aromatique dépend de la densité électronique au niveau du caarbone α et des liaisons C—H qu'il porte. Elle sera d'autant plus élevée que l'effet donneur de la chaîne est important. Ainsi les deux phénomènes sont indissociables puisque les variations de l'un sont le reflet, la conséquence directe, des variations de l'autre. Les modifications observées de ε_{00} sont donc bien dues aux variations de σ même si ces variations ne sont efficaces que parce qu'elles modifient l'état d'hyperconjugaison.

Nous avons reporté dans les deux parties de la figure 4 les données nécessaires à l'interprétation du comportement *a priori* surprenant de la courbe de protonation de la benzylamine. Ce comportement s'éclaire désormais aisément. Il est dû aux hauteurs respectives des points représentatifs sur les branches de la courbe a et à ce que le point représentatif de la première amine passe lors de la protonation d'une branche à l'autre

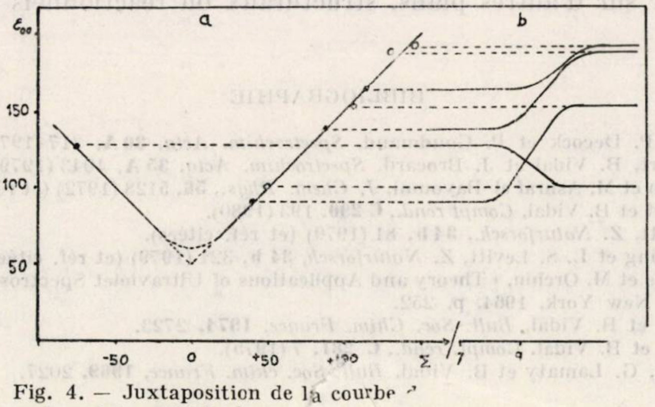

Fig. 4. — Juxtaposition de la courbe
seuls points relatifs à une
courbes de la figur
l'évolution de ces der
de la courbe $\varepsilon_{00} = f(\Sigma$
segments linéaires de
correspondent au minim

de cette courbe. On comprend au
s'allonge, quelle que soit la basicit
de moins en moins d'influence sur
de moins en moins le spectre et ε_0
de moins en moins marquées.

Intensité de la bande 00 de phénylalcoylamines dans divers solvants

$\text{Ø}-(\mathrm{CH_2})_n-\mathrm{NH_2}$	eau + NaOH	eau + acide	méthanol + acide	méthanol	cyclohexane
$n = 1$	101	128	135	95	110
2	153	91	86	145	162
3	188	139	135	178	185
4	192	165	163	186	190

Les valeurs portées ci-dessus sont en général obtenues avec une reproductibilité n'excédant pas une fourchette de deux unités. Celles relatives aux espèces en milieu acide ou basique correspondent aux paliers des courbes $\varepsilon_{00} = f(\mathrm{pH})$ obtenus pour les valeurs des pH extrêmes. La dissolution de la n-phénylbutylamine dans le milieu eau + NaOH est difficile. La valeur correspondante est peut-être sous-estimée de quelques unités.

Nous n'avons pas dans ce travail invoqué de facon spécifique les effets électroniques de champ. On sait en effet que l'intensité de la transition secondaire est surtout sensible aux perturbations de type mésomère. Dans notre cas cette perturbation mésomère est l'hyperconjugaison du méthylène α qui se trouve modulée par l'effet inductif de la chaîne. Ainsi la transition secondaire de l'ion anilinium ($\Phi\mathrm{NH_3^+}$) est très peu intense malgré un effet de champ marqué et un caractère électroattracteur notable du substituant. Il était donc ni nécessaire, ni possible, d'étudier spécifiquement un effet qui n'est pas spectroscopiquement isolable au niveau de l'intensité de la transition secondaire, malgré l'influence qu'il peut avoir sur d'autres plans, structuraux ou réactionnels par exemple.

BIBLIOGRAPHIE

[1] B. Vidal, P. Decock et P. Goudmand, *Spectrochim. Acta,* **30 A,** 317 (1974).
[2] G. Bastaert, B. Vidal et J. Brocard, *Spectrochim. Acta,* **35 A,** 1043 (1979).
[3] J. Tournon et M. Ashraf el Bayoumi, *J. Chem. Phys.*, **56,** 5128 (1972) (et réf. citées).
[4] G. Bastaert et B. Vidal, *Compt rend.*, **C 290,** 193 (1980).
[5] L. S. Levitt, *Z. Naturforsch.*, **34 b,** 81 (1979) (et réf. citées).
[6] H. F. Widing et L. S. Levitt, *Z. Naturforsch,* **34 b,** 321 (1979) (et réf. citées).
[7] H. H. Jaffe et M. Orchin, « Theory and Applications of Ultraviolet Spectroscopy » ed. Wiley, New York, 1964, p. 252.
[8] P. Decock et B. Vidal, *Bull. Soc. Chim. France,* **1974,** 2723.
[9] P. Decock et B. Vidal. *Compt. rend.*, **C 281,** 7 (1975).
[10] P. Geneste, G. Lamaty et B. Vidal, *Bull. Soc. chim. France,* **1969,** 2027.

Revue Roumaine de Chimie, 27, 7, 831–834 (1982)

AROMATIC ESTERS BY A NEW DIRECT CONDENSATION REACTION

C. I. CHIRIAC

"P. Poni" Institute of Macromolecular Chemistry
Aleea Grigore Ghica-Vodă 41 A Iași, Romania

Received October 2, 1981

By a direct condensation reaction between diacylphenylphosphites prepared "in situ" and phenols, aromatic esters are formed, avoiding, the synthesis of the acid chlorides or acid anhydrides as intermediates.

The classical syntheses of aromatic esters utilize the reactions of phenols with acyl chlorides or anhydrides. The direct reaction of aromatic acids with phenols is difficult to realize. For the synthesis of aromatic esters by direct condensation reactions, some reagents are used : *p*-toluensulfonyl chloride, [1] triarylphosphite, [2] polyphosphoric acid [3] and diarylsulfites. [2]

RESULTS AND DISCUSSIONS

Previous communications from this laboratory have shown that the diacylphenylphosphites (reactive compounds), prepared from aromatic acids and phenyldichlorophosphite, are useful for syntheses of amides [4] and hydrazides. [5]

In this work we have investigated the applicability of the diacylphenylphosphites in the synthesis of aromatic esters. Using the described procedure, [4] we have prepared "in situ" a series of diacylphenylphosphites from aromatic acids and phenyldichlorophosphite in pyridine as solvent and acceptor for hydrochloric acid. These diacylphenylphosphites reacted with phenols, affording the corresponding aromatic esters. The reaction was checked up with pure dibenzoylphenylphosphite, prepared from phenyldichlorophosphite and sodium benzoate. [4] This reaction took place under similar conditions with the reaction in which dibenzoylphenylphosphite prepared "in situ" was used. Therefore, pyridine hydrochloride (by-product), which results in the reaction with dibenzoylphenylphosphite prepared "in situ", does not affect the reaction, like in other cases. [4–6]

The diacylphenylphosphites have two reactive acyl groups, which participate in the reactions with amines [4] or hydrazines. [5] With phenols, both acyl groups participate in reaction, but at higher temperatures (135 — —145°C). As solvent, the pyridine was found to be the most suitable, because it is a very good solvent for the final products and acceptor for hydrochloric acid.

By treatment of a solution of diacylphenylphosphite (one mole), obtained "in situ" in pyridine, with a phenol (two moles) at room temperature, 4—5 hours, the yield is low. After 4—5 hours at reflux (135—145°C), the desired products result in good to moderate yields.

As a result of these investigations, we propose the following mechanism of reaction :

$$\underset{(I)}{2Ar - COOH} + C_6H_5OPCl_2 \xrightarrow[0-20°]{Py} \underset{(II)}{(Ar - COO)_2P - OC_6H_5} + 2(PyH^+Cl^-)$$

$$(II) + \underset{(III)}{2Ar' - OH} \xrightarrow[135-145°]{Py} \underset{(IV)}{2Ar - COOAr'} + C_6H_5OP(OH)_2$$

In this reaction, $C_6H_5OP(OH)_2$ and PyH^+Cl^- result as by-products, which do not affect the purity of the final products, similar to other cases.[4-6] We supposed, similar as in other cases,[2,4-7] that this reaction involves a four centre transition state (V) :

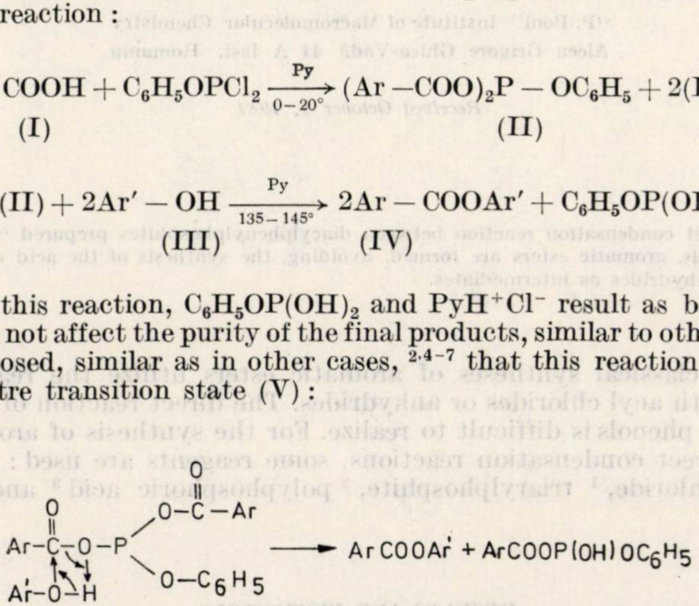

(V)

The general method for obtaining the aromatic esters (IV) consists in dissolving two moles (I) in dried pyridine, followed by addition of one mole phenyldichlorophosphite under stirring and cooling to 0° (the reaction is very exothermic). The solution thus obtained is treated with two moles + 10% excess (III). The yield was improved when we used a small excess of phenol (5—10%). After concentration up to 135°C and heating 4—5 hours at 135—145°C, the desired product was obtained in good to moderate yield. The reaction requires a large excess of pyridine to permit a good stirring, because PyH^+Cl^- precipitates during the reaction at 0—20°C ; then by treatment with (III) and heating, the solution becomes clear.

Table 1 shows the aromatic esters obtained in this way.

The large majority of the obtained aromatic esters had good melting points before recrystalisation and the yields ranged from 60 to 85% (Table 1).

By this new direct synthesis we obtained aromatic esters which are difficult to obtain by the heating of aromatic acids with phenols.

TABLE 1

Aromatic esters obtained from diacylphenylphosphites prepared "in situ"

Acid	Phenol	Esters[a]		
		Yield[b]	M.p.[c]	Lit.m.p.[d] °C
C_6H_5-COOH	C_6H_5OH	85	69—71	69—71
$p-CH_3-C_6H_4-COOH$	C_6H_5OH	83	75—77	76—77[8]
$p-CH_3O-C_6H_4-COOH$	C_6H_5OH	79	72—74	73—74[8]
$p-Cl-C_6H_4-COOH$	C_6H_5OH	60[e]	99—101[e]	100—101
$m-Br-C_6H_4-COOH$	C_6H_5OH	74	65—67	65—66
C_6H_5-COOH	β-naphthol	63[e]	105—107[e]	106—107
$p-CH_3-C_6H_4-COOH$	β-naphthol	61[e]	136—138[e]	137—138
C_6H_5-COOH	p-$CH_3-C_6H_4-OH$	65	67—69	68—70
$p-CH_3-C_6H_4-COOH$	p-$CH_3-C_6H_4-OH$	64	89—91	90—91[8]
$p-CH_3O-C_6H_4-COOH$	$p-CH_3-C_6H_4-OH$	61[e]	65—67[e]	66—67
C_6H_5-COOH	$p-Cl-C_6H_4-OH$	60[e]	85—87[e]	85—87

a) The products were identified by comparison of m.p. and IR spectra with authentic samples.

b) Yields calculated on acid employed.

c) Before recrystallization.

d) From "Beilsteins Handbuch der Organischen Chemie".

e) After recrystallization.

EXPERIMENTAL

Phenyl benzoate

To 2.44 g (0.02 mole) of benzoic acid in 10 ml dried pyridine in a 50 ml 3-necked flask, 1.4 ml (0.01 mole) of phenyldichlorophosphite[9] dissolved in 5 ml dried benzene was added slowly under stirring and cooling. The rate of addition was regulated that the temperature of reaction mixture was kept within the interval 0—10°. After stirring 2 hours at room temperature, 2.07 g (0.02 mole + 10% excess) phenol was added. Then, the solution was heated and the solvent was distilled till the temperature of the mixture rised to 135°C. The heating was continued under reflux (135—145°) for 4—5 hours. The obtained solution (still hot) was poured into a large volume of water with ice (80—100 ml) under stirring ; then treated with 10% NaOH solution till pH = 9—10. The precipitated product was collected by filtration, washed with 20—40 ml 10% HCl solution, three times with 20—30 ml water and dried at 40—45°C under vacuum. Phenyl benzoate (3.36 g) was obtained with a m.p. 69—71°C (mixed m.p. with pure product underpressed). Yield 85% calculated on benzoic acid employed. Anal. Found : C, 78.27 ; H, 4.81%. Calculated for $C_{13}H_{10}O_2$; C, 78.75 ; H, 5.08%.

Under similar conditions the other aromatic esters (presented in table 1) were prepared.

REFERENCES

[1] J. H. Brewster and C. J. Ciotti jr., *J. Amer. Chem. Soc.*, **77**, 6214 (1955).

[2] B. Iselin and W. Rittel, *Helv. Chim. Acta*, **40**, 373 (1957).

[3] A. R. Bader and A. D. Kontowicz, *J. Amer Chem. Soc.*, 75, 5416 (1953).

[4] C. I. Chiriac, *Rev. Roumaine Chim.*, **26**, 1001 (1981).

[5] C. I. Chiriac, *Rev. Roumaine Chim.*, (in press).

[6] C. I. Chiriac and J. K. Stille, *Macromolecules*, **10**, 710 (1977).

[7] H. O. Becker and K. F. Funk, *J. prakt. chem.*, **14**, 55 (1961).

[8] H. Rheinboldt, *Quimica*, **1951**, (3), 52 ; *Chem. Abstr.*, **46**, 7552 c (1952).

[9] H. Tölkmith, *J. Org. Chem.*, **23**, 1682 (1958).

Revue Roumaine de Chimie, 27, 7, 835–838 (1982)

REACTIONS OF SOME 5-OXO-2-PYRROLINES

A. I. HASHEM, M. E. SHABAN and A. F. El-KAFRAWY

Chemistry Department, Faculty of Science, Ain Shams University, Abassia, Cairo, Egypt

Received January 29, 1981

2-Aryl-4-furfurylidene-5-oxo-2-pyrrolines II react with hydrazine hydrate and benzylamine to give α-aracyl-β-(2-furyl)-acrylic acid hydrazides III and α-aracyl-β-(2-furyl)-N-benzyl-acrylamides IV respectively. The reaction of the oxopyrroline IIa with benzene in the presence of anhydrous aluminium chloride gives 4-furylphenylmethyl-5-oxo-2-phenyl-2-pyrroline V. The structures of the products are discussed in the light of their chemical and spectroscopic properties.

In a previous investigation [1], 2-aryl-4-furfurylidene-5-oxo-2-pyrrolines II were prepared by the action of gaseous ammonia in ethanol on α-furfurylidene-γ-aryl-$\Delta^{\beta,\gamma}$-butenolides I.

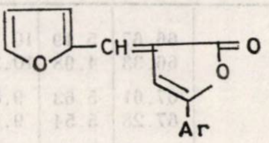

I

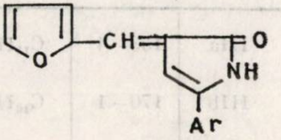

II

a ; Ar = C_6H_5-
b ; Ar = $C_6H_4CH_3(p-)$
c ; Ar = $C_6H_4OCH_3(p-)$
d ; Ar = $C_6H_4Cl(p-)$

In this investigation, the behaviour of these highly conjugated oxopyrrolines towards hydrazine hydrate, benzylamine as well as Friedel-Crafts alkylation is studied.

Hydrazine hydrate reacts with the oxopyrrolines II with the formation of α-aracyl-β-(2-furyl)-acrylic acid hydrazides III.

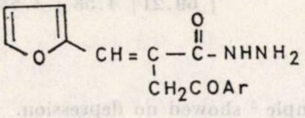

III

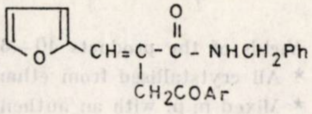

IV

a ; Ar = C_6H_5-
b ; Ar = $C_6H_4CH_3(p-)$
c ; Ar = $C_6H_4OCH_3(p-)$
d ; Ar = $C_6H_4Cl(p-)$

The proposed structure for the hydrazides III is based upon analytical data (Table 1), as well as on their infrared spectra which show an amidic carbonyl band at 1660 cm^{-1}, and ν(NH) band at 3300—3400 cm^{-1} (broad base). Moreover, an authentic sample [2] of α-phenacyl-β-(2-furyl)-acrylic acid hydrazide was prepared and shown to be identical with IIIa.

The reaction of II with benzylamine in ethanol follows a similar route with the formation of α-aracyl-β-(2-furyl)-N-benzyl-acrylamides IV.

The structure of these amides is inferred from analytical data (Table 1) and their infrared spectra which show ν(C=O) at 1670 cm^{-1} and ν(NH) at 3250—3350 (broad band). Further support for the above structure was obtained by preparing an authentic sample [2] of α-phenacyl-β-(2-furyl)-N-benzyl-acrylamide which was shown to be identical with IVa.

TABLE 1

Physical data of the hydrazides* III and the amides *IV

Compound	m.P. °C	Formula	Calcd. % (found) C	H	N
IIIa	133—4^{+}	$C_{15}H_{14}N_2O_3$	66.67 66.33	5.19 4.98	10.37 10.23
IIIb	170—1	$C_{16}H_{16}N_2O_3$	67.61 67.28	5.63 5.54	9.86 9.49
IIIc	124—5	$C_{16}H_{16}N_2O_4$	64.00 63.61	5.33 5.21	9.33 9.13
IIId	214—5	$C_{15}H_{13}ClN_2O_3$	59.11 58.83	4.27 4.14	9.20 9.08
IVa	155—6^{+}	$C_{22}H_{19}NO_3$	76.52 76.16	5.51 5.40	4.06 4.15
IVb	174—5	$C_{23}H_{21}NO_3$	76.88 76.56	5.85 5.66	3.90 3.88
IVc	183—4	$C_{23}H_{21}NO_4$	73.60 73.25	5.60 5.42	3.73 3.65
IVd	168—9	$C_{22}H_{18}ClNO_3$	69.57 69.21	4.74 4.58	3.69 3.58

Yields of the products 40—65%.

* All crytstallised from ethanol.

* Mixed m.p. with an authentic sample [2] showed no depression.

The formation of III and IV by the action of hydrazine hydrate and benzylamine respectively on the oxopyrrolines II may be represented by the following scheme :

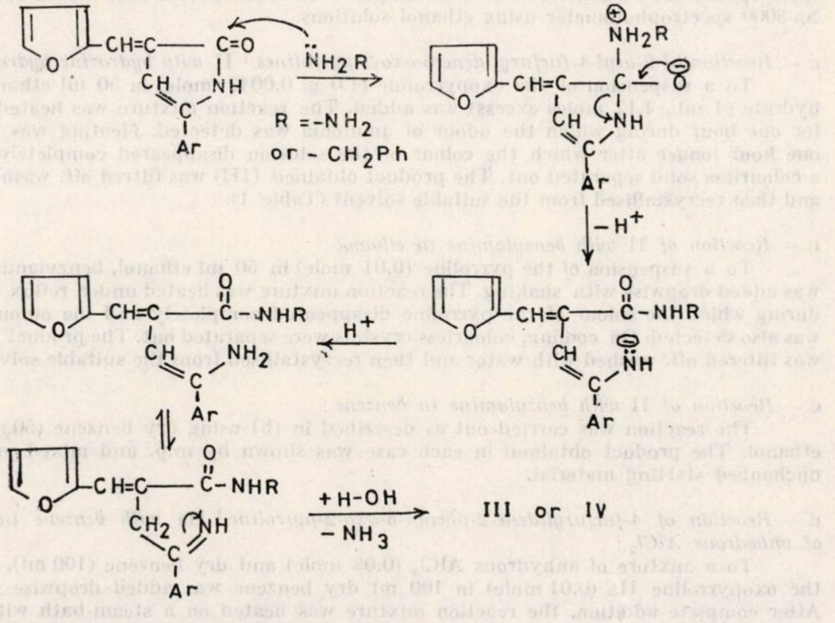
CH=C
C=O
NH₂R
CH
NH
C
Ar
R = -NH₂
or - CH₂Ph
NH₂R
CH=C
C
O
NH
Ar
-H⁺
O
CH=C
C-NHR
NH₂
H⁺
CH=C
C-NHR
NH
Ar
CH=C
C-NHR
CH₂
NH
Ar
+H-OH
-NH₃
III or IV

This proposed mechanism finds support from :

(i) The evolution of ammonia gas which was detected during the reaction.

(ii) In reaction with benzylamine, using dry benzene as a solvent instead of ethanol, the oxopyrrolines were recovered unchanged.

Under Friedel-Crafts conditions, IIa reacts with benzene in the presence of anhydrous aluminium chloride with the formation of 4-furylphenylmethyl-5-oxo-2-phenyl-2-pyrroline V.

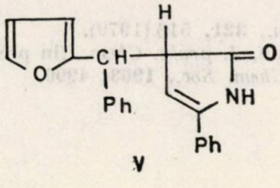
H
CH
O
Ph
NH
Ph

V

The structure of this product is based upon :

(i) Analytical data which indicate the incorporation of a phenyl group in V.

(ii) The infrared spectrum of this compound shows ν(C=O) at 1700 cm⁻¹ and ν(NH) at 3250 cm⁻¹.

(iii) Similarity with the formation [3] of 4-diphenylmethyl-5-oxo-2-phenyl-2-pyrroline.

The formation of V may be explained on the basis of 1,4-addition reaction of the α, β-unsaturated carbonyl moiety of II, with the pyrroline ring remaining intact.

EXPERIMENTAL PROCEDURE

Melting points are uncorrected. Infrared spectra were measured on a Unicam Sp 1200 spectrophotometer using KBr-wafer technique. Electronic spectra were measured on a Unicam Sp 8000 spectrophotometer using ethanol solutions.

a — *Reaction of* 2-*aryl*-4-*furfurylidene*-5-*oxo*-2-*pyrrolines*[1] II *with hydrazine hydrate in ethanol* :

To a suspension of the oxopyrroline (1.0 g, 0.0042 mole) in 50 ml ethanol, hydrazine hydrate (4 ml., 4.12 moles excess) was added. The reaction mixture was heated under reflux for one hour during which the odour of ammonia was detected. Heating was continued for one hour longer after which the colour of the solution disappeared completely. On cooling, a colourless solid separated out. The product obtained (III) was filtred off, washed with water and then recrystallised from the suitable solvent (Table 1).

b — *Reaction of* II *with benzylamine in ethanol* :

To a suspension of the pyrroline (0.01 mole) in 50 ml ethanol, benzylamine (0.02 mole) was added dropwise with shaking. The reaction mixture was heated under reflux for two hours during which the colour of the pyrroline disappeared completely and the odour of ammonia was also detected. On cooling, colourless crystals were separated out. The product obtained (IV) was filtered off, washed with water and then recrystallised from the suitable solvent (Table 1).

c — *Reaction of* II *with benzylamine in benzene* :

The reaction was carried out as described in (b) using dry benzene (50 ml) instead of ethanol. The product obtained in each case was shown by m.p. and mixed m.p. to be the unchanged starting material.

d — *Reaction of* 4-*furfurylidene*-2-*phenyl*-5-*oxo*-2-*pyrroline*[1] IIa *with benzene in the presence of anhydrous* $AlCl_3$:

To a mixture of anhydrous $AlCl_3$ (0.03 mole) and dry benzene (100 ml), a solution of the oxopyrroline IIa (0.01 mole) in 100 ml dry benzene was added dropwise with stirring. After complete addition, the reaction mixture was heated on a steam-bath with continuous stirring for 3 hours. The complex was decomposed with hydrochloric acid and the mixture steam distilled to give a yellow solid. The product obtained (V) was recrystallised from etahnol in yellow crystals ;

Yield 50%, m.p. 251–2°C (Found : C, 79.66 ; H, 5.25 ; N, 4.32. $C_{21}H_{17}NO_2$ requires C, 80.00 ; H, 5.40 ; N, 4.44%).

REFERENCES

[1] A. I. Hashem, *J. prakt. Chem.*, **321**, 516 (1979).

[2] A. I. Hashem and M. E. Shaban, *J. prakt. Chem.*, (in press).

[3] Y. S. Rao and R. Filler, *J. Chem. Soc.*, **1963**, 4996.

Revue Roumaine de Chimie, 27, 7, 839–846 (1982)

ACTION OF HYDRAZINES, HYDROXYLAMINE AND UREA ON 5-ARYL-3-CHLOROMETHYL-2-THIONO-1,3,4-OXADIAZOLES

M. ANWAR, F. I. ABDEL-HAY and A.F. HASHEM
Chemistry Department, Faculty of Science, Tanta University,
Tanta, A.R. Egypt

Received January 17, 1981

5-Aryl-3-chloromethyl-2-thiono-1,3,4-oxadiazoles III reacted with hydrazines, hydroxylamine hydrochloride, urea and thiourea forming compounds IV–IX. The structure of the newly prepared compounds was established by the IR, UV,^{1}H–NMR and MS studies.

5-Aryl-2-thiono-1,3,4-oxidiazoles I [1-3] reacted with formaldehyde to form 5-aryl-3-hydroxymethyl-2-thiono-1,3,4-oxadiazoles II. Compounds II reacted with thionyl chloride yielding 5-aryl-3-chloromethyl-2-thiono-1,3,4-oxadiazoles (III).[4]

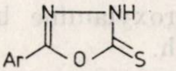
(I)

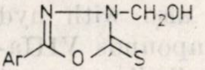
(II)

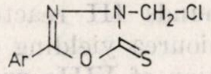
(III)

I–III, a, Ar = C_6H_5 c, Ar = $C_6H_4OCH_3$-*p*
b. Ar = $C_6H_4CH_3$-*p* d, Ar = C_6H_4Cl-*p*

The reaction of phenols and amines with 5-aryl-3-chloromethyl-2-thiono-1,3,4-oxadiazoles was the aim of a previous work.[5]

In the present investigation the action of hydrazines, hydroxylamine, urea and thiourea on the same oxadiazoles was attemped.

5-Aryl-3-chloromethyl-2-thiono-1,3,4-oxadiazoles III reacted with hydrazines, namely hydrazine hydrate, phenylhydrazine, *p*-nitrophenylhydrazine and 2,4-dinitrophenylhydrazine. The reaction proceeds normally yielding compounds IV-a-n.

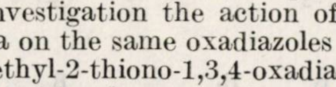
(IV)

	R	R_1		R	R_1
a,	H	H	h,	OCH_3	H
b,	H	C_6H_5	i,	OCH_3	C_6H_5
c,	H	$C_6H_4-NO_2$-*p*	j,	OCH_3	$C_6H_4-NO_2$-*p*
d,	H	$C_6H_3(NO_2)_2$2,4	k,	OCH_3	$C_6H_3(NO_2)_2$2,4
e,	CH_3	H	l,	Cl	H
f,	CH_3	C_6H_5	m,	Cl	C_6H_5
g.	CH_3	$C_6H_4-NO_2$-*p*	n,	Cl	$C_6H_4-NO_2$-*p*

Oxidation of IVh with potassium permanganate in acetic acid medium afforded the 2-oxo-1,3,4-oxadiazole (V).[5]

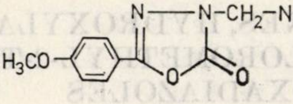

(V)

Compounds IVa, d, h and l were cyclized with elimination of hydrogen sulphide on heating in an oil-bath at 5–10°C over their melting points yielding compounds VIa-d.

Compounds VI reacted with methyl iodide forming VIIa-c.

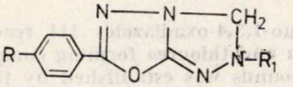

	R	R_1		R	R_1
VIa,	H	H	c,	OCH_3	H
b,	CH_3	H	d,	Cl	H
VIIa,	H	CH_3	c,	Cl	CH_3
b,	CH_3	CH_3			

Compounds III reacted also with hydroxylamine hydrochloride, urea and thiourea yielding compounds VIIIa-h.

Oxidation of VIIIe with alkaline potassium permanganate in acetic acid medium afforded IX.

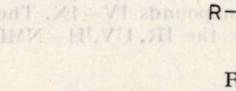

(VIII)

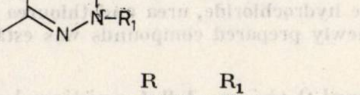

(IX)

	R	R_1		R	R_1
a,	H	OH	e,	OCH_3	OH
b,	H	$CONH_2$	f,	OCH_3	$CONH_2$
c,	H	$CSNH_2$	g,	OCH_3	$CSNH_2$
d,	CH_3	OH	h,	Cl	OH

The structure of the newly prepared compounds was confirmed by infrared, ultraviolet, nuclear magnetic resonance and mass spectral studies. The whole spectral data are presented in tables 1–4.

EXPERIMENTAL

The IR spectra were recorded with a UNICAM S.P. 1200 spectrophotometer. The KBr pellet technique was used.

The absorption spectra in UV region using ethanol as solvent were recorded with a UNICAM S.P. 800 spectrophotometer.

TABLE 1

IR-Spectral data for compounds IV–IX (KBr cm^{-1}) a) [6, 7]

Compound	ν(NH)	ν(C=N)	ν(CH_2)	ν(C=S)	ν_{asym}(C–O)	ν_{asym}(C–O)
IVa	3410^{b}	1615^{s}	1445^{vs}	1260^{s}	1070^{m}	970^{s}
IVb	3400^{b}	1620^{s}	1440^{vs}	1270^{s}	1080^{s}	985^{s}
IVd	3420^{b}	1640^{m}	1420^{s}	1330^{vs}	1080^{s}	975^{s}
IVi	3430^{b}	1615^{s}	1440^{vs}	1260^{s}	1070^{m}	970^{s}
V	3400^{b}	1620^{s}	1440^{s}	(*)	1085^{m}	985^{s}
VIa	3460^{b}	1615^{m}	1430^{s}	—	1070^{m}	975^{s}
VIb	3460^{b}	1620^{s}	1440^{vs}	—	1085^{m}	970^{vs}
VIIa	—	1630^{s}	1435^{s}	—	1085^{s}	985^{s}
VIIb	—	1625^{s}	1440^{vs}	—	1080^{vs}	980^{s}
VIIIa	3440^{b} (**)	1610	1430^{vs}	1250^{vs}	1080^{s}	970^{m}
VIIIc	3300^{s}	1640^{s}	1440^{vs}	1290^{vs}	1070^{vs}	975^{m}
VIIId	3460^{b} (**)	1615^{s}	1430^{vs}	1250^{vs}	1075^{vs}	970^{m}
VIIIe	3320^{b} (**)	1640^{m}	1445^{s}	1300^{vs}	1080^{ss}	970^{vv}
IX	3340^{b}	1615^{s}	1440^{s}	(*)	1085^{v}	990^{vs}

(a) s = strong ; m = medium ; b = broad
(*) ν (C = O) at 1720 cm^{-1}
(**)ν(NH) overlapped with νOH .

TABLE 2

UV – Spectra of compounds IV in ethanol, [6–10]
(λ max. / ε max. × 10^{-4})

Compound	π–π*phenyl	π–π*phenyl	π– π*exadiazole
IVa	210/4.80	240/4.85	283/4.95
IVb	212/4.40	235/4.60	270/4.65
IVc	—	235/4.10	350/3.80[1]
IVd	210/4.60	255/4.45	380/4.85
IVe	212/4.10	235/3.45	275/3.80
IVf	210/3.60	240/4.40	282/3.65
IVg	—	240/3.85	290/3.40[2]
IVh	—	235/4.40	275/4.85
IVi	210/4.60	240/4.00	280/3.85
IVj	212/4.85	240/4.25	290/3.85
IVk	210/4.60	250/4.40	295/3.20
IVl	210/4.20	252/3.80	282/3.60
IVm	210/4.80	235/4.20	275/3.80
IVn	210/4.25	240/4.40	290/3.85

---

[1]) Remarkable red shift owing to the presence of nitro group.

[2]) Slight red shift owing to the presence of nitro group, antagonised by the presence of substituent in phenyl ring at position 5.

TABLE 3

^{1}H—NMR—Spectral data for compounds IV—VIII*' **

Compound	Aromatic	NH	OH (1H, s)	CH_2— (2H, s)	Ar—CH_3 (3H, s)	Ar—OCH_3 (3 H, s)
IVa	7.4—8.2 (5 H, m)	8.7(3H, s) $NHNH_2$	—	5.8	—	—
IVb	6.8—8.0 (10 H, m)	10.8	—	4.4	—	—
IVc	6.8—7.7 (4H,dd)	4.4(3 H, s)	—	4.9	1.9	—
IVf	7.3—8.0 (9 H, m)	8.8(3H, s)	—	5.6	2.4	—
IVg	7.2—7.8 (8 H, m)	3.3(3 H, s)	—	5.9	2.3	—
IVh	6.5—7.7 (4 H, dd)	3.4(3 H, s)	—	4.3	—	2.3
IVi	6.9—8.1 (9 H, m)	3.9(3H, s)	—	5.8	—	1.9
VIa	7.3—8.0 (5 H, m)	3.3(1 H, s)	—	5.5	—	
VIb	7.1—7.9 (4H, dd)	3.3(1 H, s)	—	6.0	2.2	—
VIIa	7.0—7.8 (5 H, m)	—	—	6.0	2.2	—
VIIIa	7.2—7.7 (5 H, m)	4.4(1 H, s)	5.1	5.6	—	—
VIIIb	7.2—7.7 (5 H, m)	4.3(4 H, s) NH_2CONH_2	—	5.5	—	—
VIIIc	7.2—7.7 (5 H, m)	4.4(4H, s) NH_2CSNH_2	—	5.6	—	—
VIIId	7.2—7.9 (4H, dd)	2.4(1H, s)	3.6	5.8	1.6	—
VIIIe	6.9—7.9 (4H, dd)	3.8(1 H, s)	5.5	5.8	—	1.7
VIIIf	6.7—7.7 (4 H, dd)	4.5(2H, s) 5.1(2 H, s) NH_2CONH_2	—	5.7	—	—
VIIIg	6.8—7.8 (4 H, dd)	3.7(2H, s) 3.9(2 H, s) $NH_2CS\ NH_2$	—	5.4	—	2.7
VIIIh	7.3—8.2 (5H, m)	5.0(1 H, s)	(***)	5.5	—	—

---

* Chemical shifts were determined as σ ppm. in DM SO or $CDCl_3$.

** s = singlet ; d = doublet ; m = multiplet

*** The OH proton superposed with aromatic protons.

TABLE 4

Mass spectral data for compounds IV—VIII

Compound	M(m/e)	R.A.(I %)
IVa	222	35.5
IVl	256.5	50
VIb	202	70
VIc	218	100
VIIIa	223	15.5
VIIIc	266	50

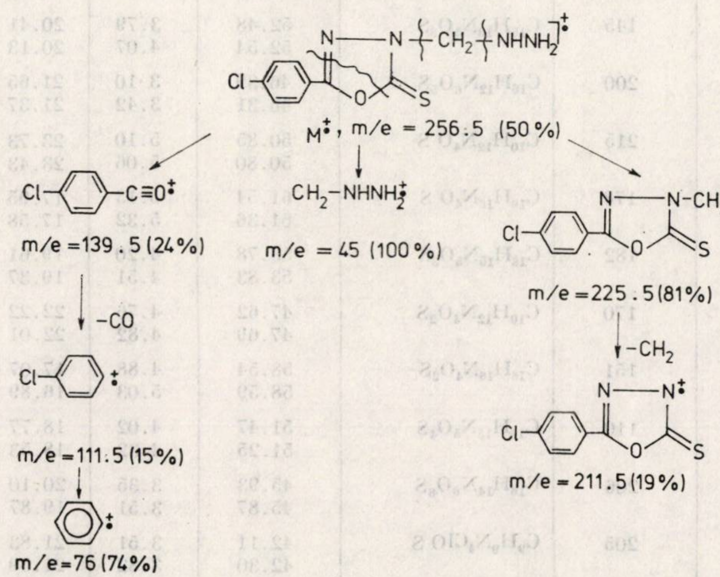

The ^{1}H— NMR spectra were recorded at 60 MHz on a Varian A—60 spectrometer.

The mass spectra were recorded on a V.G. Micromass 7070 F spectrometer operating at 70 eV using direct inlet.

All melting points are uncorrected.

Action of hydrazines on 5-aryl-3-chloromethyl-2-thiono-1,3,4- oxadiazoles III. Formation of IV

5-Aryl-3-chloromethyl-2-thiono-1,3,4-oxadiazoles III (0.01 mole) and hydrazines (0.01 mole) in 50 ml ethanol were heated under reflux for 3 hrs. The reaction mixture was concentrated, cooled and filtered. The solid obtained was recrystallized from ethanol to give IVa—n in about 90 % yields. The physical data are listed in table 5.

Oxidation of IVh with potassium permanganate

Potassium permanganate (0.46 g ; 0,003 mole) in the least amount of water was added gradually to a solution of IVh (1 g) in acetic acid (50 ml). The reaction mixture was heated on a water bath for half hr., concentrated, and cooled. The reaction mixture was poured on ice cold water, the formed precipitate was filtered off and recrystallized from ethanol to give V in 80 % yield. (See Table 5).

TABLE 5

Characterization of compounds IV and V

Compound	m.p. (°C)	Formula	Analysis % (Calcd./Found)			
			C	H	N	S
IVa	210	$C_9H_{10}N_4CS$	48.65 48.73	4.50 4.68	25.23 24.92	14.41 14.35
IVb	198	$C_{15}H_{14}N_4O\ S$	60.40 60.21	4.70 4.60	18.79 18.47	10.74 10.70
IVc	145	$C_{15}H_{13}N_5O_3S$	52.48 52.54	3.79 4.07	20.41 20.13	9.33 9.46
IVd	200	$C_{15}H_{12}N_6O_5S$	46.39 46.31	3·10 3.42	21.65 21.37	8.25 8.36
IVe	215	$C_{10}H_{12}N_4O\ S$	50.85 50.80	5.10 5.06	23.73 23.43	13.56 13.49
IVf	178	$C_{16}H_{16}N_4O\ S$	61.54 61.36	5.13 5.32	17.95 17.58	10.26 9.97
IVg	182	$C_{16}H_{15}N_5O_3S$	53.78 53.83	4.20 4.51	19.61 19.37	8.96 9.00
IVh	170	$C_{10}H_{12}N_4O_2S$	47.62 47.69	4.76 4.82	22.22 22.01	12.70 12.74
IVi	151	$C_{16}H_{16}N_4O_2S$	58.54 58.59	4.88 5.03	17.07 16.89	9.76 9.83
IVj	110	$C_{16}H_{15}N_5O_4S$	51.47 51.25	4.02 4.32	18.77 18.53	8.58 8.61
IVk	206	$C_{16}H_{14}N_6O_6S$	45.93 45.87	3.35 3.51	20.10 19.87	7.66 7.81
IVl	205	$C_9H_9N_4ClO\ S$	42.11 42.30	3.51 3.82	21.83 21.59	12.48 12.40
IVm	200	$C_{15}H_{13}N_4ClO\ S$	54.14 54.26	3.91 4.07	16.84 16.59	9.62 9.43
IVn	162	$C_{15}H_{12}N_5ClO_3S$	47.68 47.52	3.18 3.50	18.54 18.33	8.48 8.52
V	138	$C_{16}H_{16}N_4O_3$	61.54 61.32	5.13 5.26	17.95 17.76	— —

Cyclization of IVa, d, h and l

In a dry conical flask, 1 g of IV a, d, h and/or IV l, was heated in an oil-bath at 200—220°C for 3 hrs. After cooling the solid obtained was recrystallized from ethanol to give compounds VIa-d in almost quantitative yield. The physical data are shown in table 6.

Action of methyl iodide on VI

A mixture of VI (0.01 mole), and methyl iodide (0.9 ml ; 0.01 mole) and 30 ml 0.1 N alcoholic sodium hydroxide was heated on water bath for 2 hrs. The product obtained was triturated with light petrol and crystallized from benzene to give VIIa—c in about 75 % yield. The results are listed in table 6.

TABLE 6

Characterization of compounds VI and VII

Compound	m.p. (°C)	Formula	Analysis % (Calcd./found).		
			C	H	N
VIa	185	$C_9H_8N_4O$	57.45 57.31	4.26 4.51	29.79 29.68
VIb	189	$C_{10}H_{10}N_4O$	59.41 59.35	4.95 5.02	27.73 27.50
VIc	201	$C_{10}H_{10}N_4O_2$	55.0 54.8	4.59 4.68	25.69 25.43
VId	164	$C_9H_7N_4ClO$	48.54 48.31	3.15 3.40	25.17 25.01
VIIa	149	$C_{10}H_{10}N_4O$	59.41 59.21	4.95 5.07	27.73 27.72
VIIb	154	$C_{11}H_{12}N_4O$	61.11 61.00	5.56 5.62	25.93 25.87
VIIc	163	$C_{10}H_9N_4ClO$	50.74 50.51	3.81 4.05	23.68 23.69

Action of hydroxylamine, urea, and thiourea on III

A mixture of III (0.01 mole) and hydroxylamine hydrochloride, urea and/or thiourea (0.01 mole) in 50 ml ethanol was heated under reflux for 3 hrs. The reaction mixture was recrystallized from ethanol to give (VIIIa–h). Yield 80–90 %. The results are given in table 7.

Oxidation of VIIIe with potassium permanganate

The same method used for the oxidation of IVh was used. Compound IX was obtained in 75 % yield. (Table 7).

TABLE 7

Characterization of compounds VIII and IX

Compound	m.p. (°C)	Formula	Analysis % (Calcd./Found).			
			C	H	N	S
VIIIa	104	$C_9H_9N_3O_2S$	48.43 48.27	4.04 4.23	18.83 18.67	14.35 14.41
VIIIb	95	$C_{10}H_{10}N_4O_2S$	48.00 48.09	4.00 4.21	22.40 22.17	12.80 12.74
VIIIc	213	$C_{10}H_{10}N_4O\ S_2$	45.11 45.02	3.76 4.03	21.05 21.00	24.06 24.01
VIIId	110	$C_{10}H_{11}N_3O_2S$	50.63 50.42	4.64 4.82	17.72 17.53	13.50 13.48
VIIIe	104	$C_{10}H_{11}N_3O_3S$	47.43 47.26	4.35 4.52	16.60 16.39	12.65 12.60

TABLE 7 (*continued*)

Compound	m.p. (°C)	Formula	Analysis % (Calcd./Found).			
			C	H	N	S
VIIIf	108	$C_{11}H_{12}N_4O_3S$	47.14	4.29	20.00	11.43
			47.21	4.42	19.78	11.41
VIIIg	160	$C_{11}H_{12}N_4O_2S_2$	44.59	4.05	18.92	21.62
			44.50	4.31	18.96	21.29
VIIIh	193	$C_9H_8H_3ClO_2S$	41.94	3.11	16.31	12.43
			41.87	3.40	16.42	12.41
IX	141	$C_{10}H_{11}N_3O_4$	50.63	4.64	17.72	—
			50.47	4.72	17.51	—

REFERENCES

[1] E. Hoggarth, *J. Chem. Soc.*, **1952**, 4811.

[2] R. W. Young, and K. H. Wood, *J. Amer. Chem. Soc.*, **77**, 400 (1955).

[3] C. Ainworth, *J. Amer. Chem. Soc.*, **78**, 4475 (1956).

[4] I. Radha and V.R. Srinivasan, *Indian J. Chem.*, **7**, 583 (1969).

[5] M. Anwar, F. I. Abdel-Hay, M. El-Borai, and A. F. Hashem, *Rev. Roumaine Chim.*, **25**, 359 (1980).

[6] M. Anwar and I. Islam, *Bull. Tanta Sci.*, **3** (1980) in press.

[7] M. Anwar, F. I. Abdel-Hay, M. M. Abou Sekkina and I. Islam, *J. Solid State, Egypt.* (1980) in press.

[8] Yu. N. Sheinker, I. Ya. Postovskii and N. M. Voronina, *Zhur. fiz. Khim.*, **33**, 302 (1959).

[9] C. Ainworth, *J. Amer. Chem. Soc.*, **77**, 1148 (1955); *Ibid.*, **87**, 5800 (1965).

[10] M. Anwar, A. A. El-Barbary, A. A. G. Ghattas and A. F. Hashem, *Polish J. Chem.*, **526**, (1980).

Revue Roumaine de Chimie, 27, 7, 847–852 (1982)

INFLUENCE OF SUBSTITUENTS ON THE PHOTOKETONIZATION OF SOME ENOLIZABLE β-KETOESTERS IN SOLUTION

I. PETKOV and P. MARKOV
Department of Organic Chemistry, University of Sofia, Bulgaria

Received September 13, 1980

The structure dependence of the photoinduced ketonization of some β-dicarbonyl compounds in solution was examined. Differences in the photosensitivity of the compounds studied were found. The rate constants and the quantum yields of the process under consideration were determined.

Recently we have performed a study of the photochemistry of enolizable β-dicarbonyl compounds showing the existence of a process of photoinduced ketonization (e.g.[1-3]). The influence of some structural features on the observed photoconversion has already been recognized.[4] The present paper studies the effect of substituents at the α and γ carbon in the β-dicarbonyl systems as well as the type of the alkoxy group on the phenomenon observed. On the other hand, only a limited number of widely scattered and isolated UV-spectral data for the compounds under consideration are now available.[5-6] For this reason we examined their electronic spectra.

Solutions of β-ketoesters I–XX were studied by UV and IR spectroscopy. The observed UV spectral characteristics, as well as the enol content in their heptane solutions, are summarized in table 1. As seen, the position of the high intensity band related to the $\pi \rightarrow \pi^*$

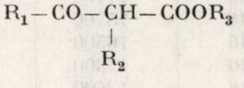

$$R_1-CO-\underset{\displaystyle R_2}{\underset{|}{CH}}-COOR_3$$

Compound	R_1	R_2	R_3
I	CH_3CH_2	H	C_2H_5
II	$CH_3(CH_2)_2$	H	C_2H_5
III	$CH_3(CH_2)_3$	H	C_2H_5
IV	$CH_3(CH_2)_4$	H	C_2H_5
V	$CH_3(CH_2)_8$	H	C_2H_5
VI	$(CH_3)_2CH$	H	C_2H_5
VII	$(CH_3)_2CHCH_2$	H	C_2H_5
VIII	$C_6H_5CH_2$	H	C_2H_5
IX	CH_3	CH_3	C_2H_5
X	CH_3	CH_3CH_2	C_2H_5
XI	CH_3	$C_6H_5CH_2$	C_2H_5

(continued)

Compound	R_1	R_2	R_3
XII	CH_3	$CH(CH_3)_2$	C_2H_5
XIII	CH_3	H	$CH(CH_3)CHCH_3$
XIV	CH_3	H	C_5H_{11}
XV	CH_3	H	$CH_2(CH_2)_6CH_3$
XVI	CH_3	H	$CH_2(CH_2)_8CH_3$
XVII	CH_3	H	C_6H_{11}
XVIII	CH_3	H	$CH_2CH{=}CHC_6H_5$
XIX	CH_3	H	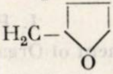
XX	CH_3	H	$H_2CC_6H_5$

transition in the β-hydroxyvinil carbonyl system is virtually independent of the type of substituents R_1, R_2 and R_3. Somewhat more noticeable is the influence of the benzyl radical, resulting in a bathochromic shift of the absorption maximum (compounds VIII and XI). The introduction of alkyl substituents at the α-carbon atom leads to analogous spectral changes (compounds IX, X, XI).

TABLE 1

UV absorption data for compounds I–XX[a]

Compound	max (nm)	ε^b	f	$E(\%)$
I	247	16300	0.429	46
II	247	17000	0.470	51
III	248	17400	0.474	50
IV	248	14800	0.383	52
V	248	12400	0.343	48
VI	246	17000	0.441	60
VII	247	17400	0.451	49
VIII	268(250)	—	—	—
IX	257	11300	0.441	15
X	252	11000	0.285	14
XI	260	11000	0.285	13
XII	245	11100	0.296	10
XIII	248	15700	0.413	46
XIV	246	16500	0.413	44
XV	240	13300	0.357	51
XVI	248	12600	0.360	54
XVII	246	16200	0.449	45
XVIII	252	29700	0.847	42
XIX	246	13000	0.331	40
XX	247	14600	0.384	51

[a] 1×10^{-4} gM·l^{-1} heptane solutions

[b] Direct measurement by bromine titration

Molar absorptivity (ε) of the enol forms varies to some extent (between 11000 and 17000). The only exception is compound XVIII, which possesses molecular absorptivity ≈ 30000. The enol content found for I—XX is in agreement with the results[5] obtained for similar β-dicarbonyl compounds.

Some features in the UV-spectral characteristics of VIII have been found. The UV-spectrum of freshly prepared heptane solution has an absorption band at 270 nm (Fig. 1, curve 1), merging gradually (curves 2, 3, 4, 5) into a maximum at 250 nm.

The observed spectral changes can be related to the existence of an equilibrium between two types of enolic species: *a* and *b*

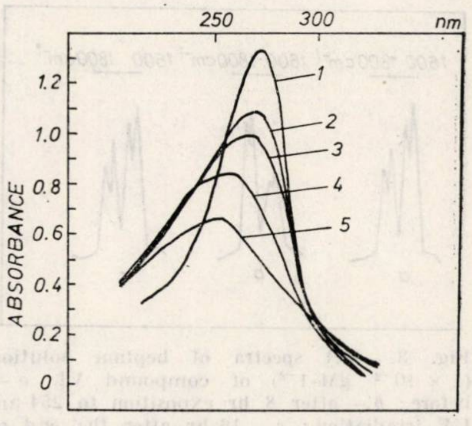

Fig. 1. — UV spectra of VIII in heptane (ca 1 × 10^{-4} gM · l^{-1}) at different times after the preparation of the solutions (curves 1—5).

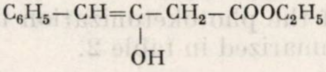

$$C_6H_5-CH=\underset{OH}{\underset{|}{C}}-CH_2-COOC_2H_5$$

a

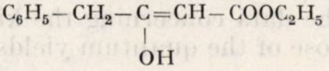

$$C_6H_5-CH_2-\underset{OH}{\underset{|}{C}}=CH-COOC_2H_5$$

b

From this standpoint, the spectral changes can be rationalized as a reflection of an alteration of the ratio between these two enol forms.

Irradiation of compounds I—XX in heptane (1 × 10^{-4} gM · l^{-1}) solution led to a substantial decrease of the content of enilic species because of the process of photoketonization. In the dark, the irradiated solutions show a gradual restoration of their original spectral characteristics.

The spectral alterations appearing as a result of the irradiation of VIII are of special interest. They are presented in Fig. 2. As one can see, the maximum at 270 nm, for a freshly prepared solution absorption decreases its intensity. Simultaneously a new low intensity band at 242 nm and a shoulder at 250 nm appear. On the other hand the irradiation of a seasoned (3.5 months) solution of the same compound led to a substantial

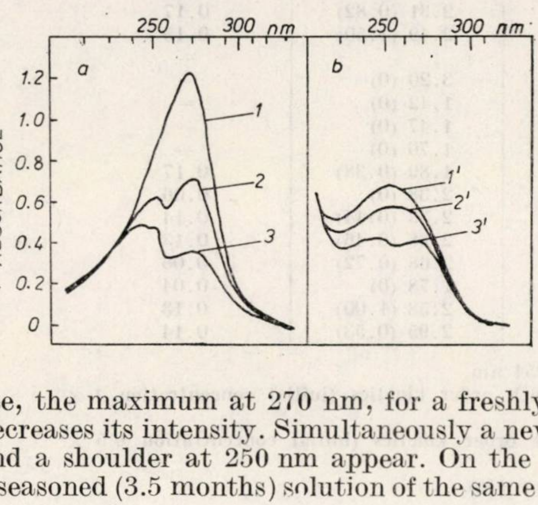

Fig. 2. — UV spectra of VIII in heptane (ca 1 × 10^{-4} gM. l^{-1}) at different times after the start of the UV (254 nm) irradiation (min): 1 — 0; 2 — 35; 3 — 65 1′ — 0; 2′ — 15; 3′ — 105. *a* — freshly prepared solution; *b* — seasoned (3.5 months) solution.

decrease of the intensity at 250 nm. Consequently one can conclude that both enol forms (*a* and *b*) of VIII are affected by the ultraviolet light. Probably the newly formed low intensity band at 242 nm is related to an $n \rightarrow \pi^*$ transition of the respective keto form.

The process of photoketonization was followed also by IR-spectroscopy. The absorption bands in the 6μ region found for compound VI before, immediately after, and at varying intervals after irradiation are shown in Fig. 3.

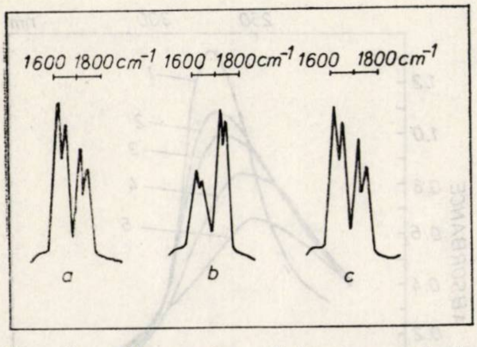

Fig. 3. — IR spectra of heptane solution (1×10^{-2} gM·l^{-2}) of compound VI. *a* — before ; *b* — after 8 hr exposition to 254 nm UV irradiation ; *c* — 16 hr after the end of irradiation

So far as the observed spectral changes are similar to those discussed previously[2] additional comments are not needed here.

The data concerning the kinetics of the photoketonization together with those of the quantum yields are summarized in table 2.

TABLE 2[a]

Rate constants and quantum yields (Φ) of the photoketonization of compounds I–XX, measured, by UV-spectroscopy

Compound	$k_{(o)} \times 10^8$[b]	$k_{(1)} \times 10^4$[c]	Φ
I	0.88 (0.98)	1.62 (0.76)	0.18
II	1.05 (0)	2.03 (0)	0.19
III	1.01 (0.53)	2.27 (0.69)	0.14
IV	2.06 (1.39)	3.27 (0.50)	0.20
V	1.69 (0)	2.06 (0.79)	0.22
VI	2.35 (0.76)	2.31 (0.82)	0.17
VII	1.26 (0.92)	2.49 (1.50)	0.15
VIII	—	—	—
IX	1.15 (0)	3.20 (0)	—
X	1.29 (0)	1.42 (0)	—
XI	1.23 (0)	1.47 (0)	—
XII	1.24 (0)	1.70 (0)	—
XIII	1.31 (0.80)	1.89 (0.38)	0.17
XIV	1.25 (0)	2.38 (0)	0.06
XV	2.06 (0.63)	2.33 (0.44)	0.14
XVI	1.36 (1.10)	2.88 (0.46)	0.13
XVII	1.59 (0)	2.68 (0.72)	0.06
XVIII	1.05 (0.94)	1.78 (0)	0.04
XIX	1.00 (0.81)	2.58 (1.00)	0.13
XX	1.97 (0.71)	2.95 (0.53)	0.14

[a] Exciting irradiation, 254 nm.

[b] Rate constant of zeroth order kinetics (initial concentration 1×10^{-4} gM·l^{-1}).

[c] Rate constant of first order kinetics (initial concentration 0.5×10^{-4} gM·l^{-1}).

( ) — Standard deviation (%).

In the region of high optical densities ($c_0 = 1 \times 10^{-4}$ gM.1^{-1}), the photoinduced transformation follows a zeroth order kinetics. At lower concentrations of the enolic form ($c_0 = 0.5 \times 10^{-4}$ gM.1^{-1}) the process satisfies the function:

$$\ln C_0^e - \ln C_t^e = kt$$

which is a solution of the rate equation for a first order kinetics. C_0^e denotes the initial concentration of the enol form and C_t 'is the concentration t min after starting the kinetic run. These results undoubtedly show that the photoketonization of enol forms of β-ketoesters proceeds as a simple type photochemical reaction.

A considerable body of evidence (Table 2) shows that the substituents (R_1, R_2, R_3) have no marked effect on the rate of photoketonization in its first (zeroth order kinetics) and second (first order kinetics) steps. But in some cases, values of $k_{(0)}$ and $k_{(1)}$ (Table 2) are particularly sensitive to the structural features of the β-ketoesters under consideration. For instance, the branching of the carbon chain of R_1 in the vicinity of the carbonyl group causes a raise of the rate of the photoconversion (compound VI). Introduction of a methylene group between the isopropyl radical and the carbonyl carbon atom diminishes the value of the respective rate constants (compound VII).

The replacement of enolic hydrogen with deuterium causes a lowering of the rate of the photoconversion. The zeroth order rate constants of nondeuterated and deuterated ethyl acetoacetate are 0.995×10^{-8} and 0.770×10^{-8} respectieyly.

The photoinduced hydrogen transfer appears to occur with a nearly constant quantum yields. The variations of the structure of the β-ketoesters results in minor differences of the values of Φ. But it must be emphasised that compounds XIV, XVII and XVIII show substantially lower quantum yields. On the other hand XVII and XVIII possess a very intensive fluorescence.[7] Consequently, one can conclude that in these cases the photophysical process of deactivation prevails and the photochemical transformation proceeds very inefficiently.

The presence of the hypsochromic shift of the UV-band, inherent in the *cis*-enol form of β-dicarbonyl system was established as a result of the UV irradiation.[8] This observation has been confirmed now.

In some cases (compounds XIII, XV, XIX) the spectral shift reaches 20 nm (Figure 4). To some extent this can be explained by the existence of a process of photoisomerization leading to the *trans*-enol form. This is in agreement with the previously established theoretical data[9] in this respect. According to Kabatchnik *et al.*[10] the band at 239 nm is due to the *trans*-enol form of α-alkylated β-ketoesters.

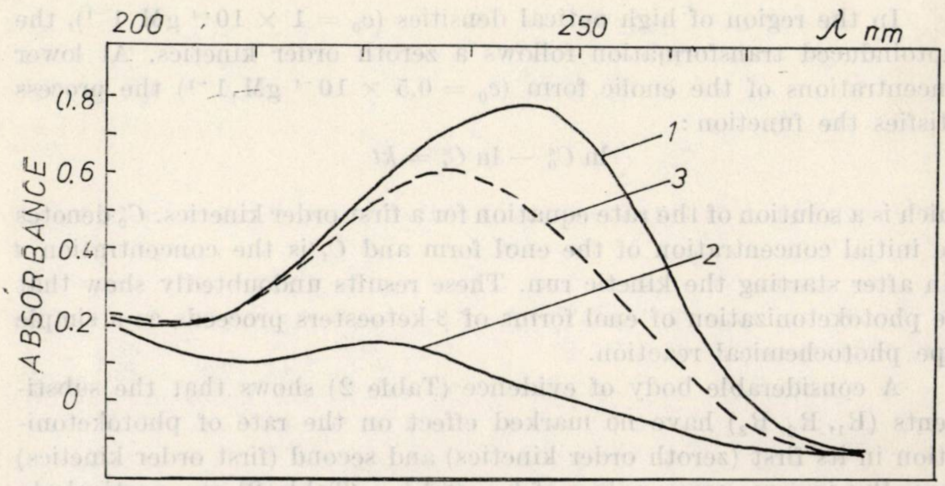

Fig. 4. — UV spectra of XIII in heptane (ca 1×10^{-4} gM.1^{-1}) : curve 1, before exposition to UV irradiation ; curve 2, after a 40 min exposition ; curve 3, 24 hr after the end of irradiation.

EXPERIMENTAL

Compounds I—XX were produced according to ref.,[11-12] and purified prior to use to a purity of 99% or higher.

Heptane (Merck, spectroscopic grade) was used as solvent. Heptane solutions with concentrations 0.5×10^{-4} and 1.0×10^{-4} gM.1^{-1} were prepared and kept in the dark until thermodynamic equilibrium between the two tautomeric forms was established. The samples (2 ml of these solutions) were thermostated at 20°C in a quartz-glass vessel and exposed to 254 nm UV irradiation under standard conditions.

UV irradiation was obtained from a Hanau medium pressure mercury arc lamp, using filters for 254 nm wavelength.

The UV absorption spectra were measured on a Specord-UV-VIS spectrophotometer using quartz cells 1.0 cm long. The IR spectra were measured on a UR-10 double beam spectrophotometer produced by Carl Zeiss-Jena. The quantum yields were determined following the procedure given by Masson *et al.*[13]. The enol content in heptane solutions of I—XX was obtained by using bromine titration measurements.[14]

REFERENCES

[1] P. Markov, L. Shishkova and Z. Zdravkova, *Tetrahedron Letters*, **39**, 4017 (1972).

[2] P. Markov and E. Radeva, *J. Photochemistry*, **4**, 179 (1975).

[3] P. Markov and I. Petkov. *Tetrahedron*, **33**, 1013 (1977).

[4] P. Markov, I. Petkov and D. Jeglova, *J. Photochemistry*, **8**, 277 (1978).

[5] Z. Bankovska, *Roczniki Chemii*, **9**, 5 (1967).

[6] F. Korte und F. Wüsten, *Liebigs Ann. Chem.*, **647**, 18 (1961).

[7] Unpublished data, P. Nikolov, I. Petkov, F. Fratev and P. Markov.

[8] D. Veierov, T. Bercovici, E. Fischer, Y. Mazur and A. Yogev, *J. Amer. Chem. Soc.*, **99**, 2723 (1977).

[9] P. Markov and F. Fratev, *Compt. rend. Acad. bulg. Sci.*, **28**, 771 (1975).

[10] M. I. Kabatchnik, S. T. Ioffe, E. M. Popov and K. V. Vatsuro, *Zhur. org. Khim.*, **31**, 2682 (1961).

[11] M. Viscontini and N. Merckling, *Helv. Chem. Acta*, **35**, 2280 (1952).

[12] C. A. Bischoff, *Ber. dtsch. chem. Ges.*, **28**, 2616 (1895).

[13] C. R. Masson, V. Boekelheide and W. A. Noyes, Jr., "Technique of Organic Chemistry", Vol. 2, Interscience, New York, 1956, p. 295.

[14] C. H. Ward, *J. Chem. Educ.*, **39** 95 (1962).

Revue Roumaine de Chimie, 27, 7, 853–857(1982)

Pd/SiO$_2$–AlPO$_4$ CATALYZED REDUCTION OF NITROBENZENES BY HYDROGEN

TRANSFER FROM CYCLOHEXENE

M.A. ARAMENDIA, V. BORAU, C. JIMENEZ and J. M. MARINAS

Departamento de Química Orgánica, Facultad de Ciencias,
Universidad de Córdoba, Spain

Received February 12, 1981

Reduction of nitrobenzene and substituted nitrobenzenes have been carried out by hydrogen from cyclohexene using a Pd/SiO$_2$–AlPO$_4$ (0.6 % *w*/*w* metal loading) catalyst. The reduction rate of electron donor-containing nitrocompounds is larger than that corresponding to electron acceptor-containing substrates.

INTRODUCTION

Although hydrogen transfer reduction processes seem to be progressively important in organic chemistry,[1] data in the literature concerning synthesis of aniline-like products by reduction of aromatic nitro-compounds are still scarce. In this sense, works by Braude and Linstead [2] using palladium-containing catalysts and different hydrogen suppliers are pioneer in this field.

Entwistle *et al.*[3–6] have sistematically studied these reactions and have undoubtedly demonstrated by TLC the existence of several molecular intermediates. Furthermore, using appropiate hydrogen suppliers molecules, it has been possible to stop the reaction at the hydroxylamine intermediate [7] or to reduce more than one nitro group of the same molecule of substrate.[6] On the other hand, Bar-Ilan *at al.*[8] have reported the reduction of nitrobenzene using 1,4-cyclohexadiene as hydrogen supplier and metallic phtalocynnines as catalysts.

In a previous paper,[9] we have shown a low-content palladium system supported on AlPO$_4$/SiO$_2$ (20 :80) acts as an efficient catalyst in the reduction of nitrobenzene and substituted nitrobenzene using triethylammonium formate as hydrogen supplier. The reduction rate of electron donor-containing nitrocompounds was smaller than that corresponding to electron acceptor-containing substrates.

In the present paper, data are reported on the reduction of the same compounds using the same catalyst but a different molecule, cyclohexene, as hydrogen supplier.

EXPERIMENTAL

The synthesis and physico-chemical characterization of the catalyst have been published elsewhere [9].

The experiments were carried out in a 50 ml, three necked flask, with refluxing refrigerent, thermometer and septum, immersed in a silicon-oil bath. When the hydrogen donor (cyclohexene) was used as a solvent itself, 1.5×10^{-2} mol nitrocompound, 7.0×10^{-2} mol cyclohexene and 0.45 g catalyst (0.56 % Pd *w/w* content) were used. If another solvent (THF) is used, 1.5×10^{-2} mol nitrocompound, 5.0 mol THF, 3.3×10^{-2} mol cyclohexene and 0.45 g catalyst were used. In both cases, the temperature was kept at 110 ± 5°C and the system magnetically stirred at 720 rpm to avoid any effect of diffussion on the reaction, up to a total reaction time of 8 h. Small portions of sample were periodicaly withdrawn through the septum and analyzed as described below.

Analysis of the products was carried out in a Hewlett-Packard 5830 gas chromatograph, equiped with flame detector, recorder and integrating units. The experimental conditions were different according to the properties of the products to be analyzed, but polyphenyl-ether or UCC columns were always used. In some cases, simultaneous GC-MS analysis with a Hewlett-Packard 59928 system was carried out.

RESULTS AND DISCUSSIONS

Blanck runs (in the same experimental conditions as used with the catalyst) did not yield any reaction product, even after 8 h reaction.

In all the cases reported here, corresponding amine was always obtained, without any GC evidence of the existence of nitroso compounds, phenylhydroxylamines or their condensation products. With *m*-dinitro-

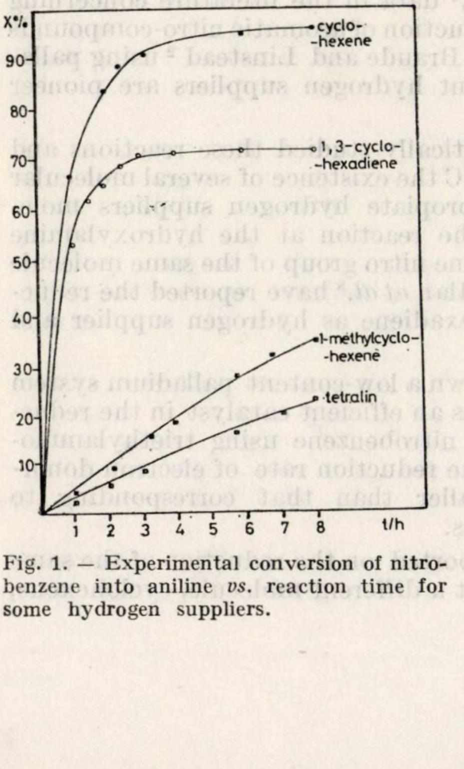

Fig. 1. — Experimental conversion of nitrobenzene into aniline *vs.* reaction time for some hydrogen suppliers.

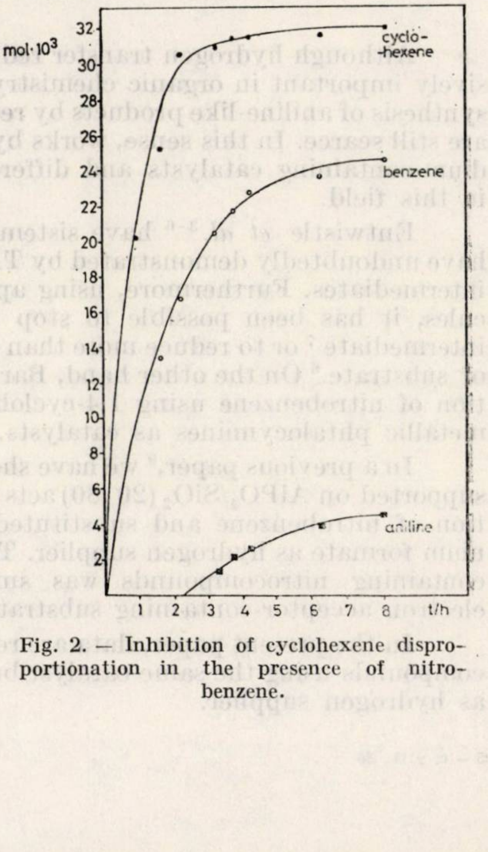

Fig. 2. — Inhibition of cyclohexene disproportionation in the presence of nitrobenzene.

benzene only one of the two nitro groups was reduced, while-*p*-nitrobenzaldehyde is mainly reduced to the corresponding *p*-aminobenzaldehyde and only traces of *p*-amine and *p*-nitrobenzylic-alcohol were detected.

When different hydrogen suppliers, namely 1,3-cyclohexadiene, cyclohexene, 1-methylcyclohexene, tetraline, α-phellandrene and limonene, were used, it was found in our experimental conditions, that the best results are obtained with cyclohexene. Fig. 1 shows the change in the conversion to aniline *vs.* reaction time for different hydrogen suppliers in the reduction of nitrobenzene. α-Phellandrene and limonene yield to less than 0.5 % conversion even after 8 h reaction.

In the presence of a catalyst, cyclohexene disproportionates to benzene cyclohexane; however, this process is inhibited if an aromatic derivative is added, as Fig. 2 shows. Once the disproportionation stops, the amount of cyclohexane remains constant, while benzene and aniline are evolved.

Table 1 summarizes the yields to amines, depending on the reaction time, when THF or cyclohexene itself are used as solvents.
For *o*-bromo-nitrobenzene a poor yield (to aniline) is obtained as a consequence of the bromine hydrogenolysis and the further poisoning of the catalyst.

TABLE 1

Conversion to amine (% mol) of some aromatic nitrocompounds. Solvent THF

Nitrocompound	1h	2h	3h	4h	5h	6h	7h
o-Nitrophenol	14.56	27.94	39.20	51.52	62.16	73.92	82.88
m-Nitrophenol	14.00	25.20	36.96	47.60	57.12	66.08	74.48
Nitrobenzene	12.88	23.52	30.80	39.20	46.48	53.20	59.92
Nitrobenzene *	23.45	35.51	44.89	55.61	63.65	70.35	76.38
p-Nitrophenol	9.52	15.68	26.88	34.16	42.00	48.15	54.88
p-Nitrotoluene	9.52	14.56	25.76	32.48	38.08	43.68	48.62
p-Nitrotoluene *	14.07	22.11	27.47	34.17	90.20	44.89	48.24
m-Dinitrobenzene	4.48	7.84	12.88	17.36	20.16	21.28	23.52
m-Dinitrobenzene *	2.68	4.69	6.70	8.04	9.38	10.05	10.72
Ethyl-p-nitroacetate	4.48	8.40	13.44	17.92	21.84	25.76	29.68
p-Nitroacetophenone	2.24	4.48	6.16	8.40	10.08	11.76	13.44
p-Nitroacetophenone *	5.36	8.71	7.37	16.08	18.76	21.44	24.12
m-Nitrobenzaldehyde	0.56	0.84	1.12	1.40	1.68	1.68	1.68
o-Nitroaniline	—	—	—	—	—	—	<0.02
m-Nitroaniline	—	—	—	—	—	—	<0.02
p-Nitroaniline	—	—	—	—	—	—	<0.02
p-Metoxynitrobenzene	—	—	—	—	—	—	<0.02

* Acting itself as a solvent (cyclohexene)

Table 2 collects the initial reduction rate (r_0) with THF or cyclohexene as solvents.

The reduction rate is nearly zero if a basic substituent (*e.g.*, $-OCH_3$, $-NH_2$) is present in the aromatic ring of the substrate, and it can be due to the presence of acid centers on the surface of the catalyst; in such a case, the original basic group in the substrate molecule together with the amino group formed along the reaction may be adsorbed on the acid centers of the catalyst, thus blocking them and leading to its deactivation.

On the other hand, the reduction rates for electron-donor containing nitrobenzenes are larger than those corresponding to electron-acceptor containing substrates. Using THF as a solvent, a good correlation ($r = 0.99$) has been obtained by plotting the Hammett parameter, σ for electron donor groups ($-OH$, $-CH_3$) in *meta-* and *para-*positions from the nitro group *vs.* $\log r_0/r'_0$, where r_0 stands for the initial reduction rate of substitued nitrobenzene, and r'_0 for that corresponding to nitrobenzene. From this graph, a value of 0.4 is obtained for the Hammett parameter ρ from the slope of the straight line. On the contrary, with electron-acceptor groups, a better correlation is obtained when plotting $\log r_0/r'_0$ *vs* instead of σ ($\rho = -1.0$ and -2.3, respectively).

TABLE 2

The initial reduction rate (r_0) with THF or cyclohexene as solvents

Nitrocompound	r_0 (mol. hr^{-1}) 10^3	Nitrocompound	r_0 (mol. hr^{-1}) 10^3
o-Nitrophenol	1.45	Ethyl-p-nitroacetate	0.35
m-Nitrophenol	1.30	*p*-nitroacetophenone	0.15
Nitrobenzene	1.10	*p*-nitroacetophenone *	0.75
Nitrobenzene *	3.70	*p*-nitrobenzaldehyde	0.07
p-Nitrophenol	1.00	*o*-nitroaniline	0.02
p-Nitrotoluene	0.95	*p*-nitroaniline	0.02
p-Nitrotoluene *	2.10	*m*-nitroaniline	0.02
m-Dinitrobenzene	0.40	*p*-metoxynitrobenzene	0.02
m-Dinitrobenzene *	0.45	*o*-bromonitrobenzene	—

* Acting itself as a solvent (cyclohexene).

According to these results, it may be concluded that there is a change in the reduction mechanism on passing from electron-donor — containing — substrates to electron-acceptor ones, these last having a major effect on the reaction rate.

TABLE 3

Conversion to aniline (% mol) of nitrobenzene

Hydrogen suppliers	1h	2h	3h	4h	5h	6h	7h	8h
Cyclohexene	66'6	83'4	90'3	90'3	93'9	94'1	95'1	95'2
1,3-Cyclohexadiene	53'3	61'5	70'3	70'3	70'3	70'3	70'3	70'3
1-Methylcyclohexene	4'6	10'0	14'6	19'3	23'3	27'2	31'8	34'6
Tetralin	3'9	6'6	9'2	11'3	14'6	16'8	20'0	22'6

It should be pointed out that the general trend in the reaction rate when studying electron-donor and electron-acceptor containing substrates reverses if triethylammonium formate is used as hydrogen supplier [9] instead of cyclohexene, despite the fact that the same Pd catalyst is used. These results suggest that both systems may play a complementary role in these reactions.

TABLE 4

Inhibition of cyclohexene disproportionation in the presence of nitrobenzene

mol. 10^3	1h	2h	3h	4h	5h	6h	7h	8h
Anilinen	*	*	1′0	2′2	3′2	4′0	4′4	4′6
Benzene	10′8	16′5	20′0	22′3	23′2	24′2	24′5	24′8
Cyclohexene	20′3	30′2	30′9	31′2	31′2	31′4	31′5	31′9

* After 2h 15 m nitrobenzene is added.

REFERENCES

[1] G. Brieger nad T. J. Nestrick, *Chem. Rev.*, **74**, 567 (1974).
[2] E. A. Braude, R. P. Linstead, and K. R. H. Wooldridge, *J. Chem. Soc.*, **1954**, 3586.
[3] I. D. Entwistle, R. A. W. Johnstone and J. Porrall, *J. Chem. Soc. Perkin I*, **1979**, 1390; Ibid., **1975**, 1424.
[4] A. E. Jackson, and R. A. W. Johnstone, *Synthesis*, **1976**, 685.
[5] I. D. Entwistle, A. E. Jackson, R. A. W. Johnstone and R. P. Telford, *J. Chem. Soc. Perkin I*, **1977**, 443.
[6] I. D. Entwistle, R. A. W. Johnstone and R. P. Telford, *Chem. Res.*, **1977**, 1382.
[7] I. D. Entwistle, T. Gilkerson, R. A. W. Johnstone and R. P. Telford, *Tetrahedron*, **34**, 213 (1978).
[8] A. Bar-Ilan and J. Manassen, "Proceedings 5th Congress Catalysis", Vol. 2, **1973**, p. 1149.
[9] M. A. Aramendía, M. S. Climent, C. Jiménez, and J. M. Marinas, *React. Kinet. Catal. Lett.*, **14**, 489 (1980).

Revue Roumaine de Chimie, **27**, *7*, 859—864 (1982)

SYNTHESIS AND BIOLOGICAL ACTIVITY OF CERTAIN DERIVATIVES OF 2,4-DIOXO-1,2,3,4-TETRAHYDROQUINAZOLINE. I

A. N. OSMAN*, M. KHALIFA*, M. A. ISMAIL**, A. E. OSSMAN** and M. G. IBRAHIM**

* Department of Organic Chemistry, Faculty of Pharmacy, University of Cairo

** Department of Pharmaceutical Chemistry, School of Pharmacy, Al-Azhar University, Cairo, A.R.E.

Received December 5, 1980

The synthesis of certain new derivatives of 2,4-dioxo-1,2,3,4-tetrahydroquinazoline is described. The structure of the products was confirmed by IR and mass spectrometry. Preliminary pharmacological screening of these compounds showed that they possess hypothermic and analgesic activities comparable to that of phenylbutazone. Compared to indomethacin, all tested compounds except one showed moderate degrees of antiinflammatory activity.

INTRODUCTION

During the past few years, the search for new non-steroidal antiinflammatory drugs has continued with growing urgency. Such drugs are important for the management of a great variety of rheumatic and other inflammatory conditions. Therefore, looking for new antiphlogistic compounds of non acidic nature, Yabuuchi *et al.* [1-3] synthesized some 2,4-dioxo-1,2,3,4-tetrahydroquinazoline derivatives having analgesic and antiinflammatory activities. Very recently, a new quinazolone drug I has been introduced into medical practice as antiinflammatory agent, under the name "Proquazone".[4]

INVESTIGATIONS, RESULTS AND DISCUSSION

On the basis of the above it has been decided to prepare some new derivatives of 2,4-dioxo-1,2,3,4-tetrahydroquinazoline having the general formula III, (Table), for screening them as antiinflammatory agents.

For the preparation of the key intermediate, 1-substituted-2,4-dioxo-1,2,3,4-tetrahydroquinazoline (II), anthranilic acid was alkylated or arylated, and then the products were cyclized by fusion with urea, using reported procedures.[5-7] Heating II with benzoyl chloride in pyridine-DMF mixture gave the corresponding 3-benzoyl derivatives (Scheme 1). The structure of these derivatives was confirmed by spectroscopic methods. Thus, the IR spectra of III (a, c, e) showed intense absorption in the 1708—1700 cm^{-1} region (benzoyl carbonyl attached at position-3). The 2,4-dioxo-1,2,3,4-tetrahydroquinazoline moiety showed two carbonyl absorption bands: one at a higher frequency in the 1750—1740 cm^{-1} region (assignable to the C = O at position-4), and the other at a lower wavenumber in the 1678—1668 cm^{-1} region (indicative of the C = O at position-2).

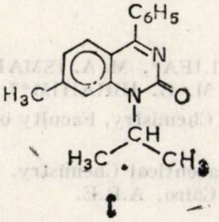

On the other hand, refluxing II with benzyl chloride in the presence of anhydrous K_2CO_3 afforded the 3-benzyl derivatives III (b, d, f).

(Scheme 1)

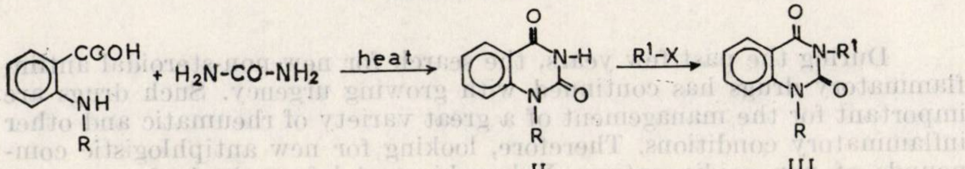

R = $-C_2H_5$;
C_5H_5- ; or
$CH_3-C_6H_4-$ (para—).

(a) R = C_2H_5-,
$R^1 = C_6H_5-CO-$;
(b) R = C_2H_5-,
$R^1 = C_6H_5-CH_2-$;
(c) R = C_6H_5-,
$R^1 = C_6H_5-CO-$;
(d) R = C_6H_5-,
$R^1 = C_6H_5-CH_2-$;
(e) R = $CH_3-C_6H_4-$(*para*—),
$R^1 = C_6H_5-CO-$;
(f) R = $CH_3-C_6H_4-$(*para*—),
$R^1 = C_6H_5-CH_2-$.

The IR spectra of the latter compounds are in full correspondence with their structures. Two carbonyl bands were shown : a lower intensity band at the higher frequency in the 1707—1690 cm^{-1} region (C = O at position-4) and a relatively higher intensity band at a lower frequency in the 1660—1645 cm^{-1} region (C = O at position-2).

Further evidence for the structure of III was obtained from the mass spectra of some members of this series. Schemes 2—4 illustrate the

(Scheme 2)

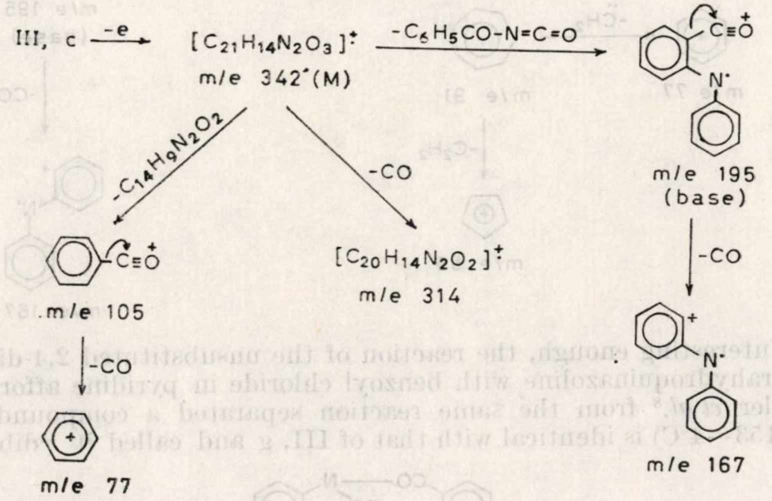
III, c
-e
$[C_{21}H_{14}N_2O_3]^{+\cdot}$
m/e 342˙(M)
$-C_6H_5CO-N=C=O$
m/e 195 (base)
$-C_{14}H_9N_2O_2$
-CO
m/e 105
$[C_{20}H_{14}N_2O_2]^{+\cdot}$
m/e 314
-CO
m/e 77
m/e 167

fragmentation patterns which could be assigned for the prominent peaks observed in the corresponding mass spectra.

(Scheme 3)

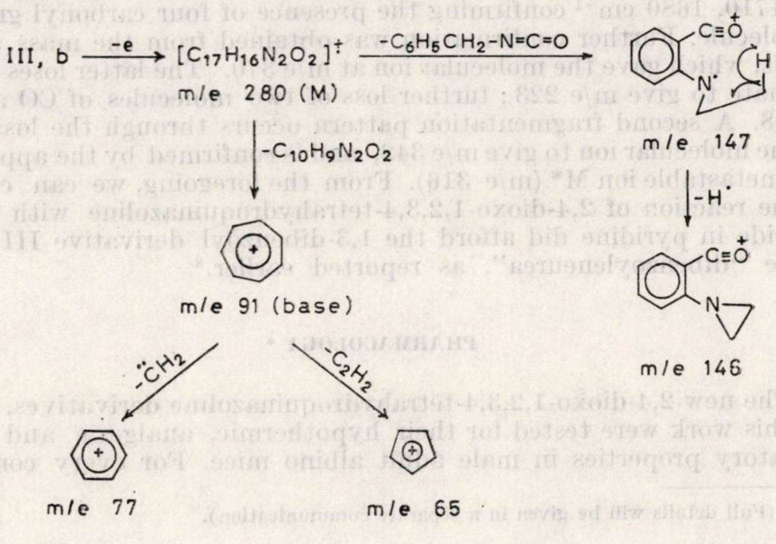
III, b
-e
$[C_{17}H_{16}N_2O_2]^{+\cdot}$
m/e 280 (M)
$-C_6H_5CH_2-N=C=O$
m/e 147
$-C_{10}H_9N_2O_2$
m/e 91 (base)
-H˙
m/e 146
$-\ddot{C}H_2$
C_2H_2
m/e 77
m/e 65

(Scheme 4)

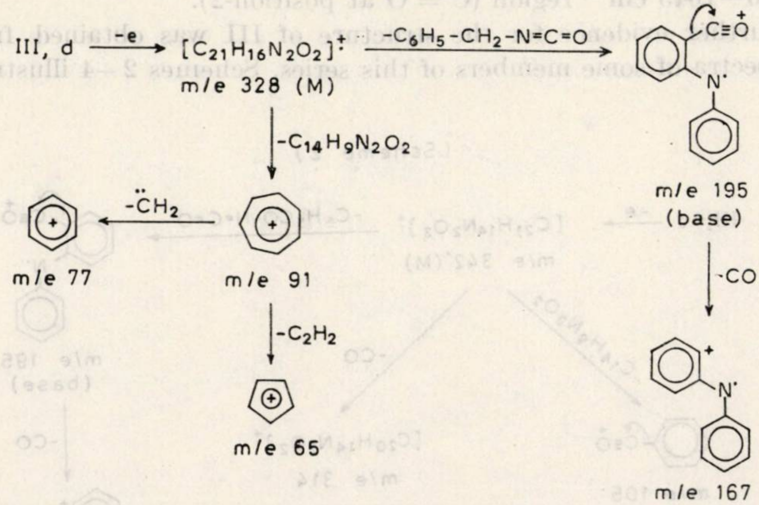

Interesting enough, the reaction of the unsubstituted 2,4-dioxo-1,2,3,4-tetrahydroquinazoline with benzoyl chloride in pyridine afforded III, g. Heller *et al.*[8] from the same reaction separated a compound, whose m.p. (153—4°C) is identical with that of III, g and called it "dibenzoyleneurea". For such a name formula IV might be proposed. Consequently, to clarify the ambiguity of the name "dibenzoyleneurea" compound III, g was subjected to IR analysis which showed the following bands : 1765, 1735, 1710, 1680 cm^{-1} confirming the presence of four carbonyl groups in the molecule. Further confirmation was obtained from the mass spectral analysis, which gave the molecular ion at m/e 370. The latter loses benzoyl isocyanate to give m/e 223; further loss of two molecules of CO afforded m/e 168. A second fragmentation pattern occurs through the loss of CO from the molecular ion to give m/e 342, and is confirmed by the appearance of the metastable ion M* (m/e 316). From the foregoing, we can conclude that the reaction of 2,4-dioxo-1,2,3,4-tetrahydroquinazoline with benzoyl chlororide in pyridine did afford the 1,3-dibenzoyl derivative III, g and not the "dibenzoyleneurea", as reported earlier.[8]

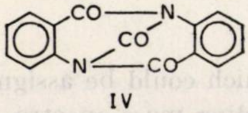

IV

PHARMACOLOGY *

The new 2,4-dioxo-1,2,3,4-tetrahydroquinazoline derivatives, obtained in this work were tested for their hypothermic, analgesic and antiinflammatory properties in male adult albino mice. For every compound three dose levels were used : 30, 60 and 90 mg/kg. All these compounds except III, b showed variable degrees of analgesic activities comparable to that of phenylbutazone. At high dose levels signs and symptoms of acute toxicity have been observed such as drowsiness and haematurea. With respect to indomethacin, these compounds showed moderate degrees of antiinflammatory activities.

---

* (Full details will be given in a separate communication).

TABLE

2,4-Dioxo-1,2,3,4-tetrahydroquinazoline derivatives III

III	Solvent of crystallization*	M.P. (°C)	Yield (%)	Molecular formula	Analysis calcd/Found		
					C	H	N
(a)	(A)	158	80	$C_{17}H_{14}N_2O_3$	69.38	4.76	9.5
					69.3	5.3	10.0
(b)	(B)	98	86	$C_{17}H_{16}N_2O_2$	72.8	5.7	10.0
					72.8	6.1	10.5
(c)	(B)	193	68	$C_{21}H_{14}N_2O_3$	73.68	4.09	8.18
					73.84	4.0	8.1
(d)	(C)	205	92	$C_{21}H_{16}N_2O_2$	76.82	4.87	8.53
					76.40	4.9	8.5
(e)	(C)	210	71	$C_{22}H_{16}N_2O_3$	74.15	4.49	7.44
					74.4	4.30	7.9
(f)	(B)	174	92	$C_{22}H_{18}N_2O_2$	77.1	5.76	8.18
					77.3	5.20	8.4
(g)	(C)	154	92	$C_{22}H_{14}N_2O_4$	71.3	3.7	7.5
					71.5	4.0	7.3

* (A) ethanol ; (B) aqueous ethanol (1 : 1) ; (C) aqueous dioxane (1 : 1).

EXPERIMENTAL

All m.p. are uncorrected and were measured using the open capillary method. Microanalyses were carried out in the microanalytical Laboratory, Faculty of Science, University of Cairo, ARE. The IR spectra were recorded on a Pye Unicam sp 1100 spectrophotometer using KBr discs. Mass spectra were performed on an Organic ms 20 AEI (70 eV), with computer read out.

Substituted-3-benzoyl-2,4-dioxo-1,2,3,4-tetrahydroquinazolines. General procedure:

Compounds III, a,c,e were prepared by heating under reflux a mixture of the appropriate 1-substituted-2,4-dioxo-1,2,3,4-tetrahydroquinazoline (II, 0.01 mole), pyridine (5 ml), dimethylformamide (5 ml) and benzoyl chloride (3 ml). Heating was continued for 2 hours, then the reaction mixture was cooled to room temperature and transferred to a beaker containing dil. HCl solution (10 ml) with stirring. The solid product which separated out was filtered off, washed with water, and dilute NaOH solution. It was finally washed several times with water, air dried and recrystallized from the suitable solvent (Table).

Substituted-3-benzyl-2,4-dioxo-1,2,3,4-tetrahydroquinazolines (Table).
General procedure:

Compounds III, b,d,f were obtained by refluxing a mixture of the suitable 1-substituted-2,4-dioxo-1,2,3,4-tetrahydroquinazoline (II, 0.01 mole), anhydrous K_2CO_3(2.0 g) and benzyl chloride (10 ml) for 6 hours. Excess benzyl chloride was then removed by distillation under reduced pressure. The residue was stirred thoroughly with water, filtered off, and air dried. The dry product was extracted several times with petroleum ether and finally was recrystallized from the appropriate solvent (Table).

REFERENCES

[1] T. Yabuuchi, M. Fujimura, A. Nakagawa and R. Kimura, Ger. offen., 2, 120, 663, 11 Nov. 1971 ; Japan. 27 Apr. 1970 ; *Chem. Abstr.*, **76**, 72548 (1972).

[2] T. Yabuuchi, M. Fujimura, A. Nakagawa and R. Kimura, Japan Kokai 7340, 788, 15 Jun. 1973 ; Appl. 1778, 926 ; 07 Oct. 1971 ; *Chem. Abstr.*, **79**, 66400 (1973).

[3] T. Yabuuchi, M. Fujimura, A. Nakagawa and R. Kimura, Japan Kokai 7340, 790, 15 Jun. 1973 ; Appl. 1778, 928 ; 07 Oct. 1971 ; *Chem. Abstr.*, **79**, 66401 (1973).

[4] H. Gubbler and M. Baggiolini, Scand. *J. Rheum. Suppl.*, **21**, 5 (1978).

[5] G. Pastor, C. Blanchard, C. Montginoul, E. Torreilles, L. Giral and A. Taxier, *Bull. Soc. Chim. France*, **1975**, 1331.

[6] A. N. Lange and F. E. Sheibley, *J. Amer. Chem. Soc.*, **55**, 2113 (1933).

[7] S. Somasekhara, V. S. Dighe and S. L. Mukherjee, *Curr. Sci.*, **37**, 529 (1968) ; *Chem. Abstr.*, **70**, 2028 (1969).

[8] G. Heller, A. Buchwarldt, R. Fucus, W. Kleinicke and J. Kloss, *J. prakt. Chem.*, **111**, 1 (1925) ; *Chem. Abstr.*, **20**, 382 (1926).

Revue Roumaine de Chimie, 27, 7, 865–877 (1982)

1,4-ARYLATION OF β-(4-CHLORO-3-METHYLBENZOYL)-ACRYLIC ACID WITH ACTIVATED HYDROCARBONS UNDER FRIEDEL-CRAFTS CONDITIONS AND SOME STUDIES ON THE PRODUCTS

M.M. MOHAMED *, M. A. El-HASHASH *,
I. ISLAM ** and O. A. ABO-BAKER **

* Department of Chemistry, Faculty of Science, Ain Shams University, Abbassia, Cairo, Egypt
** Department of Chemistry Faculty of Science (Girls), El-Azhar University, Cairo, Egypt

Received February 6, 1981

The Friedel-Crafts alkylation of *p*-xylene, *m*-xylene, *o*-xylene, ethylbenzene and *p*-cymene with β-(4-chloro-3-methylbenzoyl)-acrylic acid **(1)** gave the corresponding α-aryl-β-(4-chloro-3-methyl)-benzoylpropionic acids, **2 a-f.** The acids **2** react with acetic anhydride yielding the corresponding butenolides **3** or the ketone **4** depending on the reaction conditions. The reaction of the butenolides **3** with ammonium acetate, *p*-toluidine, cyclohexylamine, hydrazine hydrate, semicarbazide hydrochloride, hydroxylamine hydrochloride and *p*-xylene has been described. The ketone **4** condenses with diethylsuccinate in the presence of potassium *t*-butoxide to give the lactonic ester **16.**

Recently it was reported that when β-(3,4-dichloro)-benzoyl-acrylic acid was treated with aromatic hydrocarbons and aluminium chloride, addition occurred alpha to the carboxyl group.[1] In the present investigation, we have tried to augment the reactivity of the β-carbon atom toward the nucleophiles, by decreasing the polarity of the carbonyl group using two oppositely polar groups in the aromatic] ring of acid **1**.

Thus, in the treatment of β-(4-chloro-3-methylbenzoyl)-acrylic acid **(1)** with aromatic hydrocarbons, namely: *p*-xylene, *m*-xylene, *o*-xylene, ethylbenzene and *p*-cymene under the Friedel-Crafts conditions, addition occurred alpha to the carboxyl group to give the corresponding α-aryl-β-(4-chloro-3-methyl)-benzoylpropionic acids, **2 a-f.** It can be deduced that the polar effect of substituents did not play any significant role in determining the mode of addition.

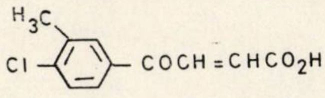

1

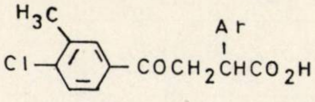

2

Ar

a, 2,5$-(CH_3)_2C_6H_3$
b, 2,4$-(CH_3)_2C_6H_3$
c, 3,4$-(CH_3)_2C_6H_3$
d, 2,3$-(CH_3)_2C_6H_3$
e, 4$-C_2H_5-C_6H_4$
f, 2$-CH_3-$5$-(CH_3)_2CH-C_6H_3$

The structure of the acids **2** was proved from their spectral data (c.f. Tables 1 and 2).

TABLE 1
IR Spectral data of the organic compounds **2**–**19**

Compd.	ν(CO), carboxylic, ketonic, amidic, γ-lactam, γ-lactone or ester	ν(CH)	ν(CH) out of plane deformation	ν(OH)	ν(NH)	ν(C=N)	ν(C=C)
2a	1705, 1685	2950 2870	880 810	3300	—	—	—
2b	1700, 1680	2950 2855	875 813	3300	—	—	—
2c	1705, 1685	2950 2850	910(1H) 840(2H's)	3255	—	—	—
2d	1705, 1690	2955 2850	890(1H) 850(2H's) 790(3H's)	3300	—	—	—
2e	1700, 1677	2950 2880	910 830	3300	—	—	—
2f	1700, 1680	2950 2870	890 835	3300	—	—	—
3a	1780	2950 2870	885 813	—	—	—	—
3b	1775	2950 2890	880 830	—	—	—	—
3c	1770	2950 2870	910(1H) 840(2H's)	—	—	—	—
3d	1762	2950 2880	890 850 790	—	—	—	—
4	1700	2930 2840	905 813	—	—	—	—
5	1740	—	—	3500	3200	—	1620
6	1749	—	—	—	—	1630	1610
7	1730	—	—	—	—	—	1620
8	1685, 1670	—	—	—	3300	—	—
9	1765	—	—	—	—	—	1615
10	1680, 1670	—	—	—	3350– 3200	—	—
11	1670, 1625	—	—	—	3200	1635	—
12	1690, 1660, 1670	—	—	—	3250 3400	—	—
13	1670, 1660	—	—	—	3250 3350	—	1610

Table 1 (continued)

Compd.	ν(CO)	ν(OH)	ν(NH)	ν(C=N)	ν(C≡N)
14	1690, 1682	—	—	—	—
15	1700	3370	3200	1635	—
16	1770, 1735	—	—	—	—
17	—	—	3300—3250	1665—1660	—
18	—	—	—	1630	—
19a	1710, 1640	—	3290	1620	—
19b	—	—	—	—	2220

TABLE 2

The ^1H-NMR spectra of compounds **2e, 3a, 11, 13, 17** and **18** in $CDCl_3$

Compd.	δ p.p.m.	Compd.	δp.p.m.
2e	1.42(t), CH_3 2.7(q), $-CH_2-$ 2.41(s), H_3C-Ar 2.8(m), $-CH_2-CO-$ 4.2(m), methine H (7.25(s) ; 7.6(m) ; 7.8(m), Ar—H's. 10.3(s), acidic H	**13**	2.3(s), 3H($p-Ar-CH_3$) 2.44(s), 3H($o-Ar-CH_3$) 2.5(s), 3H($m-Ar-CH_3$) 3.3(q), methine H 5.7—5.9, a complex pattern corresponding to ($=CH-$, NH and NH_2) (7.2(s) ; 7.3(s) ; 7.4(s) ; 7.5(d) ; 7.8(t)), 6 Ar—H.
3a	2.25(s), CH_3-Ar 2.40(s), CH_3-Ar 2.45(s), CH_3-Ar 2.1(d), methine H 6.0(d), olefinic H (7.1(d) ; 7.2(t) ; 7.6(m) ; 7.8(m)), 6 Ar—H	**17**	2.2(t), 4H(2 methylene gr's) 2.4(s), 3H($p-Ar-CH_3$) 2.43(s), 3H($o-Ar-CH_3$) 2.46(s), 3H($m-Ar-CH_3$) 6.1 (broad signal), NH (6.9(s) ; 7.4(m) ; 7.6(m) ; 7.8(m)), correspond to 6 Ar—H
11	2.3(s), CH_3-Ar 2.4(s), CH_3-Ar 2.45(s), CH_3-Ar 3.3(q),$-CH_2-$ 4.2(q), methine H 6.3 (broad signal), NH (7.1(s) ; 7.3(s) ; 7.4(d) ; 7.7(m)), 6 Ar—H	**18**	2.35(s), 3H($p-A-CH_3$) 2.42(s), 3H($o-Ar-CH_3$) 2.6(s), 3H($m-Ar-CH_3$) 2.88(m), 2H($-CH_2-Ar$) 3.7(m), 2H($-CH_2-C=N-$) (7.4(s) ; 7.46(t) ; 7.6(d) ; 7.8(d) ; 7.9(t)), 10 Ar—H

Treatment of the acids **2a, 2b, 2c** and **2d** with warm acetic anhydride yielded α-(4-chloro-3-methylphenyl)-γ-aryl-$\Delta^{\beta,\gamma}$-butenolides, **3 a-d**, respectively.

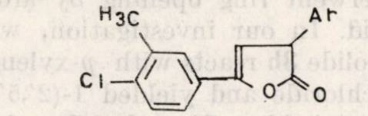

3

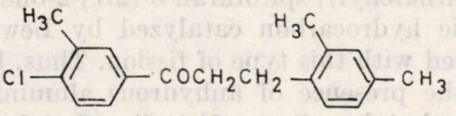

4

a, Ar = 2,5-$(CH_3)_2-C_6H_3$;
b, Ar = 2,4-$(CH_3)_2-C_6H_3$;
c, Ar = 3,4-$(CH_3)_2-C_6H_3$;
d, Ar = 2,3-$(CH_3)_2-C_6H_3$

On the other hand, treatment of the acid **2b** with boiling acetic anhydride yielded the ketone **4**; in this case decarboxylation takes place rather than dehydration.

The following data support the structure assigned for butenolide **3**:

(A) *By spectroscopy:* (c.f. Tables 1 and 2).

(B) *Chemically:*

(i) Treatment of **3b** with ammonium acetate in boiling xylene [2] yielded 2-[4′-chloro-3′-methylphenyl]-4-[2′,5′-dimethylphenyl]-2-pyrrolin-5-one **(5)**.

Carboethoxymethylation of **5** using ethyl chloroacetate in the presence of anhydrous potassium carbonate and dry acetone [3] afforded the ester **6**. From this result, we can conclude that compound **5** exists in the lactam-lactim tautomeric equilibrium.

(ii) Treatment of **3b** with *p*-toluidine in the presence of AcOH/AcONa mixture yielded 2-[4′-chloro-3′-methylphenyl]-4-[2′,4′-dimethylphenyl]-1-*p*-tolyl-2-pyrrolin-5-one **(7)**. This reaction is analogous to that of α-3-benzylidene-5-[1′-(2′-methylnaphthalenyl])-spirofuran-3-(2*H*)-2-one with the same reagent.[4]

On the other hand, **3b** reacts with cyclohexylamine in the presence of boiling ethanol to give the amidic derivative **8** together with the pyrrolinone derivative **9**.

Compound **8** was also obtained through an independent synthesis by the action of cyclohexylamine on the acid chloride of **2b**.

(iii) Butenolide **3b** reacts with hydrazine hydrate in boiling ethanol to give α-(2,4-dimethylphenyl)-β-(4-chloro-3-methylbenzoyl)-propionic acid hydrazide **(10)** together with 4-(2′,4′-dimethylphenyl)-1,4-dihydro-6-(4′-chloro-3′-methylphenyl)-3(2*H*)-pyridazinone **(11)**.

Both compounds **11** and **10** were also obtained by independent synthesis through the action of hydrazine on the acid **2b**, and on its chloride.

(iv) In this investigation the hitherto unknown reaction of semicarbazide with furanone **3b** was also realised. The butenolide **3b** reacts with semicarbazide hydrochloride in boiling pyridine and yielded α-(2,4-dimethyphenyl)-β-(4-chloro-3-methylbenzoyl)-propionic acid N-carbamoylhydrazide **(12)**, together with the pyridazinone derivatives **13**.

(v) Recently,[4] it was reported that α-3-benzylidene-5-[1′-(2′-methylnaphthalenyl)]-spirofuran-3-(2*H*)-2-one underwent ring opening by aromatic hydrocarbon catalyzed by Lewis acid. In our investigation, we agreed with this type of fission. Thus, butenolide **3b** reacts with *p*-xylene in the presence of anhydrous aluminium chloride and yielded 1-(2′,5′-dimethylphenyl) - 2 - (2′,4′-dimethylphenyl)-4-(4′-chloro-3′-methylphenyl)-1,4-butane dione **(14)**. Compound **14** was also obtained by an independent synthesis *via* the Friedel-Crafts reaction involving the chloride of **2b** and *p*-xylene.

Reactions of the butenolide **3b** with ammonium acetate, amines, hydrazine, semicarbazide and *p*-xylene are represented in the following Chart 1 :

Chart 1

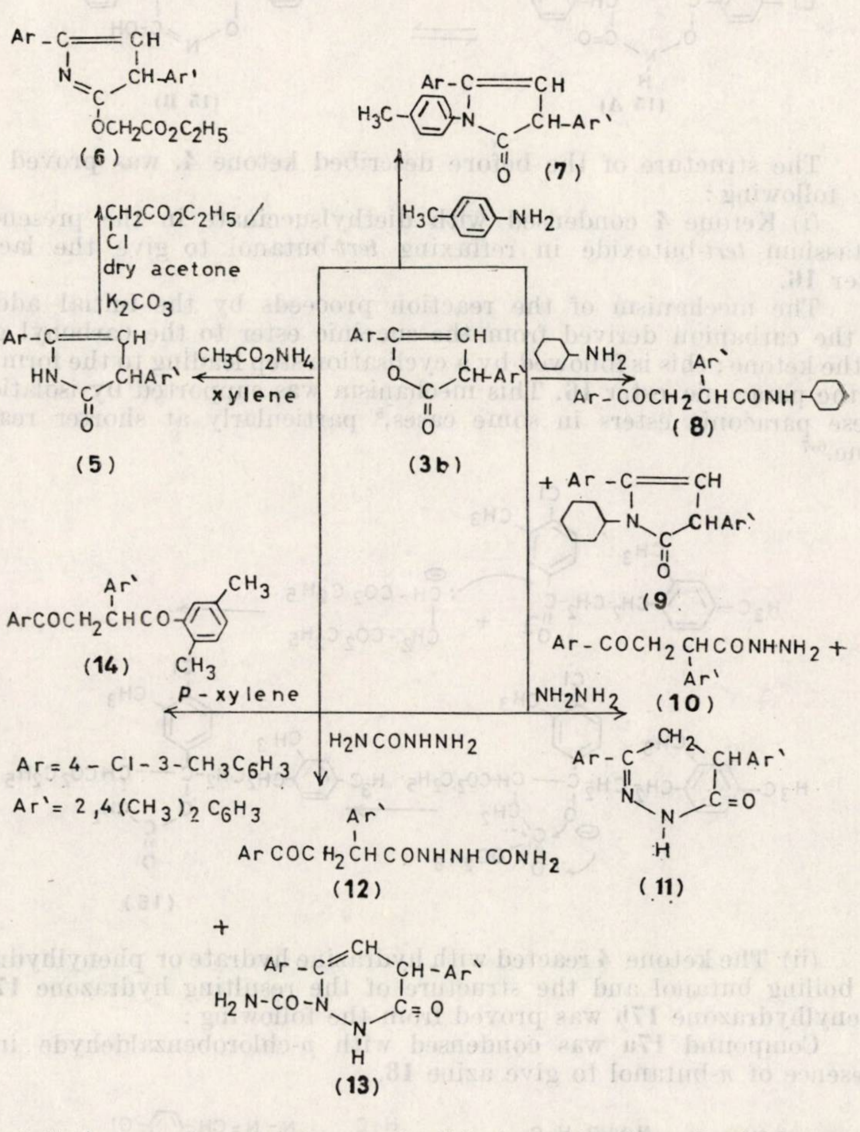
(6)
(7)
$H_3C-C_6H_4-NH_2$
$ClCH_2CO_2C_2H_5$
dry acetone
K_2CO_3
$CH_3CO_2NH_4$
xylene
(5)
(3b)
(8)
(9)
(14)
p - xylene
NH_2NH_2
(10)
$H_2NCONHNH_2$
Ar = 4 - Cl - 3 - $CH_3C_6H_3$
Ar' = 2,4 $(CH_3)_2$ C_6H_3
$ArCOCH_2CH(Ar')CONHNHCONH_2$
(12)
(11)
(13)

(vi) As a point of interest, in this investigation, the hitherto unknown reaction of hydroxylamine hydrochloride with compound **3d** was realised. Compound **3d** reacted with hydroxylamine hydrochloride in boiling pyridine to give 5-(2′,3′-dimethylphenyl)-3-(4′-chloro-3′-methylphenyl)-1,2-dihydro-2-1-oxazin-6-one **(15)**. The infrared spectrum of compound **15** suggests that the oxazinone **15** exists in the lactam-lactim tautomeric equilibrium **(15A ⇌ 15B)**.

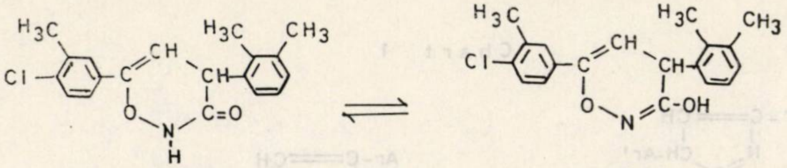

(15 A) **(15 B)**

The structure of the before described ketone **4**, was proved from the following :

(i) Ketone **4** condensed with diethylsuccinate in the presence of potassium *tert*-butoxide in refluxing *tert*-butanol to give the lactonic ester **16**.

The mechanism of the reaction proceeds by the initial addition of the carbanion derived from the succinic ester to the carbonyl group of the ketone ; this is followed by a cyclisation step leading to the formation of the paraconic ester **16**. This mechanism was supported by isolation of these paraconic esters in some cases,[5] particularly at shorter reaction time.[6,7]

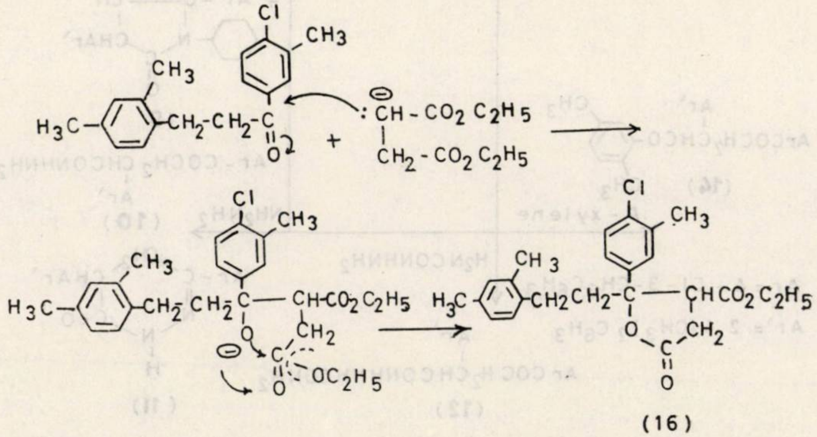

(16)

(ii) The ketone **4** reacted with hydrazine hydrate or phenylhydrazine in boiling butanol and the structure of the resulting hydrazone **17a** or phenylhydrazone **17b** was proved from the following :

Compound **17a** was condensed with *p*-chlorobenzaldehyde in the presence of *n*-butanol to give azine **18**.

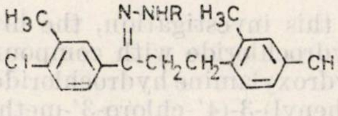

(17)

R, $a = \mathrm{H}$; $b = \mathrm{C_6H_5}$

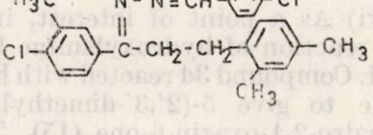

(18)

The addition of active methylene compounds to the unsaturated nitrogen compounds under the Michael reaction conditions has been also investigated. Thus, azine **18** reacted with ethyl acetoacetate and/or ethyl cyanoacetate in the presence of hydrochloric acid/ethanol mixture to give products identified as acetoacetyl or cyanoacetyl hydrazone derivatives, **19a** and **19b** respectively. These products can also be obtained by the reaction of ethyl acetoacetate and/or ethyl cyanoacetate with hydrazone **17a**.

The mechanism of formation of **19** possibly takes place by the azetidine-2-one intermediate **20** which was subsequently cleaved and finally dearylated as shown in Chart 2 :

Chart 2

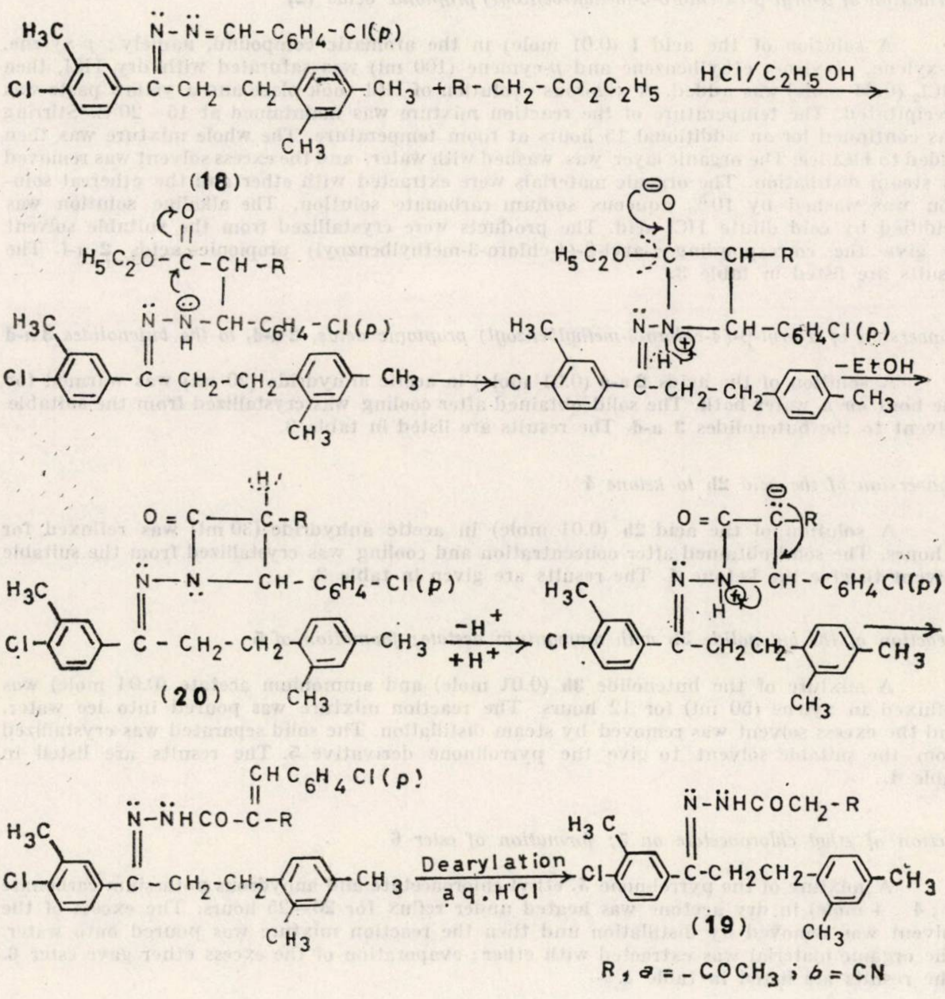
H₃C
N-N=CH-C₆H₄-Cl(p)
Cl
C-CH₂-CH₂
CH₃
+R-CH₂-CO₂C₂H₅
HCl/C₂H₅OH
CH₃
(18)
H₅C₂O-C-CH-R
O
H₃C
N-N-CH-C₆H₄-Cl(p)
H
C-CH₂-CH₂
CH₃
CH₃
H₅C₂O
C
CH-R
N-N
CH-C₆H₄Cl(p)
H
C-CH₂CH₂
CH₃
-EtOH
O=C
C-R
H
N
N
CH-C₆H₄-Cl(p)
C-CH₂-CH₂
CH₃
-H⁺
+H⁺
(20)
CH₃
O=C
C
R
N
N
CH-C₆H₄Cl(p)
H
C-CH₂CH₂
CH₃
CH₃
CHC₆H₄Cl(p)
N-NHCO-C-R
H₃C
Cl
C-CH₂-CH₂
CH₃
CH₃
Dearylation
aq.HCl
N-NHCOCH₂-R
H₃C
Cl
C-CH₂CH₂
CH₃
(19)
CH₃
R, a = -COCH₃ ; b = CN

The above results explain that the unsaturated nitrogen of *p*-chlorophenyl azoethane moiety is more reactive than the other unsaturated nitrogen toward nucleophiles. This is probably due to the inductive effect of the chlorine atom of the phenyl group.

EXPERIMENTAL

The infrared absorption spectra were determined with a Beckman[R] and Unicam SP 1000 infrared spectrophotometers using KBr wafer technique. The ^{1}H-NMR spectra were recorded with a Varian (s-60T) instrument, positions of peaks were expressed in δ-values using $CDCl_3$ as internal standard. All the melting points are uncorrected.

Friedel-Crafts alkylation of aromatic hydrocarbons with β-(4-chloro-3-methylbenzoyl) acrylic acid; formation of α-aryl-β-(4-chloro-3-methyl-benzoyl) propionic acids (**2**)

A solution of the acid **1** (0.01 mole) in the aromatic compound, namely: *p*-xylene, *m*-xylene, *o*-xylene, ethylbenzene and *p*-cymene (100 ml) was saturated with dry HCl, then $AlCl_3$ (0.04 mole) was added. A vigorous evolution of HCl took place and a yellow paste was precipitated. The temperature of the reaction mixture was maintained at 15–20°C. Stirring was continued for an additional 15 hours at room temperature. The whole mixture was then added to HCl/ice. The organic layer was washed with water, and the excess solvent was removed by steam distillation. The organic materials were extracted with ether and the ethereal solution was washed by 10% aqueous sodium carbonate solution. The alkaline solution was acidified by cold dilute HCl acid. The products were crystallized from the suitable solvent to give the corresponding α-aryl-β-(4-chloro-3-methylbenzoyl) propionic acids **2 a-f**. The results are listed in table 3.

Conversion of α-aryl-β-(4-chloro-3-methylbenzoyl) propionic acids, **2 a-d,** *to the butenolides* **3 a-d**

A solution of the acids **2 a-d** (0.01 mole) in acetic anhydride (20 ml) was warmed for one hour on a water bath. The solid obtained after cooling was crystallized from the suitable solvent to the butenolides **3 a-d**. The results are listed in table 3.

Conversion of the acid **2b** *to ketone* **4**

A solution of the acid **2b** (0.01 mole) in acetic anhydride (30 ml) was refluxed for 6 hours. The solid obtained after concentration and cooling was crystallized from the suitable solvent to give the ketone **4**. The results are given in table 3.

Reaction of the butenolide **3b** *with ammonium acetate; formation of* **5**

A mixture of the butenolide **3b** (0.01 mole) and ammonium acetate (0.04 mole) was refluxed in xylene (50 ml) for 12 hours. The reaction mixture was poured into ice water, and the excess solvent was removed by steam distillation. The solid separated was crystallized from the suitable solvent to give the pyrrolinone derivative **5**. The results are listed in table 4.

Action of ethyl chloroacetate on **5**; *formation of ester* **6**

A mixture of the pyrrolinone **5**, ethyl chloroacetate and anhydrous potassium carbonate (1 : 4 : 4 mole) in dry acetone was heated under reflux for 20–25 hours. The excess of the solvent was removed by distillation und then the reaction mixture was poured onto water. The organic material was extracted with ether; evaporation of the excess ether gave ester **6**. The results are listed in table 4.

TABLE 3

α-Aryl-β-(4-chloro-3-methylbenzoyl) propionic acids **2**, butenolides **3** and ketone **4**

Compd.	m.p.° Colour	Solvent * yield %	Formula	Analysis % Calcd.	Found
2a	180 colourless	B 85	$C_{19}H_{19}O_3Cl$	C 68.98 H 5.74 Cl 11.69	69.30 5.54 12.46
2b	165 colourless	T 77	$C_{19}H_{19}O_3Cl$	C 68.97 H 5.74 Cl 11.69	69.13 5.54 11.12
2c	215 colourless	A 55	$C_{19}H_{19}O_3Cl$	C 68.98 H 5.74 Cl 11.69	69.23 5.99 10.78
2d	192 colourless	T 17	$C_{19}H_{19}O_3Cl$	C 68.98 H 5.74 Cl 11.69	69.27 6.01 10.92
2e	125 colourless	p 100–120 52	$C_{19}H_{19}O_3Cl$	C 68.98 H 5.74 Cl 11.69	69.13 5.50 12.43
2f	118 colourless	p 80–100 40	$C_{21}H_{23}O_3Cl$	C 70.29 H 6.41 Cl 9.90	70.72 6.67 10.12
3a	215 colourless	p 100–120 53	$C_{19}H_{17}O_2Cl$	C 72.96 H 5.44 Cl 10.92	72.52 5.29 11.00
3b	235 colourless	T 75	$C_{19}H_{17}O_2Cl$	C 72.96 H 5.44 Cl 10.92	73.40 5.50 10.77
3c	265 colourless	Bu 52	$C_{19}H_{17}O_2Cl$	C 72.96 H 5.44 Cl 10.92	72.70 4.51 10.77
3d	111 colourless	p 80–100 41	$C_{19}H_{17}O_2Cl$	C 72.96 H 5.44 Cl 10.92	73.47 6.04 10.77
4	110 colourless	B 47	$C_{18}H_{19}OCl$	C 75.39 H 6.63 Cl 12.39	74.87 6.13 11.97

* B = benzene ; T = toluene ; A = glacial acetic acid ; p = petroleum ether ; Bu = butanol.

Reaction of butenolide **3b** *with p-toluidine; formation of* **7**

A mixture of **3b** (0.01 mole), *p*-toluidine (0.01 mole) and sodium acetate (0.02 mole) in 50 ml acetic acid was heated under reflux for 10 hours. The reaction mixture was poured into ice water and the solid separated was crystallized from the proper solvent to give **7** (cf. Table 4).

TABLE 4

Pyrrolinone derivatives **5**, **7** and **9**; ester **6**; amide derivative **8**; hydrazide **10**; pyridazinones **11** and **13**; N-carbamoylhydrazide **12**; dione derivative **14** and oxazinone **15**.

Compd.	m.p.° Colour	Solvent* yield %	Formula	Analysis %	
				Calcd.	Found
5	202 colourless	Bu 67	$C_{19}H_{18}NOCl$	C 73.19 H 5.77 N 4.49	73.28 5.82 4.14
6	197 colourless	B 75	$C_{23}H_{24}NO_3Cl$	C 69.43 H 6.03 N 3.52	69.71 5.84 3.67
7	174 pale yellow	T 65	$C_{26}H_{24}NOCl$	C 77.70 H 5.97 N 3.48	77.80 5.87 3.14
8	146 colourless	T 27	$C_{25}H_{30}NO_2Cl$	C 72.90 H 7.29 N 3.40	73.15 6.98 3.52
9	215 colourless	B 32	$C_{25}H_{28}NOCl$	C 76.23 H 7.11 N 3.55	75.85 6.94 3.38
10	252 colourless	B 35	$C_{19}H_{21}N_2O_2Cl$	C 66.18 H 6.09 N 8.12	66.53 6.37 7.86
11	151 pale yellow	p 100–120 23	$C_{19}H_{19}N_2OCl$	C 69.83 H 5.81 N 8.57	70.27 5.60 8.77
12	245 colourless	A 42	$C_{20}H_{22}N_3O_3Cl$	C 61.93 H 5.67 N 10.83	62.00 5.87 10.80
13	208 pale yelow	Bu 26	$C_{20}H_{20}N_3O_2Cl$	C 64.95 H 5.41 N 11.36	65.26 5.45 11.53
14	112 colourless	p 40–60 37	$C_{27}H_{27}O_2Cl$	C 77.41 H 6.45	77.64 6.74
15	173 colourless	Bu 75	$C_{19}H_{18}O_2NCl$	C 69.61 H 5.49 N 4.27	68.99 4.98 3.87

* B = benzene ; Bu = butanol ; T = toluene ; E = ethanol ; p = lightpetrol ; A = glacial acetic acid.

Reaction of the butenolide **3b** *with cyclohexylamine; formation of* **8** *and* **9**

A solution of **3b** (0.01 mole) and cyclohexylamine (0.03 mole) in 50 ml ethanol was heated under reflux for 6 hours. The product obtained on cooling was fractionally crystallized from boiling ethanol, and on recrystallization from boiling etahnol or benzene, compound **9** was obtained. The ethanol insoluble part was crystallized from toluene to give **8**. The results are listed in table 4.

Independent synthesis of **8**

An ethereal solution of the acid chloride of **2b** (0.01 mole) was added to an ethere a solution of cyclohexylamine (0.01 mole) and then heated on a steam bath for one hour. Evaporation of the excess ether and then addition of the reaction mixture onto water gave a solid substance that was crystallized from toluene and identified to be **8** by m.p. and m.m. p determinations.

Action of hydrazine hydrate on the butenolide **3b**; *formation of* **10** *and* **11**

A solution of **3b** (0.01 mole) and hydrazine hydrate (0.03 mole) in ethanol (70 ml) was heated under reflux for 6 hours. The product that separated on concentration and cooling was filtered off and fractionally crystallized from light petrol (b.p. 100—120°) to give the pyridazinone **11**. The light petrol insoluble part was crystallized from benzene and identified as the hydrazide **10** (cf. Table 4).

Independent synthesis of hydrazide **10**

An ethereal solution of the acid chloride of **2b** (0.01 mole) was treated by hydrazine hydrate (0.01 mole). The mixture was shaken well for half an hour and then heated on a steam bath for another half an hour. The ether was evaporated and the residue was poured into water, the solid separated filtered off and recrystallized from benzene to give a product identified as **10** by m.p. and m.m.p. determinations.

Independent synthesis of pyridazinone **11**

A mixture of the acid **2b** (0.01 mole) and hydrazine hydrate (0.01 mole) was refluxed in ethanol for 8 hours. The solid that separated after concentration and cooling was crystallized from light petrol (b.p. 100—120°) to give a product identified as **11** by m.p. and m.m.p determinations.

Reaction of the butenolide **3b** *with semicarbazide HCl; formation of* **12** *and* **13**

A solution of **3b** (0.01 mole) and semicarbazide NCl (0.01 mole) in pyridine (40 ml) was refluxed for five hours. The jproduct separated after pouring the solution onto ice-HCl was fractionally crystallized from boiling butanol, and on recrystallization from butanol, compound **13** was obtained. The butanol insoluble part was crystallized from glacial acetic acid to give **12**. The results are given in table 4.

Reaction of the butenolide **3d** *with hydroxylamine HCl; formation of* **15**

A mixture of **3d** (0.01 mole) and hydroxylamine HCl (0.01 mole) in pyridine (50 ml) was heated under reflux for 6 hours. The product separated after pouring the solution onto ice-HCl was crystallized from the suitable solvent to give **15** (cf. Table 4).

Reaction of the butenolide **3b** *with p-xylene; formation of* **14**

A solution of butenolide **3b** (0.01 mole) in *p*-xylene was gradually added to a suspension of anhydrous aluminium chloride (0.04 mole) in 100 ml *p*-xylene. The suspension was stirred at room temperature for 10 hours. The whole mixture was then added to HCl-ice and the excess of *p*-xylene was then removed by steam distillation. The oily residue was triturated with light petrol (b.p. 40—60°) and the solid separated was crystallized from the proper solvent to give the dione derivative **14**.

Independent synthesis of **14**

A solution of **2b** (0.01 mole) and thionylchloride (0.04 mole) was refluxed for two hours, and the excess of thionylchloride was removed by distillation under reduced pressure. The resulting acid chloride was treated with *p*-xylene (50 ml) and anhydrous aluminium chloride was added portionwise in a period of half an hour to a stirred solution. Heating was continued for two hours on a steam bath, the reaction mixture was left overnight and then the whole was added to ice-HCl. The organic layer was washed with water and the excess solvent was removed by steam distillation. The organic material was extracted with ether; evaporation of the solvent left a solid substance that crystallized from light petrol (b.p. 40—60°) to give a product which could be identified as **14** by m.p. and m.m.p. determinations (cf. Table 4).

Condensation of ketone **4** *with diethylsuccinate; formation of lactonic ester* **16**

Ketone **4** (0.01 mole) and diethylsuccinate (0.015 mole) were added to a boiling stirred solution of potassium *t*-butoxide [potassium (0.011 mole); 50 ml of *t*-butyl alcohol per g of potassium] during 30 minutes; heating was continued for 3 hours. Most of the alcohol was then removed under reduced pressure, the cooled residue was acidified with dilute hydrochloric acid and the organic material was taken up in ether. Evaporation of the neutral ethereal layer left compounds **16**. The results are listed in table 5.

TABLE 5

Lactonic ester **16**, hydrazones **17a** and **17b**; azine **18**; and acetoacetyl or cyanoacetyl hydrazone **19**

Compd.	m.p.° colour	solvent * yield %	Formula	Analysis % Calcd.	Found
16	222 colourless	B 13	$C_{24}H_{27}O_4Cl$	C 69.48 H 6.51 Cl 8.56	69.21 6.23 7.98
17a	178 colourless	B 82	$C_{18}H_{21}N_2Cl$	C 71.88 H 6.98 N 9.31	72.00 7.12 9.42
17b	192 pale yellow	M 55	$C_{24}H_{25}N_2Cl$	C 76.49 H 6.64 N 7.43	76.80 6.90 7.60
18	208 yellow	Bu 77	$C_{25}H_{24}N_2Cl$	C 70.92 H 5.67 N 6.61	70.20 5.75 6.95
19a	243 brown	A 45	$C_{22}H_{25}N_2O_2Cl$	C 68.66 H 6.50 N 7.28	68.85 6.42 6.87
19b	193 brown	T 37	$C_{21}H_{22}N_3OCl$	C 68.57 H 5.98 N 11.42	68.85 5.65 10.87

* B = benzene; M = methanol; Bu = butanol; A = acetic acid; T = toluene.

Condensation of the ketone **4** *with hydrazines ; formation of hydrazones* **1**

A mixture of the ketone **4** (0.01 mole) and hydrazine hydrate or phenyl hydrazine (0.015 mole) in 50 ml butanol was refluxed for 4 hours. The products that separated on cooling were crystallized from the suitable solvent to give hydrazones **17a** and **17b** respectively. The results are given in Table 5.

Condensation of hydrazone **17a** *with p-chlorobenzaldehyde ; formation of* **18**.

A mixture of **17a** (0.01 mole) and *p*-chlorobenzaldehyde (0.01 mole) in *n*-butanol (50 ml) was heated under reflux for six hours. The product that separated on cooling was crystallized from the proper solvent to give compound **18** (cf. Table 5).

Action of active methylene compounds on the azine **18** ; *formation of* **19**

A mixture of the azine **18** (0.01 mole) and ethyl acetoacetate or ethyl cyanoacetate (0.01 mole) in ethanol was treated with few drops of hydrochloric acid then heated under reflux for 3 hours, or left at room temperature for 7 dyes. The solution was concentrated by slow evaporation, and the solid separated was filtered off and then recrystallized from the proper solvent to give **19a** and **19b**. The results are listed in table 5.

Independent synthesis of **19**

A mixture of **18a** (0.01 mole) and ethyl acetoacetate or ethyl cyanoacetate (0.01 mole) in butanol (50 ml) was heated under reflux for 10 hours. The solid that separated after concentration and cooling was identified as **19a** or **19b** by m.p. and m.m.p. determinations.

REFERENCES

[1] M. M. Mohamed, M. A. El-Hashash and M. El-Kady, *Rev. Roumaine Chim.*, **24**, 1381 (1979)
[2] A. Essawy and A. Hamed, *Indian J. Chem.*, **15B**, 694 (1977).
[3] M. A. El-Hashash and M. El-Kady, *Rev. Roumaine Chim.*, **23**, 1981 (1978).
[4] M. Abdalla and A. Essawy, *Indian J. Chem.*, **15B**, 523 (1977).
[5] R. Robinson and E. Seijo, *J. Amer. Chem. Soc.*, **44**, 582 (1941).
[6] H. Stobbe, W. Veiweg, R. Eckert and R. Reddlien, *Liebigs Ann. Chem.*, **78**, 380 (1911).
[7] M. A. El-Hashash, M. M. Mohamed, F. A. Said and O. A. Abo-Baker, *Indian J. Chem.*, **19 B**, 107 (1980).

Revue Roumaine de Chime, 27, 7, 879–883 (1982)

THE PRINCIPLES, APPLICATIONS AND TRENDS OF FLOW INJECTION ANALYSIS FOR MONITORING CHEMILUMINESCENT REACTIONS

J. L. BURGUERA *, MARCELA BURGUERA * and A. TOWNSHEND **

* Universidad de Los Andes, Facultad de Ciencias, Departamento de Química, Mérida, Venezuela
** University of Hull, Department of Chemistry, Hull, HU6 7RX, England, U. K.

Received February 10, 1981

The rapid growth of Flow Injection Analysis which utilises chemiluminescence techniques reflects their many advantages relative to conventional procedures. The commonest chemiluminescent systems used in the liquid phase are reviewed. The basic principles of Flow Injection Anaalysis for chemiluminescent measurements are then discussed. Their applications are described in organic and inorganic compounds determination.

INTRODUCTION

A large number of chemiluminescent reactions have been reported since 1800, such as the oxidation of Grignard reagents,[1] siloxene,[2] luminol,[3] lucigenin [2] and lophine [5] among others. The early twentieth century was a period of expanding interest in chemiluminescence.[6] However, it was only in the late 1950s that analytical applications of chemiluminescence began to appear and consisted of solution and gas-phase techniques.[7,8] The use of sensitive photomultipliers has extended the list of chemiluminescent reactions. A variety of reactions, inorganic and organic as well as biochemical, are known to emit light and has been the subject of numerous investigations.[9-12]

The theory and recent developments in chemiluminescence analysis have been recently reviewed by Burguera *et al.*[13]

The possibility of using the Flow Injection Analysis technique for monitoring chemiluminescent reactions has brought additional advantages on this topic.[14] Flow Injection Analysis is based on the injection of the sample solution into a nonsegmented carrier stream of a reagent which moves in a laminar flow mode toward and through the detector.[15] In contradistinction to previously known methods, the Flow Injection Analysis technique does not require a complete mixing of the sample and reagent solutions or reaching of a chemical equilibrium.[16] The controlled dispersion of the sample zone, which takes place during its movement from the injection port to the detector, is the most important aspect of the new technique as it results in a highly reproducible readout waiting for the steady state signal.[17] The principle of Flow Injection Analysis has been succesfully applied to ion-selective, [18] spectrophotometric,[19-21] fluorimetric,[22] potentiometric [18,23] and other analytical measurements. [24,25] This technique has also been coupled with atomic absorption spectrometry.[26] Flow Injection Analysis has recently received considerable attention as a new approach for monitoring chemiluminescent signals.[27]

This paper describes the requirements, methodology and new applications of Flow Injection Analysis for measuring chemiluminescent signals. These developments are opening up many new frontiers in chemiluminescent analysis and are providing additional insight into this phenomenon.

DESIGN CONSIDERATIONS

Chemiluminescent reactions usually produce transient emissions. The intensity of chemiluminescence is proportional to the rate of the reaction that produces electronically excited states rather than to the concentration of product. Thus, in order to measure such emissions generated in a flow system, the emitting species must be within the path of the detector whilst the emission is occurring.[27] As a result, the design of a chemiluminescence detection system for Flow Injection Analysis differs from designs based on detection methods that measure concentration.[28] Fig. 1 shows a diagram of a typical Flow Injection Analysis apparatus used for chemiluminescent measurements. However, the overall system design may be different according to the chemiluminescent system studied. Burguera and Townshend designed a flow injection apparatus with two streams (solvent and reagent) for monitoring chemiluminescent signals from the triethylamine oxidation by benzoyl peroxide.[14] The sample is injected through a self-sealing rubber septum, into an acetone stream. The amine and benzoyl peroxide streams are mixed in the cell in view of the detector. A similar Flow Injection Analysis apparatus was later designed to measure chemiluminescent responses obtained from the luminol oxidation by hydrogen peroxide catalyzed by cobalt (II) and from the sulphine oxidation by sodium hypochlorite in the presence of fluorescein.[27] In this case the two reagent streams were of hydrogen peroxide and luminol or sodium hypochlorite and fluorescein for the determination of cobalt (II) or sulphide, respectively. The reaction was started by injecting the cobalt (II) or sulphide solutions, respectively, into the mixed reagent stream. The solutions passed through a coiled flow cell and the emission intensity recorded. Recently, ion-exchange resins have been used in order to determine cadmium (II) and zinc(II) selectively, monitoring the inhibiting

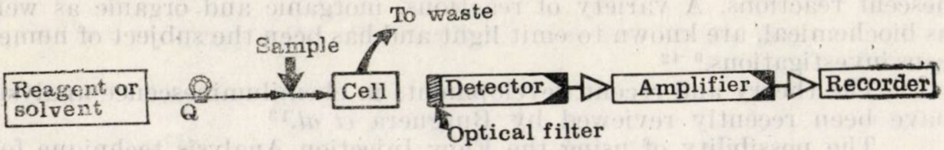

Fig. 1

effect on the chemiluminescent signal from the luminol-hydrogen peroxide-cobalt(II) system.[29] The luminol and hydrogen peroxide streams are mixed with a pre-mixed cobalt(II) and solvent stream. In the solvent stream of 0.1 N HCl and 0.5 N NaCl, an ion-exchange resin column such as Amberlite IRA 400 is inserted as shown in Fig. 2. The sample solution is injected and later the zinc(II) and cadmium(II) are eluted with chloride-containing hydroxide and diluted nitric acid solutions, respectively. The variation of the chemiluminescent signals are then recorded.[30]

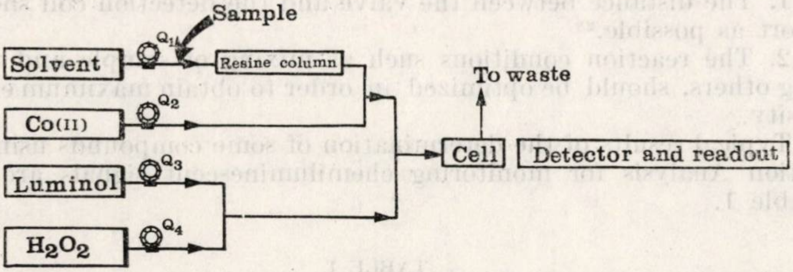

Fig. 2

Rule and Seitz [28] designed a Flow Injection Analysis apparatus in which a slug of sample is interposed in a flowing stream of reagent by use of a sampling valve. The sample mixed with the reagent in a coil downstream from the valve. A detector at the end of the coil sensed the amount of product formed. They used the luminol oxidation by hydrogen peroxide catalyzed by copper (II) for evaluating chemiluminescent detection.

It is essential that maximum light output is achieved while the analyte and reactants are in the cell in view of the detector. Fast rate chemiluminescent reactions should be observed immediately upon mixing the analyte and reactants, therefore efficient mixing is desired. The cell volume must allow a sufficient solution residence time in order to observe maximum peak height.[27] When coiled cells are used the observed intensity will depend on the fraction of the sample that is mixed in the coil in front of the detector. On increasing the coil length, more of the sample will initially contact reagent in view of the detector and the chemiluminescent intensity will be greater. After the coil reaches a certain length, adequate time is achieved for maximum emission to occur whilst the emitting solution is within view of the detector, therefore, futher increases in coil length will not lead to any increase in chemiluminescence observed.[28]

Slow rate chemiluminescent reactions will need larger cells with larger hold-up volumes. However, greater sample dispersion throughout the cell can give less effective mixing, thus diminishing and delaying the maximum intensity and broadening the signal.[14] In this case the use of longer detection coiled cells is recommended to observe all available intensity.

For any chemiluminescent reaction the larger the sample volume, more signal will be available. Higher emission is achieved with greater sample volume in a bigger cell.[27,28]

Some other important variables should be evaluated when Flow Injection Analysis is applied for chemiluminescent measurements such as : flow rate, sample dispersion, distance between the sample injection and the detection cell among others.

An optimum design of a Flow Injection apparatus for chemiluminescent measurements should follow the recommendations given below :

1. The distance between the valve and the detection coil should be as short as possible.[28]

2. The reaction conditions such as mixing of sample and reagent among others, should be optimized in order to obtain maximum emission intensity.

Typical results of the determination of some compounds using Flow Injection Analysis for monitoring chemiluminescent signals are shown in Table 1.

TABLE 1

Trace compounds determination using flow injection analysis for chemiluminescent measurements

Compound	Effect	System	Detection limit (ng ml^{-1})	Reference
Triethylamine	Reductor	Benzoyl peroxide-acetone	5.0×10^3	14
Cobalt(II)	Catalyst	Luminol-hydrogen peroxide	0.001	14
Hydrogen peroxide	Oxidant	Luminol-Copper(II)	0.003	28
Sulphide	Reductor	Sodium hypochlorite-fluorescein	0.01	27
Zinc(II)	Inhibiting	Luminol-hydrogen peroxide-cobalt(II)	0.5	29
Cadmium(II)	Inhibiting	Luminol-hydrogen peroxide-cobalt (II)	0.1	29

It has been established that Flow Injection Analysis for monitoring chemiluminescent reactions provide sensitive, precise, simple and rapid methods for the determination of some organic and inorganic compounds. The possibility of coupling Flow Injection Analysis for different chemiluminescent and bioluminescent assays is likely to be a priority in the continuing investigations on this topic.

REFERENCES

[1] E. Wedekind, *Chem. Zentr.*, **30**, 921 (1906).
[2] F. Wöhler, *Liebigz. Ann. Chem.*, **127**, 263 (1863).
[3] H. O. Albrecht, *Z. phys. Chem.*, **136**, 321 (1928).
[4] B. Radzirzenski, *Ber. dtsch. chem. Ges.*, **10**, 321 (1877).
[5] V. *Ya*. Shlyapintokh, O. N. Karpukhin, L. M. Postuikov, V. F. Tsepolov, A. A. Vichutinskil and F. V. Zakharov, in *Chemiluminescence Techniques in Chemical Reactions*, N. Emanuel (Ed)., Consultants Bureau, New York, 1968 and references therein.
[6] J. L. Burguera, *Ph. D. Thesis*, Birmingham University (1979).

[7] U. Isacsson and G. Wettermark, *Analyt. Chim. Acta*, **68**, 339 (1974).
[8] D. B. Paul, *Talanta*, **25**, 377 (1978).
[9] H. A. Neufeld, C. J. Conklin and R. D. Towner, *Analyt. Biochem.*, **12**, 303 (1965).
[10] D. H. Steadman and D. A. Tammaro, *Anal. Lett.*, **9**, 81 (1976).
[11] J. L. Burguera, *Anal. Proceed.*, **17**, 43 (1980).
[12] J. L. Burguera and A. Townshend, *Talanta*, **27**, 309 (1980).
[13] J. L. Burguera, M. Burguera and A. Townshend, *Acta Cient. Venez.*, in press.
[14] J. L. Burguera and A. Townshend, *Proceed. Anal. Div. Chem. Soc.*, **16**, 263 (1979).
[15] J. Růžička and E. H. Hansen, *Analyt. Chim. Acta*, **114**, 19 (1980).
[16] J. Růžička, in *Flow Injection Analysis Metting*, Chemical Society of the Midlands Region, University of Aston, Birmingham, U. K., April 24th., 1979.
[17] L. R. Snyder, *Analyt. Chem. Acta*, **114**, 3 (1980).
[18] K. Tóth, G. Nagy, E. Fehér, G. Horvai and E. Pungor, *Analyt. Chim. Acta*, **114**, 45 (1980).
[19] L. Nord and B. Karlberg, *Analyt. Chim. Acta*, **118**, 285 (1980).
[20] T. Yamane and T. Fukasawa, *Analyt. Chim. Acta*, **119**, 389 (1980).
[21] B. F. Reis, E. A. G. Zagatto, A. O. Jacintho, F. J. Krug and H. Bergamin, *Analyt. Chim. Acta*, **119**, 305 (1980).
[22] C. S. Lim, J. N. Miller and J. W. Bridges, *Analyt. Chim. Acta*, **114**, 183 (1980).
[23] M. Mascini and R. Giardini, *Analyt. Chim. Acta*, **114**, 329 (1980).
[24] A. Ivaska and W. F. Smyth, *Analyt. Chim. Acta*, **114**, 283 (1980).
[25] H. Kagenow and A. Jensen, *Analyt. Chim. Acta*, **114**, 227 (1980).
[26] K. Fukamachi and N. Ishibashi, *Analyt. Chim. Acta*, **119**, 383 (1980).
[27] J. L. Burguera, A. Townshend and S. Greenfield, *Analyt. Chim. Acta*, **114**, 209 (1980).
[28] G. Rule and W. R. Seitz, *Clin. Chem.*, **25**, 1635 (1979).
[29] J. L. Burguera, M. Burguera and A. Townshend, *Anal. Proceed.*, in press.
[30] J. L. Burguera, M. Burguera, F. Millán and A. Townshend, *XIV Congreso Latinoamericano de Química*, paper No. 126, San José, Costa Rica, 1—7 February, 1981.

METHOD

Apparatus and reagents: Unicam, S. P. 500 spectrophotometer, absorption cells of 1-cm light path. Quickfit quartz ground joint glassware distillation apparatus.

Sodium peroxide: Analar.

Zinc sulphate solution: Analar. Dissolve 36.0 g of zinc sulphate heptahydrate in 100 ml of distilled water.

Indicator: Dissolve 0.5 g of malachite green oxalate in 50 ml of distilled water.

Hydrochloric acid: Analar. Concentrated Sp gr. 1.19.

Sulphuric acid: Analar. Concentrated, Sp gr. 1.84. Dilute sulphuric acid (1 + 3), one volume of the concentrated acid mixed with 3 volumes of water. Dilute sulphuric acid (2 + 1), two volumes of concentrated acid mixed with 1 volume of water.

Sodium hydroxide: Analar. (20 percent m/v). Dissolve 20 g of sodium hydroxide in 100 ml of distilled water.

Sodium sulphate solution: Analar (1 percent). Make alkaline to phenolphthaline.

Reagent A: Dissolve 1.8 g of eriochrome-cyanine R in distilled water, and dilute to one litre.

Reagent B: Dissolve 0.26 g of zirconyl chloride octahydrate, or 0.220 g of zirconyl nitrate dihydrate in 50 ml distilled water. Add 700 ml concentrated hydrochloric acid to the zirconyl solution, and dilute the mixture to 1 litre with distilled water. Thus reagent should be cooled to room temperature before use.

The above zirconyl salts have a tendency to lose water and acid on storage. A preferred technique in their use is to prepare a stock solution of zirconyl salt, assay it for zirconium by precipitation with ammonia, and then use an aliquot of the stock solution when preparing repeated batches of reagents B. Reagent A and B can not be combined as a single reagent, because prior mixing produces a precipiate on prolonged storage.

Treated soda: Lime glass. Take about 250 g of glass powder in 200 ml of H_2SO_4 (1 + 2). Heat up to 70°C for an hour. Cool, filter, and wash with boiled distilled water, and dry at 150°C.

Reference solution: Ten millilitres of reagent A are added to 100 ml of distilled water. To this solution is added 10 ml of hydrochloric acid solution prepared by diluting 7 ml of concentrated acid to 10 ml with distilled water.

Standard sodium fluoride solution: Dissolve 0.221 g sodium fluoride in 1 litre of distilled water. This solution contains 100 μg Fml^{-1}.

PROCEDURE

The procedure consists of the three stages, fusion, distillation and colorimetric determination.

Fusion: Grind a rock sample to pass a 120 mesh sieve (B.S.). Dry the powder in an oven at 110°C for one to two hours, and cool it in a desiccator. Weigh 0.2 g sample in a platinium or nickel crucible. Add 2.0 g sodium peroxide (ten times of samples weight) and mix thoroughly with the sample. Place the crucible in a muffle at 350°C and raise the temperature to nearly 550°C over 1/2 or 3/4 hour. Cool to room temperature. Dissolve the frit in 100 ml of distilled water, wash the crucible with a little hot water, and add the washing to the solution. Simmer the solution for an hour to remove excess sodium peroxide. Add slowly by stirring 4 ml of zinc sulphate solution, and add 3 drops of 0.5 percent malachite green solution. Allow the precipitate to settle, otherwise there is a difficulty in recognising colour. Adjust pH between 11 and 12 by the dropwise addition of H_2SO_4 (1 + 3). At this pH the indicator is nearly colourless. If the pH is too low, readjust by the addition of 20 % NaOH. Digest the bulk precipitate of zinc silicate, zinc aluminate and hydroxide on a steam bath for about one hour. Filter through whatman No. 54 paper, and wash the precipitate several times with hot 1 % Na_2SO_4 solution. Collect the filtrate and washings in a 250 ml beaker, reduce the volume to ca 20 ml on a water bath. Transfer to a 50 ml measuring flask and make up to the mark.

Distillation: The distillation is based on a modified Willard and Winter's method.[12] Take an appropriate aliquot according to the concentration of fluoride and place it in a distillation flask. Add powdered glass (tip of spatula). Add about 30 ml H_2SO_4 (2 + 1). Mix the sample with sulphuric acid by admitting air bubbles from the steam generator. Introduce steam when the temperature reaches 130 – 135°C. Collect the distillate in a 200 ml measuring flask and make up to the mark.

Colorimetric determination: Take 50 ml of distillate or a suitable aliquot *i.e.* 0.05 to about 1.20 mg fluoride/litre. (If the concentration is less than 0.05 mg, distillate must be concentrated under alkaline conditions to a volume which will yield this concentration range if the amount of fluoride exceeds 1.20 mg. The distillate must be diluted and the results must be multiplied by the dilution factor). Add 5 ml of reagent A and 5 ml of reagent B, and mix well.

Set the spectrophotometer to zero absorbance with the reference solution. Measure the absorbance of the blank, standard and samples in a 1 cm cell at 527.5 nm.

Leave the cells in the spectrophotometer for 5 minutes, before making any measurement.

RESULTS AND DISCUSSIONS

The method under investigation has been thoroughly tested for its precision and accuracy.

PRECISION

Precision has been obtained by replicate analyses of pelitic, tourmalines, and granitic rocks.

Analysis of pelitic rocks: Three pelitic rocks, namely, WA_3 (slate) 039a and 025a (hornfels) have been analysed. 0.2 g of each sample was fused with 2.0 g of sodium peroxide and dissolved in 50 ml of distilled water. 50 ml of WA_3, 4 ml of 039a and 2 ml of 025a and 2 ml of standard solution of sodium fluoride were taken for distillation and distillates were collected in 200 ml volumetric flasks. Again 25 ml portions of 039a distillate were diluted to 50 ml with distilled water. The concentration of fluoride was determined according to the procedure outlined above.

The results given in table 1, indicate a high degree of precision. The coefficient of variation for WA_3 is 7.7 percent and the precision error at two standard deviation is only ± 0.01. For minor amounts of fluoride, < 0.2 and > 0.01 percent, this is highly satisfactory.

Analysis of tourmalines: Four samples of tourmalines (T_2, T_3, T_4 and T_5) were chosen for analysis. These represent typical sochorlites from South West England. 0.2 g of each tourmaline sample was fused with 2.0 g of sodium peroxide, dissolved in distilled water and made up to a volume of 50 ml. 5 ml of each sample solution and 2 ml of standard solution of sodium fluoride were taken for distillation, and distillates were collected in 200 ml. Fluoride contents were determined according to the procedure given above.

The results of replicate analyses of T_2 and duplicate analysis for T_3, T_4 and T_5 are given in Table 2 which are within the expected range given by Deer et al.[25] The high standard deviation of T_2 (± 0.14 at two standard deviations) is largely the result of the high reading of 0.53 giving a square of the difference of 0.017. If this result is discounted, the standard deviation of the other 5 readings is ± 0.04 *i.e.* a coefficient of variation of about 10 percent. Results from the other tourmaline specimens indicate good precision.

TABLE 1

Replicate analyses of pelitic rocks

F. Wt. P.C.

Specimen No.	Result % F		Mean value	Standard deviation	Standard error
	Analyst S. A. Khan	Analyst M. Stone	Analyst S. A. Khan	Analyst S. A. Khan	Analyst S. A. Khan
WA_3	0.06 0.06 0.06 0.06 0.06 0.06 0.06 0.07 0.07 0.07	0.060	0.06	0.005	±0.001
039a	1.65 1.67		1.66		
025a	1.69 1.76 1.70	1.70	1.71		

TABLE 2

Replicate and comparative analyses of tourmalines

F. Wt. P.C.

Specimen No.	Result % F	Mean value		Standard deviation	Standard error
	Analyst S. A. Khan	Analyst S. A. Khan	Analyst Deer,[25] et al	Analyst A. S. Khan	Analyst S. A. Khan
T_2	0.40 0.39 0.53 0.43 0.34 0.34	0.40	—	0.07	±0.03
T_3 ,,	0.37 0.37	0.37	—		
T_4 ,,	0.77 0.77	0.77	0.77		
T_5	0.36 0.36	0.36			

Analysis of granites: Three granitic rocks (E_{126}, E_1 and E_{73}) were analysed. 0.2 g of each sample was fused with 2.0 g of sodium peroxide, dissolved in distilled water and made up to a volume of 50 ml. 20 ml of E_{126}, 3 ml of E_1 and 3 ml of E_{73} and 2 ml of sodium fluoride standard solutions were taken for distillation respectively. The distillates were collected in 200 ml volumetric flask. The concentration of fluoride was determined according to the procedure given on page 870. The results are shown in Table 3. Replicate determination of E_{126} show very high precision. The coefficient of variation is about 7 percent. Replicate data for other granites (E_1 and E_{73}) indicate high precision.

TABLE 3

Replicate and comparative analyses of granites

F. Wt. P.C.

Speciemn No.	Result % F				Mean value	Standard deviation
	Analyst S. A. Khan	Analyst M. Stone	Analyst Exley [26-27]	Analyst Reid and Flett [28]	Analyst S. A. Khan	Analyst S. A. Khan
E_{126}	0.18 0.18 0.18 0.19 0.18	—	0.17	0.15	0.18	0.013
E_1	1.41 1.35	1.41	—	—	0.38	
E_{73}	0.50 0.47 0.48	—	0.45	—	0.48	

ACCURACY

Addition method: Replication indicates fairly good precision but provides no measure of accuracy. The latter can be determined only by analysing known standards, having composition similar to the sample under test. In the absence of analysed standards, the method of addition provides a useful measure of accuracy. Indeed, it is probably superior to the use of analysed standards, as the latter rarely match the composition of the sample exactly.

Controlled amounts of fluoride were added as sodium fluoride to solution of specimens, WA_3 (Slate), T_2 (Tourmaline), E_1 (Granite) and 039a (Hornfels) before distillation. The solutions were distilled and the distillates collected in 200 ml flask. A suitable aliquot was taken and determined colorimetrically according to the procedure described on page 870. The results given in Table 4 show satisfactory recovery which confirms the accuracy of the method.

TABLE 4

Recovery of fluorine

Specimen number	Fluorine added ppm	Fluorine recovered (from graph ppm)	% Recovery of fluorine
Pelitic rock Dark state (WA$_3$)	0.5	0.49	98
,,	0.5	0.50	100
Hornfels (039a)	0.5	0.49	98
Tourmaline(T$_2$)	0.05	0.05	100
,,	0.10	0.10	100
,,	0.20	0.20	100
Granite (E$_1$)	0.10	0.10	100
,,	0.10	0.10	100
,,	0.20	0.20	100

SUMMARY AND CONCLUSIONS

The proposed analytical method has been tested in eleven silicate materials. These materials represent extremes of composition. The granitic rocks represent the acid members which include also arkasic rocks and quartzites, and basic rocks include the pelites, and highly aluminus and ferruginous silica-poor materials are represented by tourmalines. Calcium-rich materials are not represented, but should find no difficulty when distillation stage is included in the method.

It is concluded that the method has the necessary precision and accuracy for the analyses of fluoride in silicate rock, over a wide range of concentrations from trace amounts to nearly two percent, by weight. It is concluded further that the method could be applied to the analyses of other rocks and minerals with no difficulty, and that the range could be extended upwards to larger percentages of fluoride.

The proposed analytical method has several attractive features. The method is simple, sensitive, accurate, and rapid. The colour reaction is almost immediate and stable, readings can be taken at any convenient time after the first five minutes. Measurements can be made with short light path. The reagents are easily obtained and prepared and are stable, requiring no special care other than moral protection from direct sunlight and evaporation. The method could also be incorporated into the analytical scheme of Shapiro and Brannock [1] and Riley [2].

The only serious feature of the method is the time taken to cover all the three major stages. With two distillation sets working (Fig. 2) it is possible to make between 8 and 12 distillations in a full day. In two days, it is possible to analyse 6 specimens in duplicate (in addition to the distillation of blanks and standards).

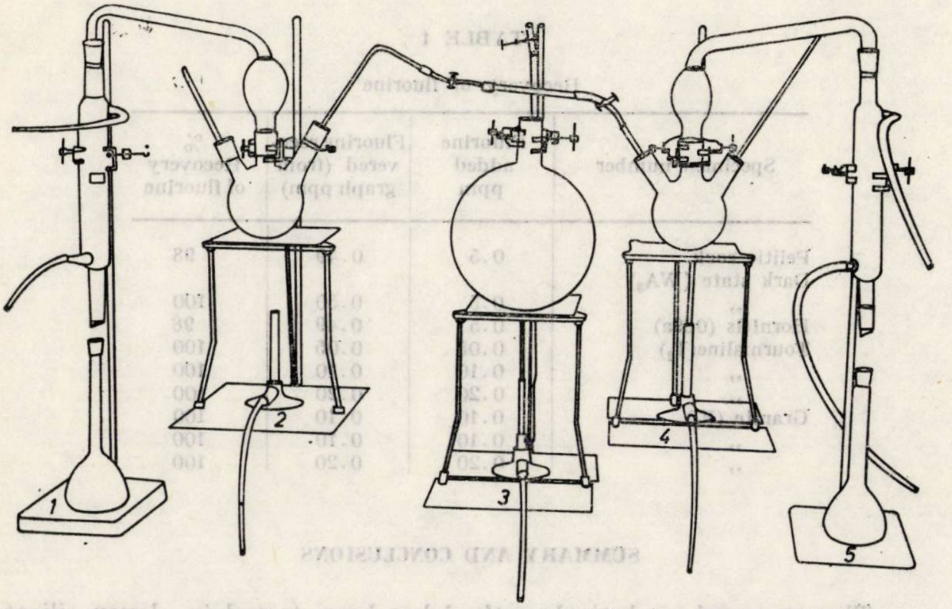

Fig. 2. – Rapid distillation apparatus for fluorine : 1. Measuring flask and condenser ; 2. Distillation flask with thermometer ; 3. Steam generator ; 4. Distillation flask with thermometer ; 5. Measuring flask and condenser.

ACKNOWLEDGEMENT. The authors are highly thankful to Professor Scott Simpson for encouragement and facilities provided for this project. We are also thankful to technical staff, Mr. J. Sanders, Mr. Raymond Ellis and Mrs. Willmington in the Department of Geology for their help at various stages of the work.

REFERENCES

[1] L. Shapiro and W. W. Brannock, *U.S. Geol. Survey Bull.* No. *1036C* (1956).
[2] J. P. Riley, *Analyt. Chim. Acta,* **19**, 413 (1958).
[3] A. I. Vogel, "A Text Book of Quantitative Inorganic Analysis", Third Edition, Longman, Green, London, 1951, p. 261.
[4] A. W. Groves, "Silicate Analysis", George Allen and Unwin Ltd, London, 1951.
[5] K. W. Powell and J. H. Saylor, *Analyt. Chem.,* **25**, 960 (1953).
[6] Sh. K. Ashratova, *Zavodskaya, Lab.,* **23**, 1064 (1957).
[7] V. I. Prokopchik and T. I. Subbotina, *At. Energy,* **21**, 415 (1966).
[8] G. L. Grenshaw and F. N. Ward, *U.S. Geol. Survey Bull.* No. *1408* 77, (1975).
[9] S. J. Hetman, *Bull. Cent. Rech. Pau.,* **10**, 663 (1976).
[10] G. I. Bebeshko, V. P. Roze and V. A. Khalizova, *Zhur. analit. Khim,* **34**, 507 (1979).
[11] Yu. G. Vlasov, Yu. E. Ermolenko, V. V. Kolodnikov and M. S. Miloshova, *Zhur. analit. Khim.,* **35**, 691 (1980).
[12] H. H. Willard and O. B. Winter, *Ind. Eng. Chem. Analyt. Ed.,* **5**, 7 (1933).
[13] F. S. Grimaldi, B. Ingram and F. Cuttita, *Analyt. Chem.,* **27**, 918 (1956).
[14] C. Chu and J. L. Schafer, *Analyt. Chem.* **27**, 1429 (1955).
[15] R. P. Howllingworth, *Analyt. Chem.,* **29**, 1130 (1957).

[16] J. P. Bonstra, *Rev. Trav. chim.*, **70**, 325 (1951).
[17] H. E. Bunsted, and J. C. Wells, *Analyt. Chem.*, **24**, 1595 (1952).
[18] S. Megregian and F. J. Maier, *J. Am. Water Works Assoc.*, **44**, 239 (1952).
[19] F. Richter, *Z. analyt. Chem.*, **124**, 161 (1942).
[20] D. Monnier, R. Voucher and P. Wenger, *Helv. Chim. Acta*, **33**, 1 (1950).
[21] J. C. Berthelay, *Ann. Fac. Sci. Univ. Chermont. Geol. Mineral*, **11**, 4 (1966).
[22] S. Megregian, *Analyt. Chem.*, **26**, 1164 (1954).
[23] W. H. Huang and W. D. Jones, *Analyt. Chem. Acta*, **37**, 508 (1967).
[24] D. F. Boltz, Editor, "Colorimetric Determination of Nonmetals", Interscience, New York, Vol. 8, 1963, p. 231.
[25] Deer, Howie and Zussman, **1**, *Analysis*, **6**, Table 52 (1962).
[26] C. S. Exley, *Analysis*, **1**, Table 6, (1959).
[27] C. S. Exley, *Analysis*, **4**, Table 6, (1959).
[28] C. Reid and J. S. Fleet, *Analysis*, **1**, 59 (1907).

LEGENDS FOR THE ROCKS

WA_3	Dark grey slate bands, Porthleven.
039a	Hornfels, from granite contract, Rainsey West Cliff.
025a	Hornfels in contact with roof of domelike mass of Tregonning granites, sea stocks, Legereath Zawn.
T_2	Shorl, from Locks Gross Sherberton Comnion.
T_3	From Luxulyanite, Luxulyan, Cornwall.
T_4	From Pegmatite, Tremearn, Cornwall.
T_5	Shorl, from Sheltor, Dartmoor.
E_{126}	Granite from St. Austell.
E_1	Ambly granite-bearing leucogranite, roof Zone, Corn Clodgy.
E_{73}	Late lithionite granite from St. Austell.

ORSZÁGOS MŰSZAKI INFORMÁCIÓS KÖZPONT ÉS KÖNYVTÁR 1883

66

TRAVAUX PARUS AUX ÉDITIONS DE L'ACADÉMIE DE LA RÉPUBLIQUE SOCIALISTE DE ROUMANIE

ELENA CEAUȘESCU, **Noi cercetări în domeniul compușilor macromoleculari** (Nouvelles recherches dans le domaine des composés macromoléculaires), 1981, 536 p.

I. G. MURGULESCU, J. PĂUN, **Introducere în chimia fizică. Vol. I. 3. Nucleu atomic, reacții nucleare, particule elementare** (Introduction à la chimie physique. Vol. I. 3. Noyau atomique, réactions nucléaires, particules élémentaires), 1982, 606 p.

ELENA JERCAN, **Analiza cromatografică** (Analyse chromatographique), 1982, 286 p.

I. G. MURGULESCU, TATIANA ONCESCU, E. SEGAL, **Introducere în chimia fizică Vol. II. 2. Cinetică chimică și cataliză** (Introduction à la chimie physique. Vol. II. 2. Cinétique chimique et catalyse), 1981, 1024 p.

V. DRĂGUȚAN, A. T. BALABAN, M. DIMONIE, **Metateza olefinelor și polimerizarea prin deschidere de inel a cicloolefinelor** (La métathése des oléfines et la polymérisation par ouverture annulaire des cyclooléfines), 1981, 254 p.

LYDIA-MARIA VAICUM, **Epurarea apelor uzate cu nămol activ. Bazele biochimice** (L'épuration des eaux résiduelles à boue active. Les bases biochimiques), 1981, 218 p.

I. GĂLĂȚEANU, **Procese și metode radiochimice în energetica nucleară** (Processus et méthodes radiochimique dans l'énergétique nucléaire), 1981, 234 p.

O. IORDACHE, **Procese polistocastice aplicate în fenomenele de transfer** (Processus polystochastiques appliqués aux phénomènes de transfert), 1981, 187 p.

CR. SIMIONESCU, VALERIA GORDUZA, **Polimeri biocompatibili și biologic activi** (Polymères biocompatibles et biologiquement actifs), 1980, 497 p.

ELENA CEAUȘESCU, **Polimerizarea stereospecifică a izoprenului** (La polymérisation stéréospécifique de l'isoprène), 1979, 307 p.

M. FLORESCU, **Metode științifice în dezvoltarea industriei chimice moderne** (Méthodes scientifiques dans le développement de l'industrie chimique moderne), 1979, 256 p.

A. T. BALABAN, I. GĂLĂȚEANU, G. GEORGESCU, LIGIA SIMIONESCU, **Compuși marcați și radiofarmaceutici cu aplicații în medicina nucleară** (Composés marqués et radiopharmaceutiques à application en médecine nucléaire), 1979, 495 p.

CONST. GH. MACAROVICI, **Analiza chimică cantitativă anorganică** (L'analyse chimique quantitative inorganique), 1979, 457 p.

I. G. MURGULESCU, E. SEGAL, **Introducere în chimia fizică. Vol. II. 1. Teoria molecular cinetică a materiei** (Introduction à la chimie physique. Vol. II. 1. La théorie moléculaire-cinétique de la matière), 1979, 1036 p.

S. STERNBERG, FL. DANEȘ, **Termodinamica chimică aplicată** (La thermodynamique chimique appliquée), 1978, 400 p.

I. G. MURGULESCU, V. EM. SAHINI, **Introducere în chimia fizică Vol. I.2. Structura și proprietățile moleculelor** (Introduction à la chimie physique. Vol. I. 2. La structure et les propriétés des molécules), 1978, 604 p.

I. ZUGRĂVESCU, MAGDA PETROVEANU, **N-ylid chemistry**, coédition avec McGraw-Hill International Book Company, U.S.A., 1977, 396 p.

I. G. MURGULESCU, **Introducere în chimia fizică. Vol. I.1. Atomi, molecule, legătură chimică** (Introduction à la chimie physique. Vol. I. 1. Atomes, molécules, liaison chimique), 1976, 560 p

ELENA CEAUȘESCU, **Research work and synthesis and characterization of macromolecular compounds. Contributions.** 1974, 251 p.

CR. SIMIONESCU, VIORICA RUSAN, V. POPA, **Chimia algelor marine** (La chimie des algues marines), 1974, 212 p., 1 pl.

I. P. INFORMAȚIA c. 2211

43 426

Lei 40

$ 70 (pour un abonnement annuel)

F 1103

ACADÉMIE DE LA RÉPUBLIQUE SOCIALISTE DE ROUMANIE

REFERÁLVA

REVUE ROUMAINE DE CHIMIE

TOME 27

N° 8

Août 1982

EDITURA ACADEMIEI REPUBLICII SOCIALISTE ROMÂNIA

Rev. Roumaine Chim.

RRCHAX, **27**, *8*, p. 895—1000 (1982), Bucarest

ACADÉMIE DE LA RÉPUBLIQUE SOCIALISTE DE ROUMANIE

COMITÉ DE RÉDACTION

Rédacteur en chef :

I.G. MURGULESCU, membre de l'Académie de la République Socialiste de Roumanie

Redacteur en chef adjoints :

A.T. BALABAN et V.EM. SAHINI, membres correspondants de l'Académie de la République Socialiste de Roumanie

Collège de rédaction :

EM. BRATU, ELENA CEAUŞESCU, ECATERINA CIORĂNESCU-NENITZESCU, CR. SIMIONESCU, membres de l'Académie de la République Socialiste de Roumanie; P. SPACU, membre correspondant de l'Académie de la République Socialiste de Roumanie; MARGARETA AVRAM, M. BANCIU, I. HAIDUC, D.I. MARCHIDAN, I. MOLDOVAN, G. NIAC et D. SĂNDULESCU

La Revue Roumaine de Chimie parait 10 fois par an. Toute commande de l'étranger pour les travaux parus aux Editions de l'Académie de la République Socialiste de Roumanie sera adressée à ILEXIM – Departamentul Export-Import Carte (Livres)/Departamentul Export-Import Presă (Revues), P.O.B. 136–137, télex 11226, 3, str. 13 Decembrie, 79517 Bucarest, Roumanie

Les manuscrits, les livres et les revues proposés en échange, ainsi que toute correspondance seront envoyés à la rédaction :

REVUE ROUMAINE DE CHIMIE

125, Calea Victoriei, 79717 Bucarest, Roumanie, téléphone 50 76 80

EDITURA ACADEMIEI REPUBLICII SOCIALISTE ROMANIA
125, Calea Victoriei, 79717 Bucarest, Roumanie, téléphone 50 76 80

REVUE ROUMAINE DE CHIMIE

ORSZÁGOS MŰSZAKI INFORMÁCIÓS *** KÖZPONT ÉS KÖNYVTÁR * 1983

Tome 27, N° 8 **Août 1982**

C. I. LEPĂDATU, The concept of electronegativity and the interelectronic repulsion energy in the vector model of the atom . . . . 897 – 899 R

EUGENE S. KRYACHKO, On water dimer structure in Coulson-Eisenberg model . . . . 901 – 904

S. El-BASIL, B. ABD El-FATTAH, M.M. El-ENANY and N. BOULOS, Cation-anion combination reactions. Molecular orbital calculations . . . . . 905 – 909

IOAN SILAGHI-DUMITRESCU, LUMINIȚA SILAGHI-DUMITRESCU and IONEL HAIDUC, Normal coordinate analysis of the vibrational spectrum of dimethyldithioarsinato anion, $(CH_3)_2AsS_2^-$ . . . . 911 – 916

MOHAMED ABDEL SALAM El ABSY, GH. MARCU, J. ZSAKÓ and CS. VÁRHELYI, Spectrophotometric and derivatographic study on some new tetradentate mixed chelates of cobalt (III) with acetylacetone derivatives . . 917 – 925

A. SYAMAL and B. K. GUPTA, New nickel (II) complexes with dibasic tridentate ONO donor ligands . . . . 927 – 930 R

V. MINCU, C. LEPĂDATU, MELANIA GUȚUL, MARIA BREZEANU and IOANA JITARU, Optical and magnetic studies of some heteronuclear complexes of nickel and zinc with hydrazine . . . . 931 – 934 R

C. I. CHIRIAC, Cyclodehydrations with phenyldichlorophosphite-dimethylformamide. A new convenient method for the synthesis of 1,3,4-oxadiazoles from diaroylhydrazines . . . . 935 – 938

M. ANAND, S. P. GUPTA, A. R. GOYAL and R. L. MITAL, Synthesis of some substituted trifluoromethyl phenothiazines and their oxidation products . . 939 – 942

C. CRISTESCU and SILVIA SITARU, *as*-Triazine derivatives with potential therapeutic action. XVI. Synthesis of 5(w-carboxy-alkyl) mercapto-6-azauridines 943 – 951

M. W. TAUSCH and P. J. PLATH, Rearrangements of $(CH)_7^+$ ions (in German) 953 – 961

M. A. HASSAN, E. A. SOLIMAN and A.A. HAMED, Synthesis and reactions of polysubstituted 2(1*H*) pyridones and pyridines . . . . 963 – 967

AGNETA CARAGHEORGHEOPOL, H. CĂLDĂRARU, GH. HUBCA, CR. OPRESCU and M. DIMONIE, Synthesis and polymerization of polyethylene glycol dimethacrylates. VII. ESR study of ethylene glycol dimethacrylate – styrene copolymers . . . . 969 – 972

LUIGI CAMPANELLA and G. de ANGELIS, Polarographic behaviour of lutidinic acid . . . . 973 – 979 Bc

Rev. Roumaine Chim. **27,** *8,* 895 – 1000 (1982) Bucharest

1983

J. HERNÁNDEZ MÉNDEZ, A. ALONSO MATEOS, E. J. MARTÍN MATEOS and C. GARCÍA de MARÍA, Gravimetric determination of gold by means of the ion pair $[AuI_4^-][(C_4H_9)_4N^+]$ (in Spanish) . . . . 981 – 986

MINODORA LECA, A new route for determining the nonpolar solubility parameters of organic solvents by gas-liquid chromatography . . . . 987 – 992

A. F. SHOUKRY, A. I. ABDEL-RAHMAN and N. T. ABDEL-GHANI, Analysis of ternary alloys containing Co(II), Ni(II) and Cu(II) . . . . . 993 – 997

SCIENTISTS AND PEACE . . . . 999 – 1000

Bc

Revue Roumaine de Chimie 27, 8, 897–899 (1982)

THE CONCEPT OF ELECTRONEGATIVITY AND THE INTERELECTRONIC REPULSION ENERGY IN THE VECTOR MODEL OF THE ATOM

C. I. LEPĂDATU

Center of Chemical Physics-ICECHIM, Spl. Independenței 202, Bucharest, Romania

Received July 11, 1981

It is shown that the electronegativity for an electronic configuration 1^N has to do with the interaction energy between a pair of identical electrons. It is also proved that the double of Mulliken's electronegativity means the energy necessary to bring a hydrogenlike couple of charges $e^- - e^-$ at a distance equal to that between the nucleus and the valence shell of the element.

1. INTRODUCTION

We have previously reported [1] that the model of the atom built from hydrogenlike shells, leads to the following expression for the electronegativity defined as the sum of the first ionization potential and electron affinity (double of Mulliken's electronegativity)

$$X = R\frac{e^2}{r_n} + A_H, \qquad (1)$$

where R is the Rydberg constant, r_n the distance from the nucleus to the valence shell of the element and A_H a constant which is the electron affinity of the hydrogen atom.

The double of Mulliken's electronegativity may be therefore interpreted as the energy necessary to reject the electron from a hydrogenlike couple of charges $e^+ - e^-$ placed at a distance equal to that between the nucleus and the valence shell of the element.

2. THE ABSOLUTE ELECTRONEGATIVITY AND THE INTERELECTRONIC REPULSION ENERGY

As we shall see below an expression similar to (1) may be also obtained from the vector model of the atom. According to that model, [2,3] the average energy of a given electronic configuration is defined as

$$E(l^N) = NI(nl) + \frac{N(N-1)}{2}\,\Pi(ll), \qquad (2)$$

where I(nl) is the sum of the kinetic and potential energy of an individual electron and $\Pi(ll)$ the interaction energy for pairs of identical electrons.

To get the ground state energy of each l^N configuration, the spin-pairing energy and the stabilization energy[3] must be added to (2). We shall consider, in the following, that the ionization process and the mechanism responsible for the electron affinity are mainly due to changes occurring in the baricenter energy of an electronic configuration.

The electronegativity defined as the sum of the ionization potential and electron affinity has the following expression:

$$X=[(E(\text{core } l^{N-1})-E(\text{core } l^{N})]+[E(\text{core } l^{N+1})-E(\text{core } l^{N})]=\Pi(ll), \qquad (3)$$

where the $\Pi(ll)$ energy is usually expressed in terms of Slater parameters [2,3]:

$$\begin{aligned}
\Pi(ss) &= F^0(ss)\\
\Pi(pp) &= F^0(pp)-\frac{2}{25}F^2(pp)\\
\Pi(dd) &= F^0(dd)-\frac{2}{63}F^2(dd)-\frac{2}{63}F^4(dd) \qquad (4)\\
\Pi(ff) &= F^0(ff)-\frac{4}{195}F^2(ff)-\frac{2}{143}F^4(ff)-\frac{1000}{5577}F^6(ff)
\end{aligned}$$

The radial integrals F^k for nodeless orbitals of Slater type may be calculated using the formula:

$$F^k = C_W\cdot C_n^k\cdot\frac{Z_{ef}e^2}{n}, \qquad (5)$$

where:

$$C_n^k=\frac{4(2n+k)!}{(2n)!(2n)!}\left[(2n-k-1)!-\sum_{r=0}^{2n+k}\frac{(2n-k-1+r)!}{r!2^{2n-k+r}}\right] \qquad (6)$$

Expression (6) has been found using a method suggested by Judd.[4] The correction C_W arises from Watson's remark.[3,5,6] F^k parameters were calculated from HFSCF radial functions and take invariably higher values as compared with the phenomenological ones. This correction is roughly equal to:

$$C_W\approx\frac{2+Q}{3+Q}, \text{ where Q is the ionic charge.}$$

From (4) and (5) one finds that:

$$\Pi(ll)=C_W\cdot K_n(ll)\,\frac{Z_{ef}e^2}{n^2}. \qquad (7)$$

where :

$$K_n(ss) = n \times C_n^0$$

$$K_n(pp) = n \times \left[C_n^0 - \frac{2}{25} C_n^2 \right], \text{ etc.} \tag{8}$$

Table 1 gives the $K_n(ll)$ values for the integer quantum numbers "n".

TABLE 1

Values for $K_n(ll)$ (for $\Pi(ll)$ in eV)

ll n	ss	pp	dd	ff
2	19.77	19.00		
3	21.07	20.18	20.49	
4	21.86	20.88	21.21	20.41
5	22.41	21.36	21.71	20.82
6	22.82	21.71	22.08	

As may be seen, the $K_n(ll)$ values given in Table 1 do not change too much with the values of "n" and "l".

From (7) and Table 1, one may see that $C_w \cdot K_n$ (11) values for n = 2, 3, are roughly close to the Rydberg constant (13.6 eV). Formula (8) and the electronegativity (3) may be therefore expressed as :

$$X \simeq \Pi(ll) \approx R \frac{e^2}{r_n}, \tag{9}$$

where $\frac{1}{r_n} = \frac{Z_{ef}}{n^2}$ is the distance between the nucleus and the valence shell of the element.

We have thus obtained an expression for the electronegativity which is similar, up to a constant, to that previously found from another model of the atom.[1]

Equation (9) may be well interpreted as the energy of a hydrogen-like couple of charges $e^- - e^-$, at a distance equal to that between the nucleus and the valence shell of the element.

REFERENCES

[1] C. I. Lepadatu, unpublished data.

[2] R. Stevenson, "Multiplet Structure of Atoms and Molecules", W. B. Saunders Comp., Philadelphia, 1965, p. 40.

[3] C. K. Jørgensen, "Modern Aspects of Ligand Field Theory", North-Holland Publ. Comp., Amsterdam, 1971, ch. 21.

[4] B. R. Judd, "Operator Techniques in Atomic Spectroscopy" Mc. Graw-Hill Book Comp., Inc. New York, 1963, Appendix 1.

[5] R. E. Watson, *Ann. Phys.*, **13**, 250 (1961).

[6] R. E. Watson and A. J. Freeman, *Phys. Rev.*, **120**, 1125, 1134 (1960).

Revue Roumaine de Chimie, 27, 8, 901–904 (1982)

ON WATER DIMER STRUCTURE IN COULSON-EISENBERG MODEL

EUGENE S. KRYACHKO
Institute for Theoretical Physics, Kiev–130, USSR 252130

Received September 1, 1980

It is shown that with including dipole-dipole, dipole-quadrupole and quadrupole-quadrupole interactions there exists a finite critical distance $R_c \simeq 1.96$ Å where the minimum-energy dimer-water-stucture transforms into the dipole-aligned one. If octupole interactions are included then no finite critical distance R_c exists.

It is known[1] that the minimum-energy water dimer structure has the form shown in Fig. 1. Obviously, the equivalent dimer structures may be obtained by any combination of the following symmetry operations: (i) rotation of $H_3O_2H_4$ with 180° about its symmetry axis; (ii) the same rotation for $H_1O_1H_2$; (iii) exchange of water molecules. Thus, we have eight equivalent stable dimer structures. As $R = R_{12}$ increases from the distance $R = R_{\min}$, the angles θ and φ decline continuously to zero, and as a result, the molecular symmetry axes become more and more nearly aligned with the oxygen – oxygen axis (see Fig. 1). Finally, at the critical distance $R = R_c$ the alignment becomes complete. This dimer structure, obviously, has the four equivalent stable structures only i.e. there is a change of symmetry in water – water interactions. For the first time Stillinger and Lemberg[1] discussed this symmetry breaking for ST2 and Popkie-Kistenmacher-Clementi water-molecule pair potentials.

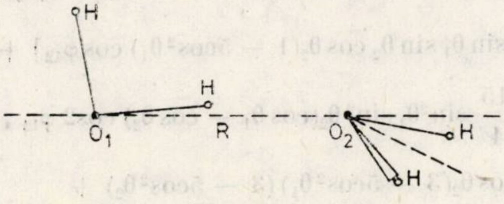

Fig. 1. — Water diner structure.

In this paper the water dimer symmetry breaking is examined in the frame of the Coulson-Eisenberg model.[2,3] In this model a water molecule is represented by the dipole, octupole and quadrupole situated on the oxygen atom. Then the water — water interaction in this model is given by the following expression

$$U=\frac{\mu^2}{R^3}U_{dd}+\frac{\mu\theta}{R^4}U_{dq}+\frac{\theta^2}{R^5}U_{qq}+\frac{\mu\Phi}{R^5}U_{do}+\frac{\vartheta\Phi}{R^6}U_{qo}+\frac{\Phi^2}{R^7}U_{qo}, \quad (1)$$

where dipole-dipole $(d-d)$, dipole-quadrupole $(d-q)$, quadrupole-quadrupole $(q-q)$, dipole-octupole $(d-o)$, quadrupole-octupole $(q-o)$, and octupole-octupole $(o-o)$ interactions are defined from the general theory of intermolecular forces :[4,5]

$$\begin{aligned}
U_{dd} &= -2\cos\theta_1\cos\theta_2+\sin\theta_1\sin\theta_2\cos\varphi_{12};\\
U_{dq} &= \frac{3}{2}\Big[\cos\theta_1(3\cos^2\theta_2-1)-\cos\theta_2(3\cos^2\theta_1-1)+\\
&\qquad 2\sin\theta_1\sin\theta_2(\cos\theta_1-\cos\theta_2)\cos\theta_{12}\Big];\\
U_{do} &= 2\cos\theta_1\cos\theta_2(6-5\cos^2\theta_1-5\cos^2\theta_2)-\\
&\qquad \frac{3}{2}\sin\theta_1\sin\theta_2(2-5\cos^2\theta_1-5\cos^2\theta_2)\cos\theta_{12};\\
U_{qq} &= \frac{3}{4}[2-6\cos^2\theta_1-6\cos^2\theta_2+18\cos^2\theta_1\cos^2\theta_2+\\
&\qquad \sin^2\theta_1\sin^2\theta_2\cos 2\varphi_{12}-16\sin\theta_1\sin\theta_2\cos\theta_1\cos\theta_2\cos\varphi_{12}];\\
U_{qo} &= \frac{5}{2}[\cos\theta_1(3-5\cos^2\theta_1)(3\cos^2\theta_2-1)-\cos\theta_2(3-5\cos^2\theta_2)(3\cos^2\theta_1-1)-\\
&\qquad -3\sin\theta_1\sin\theta_2\cos\theta_1(1-5\cos^2\theta_2)\cos\varphi_{12}+\\
&\qquad 3\sin\theta_1\sin\theta_2\cos\theta_2(1-5\cos^2\theta_1)\cos\varphi_{12}]+\\
&\qquad \frac{15}{4}\sin^2\theta_1\sin^2\theta_2(\cos\theta_1-\cos\theta_2)\cos 2\varphi_{12};\\
U_{oo} &= -5\cos\theta_1\cos\theta_2(3-5\cos^2\theta_1)(3-5\cos^2\theta_2)+\\
&\qquad \frac{45}{8}\sin\theta_1\sin\theta_2(1-5\cos^2\theta_1)(1-5\cos^2\theta_2)\cos\varphi_{12}-\\
&\qquad \frac{45}{2}\sin^2\theta_1\sin^2\theta_2\cos\theta_1\cos\theta_2\cos 2\varphi_{12}+\frac{5}{8}\sin^3\theta_1\sin^3\theta_2\cos 3\varphi_{12}.
\end{aligned} \quad (2)$$

The angles θ_1 and θ_2 define the deflection of the dipole direction for molecules one and second, accordingly, from the direction of the oxygen — oxygen axis. The angle φ_{12} represents the rotation along the oxygen —

oxygen axis required to do the dipoles into coplanarity (see Fig. 1). Dipole, quadrupole and octupole moments for the water molecule on the oxygen atom are defined as common[5] and have the following values[2,3]:

$$\mu = 1{,}855 \times 10^{-18}; \ \vartheta = 0.72 \times 10^{-26};$$

$$\Phi = 2.28 \times 10^{-34}.$$

Expanding Eq. (2) in the Taylor series for $\theta_1 \simeq 0$ and $\theta_2 \simeq 0$ we have U as a function of $x = \theta_1$ and $y = \theta_2$ up to a quadratic order in x and $y(\varphi_{12} = \pi)$:

$$U^{(1)} = \frac{\mu^2}{R^3}\left\{[-2 + x^2 + y^2 - xy] + 3\Gamma(x^2 - y^2) + 3\Gamma^2[2 - 3(x^2 + y^2) + \right.$$

$$+ 4xy] + 2\Delta[-4 + 7(x^2 + y^2) - 6xy] + 15\Gamma\Delta(x^2 - y^2) +$$

$$+ 10\Delta^2[-2 + 6(x^2 + y^2) - 9xy], \quad (3)$$

where

$$\Gamma = \frac{\vartheta}{\mu R}, \ \Delta = \beta\Gamma^2, \ \beta = \frac{\Phi\mu}{\theta^2} \simeq 8.16.$$

For $R \to \infty$, U contains the positive-definite quadratic form $x^2 + y^2 - xy$ defined by $d - d$ term, and in this approximation the dipole-aligned dimer structure is a stable one. As R decreases $U^{(1)}$ reduces to $\tilde{U}^{(1)}$:

$$\tilde{U}^{(1)} = x^2 + y^2 - xy + 3\Gamma(x^2 - y^2) + 3\Gamma^2[-3(x^2 + y^2) + 4xy] +$$

$$+ 2\Delta[7(x^2 + y^2) - 6xy] + 15\Gamma\Delta(x^2 - y^2) + 30\Delta^2[2(x^2 + y^2) - 3xy],$$

which has the following form in polar coordinates $x = r\cos\alpha$, $y = r\sin\alpha$:

$$\tilde{U}^{(1)} = r^2\left[1 - \frac{1}{2}\sin 2\alpha + 3\Gamma\cos 2\alpha + 3\Gamma^2(-3 + 2\sin 2\alpha) + \right.$$

$$\left. + 2\Delta(7 - 3\sin 2\alpha) + 15\Gamma\Delta\cos 2\alpha + 15\Delta^2(4 - 3\sin 2\alpha)\right]. \quad (4)$$

Now we consider in $\tilde{U}^{(1)}$ of Eq.(4) the terms defined by $d - d$, $d - q$ and $q - q$ interactions only. Minimizing Eq.(4) with respect to α, we find that

$$\mathrm{tg}\, 2\alpha = \frac{12\Gamma^2 - 1}{6\Gamma}.$$

Substituting this expression into $\tilde{U}^{(1)}$ $(d - d,\ d - q,\ q - q)$ we conclude that $\tilde{U}^{(1)}$ has the minimum value equal to zero when $\Gamma = \Gamma_c = 0.198$ which corresponds to the critical distance $R_c = 1.96$ Å. Note that this value of R is smaller than the distances predicted for ST2 and PKC water-molecule pair potential in 2–3 times.[1] But this is not the essence of the matter. The whole point is that this water-water interaction has the true behaviour from the viewpoint of symmetry breaking at a finite intermolecular distance R discussed above.

Including octupole terms in $\tilde{U}^{(1)}$, even confining the first, $d-o$, term we find that $\tilde{U}^{(1)}$ does not vanish i.e. the critical distance is infinite. Through quartic order in x and y, the interaction has the following form in polar coordinates :

$$\tilde{U}^2 = r^4\left[\frac{1}{12}\left(-1+\sin 2\alpha+\frac{1}{2}\sin^2 2\alpha\right)+\frac{2\Gamma}{3}(-13+2\sin^2 2\alpha)+\right.$$
$$+\Gamma^2\left(3-\frac{16}{3}\sin 2\alpha+\frac{13}{4}\sin^2 2\alpha\right)+\Delta\left(-\frac{26}{3}+\frac{4}{3}\sin^2 2\alpha+\frac{19}{4}\sin 2\alpha\right)-$$
$$\left.-\frac{5}{4}\Gamma\Delta\cos 2\alpha(13+9\sin 2\alpha)+\frac{5}{6}\Delta^2\left(-51-\frac{137}{4}\sin^2 2\alpha+51\sin 2\alpha\right)\right]. \tag{5}$$

Then

$$\tilde{U} = \tilde{U}^{(1)} + \tilde{U}^{(2)}$$

where

$$\tilde{U}^{(1)} = A(\alpha, \Gamma)r^2, \tilde{U}^{(2)} = B(\beta, \Gamma)\, r^4.$$

Minimizing $\tilde{U}$ with respect to r, we have

$$r^2 = -A(\alpha, \Gamma)/2B(\alpha, \Gamma),$$

and substituting this expression in $\tilde{U}$, we give

$$\tilde{U} = -A^2(\alpha, \Gamma)/4B(\alpha, \Gamma).$$

Without any difficulty it may be shown that $\tilde{U}$ vanishes when $A(\alpha_c, \Gamma_c) = 0$, which corresponds to the minimum of $\tilde{U}$. So, it is shown that up to the quadratic and quartic orders in $\tilde{U}$ and there exist the finite critical distance $R=1.96$ Å including $d-d$, $d-q$, and $q-q$ terms, and infinite one when we take into account octupole terms.

ACKNOWLEDGEMENT. The author is indebted to Dr. V. Ya. Antonchenko for valuable remarks and Prof. F. H. Stillinger for receiving the paper. [1]

REFERENCES

[1] F. H. Stillinger and H. L. Lemberg, *J. Chem. Phys.*, **62**, 1340 (1976).
[2] C. A. Coulson and D. Eisenberg, *Proc. Roy. Soc. London*, **A291**, 445 (1966).
[3] D. Eisenberg and W. Kauzmann, "Structure and Properties of Water", Leningrad, 1975.
[4] J. O. Hirschfelder, Ch. F. Curtiss and R. B. Bird, "Molecular Theory of Gases and Liquids", Wiley, New York, 1954.
[5] A. D. Buckingham, in "Intermolecular Interactions : from Diatomics to Biopolymers", B. Pullman, Ed., Wiley, New York, 1978.

Revue Roumaine de Chimie 27,8,905–909 (1982)

CATION-ANION COMBINATION REACTIONS. MOLECULAR ORBITAL CALCULATIONS

S. El-BASIL, B. ABD El-FATTAH, M. M. El-ENANY and N. BOULOS
Organic Chemistry Dept., Faculty of Pharmacy
Kasr El-Aini, Cairo, Egypt

Received June 12, 1980

SCF calculations are carried out on eight organic cations, four dinitrohalobenzenes and seven nucleophiles. The rate constants of these cation-anion combination reactions are correlated with certain MO quantities.

INTRODUCTION

In the past few years extensive studies have been carried out on the rates of reactions of nucleophiles with various substrates.[1–3] It has been shown[4] that all treatments that ignore solvent effects are inadequate.

In view of the tremendous amount of work and the limited success in this area, it was felt that the problem is so complicated that any general solution will be so complex as to be virtually useless.

Ritchie[5] observed, through a study of reactions of anions with a vast variety of cations, that the rates of such reactions obey the extremely simple relationship given by eqn. (1):

$$\log k = N_+ + \log k_0 \tag{1}$$

where N_+ is a parameter characteristic of nucleophile and solvent, k_o is characteristic of the cation but independent of both solvent and nucleophile; and k is the observed rate constant.

Ritchie's work included both formally charged cations, such as tropyluim,[6] aryldiazonium cations[7] and pyridinuim cations,[8] as well as nucleophilic aromatic substitution employing 2,4-dinitrohalobenzenes as substrates.[9] The present work has a two-fold purpose:

(a) To find a parameter that is intrinsic to cations and is related to k_0, and

(b) To study solvent effects on anions in an attempt to correlate their N_+ values.

Methods of calculations:

(1) Molecular orbital wave functions and energies were calculated using a slightly modified version of the SCF-PPP method. The Fock Hamil-

tonian matrix elements, within the ZDO approximation are given by eqn. (2)[10]

$$\left.\begin{aligned} F_{\mu\mu} &= H_{\mu\mu} + 1/2 P_{\mu\mu}\gamma_{\mu\mu} + \sum_{\nu} P_{\nu\nu}\gamma_{\mu\nu} \\ F_{\mu\nu} &= H_{\mu\nu} - 1/2 P_{\mu\nu}\gamma_{\mu\nu} \end{aligned}\right\} \tag{2}$$

The terms have their conventional meanings and the summation in the first equation is taken over all pi electrons.

Diagonal matrix elements, $H_{\mu\mu}$, are given by eqn. (3), viz.,

$$H_{\mu\mu} = U_{\mu\mu} - \sum_{\nu} V_{\mu\nu} \tag{3}$$

where $U_{\mu\mu}$ is the energy of an orbital Φ_{μ} in the bare field of its own atom and $V_{\mu\nu}$ represents the electrostatic interaction of an electron in Φ_{μ} and the cores of other atoms. One-electron, two-center off-diagonal terms, $H_{\mu\nu}$, were computed using an expression due to Flurry.[11] Two center electron repulsion integrals, $\gamma_{\mu\nu}$, were computed using an expression due to Nishimoto and Mataga.[12] Throughout the work geometries adopted by Dewar[13] were used.

(2) Desolvation energies of anion, E_n, were computed according to eqn. (4), due to Klopman,[14]

$$E_n = x(C^{HO})^2 R^{-1}\left(1 - \frac{1}{\in}\right)[q + 2b^2 x(C^{HO})^2] \tag{4}$$

in which $x = q - (q - 1)(0.75)^{1/2}$; $b^2 = 1/4$; $\in = 80$ (dielectric constant of water), C^{HO} is the coefficient of the atom of attack in the HOMO of the nucleophile, $q = Z = 2\sum_{occ} C^2$,Z being nuclear charge of relevant atom, and finally R is radius of anion.[14]

Correlation postulates:

Two postulates are suggested in this work:

(a) Values of k_0, found by Ritchie, that are characteristic of cation only (independent of both solvent and nucleophile) are assumed to be related to the ratio $|C^{LU}/E_{LU}|$, where C^{LU} is the coefficient of the atom of attack in the LUMO of cation and E_{LU} is the eigenvalue of its LUMO.

(b) N_+ values are directly related to the desolvation energies of nucleophiles (anions), E_n, calculated using eqn. (4).

RESULTS AND DISCUSSION

Table 1 lists values of $\ln |C^{LU}/E_{LU}|$ and $\log k_0$ for eight formally charged cations, (tropylium, four aryldiazonium cations and three pyridinium cations); as well as the four dinitrohalobenzenes as substrates in aromatic nucleophilic substitutions.

TABLE 1

Values of $\ln|C^{LU}/E_{LU}|$ and $\log k_0$ for cations

Cation	E_{LU} (ev.)	$-\ln C^{LU}/E_{LU}$	$-\log k_0$
Tropylium	−0.900	−0.99	−0.57 ± 0.15
Benzenediazonium	−2.23	1.71	1.14 ± 0.10
p-Chlorobenzenediazonium	−2.24	1.68	0.57 ± 0.18
m-Chlorobenzenediazonium	−2.20	1.69	0.08 ± 0.19
p-Methoxybenzenediazonium	−2.05	1.61	1.91 ± 0.37
N-Acetoxy, 4-methoxypyridinium	−2.78	4.4	1.86 0.22
N-Acetyl, 4-methoxypyridinium	−1.71	3.10	1.76 0.44
N-Acetyl, 4-methylpyridinium	−3.13	2.13	1.08 ± 0.40
2,4-Dinitrofluorobenzene	4.59	3.07	4.10
2,4-Dinitrochlorobenzene	5.04	3.20	6.10
2,4-Dinitrobromobenzene	7.20	3.58	6.0
2,4-Dinitroiodobenzene	6.21	4.13	7.40

Table 2 outlines values of desolvation energies of seven anions. Fig. 1 plots $\ln|C^{LU}/E_{LU}|$ vs. $\log k_0$. Considering the approximations adopted, one must consider the linearity obtained to be satisfactory (Correlation coefficient = 0.920).

It is observed that two groups are distinguished viz., the dinitrohalobenzenes and formally charged cations.

TABLE 2

Desolvation energies (E_n) and N_+ values of anions

Nucleophile	C^{HO}	q	R(au)	E_n(ev)	N_+
CH_3COO^-*	0.59	1.31	3.95(1)	1.96	1.90
CN^-	0.74	1.11	5.16	2.73	3.69
$C_6H_5NH_2$*	0.62	1.82	5.5 (2)	3.73	3.63
OH^-	1.0	1.0	2.64	5.07	4.79
Pyridine*	0.0	0.95	5.0 (3)	5.10	4.81
$NH_2 - NH_2$	.707	1.0	2.8	5.99	5.27
SO_3^{--}*	0.56	1.89	3.97 (4)	7.80	7.80

* Effective values of R are computed

(1) $R = R_C + 2R_{\ddot{C}}$

(2) $R = R_{\ddot{N}} + R_C$

(3) $R = R_{\dot{N}} + R_C$

(4) $R = R_S + 2R_{\ddot{O}}$

According to Klopman's classification of cations,[14] the latter class belongs to soft acids ($E_{LU} = -0.9$ to -2.24 ev.) while the former class is considered to be hard acids ($E_{LU} \geqslant 2$ev.). It is this class that shows the severest limitations when applying eqn. (1).[9]

The existence of a relation between $\ln|C^{LU}/E_{LU}|$ and $\log k_0$ of cations implies that there is an intrinsic factor in the cation that affects its reaction with a particular anion. Such a factor seems to be related to the overlap of the orbitals of the two reagents. This implies the existence of a certain degree of a "frontier orbital control" whence an intermediate charge transfer. For the cations studied, therefore, a completely charge-controlled mechanism seems unlikely. It is observed, in a similar series of cations, like e.g. in the aryldiazonium cations that the incorporation of electron-donating groups raises the coefficient of the nitrogen atom that carries the formal positive charge, but decreases the absolute value of E_{LU}.

The opposite effect i.e. C^{LU} is decreased but $|E_{LU}|$ is increased with electron-attracting groups. As the value of C increases the absolute value of E_{LU} decreases and vice-versa. With very strong electron-withdrawing groups the value of $|C^{LU}/E_{LU}|$ becomes very small; and the reaction with anions tends to be almost completely charge controlled.

It would, therefore, seem unreasonable to attempt including, e.g., p-nitrobenzene diazonium cation with the p-methoxy analog in the same category.

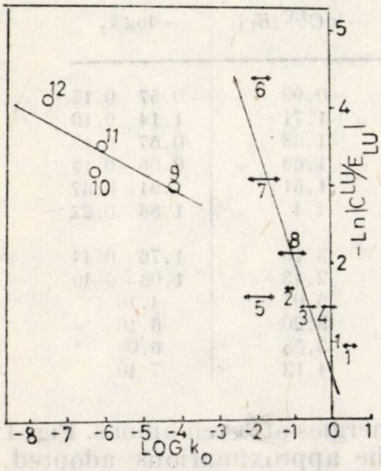

Fig. 1. — A plot of log k_0 vs. ln $|C^{LU}/E_{LU}|$ for cations. Numbers correspond to table 1. Arrow heads indicate Ritchie's average deviations in his log k_0 values.

Fig. 2 shows a plot of E_n desolvation energies of seven anions vs. their N_+ values leading to a fairly good straight-line relation (correlation coefficient = 0.925), thus supporting Ritchie's idea that the order of reactivities of anions is directly proportional to their desolvations. Ths

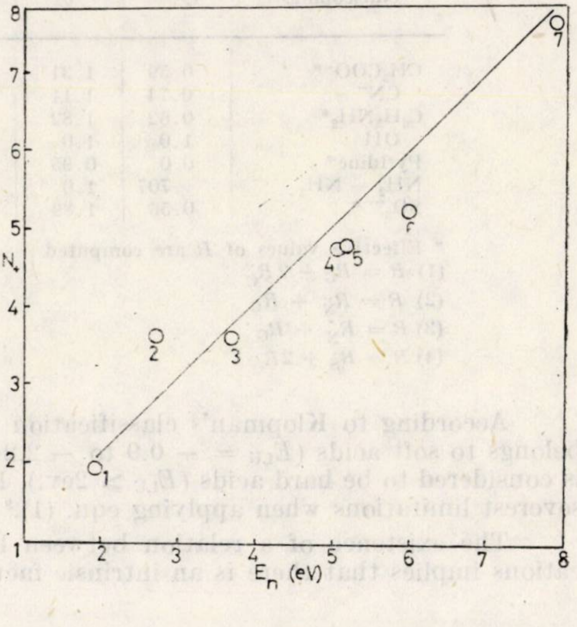

Fig. 2. — A plot of N_+ values vs. desolvation energies of anions as calculated using eqn. (4). Numbers correspond to table 2.

is also in line with Parker's[4] studies of the importance of solvents in nucleophilic substitution reactions. Throughout the calculations of E_n, a value of $b^2 = \frac{1}{4}$ is assumed, to be consistent with an intermediate charge-controlled situation[14] that seems to be prevailing in the cases studied.

One should not, however, overlook the importance of hydrogen bonds between anions and hydroxylic solvents as proposed by Parker.[4] In such a case the correlation observed might just be fortuitous.

REFERENCES

[1] C. G. Swain and C. B. Scott, *J. Amer. Chem. Soc.*, **75**, 141 (1953).

[2] J. O. Edwards, *ibid.*, **76** (1954); **78**, 1819 (1956).

[3] R. G. Pearson, *ibid.*, **89**, 1827 (1967).

[4] A. J. Parker, *Chem. Revs.*, **69**, 1 (1969).

[5] C. D. Ritchie and P. O. I. Virtanen, *ibid*, **94**, 4966 (1972).

[6] C. D. Ritchie, and P. O. I. Virtanen, *ibid*, **94**, 9463 (1972).

[7] C. D. Ritchie and D. J. Wright, *ibid.*, **93**, 6574 (1971).

[8] W. P. Jenks and M. Gilchrist, *ibid.*, **90**, 2622 (1968).

[9] C. D. Ritchie and M. Sawada, *ibid.*, **99**, 3754 (1977).

[10] J. A. Pople, *Trans. Faraday Soc.*, **94**, 1375 (1953).

[11] R. L. Flurry, Jr; E. W. Stout and J. J. Bell, *Theor. Chim. Acta*, **8**, 203 (1967).

[12] K. Nishimoto and N. Mataga, *Z. phys. Chem. (Frankfurt)*, **12**, 335 (1957).

[13] M. J. S. Dewar, "The molecular Orbital Theory of Organic Chemistry", McGraw-Hill, New York, 1969, p. 381.

[14] G. Klopman, *J. Amer. Chem. Soc.*, **80**, 223 (1969).

Revue Roumaine de Chimie, 27, 8, 911–916 (1982)

NORMAL COORDINATE ANALYSIS OF THE VIBRATIONAL SPECTRUM OF DIMETHYLDITHIOARSINATO ANION, $(CH_3)_2AsS_2^-$

IOAN SILAGHI-DUMITRESCU, LUMINIŢA SILAGHI-DUMITRESCU * and IONEL HAIDUC
Chemistry Department, Babeş-Bolyai University
*Institute of Chemistry, Cluj-Napoca, R–3400 Cluj-Napoca, Romania

Received July 1, 1981

The characteristics of the vibrational spectrum of the title compound are discussed on the basis of Normal Coordinate Analysis. Vibrational normal modes are assigned on the basis of Potential Energy Distribution. Force constants and bond orders have been calculated. The arsenic-sulfur stretchings were proven to be localised, pure group vibrations, unlike in the similar phosphorus anion, $(CH_3)_2PS_2^-$. The arsenic-sulfur force constant (2.63 mdyne/Å) suggests a relatively important degree of π-bonding, in agreement with the calculated arsenic-sulfur bond orders.

INTRODUCTION

Diorganyldithioarsinato groups, $R_2AsS_2^-$, are sulfur containing ligands with good coordinating properties relative to transition [1-7] and main group [8] metals. The spectral properties of the dithioarsinato complexes are discussed mainly with reference to central atom. [1-7] There are few data concerning the IR spectral behavior of the dithioarsinato ligands, although IR spectroscopy can be a useful tool in establishing the changes in As – S bond properties caused by the coordination of the AsS_2 group. The IR spectra of the compounds so far reported in the literature [1-8] are not based on a Normal Coordinate Analysis (NCA).

A Normal Coordinate Analysis was thus carried out here for the first representative of this class of ligands, namely the methyl derivative, $(CH_3)_2AsS_2^-$.

EXPERIMENTAL PART

The sodium salt of the dimethyldithioarsinic acid was prepared according to the literature [1,3] by passing hydrogen sulfide through an ethanolic solution of $Na[(CH_3)_2AsO_2]$ (Fluka puris) during two hours. The white crystalline product was purified by recrystallization from 50% ethanol. M. p. 170–171°C, Lit. 171°C. [1,3]

The IR spectrum of $Na[(CH_3)_2AsS_2] \cdot 2H_2O$ was recorded within the 4000–400 cm^{-1} region in KBr pellets using a UR–20 Carl Zeiss Jena spectrophotometer. The spectrum below 400 cm^{-1} was taken from the literature. [1,6]

The Infrared Spectrum

The anion $(CH_3)_2AsS_2^-$ has 27 normal modes classified according to the C_{2v} point group as:

$$\Gamma_t = 9A_1 + 5A_2 + 6B_1 + 7B_2$$

Following Boyle, [9] this representation can be separated into methyl group vibrations, Γ_{CH_3} and C_2AsS_2 skeleton vibrations, Γ_s :

$$\Gamma_{CH_3} = 5A_1 + 4A_2 + 4B_1 + 5B_2$$

$$\Gamma_s = 4A_1 + A_2 + 2B_1 + 2B_2$$

The 18 fundamental methyl vibrations transform as follows:

$$\nu(2A_1 + A_2 + B_1 + 2B_2)$$

$$\delta(2A_1 + A_2 + B_1 + 2B_2)$$

$$\tau(A_2 + B_1)$$

$$\rho(A_1 + A_2 + B_1 + B_2)$$

The IR frequencies of the dimethyldithioarsinato anion are listed in Table 1.

TABLE 1

Vibrational spectrum of $Na[(CH_3)_2AsS_2] \cdot 2H_2O$

Frequencies (cm^{-1})	Assignment	Frequencies (cm^{-1})	Assignment
80	$\delta(CAsS)$	855 sh	
108	$\delta(SAsS)$	878 s	$\rho(CH_3)$
127	$\delta(SAsC)$	910 s	$\rho(CH_3)$
210	$\delta(CAsC)$	1249 m	$\delta_s(CH_3)$
424 m	$\nu_s(AsS)$	1261 w	$\delta_s(CH_3)$
449 m	$\nu_{as}(AsS)$	1410 m	$\delta_{as}(CH_3)$
475 sh		1631 m	
524 m br		1650 sh	$\delta(OH)$
600 m	$\nu_s(AsC)$	2995 m	$\nu_s(CH_3)$
618 m	$\nu_{as}(AsC)$	3010 m	$\nu_{as}(CH_3)$
683 m br			

m = medium ; s = strong ; w = weak ; sh = shoulder ;
br = broad

The heavy As-atom separates the two methyl groups and no important coupling may arise; therefore, no splitting is expected in the CH_3 vibrations region of the spectrum. The same behavior was observed for CH_3 modes in the spectrum of dimethylarsinic acid, $(CH_3)_2As(O)OH$, as shown by Vansant et al. [10]

There are two bands in the CH_3 stretching region at 3010 and 2995 cm^{-1} due to the antisymmetric and symmetric stretchings. The band at 1410 cm^{-1} was assigned to $\delta_{as}(CH_3)$ and the two bands at 1249 and 1261 cm^{-1} to $\delta_s(CH_3)$. In the region due to the CH_3 rocking vibrations (900–800 cm^{-1}) only two bands can be observed, at 878 and 910 cm^{-1}, instead of four expected.

The vibrations of the C_2AsS_2 moiety occur in the 700—300 cm^{-1} range and are due to the As—C and As—S stretchings and deformations.

Using Gordy's rule, [11] Zingaro et al. [12] have calculated the upper limit of stretchings for the arsenic-sulfur bond at 555 cm^{-1}, due to an isolated As = S double bond, and 372 cm^{-1} as the lower limit for an As—S single bond.

According to the literature data, [1-8,13] in the dimethyldithioarsinato derivatives the ν_{as}(As—S) and ν_s(As—S) frequencies can be observed in the range 490—400 cm^{-1}. In the spectrum of $Na[(CH_3)AsS_2] \cdot 2H_2O$ the two bands occur at 449 and 424 cm^{-1}.

The arsenic (V)—carbon stretchings are expected to occur in the range 630—580 cm^{-1}.[13,14] In the infrared spectra of dimethyldithioarsinato derivatives a narrower region can be established for these stretchings, between 630 and 600 cm^{-1}. [1, 6, 13] The spectrum of $Na[(CH_3)_2AsS_2] \cdot 2H_2O$ exhibits two bands at 618 and 600 cm^{-1}, assigned to As — C antisymmetric and symmetric stretchings respectively.

CALCULATION AND DISCUSSION

As no X-ray structure determinations are reported in the literature for this class of compounds, we used a tetrahedral model with bond lengths and angles transferred from tetramethyldiarsine disulfide. [15]

In the Normal Coordinate Analysis the standard Wilson-Eliyashevich GF matrix method[16,17] has been applied, using Shimanouchi's computer programs BGLZ and LSMB [18] modified to suit the operating system of the FELIX C—256 computer available to us.

Initial force constants were transferred from trimethylarsine sulfide, $(CH_3)_3As = S$.[19] The internal coordinate system used for the calculations of G matrix elements is shown in Fig. 1.

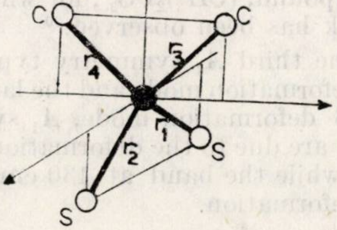

Fig. 1. — The simplified model of $(CH_3)_2AsS_2$ and internal coordinate system (r_1, r_2 : As-S ; r_3, r_4, : As—C ; α_{12} : SAsS ; α_{34} : CAsC ; α_{13}, α_{14}, α_{23}, α_{24}, α_{24} : CAsS).

The observed and calculated frequencies and their relative errors are listed in Table 2.

The assignments of the normal modes were made on the basis of the Potential Energy Distribution and by inspecting the transformation pro-

TABLE 2

Observed and calculated frequencies for $(CH_3)_2AsS_2^-$

Observed freq. (cm^{-1})	618	600	449	424	210	0	127	108	80
Calculated freq. (cm^{-1})	614	606	458	412	209	131	129	112	79
Δ(cm^{-1})	4	−6	−9	12	1	—	−2	−4	1
Δ/ν_{obsd}(%)	0.64	−1.00	−2.00	2.83	0.47	—	−1.57	−3.70	1.25

perties of the normal modes, on the basis of the symmetry coordination as given elsewhere [20] (Table 3).

The two bands at 613 and 605 cm^{-1} were assigned to As$-$C antisymmetric (B_1) and symmetric (A_1) stretchings, respectively.

TABLE 3

The potential energy distribution of the normal modes

Freq. (cm^{-1}) Coord.	613	605	458	412	209	130	128	112	79	0
As$-$S	—	1	50	49	—	—	—	4	—	—
As$-$S	—	1	50	49	—	—	—	4	—	—
As$-$C	50	49	—	1	—	—	—	—	—	—
As$-$C	50	49	—	1	—	—	—	—	—	—
α_{12}	—	—	—	—	5	—	—	75	—	—
α_{13}	—	—	—	—	2	25	25	2	25	—
α_{14}	—	—	—	—	2	25	25	2	25	—
α_{23}	—	—	—	—	2	25	25	2	25	—
α_{24}	—	—	—	—	2	25	25	2	25	—
α_{34}	—	—	—	—	85	—	—	8	—	—
Symmetry	B_1	A_1	B_2	A_1	A_1	A_2	B_2	A_1	B_1	A_1

The symmetric (A_1) and antisymmetric (B_2) As$-$S stretchings are located at 458 and 412 cm^{-1}, respectively.

All the vibrational modes are pure, group vibrations, without significant mixing within a symmetry block, unlike in the analogous phosphorus compound, $(CH_3)_2PS_2^-$, for which a high degree of coupling within the A_1 block has been observed.[20]

The third A_1 symmetry type vibration (209 cm^{-1}) is related to the CAsC deformation mode and the last one, situated at 112 cm^{-1} was assigned to SA$_s$S deformation mode, A_1 symmetry block. The bands at 128 and 79 cm^{-1} are due to the deformation of CAsS angles of B_2 and B_1 type symmetry, while the band at 130 cm^{-1} is an A_1 symmetry, infrared inactive, CAsS deformation.

Force Constants

The values of the calculated force constants are listed in Table 4. It also contains predicted values of the stretching force constants, obtained from diatomic models, on the basis of topological arguments.[21] There is a relatively good agreement between the NCA and topological force constants thus reflecting once more the localized character of the stretching normal modes.

Siebert's formula[22] predicts 2.2 mdyne/Å for the arsenic-sulfur single bond and 4.0 mdyne /Å for As = S double bond force constants, respectively. It can be noticed that our computed arsenic-sulfur force constant has an intermediate value, smaller than in $(CH_3)_3AsS$, thus suggesting a smaller degree of π-bonding. In order to have an idea about the magnitude of this contribution, the bond orders have been calculated by means of Siebert's formula [22] (Table 5). These data show that even in trimethylarsine sulfide, conventionally written as $(CH_3)_3As = S$, the arsenic-sulfur bond order does not exceed 1.34, while in the dimethyldithioarsinato anion it falls down to 1.20. This value is slightly greater than the P–S bond order in $(CH_3)_2PS_2^-$,[20] but the present data do not permit to ascertain if the difference is significant or is due to computational errors.

TABLE 4

Force constants for $(CH_3)_2AsS_2^-$ and related compounds (mdyne/Å)[a)]

	$(CH_3)_3AsS$	$(CH_3)_2AsS_2^-$		$(CH_3)_2PS_2^-$
E–S[a]	2.94	2.63	2.53[b)]	2.80
E–C	2.94	2.67	2.23[b)]	3.08
S–E–S	—	0.37		0.25
C–E–S	0.68	0.21		0.23
C–E–C	0.63	0.45		0.48
Reference	19	this work		20

[a)] E = As, P

[b)] computed by a topological method [21]

TABLE 5

Bond orders for $(CH_3)_2AsS_2^-$ and related compounds[a)]

	$(CH_3)_3AsS$	$(CH_3)_2AsS_2^-$	$(CH_3)_2PS_2^-$
E–S[a)]	1.34	1.20	1.18
E–C	1.05	0.82	1.02
References	19	this work	20

[a)] E = As, P

REFERENCES

[1] A. T. Casey, N. S. Ham, D. J. Mackey and R. L. Martin, *Austral. J. Chem.*, **23**, 1117 (1970).

[2] A. T. Casey, D. J. Mackey and R. L. Martin, *Austral. J. Chem.*, **24**, 1587 (1971).

[3] M. Forster, H. Hertel and W. Kuchen, *Angew. Chem. Int. Ed. Engl.*, **9**, 811 (1970).

[4] W. Kuchen, M. Forster and H. Hertel, *Chem Ber.*, **105**, 3310 (1972).

[5] B. J. McCormick, L. J. Featherstone, H. L. Stoklosa and J. R. Wasson, *Inorg. Chem.*, **12**, 692 (1973).

[6] E. Lindner and H. M. Ebinger, *J. Organometal. Chem.*, **66**, 103 (1974).

[7] A. T. Casey and J. R. Thackeray, *Austral. J. Chem.*, **28**, 471 (1975).

[8] L. Silaghi-Dumitrescu and I. Haiduc, *J. Organomet. Chem.*, **225**, 225 (1982).

[9] L. L. Boyle, *Spectrochim. Acta*, **28A**, 1347 (1972).

[10] F. K. Vansant, B. J. Van der Veken and M. A. Herman, *Spectrochim. Acta*, **30A**, 69 (1974).

[11] W. Gordy, *J. Chem. Phys.*, **15**, 305 (1946).

[12] R. A. Zingaro, R. E. McGlothlin and R. M. Hedges, *Trans. Faraday Soc.*, **59**, 484 (1963).

[13] R. A. Zingaro, K. J. Irgolic, D. H. O'Brien and L. J. Edmonson jr., *J. Amer. Chem. Soc.*, **93**, 5677 (1971).

[14] W. R. Cullen, G. B. Deacon and H. S. Green, *Can. J. Chem.*, **43**, 3193 (1965).

[15] N. Camerman and J. N. Trotter, *J. Chem. Soc.*, **1964**, 219.

[16] a). E. B. Wilson, *J. Chem. Phys.*, **7**, 1047 (1939); b). E. B. Wilson, J. Decius and P. Cross, "Molecular Vibrations. The Theory of Infrared Spectra and Raman Vibrations", McGraw-Hill, New-York, 1955.

[17] M. A. Eliyashevich, *Doklady Akad. Nauk., S.S.S.R.* **28**, 605 (1940); b). M. V. Volkenstein, M.-A. Eliyashevich and B.I. Stepanov, "Kolebaniya Molekul", Mir, Moskwa, 1973.

[18] T. Shimanouchi, "Computer Programs for Normal Coordinate Treatment of Polyatomic Molecules", University of Tokyo, 1968.

[19] F. L. Kolar, R. A. Zingaro and J. Lones, *J. Molec. Struct.*, **18**, 319 (1973).

[20] I. Silaghi-Dumitrescu and I. Haiduc, *Rev. Roumaine Chim.*, **25**, 814 (1980).

[21] I. Silaghi-Dumitrescu, Rev. Roum. Chim., **26**, 1441 (1981).

[22] H. Siebert, "Anwendungen der Schwingungsspektroskopie in der anorganischen Chemie", Springer Verlag, Berlin, 1966.

Revue Roumaine de Chimie 27, 8, 917–925 (1982)

SPECTROPHOTOMETRIC AND DERIVATOGRAPHIC STUDY ON SOME NEW TETRADENTATE MIXED CHELATES OF COBALT (III) WITH ACETYLACETONE DERIVATIVES

MOHAMED ABDEL SALAM El ABSY *, GH. MARCU **, J. ZSAKÓ ** and CS. VÁRHELYI **
* Nuclear Research Center, Cairo (Egypt)
** Faculty of Chemical Technology, "Babeş-Bolyai" University, Cluj-Napoca, Romania

Received February 19, 1981

A number of 22 new complex compounds of type : [Co(Ec) (amine)$_2$] X (Ec = ethylenediimino-bis-acetylacetone (ec), 1,2-propanediimino-bis-acetylacetone (pec), amine = imidazole, 3,5-lutidine) were obtained and characterized by UV and IR spectra. The interpretation of the electronic spectra, compared to those of analogous derivatives with aromatic and heterocyclic amines is attempted in terms of the ligand field theory. The mechanism of the thermal decomposition of these compounds is discussed on the basis of derivatographic data.

INTRODUCTION

Combes [1] reported that acetylacetone forms with ethylenediamine a bis-Schiff's base : ethylendiimino-bis-acetylacetone (ec. H_2). Morgan and Smith [2,3] obtained the first cobalt chelates with this reagent, the nonelectrolyte : [Co(II) (ec)$(H_2O)_2$] and some [Co(III) (ec) $(NH_3)_2$]X type salts.

In our previous papers [4,5] some [Co(ec) (amine)$_2$]X salts with aromatic amines were also obtained and characterized.

RESULTS AND DISCUSSION

Continuing the investigations in the coordination chemistry of polydentate chelating agents, we have condensed acetylacetone with other aliphatic diamines, containing 3 — 6 carbon atoms in the chain. The Schiff's bases with higher diamines, e.g. with 1,4-butane- . . . 1,5-pentane- . . . and 1,6-hexane diamine exhibit no chelating properties. The condensation product with 1,2-propanediamine : 1,2-propanediimino-bis-acetylacetone :

pec.H_2 is also a good complexing reagent. The enolic form of this Schiff's base :

$$CH_3 - C(OH){=}CH - C(CH_3){=}N - CH(CH_3) - CH_2 - N{=}$$
$$= C(CH_3) - CH{=}C(OH) - CH_3$$

is also a tetradentate chelating agent towards transition metal ions.

The oxidation of the cobalt (II) salts in the presence of ec. H_2 or pec. H_2 and aromatic and heterocyclic amines ($pK_b < 12$) leads to the formation of the [Co(Ec) (amine)$_2$]X type binary salts.

This reaction is also influenced by sterical factors. E.g. the 2- and 2,6-substituted pyridine derivatives (2-picoline, 2,6-lutidine, sym.-collidine), quinoline, isoquinoline etc. are not suitable for this purpose.

In the present paper a series of new binary complex salts of type [Co(Ec) (amine)$_2$]X (within Ec = ec or pec, amine = imindazole and 3,5-lutidine) were obtained according to the equation :

$$2Co^{2+} + 2Ec.H_2 + 4\text{ amine} + 1/2O_2 = 2[Co(Ec)(amine)_2]^+ + H_2O + 2H^+$$

From the aqueous-alcoholic solutions of the chlorides, the other salts were obtained by double decomposition reactions with alkaline salts of the halides, pseudohalides and complex acids.

It is interesting that in some cases the NCS group substitutes an amine ligand by forming a nonelectrolytic compound : [Co(Ec) (amine) (NCS)].

TABLE 1

New complex salts of the [Co(Ec) (imidazole)$_2$]X type

Formula	Aspect	Analysis		
		Calcd.		Found
[Co(ec) (imidazole)$_2$] Br	brown, rombohedral plates	Co	11.85	11.37
[Co(ec) (imidazole)$_2$]I	brown rombohedral plates	Co	10.83	10.66
[Co(ec)(imidazole)$_2$] ClO_4	yellow-brown plates	Co	11.40	11.47
		N	16.26	16.08
[Co(ec) (imidazole)$_2$] NCS	green prisms	Co	12.39	12.33
		S	6.74	6.06
[Co(pec) (imidazole)$_2$] ClO_4	irregular yellow-brown plates	Co	10.90	10.77
[Co(pec) (imidazole)$_2$]NCS	green prisms	Co	12.04	12.16
		S	6.55	6.30
[Co(ec) (imidazole)$_2$]· · [Co(DH)$_2$(NO_2)$_2$]	golden yellow plates	Co	14.76	14.65
		N	21.06	20.88
[Co(pec) (imidazole)$_2$]· · [Cr(NCS)$_4$(NH_3)$_2$]· 1/2 H_2O	brown microcryst.	Co+Cr	14.27	14.36
		S	16.50	16.37
		H_2O	3.48	3.49
[Co(pec) (imidazole)$_2$]· · [Cr(NCS)$_4$(aniline)$_2$] · $3H_2O$	brown microcryst.	Co+Cr	11.60	11.45
		S	13.40	13.28
[Co(ec) (imidazole)$_2$]·$_3$ [Cr(NCS)$_6$] · $2H_2O$	yellow-brown microcryst.	3Co+Cr	13.55	13.60
		H_2O	2.13	2.33
		S	11.39	11.60
[Co(pec) (imidazole)$_2$]·$_3$ [Cr(NCS)$_6$] · $4H_2O$	yellow-brown microcryst.	3Co+Cr	12.94	12.88
		H_2O	4.08	4.02
		S	10.88	11.00

Co determined with EDTA, S as $BaSO_4$, Co+Cr as $Co_3O_4 + Cr_2O_3$

TABLE 2

New complex salts of the [Co(Ec) (3,5-lutidine)$_2$]X type

Formula	Aspect	Analysis		
		Calcd.		Found
[Co(ec) (lutidine)$_2$] BF$_4$	gold-yellow long prisms.	Co	10.12	10.3
[Co(pec) (lutidine)$_2$]· · BF$_4$ · H$_2$O	yellow-brown needles.	Co	9.59	9.87
		N	9.12	9.30
		H$_2$O	2.93	3.09
[Co(ec)(lutidine)$_2$] · ClO$_4$	yellow-orange fine needles.	Co	9.91	10.16
		N	9.41	9.65
[Co(pec) (lutidine)$_2$]· ClO$_4$ · 1/2 H$_2$O	brown micro- cryst.	Co	9.54	9.35
		H$_2$O	1.46	2.03
[Co(ec) (lutidine)$_2$]I	brown ,fine needles.	Co	9.47	9.57
		N	9.00	9.25
[Co(pec) (lutidine)$_2$] I	gold-yellow prisms.	Co	9.26	9.09
[Co(ec) (lutidine)$_2$] · picrate	irregular yellow cryst.	Co	8.15	8.21
		N	13.55	13.44
[Co(pec) (lutidine)$_2$] · picrate	irregular yellow microcryst.	Co	7.99	7.91
[Co(ec) (lutidine)$_2$]· [Cr(NCS)$_4$(aniline)$_2$] · H$_2$O	red-violet micro-cryst.	Co+Cr	11.27	11.24
		H$_2$O	1.83	1.82
		S	13.02	13.37
[Co(pec) (lutidine)$_2$]· [Cr(NCS)$_4$(aniline)$_2$] · H$_2$O·	red-violet-micro-cryst.	Co+Cr	11.17	11.16
		H$_2$O	1.80	2.02
		S	12.85	12.64
[Co(ec) (lutidine) (NCS)] · H$_2$O	green microcryst.	Co	12.69	12.93
		H$_2$O	2.70	2.93
		S	6.90	6.82
[Co(pec) (lutidine) (NCS)].	green microcryst.	Co	12.79	12.41
		S	6.96	7.16

Infrared spectra. Ueno and Martell[6,7] mentioned the ν(C = N) frequencies and the enolic ν(C—O) frequencies of the free ec. H$_2$ to be shifted towards lower wavenumbers in the spectra of the Ni(ec), Pd(ec) and Cu(ec) from 1615 to 1510—25 cm^{-1}, and from 1140—45 to 1110—15 cm^{-1}, respectively.

In the case of the [Co(Ec) (amine)$_2$]X complexes these frequencies were found at 1520 (v.s.) and 1105 (s) cm^{-1}.

This indicates strong Co—N and Co—O covalent bonds. The ν(C=N) frequencies of the NCS group appear at 2080 — 2085 cm^{-1} indicating a Co—NCS bond through the N-atom.[8]

Electronic spectra of 17 complexes have been recorded in the region comprised between 12 000 and 50 000 cm^{-1}. The positions of the absorption bands are presented in table 3, together with the logarithm of the molar absorptivities corresponding to the absorption maxima and to the inflexion points (the last ones being marked by i).

As seen from table 3, the spectra of [Co(ec) (amine)$_2$]X type complexes are very similar to each other, including a crystal field (CF), transition band (band *B*), and four charge transfer (CT) or ligand bands . The [Co(Ec) (amine) (NCS)] type complexes possess approximately the same five bands. Besides these, they have also a very weak CF transition band at about 13000 cm^{-1}, marked mostly by an inflexion point. Some of them have also one more CT band, band *D*.

TABLE 3

Electronic spectra of some complexes studied (Wavenumbers of the absorption bands (in $10^3 \times cm^{-1}$) and logε values)

No.	Compound	Band						
		A	B	C	D	E	F	G
1	[Co(ec) $(NH_3)_2$] ClO_4	—	24.6i	29.9	—	37.4i	42.5	45.8
2	[Co(pec) $(aminothiaz)_2$]I	—	24.0i	29.3	—	34.0i	39.4i	44.3
			2.84	3.78	—	3.93	4.48	4.70
3	[Co(ec) $(m\text{-toluidine})_2$]I	—	23.1	29.3	—	36.4i	44.1	49.4
4	[Co(ec) $(aniline)_2$] ClO_4	—	23.0	29.5	—	36.0i	42.6	44.4i
5	[Co(ec) $(\beta\text{-naphtylamine})_2$] BF_4	—	23.2i	29.7	—	34.6i	42.4	45.2i
6	[Co(ec) $(\alpha\text{-naphtylamine})_2$] BF_4)	—	23.5i	30.5	—	34.0	41.8	46.0
7	[Co(ec) $(imidazole)_2$] I	—	23.7	29.6	—	34.5i	38.6i	45.2
			2.83	3.83		3.51	4.05	4.55
8	[Co(ec) $(3,5\text{-lutidine})_2$]I	—	22.7	29.5	—	34.1i	38.1	45.9
			2.82	3.83		3.77	4.23	4.75
9	[Co(pec) $(3,5\text{-lutidine})_2$]I	—	22.5	29.5	—	34.1i	38.0	45.7
			2.83	3.82		3.71	4.29	4.73
10	[Co(pec)($(\beta\text{-picoline})_2$] ClO_4	—	22.5	29.4	—	37.1i	41.1	46.0
11	[Co(ec) $(pyridine)_2$] I	—	23.0i	29.8	—	35.7i	38.0i	44.0
12	[Co(ec) (aminothiazole)(NCS)]	13.0i	24.0i	29.5	—	34.2i	39.5i	45.5
		1.81	2.76	3.67	—	3.79	4.28	4.46
13	[Co(pec) (aminothiazole) (NCS)]	13.01	23.5i	29.2	—	33.8i	39.2i	45.3
		1.79	2.81	3.82	—	3.86	4.31	4.50
14	Co(pec) (imidazole) (NCS)]	13.0	24.1	28.4i	30.7	33.0	41.9	45.8
		1.24	2.74	3.50	3.94	3.84	4.02	4.19
15	[Co(ec) (lutidine) (NCS)]	13.0i	22.7	29.5	34.0i	36.3i	38.1	47.0
		1.22	2.67	3.66	3.48	4.00	4.15	4.57
16	[Ni(ec)]	17.5	27.5i	28.6	33.0i	37.7	42.3	47.5
		1.90	3.68	3.71	3.64	4.11	4.41	4.35
17	[Cu(ec)]	15.5	26.0i	—	33.0i	34.0	41.8	48.2
		1.74	2.31		4.19	4.25	3.97	3.85
	mean of 1–6	—	23.6	29.7	—	35.4	42.1	45.8
	mean of 7–11	—	22.9	29.6	—	35.1	38.8	45.4

i – inflexion point

The spectra of Ni(ec) and Cu(ec) differ very much from those of the Co complexes. Both bands *A* and *B* are strongly shifted towards higher wavenumbers.

In order to study the influence of the ligands, the spectra of the $[Co(Ec)(amine)_2]X$ type complexes have been compared. Presumably the nature of Ec cannot have an important effect, since pec has only a CH_3 group more as compared to ec and this substituent is not directly linked to the co-ordinated N-atom. Spectra of compounds **8** and **9** seem to be in agreement with this presumption.

The amine ligands are of two main types, viz. in compounds **1** – **6** they are ammonia and aromatic amines, but in compounds **7**–**11** the co-ordinated N-atom is a member of an aromatic ring system. By calculating the mean values of the wavenumbers of the five bands separately for the above mentioned two classes (see table 3), one can observe all the wavenumbers, but especially those of bands *B* and *F* to be shifted towards lower values in the case of compounds **7**–**11** as compared to compounds **1**–**6**. Presumably, this effect is due to the metal-ligand (Ec) π-bonds, which are weakened in the case of heterocyclic amine ligands.

An attempt has been made to give a semiquantitative interpretation of this phenomenon. Since the complexes studied have a very low symmetry, the discussion of the spectral transitions is quite difficult. Nevertheless, several very rough simplifications allow to give an interpretation for the influence of the amine ligands. Let us suppose the local symmetry in the vicinity of the central atom to be a tetragonal one (D_{4h}). In this assumption, the same approach can be used as with the $[\mathrm{Co(DH)_2(amine)_2}]^+$ type complexes discussed in our earlier paper,[9] i.e. one can presume the two spinallowed CF transition bands of the octahedral Co^{3+} complexes, having the wavenumbers

$$^1A_{1g} \rightarrow {}^1T_{1g} : \tilde{\nu}_1(O_h) = 10\,Dq - C \tag{1}$$

$$^1A_{1g} \rightarrow {}^1T_{2g} : \tilde{\nu}_2(O_h) = 10Dq + 16B - C \tag{2}$$

to be splitted into two bands each, viz.

$$^1A_{1g} \rightarrow {}^1E_g^+ : \tilde{\nu}_1(\mathrm{I}) = 10Dq - \frac{35}{4}\,Dt - C \tag{3}$$

$$^1A_{1g} \rightarrow {}^1A_{2g} : \tilde{\nu}_1(\mathrm{II}) = 10\,Dq - C \tag{4}$$

$$^1\mathrm{A}_{1g} \rightarrow {}^1B_{1g} : \tilde{\nu}_2(\mathrm{I}) = 10Dq - 4Ds - 5Dt + 16B - C \tag{5}$$

$$^1A_{1g} \rightarrow {}^1E_g^- : \tilde{\nu}_2(\mathrm{II}) = 10Dq + 2Ds - \frac{25}{4}\,Dt + 16B - C \tag{6}$$

Even if the 4 bands (3) — (6) are experimentally observed, their wavenumbers are not sufficient for determining the *Dq* crystal field parameter, the *Dt* and *Ds* tetragonal perturbation parameters, as well as the *B* and *C* Racah parameters. This difficulty can be avoided by recording the spectrum of the octahedral parent compound of the tetragonal compound studied and by presuming $Dq(O_h) = Dq(D_{4h})$.

In the case of the Ec complexes studied, this possibility does not exist since Ec are tetradentate ligands. On the other hand, the electronic spectra of the complexes studied contain a single CF band, viz. band *B*, which is not split.

In this situation the following presumptions and rough approximations have been made :

1. The splitting of the $^1A_{1g} \rightarrow {}^1T_{1g}$ band is presumed not to be large enough to be resolved by the apparatus used and the wavenumber of the band *B* is considered to be the arithmetical mean of $\tilde{\nu}_1(\mathrm{I})$ and $\tilde{\nu}_1(\mathrm{II})$, i.e.

$$\tilde{\nu}_B = \frac{\tilde{\nu}_1(\mathrm{I}) + \tilde{\nu}_1(\mathrm{II})}{2} \tag{7}$$

2. The other CF band is presumed to be masked by the CT band *C*. Since this band is perfectly symmetric, the wavenumber of the CF band is

assumed to be equal to $\tilde{\nu}_C$. The splitting of the ${}^1A_{1g} \rightarrow {}^1T_{2g}$ band cannot be observed with other complexes either,[10] which allows to make the following presumption

$$\tilde{\nu}_2(\mathrm{I}) = \tilde{\nu}_2(\mathrm{II}) = \tilde{\nu}_C \tag{8}$$

3. The Dq crystal field parameter and the C Racah parameter are presumed to have the same value in tetragonal CF as in octahedral one, i.e.

$$Dq(O_h) = Dq(D_{4h}) \text{ and } C(O_h) = C(D_{4h}) \tag{9}$$

By using conditions (7) — (9), relations (1) — (6) give for the Racah parameter B the following expression :

$$B = \frac{3\tilde{\nu}_C + \tilde{\nu}_1(O_h) - 4\tilde{\nu}_B}{48} \tag{10}$$

The value of the unknown octahedral wavenumber $\tilde{\nu}_1(O_h)$ must be chosen arbitrarily.

Since Eqs(1) and (3) give

$$Dt = \frac{4}{35}[\tilde{\nu}_1(O_h) - \tilde{\nu}_1(\mathrm{I})]$$

the maximum value of $\tilde{\nu}_B$ has been taken for $\tilde{\nu}_1(O_h)$ in order to ensure positive values for the perturbation parameter Dt, i.e. calculations have been made by using the hypothetic value : $\tilde{\nu}_1(O_h) = 25\ 000\ \mathrm{cm}^{-1}$. The Racah parameter values calculated by means of formula (10) are given in table 4.

TABLE 4

The Racah parameter B and the percentage of the covalent character $100(1-\beta)$ for some $[\mathrm{Co(Ec\ (amine)_2]X}$ type complexes

Compound	B cm^{-1}	$100(1-\beta)$	pK_b
$[\mathrm{Co(ec)\ (NH_3)_2]ClO_4}$	340	68.1	4.75
$[\mathrm{Co(pec)\ (aminothiazole)_2]I}$	352	66.9	8.78
$[\mathrm{Co(ec)\ (m\text{-}toluidine)_2]I}$	427	59.9	9.34
$[\mathrm{Co(ec\ (aniline)_2]ClO_4}$	448	57.9	9.42
$[\mathrm{Co(ec)\ (\beta\ naphtylamine)_2]BF_4}$	444	58.3	9.70
$[\mathrm{Co(ec)\ (\alpha\ naphtylamine)_2]\ BF_4}$	469	56.0	10.00
$[\mathrm{Co(ec)\ (imidazole)_2]I}$	396	62.8	6.92
$[\mathrm{Co(ec)\ (3,5\text{-}lutidine)_2]I}$	473	55.6	7.10
$[\mathrm{Co(pec)\ (3,5,\text{-}lutidine)_2]I}$	490	54.0	7.10
$[\mathrm{Co(pec)\ (\beta\text{-}picoline)_2]\ ClO_4}$	490	54.0	8.32
$[\mathrm{Co(ec)\ (pyridine)_2]\ I}$	467	56.2	8.74

By using the B values obtained, the nephelauxetic ratio

$$\beta = \frac{B}{B_0}$$

as well as the "percentage of the covalent character" can be calculated as $100\,(1-\beta)$, where B_0 stands for the Racah parameter of the gaseous Co^{3+} ion. For this magnitude the $B_0 = 1065\ cm^{-1}$ value has been taken.[11]

Results obtained are presented in the same table 4, together with the basicity constants of the co-ordinated amines. As seen, the values obtained for the percentage of the covalent character are too high. In the case of Co(III) complexes with all the 6 ligands bonded through N-atoms to the central ion this value is comprised between 50 and 60 %.[12] In our complexes 2 of the 6 co-ordinated atoms are 0-atoms, which must reduce the covalent character of the bonds. These high values are not surprising if one takes into account that for $\tilde{\nu}_1(O_h)$ an arbitrarily chosen value has been used. Nevertheless, our results can be compared to each other and one can observe the percentage of the covalent character to increase almost in the same order as the nucleophilic character of the co-ordinated amine increases. But this tendency appears separately with primary amines and ammonia and separately with the heterocyclic ligands. In the case of the latter ones the percentage of the covalent character is much less than expected on the basis of the pK_b value. This effect reveals the importance of the Co—Ec π-bonds, which become weaker if the co-ordinated N-atom belongs to an aromatic ring system.

The *thermal decomposition* of four [Co(Ec) $(amine)_2$]X, of two [Co(Ec) (amine)NCS] type and of the [Cu(ec)] complexes has been studied by means of derivatography. The TG curves show no weight loss stop corresponding to the formation of a well defined, relatively stable intermediate. Derivation of kinetic parameters from the TG curve is not possible either, owing to the irregular shape of these curves.

Some of the compounds studied contain crystallization water. This water is lost in a separate stage only in the case of [Co(ec) $(py)_2$] I. H_2O. This reaction is marked by an endothermal peak on the DTA curve, at 105°C. [Co(ec) $(aminothiazole)_2$] I. 1.5 H_2O, [Co(ec) $(aminothiazole)_2$] Cl. 4 H_2O, [Co(pec) (aminothiazole) (NCS)]. H_2O and [Co(ec)(lutidine) (NCS)]. H_2O lose their crystallization water beginning from about 80—100°C but the end of this dehydration process is not marked even by an inflexion point on the TG curves and no well defined endothermal peak appears on the DTA curves excepting the [Co(ec) $(aminothiazole)_2$]Cl. $4H_2O$ complex, where the loss of three H_2O molecules is marked by an inflexion point on the TG curve and by an endothermal peak at 105°C on the DTA curve.

The TG curves of all Co complexes studied have a similar shape: after a first rapid decomposition stage no plateau appears, but the decomposition rate becomes smaller. After this slow stage a new rapid decomposition stage appears up to the total decomposition of the complex at about 600—640°C. The [Cu(ec)] complex gives a completely different TG curve. Its decomposition occurs in a single, relatively rapid stage between 200 and 340°C.

The total weight loss and the weight loss during the first rapid decomposition stage are presented in table 5.

TABLE 5

Characteristics of the thermal decomposition of the complexes studied. (Sample weight : $m =$ 20 mg, heating rate : $q = 20$ K/min)

Compound	weight loss, mg		final product	endothermal DTA peaks, t°C	exothermal DTA peaks, t°C
	up to 650 °C	in the first rapid decomposition stage			
[Co(ec) $(py)_2$]I. H_2O	17.4	4.4	Co_3O_4	(160), 205	480
[Co(ec) $(aminothiazole)_2$] I.1.5H_2O	17.8	6.8	Co_3O_4	170	(300), 580
[Co(ec) $(aminothiazole)_2$]Cl. 4H_2O	16.4	10.0	1/3 Co_3O_4+ $CoCl_2$	160	(320) 590
[Co(ec) $(imidazole)_2$] NCS	14.6	10.5	1/3Co_3O_4+ $CoSO_4$	230	(310), (375), (480) 580
[Co(ec) (lutidine)(NCS)]· H_2O	12.8	8.2	1/3Co_3O_4+ $CoSO_4$	—	(275), (390), (460) 550
[Co(pec) (aminothiazole) (NCS)]· H_2O	13.4	8.1	1/3Co_3O_4+ $CoSO_4$	—	(280), (400), (450) 590
[Cu(ec)]	16.4	16.4	CuO	—	(260) 310

The same table contains also the approximate composition of the final product of the thermal decomposition as well as the position of the endothermal and exothermal peaks on the DTA curves. If several peaks appear, the smaller ones are indicated in parantheses.

As seen, the final product of [Co(ec) $(py)_2$]I, 1.5 H_2O and of [Co(ec) $(aminothiazole)_2$]I. 1.5 H_2O is Co_3O_4, but from [Co(ec) $(aminothiazole)_2$]Cl. 4 H_2O also $CoCl_2$ is formed and the NCS containing complexes yield $CoSO_4$, too. It is interesting, that the first stage of the [Co(Ec) $(amine)_2$]X type complexes is an endothermal process, but with the [Co(Ec) (amine) (NCS)] type complexes, as well as with [Cu(ec)], only exothermal processes occur. This suggests the idea that the endothermal process might be a deamination reaction leading to the formation of a nonelectrolytic [Co(Ec) (amine)X] type complex. This hypothesis is in agreement with the very similar shape of the DTA curves of all the NCS — containing complexes. At higher temperatures all these compounds give three lower and higher exothermal peaks at about the same temperatures.

It is obvious that the exothermal peaks are very similar, but the DTA curve of [Co(ec) $(imidazole)_2$]NCS. H_2O presents also an endothermal peak, presumably corresponding to the above mentioned deamination reaction.

EXPERIMENTAL PART

[Co(Ec) (amine)$_2$]. Cl-solutions. 0.1 mol $CoCl_2$ in 250 ml water was treated with a mixture of 0.1 mol ec. H_2 (pec.H_2) and 0.25 mol imidazole (3,5-lutidine) in 300 ml dil. methanol (1 : 1). The solution was oxidized by air bubbling during 6–8 hours, filtered off, and the brown solutions used for double decomposition reactions. *[Co(Ec) (amine)$_2$] X — salts.* 10 mmoles of [Co(Ec)(amine)$_2$] Cl in 50 ml solution were treated with an excess of 3 — 10 % KI, KBr, KCNS, $NaClO_4$, $NaBF_4$, picric acid, $NH_4[Cr(NCS)_4(amine)_2]$, $K_3(Cr(NCS)_6]$. The obtained cryst. products were filtered off, after 15–30 min. standing, washed with ice cooled water and dried on air.
The *electronic spectra* have been recorded by means of a Specord recording spectrophotometer, in methanol.

The *derivatograms* were recorded with a Derivatograph MOM (Hungary) ; sample weight : 20–100 mg, heating rate : 20°/min.

REFERENCES

[1] A. Combes, *Compt. rend.*, **108**, 1252 (1889).
[2] G. T. Morgan and D. M. Smith, *J. Chem. Soc.*, **125**, 1996 (1924).
[3] G. T. Morgan and D. M. Smith, *J. Chem. Soc.*, **127**, 2030 (1925).
[4] Gh. Marcu, Cs. Várhelyi and I. Müller, *Rev. Roumaine Chim.*, **17**, 711 (1972).
[5] Gh. Marcu, Cs. Várhelyi and I. Müller, *Stud. Univ. Babeș-Bolyai, Chem.*, **19** (2), 13 (1974).
[6] K. Ueno and A. E. Martell, *J. Phys. Chem.*, **59**, 998 (1955).
[7] K. Ueno and E. A. Martell, *J. Phys. Chem.*, **60**, 1270 (1956).
[8] M. Chamberlain and J. C. Bailar, *J. Amer. Chem. Soc.*, **81**, 6412 (1959).
[9] J. Zsakó, J. Sata and Cs. Várhelyi, *Rev. Roumaine Chim.*, **18**, 1759 (1973).
[10] R. A. D. Wendthworth and T. S. Piper, *Inorg. Chem.*, **4**, 709 (1965).
[11] M. Bán and J. Császár, *Acta Chim. Acad. Sci. Hung.*, **57**, 153 (1968).
[12] J. Császár and M. Bán "Optikai színkép, ligandumtér-elmélet, komplex szerkezet", Akadémiai Kiadó, Budapest, 1973, p. 240.

Revue Roumaine de Chimie, 27, 8, 927–930 (1982)

NEW NICKEL (II) COMPLEXES WITH DIBASIC TRIDENTATE *ONO* DONOR LIGANDS

A. SYAMAL[a*] and B. K. GUPTA[b]

[a]Department of Applied Sciences and Humanities, Kurukshetra University, Kurukshetra 132119, Haryana
[b]Department of Chemistry, Regional Engineering College, Kurukshetra 132119, Haryana, India

Received April 20, 1981

The synthesis of several new nickel (II) complexes with the Schiff bases derived from *ortho*-aminobenzylalcohol and salicylaldehyde, 5-bromosalicylaldehyde, 3-methoxysalicylaldehyde, 3-ethoxysalicylaldehyde, 3,5-dichlorosalicylaldehyde or 2-hydroxy-1-naphthaldehyde, are described. The Schiff bases behave as dibasic, tridentate ONO donor ligands and form complexes of the $[Ni(H_2O)_3L]$ type (where LH_2 = dibasic, tridentate Schiff base). The complexes have been characterized on the basis of elemental analysis, electrical conductance, molecular weight, IR and electronic spectra, and magnetic susceptibility measurements. The magnetic moments of the complexes are in the 2.95–3.35 B. M. range, indicating octahedral structures. The electronic spectra of the complexes reveal bands at around 10000, 16000 and 29000 cm^{-1} due to the $^3A_{2g} \rightarrow {}^3T_{2g}$, $^3A_{2g} \rightarrow {}^3T_{1g}$(F) and $^3A_{2g} \rightarrow {}^3T_{1g}$(P) transitions, respectively, characteristic of octahedral structure. The $\nu(C = N)$, $\nu(C - O)$ (phenolic), $\nu(C - O)$ (alcoholic) and $\nu(O - H)$ bands of the ligands have been followed in order to find out the coordination sites of the ligands.

INTRODUCTION

There has been considerable research interest in the metal complexes of dibasic, tridentate ligands which force the metal (II and III) ions to form dimetallic complexes with unusual magnetic properties.[1–3] Such studies have mostly veered around $S = 1/2$ systems and far fewer studies have been reported on other spin systems, like $S = 1$, 3/2 or 5/2. Our studies on the magnetic properties of transition metal complexes with $S=1/2$ systems of dibasic, tridentate ligands have given interesting results.[3,4] This prompted us to extend our studies on dibasic tridentate ligands to nickel (II), an $S = 1$ system. In this paper we describe new nickel (II) complexes of the Schiff bases (I) derived from *ortho*-aminobenzylalcohol and salicylaldehyde, 5-bromosalicylaldehyde, 3-methoxysalicylaldehyde, 3-ethoxysalicylaldehyde, 3,5-dichlorosalicylaldehyde or 2-hydroxy-1-naphthaldehyde.

---

* For correspondence.

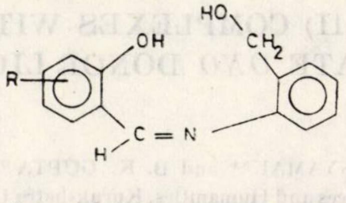

I. R = H, 5-BROMO, 3-METHOXY, 3-ETHOXY, 3,5- DICHLORO AND 5,6-BENZO.

EXPERIMENTAL

Materials and methods

Nickel (II) acetate tetrahydrate was obtained from E. Merck (Germany). Salicylaldehyde was purchased from Sarabhai M. Chemicals. 5-Bromosalicylaldehyde, 3-ethoxysalicylaldehyde and *ortho*-aminobenzylalcohol were purchased from Aldrich Chemical Co. (U.S.A.). 3,5-Dichlorosalicylaldehyde was of Eastman Kodak Co.(U.S.A.). 3-Methoxysalicylaldehyde and 2-hydroxy-1-naphthaldehyde were obtained from Fluka AG (Switzerland).

Physical measurements

The metal content was determined gravimetrically as bis (dimethylglyoximato) nickel (II). The carbon and hydrogen analyses were done by Ciba Geigy Research Center, Bombay. Nitrogen analyses were done microanalytically. Conductance measurements were done in methanol (10^{-3} M) with the help of a Toshniwal Conductivity bridge (Model LO1—02A) and a dip type cell calibrated with KCl solutions. Molecular weights were determined by the Rast method and diphenyl was used as the solvent. The infrared spectra were recorded in KBr pellets using a Perkin Elmer 257 Infrared Spectrophotometer, calibrated with polystyrene. The magnetic susceptibilities were determined by the Gouy method, at room temperature, and $Hg[Co(NCS)_4]$ was used as standard. The susceptibilities were corrected for diamagnetism and temperature independent paramagnetism contributions. The electronic absorption spectra were recorded in $CHCl_3$ on a Beckman DU2 Spectrophotometer with 10 mm matched quartz cells.

General method of synthesis of the complexes

The nickel (II) acetate tetrahydrate (1.25 g, 0.005 mole) was dissolved in 95 % ethanol (10 ml) and was added to an ethanol (95 %) solution of the appropriate Schiff base (0.005 mole in 10—20 ml). The mixture was refluxed for 4 hrs on a waterbath. The solid compound separated after partial evaporation of the solvent under a fan and this was suction filtered, washed with ethanol, recrystallized from 95 % ethanol and dried *in vacuo* at room temperature. Yield = 60 %. The analytical data are given in table 1.

RESULTS AND DISCUSSION

The Schiff bases, I derived from *ortho*-aminobenzylalcohol and salicylaldehyde or substituted salicylaldehydes react with the Ni^{2+} ions to form 1 : 1 metal : ligand complexes. The remaining coordination positions are occupied by three water molecules and the complexes are of the $[Ni(H_2O)_3L]$ type. The complexes exhibit low molar electri cconductance values (6 —10 ohm^{-1} cm^2 $mole^{-1}$) in methanol and this is indicative of

TABLE 1

Analytical molecular weight, IR, electronic spectra and magnetic moment data of nickel (II) complexes [a, b, c]

Complex	Found (Calcd.)				Mol. wt. Found (Calcd.)	IR spectra			Electronic spectra	$\mu_{eff.}$ M. B. (temp.) °K
	Ni %	C%	H %	N %		ν(C–O) (alcoholic) complex (ligand)	ν (C–0) (phenolic) complex (ligand)	ν(C=N) (complex ligand)	$\nu_{max.}$ (∈)[d]	
$[Ni(H_2O)_3$ (sal-OABA)]	17.1 (17.45)	49.6 (49.70)	4.7 (5.03)	4.3 (4.14)	328 (338)	1175 (1190)	1555 (1530)	1605 (1615)	10750(18), 15900(20), 28600(16)	2.95 (291)
$[Ni(H_2O)_3$ (5-bromosal--OABA)]	14.3 (14.15)	42.7 (40.29)	3.4 (3.84)	3.6 (3.36)	390 (417)	1170 (1200)	1540 (1515)	1595 (1620)	10690(22), 15650 (22), 29850 (18)	3.35 (292)
$[Ni(H_2O)_3$ (3-methoxysal--OABA)]	15.6 (16.03)	46.9 (48.91)	4.2 (5.16)	3.5 (3.80)	358 (368)	1175 (1200)	1545 (1540)	1600 (1610)	10800(13), 16000(14), 30300(13)	3.10 (293)
$[Ni(H_2O)_3$ (3-ethoxysal--OABA)]	15.2 (15.44)	52.7 (50.26)	5.5 (5.50)	3.6 (3.66)	344 (382)	1180 (1190)	1555 (1545)	1595 (1615)		3.20 (291)
$[Ni(H_2O)_3$(3,5-dichlorosal -OABA)]	14.6 (14.50)	43.8 (41.28)	3.6 (3.68)	3.6 (3.44)	393 (407)	1180 (1200)	1515 (1510)	1600 (1630)		3.22 (291)
$[Ni(H_2O)_3$ (hydrox-OABA)	15.0 (15.21)	53.1 (55.67)	4.5 (4.90)	3.9 (3.61)	351 (388)	1170 (1215)	1535 (1530)	1590 (1620)	10600(15), 15750(16), 29400(14)	3.18 (293)

a) Abbreviations ; sal = salicylaldehyde, 5-bromosal=5-bromosalicylaldehyde, 3-methoxysal=3-methoxysalicylaldehyde, 3-ethoxysal= = 3-ethoxysalicylaldehyde, 3,5-dichlorosal = 3,5-dichlorosalicylaldehyde, and hydrox = 2-hydroxy-1-naphthal-dehyde.

b) All IR and electronic spectral data are in cm^{-1}.

c) Magnetic moment was calculated using the Curie equation :$\mu_{eff} = 2.83\ (\chi_M^{corr} \times T)^{\frac{1}{2}}$ M. B.

d) Molar extinction coefficient in $[1.mole^{-1}\ cm^{-1}]$.

non-electrolytic nature of the complexes. The molecular weight data indicate the monomeric nature of the complexes.

The measured magnetic moments of the complexes are in the 2.95 – 3.35 B. M. range, which is in the usual range (2.9 –3.4 B.M.) observed for the majority of nickel (II) complexes with octahedral structure.[5] The complexes exhibit three ligand field bands, at around 10000, 16000 and 29 000 cm^{-1}, assigned to the transitions $3_{A_{2g}} \to 3_{T_{2g}}$, $3_{A_{2g}} \to 3_{T_{1g}}(F)$ and $3_{A_{2g}} \to 3_{T_{1g}}$ (P), respectively, in an octahedral symmetry.[5] The low molar extinction coefficient values (13 –22 l. $mole^{-1}$ cm^{-1}) are also the characteristic of octahedral nickel (II) complexes. In the IR spectra the free Schiff bases (I) reveal a medium intense band at ~ 2700 cm^{-1}, characteristic of intramolecularly hydrogen bonded OH group. In the complexes this band is absent and this is indicative of the breaking of the hydrogen bonding and consequent deprotonation of the OH groups. A band at ~3200 cm^{-1} can be assigned to the ν(OH) stretch of coordinated water. The ν(C –O) (alcoholic) stretch of the ligands occurs in the 1199 – 1215 cm^{-1} range (Table 1). This band shifts to lower wavenumber indicating the involvement of the alcoholic oxygen atom in coordination.[6] The ligands exhibit the ν(C –O) (phenolic) stretch in the range 1510 –1545 cm^{-1}. On complexation this band shifts to higher wavenumber, indicating the phenolic oxygen coordination of the ligands.[7] The ν(C=N) stretch of the ligands occurring at 1615 –1630 cm^{-1} undergoes negative shift and this indicates the nitrogen coordination of the azomethine group.[8] Thus, the IR data indicate that the ligands are behaving as ONO donor tridentate ligands.

The intent of this was to synthesize the $[NiL]_2$ type complexes which might be involved in magnetic exchange, similar to $[VOL]_2$ and $[CuL]_2$ complexes.[3,4] But, in reality, only complexes of the $[Ni(H_2O)_3L]$ type were formed. The molecular weight and magnetic moment data indicate magnetically dilute nature of the complexes.

ACKNOWLEDGEMENT. The authors are indebted to University Grants Commission, New Delhi 11 0002 for support of this work.

REFERENCES

[1] W. E. Hatfield and R. Whyman, *Transition Met. Chem.*, **5**, 47 (1969).

[2] D. J. Hodgson, *Progr. Inorg. Chem. Chem.*, **19**, 173 (1975).

[3] A. Syamal, *Coord. Chem. Rev.*, **16**, 309 (1975).

[4] C. C. Lee, A. Syamal and L. J. Theriot, *Inorg. Chem.*, **10**, 1669 (1970); G. O. Carlisle, A. Syamal, K. K. Ganguli and L. J. Theriot, *J. Inorg. Nuclear Chem.*, **34**, 2761 (1972); A. Syamal, E. F. Carey and L. J. Theriot, *Inorg. Chem.*, **12**, 245 (1973); A. Syamal and L. J. Theriot, *J. Coord. Chem.*, **2**, 193, 241 (1973); A. Syamal *Indian J. Chem.*, **11**, 363 (1973); A. Syamal and K. S. Kale, *Indian J. Chem.*, **15A**, 431 (1977), **16A**, 46(1978), *Transition Met. Chem.*, **4**, 298 (1979), *Inorg. Chem.*, **18**, 992 (1979), *Indian J. Chem.*, **19A**, 225 (1980); A. Syamal, *Transition Met. Chem.*, **5**, 220 (1980).

[5] F. A. Cotton and G. Wilkinson, "Advanced Inorganic Chemistry", Wiley Eastern, New Delhi, 1972, p. 881–882.

[6] H. H. Freedman, *J. Amer. Chem. Soc.*, **83**, 2900 (1961); K. Ueno and A. E. Martell, *J. Phys. Chem.*, **59**, 998 (1955).

[7] G. E. Batley and D. P. Graddon, *Austral. J. Chem.*, **20**, 877, 885 (1967).

[8] F. Maggio, T. Pizzino, V. Romano and G. Dia, *J. Inorg. Nuclear Chem.*, **38**, 602 (1976).

Revue Roumaine de Chimie, 27, *8*, 931–934 (1982)

OPTICAL AND MAGNETIC STUDIES OF SOME HETERONUCLEAR COMPLEXES OF NICKEL AND ZINC WITH HYDRAZINE

V. MINCU, C. LEPĂDATU, MELANIA GUȚUL, MARIA BREZEANU
and IOANA JITARU
The Polytechnic Institute Bucharest, Department of Chemistry, Laboratory of Inorganic Chemistry, 3–5 Polizu str., Bucharest, Romania

Received June 18, 1980

The electronic spectra and the magnetic proprieties of some $NiZn(N_2H_4)_6(SO_4)_2$, $NiZn(N_2H_4)_6(NO_3)_4$ and $NiZn(N_2H_4)_4Cl_4$ complexes are interpreted in order to obtain information on the coordination geometry of Ni(II) ion in polynuclear complexes containing hydrazine as ligand. It has been concluded that Ni(II) ion within these complexes is octahedrally coordinated, having a high spin d^8 electronic configuration with two uncoupled electrons.

The synthesis and characterization (IR spectroscopy, X-Ray diffraction) of complexes containing hydrazine, $NiZn(N_2H_4)_6(SO_4)_2$ $NiZn(N_2H_4)_6(NO_3)_4$ and $NiZn(N_2H_4)_4Cl_4$, were previously reported. [1–3]

This paper presents the optical and magnetic studies carried on[6] these complexes, in order to obtain information concerning their stereochemistry.

RESULTS AND DISCUSSION

The reflectance electronic spectra of $NiZn(N_2H_4)_6(SO_4)_2$, $NiZn(N_2H_4)$ $(NO_3)_4$ and $NiZn(N_2H_4)_4Cl_4$ have been recorded. This is the only technique to be used, because these complexes decompose in solution. [4]

Fig. 1 and table 1 give the electronic spectra and the spectral parameters for $NiZn(N_2H_4)_6(SO_4)_2$, $NiZn(N_2H_4)_6(NO_3)_4$,$Ni Zn(N_2H_4)_4Cl_4$ and for comparison some Nickel complexes containing hydrazine, reported in the literature. [5]

As may be easily seen, these spectra are very similar in the shape and position of the absorption bands, which may be interpreted assuming an octahedral coordination geometry for all Nickel(II) complexes.

The spectrum of $NiZn(N_2H_4)_4Cl_4$ and also that of $Ni(N_2H_4)_2Cl_2$ contains absorption maxima shifted (excepting ν_1) towards longer wavelengths, if they are compared with those of the chromophore $[Ni(II)(N_2H_4)_6]^{2+}$. This shift is undoubtedly due to the presence of two chlorines instead of a hydrazine molecule. This fact may be explained by the so-called ligand field strength, which is higher for hydrazine (nitrogen as ligator) as compared with that of chloride ion, if we look at their position in the spectrochemical series. [6-7] This interpretation is in agreement with the colour modification of the compounds from light violet $[Ni(II)N_6]$ to gray-blue $[Ni(II)N_4Cl_2]$. [7]

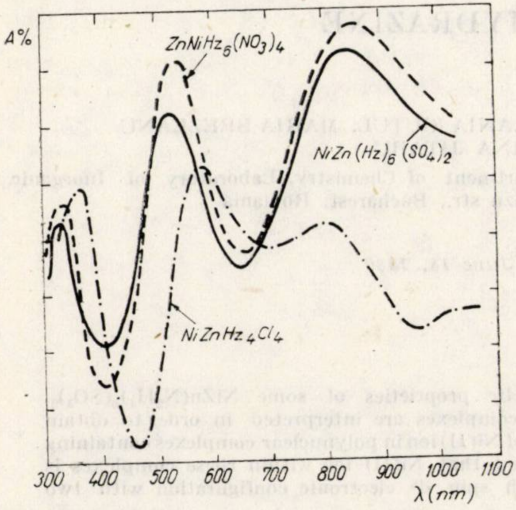

Fig. 1. — Electronic spectra of some polynuclear Ni(II) complexes containing hydrazine as ligand.

TABLE 1

Reflectance spectra of Nickel—hydrazine complexes

Complex	Transitions			Colour
	ν_1 $^3T_{2g} \leftarrow {}^3A_{2g}$	ν_2 $^3T_{1g} \leftarrow {}^3A_{2g}$	ν_3 $^3T_{1g}(P) \leftarrow {}^3A_{2g}$	
$NiZn(N_2H_4)_6(SO_4)_2$	(11764)	18518	29240	light violet
$NiZn(N_2H_4)_6(NO_3)_4$	(11560)	18518	29240	light violet
$NiZn(N_2H_4)_6Cl_2$[7]	(11700)	18125	29000	light violet
$NiZn(N_2H_4)_4Cl_4$	(12195)	17980	27000	gray-blue
$Ni(N_2H_4)_2Cl_2$[7]	(12376)	16775	26750	gray-blue

For an electronic configuration d^8, in an octahedral coordination geometry, the three spin-allowed d—d transitions, according to a strong field coupling, are the following :[8]

$$\nu_1[{}^3T_{2g} \leftarrow {}^3A_{2g}] = 10\,D_q$$

$$\nu_2[{}^3T_{1g} \leftarrow {}^3A_{2g}] = 15D_q + 7.5B - 1/2\;[225B^2 + 100\,D_q^2 - 180\,D_qB]^{1/2}$$

$$\nu_3[{}^3T_{1g}(P) \leftarrow {}^3A_{2g}] = 15D_q + 7.5B + 1/2\;[225B^2 + 100D_q^2 - 180D_qB]^{1/2}$$

As the first transition ν_1 is not well localized in the electronic spectra of the complexes, 10 D_q and B have been fitted from ν_2 and ν_3, according to König's proposed method.[9]

$$10D_q = 1/3\;(2\nu_2 - \nu_3) + 5B$$

$$B = 1/510\;\;[7(\nu_3 - 2\nu_2) + 3\;\{81\nu_3^2 - 16\nu_2(\nu_2 - \nu_3)\}^{1/2}]$$

Table 2 summarizes the 10 D_q, B and β (nephelauxetic ratio) for the complexes.

One may observe (in Table 2) that $B_{\text{complex}} < B_{0\text{Ni(II)}}$.[10] This fact suggests a mean covalency degree for Ni(II) — (N) hydrazine bonds.

TABLE 2

Spectral parameter values of octahedral Nickel—hydrazine complexes

Complex	$10D_q$ (cm^{-1})	B(cm^{-1})	β*
$NiZn(N_2H_4)_6(SO_4)_2$	11892	805	0.77
$NiZn(N_2H_4)_6(NO_3)_4$	11802	835	0.80
$NiZn(N_2H_4)_4Cl_4$	10894	820	0.79

*$B_{0\text{Ni(II)}} = 1040\ cm^{-1}$

Table 3 gives, in the first raw, the experimental magnetic moments. The magnetic moments were also theoretically calculated using the expression :[11]

$$\mu_{\text{eff}} = \mu_s\left(1 - \frac{4\lambda}{10D_q}\right)$$

where μ_s — is the spin only magnetic moment (2.83 B.M. for Ni(II));

TABLE 3

Experimental and calculated values of magnetic moments (25°C) and contributions from spin-orbit coupling

Complex	$\mu_{\text{eff. exp.}}$(B.M)	$\mu_{\text{eff. calc.}}$(B.M)	Orbital contributions (B.M)
$NiZn(N_2H_4)_6(SO_4)_2$	3.24±0.04	3.13	0.30
$NiZn(N_2H_4)_6(NO_3)_4$	3.18±0.04	3.13	0.30
$NiZn(N_2H_4)_4Cl_4$	3.16±0.04	3.16	0.33

λ — the spin-orbit coupling ($\lambda = -315\ \text{cm}^{-1}$ for Ni (II));
$10D_q$ — splitting parameter.

The calculated values are given in the second raw of table 3. The experimental values assumed by the magnetic moments show that the complexes are paramagnetic, corresponding to a high spin d^8 configuration in an octahedral environment (two unpaired electrons).

It is well known that the two paramagnetic species of Ni(II), octahedral and tetrahedral, have magnetic moments with only 10% orbital contribution. For the tetrahedral one, the orbital contribution is somewhat higher, the typical effective magnetic moment being, at the room temperature, between 3.6 and 4.0 B.M.[12] As may be seen in table 3, the experimentally found magnetic moments for our complexes take values within 3.16–3.24 B.M., typical for Ni(II) in an octahedral environment. These values agree with those calculated using spectral data.

EXPERIMENTAL

The visible reflectance spectra of the finely powdered solids were measured on a Beckman D K–2 spectrophotometer fitted with a standard reflectance attachment and Magnesium oxide as reference.

Magnetic susceptibility measurements were made using the Faraday method, with a $Hg[Co(SCN)_4]$ Standard.

The magnetic moment was calculated according to the expression

$$\mu = 2.83\,(\chi'_m T)^{1/2}, \text{ where } \chi'_m = \chi_m - \chi_{\text{dia}}\,;\ \chi_{\text{dia}N_2H_4} = -201 \times 10^{-6}\,;^{13}$$

$$\chi_{\text{diaNi}} = -12.5 \times 10^{-6}\,;\ \chi_{\text{diaZn}} = -13.5 \times 10^{-6}\,;\ \chi_{\text{dia}SO_4} = -33.6 \times 10^{-6}\,;\ \chi_{\text{dia}NO_3} = -14.2 \times 10^{-6}\,;$$

$$\chi_{\text{diaCl}} = -40.2 \times 10^{-6}\ \text{ucgs.}^{14}$$

REFERENCES

[1] M. Brezeanu and M. Guţul, *Bul. Inst. Politeh. Bucureşti*, **39**, 65 (1977).
[2] M. Munteanu, M. Guţul and M. Brezeanu, *Bul. Inst. Politeh. Bucureşti*, **40**, 41 (1978).
[3] C. Mandravel, M. Brezeanu and M. Guţul, *Bul. Inst. Politeh. Bucureşti*, **41**, 45 (1979).
[4] E. C. Gilbert and W. H. Evans, *J. Amer. Chem. Soc.*, **73**, 3517 (1951).
[5] R. Tsuchiya, M. Yonemura, A. Uehara and E. Kyuno, *Bull. Chem. Soc. Japan*, **47**, 660 (1974).
[6] C. Furlani, G. Mattogno, A. Monaci and F. Tarli, *Inorg. Chim. Acta*, **4**, 187 (1970).
[7] R. Tsuchiya, S. Joba, A. Uehara and E. Kyuno, *Bull. Chem. Soc. Japan*, **46**, 1454 (1973).
[8] A. B. Lever "Inorganic Electronic Spectroscopy", Ed. Elsevier, New York, 1968, p. 183.
[9] E. König, *Structure and Bonding*, **9**, 175 (1971).
[10] S. Griffith, "The Theory of Transition Metal-Ions", Cambridge Univ. Press, Cambridge, 1960, p. 310.
[11] B. N. Figgis, "Introduction to Ligand Fields", Intersc. Publ., New York, 1966, p. 265, 281.
[12] B. N. Figgis and J. Lewis, "Progress in Inorganic Chemistry", vol. 6, Editor F. A. Cotton, Cambridge, 1964, p. 207.
[13] M. Turkevich and P. W. Selwood, *J. Amer. Chem. Soc.*, **63**, 1077 (1971).
[14] G. Foex, "Constantes Selectionnees Diamagnetisme at Paramagnetisme", vol. 7, Ed. Mason, Paris, 1957, p. 223.

Revue Roumaine de Chimie, 27, *8*, 935–938 (1982)

CYCLODEHYDRATIONS WITH PHENYLDICHLOROPHOSPHITE-DIMETHYLFORMAMIDE. A NEW CONVENIENT METHOD FOR THE SYNTHESIS OF 1,3,4-OXADIAZOLES FROM DIAROYLHYDRAZINES

C. I. CHIRIAC
"P. Poni" Institute of Macromolecular Chemistry, Aleea Gr. Ghica Vodă 41 A Iaşi, Romania

Received October 2, 1981

Various substituted 1,3,4-oxadiazoles are prepared in good yields by a cyclodehydration reaction with the new adduct phenyldichlorophosphite-dimethylformamide, under mild conditions.

Since Stollé[1] first prepared 2,5-diphenyl-1,3,4-oxadiazole from N, N′-dibenzoyl-hydrazine by dehydration at 250–300°C, numerous dehydrating reagents have been used in an effort to decrease the harshness of the reaction conditions.

The dehydrating reagents which have tested are: phosphorus oxychloride,[2-4] thionyl chloride,[5] ethyl ortoformate,[6] thionyl chloride in nitrobenzene[7] and aluminium chloride in nitrobenzene.[8] Various disadvantages are associated with these reagents: the long reflux time, the high temperature, or the low yield.

RESULTS AND DISCUSSIONS

Previous communications from this laboratory have shown that phenyldichlorophosphite is a useful reagent in syntheses of amides[9] or hydrazides.[10]

In this work, we have investigated the applicability of phenyldichlorophosphite in dimethylformamide (DMF) as reagent in the cyclodehydration of diaroylhydrazines to substituted 1,3,4-oxadiazoles. Thus by heating at 100–110°C one mole of dibenzoylhydrazine with one mole of phenyldichlorophosphite in excess DMF, 2,5-diphenyl-1,3,4-oxadiazole resulted (yield 91%). When we used only 0.5 mole of phenyldichlorophosphite, the yield was 40–50%. Therefore, only one chlorine atom is reactive. The second becomes reactive at higher temperatures (120–140°C), but the purity of the obtained oxadiazoles is more reduced.

It is well known that by the reaction between DMF and different reactive compounds containing chlorine, the following adducts result:

With $SOCl_2$, $[(CH_3)_2N^+=C(H)Cl]^{(+)}Cl^{(-)}$,[11]

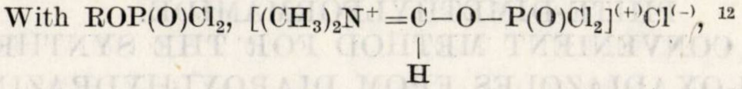

With $ROP(O)Cl_2$, $[(CH_3)_2N^+=\underset{\displaystyle H}{\underset{|}{C}}-O-P(O)Cl_2]^{(+)}Cl^{(-)}$, [12]

With $POCl_3$, $[(CH_3)_2N^+=CH-O-P(O)Cl_2]^{(+)}Cl^{(-)}$. [13]

Phenyldichlorophosphite having reactive chlorine, reacts with DMF, giving a new adduct. By the reaction between phenyldichlorophosphite (1 mole) and DMF (1 mole), 3 hours at room temperature, this adduct precipitates by cooling. The product being hygroscopic, it was collected very fast by filtration, washed with anhydrous ethylic ether and dried under vacuum (m.p. 86 – 88°). The analysis of chlorine, phosphorus and nitrogen correspond for the following structure:

$[(CH_3)_2N^+=CH-O-P(Cl)OC_6H_5]^{(+)}Cl^{(-)}$, similar to other cases. [12,1] On the other hand, DMF is a very good solvent for the products of reaction.

We supposed, similar as in other cases, [12,14,15] that this reaction involves two transition states (II) and (III):

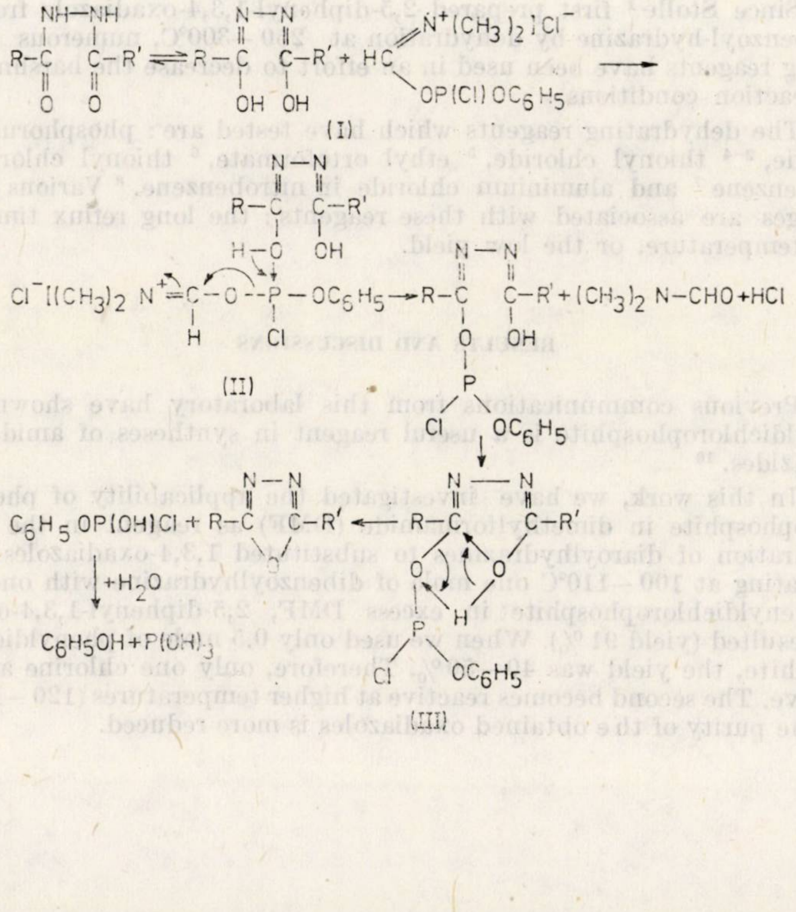

In this reaction, $C_6H_5OP(OH)Cl$ which results as by product, does not affect the reaction, like in other cases.[9,10]

The cyclodehydration reaction of diaroylhydrazines takes place with phenyldichlorophosphite without DMF, but the presence of a good solvent is necessary because the products have aromatic structure with low solubility and high melting points. In this case the reaction involves only the transition state (III).

In a typical procedure, one mole of phenyldichlorophosphite was added slowly to dried DMF cooled to 0 –5°C. After two-hour stirring at room temperature, one mole (I) was added and heated four hours at 100 –110°C. At room temperature, the yield is low. The obtained product is precipitated with water and ice, when $C_6H_5O-P(OH)Cl$ (by product) is transformed in C_6H_5OH and $P(OH)_3$. The yields of this method ranged from 74 to 93% (Table 1).

TABLE 1

Substituted 1, 3, 4-oxadiazoles obtained from diaroylhydrazines using the phenyldichlorophosphite – DMF adduct

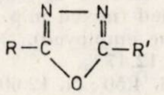

R	R′	Oxadiazoles[a]		
		Yield[b] %	M.p.[c] °C	Reported m.p.°C
3-Bromophenyl	3-Bromophenyl	86	181–183	181–183[16]
4-Methoxyphenyl	4-Methoxyphenyl	88	166–168	166–167[16]
4-Methylphenyl	4-Methylphenyl	93	174–176	175[16]
Phenyl	Phenyl	91	139–140	139–140[1]
Phenyl	4-Nitrophenyl	74	204–207	207–209[17]
Phenyl	4-Methoxyphenyl	91	145–147	146[17]
Phenyl	4-Chlorophenyl	81	161–163	162[17]
4-Chlorophenyl	4-Chlorophenyl	78	240–242	242–243[18]
Phenyl	4-Bromophenyl	76	166–168	167[17]

[a] The products were identified by comparison of m.p. and IR spectra with authentic samples.
[b] Yields calculated on diaroylhydrazines employed.
[c] Before recrystallization.

Using this new adduct between phenyldichlorophosphite and DMF (reactive compound), we obtained substituted 1,3,4-oxadiazoles in high yields.

EXPERIMENTAL

Phenyldichlorophosphite-DMF adduct

To 7.31 g (0.1 mole) dried DMF in a 50 ml three-necked flask, 18.9 g (14 ml ; 0.1 mole of phenyldichlorophosphite were added slowly under stirring and cooling. After stirring 2—3 hours at room temperature, the product began to precipitate. After stirring (1 h) under cooling, the product was collected by filtration and washed (very fast) with anhydrous cold ethylic ether (50—70 ml), because it is hygroscopic. After drying 3—4 hours under vacuum, 22.2 g adduct with m.p. 86—88°C were obtained. Yield 84%.

Anal. Found : Cl, 27.06 ; P, 11.12 ; N, 5.96%.

Calculated for : $C_9H_{12}Cl_2NO_2P$; Cl, 26.48 ; P, 11.56 ; N, 5.22%.

2,5-Diphenyl-1,3,4-oxadiazole

To 15 ml dried DMF in a 50 ml three-necked flask, 1.4 ml (0.01 moles) of phenyldichlorophosphite [19] were added slowly under stirring and cooling. After stirring two hours at room temperature, 2.4 g (0.01 moles) dibenzoylhydrazine were added. Then, this solution was heated four hours at 100—110°C. At the end of reaction, the obtained solution was poured into a large volume of water with ice (50—70 ml) under stirring, when the desired product precipitated. The solution was treated with 10% NaOH solution till pH = 9—10 and the product was collected by filtration, washed with 30—40 ml 10% HCl solution, three times with 20—30 ml water and dried under vacuum at 100—110°C. 2,5-Diphenyl-1,3,4-oxadiazole 2.02 with m.p. 139—140°C was obtained (mixed m.p. with pure product underpressed). Yield 91% (calculated on dibenzoylhydrazine employed).

Anal. Found : C, 75.23 ; H, 4.31 ; N, 12.47%

Calculated for $C_{14}H_{10}N_2O$; C, 75.60 ; H, 4.50 ; N, 12.60%.

Under similar conditions, the other oxadiazoles (presented in table 1) were prepared in good yields from the corresponding diaroylhydrazines.

REFERENCES

[1] R. Stollé, *Ber. dtsch. chem. Ges.*, **32**, 797 (1897).

[2] A. P. Grekov and L. N. Kulakova, *Zhur. obshcei. Khim.*, **29**, 3054 (1959) ; *Chem. Abstr.*, **54**, 13108 (1960).

[3] A. P. Grekov and R. S. Azen, *Zhur. obshcei Khim.*, **29**, 1955 (1959) ; *Chem. Abstr.*, **54** 9898 (1960).

[4] F. N. Hayes and B. S. Rogers, *J. Amer. Chem. Soc.*, **77**, 1850 (1955).

[5] Ciba Ltd., British patent 816, 750 (July 15, 1959) ; *Chem. Abstr.*, **54**, 3457 (1960).

[6] G. Ainsworth, U.S. Pat. 2, 733, 245 ; *Chem. Abstr.*, **50**, 12.115 (1956).

[7] N. S. Dokunikhin, *Zhur. priklad. Khim.*, **32**, 664 (1959).

[8] W. Müeller, U. S. Pat. 2, 838, 520 ; *Chem. Abstr.* **52**, 17.290 (1958).

[9] C. I. Chiriac, *Rev. Roumaine Chim.*, **26**, 1001 (1981).

[10] C. I. Chiriac, *Rev. Roumaine Chim.*, **27**, 411 (1982).

[11] H. H. Bosshard, *Helv. Chim. Acta*, **42**, 1658 (1959).

[12] F. Cramer and M. Winter, *Chem. Ber.* **94**, 990 (1961).

[13] H. Brederek, *Chem. Ber.*, **92**, 837 (1959).

[14] H. M. Walborsky and G. E. Niznik, *J. Org. Chem.*, **37**, 187 (1972).

[15] E. A. Lawton and D. D. McRitchie, *J. Org. Chem.*, **24**, 26 (1959).

[16] E. Baltazzi and A. J. Wysocki, *Chem. Ind.*, **26**, 1080 (1963).

[17] A. P. Grekov and L. M. Kulakova, *Zhur. obshcei Khim.*, **29**, 3055 (1959) ; *Chem. Abstr.*, **54**, 131.089 (1960).

[18] F. N. Hayes and D. G. Ott, *J. Amer. Chem. Soc.*, **77**, 1851 (1955).

[19] H. Tölkmith, *J. Org. Chem.*, **23**, 1682 (1958).

Revue Roumaine de Chimie, **27**, *8*, 939–942(1982)

SYNTHESIS OF SOME SUBSTITUTED TRIFLUOROMETHYL-PHENOTHIAZINES AND THEIR OXIDATION PRODUCTS

M. ANAND[a], S. P. GUPTA[a], A. R. GOYAL[b] and R. L. MITAL [b]*
[a] D. N. College, Meerut, India
[b] Chemical Laboratories, University of Rajasthan, Jaipur, India

Received March 10, 1980

2-Trifluoromethyl-7-isopropoxy-8-methoxyphenothiazine-10-propionic acid (III) has been synthesized by N-alkylation of 2-trifluoromethyl-7-isopropoxy-8-methoxy phenothiazine (1) with acrylonitrile. III was oxidized with 30% H_2O_2 and hydrolyzed with conc. hydrochloric acid to give 2-trifluoromethyl-7-hydroxy-8-methoxy phenothiazine-10-propionic acid-5-oxide (V).

Recent studies on the metabolism of chlorpromazine [1-4] have initiated an interest among the psychopharmacologists to synthesize highly potent metabolites of triflupromazine (Triflupromazine is the generic name of 2-trifluoromethyl-10-(3-dimethylaminopropyl)-phenothiazine; in USA and UK it is sold as Vesprin, while in India as Siquil), because the literature is deplete of the triflupromazine studies.

Since 1957 triflupromazine has been extensively used as tranquilizer and neuroleptic,[5] but the mode of its action is still equivocal. In order to elucidate the therapeutic mechanism of the drug, the availability of the reference standard is indispensable. [6] Sulfoxides are the chief degraded products of psychopharmacological drugs metabolism.[7] Therefore, in the present investigation we have synthesized 2-trifluoromethyl-7-hydroxy-8-methoxy phenothiazine-10-propionic acid-5-oxide, a probable metabolite [1,8] of triflupromazine reported from biological materials. This derivative may be useful in studies concerning the isolation and identification of triflupromazine metabolites.

2-Trifluoro-7-isopropoxy-8-methoxyphenothiazine (I) has been synthesized by isopropylation of 2-trifluoromethyl-8-methoxy-phenothiazine-7-ol [9] with 2-bromopropane. Compound I on N-alkylation with acrylonitrile in the presence of Triton B gave 2-trifluoromethyl-7-isopropoxy-8-methoxy-10-(2-cyano ethyl)-phenothiazine (II), which on complete basic hydrolysis gave 2-CF_3-7-isopropoxy-8-methoxy phenothiazine-10-propionic acid (III). III was further oxidized with 30% H_2O_2 and hydrolysed with hydrochloric acid to give the desired product 2-trifluoromethyl-7-hydroxy-8-methoxy-phenothiazine-10-propionic acid-5-oxide (V).

---

* Correspondence author : Prof. R. L. Mital, B—8, Ganesh Marg, Bapu Nagar, Jaipur—302004 (India)

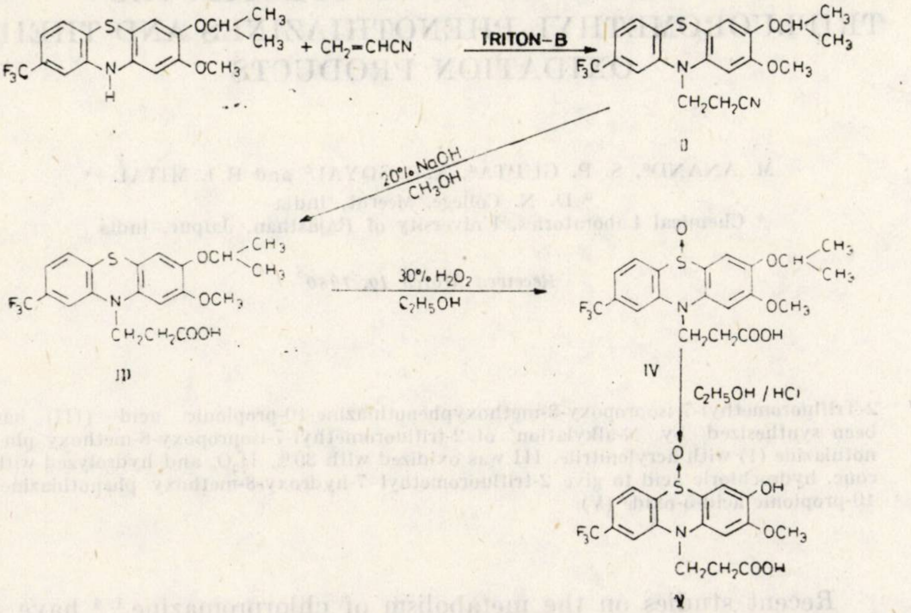

EXPERIMENTAL

All melting points are uncorrected and the reactions have been carried out under dry nitrogen atmosphere. The compounds are sensitive towards light and hence are kept in coloured bottles flushed with nitrogen. The purity of the compounds has been checked by elemental analysis and TLC behaviour. A mixture of polar and nonpolar solvents was used for chromatography. The IR spectra were recorded for KBr Wafer on Perkin Elmer—577 spectrophotometer.

Synthesis of 2-trifluoromethyl-7-isopropoxy-8-methoxy phenothiazine (I):

To a mixture of 2-trifluoromethyl-8-methoxy phenothiazin-7-ol (0.01 mole) sodium dithionite (0.5 g.) and 20 ml of 10% ethanolic potassium hydroxide solution was added 2-bromopropane (0.014 mole). The reaction mixture was refluxed for 8 hrs and poured into 150 ml cold water. The yellow solid was extracted with diethyl ether, washed with water and dried (Na_2SO_4). The solvent was stripped off at reduced pressure to half of its volume and trituration done with pet. ether (60—80°). The light yellow solid was filtered and recrystallized from benzene to give the desired product I (Table 1).

2-Trifluoromethyl-7-isopropoxy-8-methoxy-10-(2-cyanoethyl)-phenothiazine (II)

To a mixture of I (0.015 mole) in 26 ml anhyd. benzene, 0.5 ml of triton B (40% benzyl trimethyl ammonium hydroxide in methanol) was added dropwise a solution of acrylonitrile (0.045 mole) in benzene. The temperature of reaction was maintained around 65°C and stirred for an hour. The mixture was extracted with methyl alcohol, decolourized with Darco G—60 and filtered. The filtrate was allowed to stand at room temperature for crystallization. The drak grey solid was recrystallized from ethanol-benzene to afford the light grey crystals of II (Table 1).

TABLE *1*

Analytical data of 2-trifluoroethyl-8-methoxy-7, 10-disubstituted phenothiazines

Comp.	Mol. formula of compound	M. p. (°C)	Yield (%)	Elemental Analysis*				IR data ν/cm^{-1}			
				Calc. %		Found %		(i)	(ii)	(iii)	(iv)
				N	S	N	S				
I.	$C_{17}H_{61}NO_2$ SF_3	165	70	3.94	9.01	3.89	9.07	3320	—	1065	—
II.	$C_{20}H_{19}N_2O_2$ SF_3	161	67	6.86	7.84	6.84	7.79	—	—	1070,	—
III.	$C_{20}H_{20}NO_4$ SF_3	148	55	3.28	7.49	3.34	7.53	—	1680	1085	—
IV.	$C_{20}H_{20}NO_5$ SF_3	168	65	3.16	7.22	3.18	7.30	—	1690	1060	995
V.	$C_{17}H_{14}NO_5$ SF_3	189	45	3.49	7.98	3.43	7.99	—	1675	3690	990

* Satisfactory analysis for C and H were also obtained.

** (i) ν(NH) stretch ; (ii) ν(C = O) ; (iii) peak due to 7 substitution (iv) S→0 str.

2-Trifluoromethyl-7-isopropoxy-8-methoxy phenothiazine-10-propionic acid (III)

To a well stirred solution of II (0.012 mole) in 50 ml methanol was added gradually 15 ml of 25% sodium hydroxide solution and refluxed for 15 hrs. The resulting brown suspension was poured into 150 ml of cold water and acidified with dil-HCl. The contents were extracted with ether, washed with water and dried ($MgSO_4$).

The solvent was stripped off at reduced pressure to give a brown solid. Crystallization from acetone provided light brown flakes of III (Table I).

2-Trifluoromethyl-7-isopropoxy-8-methoxy-phenothiazine-10-propionic acid-5-oxide(IV)

To a mixture of III (0.01 mole) in 40 ml ethanol and 75 ml acetone was added dropwise 30% hydrogen peroxide (6.6 ml). The mixture was refluxed gently for 5 hrs. The volume of the solution was reduced to half cooled and poured into water. The contents were extracted with ether, dried (Na_2SO_4) and concentrated to give light pink solid. Crystallization from chloroform-ethanol (1 : 1) gave shining white flakes of IV (Table I).

2-Trifluoromethyl-7-hydroxy-8-methoxy phenothiazine-10-propionic acid-5-oxide (v)

A mixture of IV (0.01 mole), ethanol (20 ml) and 100 ml hydrochloric acid was refluxed for an hour, cooled to room temperature and filtered into 300 ml cold water. The pH of the solution was adjusted to 8 with 10% sodium hydroxide solution. The pink gum was taken up in diethyl ether, dried ($MgSO_4$) and decolourized with Darco G – 60. The solvent was stripped off in vacuo and gave pale-yellow flakes of V. Recrystallized from acetone.

ACKNOWLEDGEMENT: Thanks are due to the C.S.I.R., New Delhi for awarding a Senior Fellowship to one of us (M. Anand).

REFERENCES

[1] D. Johnson and C. F. Rodriguez, *Life Science*, **5**, 1283 (1966).

[2] R. L. Young, J. J. Ross jr. and Q. R. Maass, *Nature*, **183**, 1396 (1959).

[3] E. A. Nodiff, M. Hausman and A.A. Manian, *J. Heterocyclic Chem.*, **4**, 239 (1967).

[4] P. N. Kaul and P. R. Pabrai, *Arch. Int. Pharmac. Therp.*, **206**, 325 (1973).

[5] H. L. Yale, F. Sowinski and J. Bernstein, *J. Amer. Chem. Soc.*, **79**, 4375 (1957).

[6] U. Brayer and G. Schmalzing, *Drug Metabolism and Disposition*, **5**, 97 (1977).

[7] M. I. Kelsey and E. A. Moscateeli, *J. Chromatogr.*, 85, 65 (1973).

[8] A. A. Manian, N. Watman, M. L. Steinberg and J. P. Bucly, *Life Sci.*, **7**, 731 (1968).

[9] R. L. Mital, M. Mital, A. P. Shukla, S. Mital and V. Laxmi, *Indian J. Chem.*, **15B**, 1145 (1977).

Revue Roumaine de Chimie 27, 8, 943–951 (1982)

as-TRIAZINE DERIVATIVES WITH POTENTIAL THERAPEUTIC ACTION. XVI*

SYNTHESIS OF 5(ω-CARBOXY-ALKYL) MERCAPTO-6-AZAURIDINES

C. CRISTESCU and SILVIA SITARU
Chemical-Pharmaceutical Research Institute, Sos. Vitan 112, 74351 Bucharest 3, Romania

Received July 1, 1981

5-Mercapto-6-azauracil (I) reacts in aqueous medium with ω-haloalkoxyalkyl derivatives giving 5-(ω-carbalkoxyalkyl)mercapto-6-azauracils (II). Treatment of II with hexamethyldisilazane led to 2,4-bis(trimethylsilyloxy) derivatives (III). These were condensed with 1-0-acetyl-2,3, 5-tri-0-benzoyl-D-ribofuranose in the presence of anhydrous stannic chloride to afford the corresponding blocked-nucleoside (IV). Under the action of sodium methoxide, derivatives IV were debenzoylated with the formation of the 5(ω-carboxyalkyl) mercapto-6-azauridines (VI) or 5(ω-carbalcoxyalkyl)mercapto-6-azauridines (V).

In connection with our synthetic works [1, 2] in the field of anomalous nucleosides, we describe the synthesis of nucleosides derived from 5(ω-carboxyalkyl) mercapto-6-azauracils.

The research on 5(ω-carboxyalkyl) mercapto-6-azauridines, was undertaken in an attempt to find substances with improved pharmacological and therapeutic properties as compared to 5-mercapto-6-azauracil. The study was stimulated by the assumption that the carboxyalkyl group, especially by multicarbon formation, may favourably effect the transport of a substance of this type in macroorganism, especially through the cellular membrane.

We have investigated the synthesis of these nucleosides by applying the Friedel-Crafts-catalyzed silyl Hilbert-Johnson reaction. [3,4]

5-Mercapto-6-azauracil [5] (I) reacts in aqueous medium with ω-halocarbalcoxyalkyl derivatives leading to 5(ω-carbalcoxyalkyl) mercapto-6-azauracils (IIa-c). Treatment of II with hexamethyldisilazane in the presence of traces of trimethylchlorosilane, under reflux, afforded the corresponding 2,4-bis(trimethylsilyloxy)-5(ω-carbalcoxyalkyl) mercapto-6-azauracils (IIIa –c). Condensation of III with 1-0-acetyl 1-2, 3, 5-tri-0-benzoyl-D-ribofuranose [6] in dry 1,2-dichloroethane, at room temperature, in the presence of anhydrous stannic chloride gives only the N-glycosides in 80 – 85 % yield.

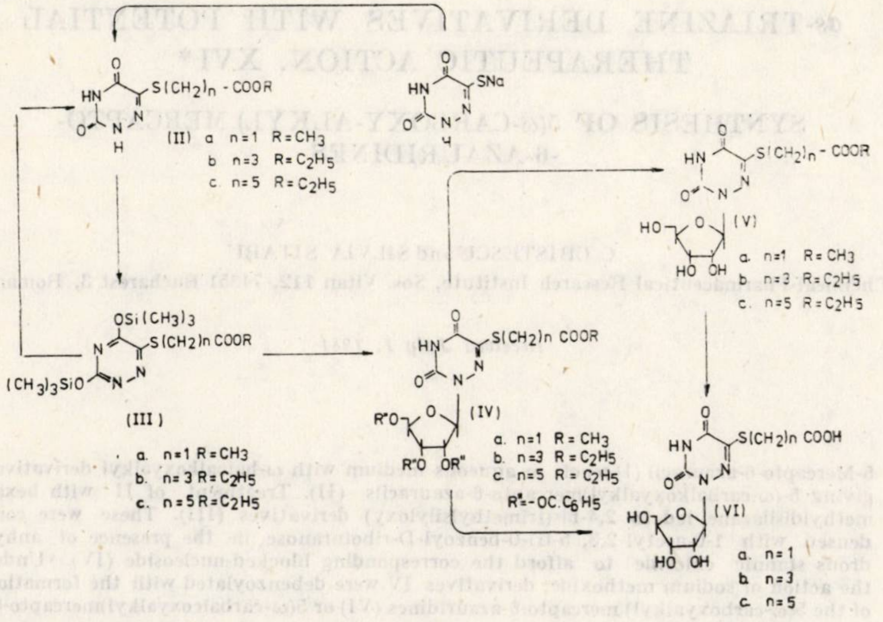

Scheme 1

The resulting blocked nucleosides (IV a – c) were deacylated by the methoxide catalyzed transesterification to yield the 5-(ω-carbalcoxyalkyl) mercapto-6-azauridines (Va-c), or 5-(ω-carboxyalkyl) mercapto-6-azauridines (VIa-c) after hydrolysis of the esters.

The assignment of carbohydrate moiety to the N-1-position of 5-substituted-6-azauracil ring is based on the fact that the nucleosides (V) or (VI) exhibit a hypsochromic shift of the absorption maximum in the ultraviolet spectrum by passing from acidic to basic media. This is a typical behaviour for N_1-substituted 6-azauracils.[7,8]

In the infrared spectrum of the tri-O-benzoyl-derivatives (IVa – c) the intense absorption of the acyl groups overlaps a considerable number of bands of the heterocyclic and the sugar parts of the molecule. As a consequence of these overlaps the spectra show fewer bands. The carbonyl groups absorb in the 1723 ± 10 cm $^{-1}$ region. The absorption bands of acyl group, linked to the ribose residue are 1260 ± 10 cm^{-1}, 1315 ± 5 cm^{-1} (C.CO) and 1090 ± 10 cm^{-1}, 1170 ± 10 cm^{-1} (CO.O), respectively. In the spectra of all tri-0-benzoyl derivatives and nucleosides (V) or (VI), three bands regularly occurred (1099, 1128 and 1237 cm^{-1}). These bands are probably due to the strong absorption of the ribose component.[9,10]

The anomeric protons of the nucleosides IV, V and VI, appear in ^{1}H – NMR spectra as a doublet at $\delta = 6.05 - 6.55$ p.p.m., with a coupling constant 2 – 3.2 Hz. The position of the signal indicated that the nucleosides may be the β-anomer by comparison with the ^1H—NMR spectra of other nucleosides of this type [11–15].

ANTITUMOR EFFECTS

The results obtained from the testing of compounds prepared in this investigation are shown partly in table 1. The testing was performed under the auspices of the National Cancer Institute, Bethesda, Maryland. The ratio (T/C) of the survival times (T) of the treated animals and the survival times of the control animals (C) is used as a measure of the effectiveness of the treatment. An increase in average survival times for six animals of 25 % (T/C, 125 %) is considered to be statistically significant of the antitumor activity for several tumor systems according to criteria used by the National Cancer Institute. [16]

TABLE 1

Screening data

Compound	Test system[b]	Dose mg/kg	Survivors	Animal wt. in g (T— C)[d]	Survival days (T/C)	T/C %
II a	LE	200	6/6	—0,7	8.3/9.0	92
		100	6/6	0.1	8.5/9.0	94
		50	6/6	—0,8	9.3/9.0	103
		25	6/6	—0.3	9.0/9.0	100
		12,5	6/6	—0.1	8.8/9.0	97
II b	LE	400	6/6	—0.8	7.7/8.8	87
		200	6/6	—1.0	8.3/9.0	92
		100	6/6	—0.4	8.2/9.0	91
		50	6/6	—0.1	8.7/9.0	96
		25	6/6	—0.2	9.2/9.0	102
		12,5	6/6	—0.2	9.0/9.0	100
II c	LE	400	6/6	—1.5	8.2/8.8	93
		200	6/6	—0.9	9.2/9.0	102
		100	6/6	—0.7	9.2/9.0	102
		50	6/6	—0.4	8.3/9.0	90
		25	6/6	0.1	9.3/9.0	103
		12.5	6/6	0.0	9.2/9.0	102
IV a	LE	200	6/6	—1.3	8.3/9.4	88
		100	6/6	—1.1	8.5/9.4	90
		50	6/6	—0.1	8.8/9.4	93
		25	6/6	—0.9	9.5/9.4	101
		12.5	6/6	—1.3	8.7/9.4	92
IV b	LE	200	6/6	—1.4	8.7/9.4	92
		100	6/6	—1.6	8.3/9.4	88
		50	6/6	—0.3	8.8/9.4	93
		25	6/6	—0.6	8.5/9.4	90
		12.5	6/6	—0.7	8.8/9.4	93

a. Only a part of the data is presented

b. LE — L 1210 Lymphoid leukemia.

c. Average weight change of test group (T) minus average weight change of control (C) animals in grams.

Table 1 (continued)

Compound	Test sistem[b]	Dose mg/kg	Survivors	Animal wt· in g (T−C)[d]	Survival days (T/C)	T/C %
IV c	LE	200	6/6	−1.9	9.8/9.1	107
		100	6/6	−1.5	9.7/9.1	106
		50	6/6	−0.2	8.7/9.1	95
		25	6/6	−0.3	9.8/9.1	107
		12.5	7/6	−0.7	9.2/9.1	101
V b	LE	400	6/6	−0.1	8.3/8.8	94
		200	6/6	−0.4	9.3/8.9	104
		100	6/6	−0.6	8.8/8.9	98
		50	6/6	0.0	9.0/8.9	101
		25	6/6	−0.2	9.0/8.9	101
		12.5	6/6	−0.2	9.0/8.9	101
V c	LE	200	6/6	−0.3	8.7/8.9	97
		100	6/6	−0.7	9.2/8.9	103
		50	6/6	−0.3	9.3/8.9	104
		25	6/6	−0.2	8.8/8.9	98
		12.5	6/6	−0.2	9.2/8.9	103
VI b	LE	200	6/6	−1.0	9.0/8.9	101
		100	6/6	−0.9	9.0/8.9	101
		50	6/6	−0.7	9.3/8.9	104
		25	6/6	−0.5	9.3/8.9	104
		12.5	6/6	−0.4	9.3/8.9	104
VI c	LE	200	6/6	−0.6	9.3/8.9	104
		100	6/6	−0.7	9.3/8.9	104
		50	6/6	−0.6	9.3/9.8	104
		25	6/6	0.0	9.3/8.9	104
		12.5	6/6	−0.2	10.0/8.9	112

From the testing data available till now it is evident that this series of compounds possesses a reduced activity as inhibitory agents in L 1210 Lymphoid Leukemia.

EXPERIMENTAL

The melting points were determined with a heating microscope plate and are not corrected. Samples for analysis and spectral measurement were dried at 30°/0.1 mm Hg, for 8 hours over P_2O_5. Paper chromatography was performed by the ascending tehnique on Schleicher & Schüll 2043 bmgl paper in the solvent systems: 1-butanol-acetic acid-water (4 : 1 : 1), A, propan 2-ol-water-conc. ammonia (16 :4 :1) B, 1-butanol-water (86 :14) C. Detection of the compounds was performed visually in ultraviolet light (254 nm) after spraying with 0.002% fluoresceine (in ethanol). Thin layer chromatography (tlc) was performed on precoated silicagel plates 60 F_{254} (Merck) in the solvent systems; benzene-ethyl acetate (7 : 3) D, benzene-methanol (9 : 1) E and benzene-methanol (1 : 1) F. The spots were detected visually in ultraviolet light (254 nm). Preparative column chromatography was performed on a LKB column of silicagel 60 (70—230 mesh ASTM) Merck, a flow-rate of 2.5 ml per minute being maintained. The fractions were collected at 10 minutes intervals. Optical rotation was measured on a Hilger-Watts automatic polarimeter. Ultraviolet spectra of products were measured on a Unicam Sp 1800 Ultraviolet Spectrophotometer. The infrared spectra were recorded with a C. Zeiss-Jena UR20 Infrared Spectrophotometer. The NMR spectra were recorded at 60 MHz on a Varian EM 360 Spectrophotometer in the indicated solvents and the chemical shifts are reported in parts per million (δ) with tetramethylsilane (TMS) or sodium 2,2-dimethyl-2-silapentane-5-sulfonate (DSS) as internal standard.

5-(1-Carbomethoxymethyl)mercapto-6-azauracial (IIa)

4.06 g (20 mM) 5-mercapto-6-azauracil sodium salt (I) was dissolved at 35°C in 50 ml water. A solution of methyl chloroacetate (2.39 g ; 22mM) in ethanol (25 ml) was added. The mixture was stirred at 70°C for 1 hour, cooled at 4°C overnight and filtered. The product was recrystallized from ethanol to yield 3.90 g (90 %) of IIa with m.p. 207—209°C. The analytical sample melted at 209—210°C (from ethanol). The following Rf values were recorded : 0.60 (A), 0.27 (B), 0.59 (C), 0.07 (D), 0.33 (E), 0.75 (F) ; $IR_{(KBr)}$; 1666, 1720 cm^{-1} $\bar{\nu}(C{=}O)$; 2926 cm^{-1} $\bar{\nu}$ as (CH_2) ; 2826 cm^{-1} $\bar{\nu}s(CH_2)$; $UV_{(Ethanol)}$ 306 nm (logε 3.81).

Calcd. $C_6H_7N_3O_4S$:C, 33.17 ; H, 3.24 ; N, 19.34 ; S, 14.76 %

Found C, 33.20 ; H,3.25 ; N, 19.41 ; S, 14.72 %

5-(3-Carbethoxypropyl)mercapto-6-azauracil (IIb)

Starting material I (2.03 g, 10 mM) was dissolved at 40°C in water (20 ml). A solution of ethyl 4-chlorobutyrate (1.5 g 10 mM) in ethanol (15 ml) was added. The mixture was stirred at 70°C for 3 hours, cooled at 4°C overnight and filtered. The product was recrystallized from ethanol to yield 2.38 g (92 %) of IIb with m.p. 202 — 203°C. The analytical sample melted at 203—204°C (from ethanol). Rf ; 0.79 (A), 0.55 (B), 0.58 (C), 0.23 (E), 0.79 (F) ; $IR_{(KBr)}$: 1673, 1713 cm^{-1} $\bar{\nu}(C{=}O)$; 2927 cm^{-1} $\bar{\nu}$ as (CH_2) ; 2800 cm^{-1} $\bar{\nu}s(CH_2)$; $UV_{(Ethanol)}$: 309 nm (logε = 3.81).

Calcd. $C_9H_{13}N_3O_4S$:C, 41.69 ; H, 5.05 ; N, 16.20 ; S, 12.36 %

Found : C, 41.80 ; H, 5.10 ;N, 16.30 ; S, 12.40 %

5(5-Carbethoxypentyl) mercapto-6-azauracil (IIc)

Starting material I (4.06 g, 20 mM) was dissolved at 40°C in water (50 ml). A solution of ethyl 6-bromocaproate (4.46 g, 20 mM) in ethanol (25 ml) was added. The mixture was stirred at 70°C for 4 hours, cooled at 4°C overnight and filtered. The product was recrystallized from ethanol to yield 5.15 g (90 %) of IIc with m.p. 192—193°C. The analytical sample melted at 193—194° (from ethanol). Rf : 0.79 (A), 0.63 (B), 0.81 (C), 0.14 (D), 0.43 (E) ; $IR_{(KBr)}$: 1691, 1717 cm^{-1} $\bar{\nu}(C = 0)$; 2945 cm^{-1} $\bar{\nu}as(CH_2)$; 2858 cm^{-1} $\bar{\nu}s(CH_2)$; $UV_{(Ethanol)}$: 312 nm (logε 3.84).

Calcd. $C_{11}H_{17}N_3O_4S$:C, 45.97 ; H, 5.96 ; N, 14.62 ; S, 11.15 % Found : C, 45.80 ; H, 5.70 ; N, 14.82 ; S, 11.25 %

5-Substituted-2,4-bis(trimethylsilyloxy)-6-azauracil (IIIa-c)

A mixture of 5-substituted-6-azauracil (IIa—c) (25 mM), hexamethyldisilazane (20 ml) and trimethylchlorosilane (1 ml) was refluxed for 2 hours, until a clear solution was obtained.

TABLE 2

5-Substituted-2, 4-bis(trimethylsilylosxy)-6-azauracil

Compd.	R	B.p., (mm)	Yield %
III-a	$-S-CH_2-COOCH_3$	170—172 (1.3)	96
III-b	$-S-(CH_2)_3-COOC_2H_5$	200—202 (1.2)	94
III-c	$-S-(CH_2)_5-COOC_2H_5$	210—212 (1.2)	96

The excess of hexamethyldisilazane was removed under vacuum at 15 mmHg and the viscous oily residue was distilled under reduced pressure to give 5-substituted-2,4-bis(trimethylsilyloxy)-6-azauracil, with the properties indicated in table 2.

1(2′ 3′,5′,-tri-0-benzoyl-β-D-ribofuranosyl)-5-(1-carbomethoxymethyl) mercapto-6-azauracil (IV a)

3.28 g (9mM) of IIIa in dry 1,2-dichloroethane (50 ml) was added to 3.62 g (7.2 mM) 1-0-acetyl-2, 3, 5-tri-0-benzoyl-D-ribofuranose, previously dissolved in 1,2-dichloroethane (150 ml). The mixture was stirred 14 hours at room temperature in the presence of anhydrous stannic chloride (1.40 g, 5.4 mM). The solution was treated with saturated sodium hydrogen carbonate aqueous solution (100 ml) and the organic phase was filtered over Celite 535, dried (sodium sulphate) and evaporated. The residue was dissolved in benzene and applied to a silicagel column (60 g). The column was washed with benzene and eluted with a mixture of benzene-ethyl acetate (9 : 1). Fractions containing the product were pooled and evaporated. The residue (4.70 g, 83 %) was chromatographically homogeneous. The following Rf values were recorded : 0.85 (A), 0.72 (B), 0.84 (C), 0.52 (D), 0.73 (E) ; $[\alpha]_D^{25}$: – 53.5° (c 2, chloroform) ; $IR_{(CHCl_3)}$; 1720cm^{-1} $\bar{\nu}$ (C=0) ; 1260, 1313 cm^{-1} $\bar{\nu}$ (C.CO) ; 1080, 1173 cm^{-1} $\bar{\nu}$(CO.O) ; 2926 cm^{-1} $\bar{\nu}$ as (CH_2) ; (2820 cm^{-1} $\bar{\nu}$s(CH_2) ; $UV_{(Ethanol)}$: 230 nm (log ε 4.69) and 304 nm (logε3.86) ; $NMR_{(CDCl_3)}$6.55 (1 H, d, $J_{1', 2'}$ = 2,4 Hz, 1$H_{1'}$).
Calcd. $C_{32}H_{27}N_3O_{11}S$:C, 58.08 ; H, 4.11 ; N, 6.35 ; S, 4.84% : Found : C, 58.12 ; H, 4.20 ; N 6.30 ; S, 4.70%

1(2,3,5,-tri-0-benzoyl-β-D-ribofuranosyl)-5(3-carbethoxypropyl)mercapto-6-azauracil (IVb)

A clear solution of 7.59 g (18.8 mM) of IIIb in dry 1,2-dichloroethane (50 ml) was added to 7.59 g (15 mM) 1-0-acetyl-2, 3, 5-tri-0-benzoyl-D-ribofuranose, previously dissolved in dry 1,2-dichloroethane (150 ml). The mixture was stirred 12 hours at room temperature in the presence of anhydrous stannic chloride (2.92 g, 11.2 mM). The solution was treated with saturated sodium hydrogen carbonate aqueous solution (100 ml) and the organic phase was filtered over Celite 535, dried on sodium sulphate and evaporated. The residue was chromatographed on a column of silicagel (120 g) with benzene and benzene-ethyl acetate (95 : 5 v/v).Fractions containing the product were combined and evaporated. The residue (8.97, g, 85%) was chromatographically homogeneous. The following Rf values were recorded 0.86 (A), 0.72 (B), 0.78 (C), 0.40 (D), 0.49 (E) ; $[\alpha]_D^{25}$:-60.6° (c2, Chloroform) ; $IR_{(CHCl_3)}$: 1700 cm^{-1} $\bar{\nu}$(C=O) ; 1243, 1313 cm^{-1} $\bar{\nu}$(C.CO) ; 1100, 1140 cm^{-1} $\bar{\nu}$(CO.O) ; 2926 cm^{-1} $\bar{\nu}$ as(CH_2) ; 2800 cm^{-1} $\bar{\nu}$ s(CH_2) ; $UV_{(Ethanol)}$: 230 nm (logε 4.64) and 304 nm (logε 3.80) ; $NMR_{(CDCl_3)}$: 6.53 (1 H, d, $J_{1',2'}$=2.66 Hz, 1 $H_{1'}$).
Calcd. $C_{35}H_{33}N_3O_{11}S$: C, 59.76 ; H, 4.72 ; N, 5.97 ; S, 4.55% ; Found : C, 59.82 ; H, 4.90 ; N, 5.92 ; S, 4.70%.

1(2′,3′,5′-tri-0-benzoyl-β-D-ribofuranosyl)-5(5-carboethoxypentyl)mercapto-6-azauracil (IVc)

A solution of 3.63 g (7.2 mM) of 1-0-acetyl-2, 3, 5-tri-0-benzoyl-D-ribofuranose in dry 1,2- dichloroethane (100 ml) was added to a clear solution of 3.92 g (9 mM) of IIIc in dry 1,2-dichloroethane (100 ml). The mixture was stirred at room temperature for 16 hours in the presence of anhydrous stannic chloride (1.4 g, 5.4 mM). The solution was treated with saturated sodium hydrogen carbonate aqueous solution and the organic phase was filtered over Celite 535 and dried (sodium sulphate). The solvent was evaporated in vacuum and the residue was passed through a column of silicagel (60 g) packed in benzene and eluted with benzene and benzene-ethyl acetate (95 : 5 v/v). The major, UV and sugar positive fractions were collected and the solvent was evaporated in vacuum to give 4.84 g (85%) of the pure product IVc as a foam. The following Rf values were recorded : 0.90 (A), 0.77 (B), 0.89 (C), 0.58 (D), 0.77 (E) ; $[\alpha]_D^{25}$; – 55.8°C (c 1, chloroform) ; $IR_{(CHCl_3)}$: 1733 cm^{-1} $\bar{\nu}$(C=0) ; 1274, 1320 cm^{-1} $\bar{\nu}$ (C.CO) ; 1095, 1183 cm^{-1} $\bar{\nu}$(CO.O) ; (2945 cm^{-1} $\bar{\nu}$ as $(CH)_2$; 2860 cm^{-1} $\bar{\nu}$s CH_2) ; $UV_{(Ethanol)}$: 230 nm (logε4.80) and 304 nm (logε 3.70) ; ^1H — $NMR_{(CHCl_3)}$: 6.19 (1 H, d, $J_{1', 2'}$ = 2.5 Hz, 1 $H_{1'}$).
Calcd. $C_{37}H_{37}N_3O_{11}S$: C, 60.70 ; H, 5.09 ; N, 5.76 ; S, 4.38% Found : C, 60.80 ; H, 5.15 ; N, 5.42 ; S, 4.22%

5(1-Carbomethoxymethyl)mercapto-6-azauridin (Va)

A mixture of the protected nucleoside IVa (1 g, 1,5 mM) 0.1 N sodium methoxide (15 ml) and dry methanol (55 ml), was stirred at reflux for 1 hour. The clear solution was treated at room temperature whit DOWEX 50W ×8 (H^+) at pH 4.5–5, filtered and evaporated in vacuum. The resulting oil was treated with water (50 ml) and extracted with ethyl acetate-ether (2 : 1 v/v). The aqueous layer was evaporated in vacuum (40°C) and the residue crystallized from water. Yield 0.48 g (92%) of compound V-a, mp 160–162°C ; Rf 0.35 (A), 0.28 (B), 0.04 (C), 0.61 (F) ; $[\alpha]_D^{25}$: $-20.7°$ (c5, water) ; $IR_{(KBr)}$: 1720 cm^{-1} $\bar{\nu}(C{=}O$;) 2926cm^{-1} $\bar{\nu}as(CH_2)$; 2800 cm^{-1} $\bar{\nu}s(CH_2)$; UV : $\lambda_{max.(0.1N\ hdrochloric\ acid)}$ 306 nm (logε3.80) ; $\lambda_{max.(0.1\,N\ sodium\ hydroxide)}$ 302 nm (logε 3.71) ; $^1H-NMR_{(D_2O,\ DSS)}$: 6.11 (1 H, d, $J_{1,2} = 2$ Hz, $1H_{1'}$).

Calcd. $C_{11}H_{15}N_3O_8S$: C, 37.84 ; H, 4.32 ; N, 12.02 ; S, 9.17% Found : C, 37.86 ; H, 4.30 ; N, 12.06 ; S, 9.21%

5(3-Carbethoxypropyl)mercapto-6-azauridin(Vb)

A mixture of IVb (2.11 g, 3 mM), 0.1 N sodium methoxide (30 ml) and dry methanol (50 ml) was stirred 1 hour at reflux. The clear solution was treated, at room temperature, with DOWEX 50W × 8 (H^+) at pH 5, filtered and evaporated in vacuum. The oil residue was dissolved in water (70 ml) and extracted with ethyl acetate-ether (2 : 1 v/v). The aqueous layer was evaporated in vacuo at 40°C. The residue was crystallized from water, yielding 1.03 g (88%) of product V-b with m.p. 74 – 75°C ; Rf 0.50 (A), 0.39 (B), 0.18 (C), 0.67 (F) ; $[\alpha]_D^{25}$: -11.2°C (c 1.95, water) ; $IR_{(KBr)}$: 1733 cm^{-1} $\bar{\nu}(C{=}O)$; 2926 $cm^{-1}\bar{\nu}as(CH_2)$; 2800 $cm^{-1}\bar{\nu}s\ (CH_2)$ UV : $\lambda_{max.(0.1N\ hydrochloric\ acid)}$ 314 nm (logε 3.82) ; $\lambda_{max.\ (sodium\ hydroxide)}$ 304 nm (log ε 3.74) ; $^1H-NMR_{(D_2O,\ DSS)}$: 6.20 (1 H, d, $J_{1,2} = 3$ Hz, 1 $H_{1'}$).

Calcd. $C_{14}H_{21}N_3O_8S$: C, 42.96 ; H, 5.40 ; N, 10.73 ; S, 8.19% Found : C, 42.92 ; H, 5.43 ; N, 10.78 ; S, 8.21%

5(5-Carbetoxypentyl)mercapto-6-azauridin(Vc)

This compound was obtained starting from IVc (1.5 mM) and following exactly the procedure reported for the synthesis of compounds Va and Vb described above. The product Vc was crystallized from water to give a pure crystalline compound in 89% yield, with m.p. 119–120°C. The following Rf values were recorded 0.59 (A), 0.53 (B), 0.50 (C), 0.59 (F) ; $[\alpha]_D^{25}$: -10.8°C (c 1, water) ; $IR_{(KBr)}$: 1700 cm^{-1} $\bar{\nu}$ (C=O), 2930 cm^{-1} $\bar{\nu}as\ (CH_2)$; 2853 cm^{-1} $\bar{\nu}s\ (CH_2)$; UV : $\lambda_{max.(0.1N\ hydrochloric\ acid)}$ 314 . nm (log ε 3.81) ; $\lambda_{max.\ (0.1N\ sodium\ hydroxide)}$ 304 nm (log ε 3.73) ; $NMR_{(D_2O,DSS)}$: 6.11 (1 H, d, $J_{1',\,2'} = 2.0$ Hz, 1 $H_{1'}$).

Calcd. : $C_{16}H_{25}N_3O_8S$: C, 45.85 ; H, 6.00 ; N, 10.01 ; S, 7.64% Found : C, 45.85 ; H, 5.97 ; N, 10.05 ; S, 7.69%

5(1-Carboxymethyl) mercapto-6-azauridin (VIa)

METHOD 1

A mixture of the blocked nucleoside IVa (1 g, 1.5 mM), 1 N sodium methoxide (3 ml) and dry methanol (50 ml), was stirred at reflux 1 hour. The solvent was evaporated in vacuum and the resulting oil was dissolved in water (25 ml) and extracted with ethyl acetate-ether (2 : 1 v/v). The aqueous layer was corrected to pH 12 with sodium hydroxide and allowed to stand at room temperature with occasional stirring for 3 hours. The alkaline solution was treated with DOWEX 50W×8(H^+) at pH2, filtered and evaporated *in vacuo*. The residue crystallised from ethanol yielded 0.452 g (90%) of compound VIa with m.p. 223–224°C, Rf 0.21 (A), 0.09 (B), 0.01 (C), 0.18 (F) ; $[\alpha]_D^{25}$: -26.8°C (c5, water) ; $IR_{(KBr)}$: 1665, 1700 cm^{-1} $\bar{\nu}(CO)$; 2920 cm^{-1} $\bar{\nu}$ as(CH_2) ; 2826 cm^{-1} $\bar{\nu}s(CH_2)$; UV : $\lambda_{max.(0.1\ N\ hydrochloric\ acid)}$ 309 nm (log ε 3.74) ; $\lambda_{max.(0.1N\ sodium\ hydroxide)}$ 298 nm (logε 3.68) ; $NMR_{(D_2O,\ DSS)}$: 6.05(1 H, d, $J_{1',2'} = 3.25$ Hz, $1H_{1'}$).

Calcd. $C_{10}H_{13}N_3O_8S$: C, 35.82 ; H, 3.90 ; N, 12.53 ; S, 9. 56% Found : C, 35.88 ; H, 3.95 ; N, 12.60 ; S, 9.50%

METHOD 2

Nucleoside Va (0.1 g) was dissolved in water (10 ml) and 1 N sodium hydroxide was added at pH 12. The mixture was allowed to stand at room temperature for 3 hours. The alkaline solution was treated with DOWEX 50W × 8 (H^+) at pH 2, filtered, evaporated in vacuum and the residue crystallised from ethanol. Yield 0.088 g (92%) of compound VIa, with m.p. 223–224°C, without depression on admixture with the product prepared by method 1. The infrared and ultraviolet spectra, tlc and paper chromatography of the two samples were identical.

5(3-Carboxypropyl)mercapto 6-azauridin(VIb)

A mixture of the blocked nucleoside IVb (2.11 g ; 3 mM) ; dry methanol (50 ml) and 1 N sodium methoxide (6 ml), was stirred at reflux 1 hour. The solvent was evaporated *in vacuo* and the resulting oil was dissolved in water (50 ml) and extracted with ethyl acetate-ether (2 : 1 v/v). The aqueous layer was corrected to pH 12 with sodium hydroxide and allowed to stand at room temperature for 3 hours. The alkaline solution was treated with DOWEX 50W × 8 (H^+) at pH 2, filtered and evaporated in vacuum. The residue crystallised from 2-propanol. Yield 0.93 g (88 %) of compound VIb with m.p. 140–141°C. The following Rf values were recorded 0.38 (A), 0.13 (B), 0.02 (C), 0.34 (F) ; $[\alpha]_D^{25}$: − 10.3°C (c 1.95, water) ; $IR_{(KBr)}$: 1700 cm^{-1} $\bar{\nu}(CO)$; 2930 cm^{-1} $\bar{\nu}as\ (CH_2)$; 2800cm^{-1} $\bar{\nu}s(CH_2)$; UV : $\lambda_{max.(0.1N\ hydrochloric\ acid)}$ 314 nm (log ε3.80) ; $\lambda_{(max.0.1N\ sodium\ hydroxyde)}$ 304 nm (log ε 3.72) ;

$^1H-NMR_{(D_2O,\ DSS)}$;6.2 (1 H, d, $J_{1',\,2'}$ = 3 Hz, 1 H_1).

Calcd. $C_{12}H_{17}N_3O_8S$: C, 39.66 ; H, 4.71 ; N, 11.56 ; S, 8.82% Found : C, 39.62 ; H, 4.78 ; N, 11.54 ; S, 8.80%

5(5-Carboxypentyl)mercapto-6-azauridian (VIc)

This compound was obtained starting from IVc or Vc (1.5 mM) and following exactly the procedure reported for the synthesis of compounds VIa and VIb described above. The product VIc was crystallised from 2-propanol to give a pure crystalline compound in 85% yield with m.p. 142–143°C; Rf. 0.51 (A), 0.19 (B), 0.18(C), 0.34 (F); $[\alpha]_D^{25}$: − 19.2°C (c 1, water); $IR_{(KBr)}$: 1700 cm^{-1} $\bar{\nu}(CO)$; 2926 cm^{-1} $\bar{\nu}as\ (CH_2)$; 2853 cm^{-1} $\bar{\nu}s\ (CH_2)$; UV: $\lambda_{max.(0.1N\ hydrochloric\ acid)}$ 314 nm (logε3.72) ; $\lambda_{max.(0.1\ N\ sodium\ hydroxide)}$ 300 nm (log ε 3.73)

$^1H-NMR_{(D_2O,DSS)}$ 6.13 (1 H, d, $J_{1',2'}$ = 3.1Hz ; $1H_{1'}$).

Calcd. $C_{14}H_{27}N_3O_8S$: C, 42.96 ; H, 5.40 ; N, 10.73 ; S, 8.19% Found : C, 43.10 ; H, 5.30 ; N, 10.80 ; S, 8.25%

ACKNOWLEDGEMENT. The authors gratefully acknowledge the help of National Cancer Institute, Bethesda, Md, USA, for antitumor screening data, Mrs. Chem. Veronica Vişan of the Analytical Department of our Institute for recording the IR and UV spectra, Mrs. Pharm. Cornelia Ioan for elemental analyses and Dr. D. Ionescu for NMR spectra.

REFERENCES

* Part XV, C. Cristescu, *Monatsh.* **108**, 1455 (1977).

[1] C. Cristescu, *Rev. Roumaine Chim.*, **20**, 1287 (1975).

[2] C. Cristescu and S. Sitaru, Unpublished results.

[3] U. Niedbala and H. Vorbrüggen, *Angew. Chem. Internat. Edit.*, **9**, 461 (1970).

[4] U. Niedbala and H. Vorbrüggen, *J. Org. Chem.*, **39**, 3654 (1974).

[5] C. Cristescu and J. Marcus, *Pharmazie*, **16**, 135 (1961).

[6] E. F. Recondo and R. Rinderknecht, *Helv. Chem. Acta.*, **42**, 1171 (1959).

[7] J. Johnas and J. Gut, *Coll. Czech. Chem. Comm.*, **26**, 2155 (1961).

[8] K. V. Zee-Cheng and C. C. Cheng, *J. Org. Chem.*, **27**, 976 (1962).

[9] C. L. Angell, *J. Chem. Soc.*, **1961**, 504.

[10] J. Pitha and J. Zemlika, *Coll. Czech. Chem. Comm.*, **29**, 410 (1964).

[11] J. Beranek, *Coll Czech. Chem. Comm.*, **34**, 618 (1969).

[12] M. P. Sweizer E. B. Banta, J. T. Witkowsky and R. K. Robins, *J. Amer. Chem. Soc.*, **95**, 3770 (1973).

[13] D. J. Wood, F. E. Hruska, R. Mynott and R. H. Sarma, *Canad. J. Chem.*, **51**, 2571 (1973).

[14] J. D. Stewens and H. G. Fletcher, *J. Org. Chem.*, **33**, 1799 (1968).

[15] F. E. Hruska, A. A. Grey and I. C. Smith, *J. Amer. Chem. Soc.*, **92**, 4088 (1970).

[16] Instruction Booklet 14 "Screening Data Summary Interpretation and Outline of Current Screen", Drug Evaluation Branch, Division of Cancer Treatment, National Cancer Institutue, Bethesda, Md., 1979.

Revue Roumaine de Chimie 27, 8, 953–961 (1982)

UMLAGERUNGEN IN $(CH)_7^+$-CARBOKATIONEN

M. W. TAUSCH und P. J. PLATH
Forschungsgruppe „Angewandte Katalyse"
Universität Bremen
Bibliothekstraße, NW 2
D-2800 Bremen 33

Eingegangenam 25 März 1981

Die kontinuierliche Negation des Graphen, der den Zusammenhang in einem chemischen System abbildet durch sein Komplement bezüglich des vollständigen Graphen wird herangezogen, um die topologischen Verwandtschaftgrade in einigen ausgewählten kationischen 7-Zentrensystemen zu definieren und zu berechnen. Diese gestatten es, topologisch begünstigte Valenzisomerisierungen zwischen den untersuchten Kationen vorauszusagen. Die Neigung der $(CH)_7^+$-Systeme zur monocyclischen Bindungsdelokalisation wird modelltheoretisch begründet.

The continual negation of the graph, which represents the connectivity of a chemical system by its complement to the complete graph is used both to define and calculate the topological degrees of relationship in several selected cationic 7-membered-systems. This allows for predictions to be made concerning the topologically favoured valenceisomerisations of the investigated cations. The tendency of $(CH)_7^+$-systems to the monocyclic bond-delocalisation is theoretically established.

1. EINFÜHRUNG

Seit dem ersten Nachweis eines Tropyliumsalzes im Jahre 1954 [1a] wurde in einer Vielzahl von Arbeiten über die aromatischen Eigenschaften des $(CH)_7^+$ Ringes berichtet. [1b,1c] Das Tropyliumkation existiert in Lösung weitgehend „frei", denn NMR-Messungen [2] lassen darauf schließen, daß es keine Assoziationseffekte mit dem Gegenion, wohl aber Wechselwirkungen mit dem Lösungsmittel gibt. Seine besondere Stabilität wird dadurch dokumentiert, daß alle anderen $(CH)_7^+$ Ionen, egal aus welchen Praecursoren sie erzeugt werden, letztlich die Struktur des Tropylium-Ions annehmen. [3,4] Balaban und Rouvray zeigten vor kurzem, [5] daß in organischen Kationen mit delokalisierten Bindungen die kreisförmige Struktur keineswegs notwendigerweise die günstigste ist. Eine Analyse der $(CH)_7^+$ — Kationen auf topologischer Basis soll nun zeigen, warum und wie sich die Valenzisomeren des Tropyliums gegenseitig ineinander umlagern und wie aus der Sicht unseres Modells die besondere Stabilität des $(CH)_7^+$ Ringes zu begründen ist.

2. ANMERKUNGEN ZUM MODELL

Gerüstumlagerungen in Carboniumionen wurden bisher hauptsächlich durch 1,2-Bindungsverschiebungen des Wagner-Meerwein Typs beschrieben.[1b, 6] Es gibt aber auch Fälle, wo sie als pericyclische, den Woodward-Hoffmann Regeln gehorchende Prozesse beschrieben werden.[1c,7]

Die chemische Reaktion als einen quasiadiabatischen Übergang[8] von der Potentialhyperfläche des Edukts auf die des Produkts auffassend, verzichten wir in unserem Modell[9] darauf, der Reaktion einen bestimmten Weg, etwa den über einen pericyclischen Zustand, aufzuzwingen. Das Neue zu allen bisherigen Modellen besteht in der Hypothese, daß bei einer konzertierten Valenzisomerisierung alle Zentren des reagierenden Systems paarweise miteinander in Wechselwirkung stehen. Für den Übergangszustand der Valenzisomerisierung zwischen Dewar-Benzol und Benzol ist demnach nicht die pericyclische Struktur C_4 relevant, sondern eine Struktur des Typs G_E^* (oder G_P^*) mit der ihr zugeordneten Matrix[9,10]: Das tragende Gerüst im *Konnektivitätsgraphen* G_E^* ist offensichtlich isomorph[11] mit dem „ σ-Gerüst'' im Dewar-Benzol, hat aber in unserem Modell einen dynamischen Charakter :

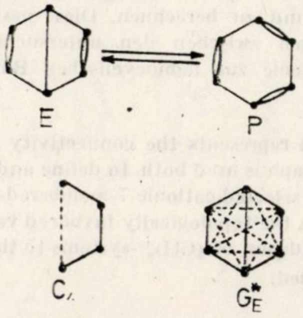

$$\begin{bmatrix} 0 & (\frac{1}{1})^R & (\frac{1}{2})^R & (\frac{1}{1})^R & (\frac{1}{2})^R & (\frac{1}{1})^R \\ (\frac{1}{1})^R & 0 & (\frac{1}{1})^R & (\frac{1}{2})^R & (\frac{1}{3})^R & (\frac{1}{2})^R \\ (\frac{1}{2})^R & (\frac{1}{1})^R & 0 & (\frac{1}{1})^R & (\frac{1}{2})^R & (\frac{1}{3})^R \\ (\frac{1}{1})^R & (\frac{1}{2})^R & (\frac{1}{1})^R & 0 & (\frac{1}{1})^R & (\frac{1}{2})^R \\ (\frac{1}{2})^R & (\frac{1}{3})^R & (\frac{1}{2})^R & (\frac{1}{1})^R & 0 & (\frac{1}{1})^R \\ (\frac{1}{1})^R & (\frac{1}{2})^R & (\frac{1}{3})^R & (\frac{1}{2})^R & (\frac{1}{1})^R & 0 \end{bmatrix}$$

Konnektivitätsmatrix $\underline{\underline{R}}$

Wenn man bei der oben genannten Reaktion alle Valenzstrichformeln, die sich für das Edukt und Produkt schreiben lassen, als Graphen A_i $(i = 1, 2, \ldots, k)$ mit Doppelkanten darstellt, so ergibt die Kantenvereinigung[12] aller dieser Graphen (zu denen auch A_E und A_P gehören) den *Molekülreaktionsgraphen* M.[12, 13, 14] Bei der hier betrachteten Valenzisomerisierung gibt es einige Bindungen, die in allen möglichen Valenzstrichformeln des Edukts und des Produkts vorkommen. Diese bilden den

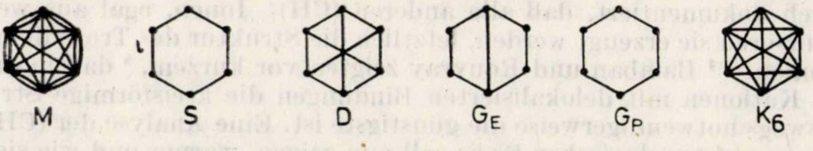

unveränderlichen Teil bei dem Umlagerungsprozeß und sind im *statischen Graphen S* abgebildet. Die restlichen Kanten aus M stellen Bindungen dar, die nur in ganz bestimmten Edukt- oder Produktformeln auftreten. Sie bilden den veränderlichen Teil bei der Umlagerung und konstituieren den *dynamischen Graphen D*.[13, 14] Mit der Annahme, daß jede Struktur A_i zeitlich realisierbar ist (die Valenzstrichformel drückt eine aktualisierbare Eigenschaft des chemischen Systems aus), können aus D durch Kantenschnitt mit den Graphen A_i k Unterstrukturen gebildet werden, die einen

„dynamischen Charakter" haben. Im obigen Beispiel erhält man auf diese Weise nur zwei nichtisomorphe *Teilgraphen* G_E *und* G_P *des dynamischen Graphen* D, die aber in ihrer Bedeutung nichts mit dem „starren σ-Gerüst" zu tun haben. Eine dynamische Teilstruktur wie G_E oder G_P tritt bei einer konzertierten Reaktion als zeiltich realisierbare Grenzsituation von G_E^* (bzw. G_P^*) bei dem Parameterwert $R \rightarrow \infty$ auf [9]. Für den anderen Grenzwert des Parameters ($R = 0$) ist die Situation des K_6 erreicht. In der Situation, in der der vollständige Graph das System beschreibt, ist die Wirkung von G_E auf das Reaktionsgeschehen gänzlich ausgelöscht und zwar dadurch, daβ das Komplement [10] von G_E jetzt den gleichen Anteil an der Reaktion hat wie G_E selbst. Die Afirmation (G_E) und deren Negation (G_E) sind also in ihren Gewichten gleich. Selbst wenn diesem Zustand eine maximale Informationsentropie entspricht [16], ist er seiner Nichtplättbarkeit wegen sehr unwahrscheinlich. Dem Streben nach maximaler Informationsentropie der molekularen Struktur wirkt die mit kleiner werdendem Wert R verbundene Erhöhung der Dimension des graphentheoretischen Fractals [17] entgegen. Ehe G_E^* mit kleiner werdendem R die maximale Informationsentropie erreicht hat, weicht es in die Struktur G_P^* aus oder „fällt" in seine alte Struktur zurück, beginnt also zu fluktuieren.

Die Leichtigkeit, mit der allgemein ein Übergang $G_1 \rightleftarrows G_2$ stattfindet, ist daran zu messen, wie weit eine dieser beiden Strukturen, als Konnektivitätsgraph G_1^* bzw. G_2^* dargestellt, in Richtung K_n gehen muß, um in eine Situation zu kommen, aus der sie mit gleichen Chancen in G_1 oder G_2 „zurückfallen" kann. Die Länge dieses Weges wird durch den Parameter R beschrieben (je größer R, desto kürzer der Weg). Die Übergangssituation ist dann erreicht, wenn die Summen der Eigenwertdifferenzen zwischen G_1^* (oder G_2^*) und G_1 bzw. G_2 gleich sind. Das entspricht der in Abbildung 1 mit $R_{1,2}$ gekennzeichneten Situation. Vergleicht man Konnektivitätsgraphen verschiedener dynamischer Teilgraphen mit einem ganzen Satz von einfachen, zusammenhängenden Graphen (die als dynamische Teilstrukturen chemischer Systeme in Frage kommen), wobei für alle diese Graphen gilt : $G_i \subset K_n$, so läßt sich anhand des Kreuzungsverhaltens der Kurven „$G_i^* - G_j$" (s. Abb. 1) auf die *topologischen Verwandtschaftsverhältnisse* der untersuchten Strukturen schließen.

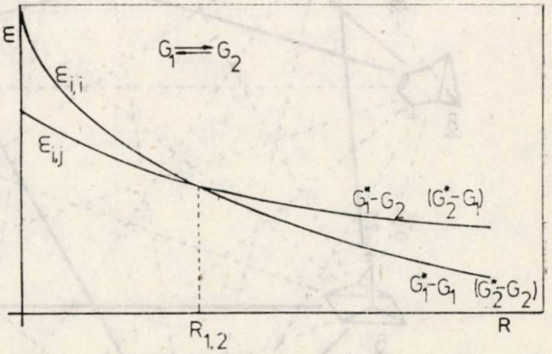

Abb. 1. — Übergangssituation im Modell des Konnektivitätsgraphen

3. ERGEBNISSE FÜR (CH)$_7^+$-SYSTEME

Von den 18 möglichen (CH)$_7^+$-Kationen [18] wurden zunächst die 8 aus Abbildung 2 betrachtet, die entweder schon als relativ beständige Systeme nachgewiesen oder als Zwischenstufen bei deren Umlagerungen in Betracht gezogen worden sind[1c, 4, 16]. Das Kation **5** interessierte wegen der dafür vorausgesagten Automerisierungsmöglichkeit. Obwohl es sich bei **7** nicht um ein $(CH)_7^+$-System handelt, wurde es in die Analyse mit einbezogen, weil die Umlagerung $\mathbf{7} \rightarrow \mathbf{1}$ experimentell bekannt ist und theoretisch bereits untersucht wurde.[19]

Die Carbokationen **1** – **9** (s. Abb. 2) wurden durch ihre entsprechenden Teilgraphen G_i (isomorph zu den σ-Gerüsten) und den dazugehörigen Konnektivitätsgraphen G_i^* dargestellt. Für die Konnektivitätsgraphen wurden die Eigenwertspektren zwischen $R = 15$ und $R = 0$ (Schrittweite 0,2) berechnet. Jedem dieser R-Werte entsprechend wurden die „Spektrendifferenzen $G_i^* - G_j$ „zwischen dem entsprechenden Konnektivitätsgraphen G_i^* und allen neun dynamischen Teilgraphen G_j wie folgt bestimmt:

$$\varepsilon_{ij} = G_i^* - G_j = \frac{1}{7} \sum_{k=1}^{7} | x_{i,k}(R) - x_{j,k}(\infty) | \qquad \text{für } j = 1,2, \ldots, 9 \quad i = 1,2, \ldots, 9$$

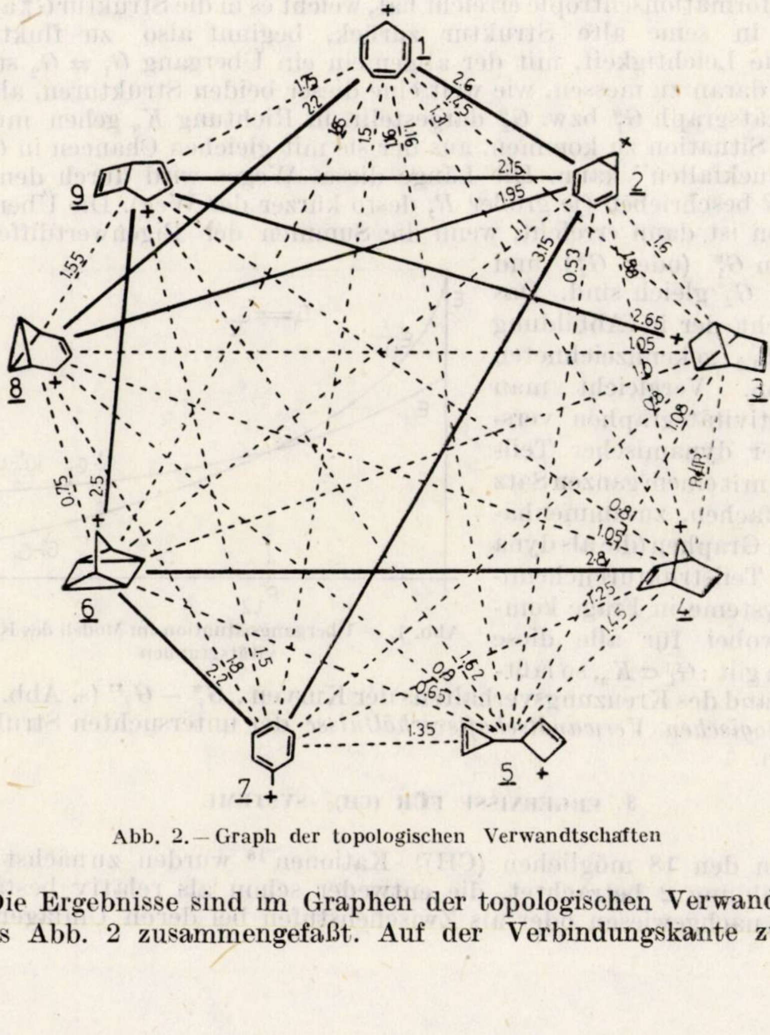

Abb. 2. – Graph der topologischen Verwandtschaften

Die Ergebnisse sind im Graphen der topologischen Verwandtschaften aus Abb. 2 zusammengefaßt. Auf der Verbindungskante zwischen zwei Ionen i und j steht jeweils der R-Wert, bei dem entweder G_i^* oder G_j^* gleichstark von G_i und G_j abweicht, d.h. $\varepsilon_{i,i} = \varepsilon_{i,j}$ oder $\varepsilon_{j,j} = \varepsilon_{j,i}$.

Die energetische Situation der betrachteten Kationen im Grundzustand kann durch ΔS-Werte [20] charakterisiert werden. Diese geben an, um wieviel die Energie eines Systems im Grundzustand der Struktur $G_i^*(R)$ günstiger ist, als die des Systems im „Grundzustand" von K_7 wäre :

$$\Delta S_i = \frac{1}{7}\left[\sum_{j=1}^{3} 2\cdot x_{i,j}(R) - \sum_{j=1}^{3} 2\cdot x_{K,j}\right]$$

j : Laufindex für die ersten drei Eigenwerte

i : bezieht sich auf den Konnektivitätsgraphen G_i^*

K : bezieht sich auf K_7

Unsere ΔS-Werte haben analoge Bedeutung wie die Delokalisationsenergie in der HMO-Interpretation [21] und korrelieren linear mit den topologischen Resonanzenergien. [22] Für einige Werte des Parameters R sind die Abweichungen ΔS in der Tabelle 1 zusammengefaßt :

TABELLE 1

ΔS-Abweichungen bei unterschiedlichen R-Werten

	1	**3**	**4**	**9**	**5**	**2**	**6**	**8**	**7**
$\Delta S(\mathrm{R} \to \infty)$	0.141	0.122	0.098	0.129	0.099	0.237	0.321	0.321	0.103
$\Delta S(R = 5)$	0.149	0.121	0.101	0.133	0.096	0.238	0.311	0.318	0.108
$\Delta S(R = 3{,}5)$	0.159	0.120	0.103	0.137	0.092	0.237	0.292	0.314	0.114
$\Delta S(R = 2)$	0.170	0.110	0.102	0.136	0.076	0.223	0.240	0.285	0.121
$\Delta S(R = 1)$	0.145	0.083	0.083	0.111	0.051	0.172	0.165	0.213	0.104

4. DISKUSSION DER ERGEBNISSE

a. Topologische Verwandtschaften und konzertierte Übergänge in $(CH)_7^+$ - Kationen

Der topologische Verwandtschaftsgrad zweier Strukturen ist in Abb. 2 durch die Zahl auf der entsprechenden Verbindungskante charakterisiert. Zur leichten Übersicht wurden die näher verwandten Strukturen mit fetten Linien verbunden. Dem Prinzip der minimalen Strukturveränderung folgend, müßte ein konzertierter Übergang zwischen zwei Strukturen umso leichter stattfinden, je größer der topologische Verwandtschaftsgrad zwischen ihnen ist. Unter diesem Aspekt liefert die Abbildung 2 folgende Aussagen :

1. Das Cyclopropenyl-Cyclobuteniumion **5** hat keine „nähere Verwandte", sollte also nur schwer konzertiert in eine andere der hier untersuchten Strukturen übergehen. Es sollte daher bevorzugt entartete Umla-

gerungen (Automerisierungen) geben, bei denen die dynamischen Teilgraphen des Edukts und des Produkts isomorph sind. Chemisch bedeutet das eine Eerhaltung der Struktur, aber eine Vermischung der C-Atome. Balaban[6] hat für **5** auch schon die Automerisierungsmöglichkeit vorausgesagt, aber experimentell konnte das sehr instabile Ion **5** (s. weiter) noch nicht nachgewiesen werden.

2. Die Umlagerung des Benzyl-Kations **7** in das Tropylium-Kation **1** kann leicht, aber nicht konzertiert, über das Norcaradienyl-Kation **2** ablaufen :

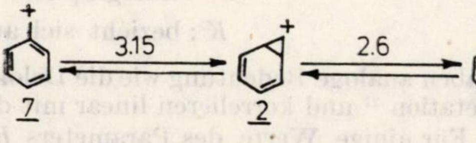

Es ist schon länger bekannt [23], daß in den Massenspektren von C_7H_8-Kohlenwasserstoffen ein Peak bei $m/e = 91$ auftritt, der dem $(C_7H_7)^+$ zugeordnet wurde. Unter den drastischen Bedingungen des Massenspektrometers nehmen die aus verschiedenen Vorgängern (Toluol, Norbornadien) primär entstandenen Kationen sehr schnell die Struktur von **1** an[24]. Nach unseren Ergebnissen (s. Abb. 2) gibt es für das Norbornadienyl-Kation **4** zwei Möglichkeiten, um in Vierstufenprozessen in **1** überzugehen. Jeder dieser beiden Wege beinhaltet das Ion **2** als direkte Vorstufe von **1**. Durch Eichung unserer ΔS-Einheiten mit der experimentellen Delokalisationsenergie des Benzols [20] (35.9 kcal/mol) und Anwendung auf die $(CH)_7^+$-Kationen, erhalten wir für die Exothermiziztät des Prozesses **7 → 1** einen Wert von -8.06 kcal/mol und für die Umlagerung **4 → 1** -9.12 kcal/mol. Experimentelle Daten [25] für die Umlagerung des Benzyl-Kations in das Tropylium-Kation lassen auf $\Delta H = -7$ kcal/mol schließen. MINDO/3 Berechnungen von Dewer et al. [19] deuten bei der Umlagerung **7→1** ebenfalls auf eine Favorisierung des Reaktionsweges über die Zwischenstufe **2** hin, aber die Gesamtreaktion müßte ihren Berechnungen zufolge sehr viel exothermer (-24.8 kcal/mol) sein.

3. Die Kationen **4** (Norbornadienyl), **6** (Quadricyclyl), **2** (Bicyclo [3.2.0]-heptadienyl) und **3** (Tricyclo [3.2.0.0.] – heptenyl) weisen enge topologische Verwandtschaften auf. Folgende (fett markierte) Umlagerungen sollten daher leicht und konzertiert stattfinden :

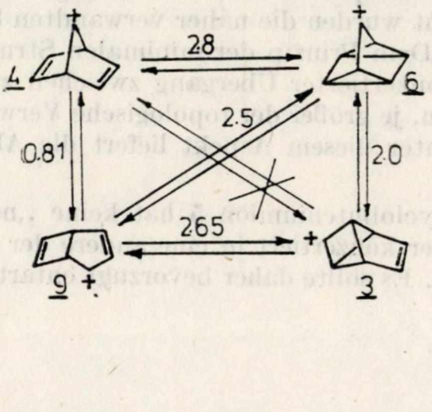

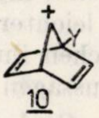

Die Bevorzugung dieser Gerüstumlagerungen ist sowohl für die $(CH)_7^+$-Kationen selbst, als auch für die entsprechenden Ketone (Norbornadienon, etc.) experimentell bekannt. [3, 4, 26, 27] Einigermaßen stabil sollten unter diesen vier Ionen nur **4** und **9** sein (vergl. Begründung im folgenden Teil dieser Arbeit). Bei der Erzeugung der Kationen **4**, **6** und **9** aus den entsprechenden Alkoholen konnten zwischen -150^0 und -50^0C tatsächlich nur **4** und **9** NMR-spektroskopisch identifiziert werden, [4, 26] aber gleichzeitig wird eine sehr große Beweglichkeit im Norbornadienyl-Kation beobachtet: außer „bridge flipping" finden auch zwei tiefgreifende Umlagerungen statt, bei denen der Substituent Y in **10** nicht nur auf dem Fünferring (1, 2, 3, 4, 5), sondern auch auf allen 7C-Atomen des C-Gerüstes „herumklettert". Beide Umlagerungen sind entartet, denn das Norbornadiengerüst bleibt erhalten. Das Verhalten verschiedener Y-substituierter Kationen, die aus den Vorgängern von **4** und **9** erzeugt wurden, spricht dafür, daß die entartete Gerüstumlagerung von **4** nicht konzertiert, sondern über **9** als Zwischenstufe verläuft. Aufgrund unserer Ergebnisse müssen wir hinzufügen, daß in dieser nicht-konzertierten Art auch **6**, **9** und **3** fluktuieren müssen (für **9** wurde schon Fluktuationsmöglichkeit vorausgesagt [6]), und daß der Übergang **4**→**9** sehr unwahrscheinlich konzertiert abläuft (s. Abb. 2 und obiges Schema). Die Zwischenstufe zwischen **4** und **9** kann eine Struktur sein, deren Konnektivitätsgraph das Grundgerüst des Quadricyclyl-Kations **6** hat. Da die „long life" Bedingungen der hier diskutierten Ionen so extrem sind (sehr tiefe Temperaturen), werden bei Gerüstumlagerungen oberhalb $-50°$C und erst recht bei positiven Temperaturen die Zwischenstufen nicht-konzertierter Reaktionen durch die dann konkurrierenden konzertierten Prozesse verwischt.

4. Die Umlagerungen des instabilen Gerüstes **3**, die zu den Gerüsten aus **4** und **9** führen, [26,27,28] sollten nicht-konzertiert mit **1** als erster Zwischenstufe ablaufen. Hierzu gibt es noch keine detaillierten Experimentaldaten [26].

5. Das Quadricyclyl-Kation **6** konnte in Lösung noch nie nachgewiesen werden, weil es sich sofort in die topologisch verwandeten Ionen **4** und **9** umlagert [4] (s. Abb. 2). Auch das Quadricyclanon zeigt entsprechende Gerüstumlagerungen. [27,28] Die von Prinzbach et all. [27] beobachtete Umlagerung des Quadricyclanons in das valenzisomere Keton mit dem Gerüst **8** könnte über **9** und **2** in einem Dreistufenprozeß stattfinden.

b. Relative Stabilitäten der $(CH)_7^+$-Kationen

In der Tabelle 1 wurden die neun untersuchten Kationen in drei Klassen eingeteilt: Die Kationen **1**, **3**, **4**, **9** und **5** enthalten keine kondensierten C_3-Ringe, **2**, **6** und **8** enthalten solche Ringe; **7** steht am Rand der Tabelle, weil es kein $(CH)_7^+$-System ist. Unter allen Kationen aus der ersten Klasse hat das Tropylium-Kation **1** bei $R \to \infty$ den höchsten „ ΔS-Wert". Dies entspricht in der HMO-Auffassung der höchsten Delokalisationsenergie und damit der größten Stabilität. Vergleicht man aber die ΔS-Werte von **1** und von einem Kation aus der zweiten Klasse, so ist **1** scheinbar das instabilere Ion. Hier muß berücksichtigt werden, daß bei kleiner werdenden R-Werten für einige der untersuchten Kationen die ΔS-Werte monoton abnehmen, während sie für andere durch ein Maximum gehen (s. Tab. 1). Eine genauere Analyse der ΔS-Werte bei unterschiedlichen Werten des Parameters R zeigt, daß bei der Überführung von **1** in den vollständigen Graphen K_7, das Tropylium-Ion immer stabiler wird (s. Tab. 1). Die ΔS-Werte steigen bis zum Parameterwert $R = 2$, wo sogar schon die ,,leichten Übergänge'' abgeschlossen sind, ständig an. Das bedeutet, daß die Kreisstruktur, die elektronisch durch sp^2-hybridisierte C-Atome realisiert werden kann, bei einer Anzahl von 7 Zentren und einer ,,Besetzung mit 6 Elektronen'' eine besonders günstige topologische Situation darstellt : Bei Störung im Sinne ihrer Negierung durch ihr Komplement gewinnt sie an ,,Delokalisationsenergie'' (ΔS steigt) und gleichzeitig auch an ,,molekülinnerer Entropie'' (Annährung an K_7). Das ist nicht eine allgemeine Eigenschaft aller Ringstrukturen : Das hypothetische antiaromatische Cyclohepattrienyl-Anion verhält sich umgekehrt und das ebenfalls antiaromatische Cyclopentadienyl-Kation hat für alle R-Werte negative Werte $\Delta S < 0$.

Chemische Systeme, die sich wie die hier untersuchten Kationen verhalten (Ringstruktur im Grundzustand hat wachsende ΔS-Werte bei fallenden R-Werten) neigen offensichtlich zu ringförmigen und nicht polycylischen Strukturen, selbst wenn man für polycyclische Strukturen größere topologische Resonanzenergien [22] (bei uns ΔS-Werte) erhält.

In der Reihenfolge der Stabilitäten sollten **4** und **9** folgen (s. Tab. 1). Diese sind tatsächlich die $(CH)_7^+$-Kationen, die neben **1** bisher am besten beobachtet werden konnten. [4,26] Die größere Anzahl der nahen topologischen Verwandten von **9** im Vergleich zu **4** (s. Abb. 2) könnte dafür verantwortlich gemacht werden, daß das Norbornadienyl-Kation scheinbar stabiler ist.

Die Kationen **3** und **5** sollten sehr instabil sein. Ihr Nachweis und die Beobachtung ihrer Eigenschaften erfordern wahrscheinlich sehr tiefe Temperaturen und ist bisher nicht gelungen.

Das Norcaradienyl-Kation **2** hat zwar unter den Kationen der zweiten Klasse den kleinsten ΔS-Wert, ,,stabilisiert'' sich aber anfänglich mit kleiner werdenden R-Werten.

Obwohl **6** und **8** für $R \to \infty$ den gleichen ΔS-Wert haben, sollte **8** etwas stabiler als das Quadricyclyl-Kation sein, denn sein ΔS-Wert fällt langsamer. Die experimentallen Beobachtungen [4,26,29] scheinen diese Aussage zu bestätigen.

5. SCHLUSSBEMERKUNG

In allen diesen Betrachtungen zur Stabilität und zu Umlagerungsmöglichkeiten wurden Fragen betreffend den Einfluß von Substituenten am Gerüst, Polarität und chemische Beschaffenheit des Reaktionsmediums sowie sterische Verhältnisse nicht gestellt. Ebenfalls wurde bei den Umlagerungen nicht nach der Art der zur Reaktion nötigen Aktivierung (thermisch, photochemisch) gefragt. Daß zwischen experimentellem Datenmaterial und unseren Voraussagen trotzdem eine gute Übereinstimmung besteht, zeigt deutlich, welchen Rang die topologische Beschaffenheit eines Systems für die Bestimmung seines chemischen Verhaltens einnimmt.

LITERATURVERZEICHNIS

[1] a. W. v. E. Doering und L. H. Knox, *J. Amer. Chem. Soc.*, **76**, 3203, (1954) b. G. A. Olah und P. v. R. Schleyer, „Carbonium Ions", vol. II Wiley-Interscience, New York. c. R. E. Leone und P. v. R. Schleyer, *Angew. Chem.*, **82**, 22, 889 (1970).

[2] R. H. Cox, L. W. Harrison und W. K. Austin Jr., *J. Phys. Chem.*, **77**, *2*, 200, (1973).

[3] J. Winkler und F. W. Mc Lafferty, *J. Amer. Chem. Soc.*, **95**, 7533 (1973).

[4] R. K. Lustgarten, M. Brookhardt und S. Winstein, *J. Amer. Chem. Soc.*, **94**, 2347 (1972) s. dort auch weitere Lit.

[5] A. T. Balaban und T. H. Rouvray, *Tetrahedron*, **36**, 1851, (1980).

[6] A. T. Balaban, *Rev. Roumaine Chim.*, **22**, *2*, 243, (1977). s. dort weitere Lit.

[7] G. Maier, „Valenzisomerisierungen", Verl. Chemie, Weinheim/Bergstr. (1972).

[8] H. Metiu, J. Ross und G. M. Whitesides, *Angew. Chem.*, **91**, 5, 363, (1979).

[9] M. W. Tausch, E. C. Haß und P. J. Plath, *Match*, **7**, 289, (1979).

[10] M. W. Tausch und P. J. Plath, *Z. Naturf.* zur Publikation angenommen –

[11] F. Harary, „Graphentheorie", R. Oldenbourg Verl., München, 1974.

[12] E. C. Haß und P. J. Plath, *Bremer Briefe zur Chemie*, **II**, 2, 3, (1978).

[13] U. Döring und P. J. Plath, *Match*, **1**, 151 (1975).

[14] E. C. Haß und P. J. Plath, *Match*, **1**, 141 (1975).

[15] H. Primas und W. Gans, *Erfahrung und Denken*, **56**, 15 (1979).

[16] P. J. Plath, in "Applic. of MO-Theory in Org. Chem." (Hrsg. I. G. Csizmadia) Elsevier Scient. Publ. Comp. 1977, 604–617 p.

[17] J. Krüger, *Wifo* (*Akad. Wiss. DDR*), **29**, 9, 344 (1979).

[18] A. T. Balaban, *Rev. Roumaine Chim.*, **19**, 1611 (1974).

[19] C. Cone, M. J. S. Dewar und D. Landmann, *J. Amer. Chem. Soc.*, **99**, 372 (1977).

[20] M. W. Tausch und P. J. Plath, *Bremer Briefe zur Chemie*, **II**, 30 (1978).

[21] E. Heilbronner und H. Bock, „Das HMO Modell und seine Anwendungen, Verl. Chemie, BERLIN, 1968.

[22] I. Gutman, *Theor. Chim. Acta*, **56**, 89 (1980).

[23] J. T. Bursey, M. M. Bursey und D. G. I. Kingston, *Chem. Rev.*, **73**, 191 (1973).

[24] J. C. Traeger und R. G. Mc Loughlin, *J. Chem. Amer. Soc.*, **99**, 735 (1977).

[25] J. L. Franklin, J. G. Dillard, H. M. Rosenstock, J. T. Herron, K. Draxl und F. H. Field, *Natl. Stand. Ref. Data Ser., Natl. Bus. Stand.*, No. **26**, (1969).

[26] H. Volz, J. H. Shin, H. Prinzbach, H. Babsch und M. Christl, *Tetr. Lett.*, **14**, 1247 (1978).

[27] H. Prinzbach, H. Babsch und H. Fritz, *Tetr. Lett.*, **25**, 2129, (1976) s. dort auch weitere Lit.

[28] H. P. Figeys, M. Destrebeeq und G. Van Lommen, *Tetr. Lett.*, **21**, 2369 (1980).

[29] M. Christl und G. Freitag, *Angew. Chem.*, **88**, 15, 508 (1976).

LITERATURVERZEICHNIS

[1] a. W. v. E. Doering und L. H. Knox, J. Amer. Chem. Soc., **76**, 3203, (1954) b. G. A. Olah und P. v. R. Schleyer, „Carbonium Ions", vol. II Wiley-Interscience, New York. c. H. E. Leone und P. v. R. Schleyer, Angew. Chem., **82**, 22, 889 (1970).

[2] R. H. Cox, L. W. Harrison und W. K. Austin Jr., J. Phys. Chem., **77**, 2, 200, (1973).

[3] L. Winkler und F. W. McLafferty, J. Amer. Chem. Soc., **95**, 7533 (1973).

[4] R. K. Lustgarten, M. Brookhardt und S. Winstein, J. Amer. Chem. Soc., **94**, 2347 (1972) s. dort auch weitere Lit.

[5] A. T. Balaban und D. H. Rouvray, Tetrahedron, **36**, 1851, (1980).

[6] A. T. Balaban, Rev. Roumaine Chim., **22**, 2, 243, (1977) s. dort weitere Lit.

[7] G. Maier, „Valenzisomerisierungen", Verl. Chemie, Weinheim/Bergstr. (1972).

[8] H. Mettin, J. Ross und G. M. Whitesides, Angew. Chem., **91**, 5, 363, (1979).

[9] M. W. Tausch, E. C. Hass und P. J. Plath, Match, **7**, 289, (1979).

[10] M. W. Tausch und P. J. Plath, Z. Naturf., zur Publikation angenommen.

[11] F. Harary, „Graphentheorie", R. Oldenbourg Verl., München, 1974.

[12] E. C. Hass und P. J. Plath, Bremer Briefe zur Chemie, H. 2, 3, (1978).

[13] U. Döring und P. J. Plath, Match, **1**, 151 (1975).

[14] E. C. Hass und P. J. Plath, Match, **1**, 141 (1975).

[15] H. Primas und W. Gans, Erfahrung und Denken, **56**, 13 (1979).

[16] P. J. Plath, in "Applic. of MO-Theory in Org. Chem." (Hrsg. I. G. Csizmadia) Elsevier Scient. Publ. Comp., 1977, 604—617 p.

[17] I. Krüger, Wiss. (Akad. Wiss. DDR), 29, 9, 344 (1979).

[18] A. T. Balaban, Rev. Roumaine Chim., **19**, 1611 (1974).

[19] C. Cone, M. J. S. Dewar und D. Landman, J. Amer. Chem. Soc., **99**, 372 (1977).

[20] M. W. Tausch und P. J. Plath, Bremer Briefe zur Chemie, H. 30 (1978).

[21] E. Heilbronner und H. Bock, „Das HMO Modell und seine Anwendungen, Verl. Chemie, BERLIN, 1968.

[22] I. Gutman, Theor. Chim. Acta, **58**, 89 (1980).

[23] J. T. Bursey, M. M. Bursey und D. G. I. Kingston, Chem. Rev., **73**, 191 (1973).

[24] J. C. Traeger und R. G. McLoughlin, J. Chem. Amer. Soc., **99**, 7351 (1977).

[25] J. L. Franklin, J. G. Dillard, H. M. Rosenstock, J. T. Herron, K. Draxl und F. H. Field, Natl. Stand. Ref. Data Ser., Natl. Bur. Stand., No. **26**, (1969).

[26] H. Volz, J.-H. Shin, H. Prinzbach, H. Babsch und M. Christl, Tetr. Lett., **14**, 1247 (1978).

[27] H. Prinzbach, H. Babsch und H. Fritz, Tetr. Lett., **25**, 2129, (1976) s. dort auch weitere Lit.

[28] H. R. Pieys, M. Desterbecq und G. Van Lommen, Tetr. Lett., **21**, 2359 (1980).

[29] M. Christl und G. Freitag, Angew. Chem., **88**, 15, 508 (1976).

Revue Roumaine de chimie, 27, 8, 963–967 (1982)

SYNTHESIS AND REACTIONS OF POLYSUBSTITUTED 2(1*H*)PYRIDONES AND PYRIDINES

M. A. HASSAN, E. A. SOLIMAN and A. A. HAMED
Chemistry Department, Faculty of Science, Ain Shams University, Cairo, Egypt

Received March 20, 1981

1,2-Dihydro-6-methyl-2-oxo-nicotinonitrile (I) was converted to 2-acyl-2(*H*) pyridones (II) by the action of Grignard reagents, and to 2-chloro-6-methyl-nicotinonitrile (VI) by the action of phosphorus oxychloride. II and VI are the key intermediates for synthesis of new polysubstituted 2(1*H*) pyridones and pyridines. The structures of all new compounds were established by IR, ^{1}H-NMR, and mass spectroscopy.

As well known[1,2] 2(1*H*) pyridones exist in the lactam-lactim tautomeric mixture in which the lactam form predominates due to stabilization by chelation. 1,2-Dihydro-6-methyl-2-oxo-nicotinonitrile (I) [Fluka product No. 28530] was converted to 3-acyl-6-methyl-2(1*H*)pyridones (IIa-c) by the action of Grignard reagents. [3]

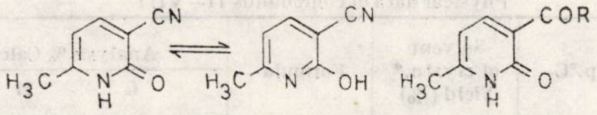

I

II

a) $R = CH_3$

b) $R = C_6H_5$

c) $R = \text{cycl. } C_5H_9$

Condensation of 3-acetyl-6-methyl-2(1*H*)pyridone (II*a*) with aromatic aldehydes gave 3-cinnamoyl-6-methyl-2(1*H*) pyridones (IIIa and b). Treatment of IIb or IIIa with phenylhydrazine gave 1,3-diphenyl-6-methyl-pyrazolo-5,4,-*b*-pyridine IV or 3-5-(*p*-tolyl)-1-phenyl-2-pyrazolin-3-yl-6-methyl-2(1*H*)-pyridone (V) respectively.

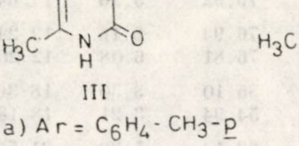

III

a) $Ar = C_6H_4-CH_3-\underline{p}$

b) $Ar = C_6H_4-Cl-\underline{p}$

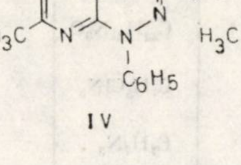

IV

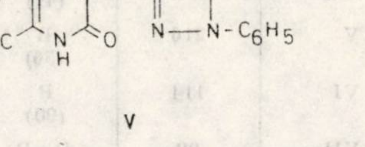

V

On the other hand, heating of 1,2-dihydro-6-methyl-2-oxonicotinonitrile (I) with phosphorus oxychloride gave 2-chloro-6-methyl-nicotinonitrile (VI).[4] Treatment of VI with sodamide or amines gave 2-amino or alkylamino-6-methyl-nicotino-nitriles (VIIa-c). Also reaction of potassium salt of I with alkyl halides or treatment of VI with sodium alkoxides yielded 2-alkoxy-6-methyl-nicotinonitriles (VIIIa-d).

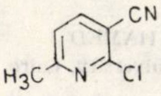

VI

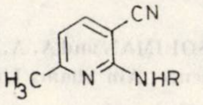

VII

a) $R = H$

b) $R = C_6H_5-CH_2$

c) $R = CH_2-C_6H_4-OCH_3$-p

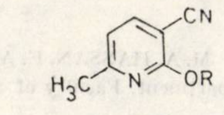

VIII

a) $R = CH_3$

b) $R = C_2H_5$

c) $R = C_6H_5-CH_2$

d) $R = CH_2CO_2C_2H_5$

EXPERIMENTAL

All melting points are uncorrected. IR spectra were obtained using a Beckman IR–20A spectrophotometer using KBr wafer technique ; ^{1}H-NMR spectra were determined by BRUKER WP-80CW spectrophotometer, and mass spectra were obtained using a Hewlett-Packard 5980 A spectrophotometer by direct introduction technique. The physical data of all new compounds are listed in table 1 and the spectral data are listed in table 2.

TABLE 1

Physical data of compounds II–VIII

Compd.	m.p.°C	Solvent of crystn.* Yield (%)	Formula	Analysis % Calcd/Found		
				C	H	N
IIa	198	B+P (46)	$C_8H_9NO_2$	63.56 63.38	6.00 5.88	9.27 9.17
IIb	211	B+M (68)	$C_{13}H_{11}NO_2$	73.22 73.12	5.20 5.16	6.57 6.38
IIc	174	B (63)	$C_{12}H_{15}NO_2$	70.22 70.08	7.37 7.26	6.82 6.69
IIIa	219	B (74)	$C_{16}H_{15}NO_2$	75.87 75.80	5.97 5.89	5.53 5.48
IIIb	216	B (67)	$C_{15}H_{12}ClNO_2$	65.82 65.76	4.42 4.40	5.12 5.09
IV	207	B (47)	$C_{19}H_{15}N_3$	79.98 79.92	5.30 5.26	14.73 14.64
V	216	B (56)	$C_{22}H_{21}N_3O$	76.94 76.81	6.16 6.08	12.24 12.20
VI	114	P (90)	$C_7H_5ClN_2$	55.10 54.94	3.30 3.21	18.36 18.18
VIIa	99	B+P (43)	$C_7H_7N_3$	63.14 63.08	5.30 5.16	31.56 31.38

TABLE 1 (continued)

Compd.	m.p. °C	Solvent of crystn.* Yield (%	Formula	Analysis % Calcd / Found C	H	N
VIIb	124	B+P (77)	$C_{14}H_{13}N_3$	75.31 75.19	5.87 5.80	18.82 18.76
VIIc	118	B+P (65)	$C_{15}H_{15}N_3O$	71.12 71.02	5.97 5.83	16.59 16.48
VIIIa	85	P (79)	$C_8H_8N_2O$	64.85 64.72	5.44 5.40	18.91 18.77
VIIIb	93	P (70)	$C_9H_{10}N_2O$	66.65 66.61	6.21 6.07	17.27 17.16
VIIIc	106	B+P (62)	$C_{14}H_{12}N_2O$	74.98 74.82	5.39 5.27	12.49 12.41
VIIId	126	B+P (58)	$C_{11}H_{12}N_2O_3$	59.99 59.89	5.49 5.41	12.72 12.67

* B = Benzene, M = Methanol ; P = Light petrol (B. p. 40 – 60°C).

TABLE 2

Spectral data of compounds II – VIII

Compd.	IR Spectra ν(cm⁻¹)*	¹H–NMR spectra(*) (δ in ppm)/acetone–d_6	Mass spectra m/e (abundance) %
IIa	1550, 1615, 1675, 2780, 2980, 3300	1.5*b*, 2.42*s* (CH_3), 2.57*s*($COCH_3$), 5.85*d* (β–CH), 8.1*d*(γ–CH).	108(27), 137(100), 151(48)
IIb	1565, 1590, 1620, 1640, 1670, 2840-3140, 3300, 3460 *b*	1.58 *b*(NH), 2.16 *s*(CH_3), 6.13*d*(β-CH), 7.38 *m* (C_6H_5), 8.00*d*(γ–CH)	108(30), 137(100), 213(17)
IIc	1555, 1620, 1650, 1675, 2790–3130, 3315, 3475*b*	1.8*m*(C_5H_9), 2.43 *s*(CH_3), 4.08*b*(NH), 6.15*d*(β–CH), 8.05d(γ–CH)	108(17), 137(100), 205(15)
IIIa	1550, 1590, 1610, 1645, 1665, 2800–3100, 3450*b*	1.55*b*(NH), 2.35*s*(CH_3), 2.45*s*(CH_3), 6.2*d*(β–CH), 7.05*d* × *d*(CH=CH), 7.4–7.9 dxd(C_6H_4), 8.18 *d*(γ–CH)	108(20), 117(100), 137(40), 225(36), 239(60), 253(48)
IIIb	1550, 1590, 1620, 1650, 1670, 2850-3100, 3440*b*	1.52*b*(NH), 2.45*s*(CH_3), 6.13*d*(β–CH), 7.18*d* × *d* (CH=CH), 7.52–7.94 *d* × *d* (C_6H_4), 8.16*d*(γ-CH)	108(84), 137 (100), 245.5(47), 273 (93)
IV	1590, 1000, 2840-3140	2.4*s*(CH_3), 6.2*d*(β–CH) 7.08–7 ; 33*m*(1,3–C_6H_5), 7.6*d*(γ–CH)	77(100), 208(10), 285(16)
V	1550, 1600, 1620, 1650, 2800–2930, 3450*b*	1.8*t*(CH), 2.05*s*(CH_3), 2.33*d*(CH_2), 2.75*s*(CH_3), 3.03*b*(NH), 6.1*d*(β–CH), 7.1–7.32 *d* × *d*(C_6H_4), 8.08 *d* (γ–CH)	252(100), 343 (34)
VI	1595, 2240, 3060 3100	2.85*s* (CH), 7.1*d*(β–CH), 7.8*d*(γ–CH)	117(100), 152 (58)

TABLE 2 (continued)

Compd.	IR Spectra ν(cm^{-1})*	^{1}H–NMRspectra (*) (δ in ppm)/ acetone–d$_6$	Mass spectra m/e (abundance %)
VIIa	1560,1600, 2240, 2860–3080, 3460	2.55*s*(CH$_3$), 5.2*b*(NH$_2$), 6.2*d*(β–CH), 7.8*d*(γ–CH)	107(100),117(52), 133(21)
VIIb	1510, 1580, 2210, 2940–3080, 3360	2.43*s*(CH$_3$), 4.68*d*(CH$_2$), 5.33*b*(NH), 6.45*d*(β–CH), 7.02–7.25*m*(C$_6$H$_5$), 7.5*d*(γ–CH)	107(100), 117(14), 146(8), 223(40)
VIIc	1510, 1600, 2210, 2850–3085, 3395	2.35*s*(CH$_3$), 3.7*s*(OCH$_3$), 4.53*d*(CH$_2$), 5.08*b*(NH), 6.33*d*(β–CH), 6.7–7.15*d* × *d* (C$_6$H$_4$), 7.38d(γ–CH)	121(100), 253 (18)
VIIIa	1580, 1600, 2240, 2880–3080	2.53*s* CH$_3$), 4.0*s*(OCH$_3$), 6.75*d*(β–CH), 7.68*d*(γ–CH)	117(100), 148(60),
VIIIb	1575, 1595, 2230, 2905–3090	1.43*t*(CH$_3$), 2.48*s*(CH$_3$), 4.43*q*(CH$_2$), 6.73*d*(β–CH), 7.68*d*(γ–CH)	107(100), 117(51), 136(53), 162(29)
VIIIc	1560, 1590, 2230, 2920–3090	2.35*s*(CH$_3$), 5.3*s*(CH$_2$), 6.05*d*(β–CH), 7.1–7.38*m* (C$_6$H$_5$), 7.63*d*(γ–CH)	91(100),107(18), 117(17), 198(9),
VIIId	1560, 1585, 1740, 2230, 2930–3095	1.5*t*(CH$_3$), 2.35*s*(CH$_3$), 3.75*q* (CH$_2$), 4.8*s*(OCH$_2$), 6.1*d*(β–CH), 7.68*d*(γ–CH)	117(68),147(100), 175(53), 220(17)

*b = broad ; d = doublet ; m = multiplet ; q = quartet ; s = singlet ; t = triplet.

3-Acyl-6-methyl-2(1*H*)pyridones (IIa-c)

To a suspension of I (0.01 mol) in dry ether (50 ml) was added an ethereal solution of methylmagnesium iodide, phenyl, or cyclopentylmagnesiumbromide (0.04 mol). The reaction mixture was refluxed on a steam-bath for 4 hrs., set aside overnight at room temperature, and then decomposed with cold solution of hydrochloric acid (10 %). The solid product was filtered off and crystallized from the proper solvent to give II a-c as yellow crystals.

3-Cinnamoyl-6-methyl-2(1*H*)pyridones (IIIa and b)

To a solution of IIa (0.01 mol) in alcoholic KOH (4 %) *p*-methyl or *p*-chlorobenzaldehyde (0.01 mol) was added and the reaction mixture was left overnight at room temperature. The solid obtained was filtered off and crystallized from benzene to give IIIa or b as yellow crystals.

1,3-Diphenyl-6-methyl-pyrazolo-5, 4-b-pyridine(IV) or 3-(1-phenyl-5-(*p*-tolyl)-2-pyrazolin-3-yl-6-methyl-2(1*H*)pyridone (V)

A solution of IIb or IIIa (0.01 mol), phenylhydrazine (0.01 mol), and ethanol (50 ml) was refluxed for 4 hrs. The solid product obtained after concentration and cooling was filtered off and crystallized from benzene to give IV or V as yellow crystals.

2-Chloro-6-methyl-nicotinonitrile (VI)

A mixture of I (10.0 g) and phosphorus oxychloride (50 ml) was heated on a steam-bath for 2 hrs. The reaction mixture was poured gradually into crushed ice with stirring. The solid which separated was filtered off and crystallized from light petrol (80–100°C) to give VI (10.5g) as colourless crystals, m.p. 114–5°C.

2-Amino (or alkylamino)-6-methyl-nicotinonitriles (VIIa-c)

A mixture of VI (0.01 mol) and sodamide, benzyl or *p*-methoxybenzylamine (0.012 mol) was heated at 130°C in a sealed tube for 6 hrs. The reaction mixture was triturated with dilute hydrochloric acid (10 %) and the solid product was washed by sodium bicarbonate solution (10 %), dried and crystallized from suitable solvent to give VIIIa-c as colourless crystals.

2-Alkoxy-6-methylnicotinonitriles (VIIIa-c) and ethyl(3-cyano-6-methyl-2-pyridyl)oxy acetate (VIIId)

Method 1. A mixture of the potassium salt of I (0.01 mol), absolute ethanol (50 ml), and methyl iodide, ethyl iodide, benzyl chloride or ethyl bromoacetate (0.01 mol) was refluxed for 4 hrs. The colourless crystals which separated upon concentration and cooling were filtered and crystallized from the proper solvent to give VIIIa-d respectively as colourless crystals.

Method 2. A mixture of VI (0.01 mol) and sodium methoxide, ethoxide, or benzyloxide (0.01 mol) in corresponding alcohol (30 ml) was refluxed for 3 hrs. The reaction mixture was concentrated and poured into water (100 ml). The solid obtained was filtered off and crystallized from the proper solvent to give VIIIa-c as colourless crystals.

REFERENCES

[1]. A. Albert and E. Spinner, *J. Chem. Soc.*, **1960**, 1221.
[2]. E. Spinner and J. C. B. White, *J. Chem. Soc.*, **1966**, 991.
[3]. A. Sammour, A. Raouf, M. El-Kasaby and M. Hassan, *J. prakt, Chem.* **315**, 1175 (1973).
[4]. L.A. Perez-Medina, R. P. Mariella and S. M. McElvain, *J. Amer. Chem. Soc.*, **69**, 2574 (1947).

Revue Roumaine de Chimie, 27, 8, 969–972 (1982)

SYNTHESIS AND POLYMERIZATION OF POLYETHYLENE GLYCOL DIMETHACRYLATES. VII[1]

ESR STUDY OF ETHYLENE GLYCOL DIMETHACRYLATE–STYRENE COPOLYMERS

AGNETA CARAGHEORGHEOPOL*, H. CĂLDĂRARU*, GH. HUBCA**, CR. OPRESCU** and M. DIMONIE**

* Centre of Physical Chemistry – ICECHIM, Splaiul Independenţei 202, Bucharest, Romania.

** Polytechnical Institute of Bucharest, Laboratory of Macromolecular Technology, Calea Victoriei 149, Bucharest, Romania.

Received September 30, 1981

An ESR study of ethylene glycol dimethacrylate–styrene copolymers is presented. These investigations pointed out the influence of the physical properties of the system (network density, viscosity, monomer molecule dimensions) on the composition of the copolymers in the limiting conversion range.

INTRODUCTION

In an earlier paper the kinetics of copolymerization reaction of polyethyleneglycol dimethacrylates with styrene has been investigated.[1] As the reaction proceeds and a three dimensional polymer network is formed the viscosity increases and the system gradually changes from liquid to gel and finally to glassy state.[2,3]

An ESR study of these systems was undertaken for the third stage (conversion ~ 50 %), when the systems are glassy, and the macroradicals are trapped in the polymer network.

EXPERIMENTAL

Polymer samples of the following types : polyethylene dimethacrylate, polydiethylene glycol dimethacrylate, copolymers of styrene — divinylbenzene, ethylene dimethacrylate — styrene and ethylene dimethacrylate — divinylbenzene were obtained by polymerization directly in the sample tubes ; the molar ratios of the monomers are indicated in table 1. The polymerization was accomplished in vacuum (10^{-3} torr) at 70°C for 1 hour, using methyl ethyl ketone peroxide (2 %) as initiator.

The ESR spectra were recorded on a JES — 3 B (JEOLCO) spectrometer with 100 KHz modulation, at room temperature. The parameters of the spectra were measured by comparison with a Mn^{2+} sample.

TABLE 1

The molar ratios of the monomer in the copolymer sublayer and the corresponding type of radicals trapped at limiting conversion

Ethylene dimethacrylate : styrene	Type of radical	Ethylene dimethacrylate : divinylbenzene	Type of rapical
100 : 0	I	100 : 0	I
80 : 20	I	70 : 30	I
50 : 50	I	50 : 50	I
40 : 60	—	40 : 60	I + II
		33 : 67	II
		25 : 75	II
20 : 80	—	20 : 80	II
		0 : 100	

RESULTS AND DISCUSSIONS

Samples of the homopolymers of ethylene dimethacrylate and diethylene glycol dimethacrylate showed the well known "conventional 9 line" ESR Spectrum (Figure 1) characteristic of γ — irradiated poly(methyl methacrylate) and of trapped radical in the copolymer of ethylene dimethacrylate — methy methacrylate.[4]

This spectrum was assigned to the chain propagating radical[5] (I)

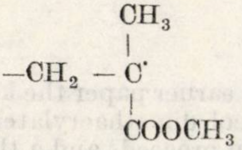

$$-CH_2-\overset{\overset{\displaystyle CH_3}{|}}{\underset{\underset{\displaystyle COOCH_3}{|}}{C^{\cdot}}} \qquad (I)$$

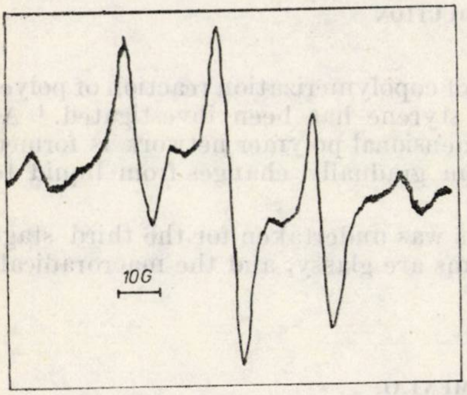

Fig. 1. — ESR spectrum of polyethylene dimethacrylate.

The observed spectral pattern is due to interaction with a free rotating methyl group and two methylene protons. The alternation of the line width could be interpreted as being due to line broadening caused by hindered oscillation of the methylene group around a tilt equilibrium conformation, or a distribution of the tilt angle value in the irregular environment of the polymer matrix.

The ESR spectrum of styrene -divinylbenzene copolymer consisted of an incompletely resolved triplet pattern ($a_H \sim 20$ G, $g = 2.002$) (Fig. 2).

As expected, the spectrum is similar to that found in γ — irradiated polystyrene, which was assigned to structure (II).

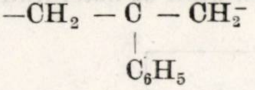

$$-CH_2-\underset{\underset{C_6H_5}{|}}{\dot{C}}-CH_2^- \qquad (II)$$

Verma and Peterlin [6] concluded that the methylene protons are non-equivalent, the corresponding *hf* splittings being 20 G and 5 G, respectively.

Studying the copolymer of the diester with styrene at different molar ratios the following behaviour was noticed : at molar ratios diester : styrene$\geqslant$1 only the ESR spectrum of the methacrylate radical (I) was observed, while for molar ratios styrene : diester $>$1, no radicals appeared (Table 1).

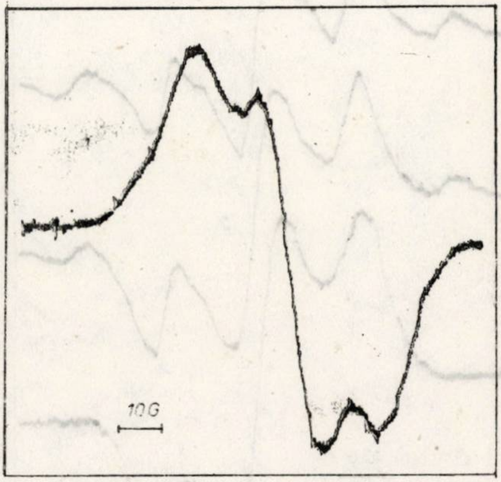

Fig. 2. — ESR spectrum of styrene — divinylbenzene copolymer.

In the former case, owing to the large amount of diester and to its higher reactivity as compared to styrene the copolymer becomes richer in diester and macroradicals of type (I) will prevail ; at limiting conversion a very dense three-dimensional network is formed and the macroradicals are trapped. When the composition in sublayer is rich in styrene, radicals of type (II) are expected. The fact that no radicals were actually observed can be related to their disappearance in recombination reaction. In this case the three dimensional network is looser and the smaller styrene molecules diffuse more easily toward the growing macroradicals. Thus, at high conversions the macroradical chains are formed mostly of styrene units : these chains are more flexible and allow recombination reactions.

In order to follow the evolution of both radicals (I) and (II), at different monomer ratios, styrene was replaced by divinylbenzene, a molecule having the same radical center (similar reactivity) and two reaction sites. In this case, regardless of monomer ratios, a dense polymer network is expected to be formed and the corresponding radicals should be trapped. Indeed, for this copolymer, radicals (I) and (II) were evidenced for the entire range of molar ratios (Table 1). Since the g and a_H parameters of radicals (I) and (II) are close, their spectra overlap in central region ; therefore a quantitative estimation of their ratios was not attempted. Radical (I) was evidenced by its outer lines, while the increased intensity of the central lines was an indication for the presence of radical (II) (Fig. 3).

The appearance of radical (II) in divinylbenzene copolymer at high divinylbenzene proportions, as compared to the lack of the same radical for the same proportions of styrene stresses the importance of chain mobility for the recombination reaction of macroradicals.

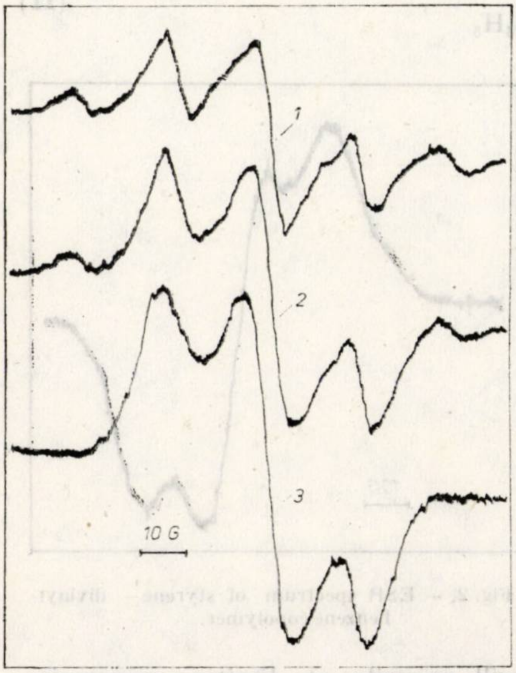

Fig. 3. — ESR spectra obtained at different molar ratios of ethylene dimethacrylate : divinylbenzene : 1 — ethylene dimethacrylate : divinylbenzene = 70 : 30 ; 2 — ethylene dimethacrylate : divinylbenzene = 40 : 60 ; 3 — ethylene dimethacrylate : divinylbenzene = 20 : 80.

Radical (I) was observed at lower ethylene dimethacrylate : divinyl benzene ratio (40 :60) than in ethylene dimethacrylate-styrene copolymer· This fact indicates the influence of the physical properties of the system (network density, viscosity, monomer molecule dimensions) on the composition of the copolymers in the limiting conversion range.

REFERENCES

[1] Part. VI. Gh. Hubca, Cr. Oprescu, A. Caragheorgheopol, H. Căldăraru, D. Racoţi and M. Dimonie, *Rev. Roumaine Chim.*, **27**, 659 (1982).

[2] Part. IV. Gh. Hubca, Cr. Oprescu, Gh. Drăgan and M. Dimonie, *Rev. Roumaine Chim.*, **27**, 433 (1982).

[3] G. V. Korolev, L. I. Mahonina and A. A. Berlin, *Vysokomol, Soedineniya* **3**, 198 (1961).

[4] N. M. Atherton, H. W. Melville and D. H. Whiffen, *Trans. Faraday Soc.* **54**, 1300 (1958).

[5] M. Iwasaki and Y. Sakai, *J. Polymer Sci*, **A**— **1**, 1537 (1969), and literature cited therein.

[6] G. P. S. Verma and A. Peterlin, *J. Polymer Sci*, **B 7**, 587 (1969).

Revue Roumaine de Chimie, 27, 8, 973–979 (1982)

POLAROGRAPHIC BEHAVIOUR OF LUTIDINIC ACID

LUIGI CAMPANELLA and G. de ANGELIS
Institute of Analytical Chemistry — University of Rome, Italy

Received March 25, 1981

Polarographic and oscillopolarographic behaviour of lutidinic acid is characterized by the presence of three waves and four peaks. True reduction processes and catalytic ones are observed and adsorption phenomena evidenced. Nature of the electrode reactions is studied and analytical aspects discussed.

Pyridinecarboxylic acids are characterized by a polarographic behaviour pointed out by the presence both of true reduction waves and of catalytic ones, these latter ascribed to the hydrogen discharge. In the case of the monocarboxylic acids the reduction waves fall generally at more negative values of potential than the catalytic ones; the opposite occurs in the case of pyridinedicarboxylic acids. Catalyzing action seems to be due especially to the protonated cationic species (protonation level = + 1) of the acids both directly and through a recombination process between hydrogen ions and the species of the acids at lower protonation degree, to which a partial kinetic character of some waves is added. Adsorption phenomena evidenced by post-waves are also observed. Ilkovic equation is obeyed, at least by one wave for each acid, quantitative polarographic analysis so being possible. The above conclusions are drawn from literature [1-4] and from our preceding experimental results about 2-pyridinecarboxylic acid (picolinic),[5] 3-(nicotinic),[6] 4-(isonicotinic),[7] 2,3-(quinolinic),[8] 2,5-(isocinchomeronic),[9] 2,6-(dipicolinic),[10] 3,4-(cinchomeronic)[11] [12] pyridinecarboxylic acids in the progress of a program to which this paper dealing with lutidinic acid belongs too. Lutidinic or 2,4-pyridinedicarboxylic acid was never polarographically studied till today, the only information being due to a paper by Pozdeeva and Novikov who evidenced only one polarographic wave with $E_{1/2} = -1.71$ V in 0.1 M tetramethylammonium iodide. [1] This acid can be obtained as a white crystalline solid by oxidation of substituted pyridines and recrystallization from water of the obtained compound. Its dissociation constants were determined by Canic [13] and Yamasaki and Yasuda [14] in water and by Hopff and Krilger [15] in 80% cellosolve solution (Table 1).

TABLE 1

Dissociation constants of lutidinic acid

Solvent	$(H_2PC \overset{pK_1}{\rightleftarrows} HPC^- + H^+)$	$(HPC^- \overset{pK_2}{\rightleftarrows} PC^{--} + H^+)$	Reference
water	2.17	5.09	13
water	2.23	4.71	14
80 % cellosolve	4.72	6.48	15

EXPERIMENTAL

Materials : Lutidinic acid supplied by Phalts-Bauer Inc. recrystallized from water.

The study was carried out at 25.0 ± 0.5 °C in aqueous solutions, whose free acidity was varied from very high values (about 2 M $HClO_4$) up to pH 10, with NaClO 0.5 M as supporting electrolyte and citric buffer as buffering agent. For the experiments at high acidity the ionic strength was buffered at 2.0 M with $NaClO_4$ and $HClO_4$. The solutions were prepared by dissolving in distilled water weighed amounts of lutidinic acid (dried at 115°C) in order to have concentrations of about 10^{-3} M.

Apparatus : AMEL (Milan, Italy) polarograph (mod. 461) with pen recording and with a dropping mercury electrode having at open circuit the following characteristics $m = 0.915$ mg s^{-1}, $t = 3.0$ s (obtained by a hammer), $r = 0.052$ mm ; oscillopolarograph AMEL (mod. 448), dropping time 8 s, waiting time 6 s, measurement time 2s ; pH meter Electroscan Beckman 30 equipped with usual glass and satured calomel electrodes (SCE).

The scanning rate of the potential in the polarographic experiments was 0.2 V/min ; in the oscillopolarographic ones it was varied within the range 0.25 ÷ 25.0 V/s ; if not otherwise stated it must be considered as 1.0 V/s.

RESULTS

Lutidinic acid shows two cathodic polarographic waves, the first one of which deformed by the probable overlapping of two different processes. The existence evidenced pH range is limited on one side by $[H^+] = 2.8$ M for both the waves and on the other by pH 8 and 3.6 respectively for the first and the second wave. The height maximum falls at pH 4 (first wave) and 1,5 (second wave), the first wave being in all the range higher than the second one (Fig. 1,2). Half wave potential at pH = 1.2 is − 0.704 V vs SCE for the first wave and − 0.916 V vs SCE for the second one. As pH increases $E_{1/2}$ shifts towards more negative values with a slope $\Delta E_{1/2}/\Delta pH = -30$ and − 60 mV/pH respectively for the two waves. In very acid medium ($[H^+] = 2M$) $E_{1/2}$ is respectively − 0.600 and − 0.880 vs SCE for the first and second wave with $\Delta E_{1/2}/\Delta pH = 0$. The first wave appears and results to be irreversible both from logarithmic analysis and from the variations of $E_{1/2}$ with the concentration ($\Delta E_{1/2}/\Delta c = 10$ V/M) ; two electrons are involved in it as shown by coulometric analysis ; the second wave is on the contrary reversible at both the checks with two electrons involved. Ilkovic law is obeyed by both the waves, but the slope and so the sensitivity of possible polarographic quantitative analysis is higher for the first than for the second wave. If experimental temperature is decreased the first wave change its shape up to the formation of a post-wave with $E_{1/2}$ more negative than that one of the generating for about 80 mV. Temperature coefficients of the first wave current are 2 and 3 % respectively at pH 1.0 and 4.2 and 0 %, 2 %, 6 % and 2 % again for the second wave at pH 1.0 for the corresponding temperature intervals 0 – 5°C, 5 – 30°C, 30 – 40°C, 40 – 50°C. $E_{1/2}$ values do not depend on temperature. The addition of surface active agents results in a lowering of the height of both the waves and in the disappearance of the post wave evidenced at temperatures between 0 and 10°C. Increasing ionic strength reduces current values but does not affect $E_{1/2}$ of the two

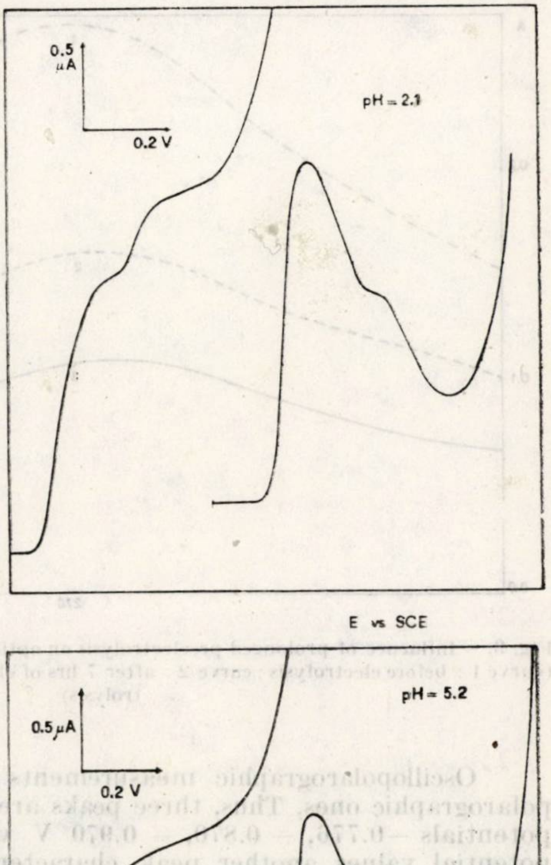

Figs 1 and 2. – Direct and derivative polarographic curves of lutidinic acid solutions at different pH values.

waves. The same effects are observed when polarographic curves are recorded after prolonged preelectrolysis in polarographic conditions on large area cathodes; to these effects a decreasing of optical density is corresponding (Fig. 3).

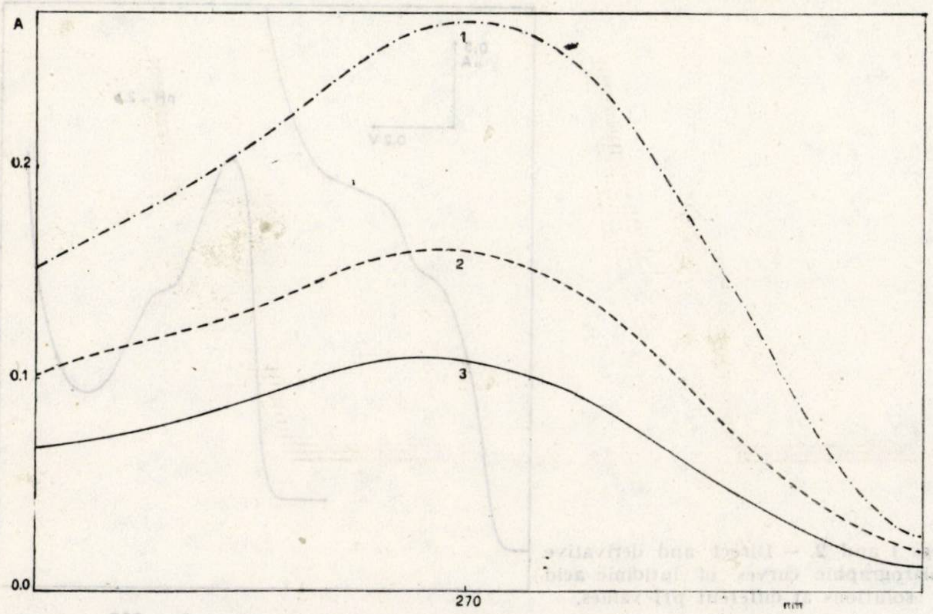

Fig. 3. — Influence of prolonged preelectrolysis on optical W density of lutidinic acid solutions (curve 1 : before electrolysis ; curve 2 : after 7 hrs of electrolysis ; curve 3 ; after 24 hrs of electrolysis)

Oscillopolarographic measurements substantially agree with the polarographic ones. Thus, three peaks are observed at pH 1.2 with peak potentials −0.776, − 0.870, − 0.970 V vs SCE and at more negative potential values another peak characterised by current values higher than those of the preceeding peaks for about 10^3 times can be recorded, its shape changing in that one of a polarographic step when experimental pH is higher than 4. Current values are lowered by decreasing free acidity. Concentration variations affect moderately E_p values while they modify current values in order that Randles and Sevcik equation ensuring proportionality between current and concentration is obeyed (Fig. 4). Potential scanning rate (V) and peak potential and current are related by equations of similar form : $E_p = kV^n$, $I_p = k'V^m$, where n and m assume the following values for the observed peaks :

	pH 1.2		pH 3.6		pH 4.6	
peak	*n*	*m*	*n*	*m*	*n*	*m*
I	0.6	0.75	0.15	0.65	0	0.65
II	0.6		0.15		0	

III	0	0	0	1	—	1
IV	—	—	0.5	—	0.55	

for 1V/s $< V <$ 7 V/s I_p decreases with increasing scanning rate, for V $>$ $>$ 7V/s I_p remains constant.

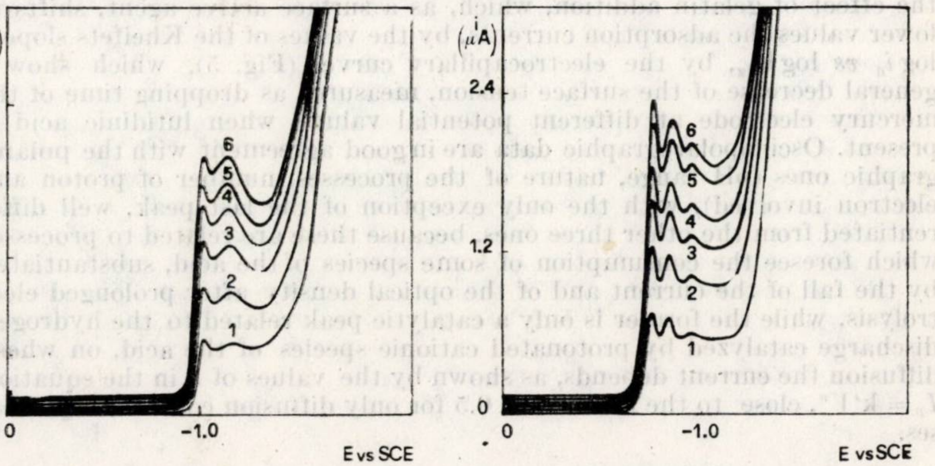

Fig. 4. — Influence of concentration variations on oscillopolarographic curves of lutidinic acid solutions (concentration values increasing from down to up: 1.0, 2.2, 2.7, 3.1, 3.4 × 10^{-3}M; pH = 1.2 on the right and 4.2 on the left)

DISCUSSION

On the basis of the decribed results and of the consideration of the acid equilibria the following processes can be hypothesized for the three waves, i.e. the two normal waves and the adsorption post-wave:

$$[H^+]\uparrow \quad \begin{array}{l} H_3PC^+ + H^+ + 2e \rightarrow H_2PC(H_2) \\ H_2PC + H^+ + 2e \rightarrow HPC^-(H_2) \\ HPC^- + H^+ + 2e \rightarrow PC^{--}(H_2) \end{array} \qquad \text{first wave and peak}$$

$$[H^+]\uparrow \quad \begin{array}{l} H_3PC^+ + 2H^+ + 2e \rightarrow H_3PC(H_2) \\ H_2PC + 2H^+ + 2e \rightarrow H_2PC(H_2) \end{array} \qquad \text{second wave and peak}$$

$$[H^+]\uparrow \quad \begin{array}{l} (H_3PC^+)_{ads} + 2H^+ + 2e \rightarrow H_3PC^+(H_2) \\ (H_2PC)_{ads} + 2H^+ + 2e \rightarrow H_2PC(H_2) \end{array} \qquad \text{third wave and peak}$$

$$H_3PC^+ + 1e \rightarrow 1/2\, H_2 + H_2PC \qquad \text{fourth peak (high currents)}$$

where for H_2PC lutidinic acid is indicated, for $X(H_2)$ a dehydroderivative compound of a species X, for X(ads) the species X in adsorbed phase and with $[H^+]\uparrow$ solutions at increasing acidity degree. As it can be seen the third wave is an adsorption post-wave, its nature being well evidenced by the fact that the wave appears with decreasing temperature. Also for the following two processes the current is not only diffusion controlled but contains an adsorption component as shown by the high values of the temperature coefficient of the limiting current, especially for the first wave, by the effect of gelatin addition, which, as a surface active agent, shifts to lower values the adsorption currents, by the values of the Kheifets slope [16] $\log i_d$ *vs* $\log h_{Hg}$, by the electrocapillary curves (Fig. 5), which show a general decrease of the surface tension, measured as dropping time of the mercury electrode at different potential values, when lutidinic acid is present. Oscillopolarographic data are in good agreement with the polarographic ones (pH range, nature of the processes, number of proton and electron involved), with the only exception of the last peak, well differentiated from the other three ones, because these are related to processes which foresee the consumption of some species of the acid, substantiated by the fall of the current and of the optical density after prolonged electrolysis, while the former is only a catalytic peak related to the hydrogen discharge catalyzed by protonated cationic species of the acid, on whose diffusion the current depends, as shown by the values of n in the equation $I_p = k' V^n$, close to the theoretical 0.5 for only diffusion controlled processes.

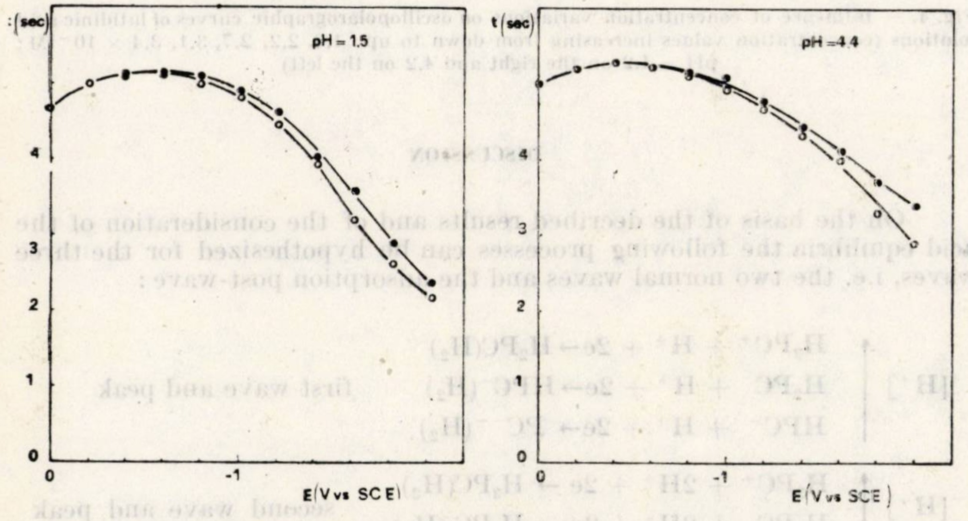

Fig. 5. — Electrocapillary curves at the indicated pH values in the presence (curves down) and in the absence (curves up) of lutidinic acid ($c = 10^{-3}$ M).

More from the study of the variations of the current of the first peak with the free acidity it can be calculated as 0.25 the value of pK for the protonation equlibrium (Fig. 6)

$$H_2PC + H^+ \rightarrow H_3PC^+$$

Finally the observation that Ilkovic and Randles-Sevcik equations ensuring proportionality respectively between wave or peak current and lutidinic acid concentration are followed at least for one process shows the possibility of quantitative polarographicanalysis for the considered acid.

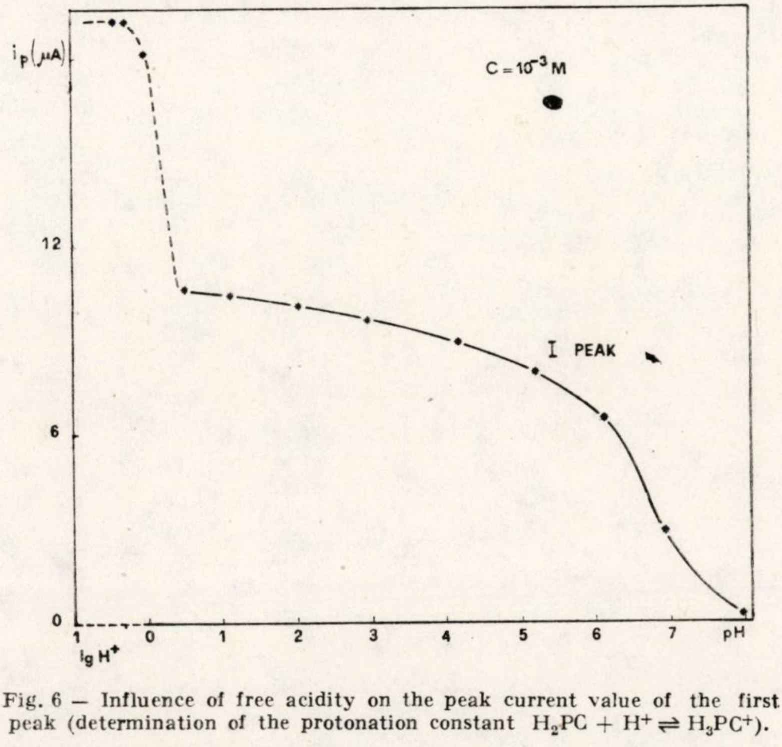

Fig. 6 — Influence of free acidity on the peak current value of the first peak (determination of the protonation constant $H_2PC + H^+ \rightleftharpoons H_3PC^+$).

ACKNOWLEDGEMENT. Work carried out with the aid of Italian CNR

REFERENCES

[1] A. G. Pozdeeva and E. G. Novikov, *Zhur. priklad Khim.*, **40**, 213 (1967).
[2] J. Volke and V. Volkova, *Coll. Czech. Chem. Comm.*, **20**, 908 (1955).
[3] J. Volke and V. Volkova, *Coll. Czech. Chem. Comm.*, **20**, 1332 (1955).
[4] J. Volke, *Chem. Listy*, **49**, 1236 (1955).
[5] L. Campanella and G. De Angelis, *Rev. Roumaine Chim.*, **16**, 545 (1971).
[6] L. Campanella, P. L. Cignini and G. De Angelis, *Rev. Roumaine Chim.*, **18**, 1269 (1973).
[7] L. Campanella and G. De Angelis, *Rev. Roumaine Chim.*, **17**, 1087 (1972).
[8] L. Campanella, P. L. Cignini and F. Croce, *Rev. Roumaine Chim.*, **20**, 855 (1975).
[9] L. Campanella, P. L. Cignini and G. De Angelis, *Rev. Roumaine Chim.*, **18**, 1649 (1973).
[10] L. Campanella, E. Chiacchierini and M. Palchetti, *Rev. Roumaine Chim.*, **17**, 647 (1972).
[11] L. Campanella, M. T. Benignetti and P. Mazzoni, *Rev. Roumaine Chim.*, **24**, 493 (1979).
[12] L. Campanella, *Rev. Roumaine Chim.*, **24**, 1203 (1979).
[13] V. D. Canic, *Ber. chem. Ges. Belgrad*, **20**, 29 (1957).
[14] K. Yamasaki and K. Yasuda, *Naturwiss*,. **41**, 84 (1918).
[15] H. Hopff and A. Krilger, *Helv. Chim. Acta*, **44**, 1058 (1961).
[16] L. Ya. Kheifets, *Zhur. analit. Khim.*, **20**, 355 (1965).

Revue Roumaine de Chimie 27, 8, 981–986 (1982)

DETERMINACIÓN GRAVIMÉTRICA DE ORO MEDIANTE LA FORMACIÓN DEL PAR IÓNICO $[AuI_4^-]$ $[(C_4H_9)_4N^+]$

J. HERNÁNDEZ MÉNDEZ, A. ALONSO MATEOS, E. J. MARTÍN MATEOS y
C. GARCÍA de MARÍA
Departamento de Química Analítica. Facultad de Química. Universidad de Salamanca.
España

Recibido el 26 de Febrero de 1981

El complejo tetraiodoaurato (III) forma con el ion tetrabutilamonio un compuesto de asociación iónica insoluble en agua. En las condiciones experimentales deducidas en este trabajo, este compuesto presenta una estequiometría definida, $[AuI_4^-][(C_4H_9)_4N^+]$, y puede servir para la determinación gravimétrica de oro. El factor gravimétrico 0.2079, es más favorable que todos los que aparecen en bibliografia y permite determinar cantidades de oro del orden de 20 mg con un error inferior al 0.6 %. Se propone un procedimiento con el que quedan eliminadas la mayor parte de las interferencias.

The tetraiodoaurate (III) complex forms a water insoluble ionic-association compound with the tetrabutylammonium ion. This compound shows a definite stoichiometric composition $[AuI_4^-]$ $[(C_4H_9)_4N^+]$, at the optimal deduced conditions. So that, this compound can be used for the gravimetric determination of gold. The very favourable gravimetric factor, 0.2079, enables us to determine gold amounts in the order of 20 mg with a smaller than 0.6 % error. An almost without interferences procedure is proposed.

INTRODUCCIÓN

Los métodos de determinación gravimétrica de oro pueden clasificarse en dos grupos perfectamente diferenciados: 1. *Reducción a metal:* comprende los procedimientos basados en la utilización de agentes reductores que depositan el oro en estado metálico, el cual es pesado posteriormente. Estos métodos presentan diversos inconvenientes: por un lado el factor gravimétrico no es favorable; por otro, el oro se obtiene en partículas muy pequeñas que se adhieren con facilidad a las paredes de los recipientes. Entre los reductores utilizados están: ácido oxálico, sulfato ferroso, dióxido de azufre, peróxido de hidrógeno, cloruro estannoso, dimetilglioxima y ácido fórmico. II. *Precipitación con reactivos orgánicos:* este grupo comprende los procedimientos basados en la precipitación del oro en forma de sal orgánica insoluble. Generalmente, los precipitados formados no son estequiométricos, por lo que se requiere su ignición hasta metal.

Las sales de amonio cuaternario solubles en agua dejan en solución un catión voluminoso capaz de formar, con aniones también voluminosos, compuestos de asociación iónica que poseen a veces las propiedades necesarias (baja solubilidad, estequiometría, estabilidad, etc) para ser utilizadas como forma pesable en gravimetría. En cualquier caso presentan factores gravimétricos favorables debido a su elevado peso molecular.

Los trabajos encontrados en bibliografía acerca de la utilización de estos compuestos son escasos. Así, el yoduro de trimetilfenilamonio fue utilizado por primera vez por Pass y Ward[1] en un método volumétrico de determinación de cadmio; posteriormente Burkhalter y Solarek[2] lo utilizaron en el análisis volumétrico de bismuto y por último White y Zuber[3] en la determinación gravimétrica de oro, pesando al final el par iónico formado resultando un factor gravimétrico de 0.2342.

En este Departamento se inició hace unos años una línea de trabajo sobre la utilización analítica de las sales de amonio cuaternario. En el primer trabajo publicado[4] se realizó la determinación de Pb(II) por precipitación de su complejo $Pb(SCN)_3^-$ con cloruro de tetrabutilamonio y posterior determinación volumétrica del SCN^- de dicho compuesto mediante reacciones de amplificación.

En el presente trabajo se estudia la precipitación del complejo tetraiodoaurato (III) y su aplicación a la determinación gravimétrica de oro.

PARTE EXPERIMENTAL

Reactivos

Soluciones de Au(III) preparadas a partir de oro metálico de 99.99 % de pureza (Merck) disuelto en agua regia, con eliminación del ácido nítrico en exceso por colentamiento hasta casi sequedad y posterior dilución. Soluciones de yoduro de tetrabutilamonio 0.025 M, 0.05 M y 0.1 M preparadas a partir del producto sólido (BDH). Soluciones de diferentes cationes metálicos para el estudio de interferencias, preparadas a partir de los respectivos productos sólidos en calidad R. A. Acido nítrico, sulfúrico y clorhídrico en calidad R. A.así como yoduro potásico y citrato sódico.

APARATOS

Además del material corriente de laboratorio se utilizó una estufa de vacío marca Ionos 300 en la que se trabajó a una presión de 690 mmHg.

PROCEDIMIENTO

Se forma el complejo tetrayodoaurato (III) mediante adición de exceso de yoduro potásico en forma sólida sobre la solución que contiene oro y se lleva a cabo la precipitación por posterior adición de la sal de amonio cuaternario. Los precipitados así obtenidos se filtran, lavan y secan operando en todos los casos en las condiciones óptimas deducidas. Exceptuando la variable en estudio se operó siempre en las siguientes condiciones : Au(III) puesto, 78.32 mg ; IK 0.7—1 M ;amonio cuaternario 0.1M : pH = 5 : volumen aproximado 25 ml.

RESULTADOS Y DISCUSION

Características morfológicas del precipitado

Al añadir cloruro de tetrabutilamonio sobre el complejo yodurado se forma un precipitado pardo-naranja que se deposita fácilmente, dando por agitación partículas mayores, fáciles de filtrar. Si la precipitación se lleva a cabo en medio ácido se observa la aparición de I_2, por lo que, en principio, se trabaja al pH de los reactivos, próximo a 5. En cuanto a la influencia de la temperatura en la obtención de un mejor precipitado se refiere, se comprueba que la morfología del mismo mejora a bajas temperaturas, como era de esperar debido al caracter tensoactivo del reactivo precipitante. Además, al aumentar la temperatura de la solución y hacerlo la tensión superficial, el riesgo de que parte del precipitado quede adherido a las paredes del recipiente es mayor.

Influencia de la temperatura de secado

A fin de conocer el comportamiento térmico del precipitado, se preparan diferentes muestras que una vez filtradas y lavadas se someten a temperaturas comprendidas entre 20 y 70°C operando en estufa de vacio a 690 mmHg. El peso final obtenido es prácticamente el mismo para temperaturas comprendidas entre 20 y 50°C, disminuyendo gradualmente por encima de estos valores, debidos a la descomposición de la sal de amonio cuaternario. El sólido obtenido, una vez secado, no es higroscópico.

Influencia del pH

Se efectua un estudio de la influencia del pH operando a valores comprendidos entre 1 y 6. Estos valores se logran mediante adición cuidadosa de ClH o NH_3 y posterior medida potenciométrica. Los precipitados obtenidos, una vez filtrados se lavan con tolueno para disolver el posible I_2 formado por oxidación atmosférica y se secan a 50°C hasta peso constante. Los resultados obtenidos se muestran en la Tabla 1 y de ellos se deduce, como era de esperar, que cuanto más ácido es el medio menor es el peso del precipitado, como consecuencia de la disminución de la concentración de Au(III) por reacción de óxido-reducción con el yoduro. Estos resultados indican igualmente que a partir de pH 4 no se produce, al menos de modo apreciable, esta reacción de óxido-reducción.

TABLA 1

Influencia del pH del medio

pH	Precipitado mg
1	200.2
2	260.6
3	300.4
4	376.6
5	376.9
6	376.2

Influencia de la concentración de amonio cuaternario

Para el estudio de la influencia de esta especie se modifica su concentración entre 0.4 y 2.0 mmoles (en los 25 ml de solución). Los precipitados obtenidos se lavan primero con agua y después con tolueno, secándose hasta peso constante a 50°C. Los resultados obtenidos (Tabla 2) ponen de manifiesto que al aumentar la

TABLA 2

Influencia de la concentración$(Bu)_4N^+$

$(Bu)_4N^+$ milimoles	Precipitado mg
0.4	160.6
0.8	240.8
1.2	350.6
1.6	376.9
1.8	376.6
2.0	376.9

concentración de $(But)_4N^+$ aumenta también el peso del precipitado hasta que la sal de amonio alcanza el valor de 1.6 mmoles (0.03 M), valor a partir del cual la cantidad de precipitado se mantiene constante.

Se pueden poner concentraciones superiores de sal de amonio cuaternario, pero no es conveniente realizar la precipitación en presencia de grandes excesos de esta especie, ya que se contamina el precipitado, requiriéndose entonces reiterados lavados del mismo. En ninguno de los casos estudiados se apreció la aparición de I_2 en la solución.

Influencia de la concentración de yoduro

De forma análoga a lo que ocurre al variar la concentración de $(Bu)_4N^+$, al estudiar la influencia de la concentración de IK (Tabla 3), también se observa un aumento de la cantidad de precipitado obtenido al incrementar la concentración de yoduro : a partir de 0.16 M los valores de los pesos se hacen constantes. Teniendo en cuenta la concentración de Au(III) puesto y suponiendo que se forma el anion AuI_4^-, la cantidad de I^- libre necesaria para obtener peso constante resulta ser de 0.1 M.

TABLA 3

Influencia de la concentración de IK

IK milimoles	Precipitado mg
1.6	160.6
2.0	202.4
2.4	210.6
3.4	302.4
4.0	376.4
4.5	376.9
5.0	376.4

Para todas las concentraciones de yoduro estudiadas, tanto el color como el aspecto del precipitado son idénticos, de lo que podría deducirse que en todos los casos el compuesto de asociación iónica formado es el mismo. Este hecho no es de extrañar, dadas las escasas posibilidades de formación de otros complejos yodurados de oro que presenten cargas negativas.

Determinación del factor gravimétrico

Teniendo en cuenta las condiciones óptimas deducidas en los apartados anteriores se ha procedido a determinar el factor gravimétrico del sólido obtenido operando en las siguientes condiciones : pH = 5, $(Bu)_4N^+$ 0.1 M ; IK 0.16 – 0.3 M ; volumen total 25 ml en todos los casos.

Se preparan soluciones conteniendo Au(III) en cantidades variables entre 40 y 90 mg, procediéndose a su precipitación en las condiciones indicadas, : se secan los precipitados a 50°C en estufa de vacío.

A partir de los datos correspondientes a siete experiencias se obtiene un valor medio para el factor gravimétrico de 0.2079 que corresponde al valor teórico calculado para la estequiometría $AuI_4(But)_4N$:

$$\bar{X} \pm \frac{ts}{N} (90\,\% \text{de P}) = 0.2079 \pm 0.0004$$

Valor teórico para $AuI_4(Bu)_4N = 0.2083$

Margen de aplicabilidad

Con el fin de determinar el margen de aplicabilidad a la determinación gravimétrica de oro, se preparan soluciones conteniendo entre 18 y 199 mg de dicho metal como complejo clorurado y, después de formar el complejo yodurado, se precipita con sal de amonio cuaternario en las condiciones experimentales adecuadas. Los resultados se muestran en la Tabla 4 y como puede comprobarse, para cantidades de oro superiores a 20 mg se obtienen siempre resultados satisfactorios con errores inferiores al 0.6 %.

TABLA 4

Margen de aplicabilidad del método

Au^{3+}		Error %
Puesto mg	Encontrado mg	
19.68	19.90	1.12
39.36	39.59	0.58
59.04	58.96	0.14
78.32	77.92	0.51
98.39	98.35	0.04
18.00	18.30	1.60
36.00	35.84	0.44
54.00	53.76	0.44
72.00	72.40	0.56
90.00	89.89	0.12
25.10	25.25	0.58

Para comprobar la exactitud y precisión del método, se realizan 16 determinaciones sobre otras tantas disoluciones conteniendo 39.36 mg de oro, resultando una desviación estandar relativa de 0.64 %.

El valor experimental de „t" calculado a partir del valor medio experimental y del considerado como verdadero (39.36) es de 0.31, lo que indica una probabilidad mayor del 75 % de encontrar mediante este procedimiento el valor verdadero. La expresión correcta del resultado para un margen de fiabilidad del 90 % es ÷ 0.11 mg.

Estudio de interferencias

Teniendo en cuenta el mecanismo de la reacción, es de esperar la interferencia de todos aquellos iones metálicos que puedan formar precipitados o complejos aniónicos con yoduro o que sean suficientemente oxidantes para pasar el yoduro a iodo. No deben interferir los cationes que no presenten estas propiedades. En este sentido se ha comprobado la no interferencia de Al, Ca, Sr, Mg, Ni, Co, Zn, Mn(II), Cr(III), Cu(II) y Fe(III) — estos dos últimos en presencia de citrato-y, como era de esperar, constituyen interferencia positiva Bi(III), Pb(II), Pd(II), Pt(IV), Ag(I), Cd(II), Tl(I), Sn(IV) y los iones del mercurio.

De todos los cationes interferentes Tl(I) y Ag(I) se separan por precipitación con cloruro en el proceso de disolución de la muestra en agua regia. Después de este paso quedan en disolución Cd(II), Bi(III), Au(III), Pd(II), Hg(II) y parcialmente Pb(II) como complejos clorurados. De todos estos complejos, solamente los de Bi, Au y Hg precipitan como complejos de asociación iónica con cloruro de tetrabutilamonio, siendo éste un procedimiento para separar oro de paladio y platino, elementos que le acompañan corrientemente en sus aleaciones. En la disolución obtenida disolviendo este precipitado en medio ácido se puede llevar a cabo la determinación de Au(III) con yoduro de tetrabutilamonio según el procedimiento descrito. En estas condiciones solamente interfieren Bi(III) y los iones del mercurio.

BIBLIOGRAFIA

[1] A. Pass, y A. M. Ward, *Analyst*, **58**, 667 (1933).

[2] T. S. Burkhalter, y J. F. Solarek *Analyt. Chem.*, **25**, 1125 (1953).

[3] W. W. White, y J. R. Zuber *Analyt. Chem.*, **36**, 2363 (1964).

[4] J.Hernandez-Mendez, A. Alonso-Mateos, E. J. Martin-Mateos, *Analyt. Chim Acta*, **111**, 327 (1979).

Revue Roumaine de Chimie, 27, 8, 987–992 (1982)

A NEW ROUTE FOR DETERMINING THE NONPOLAR SOLUBILITY PARAMETERS OF ORGANIC SOLVENTS BY GAS-LIQUID CHROMATOGRAPHY

MINODORA LECA

Polytechnic Institute of Bucharest, Chemistry Department, Blvd Republicii 13, Romania

Received February 18, 1981

Using the relations between ln V_g and polarizability and ln V_g and molar volumes for n-alkanes, a new way to determine the nonpolar solubility parameter of linear organic solvents from chromatographic retention data on squalane as stationary phase has been developed. This demonstrates the validity of gas-liquid chromatography as a method to determine the nonpolar solubility parameters of volatile compounds. The method is fast, has a high accuracy, requires small amounts of substance, and allows the correction of the nonpolar solubility parameters determined from homomorphism charts.

Gas-liquid chromatography (GLC) has proved to be an accurate technique for measuring thermodynamic properties of very concentrated polymer solutions.[1–5] One of the most important and interesting problems is the identification of various types of intermolecular force interactions between polymer and solute and the determination of their contributions.

Intermolecular interactions between polar molecules are due to the following types of forces: (a) London dispersion forces; (b) permanent dipol moments; (c) quadrupoles and higher multipole moments; (d) hydrogen bonding, charge transfer and coordination forces. Interactions due to the latter types of forces are usually referred to as specific interactions.[6]

Assuming that the cohesive energy $-E$ arises from contributions due to the dispersion or nonpolar interactions $-E_d$, polar interactions (*b* and *c* types) $-E_p$ and hydrogen bonding or similar specific interactions (type *d*) $-E_h$, it can be written as:

$$-E = -E_d - E_p - E_h \tag{1}$$

The square root of the cohesive energy density (CED) was named by Hildebrand[7] solubility parameter. The total solubility parameter δ is related then to the partial solubility parameters δ_d, δ_p, δ_h due to the above contributions by the following relationship:[8,9]

$$\delta^2 = \delta_d^2 + \delta_p^2 + \delta_h^2 \tag{2}$$

The intermolecular forces operating in solutions depend mainly on the chemical composition of the solution components. Thus, if one of the two component mixtures — solute or solvent — is nonpolar, interactions are due to the induced dipole moments that arise from the short lived perturbation of the electron position during or near collision. Interactions due to the dispersion forces are always present in any solute-solvent system. Consequently, using a convenient nonpolar stationary phase the interactions due to the dispersion forces and the corresponding solubility parameters for polar solvents can be obtained from gas-liquid chromatographic data.

RESULTS AND DISCUSSION

The solubility parameter due to the dispersion forces or the nonpolar solubility parameter δ_d have been estimated on the homomorph principle.[10,11] The homomorph of a polar compound is a nonpolar molecule having nearly the same size and shape as that of the polar one. This was applied to the vaporization energy of polar and hydrogen-bonded liquids. The nonpolar component of the vaporization energy of a polar liquid is taken as the experimentally total vaporization energy of the homomorph at the same reduced temperature. Of course, the molar volumes should also be equal for this comparison. This empirical basis for estimating δ_d does not give very accurate results, thus limiting the accuracy of δ_p and δ_h values calculated from equation (2). The values calculated by this procedure were modified for solvents containing halogen or sulfur atoms.[8]

To improve the results, correlations between δ_d and other physical quantities were searched. Keller et al.[12] have recommended an alternative, more fundamental approach to predicting dispersion contribution, based on a relationship between δ_d and the Lorentz-Lorenz refractive index function $\frac{n^2-1}{n^2+2}$ for both nonpolar and slightly polar compounds. Koehnen et al.[13] have found a linear relation between δ_d and n. They also have obtained, using a Lennard-Jones potential for the interaction between the molecules, a relation between the dispersion contribution to the surface tension γ_L^d and δ_d. Both relations were applied to a number of slight polar, polar and hydrogen bonding solvents giving good results.

In a previous paper[14] we suggested the determination of δ_d from gas-liquid chromatographic data. Using squalane—the least selective for n-hydrocarbons[15] — as nonpolar stationary phase, a linear relationship exists between ln V_g (specific retention volume) and carbon numbers C in the normal hydrocarbon series. The data for the $C_5 - C_9$ hydrocarbons (Table 1) give the following equation at the given column temperature (84.5°C) :

$$C = 1.29 + 1.22 \ln V_g \tag{3}$$

The apparent carbon number of a polar linear compound on n-hydrocarbon scale C can be determined by Huebner method,[16] introducing the retention data in equation (3). These apparent carbon numbers are nothing

TABLE 1

Physical quantities and retention data for n-hydrocarbons

Hydrocarbon	V, cm³/mol	$\alpha \times 10^{24}$, cm³	δ, (cal/cm³)$^{1/2}$	$\ln V_g$	α^2	$(\alpha^2/V)^{1/2}$
n-Pentane	116·21	9.63	7.05	3.027	92.74	0.893
n-Hexane	131.60	11.85	7.27	3.858	140.42	1.033
n-Heptane	147.50	13.71	7.42	4.684	187.96	1.129
n-Octane	163.50	15.54	7.55	5.404	241.49	1.215
n-Nonane	179.70	17.42	7.65	6.303	303.46	1.299

else than the homomorphs of the corresponding polar compounds. Energies of vaporization and molar volumes at 25°C being linear function on carbon numbers in the homologous series, the following relation has been found between δ_a and carbon numbers of n-hydrocarbons:

$$(\delta_a)_{25^\circ\mathrm{C}} = \left(\frac{-118 + 1180\,C}{36.31 + 15.91\,C}\right)^{1/2} \tag{4}$$

The C of a polar compound once known, δ_a can be determined (table 2, column 4).

It should be thought that correlation of energies of vaporization and molar volumes at 25°C with apparent carbon numbers of polar compounds at column temperature would give erroneous results for δ_a. But it is well known that C are independent of column temperature and then the correlation is proper. The relation for δ_a at column temperature has been determined to verify that:

$$(\delta_a)_{84.5\,^\circ\mathrm{C}} = \left(\frac{-1326.5 + 1202.5\,C}{50.17 + 15.74\,C}\right)^{1/2} \tag{5}$$

The results are given in table 2, column 5. Then, using the relation $(\delta_a)_{25^\circ\mathrm{C}} - (\delta_a)_{84.5\,^\circ\mathrm{C}}$:

$$(\delta_a)_{25^\circ\mathrm{C}} = 3.6 + 0.575\ (\delta_a)_{84.5} \tag{6}$$

$(\delta_a)_{25^\circ\mathrm{C}}$ were determined (table 2, column 6). The difference between δ_a, calculated in this way, and δ_a, calculated using equation (4), does not exceed ± 0.03 (cal/cm³)$^{1/2}$.

Apparent carbon numbers of polar compounds (see column 3 of table 2) determined by gas-liquid chromatography are a better approximation of the homomorphs and need no correction for solvents containing halogen atoms.

We want to present here another way to revaluate gas-chromatographic data for determination of δ_a.

TABLE 2

Retention data, apparent carbon numbers, δ_d from equations (4), (5), (6), and (12) and literature data for the studied compounds

Compound	$\ln V_g$	C	δ_d (cal/cm^3)$^{1/2}$				
			eqn. 4	eqn. 5	eqn. 6	eqn. 12	Literature [a]
Alcohols							
CH_3OH	1.823	3.51	6.61	5.24	6.58	6.30	7.42 ; 7.75^{d} ; $7.14^{d'}$
C_2H_5OH	2.450	4.28	6.88	5.70	6.87	6.78	7.73 ; 6.80^{c} ; $7.45^{d'}$
n-C_3H_7OH	3.283	5.30	7.14	6.15	7.12	7.11	7.75 ; 7.79^{d} ; $7.68^{d'}$
n-C_4H_9OH	4.111	6.30	7.32	6.47	7.32	7.32	7.81 : 7.79^{d} ; $7.81^{d'}$
n-$C_5H_{11}OH$	4.983	7.37	7.47	6.73	7.48	7.48	7.81 ; 7.87^{d} ; $7.91^{d'}$
n-$C_6H_{13}OH$	5.660	8.19	7.57	6.90	7.57	7.57	7.75
n-$C_7H_{15}OH$	6.456	9.17	7.66	7.06	7.67	7.65	7.70
n-$C_8H_{17}OH$	7.286	10.2	7.74	7.20	7.75	7.73	7.88
Halogenated compounds							
n-C_3H_7Cl	3.241	5.24	7.12	6.12	7.11	7.10	7.75 ; 7.30^{c}
CH_2Cl_2	2.963	4.90	7.04	5.99	7.03	7.01	8.52 ; $8.05^{d'}$
$C_2H_4Cl_2$	3.988	6.15	7.30	6.43	7.29	7.30	8.50 ; $8.25^{d'}$
C_2H_5Br	3.011	4.95	7.05	6.01	7.05	7.02	—
$C_2H_4Br_2$	5.361	7.83	7.53	6.83	7.55	7.53	8.10
CH_2I_2	6.348	9.03	7.65	7.04	7.66	7.64	—
Aldehydes							
CH_2O	2.020	3.75	6.70	5.40	6.66	6.49	7.55^{d} ; $7.37^{d'}$
CH_3CHO	2.687	4.57	6.96	5.84	6.94	6.90	—
C_2H_5CHO	3.393	5.43	7.16	6.19	7.15	7.15	—
$C_6H_{13}CHO$	5.953	8.55	7.60	6.96	7.61	7.60	—
Ketones							
$(CH_3)_2CO$	2.529	4.37	6.91	5.75	6.89	6.82	7.58 ; 7.68^{d} ; $7.42^{d'}$
$(C_3H_8)_2CO$	3.419	5.46	7.16	6.20	7.16	7.16	7.77 ; 7.70^{d}
Amines							
$C_4H_9NH_2$	4.396	6.65	7.37	6.56	7.37	7.38	—
$C_2H_4(NH_2)_2$	4.443	6.71	7.38	6.58	7.38	7.39	7.30
$(CH_3)_2NH$	2.765	4.65	6.98	5.88	6.97	6.93	—
$(C_2H_5)_2NH$	3.228	5.23	9.12	6.12	7.11	7.10	7.30^{b} ; 7.84^{d} ; $7.68^{d'}$
Miscellaneous							
$(C_2H_5)_2O$	2.823	4.73	7.00	5.92	6.99	6.95	7.05 ; 7.30^{c} ; 7.25^{d} ; $7.37^{d'}$
CH_3NO_2	2.842	4.76	7.01	5.93	7.00	6.96	8.03 ; 7.70^{b} ; 7.30^{c} ; 8.22^{d} ; $7.64^{d'}$
HOC_2H_4Cl	4.086	6.27	7.31	6.46	7.31	7.32	—

[a] C. M. Hansen, *J. Paint Technol.*, **39**, 104 (1967).

[b] C. M. Hansen and K. Skaarup, *J. Paint Technol.*, **39**, 505 (1967).

[c] R. A. Keller, B. L. Karger and L. R. Snyder, *Gas Chromatogr., Proc., Int. Symp. (Europe)*, **8**, 125 (1970).

[d] D. M. Koehnen and C. A. Smolders, *J. Appl. Polymer Sci.*, **19**, 1163 (1975), from refractive indexes.

[d'] *ibid.*, from surface tensions.

The main idea is that the interaction energy between nonpolar molecules is dependent on the polarizability. This dependence for dispersion interactions between like molecules is given by the London expression :

$$E_d = -3\alpha^2 I/4r^6 \tag{7}$$

where α is the polarizability of the molecule, I — its ionization potential, and r — the distance between the two molecules. Since I normally varies only slightly from one component to another, E_d should be approximately proportional to α^2 and δ_d to $\alpha/V^{1/2}$, V being the molar volume.

The energy of vaporization of a solute from the stationary phase is equal to its energy of vaporization due to the dispersion forces if the stationary phase is nonpolar. The enthalpy of vaporization from the stationary phase $\overline{H}_{s\to v}$ is related to the specific retention volume V_g of the solute by the relation :

$$\mathrm{d}\ln V_g = -\frac{H_{s\to v}}{RT^2}\,\mathrm{d}T \tag{8}$$

that is it is proportional to ln V_g. It follows then that a linear relationship has to exist between the values ln V_g of n-hydrocarbons on squalane and their α^2 values. Taking the data for n-alkanes given in table 1 a linear relation was obtained indeed, excepting for n-nonane. This agrees with the unreliability of Hildebrand rule, from which most of the δ values were estimated, for the normal hydrocarbons above n-octane and led us to limit our option to compounds containing eight or fewer alkyl carbon atoms. We obtained the following relation for the first four hydrocarbons at column temperature :

$$\alpha^2 = -97.11 + 61.926 \ln V_g \tag{9}$$

The data of table 1 show also a linear relation between δ_d and $\alpha/V^{1/2}$, as expected :

$$\delta_d = 5.66 + 1.555\frac{\alpha}{V^{1/2}} \tag{10}$$

with δ for n-nonane again below the line. For n-hydrocarbons V is a linear function of ln V_g :

$$V = 56.29 + 19.63 \ln V_g \tag{11}$$

and δ_d can be expressed as a function of ln V_g only :

$$\delta_d = 5.66 + \left(\frac{-234.81 + 149.74\ln V_g}{56.29 + 19.63 \ln V_g}\right)^{1/2} \tag{12}$$

The results obtained for the compounds we have examined are shown in table 2, together with available literature data.

The δ_a values obtained using relations (12) and (4) are practically identical, excepting for the low boiling temperature compounds, the maximum difference reaching the value 0.31 $(cal/cm^3)^{1/2}$ for methanol. This demonstrates the reliability of gas-liquid chromatographic method for determination of δ_a.

Table 2 further indicates the conflicting data existing in the literature for δ_a. Our values coincide with those in the literature in a few cases only. The agreement with Keller et al.[12] data is better, but unfortunately we used very few common compounds. It seems that the homomorph charts supraevaluate the δ_a values.

The gas-liquid chromatographic method supplies thus a fast and accurate method to determine the δ_a values of linear polar organic solvents.

Selecting adequate nonpolar references the method can be extended to determine the nonpolar solubility parameters of solvents having any molecular shape.

The experimental part is described in the paper.[14]

REFERENCES

[1] A. J. B. Cruickshank, M. L. Windsor, and C. L. Young, *Proc. Roy Soc., Ser. A*, **295**, 259 (1966).

[2] A. J. B. Cruickshank, W. B. Gainey, and C. L. Young, *Trans. Faraday Soc.*, **64**, 337 (1968).

[3] E. F. Meyer, *J. Chem. Educ.*, **50**, 191 (1973).

[4] O. Smidsrød and J. Guillet, *Macromol.*, **2**, 272 (1969).

[5] W. R. Summers, Y. B. Tewary, and H. P. Schreiber, *Macromol.*, **4**, 356 (1971).

[6] S. Dinçer and D. C. Bonner, *Macromol.*, **11**, 107 (1978).

[7] J. H. Hildebrand and R. L. Scott, "The Solubility of Non-Electrolytes", 3rd ed., Dover, New York, 1949.

[8] C. M. Hansen, *J. Paint Technol.*, **39**, 104 (1967).

[9] C. M. Hansen and K. Skaarup, *J. Paint Technol.*, **39**, 505 (1967).

[10] R. F. Blanks and J. M. Prausnitz, *Ind. Eng. Chem., Fundamentals*, **3**, 1 (1964).

[11] C. M. Hansen, *Ind. Eng. Chem., Product Research and Development*, **8**, 2 (1969).

[12] R. A. Keller, B. L. Karger, and L. R. Snyder, *Gas Chromatogr., Proc. Int. Symp. (Europe)*, **8**, 125 (1970).

[13] D. M. Koehnen and C. A. Smolders, *J. Appl. Polymer Sci.*, **19**, 1163 (1975).

[14] M. Leca, M. Surmeian, and L. Groswald-Cremer, *Rev. Chim. (București)*, **30**, 172 (1979).

[15] H. M. Tenney, *Analyt. Chem.*, **30**, 2 (1958).

[16] V. R. Huebner, *Analyt. Chem.*, **34**, 488 (1962).

Revue Roumaine de Chimie, 27, 8, 993–997 (1982)

ANALYSIS OF TERNARY ALLOYS CONTAINING Co(II), Ni(II) and Cu(II)

A. F. SHOUKRY*, A. I. ABDEL-RAHMAN and N.T. ABDEL-GHANI
Chemistry Department, Faculty of Science, University of Cairo, Egypt

Received April 20, 1981

Nitrosochromotropic acid, 4-5-dihydroxynaphthalene-2-7-disulphonic acid-3-nitroso, was found to be a precise visual indicator in EDTA titrations of Co(II), Ni(II) and Cu(II) cations. A number of alloys containing these cations were analysed. These alloys are "Conico" (50 % Cu, 29 % Co & 21 % Ni), "Colorado Metal" (57 % Cu, 25 % Ni & 18 % Zn), "German Silver" (55 % Cu, 20 % Ni and 25 % Zn), "Nickel Silver Grade A" (65 % Cu, 18 % Ni and 17 % Zn), "Nickel Silver Grade B" (55 % Cu, 18 % Ni and 27 % Zn) and "Nickel Silver Rolling" (49 % Cu, 12 % Ni and 39 % Zn).

Nitrosochromotropic acid (NCA) complexes with a number of metal ions were studied.[1-3] Copper was determined[4] and its alloy with zinc and tin was analysed[5] using NCA as a metallochromic indicator. The present work comprises EDTA titrations involving the utilisation of NCA as indicator for the analysis of a number of industrially important alloys[6] including Conico (50 % Cu, 29 % Co and 21 %Ni) which is used in making magnets for electrical equipments. Colorado Metal (57 % Cu, 25 % Ni and 18 % Zn) utilised for the production of electrical resistance and corrosion resistant parts of some machines, German Silver (55 % Cu, 20 % Ni and 25 % Zn), Nickel Silver Grade A (65 % Cu, 18 % Ni and 17 % Zn) and Nickel Silver Grade B (55 % Cu, 18 % Ni and 27 % Zn). The last three alloys are used for making cutlery, cheap jewelry, resistance wire and are fairly good corrosion resistants. Nickel Silver Rolling alloy (49 % Cu, 12 % Ni and 39 % Zn) used for the manufacture of sheets, rolled parts and corrosion resistant products is also analysed.

EXPERIMENTAL

NCA was prepared as previously described[3] and its composition and purity were confirmed by chemical and IR-analysis. All other chemicals were of Analar grade provided by BDH, England. The 0.001 M solutions of Co(II), Ni(II) and Cu(II) nitrates were prepared by diluting previously standardised[7] 0,05 M stock solutions. For testing the interfering effect, solutions containing 1 mg anion or cation were used. The alloys were dissolved by the usual technique of aqua regia.

The EDTA titrations were carried out using a 5 ml 1/50 microburette. The EDTA solution was always two times as concentrated as the metal ion to be titrated. The titration was characterized by a sharp colour change from violet, purple or orange red to yellow in the case of Co^{2+}, Ni^{2+} and Cu^{2+}, respectively at pH 10 and from orange red to yellow in the case of Cu^{2+}

at pH 5. Among the universal, acetate and hexamine buffers, the modified Britton and Robinson universal one was the best. The required buffers were prepared after reported methods[8] using Corning pH meter 113.

The formation and composition of NCA complexes with Co(II), Ni(II) and Cu(II) were studied spectrophotometrically in the visible range (300—700 nm) using SP—1750 Pye-Unicam recording spectrophotometer.

RESULTS AND DISCUSSION

The optimal pH values for development of the violet complexes of NCA with Co(II) and Cu(II) are 10 and 5, respectively. At pH 10, NCA also forms purple complex with Ni(II) and orange red complex with Cu(II) (Table 1). At the recommended pH values, the absorption spectra of the yellow NCA measured against water and those of the complexes measured tagains water and ligand, show that the complexes exhibit invariably absorption maxima well separated from the maxima of the NCA (Table 1). Representative spectra are shown in Fig. 1.

All complexes are formed instantaneously and their absorbances remain constant for 24 hrs. Limits of obedience to Beer's law and the absorptivities of the complexes are given in Table 1.

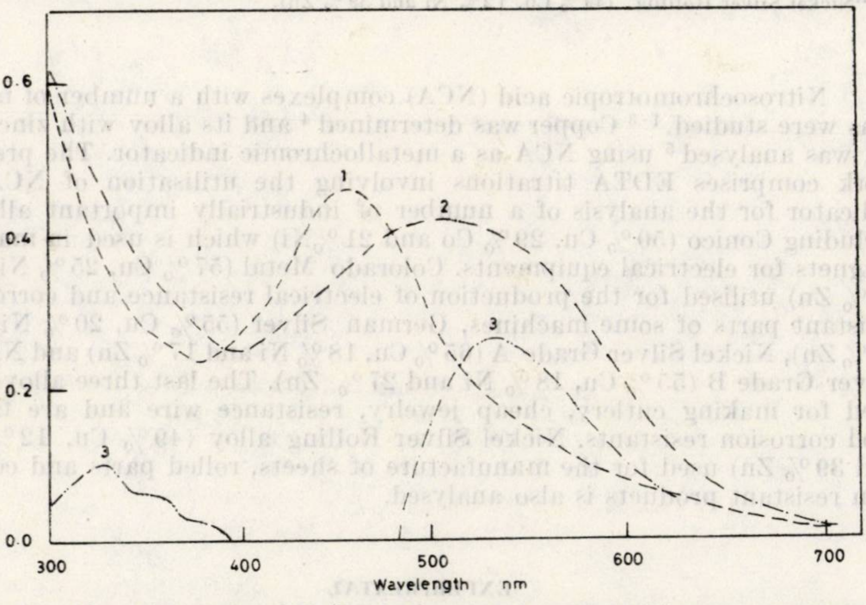

Fig. 1.— Absorption spectra of 10^{-4}M solutions of NCA and its Ni(II) complex at pH 10 : 1.NCA against water ; 2. 1:1 (M: L) complex against water ; 3. 1: 1 (M : L) complex against NCA.

Investigation of the complexes by the conventional molar ratio, continuous variation and slope ratio methods is represented by the results given in table 2. The logarithmic values of the stability constants of the complexes as calculated from the molar ratio and continuous variation methods [9] are also listed.

TABLE 1

Optimal pH, λ max, obedience to Beer's law and optimum concentration range for the EDTA titrations

M pH	Colour	NCA λ max nm	Complex		Beer's law ppm	Optimum concentration range	
			Blank water λ max nm	Blank ligand λ max nm		λ max	Molar
Co 10	Violet	453	575	610	0.23–2.36	7756	$0.5\times10^{-4}-0.95$
Ni 10	Purple	453	510	530	0.25–2.50	8200	$10^{-3}-0.85$
Cu 10	Orange red	440	500	520	0.29–3.68	8350	$10^{-3}-0.80$
5	Violet	453	540	560	0.32–3.48	7142	$0.5\times10^{-4}-0.95$

TABLE 2

The apparent stability constants of metal ion complexes with NCA

Complex	pH	Molar ratio	n	log β_n
Co–NCA	10	1:2	2	7.54
		1:3	3	11.53
Ni–NCA	10	1:1	1	4.29
		1:3	3	11.52
Cu–NCA	10	1:2	2	7.99
	5	1:3	3	12.51

A systematic study of the influence of foreign ions can be summarised as follows:

For cobalt complexes: Li^+, Na^+, K^+, Ba^{2+}, Sr^{2+}, Hg^{2+}, Cd^{2+}, Mn^{2+}, Zn^{2+}, Pb^{2+}, Fe^{3+}, Al^{3+}, Ga^{3+}, Bi^{3+}, Cl^-, Br^-, I^-, CH_3COO^-, NO_3^-, SO_4^{2-}, $B_4O_7^{2-}$ and PO_4^{3-} have almost no influence when present in 20-fold amounts relative to cobalt. Ca^{2+}, Ni^{2+}, Cu^{2+}, UO_2^{2+}, In^{3+}, Cr^{3+}, Th^{4+}, oxalate, succinate, EDTA and CDTA interfere.

For nickel complexes: Li^+, Na^+, K^+, Ca^{2+}, Ba^{2+}, Sr^{2+}, Cd^{2+}, Mn^{2+}, Pd^{2+}, Zn^{2+}, Al^{3+}, Ga^{3+}, In^{3+}, Cl^-, Br^-, I^-, CH_3COO^-, NO_3^-, SO_4^{2-}, and $B_4O_7^{2-}$ do not interfere when present up to 20-fold amount. Hg^{2+}, Co^{2+}, Cu^{2+}, UO_2^{2+}, Bi^{3+}, Cr^{3+}, Fe^{3+}, Th^{4+}, oxalate, succinate, EDTA and CDTA interfere.

For copper complexes: Li^+, Na^+, K^+, Ca^{2+}, Ba^{2+}, Sr^{2+}, Cd^{2+}, Mn^{2+}, Zn^{2+}, Pb^{2+}, Al^{3+}, Ga^{3+}, In^{3+}, Cl^-, Br^-, I^-, CH_3COO^-, NO_3^-, SO_4^{2-}, $B_4O_7^{2-}$, and PO_4^{3-} in 20-fold amounts do not interfere. Hg^{2+}, Co^{2+}, Ni^{2+}, UO_2^{2+}, Cr^{2+}, Bi^{2+}, Fe^{3+}, Th^{4+}, oxalate, succinate, EDTA and CDTA interfere.

The use of NCA as metallochromic indicator. At pH 10, NCA can be used as visual indicator in normal EDTA titration of Co(II), Ni(II) and Cu(II) ion solutions. The equivalent point is characterized by sharp colour change from violet, purple or orange red to yellow in the case of the three cations, respectively. On the other hand, at pH 5, copper only can be titrated with EDTA using NCA as indicator. The end point in this case shows a sharp colour change from violet to yellow. The results of the determinations show high accuracy and precision as the standard deviation does not exceed ± 0.05 in any case. The sharpness of the stability constants of the metal ion complexes of EDTA[10] (log k_1 = 18.8, 18.5 and 16.1 for Co(II), Ni(II) and Cu(II) complexes at pH 10, respectively) with those obtained for their complexes with NCA (Table 2). It is clear that the EDTA complexes have much higher log k_1^r than log β_n (where n is the maximum number of NCA molecules per metal ion) of the corresponding NCA complexes.

The difference (log k_1^r − log β_n) amounts to 7.27, 6.98 and 8.11 in the case of Co(II), Ni(II) and Cu(II) complexes, at pH 10, respectively. This explains why NCA can be used as excellent metallochromic indicator for titration of these metal ions.

Binary mixtures of Co^{2+} and Cu^{2+} or Ni^{2+} and Cu^{2+} are analysed by performing EFTA titrations at different pH values using NCA as indicator. The metal content was determined by titrating the mixture, at pH 10, with EDTA in the presence of NCA as indicator. The equivalence point is colour change from reddish-violet to yellow in the case of $Co^{2+} - Cu^{2+}$ mixture and from purple-red to yellow in the case of $Ni^{2+} - Cu^{2+}$ mixture. To determine the content of Cu^{2+} ions only in each of the two mixtures, the pH value of another solution portion is adjusted to 5 and then titrated with EDTA using NCA as indicator. The end point is sharp colour change from violet to yellow.

Analysis of the alloys. To analyse the Conico alloy (50 % Cu, 29 % Co and 21 % Ni) the pH value of the solution is adjusted to 10 and Ni^{2+} is separated and determined gravimetrically using dimethylglyoxime as a precipitating agent. The filtrate which contains Co^{2+} and Cu^{2+} is divided into two portions and analysed as described above. The results are given in Table 3.

TABLE 3

Determination of Co(II) and Cu(II) in some alloys by EDTA titrations using NCA as indicator

Alloy	pH	Results
Conico	10	Co % Calc. = 29.00, Found = =28.80±0.07.
	5	Cu % Calc. = 50.00, Found = = 49.93±0.04
German silver	10	Cu % Calc. = 55.00, Found = = 55.08±0.05
Nickel silver rolling	10	Cu % Calc. = 49.00, Found = = 48.96±0.07

Other alloys which are analysed by separating nickel dimethylglyoximate are Colorado Metal, German Silver, Nickel Silver Grade A, Nickel Silver Grade B and Nickel Silver Rolling. In all these alloys, copper is determined by EDTA titration using NCA as indicator in the presence of

Zn^{2+} which does not interfere. The total metal ion concentration is determined by adding a known excess of EDTA solution and back titrating, potentiometrically, the excess EDTA with standard zinc solution. Representative results of the analysis of alloys are given in Table 3. The standard deviation values are calculated from 10 determinations in each case.

REFERENCES

[1] S. K. Datta and P. Ghose, *Naturwiss*, **45**, 516 (1958).
[2] A.C.S. Costa, *Anais Assoc. Brasil Quim*, **20**, 85 (1961).
[3] L. Sommer and J. Haki, *Mikrochim. Technoanal. Acta*, **1963**, 270.
[4] A. B. Sen and T. S. Srivastava *Z. analyt. Chem.*, **187**, 401 (1962).
[5] S. K. Datta and S. N. Saha, *Indian J. Appl. Chem.*, **27**, 7 (1964).
[6] N. E. Woldman, "Engeneering Alloys" 5th Ed., Van Nostrand, Reinhold, New York, 1973.
[7] F. J. Welcher, "The Analytical Uses of Ethylenediaminetetraacetic Acid", Princeton, Van Nostrand, New York, 1965.
[8] H. T. S. Britton, "Hydrogen Ions" 4th Ed., Chapman & Hall, London, 1952.
[9] A. E. Harvey and D. L. Manning, *J. Amer. Chem. Soc.*, **72**, 44 (1950).
[10] F. Basolo and R. G. Pearson, "Mechanism of Inorganic Reactions", Wiley, London, 1960.

SESSION OF THE ACADEMY OF THE SOCIALIST REPUBLIC OF ROMANIA OF JUNE 16, 1982

Address by Prof. Dr. V.E. SAHINI,
corresponding member of the Academy

The remarkable scientific and technological development at the end of this century, the almost pathological character of the arms race and mainly of the nuclear arms race, has made of the most valuable asset of mankind, i.e., peace, a function of the precarious stability of the atomic terror. If we were to believe the Latin saying *Si vis pacem para bellum,* it would seem that the aspiration for peace is stronger today than ever before ! Indeed, never were arsenals more piled up with arms of such great technicality and power of destruction. The insane arms race hovers like a gloomy spectre over the destiny of civilization and it urges us to reflect in a responsible manner upon the very disturbing problems involved by the use of modern science and technology to other ends than the progress of humanity.

Nowadays, peace is strictly conditioned by the global interdependence among states, and none of these states is invulnerable anymore. This situation is expected to generate a deep sense of solidarity among peoples, a clear-sighted analysis showing that mankind is going through a nightmare of impeding total destruction, that risks are admitted in cold blood, that an important share of the financial, economic, scientific and technical effort goes to war preparations. A significant part of the world's specialists are involved in activities of arms research and production, a state of things that seriously questions the spiritual and moral values of today's intelligentsia. Scientific progress has always posed important ethical problems. More than ever before, these problems cannot be overcome without taking into account the value of human life, without the individual endeavour to re-define oneself, to clear up one's own position versus other human beings, to reconsider more deeply and far-reaching the sense of one's belonging to humanity. That is why Kant's categorical imperative — a highly moral law and a profound expression of human solidarity, of respect for human dignity — has never been more topical than it is today.

After the painful experience of the last two world wars, the fatalist acceptance of the imminence of a new conflagration, no mater how "modest" and "local" it might be at the beginning, is absurd. One cannot be at ease when one comes to think that the huge military "investment" made over the past few decades, can only push us to disaster, if efficient means able to neutralize this terrible force of destruction cannot be found. Securing peace, not merely as the absence of war, but as the most genuine expression of what is human in people, cannot be achieved by speeding up the arms race, but by stopping it altogether, by disarmament and arms control, by political solutions searched for at government level, by the involvement of the broad masses of people, by an appeal to public conscience. Avoiding armed conflicts means ensuring the conditions capable to eradicate the causes generating them such as economic underdevelopment, social injustice, famine a.s.o. In a world of contradictions, in which state aggression and assault upon the individual persons though indignantly condemned continue to be current events, the mobilization of public opinion and, first and foremost, of scientists, who have a great responsibility for the future of mankind, is of paramount importance for the implementation of the most effective means to control the huge destructive power of arms, of nuclear ones, in particular.

As intellectuals, we start by acknowledging that especially today peace must be viewed as one of the highest achievements of human culture and that maintaining peace is a moral imperative requiring the material and moral effort of the whole society.

Scientists in general and those working in the area of the natural and technical sciences, in particular, enjoy a high moral credit and have a great responsibility due to the spectacular results of their work : also, due to them the ethic value has come to be considered the primordial asset of any human activity, therefore they can be justified only provided they are placed in the service of mankind. In order to do credit to its calling, science must intertwine with conscience and in this way commit itself to the defence of peace, to the use of its achievements for the benefit of mankind, of life, of progress and civilization.

ORSZÁGOS MŰSZAKI INFORMÁCIÓS KÖZPONT ÉS KÖNYVTÁR
88

NOTE POUR LES AUTEURS

La Revue Roumaine de Chimie publie des articles en anglais, français, russe, allemand ou espagnol. Les auteurs sont priés d'envoyer des articles et des comptes rendus inédits.

Les manuscrits seront dactylographiés à double interligne. La bibliographie, les tableaux et la légende des figures seront placés après le texte.

Si l'article fait partie d'une série numérotée, la partie précédente sera donnée comme première référence.

Chaque article sera précédé d'un résumé comprenant quinze lignes au maximum.

Les références bibliographiques dans le texte seront faites par des exposants sans parenthèses et paraîtront à la fin de l'ouvrage.

Les publications périodiques mentionnées dans la bibliographie seront présentées suivant les prescriptions internationales : le nom de l'auteur précédé de l'initiale du prénom, le titre du périodique abrégé conformément à « Chemical Abstracts » et souligné par une ligne, le numéro du tome indiqué par des chiffres arabes et souligné par deux lignes, suivi de la première page de l'article ; à la fin, l'année de la parution sera placée entre parenthèses. Le numéro de la revue ne sera pas indiqué si les pages du volume sont numérotées consécutivement.

Les textes des livres ou traités inclueront : le nom des auteurs, l'initiale du prénom, le titre du livre entre guillemets et sans être souligné, le numéro du tome précédé par l'abréviation « vol. » (ou «Bd. »), le numéro de l'édition, les éditions (the publisher), la localité de la parution du livre, l'année de la parution et la page de la référence précédée(s) par l'abréviation « p » (ou « S»).

Les brevets seront indiqués comme suit : l'auteur ou la firme le pays et le numéro du brevet, la date et la revue (*Chem. Abstr.*). Par ex. : M. Jones (to Union Carbide Co.), Brit. Pat. 601 238, 2 sept. 1959 ; cf. *Chem. Abstr.*, **54**, 12808 (1960).

Si la référence n'a pas été lue en original, on indiquera aussi la revue de références consultée.

Les diagrammes seront tracés à l'encre de Chine sur papier calque. Les tableaux et les figures (en nombre strictement nécessaire) ainsi que les courbes dans les figures seront numérotés par des chiffres arabes. Leur explication sera donnée dans la légende des figures. Prière de ne pas inscrire les mêmes données dans les tableaux et les figures. Chaque tableau aura un titre. On indiquera dans le texte la place approximative des tableaux et des figures. Les formules chimiques seront incluses dans le texte ; en outre, elles seront transcrites sur papier calque, à l'encre de Chine.

Les auteurs sont priés d'indiquer les caractères italiques (en soulignant les lettres au crayon), ainsi que tout autre caractère spécial ; les préfixes *ortho*, *meta*, *para*, *cis*, *trans*, etc. seront soulignés pour indiquer leurs caractères italiques et ne seront jamais écrits avec des majuscules.

Aucune correction à la main ne sera admise sur le manuscrit. Les corrections seront tapées à la machine. Les lettres grecques ou d'autres symboles spéciaux seront insérés à la main à l'encre clairement.

Le manuscrit sera signé par l'auteur.

Le titre-courant aura 50 lettres au maximum.

L'entière responsabilité du contenu des articles appartient aux auteurs.

Sur demande on peut obtenir une note plus complète.

PRINTED IN ROMANIA

933 FEB 17

TRAVAUX PARUS AUX ÉDITIONS DE L'ACADÉMIE DE LA RÉPUBLIQUE SOCIALISTE DE ROUMANIE

ELENA CEAUŞESCU, **Noi cercetări în domeniul compuşilor macromoleculari** (Nouvelles recherches dans le domaine des composés macromoléculaires), 1981, 536 p.

I.G. MURGULESCU, RODICA VÎLCU, **Introducere în chimia fizică, Vol. III. Termodinamica chimică** (Introduction à la chimie physique, Vol. III, Thermodynamique chimique), 1982, p. 626.

I.G. MURGULESCU, J. PĂUN, **Introducere în chimia fizică, Vol. I.3. Nucleul atomic, reacţii nucleare, particule elementare** (Introduction à la chimie physique. Vol. I.3. Noyau atomique, réactions nucléaires, particules élémentaires), 1982, 606 p.

ELENA JERCAN, **Analiza cromatografică** (Analyse chromatographique), 1982, 286 p.

I.G. MURGULESCU, TATIANA ONCESCU, E. SEGAL, **Introducere în chimia fizică, vol. II. Cinetică chimică şi cataliză** (Introduction à la chimie physique. Vol. II. 2, Cinetique chimique et catalyse, 1981, 1024 p.

V. DRĂGUŢAN, A.T. BALABAN, M. DIMONIE, **Metastaza olefinelor şi polimerizarea prin deschidere de inel a cicloolefinelor** (La métathese des oléfines et la polymerization par ouverture annulaire des cycloolefines), 1981, 254 p.

LYDIA-MARIA VAICUM, **Epurarea apelor uzate cu nămol activ. Bazele biochimice** (L'épuration des eaux résiduelles à boue active. Les bases biochimiques), 1981, 218 p.

I. GĂLĂŢEANU, **Procese şi metode radiochimice în energetica nucleară** (Processus et méthodes radiochimiques dans l'énergetique nucléaire), 1981, 234 p.

OCTAVIAN IORDACHE, **Procese polistocastice aplicate la fenomenele de transfer** (Processus polystochastiques appliqués aux phenomenes de transfert), 1981, 186 p.

CR. SIMIONESCU, VALERIA GORDUZA, **Polimeri biocompatibili şi biologic activi** (Polymères biocompatibles et biologiquement actifs), 1980, 479 p.

CONST. GH. MACAROVICI, **Analiza chimică cantitativă anorganică** (L'analyse chimique quantitative inorganique), 1979, 457 p.

M. FLORESCU, **Metode ştiinţifice în dezvoltarea industriei chimice moderne** (Méthodes scientifiques dans le développement de l'industrie chimique moderne), 1979, 256 p.

A.T. BALABAN, I. GĂLĂŢEANU, G. GEORGESCU, LIGIA SIMIONESCU, **Compuşi marcaţi şi radiofarmaceutici cu aplicaţii în medicina nucleară** (Composés marqués et radiopharmaceutiques à application en médecine nucléaire), 1979, 495 p.

I.G. MURGULESCU, E. SEGAL. **Introducere în chimia fizică, vol. II.1. Teoria molecular-cinetică a materiei** (Introduction à la chimie physique. Vol. II.1. La théorie moléculaire-cinétique de la matière), 1979, 1036 p.

S. STERNBERG, FL. DANEŞ, **Termodinamica chimică aplicată** (La thermodynamique chimique appliquée), 1978, 400 p.

I.G. MURGULESCU, V.EM. SAHINI, **Introducere în chimia fizică. Vol. I.2. Structura şi proprietăţile moleculelor** (Introduction à la chimie physique. Vol. I. 2. La structure et les proprietes des molecules), 1978, 604 p.

I. ZUGRĂVESCU, MAGDA PETROVANU, **N-ylid chemistry,** coédition avec McGraw-Hill International Book Company, U.S.A., 1977, 396 p.

I.G. MURGULESCU, **Introducere în chimia fizică. Vol. I.1. Atomi, molecule, legătură chimică** (Introduction a la chimie physique, Vol. I.1.) Atomes, molécules, liaison chimique), 1976, 560 p.

ELENA CEAUŞESCU, **Research work on synthesis and characterization of macromolecular compounds. Contributions**, 1974, 251 p.

CR. SIMIONESCU, VIORICA RUSAN, V. POPA, **Chimia algelor marine** (La chimie des algues marines), 1974, 212 p., 1 pl.

I. P. Informaţia c. 2415

43 426

Lei 40

$ 70 (pour un abonnement annuel)

F 1103
04
Vegyészet

ACADÉMIE DE LA RÉPUBLIQUE SOCIALISTE DE ROUMANIE

REFERÁLVA
R

REVUE ROUMAINE DE CHIMIE

TOME 27

N°s 9 – 10

Septembre – Octobre 1982

EDITURA ACADEMIEI REPUBLICII SOCIALISTE ROMÂNIA

| Rev. Roumaine Chim. | RRCHAX, **27**, *9 – 10*, p. 1001–1082 (1982) **Bucarest**

ACADÉMIE DE LA RÉPUBLIQUE SOCIALISTE DE ROUMANIE

COMITE DE RÉDACTION

Rédacteur en chef :

I. G. MURGULESCU, membre de l'Académie de la République Socialiste de Roumanie

Rédacteurs en chef adjoints :

A. T. BALABAN et V. EM. SAHINI, membres correspondants de l'Académie de la République Socialiste de Roumanie

Collège de rédaction :

EM. BRATU, ELENA CEAUȘESCU, ECATERINA CIORĂNESCU-NENITZESCU, CR. SIMIONESCU, membres de l'Académie de la République Socialiste de Roumanie ; P. SPACU, membre correspondant de l'Académie de la République Socialiste de Roumanie ; MARGARETA AVRAM, M. BANCIU, I. HAIDUC, D. I. MARCHIDAN, I. MOLDOVAN, G. NIAC et D. SĂNDULESCU

La Revue Roumaine de Chimie paraît 10 fois par an. Toute commande de l'étranger pour les travaux parus aux Editions de l'Académie de la République Socialiste de Roumanie sera adressée à ILEXIM – Departamentul Export–Import Carte (Livres)/ Departamentul Export–Import Presă (Revues), P.O.B. 136–137, télex 11226, 3, str. 13 Decembrie, 79517 Bucarest, Roumanie

Les manuscrits, les livres et les revues proposés en échange, ainsi que toute correspondance seront envoyés à la rédaction :

REVUE ROUMAINE DE CHIMIE

125, Calea Victoriei, 79717 Bucarest, Roumanie, téléphone 50 76 80

EDITURA ACADEMIEI REPUBLICII SOCIALISTE ROMÂNIA
125, Calea Victoriei, 79717 Bucarest, Roumanie, téléphone 50 76 80

REVUE ROUMAINE DE CHIMIE

ORSZÁGOS MŰSZAKI INFORMÁCIÓS KÖZPONT ÉS KÖNYVTÁR
1983

Tome 27, N°s 9–10 Septembre–Octobre, 1982

S. STERNBERG and V. BRÂNZOI, Polarization behaviour of stainless steel, type W. 1.4541 in $R-OH + HCl$ anhydrous solution . . . . 1003–1008 R

D. GEANĂ and F. DANEȘ, Application of *Kuhn–Tucker* conditions to the problem of chemical and phase equilibrium 1009–1023

EDUARDO A. CASTRO and FRANCISCO M. FERNÁNDEZ, Semiempirical prediction of ionization potentials . . . . 1025–1027 BC

C. GHIRVU, ANA ONU and GH. IONIȚĂ, Spectral study of the influence of polystyrene in benzene solutions on the α, α'-diphenyl-β-picrylhydrazyl (DPPH) radical 1029–1033

C. I. LEPĂDATU, On a formula of Racah and Shadmi for the interelectronic repulsion parameters 1035–1036

M. BANCIU, A. T. BALABAN, C. DRĂGHICI and RODICA VLAD, Synthesis of pyrylium salts with an annelated dibenzo [*f*, *i*] bicyclo [3.2.2.] nona-6,8-diene skeleton (oxonia-homotriptycenes) and their reactions with nucleophiles 1037–1046

A. GARCÍA, RASO, J. V. SINISTERRA and J. M. MARINAS, Hydrolysis of *n*-alkyl salicilates catalysed by activated barium hydroxides (in Spanish) 1047–1054 C

CR. SIMIONESCU, CLEOPATRA VASILIU-OPREA and CLAUDIA NEGULIANU, Mechanochemical synthesis of some polychelates on polyamidic support (in Russian) 1055–1066

A. J. ALLER, Indium determination in aluminium alloys by atomic absorption and emission spectrometry (in Spanish) . . . . 1067–1078 C

BOOK REVIEWS 1079–1080

SCIENTISTS AND PEACE 1081–1082

Rev. Roumaine Chim. **27**, *9–10*, 1001–1082 (1982) Bucarest

Revue Roumaine de Chimie, 27, *9–10*, 1003–1008 (1982)

POLARIZATION BEHAVIOUR OF STAINLESS STEEL, TYPE W.1.4541 IN R–OH + HCl ANHYDROUS SOLUTION

S. STERNBERG and B. BRÂNZOI
Department of Physical Chemistry and Electrochemistry, National Institute of Chemistry, Bucharest, Str. Polizu 1. Romania

Received September 16, 1981

The polarization behaviour of stainless steel type W. 1. 4541 in R—OH + HCl anhydrous solution (where R = CH_3 ; C_2H_5 ; C_3H_7 ; C_4H_9 ; C_5H_{11}) was studied by the potentiostatic method. The increase in HCl concentration and temperature led to an increase of the corrosion rate, whereas increase of the hydrocarbonate chain length led to a decrease of the corrosion rate.

INTRODUCTION

Corrosion in organic solvents has received considerable attention due to the great number of organic systems used in technology. Corrosion is mainly due to environmental impurities, resulting from the manufacturing process or the degradation reactions after prolonged use of the solvents. [1]

The most frequently met impurities are : water, acids and the high valence halogens of metal ions. Hence, it is imperative to determine the dependence of the corrosion rate on the concentration of impurities.

The present paper reports on the influence of different quantities of hydrochloric acid and temperature on the polarization behaviour of stainless steel, type W. 1. 4541 in anhydrous R–OH (where R = CH_3 ; C_2H_5 ; C_3H_7 ; C_4H_9 ; C_5H_{11}).

EXPERIMENTAL

The polarization curves were plotted by the potentiostatic method. The device is shown in figure 1.

In all the experiments, the electrochemical polarization was started about 30 minutes after immersion of the working electrode (L) to permit stabilization of the steady-state potential. The potential was changed in steps with the QTK potentiometer and maintained at a constant value by the Wenking potentiostate (W). The value of the current appearing in the external circuit after adjustment of the potential step was determined by measuring the voltage on the standard resistance (SR) with an electronic voltmeter (E.V.). The working electrode potential was always measured with respect to the saturated calomel electrode and was represented graphically as a function of the current that appeared in the external circuit. Thus, the anodic or cathodic polarization curves were obtained as a function of the direction in which the potential of the working electrode varied.

The electrochemical cell, electrode assembly and the method for obtaining hydrochloric acid gas and R—OH + HCl anhydrous solutions have been described in detail in an earlier paper.[1] Prior to each determination, the working electrode was mechanically ground and polished with emery paper of varied granulation up to mirror-luster, degreased in benzene at boiling temperature for 5 min in order to remove all traces of fat and abrasive powder remaining on the surface after polishing. The samples were then electropolished following the recipes used in research and industry[2,3] for various metals. After electrical polishing, the working electrode used to be washed in anhydrous alcohol, afterwards in solution to be tested and only then introduced in the cell for electrochemical polishing. The solution to be tested had been previously deaerated with argon for one hour and deaeration continued throughout the determination.

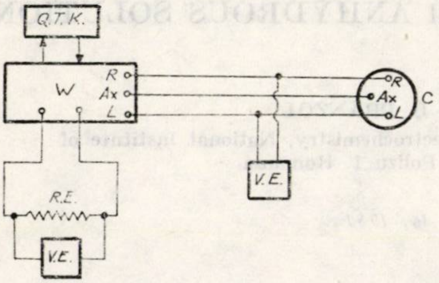

Fig. 1. — Scheme of the potentiostatic device.

The solution in the cell was introduced in a UM—210 thermostat, which can be adjusted to a tenth of degree at the constant temperature.

The polarization curves were recorded always starting from the mixed potential at steady-state. The determinations were repeated with each solution until a good reproducibility of the results was obtained. On plotting the polarization curves, account was kept of the fact that prolonged anodic polarization might give rise to changes at the level of the surface asperities which would imply parallel translation of the Tafel slopes. This effect can be eliminated[4,5] by first tracing the cathodic polarization curves and then the anodic ones, method used in the present paper.

RESULTS AND DISCUSSION

Figure 2 shows the anodic and cathodic polarization curves obtained by the potentiostatic technique of stainless steel, type W. 1. 4541 in anhydrous $CH_3OH + HCl$ solution.

Increase in hydrochloric acid concentration shifts the curves towards more negative potentials (an almost parallel shift), increases the corrosion rate and the value of the limit diffusion current.

Similarly, analysis of the polarization curves shows that no passive — active transition up to very high currents was observed. This could be explained by the presence of hydrochloric acid that prevents the formation of the passive film and accelerates the process of anodic dissolution, the more the greater is the concentration of chlorine ions. It is assumed that halogen ions participate by competitive adsorption in the reactions on the metal — electrolyte interface which form chemisorbed films that satisfy the surface affinity for oxygen atoms or alcohol molecules.[6,7] The specific adsorption of those anions reduces the potential energy barrier necessary for transition from the metal phase in solution therefore acceleration of the process of anodic dissolution. The kinetic parameters of corrosion obtained from the polarization curves are shown in table 1.

Analysis of the density current-potential curves in figure 2 shows that at lower overvoltage values the Tafel relation is met with (linear dependence) indicating that both the anodic and the cathodic reaction are controlled by activation.

At high overvoltage, a limit diffusion current appears on the anodic polarization curve, suggesting that at higher densities of current, the hydrochloric acid transport on the electrode surface gradually becomes rate-determinant (concentration polarization). For this reason, the electrode surface cannot be completely covered by adsorbed chlorine ions and hence the solvent molecule may participate directly in the mechanism of metal dissolution by its oxidation products at the free positions on the electrode surface. Methanol oxidation on the chlorine ion-free portions combined with the participation of oxidation products in dissolution of the metal and increase of the transport rate of chlorine ions on the electrode surface with increase of the potential, explain why the limit diffusion current cannot always be well defined. Moreover, the foregoing data explain why the value of the limit diffusion current decreases with reduction of the hydrochloric acid concentration (Table 1).

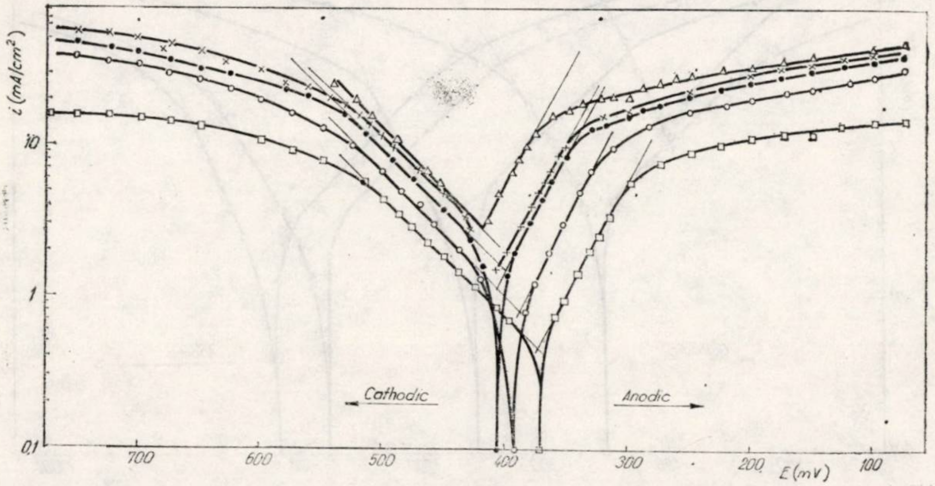

Fig. 2. — Anodic and cathodic polarization curves of stainless steel, W. 1. 4541, in anhydrous $CH_3OH + HCl$ solution : (△) $CH_3OH + 2NHCl$; (×) $CH_3OH + 1.5NHCl$; (●) $CH_3OH + 1$ NHCl ; (○) $CH_3OH + 0.5$ NHCl ; (□) $CH_3OH + 0.1$ NHCl.

INFLUENCE OF NATURE AND LENGTH OF HYDROCARBONATE CHAIN ON THE POLARIZATION BEHAVIOUR OF STAINLESS STEEL, TYPE W.1. 4541

The polarization curves of stainless steel, type W. 1. 4541 in anhydrous solutions of inferior alcohols were likewise obtained at the same hydrochloric acid concentration (Fig. 3).

Lowering of the corrosion rate (i_{corr}) and density of the limit diffusion current was observed with increase in the length of the hydrocarbonate chain. This effect is due, as already shown, to reduction of the dielectric constant and to parallel diminution of the protic character of alcohols. In point of fact, increase in the length of the hydrocarbonate chain increases viscosity, lowers the diffusion coefficient and the specific conductivity coefficient, resultig in decrease of the aggressive character of the medium.

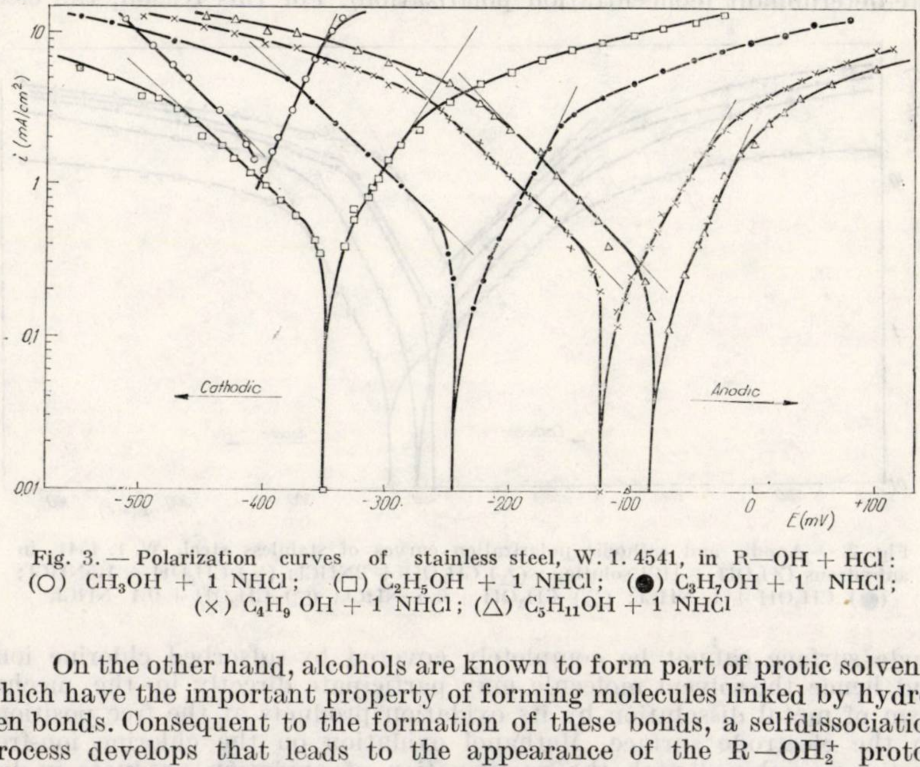

Fig. 3. — Polarization curves of stainless steel, W. 1. 4541, in R—OH + HCl : (○) $CH_3OH + 1$ NHCl ; (□) $C_2H_5OH + 1$ NHCl ; (●) $C_3H_7OH + 1$ NHCl ; (×) C_4H_9 OH + 1 NHCl ; (△) $C_5H_{11}OH + 1$ NHCl

On the other hand, alcohols are known to form part of protic solvents which have the important property of forming molecules linked by hydrogen bonds. Consequent to the formation of these bonds, a selfdissociation process develops that leads to the appearance of the $R-OH_2^+$ proton solvates, which are the main corrosive agents.

With the increase in the length of hydrocarbonate chain of alcohol, steric prevention of the above process takes place and hence, the number of $R-OH_2^+$ proton solvates will be lower, their mobility will likewise diminish and consequently, the aggressiveness of the medium too. This explains the shift of corrosion potentials towards more positive values and diminution of the corrosion current density with increase in the length of the hydrocarbonate chain (Table 1).

TABLE 1

Kinetic parameters of corrosion of stainless steel type W. 1. 4541 in R—OH + HCl at 20°C

Solution	i_{corr}	$P_{mm/an}$	Tafel slopes b_a	$-b_c$	$-E_{corr}$	i_{LD}
			mV		mV	mA/cm²
$CH_3OH + 1$ NHCl	1.44	17.05	62.5	125	359	16
$C_2H_5OH + 1$ NHCl	0.45	4.5	72	130	343	7
$C_3H_7OH + 1$ NHCl	0.3	3.55	62	132	220	5.4
$C_4H_9OH + 1$ NHCl	0.22	2.6	75	128	112	3.8
$C_5H_{11}OH + 1$ NHCl	0.18	2.13	60	120	65	3.2

The table also shows marked decrease in the density of the limit diffusion current with increase of the hydrocarbonate chain length. This can be explained, as mentioned, by the increased viscosity and diminished diffusion coefficient which will lower the transport rate of aggressive ions on the metal surface and of the corrosion products on the metal surface in solution.

THE INFLUENCE OF TEMPERATURE

Furthermore, the polarization behaviour of stainless steel, W.1. 4541, in $CH_3OH + 1NHCl$ anhydrous solution was studied at various temperatures. The experimental results given in figure 4 and table 2 show the increase of corrosion density current with the increase of temperature.

TABLE 2

Dependence of the corrosion rate of W. 1. 4541 steel in $CH_3OH + 1$ NHCl anhydrous solution on temperature

Solution	t°C	i_{corr} mA/cm²	$\frac{i_t}{i_{20}}$	Apparent energy of activation cal/mol
$CH_3OH + 1$ NHCl	20	1.44	1	7622
	35	1.9	1.32	
	45	3.1	2.15	
	55	5.8	4.03	

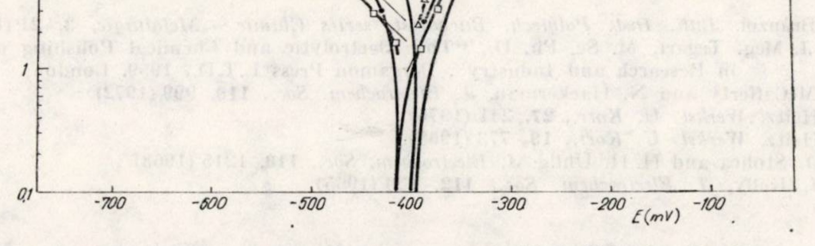

Fig. 4. — Polarization curves of stainless steel, W. 1. 4541, in $CH_3OH + 1$ NHCl at various temperatures: (□) $t = 25$°C; (●) $t = 35$°C; (×) $t = 45$°C; (△) $t = 55$°C.

Plotting the logarithm of the corrosion current density as a function of $1/T$ results in a straight line in keeping with the Arrhenius equation:

$$i_{corr} = A \exp(-E/RT) \text{ or } \ln i_{corr} = \ln A - E/RT$$

The value of apparent activation energy, 7622 cal/mol, was calculated from the slope of the straight line obtained. The i_t/i_{20} ratio indicates how many times the corrosion rate increases at a given temperature as compared to the corrosion rate in the same medium at 20°. Table 2 presents the values of i_t/i_{20} ratio and that of the apparent activation energy. Analysis of the i_t/i_{20} values shows, as already mentioned, increase of the corrosion rate with temperature, the highest value being reached at 55°C when $i_t/i_{20} = 4$.

After each experiment, the working electrode was examined by metallographic microscopy which revealed pitting corrosion of its surface at all the temperatures studied.

CONCLUSIONS

From the physico-chemical viewpoint, both corrosion in protic organic solvents and corrosion in aqueous solutions belong to the processes taking place at metal/ liquid phase interface.

In anhydrous R—OH + HCl solution, the increase of hydrochloric acid concentration leads to a marked increase in the densities of the corrosion current and of the limit diffusion current.

Increase of the hydrocarbonate chain length shifts the corrosion potentials towards more posistive values and decreases the corrosion current density and limit diffusion current density.

In anhydrous CH_3OH + HCl solution, elevation of the temperature results in a marked increase of the corrosion rate and density of the limit diffusion current.

Metallographic analysis of the electrode surface showed pitting in all cases.

REFERENCES

[1] V. Brânzoi, *Bull. Inst. Polytech. Bucharest, series Chimie — Metalurgie*, **3**, 21 (1978).
[2] W. J. Meg. Tegart, M. Sc. Ph. D., "The Electrolytic and Chemical Polishing of Metals in Research and Industry", Pergamon Press L.T.D., 1959, London.
[3] E. McCafferty and N. Hackerman, *J. Electrochem. Soc.*, **119**, 999 (1972).
[4] E. Heitz, *Werkst. U. Korr.*, **27**, 241 (1976).
[5] E. Heitz, *Werkst. U. Korr.*, **19,** 773 (1968).
[6] N. D. Stolica and H. H. Uhlig, *J. Electrochem. Soc.*, **110**, 1215 (1968).
[7] E. J. Kelly, *J. Electrochem. Soc.*, **112**, 124 (1965).

Revue Roumaine de Chimie, 27, *9–10*, 1009–1023 (1982)

APPLICATION OF *KUHN–TUCKER* CONDITIONS TO THE PROBLEM OF CHEMICAL AND PHASE EQUILIBRIUM

D. GEANĂ and F. DANEȘ

Dept. Physical Chemistry, Polytechnic Institute
Bucharest, str. Polizu 1, Romania

Received December 29, 1980

The paper presents a transformation of the problem of chemical equilibrium for multiphase systems to a nonlinear program with inequalities constraints. The application of Kuhn-Tucker conditions of optimum leads to a rigorous theoretical formalism of chemical equilibrium, including the cases of indifferent, degenerated and totally displaced equilibria. An analysis of Kuhn-Tucker conditions for some practical systems is presented.

INTRODUCTION

It is known [1,2] that the problem of chemical equilibrium (PCE) in multicomponent and multiphase systems is equivalent to a nonlinear mathematical program (or an optimization problem).

For single phase systems (e.g. gaseous) a series of solving methods reviewed in [3,4] has been developed. More recently, PCE in such systems has been discussed on the basis of geometric programming methods. [5,6] A series of papers in the last decade has considered the simultaneous chemical and phase equilibrium [1,2,7–15]. The problem of restricted equilibrium was considered too. [16]

This work presents a transformation of PCE for multiphase systems, similar to that suggested elsewhere. [17] The transformation leads to a nonlinear program with inequalities constraints to whom one can apply the conditions of optimum known as the Kuhn-Tucker theorems. It is thus possible to develop a rigorously theoretical formalism of PCE including the cases of indifferent, degenerated and totally displaced equilibrium. The application of Kuhn-Tucker conditions to some systems is analysed in detail.

A TRANSFORMATION OF PCE

The PCE in a system with C components, M elements, and F phases can be formulated for T and P constants as:

$$\min G = \sum_{i=1}^{C} n_i \mu_i \qquad (1)$$

subject to

$$\sum_{i=1}^{C} a_{ki} n_i = b_k \qquad (k = 1, 2, \ldots M) \tag{2}$$

$$n_i \geqslant 0 \qquad (i = 1, 2, \ldots C) \tag{3}$$

If we denote by **A** — the "atomic matrix" of a reaction system (of elements a_{ki}), **N** — the column vector of mole numbers and **B** — the vector of chemical elemental abundances, eq. (2) can be written in a matrix form:

$$\mathbf{AN} = \mathbf{B} \tag{4a}$$

It must be mentioned that we mean herein by "component" a chemical species which appears in a phase. When the same species appears in a second phase this is a "new" component. Generally, the number of components is greater or at least equal to the number of chemical species in the system. In other papers [11, 15] the distinction between "component" and "species" was made by double indexing (for species and phase). The nomenclature is still different with other authors, e.g. one treats chemical substances with different phase designations as "distinct chemical species".

It is assumed that "atomic" matrix of dimensions $M \times C$ has the rank M. The vector **B** can be calculated from:

$$\mathbf{B} = \mathbf{AN}^0 \tag{4b}$$

where $\mathbf{N}^0$ is the column vector of initial amounts (mole) of components, n_i^0. Eq. (4a) becomes:

$$\mathbf{AN} = \mathbf{AN}^0$$

The matrix **A** allows for obtaining a stoichiometric matrix by the relation:

$$\mathbf{WA}^{\mathrm{T}} = 0 \tag{5}$$

where **W** is of dimensions $\mathcal{R} \times C$. Its elements are the stoichiometric coefficient, ν_{ji}, of the components i in reaction j. The superscript T denotes a transposition. It is worth mentioning that we mean by reactions not only the chemical ones but also the processes of transfer of species between the phases. The reactions take place therefore "between the components". Another formulation of PCE in multiphase systems by considering only chemical reactions ("between the species") was discussed elsewhere. [2]

Matrix **W** can be partitioned in two matrices:

$$\mathbf{W} = \mathbf{W}_1 | \mathbf{W}_2 \tag{6}$$

having the dimensions $\mathcal{R} \times \mathcal{R}$ and $\mathcal{R} \times (C - \mathcal{R})$ respectively.

Likewise, matrix $\mathbf{A}$ can be partitioned

$$\mathbf{A} = \mathbf{A}_1 | \mathbf{A}_2 \tag{7}$$

the submatrices having the dimensions $M \times (C - M)$ and $M \times M$ respectively. In the assumed case, (rank $\mathbf{W} = M$) there is the relation: $\mathscr{R} = C - M$. Eq. (5) becomes:

$$\mathbf{W}_1\mathbf{A}_1^{\mathrm{T}} + \mathbf{W}_2\mathbf{A}_2^{\mathrm{T}} = 0$$

or

$$\mathbf{W}_2\mathbf{A}_2^{\mathrm{T}} = - \mathbf{W}_1\mathbf{A}_1^{\mathrm{T}}$$

It results:

$$\mathbf{W}_2 = - \mathbf{W}_1\mathbf{A}_1^{\mathrm{T}}(\mathbf{A}_2^{\mathrm{T}})^{-1} \tag{8a}$$

A stoichiometric matrix is obtained for example, taking $\mathbf{W}_1 = \mathbf{I}$, where $\mathbf{I}$ is matrix unity of dimensions $\mathscr{R} \times \mathscr{R}$.

Eq. (8a) becomes:

$$\mathbf{W}_2 = - \mathbf{A}_1^{\mathrm{T}}(\mathbf{A}_2^{\mathrm{T}})^{-1} \tag{8b}$$

and the stoichiometric matrix is:

$$\mathbf{W} = \mathbf{I} | \mathbf{W}_2 \tag{8c}$$

The matrix equations (6, 8a) or (8b, c) give the possibility of a transformation of PCE (1–3). Thus eq. (4c) can be written in the form:

$$\mathbf{A}_1\mathbf{N}_1 + \mathbf{A}_2\mathbf{N}_2 = \mathbf{A}_1\mathbf{N}_1^0 + \mathbf{A}_2\mathbf{N}_2^0 \tag{9}$$

considering the corresponding partitions of the vectors $\mathbf{N}$ and $\mathbf{N}^0$. From (9) results:

$$\mathbf{N}_2 = \mathbf{A}_2^{-1}\mathbf{A}_1\mathbf{N}_1^0 + \mathbf{N}_2^0 - \mathbf{A}_2^{-1}\mathbf{A}_1\mathbf{N}_1 \tag{10}$$

From eq. (8a) one obtains:

$$\mathbf{A}_2^{-1}\mathbf{A}_1 = - \mathbf{W}_2^{\mathrm{T}}(\mathbf{W}_1^{\mathrm{T}})^{-1} \tag{11}$$

Combining eq. (10) and (11):

$$\mathbf{N}_2 = \mathbf{N}_2^0 + \mathbf{W}_2^{\mathrm{T}}(\mathbf{W}_1^{\mathrm{T}})^{-1}(\mathbf{N}_1 - \mathbf{N}_1^0) \tag{12a}$$

It is possible to introduce the vector:

$$\mathbf{E} = (\mathbf{W}_1^{\mathrm{T}})^{-1}(\mathbf{N}_1 - \mathbf{N}_1^0) \tag{13a}$$

eq. (12a) becoming:

$$\mathbf{N}_2 = \mathbf{N}_2^0 + \mathbf{W}_2^{\mathrm{T}}\mathbf{E} \tag{12b}$$

Rearranging eq. (13a):

$$\mathbf{N}_1 = \mathbf{N}_1^0 + \mathbf{W}_1^T\mathbf{E} \tag{13b}$$

and with the partition of **N**:

$$\mathbf{N} = \mathbf{N}^0 + \mathbf{W}^T\mathbf{E} \tag{14}$$

Eq. (14) represents the expression for defining the vector **E** of De Donder variables $\xi_j (j = 1, 2 \ldots \mathscr{R})$ (called also reaction extents or progress variables). It is worth mentioning that (14) is rigorously obtained on the basis of "atomic" matrix of the system.

Eq. (14) can be written using the elements of vector **N**:

$$n_i = n_i^0 + \sum_{j=1}^{\mathscr{R}} \nu_{ji}\,\xi_j \tag{15}$$

Substituting in eq. (1) and (3) one obtains the transformed PCE:

$$\min G(\mathbf{E}) = \sum_{i=1}^{C}\left(n_i^0 + \sum_{j=1}^{\mathscr{R}} \nu_{ji}\,\xi_j\right)\mu_i(\mathbf{E}) \tag{16}$$

$$n_i(\mathbf{E}) = n_i^0 + \sum_{j=1}^{\mathscr{R}} \nu_{ji}\xi_j \geqslant 0 \tag{17}$$

where by $G(\mathbf{E})$, $\mu_i(\mathbf{E})$ and $n_i(\mathbf{E})$ was designed the functional dependence of variables ξ_j $(j = 1, 2 \ldots \mathscr{R})$. For pure condensed phases μ_i are independent of **E** being reduced to standard potentials.

The transformed PCE results as a nonlinear program with inequalities constraints:

$$\min_{\mathbf{E}}\{G(\mathbf{E})\,|\,n_i(\mathbf{E}) \geqslant 0,\ i = 1, 2, \ldots C\} \tag{18}$$

In comparison with formulation (1—3), the problem (18) has a smaller number of variables ($\mathscr{R} < C$) and is subjected to only inequalities constraints.

APPLICATION OF KUHN-TUCKER CONDITIONS TO TRANSFORMED PCE

In the branch of nonlinear programming, the Kuhn-Tucker conditions [18–20] represent some of the most important theoretical results. In what follows we will use the necessary Kuhn-Tucker conditions for a local optimum with inequalities constraints. These conditions must be satisfied by the transformed PCE (18).

The inequalities (18) can be transformed in equalities by introducing auxiliary real variables χ_i $(i = 1, 2, \ldots C)$. Restrictions (17) become:

$$-\,n_i(\mathbf{E}) + \chi_i^2 = 0 \tag{19}$$

It is possible to apply the method of multipliers and to build the Lagrange's function:

$$L(\mathbf{E}, \chi_i, \lambda_i) = G(\mathbf{E}) + \sum_{i=1}^{C} \lambda_i[-n_i(\mathbf{E}) + \chi_i^2] \tag{20}$$

The conditions for optimum are:

$$\frac{\partial L}{\partial \xi_j} = \frac{\partial G}{\partial \xi_j} - \sum_{i=1}^{C} \lambda_i \frac{\partial n_i}{\partial \xi_j} = 0 \quad (j = 1, 2, \ldots \mathscr{R}) \tag{21a}$$

$$\frac{\partial L}{\partial \lambda_i} = -n_i(\mathbf{E}) + \chi_i^2 = 0 \qquad (i = 1, 2 \ldots C) \tag{21b}$$

$$\frac{\partial L}{\partial \chi_i} = 2\lambda_i \chi_i = 0 \qquad (i = 1, 2 \ldots C) \tag{21c}$$

The auxiliary variables χ_i can be eliminated. From (32) results that for each i, $n_i(\mathbf{E}) = 0$ only when $\chi_i = 0$. From (21b, c) one obtains:

$$\lambda_i n_i(\mathbf{E}) = 0 \tag{21d}$$

It results:

$$\frac{\partial G}{\partial \xi_j} - \sum_{i=1}^{C} \lambda_i \frac{\partial n_i}{\partial \xi_j} = 0 \quad (j = 1, 2, \ldots \mathscr{R}) \tag{22a}$$

$$n_i(\mathbf{E}) \geqslant 0 \qquad (i = 1, 2, \ldots C) \tag{22b}$$

$$\lambda_i n_i(\mathbf{E}) = 0 \qquad (i = 1, 2, \ldots C) \tag{22c}$$

According to Kuhn-Tucker theorem [18-20] one must take additionally the conditions:

$$\lambda_i \geqslant 0 \tag{22d}$$

The relations (22a–d) are the Kuhn-Tucker (KT) conditions necessary for an optimum with inequalities constraints. These conditions become necessary and sufficient conditions for a global optimum when the objective function and the restrictions are convex. A rigorous treatment of KT conditions can be found, for example in [18-20]. The geometric meaning of KT conditions for PCE is that an equilibrium point ($\mathbf{E}_e$) with inequalities restrictions corresponds to the situation when the gradient vector of the free enthalpy function, $\nabla G(\mathbf{E}_e)$, is in the cone generated by the gradient vectors of active constraints, $\nabla n_i(\mathbf{E}_e)$. In terms of linear algebra this means that $\nabla G(\mathbf{E}_e)$ is a linear nonnegative combination of the form :

$$\nabla G(\mathbf{E}_e) = \sum_{i \in \mathcal{I}} \lambda_i \cdot \nabla n_i(\mathbf{E}_e) \tag{23}$$

where $\lambda_i > 0$, $i \in \mathcal{I}$ the set of active constraints *).

These results can be reformulated for considering all restrictions by defining the coefficients $\lambda_i = 0$ for $n_i(\mathbf{E}_e) > 0$. One observes that $\lambda_i > 0$ if $n_i(\mathbf{E}_e) = 0$, and $\lambda_i = 0$ if $n_i(\mathbf{E}_e) > 0$, i.e. the KT conditions (22c).

For the transformed PCE, eqs (22a—d) become :

$$\Delta^r G_j = \sum_{i=1}^{C} \nu_{ji} \mu_i = \sum_{i=1}^{C} \nu_{ji} \lambda_i \qquad (j = 1, 2 \ldots \mathcal{R}) \tag{24a}$$

$$n_i^0 + \sum_{j=1}^{\mathcal{R}} \nu_{ji} \xi_j \geqslant 0 \qquad (i = 1, 2 \ldots C) \tag{24b}$$

$$\lambda_i \left(n_i^0 + \sum_{j=1}^{\mathcal{R}} \nu_{ji} \xi_j \right) = 0 \tag{24c}$$

$$\lambda_i \geqslant 0 \tag{24d}$$

Eqs (24a—d) represent KT conditions for PCE. The physical meaning of these conditions is discussed in what follows. As far as we know, KT conditions were not previously formulated and used in relation to PCE.

APPLICATION OF KT CONDITIONS TO PCE IN SINGLE REACTION SYSTEMS

In single reaction systems, eqs (14, 15) reduce to the simple form : $n_i = n_i^0 + \nu_i \xi$. Empirically one establishes the existence of 5 types of equilibrium at T, P constants :

a) degenerate ("D") for which a shift from the initial composition $\mathbf{n}_i^0$ is not possible because at least a reactant and a product are initially not present in the system. In consequence $\xi = 0$, and the KT conditions are :

$$n_i = n_i^0 > 0 ; \quad \lambda_i = 0 \text{ for the present components}$$

$$n_i = n_i^0 = 0 ; \quad \lambda_i > 0 \text{ for the absent components}$$

$$\Delta^r G = \sum_{i=1}^{C} \nu_i \lambda_i \in (-\infty, \infty) \text{ without a defined sign.}$$

---

*) The active constraints are those fulfilled with zero.

b) intermediate (middle) ("M") for which all the components coexist in the systems. KT conditions are:

$$n_i = n_i^0 + \nu_i\xi > 0\,; \quad \lambda_i = 0 \qquad (i = 1, 2 \ldots C)$$

$$\Delta^r G = \sum_{i=1}^{C} \nu_i\lambda_i = 0$$

The equilibrium point is found in the range of constraints. KT conditions reduce to the well-known thermodynamic equilibrium condition.

c) totally displaced to left ("L") for which at least one reaction product is absent from the system. It may be the case of heterogeneous equilibrium with pure condensed phases. KT conditions become:

$$n_i = n_i^0 + \nu_i\xi > 0\,; \quad \lambda_i = 0 \ \forall_i \text{ with } \nu_i < 0$$

$$n_i = n_i^0 + \nu_i\xi = 0\,; \ \lambda_i > 0 \text{ for at least a product } (\nu_i > 0).$$

Thus,

$$\Delta^r G = \sum_{i=1}^{C} \nu_i\lambda_i > 0 \text{ (reduced only to absent products } \nu_i > 0)$$

The equilibrium point is found on the frontier of feasible region, at least one product (pure condensed phase) being consumated in reaction.

d) totally displaced to right ("R") for which at least one reactant is absent from the system ($\nu_i < 0$). It is the opposite case of (c). KT conditions are:

$$n_i = n_i^0 + \nu_i\xi > 0\,; \ \lambda_i = 0 \ \forall_i \text{ with } \nu_i > 0$$

$$n_i = n_i^0 + \nu_i\xi = 0\,; \ \lambda_i > 0 \text{ for at least a reactant } (\nu_i < 0)$$

It results:

$$\Delta^r G = \sum_{i=1}^{C} \nu_i\lambda_i < 0 \text{ (reduced only to absent reactants, } \nu_i < 0)$$

The equilibrium point is also on the frontier of the feasible range, at least one reactant (pure condensed phase) is consumated in reaction.

e) indifferent ("I") for which the chemical equilibrium is realized at all compatible stoichiometric compositions. For this case

$$\Delta^r G = \sum_{i=1}^{C} \nu_i\lambda_i = 0 \text{ (for a set of points } n_i)$$

Excepting the case "I" one can differentiate between the equilibrium types using the KT conditions. For including this case it is necessary to introduce in addition to KT conditions a new criterion. With usual notations $\Delta^r G^0 = \sum_{i=1}^{C} \nu_i\mu_i^0 = -RT \ln K$, and considering the activity function:

$$Q = \prod a_i^{\nu_i} - K \ (i = 1, 2 \ldots C) \tag{25}$$

it results

$$\Delta^r G = \sum_{i=1}^{C} \nu_i \lambda_i = RT \ln(Q/K + 1) \tag{26}$$

taking into account the relation of chemical potential $\mu_i = \mu_i^0 + RT \ln a_i$. From eq. (26) one can observe that $\Delta^r G$ is positive, zero, negative or nondefined as well as Q. The criterion which allows for differentiating the case "I" consists in the derivative $\mathrm{d}Q/\mathrm{d}\xi$. This is surely a consequence of the thermodynamic condition of equilibrium stability [21,22] (and of indifferent state): $\partial^2 G/\partial \xi^2 = \partial(\Delta^r G)/\partial \xi \geqslant 0$.

The algorithm for complete differentiating of the 5 types of equilibrium is:

$$\Delta^r G = \sum \nu_i \lambda_i = 0 ; \quad Q = 0 ; \quad \mathrm{d}Q/\mathrm{d}\xi = 0 \qquad (\text{"}I\text{"}) \tag{27a}$$

$$\Delta^r G = \sum \nu_i \lambda_i = 0 ; \quad Q = 0 ; \quad \mathrm{d}Q/\mathrm{d}\xi > 0 \qquad (\text{"}M\text{"}) \tag{27b}$$

$$\Delta^r G = \sum \nu_i \lambda_i < 0 ; \quad Q < 0 ; \quad \mathrm{d}Q/\mathrm{d}\xi \geqslant 0 \qquad (\text{"}R\text{"}) \tag{27c}$$

$$\Delta^r G = \sum \nu_i \lambda_i > 0 ; \quad Q > 0 ; \quad \mathrm{d}Q/\mathrm{d}\xi \geqslant 0 \qquad (\text{"}L\text{"}) \tag{27d}$$

$$\Delta^r G = \sum \nu_i \lambda_i \in (-\infty, \infty) ; \ Q \in (-\infty, \infty) ; \mathrm{d}Q/\mathrm{d}\xi \geqslant 0 \qquad (\text{"}D\text{"}) \tag{27e}$$

The equilibrium composition will be calculated as follows:

— in the case "M" by solving eq. $Q(\xi) = 0$

— in the case "R": $\xi = \inf(-n_i^0/\nu_i), \ \forall_i, \ \nu_i < 0$

— in the case "L": $\xi = -\inf(n_i^0/\nu_i), \ \forall_i, \ \nu_i > 0$

— in the case "D": $\xi = 0$

— in the case "I": it is allowable each ξ between the limits of the cases "R" and "L".

Example 1

Consider the reaction $A(s) \rightleftharpoons B(s') + C(g)$ where A and B are two pure solids and C is a pure gas, for example $CaCO_3(s) \rightleftharpoons CaO(s') + CO_2(g)$.

The values of n_i are: $n_A = n_A^0 - \xi$, $n_B = n_B^0 + \xi$; $n_C = n_C^0 + \xi$ and the activities (assuming an ideal gas) are

$$a_A = a_B = 1 \quad \text{and} \quad a_C = P$$

From (25) it results:

$$Q = P - K \text{ and } \mathrm{d}Q/\mathrm{d}\xi = 0$$

Taking into account eqs (27a—e), the following equilibria types are possible as a function of temperature and pressure:

"L" or "D", if $Q > 0$ (i.e. $P > K$)

"R" or "D", if $Q < 0$ (i.e. $P < K$)

"I" or "D", if $Q = 0$ (i.e. $P = K$)

A discrimination between the above cases is possible based on KT conditions and considering the initial amounts n_i^0. In Table 1 the arising situations of equilibria are displayed.

TABLE 1

Equilibrium in the system $A(s) \rightleftharpoons B(s') + C(g)$

Initial composition	λ_i	Q	ξ	Type
$n_A^0 = 0,\ m = 0$*	$\lambda_A > 0,\ \lambda_{B(C)} > 0$ $\lambda_{C(B)} > 0$	$(-\infty, \infty)$	0	*“D”*
$n_A^0 > 0$ or $m > 0$	$\lambda_A > 0,\ \lambda_B = \lambda_C = 0$	<0	n_A^0	*“R”*
	$\lambda_A = \lambda_B = \lambda_C = 0$	0	$[-m,\ n_A^0]$	*“I”*
	$\lambda_A = 0$ $\lambda_{B(C)} > 0,\ \lambda_{C(B)} = 0$	>0	$-m$	*“L”*

* $m = \inf(n_B^0, n_C^0)$

Example 2

Consider the reaction $A(s) + B(g) \rightleftharpoons C(s') + D(g)$ in which A and C are components in pure condensed phases and B and D form a mixture phase (e.g. an ideal gaseous mixture). Such a reaction is $ZnO + H_2 \rightleftharpoons Zn + H_2O$.

From eq. (15) one obtains:

$$n_A = n_A^0 - \xi;\quad n_B = n_B^0 - \xi;\quad n_C = n_C^0 + \xi;\quad n_D = n_D^0 + \xi \tag{28}$$

and the activities are:

$$a_A = a_C = 1;\ a_B = P(n_B^0 - \xi)/(n_B^0 + n_D^0);\ a_D = P(n_D^0 + \xi)/(n_B^0 + n_D^0)$$

Eq. (25) yields:

$$Q = \frac{n_D^0 + \xi}{n_B^0 - \xi} - K \tag{29a}$$

and the differentiation gives

$$\frac{dQ}{d\xi} = \frac{n_B^0 + n_D^0}{(n_B^0 - \xi)^2} \tag{29b}$$

With the exception of the (degenerated) case in which $n_B^0 + n_D^0 = 0$, it results from (29b) that $dQ/d\xi > 0$ and consequently the *“I”* equilibrium will not be realized.

The equilibria *“M, L, R”* can be determined by applying the conditions (27 b, c, d).

a) Equilibrium "*M*": from relations (27b, 29a) it results $\xi = (n_B^0 K - n_D^0)/(K+1)$.

Substitution in (28) gives:

$$n_A = \frac{(n_A^0 - n_B^0)K + (n_A^0 + n_D^0)}{K+1}; \quad n_B = \frac{n_B^0 + n_D^0}{K+1}$$

$$n_C = \frac{(n_C^0 + n_B^0)K + (n_C^0 - n_D^0)}{K+1}; \quad n_D = \frac{K(n_B^0 + n_D^0)}{K+1}$$

For the components B and D, KT conditions, $\lambda_i = 0$ $(i = B, D)$, are always fulfilled (excepting the degenerated case). For the components A and C, $\lambda_i = 0$ if $n_i > 0$ $(i = A, C)$. Denoting

$$x = (n_B^0 K - n_D^0)/(K+1) \tag{30}$$

the "*M*" equilibrium $(\lambda_i = 0,\ i = A, B, C, D)$ arises when:

$$-n_C^0 < x < n_A^0$$

b) Equilibrium "*L*": substituting in (29a) ξ from $n_D = n_D^0 + \xi$, one obtains

$$Q = \frac{n_D}{n_B^0 + n_D^0} - K$$

so that, excepting the case when $n_B^0 + n_D^0 = 0$ (degenerated) it results

$$\lim_{n_D \to 0} Q < 0$$

This is not compatible with the condition (27d) which defines the case "*L*" $(Q > 0)$. As a consequence $n_D > 0$, $\lambda_D = 0$ and $n_C = 0$, $\lambda_C > 0$. From (28) and (29a) one derives successively:

$$\xi = -n_C^0 \text{ and } Q = \frac{n_D^0 - n_C^0}{n_B^0 + n_C^0} - K$$

It follows that the KT condition $(\lambda_C > 0,\ Q > 0)$ is satisfied only for $x < -n_C^0$ (considering eq. 30).

c) Equilibrium "*R*": one can demonstrate similarly that $n_B > 0$ with KT condition $n_A = 0$, $\lambda_A > 0$, $Q < 0$. From (28) $\xi = n_A^0$ and

$$Q = \frac{n_D^0 + n_A^0}{n_B^0 - n_A^0} - K$$

KT condition is satisfied when $n_A^0 < x$.

In conclusion, for the considered reaction the equilibria "*L*, *M* or *R*" are realized depending on the values of the function x defined by eq. 30. Table 2 presents all the discussed types of equilibrium.

TABLE 2

Equilibrium in the system $A(s) + B(g) \rightleftharpoons C(s') + D(g)$

x Values	λ_i	Q	ξ	Type
$(-\infty, -n^0_C)$	$\lambda_A = \lambda_B = \lambda_D = 0$ $\lambda_C > 0$	> 0	$-n^0_C$	"*L*"
$(-n^0_C, -n^0_A)$	$\lambda_A = \lambda_B = \lambda_C = \lambda_D = 0$	$= 0$	x	"*M*"
(n^0_A, ∞)	$\lambda_B = \lambda_C = \lambda_D = 0$ $\lambda_A > 0$	< 0	n^0_A	"*R*"

APPLICATION OF KUHN-TUCKER CONDITIONS TO PCE IN SYSTEMS WITH SEVERAL REACTIONS

As in the systems with a single reaction, the application of KT conditions allows for defining the equilibrium types: "I_j", "D_j", "M_j", "R_j", "L_j" for each independent reaction j.

Defining the function $Q_j(a_i)$:

$$Q_j = \prod_i a_i^{\nu_{ji}} - K_j \quad (j = 1, 2 \ldots \mathscr{R}) \tag{31}$$

and using KT conditions one arrives at relations similar to (27a—e). The analysis is complicated because the choice of a set of independent reaction is arbitrarily.

Example 3

Consider a system with 3 phases, a pure condensed phase c (component 1), another one c′ (component 2) and a gaseous phase (g) containing the components 3, 4, 5 (for example an ideal gaseous mixture). Based on eqs (8a—c) one obtains a set of reactions, e.g. $A_1(c) + A_3(g) \rightleftharpoons A_4(g)$ and $A_2(c') + A_3(g) \rightleftharpoons A_5(g)$. Such a case is given by components C(s), S(1), O_2(g), CO_2(g) and SO_2 (g) taken in order $A_1 - A_5$. With indexes 1, 2, 3 for the elements C, S and O respectively, the "atomic" matrix is:

$$\mathbf{A} = \left\| \begin{array}{cc|ccc} 1 & 0 & 0 & 1 & 0 \\ 0 & 1 & 0 & 0 & 1 \\ 0 & 0 & 2 & 2 & 2 \\ \multicolumn{2}{c}{\mathbf{A}_1} & \multicolumn{3}{c}{\mathbf{A}_2} \end{array} \right\| \quad \text{and} \quad (\mathbf{A}_2^T)^{-1} = \left\| \begin{array}{ccc} -1 & 1 & 0 \\ -1 & 0 & 1 \\ 0.5 & 0 & 0 \end{array} \right\|$$

Using eqs (8a–c) one obtains a stoichiometric matrix

$$\mathbf{W} = \left\| \begin{array}{rr:rrr} -1 & 0 & -1 & 1 & 0 \\ 0 & -1 & -1 & 0 & 1 \end{array} \right\|$$

Considering $\mathbf{W}_1 = \left\| \begin{array}{rr} -1 & 0 \\ 0 & 1 \end{array} \right\|$

The reactions are:

$$\mathrm{C(s)} + \mathrm{O_2(g)} \rightleftharpoons \mathrm{CO_2(g)} \text{ and } \mathrm{S(1)} + \mathrm{O_2(g)} \rightleftharpoons \mathrm{SO_2(g)}$$

The mole numbers are (from eqs 14, 15):

$$n_1 = n_1^0 - \xi_1 ;\ n_2 = n_2^0 - \xi_2 ;\ n_3 = n_3^0 - \xi_1 - \xi_2 ;\ n_4 = n_4^0 + \xi_1 ;$$
$$n_5 = n_5^0 + \xi_2 \tag{32a – e}$$

the activities being:

$$a_1 = a_2 = 1 ;\ a_3 = n_3 P/n ;\ a_4 = n_4 P/n ;\ a_5 = n_5 P/n$$

where

$$n = n_1^0 + n_2^0 + n_3^0 \tag{33}$$

The functions Q_j, defined by (31), are:

$$Q_1 = \frac{n_4^0 + \xi_1}{n_3^0 - \xi_1 - \xi_2} - K_1 ;\quad Q_2 = \frac{n_5^0 + \xi_2}{n_3^0 - \xi_1 - \xi_2} - K_2 \tag{34}$$

The partial derivatives of the functions Q_j result after a combination with (32 d, e):

$$\frac{\partial Q_1}{\partial \xi_1} = \frac{n_3 + n_5}{n_3^2} ;\quad \frac{\partial Q_1}{\partial \xi_2} = \frac{n_4}{n_3^2} ;\quad \frac{\partial Q_2}{\partial \xi_1} = \frac{n_5}{n_3^2} ;\quad \frac{\partial Q_2}{\partial \xi_2} = \frac{n_3 + n_4}{n_3^2} \tag{35a–e}$$

It will be shown that the amounts n_3, n_4, n_5 of the components in the gas phase cannot be zero but all 3 simultaneously. Thus, if eqs (34) are written:

$$Q_1 = \frac{n_4}{n_3} - K_1 ;\ Q_2 = \frac{n_5}{n_3} - K_2$$

one observes that

I if $n_4 = 0 < n_3$ then $Q_1 < 0$
II if $n_5 = 0 < n_3$ then $Q_2 < 0$
III if $n_3 = 0 < n_4$ then $Q_1 > 0$
IV if $n_3 = 0 < n_5$ then $Q_2 > 0$

The last two inequalities are justified because n_3 tends to zero only by positive values.

On the other side the KT conditions lead for the above situations to the inequalities: $\lambda_4 > 0$ and $Q_1 > 0$ (I), $\lambda_5 > 0$ and $Q_2 > 0$ (II), $\lambda_3 > 0$ and $Q_1 < 0$(III), $\lambda_3 > 0$ and $Q_2 < 0$ (IV) which are contradictorily to the first series of inequalities. It should be concluded that, excepting the degenerated case:

$$n_3 > 0,\ n_4 > 0 \quad \text{and} \quad n_5 > 0 \ (\text{with } \lambda_3 = \lambda_4 = \lambda_5 = 0) \tag{36}$$

and the alternatives $n_i = 0$ and $n_i > 0$ are possible only for the components $i = 1, 2$ (condensed phases).

From (36), after substitution in (35a–e), one observes also that $(\partial Q_j / \partial \xi_k) > 0$. Therefore no reaction can be in an "I" equilibrium. The equilibria "L_1 and L_2" are also impossible because are in contradiction with inequalities (42 b, c). It results – excepting the degenerated cases – the following 4 combinations of reaction equilibria:

a) "M_1M_2" – in this case $(n_1 > 0,\ \lambda_1 = 0,\ Q_1 = 0) \cap (n_2 > 0,$ $\lambda_2 = 0,\ Q_2 = 0)$. From relations $Q_1 = 0$, $Q_2 = 0$ one obtains:

$$\xi_1 = -n_4^0 + nK_1/(K_1 + K_2 + 1); \quad \xi_2 = -n_5^0 + nK_2/(K_1 + K_2 + 1) \tag{37}$$

where n is given by (33). KT conditions, $\lambda_1 = \lambda_2 = 0$ are satisfied when:

$$\begin{gathered}[(K_1 + K_2 + 1)(n_1^0 + n_4^0) - K_1 n > 0] \cap \\ \cap\, [(K_1 + K_2 + 1)(n_2^0 + n_5^0) - K_2 n > 0]\end{gathered} \tag{38}$$

b) "M_1R_2" – this corresponds to $(n_1 > 0,\ \lambda_1 = 0,\ Q_1 = 0) \cap (n_2 = 0,$ $\lambda_2 > 0,\ Q_2 < 0)$. From $Q_1 = 0$ and $n_2 = 0$ it results:

$$\xi_1 = \frac{K_1(n_3^0 - n_2^0) - n_4^0}{K_1 + 1}; \quad \xi_2 = n_2^0 \tag{39}$$

KT conditions $\lambda_1 = 0$ and $\lambda_2 > 0$ are realized when:

$$[K_1\,(n_1^0 + n_2^0 - n_3^0) + (n_1^0 + n_4^0) > 0] \cap [(K_1 + K_2 + 1)(n_2^0 + n_5^0) - K_2 n > 0] \tag{40}$$

from $n_1 > 0$ and $Q_2 < 0$.

c) "R_1M_2" – this case corresponds to $(n_1 = 0,\ \lambda_1 > 0,\ Q_1 < 0) \cap$ $\cap\, (n_2 > 0,\ \lambda_2 = 0,\ Q_2 = 0)$. From $n_1 = 0$ and $Q_2 = 0$ one obtains:

$$\xi_1 = n_1^0; \quad \xi_2 = \frac{K_2(n_3^0 - n_1^0) - n_5^0}{K_2 + 1} \tag{41}$$

and the conditions ($n_2 > 0$ and $Q_1 < 0$):

$$[K_2(n_1^0 + n_2^0 - n_3^0) + (n_2^0 + n_5^0) > 0] \cap$$
$$\cap\, [(K_1 + K_2 + 1)(n_1^0 + n_4^0) - K_1 n < 0] \tag{42}$$

d) "R_1R_2" – this case arises when ($n_1 = 0$, $\lambda_1 > 0$, $Q_1 < 0$) $\cap$ $\cap$ ($n_2 = 0$, $\lambda_2 > 0$, $Q_2 < 0$), From $n_1 = 0$ and $n_2 = 0$ it follows:

$$\xi_1 = n_1^0; \quad \xi_2 = n_2^0 \tag{43}$$

and the conditions ($Q_1 < 0$ and $Q_2 < 0$):

$$[K_1(n_1^0 + n_2^0 - n_3^0) + (n_1^0 + n_4^0) < 0] \cap$$
$$\cap\, [K_2(n_1^0 + n_2^0 - n_3^0) + (n_2^0 + n_5^0) < 0] \tag{44}$$

The equilibrium composition n_i, $i \in [1, 5]$ is calculated from (32a–e) with ξ_1, ξ_2 given by (37), (39), (41) or (43) for the corresponding case. The establishment of each type of equilibrium is made on the basis of K_1, K_2 values and of initial amounts n_i^0 using double inequalities (38), (40), (42) or (44) respectively.

Similar analysis may be given for more complicated systems, for example with several mixed phases. A discussion of such systems will be the object of a future work.

During the revision of this paper we received Professor Smith's reviews on computational aspects of chemical equilibrium in complex systems.[23] His "P_3 and P_4 formulation" of PCE are similar to our formulations given in [17,2] and in this work. We called such transformations of PCE, "ξ formulations".

REFERENCES

[1] R. Gautam and W. D. Seider, *A.I.Ch.E.J.*, **25**, 991, 999, 1006 (1979).

[2] D. Geană, *Rev. Roumaine Chim.*, **26**, 363 (1981).

[3] F. van Zeggeren and S. H. Storey, "The Computation of Chemical Equilibria", Cambridge Univ. Press, London, 1970.

[4] R. Holub and P. Vonka, "The Chemical Equilibrium of Gaseous Systems" Academia, Prague, 1975.

[5] R. J. Duffin, E. L. Peterson and C. Zener, "Geometric Programming-Theory and Applications", Wiley, New York, 1967.

[6] J. J. Dinkel and R. Lakshmanan, *Comput. Chem. Engng.*, **1**, 41 (1977).

[7] G. Eriksson, *Chem. Scr.* **4**, 193 (1973); **8**, 100 (1975); *Analyt. Chim. Acta*, **112**, 375 (1979).

[8] J. H. Dluzniewski and S. B. Adler, *I. Chem. E. Sympos. Series No. 5, Int. chem. Eng. (London)*, **4**, 21 (1972).

[9] R. V. Sanderson and H. H. Y. Chien, *Ind. Eng. Chem. Process Des. Dev.*, **12**, 81 (1973).

[10] B. George, L. P. Brown, C. H. Farmer, P. Buthod and F. S. Manning, *Ind. Eng. Chem. Process Des. Dev.*, **15**, 372 (1976).

[11] D. Geană, *Rev. Chim. (Bucureşti)*, **29**, 1171 (1978).

[12] A. K. Lahiri, *Fluid Phase Equil.*, **3**, 113 (1979).

[13] H. S. Caram and L. E. Scriven, *Chem. Eng. Sci.*, **31**, 163 (1976).

[14] H. G. Othmer, *Chem. Eng. Sci.*, **31**, 993 (1976).

[15] R. A. Heidemann, *Chem. Eng. Sci.*, **33**, 1517 (1978).

[16] P. H. Bjornborn, *Ind. Eng. Chem. Fundam.*, **14**, 102 (1975); *A. I. Ch. E. J.*, **23**, 285 (1977).

[17] D. Geană, *Rev. Roumaine Chim.*, **26**, 43, 1365 (1981).

[18] H. W. Kuhn and A. W. Tucker, in "Proc. Sec. Berkley Symp. on Mathemat., Statist. and Probability", (J. Neymen ed.), Univ. California Press, 1951.

[19] M. Dragomirescu and M. Maliţa, "Programa neliniară", Ed. Ştiinţifică, Bucureşti, 1972.

[20] V. Dumitru, "Programare neliniară", Ed. Academiei, Bucureşti, 1975.

[21] I. Prigogine and R. Defay, "Chemische Thermodynamik", VEB Deutscher Verlag, Leipzig, 1962.

[22] J. G. Kirkwood and I. Oppenheim, "Chemical Thermodynamics", McGraw-Hill, NewYork, 1961.

[23] W. R. Smith, in "Theoretical Chemistry, Advances and Perspectives", vol. 5, Academic Press, New York, 1980; *Ind. Eng. Chem. Fundamen.*, **19**, 1 (1980).

Revue Roumaine de Chimie, 27, *9–10,* 1025–1027 (1982)

SEMIEMPIRICAL PREDICTION OF IONIZATION POTENTIALS

EDUARDO A. CASTRO and FRANCISCO M. FERNÁNDEZ
INIFTA, Sección Quimica Teorica, Suc. 4 — C.C. Nº 16, La Plata 1900, Argentina

Received May 27, 1981

Ruedenberg's and Robinson and Schaad's approximations for total electronic SCF energies are used in the calculation of ionization potentials. Results are analysed with respect to experimental values as well as in connection with other calculation schemes.

Two very simple relationships have recently been proposed to calculate total electronic Self-Consistent-Field (SCF) energies from orbital electronic SCF energies. Ruedenberg[1] has proposed an empirical relation between Hartree-Fock (HF) orbital energies e_s and the total HF–SCF energy E

$$E = 1.55 \sum_s n_s e_s \tag{1}$$

where n_s is the s-th orbital occupation number. From the combination of the rigorous HF formula for E

$$E = \sum_s n_s e_s + V_{nn} - V_{ne} \tag{2}$$

and the Politzer's[2] approximate relation

$$E = \frac{3}{7}(V_{ne} + 2V_{nn}) \tag{3}$$

where V_{ee} is the total electronic repulsion energy, V_{nn} is the total nuclear repulsion energy, and V_{ne} denotes the total nuclear-electronic attraction energy. Ruedenberg deduced the formula but he suggested

$$E = 1.5 \sum_s n_s e_s \tag{4}$$

that Eq. (1) was a better empirical relation for the total energy. Eq. (3) is approximately satisfied for molecules at equilibrium nuclear separations[2], so that Eq. (1) is valid for atoms and molecules at their equilibrium configurations. Robinson and Schaad[3,4] have proposed another calculation scheme which preserves the simplicity of Ruedenberg's formula and, furthermore, is it valid for any geometric configuration, equilibrium nuclear separations or not. This equation gives the electronic energy as 1/4 times the sum of orbital energies of a scaled system obtained by doubling each nuclear charge and halving each internuclear distance in the original molecule. Then, nuclear repulsion V_{nn} is added to get total SCF energy. The formula was deduced from a Z^{-1} perturbation method and has the form

$$E(Z, R) = 0.25 \sum_s n_s e_s (2Z, R/2) + V_{nn} \qquad (5$$

Both approximations have been numerically tested by several authors [5-25] and the results showed different degrees of agreement between SCF and empirical calculated energies. Rao and Sen [10] have recently tested the approximations (1) and (5) for the isoelectronic atomic series containing 2—18 electrons, based on the SCF wavefunctions given by Clementi and Roetti. [26] They found that Robinson and Schaad's formula (5) is superior to the Ruedenberg's relation (1). In spite of the fact that there exist several comparisons for total energies, this is not true for the calculations of experimentally observable quantities. Such a kind of comparison would offer us a more direct measure of the goodness and accuracy of them. For that reason we have believed of interest to supplement Rao and Sen's comparison, making a calculation of atomic ionization energies and confronting them with available experimental data. The ionization energies of the light atoms were measured in the early days of the atomic theory by Hertz. [27] His results were improved over the years and at the present there are very accurate experimental values. Theoretically, the ionization energy may be obtained from the difference between the ionization term energies and the ground state energy of the atom. We have employed Eqs (1) and (5) to calculate the ionization energies of atoms with $Z = 3$ up to $Z = 16$. Results are presented in Table 1 together with experimental values and other ionization potentials calculated recently by Brandus [28] and by us [29] for comparison purposes. We can see that results obtained from Eqs (1) and (5) (columns 2 and 3) are definitely incorrect. Ruedenberg's relation predicts that atoms are unstable with respect to ionized species, and similar results follow from Robinson and Schaad's approximation, except the first three members of the series. On the contrary, from exact SCF data (fourth column) as well as from more elaborate approximations (column 5 and 6) we obtain accurate enough results which are in a very good agreement with experimental values (column 7).

As final conclusion we can not deny the importance and value of the use of additive-like relationships for electronic total energies, because there are several fields where they could be applied with success.[30] However, special care has to be exercised in their applications and matching against experimental data, whenever possible, would be made in order to get a deeper insight into the qualities and ranges of applicability of these approximate formulae.

TABLE 1

Atomic ionization energy (atomic units)

Atom	Eq. (1)	Eq. (5)	SCF data[26]	Brandus[28]	Castro et al.[9]	Experimental[39]
Li	0.12	−0.67	0.20	0.21	0.20	0.20
Be	0.16	−1.33	0.30	0.29	0.31	0.35
B	0.02	−2.22	0.29	0.36	0.30	0.31
C	−0.00	−3.22	0.40	0.42	0.41	0.42
N	−0.27	−4.60	0.34	0.47	0.57	0.54
O	−0.07	−5.71	0.66	0.50	0.84	0.50
F	−0.42	−7.58	0.58	0.56	1.50	0.70
Ne	−0.51	−9.28	0.73	0.59	0.71	0.80
Na	−0.68	−4.04	0.18	0.26	0.13	0.19
Mg	−0.75	−5.03	0.24	0.33	0.26	0.28
Al	−1.12	−5.24	0.20	0.30	0.21	0.22
Si	−1.19	−6.45	0.28	0.45	0.29	0.30
P	−1.44	−7.72	0.25	0.51	0.25	0.40
S	−1.31	−9.01	0.48	0.57	0.44	0.38

REFERENCES

[1] K. Ruedenberg, *J. Chem. Phys.*, **66**, 375 (1977).
[2] P. Politzer, *J. Chem. Phys.*, **64**, 4239 (1976).
[3] B. H. Robinson and L. J. Schaad, *J. Chem. Phys.*, **59**, 6189 (1973).
[4] L. J. Schaad, B. H. Robinson and B. A. Hess, Jr., *J. Chem. Phys.*, **67**, 4616 (1977).
[5] C. S. Sharma and C. A. Coulson, *Proc. Phys. Soc. (London)*, **80**, 81 (1962).
[6] E. A. Castro, *Anal. Asoc. Quīm. Argentina*, **66**, 173 (1978).
[7] E. A. Castro, *Int. J. Quantum Chem.*, **15**, 355 (1979).
[8] E. A. Castro, *Rev. Roumaine Chim.*, **25**, 41 (1980).
[9] E. A. Castro, L. Villata and F. M. Fernandez, *J. Chem. Phys.*, **74**, 592 (1981).
[10] C. V. Rao and K. D. Sen, *J. Chem. Phys.*, **70**, 586 (1979).
[11] K. D. Sen, *J. Phys. B : Atom. Molec. Phys.*, **12**, L287 (1979).
[12] P. Politzer and K. C. Daiker, *Int. J. Quantum Chem.*, **14**, 245 (1978).
[13] D. B. Boyd, *J. Chem. Phys.*, **67**, 1787 (1977).
[14] E. B. Priestley and S. Fraga, Canad. J. Phys., **44**, 1933 (1966).
[15] S. T. Wu, *J. Chem. Phys.*, **69**, 4709 (1978).
[16] A. Francis and L. Pujol, *J. Chem. Phys.*, **71**, 1066 (1979).
[17] M. M. Heaton, *J. Chem. Phys.*, **70**, 4435 (1979).
[18] T. Anno, *J. Chem. Phys.*, **69**, 2936 (1978).
[19] T. Anno and Y. Sakai, *J. Chem. Phys.*, **70**, 2579 (1979).
[20] P. Politzer, *J. Chem. Phys.*, **69**, 491 (1978).
[21] P. Politzer, *J. Chem. Phys.*, **70**, 1067 (1979).
[22] M. A. Whitehead, *J. Chem. Phys.*, **69**, 497 (1978).
[23] T. Anno, *J. Chem. Phys.*, **72**, 782 (1980).
[24] R. G. Parr and S. R. Gadre, *J. Chem. Phys.*, **72**, 3669 (1980).
[25] J. F. Mucci and N. H. March, *J. Chem. Phys.*, **71**, 1495 (1979).
[26] E. Clementi and C. Rosetti, *At. Data and Nucl. Data Tables*, **14**, 177 (1974).
[27] G. Hertz, *Z. Physik.*, **95**, 408 (1919).
[28] L. Brandus, *Rev. Roumaine Phys.*, **24**, 559 (1979).
[29] E. A. Castro and F. M. Fernández, *Chemica Scripta* (in press).
[30] E. A. Castro and F. M. Fernández, *Folia Chimica Theoretica Latina* (submitted for publication).
[31] C. E. Moore, "Ionization Potentials and Ionization Limits Derived from the Analysis of Optical Spectra, NSRDS – NBS 34", National Bureau of Standards, U.S.A., 1970.

Revue Roumaine de Chimie, 27, *9–10*, 1029–1033 (1982)

SPECTRAL STUDY OF THE INFLUENCE OF POLYSTYRENE IN BENZENE SOLUTIONS ON THE α, α′-DIPHENYL-β-PICRYLHYDRAZYL (DPPH) RADICAL

C. GHIRVU, ANA ONU and GH. IONIȚĂ

Polytechnic Institute of Jassy, Faculty of Chemical Technology, Department of Physical Chemistry, Splai Bahlui 71, Jassy 6600, Romania

Received February 12, 1981

The influence of polystyrene in benzene solutions on the DPPH radical has been investigated by ultraviolet (UV) and visible (VIS) spectroscopy. The time diminution of the amount of free radical as a function of the concentration and age of the polystyrene in benzene solutions has been revealed and the observed phenomena explained.

INTRODUCTION

As well known, the DPPH free radical has a great stability both in the crystalline and in benzene solutions due to its electronic structure.[1–4] Therefore, this radical was extensively studied by ESR spectrometry, being used as standard for the *g* factor and for the spectral intensity.

The intense colour of the hydrazyl radicals solutions was allowed to the presence of ionic forms in solution,[5] but the MO calculations of the $\pi \rightarrow \pi^*$ transition energies for some of these radicals pointed out that the absorption in the visible spectrum is due to the unpaired electron,[6] the contribution of the ionic forms being insignificant.[7]

The aim of this paper is the study of the UV – VIS spectra of the DPPH free radical in polystyrene in benzene solutions. The spectra of DPPH free radical in these solutions pointed out that the amount of radical was diminished both by the polystyrene concentration and the age of solutions. These observations could be used for the characterization of the polymer solutions.

EXPERIMENTAL PART

The spectra of the DPPH free radical were investigated by using four solutions of polystyrene in benzene (1.5 ; 1 ; 0.5 and 0.25 g/dl). As polystyrene we used a standard polymer of molecular weight 150,000 as well as a Romanian one of molecular weight 37,200 g/mol. The solutions of polystyrene in benzene were used after 2, 30 and 90 days after the preparation.

The final solutions of $0.5 \cdot 10^{-3}$ M in DPPH (BDH Laboratory Reagents), were prepared by mixing a solution of DPPH in benzene with polystyrene in benzene solutions. The visible spectra (350 – 800 mμ) were recorded by using a Karl Zeiss Jena UV – VIS spectrophotometer.

All the spectra are similar, nevertheless the diminution of amount of the free radical in time depends on the concentration of polystyrene in benzene solutions. This observation is illustrated in Figure 1, where the time dependence of the optical density corresponding to the absorption maximum (525 mμ) was represented.

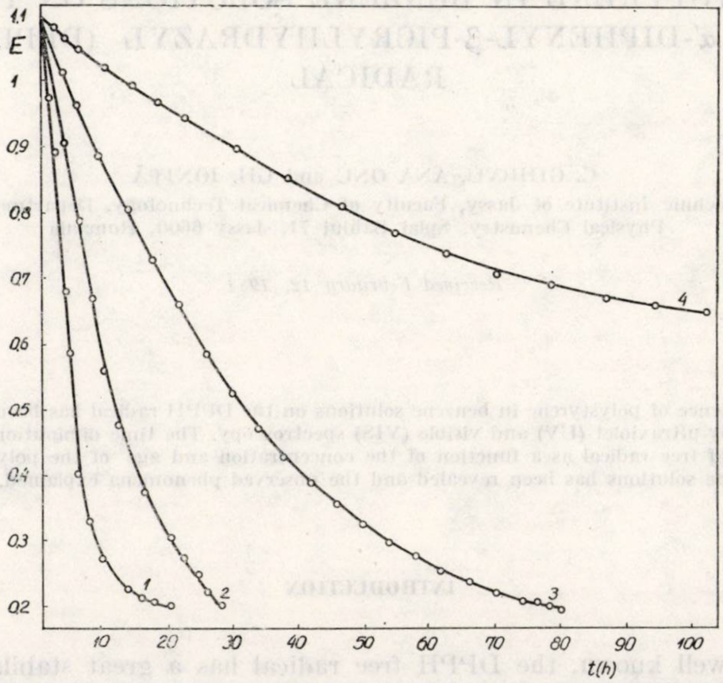

Fig. 1. – The diminution of the amount of DPPH free radical in fresh solutions of polystyrene in benzene: *1.* concentration of polystyrene in benezene solution 1.5 g/dl; *2.* concentration 1.0 g/dl; *3.* concentration 0.5 g/dl; *4.* concentration 0.25 g/dl.

The dependence of the diminution of the radical concentration as a function of the age of the polystyrene in benzene solution is given both in Figure 2 and Table 1.

DISCUSSION OF THE RESULTS

The first thing to be explained was the time diminution of the amount of free radical. First, we assumed a possible chemical interaction between radical and the rests of initiator, monomer or other impurities of solution, but the purification of polystyrene by reprecipitation with methanol did not support this explanation. Therefore, we looked for another possibility of the radical transformation. So the DPPH → $DPPH_2$ chemical transformation was presumed as a consequence of a capture of an hydrogen atom by the free radical and its transition to the corresponding hydrazine. To verify this supposition, we extended spectral

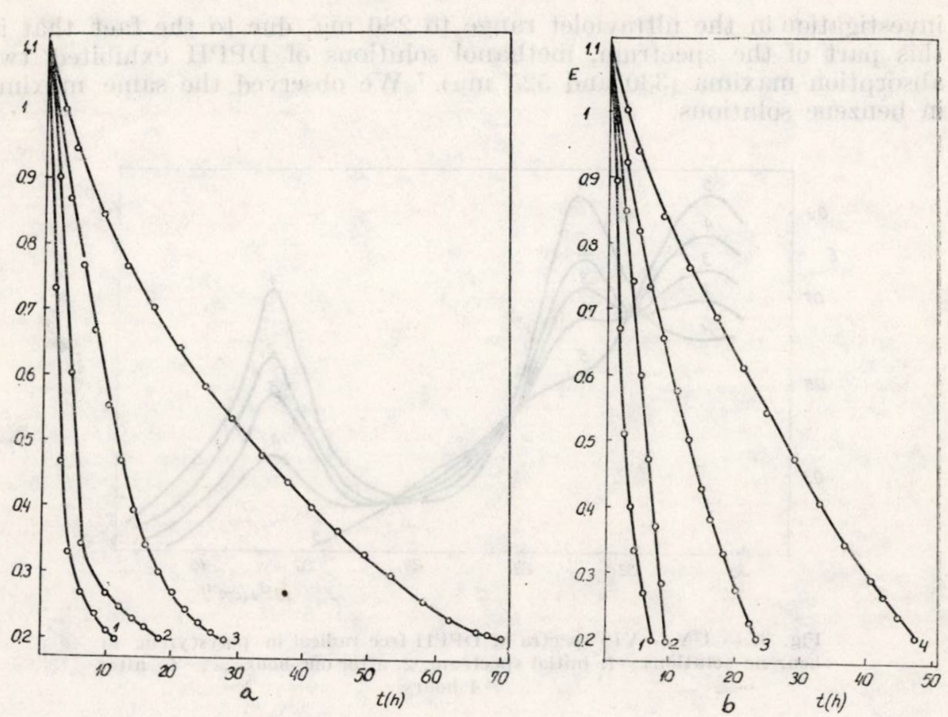

Fig. 2. — Time diminution of the amount of DPPH free radical in polystyrene in benzene solutions : a. 30 days after the preparation of polystyrene in benzene solution ; b. 90 days after the preparation of polystyrene in benzene solution. Other indications are the same as in Figure 1.

TABLE 1

The disappearance of DPPH free radical as a function of concentration and age of the polystyrene solutions

Concentration of polystyrene in benzene solutions (g/dl)	Concentration of DPPH in polystyrene in benzene solutions mol/l	Age of polystyrene solutions (days)	Disappearance time of radical (h)
1.5	$0.5 \cdot 10^{-3}$	fresh	20
		30	12
		90	7
1.0	$0.5 \cdot 10^{-3}$	fresh	28
		30	18
		90	9
0.5	$0.5 \cdot 10^{-3}$	fresh	80
		30	28
		90	23
0.25	$0.5 \cdot 10^{-3}$	fresh	>120
		30	70
		90	47

investigation in the ultraviolet range to 280 mμ, due to the fact that in this part of the spectrum, methanol solutions of DPPH exhibited two absorption maxima (330 and 525 mμ). [7] We observed the same maxima in benzene solutions.

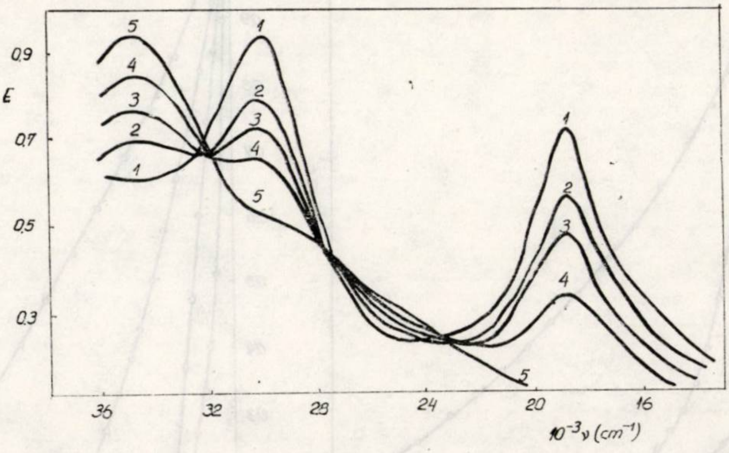

Fig. 3. — UV — VIS spectra of DPPH free radical in polystyrene in benzene solutions : *1.* initial spectrum, *2.* after one hour, . . . *5.* after 4 hours.

The investigation of DPPH free radical spectra using polystyrene in benzene solutions pointed out that the intensity of the two absorption bands of DPPH became smaller in time. However, a new band, located at 290 mμ, whose intensity grew up in time, appeared (Figure 3).

We assigned this absorption band to the DPPH$_2$ hydrazine in methanol solution, this band being localized around 320 mμ. [7] To verify this assertion, the corresponding hydrazine was prepared by reducing the radical with hydroquinone. [8] The electronic spectra were recorded in methanol solutions. On the other side, from the final mixture of DPPH in polystyrene in benzene solution, obtained after the disappearance of the radical, the polystyrene was precipitated with methanol then, after filtration, the solution was evaporated to remove benzene and methanol. The obtained residue was again dissolved in methanol and a solution of DPPH$_2$ in hydroquinone and methanol was added. The obtained spectra exhibited an absorption band located at the same wavelength but of a great intensity.

Therefore, the diminution of the radical concentration in polystyrene in benzene solutions is due to its transformation into the corresponding DPPH$_2$ hydrazine. Our conclusion is] also supported by the observation that the intensity of absorption band of the solution resulted after the disappearance of the radical was increasing when a DPPH$_2$ in polystyrene solution was added.

Finally, it should be mentioned that the spectrum of methanol solution of the residue obtained by evaporation of the solution, when the polystyrene was removed, was the same as that presented for $DPPH_2$ in reference 7.

The influence of the concentration of polystyrene in benzene solutions on the diminution time of the radical could be explained by the fact that an increase of polystyrene concentration in benzene solution will increase the rate of collision between the DPPH and polystyrene molecules. Therefore, the probability of DPPH → $DPPH_2$ transformation will also increase.

As concerns the dependence of the diminution time of the radical as a function of molecular weight we observed that the amount of radical diminished faster when we used polystyrene of molecular weight 37,200 g/mol as compared with the case when we used polystyrene of molecular weight 354,200 g/mol. This observation is illustrated in Figure 4.

This investigation suggests that the molecular weight of polystyrene in benzene solutions is diminished in time by the electromagnetic radiation. Therefore we proceeded to the measurements of molecular weights by the osmotic pressure method. These measurements have pointed out that the molecular weight of polystyrene was two times smaller in a 30 days' old solution than in a fresh one.

We can conclude that the stability of DPPH radical in polymer solutions is influenced both by the concentration of the polymer solutions and the molecular weight of polymer. Therefore, the spectral study of the radical in polymer solutions could supply information on the polymer structure in solution.

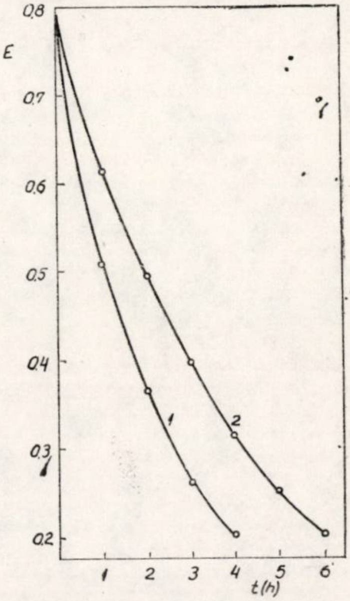

Fig. 4. — Diminution of the amount of radical as a function of molecular weight: 1. polystyrene of molecular weight 37,200; 2. polystyrene of molecular weight 354,200.

REFERENCES

[1] I. Ursu, "Rezonanţă Electronică de Spin", Ed. Academiei R.S.R., Bucureşti, 1965, p. 209—213; I. G. Murgulescu and V. Em. Sahini, "Introducere în chimia fizică, vol. I, 2", Ed. Academiei R.S.R., Bucureşti, 1978, p. 333—355.

[2] A. N. Holden, C. Kittel, F. R. Merritt and W. A. Yager, *Phys. Rev*. **77**, 147 (1950).

[3] V. W. Cohen, C. Kikuchi and J. Turkevich, *Phys. Rev*., **85**, 379 (1952).

[4] C. Kikuchi and W. M. Cohen, *Phys. Rev*., **93**, 394 (1954); I. Anghelache, D. Sădulescu and V. Vântu, *Rev. Roumaine Chim*., **16**, 1901, (1971).

[5] R. O. Matevosian, L. V. Holevinskaya and A. K. Chirikov, *Zur. org. Khim*, **1**, 1703 (1965).

[6] V. A. Gubanov, L. A. Pereljaeva, A. K. Chirchov and R. O. Matevosian, *Theor. Chim. Acta*, **18**, 177(1970).

[7] V. A. Gubanov, L. A. Pereljaeva, A. K. Chircov, G. N. Yastchenko and R. O. Matevosian, *Internat. J. Quantum Chem*., **5**, 513 (1971).

[8] C. D. Neniţescu, "Chimie Organică", vol. II, Ed. Didactică şi Pedagogică, Bucureşti, 1966, p. 590.

polystyrene was removed, was the same as that presented for $DPPH_2$ in reference [7].

The influence of the concentration of polystyrene in benzene solutions on the diminution time of the radical could be explained by the fact that an increase of polystyrene concentration in benzene solution will increase the rate of collision between the DPPH and polystyrene molecules. Therefore, the probability of $DPPH \rightarrow DPPH_2$ transformation will also increase.

As concerns the dependence of the diminution time of the radical as a function of molecular weight we observed that the amount of radical diminished faster when we used polystyrene of molecular weight 37,200 g/mol as compared with the case when we used polystyrene of molecular weight 354,200 g/mol. This observation is illustrated in Figure 4.

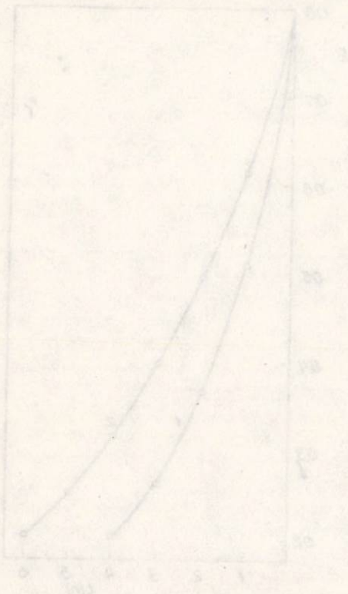

Fig. 4. – Diminution of the amount of radical as a function of molecular weight : 1, polystyrene of molecular weight 37,200; 2, polystyrene of molecular weight 354,200.

This investigation suggests that the molecular weight of polystyrene in benzene solutions is diminished in time by the electromagnetic radiation. Therefore we proceeded to the measurements of molecular weights by the osmotic pressure method. These measurements have pointed out that the molecular weight of polystyrene was two times smaller in a 30 days' old solution than in a fresh one.

We can conclude that the stability of DPPH radical in polymer solutions is influenced both by the concentration of the polymer solutions and the molecular weight of polymer. Therefore, the spectral study of the radical in polymer solutions could supply information on the polymer structure in solution.

REFERENCES

[1] I. Ursu, "Rezonanța Electronică de Spin", Ed. Academiei R.S.R., București, 1965, p. 209–213; I. G. Murgulescu and V. Em. Sahini, "Introducere în chimia fizică", vol. I, 2, Ed. Academiei R.S.R., București, 1978, p. 352–355.
[2] A. N. Holden, C. Kittel, F. R. Merritt and W. A. Yager, Phys. Rev., 77, 147 (1950).
[3] W. Cohen, C. Kikuchi and J. Turkevich, Phys. Rev., 85, 379 (1952).
[4] C. Kikuchi and W. M. Cohen, Phys. Rev., 93, 394 (1954); I. Angelescu, D. Săndulescu and V. Vasile, Rev. Roumaine Chim., 16, 1901 (1971).
[5] R. O. Matevosian, L. V. Holevinskaya and A. K. Chirkov, Zh. org. Khim. 1, 1703 (1965).
[6] V. A. Gubanov, L. A. Pereliaeva, A. K. Chirkov and R. O. Matevosian, Theor. Chim. Acta, 18, 177 (1970).
[7] V. A. Gubanov, L. A. Pereliaeva, A. K. Chirkov, G. N. Yastrebova and R. O. Matevosian, Internat. J. Quantum Chem., 5, 513 (1971).
[8] C. D. Nenitzescu, "Chimie Organică", vol. II, Ed. Didactică și Pedagogică, București, 1966, p. 390.

Revue Roumaine de Chimie, 27, *9–10*, 1035–1036 (1982)

ON A FORMULA OF RACAH AND SHADMI FOR THE INTERELECTRONIC REPULSION PARAMETERS

C. I. LEPĂDATU
Center of Chemical Physics – ICECHIM
Spl. Independenţei 202, Bucharest, Romania

Received July 11, 1981

An empirical formula of Racah and Shadmi for the interelectronic repulsion parameter B is theoretically proved. The proof makes use of three types of atomic orbitals (Slater, Clementi-Raimondi and Burns).

Many years ago, Racah and Shadmi [1] reported an empirical formula for the interelectronic repulsion parameter B $(3d^n)$, found from the spectral data

$$B(3d^n) \simeq 80Z + 95Q - 1295\ (\mathrm{cm}^{-1}), \tag{1}$$

where Z is the atomic number and Q the oxidation state of the element. The aim of this note is to prove the validity of this empirical relationship. We express firstly the B parameter in terms of Slater-Condon ones [1]

$$B = \frac{1}{49}F^2 - \frac{5}{441}F^4, \tag{2}$$

where

$$F^k(n_i, n_j) = \iint R^2_{n_i} R^2_{n_j} \frac{r^k_<}{r^{k+1}_>} r_i^2 r_j^2 dr_i dr_j \tag{3}$$

The radial integrals $F^k(n_i, n_j)$ may be calculated using the radial parts of the nodeless atomic orbitals

$$R_n = N_n r^{n-1} e^{-\zeta r}, \tag{4}$$

where N_n is the normalization factor, n the principal quantum number and $\zeta = Z_{ef/n}$, Z_{ef} being the screened nuclear charge. Substituting (4) for (3) and using a suggestion given by Judd, [2] we find

$$F^k = \frac{4(2n+k)!}{(2n)!\,(2n)!}\left[(2n-k-1)! - \sum_{r=0}^{2n+k} \frac{(2n-k-1+r)!}{r!\,2^{2n-k+r}}\right], \tag{5}$$

where k = 2, 4, etc.

From (2) and (5) we obtain a very simple expression for B

$$B(3d^n) = 129.73\, Z_{ef}\, (cm^{-1}) \tag{6}$$

The screened nuclear charge may be calculated according to the following relationship derived from the Slater rules [3]

$$Z_{Slater} = 0.65\ Z + 0.35 Q - 8.95 \tag{7}$$

If Clementi-Raimondi atomic orbitals[4] are used, the effective nuclear charge may be estimated from the following expression, which is equivalent with the rules given by the mentioned authors

$$Z_{C-R} = 0.7307\ Z + 0.2693\ Q - 8.4727 \tag{8}$$

For Burns orbitals, [5] the nuclear charge may be calculated as follows

$$Z_{Burns} = 0.65\ Z + 0.35\ Q - 7.85 \tag{9}$$

From (6) – (9), we find the following expressions for the interelectronic repulsion parameter B (in cm^{-1})

$$\begin{aligned} B(3d^n)_{Slater} &= 84.32\ Z + 45.40\ Q - 1161.08 \\ B(3d^n)_{C-R} &= 94.79\ Z + 34.93\ Q - 1099.16 \qquad (10) \\ B(3d^n)_{Burns} &= 84.32\ Z + 25.94\ Q - 1018.38 \end{aligned}$$

As may be seen, the theoretical expressions obtained with three different types of atomic orbitals widely used in the literature, may be favourably compared with the Racah-Shadmi formula. The agreement is better for the neutral elements ($Q = 0$).

REFERENCES

[1] J. S. Griffith, "The Theory of Transition Metal Ions", Cambridge, Univ. Press., 1964.

[2] B. R. Judd, "Operator Technique in Atomic Spectroscopy", Mc. Graw-Hill Comp., Inc., New York, 1963, Appendix 1.

[3] C. I. Lepadatu, unpublished data.

[4] E. Clementi and D. L. Raimondi, *J. Chem. Phys.*, **38**, 2686 (1963).

[5] G. Burns, *J. Chem. Phys.*, **41**, 1521 (1964).

Revue Roumaine de Chimie 27, *9–10*, 1037–1046 (1982)

SYNTHESIS OF PYRYLIUM SALTS WITH AN ANNELATED DIBENZO[*f*, *i*]BICYCLO[3.2.2]NONA-6,8-DIENE SKELETON (OXONIA-HOMOTRIPTYCENES) AND THEIR REACTIONS WITH NUCLEOPHILES

M. BANCIU, A. T. BALABAN, C. DRĂGHICI and RODICA VLAD
Laboratory of Organic Chemistry — TCH, Polytechnic Institute, 76206 Bucharest 16, Romania

Received February 15, 1982

The reaction between acetophenone and the hydroxymethylene ketone **2** (synthesized by formylation of the known ketone **1**) in the presence of perchloric acid afforded two isomeric pyrylium salts **3** and **4**, the former main product **3** being isolated as a pure substance. The reaction of the mixture of **3** and **4** with methylamine or ammonia afforded mixtures of pyridinium salts **6** and **7** or of pyridines **8** and **9**, respectively ; in both cases the main products **6** and **8** could be isolated in pure state. From the reaction of the pyrylium salts mixture **3** + **4** with aniline the N-phenylpyridinium perchlorate **5** was obtained.

The structures of the new compounds **3**–**9** and the reaction mechanisms are discussed.

INTRODUCTION

In another paper from this laboratory [1] aiming to develop the chemistry of dibenzo[*f*, *i*]bicyclo[3.2.2]nona-6,8-dien-2-one (**1**), previously obtained by us, [2] the synthesis of the tautomeric hydroxymethyleneketone ⇄ β-ketoaldehyde **2** was described. In the same paper, [1] convincing spectral evidence was brought in order to demonstrate the existence of this compound in the enolic form **2b.**

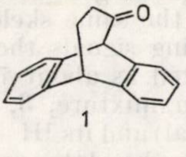
1

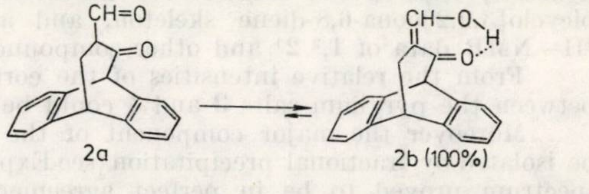

2a
2b (100%)

In this paper we describe the synthesis of two isomeric pyrylium salts (oxonia-homotriptycene derivatives) starting from this hydroxymethylene ketone **2b**, as well as further reactions of these pyrylium salts with nucleophiles. The growing interest in pyrylium salts chemistry is illustrated by the numerous recent applications and reviews. [3–7]

RESULTS AND DISCUSSION

The synthesis of the pyrylium salts was performed by the condensation of β-ketoaldehyde **2** with a ketone possessing a reactive α-CH_2 group. [3] This type of reaction goes back to Dilthey [8] who first condensed 1,3-diketones with ketones having an α-methyl(ene) group, but has received revived interest, [9,10] especially after Dorofeenko and Junghietu[10] showed that it gives good results with hydroxymethyleneketones (β-ketoaldehydes).

The reaction of the hydroxymethylene ketone **2b** [1] with acetophenone in acetic acid (1.5 hours at 100 — 105°) in the presence of perchloric acid gives rise to a yellowish-green solid product (yield 18 %).

The IR spectrum of the solid demonstrates, through the characteristic ClO_4^- bands at 625 and 1100 cm^{-1}, the formation of pyrylium perchlorate(s).

The relatively complex ^1H-NMR spectrum (in $F_3C-COOH$) — see Experimental — could be separated in two simple spectra corresponding to two isomeric pyrylium salts **3** and **4**, taking into account the pattern of the signals as well as their relative intensities.

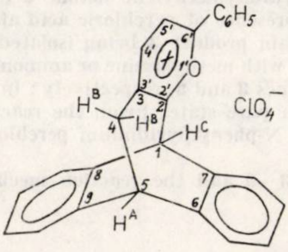

3

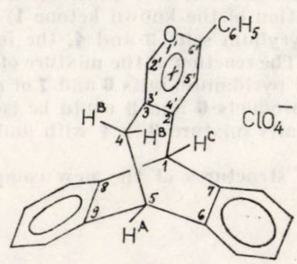

4

The assignment of the signals is given in Table 1. A confirmation of these attributions comes out from a double resonance experiment: when the quintet at about 4.5 ppm was irradiated, the doublets at 3.27 and 3.5 ppm were converted into singlets (H^B from **3** and **4**) and when the doublets at 3.27—3.5 ppm were irradiated, the quintet at 4.3—4.6 ppm was converted into a doublet, protons H^A from **3** and **4** giving singlet signals under these conditions. The pattern and the positions of the doublets, triplets and singlets are characteristic for the dibenzo[*f*, *i*] bicyclo[3.2.2]nona-6,8-diene skeleton, and are in good agreement with ^1H-NMR data of **1**,[2] **2**[1] and other compounds with the same skeleton. [2]

From the relative intensities of the corresponding signals the ratio between the pyrylium salts **3** and **4** could be evaluated as about 70 : 30.

Moreover the major component of the reaction mixture, **3**, could be isolated by fractional precipitation (see Experimental) and its ^1H-NMR spectrum proved to be in perfect agreement with the data assigned from the spectrum of the mixture of **3** and **4**.

Another proof (an indirect one) that the major isomer has structure **3** comes out from the reaction with different nucleophiles (v. infra) in which the major isomers — having undoubtfully proved structures — are always those corresponding to the pyrylium salt **3**.

From the above results it follows that the reaction of **2** with acetophenone takes place in two ways affording the two isomeric pyrylium salts **3** and **4**:

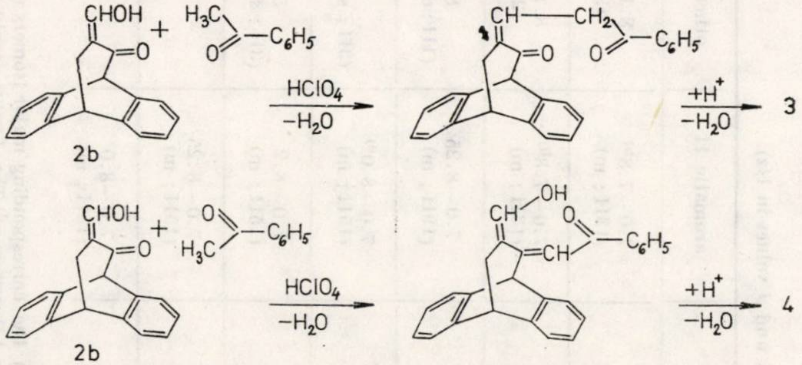

The formation of **3** in larger amounts than **4** could be attributed to higher reactivity of the aldehydic (hydroxymethylenic) group as compared to the ketonic group from **2**.

The mixture of pyrylium salts was then converted with primary amines into pyridinium salts. [4,6,7]

Reaction of the mixture of **3** and **4** with aniline afforded in 32% yield, after long standing in the refrigerator, a white solid. The ^1H-NMR spectrum (Table 1) suggests that the product is a unitary compound, for which the structure **5** is proposed (probably the pyridinium salt corresponding to the minor pyrylium component **4** remains soluble in the reaction mixture; see Experimental).

The signals at 3.66; 4.46 and 5.28 ppm are characteristic for H^B, H^A and H^C respectively. The confirmation of the structure **5**, especially the position of the N atom, was brought starting from the observation that in the multiplet at 7.0–8.25 ppm a doublet could be easily seen at 8.17 ppm ($J = 8.5$ Hz). This doublet could be a part of an AB-system corresponding to H^D and H^E. In order to prove this assumption, the ^1H-NMR spectrum (in CH_2Cl_2) was followed in the presence of increasing amounts of $Eu(fod)_3$ as shift reagent. It had been previously demonstrated that europium chelates cause induced shifts in ^1H-NMR spectra of pyridinium salts. [11,12] In the present spectra the characteristic quartet of the AB-system begins to appear at a 0.22 ratio $Eu(fod)_3/\mathbf{5}$ and becomes totally separated from the remaining aromatic proton multiplet at a 0.47 molar ratio $Eu(fod)_3/\mathbf{5}$. It must be stressed that the coupling constant of 8.5 Hz is characteristic [13] for an *ortho*-coupling $^3J_{45}$ bringing thus another confirmation for structure **5**. (In a pyridinium salt corres-

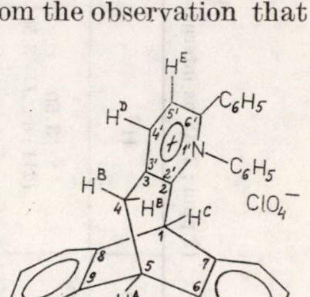

5

TABLE 1

^{1}H–NMR data for compounds **3**–**9**[a)]

(δ ppm ; TMS as internal standard ; number of protons, multiplicity and J values in Hz)

Compound (solvent)	H^B	H^A	H^C	aromatic H	other signals
Pyrylium salt **3** (TFA)	3.50 (2H ; d ; J = 3.5)	4.50 (1H ; t ; J=3.5)	5.50 (1H ; s)	7.0–7.8[b)] (13H ; m)	8.1–8.5[b)] (2H ; m)
Pyrylium salt **4** (TFA)	3.27 (2H ; d ; J=3.5)	4.36 (1H ; t ; J=3.5)	5.47 (1H ; s)	7.0–7.8[b)] (13H ; m)	8.1–8.5[b)] (2H ; m)
N-Phenylpyrydinium salt **5** (TFA)	3.66 (2H ; d ; J=3.5)	4.46 (1H ; t ; J=3.5)	5.28 (1H ; s)	7.0–8.25 (19H ; m)	8.17[c)] (1H ; d ; J=8.5Hz)
N-Methylpyridinium salt **6** ($CDCl_3$)	3.40 (2H ; d)[d)]	4.31 (1H ; t)[d)]	6.10 (1H ; s)	7.0–8.0[e)] (15H ; m)	4.60 (3H ; s ; CH_3–N)
N-Methylpyridinium salt **7** ($CDCl_3$)	3.15 (2H ; d)[d)]	4.17 (1H ; t)[d)]	6.05 (1H ; s)	7.0–8.2 (15H ; m)	5.15 (3H ; s ; CH_3–N)
Pyridine **8** ($CDCl_3$)	3.20 (2H ; d ; J=3.5)	4.23 (1H ; t ; J=3.5)	5.37 (1H ; s)	7.0–8.25 (15H ; m)	–
Pyridine **9** ($CDCl_3$)	2.97 (2H ; d ; J=3.5)	4.12 (1H ; t ; J=3.5)	5.20 (1H ; s)	7.0–8.0 (15H ; m)	–

[a)] The data for compounds **4**, **7** and **9** were extracted from the spectra of mixtures with the corresponding major isomers (**3**, **6**, respectively **8**) ; [b)] The signals from 7.0–8.5 of **3** and **4** are superimposed on each other ; [c)] A part of an AB-system ; [d)] The J values could not be determined exactly ; [e)] The AB–system of pyridinium protons visible with $Eu(fod)_3$

ponding to **4** the protons H^D and H^E would be in *para*-positions and, consequently, they should have a much smaller coupling constant, $^5J_{25}$ of 1.0—1.5 Hz. [13]

The reaction of the mixture of pyrylium salts **3** and **4** with methylamine in methanol solution afforded — in about 35 % yield — a yellow solid whose ^1H-NMR spectrum indicated a mixture of two isomeric N-methylpyridinium perchlorates **6** and **7**.

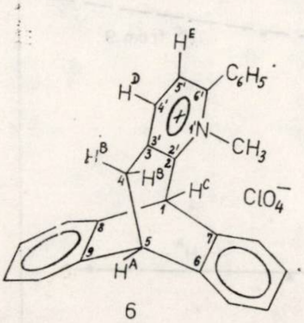

6

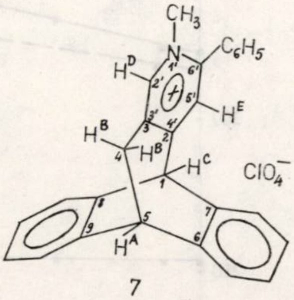

7

The assignment of the signals was made similarly as for the pyrylium salts **3** and **4** (Table 1). From the spectrum a 75 : 25 ratio of **6** : **7** could be calculated. The major component **6** could be isolated as a pure compound (see Experimental). Its ^1H-NMR spectrum is also in perfect agreement with that assigned from the spectrum of the crude reaction mixture. The ^1H-NMR spectra of **6** recorded in the presence of $Eu(fod)_3$ indicated characteristic induced shifts for different protons in agreement with the proposed structure. Moreover, the characteristic AB-system of two *ortho*-pyridinium protons ($J = 8.5$ Hz) occurs at a 0.8 molar ratio $Eu(fod)_3/$**6** bringing thus another evidence in favour of the structure **6**. The molar induced shifts for the other protons are in the following order: $H^C > CH_3 > H^B > H^A$.

The reaction of pyrylium salts with ammonia[4-7] was also investigated.

When a methanolic solution of **3** and **4** (as a mixture obtained as above) was treated with an excess of aqueous ammonia an orange-coloured solid was obtained in about 50 % yield. The ^1H-NMR spectrum indicates that the product is a mixture of two pyridines **8** and **9** in about 75 : 25 ratio.

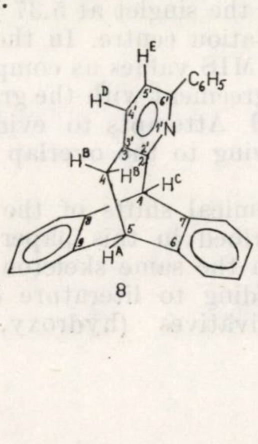

8

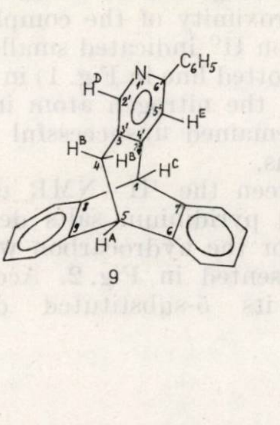

9

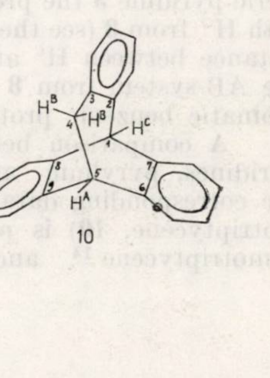

10

On treating a concentrated benzenic solution of the mixture of **8** and **9** with *n*-heptane, a unitary product precipitates. Its ^1H-NMR spectrum (Table 1) is in agreement with the structure **8**. A confirmation of this structure **8** results from the spectra recorded in the presence of Eu (fod)$_3$ (Fig. 1). As expected, among the protons bonded to saturated carbons, the greatest MIS value was observed for the singlet at 5.37 ppm because H^C lies in the proximity of the complexation centre. In the isomeric pyridine **9** the proton H^C indicated smaller MIS values as compared with H^C from **8** (see the dotted line in Fig. 1) in agreement with the greater distance between H^C and the nitrogen atom in **9**. Attempts to evidence the AB-system from **8** remained unsuccessful owing to the overlap with aromatic benzenic protons.

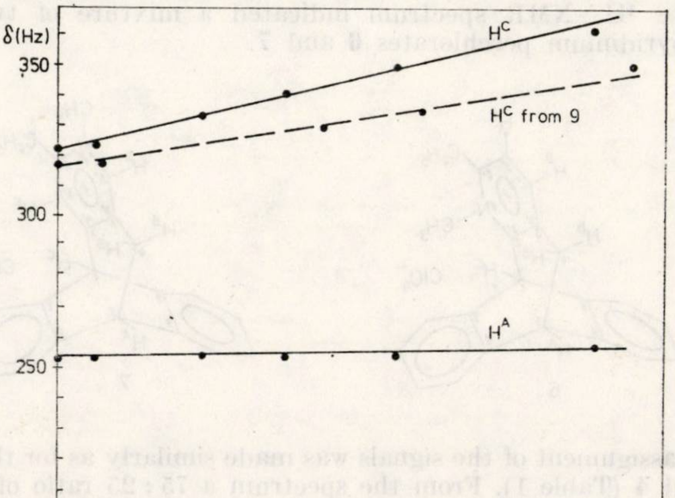

Fig. 1. — Variation of δ values for characteristic protons of pyridine **8** as a function of the molar ratio Eu(fod)$_3$/**8**. The calculated molar induced shifts are : H^A, 10.9 ; H^B, 17.4 ; H^C, 116.5 Hz. The dotted line corresponds to H^C from the isomeric pyridine **9**.

A comparison between the ^1H-NMR chemical shifts of the new pyridines, pyrylium- and pyridinium salts described in this paper and the corresponding data for the hydrocarbon with the same skeleton (homotriptycene, **10**) is presented in Fig. 2. According to literature data, homotriptycene [14] and its 5-substituted derivatives (hydroxy, [14,15] chloro,[14] alkoxy[14] or acetoxy[14]) present consistent data for the H^A, H^B and H^C protons.

The known and the new compounds with homotriptycene skeletons from Fig. 2 present all a unified pattern of H^A, H^B and H^C chemical shifts as well as of coupling constants.

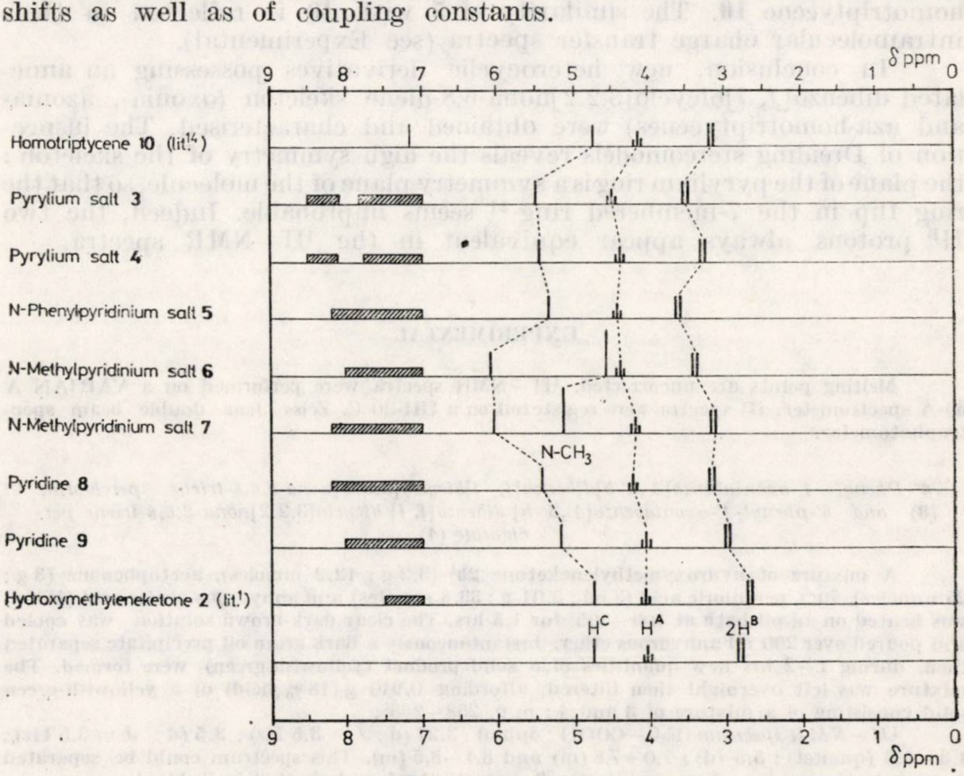

Fig. 2. — Correlation of ^{1}H—NMR spectra of compounds **2**—**10**.

An intriguing observation is the different shielding of the N-methyl protons in the two pyridinium salts **6** and **7**. The higher field resonance observed for the N-methyl protons in **6** is contrary to the calculated effect following the Johnson — Bovey diagram[16] (a deshielding of —0.6 ppm is calculated as the effect of the two benzene rings*) for the central point of the freely rotating methyl group, as indicated by other authors[17]), while the effect for the methyl protons in **7** is negligible. A qualitatively similar (but quantitatively smaller) deshielding for the N-methyl in **6** results from the Haigh — Mallion tables.[18] However, this discrepancy between theory and experiment is probably not due to erroneous structural or spectral assigments, but to the poor predictive ability of the calculated (de)shieldings. Indeed, criticism of the Johnson — Bovey and Haigh — Mallion data has recently been voiced by Mallion himself.[19]

---

*) The effect of the phenyl group adjacent to the heteroatom is assumed to be equal for both isomers, especially since in neither of them is there any reason to suppose different tilting angles between the pyridinium and phenyl rings.

The value of the coupling constant between the bridgehead proton H^A and the geminal protons H^B (experimental value 3.5 Hz, Table 1) is in good agreement with the calculated value [20] of 3.3 Hz for a normal dihedral angle of 60°, as well as with the reported value of 3.8 Hz [14] for homotriptycene **10**. The similarity of **5** with **10** is reflected in their intramolecular charge transfer spectra (see Experimental).

In conclusion, new heterocyclic derivatives possessing an annelated dibenzo[*f*, *i*]bicyclo[3.2.2]nona-6,8-diene skeleton (oxonia-, azonia- and aza-homotriptycenes) were obtained and characterised. The inspection of Dreiding stereomodels reveals the high symmetry of the skeleton: the plane of the pyrylium ring is a symmetry plane of the molecule, so that the ring flip in the 7-membered ring [21] seems improbable. Indeed, the two H^B protons always appear equivalent in the ^1H-NMR spectra.

EXPERIMENTAL

Melting points are uncorrected. ^1H-NMR spectra were performed on a VARIAN A 60-A spectrometer. IR spectra were registered on a UR-20 C. Zeiss Jena double beam spectrophotometer.

6′-Phenyl—1′-oxoniabenzo[2′,3′-*b*]*dibenzo*[*f, i*]*bicyclo*[3.2.2]*nona-2,6,8-triene perchlorate* (**3**) *and 6′-phenyl-1′-oxoniabenzo*[4′,3′-*b*] *dibenzo*[*f, i*] *bicyclo*[3.2.2]*nona-2,6,8-triene perchlorate* (**4**).

A mixture of hydroxymethyleneketone **2b**[1] (3.2 g ; 12.2 mmoles), acetophenone (3 g ; 25 mmoles), 70 % perchloric acid (3 ml ; 5.01 g ; 33.8 mmoles) and anhydrous acetic acid (15 ml) was heated on an oil bath at 100—105° for 1.5 hrs. The clear dark-brown solution was cooled and poured over 200 ml anhydrous ether. Instantaneously a dark green oil precipitate separated then, during 1—2 hrs new quantities of a solid product (yellowish-green) were formed. The mixture was left overnight then filtered, affording 0.910 g (18 % yield) of a yellowish-green solid consisting of a mixture of **3** and **4** ; m.p. 258—268°.

^1H-NMR spectrum ($F_3C-COOH$; δppm) : 3.27 (d ; $J = 3.5$ Hz) ; 3.5 (d ; $J = 3.5$ Hz) ; 4.3—4.6 (quintet) ; 5.5 (d) ; 7.0—7,8 (m) and 8.1—8.5 (m). This spectrum could be separated in two simple spectra, characteristic for **3** respectively **4** as indicated in Table 1.

From the ratio of integrals of the signals at 3.27 and 3.50 ppm the ratio of **3** to **4** was determined to be 70 : 30.

In an experiment conducted as above the reaction mixture was decanted immediately after the separation of the dark green precipitate. In the separated clear liquid a yellowish-green precipitate begins soon to separate. After filtration this solid indicated a m.p. of 275—277°. The ^1H-NMR spectrum demonstrated the existence of only one pyrylium salt, namely **3** (the spectrum is identical with those presented in Table 1 for **3**).

Found : Cl, 7.71 ; $(C_{29}H_{19}O)^+ClO_4^-$ requires Cl, 7.92 %.

IR-spectrum (KBr ; cm^{-1}) : 626s, 693m, 734m, 786m, 1096vs, 1384m, 1478vs, 1501s, 1606s, 2930w, 3072w and 3110w.

Electronic spectrum (CH_2Cl_2)$\lambda_{max}^{nm}(\varepsilon_{max})$: 260 (9500), 397 (27000), 495 (30).

1′,6′-Diphenyl-1′-azoniabenzo[2′, 3′-*b*]*dibenzo*[*f,i*]*bicyclo*[3.2.2]*nona-2, 6, 8-triene perchlorate* (**5**) (*or 1′,6′-diphenyl-1′-azoniahomotriptycene perchlorate*)

A mixture of pyrylium salts **3** and **4** obtained as described before (0.5 g ; 1.1 mmoles) dissolved in methanol (10 ml) was treated with an excess of aniline and allowed to react at 30—40° for one hour. Then 0.2 ml of acetic acid was added and the solution was kept at 30—40° for another two hours. The reaction mixture was kept in a refrigerator. After a week, small quantities of a yellowish brown solid were precipited. Through filtration a yellowish-white solid, **5** (0.1 g ; 17 %) with a m.p. 208°—211° was obtained, then after two weeks at 0° a new crop of **5** (0.09 g ; 15.5 %) was obtained.

IR-spectrum (CH_2Cl_2 ; cm^{-1}) ; 1098vs, 1390w, 1481m, 1499m, 1572w, 1607m, 2925w and 3072w.

^1H-NMR spectrum (see Table 1).

Electronic spectrum (CH_2Cl_2)$\lambda^{nm}_{max}(\varepsilon_{max})$: 317.5 (9400), 392 (140). The shoulder with low absorbance at long wavelength in this spectrum and in the spectrum of **3** is due to charge transfer from benzenoid rings to the pyridinium (in **5**) or pyrylium ring (in **3**) by analogy with tropylium.[22]

1′-Methyl-6′-phenyl-1′-azoniabenzo [2′,3′-b]dibenzo[f, i]bicyclo[3.2.2]nona-2,6,8-triene perchlorate (**6**) *and 1′-methyl-6′-phenyl-1′-azoniabenzo[4′, 3′-b]dibenzo[f, i]bicyclo[3.2.2] nona-2, 6, 8-triene perchlorate* (**7**)

Over a mixture of pyrylium perchlorates **3** and **4** (obtained as described above, 200 mg ; 0.45 mmoles) an excess of saturated methanolic solution of methylamine was added. The orange-red mixture was heated on reflux for two minutes then filtered from some unsoluble residue (17 mg) which was not further investigated. The filtrate was treated with 1 ml acetic acid then diluted with ethyl ether (200 ml). Cooling of this solution (0°) produces the precipitation of a yellow solid (52 mg ; 25 %) m.p. 167–185°, consisting of a 75 : 25 mixture of **6** and **7**.

IR spectrum (CH_2Cl_2 ; cm^{-1}) : 1099vs, 1482m, 1572w, 1610 w, 2931w, 3048w and 3078w.

^1H-NMR spectrum (see Table 1).

The mother liquors from the last filtration were left overnight in a refrigerator affording a yellow solid (20 mg ; 9.7 %), m.p. 173–176°. The ^1H-NMR spectrum (Table 1) indicates the presence of a unitary compound, **6**.

6′-Phenyl-1′-pyridino[2′, 3′-b]dibenzo[f, i]bicyclo[3.2.2]nona-2,6,8-triene (**8**) *and 6′-phenyl-1′-pyridino[4′, 3′-b]dibenzo[f,i]bicyclo[3.2.2]nona-2,6,8-triene* (**9**).

Over a mixture of pyrylium salts **3** and **4** (500 mg ; 1.1 mmoles) obtained as described above, 10 ml methanol then 5 ml conc. aqueous solution of ammonia were added with stirring. The reaction mixture was heated at 40–50° for two minutes then a new quantity (2 ml) of ammonia was added. The mixture was filtered from a small quantity (33 mg) of unsoluble material which was not further examined. The clear filtrate was diluted with cold water (until opalescence occurs) then cooled in ice. The orange solid precipitate formed was filtered affording 165 mg (43 %) of a 75 : 25 mixture of pyridines **8** and **9**, m.p. 113–126°.

^1H-NMR spectrum (see Table 1).

The mother liquors from the last filtration were left overnight in a refrigerator affording a new crop (25 mg ; 6.5 %) of pyridines **8** and **9**, m.p. 108–114°.

A sample of the mixture of **8** and **9** (80 mg) obtained as described above was disolved in 2 ml anhydrous benzene. Over the clear brown solution *n*-heptane (5 ml) was added with stirring. The light yellow crystalls formed were filtered affording the pure isomer **8** (35 mg), m.p. 114–115°.

IR spectrum (CCl_4 ; cm^{-1}) : 982w, 1180m, 1208m, 1361m, 1465m, 1482m, 1618w, 1646m, 2830w, 2918m, 2960w, 3022m and 3078m.

^1H-NMR spectrum (see Table 1).

ACKNOWLEDGMENT : We express our thanks to Professor Ecaterina Ciorănescu for helpful discussions and to Dr. M. Gheorghiu for recording some NMR spectra.

REFERENCES

[1] M. Banciu, *Rev. Roumaine Chim.*, **27**, 769 (1982).

[2] E. Ciorănescu, M. Banciu, R. Jelescu, M. Elian and C. D. Nenitzescu, *Tetrahedron Letters*, **1969**, 1871 ; *Rev. Roumaine Chim.* **14**, 911 (1969).

[3] G. N. Dorofeenko, E. I. Sadekova and E. V. Kuznetzov, "Preparativnaya khimia pirilievyh solei", Izd. Rostovskogo Univ., Rostov, 1972, p. 29.

[4] K. Dimroth and K. H. Wolf, in "Newer Methods of Preparative Organic Chemistry" (editor W. Foerst), Academic Press, New York, 1964, vol. 3, p. 357.

[5] A. T. Balaban, W. Schroth and G. Fischer, *Adv. Heterocyclic Chem.*, **10**, 241 (1969).

[6] A. T. Balaban, A. Dinculescu, G. N. Dorofeenko, G. W. Fischer, A. V. Koblik, V. V. Mezheritskii and W. Schroth, "Pyrylium Salts. Syntheses, Reactions and Physical Properties", *Adv. Heterocyclic Chem.*, Suppl. 2, 1982, Academic Press, New York, 1982.

[7] A. T. Balaban, in "New Trends in Heterocyclic Chemistry" (editors R. B. Mitra *et. al.*) Elsevier, Amsterdam, 1979, (Studies in Organic Chemistry, No. 3) p. 79.

[8] W. Dilthey and J. Fischer, *Ber. dtsch. chem. Ges.*, **57**, 1653 (1924).

[9] W. Schroth and G. Fischer, *Z. Chem.*, **3**, 147, 277 (1963).

[10] G. N. Dorofeenko and G. I. Junghietu, *Zhur. obshchei. Khim.*, **35**, 589 (1965).

[11] A. T. Balaban, *Tetrahedron Letters*, **1978**, 5055.

[12] K. B. Lipkowitz, T. Chevalier, B. P. Mundy and J. J. Theodore, *Tetrahedron Letters*, **1980**, 1297.

[13] P. Sándor and L. Radics, *Org. Magn. Reson.*, **14**, 98 (1980).

[14] S. J. Cristol and D. K. Pennelle, *J. Org. Chem.*, **35**, 2357 (1970).

[15] I. I. Brunovlenskaia, T. A. Gudasheva and V. R. Shvarchenko, *Zhur, org. Khim.*, **10**, 1495 (1974).

[16] C. E. Johnson Jr. and F. A. Bovey, *J. Chem. Phys.*, **29**, 1012 (1958).

[17] H. A. P. De Jongh and H. Wynberg, *Tetrahedron*, **21**, 515 (1965).

[18] C. W. Haigh and R. B. Mallion, *Org. Magn. Reson.*, **4**, 203 (1972).

[19] R. B. Mallion, *J. Chem. Phys.*, **75**, 793 (1981); see also: R. B. Mallion in "Nuclear Magnetic Resonance Spectroscopy in Molecular Biology" (editor B. Pullman), Reidel Publ. Co., Dordrecht, Holland, 1978, p. 183; R. B. Mallion, *Pure Appl. Chem.*, **52**, 1541 (1980); C. W. Haigh and R. B. Mallion, *Progress in Nuclear Magnetic Resonance Spectroscopy*, **13**, 303 (1979); R. B. Mallion, in "Specialist Periodical Report on Nuclear Magnetic Resonance" (editor R. K. Harris), The Chemical Society, London, 1975, vol. 4, p. 50.

[20] E. Pretsch, T. Clerc, J. Seibl and W. Simon, "Tabellen zur Strukturaufklärung organischer Verbindungen", Springer, Berlin, 1976, p. H 25.

[21] W. Tochtermann, *Top. Curr. Chem.*, **15**, 378 (1970).

[22] A. Tajiri, M. Hatano, T. Nakazawa and I. Murata, *Chem. Phys. Letters*, **76**, 490 (1980); T. Nakazawa, N. Abe, K. Kubo and I. Murata, *Tetrahedron Letters*, **1979**, 4995; T. Nakazawa and I. Murata, *J. Amer. Chem. Soc.*, **99**, 1996 (1977).

Revue Roumaine de Chimie, 27, *9—10*, 1047—1054 (1982)

HIDROLISIS DE SALICILATOS DE *n*-ALQUILO CATALIZADA POR HIDROXIDOS DE BARIO ACTIVADOS

A. GARCIA RASO, J. V. SINISTERRA y J. M. MARINAS

Departamento de Química Orgánica, Facultad de Ciencias, Universidad de Palma de Mallorca
Islas Baleares (España)

Recibido el 24 avril de 1981

Se estudia la aplicabilidad de nuevos catalizadores de $Ba(OH)_2$ activados a la hidrólisis de salicilatos de *n*-alquilo, mediante los cuales se consiguen en condiciones óptimas, rendimientos prácticamente cuantitativos en todos los casos estudiados, operando en fase heterogénea sólido-líquido. Estos catalizadores son capaces de hidrolizar selectivamente estos esteres frente a otros de similares características (benzoatos y acetatos de *n*-alquilo). Se propone como mecanismo de hidrólisis de los salicilatos de *n*-alquilo en fase heterogénea el $B_{Ac}2$, aportándose pruebas que excluyen el mecanismo $B_{A1}2$.

The application of new activated Ba $(OH)_2$ catalysts to hydrolysys of *n*-alkyl salicilates is studied. In all cases, quantitative yields are obtained at optimum conditions, working in heterogeneous phase (solid-liquid). These catalysts can hydrolyse selectively these esters and not others that present similar characteristics (*n*-alkyl benzoates and acetates). The $B_{Ac}2$ mechanism is proposed. It is experimentally verified that $B_{A1}2$ mechanism is not existent working in heterogeneous phase (solid-liquid).

INTRODUCCION

Los procesos de esterificación e hidrólisis de ácidos alifáticos y aromáticos han sido ampliamente estudiados desde los comienzos de los mecanismos de reacción. Dentro de esta línea han sido efectuados por nuestro equipo de investigación diversos procesos de esterificación en fase heterogénea, tanto sólido-líquido como sólido-gas[1,2]. Recientemente se han obtenido en nuestros laboratorios una serie de catalizadores básicos, de hidróxido de bario, resistentes a la desactivación por el CO_2 atmosférico y que han sido aplicados con éxito a diversas reacciones orgánicas, tales como la transposición bencilo-ácido bencílico [3], síntesis de Williamson de éteres [3], condensación aldólica [3], condensación de Claisen-Schmidt [4], etc.

PARTE EXPERIMENTAL

I. Síntesis de los catalizadores

Todos los catalizadores son hidróxidos de bario que han sido obtenidos por calcinación del $Ba(OH)_2 \cdot 8H_2O$ comercial (Probus) a temperatura conveniente. Este proceso fue efectuado al aire y durante 3 h. Los catalizadores han sido denominados con la letra C seguida de la

temperatura de calcinación y pueden conservarse sin pérdida apreciable de actividad durante meses dentro de un desecador que contenga NaOH en pastillas [3].

II. Propiedades químico-texturales

El contenido en Ba^{2+}(% en peso) se determinó trabajando con un aparato de absorción atómica Perkin-Elmer modelo 703, utilizando llama acetileno- aire y mediante el empleo de la espectrofotometría de emisión. Se pesan entre 40 y 60 mg de catalizador y sobre él se añaden unas gotas de HCl, a fin de transformarlos en el correspondiente $BaCl_2$, mucho más soluble en agua. Después se diluyen hasta 1 litro a fin de introducirlos en el rango de concentraciones deseado.

Las superficies específicas se han calculado mediante el método BET por adsorción de N_2.

La basicidad (meq/g) se midió utilizando una variación del método de Berodin [5]. Este método consiste en poner en contacto durante 1 hora y con agitación, una disolución de ácido benzoico de concentración perfectamente conocida con una cantidad conocida de catalizador (entre 10 y 25 mg). Al final de este tiempo se procede a la filtración de la disolución a través de lana de vidrio resultando así disoluciones transparentes sobre las que se procede a la medición del valor de la absorbancia * a la longitud de onda correspondiente al máximo de la banda K del ácido benzoico ($\lambda = 273$ nm)

La recta de calibrado obtenida fue (1) :

$$\text{Absorbancia (D.O.)} = 878\,[PhCO_2H] + 0{,}0021 \qquad (1)$$

$$r^2 = 0{,}999$$

Finalmente, la basicidad es calculada mediante la fórmula (2) :

$$\text{Basicidad (meq/g)} = (A_i - A_f)\,V/\varepsilon g \qquad (2)$$

donde :

A_i = absorbancia inicial de la disolución valorante (para nuestro caso concreto fue de $1{,}412 \pm 0{,}002$ D.O.)

A_f = absorbancia final de la disolución valorante

V = volumen (en ml) de disolución de agente valorante.

ε = pendiente de la recta de calibrado [(1)]

g = gramos de catalizador

III. Hidrólisis de salicilatos de n-alquilo

En un matraz de fondo redondo de 100 ml de capacidad se introducen 16,5 mmoles del correspondiente salicilato de *n*-alquilo, 25 ml de etanol y 6 g de catalizador C—200. Se calienta a ebullición y con agitación continuada por espacio de 40 minutos y al final de los mismos se vierte el contenido del matraz caliente sobre un vaso de precipitados previamente enfriado en hielo y se procede a la adición lenta y con agitación vigorosa de HCl 3N a fin de disolver el catalizador. El precipitado que queda sin disolver es de ácido salicílico, el cual se filtra y se recristaliza en agua hirviendo. El rendimiento en todos los casos estudiados es prácticamente cuantitativo ($\geqslant 98\,\%$)**.

Las correspondientes hidrólisis de acetatos y benzoatos de *n*-alquilo condujeron en las condiciones de reacción a la recuperación total del ester inalterado.

RESULTADOS Y DISCUSION

I. Catalizadores

Les propiedades químico-texturales de todos los catalizadores estudiados se muestran en la Tabla 1. De la observación de la misma po-

---

(*) — Las mediciones en el UV fueron realizadas en un espectrofotómetro Zeiss DMR11, utilizando una anchura de rendija de 0,6 nm.

(**) — El catalizador de $Ba(OH)_2 \cdot 8H_2O$ comercial se ha comprobado que conduce a inferiores resultados [3].

demos notar que : i) El % de Ba^{2+} (en peso) para todos los catalizadores es idéntico (dentro del error experimental). Por esta razón, pueden ser representados mediante una fórmula empírica que estaría comprendida entre dos estructuras límite — $Ba(OH)_2 \cdot 1{,}5H_20$ ($\%Ba^{2+} = 69{,}2\,\%$) y $Ba(OH)_2 \cdot H_2O$($\%Ba^{2+} = 72{,}5\,\%$). ii) La superficie específica es en todos los casos muy pequeña pero, del mismo orden que la de otros catalizadores básicos que realizan procesos en fase heterogénea (sólido-líquido) [6]. iii) En general, un *aumento* en la temperatura de calcinación provoca una *disminución global* de las propiedades químico-texturales.

TABLA 1

Propiedades químico-texturales de los catalizadores

Catalizador	% Ba^{2+} (en peso)	Superficie específica (m^2/g)	Basicidad (meq/g)
C—O*	43±1	1.4±0.1	0.74±0.02
C—200	70±3	1.9±0.1	1.63±0.05
C—300	71±3	1.4±0.1	1.52±0.05
C—400	71±3	1.2±0.1	1.15±0.03
C—500	71±3	1.0±0.1	0.78±0.02
C—600	71±3	0.4±0.1	0.40±0.01

* — Conel nombre C — O queremos describir al catalizador de $Ba(OH)_2 \cdot 8H_2O$ comercial.

La basicidad ha sido determinada utilizando etanol como disolvente de valoración. La razón de esto es que se ha comprobado que para que tenga lugar la hidrólisis se requiere el empleo de disolventes oxigenados (etanol, THF, dioxano, etc). Esta no se produce al utilizar disolventes apróticos apolares no oxigenados, tales como benceno, tolueno, *n*-hexano, etc.

Estos catalizadores son, por otra parte, muy reproducibles ya que conducen a idénticos valores de conversión al variar ostensiblemente variables de calcinación tales como el tiempo de calcinación o la velocidad de calefacción hasta alcanzar la temperatura óptima de calcinación (ver Tablas 2 y 3).

II. Optimización de las condiciones de reacción

En la Figura 1 podemos apreciar para todos los catalizadores estudiados la variación del rendimiento (% molar) en ácido salicílico frente a la cantidad de catalizador. De la observación de la Figura 1 podemos notar : i) El mejor de los catalizadores es el calcinado a más baja temperatura, lo cual está de acuerdo con los resultados obtenidos para otras reacciones catalizadas por hidróxidos de bario activados [4]. ii) Se requiere una cantidad mínima de catalizador para que la reacción tenga lugar. Con todo, se ha comprobado que esta zona inicial de la gráfica es ficticia[3] ya que depende de la cantidad de ester (moles totales añadidos) objeto de hidrólisis. Así, al disminuir ésta, las

TABLA 2

Variación de la conversión en ácido salicílico (% molar) con respecto al tiempo de calcinación. (catalizador C—200)

Tiempo de calcinación (h)	Rendimiento (%)
<2	No reproducible
2.5	60±4
3	63±2
4	63±2
5	63±2
7	63±2

Las condiciones de reacción han sido: (Catalizador = 3g, habiéndose tardado en alcanzar la temperatura de calcinación óptima — 200°C — un tiempo de 30 minutos)

TABLA 3

Variación de la conversión (% molar) en ácido salicílico con respecto a la velecidad de incremento de temperatura hasta la óptima de calcinación (200°C)

Tiempo en alcanzar 200°C (min)	Rendimiento (%)
9	63±2
15	63±2
20	64±2
30	63±2
40	63±2
50	62±2
60	63±2
67	64±2
75	63±2

Las condiciones de reacción han sido: (Catalizador = 3 g calcinados durante 3 h).

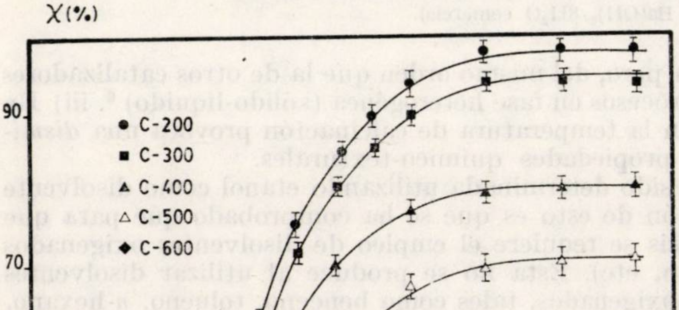

Fig. 1.—Conversión (%molar) en ácido salicílico en función de los gramos de catalizador, para todos los catalizadores estudiados.

curvas de conversión (% molar) frente a los gramos de catalizador van tendiendo hacia el origen manteniéndo el mismo hábito. Debido a este comportamiento, y al hecho de que al trabajar a cortos tiempos de reacción se produce adsorción de reactivo pero no ácido salicílico, producto final de la reacción, es por lo que proponemos como posible explicación el hecho de que la basicidad medida por aplicación del método anteriormente indicado[5] es distinta a la basicidad real de nuestro sistema en el proceso en cuestión, ya que a la basicidad medida habría que sustraer un término que sería debido la basicidad que emplea el catalizador en la adsorción no reactiva del salicilato de n-alquilo de que se trate. Esto podría representarse de la siguiente forma:

$$B_{\text{real}} = B_{\text{medida}} - B_{\text{no reactiva}} \text{ (en eq/1)} \qquad (3)$$

iii) La conversión límite está relacionada directamente con la basicidad (meq/g) de cada uno de los sistemas catalíticos estudiados, como puede apreciarse al comparar los valores del máximo de rendimientos para cada catalizador con la basicidad de los mismos (vease Tabla 1).

III. Cálculo de la ecuación cinética

Primeramente procedimos a conocer la influencia del agua en el proceso de hidrólisis. Los resultados experimentales aparecen representados en la Tabla 4 en donde podemos observar que no existe variación en la conversión a ácido salicílico al variar de forma notoria el contenido de agua presente en el sistema.

Es decir, nos encontramos en condiciones de pseudo-orden cero en agua, lo cual puede entreverse fácilmente al evaluar la relación existente entre moles de ester a hidrolizar y moles de agua presentes. Así, en las condiciones experimentales en que se han llevado a cabo todas nuestras experiencias tenemos:

Cantidad de ester a hidrolizar = 16,5 mmoles
Cantidad de agua presente:
Por el disolvente (25 ml EtOH ($4\,\%$ H_2O) = 55,6 mmoles
Por el catalizador ($Ba(OH)_2 \cdot H_2O$*) = 10,6 mmoles
66,2 mmoles

De donde puede apreciarse que la cantidad de agua presente es muy superior a la de ester (moles H_2O moles ester = 4).

TABLA 4

Estudio de la influencia de la adición de agua al seno de reacción en el rendimiento de la hidrólisis, para el catalizador C—200. (ester utilizado = salicilato de metilo)

% H_2O (en peso)/100 ml disolución	Rendimiento (%)
0.5	84±1
1	84±1
2	84±1
3	85±1
4	84±1
5	84±1
6	83±2
8	83±2
10	82±3
12	84±4
13	81±4
14	82±4
15	80±4
16	78±5
17	75±7

El error relativo en el % de H_2O es en todos los casos inferior al 1 %.

Las condiciones de reacción en las que se han llevado a cabo todas estas reacciones son: (tiempo de reacción = 40 min; $B_{\text{real}} = 0.163$ eq/l; gramos de catalizador = 4g).

(*) —Recuérdese que los catalizadores poseen una fórmula empírica comprendida entre $Ba(OH)_2 \cdot H_2O$ y $Ba(OH)_2 \cdot 1{,}5H_2O$ y que se requieren como mínimo 2 g, al utilizar 16,5 mmoles de ester, para que la reacción tenga lugar.

Con todo, a fin de evaluar si realmente el agua influía de forma directa en la ecuación cinética se procedió a trabajar en las condiciones donde la relación (moles H_2O/moles ester) fuera la menor posible, para ello se efectuaron experiencias con etanol anhidro (contenido aproximado de agua = 0,5 %). Entonces :

Cantidad de ester a hidrolizar = 16,5 mmoles
Cantidad de agua presente :
Por el disolvente (25 ml EtOH (0,5 % H_2O)) = 6,9 mmoles
Por el catalizador = 10,6 mmoles
17,5 mmoles

Donde, podemos apreciar que en el peor de los casos esta relación será de aproximadamete 1, ya que el agua que aporta el catalizador eleva, en este caso, de forma notable el contenido de la misma en el sistema. Como, a pesar de estas condiciones, los resultados experimentales seguían siendo análogos con los anteriormente obtenidos es por lo que hemos optado por considerar como nula la influencia del agua en el paso lento de la reación.

Entonces, la representación de los datos cinéticos — para el caso del catalizador C—200 que es el más activo — ajustados a cinéticas de primer orden conduce a rectas, cuyos valores de las pendientes vienen representados en la Tabla 5.

Así, la ecuación cinética obtenida será del tipo :

$$v = k\ (\text{ester}) \qquad (4)$$

que nos indica que es de primer orden en reactivo.

TABLA 5

Valores de las constantes pseudocinéticas para la hidrólisis del salicilato de metilo. Temperatura de reacción = 78 ± 1°C

B_{real} (eq/1)	$K \cdot 10^2 (\text{min}^{-1})$
0.163±0.001	5.6±0.5
0.148±0.001	4.6±0.4
0.128±0.001	3.5±0.3
0.112±0.001	2.4±0.2
0.092±0.001	$1.8 \pm 0.1_5$
0.074±0.001	1.2±0.1
0.059±0.001	0.67±0.05

Seguidamente se trató de evaluar la influencia del catalizador en la ecuación cinética global del proceso de hidrólisis. La representación, mediante el cálculo de las velocidades iniciales (v_0), trabajando en condiciones de pseudo-orden 0 en ester salicílico condujo a la siguiente recta :

$$\ln v_0 = -1{,}57 + 2{,}08 \ln (B_{\text{real}}) \qquad (5)$$

$$r^2 = 0{,}98$$

El valor de la pendiente nos indica que el catalizador entrará a formar parte en la ecuación cinética global en forma cuadrática. En efecto, la representación de las constantes pseudocinéticas (k) frente a $(B_{\text{real}})^2$ conduce a una recta que pasa por el origen, resultando descrito así el proceso lento para la hidrólisis de salicilatos de n-alquilo mediante una ecuación del tipo :

$$v = K\ (\text{ester})\ (\text{catalizador})^2 \qquad (6)$$

donde :

$$K = 2{,}1 \pm 0{,}2\ \text{l}^2\ \text{eq}^{-2}\ \text{min}^{-1}$$

Por otra parte, los parámetros de activación aparentes * resultan ser:

$$E_a = 20 \pm 2 \text{ Kcal/mol}$$

$$PZ = 1 \pm 1 \text{ l}^2 \text{ eq}^{-2} \text{ min}^{-1}$$

IV. Mecanismo de la reacción

Dada la ecuación cinética obtenida:

$$v = K \text{ (ester) (catalizator)}^2 \tag{6}$$

y considerando que: i) Cuando la reacción se efectúa en fase homogénea, Unterhalt[7] define un primer paso rápido como el correspondiente a la formación del anión fenoxicarboxilato de n-alquilo. ii) Al trabajar a cortos periodos de tiempo y baja temperatura o incluso, con poco catalizador podemos conseguir el fenómeno de la adsorción sin que se produzca la reacción. iii) Hemos comprobado que se hidrolizan selectivamente los salicilatos de n-alquilo, pero no los benzoatos ni acetatos correspondientes. Por todo esto, podemos reestructurar la ecuación cinética (6) en las formas (7) y (8):

$$v = K \text{ ((ester) (catalizador)) (catalizador)} \tag{7}$$

ó

$$v = K \text{ (ester adsorbido) (catalizador)} \tag{8}$$

ecuaciones de segundo orden que nos pueden representar, en principio, un mecanismo $B_{\text{Ac}}2$ ó $B_{\text{Al}}2$. Con todo, antes de distinguir entre ambos, se procedió a evaluar el paso lento de la reacción, ya que al presentar la hidrólisis un patrón típico $Ad_N - E$, tanto el primero como el segundo paso podrían representar la ecuación cinética propuesta. Los resultados al cambiar la naturaleza del alcohol (Figura 2) ponen de manifiesto su nula influencia en el proceso, pués se obtienen siempre las mismas conversiones independientemente de la naturaleza del alcohol. Ello parece indicar que la salida del grupo alcóxido deberá tener lugar

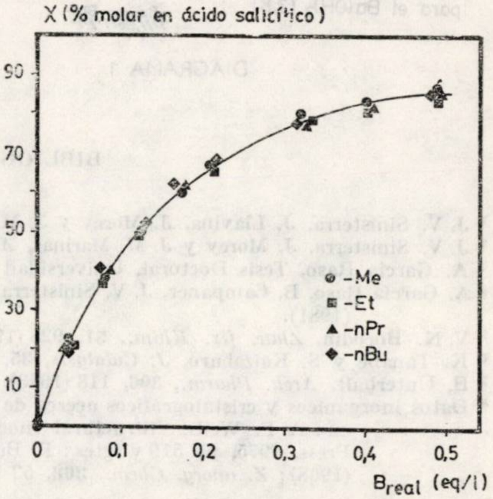

Fig. 2. — Influencia del resto alcoholico en la hidrólisis de salicilatos de n-alquilo.

(*) — Estos parámetros son válidos entre 62°C y 78°C que es la zona de trabajo donde han sido obtenidos.

en el paso rápido ya que la reacción no se afecta al modificarlo y, por tanto, anula la eliminación como paso lento de la hidrólisis estudiada.

Ningún análisis efectuado (por cromatografía de gases) sobre el crudo de reacción puso de manifiesto la existencia de éteres del tipo EtOR que se formarían según un proceso $B_{Al}2$ (vease Diagrama 1) lo cual nos inclina a descartar dicho mecanismo proponiendo como mecanismo más probable de hidrólisis de salicilatos de *n*-alquilo en fase heterogénea sólido-líquido catalizada por $Ba(OH)_2$ activados, el $B_{Ac}2$ que es, por otra parte, el que ocurre generalmente en todas las hidrólisis básicas catalizadas por bases fuertes. En el diagrama 2 se visualiza el paso lento de Ad_N propuesto. En dicho diagrama, por centro de reacción y centro de anclaje entendemos dos centros activos del hidróxido de bario y únicamente han sido denominados de esta forma con el fin de visualizar más claramente el paso lento de la hidrólisis.

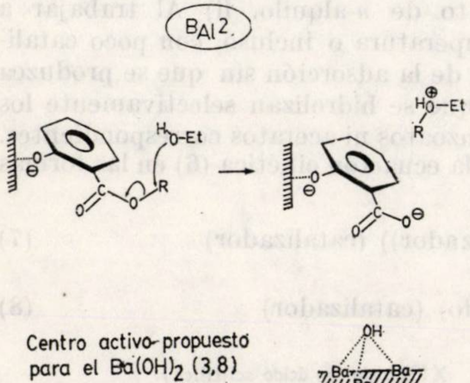
$B_{Al}2$
H
O-Et
R
C
O
⊖
$H\overset{\oplus}{O}-Et$
R
O⊖
Centro activo propuesto para el $Ba(OH)_2$ (3,8)
OH
Ba
Ba
Ba

DIAGRAMA 1

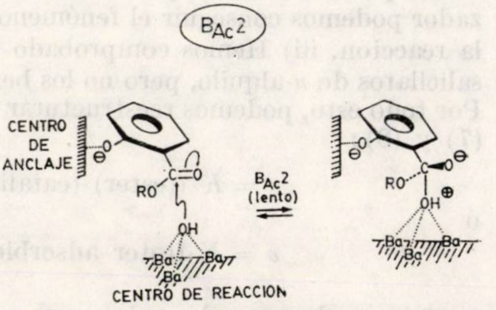

DIAGRAMA 2

BIBLIOGRAFIA

[1] J. V. Sinisterra, J. Llavina, J. Morey y J. M. Marinas, *Rev. Roumaine Chim.* (en prensa).

[2] J. V. Sinisterra, J. Morey y J. M. Marinas, *Afinidad,* **1979,** 305.

[3] A. García Raso, Tesis Doctoral. Universidad de Palma de Mallorca (1981).

[4] A. García Raso, B. Campaner, J. V. Sinisterra y J. M. Marinas, *Anales de Química,* **77C,** 222 (1981).

[5] V. N. Borodin, *Zhur. fiz. Khim.,* **51,** 928 (1977).

[6] K. Tanabe y S. Kaizaburo, *J. Catalysis,* **35,** 247 (1974).

[7] B. Unterhalt, *Arch. Pharm.,* **306,** 118 (1973).

[8] Datos inorgánicos y cristalográficos acerca de la estructura del hidróxido de bario aparecen en : A. F. Wells, "Structural Inorganic Chemistry" (4ª Edición). Ed. Claredon Press, 1975, pg 519 y sgtes ; P. Buck y H. Baernighausen, *Acta Cryst.,* **B24**, 1705 (1968) ; *Z. anorg. Chem.,* **368,** 53 (1969).

Revue Roumaine de Chimie, 27, *9–10,* 1055–1066 (1982)

МЕХАНОХИМИЧЕСКИЙ СИНТЕЗ НЕКОТОРЫХ ПОЛИХЕЛАТОВ НА ПОЛИ-АМИДНОЙ ОСНОВЕ

КР. СИМИОНЕСКУ, КЛЕОПАТРА ВАСИЛИУ-ОПРЯ
и КЛАУДИЯ НЕГУЛИАНУ

Кафедра органической и высокомолекулярной химии, Ясский политехнический институт, Румыния

Получена 25 мая 1981 г.

Предметом настоящей работы является механохимический синтез некоторых макромолекулярных комплексов с использованием поли-ε-капролактама в качестве основы. Активация процесса комплексообразования была осуществлена в переменном механическом поле посредством вибрационного размола. Было исследовано влияние на эффективность реакции таких факторов, как продолжительность механического воздействия и количество агента комплексообразования. Полученные продукты обладают повышенными электрическими и термическими свойствами по сравнению с поли-ε-капролактамом, использованным в качестве основы.

In this paper the mechanochemical synthesis of some macromolecular complexes using poly-ε-caprolactam as support was studied. Activation of complexation process was achieved in variable mechanical field by vibratory milling. The influence of some factors, as : time of mechanical stress and amount of complexation agent was carried out. The obtained products have higher electrical and thermal properties than poly-ε-caprolactam used as support.

I. ВВЕДЕНИЕ

Прогресс химии комплексных соединений и перспективы исследования в этой области обусловлены широкой применяемостью этих соединений в самых различных областях науки и техники, а именно, в конструкции космических кораблей и искусственных спутников, в радиотехнике, медицине, биологии и т.д. Такая широкая применяемость является следствием некоторых весьма ценных свойств этих соединений, из которых следует упомянуть следующие: высокая термостойкость к действию разбавленных растворов кислот и оснований, хорошее сцепление с металлическими поверхностями, стеклом и пластмассами, полупроводниковые свойства и т.д.

Хотя в настоящее время на различных макромолекулярных матрицах получают поликомплексы, они не получили широкого употребления, либо из-за сложности синтезов, либо в силу труднодостижимости полученных продуктов. $^{1-6}$ В этом смысле, особенный интерес представляет механохимический метод.

Механическая энергия, воздействующая в самых различных формах (вибрационный размол, вальцевание, криолиз, принудительное прохождение через капилляры и т.д.) на структуру полимеров, расходуется в первую очередь на деформацию макромолекулярных цепей, что в энергетическом смысле соответствует переходу последних в механовозбуждённое состояние, а в дальнейшем, путем концентрирования на дефектах, расположенных в определенных малых объёмах, эта энергия способствует расщеплению химических связей с образованием активных частиц, обычно радикального характера. Эти превращения придают продуктам, подвер접нным механическому воздействию, повышенный химический потенциал, следовательно, широкие возможности химического превращения путём реакций с различными партнерами, специально введёнными в реакционную среду. Исходя из этого, удалось получить механохимическим путём некоторые новые полихелаты. $^{7-11}$

Настоящая работа исследует механохимический синтез и свойства некоторых комплексов на полиамидной основе, полученных при помощи вибрационного размола. В качестве лигандов выступали фрагменты деструкции поли-ε-капролактама, подвержённого вибрационному размолу в присутствии агента комплексообразования $M_nCI_2.4H_2O$. Поли-ε-капролактам, используемый в качестве полимера-основы для процесса комплексообразования, содержит вдоль макромолекулярной цепи электроотрицательные элементы (кислород и азот), которые обладают парами свободных электронов. Последние придают вышеупомянутым элементам способность дополнительного образования координационных связей, используя свободные орбитали и комплексообразующих центров, а именно M_n^{2+}.

II. ЭКСПЕРИМЕНТАЛЬНАЯ ЧАСТЬ

II.1. ПРИНЯТЫЕ СПОСОБЫ ПРОВЕДЕНИЯ ЭКСПЕРИМЕНТАЛЬНЫХ РАБОТ

I.1. Синтез полихелатов

Процесс механохимического комплексообразования был осуществлён в лабораторной мельнице модели LS-60, производства фирмы KEFAMA KATZHÜTTE, THÜRINGEN, ГДР, имеющей камеры и размалывающие шары из нержавеющей стали, вентили для ввода и удаления газов, рубашку для термостатирования. Поли-ε-капролактам в виде зёрен был подвержён механической обработке, после превращения его в порошок путём растворения в м-крезоле при температуре 80°C и последующего осаждения метанолом. После фильтрации, полимер был экстрагирован до постоянного веса при помощи агента осаждения, с целью полного удаления использованного растворителя. Полученный таким образом материал был подвержён сушке при температуре 105°C и тонкому измельчению.

Агент комплексообразования — неорганическая соль $M_nCl_2\cdot 4H_2O$ в кристаллическом состоянии, химически чистая — был введён в камеры для размалывания вместе с полимерным порошком и необходимым количеством шаров. Сосуды были герметически закрыты, затем была проведена поочередная эвакуация воздуха при помощи разрежения и многократная промывка очищенным азотом. Последний и составил в итоге атмосферу реакционной среде. Температура поддерживалась постоянной, 20±2°C, при помощи циркуляции воды через рубашки камер. Реакция механохимического комплексообразования была проведена при степени заполнения $\eta = 0{,}4\%$, в расчёте на полимер-основу. Количество поли-ε-капролактама взятого для реакции было равно 10 г. В качестве размалывающих тел были использованы шары из нержавеющей стали V_2A, диаметром $\Phi = 0{,}9$ см.

I.2. Очищение продуктов реакции

После окончания реакции, продукты реакции были количественно извлечены из камер для размола путём смывания метанолом — растворителем агента комплексообразования ($M_nCl_2 \cdot 4H_2O$), после чего проводилось их очищение, экстрагируя их в аппарате «Сокcхлет» той же жидкостью для удаления избытка металлической соли, не вошедшей в реакцию.

Экстрагирования были проведены до постоянного веса, после чего пробы были высушены и взвешены для определения конверсии. Для лучшего очищения продуктов реакции от случайных следов железа, которые неминуемо появляются в массе полимера во время размола, пробы растворялись в м- крезоле при температуре 80°C на водяной бане, в течение шести часов, с отношением полихелат: крезол = 1/50 (весовых частей). После фильтрации, осаждения и экстракции в аппарате «Сокcхлет» метанолом, для удаления м-крезола, продукты реакции были охарактеризованы химически и спектрально.

I.3. Записывание ИК-спектров

Записывание ИК-спектров, соответствующих полихелатам, полученным описанным механохимическим методом, было осуществлено при помощи аппарата SP-200 UNICAM, с использованием метода таблетирования бромистым калием.

I.4. Записывание спектров ЭПР

Спектры электронного парамагнитного резонанса полихелатов, синтетизированных механохимическим путём, были записаны для твёрдых, проб, при помощи спектрометра, осуществлённого в Институте атомной физики в Бухаресте.

I.5. Термостойкость

Термическое поведение комплексов, полученных вибрационным размолом, исследовалось двумя способами, а именно: 1) путём выдержки проб в печи, при температуре 1000°C, в воздушной атмосфере, 2) путём термогравиметрического и термодифференциального анализа, с использованием аппарата типа ,,Паулинг-Ердели-Паулинг'', работающего в диапазоне температур 20—900°C, в воздухе, со скоростью 9°C/мин.

I.6. Удельная электрическая проводимость

Удельная электрическая проводимость полихелатов, синтетизированных описанным механохимическим методом была определена в интервале температур 30—180°C, в воздухе, при помощи мегаомметра марки Тесла.

Измерения удельной проводимости проводились на таблетках диаметром 0,9 мм, полученных путём прессования при давлении 10т/см².

II.2. ВЛИЯНИЕ НЕКОТОРЫХ ФАКТОРОВ НА ЭФФЕКТИВНОСТЬ ПРОЦЕССА МЕХАНОХИМИЧЕСКОГО КОМПЛЕКСООБРАЗОВАНИЯ ПОЛИ-ε-КАПРОЛАКТАМА С $M_nCl_2 \cdot 4H_2O$

2.1. Продолжительность размола

Влияние продолжительности размола, отражающее по сути дела влияние количества механической энергии, переданной системе во время обработки, исследовалось в широком диапазоне, от 24 до 144 часов, с использованием реакционной смеси, состоящей из 10 г поли-ε-копролактама и 5 г $M_nCl_2 \cdot 4H_2O$.

Образование полихелатов изучалось: а) путём определения изменения процентного содержания азота сравнительно с его содержанием в полимере-основе, б) путём измерения характеристической вязкости растворов, полученных из продуктов, синтетизированных при различных значениях продолжительности и в) путём определения степени превращения $\left(X\% = \frac{a}{б}\cdot 100\right.$, где: a — полученное в определённый момент процесса количество продукта, нерастворимого в агенте экстрагирования, в граммах, $б$ — количество смеси, подвёргшееся обработке в течение различных интервалов времени$\left.\right)$. Полученные результаты представлены на рис. 1.

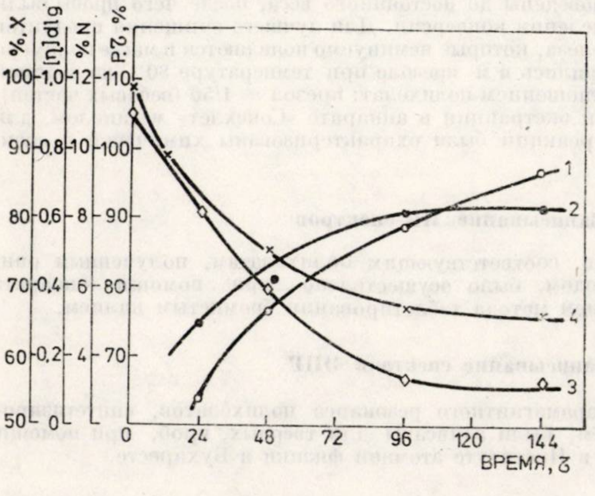

Рис. 1. — Влияние продолжительности размола на процесс комплексообразования поли-ε-капролактама с $M_nCl_2 \cdot 4H_2O$, при отношении лиганд/соль = 10 г/5г; 1 — Изменение степени превращения в продукт, нерастворимый в агенте экстрагирования, $X\%$; 2 — Изменение процентного содержания фракции, растворяемой в м-крезоле, получающейся при растворении продукта реакции; 3 — Изменение величины $[\eta]$, соответствующей растворимой фракции; 4 — Изменение процентного содержания азота % в растворимой фракции.

Как видно из вышеуказанных условий, при увеличении продолжительности механической обработки, степень превращения прогрессивно возрастает от значения 54,2%, соответствующего продолжительности активации 24 часа, до значения 87,8%, соответствующего продолжительности 144 часа. При проведении процесса комплексообразования с возрастающими продолжительностями активации, процентное содержание азота постепенно уменьшается в механохимически синтетизированном полихелате (рис. 1, кривая 4) из-за всё более эффективной координации с металлическими центрами M_n^{2+}, что отражается в элементном составе нового продукта.

Указания, касающиеся молекулярного веса лиганда были получены путём определения изменения характеристической вязкости ($[\eta]$), которая на графике имеет вид кривой, ординаты которой возрастают с увеличением продолжительности (рис. 1, кривая 3).

На рис. 1 показано также и изменение процентного содержания фракции, растворимой в м-крезоле. Для исследуемых продолжительностей это содержание менялось от 75 до 93%.

2.2. Количество комплексообразующего агента

Количество неорганической соли ($M_nCl_2 \cdot 4H_2O$), источника комплексообразующих центров, является другим важным фактором, имеющим решающую роль в эффективности механохимического комплексообразования. Влияние этого параметра было исследовано при проведении ряда размолов, в которых все остальные параметры поддерживались постоянными и изменению подлежало лишь количество M_nCl_2, от 0,1 до 5 г. Продолжительность механического воздействия была 48 часов. Полученные данные, касающиеся влияния этого параметра, представлены на рис. 2.

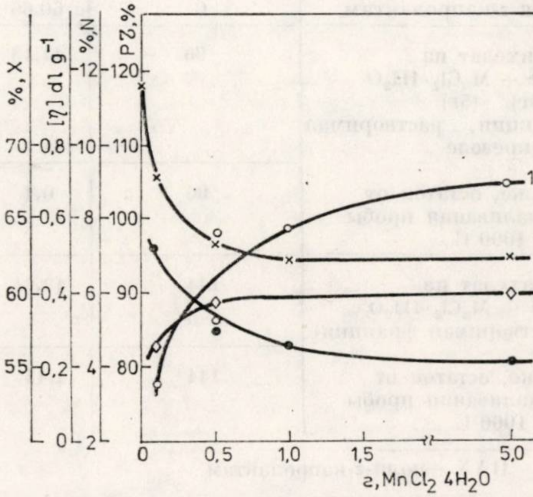

Рис. 2.— Влияние количества неорганической соли ($M_nCl_2 \cdot 4H_2O$) на эффективность процесса механохимического комплексообразования между поли-ε-капролактамом и хлористым марганцем: 1. Изменение степени превращения X% в продукте, нерастворимом в экстрагирующей среде; 2. Изменение процентного содержания фракции, растворяемой в-м-крезоле; 3. Изменение характеристической вязкости, соответствующей фракции, растворяемой в м-крезоле; 4. Изменение процентного содержания азота в растворимых фракциях.

Наблюдается прогрессивное возрастание степени превращения (X%), которое определяет уменьшение процентного содержания растворяемой в м-крезоле фракции полихелатов, синтетизированных с возрастающими количествами неорганической соли ($M_nCl_2 \cdot 4H_2O$) (рис. 2, кривые 1,2). Как следствие, наблюдается уменьшение процента азота (рис. 2, кривая 4) и увеличение вязкости ([η]) различных растворимых фракций, полученных из продуктов механохимического комплексообразования с различными количествами неорганической соли (рис. 2, кривая 3).

II.3. ОХАРАКТЕРИЗОВАНИЕ МЕХАНОХИМИЧЕСКИ СИНТЕТИЗИРОВАННЫХ ПОЛИХЕЛАТОВ

Продукты, полученные в процессе механохимического комплексообразования поли-ε-капролактама с хлористым марганцем ($M_nCl_2 \cdot 4H_2O$) были охарактеризованы химически (путем: а — элементного анализа, б — определения азота при помощи Киелдхалого метода и в — определения остатка, полученного при сжигании проб в печи, при температуре 1000°C) и спектрально (поглощение в ИК — области).

Данные, полученные при элементном анализе, представлены в таблице 1.

Видно, что вследствие реакции комплексообразования, процентное отношение между различными составными элементами макромолекулярных цепей полихелатов (C, H, N, и т.д.) претерпевают заметные изме-

ТАБЛИЦА 1

Результаты элементарного анализа некоторых комплексов, полученных механохимическим способом в системе «поли-ε-капролактам и $M_nCl_2 \cdot 4H_2O$»

Проба	Продолжительность механической обработки, в часах	Элементный состав			
		C%	H%	C%	Остаток, %
Поли-ε-капролактам	0	60,66	8,65	11,55 —	—
Полихелат из ПА^x + $M_nCl_2 \cdot 4H_2O$ (10г) (5г) Фракция, растворимая в м-крезоле	96	44,13	5,66	5,41 2,75	29,9
То же, остаток от прокаливания пробы при 1000°С	96	0,1	—	менее 1 —	99,82
Полихелат из ПА^x + $M_nCl_2 \cdot 4H_2O$ (Растворимая фракция)	144	43,94	6,47	5,34 2,72	27,8
То же, остаток от прокаливания пробы при 1000°С	144	1,44	2,15	— 1,39	—

ПА^x —поли-ε-капролактам.

нения. Так, например, процент углерода падает от значения 60,66%, полученного для поли-ε-капролактама, до значения 43,94%, соответствующего продукту, синтетизированному при продолжительности вибрационного размола, равной 144 часа.

Представленные в таблице 1 результаты элементного анализа, касающиеся процентного содержания азота, находятся в полном соответствии со значениями, полученными методом Киелдхаля (рис. 1, кривая 4 и рис. 2, кривая 4).

При дальнейшем рассмотрении данных элементарного анализа, представленных в таблице 1, привлекает к себе внимание тот факт, что в результате термического разложения механохимически синтетизированных продуктов в сжигающей печи, при температуре 1000°С, образуется остаток, процент которого, при некоторых условиях синтеза (большая продолжительность размола — 96 или 144 часа, или большие количества неорганической соли — 5г) достигает довольно высокие значения. Необходимо подчеркнуть, что этот продукт термического разложения не может быть отождествлён ни с одной из окисленных, неорганических форм марганца и использован в расчётах для определения процентного содержания металла. Такие попытки ведут к сильно преувеличенным результатам. Кроме того, элементарный анализ, проведённый путём сжигания остатка в потоке кислорода, указывает на следы углерода и азота (таблица 1). На основании этого результата можно заключить, что полихелат содержит термостойкую фракцию, которая не разлагаеся до 1000°С.

Полихелаты, полученные в результате процесса механохимического комплексообразования поли-ε-капролактама с хлористым марганцем, были исследованы также и спектроскопически, в инфракрасной области (рис. 3).

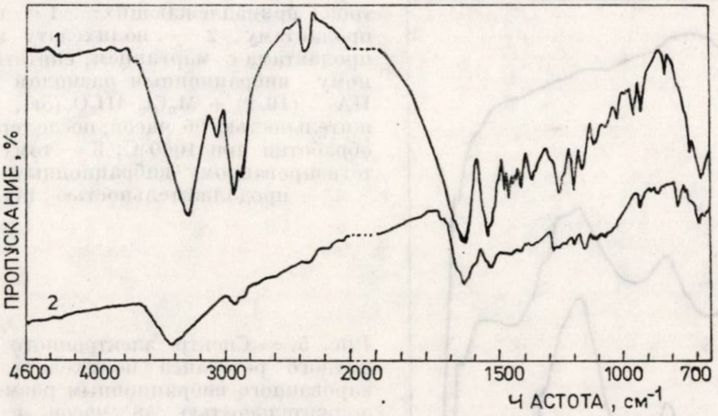

Рис. 3.—ИК-спектры: 1 — поли-ε-капролактама, полимера-основы; 2— полихелата, синтетизированного механохимически, путём вибрационного размола в системе ПА (10г) + $M_nCl_2\cdot4H_2O$ (5г), в течение 96 часов, в инертной среде.

Детальное рассмотрение спектра, принадлежащего полихелату, синтетизированному при продолжительности 96 часов (рис. 3, кривая 2) показывает следующие характеристики: 1 — присутствие полос, характерных для полиамидов (—H при 3200 см$^{-1}$; —CH$_2^-$ при 2970 см$^{-1}$; —CO—N—H — при 1540 и 1630 см$^{-1}$); 2 — исчезновение многочисленных полос, присущих полимеру-основе, что указывает на интимное изменение его структуры.

ИК-спектры были использованы и для охарактеризования остатков, полученных после термической обработки в воздухе, при температуре 1000°C (рис. 4). В ИК-спектрах этих продуктов, в области 650—200см$^{-1}$, можно наблюдать появление новых полос — при 300, 450, 500 см$^{-1}$ — которые могут быть объяснены, с одной стороны, существованием хелатных кольцов, а с другой — присутствием галогенов и металлических ионов, введённых в полимер реакцией комплексообразования.[12,13]

Введение металла в структурные единицы полихелатов, синтетизированных механохимическим способом, было установлено также и при помощи спектров электронного парамагнитного резонанса, которые характеризуют эти продукты как парамагнитные.

Форма полученного спектра (рис. 5) указывает на наложение сигнала марганца, связанного комплексообразованием на сигнал железа, которое переходит со стенок аппаратуры и также входит в реакцию с лигандами полиамидного типа.

Полученный спектр не имеет форму, характерную для продуктов, содержащих марганец координационно. Это изменение имеет две причины: 1 — у подвергаемого анализу продукта, концентрация парамагнитных центров имела гораздо более высокие значения, чем требуемые методом ЭПР (более 5% по сравнению с 10^{-1}% М) и 2 — сигнал марганца налагается на сигнал железа, которое в условиях механохимического синтеза отщепляется в тонком и сильно активированном состоянии и также участвует в реакции с лигандами полиамидного типа. Способность железа к комплексообразованию с гетероцепными и полиэфирными полимерами была доказана нами в ряде предыдущих работ.[7-11]

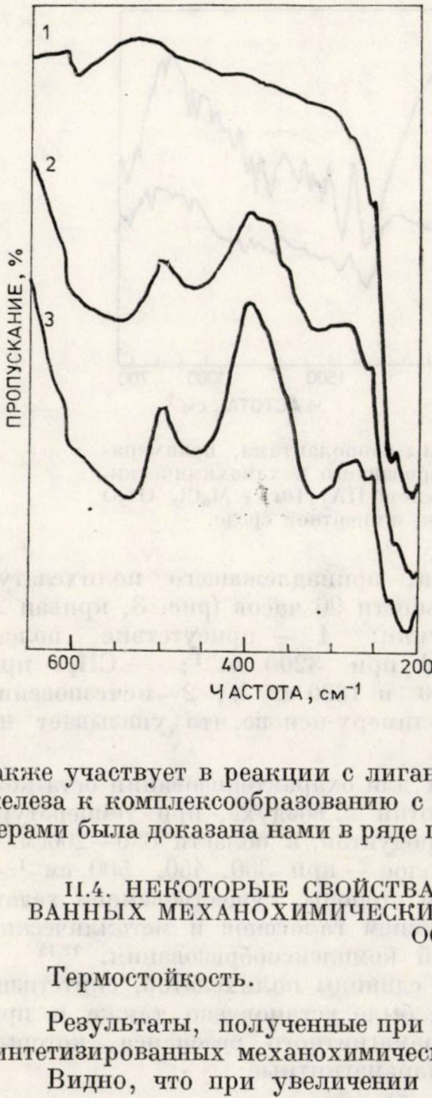

Рис. 4. — Область 650—400 см$^{-1}$ ИК-спектров, принадлежающих: 1 — поли-ε-капролактаму; 2 — полихелату поли-ε-капролактама с марганцем, синтетизированному вибрационным размолом в системе ПА (10 г) + $M_nCl_2\cdot 4H_2O$ (5г), продолжительностью 96 часов, после термической обработки при 1000°С; 3 — тому же, синтетизированному вибрационным размолом продолжительностью 144 часа.

Рис. 5. — Спектр электронного парамагнитного резонанса полихелата, синтетизированного вибрационным размолом продолжительностью 48 часов в системе: поли-ε-капролактам (10г) + $M_nCl_2\cdot 4H_2O$(5г).

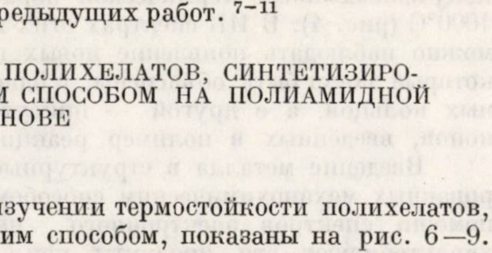

II.4. НЕКОТОРЫЕ СВОЙСТВА ПОЛИХЕЛАТОВ, СИНТЕТИЗИРОВАННЫХ МЕХАНОХИМИЧЕСКИМ СПОСОБОМ НА ПОЛИАМИДНОЙ ОСНОВЕ

Термостойкость.

Результаты, полученные при изучении термостойкости полихелатов, синтетизированных механохимическим способом, показаны на рис. 6—9.

Видно, что при увеличении продолжительности размола (рис. 6) и количества комплексобразующего агента (рис. 7) термостойкость продуктов реакции улучшается. Так, рассматривая влияние продолжительности размола на процентное отношение термостойкого продукта при 900°С, можно установить, что самым выгодным в этой точки зрения является полихелат, синтетизированный при продолжительности обработки 144 часа. Нетрудно заметить, что при температурах около 500°С, поли-ε-капролактам теряет приблизительно 88% веса (рис. 6, кривая 1), в то время как комплексы, синтетизированные при продолжительностях 48, 96 и 144 часа теряют 57–54%.

Комплексы не плавятся, а разлагаются постепенно под действием тепла.

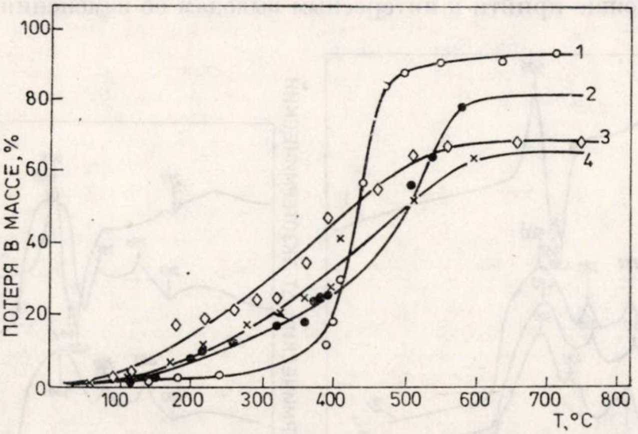

Рис. 6. — Изменение весовых потерь с температурой разложения, при различных продолжительностях процесса механохимического синтеза: 1 — поли-ε-капролактам, 2 — комплекс, синтетизированный механохимически в системе ПА (10 г) $+M_nCl_2 \cdot 4H_2O$ (5г) при продолжительности обработки 48 часов; 3 — то же, 96 часов; 4 — то же, 144 часа.

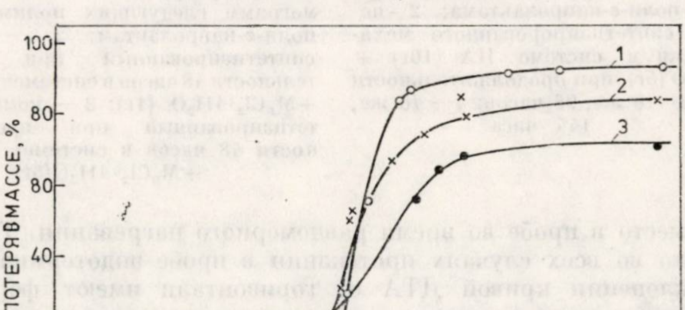

Рис. 7. — Изменение весовых потерь с температурой разложения при различных количествах комплексообразующего агента: 1 — поли-ε-капролактам; 2 — полихелат, синтетизированный вибрационным размолом в системе ПА (10г) $+ M_nCl_2 \cdot 4H_2O$ (1 г), при продолжительности 48 часов; 3 — то же, но с количеством $M_nCl_2 \cdot 4H_2O$ равным 5 г.

Данные, представленные на рис. 7, показывают термическое поведение продуктов, синтетизированных с различными (возрастающими) количествами хлористого марганца. Самым стойким является полихелат, полученный при употреблении 5г хлористого марганца (рис. 7, кривая 3).

Известно, что изучая вид кривых ДТА для различных полимеров, следовательно и для комплексов, синтетизированных в вышеуказанных условиях, можно прийти к интересным выводам об изменениях энтальпии, имеющих место в пробе во время равномерного нагревания. Так, исходя из того, что во всех случаях протекания в пробе эндотермических процессов отклонения кривой ДТА от горизонтали имеют форму пиков, направленных вниз, а в случае протекания экзотермических процессов — форму пиков, направленных вверх, можно прийти к выводу, что в комплексах, полученных механохимическим путём, имеет место большое число экзотермических превращений, в отличие от исходного полиамида, в котором, согласно записанным данным, протекают лишь три различимых процессе, а именно: плавление при температуре 212°C, эндотермический процесс, достигающий максимума при температуре 420°C и состоящий в деструкции полимера и, наконец, энзотермическое горение до полного исчезновения пробы.

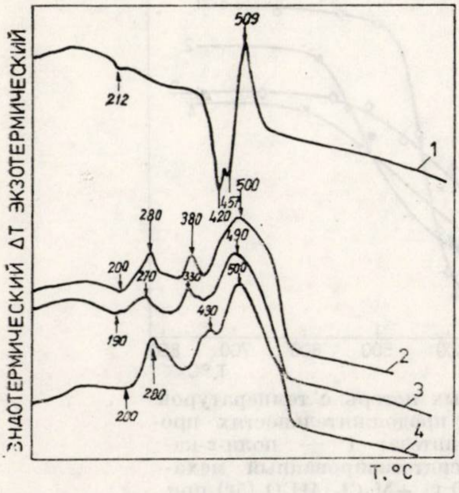

Рис. 8. — Влияние продолжительности размола на вид термограмм следующих проб: 1—поли-ε-капролактама; 2—полихелата, синтетизиророванного механохимически в системе ПА (10г) + $+MC_2\cdot 4H_2O$ (5г), при продолжительности 48 часов; 3—то же, 96 часов; 4— то же, 144 часа.

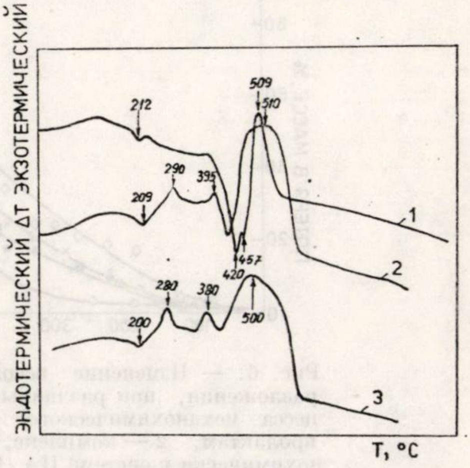

Рис. 9. — Влияние количества комплексообразующего агента на вид термограмм следующих полимеров: 1 — поли-ε-капролактам; 2 — комплекс, синтетизированный при продолжительности 48 часов в системе: ПА (10г) + $+M_nCl_2\cdot 4H_2O$ (1г); 3 — комплекс, синтетизированный при продолжительности 48 часов в системе: ПА (10г) + $+M_nCl_2\cdot 4H_2O$(5г).

Температура плавления поли-ε-капролактама (212°C), взятая из соответствующей термограммы (рис. 9, кривая 1), полностью соответствует данным из литературы.

Расчёт энергии активации термического разложения полихелата, синтетизированного вибрационным размолом из 10 г поли-ε-капролактама и 5 г хлористого марганца, при продолжительности размола 144 часа, даёт значение 35,99 Ккал/моль, что больше чем у исходного полиамида, для которого было найдено значение 32,9 Ккал/моль.

Высокая термостойкость комплексов, синтетизированных механохимическим способом из исходной смеси, состоящей из поли-ε-капролактама и хлористого марганца, объясняется как привязыванием ионов металла к фрагментам деструкции полимера, так и замыканием хелатных кольцов между лигандом и комплексообразующим центром.

Рис. 10. — Изменение процентного содержания азота (%) (кривая 2), термостойкого остатка (кривая 1), энергии активации удельной электрической проводимости (E, эВ) (кривая 3) для полимеров, синтетизированных из 10 г поли-капролактама и 5 г $M_nCl_2 \cdot 4HO_2$, в зависимости от количества комплексообразующего агента.

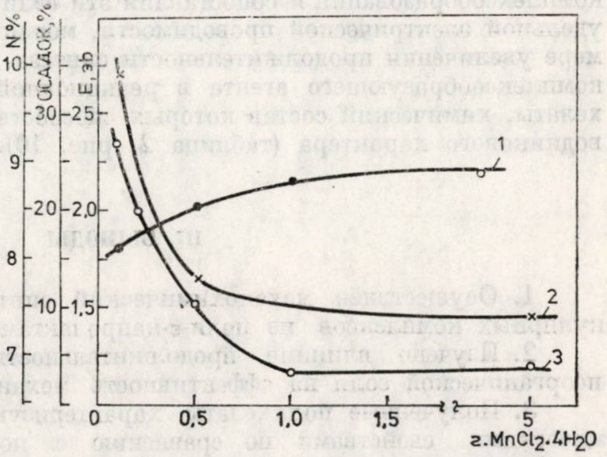

Удельная электрическая проводимость.

Благодаря введению металлических ионов путём комплексообразования, полученные полихелаты позволяют прохождение электрического тока и ведут себя как полупроводники.

Значение удельной проводимости зависит от условий синтеза, а именно: продолжительности размола и количества комплексообразующего агента (рис. 10, таблица 2).

ТАБЛИЦА 2

Значения удельной электрической проводимости и энергии активации, соответствующие полихелатам, синтетизированным механохимическим путём из 10 г ПА и 5 г $M_nCl_2 \cdot 4H_2O$

Полимер	Продолжительность размола в часах	Удельная электрическая проводимость ($ом^{-1} \cdot см^{-1}$)	Энергия активации удельной электрической проводимости, E(эВ)
ПА + $M_nCl_2 \cdot 4H_2O$	48	$(5{,}6 \cdot 10^{-7})_{170°C} - (3 \cdot 10^{-10})_{62{,}9°C}$	1,50
(10г) (5г)	96	$(7{,}8 \cdot 10^{-8})_{155{,}3°C} - (3{,}12 \cdot 10^{-10})_{62{,}9°C}$	1,51
	144	$(4{,}0 \cdot 10^{-7})_{154{,}25°C} - (3{,}68 \cdot 10^{-9})_{63{,}95°C}$	—

Изменение удельной проводимости с температурой в интервале 30—150°C следует экспоненциальному закону, который имеет следующую форму:

$$\sigma_T = \sigma_0(-E/RT)$$

5 – с. 2442

Значения удельной электрической проводимости определялись для синтетизированных в различных условиях полихелатов, как видно из таблицы 2 и рис. 10.

Рассматривая изменения процентного содержания азота и процентного содержания термостойкого остатка, получаемого при термическом разложении продукта, как критерии эффективности механохимического комплексообразования и сопоставляя эти величины с энергией активации удельной электрической проводимости, можно прийти к выводу, что по мере увеличения продолжительности синтеза, соответственно, количества комплексообразующего агента в реакционной среде, образуются полихелаты, химический состав которых способствует усилению их полупроводникового характера (таблица 2, рис. 10).

III. ВЫВОДЫ

1. Осуществлён механохимический синтез некоторых макромолекулярных комплексов из поли-ε-капролактама и хлористого марганца.
2. Изучено влияние продолжительности размола и количества неорганической соли на эффективность механохимической реакции.
3. Полученные полихелаты характеризуются более высокими термическими свойствами по сравнению с поли-ε-капролактамом-основой и обладают свойствами полупроводников.

ЛИТЕРАТУРА

[1] Г. Г. Скворцова, Е. С. Домнина, И. Н. Ивлев и Н. Н. Кипанина, *Ж. общей хим.*, 1593 (1976).

[2] G. Bidermann u P. Siedl, *Makromol, Chem.*, **177**, 631 (1976).

[3] A. K. Khalid u P. Holt, *Makromol. Chem.*, **177**, 311 (1976).

[4] B. Valenti, *Macromolecules*, **9**, 177 (1976).

[5] В. А. Кабанов, *Д.А.Н. С.С.С.Р.*, **230**, 139 (1976).

[6] Tsuchide Nishilearva, *J. Polymer Sci*; *Polym. Chim.* **14**, 520 (1976).

[7] Cr. Simionescu, Cl. Vasiliu-Oprea u Cl. Negulianu, *Makromol. Chem.* **163**, 75 (1973).

[8] Cr. Simionescu, Cl. Vasiliu-Oprea u Cl. Negulianu, Patent rom. 69467, 20. I. 1971.

[9] Cr. Simionescu, Cl. Vasiliu-Oprea u Cl. Negulianu, *Makromol. Chem.* **48**, 155 (1971).

[10] Cl. Negulianu, Диссертация, Яссы, 1975.

[11] Cr. Simionescu, Cl. Vasiliu-Oprea u Cl. Negulianu, *Angew. Makromol. Chem.*, **44**, 17 (1975).

[12] M. Avram u D. Gh. Mateescu, “Spectroscopia în infraroşu. Aplicaţii în chimia organică”, Ed. Tehnică, Bucureşti, 1966.

[13]. I. Pogany u M. Banciu, “Metode fizice în chimia organică”, Ed. Ştiinţifică, Bucureşti, 1972.

Revue Roumaine de Chimie, 27, 9–10, 1067–1078 (1982)

DETERMINACIÓN DE INDIO EN ALEACIONES BASE ALUMINIO MEDIANTE LAS TÉCNICAS DE ABSORCIÓN ATÓMICA Y FOTOMETRIA DE LLAMA

A. J. ALLER*
Departamento de Química Analítica
Universidad de Valladolid
Valladolid, España

Recibido el 25 de Marzo de 1981

Se describe un método para la determinación de indio en aleaciones base aluminio, mediante las técnicas de absorción atómica y fotometria de llama, en las que se utiliza el lantano para suprimir el efecto de matriz. Al mismo tiempo se comparan los resultados obtenidos con dos tipos de llama diferentes, aire-acetileno y óxido nitroso-acetileno. Se estudian los efectos producidos por varios cationes y aniones. La reproducibilidad del método presentado y el error en la determinación se examinan estadísticamente.

A method is described for the determination of indium in aluminium alloys by both atomic absorbtion and emission spectrometry, in which lanthanum is used to suppress the matrix effect, and the results obtained with two flame types, air-acetylene and nitrous oxide-acetylene, are compared. The effects of some cations and various anions have been studied. The reproducibility achieved by the instrument, and the errors attributable to uneven distribution of the results in determinations of indium are examined statistically.

Dado que el indio es un elemento de reciente aplicación en las aleaciones base alumino, no es fácil encontrar en el mercado patrones analíticos susceptibles de ser utilizados como contraste en la Espectrometria de Emisión por lo que su determinación mediante la citada técnica es dificil de realizar al carecer de línea analítica de calibrado. Es por esto, y porque en ocasiones es necesario contrastar los posibles patrones adquiridos, por lo que la Empresa Nacional del Aluminio (ENDASA) nos ha solicitado la puesta a punto de un método capaz de determinar dicho elemento en las aleaciones base aluminio preparadas en sus propias factorias.

A través de los muchos años de experimentación se han utilizado distintas técnicas en la determinación del indio.[1] Sin embargo, es escasa la documentación bibliográfica referente a la determinación del susodicho elemento en este tipo de aleaciones, mediante la técnica de absorción atómica; lo prueba el hecho de no haber encontrado más que el trabajo de

---

*** Dirección actual : Polvos Metálicos, S.A. (POLMETASA), Avda. de Alava, 30, Mondragón, Guipuzcoa (ESPAÑA)**

Hoehn y col. [2] en el que determinan una serie de elementos traza en aluminios de alta pureza, mediante la técnica de absorción atómica, previa concentración de los elementos mediante una disolución parcial de la matriz en presencia de mercurio. El mismo tipo de trabajo ha sido desarrollado por Jackwerth y col. [3].

No obstante, existen otra serie de trabajos en los que se determina indio en una matriz diferente al aluminio, los cuales son también de interés; son ejemplos de ellos, el trabajo de Langmyhr y col. [4], en el cual se indica la determinación de trece elementos traza, entre ellos el indio, en concentrados de rocas fosfatadas. Jackwerth y col . [5] determinan por absorción atómica varios elementos minoritarios en sales de cobre mediante preconcentración por precipitación de la matriz como sulfuro de cobre. Un trabajo similar es el de Balandina y col. [6] los cuales determinan las impurezas en oro de alta pureza, utilizando siempre esta técnica. Marks y col. [7] determinan varios elementos traza en una matriz compleja.

Un estudio en cierta medida semejante al que se realiza aquí es el de Nakahara y col.[8] pues determinan indio en diversas llamas, realizando así un trabajo comparativo y estudiando también sus posibles interferencias. De la misma índole es el trabajo desarrollado por Fujiwara y col. [9] los cuales realizan un estudio sobre las interferencias originadas por los ácidos en la determinación del indio por absorción atómica, así como el de Haraguchi y col. [10]

Gran interés presentan los trabajos referentes al empleo de algunos elementos como contrainterferentes, debidos a Belcher y col. [11]; Adams y col. [12]; Trent y col. [13] y Pittis [14] sobre la adición de tricloruro de lantano en cantidades variables como relajante, y los debidos a David [15] y Willis [16] que proponen el calcio y el estroncio como elementos correctores.

Podemos constatar que no existe un método de análisis de indio aplicable a los distintos tipos de aleaciones base aluminio, por lo que pensamos es de gran interés poner a punto un nuevo método dado el creciente interés del indio en este tipo de aleaciones.

Para ello, nos proponemos obtener los parámetros experimentales adecuados a tal fín, así como conocer las posibles interferencias, tanto de los elementos minoritarios como las debidas al efecto de matriz. Conocidas estas, su corrección resulta obligatoria. Pretendemos utilizar tres elementos como agentes contrainterferentes : lantano, calcio y estroncio. Así mismo, se utilizan y comparan dos técnicas : absorción atómica y fotometria de llama, utilizando en ambas dos tipos differentes de llama : aire-acetileno y óxido nitroso-acetileno. Hemos de indicar que las longitudes de onda utilizadas son : en absorción atómica la de 303.9 nm, mientras que en fotometria de llama es la de 451.1 nm.

RESULTADOS

Estudio de las interferencias

Hemos podido comprobar que en la determinación del indio, existe un amplio intervalo de respuesta lineal. Sin embargo, hay que tener en cuenta que además de la posible interferencia debida al efecto de matriz del aluminio, existen en este tipo de aleaciones, ó pueden existir, otros muchos elementos aleantes, por lo que conviene conocer su posible influencia. El estudio llevado a cabo para conocer lo interferencia de los distintos elementos nos proporcionó los resultados siguientes.

TABLA 1

Valores obtenidos para el rango de linearidad, límite de detección y sensibilidad, con cada una de las técnicas y llamas utilizadas

	F.E.S.		A.A.S.	
	A—A	N—A	A—A	N—A
Rango de linearidad, ppm	0—10	0—15	0—40	0—30
Límite de detección, ppm	0.50	0.02	0.80	1.50
Sensibilidad, ppm	0.046	0.013	0.160	0.440

Se ha considerado que un elemento presenta interferencia cuando existe una desviación en el valor de la absorbancia, con respecto al valor de la absorbancia de soluciones de indio solo, igual ó mayor al dos por ciento.

Hemos agrupado los elementos ensayados en tres grupos :

— elementos que no interfieren
— elementos cuya interferencia se presenta únicamente para grandes concentraciones (mayores de 5000 p.p.m.)
— elementos que interfieren en todo el rango de concentraciones estudiado

Los resultados son los siguientes :

Técnica de absorción atómica :

Llama aire-acetileno :

a. — Elementos que no interfieren : dentro de este grupo y en las condiciones instrumentales indicadas en el apartado PARTE EXPERIMENTAL, hemos encontrado que no presentan interferencia los elementos : Pb(II), Sn(II), Hg(II), Cd(II) y Cu(II).

b. — Elementos que interfieren a altas concentraciones : Al(III), Bi(III), Ni(II), Co(II), Mn(II), Cr(III), Mg(II), Na(I), Ba(II), V(V), Ti(III) Zr(IV), Sr(II) y La(III).

c. — Elementos que interfieren a cualquier concentración : F(III), Zn(II), P(V), As(V), Sb(V), W(VI), Mo(VI), Te(IV), y Ca(II) (Absorbancia inferior al 10 %).

Llama óxido nitroso-acetileno :

a. — No interfieren : Pb(II), Sn(II), Hg(II), Cd(II), Cu(II), Bi(III), Fe(III), Ni(II), Co(II), Zn(II), Cr(III), Ba(II), P(V), As(V), Sb(V), Ti(III) Zr(IV), Te(IV) y Sr(II).

b. — Interfieren a altas concentraciones : Al(III), Mn(II), Mg(II), Na(I), Mo(VI), V(V), Ca(II) y La(III).

c. — Interfieren a cualquier concentración : W(VI).

A la vista de estos resultados, destacaremos que con la llama óxido nitroso-acetileno se consigue eliminar una mayor cantidad de elementos interferentes, y aquellos que perturban aún, su efecto tiene lugar a altas concentraciones exclusivamente.

Hay que indicar también que las interferencias se han estudiado para tres concentraciones de indio, 5, 10 y 20 p.p.m., observándose siempre que todos aquellos elementos interferentes ejercen un efecto más pequeño cuando se disminuye la concentración de indio. Por esto, es conveniente realizar las dilucciones oportunas para que estas interferencias se vean disminuidas. Por ejemplo, el wolframio presenta interferencia únicamente para las concentraciones de 10 y 20 p.p.m., mientras que no tienen efecto alguno cuando se utiliza una solución de 5 p.p.m. de indio.

El tipo de interferencia en los elementos del segundo grupo (interfieren a altas concentraciones), será en todos ellos del tipo de matriz. Mientras que en los del tercer grupo, pueden presentarse dos casos :

a : La producida por el hierro, cinc y calcio, por ejemplo, y

b : La originada por el resto de los elementos de este grupo.

En el primer caso, estos elementos presentan un aumento de las absorbancias para concentraciones bajas de interferente (hasta 100 p.p.m.), mientras que para concentraciones superiores a las indicadas se observa una disminución.

Los elementos de este grupo segundo, presentan una interferencia constante a bajas concentraciones (hasta 1000 p.p.m.) observándose una disminución en las absorbancias a medida que aumenta la concentración, debido probablemente a un efecto de matriz. A este grupo también pertenece la interferencia producida por el aluminio.

Para la llama óxido nitroso-acetileno, el aluminio y el molibdeno presentan una disminución de la absorbancia, mientras que el resto de los cationes ejercen un aumento. Técnica de fotometria de llama :

Llama aire-acetileno :

a. — No interfieren : Zn(II), Tl(I), Co(II), As(V), Cr(III), Mn(II), Cu(II), Mg(II), Sb(V), Sn(II), Pb(II), Te(IV), Bi(III), Li(I), Cd(II) y Fe(III).

b. — Interfieren a grandes concentraciones : V(V), Mo(VI), W(VI), P(V), Ti(III), Sr(II), Ca(II), Ba(II), La(III), Hg(II) y Na(I).

c. — Interfieren en todo el rango de concentraciones : Al(III).

Llama óxido nitroso-acetileno :

a. — No interfieren : Hg(II), Tl(I), Te(IV), Li(I), As(V), Zr(IV), Ni(II), Cu(II), Zn(II), Sb(V), Bi(III), Co(II), Fe(III), Sn(II), Cd(II), Mg(II), Mn(II) y Pb(II).

b. — Interfieren a grandes concentraciones : Na(I), Ba(II), Ti(III), Cr(III), Ca(II), Sr(II), La (III), Ce(III), V(V), Mo(VI), W(VI), y P(V).

c. — Interfieren en todo el rango : Al(III).

La interferencia que presentan los elementos del segundo grupo, comienza a ser importante, para concentraciones de indio de 5 p.p.m., a 200 p.p.m. de elemento interferente, encontrándose dos tipos diferentes de interferencia. La presentada por el bismuto, mercurio y cinc, la cual disminuye las absorbancias para altos contenidos de elemento, asemejándose a un efecto de matriz ; y la presentada por el resto de los elementos, los cuales aumentan, contrariamente a los anteriores, las absorbancias a medida que crece su concentración. Este tipo de interferencia también es la presentada por el aluminio, y es debido a que la matriz presenta emisión de luz a esta longitud de onda. (Las lectures obtenidas con la técnica de Fotometria de llama las hemos transformado en absorbancias, por eso en los párrafos anteriores hacemos referencia a las absorbancias y no a las medidas de emisión).

Hay que indicar que con esta técnica se presenta el caso contrario al que se presentaba con la técnica de absorción atómica, y es que en la fotometria de llama, la interferencia de los elementos correspondientes disminuye al aumenter la concentración de indio, mientras que en absorción atómica aumentan.

Podemos hacer notar que las interferencias encontradas en asta técnica son muy pequeñas, aunque algo mayores que para la absorción atómica. Para la mayoria de los elementos, podemos afirmar que son ignorables, dadas las concentraciones tan bajas en que aparecen en este tipo de aleaciones.

Con la llama aire-acetileno se disminuyen considerablemente las interferencias, al contrario que en la técnica de absorción atómica. Solamente presentan mayor interferencia en este tipo de llama los elementos fácilmente ionizables.

En las gráficas 1, 2, 3 y 4 se presentan algunas de las interferencias encontradas para la técnica de fotometria de llama. Las figuras 2 y 3

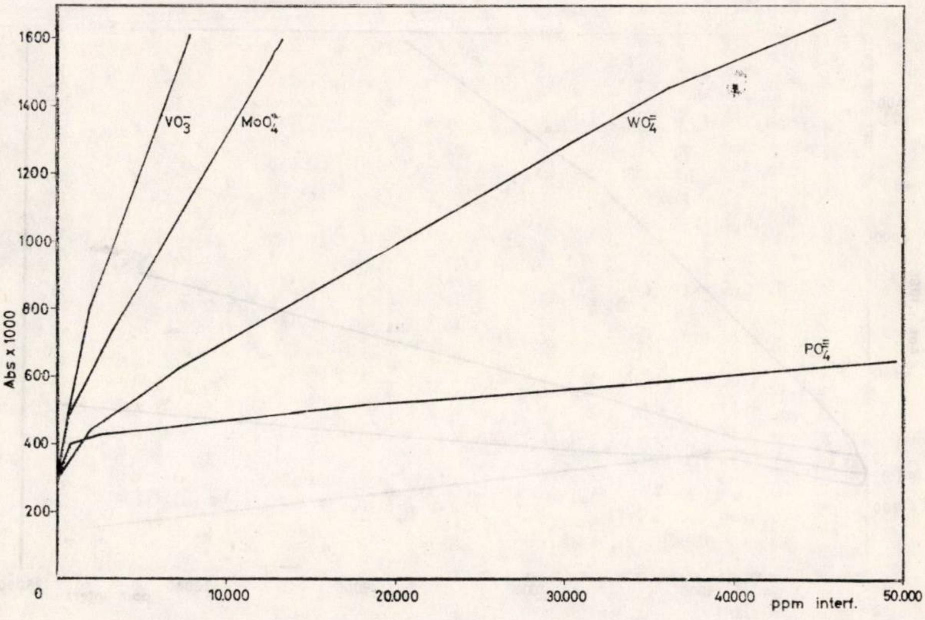

Fig. 1. — Interferencia de los aniones, sobre 10 p.p.m. de indio con llama óxido nitroso-acetileno y utilizando la técnica de fotometria de llama.

corresponden a la llama aire-acetileno, mientras que las figuras 1 y 4 han sido obtenidas con la llama óxido nitroso-acetileno. No hemos querido representar ninguna interferencia relativa a la técnica de absorción ató-

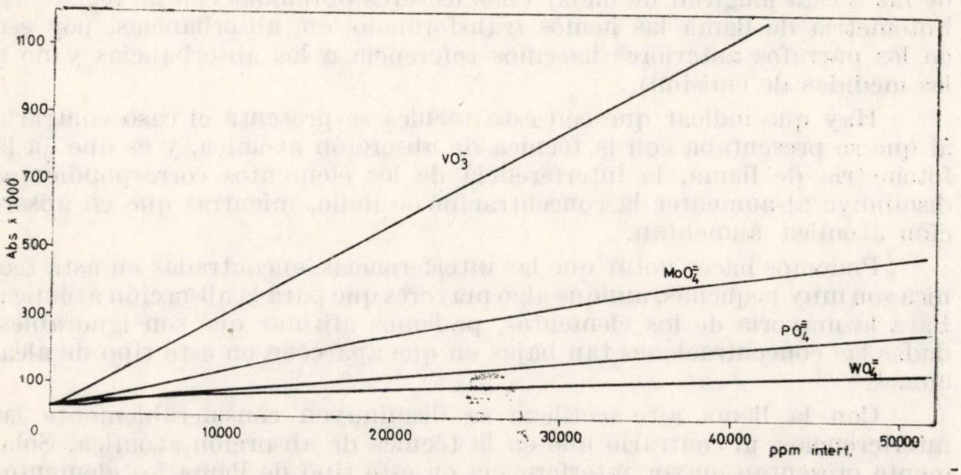

Fig. 2. — Interferencia de los aniones, sobre 10 p.p.m. de indio con llama aire-acetileno y utilizando la técnica de fotometria de llama.

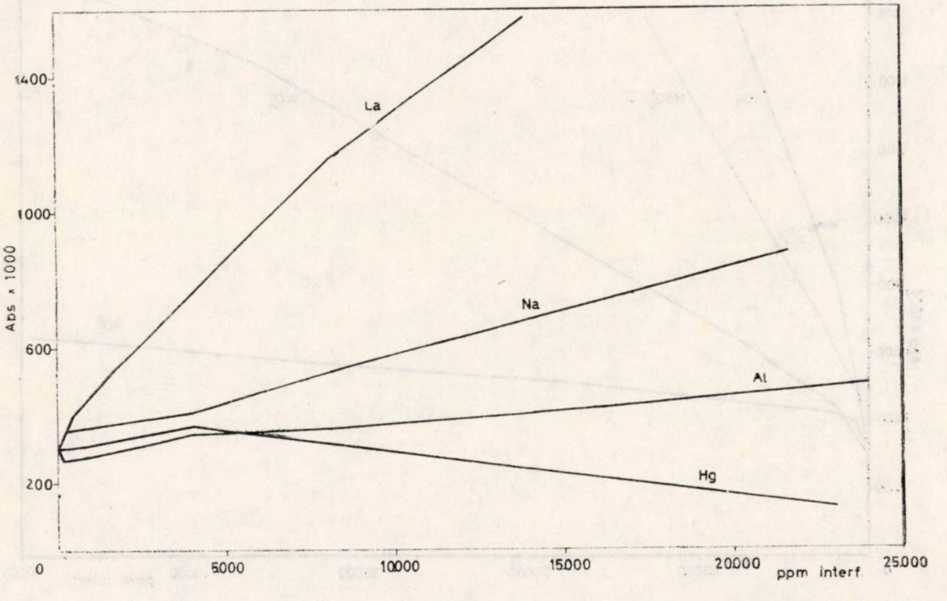

Fig. 3. — Interferencia de los cationes, sobre 10 p.p.m. de indio con llama óxido nitroso-acetileno y utilizando la técnica de fotometria de llama.

mica puesto que todas las interferencias indicadas anteriormente lo son, pero con un valor relativo inferior al 10 %, por lo que no hemos creido oportuno incluirlas.

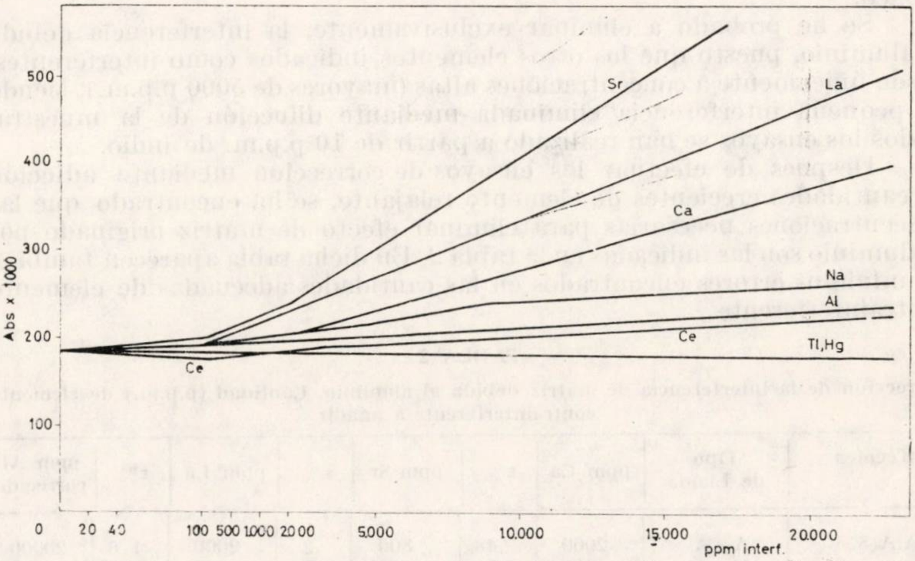

Fig. 4. — Interferencia de los cationes, sobre 10 p.p.m. de indio con llama aire-acetileno y utilizando la técnica de fotometria de llama.

Corrección de las interferencias

Con el fín de eliminar ó llevar a una forma constante las interferencias originadas por el efecto de matriz del aluminio, se han intentado resolverlas mediante adiciones de un elemento contrainterferente.

Los métodos que han sido utilizados para eliminar las interferencias incluyen los siguientes:

a. — Creación de una matriz semejante al problema, en las muestras de calibrado.
b. — Utilización de la llama óxido nitroso-acetileno
c. — Utilización de una llama aire-acetileno oxidante ó reductora.
d. — Separación del indio mediante extracción con disolventes
e. — Utilización de agentes relajantes

En el primer caso, la matriz puede ser muy compleja conteniendo elementos en un amplio rango de concentraciones por lo que puede presentarse una sobrepresión con la consiguiente pérdida en la sensibilidad; por otra parte, en la mayor parte de las ocasiones no se conoce la composición de la matriz del problema. Con el uso de la llama óxido nitroso-acetileno se obtendrá en la mayoria de los casos una pérdida de sensibilidad y un aumento en la inestabilidad de las lecturas. Las mismas desventajas ofrece el empleo de la llama aire-acetileno oxidante ó reductora. El empleo de un procedimiento de separación con disolventes proporciona un método más largo y al mismo tiempo se aumentan las posibles fuentes de error, no siendo normalemente recomendado ya que también puede necesitarse una previa preconcentración. Por estas razones hemos preferido el empleo de los agentes contrainterferentes. Se han empleado tres elementos : calcio, estroncio y lantano, con el fín de comparar su eficacia y elegir el más idóneo.

Se he probado a eliminar exclusivamente, la interferencia debida al aluminio, puesto que los otros elementos indicados como interferentes, lo son únicamente a concentraciones altas (mayores de 5000 p.p.m.), siendo su pequeña interferencia eliminada mediante dilucción de la muestra. Todos los ensayos se han realizado a partir de 10 p.p.m. de indio.

Después de efectuar los ensayos de corrección mediante adicción de cantidades crecientes de elemento relajante, se ha encontrado que las concentraciones necesarias para eliminar efecto de matriz originado por el aluminio son las indicadas en la tabla 2. En dicha tabla aparecen también los mínimos errores encontrados en las cantidades adecuadas de elemento contrainterferente.

TABLA 2

Corrección de la interferencia de matriz debida al aluminio. Cantidad (p.p.m.) de elemento contrainterferente a añadir

Técnica	Tipo de Llama	ppm Ca	ε%	ppm Sr	ε%	ppm La	ε%	ppm Al corregido
A.A.S.	A−A	2000	4	800	2	2000	1.6	20000
	N−A	200	5	200	1.5	100	1.3	” ”
F.E.S	A−A	2000	4	1000	0.9	800	0.7	” ”
	N−A	2000	3	900	0.7	1000	0.3	” ”

El elemento que mejores resultados proporciona es el lantano, debido entre otras cosas a una mayor estabilidad de la llama. Es por esto por lo que se prefiere a los demás. El estroncio proporciona unos resultados casi semejantes al lantano. Los peores valores se han obtenido con el calcio.

Aplicación al análisis de una serie de aleaciones base aluminio

Para comprobar la aplicabilidad del método propuesto, en este tipo de aleaciones, se ha verificado la determinación de indio en varias muestras de composición conocida. Los resultados se encuentran reflejados en la tabla 3.

TABLA 3

Resultados de la determinación de indio en una aleación base aluminio, mediante el método propuesto

Tipo de aleación	% de In presente	% de In encontrado			
		F.E.S.		A.A.S.	
		A−A	N−A	A−A	N−A
L−3710	0.028	0.028	0.028	0.027	0.026
L−3721	0.026	0.025	0.025	0.025	0.024
L−3731	0.025	0.026	0.025	0.024	0.028
L−3741	0.028	0.027	0.028	0.027	0.027
L−3751	0.030	0.030	0.030	0.029	0.031

Control estadístico del método

Para establecerlo efectuamos un control sobre el error en la determinación y sobre la reproducibilidad. Estos controles se han llevado a cabo en ambas técnicas.

Error en la determinación : El error lo determinamos según la técnica operatoria propuesta, valorando distintas soluciones cuyo contenido en indio estaba presente entre 1 y 10 p.p.m. En la tabla 4 se recogen los resultados obtenidos.

TABLA 4

Cálculo del error medio en la determinación
(Cada valor es el resultado de promediar siete determinaciones)

ppm de In colocadas	Error medio, %			
	F.E.S.		A.A.S.	
	A−A	N−A	A−A	N−A
0.84	1.25	1.33	1.31	1.03
1.40	0.43	0.40	0.86	0.97
3.35	0.23	0.18	0.37	0.45
5.74	0.38	0.29	0.34	0.36
8.41	0.26	0.25	0.56	0.66

Reproducibilidad ; Para determinar la reproducibilidad de los métodos propuestos, se determinaron dos series de siete muestras cada una, conteniendo la primera 2 p.p.m. de indio y la segunda 7 p.p.m.. Después de aplicar a los distintos datos obtenidos el cálculo de errores, encontramos los valores de la media, desviación típica, desviación sobre la media y el error relativo sobre el valor medio para cada una de las dos series, recogidos en la tabla 5.

TABLA 5

Cálculo de la reproducibilidad del método
(Cada valor es el promedio de siete determinaciones)

Técnica de absorción atómica :

ppm In colocados	$\sigma . 10^{-3}$		$\sigma_m . 10^{-3}$		ε,%	
	A−A	N−A	A−A	N−A	A−A	N−A
3.1	25	21	11	6	0.83	0.67
5.3	21	18	8	6	0.42	0.36

Técnica de fotometria de llama :

ppm In colocados	$\sigma . 10^{-3}$		$\sigma_m . 10^{-3}$		ε, %	
	A−A	N−A	A−A	N−A	A−A	N−A
1.4	5	6	4	2	0.35	0.41
2.5	6	8	5	3	0.24	0.32

σ = Desviación típica
σ_m = Desviación media
ε = Error relativo sobre el valor medio

DISCUSION

Conviene considerar, en primer lugar, que la llama no solamente es una fuente de calorias, sino también un medio donde tienen lugar una serie de reacciones muy complejas cuya naturaleza no se conoce muy bién. El comburente y el combustible son de hecho reactivos cuya composición, concentración y pureza, tienen cierta influencia sobre la atomización. Por esto, es probable que cierto tipo de interferencias desaparezcan cuando se modifican estas características del medio. No obstante, es dificil hacerlo sin modificar la sensibilidad ó la estabilidad de la medida, es por esto por lo que nosotros hemos realizado todas las experiencias para un mismo medio, ya que este medio elegido era el de mejores características para la atomización del indio.

En las interferencias estudiadas, podemos observar que los aniones afectan tanto a la absorción como a la emisión (Mo, W, V, P, etc.). Esto es debido a la eliminación de la llama de los átomos en el estado fundamental. En la interferencia producida por los cationes observaremos que en la fotometria de llama, existen algunas, de las cuales está libre la absorción. En la emisión, la presencia de átomas de otros elementos afecta a la temperatura de la llama, y al número de electrones libres, por lo que varios estados son excitados en cantidades relativas muy diferentes. La absorción, sin embargo, está libre de esto, ya el estado fundamental para la absorción está tan altamente poblado, que la pequeña diferencia en la población puede originarse por variaciones en la llama, debidas a otros elementos.

En la mayor parte de las interferencias se observa un aumento en la absorción ó emisión, debido a que la neuva combinación del elemento es más fácilmente ionizable que la sal de referencia.

Podemos concluir indicando que las interferencias desaparecen cuando la temperatura de la llama es suficientemente elevada (absorción atómica), la cual nos lleva a generalizar el empleo de la llama óxido nitroso-acetileno la cual posee el único inconveniente de ser más inestable y de ionizar fuermente ciertos elementos (en fotometria de llama). Aunque las cosas parece ser que son más complejas, puesto que hemos obtenido una mayor sensibilidad en absorción atómica para la llama aire-acetileno frente a la llama óxido nitroso-acetileno, debido probablemente a un aumento en la ionización de los átomas en esta segunda llama.

Con la primera llama, se obtiene menos ruido de fondo, con lo que se mejora la relación señal/ruido, y el límite de detección llega hasta 0.8 p.p.m. de indio. Ver tabla 1.

Cuando se hace uso de la técnica de fotometria de llama ocurre lo contrario, se alcanza mayor sensibilidad con la llama óxido nitroso-acetileno. Hay que destacar que la línea analítica utilizada en esta técnica ($\lambda = 451.1$ nm) es diferente a la utilizada en absorción atómica ($\lambda = 303.9$ nm).

Comparando ambas técnicas, se obtienen mejores resultados tanto en la sensibilidad como en el límite de detección, haciendo uso de la fotometria de llama, a pasar de existir un ligero aumento en las interferencias.

CONCLUSION

De las interferencias producidas por el efecto de matriz del aluminio, tanto en la emisión como en la absorción del indio, pueden ser eliminadas mediante la adición de cantidades adecuadas de lantano ó estroncio.

Hemos podido comprobar la utilidad del método descrito, para su empleo en el análisis de indio en aleaciones base aluminio, para concentraciones de aquel superiores a 0.005 %, si bien utilizando la técnica de emisión puede llegarse hasta 0.001 %; aunque estos valores pueden disminuirse aún más partiendo de una pesada superior a 1 g.

Se propone como técnica más adecuada la fotometria de llama por su mejor sensibilidad y menor límite de detección Así mismo, para el uso de esta técnica se recomienda la llama óxido nitroso-acetileno, mientras que para la técnica de absorción atómica es preferible la llama aire-acetileno.

EXPERIMENTAL

Soluciones e Instrumentación

Reactivos : Todos los reactivos empleados han sido de calidad para absorción atómica. Se ha hecho uso de agua desionizada para las disoluciones. Las disoluciones de indio se han realizado a partir de indio metálico, disuelto en ácido clorhidrico dil. (1 : 1). Las disoluciones de aluminio se prepararon a partir de cloruro de aluminio. Para el resto de los iones interferentes se ha partido del cloruro ó del óxido correspondiente.

Equipo : Se ha empleado un equipo Pye Unicam SP 1900 de doble haz. Como fuente espectral de indio se ha utilizado una lámpara de cátodo hueco para la técnica de absorción atómica, y la llama ha sido la fuente de excitación atómica.

Las condiciones instrumentales más idóneas, han sido las siguientes :

	F.E.S.^{a}		A.A.S.^{b}	
	A−A^c	N−A^d	A−A^c	N−A^d
longitud de onda, nm	451.1	451.1	303.9	303.9
sensibilidad del selector	400	300	360	360
slit, mm	0.20	0.20	0.20	0.20
altura quemador, cm	1.5	1.0	1.5	1.5
flujo acetileno, l/min	0.700	4.400	1.000	4.500
flujo aire, l/min	4.700	—	4.700	—
flujo óxido nitroso, l/min	—	4.900	—	4.900
tiempo integración, min	1.0	1.0	1.0	4.0

a : Fotometria de llama
b : Absorción atómica
c : aire-acetileno
d : óxido nitroso-acetileno

Descripción del método

Realizado el estudio previo experimental, en el que se ha llevado a cabo la determinación de todas las posibles interferencias del indio en ambas técnicas, así como sus posibles correcciones, proponemos un método para la determinación de indio en aleaciones base aluminio.

Pesar 1 g de muestra en virtutas y desengrasadas. Disolver esta cantidad en 10 ml de ClH dil. (1 : 1). Hervir durante algunos minutos hasta que la solución quede perfectamente clara. Añadir la cantidad de elemento contrainterferente indicado en la tabla 2. Enrasar a 50 ml y llevar esta solución al aparato de absorción, comparando los resultados con los de la curva de calibrado. De aquí se obtienen las p.p.m. de indio presentes en la solución.

Línea de calibrado

Para realizar la línea de calibrado se partió de indio metálico disuelto en ClH dil. (1 : 1). Esta línea presenta un comportamiento lineal dependiente de la técnica y llama que se utilice. El rango de concentración aconsejable es el recomendado en la tabla 1.

Los límites de detección y la sensibilidad se han efectuado a partir de las disoluciones de patrones de indio, ya que las determinaciones posteriores se compararán con esta línea de calibrado. Los valores obtenidos para estos dos factores aparecen en la tabla 1.

AGRADECIMIENTO: El autor está agradecido al Dr. Don Mariano de Andrés, de la Empresa Nacional del Aluminio (E.N.D.A.S.A.) de Valladolid, por su atenta ayuda en la consecución de las muestras y patrones.

BIBLIOGRAFIA

[1] A. I. Busev, ,,The Analytical Chemistry of Indium'', Pergamon Press, New York, 1962.
[2] R. Hoehn ; L, Jackwerth y k.Koos, *Spectrochim. Acta, Parte B*, **29(b)**, 225 (1974).
[3] E. Jackwerth, J. Messerschnidt y R. Hoehn, *Analyt. Chim. Acta*, **94**, 225 (1977).
[4] F. J. Langmyhr, R. Solberg y Y. Thomassen, *Analyt. Chim. Acta*, **92**, 105 (1977).
[5] E. Jackwerth y P. G. Willmer, *Z. analyt. Chem.*, **279**, 23 (1976).
[6] N. S. Balandina ; V. P. Kharapai y I. G. Yudelevich, *Zhur. analit. Khim.*, **31**, 265 (1976).
[7] J. I. Marks, y G. Welcher, *ASTM Spec. Tech. Publ.*, **618**, 11 (1977).
[8] T. Nakahara, y S. Musha, *Analyt. Chim. Acta*, **80**, 47 (1975).
[9] K. Fujiwara ; H. Haraguchi y K. Fuwa, *Analyt. Chem.*, **47**, 1670 (1975).
[10] H. Haraguchi y K. Fuwa, *Bull. Chem. Soc. Japan*, **48**, 3056 (1975).
[11] C. P. Belcher y K. A. Brooks, *Analyt. Chim. Acta.*, **29**, 202 (1963).
[12] P. B. Adams y W. O. Passmore, *Analyt. Chem.*, **38**, 630 (1966).
[13] D. Trent y W. Slavin, *Atom Absorp. Newsletter*, **3**, 118 (1964).
[14] F. Pitts, *Analyt. Chim. Acta*, **50**, 181 (1964).
[15] D. J. David, *Analyst*, **87**, 576 (1962).
[16] J. B. Willis, *Analyt. Chim. Acta*, **33**, 556 (1961).

Revue Roumaine de Chimie, 27, 9–10, 1079–1080 (1982)

COMPTES RENDUS

ADVANCES IN POLYMER SCIENCE, Volume 41 "POLYMER PRODUCTS" Springer-Verlag, Berlin, Heidelberg, New York, 1981, 186 pages

This book is a very interesting work about the new polymers with well-defined chemical structure which have been synthesized during the last decade.

The first chapter written by Kuchi Takemoto and Yoshiaki Inaki, "Synthetic nucleic acid analogs" (52 pages and 84 references), studies the preparation and polymerization of derivatives of nucleic acid bases, their biomimetic significance and application and the specific base-base interactions between the nucleic acid analogs.

The study of functional monomers and polymers containing heterocyclic moieties, which may be used as polymeric drugs and other biomaterials, provides a novel route in the field of macromolecular chemistry and biochemistry.

Poly-N-vinyl derivatives of nucleic acid bases were prepared by polymerizing the corresponding monomers. The base-base interaction between two polymer chains was studied by UV spectroscopy and the intramolecular interaction between adenine residues in a polymer chain was investigated by emission and UV spectroscopy. Polyacrylates and polymethacrylates containing nucleic acid bases are obtained by free-radical polymerization, by anionic polymerization and by polymer reactions with cyclic compounds of uracil and thymine. The kinetics of copolymerization of vinyl-type monomers bearing complementary nucleic acid bases (β-methacryloyloxyethyl adenine and β-methacryloyloxyethyl uracil) in different solvents, using AIBN as the initiator and the kinetics of template polymerization of atactic poly-1-(β-methacryloyloxyethyl) thymine has been investigated. The degree of intramolecular self-association of the bases was estimated from photodimerization study of thymine bases along the polymer chain. Recently, graft copolymers of nucleic acid bases onto polyethylenimine have been prepared for interferon inducers (The interferon inducers can prevent or regress certain tumors). Poly-L-lysine derivatives containing pendant nucleic acid bases were prepared by polymerization and by polymer reaction of carboxy ethyl derivatives of the base onto poly-L-lysine.

The formation and stoichiometry of the polymer complex between nucleic acid analogs are affected by the base-base distance in the polymer chain and by the nature of the polymer backbone (flexibility, steric regularity, electric charge and branching). In the case of the poly-L-lysine derivatives, the formation of polymer complexes is affected by their helical content.

Other synthetic nucleic acid analogs (polyvinylpyridine derivatives, polystyrene derivatives, polyvinyl alcohol derivatives and polyaddition type polymers) are also reviewed.

The second chapter "Statistical theory of polymeric lyotropic liquid crystals", written by Alexander Yu. Grosberg and Alexei R. Khokhlov is a theoretical study (44 pages and 46 references) on the liquid-crystalline phase in solutions of completely stiff and semiflexible macromolecules. The first part of the work is devoted to the investigation of the phase diagram for the liquid-crystalline transition in the solution of completely stiff macromolecules by a method which combines both the Onsager and the Flory methods. This method is applied for the study of the phase diagram in the solution of semiflexible macromolecules. In the last two sections the intramolecular liquid-crystalline ordering for semiflexible and relatively short chains is discussed.

The third chapter "Interpolymer complexes" is written by Esen A. Bekturov and Larisa A. Bimendina. The article contains 48 pages and 178 references.

The study of interpolymer complexes is a new field of the macromolecular chemistry. The polymer-polymer complexes possess properties which are essentially different from those of the initial components. Interpolymer complexes may be obtained by two main methods: from pre-existing chemically and structurally complementary macromolecules and by matrix polymerization. Interpolymer complexes can be divided into four classes: stereocomplexes, polyelectrolyte complexes, complexes stabilized by hydrogen bonds and coordination complexes. Hydrophobic interactions play an important role in stabilization of polyelectrolyte complexes and of complexes with hydrogen bonds. The problems of complex formation are discussed. Formation of interpolymer complexes has a cooperative nature: i.e. it occurs within a narrow range of molecular weight, solvent composition, pH, temperature, etc. There may exist two types of equilibria in cooperative interpolymer reaction: on a macromolecular level and inside the complex particles. In the study of complex formation the principles of equilibrium thermodynamics may be used. The resemblance of polyelectrolyte complex formation and cooperative transition in DNA molecules are pointed out. The selectivity and the cooperativity in reactions are studied. In the last part of the work, the applications of polymer-polymer complexes are considered. The polyelectrolyte complexes may be used for preparation of transparent and electroconductive plates for illuminating and heating, for preparing semipermeable membranes of definite permeability and selectivity, and also as separators in galvanic and storage batteries. Polyelectrolyte complexes are also of great interest in medicine. Interpolymer complexes may be applied for preparation of "chemical muscles" transforming chemical energy into electrical and mechanical energy.

The chapter "Linear polymers containing transition metals in the main chain" (29 pages and 56 references) is written by Nobue Hagihara, Kenkichi Sonogashira, Shigetoshi Takahashi.

There exists a number of many potential practical applications of linear polymers containing transition metals in the main chain. Recently, because of their high-temperature stability and radiation resistance, a number of organometallic polymers containing metallocenes and metallocene analogues has been studied. The authors present the linear "Werner-type" coordination polymers which can exist as a stable form in solution. The polymers obtained by polycondensation between bischelating ligands and bisfunctional metal salts are thermally stable and can be used for the preparation of good conductors or semiconductors. The polymers obtained by polycondensation between bifunctional metal complexes and bifunctional organic amines and by insertion of transition metal ions into polymer ligands are reviewed. In the main part of this article the polymers containing sigma-bonded transition metals in the main chain are reported. They include a new class of soluble metal-poly-yne polymers, which have been studied in the authors' laboratory. The metal-poly-yne polymers are soluble in a variety of organic solvents. The high solubility of these polymers may be attributed to bulky substituents on phosphorus which cover the backbone and decrease intermolecular interactions between macromolecules. The metal-poly-yne polymers are fairly stable in air in the solid state and show considerable thermal stability. The study of solution properties indicates a rod-like structure for these polymers. The poly-yne polymers are lyotropic liquid-crystalline materials.

Kristiana Goşa

Revue Roumaine de Chimie, 27, *9–10*, 1081 (1982)

SCIENTISTS AND PEACE

I could hardly have thought, at the end of World War II, after all those atrocities and pains that peoples would so soon consider triggering a new war as a possibility. Wheather this war is to be waged with conventional or nuclear weapons, *clean* or *dirty*, it amounts to the same shadow of death over life.

As a researcher in the field of science and technology, I express, together with my fellows from the Center of Physical Chemistry, our staunch stand for peace and join those who defend the fundamental rights of the peoples — life, peace, a free and dignified existence — endeavouring to stop the arms race and accomplish disarmament.

We support disarmament, first and foremost nuclear disarmament, we stand for firm promotion of a peaceful policy as put forward by Romania. The considerable sums of money, obtained from military cuts, could be used for improving the living conditions, for developing fundamental researches or control and eradicate such diseases as cancer.

Like my research fellows, I signed the Appeal of the Romanian People addressed to the special session of the United Nations Organization devoted to disarmament and I am appealing now through this journal, to all my friends and colleagues from abroad to spare no efforts in safeguarding peace, in saving us all, in saving that miracle called life.

All of us engaged in scientific research share a great responsibility; we are called to play a special role in building up a united Europe, in which all the nations, irrespective of their social system could cooperate on an equal footing grounded on mutual respect, with each nation developing in freedom and independence without any foreign interference.

Let us remember that life, spiritual and material values are difficult to create. Therefore let us do everything in our power to stop anybody who might waste or destroy them.

Dr. Chem. D. I. MARCHIDAN
ICECHIM—Center of Physical
Chemistry, Bucharest

NOTE POUR LES AUTEURS

La Revue Roumaine de Chimie publie des articles en anglais, français, russe, allemand ou espagnol. Les auteurs sont priés d'envoyer des articles et des comptes rendus inédits.

Les manuscrits seront dactylographiés à double interligne. La bibliographie, les tableaux et la légende des figures seront placés après le texte.

Si l'article fait partie d'une série numérotée, la partie précédente sera donnée comme première référence.

Chaque article sera précédé d'un résumé comprenant quinze lignes au maximum.

Les références bibliographiques dans le texte seront faites par des exposants sans parenthèses et paraîtront à la fin de l'ouvrage.

Les publications périodiques mentionnées dans la bibliographie seront présentées suivant les prescriptions internationales : le nom de l'auteur précédé de l'initiale du prénom, le titre du périodique abrégé conformément à « Chemical Abstracts » et souligné par une ligne, le numéro du tome indiqué par des chiffres arabes et souligné par deux lignes, suivi de la première page de l'article ; à la fin, l'année de la parution sera placée entre parenthèses. Le numéro de la revue ne sera pas indiqué si les pages du volume sont numérotées consécutivement.

Les textes des livres ou traités inclueront : le nom des auteurs, l'initiale du prénom, le titre du livre entre guillemets et sans être souligné, le numéro du tome précédé par l'abréviation « vol. » (ou « Bd. »), le numéro de l'édition, les éditions (the publisher), la localité de la parution du livre, l'année de la parution et la page de la référence précédée (s) par l'abréviation « p » (ou „S").

Les brevets seront indiqués comme suit : l'auteur ou la firme, le pays et le numéro du brevet, la date et la revue *(Chem. Abstr.)*. Par ex. : M. Jones (to Union Carbide Co.), Brit. Pat. 601 238, 2 Sept. 1959 ; cf. *Chem. Abstr.*, **54**, 12808 (1960).

Si la référence n'a pas été lue en original, on indiquera aussi la revue de références consultée.

Les diagrammes seront tracés à l'encre de Chine sur papier calque. Les tableaux et les figures (en nombre strictement nécessaire), ainsi que les courbes dans les figures seront numérotés par des chiffres arabes. Leur explication sera donnée dans la légende des figures. Prière de ne pas inscrire les mêmes données dans les tableaux et les figures. Chaque tableau aura un titre. On indiquera dans le texte la place approximative des tableaux et des figures. Les formules chimiques seront incluses dans le texte ; en outre, elles seront transcrites sur papier calque, à l'encre de Chine.

Les auteurs sont priés d'indiquer les caractères italiques (en soulignant les lettres au crayon), ainsi que tout autre caractère spécial ; les préfixes *ortho*, *meta*, *para*, *cis*, *trans*, etc. seront soulignés pour indiquer leurs caractères italiques et ne seront jamais écrits avec des majuscules.

Aucune correction à la main ne sera admise sur le manuscrit. Les corrections seront tapées à la machine. Les lettres grecques ou d'autres symboles spéciaux seront insérés à la main à l'encre clairement.

Le manuscrit sera signé par l'auteur.

Titre-courant aura 50 lettres au maximum.

L'entière responsabilité du contenu des articles appartient aux auteurs.

Sur demande on peut obtenir une note plus complète.

PRINTED IN ROMANIA

1983 FEB 17

TRAVAUX PARUS AUX ÉDITIONS DE L'ACADÉMIE DE LA RÉPUBLIQUE SOCIALISTE DE ROUMANIE

ELENA CEAUŞESCU, **Noi cercetări în domeniul compuşilor macromoleculari** (Nouvelles recherches dans le domaine des composés macromoléculaires), 1981, 536 p.

I. G. MURGULESCU, RODICA VÎLCU, **Introducere în chimia fizică. Vol. III. Termodinamica chimică** (Thermodynamique chimique), 1982, 626 p.

I. G. MURGULESCU, J. PĂUN, **Introducere în chimia fizică. Vol. I. 3. Nucleul atomic, reacţii nucleare, particule elementare** (Introduction à la chimie physique. Vol. I.3. Noyau atomique, réactions nucléaires, particules élémentaires), 1982, 606 p.

ELENA JERCAN, **Analiza cromatografică** (Analyse chromatographique), 1982, 286 p.

I. G. MURGULESCU, TATIANA ONCESCU, E. SEGAL, **Introducere în chimia fizică. Vol. II.2. Cinetică chimică şi cataliză** (Introduction à la chimie physique. Vol. II.2. Cinétique chimique et catalyse), 1981, 1024 p.

V. DRĂGUŢAN, A. T. BALABAN, M. DIMONIE, **Metateza olefinelor şi polimerizarea prin deschidere de inel a cicloolefinelor** (La métathèse des oléfines et la polymérisation par ouverture annulaire des cyclo-oléfines), 1981, 254 p.

LYDIA-MARIA VAICUM, **Epurarea apelor uzate cu nămol activ. Bazele biochimice** (L'épuration des eaux résiduelles à boue active. Les bases biochimiques), 1981, 218 p.

I. GĂLĂŢEANU, **Procese şi metode radiochimice în energetica nucleară** (Processus et méthodes radiochimiques dans l'énergétique nucléaire), 1981, 234 p.

O. IORDACHE, **Procese polistocastice aplicate în fenomenele de transfer** (Processus polystochastiques appliqués aux phénomènes de transfert), 1981, 187 p.

CR. SIMIONESCU, VALERIA GORDUZA, **Polimeri biocompatibili şi biologic activi** (Polymères biocompatibles et biologiquement actifs), 1980, 479 p.

ELENA CEAUŞESCU, **Polimerizarea stereospecifică a izoprenului** (La polymérisation stéréospécifique de l'isoprène), 1979, 307 p.

M. FLORESCU, **Metode ştiinţifice în dezvoltarea industriei chimice moderne** (Méthodes scientifiques dans le développement de l'industrie chimique moderne), 1979, 256 p.

A. T. BALABAN, I. GĂLĂŢEANU, G. GEORGESCU, LIGIA SIMIONESCU, **Compuşi marcaţi şi radiofarmaceutici cu aplicaţii în medicina nucleară** (Composés marqués et radiopharmaceutiques à application en médecine nucléaire), 1979, 495 p.

CONST. GH. MACAROVICI, **Analiza chimică cantitativă anorganică** (L'analyse chimique quantitative inorganique), 1979, 457 p.

I. G. MURGULESCU, E. SEGAL, **Introducere în chimia fizică. (Vol. II.1. Teoria molecular cinetică a materiei** (Introduction à la chimie physique. Vol. II.1. La théorie moléculaire-cinétique de la matière), 1979, 1036 p.

S. STERNBERG, FL. DANEŞ, **Termodinamica chimică aplicată** (La thermodynamique chimique appliquée), 1978, 400 p.

I. G. MURGULESCU, V. EM. SAHINI, **Introducere în chimia fizică. Vol. I.2. Structura şi proprietăţile moleculelor** (Introduction à la chimie physique. Vol. I.2. La structure et les propriétés des molécules), 1978, 604 p.

I. ZUGRĂVESCU, MAGDA PETROVANU, **N-ylid chemistry**, coédition avec McGraw-Hill International Book Company, U.S.A., 1977, 396 p.

I. G. MURGULESCU, **Introducere în chimia fizică.Vol. I.1. Atomi, molecule, legătură chimică** (Introduction à la chimie physique. Vol. I.1. Atomes, molécules, liaison chimique), 1976, 560 p.

ELENA CEAUŞESCU, **Research work on synthesis and characterization of macromolecular compounds. Contributions**, 1974, 251 p.

CR. SIMIONESCU, VIORICA RUSAN, V. POPA, **Chimia algelor marine** (La chimie des algues marines), 1974, 212 p., 1 pl.

I.P. INFORMAŢIA c. 2442

43 426

Lei 40

$ 70 (pour un abonnement annuel)

F 1103
Vegyészet
R

ACADÉMIE DE LA RÉPUBLIQUE SOCIALISTE DE ROUMANIE

REVUE ROUMAINE DE CHIMIE

REFERÁLVA

TOME 27

N°s 11 – 12

Novembre – Décembre 1982

EDITURA ACADEMIEI REPUBLICII SOCIALISTE ROMÂNIA

Rev. Roumaine Chim. RRCHAX, **27**, *11–12*, p. 1083 – 1170 (1982), Bucarest

ACADÉMIE DE LA RÉPUBLIQUE SOCIALISTE DE ROUMANIE

COMITÉ DE RÉDACTION

Rédacteur en chef:

I. G. MURGULESCU, membre de l'Académie de la République Socialiste de Roumanie

Rédacteurs en chef adjoints:

A. T. BALABAN et V. EM. SAHINI, membres correspondants de l'Académie de la République Socialiste de Roumanie

Collège de rédaction:

EM. BRATU, ELENA CEAUŞESCU, ECATERINA CIORĂNESCU-NENITZESCU, CR. SIMIONESCU, membres de l'Académie de la République Socialiste de Roumanie; P. SPACU, membre correspondant de l'Académie de la République Socialiste de Roumanie; MARGARETA AVRAM, M. BANCIU, I. HAIDUC, D. I. MARCHIDAN, I. MOLDOVAN, G. NIAC et D. SĂNDULESCU

La Revue Roumaine de Chimie paraît 10 fois par an. Toute commande de l'étranger pour les travaux parus aux Editions de l'Académie de la République Socialiste de Roumanie sera adressée à ILEXIM — Departamentul Export — Import Carte (Livres)/Departamentul Export — Import Presă (Revues), P.O.B. 136—137, télex 11226, 3, str. 13 Decembrie, 79517 Bucarest, Roumanie

Les manuscrits, les livres et les revues proposés en échange, ainsi que toute correspondance seront envoyés à la rédaction :

REVUE ROUMAINE DE CHIMIE
125, Calea Victoriei, 79717 Bucarest, Roumanie, téléphone 50 76 80

EDITURA ACADEMIEI REPUBLICII SOCIALISTE ROMÂNIA
125, Calea Victoriei, 79717 Bucarest, Roumanie, téléphone 50 76 80

REVUE ROUMAINE
DE
CHIMIE

ORSZÁGOS MŰSZAKI INFORMÁCIÓS KÖZPONT ÉS KÖNYVTÁR

Tome 27, N°s 11–12 Novembre — Décembre 1982

S. STERNBERG, I. LINGVAY and T. VIŞAN, The cathodic reactions on silicon electrode in molten potassium nitrate . . . . 1085–1089 R

I. TEOREANU and V. MOLDOVAN, On the hardening structures developed in the system Portland cement-water . . . . 1091–1098 R

ADRIAN VOLCEANOV and ALIN BĂRBULESCU, Effective hybridization of oxygen orbitals in SiO_2 . . . . 1099–1103 Bc

DANUTA M. CZAKIS-SULIKOWSKA and JOANNA RADWANSKA-DOCZEKALSKA, Thermal decomposition of the 2,2′-bipyridine and 4,4′-bipyridine compounds with bismuth, antimony and tin chlorides 1105–1108

R. P. VARMA and A. K. VIRMANI, Studies on physical properties of cadmium soaps. I. Infrared, solubility, conductivity and viscosity studies in water 1109–1115 C

R. P. VARMA and P. K. JAIN, Studies on the behaviour of cobalt and calcium soaps. III. Viscosity and surface tension studies in alcohols . . . . 1117–1123 C

IOSIF SCHIKETANZ, ALEXANDRU T. BALABAN and ECATERINA CIORĂNESCU, Aminoketone and oxazole synthesis. VII. Conversion of bis-azlactones into bis-oxazoles 1125–1129

MANOHAR V. KULKARNI and VEMANNA D. PATIL, Synthesis of pharmacologically active benzimidazoles . . . . 1131–1139 R

GH. IONESCU, F. MATEI and AL. DUCA, Contributions to the kinetical-analytical study on the CN^--traces determination based on its inhibitory effect (in German) 1141–1150

BOOK REVIEWS 1151–1152

AUTHOR INDEX 1153–1163

SUBJECT INDEX 1165–1170

Rev. Roumaine Chim. **27**, *11–12*, 1083–1170 (1982), Bucarest

Revue Roumaine de Chimie, 27, *11–12*, 1085–1089 (1982)

THE CATHODIC REACTIONS ON SILICON ELECTRODE IN MOLTEN POTASSIUM NITRATE

S. STERNBERG*), I. LINGVAY**) and T. VIŞAN*)

*) Department of Physical Chemistry & Electrochemical Technology, Polytechnic Institute Bucharest, Calea Griviţei 132.

**) Radio Parts and Semiconductors Factory, Bucharest, Romania

Received September 30, 1981

The cathodic process on n-type and p-type silicon electrodes in molten KNO_3 has been investigated under potentiostatic and galvanostatic conditions. A detailed description of the experimental set-up and the pretreatment of the silicon disk electrodes have been presented. The polarization curves on silicon with different concentrations of the charge carriers have been discussed and compared with Pt electrode curves. A mechanism for the formation and cathodic dissolution of a SiO_2 insulating film has been proposed.

The study of electrochemical processes on semiconductor electrode is related to the increasing requirements for new energy sources, e.g. photoelectrochemical solar cells.

The electrochemical behaviour of the monocrystal silicon electrode in aqueous solutions was largely analysed in the specialty literature.[1,2] There are only few papers[3,4] which dealt with the electrode reaction study on semiconductor silicon in molten salts.

It is well known that the strong oxidizing character of molten alkali nitrates in the cathodic reduction processes on metallic electrodes corresponds to the reaction [5–8]

$$NO_3^- + 2e = NO_2^- + O^{2-} \qquad (1)$$

Hence, it is interesting to verify the stability of semiconductor silicon during electrolysis in these molten electrolytes. The present paper reports on the investigation of cathodic polarization in molten potassium nitrate on monocrystal silicon electrodes. This study is based upon the potentiostatic and the galvanostatic determinations under steady conditions.

EXPERIMENTAL

Potentiostatic determination were performed by the usual technique using a Radelkis potentiostat, type OH–405. Galvanostatic experiments were also carried out with a transistored galvanostat (current pulse generator) designed and constructed in our laboratory. Its electronic circuitry is shown in Fig. 1. In this arrangement the current was adjusted and maintained constant within the $10\ \mu A \div 100$ mA range with a stability better than 1.5 %, for the impedance variations of the electrolysis cell between 0.5 and 600 Ω.

Cathodic potentials were read with a high-impedance input electronic voltmeter Philips, type PM 2440, and simultaneously recorded by an Orion type NE−230 recorder with time base. No corrections for the possible ohmic potential drops were applied.

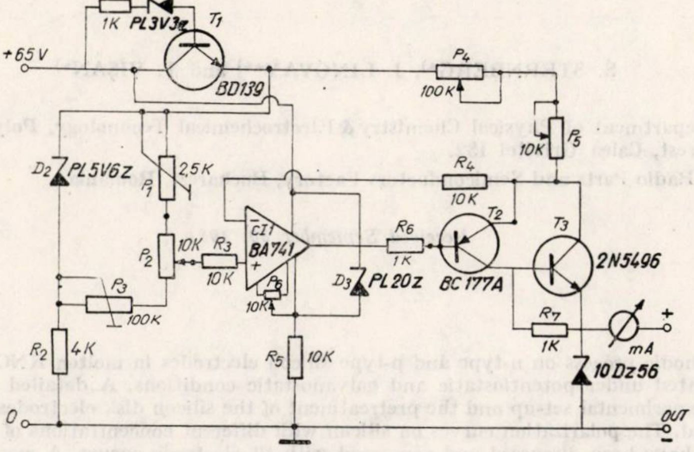

Fig. 1. — Block diagram of the galvanostat (current pulse generator).

The employed electrolysis cell was made of Rasotherm glass following the already described design.[8,9] The working disk electrode of n-type or p-type semiconductor silicon (with different charge carriers concentrations and resistivity of $10^{-2} \div 10^{2}\ \Omega\cdot$cm) raised special problems. Monocrystal silicon (111) disks of 1−2 mm thickness were sealed in a Pyrex glass tube as shown in Fig. 2. The electric contact for cathodic polarization at silicon disk was achieved by the copper wire immersed in low melting Pb−Sn alloy.

In order to prevent a rectifier contact molten Pb−Sn alloy/silicon, the inside sides of the n-type silicon disks were doped by diffusion with phosphorus from $POCl_3$, at 1255°C. Similarly, the inside sides of the p-type silicon disks were also saturated with boron by painting with B_2O_3 and heating up at the same high temperature (1255°C). The reaction products formed during thermal diffusion were moved by a special electrochemical treatment.[10]

The silicon slices nn^+ and pp^+ this way doped were metallized by chemical deposition of nickel and also by gold electrodeposition in aqueous solutions. Once the whole electrode assembled as in Fig. 2, prior to each experiment the surface renewal of the silicon disk was accomplished. The electrode was pretreated as follows : a) etched in a 10 :1 mixture of HNO_3 (70 %) and HF(50 %), b) etched in HF(50 %) solution, and c) rinsed in distilled water 3 or 4 times.

For the results comparison, the cathodic polarization curve on a Pt sheet of 1 cm^2 area was also determined. A Pt sheet of 3 cm^2 surface area and an Ag wire/0.01 M $AgNO_3$ in 1 kg KNO_3 melt served as the counterelectrode and the reference electrode, respectively.

As molten electrolyte KNO_3 chemical reagent of p.a. grade quality was used. All experiments were carried out at constant temperature of 400°C.

RESULTS AND DISCUSSION

During the galvanostatic measurements sudden variations of cathodic potential were repeatedly recorded (Fig. 3). The appearence of the maximum and minimum potentials in the potential-time curves could be attributed to the presence of a high electric insulating film on the silicon surface which is successively formed and dissolved.

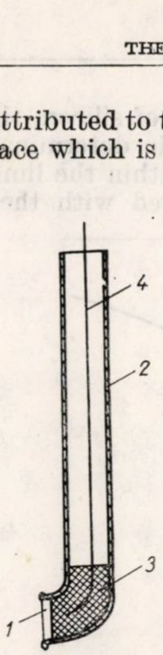

Fig. 2. — Detail of the working electrode; 1. silicon disk; 2. Pyrex glass tube; 3. Pb—Sn alloy; 4. copper wire.

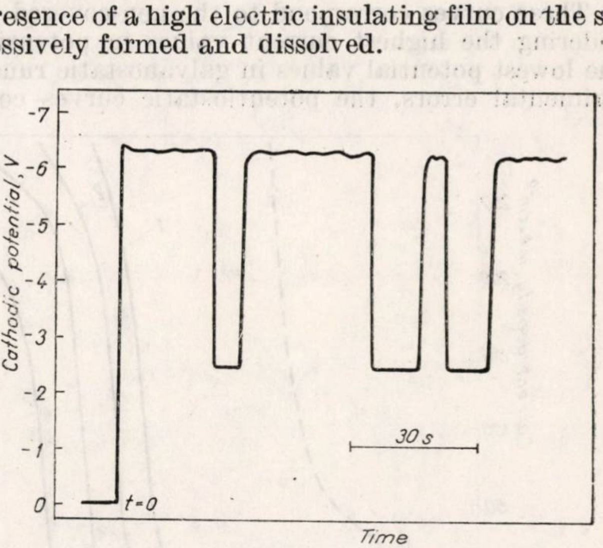

Fig. 3. — Typical galvanostatic potential-time curve on p-type silicon in KNO_3 melt; resistivity — 60 Ω.cm; current density — 100 $mA.cm^{-2}$; T. = 400°C.

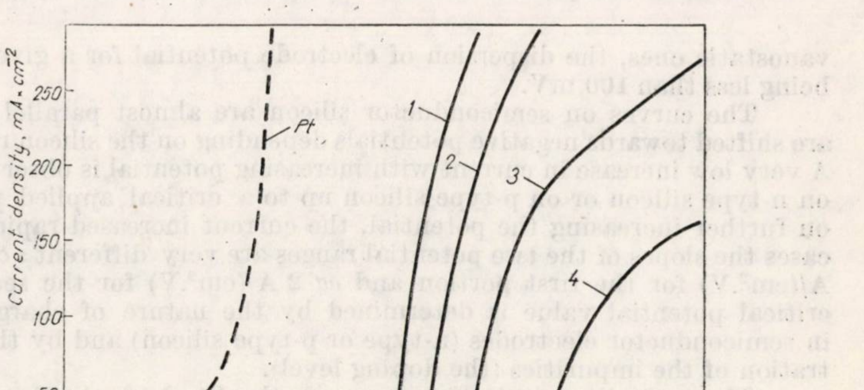

Fig. 4. — Polarization curves obtained potentiostatically and galvanostatically on p-type silicon (various resistivities) and platinum in molten KNO_3. 1. 0.014 Ω.cm; 2. 10 Ω.cm; 3. 60 Ω.cm; 4. 300 Ω.cm.

In the potentiostatic measurements low and high values of current were obtained at any cathodic potential.

Figures 4 and 5 give the obtained polarization curves.

These curves correspond to the non-covered state of silicon, that is considering the highest current values in potentiostatic determinations or the lowest potential values in galvanostatic runs. Within the limits of experimental errors, the potentiostatic curves concurred with the galvanostatic ones, the dispersion of electrode potential for a given current being less than 100 mV.

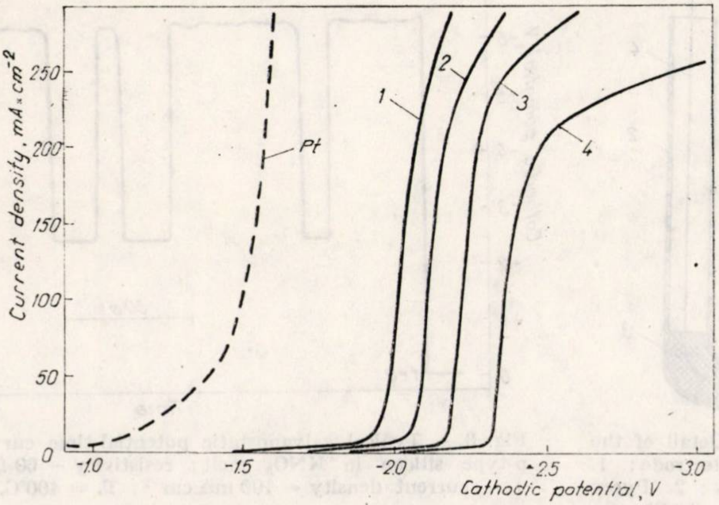

Fig. 5. — Polarization curves obtained potentiostatically and galvanostatically on n-type silicon (various resistivities) and platinum in molten KNO_3·1·0·018 Ω·cm ; 2·1 Ω·cm ; 3·30 Ω·cm ; 4·65 Ω·cm.

The curves on semiconductor silicon are almost parallel and they are shifted towards negative potentials depending on the silicon resistivity. A very low increase in current with increasing potential is observed either on n-type silicon or on p-type silicon up to a critical applied potential; on further increasing the potential, the current increased rapidly. In all cases the slopes of the two potential ranges are very different : *ca* 5×10^{-5} A/(cm^2.V) for the first portion and *ca* 2 A/(cm^2.V) for the second. The critical potential value is determined by the nature of charge carriers in semiconductor electrodes (n-type or p-type silicon) and by the concentration of the impurities (the doping level).

The cathodic polarization curve on the Pt electrode also presented in Figures 4 and 5 shows a very low overpotential.

The unexpected cathodic behaviour of silicon in KNO_3 melt may be explained by the presence of SiO_2 film. We consider that the insulating oxide-film is chemically formed by immersion of silicon disks in the oxidizing KNO_3 melt according to reaction

$$Si + 2\ KNO_3 = SiO_2 + 2\ KNO_2 \qquad (2)$$

At cathodic polarization, reaction (1) takes place followed by the SiO_2 dissolution

$$SiO_2 + O^{2-} = SiO_3^{-2}(\text{soluble}) \qquad (3)$$

Up to a new chemical formation of the SiO_2 film, there may be considered to carry on either reaction (1) or one of the following electrochemical reactions

$$Si + 2\,NO_3^- + e = SiO_3^{2-} + NO_2^- + NO \tag{4}$$

$$Si + 3\,NO_3^- + 2e = SiO_3^{2-} + 3\,NO_2^- \tag{5}$$

Thus, the possible cathodic reduction of NO_3^- to NO_2^- corresponding to reaction (1), would proceed without the direct participation of silicon. The most probable path is this reaction.

The sudden (unexpected) current increase can be likewise explained by the metallization of the semiconductor electrode owing to the potassium ions. Under these conditions, the kinetic braking, characteristic of the semiconductor electrode, does not occur and the electrodes work similarly to a metallic conductor.

CONCLUSIONS

On the basis of the polarization curves in molten KNO_3 we concluded that cathodic overpotential appears to be substantially higher for silicon electrodes (n-type or p-type silicon) than for the Pt electrode. The cathodic curves can clearly be divided into two potential regions, with very different $d\,i/d\,\eta$ slope values. It was observed that the silicon has an approximate stability in KNO_3 melt, an oxide-film being successively formed and dissolved by cathodic polarization. A reaction path for this mechanism was proposed.

REFERENCES

[1] J. I. Carasso and M. M. Faktor, in "The Electrochemistry of Semiconductors", (Edited by P. J. Holmes) Academic Press, London, 1962.

[2] T. Erdey-Gruz, "Kinetics of Electrode Processes", Akademiai Kiadó, Budapest, 1972.

[3] V. A. Tyagay, E. V. Panov, Yu. K. Delimarskiy, I. A. Stepanova and Yu. M. Shirshov, *Elektrokhimiya*, **14**, 1674 (1978).

[4] V. A. Tyagay, A. V. Gorodyskiy, I. A. Stepanova, E. V. Panov and Yu. M. Shirshov, *Elektrokhimiya*, **14**, 1682 (1978).

[5] H. S. Swofford, Jr. and H. A. Laitinen, *J. Electrochem. Soc.*, **110**, 814 (1963).

[6] H. E. Bartlett and K. E. Johnson, *J. Electrochem. Soc.*, **114**, 64 (1967).

[7] K. E. Johnson and P. S. Zacharias, *J. Electrochem. Soc.*, **124**, 448 (1977).

[8] S. Sternberg and T. Vişan, *Electrochim. Acta*, **26**, 75 (1981).

[9] I. Lingvay, Romanian Patent No. 66.653/1 Dec. 1977.

[10] I. Lingvay, F. Daneş, and M. Scârlete, to be published.

Revue Roumaine de Chimie, 27, 11–12, 1091–1098 (1982)

ON THE HARDENING STRUCTURES DEVELOPED IN THE SYSTEM PORTLAND CEMENT-WATER

I. TEOREANU * and V. MOLDOVAN **

* Polytechnical Institute Bucharest, Polizu, 1

** Institute for Construction Bucharest, Lacul Tei, 124, Bucharest, Romania

Received April 22, 1982

Matrix (cement-stone) represents the fundamental support of concrete properties. Theoretical considerations and experimental results referring to the hardening structures of cement-water system are presented. The emergence and development of the structural and mechanical properties of hardened cement are the result of development coagulation, crystallization and polycondensation structures. The mechanisms of crystallization in homogeneous and heterogeneous systems are examinated. Theoretical analysis and experimental data underline the role of polycondensating calcium hydrosilicates. The disperse-coherent and polyphase character in correlation with the nature of the hydration products make us conclude that water under different forms is very important in the cohesion of hardened cement and its mechanical properties.

INTRODUCTION

The properties of concrete as a composite material depend on the characteristics of the matrix and the aggregates, and on the adhesion (and cooperation) between them. But the matrix is the essential frame which determines the properties of the system as a whole.

The mechanism underlying the mechanical behaviour of the matrix (of hardened binders and, in particular, of hydraulic binders), is still under discussion. The main factors which influence it are thought to be either the intermolecular or the interphase forces which generate in the system zones of weak interconnections between its components, or the porosity of the system considered as an assembly of essential structural defects (the cement stone is different from the compact rocks only because the values of porosity are rather great, binding forces being mainly ionic or covalent).

In order to explain the mechanical strength of hardened cement one must keep in mind that its complex structure is a system in evolution. The emergence and development of the mechanical and structural features of hardened cements are a result of the processes of hydration-hydrolysis of the mineralogic constituents, which generate structures of coagulation, crystallization and polycondensation.

THEORY AND EXPERIMENTAL DATA

Coagulation structures have an important influence on the properties of the hardened cement. A certain time period after the cement had been mixed with water, the coagulation structures of the freshly-formed gel structures are of paramount importance in determining the behaviour of the system. The structures formed within this time interval (which apparently lasts for a while after the beginning of the setting process) can be destroyed reversibly; thus, the physical-mechanical properties of the hardening system can be improved in this stage, as a rather compact coagulation structure (for example, after revibration) replaces the former loose packing. Another way to do it is to use the peptizing action of superplasticizers.

The rheologic coefficients of cement pastes show that the cohesion increases with time. Until the setting begins, the paste behaves as a pseudoplastic fluid (Fig. 1, curves 1 and 2); after this moment, a sharp increase is recorded in the rheological parameters, and the rheologic curve shows that the system is structured. In M_1, M_2, M_3 the structures are destroyed by tangential stress τ_1, τ_2, τ_3, respectively, and the system becomes pseudoplastic again, as shown by the curve 5′. The dashed area between curves 5 and 5′ is proportional to the degree of structuring developed after a certain time of hardening (starting from the moment of mixing of cement with water). For a given system, this degree is a function of time denoted by $\psi_s(t)$. Its value is important in assessing the amount of structure developed in the initial stage of hardening of cement-water pastes, when the coagulation structures determine the behaviour of the system.

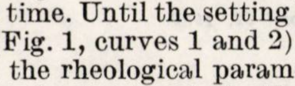

Fig. 1. — Variation in time (t) of rheological coefficients
$1 \cdot t = 0$; $2 \cdot t = 1$ h;
$3 \cdot t = 2$ h; $4 \cdot t = 3$ h;
$5 \cdot t = 3$h 30 min.

The mechanical strengths of the systems possessing only coagulation structures are practically null, as in the coagulation structures the forces between particles are weak Van der Waals-London bonds.

The crystallization structures are formed from the first-stage coagulation structures. Some non-gellic, crystalline hydration products can develop crystalline structures independently; no previous coagulation structures are noted in their case. Therefore the crystallization phenomena in the hardening of binders are both solid-state and solution processes. First, a nucleation step occurs, followed by crystal growth and formation of a three-dimensional lattice. According to Rebinder [1], the latter step is a two-stage process. In the first stage, a crystalline skeleton is formed, and the small crystals of hydrated compounds exhibit concretion contacts. These crystals may eventually grow. In the second stage no new crystals result, but the pre-formed skeleton is covered by concretions. On the one side, the crystalline structure is strengthened, and on the other, internal tensile forces appear as the freely growing crystals are randomly interconnected and consequently the tensions in the structure cannot relax themselves. In this approach, the kinetics of the nucleation and crystal growth processes is very important for the strength of the three-dimensional hardening structures, and an optimum reaction rate exists for both processes.

If the nucleation is homogeneous, the formation kinetics of critical nuclei can be described, as a general form, according to a simplified model, by the following equation:

$$I = I_0 \exp\left(-\frac{\Delta G^*}{KT}\right), \tag{1}$$

where

I_0 is pre-exponential factor;
ΔG^* — thermodynamic barrier of nucleation (maximum variation of the free energy of the system, which corresponds to the critical nuclei);
K — Boltzmann constant;
T — absolute temperature.

The thermodynamic barrier of nucleation is given, for any shape of crystallization germs, by the equation:

$$\Delta G^* = K_\Psi \frac{\sigma_{1,2}^3}{3(\Delta G_v)^2}, \tag{2}$$

where

K_Ψ is the coefficient of shape of crystallization nuclei;
$\sigma_{1,2}$ — the surface energy at the interface between "mother" phase (the phase in which crystallization occurs) and new, crystallizing phase;
ΔG_v — the variation in the volume free energy (determined by the ordered arrangement in the new phase).

The variation of the volume free energy upon crystallization from solutions at a constant temperature can be defined by the degree of supersaturation in hydration products of the "mother" solution:

$$\Delta G_v = -\frac{KT}{V_2} \ln \alpha_i, \tag{3}$$

where

V_2 is the partial volume of the crystallized phase;
α_i — the degree of supersaturation in the solution.

In the case of solid phase crystallization, the changes in the volume free energy must be adjusted by taking into consideration the free energy changes determined by the elastic stresses developed in the formation process of the lattice (ΔG_ε). These stresses are a consequence of the volume changes accompanying in most cases the phase transformations.

Considering the facts discussed above, the following equations can be written for the formation rate of the crystallization nuclei of critical size :

— crystallization from solutions

$$I = I_0 \exp - \left[\frac{K_\Psi \sigma_{1,2}^3}{3KT \left(\frac{KT}{V_2} \ln \alpha_i \right)^2} \right] \tag{4}$$

— solid-phase crystallization

$$I = I_0 \exp - \left[\frac{K_\Psi \sigma_{1,2}^3}{3KT(\Delta G_v + \Delta G_\varepsilon)^2} \right] \tag{5}$$

where all terms have already described meanings.

Analyzing the equations which describe the nucleation rate one can note that the most important factors are : the energy of the interface between nuclei and the "mother" phase ; the supersaturation of the "mother" solution ; the stresses accumulated in the newly formed lattices. As the former decreases and the latter increases, at constant temperature, the nucleation processes are much faster. As shown above, an optimum value of the nucleation rate exists ; the factors affecting it can be consequently monitored in such a manner as to obtain the best results for a given hardened system.

When foreign interfaces are present, the process is deeply affected. The appearance of such interfaces (both anhydrous and hydrated) in the process of hardening of binders and their influence on the nucleation phenomena cannot be ignored. On the basis of a simplified model, for the thermodynamic barrier of the heterogeneous nucleation, holds the following relationship :

$$\Delta G^* = K_\Psi \frac{\sigma_{1,2}^3}{3(\Delta G_v)^2} \cdot \frac{2 - 3\cos\theta + \cos^3\theta}{4} \tag{6}$$

where θ is the contact angle between the crystallizing phase and a foreign solid surface.

From (6) results that for $0 < \theta < 180°$, the rate of heterogeneous nucleation is accelerated ; when the surface of the foreign solid interface is strongly wetted by the crystallizing phase, the thermodynamic barrier of nucleation becomes negligible (for $\theta = 0$, $\Delta G^* = 0$) ; this case is favoured by a similarity in the lattices involved in the process.

The rate of crystal growth can be expressed in a general form by :

$$v = v_0 \exp\left(- \frac{\Delta G_a}{KT} \right) \left[1 - \exp\left(- \frac{\Delta G'_a}{KT} \right) \right], \tag{7}$$

where:

ΔG_a is the thermodynamic barrier of crystal growth;

$\Delta G'_a$ -- kinetic barrier;

v_0 — the pre-exponential factor.

The rate of crystal growth can be expressed in the case of crystallization from solutions with respect to supersaturation. According to a simplified model (see [2]), the equation is:

$$v = K_0 \frac{\exp(-24/KT)}{(\ln \alpha_i)^4} \exp\left[-\frac{\psi/KT)^2}{\ln \alpha_i}\right], \tag{8}$$

for high values of α_i; and for low values of α_i the equation is:

$$v = A_0 \exp -\left(\frac{\Delta G_a}{KT}\right)(\alpha_i - 1). \tag{9}$$

In equations (8) and (9), K_0 and A_0 are pre-exponential factors: ψ — energy of a single molecular band; ΔG_a — activation energy of diffusion processes.

The rate of crystal growth is mostly influenced by roughly the same factor as the nucleation phenomena. The correlation of the optimum value ranges of these factors aiming at convenient rates of the elementary steps of the crystallization process should have a desirable effect on the mechanical properties of the hardening structures, but this problem is still under study, both theoretically and experimentally.

The ionic and covalent bonds in the crystallization structures play an essential role in the mechanical strength of the hardened binders. The formation of a strength structure in the nucleation and growth of crystals, their state of stresses and mechanical behaviour are strongly determined by the degree of coherence between the crystal lattices in contact. According to the relative values of lattice parameters of the phases in contact, the interfaces between the latter can be: coherent (epitaxy occurs), semi-coherent (dislocations and stresses are noted) and non-coherent; in the latter case, the interface energy plays an important role in determining the properties of the hardened cement.

The three-dimensional crystal lattices can originate from system of polycondensed hydrocompounds. As the hydration-hydrolysis process advances, *crystallization-polycondensation structures* may result. They strengthen the system, as the ionic and the covalent binding forces are getting more important.

The occurrence, the degree of polycondensation and the relative amounts of different classes of silicates in silicate binder systems during hardening has been experimentally estimated.[3-7] Starting from these results, a stochastic model describing the irreversible discrete steps of the polycondensation process, in the particular case of the calcium silicates found in portland cement clinker, has been developed [8].

Assuming that the polycondensation process starts from monomers and proceeds by a succession of monomer additions, and that the successive steps are independent of each other, its kinetics is described by the equation:

$$\frac{\partial P_n(t)}{\partial t} = -\lambda(n, t)\, P_n(t) + \lambda(n-1, t)\, P_{n-1}(t), \tag{10}$$

where:

$P_n(t)$ is the probability of a polycondensation degree which equals n at the time t (if at the beginning $n = 1$)

$\lambda(n, t)$ — the intensity of the process at the time t corresponding to a polycondensation degree of n.

The parameter $\lambda(n, t)$ is analogous to the rate constants of the processes treated according to a determinist approach (as, e.g., in chemical kinetics). Assuming that the polycondensation is characterized by two synthetic parameters: β — percent decrease of the intensity of the phenomenon when the polycondensation degree increases by one unit, time being constant $\left(\beta = -\frac{1}{\lambda}\left(\frac{\partial\lambda}{\partial n}\right)t\right)$, and γ = percent decrease of the intensity of the phenomenon when the polycondensation degree is constant $\left(\gamma = -\frac{1}{\lambda}\left(\frac{\partial\lambda}{\partial t}\right)n\right)$, the following equation results:

$$\lambda(n, t) = e^{-\beta n} . \mathrm{e}^{-\gamma t} \tag{11}$$

Accordingly, the solution of equation (10) becomes:

$$P_n(t) = \mathrm{e}^{-\int_0^t \lambda(n, t)\,\mathrm{d}t} . \int_0^t \lambda(n-1, t)\, P_{n-1}(t)\, \mathrm{e}^{\int_0^t \lambda(n, t)\,\mathrm{d}t} . \mathrm{d}t \tag{12}$$

Putting $\beta = 2/3$ and $\gamma = 1/3$, the graphic integration gives the results shown in Fig. 2, against the data reported by Lentz [3] for the case of $3CaO.SiO_2$ (from Lentz's data one cannot tell which are the relative amounts of trimer, tetramer etc., found in the polysilicate; for this reason, the comparison has its limits).

$Ca(OH)_2$ plays a part in the polycondensation of hydrosilicates, which is important in the formation of polycondensation structures.

The extremely complex composition of cement, the multitude of hydration products and their formation kinetics generate the main features of the structure of hardened cement: it is a heterogeneous polydisperse system, where the hydration products exhibit concretions (Fig. 3) whose dispersion depends on the composition of cement and on the kinetics of the hydration-hydrolysis processes.

The chemical similarity (regarding the HO^- groups) and the tetrahedral coordination of the majority of hydration products and those of water mean that the latter is very important for the cohesion of the hardened cement. The water — intermediated binding forces are epitaxial bonds with different intensities.

In Fig. 4 are shown the DTA and TG curves for a portland cement paste hardened for 28 days in a wet atmosphere. The weight losses between 50 and 800°C (41,7 %) are continuous; more important losses are recorded between 50 and 240°C (water losses from cement gels and decomposition of some calcium aluminate hydrates or sulphataluminate hydrates), 290 and 380°C (particulary the dehydration of calcium aluminate hydrates), 460 and 580°C (calcium hydroxide decomposition) and between 760 and 790°C (hydrosilicate decomposition, decarbonation). These results, corroborated with IR spectrometry data [9] lead to the conclusion that no well-defined limits can be drawn between the different types of water. Sometimes, the HO^- groups begin to be eliminated before all H_2O molecules have been eliminated, as shown by the IR data. This is explained as

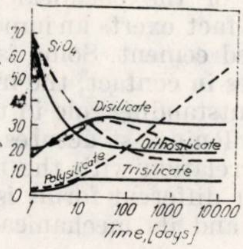

Fig. 2. — Variation of the concentration of polysilicates hydrates in the C_3S pastes. — own experimental data ; – – – Lentz[8]

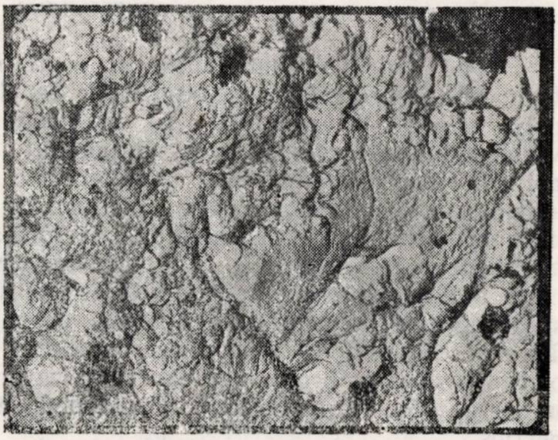

Fig. 3. — Microstructure of the hardened portland cement paste; 30 days, (5000 X).

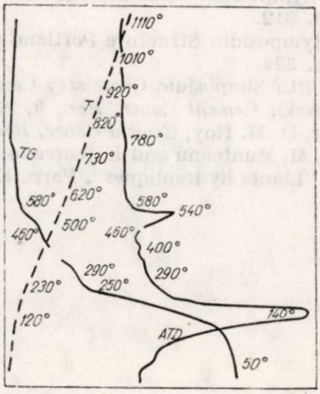

Fig. 4. — Differential thermal and thermalgravimetric curves of portland cement paste at 30 days of hydration.

follows: as the number of molecules of absorbed water decreases, the energy characterizing their bond with the solid phases increases, and finally becomes higher than the energy required for dehydroxilation.

CONCLUSIONS

The hydrated compounds in portland cement are a result of the hydration-hydrolysis processes. They develop coagulation-crystallization-polycondensation structures. In the coagulation structures the Van der Waals-London forces are very important, but as the crystallization and polycondensation structures develop, the share of the chemical (ionic and covalent) bonds increases substantially. This fact exerts an important influence on the mechanical properties of hardened cement. Some factors, as the degree of coherence of the crystal structures in contact, the microscopic and macroscopic defect state etc. play an outstanding role in understanding the mechanical properties of the hardening structures. The disperse coherent and polyphase character in correlation with the nature of the hydration products mean that water under different forms is very important for the cohesion of hardened cement and its mechanical properties.

REFERENCES

[1] P. A. Rebinder, *Kolloid. Zhur.*, **17**, 107 (1955).

[2] A. F. Polak, "Tverdenie monomineralnyh viajushcih vecestv", Moskva, Stroiizdat, 1966.

[3] W. Lentz, "Symposium Structure Portland Cement Paste and Concrete", Washington, 1969, p. 312.

[4] H. Funk, "Symposium Structure Portland Cement Paste and Concrete", Washington, 1969, p. 324.

[5] H. Funk, "Fifth Simposium Chemistry Cement", Tokyo, 1968.

[6] E. E. Lachowski, *Cement Concr. Res.*, **9**, 337 (1979).

[7] A. K. Sarkar, D. M. Roy, *Cement Concr. Res.*, **9**, 343 (1979).

[8] O. Iordache, M. Munteanu and I. Teoreanu, *Rev. Roumaine Chim.*, **18**, 239 (1973).

[9] H. Lafuma, "Liants hydrauliques", Paris, Dunod, 1963, p. 16.

Revue Roumaine de Chimie, 27, *11–12*, 1099–1103 (1982)

EFFECTIVE HYBRIDIZATION OF OXYGEN ORBITALS IN SiO_2

ADRIAN VOLCEANOV and ALIN BĂRBULESCU
Polytechnic Institute, Bucharest,
Splaiul Independenţei 313, Romania

Received February 12, 1981

The effective hybridization of oxygen in SiO_2 was calculated starting from linear combination of *s* and *p* non-equivalent orbitals, as a function of Si—O—Si angles experimentally determined.

1. INTRODUCTION

The twofold coordination of oxygen in SiO_2 implies its covalent participation, and therefore a certain orientation in space for the bonding hybrid orbitals. The observed Si—O—Si angles for different polymorphic varieties of SiO_2 are not, however, in accordance with the symmetry requirements imposed by the hybrid orbitals of the type sp^n ($n = 1, 2, 3$). This fact has determined the statement that for Si—O—Si angles between 120° and 180°, there must be some intermediate hybridization states between an sp^2 and *sp* type of hybridization [1]. This work reports the effective hybridization state of oxygen in different polymorphs of SiO_2 on the basis of the values of Si—O—Si angles, analogous to the methodology used in organic chemistry [2].

2 PRELIMINARIES

The relations used for determining the effective hybridization of oxygen can be obtained from the required condition of orthogonality for two hybrid orbitals, considered as simple vectors. Therefore, every hybrid of the *sp* type (bonding or non-bonding orbitals), which has a maximum in a certain direction "*i*", has to be of the form [3]:

$$\varphi_i = s + \lambda_i p_i \tag{1}$$

in which the coefficient λ_i shows the relative share of *s* and *p* orbitals.

A second hybrid orbital joined to "*j*" direction, which forms an θ_{ij} angle with direction "*i*" (see Fig. 1), will be of the form:

$$\varphi_j = s + \lambda_j p_j \tag{2}$$

It is easy to demonstrate [3] that the relationship between hybridization coefficients λ_i, λ_j and angle θ_{ij} is to be

$$1 + \lambda_i \lambda_j \cos\theta_{ij} = 0 \tag{3}$$

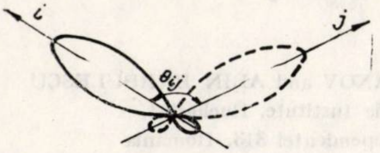

Fig. 1. — The relative position of two hybrid orbitals.

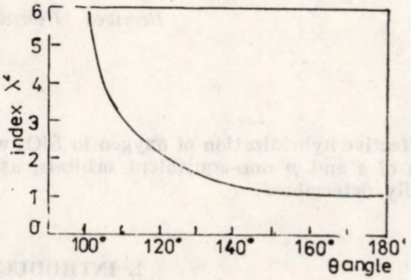

Fig. 2. — Hybridization index *versus* Si—O—Si angles.

If the hybrid orbitals are equivalent, i.e. $\lambda_i = \lambda_j = \lambda$, we can write (3) as

$$1 + \lambda^2 \cos\theta_{ij} = 0 \tag{4}$$

Thus the formula used in organic chemistry for determining the effective hybridization of carbon in aliphatic compounds results.[2,4]

The dependence between the θ_{ij} as shown in Fig. 1 (which can be experimentally determined [5]) and hybridization (denoted by λ^2) is shown in Fig. 2.

3. EFFECTIVE HYBRIDIZATION OF OXYGEN ORBITALS

From (3) and (4) we are able to estimate the hybridization coefficient, which is used for calculating the percentage of character "*s*" and "*p*" in each hybrid orbital [2], and thus to determine the effective hybridization of oxygen in SiO_2 (and generally in any oxidic compounds). So,

$$\%\, s \text{ in each hybrid orbital} = 100/(1 + \lambda^2) \tag{5}$$

$$\%\, p \text{ in each hybrid orbital} = \lambda^2/(1 + \lambda^2)\cdot 100 \tag{5'}$$

Because the percentage of total "*s*" character has to be equal to 100 % (or "*s*" orbital), we can write

$$\sum_{k=1}^{n} \frac{100}{1 + \lambda_k^2} = 100 \tag{6}$$

where n is equal to the number of the formed hybrid orbitals (in the case of oxygen four).

We can observe that λ can take any value between zero (a pure "s" orbital) and infinite (a pure "p" orbital). The intermediate values can be estimated with relations (3) and (4).

4. BONDING AND NON-BONDING HYBRID ORBITALS OF OXYGEN IN SiO_2

a) BONDING HYBRID ORBITALS

The value $\theta_{ij} = 144°$, for angle Si—O—Si from α-quartz, together with the equivalence of Si—O—Si bonds, allows us to estimate the hybridization coefficient λ_l^2 ("l" denotes that hybrids are used for bonding) using (4), which leads to the value

$$\lambda_l^2 = 1.236$$

It results that oxygen uses two bonding hybrids of the $sp^{1.236}$ type for achieving Si—O bond (it is easy to see that every hybrid can be described formally as a hybrid of the sp^{λ^2} type).

Relations (5), (5′) permit us to estimate the percentage of character, "s" and "p" of the hybrids, as follows :

$$\% s = 44.85\,\%$$
$$\% p = 55.15\,\%$$

For other polymorphic forms, the results are shown in Table 1.

b. NON-BONDING HYBRID ORBITALS

There is one more problem to solve, namely the two pairs of non-bonding electrons of oxygen. Also, we can consider that the non-bonding orbitals are equivalent.

Relation (6) permits the estimation of the hybridization coefficient of the non-bonding hybrid orbitals, if they exist, thus

$$2\,\frac{100}{1 + 1.236} + 2\,\frac{100}{1 + \lambda_n^2} = 100$$

This leads to $\lambda_n^2 = 18.391$

(indeed "n" is used for denoting the non-bonding hybrids), that is an $sp^{18.391}$ type of hybridization.

The percentage of s and p character is easy to calculate relations (5), (5′) :

$$\% s = 5.15\,\%$$
$$\% p = 94.85\,\%$$

TABLE I

Types of hybridization for polymorphic forms of SiO_2

Polymoprhic forms of SiO_2 ÷	Angle Si – O – Si (°) Ref. [5]	Percentage of orbitals				Hybridization			
		Bonding		Non-bonding		Index, λ^2		Type, sp^{λ^2}	
		s %	p%	s %	p%	Bonding	Non-bonding	Bonding	Non-bonding
α-quartz	144	44.85	55.15	5.15	94.85	1.236	18.391	$sp^{1.236}$	$sp^{18.391}$
β-quartz	162	48.74	51.25	1.25	98.74	1.051	78.821	$sp^{1.051}$	$sp^{78.821}$
β-trydimite	156	47.74	52.26	2.26	97.74	1.094	43.28	$sp^{1.094}$	$sp^{43.28}$
α-cristobalite	147	45.62	54.37	4.58	95.42	1.192	21.833	$sp^{1.192}$	$sp^{21.83}$
β-cristobalite	180	50	50	0	100	1.0	∞	sp^1	orbitals p pure
Koesite	120	33.33	66.67	33.3 0	66.7 100	2	2 different hybrid orbitals		sp^2
Keatite	156	47.74	52.74	2.26	97.74	1.094	43.28	$sp^{1.094}$	$sp^{43.28}$

The angle between these non-bonding hybrids (proceeding from (4)) was found to be $\theta_n = 93°$.

In accordance with these results, we state that the non-bonding orbitals of oxygen are not pure "*p*" orbitals, as it is usually considered, but they are weakly hybridized, for achieving maximal covering of bonding orbitals, in the best power conditions permitted by oxygen electronic state.

5. CONCLUSIONS

1. The effective hybridization of oxygen depending on Si—O—Si angles, for some polymorphs of SiO_2, was calculated.

2. The fact was emphasized that the non-bonding orbitals of oxygen bonded in SiO_2 are, in most cases, weakly "*p*" hybridized orbitals and not pure "*p*" ones.

REFERENCES

[1] P. Baltă and E. Baltă, "Introduction to the Physical Chemistry of the Vitreous State", Abacus Press, London 1976, p. 149.

[2] J. Hendrickson, D. J. Cramm and G. S. Hammond, "Chimie organică", Ed. St. şi Enciclop., Bucureşti, 1976, pp. 80—82.

[3] I. G. Murgulescu, "Introducere în chimia fizică", vol. I.1, Ed. Academiei R.S.R., Bucureşti, 1976, cap. XXII—6.

[4] Fl. Badea and Fl. Kerak, "Stereochimie", Ed. Ştiinţifică, Bucureşti, 1974, pp. 23—28.

[5] K. Hübner, *Phys. Stat. Sol. (a)*, **40**, 487 (1977).

Revue Roumaine de Chimie, 27, 11–12, 1105–1108 (1982)

THERMAL DECOMPOSITION OF THE 2,2′-BIPYRIDINE AND 4,4′-BIPYRIDINE COMPOUNDS WITH BISMUTH, ANTIMONY AND TIN CHLORIDES

DANUTA M. CZAKIS-SULIKOWSKA and JOANNA RADWANSKA-DOCZEKALSKA
Institute of General Chemistry, Technical University,
90 924 — Łódź, Poland

Received December 29, 1980

The thermal decompositions of the complexes bipy$\cdot H_2SnCl_4$, bipy$\cdot H_2MCl_5$ (bipy = = 2–bipy or 4–bipy, M = Bi^{+3}, Sb^{3+}), 4-bipy$\cdot H_2SnCl_6$ and 4-bipy$\cdot HSbCl_6$ were studied. A higher thermal stability was observed for 4,4′-bipyridine complexes.

INTRODUCTION

Although the 2,2-bipyridine (2-bipy) and 4,4′-bipyridine (4-bipy) compounds with bismuth (III), antimony (III), tin (II) and tin (IV) halides have been prepared by a number of workers,[1–11] the systematic study of their thermal decomposition has not been done. Previously we prepared crystalline complexes of the composition 2-bipy$\cdot H_2BiCl_5$, 4-bipy$\cdot H_2BiCl_5$, 2-bipy$\cdot H_2SbCl_5$, 4-bipy$\cdot H_2SbCl_5$, 2-bipy$\cdot H_2SnCl_4$, 4-bipy$\cdot H_2SnCl_4$ and 4-bipy$\cdot H_2SnCl_6$ and determined their IR spectra and other physical properties. [12] The subject of this paper is the thermal decomposition of these compounds and 4-bipy$\cdot HSbCl_6$, which at present was isolated. The mechanism of thermal decomposition of these compounds has been established.

EXPERIMENTAL

Preparation. All the syntheses were carried out with analytical grade reagents. The complexes investigated were obtained by the methods described earlier.[12]

The crystalline complex 4-bipy$\cdot HSbCl_6$ was also prepared from $SbCl_5$ by standard procedure [12] giving the following results of chemical analysis : theor : 24.76 % Sb (exp. 25.25 %), 43.26 % Cl (43.10 %), 5.70 % N/5.10 %/, 24.43 % C (24.90 %), 1.85 % H (2.00 %). In the product obtained, antimony(V) was determined by solvent extraction with rhodamin B.[13] Nitrogen carbon and hydrogen were determined by microcombustion, chlorides — by Volhard method.

Apparatus and procedure. The thermal decomposition studies were made using the derivatograph OD–102/1500°C with α-Al_2O_3 as the inert substance. Other operating conditions were : T_{max}400°C or 600°C ; heating-rate 7,9°C/min ; the mass sample — 50 mg ; sensitivity : TG — 100 mg ; DTA — 1/2 and DTG — 1/15.

The thermal decomposition of the compounds isolated has been investigated in the presence of air. The composition of the intermediate compounds formed at various stages of the thermal decomposition was evaluated by calculation from weight losses, observed on the TG curves.

RESULTS AND DISCUSSION

Thermal decomposition of 2,2′-bipyridine and 4,4′-bipyridine complexes with chlorides of bismuth (III), antimony (III), antimony (V), tin (II) and tin (IV) occurs stepwise. This is confirmed by a number of endothermic peaks on DTA curves, all due to endothermic reactions. The exothermic peaks were observed only when BiOCl and $SbOCl_3$ are partially formed. Mass changes on the TG curves are clear and can be subjected to quantitative interpretation. The error in results, determined thermogravimetrically, in comparison with theoretical value was equal to ca 1.5 %. Thermal decomposition curve of $2\text{-bipy}\cdot H_2SbCl_5$ is illustrated, as an example, in the Figure.

At the first stage of heating, HCl is liberated and intermediate compounds of the type $\text{bipy}.SnCl_2$, $\text{bipy}\cdot MCl_3$ ($M = Bi^{3+}, Sb^{3+}$, bipy = = 2-bipy or 4-bipy), $4\text{-bipy}\cdot SnCl_4$ and $4\text{-bipy}\cdot SbCl_5$ are formed. The intermediate compounds $2\text{-bipy}\cdot SbCl_3$, $2\text{-bipy}\cdot BiCl_3$[1] and $2\text{-bipy}\cdot SnCl_4$[11] were obtained as stable complexes by preparative methods. The elimination of HCl in the first or in the first and second stages was interpreted as being due to dissociation, e.g.:

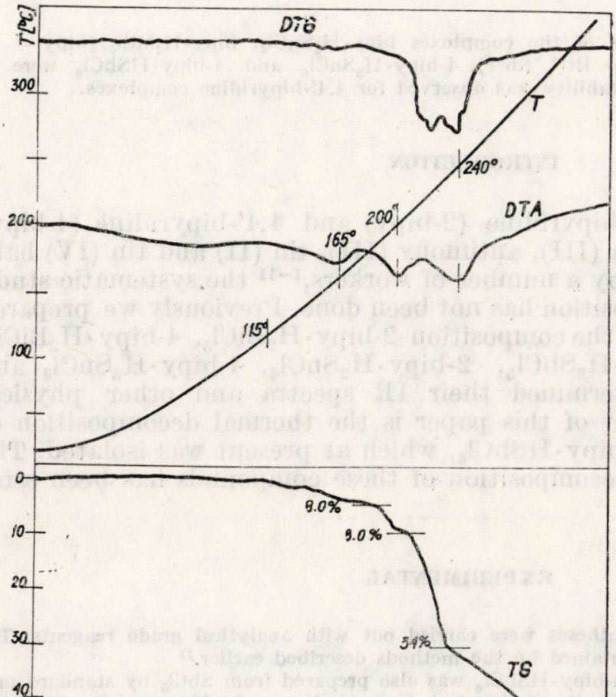

Fig. — Derivatogram of $2\text{-bipy}\cdot H_2SbCl_5$.

$$2\text{-bipy}\cdot H_2SnCl_4 \rightarrow 2\text{-bipy}\cdot SnCl_2 + 2\,HCl$$

In the following stage they lose bipyridine and are converted to metal chlorides. In the final stage $SnCl_4$, $BiCl_4$, $SbCl_3$ and $SbCl_5$ are evaporated with partial formation of BiOCl, SbOCl and $SbOCl_3$, which were isolated and confirmed by analysis of metal content.

The compounds investigated can be classified into 2 groups on the basis of their decomposition patterns.

Group A. The $\text{2-bipy}\cdot H_2MCl_5$ ($M = Bi^{3+}$, Sb^{3+}) complexes decompose according to the following scheme:

$$\text{2-bipy}\cdot H_2MCl_5 \xrightarrow{\text{I}} \text{2-bipy}\cdot HMCl_4 \xrightarrow{\text{II}} \text{2-bipy}\cdot MCl_3 \longrightarrow$$

$$\xrightarrow{\text{III}} MCl_3 \xrightarrow[\text{evaporate } MCl_3]{\text{IV}} \text{trace of MOCl}$$

In Group B, the general pyrolysis pattern consisted of the following sequence:

$$\text{bipy}\cdot H_2SnCl_4 \xrightarrow{\text{I}} \text{bipy}\cdot SnCl_2 \xrightarrow{\text{II}} SnCl_2$$

where: bipy = 2-bipy or 4-bipy.
and

$$\text{4-bipy}\cdot H_2MCl_{n+2} \xrightarrow{\text{I}} \text{4-bipy}\cdot MCl_n \xrightarrow{\text{II}} MCl_n \xrightarrow[\text{evaporate MCln}]{\text{III}} \text{trace of BiOCl}$$

or SbOCl
where: $M = Bi^{3+}$, Sb^{3+}, $n = 3$ and Sn^{4+}, $n = 4$.

The thermal decomposition of $\text{4-bipy}\cdot HSbCl_6$ occurs analogously in three stages.

In the case of complexes with ligand isomerism higher thermal stability is observed for 4,4′-bipyridine complexes. The starting temperatures of decomposition for this type of complexes are:

$\text{2-bipy}\cdot H_2BiCl_5$	$\text{4-bipy}\cdot H_2BiCl_5$
215°C	250°C
$\text{2-bipy}\cdot H_2SbCl_5$	$\text{4-bipy}\cdot H_2SbCl_5$
115°C	130°C
$\text{2-bipy}\cdot H_2SnCl_4$	$\text{4-bipy}\cdot H_2SnCl_4$
146°C	190°C

The higher thermal stability observed for complexes with 4,4′-bipyridine is assigned to the fact that this ligand favours polymeric structures.[14,15]

From the above comparison it follows that the thermal stability of the compounds investigated is influenced by the nature of metal ion. The antimony (III) complexes exhibit lower thermal stability than the corresponding compounds of bismuth (III) and tin (II). Also higher thermal stability of the compounds containing central ion in higher oxidation states is observed. The order of decreasing thermal stability is:

Bi/III/ > Sn/II/ > Sb/III/ — for 2-bipy complexes

and

Bi/III/ > Sn/IV/ > Sn/II/ > Sb/V/ > Sb/III/ — for 4-bipy complexes.

The thermal stability increasing from Sb(III) to Bi(III) is consistent with the increasing preference for higher coordination numbers down the group VA. This trend is observed in the case of ionization of the complexes 2-bipyMX_3 in nitrobenzene to $[\text{2-bipy}\cdot MX_2]^+X^-$($M$ = As(III), Sb(III), Bi(III), $X = Cl^-, Br^-$ and I^-).[1] The decreasing thermal stability for metals in low oxidation states, may be also due — among other causes — to the occurrence of a free electron pair ns^2 in the valence shell of these elements.

REFERENCES

[1] W. R. Roper and C. J. Wilkins, *Inorg. Chem.*, **3**, 500 (1964).
[2] S. P. Sinha, *Z. Chem.*, **4**, 150 (1964).
[3] G. J. Sutton, *Austral. J. Chem.*, **11**, 415 (1958).
[4] P. P. Popov, *Trudy Tomskogo Univ.*, **126**, 146 (1956).
[5] J. A. Allison and F. G. Mann, *J. Chem. Soc.*, **1949**, 2915.
[6] N. N. Greenwood and J. N. Ruddick, *J. Chem. Soc.*, A, **1967**, 1679.
[7] J. R. Beatie, G. P. McQuillan, L. Rule and M. Webster, *J. Chem. Soc.*, **1963**, 1514.
[8] M. A. Mullins and C. C. Curran, *Inorg. Chem.*, **6**, 2017 (1967).
[9] G. Matsubayashi, Y. Kawasaki, T. Tanaka and R. Okawara, *J. Inorg. Nuclear Chem.*, **28**, 2937 (1966).
[10] M. Komura, Y. Kawasaki, T. Tanaka and R. Okawara, *J. Organometal. Chem. Amsterdam*, **4**, 308 (1965).
[11] W. R. McWhinnie and J. D. Miller, *Advances in Inorg. Chem. and Radiochemistry*, **12**, 135 (1969).
[12] D. M. Czakis-Sulikowska and J. Radwańska-Doczekalska, *Ann. Soc. Chim. Polonorum*, **48**, 1379 (1974).
[13] G. Charlot, "Les Méthodes de la Chimie Analytique. Analyse Quantitative Minérale", Masson et Cie, Paris 1961.
[14] T. R. Musgrave and C. E. Mattson, *Inorg. Chem.*, **7**, 1433 (1968).
[15] J. R. Ferraro and K. C. Davis, *Inorg. Chem.*, **8**, 685 (1969).

Revue Roumaine de Chimie, 27, *11–12*, 1109–1115 (1982)

STUDIES ON PHYSICAL PROPERTIES OF CADMIUM SOAPS. I.

INFRARED, SOLUBILITY, CONDUCTIVITY AND VISCOSITY STUDIES IN WATER

R. P. VARMA and A. K. VIRMANI *

Department of Chemistry, D. A. V. College, Muzaffarnagar—251001, India

Received August 8, 1979
Revised April 10, 1982

Infrared spectra of cadmium soaps show the absence of water of crystallization. Solubility measurement of these soaps in water at different temperatures, the values of apparent heat and entropy of solution confirm the existence of micellar aggregates above Krafft point. The CMC has been determined by conductivity and viscosity methods. Dissociation constant, K, molecular conductivity at infinite dilution, λ_∞, heat of dissociation, ΔH° and free energy and entropy of dissociation, ΔG° and ΔS° respectively have been calculated using conductivity data. Several viscosity equations have been applied for soap solutions and the activation parameters of viscous flow have been calculated.

INTRODUCTION

Cadmium soaps are used [1] in the preparation of colourless and coloured lustres by dry and wet methods. The effect of these soaps on the development of microporosity in activated C prepared from polyvinyl chloride (PVC) with soaps has been determined.[2] The role of cadmium soaps as a stabilizer [3] and the mechanism of the thermal stabilization of PVC with soap and epoxy plasticizers have been studied. [4] It has been observed[5] that surfactant accelerates the preparation of cadmium soaps in water. Recently the solubility of cadmium laurate in water has been reported.[6]

In view of the important industrial applications and the fact that the references on physical properties of these soaps are rare, the present study has been initiated. Cadmium soaps (valerate and caproate) have been prepared and characterized by infrared studies. Solubility, conductivity and viscosity of these soaps in water have been measured with a view to study the micellar aggregation and to determine various parameters under different conditions.

---

* Present address: Department of Chemistry, S. D. College, Muzaffarnagar, 251001, India.

EXPERIMENTAL

MATERIALS

Merck or B.D.H. reagent grade cadmium carbonate, n-caproic and valeric acids were used. The fatty acids were purified by distillation under reduced pressure. Conductivity water was prepared in a glass apparatus, and in all cases, freshly distilled (alkaline potassium permanganate) was used.

The calculated amount of cadmium carbonate was suspended in water and the same was heated to about 80°C. The required amount of acid was added in portions to the suspension under constant stirring. After the evolution of CO_2 had ceased the product was purified by recrystallization from alcohol and then dried in vacuum.

Soaps were analysed[7] for their metal content and were found : 35.60 % (Theo. 35.75 %) in valerate and 32.72 % (Theo. 32.83 %) in caproate.

APPARATUS AND PROCEDURE

Infrared spectra of soaps were recorded on Beckman IR 20 using KBr pellets. Solubility of soaps in water was measured by preparing saturated solutions at different temperatures. The thermostat was controlled to within ±0.5°C. Clear supernatant saturated solution was taken only when the equilibrium was attained (after 2–3 hrs) with pipette, evaporated, dried and weighed. The apparatus and procedure of conductivity and viscosity measurements were the same as reported earlier.[8,9]

RESULTS AND DISCUSSION

INFRARED SPECTRA

Infrared spectra of cadmium soaps have been recorded and tentative assignments of some important vibrations have been made (Table 1). Two absorption bands of COO^- group corresponding to symmetric and asymmetric vibrations are found at 1410–20 cm^{-1} and 1540 cm^{-1} instead

TABLE 1

Some of the characteristic absorption frequencies (cm^{-1}) of cadmium soaps

	Valerate	Caproate
Rocking CH_2	710(vw)	715(w)
Out of plane deformation CH	850 (vw)	765 (vw), 860 (vw)
Stretching C–C–	1100 (vw)	1105 (s)
Progression bands	1175(vw), 1230(vw), 1310(vw)	1220(vw),1260(vw), 1280(vw),1320(vw), 1340(vw)
Symmetric stretching COO^-	1420(mb)	1410(m)
Asymmetric stretching COO^-	1540(ms)	1540(m)
Out of plane stretching CH_2	2860(s)	2870(vs)
Inphase stretching CH_2	2920(s), 2950(vs)	2940(vs), 2960(vs)

Key to abbreviation — vw = very weak ; m = medium ; s = strong ;
vs = very strong ; ms = medium strong ;
w = weak ; mb = medium broad.

of one observed at 1710 cm^{-1} in fatty acids. This occurs due to the formation of soaps. These spectra show no peak between 3590 and 3650 cm^{-1} which is due to the absence of water of crystallization. This confirms the conclusion drawn for chemical analysis of soaps.

SOLUBILITY

Solubility of soaps (Table 2) shows that valerate dissolves more than caproate. At low temperatures the solubility of soaps is low but this increases slowly with increase in temperature. With narrow range of temperature, solubility increases rapidly and the temperature (45°C for both soaps) at which the abrupt change occurs is called the Krafft point. This behaviour is the characteristic of micelle forming substances. The low solubility is due to soap molecules and the formation of soap micelles increases the solubility abruptly.

TABLE 2

Solubility and constants *A* and *B* of cadmium soaps in water at different temperatures (35—50°C)

Temp. (°C)	Valerate			Caproate		
	Sol. × 10^2 (moles litre^{-1})	*A*	*B*	Sol. × 10^2 (moles litre^{-1})	*A*	*B*
35	0.972	1.64	0.25	0.445	1.44	0.30
40	1.020	1.68	.25	.488	1.46	.30
45	1.065	1.70	.25	.525	1.49	.30
50	1.096	1.73	.23	.579	1.52	.28
55	1.155			.667		
60	1.193			.695		

The apparent heat of solution, ΔH_{sol}, can be calculated by the following relationship

$$\Delta H_{\text{sol}} = RT^2 \left[\frac{\mathrm{d} \ln S}{\mathrm{d} T} \right] \tag{1}$$

where S is the solubility in moles litre^{-1} and other terms have their usual significances. The values of ΔH_{sol} (Table 3) for valerate are lower than caproate and differ appreciably below and above K.P.

Since this process of soap can be considered as isotherm equilibrium reaction, the free energy, ΔG_{sol}, is equal to zero. Therefore, the entropy of solution, ΔS_{sol}, can be calculated as follows :

$$\Delta S_{\text{sol}} = \Delta H_{\text{sol}} / T \tag{2}$$

The variation of ΔS_{sol} is similar to ΔH_{sol} and thus confirms the micellar aggregation of soaps.

Table 3

Thermodynamic parameters of cadmium soaps at 35°C

Method	Parameter	Valerate	Caproate
Solubility	ΔH_{sol} (kJ.mole^{-1})		
	Above K.P.	5.73	15.31
	Below K.P.	8.62	18.20
	ΔS_{sol} (JK^{-1} mole^{-1})		
	Above K.P.	18.62	0.50
	Below K.P.	27.96	0.59
Conductivity	ΔE_{λ} (kJ.mole^{-1})		
	Above CMC	10.54	13.39
	Below CMC	7.66	8.62
	$\Delta H°$ (kJ.mole^{-1})	6.69	9.58
	$\Delta G°$ (kJ.mole^{-1})	−3.06	−30.96
	$\Delta S°$ (JK^{-1} mole^{-1})	96.23	100.70

CONDUCTIVITY

Specific conductance, k, of aqueous soap solutions has been studied at different temperatures (35−50°C). The plots (Fig. 1) of k vs. C show an intersection of two straight lines at a definite concentration i.e., 0.005 M and 0.003 M indicating CMC for valerate and caproate respectively which is independent of temperature.

The plots of molecular conductance, λ vs. $C^{1/2}$ are concave upwards which show the weak electrolyte behaviour of soaps. An average values of activation energy of conductance, ΔE_{λ} have been calculated from the linear plots of $\log\lambda$ vs. $1/T$. The values of ΔE_{λ} (Table 3) show a large difference in the values below and above CMC supporting the micelle formation in the soap solutions.

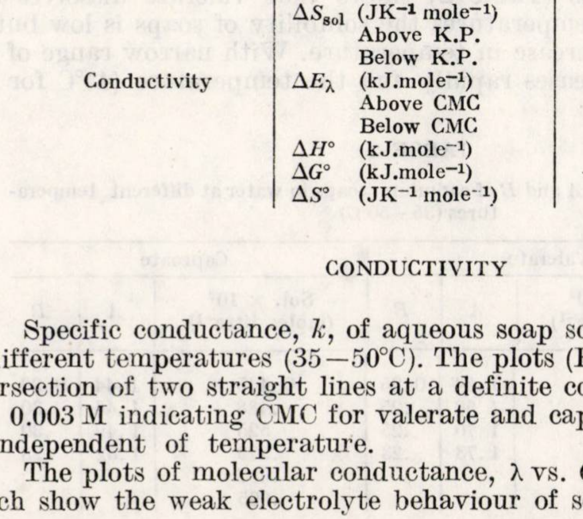

Fig. 1. — Plots of specific conductance, k (ohm^{-1} cm^{-1}), viscosity, η (millipoise) and d, density (g ml^{-1}) vs. concentration, C (moles litre^{-1}) of cadmium caproate in water at 35°C.

The linear plots of $\log \lambda$ vs. $\log C$ show that λ can be related with C as follows:

$$\log \lambda = A + B \log C \tag{3}$$

where A and B are constants.

Constant A (Table 2) increases with increasing temperature and these values of valerate are higher than caproate. Constant B (Table 2) is found to be independent of temperature which shows that the CMC is unaffected by temperature.

Values of K and λ_∞ have been evaluated graphically from Kraus and Bray's type expression.[8] Dissociation constant (Table 4) of valerate is higher than caproate and these values of soaps decrease with increasing temperature. The heat of dissociation, ΔH°, has been calculated from the linear plots of $\log K$ vs. $1/T$. The free energy, ΔG° has been calculated from the relationship:

TABLE 4

Values of dissociation constant, K, and molecular conductance at infinite dilution, λ_∞ of cadmium soaps in water at different temperatures (35–50°C)

Temp. (°C)	Valerate		Caproate	
	$K \times 10^6$	$\lambda_\infty \times 10^{-2}$	$K \times 10^6$	$\lambda_\infty \times 10^{-2}$
35	6.530	3.50	5.492	3.08
40	6.216	3.72	5.148	3.27
45	6.022	3.91	4.880	3.45
50	5.880	4.08	4.140	3.87

$$\Delta G^\circ = RT \ln K \tag{4}$$

where K is the dissociation constant.

The values of entropy, ΔS°, have also been obtained from ΔH° and ΔG° and are recorded in Table 3.

Molecular conductance at infinite dilution (Table 4) increases with increasing temperature due to increase in ionic mobility. It is found that λ_∞ values of valerate are higher than caproate due to higher mobility of valerate ion in the soap.

VISCOSITY

The plots (Fig. 1) of viscosity vs. soap concentration indicate that a point is reached at which the discontinuity occurs and the viscosity increases at a slower rate. The concentrations at the inflection point, i.e. CMC values are the same as observed by conductivity measurements.

Viscosity data of aqueous soap solutions have been satisfactorily represented in the wide range of concentration (Table 5) by the Vand[10] and Moulik[11] equations. The parameters, i.e. molar volume in litre mole^{-1}, $\bar{V}$, interaction coefficient, Q, and Moulik's constants, M and K', have been calculated. These parameters (Table 5) decrease with increasing temperature. Arrhenius equation has been used[12] to calculate the values

TABLE 5

Viscosity parameters for cadmium soaps in water

Temp. (°C)	Tested conc. limit (moles litre^{-1})	Valid zones (moles litre^{-1})	$\bar{V}$	Q	M	K'
Valerate						
35	0.001–0.010	0.005–0.01	0.57	−8.76	1.015	110
40	0.001–0.010	0.005–0.01	0.51	−11.86	1.013	105
45	0.001–0.010	0.005–0.01	0.41	−19.32	1.010	85
50	0.001–0.010	0.005–0.01	0.33	−27.19	1.007	80
Caproate						
35	0.0008–0.006	0.002–0.006	0.84	−4.76	1.009	440
40	0.0008–0.006	0.002–0.006	0.76	−7.89	1.007	420
45	0.0008–0.006	0.002–0.006	0.65	−13.84	1.005	400
50	0.0008–0.006	0.002–0.006	0.57	−21.05	1.002	390

of ΔH^* (Table 6). Entropy of activation, ΔS^* has been calculated[12] and then free energy of activation, ΔG^* is obtained from Gibb's equation at 35°C.

ΔH^* and ΔS^* values (Table 6) both show a little change below CMC, but above this concentration there is an appreciable increase. The increase in ΔH^* indicates less fluidity which shows structured solvent and micellar

TABLE 6

Activation parameters for fluidity of cadmium soaps in water at 35°C

Conc. of soap (moles litre^{-1})	Valerate			Caproate		
	$-\Delta H^*$ (kJ. mole^{-1})	$-\Delta S^*$ ($\text{JK}^{-1}\ \text{mole}^{-1}$)	$-\Delta G^*$ (kJ. mole^{-1}	$-\Delta H^*$ (kJ. mole^{-1})	ΔS^* ($\text{JK}^{-1}\ \text{mole}^{-1}$)	$-\Delta G^*$ (kJ. mole^{-1})
0.001	14.81	29.07	5.86	15.31	29.09	6.36
0.002	14.89	29.08	5.94	15.39	29.11	6.44
0.003	15.02	29.09	6.07	15.44	29.12	6.50
0.004	15.10	29.11	6.15	15.48	29.14	6.53
0.005	15.31	29.12	6.28	15.56	29.15	6.61
0.006	15.48	29.14	6.53	15.69	29.17	6.69
0.008	15.69	29.15	6.69	—	—	—
0.010	15.86	29.17	6.90	—	—	—

aggregation. The plots of ΔG^* vs. C are linear above CMC, therefore, solvent-solute aggregation is not occurring, but micelle remains in overall surroundings, because the non-linear plots show the solvent-solute aggregation[13] in the system.

ACKNOWLEDGEMENT. We appreciate the laboratory facilities provided by College authorities and the advice given by Dr. K. N. Mehrotra.

REFERENCES

[1] J. S. Yang, K. J. Lee and S. D. Han, *Guklip Kongop Yonguso Yongu Pogo*, **23**, 53 (1973).

[2] R. Tsunoda and S. Takeshita, *Ind. Res. Inst. Kanagawa Prefect*, **10**, 1795 (1975).

[3] E. Czako, Z. Vymazal and J. Stepek, *Vys. Sk. Chem. Tedinol. Prague, Czech. Plastykauc.* **12**, 259 (1975).

[4] D. F. Anderson and D. A. Mckendie, *J. Polym. Sci. Part A – 1*, **8**, 2905 (1970).

[5] L. F. Scott, H. D. Strachan, and C. M. McCloskey, *Fr. Demande.*, 2, 261, 335, 12 Sep. (1975); Appl. 7405, 732, 20 Feb. (1974); 29 pp.

[6] W. U. Malik and A. K. Jain, *J. Colloid and Interface Sci.*, **31**, 460 (1969).

[7] A. I. Vogel, "A Text Book of Quantitative Inorganic Analysis", Ed. 3rd Longman, 1961, p. 444.

[8] R. P. Varma and K. Kumar, *Cellulose Chem. Technol.*, **9**, 23 (1975).

[9] R. P. Varma and P. Bahadur, *Cellulose Chem. Technol.*, **9**, 393 (1975).

[10] V. Vand, *J. Phys. Colloid. Chem.*, **52**, 277 (1948).

[11] S. P. Moulik, *J. Phys. Chem.*, **72**, 4682 (1968).

[12] R. P. Varma and K. Kumar, *J. Am. Oil Chem. Soc.*, **54**, 156 (1977).

[13] J. C. Macdonald, J. Serphillips and J. J. Guerrera, *J. Phys. Chem.*, **77**, 370 (1973).

REFERENCES

[1] J. S. Yang, K. J. Lee and S. D. Han, Onhak Konghak Yongso Yongu Pogo, 23, 53(1975).

[2] H. Tsunoda and S. Takeshita, Ind. Res. Inst. Kanagawa Prefect. 16, 128 (1975).

[3] L. Cosko, Z. Vymazal and J. Stepek, Vys. Sk. Chem. Technol. Prague, Czech. Plastpace. 12, 289(1975).

[4] D. K. Anderson and D. A. McKenzie, J. Polym. Sci. Part A—1, 8, 2905 (1970).

[5] L. F. Scull, H. D. Strachan, and C. M. McCloskey, Fr. Demande, 2, 261, 335, 12 Sep (1975); Appl. 7405, 737, 20 Feb. (1974); 29 pp.

[6] W. U. Malik and A. K. Jain, J. Colloid and Interface Sci., 31, 180 (1969).

[7] A. I. Vogel, "A Text Book of Quantitative Inorganic Analysis", Ed. 3rd Longman, 1961, p. 444.

[8] R. P. Varma and K. Kumar, Cellulose Chem. Technol. 9, 11 (1975).

[9] R. P. Varma and P. Bahadur, Cellulose Chem. Technol., 9, 303 (1975).

[10] V. Vand, J. Phys. Colloid. Chem., 52, 277 (1948).

[11] S. P. Moulik, J. Phys. Chem., 72, 4682(1968).

[12] R. P. Varma and K. Kumar, J. Am. Oil Chem. Soc., 54, 156 (1977).

[13] J. C. Macdonald, J. Serphillips and J. J. Guerrera, J. Phys. Chem., 77, 370 (1973).

Revue Roumaine de Chimie, 27, 11–12, 1117–1123 (1982)

STUDIES ON THE BEHAVIOUR OF COBALT AND CALCIUM SOAPS. III.[1]

VISCOSITY AND SURFACE TENSION STUDIES IN ALCOHOLS

R. P. VARMA and P. K. JAIN
Department of Chemistry, D.A.V. College, Muzaffarnagar—251001, India

Received July 12, 1979
Revised August 10, 1982

Studies of viscosity and surface tension of soap solutions in methanol, 1-butanol and 3-methyl-1-butanol show the micelle forming nature of soaps. The values of CMC vary in alcohols but are found independent of temperature. Vand and Moulik equations are applicable to viscosity data above CMC. The effect of temperature and concentration of soaps on fluidity of solutions are discussed and various thermodynamic parameters of viscous flow i.e. ΔH^*, ΔS^* and ΔG^* are evaluated. The surface tension results are explained on the basis of the Langmuirs equation. Surface areas covered by the soap micelle formed from 1 mol. of the soap are calculated at different temperatures (35–50°C).

INTRODUCTION

In continuation of our studies on conductivity,[1] solubilization [2] and solubility [3] of cobalt and calcium soaps in alcohols to elucidate the micellar aggregation, we report in this communication, the viscosity and surface tension studies in these solvents. The purpose of this study is to (a) confirm the results obtained in the previous studies, (b) test the applicability of viscosity equations, (c) calculate the thermodynamic parameters of viscous flow, ΔH^*, ΔS^* and ΔG^* and study the surface behaviour of soaps.

EXPERIMENTAL

The chemicals were purified and the soaps prepared by the methods described elsewhere.[4,5] The procedure and apparatus used to measure the viscosity and surface tension of soap solutions were the same as reported earlier.[6,7]

RESULTS AND DISCUSSION

VISCOSITY

Viscosity, η, of calcium and cobalt soaps soluble in methanol, 1-butanol and 3-methyl-1-butanol has been studied at different temperatures (35–50°C). The plots (Fig. 1) of η vs. C show an intersection of two straight lines at CMC which varies in different alcohols but the same is found to be independent of temperature. The values of CMC in alcohols obtained by this method are in complete agreement as determined earlier.[1]

The extrapolated values of η_0 are independent of the nature of soap and are in complete agreement with the corresponding experimental values of the solvent. This shows that soap molecules do not aggregate to an appreciable extent below CMC whereas there is a marked change in the aggregation at CMC.

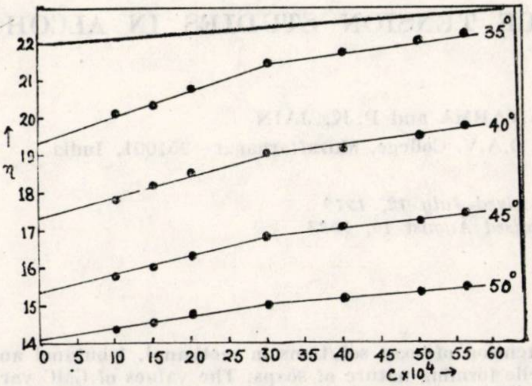

Fig. 1. — Plot of viscosity, η (millipoise) vs. concentration, C (moles dm^{-3}) of cobalt oleate in 1-butanol at 35–50°C.

Viscosity data have been examined in the light of Vand [8] and Mouliks [9] equations. Both equations are found to be linear in a limited range of concentration above CMC (Table 1). The parameters of these equations have been calculated from linear plots and are given in table 1.

Molar volume, $\bar{V}$, decreases with increasing temperature. It is found that $\bar{V}$ of calcium is higher than the corresponding cobalt soaps in methanol and 1-butanol. A comparison of $\bar{V}$ values of cobalt laurate in different solvents shows the following order:

1-butanol > methanol > 3-methyl-1-butanol

The interaction coefficient, Q, decreases with increasing temperature in methanol and 1-butanol. Both cobalt soaps in 3-methyl-1-butanol and oleate in 1-butanol show an increase in Q with rise in temperature. It is found that the values of Q of cobalt laurate are higher than the oleate in 3-methyl-1-butanol and calcium laurate in methanol. In 1-butanol these values vary for different soaps as follows:

Calcium oleate > cobalt oleate > cobalt laurate

Moulik's constants, M and K^1, (Table 1) decrease with increasing temperature. Constant K^1 of cobalt oleate increases with increasing temperature in 3-methyl-1-butanol.

From these equations the viscosity can not be calculated without having knowledge of these parameters which can not be evaluated theo-

TABLE 1

Viscosity parameters of soap solutions in alcohols at 35–50°C

Alcohols	Temperature	Tested conc. limit (moles dm^{-3})	Valid zones (moles dm^{-3})	$\bar{V}$	$-Q$	M	$K' \times 10^{-3}$
Methanol	Cobalt laurate						
	35	0.0006–0.010	0.004–0.010	31.54	18.55	1·198	74.0
	40	0.0006–0.010	0.002–0.010	15.66	21.08	1.132	70.0
	45	0.0006–0.010	0.004–0.010	13.82	21.72	1.120	66.0
	50	0.0006–0.010	0.002–0.010	6.91	28.23	1.064	60.00
	Calcium laurate						
	35	0.0002–0.0015	0.0004–0.0015	60.33	35.64	1.088	13.0
	40	0.0002–0.0015	0.0006–0.0015	46.51	40.85	1.065	19.0
	45	0.0002–0.0015	0.0004–0.0015	32.70	42.05	1.055	14.0
	50	0.0002–0.0015	0.0004–0.0015	25.33	42.44	1.052	12.0
1-Butanol	Cobalt laurate						
	35	0.0002–0.0030	0.0010–0.0030	45.05	32.57	1.086	9.6
	40	0.0002–0.0030	0.0010–0.0030	18.97	34.26	1.053	7.8
	45	0.0002–0.0030	0.0010–0.0030	15.10	34.43	1.042	5.6
	50	0.0002–0.0030	0.0010–0.0030	7.26	35.13	1.023	4.4
	Cobalt oleate						
	35	0.0010–0.0056	0.0030–0.0056	16.81	14.58	1.218	4.4
	40	0.0010–0.0056	0.0030–0.0056	13.82	6.52	1.174	3.6
	45	0.0010–0.0056	0.0030–0.0056	10.59	5.67	1.137	3.3
	50	0.0010–0.0056	0.0030–0.0056	6.91	4.34	1.082	3.1
	Calcium oleate						
	35	0.0004–0.006	0.003–0.006	23.49	2.13	1.305	11.5
	40	0.0004–0.006	0.003–0.006	22.57	3.10	1.295	8.5
	45	0.0004–0.006	0.004–0.006	20.26	3.70	1.280	7.2
	50	0.0004–0.006	0.003–0.006	18.88	5.30	1.230	5.5
3-Methyl-1--1-butanol	Cobalt laurate						
	35	0.0020–0.012	0.006–0.012	5.81	17.22	1.096	0.6
	40	0.0020–0.012	0.006–0.012	3.28	12.97	1.064	0.57
	45	0.0020–0.012	0.006–0.012	2.76	10.86	1.056	0.53
	50	0.0020–0.012	0.006–0.012	2.24	7.81	1.049	0.47
	Cobalt oleate						
	35	0.0020–0.010	0.006–0.010	7.94	20.47	1.108	0.58
	40	0.0020–0.010	0.004–0.010	5.81	17.22	1.093	0.64
	45	0.0020–0.010	0.006–0.010	4.31	12.76	1.078	0.71
	50	0.0020–0.010	0.004–0.010	3.39	7.37	1.069	0.75

retically, therefore graphical testing has been performed. The evaluated parameters can be useful to calculate the solution viscosity. Viscosity-temperature are related exponentially with Arrhenius equation. The values of ΔH^* have been calculated from the plots of $\log \eta$ vs. $1/T$ and are recorded in Table 2. The temperature dependence of reciprocal viscosity (fluidity), $1/\eta$, has also been evaluated in terms of Eyrings'equation.[10]

TABLE 2

Thermodynamic parameters for fluidity of cobalt laurate in alcohols

Alcohol	Conc. of soap (mole dm^{-3})	$-\Delta H^*$ kJ $mole^{-1}$	$-\Delta S^*$ JK^{-1} $mole^{-1}$	ΔG^* kJ $mole^{-1}$
Methanol	0.001	10.91	68.37	10.15
	0.002	12.15	72.55	10.20
	0.004	12.25	73.07	10.24
	0.008	12.44	73.76	10.28
	0.010	12.64	74.39	10.29
1-Butanol	0.0004	17.61	108.07	15.68
	0.0006	17.99	109.45	15.72
	0.0010	18.18	110.12	15.74
	0.0015	18.38	110.79	15.75
	0.0020	18.57	111.46	15.76
	0.0030	18.76	112.26	15.81
3-Methyl-1--butanol	0.002	23.36	130.54	16.85
	0.003	23.55	131.25	16.88
	0.004	23.75	131.96	16.90
	0.005	23.85	132.34	16.93
	0.006	23.94	132.72	16.95
	0.008	24.13	133.39	16.96
	0.010	24.32	134.09	16.99
	0.012	24.52	134.81	17.02

Entropy of viscous flow, ΔS^*, has been calculated and then free energy, ΔG^*, is obtained from Gibb's equation at 35°C.

The plots of ΔH^* vs. C show a change at CMC and the rate becomes slow but increases rapidly at higher concentration. ΔH^* measures energy barrier to the fluid motion and increase in this parameter shows less fluidity and thus confirms structured solvent and micellar aggregation.

The variation of ΔS^* with soap concentration is similar to that of ΔH^*. Free energy of viscous flow ΔG^* controls the rate of flow in fluid process and the non-linear variation of ΔG^* with solute concentration indicates the solute-solvent interaction [11] as the principal kinetic entity. Here the plots of ΔG^* vs. C are linear, which confirms that no solute-solvent interaction occurs but soap forms micellar aggregates in the solution. The slopes of ΔG^* vs. C plots for different soaps in alcohols are : methanol : cobalt laurate 41.8, and calcium laurate 209.2, 1-butanol : cobalt laurate 167.4, cobalt oleate 209.2, and calcium oleate 460.2 and 3-methyl-1-butanol : cobalt laurate 50.2 and cobalt oleate 66.9 kJ mol^{-2} dm^3. It is found that the slopes of calcium soaps are higher than cobalt soaps.

SURFACE TENSION

Surface tension, γ (dynes, cm^{-1}) of soap solutions in alcohols decreases with increasing temperature and soap concentration. This decrease in the surface tension in the presence of soaps is due to the decreasing effects in the surface energy of the solvents. This indicates the surface active behaviour of soaps. The plots of γ vs. C show a rapid fall upto CMC and then decrease very slowly with addition of higher concentration of soap.

The surface tension data have been interpreted by the following[12] equation

$$\frac{\gamma}{\gamma_0} = 1 - \frac{KTn_s}{\gamma_0} \ln\left(1 + \frac{n_2}{K}\right) \tag{1}$$

Where n_s is the number of exposed solvent sites per cm^2 of its surface, n_2 is the concentration of the substrate molecule cm^{-1} in bulk, K is a constant for the solvent and other terms have their usual significance.
On substituting,

$$\frac{KTn_s}{\gamma_0} = X \text{ and } \frac{n_2}{K} = \frac{C}{Y}$$

one obtains

$$\gamma/\gamma_0 = 1 - X \ln (1 + C/Y) \tag{2}$$

Where X and Y are constants. On applying the condition $C/Y >>> 1$, the following approximate expression which Langmuir[13] showed to apply at high solute concentration and in condition of surface saturation was obtained

$$\gamma/\gamma_0 = 1 - X \ln C/Y \tag{3}$$

Where γ and γ_0 are the surface tensions of solutions of concentration C and of pure solvent respectively. Equation (3) can also be written as:

$$\gamma = \gamma_0(1 + X \ln Y) - X\gamma_0 \ln C \tag{4}$$

The plots (Fig. 2) of γ vs. log C are linear, which shows the applicability of equation (4). The values of X, and Y have been calculated from the γ-log C plots and are given in tables 3 and 4.

Constant X is found to be independent of temperature in methanol but increases with rise in temperature in other alcohols. A comparison of results shows that X for cobalt soaps in alcohols is higher than calcium soaps. This indicates that the number of exposed solvent site per cm^2 in the presence of cobalt soap is higher.

The values of constant Y (Table 4) decrease with increase in temperature in methanol but increase in other alcohols. The increasing value of constant Y with increase in temperature in 1-butanol and 3-methyl-1-

butanol may be due to increase in substrate molecules per ml in the bulk. It may be pointed out that the values of both the constants X and Y are higher for oleates in 1-butanol but lower in 3-methyl-1-butanol.

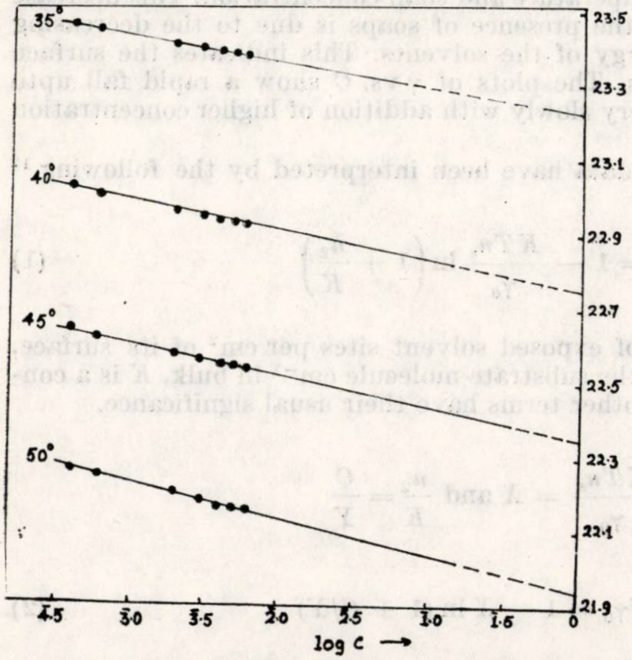

Fig. 2. — Plot of surface tension, γ (dynes cm^{-1}) vs. Logarithm of concentration (moles litre^{-1}), log C of calcium oleate in 1-butanol at different temperatures (35—50°C).

TABLE 3

Values of constant X of soaps in alcohols at 35—50°C

Solvent	Soap	$X \cdot 10^3$			
		35°C	40°C	45°C	50°C
Methanol	Cobalt laurate	3.480	3.464	3.455	2.814
	Calcium laurate	2.456	2.547	2.646	2.757
1-Butanol	Cobalt laurate	1.419	1.509	1.693	1.918
	Cobalt oleate	3.764	3.896	4.313	4.545
	Calcium oleate	1.135	1.477	1.660	1.884
3-Metyl-1-butanol	Cobat laurate	4 569	4.972	5.352	5.765
	Cobalt oleate	2 029	2.603	2.742	3.018

TABLE 4

Values of constant Y of soaps in alcohols at 35—50°C

Solvent	Soap	$Y \cdot 10^4$			
		35°C	40°C	45°C	50°C
Methanol	Cobalt laurate	11.450	4.285	1.280	1.207
	Calcium laurate	0.681	0.562	0.464	0.316
1-Butanol	Cobalt laurate	0.173	0.365	0.499	1.081
	Cobalt oleate	4.272	4.835	5.143	5.473
	Calcium oleate	2.587	3.085	3.434	4.869
3-Methyl-1-butanol	Cobalt laurate	7.499	9.991	12.936	15.087
	Cobalt oleate	3.381	6.925	8.420	8.519

On differentiating equation (4) and substituting the results in Gibb's adsorption equation, the excess concentration of solute per unit area of surface is found to be

$$\Gamma = \frac{1}{A} = \frac{X\gamma_0}{RT}$$

or

$$A = \frac{RT}{X\gamma_0} \tag{5}$$

The surface area, *A*, occupied by the micelle formed by 1 mol of the soap has been found (Table 5) to increase with increase in temperature in methanol but it decreases in other alcohols. The surface area for calcium soaps is higher than the corresponding cobalt soaps.

TABLE 5

Values of area *A* of soaps in alcohols at 35 − 50°C

Solvent	Soap	$A.10^{-10}$ cm²			
		35°C	40°C	45°C	50°C
Methanol	Cobalt laurate	34.690	36.699	38.856	50.486
	Calcium laurate	49.144	49.942	50.740	51.538
1-Butanol	Cobalt laurate	76.928	74.913	68.932	62.895
	Cobalt oleate	29.008	28.998	27.061	26.543
	Calcium oleate	96.157	76.510	70.310	64.022
3-Methyl-1-butanol	Cobalt laurate	24.571	23.660	22.839	22.088
	Cobalt oleate	55.322	47.339	44.534	42.186

ACKNOWLEDGEMENT. We appreciate the advice given by K. N. Mehrotra and facilities provided by the College authorities. One of us (P.K.J.) is thankful to C.S.I.R., New Delhi for the award of Junior Research Fellowship.

REFERENCES

[1] R. P. Varma and P. K. Jain, *Pol. J. Chem.*, **54**, 561 (1980).

[2] R. P. Varma and P. K. Jain, *J. Indian Chem. Soc.*, **LVIII**, 277 (1981).

[3] R. P. Varma and P. K. Jain, *J. Indian Chem. Soc.*, (Communicated).

[4] R. P. Varma and K. Kumar, *Colloid and Polymer Sci.*, **256**, 266 (1978).

[5] R. P. Varma, K. Singh and H. Singh, *Bull. Chem. Soc. Japan*, **51**, 1530 (1978).

[6] R. P. Varma and K. Kumar, *J. Am. Oil Chem. Soc.*, **54**, 156 (1977).

[7] R. P. Varma and K. Kumar, *Rev. Roumaine Chim.*, **24**, 757 (1979).

[8] V. Vand, *J. Phys. Colloid Chem.*, **52**, 277 (1948).

[9] S. P. Moulik, *J. Phys. Chem.*, **72**, 4682 (1968).

[10] S. Glasstone, K. J. Laidler and H. Eyring, "*Theory of rate process*". McGraw Hill, New York, N. Y. Chapter, 9, pp. 477 (1941).

[11] J. C. Macdonald, J. Serphillips and J. J. Guerrera, *J. Phys. Chem.*, **77**, 330 (1973).

[12] E. A. Moelwyn Hughes, "Physical Chemistry" 2nd ed. Pergamon Press, London, 978 (1961).

[13] I. Langmuir, *J. Amer. Chem. Soc.* **39**, 1848 (1917).

Revue Roumaine de Chimie, 27, *11–12*, 1125–1129 (1982)

AMINOKETONE AND OXAZOLE SYNTHESIS. VII[1].

CONVERSION OF BIS-AZLACTONES INTO BIS-OXAZOLES

IOSIF SCHIKETANZ, ALEXANDRU T. BALABAN and ECATERINA CIORĂNESCU
Organic Chemistry Department, Polytechnic Institute, Bucharest, Romania

Received April 29, 1982

From terephthaloyl dichloride we prepared N,N′-terephthaloyl-bis(glycine) 8 and hence the known bis-azlactone 10. This compound substitutes electrophilically two moles of aromatic hydrocarbons ArH (benzene, toluene, *p*-xylene) in the presence of anhydrous aluminium chloride affording bis-(acylaminoketones) 11, whose dehydration yields 2,2′-(*p*-phenylene)-bis(5-aryloxazoles) 12 in good yields. This new synthesis of bis-oxazoles ought to be applicable to various aromatics ArH able to undergo electrophilic acylaminoacylation.

INTRODUCTION

In previous papers of this series,[1,2] it was shown that arenecarboxylic acids **1** can be converted into α-acylamino ketones **5** and hence into oxazoles **6**. This reaction involves :

(i) acylation of glycine **2** ;

(ii) dehydration of the resulted acylaminoacetic acid **3** to the azlactone (2-substituted 5-oxazolone) **4** ;

(iii) acylaminoacylation of an aromatic compound ArH in the presence of anhydrous aluminium chloride ; and

(iv) dehydration of the acylamino ketone **5** to the oxazole **6** (usually under the action of phosphorus oxychloride).

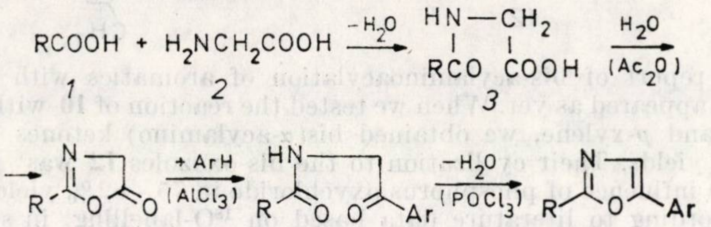

A NEW SYNTHESIS OF BIS-OXAZOLES

Taking into account that a review on advances in oxazole chemistry published in 1974 qualified this method as excellent,[3] we endeavoured to widen the scope of this reaction. The present paper extends this reaction to dicarboxylic acids and presents a new synthesis of bis-oxazoles.

Some of these bis-oxazoles have various applications for liquid scintillation counting (as secondary solutes) or for dye lasers, owing to their strong fluorescence.

As dicarboxylic acid, we employed terephthalic acid **7**. The synthesis of N,N′-terephthaloyl-bis(glycine) **9** from terephthaloyl dichloride **8** proceeded smoothly according to known procedures. The dehydration of **9** to the bis-azlactone **10** was tested under two conditions :

(a) using dicyclohexylcarbodiimide, the reaction had poor reproducibility, and the resulting dicyclohexylurea could not be removed easily from the product ;

(b) however, with hot acetic anhydride under conditions similar to those described in the literature,[4] the known bis-azlactone **10** was obtained in good yield.

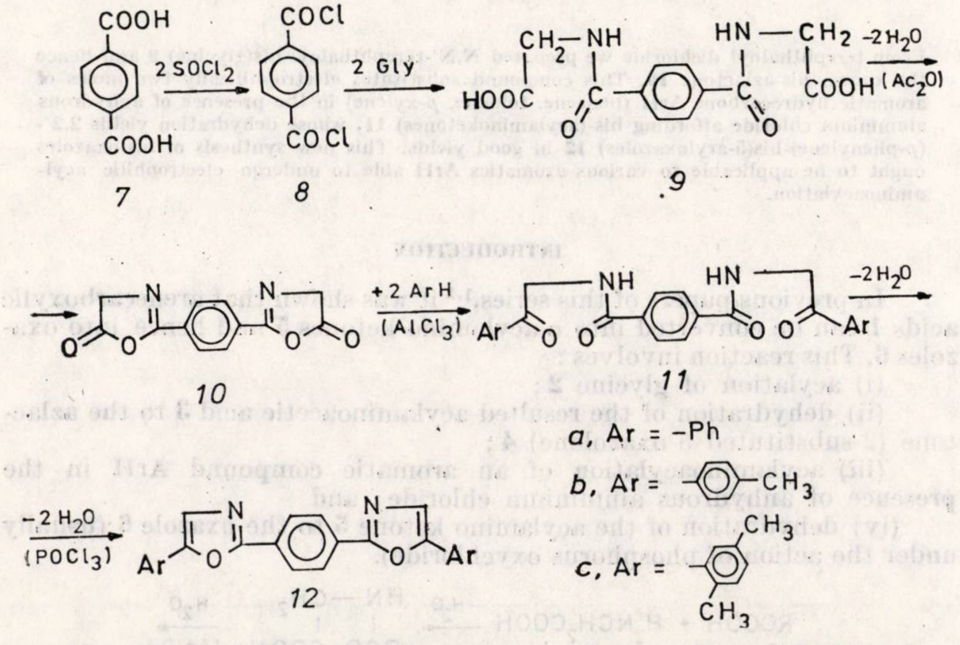

No report of bis-acylaminoacylation of aromatics with bis-azlactones has appeared as yet. When we tested the reaction of **10** with benzene, toluene, and *p*-xylene, we obtained bis(α-acylamino) ketones **11a—c** in 70—80% yields. Their cyclization to the bis-oxazoles **12** was performed under the influence of phosphorus oxychloride in 75—82% yield.

According to literature data based on ^{18}O-labelling, in such cyclizations the amidic oxygen is conserved in the oxazole, and the ketonic oxygen is lost as water.[5]

SPECTROMETRIC DETERMINATIONS

The IR spectrum of the dicarboxylic acid **9** (potassium bromide pellet) has strong bands at 3300 (NH stretching), 1710 (C=O stretching), 1640, 1550 and 1250 cm^{-1}. Its ^{1}H—NMR spectrum in dimethylsulfoxide-d$_6$

(DMSO-d_6) presents the CH_2 protons as a broadened singlet at $\delta = 4.07$ ppm with coupling due to the NH group ; the NH proton appears as a triplet at 9.07 ppm ($J = 5$ Hz) ; this coupling is no longer visible on decoupling or in the ND-derivative obtained on equilibration with deuterium oxide. The aromatic protons appear as a singlet at 8.07 ppm. Interestingly, the area of the NH triplet peak is lower than expected, suggesting some dynamic intramolecular hydrogen bonding as in **13**. Indeed, the carboxyl proton signal is centered at 4.73 ppm and is extremely broad. Similar phenomena (lower NH intensity, broadened COOH peak) are shown by the ^1H-NMR spectra of hippuric acid in DMSO$-d_6$.

The IR spectrum of the bis-azlactone **10** presents, in agreement with literature data,[4] strong bands at 1820 and 1665 cm^{-1}. The low solubility of this bis-azlactone in DMSO$-d_6$ precludes recording its ^1H-NMR spectrum in this solvent. Interestingly, the ^1H-NMR spectrum in trifluoroacetic acid (TFA) shows immediately after dissolution only two equally intense singlets at 5.05 and 8.58 ppm corresponding to the CH_2 and aromatic protons, respectively. However, upon standing at room temperature, the ^1H-NMR spectrum undergoes a gradual change : after one week the aromatic protons are almost completely replaced by an A_2B_2 pattern at 8.47 and 8.22 ppm, while along with one CH_2 singlet at the same field as before, the second CH_2 group appears as an AB system at 4.45 and 4.67 ppm with $J = 8$ Hz (geminal coupling), indicating the probable formation of **14**.

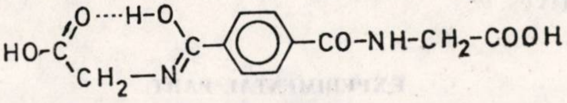

13

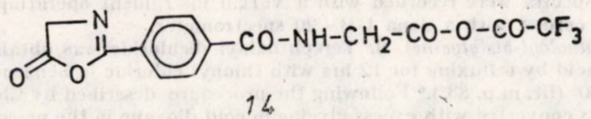

14

The IR spectra of acylamino ketones **11** in KBr pellets have strong bands at 3300 cm^{-1} (NH stretching) and 1640 cm^{-1}, and two medium-strong bands at 1690 and 1705 cm^{-1} for the C=O stretching. The ^1H-NMR spectrum of the bis(α-acylamino) ketone **11 c** in $CDCl_3$ presents the methyl peaks at 2.40 and 2.53 ppm, the methylene group as a doublet ($J = 4$ Hz) at 4.15 ppm, the *p*-phenylene protons as a singlet at 8.03 ppm, and the xylyl aromatic protons as a multiplet at 7.2–7.7 ppm.

The IR spectra of the bis-oxazoles **12** do not present salient features. Their ^1H-NMR spectra are presented in Table 1 with the respective assignments. All spectral data and melting points agree with the structure and literature data (NMR data were not indicated in the literature).

CONCLUSION AND PERSPECTIVES

In conclusion, the method presented here is an attractive one for obtaining bis-oxazoles **12** with various aryl groups, especially derived from hydrocarbons with more extended conjugation. Indeed, in comparison with the classical methods which prepare POPOP (**12 a**) and its derivatives starting from an α-acylamino ketone possessing the Ar group, and effecting a reaction with terephthaloyl dichloride **8** to obtain the bis-(α-acylamino) ketone **11**, carrying thus the Ar groups through many steps, in our method the Ar group is introduced last. This fact has several advantages, one of which is that the overall yield is good (55–65% with respect to the bis-azlactone **11**).

TABLE 1

^{1}H–NMR Spectra (δ values, ppm) of bis-oxazoles **12** in trifluoroacetic acid[a]

Compound	Aromatic protons		Methyl protons	
12 a	7.7–8.0 m (10 H)		—	—
12 b	7.83 d (4H)	7.50 d (4H)	2.50 s (6H)	—
12 c	7.77 m (2H)	7.47 m (4H)	2.50 s (6H)	2.63 s (6H)

[a] In addition, all three compounds present a singlet (4H) at 8.66 ppm (*p*-phenylene protons) and a singlet (2H) at 8.06 ppm (oxazole 4-proton).

The method ought to be easily generalizable to any aromatic system ArH which is able to undergo acylaminoacylation under the conditions used in this and previous papers, i. e. a variety of hydrocarbons and substituted derivatives.[1,2]

EXPERIMENTAL PART

^{1}H–NMR Spectra were recorded with a Varian instrument operating at 60 MHz. The IR spectra were recorded with a Jena UR–20 spectrometer.

N,N′-Terephthaloyl-bis(glycine), **9.** Terephthaloyl dichloride was obtained in 80% yield from terephthalic acid by refluxing for 12 hrs with thionyl chloride in benzene in the presence of pyridine. M.p. 80° (lit. m.p. 83°).[6] Following the procedure described by Cleaver and Pratt,[4] the dichloride **8** was converted with excess glycine in cold dioxane in the presence of magnesium oxide into **9**, m. p. (crude) 245–250° in 90% yield. The dicarboxylic acid **9** may be recrystallized from water yielding a product with m.p. 266–268°C in agreement with literature data.[4] Spectrometric data were discussed in the text.

*2,2′-*p*-Phenylene-bis[5(4H)-oxazolone]*, **10.** The bis-azlactone **10** was obtained from **9** and acetic anhydride according to literature data [4] in 75% yield. M.p. (dec.) 245° (from dioxane). In addition to the IR bands described in the literature [4] and in the text above, it presents also the following main bands (KBr pellet): 1330 vs, 1265 s, 1150 s, 1055 s, 1020 s, 890 s cm^{-1}. NMR data were discussed in the text.

Preparation of bis(α-acylamino) ketones **11.** The aromatic hydrocarbon ArH (benzene, toluene or *p*-xylene) was used as solvent in large excess (50 ml). The bis-azlactons **10** (1.22 g, 5 mmol) and anhydrous freshly sublimed aluminium chloride (4.0 g, 30 mmol) were added, and the mixture was heated at 80° on the water bath with mechanical stirring for 6 hrs. The cooled mixture was then decomposed with dilute hydrochloric acid, and the crystalline product was filtered off. By evaporating the organic layer, an additional small amount of product **11** may be obtained. The yields are presented in Table 2, together with melting points compared with literature data.

11 a, Ar = Ph, m.p. (crude) 254°, recrystallized from dioxane.

11 b, Ar = p-tolyl, m.p. (crude) 272°, recrystallized similarly.

11 c, Ar = 2,5-dimethylphenyl, m. p. (crude) 160°, recrystallized from toluene because it is too soluble in dioxane. Found : N, 6.45. Calcd. for $C_{28}H_{28}N_2O_4$: N, 6.14%.

*Preparation of 2,2′-(*p*-phenylene)-bis(5-aryloxazoles)*, **12.** The bis(α-acylamino) ketones **11** (1.5 g) were refluxed for 12 hrs with 50 ml phosphorus oxychloride, then the excess $POCl_3$

TABLE 2

Melting points and reaction yields (relative to azlactone **10**) of bis(α-acylamino) ketones **11** and of bis-oxazoles **12**[a]

Comp.	Aminoketone **11**			Oxazole **12**		
	Yield	Melting point °C		Yield[a]	Melting point °C	
	%	Found	Lit. Ref.	%	Found	Lit. Ref.
a	81	265–8[b]	262–8 [7] 255–60 [8]	65	240[c]	237–8[7] 253–6[8] 243–4[9,10]
b	70	278[b]	281–3 [9]	57	250[c]	250–2[9] 254–5[11] 259–60[12]
c	71	170–2[c]	— —	56	220–2[c]	231–3[12]

[a] The latter yield is the total yield ; for obtaining the yield of the step **11→12**, the latter yield should be divided by the former.

[b] From dioxane.

[c] From toluene.

was distilled off at normal pressure and the residue was poured on ice-water. The crystalline product was filtered off and recrystallized from toluene. Melting points and overall yields based on the bis-azlactone **10** are presented in Table 2.

12 a, Ar = Ph (POPOP) : found, C, 78.93 ; H, 4.38. Calcd. for $C_{24}H_{16}N_2O_2$:C, 78.93 ; H, 4.35 %.

12 b, Ar = *p*-tolyl : found, C, 79.14 ; H, 5.43. Calcd. for $C_{26}H_{20}N_2O_2$:C, 79.57 ; H, 5.14 %.

12 c, Ar = 2,5-dimethylphenyl : found, C, 79.40 ; H, 5.73. Calcd. for $C_{28}H_{24}N_2O_2$:C 79.97 ; H, 5.75 %.

ACKNOWLEDGEMENTS. Thanks are expressed to Drs. M. D. Gheorghiu and F. Chiraleu for the ^{1}H–NMR spectra and to Mrs. Todan for the IR spectra.

REFERENCES

[1] Preceding part in the series (which had a shorter name, "Aminoketone Synthesis") : A. T. Balaban, L. Bîrlădeanu, I. Bally, P. T. Frangopol, M. Mocanu and Z. Simon, *Tetrahedron*, **19**, 2199 (1963).

[2] A. T. Balaban, I. Bally, P. T. Frangopol, M. Băcescu, E. Ciorănescu and L. Bîrlădeanu, *Tetrahedron*, **19**, 169 (1963) ; E. Ciorănescu, L. Birlădeanu, A. T. Balaban and P. T. Frangopol, *Rev. Chim. Acad. R. P. Roumaine*, **7**, 755 (1962) ; P. T. Frangopol, A. T. Balaban, L. Bîrlădeanu and E. Ciorănescu, *Tetrahedron*, **16**, 59 (1961) ; E. Ciorănescu and L. Bîrlădeanu, *Izvest. Akad. Nauk. S.S.S.R. Otdel. Khim. Nauk*, **1961**, 149.

[3] R. Lakhan and B. Ternai, *Adv. Heterocyclic Chem.*, **17**, 100 (1974).

[4] C. S. Cleaver and B. C. Pratt, *J. Amer. Chem. Soc.*, **77**, 1544 (1955).

[5] M. P. Demchenko, *Teor. Eksper. Khim. Akad. Nauk. Ukr. S.S.R.*, **1**, 408 (1965) ; *Chem. Abstr.*, **63**, 13004 a (1965).

[6] P. Carré and D. Liebermann, *Compt. rend.*, **199**, 1422 (1934).

[7] F. N. Hayes, B. S. Rogers and D. G. Ott, *J. Amer. Chem. Soc.*, **77**, 1850 (1955).

[8] D. L. Dhane, K. A. Noras and A. U. Mushrif, *Indian J. Chem.*, **13**, 858 (1975) ; *Chem. Abstr.*, **83**, 206143 (1975).

[9] S. D. Paul, D. L. Dhane, K. A. Noras and A. U. Mushrif, *Indian J. Chem.*, **49**, 579 (1972) ; *Chem. Abstr.*, **77**, 114285 (1972).

[10] N. A. Adrova and M. M. Kota, *Izvest. Akad. Nauk. S.S.S.R., Otdel. Khim. Nauk.*, **1957**, 758.

[11] G. Vasvari, *Magy. Tud. Akad. Kozp. Kem. Kutato Int. Kozlemeny*, No. 8, 123 (1966) ; *Chem. Abstr.*, **65**, 3198 (1966).

[12] D. Walker and T. D. Waugh, *J. Heterocyclic Chem.*, **1**, 72 (1964).

Revue Roumaine de Chimie, 27, 11—12, 1131—1139(1982)

SYNTHESIS OF PHARMACOLOGICALLY ACTIVE BENZIMIDAZOLES

MANOHAR V. KULKARNI and VEMANNA D. PATIL
Department of Chemistry, Karnatak University, Dharwad—580003
India

Received July 30, 1980

Halonitrobenzenes and 4-bromomethyl coumarins have reacted with 5,6-dimethyl-2-mercaptobenzimidazole to yield the sulfides. Various 2-benzimidazolylmercaptoacetohydrazones have been synthesised and their antimicrobial properties have been reported. 2-Arylidene and 2-heteroarylidene 6,7-dimethyl benzimidazothiazol-3-(2H)-ones have been synthesised and their mass spectral fragmentation pattern has been discussed.

The presence in vitamin B_{12} and its purine antagonistic nature have made the 5,6-dimethylbenzimidazole moiety the most prominent amongst the innumerable imidazole derivatives of biological significance. 2-Alkylsulfides and 2-arylnitrosulfides of benzimidazole are well known for their fungicidal activity.[1,2] Recently Budeanu et al.[3] reported the cytostatic action of benzimidazole-2-mercaptoacetohydrazide and hydrazones on experimental tumors. 2-Arylidene benzimidazolothiazoles have been reported to possess antimicrobial[4] and anticonvulsant[5] properties.

The above observations prompted the synthesis of some physiologically important analogues of these compounds by introducing the 5,6-dimethylbenzimidazole moiety as potential fungicides and bactericides.

CHEMISTRY

5,6-Dimethyl-2-mercaptobenzimidazole (I)[6,7] reacted with halonitrobenzenes in refluxing alcohol in the presence of sodium hydroxide and the resulting sulfides (II) were obtained in good yields and are described with their analytical data in table 1. Heterocyclic sulfides (III) were prepared by the reaction of (I) with 4-bromomethylcoumarins,[8-10] in dry dioxan and are represented with their analytical and IR spectral data in table 2. These reactions are given under Scheme A.

The mercaptoacetic ester (IVa) obtained by the reaction of (I) with chloroethylacetate was not isolated and the resulting solution was directly treated with hydrazine hydrate to get the hydrazide (IVb). The hydrazones (IV) were obtained easily in refluxing ethanol by condensation with aldehydes, and are represented with their physical constants and IR data in table 3.

2-Arylidene and 2-heterarylidene-6,7-dimethyl benzimidazolthiazole 3-(2H)-ones (V) were prepared according to the method of Chaudhary et al.[4] The analytical and IR spectral data of compounds (IV) are represented in table 4. The reactions are shown in Scheme B.

TABLE 1

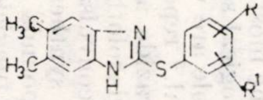

R	R^1	M.P.°C	Yield %	Formula	Analysis					
					Required			Found		
					C	H	N	C	H	N
2′-Nitro	4′-Nitro	154–5	82	$C_{15}H_{12}N_4O_4S$	52.32	3.48	16.27	52.14	3.31	16.51
2′-Nitro	H	245–6	75	$C_{15}H_{13}N_3O_2S$	60.20	4.34	14.04	60.04	4.20	13.84
4′-Nitro	2′-Chloro	210	79	$C_{15}H_{12}N_3ClO_2S$	53.97	3.59	12.59	53.71	3.40	12.71
2′-Nitro	4′-Chloro	300	80	$C_{15}H_{12}N_3ClO_2S$	53.97	3.59	12.59	53.69	3.24	12.29
2′-Nitro	4′-Methyl	107	75	$C_{16}H_{15}N_3O_2S$	61.34	4.79	13.41	61.02	4.61	13.21

IR spectra (KBr) showed : 3390–3420 (N–H) ; 1600–1620 (C=N) ; 1520–1580 (C=C) cm^{-1} bands.

TABLE 2

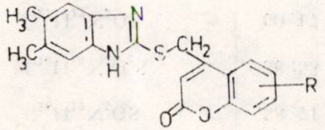

R	M.P.°C	Yield %	Formula	Analysis Required C	H	N	Found C	H	N	IR spectra (Nujol) N−H	C=O
6′-Methyl	207[a]	65	$C_{20}H_{18}N_2O_2S$	68.57	5.14	8.00	68.25	4.74	7.74	3263	1700
7′-Methyl	141−2[b]	70	$C_{20}H_{18}N_2O_2S$	68.57	5.14	8.00	68.84	5.31	8.24	3420	1700
6′-Methoxy	230[a] (dec)	72	$C_{20}H_{18}N_2O_3S$	65.57	4.91	7.65	65.24	4.61	7.42	3375	1705
7′-Methoxy	170−1[b]	71	$C_{20}H_{18}N_2O_3S$	65.57	4.91	7.65	65.24	4.70	7.82	3350	1700
6′-Chloro	250[c]	68	$C_{19}H_{15}N_2ClO_2S$	61.53	4.04	7.55	61.31	3.81	7.39	3360	1705
7′-Chloro	258[a]	73	$C_{19}H_{15}N_2ClO_2S$	61.53	4.04	7.55	61.81	3.73	7.24	3400	1705

a = ethanol or aqueous ethanol ; b = benzene ; c = acetic acid

TABLE 3

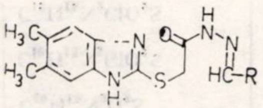

R	M.P.°C	Yield %	Formula	Analysis					
				Required			Found		
				C	H	N	C	H	N
Phenyl	258–9	80	$C_{18}H_{18}N_4OS$	63.90	5.32	16.56	63.71	5.14	16.41
Anisyl	243	75	$C_{19}H_{20}N_4O_2S$	61.95	5.43	15.21	61.64	5.33	15.04
Salicyl	269–70	76	$C_{18}H_{18}N_4O_2S$	61.01	5.08	15.81	60.94	5.29	15.98
Cinnamyl	255	72	$C_{20}H_{20}N_4OS$	65.93	5.49	15.38	65.61	5.64	15.79
2-Pyrryl	225	73	$C_{16}H_{17}N_5OS$	58.71	5.19	21.40	58.50	5.04	21.12
2-Furyl	235 (dec)	79	$C_{16}H_{16}N_4O_2S$	58.53	4.87	17.07	58.34	4.65	17.34
3-Pyridyl	293	75	$C_{17}H_{17}N_5OS$	60.17	5.01	20.64	59.94	5.34	20.31

IR spectra : (KBr) showed 3385–3420 (N–H), 1680–1710 (C=0) ; 1600–1620 (C=N) 1580–1520 (C=C) cm^{-1} bands

TABLE 4

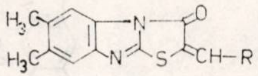

R	M.P.°C	Yield %	Formula	Analysis						IR (Nujol) cm^{-1}	
				Required			Found				
				C	H	N	C	H	N	C = O	C = N
p-Tolyl	270	80	$C_{19}H_{16}N_2OS$	71 .25	5 .00	8 .75	70 .92	4 .82	8 .51	1710	1620
p-Nitro-phenyl	300	82	$C_{18}H_{13}N_3O_3S$	61 .53	3 .70	11 .96	61 .34	3 .51	11 .63	1710	1605
Cinnamyl	242−4	79	$C_{20}H_{16}N_2OS$	72 .28	4 .81	8 .43	72 .04	4 .64	8 .19	1700	1600
3-Pyridyl	270	75	$C_{17}H_{13}N_3OS$	66 .44	4 .23	13 .68	66 .18	4 .02	13 .34	1720	1590
4-Pyridyl	300	70	$C_{17}H_{13}N_3OS$	66 .44	4 .23	13 .68	66 .24	4 .18	13 .48	1715	1600
2-Furyl	248−9	72	$C_{16}H_{12}N_2O_2S$	64 .86	4 .05	9 .46	64 .61	3 .75	9 .21	1715	1610

In the case of arylnitrosulfides (II) and the hydrazones (IV) the characteristic IR absorption bands are mentioned at the bottom of each table.

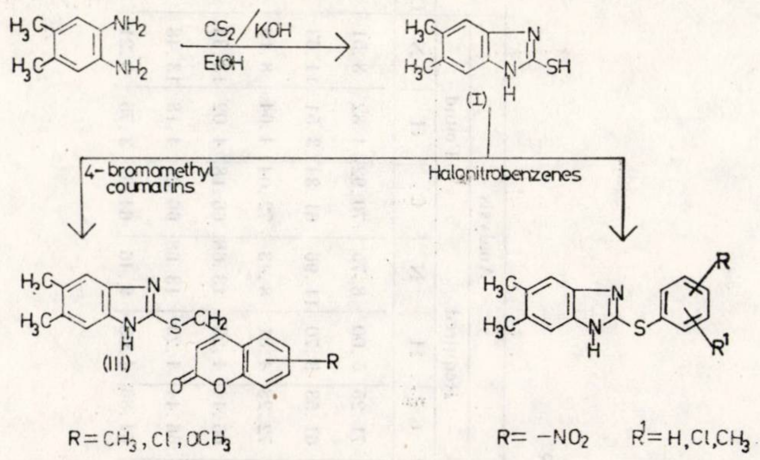
CS2 / KOH
EtOH
(I)
4-bromomethyl coumarins
Halonitrobenzenes
(III)
R = CH3, Cl, OCH3
R = -NO2
R1 = H, Cl, CH3

Scheme-A

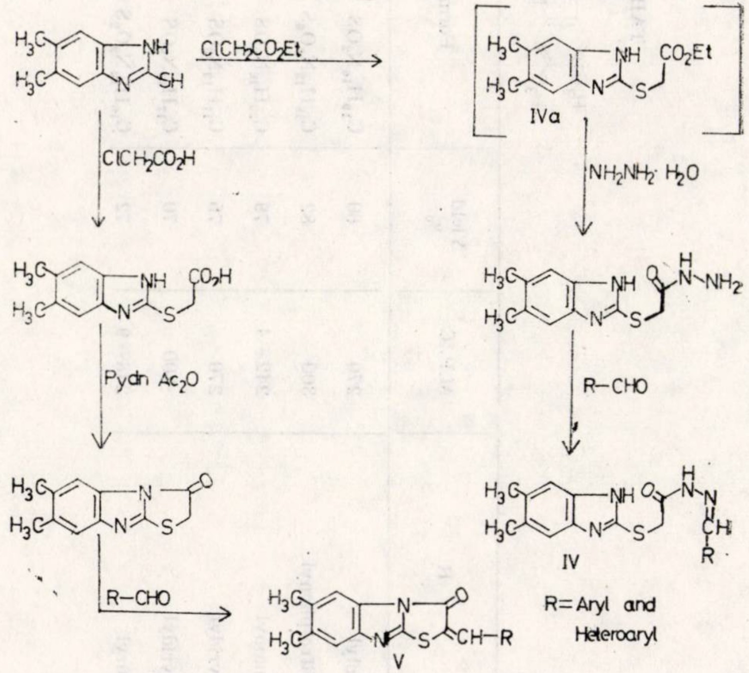
ClCH2CO2Et
IVa
ClCH2CO2H
NH2NH2·H2O
Pydn Ac2O
R-CHO
R-CHO
IV
V
R = Aryl and Heteroaryl

Scheme-B

The mass spectrum of compounds (V) where Ar = Ph, exhibited the molecular ion $M^{+\cdot}$ as the base peak. The expected peaks due to $M+2$, $M+1$, ions and to $M-H$, $M-CH_2$, $M-CO$, $M-(H+CO)$ and $M-(CO+CH_3)$ fragmentations were observed at m/e values 308, 307, 305, 291, 278, 277 and 263 respectively, which can be seen in the bar graph. The other fragmentations are given in scheme 1.

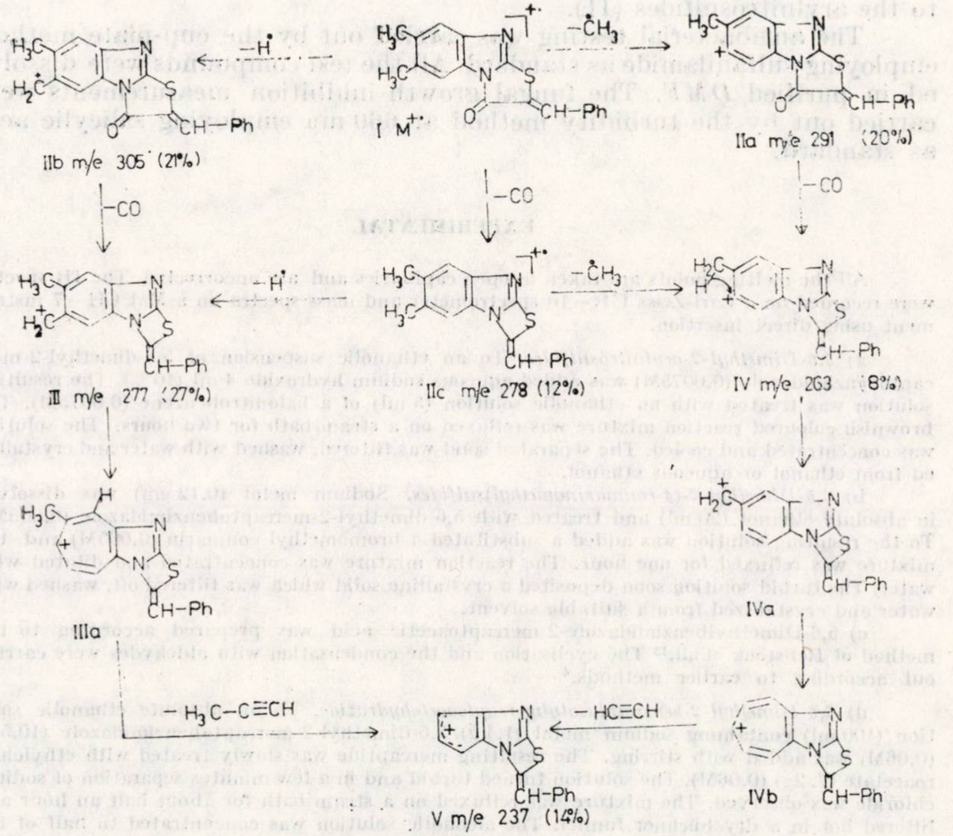
IIb m/e 305 (21%)
−H·
$M^{+\cdot}$
−ĊH₃
IIa m/e 291 (20%)
−CO
−CO
−CO
III m/e 277 (27%)
−H·
IIc m/e 278 (12%)
−ĊH₃
IV m/e 263 (8%)
IVa
IIIa
−H₃C−C≡CH
−HC≡CH
V m/e 237 (14%)
IVb
CH−Ph

The molecular ion $M^{+\cdot}$ can break up in three ways to give the daughter ions IIa, IIb and IIc by the loss of methyl radical, hydrogen radical and a molecule of carbon monoxide respectively.

The ions IIc and IIa may eliminate a methyl radical and carbon monoxide molecule respectively resulting in the even-electron ion IV. On the other hand the ion IIc may lose a hydrogen radical to give the ion III which after ring expansion [11] and elimination of a methyl acetylene molecule ends up in ion V. The ion IV undergoes hybride ion transfer resulting in the ion IVa which can undergo similar ring expansion to give IVb which eliminates a molecule of acetylene to end up in ion V.

SCREENING RESULTS

ANTIMICROBIAL ACTIVITY

All the compounds synthesised during the present investigation were screened for antimicrobial activity against *S. aureus*, *E. coli*. *A. niger* and *C. albicans*. Amongst the test compounds the hydrazide IVa was more active against *A. niger* than the hydrazones IV. Introduction of the coumarin moiety did not enhance the antimicrobial activity compared to the arylnitrosulfides (II).

The antibacterial testing was carried out by the cup-plate method employing sulfanilamide as standard. All the test compounds were dissolved in purified *DMF*. The fungal growth inhibition measurements were carried out by the turbidity method at 660 mμ employing salicylic acid as standard.

EXPERIMENTAL

All the melting points are taken in open capillaries and are uncorrected. The IR spectra were recorded on a Carl-Zeiss UR—10 spectrometer and mass spectra on a Mat CH—7 instrument using direct insertion.

a) *5,6-Dimethyl-2-arylnitrosulfides.* To an ethanolic suspension of 5,6-dimethyl-2-mercaptobenzimidazole (0.0075M) was added aqueous sodium hydroxide 4 ml (10%). The resulting solution was treated with an ethanolic solution (5 ml) of a halonitrobenzene (0.0075M). The brownish coloured reaction mixture was refluxed on a steam bath for two hours. The solution was concentrated and cooled. The separated solid was filtered, washed with water and crystallised from ethanol or aqueous ethanol.

b) *5,6-Dimethyl-2-(4-coumarinomethyl)sulfides.* Sodium metal (0.12 gm) was dissolved in absolute ethanol (20 ml) and treated with 5,6-dimethyl-2-mercaptobenzimidazole (0.005M). To the resulting solution was added a substituted 4-bromomethyl coumarin (0.005M) and the mixture was refluxed for one hour. The reaction mixture was concentrated and diluted with water. The turbid solution soon deposited a crystalline solid which was filtered off, washed with water and crystallized from a suitable solvent.

c) 5,6-Dimethylbenzimidazole-2-mercaptoacetic acid was prepared according to the method of Rebstock et all.[12] The cyclisation and the condensation with aldehydes were carried out according to earlier methods.[4]

d) *5,6-Dimethyl-2-benzimidazolylmercaptoacetohydrazide.* To an absolute ethanolic solution (100 ml) containing sodium metal (1.4 g) 5,6-dimethyl-2-mercaptobenzimidazole (10.5 g) (0.06M) was added with stirring. The resulting mercaptide was slowly treated with ethylchloroacetate (7. 2g) (0.06M). The solution turned turbid and in a few minutes separation of sodium chloride was observed. The mixture was refluxed on a steam bath for about half an hour and filtered hot in a dry büchner funnel. The alcoholic solution was concentrated to half of the original volume and hydrazine hydrate 15 ml (0.3M) was added, and the solution refluxed for twenty hours on a steam bath and cooled in ice. The separated solid was filtered off, washed with water and recrystallised from alcohol, m.p. 199°C. Yield 9 gms (60%).

Found : C, 52.64 ; H, 5.39 ; N, 22.30 ; $C_{11}H_{14}N_4OS$,

requires : C, 52.80 ; H, 5.60 ; N, 22.40.

The spectrum (Nujol) showed 1690 ($>C=0$) : 1620 ($C=N$) ;

3350—3400 (NH) cm^{-1} bands.

e) *5,6-Dimethyl-2-benzimidazolylmercaptoacetohydrazones.* To an ethanolic solution of 5,6-dimethyl-2-benzimidazolylmercaptoacetohydrazide (0.005M) (1.25 g), was added an aromatic aldehyde (0.006M) and the mixture refluxed on a steam bath for three hours. The solution was filtered hot from the suspended impurities, concentrated and cooled. The separated solid was filtered off, washed with water (100 ml) and crystallised from alcohol.

ACKNOWLEDGEMENTS. We thank Prof. E. S. Jayadevappa, Head of the Department of Chemistry, for his encouragement and Sri. V. A. Desai for microanalysis. One of us (M.V.K) thanks UGC, New Delhi for a Junior Research Fellowship.

REFERENCES

[1] S. Nakajima, I. Tanaka, T. Seki and T. Anmo, *Yakugakuzasshi*, **78**, 1378 (1958); *Chem. Abstr.*, **53**, 8124 (1959).

[2] S. P. Gupta and Rani, *J. Indian Chem. Soc.*, **54**, 478 (1977).

[3] C. H. Budeanu, G. Rusu, Z. Cojocaru and C. Nistor, *Rev. Med. Chir.*, **80**, 605 (1976); *Chem. Abstr.*, **87**, 102330 (1976).

[4] H. S. Chaudhary, C. S. Panda and H. K. Pujari, *Indian J. Chem.*, **8**, 10 (1970).

[5] S. P. Singh, S. S. Parmar and B. R. Pandey, *J. Heterocyclic Chem.*, **14**, 1093 (1977).

[6] J. A. Van. Allan and B. D. Deacon, *Coll. Org. Synth.*, **4**, 569 (1963).

[7] K. Takatori, Y. Yamada and G. Kawashima, *J. Pharm. Soc., Japan*, **75**, 881 (1955); *Chem. Abstr.*, **50**, 49209 (1956).

[8] Y. S. Agasimundin and S. Siddappa, *J. Kar. Univ. Sci.*, **15**, 1 (1970).

[9] B. B. Dey and K. Radhabai, *J. Indian Chem. Soc.*, **11**, 635 (1934).

[10] M. V. Kulkarni and V. D. Patil, *Arch. Pharm.* (Weinheim) Communicated.

[11] S. O. Lawesson, G. Schroll, J. H. Bowie and R. G. Cooks, *Tetrahedron*, **24**, 1875 (1968).

[12] T. L. Rebstock, C. D. Ball, C. L. Hammer and H. M. Sell, *J. Amer. Chem. Soc.*, **78**, 5831 (1956).

Revue Roumaine de Chimie, 27, *11–12*, 1141–1150(1982)

BEITRÄGE ZUM KINETISCH-ANALYTISCHEN STUDIUM ÜBER DIE BESTIMMUNG VON CN^--SPUREN AUF GRUND DER HEMMUNGSWIRKUNG

GH. IONESCU, F. MATEI und AL. DUCA
Technische Hochschule „Gheorghe Asachi“ Iassy, Fakultät für Chemische Technologie, Splai Bahlui stînga 71, Rumänien

Eingegangen am 24. Januar 1981

Die Hemmwirkung von CN^- auf die katalytische Funktion der Ag^+-und Co^{2+}-Ionen in den Umsetzungen Sulfanilsäure-$S_2O_8^{2-}$-Äthylendiamin bzw. Gallussäure-Sauerstoff wurde theoretisch mit der Reaktionsgeschwindigkeit in Wechselbeziehung gebracht. Bei Vergleich der von den Verfassern erhaltenen Versuchsergebnisse wurde die theoretische Gleichung überprüft, welche die Konstante die Reaktionsgeschwindigkeit mit der Hemmstoffkonzentration in Beziehung bringt. Die Bedingung der Geradlinigkeit dieser Gleichung stellt ein Kriterium vor, die Zusammensetzung des stabilen Komplexes Katalysator/Hemmstoff zu bestimmen. Gleichzeitig bedeutet die Beziehung Geschwindigkeitskonstante-Hemmstoffkonzentration eine nützliche und bequeme Eichfunction für die Hemmstoffanalyse mittels der kinetischen Methode, welche die angefülnten katalytischen Reaktionen verwendet.

The inhibitory effect of CN^--ion *versus* catalytic action of Ag^+-and Co^{2+}-ions in sulphanylic acid-$S_2O_8^{2-}$-ethylenediamine and gallic acid—oxygen reactions was theoretically correlated with reaction rate. Using the experimental data obtained by the authors, the theoretical equation which correlates the reaction rate constant with the inhibitor concentration was verified. The linearity condition of this equation shows a typical criterion of establishing the stable complex composition of the cytalyst/inhibitor type. Simultaneously, the previous equation represents a useful and convenient calibration function in order to analyse the inhibitor kinetically, using the specified catalytic reactions.

1. EINFÜHRUNG

Die qualitative und quantitative Analyse geringer Konzentrationen von CN^--Ionen (Spurenmengen) ist von besonderer Bedeutung für die Bestimung des Grades der Verunreinigung von Wasser mit einfachen oder komplexen Zyaniden sowie des Luftraums durch sowohl Zyanwasserstoff.

Wegen der ausservordentlichen Giftigkeit sowohl des Zyanions wie auch des Zyanwasserstoffs sind in den Standardbestimmungen der verschiedenen Länder sehr niedrige zulässige Grenzwerte in Luft, Wasser oder Nahrungsmitteln vorgesehen. So z.B. empfichlt die Weltorganisation für das Gesundheitswesen[1] dass Haushaltswasser nicht mehr als 0,01 p.p.m.CN^- enthalten soll; der Luftraum darf in den Vereinigten Staaten von Amerika[2] höchstens 10 p.p.m. enthalten, u.s.f. In der S. R. Rumänien beträgt die zulässige Höchstkonzentration in Wasser 0,01 mg CN^-/l und in Luft 10 mg HCN/m^3.[3-4]

Solche sehr geringe Konzentrationen (Spuren) beanspruchen sehr empfindliche Teste zur Entdeckung und Bestimmung von Zyan. Die Hauptmenge dieser Teste ist in den folgenden Klassen eingeordnet :[5] massanalytische Methoden, polarographische Methoden, Gaschromatographie, kinetische Methoden.

Der Hemmungseffekt des CN^--Ions, der sich in gewissen von Metallionen katalysierten Umsetzungen bekundet,[6-9] liegt seiner Analyse mittels der kinetischen Methode zugrunde. Andere Effekte des Zyanions, die für seine Bestimmung durch die kinetische Methode verwentbar erscheinen, sind : der katalytische Effekt,[10-11] der aktivierende Effekt[12] sowie der Modifizierungseffekt von katalytischen Polarographieströmen.[13-14]

In die vorliegenden Arbeit werden die Verfasser einige Versuchsergebnisse über die Bestimmung des CN^--Ions mittels der kinetischen Methode interpretieren, wobei der Hemmungseffekt dieses letztern auf die Indikatorreaktionen zugrunde wurde : Sulfanilsäure-$S_2O_8^{2-}$-Äthylendiamin-Ag^+[7] und Co^{2+}-O_2-Gallussäure.[9,15]

2. THEORETISCHER TEIL

Die Metallionen Co^{2+} und Ag^+ bilden mit dem Liganden CN^- besonders stabile Komplexverbindungen,[16] wobei die Stabilitätskonstante des Co^{2+}/CN^--Komplexes von der Ordnung 10^{19}, jene des Ag^+/CN^--Komplexes von der Ordnung 10^{21} sind. Demgemäss werden die katalytische Einwirkung des Co^{2+}-Ions auf die Selbsoxydierung der Gallussäure und die des Ag^+-Ions auf die Oxydation von Sulfanilsäure mit Persulfaten in Gegenwart des CN^--Ions fühlbar verringert sein, da dieses einen denflichen Hemmungseffekt aufweist, insoweit die mit den zwei Metallionen gebildeten Komplexe katalytisch wirkungslos sind.

Um die Versuchsergebnisse über diesen Hemmungseffekt kinetisch zu interpretieren,[7,9] bezeichnet man mit „X" die Konzentration des Oxydationsproduktes des organischen Reaktanten (Sulfanilsaüre, Gallussäure), die Geschwindigkeit der katalysierten Reaktion (Sulfanilsäure-$S_2O_8^{2-}$-Äthylendiamin-Ag^+ ; Gallussäure-Sauerstoff-Co^{2+}) kann in folgender Form beschrieben werden :

$$\frac{\mathrm{d}X}{\mathrm{d}t} = [k_0 + k_c \cdot c_0(\mathrm{M}^{m+})] \cdot c(R) \qquad (1)$$

(hier sind : $\mathrm{d}X/\mathrm{d}t$ = Reaktionsgeschwindigkeit ; k_0 = spezifische Geschwindigkeit der nichtkatalysierten Reaktion ; k_c = spezifische Geschwindigkeit der katalysierten Reaktion ; $c_0(\mathrm{M}^{m+})$ = Gesamtkonzentration des Katalysator-Ions mit der Aufladung „$m+$" ; $c(R)$ = Konzentration des organischen Reaktanten in der Zeit „t".

Durch die Reaktion

$$\mathrm{M}^{m+} + n\mathrm{CN}^- = [\mathrm{M}(\mathrm{CN}^-)_n]^{m-n} \qquad (2)$$

wird ein Komplex gebildet, in welchem das Katalysator-Ion gebunden ist. Die Hemmwirkung des CN^--Ions, welches das Katalysator-Ion im katalytisch unwirksamen Komplex bindet, wird die Reaktionsgeschwindigkeit mit einem der Konzentration des im Komplex gebundenen Katalysator-Ions entsprechenden Term verringern. Die Stabilitätskonstante ist:

$$\beta = \frac{c(K)}{c(M) \cdot c^n(CN^-)} \tag{3}$$

In der Gleichung (3) sind $c(K)$, $c(M)$ und $c(CN^-)$ die Gleichgewichtskonzentrationen des Komplexes, des Katalysators bzw. des Hemmungsfaktors. Die Reaktionsordnung des Katalysators aus dem Komplex sei gleich 1, wie auch die Reaktionsordnung des freien Katalysators. Folglich wird die Gesamtgeschwindigkeit der Reaktion bei gleichzeitiger Anwesenheit des Katalisators und des Hemmungsfaktors folgendermassen auszudrücken sein,

$$\frac{dX}{dt} = [k_0 + k_c \cdot c_0(M^{m+}) - k_i' \cdot c(K)] \cdot c(R) \tag{4}$$

wobei k_i' = spezifische Geschwindigkeit, die der Hemmwirkung des CN^--Ions entspricht.

Eerhellt aus Gleichung (3) die Konzentration des Komplexes und aus der Bilanzformel des Katalysators ergibt sich die Konzentration des Katalysators:

$$c(K) = \beta \cdot c(M^{m+}) \cdot c^n(CN^-) \tag{5}$$

$$c(M^{m+}) = c_0(M^{m+}) - c(K) \tag{6}$$

Auf Grund der Umsetzung (2) kann die Katalysatorkonzentration auch durch die folgende Gleichung ausgedrückt werden:

$$c(M^{m+}) = \frac{c_0(CN^-) - c(CN^-)}{n} = c(K) \tag{7}$$

wobei $c_0(CN^-)$ die Gesamtkonzentration des Hemmungsfaktors vorstellt. Aus den Formeln (6) und (7) folgt,

$$c(M^{m+}) = c_0(M^{m+}) - \frac{c_0(CN^-)}{n} - \frac{c(CN^-)}{n} \tag{8}$$

und durch Kombination der Formeln (5) und (8) erhält man für die Komplexkonzentration:

$$c(K) = \beta \cdot c^n(CN^-) \cdot \left[c_0(M^{m+}) - \frac{c_0(CN^-)}{n} - \frac{c(CN^-)}{n} \right] \tag{9}$$

Durch die Substitution der Konzentration $c(K)$ aus Gleichung (9) in Gleichung (4) der Geschwindigkeit der gehemmten Reaktion, verwandelt sich die kinetische Formel, wie folgt :

$$\frac{\mathrm{d}X}{\mathrm{d}t} = \left\{k_0 + k_c \cdot c_0(\mathrm{M}^{m+}) - k_i' \cdot \beta \cdot c^n(\mathrm{CN}^-)\left[c_0(\mathrm{M}^{m+}) - \frac{c_0(\mathrm{CN}^-)}{n} + \frac{c(\mathrm{CN}^+)}{n}\right]\right\} \cdot c(R) \tag{10}$$

Nach Entwicklung der Klammernausdrücke in Formel (10) ergeben sich zwei Glieder folgender Form : $+k_i' \cdot \beta \cdot c^n(\mathrm{CN}^-) \cdot c_0(\mathrm{CN}^-)/n$ und $-k_i' \cdot \beta \cdot c_0^n(\mathrm{CN}^-) \cdot c(\mathrm{CN}^-)/n$. Da die Konzentration des Ions M^{m+} aus dem Verbande des Komplexes im Vergleiche mit der Gesamtkonzentration des Hemmungsfaktors gering ist, kann man die Annäherung anschreiben :

$$c(\mathrm{CN}^-) \cong c_0(\mathrm{CN}^-) \tag{11}$$

infolgedessen reduzieren die erwähnten Glieder einander.

Die Reaktionsgeschwindigkeit wird gleich dem Ausdrucke :

$$\frac{\mathrm{d}X}{\mathrm{d}t} = [k_0 + k_c \cdot c_0(\mathrm{M}^{m+}) - k_i' \cdot c_0^n(\mathrm{CN}^-)] \cdot c(\mathrm{R}) \tag{12}$$

wo $k_i = \beta \cdot k_i' \cdot c_0(\mathrm{M}^{m+})$.

Die katalytischen Indikatorreactionen erfordern kleine Konzentrationen des organischen Reaktanten R. Diese Eigentümlichkeit ist von Bedeutung, da die Anwendung der spektrophotometrischen Bestimmungsmethode der Reaktionsgeschwindigkeit das LAMBERT-BEER-Gesetz einbegrift ; dieses Gesetz ist im allgemeinen bei niedrigen Konzentrationen des photoabsorbierenden Stoffes (des Indikatorstoffes) gültig.

Wird das Oxydationsprodukt des Reaktanten R als Indikatorsubstanz angesehen, dann ist die Konzentration „X“ derselben mit der Absorbanz „A“ der Lösung in Wechsebeziehung und zwar gemäss der Formel : $A = \varepsilon \cdot b \cdot X$, ($b$ = Kuvettenstärke). Die Gültigkeit dieser Beziehung bedinkt folgende Substitutionen : $\mathrm{d}X/\mathrm{d}t = \mathrm{d}A/\varepsilon \cdot b$; $c(R) = c_0(R) - X = c_0(R) - A/\varepsilon \cdot b$. So erhält die Gleichung (12) folgende Form :

$$\frac{\mathrm{d}A}{\mathrm{d}t} = [k_0 + k_c \cdot c_0(\mathrm{M}^{m+}) - k_i \cdot c_0^n(\mathrm{CN}^-)] \cdot [\varepsilon \cdot b \cdot c_0(R) - A] \tag{13}$$

Die Höchstkonzentration des Oxydationsproduktes wird durch $X_{\max} = c_0(R)$ ausgedrückt ; die Formel $\varepsilon \cdot b \cdot c_0(R)$ stellt die Höchstabsorbanz der Lösung vor ($A_{\max}$). Führt man diese Notierung in die Gleichung (13) in, so erhält man :

$$\frac{\mathrm{d}A}{\mathrm{d}t} = [k_0 + k_c \cdot c_0(M^{m+}) - k_i \cdot c_0^n(\mathrm{CN}^-)] \cdot (A_{\max} - A) \tag{14}$$

Die experimentelle kinetische Gleichung hat die Form :

$$\frac{dA}{dt} = k_{\exp}(A_{\max} - A) \qquad (15)$$

Vergleicht man Gleichungen (14) und (15), so ergibt sich für $k_{\exp}$ der Ausdruck :

$$k_{\exp} = k_0 + k_c \cdot c_0(\mathrm{M}^{m+}) - k_i \cdot c_0^n(\mathrm{CN}^-) \qquad (16)$$

Den Wert der Grösse $k_{\exp}$ kann man durch die Interpretation der Versuchsergebnisse Absorbanz (A) – Zeit (t) erhalten. In diesem Zweck erhält man die integrale kinetische Gleichung durch Integration der Formel (14) in folgender Weise :

$$\frac{dA}{A_{\max} - A} = k_{\exp} \cdot dt$$

$$\ln(A_{\max} - A) = \ln A_{\max} - k_{\exp} \cdot t \qquad (17)$$

In der Gleichung (17) stellt $k_{\exp}$ die Neigung der Geraden in den Koordonaten $\ln(A_{\max} - A)$ und t vor.

Vom Standpunkte der kinetischen Analyse des Hemmungsfaktor Gleichung (16) ergibt sich, dass die Grösse $k_{\exp}$ eine Funktion der Gesamtkonzentration desselben ist. Der Grad „n" der Funktion hängt von der Zusammensetzung des stabilen Komplexes ab, welcher sich aus dem Katalysator und dem Hemmungsfaktor bildet. Die Hauptfaktoren, welche diese Zusammensetzung bestimmen, sind : Oxydationsstufe, durchmesser und elektronischer Aufbau des Katalysator-Ions und des Liganden, Natur des Reaktionsmediums (pH, Ionenstärke, Dipolmoment, Dielektrizitätskonstante), sowie Anwesenheit anderer Liganden.[17] Folglich kann „*n*" sogar für dasselbe Ionenpaar Katalysator-Ligand variieren.

Die Zahlenmässige Bestimmung dieser Grösse bildet ein verhältnismässig schwieriges Problem. Die Gleichung (16) bietet ein Kriterium für die Bestimmung aus kinetischen Versuchsergebnissen. Gemäss dieser Gleichung soll die Funktion $k_{\exp} - c_0^n(\mathrm{CN}^-)$ geradlinig verlaufen. Nimmt man für „*n*" verschiedene Werte an, wird man also als korrekten Wert jenen Wert auswöhlen, welcher der Bedingung der Geradlinigkeit der spezifizierten theoretischen Funktion entspricht.

Das Volumen der Berechnungen, die von diesem kinetischen Bestimmungskriterium der Zusammensetzung des Katalysator-Hemmungsfaktor-Komplexes erfordet wird, bildet heutzutage kein Hindernis, da di notwendigen Berechnungen an der Rechenmaschine programiert werden können. Ausserdem kann „*n*" nur gange und positive Werte im Bereiche (0 . . . 6) zulassen ; Bruchzahlen, negative Werte oder Werte über 6 sind physikalisch sinnlos.

3. VERSUCHSERGEBNISSE UND DISKUSSION

Zur Überprüfung der Übereinstimmung zwschen Theorie und Erfahrung verwendeten die Verfasser die Redox-Indikator-Reaktion : Sulfanilsäure-$S_2O_8^{2-}$-Äthylendiamin-Ag^+—CN^- und Gallussäure—O_2—Co^{2+}-CN^-.[7,9,15]

3.1. DIE UMSETZUNG Ss-$S_2O_8^{2-}$-ÄTHYLENDIAMIN (ÄN)—Ag^+—CN^-

Die für den Ablauf der katalytischen Umsetzung nötigen Optimalbedingungen Ss—$S_2O_8^{2-}$—Än—Ag^+ wurden im Fachschriftum veröfentlicht.[7,18] Diese Bedingungen wären : pH=9.4 ; $c(Ss)=2.10^{-3}M$; $c(S_2O_8^{2-})=2,5\cdot 10^{-2}$ M und c(Än) = $7,8,10^{-4}$M.

Die Hemmungswirkung des CN^--Ions wurde spektrophotometrisch untersucht, wobei die Absorbanz des Reaktionsmediums und die dem Oxydationsprodukt der Supfanilsäure zukommende Absorbanz gemessen wurden. Demgamäss kamen zu den angeführten Optimalbedingungen noch die folgenden : $\lambda = 324$ nm ; Kuvettenstärke $(b) = 1$ cm ; 25°C. Die Primären Versuchsergebnisse, Absorbanz-Reaktionsdauer, sind auf Tab. 1 für eine konstante Katalysatorkonzentration $c(Ag^+) = 5.10^{-7}M$ (54 ng/cm^3) und bei verschiedenen Hemmstoffkonzentrationen dargestellt.

Die Versuchsergebnisse aus Tab. 1, graphisch in den Koordonaten, $\ln(A_{max} - A)$-Zeit, interpretiert führten zur Schlussfolgerung dass die theoretische Gleichung (17) befolgt ist. Die Neigung der erhaltenen Geraden stellt gemäss dieser Gleichung die kinetische Grösse k_{exp} vor. Die Werte derselben sind in Tab. 1 eingetragen. Mit Hilfe dieser Angaben und der entsprehenden Werte Hemmstoffkonzentration wurde der Wert des Exponenten „n" bestimmt, für den die Gleichung (16) eine geradlinige Funktion in den Koordonaten $k_{exp} - c_0^n(CN^-)$. Es wurde festgestellt, dass diese Bedingung für $n = 1$ gegeben ist, Bild 1. Was nun die Analyse des Hemmstoffes CN^- durch die kinetische Methode angeht, stellt diese geradlinige Funktion ein nützliches Eichdiagramm vor.

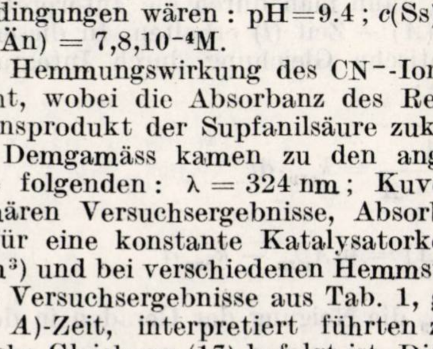

Bild 1 — Überprüfung der Geradlinigkeit der Funktion $k_{exp} - c_0^n(CN^-)$ für die Reaktion Ss—$S_2O_8^{2-}$—En—Ag^+—CN^-, $(n = 1)$.

Bei der statistischen Verarbeitung[19] der Angaben $k_{exp} - c_0^n(CN^-)$, die in Tab. 1 eingetragen sind, erhielt man die Gleichung der Eichcurve in folgender Form :

$$10^5 \cdot k_{exp} = 14,5 - 1,23 \cdot [10^7 \cdot c_0(CN^-)], s^{-1} \tag{18}$$

$(n = 5 ; P = 95\,\% ; s_0^2 = 0,174, s^2 ; \Delta a = 0,9, s^{-1} ; \Delta b = 0,18, 1/mol.s)$

TAB. 1

Versuchsergebnisse, Absorbanz-Zeit, über die Hemmwirkung von CN^- auf die Katalysatorwirkung von Ag^+ (*)

$10^7 \cdot c_0(CN^-)$, mol/l									
0,00		2,40		4,80		7,20		9,60	
τ, (s)	A	τ, (s)	A	τ, (s)	A	τ, (s)	A	τ, (s)	A
100	0,049	200	0,073	200	0,053	300	0,055	400	0,0385
200	0,096	300	0,109	400	0,104	500	0,104	700	0,068
300	0,142	400	0,143	600	0,154	700	0,127	900	0,085
400	0,186	500	0,177	800	0,201	900	0,162	1200	0,112
500	0,228	700	0,241	1000	0,246	1100	0,195	—	—
$k_{exp} = 14,9.10^{-5}s^{-1}$		$k_{exp} = 11,3.10^{-5}s^{-1}$		$k_{exp} = 8,10.10^{-5}s^{-1}$		$k_{exp} = 5,70.10^{-5}s^{-1}$		$k_{exp} = 2,92.10^{-5}s^{-1}$	

---

*) $A_{max} = 1,45$, für eine Konzentration von $2,0.10^{-3}$M des Reaktionsproduktes, welches durch vollständige Oxydation der Sulfanilsäure aus der Lösung erhalten wurde.

TAB. 2

Versuchsergebnisse, Absorbanz-Zeitdauer, über die Hemmwirkung von CN^- auf die katalytische Einwirkung von Co^{2+}(**).

$10^6 \cdot c_0(CN^-)$, mol/l									
0,00		6,385		9,115		10,961		13,615	
τ, (s)	A	τ, (s)	A	τ, (s)	A	τ, (s)	A	τ, (s)	A
36	0,250	45	0,250	50	0,250	60	0,250	35	0,200
49	0,300	54	0,300	65	0,300	76	0,300	93	0,250
58	0,350	67	0,350	78	0,350	95	0,350	116	0,300
72	0,400	83	0,400	98	0,400	118	0,400	142	0,350
87	0,450	100	0,450	117	0,450	142	0,450	178	0,400
$k_{exp} = 1,275.10^{-2}s^{-1}$		$k_{exp} = 1,08.10^{-2}s^{-1}$		$k_{exp} = 0,93.10^{-2}s^{-1}$		$k_{exp} = 0,78.10^{-2}s^{-1}$		$k_{exp} = 0,52.10^{-2}s^{-1}$	

(**) $A_{max}=0,675$, für eine Konzentration von $1,6.10^{-3}$M des Reaktionsproduktes, welches durch die vollständige Oxydation der Gallussäure aus der Lösungerhalten wurde.

3.2. DIE UMSETZUNG GALLUSSÄURE(Gs)$-O_2-Co^{2+}-CN^-$

Die günstigsten Bedingungen für die Abwicklung der katalytischen Reaction Gs$-O_2-Co^{2+}$ wurden von den Verfassern in einer früher voröffentlichten Arbeit[15] festgestelt und sind :pH=10,3 ; c(Gs) = 1,6.10^{-3}M. Das spektrophotometrische Studium der Reaktion wurde bei 20°C durchgeführt, wobei eine Küvette der Stärke b = 1 und eine Wellenlänge λ = 342 nm (Wellenlänge des ersten Absorptionsmaximums des Oxydationsproduktes de Gallussäure) angewendet wurden.

Die primären Versuchsergebnisse Absorbanz-Reaktionsdauer, sind in Tab. 2 vorgelegt. Es wurden eine konstante Konzentration des Katalysators, $c(Co^{2+})$ = 1,08.10^{-6}M (63,5 ng/cm^3) und verschiedene Konzentrationen des Hemmstoffes CN^- eingehalten.

Die Versuchsergebnisse aus Tab. 2 graphisch in den Koordonaten ln $(A_{max}-A)$-Zeit interpretiert, ergaben die Schlussfolgerung, dass die theoretische Gleichung (15) erfüllt ist. Die Grösse k_{exp} beschreibt die Neigung dieser Geraden und hat die in Tab. 2 eingetragenen Werte, die den verschiedenen Konzentrationen des Hemmstoffes entsprechen. Mit Hilfe dieser Angaben wurde der Exponent „n" aus der Gleichung (16) bestimmt, für welche die Funktion $k_{exp} - c_0^n(CN^-)$ eine Gerade vorstellt Gemäss. Bild 2 entspricht der Wert $n = 2$ der Bedingung der Geradlinigkeit der Funktion.

Die Gerade in den Koordonaten $k_{exp} - c_0^2(CN^-)$ kann bequem als Eichdiagramm für die CN^--Analyse mittels der kinetischen Methode verwendet werden. Die Gleichung dieser Geraden wurde durch die statistische Verarbeitung der Versuchsergebnisse[20] $k_{exp}-c_0(CN^-)$ aus Tab. 2 erhalten und hat die Form :

$$10^2 \cdot k_{exp} = 1{,}26 - 4{,}02 \cdot 10^{-3} \cdot [10^6 \cdot c_0(CN^-)]^2, \text{ s}^{-1} \qquad (19)$$

$$(n = 5 ; p = 95\,\% ; s_0^2 = 1{,}39.10^{-4}, \text{ s}^2 ; \Delta a = 3.10^{-2}, \text{ s}^{-1} ; \Delta b = 2{,}9.10^{-4}, \text{ l/mol.s})$$

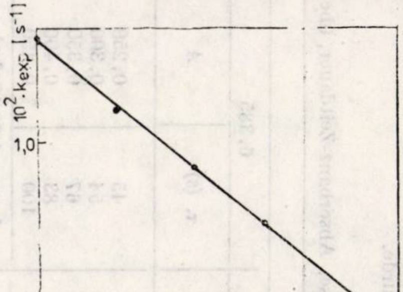

Bild 2 — Überprüfung der Geradlinigkeit der Funktion $k_{exp} - c_0^n(CN^-)$ für die reaktion Gs$-O_2-Co^{2+}-CN^-$, (n = 2).

3.3. ANWENDBARKEITS PRÜFUNG DER DURCH GLEICHUNG (11) ZUM AUSDRUCK GEBRACHTEN ANNÄHERUNG

Auf Grund der durch Gleichung (11) angegebener Annäherung wurden die aus der Entwicklung der Gleichung (10 ergebenen Termausdrücke $+k_i' \cdot \beta \cdot c_0(CN^-) \cdot c^n(CN^-)/n$ und $-k_i' \cdot \beta \cdot c_0^n(CN^-) \cdot c(CN^-)/n$ reduziert. Die

Reduzierung dieser Termausdrücke haben die Folgerung der Endgleichung (16) möglich gemacht.

Die in Paragraph 3.1 u. 3.2 dargestellte experimentelle Auslegung, führte zu den Werten 1 bzw. 2 für „n“. Für den Fall $n = 1$, sind die reduzierten Termausdrücke mathematisch vollkommen gleich. Für $n = 2$ muss der Aproximationsgrad festgelegt werden, d.h. das der maximale Wert der initialen Konzentration des CN^--Inhibitors festgestellt werden muss, wo aus praktischen Standpunkt, die Gleichung (16) noch zulässigen CN^--Bestimmungsfehler führt.

Zu diesem Zweck wurde die kinetische Grösse $10^2 \cdot k_{exp}$ der Indikatorreaktion Gallussäure (Gs)-Sauerstoff(O_2)$-Co^{2+}$ bei einigen Co^{2+} Konzentrationen unter dem Paragraph 3.2 angegebenen identischen Bedingungen, aber in Abwesenheit des CN^--Inhibitor bestimmt.

Da die Funktion $10^2.k_{exp} - c_0(Co^{2+})$ eine lineare Abhängigkeit darstellt wurde diese nachträglich zur Konzentrationbestimmung Co^{2+} Iones im katalitischen inaktiven Komplex Co^{2+}/CN^- angewandt, eine Bestimmung die zur Gewinnung der in Tab. 3 dargestellten Daten notwendig ist.

Aus Tab. 3 überprüften Daten geht hervor dass für ungefähr 1,5 eingetlichen Konzentrationsdekaden von CN^- die Annäherungen $c(CN^-) \cong c_0(CN^-)$ und $k_i' \cdot \beta \cdot c_0^2(CN^-) \cdot c(CN^-)/n \cong k_i' \cdot \beta \cdot c_0(CN^-) \cdot c^2(CN^-)$

TAB. 3

Zur Festlegung des Anwendungsgrades der Gleichung (11) notwendig Versuchsdaten und Berechnungen.

$10^6.c_0(Co^{2+})$, in Abwesenheit von CN^-, (M)	1,10	0,90	0,70	0,50	0,30
$10^2.k'_{exp}$, in Abwesenheit von CN^-, (s^{-1})	1,28	1,04	0,81	0,58	0,36
$10^6.c_0(CN^-)$, (M)	0,00	0,639	9,12	10,96	13,62
$10^2.k''_{exp}$*), in Gegenwart von CN^-, (s^{-1})	1,26	1,08	0,93	0,78	0,52
$10^6.c(Co^{2+})$**), frei, in Gegenwart von CN^-, (M)	1,06	0,94	0,81	0,67	0,445
$10^6.c(CN^-)$***) $= 2.10^6[c_0(Co^{2+}) - c(Co^{2+})]$, (M)	0,0	2,4	5,0	7,8	10,8
$10^6.c(CN^-)$****) $= 10^6[c_0(CN^-) - c(CN^-)]$, (M)	0,0	6,15	8,62	10,18	12,54
$\delta\% = 10^2[c_0(CN^-) - c(CN^-)]/c_0(CN^-)$	0,0	3,8	5,5	7,1	7,9
$A = 10^{16}.c_0(CN^-).c^2(CN^-),(M)^3$	0,0	2,41	6,77	11,36	21,39
$B = 10^{16}.c^2_0(CN^-).c(CN^-),(M)^3$	0,0	2,51	7,56	12,23	23,24
$\delta\% = 10^2(B - A)/B$	0,0	3,7	5,4	7,1	7,9

---

*) siehe Tab. 2 ; **) durch Interpolierung der Werte $10^2.k''_{exp}$ auf der Gerade $10^2.k''_{exp} - c_0(Co^{2+})$; ***) Konzentration des im Komplex Co^{2+}/CN^- gebundenen CN^- Iones für $n = 2$; ****) Konzentration der freien CN^- Iones.

mit einem maximal 8 %igem Fehler gültig sind. Dieser Fehler ist für eine Konzentrationsbestimmung in Grösse der Mikrogramme (μg) von CN^- in einem relativ komplexen kinetischen System wie die angewandte Indikator reaktion zulässig.

4. SCHLUSSFOLGERUNGEN

Die Hemmwirkung des CN^--Ions auf die katalytische Funktion von Ag^+ und Co^{2+} bei den Oxydierungsvorgängen Sulfanilsäure-$S_2O_8^{2-}$ bzw. Gallussäure-O_2 kann kinetisch mittels einer Gleichung der Form $k_{exp} = a - b \cdot c_0^n(CN^-)$ beschrieben werden. Die Grösse k_{exp} stellt die Neigung der Geraden in den Koordonaten $\ln(A_{max} - A)$ und Zeit vor. Aus der Bedingung der Geradlinigkeit der Funktion $k_{exp} - c_0^n(CN^-)$ lässt sich der Wert des Exponenten „n“ bestimmen, welcher die Anzahl der hemmenden Ionen angibt, die einem Katalysator-Ion im stabilen Komplex Katalysator-Hemmstoff zukommt.

Was die Analyse des Hemmstoffes CN^- mittels der kinetischen Methode betrifft, bedeuten die abgeleiteten liniaren Gleichungen (18) und (19) nützliche und bequeme Eichdiagramme.

LITERATUR

[1] World Health Organization, „International Standards for Drinking Water“, Geneva, 1958.
[2] M. B. Jakobs, „The Analytical Chemistry of Industrial Poisons, Hazards and Solvents”, Second Edition, Interscience Publishers Inc., New York, 1949.
[3] STAS 4706/1966.
[4] Normele M.I.Ch., 1974, p. 82.
[5] L. S. Bark u. H. G. Higson, *Analyt. Chem.*, **88**, 751 (1963).
[6] H. A. Mottola u. H. Freiser, *The Analyst*, **40**, 1266 (1968).
[7] Gh. Ionescu u. Al. Duca, *Bul. Inst. Politeh. Iași*, **21**, 25 (1975).
[8] Z. Gregorovicz u. T. Suwinska, *Chem. Analit.*, **19**, 447 (1974).
[9] Gh. Ionescu, Al. Duca u. F. Matei, *Chem. Analit.*, **25**, 223 (1980).
[10] F. Feigl. u. A. Caldas, *Mikrochim. Acta*, **3**, 992 (1955).
[11] E. I. Poziomek, M. E, Kronenberg u. E. Haringa, *Rec. Trav. chim.*, **85**, 834 (1966).
[12] D. Mealor u. A. Towshend, *Talanta*, **15**, 1477 (1968).
[13] V. F. Toropova u. A. Averko-Antonovici, *Zhur. analit. khim.*, **26**, 2437 (1971).
[14] V. F. Toropova u. A. Averko-Antonovici, *Zhur. analit. khim.*, **26**, 116 (1972).
[15] Gh. Ionescu, Al. Duca u. N. Aelenei, *Bul. Inst. Politeh. Iași*, **22**, 23 (1976).
[16] K. B. Yatzimirski u. V. P. Vasiliev, „Konstanty nestoikostj komplexnyh soedinenij“, Izd. Akad. Nauk S.S.S.R., Moskva, 1959, p. 126.
[17] K. B. Yatzimirski u. V. P. Vasiliev, „Konstanty nestoikostj komplexnyh soedinenij“, Izd. Akad. Nauk S.S.S.R., Moskva, 1959, p. 64.
[18] P. Bonçev, *Mikrochim. Acta*, **6**, 1104 (1970).
[19] K. Doerffel, „Statistik in der analytischen Chemie“, Leipzig, 1966, p. 176.
[20] C. Liteanu u. I. Râcă, “Teoria și metodologia statistică a analizei urmelor“, Ed. Scrisul Românesc, Craiova 1979, cap. 2.7 u. 5.7.

Revue Roumaine de Chimie, 27, *11–12*, 1151 (1982)

COMPTES RENDUS

"Advances in Polymer Science". Volume 42, "New Polymerization Reactions". Springer Verlag, Berlin, Heidelberg, New York, 1982, 172 pages.

The first chapter of the book, "Four-Center Photopolymerization in the Crystalline State" (49 pages, 81 references) is written by M. Hasegawa from the University of Tokyo. In the title reactions conjugated diolefins are photochemically stepwise polymerized in solid, crystalline state affording linear polymers containing cyclobutane rings in their main chain. All the polymers obtained are highly crystalline and three dimensionally oriented with 1,3-*trans*-cyclobutane and 2,4-phenylene groups alternating in the main chain. The first four-center photopolymerization was described by M. Hasegawa in 1967, and in 1978 Lahav and co-workers realized an absolute asymmetric synthesis of chiral oligomeric crystals by four-center polymerization of achiral monomers.

The different monomers and the preparation of polymers are presented. The elucidation of the chemical structure of polymers using the IR and NMR spectroscopy is shortly stressed. A special heading is devoted to polymerization mechanism and includes the reaction kinetics, the effect of wavelength of exciting light, the quantum yield and the matrix effect. Special attention is paid to the crystallographic aspects and to changes of morphology and thermodiagram in the course of polymerization. Some important physical and chemical properties of polymers are also described.

The second chapter: "Macrozwitterion Polymerization" (55 pages, 71 references) is written by D. S. Johnston from Trinity College, Dublin. In macrozwitterion polymerizations the counterion is *covalently bound* to the chain (and not ionically as in the majority of ionic polymerizations). A comprehensive literature review of this relatively unexplored area of polymer chemistry is given. The attention is drawn to different monomer classes such as : vinyl, carbonyl and strained ring derivatives, to initiators e.g. tertiary amines, phosphines, phosphites etc. and to charge cancellation polymerizations.

In an attempt "to construct a general scheme into which as many as possible of the conclusions reached about macrozwitterion polymerizations can be fitted", some essential problems concerning the mechanism of polymerization are discussed underlining the importance of covalent initiators, of chemically inert salts, of solvents etc.

The third contribution from the book, "Ring-Opening Polymerization" (31 pages, 203 references) is written by Y. Yokoyama and H. K. Hall from University of Arizona, Tucson. The paper presents the polymerization mechanism and polymerizability of bicyclic compounds containing oxygen atoms and is limited to atom- and bond-bridged bicyclic monomers (leading references concerning the related compounds are also given).

A complete tabular survey concerning the polymerization of bicyclic ethers, ketals and orthoesters is given. Different thermodynamical data are correlated with strain energies in order to discuss the thermodynamical polymerizability. The conformation of monomers and polymers is detailed, paying special attention to the gauche and anomeric effects (the preference of the synclinal-gauche-conformation to the anti periplanar one is known as "anomeric effect"). The kinetic data and the mechanism of polymerization are also briefly described. Some medical application of such polymers are also stressed.

The last chapter of the book : "Structural and Chemical Modifications of Cellulose by Graft Copolymerization" (27 pages, 104 references) is written by B. P. Morin, I. P. Breusova and (the late) Z. A. Rogovin from Moscow Textile Institute. The paper reviews the influence of cellulose structure and of the chemical structure of the grafted polymer on the kinetics of graft polymerization of cellulose. Then the kinetics of chemically initiated graft polymerization and its features arising from the heterogeneous nature of the process are presented. A special part is devoted to technological aspects as well as to basic trends in the development of the commercial process of graft polymerization of cellulose. Finally polymer-analogous conversions of functional groups in polymer chains grafted to cellulose are briefly mentioned.

The author index for volumes 1–42 of the series ends this interesting book which presents some very recent and important reactions in polymer science.

M. Banciu

COMPTES RENDUS

"Advances in Polymer Science", Volume 42, "New Polymerization Reactions". Springer Verlag, Berlin, Heidelberg, New York, 1982, 172 pages.

The first chapter of the book, "Four-Center Photopolymerization in the Crystalline State" (49 pages, 81 references) is written by M. Hasegawa from the University of Tokyo. In the title reactions conjugated diolefins are photochemically stepwise polymerized in solid, crystalline state affording linear polymers containing cyclobutane rings in their main chain. All the polymers obtained are highly crystalline and three dimensionally oriented with 1,3-trans-cyclobutane and 2,4-phenylene groups alternating in the main chain. The first four-center photopolymerization was described by M. Hasegawa in 1967, and in 1978 L. Addadi and co-workers realized an absolute asymmetric synthesis of chiral oligomeric crystals by four center polymerization of achiral monomers.

The different monomers and the preparation of polymers are presented. The elucidation of the chemical structure of polymers using the IR and NMR spectroscopy is shortly stressed. A special heading is devoted to polymerization mechanism and includes the reaction kinetics, the effect of wavelength of exciting light, the quantum yield and the matrix effect. Special attention is paid to the crystallographic aspects and to changes of morphology and thermodiagram in the course of polymerization. Some important physical and chemical properties of polymers are also described.

The second chapter "Macrozwitterion Polymerization" (65 pages, 71 references) is written by D. S. Johnston from Trinity College, Dublin. In macrozwitterion polymerizations the counterion is covalently bound to the chain (and not ionically as in the majority of ionic polymerizations). A comprehensive literature review of this relatively unexplored area of polymer chemistry is given. The attention is drawn to different monomer classes such as vinyl, carbonyl and strained ring derivatives, to initiators e.g. tertiary amines, phosphines, phosphites etc. and to charge cancellation polymerizations.

In an attempt "to construct a general scheme into which as many as possible of the conclusions reached about macrozwitterion polymerizations can be fitted", some essential problems concerning the mechanism of polymerization are discussed underlining the importance of covalent initiators, of chemically inert salts, of solvents etc.

The third contribution from the book, "Ring-Opening Polymerization" (31 pages, 203 references) is written by Y. Yokoyama and H. K. Hall from University of Arizona, Tucson. The paper presents the polymerization mechanism and polymerizability of bicyclic compounds containing oxygen atoms and is limited to atom- and bond-bridged bicyclic monomers (leading references concerning the related compounds are also given).

A complete tabular survey concerning the polymerization of bicyclic ethers, ketals and orthoesters is given. Different thermodynamical data are correlated with strain energies in order to discuss the thermodynamical polymerizability. The conformation of monomers and polymers is detailed, paying special attention to the gauche and anomeric effects (the preference of the synclinal-gauche-conformation to the anti periplanar one is known as "anomeric effect"). The kinetic data and the mechanism of polymerization are also briefly described. Some medical application of such polymers are also stressed.

The last chapter of the book "Structural and Chemical Modifications of Cellulose by Graft Copolymerization" (27 pages, 104 references) is written by B. P. Morin, I. P. Breusova and (the late) Z. A. Rogovin from Moscow Textile Institute. The paper reviews the influence of cellulose structure and of the chemical structure of the grafted polymer on the kinetics of graft polymerization of cellulose. Then the kinetics of chemically initiated graft polymerization and its features arising from the heterogeneous nature of the process are presented. A special part is devoted to technological aspects as well as to basic trends in the development of the commercial process of graft polymerization of cellulose. Finally polymer-analogous conversions of functional groups in polymer chains grafted to cellulose are briefly mentioned.

The author index for volumes 1 – 42 of the series ends this interesting book which presents some very recent and important reactions in polymer science.

M. Dimonie

INDEX DES AUTEURS

A.

ABD EL-FATTAH B., voir El-BASIL S. 905
ABDEL-GHANI N. T., voir SHOUKRY A. F. 993
ABDEL-HAY F. I., voir ANWAR M. 839
ABDEL-RAHMAN A. E., and A. M. MAHMOUD, H. A. El-SHERIEF, A. G. GHATTAS, Synthesis of some 1, 3, 4-thiadiazole derivatives with antibacterial activity 781
ABDEL-RAHMAN A. I., voir SHOUKRY A. F. 993
ABDEL SALAM El ABSY M. and GH. MARCU, J. ZSAKÓ, CS. VÁRHELYI, Spectrophotometric and derivatographic study on some new tetradentate mixed chelates of cobalt (III) with acetylacetone derivatives 917
ABDEL-WAHAB A. A., voir El-EZBAWY S. R. 537
ABO-BAKER O. A., voir MOHAMED M. M. 865
ABOU El-NOUR F., voir BARAKAT N. 261
AGARWAL S. C. and SMT. P. L. AGARWAL, V. B. AGARWAL, VIBHAKAR DWIVEDI, Kinetics and mechanism of Cu(II)-catalysed oxidation of acetone by the peroxodisulphate ion 265
AGARWAL S. P. L., voir AGARWAL S. C. 265
AGARWAL V. B., voir AGARWAL S. C. 265
Al-AASAR N. K., voir MOUSSA G. E. M. 549
ALLER A. J., Indium determination in aluminium alloys by atomic absorption and emission spectrometry (in Spanish) 1067
AMER M. H., voir MASOUD M. S. 235
ANAND M. and S. P. GUPTA, A. R. GOYAL, R. L. MITAL, Synthesis of some substituted trifluoromethyl-phenothiazines and their oxidation products 939
ANGELIS G. DE, voir CAMPANELLA L. 973
ANWAR M. and F. I. ABBEL-HAY, A. F. HASHEM, Action of hydrazines, hydroxylamine and urea on 5-aryl-3-chloromethyl-2-thione-1, 3, 4-oxadiazoles 839
APOSTOL M., voir CĂLUŞARU A. 175
ARAMENDIA M. A. and V. BORAU, C. JIMENEZ, J. M. MARINAS, Pd/SiO_2-AlPO_4 catalyzed reduction of nitrobenzenes by hydrogen. Transfer from cyclohexene 853
ARVAY ZS., voir RĂZUŞ A. C. 423

B.

BADAMI B. V. and GURUBASAV S. PURANIK, Reactions of sydnones 281
BAHADUR P. and K. SINGH, Solubilization of alkanols in the presence of alkaline earth metal soaps 485
— , voir SINGH S. P. 803
BALABAN A. T., voir BANCIU M. 1037
— , voir HERDAN J. 69
— , voir MOŢOC I. 735
— and M. PARASCHIV, Molecular complexes with aromatic cations as electron acceptors. V. Inter- and intramolecular charge transfer of amino-substituted pyridinium salts evidenced by electronic absorption spectra 513
— , voir SCHIKETANZ I. 1125
BANCIU M., Photochemical ring contraction of 3-diazo-dibenzo [*f*, *i*] bicyclo [3.2.2] nona-6, 8-dien-2-one 769
— and M. ELIAN, PHAN LE THUY, C. DRĂGHICI, ECATERINA CIORĂNESCU, Synthesis and pyrolysis of dibenzo [*c*, *e*] tricyclo $[5.3.0.0^{2,10}]$ deca-3, 5, 8-triene, a new dibenzo $(CH)_{10}$ hydrocarbon 19

— and A. T. BALABAN, C. DRĂGHICI, RODICA VLAD, Synthesis of pyrylium salts with an annelated dibenzo [*f*, *i*] bicyclo 3.2.2 nona-6, 8-diene skeleton (oxoniahomotriptycenes) and their reactions with nucleophiles 1037
BANERJEE D. K. and V. MATEI, V. VANTU, Kinetic studies of the pyrolysis of some alkylbenzenes 621
BĂNICA F. G., voir QILONG L. 443
— , voir QILONG L. 615
BARAKAT N. and F. ABOU El-NOUR, N. SHAHEEN, Quantitative spectrophotographic estimation of zirconium by chemical enrichment 261
BĂRBULESCU A., voir VOLCEANOV A. 1099
BASYOUNI M. N., voir MOUSSA G. E. M. 549
BENDIC C., voir SAHINI V. E. 129
BERCARU A. M., voir DĂNEŢ A. F. 459
BICĂ I., voir ENE R. 609
BORAU V., voir ARAMENDIA M. A. 853
BOULOS N., voir EL-BASIL S. 905
BRÂNZOI V., voir STERNBERG S. 217
— , voir STERNBERG S. 1003
BREŢCANU D., voir CONTINEANU I. 55
BREZEANU M., voir MINCU V. 931
— , voir MUNTEANU G. 727
— , voir SEGAL E. 137
BURGUERA J. L. and MARCELA BURGUERA, A. TOWNSHEND, The principles, applications and trends of flow injection analysis for monitoring chemiluminescent reactions 879
BURGUERA, M., voir BURGUERA J. L. 879
BURON C. S., voir MENDEZ J. H. 491

C.

CĂLDĂRARU H., voir CARAGHEORGHEOPOL A. 969
— , voir HUBCA GH. 659
CĂLDĂRARU M., voir IONESCU N. I. 75
CALU C. and E. DONIGA, Amperometric determination of thiamine 667
CALU N. and EUGENIA SAVIUC, TEODORA POPOVICI, Study of the Fe(III)-3-hydroxypyridine N-oxide system 385
CĂLUŞARU A. and M. APOSTOL, Charge transfer by quantum tunneling across the separation interface of two media using perturbation formalism 175
— , voir QUILONG L. 443
— , voir QUILONG L. 615
CAMPANELLA L. and G. de ANGELIS, Polarographic behaviour of lutidinic acid 973
— and T. FERRI, M. GABRIELLI, Liquid membrane electrodes for benzoic acid determination 681
CARAGHEORGHEOPOL A. and H. CĂLDĂRARU, GH. HUBCA, CR. OPRESCU, M. M. DIMONIE, Synthesis and polymerization of polyethylene glycol dimethacrylates. VII. ESR study of ethylene glycol dimethacrylate-styrene copolymers 969
— , voir HUBCA GH. 659
CASTRO E. A. and F. M. FERNANDEZ, Semiempirical prediction of ionization potential 1025
CETINA R., voir RUBIO M. 285
CHIFU E., voir FINTA Z. 191
— and MARIA TOMOAIA-COTIŞEL, Mixed films of retinyl palmitate with lipids at the air-water interface 27
— and IOAN STAN, Surface mobility of surfactant solutions. X. *Marangoni* flow against gravity forces 703
CHIRALEU F., voir GEORGESCU F. 635
CHIRIAC A. and VERONICA CHIRIAC, S. HOLBAN, I. MOŢOC, Z. SIMON, Quantitative structure—activity relations with the MTD-procedure for plant growth regulating optically active acetic acid derivatives 561
CHIRIAC, C. I., A new method for the synthesis of aromatic amides directly from acids 747

— , A new synthesis of hydrazides by a direct condensation reaction 411
— , Aromatic esters by a new direct condensation reaction 831
— , Aromatic esters by a new direct condensation reaction using triaryl borates 533
— , Cyclodehydrations with phenyldichlorophosphite-dimethylformamide. A new convenient method for the synthesis of 1, 3, 4-oxadiazoles from diaroylhydrazines 935
CHIRIAC V., voir CHIRIAC A. 561
CIOCHINĂ A., voir VÎLCU R. 313
CIORĂNESCU E., voir BANCIU M. 19
— , voir SCHIKETANZ I. 1125
CIUBOTARIU D., voir RADULY S. 121
COCHECI V. and LUCIAN NEGULESCU, FRANCISC KLEPP, Contributions to the calculation of ion exchange equilibrium in water demineralization process . . 37
CONSTANTINESCU E. and HILDEGARD DENGEL, Thermogalvanic cells with aqueous rubidium chloride solutions (in German) 47
CONSTANTINESCU M., voir ZUCA ȘT. 161
CONȚESCU CR. and M. I. VASS, On the dipole moment of Cu, Ag and Au atoms adsorbed on different tungsten planes 59
CONTINEANU I. and D. BREȚCANU, D. I. MARCHIDAN, The enthalpies of combustion and formation of 3-amino-4-methoxyacetanilide and 3-(N-β-cyanoethyl)-amino-4-methoxyacetanilide. 55
— and L. WAGNER, L. STĂNESCU, D. I. MARCHIDAN, The enthalpies of combustion and formation of *o*-phenylenediamine urea, and 2-hydroxy benzamidazole (in German). 205
CONTINEANU M., voir ONCESCU T. 95
COSTA A., voir DEYA P. M. 401
COSTEANU G., voir LANDAUER O. 603
CRISTESCU C. and S. SITARU, *as*-Triazine derivatives with potential therapeutic action. XVI. Synthesis of 5-(ω-carboxy-alkyl) mercapto-6-azauridines 943
CUETO G. L., voir MENDEZ J. H. 491
CZAKIS-SULIKOWSKA D. M. and J. RADWANSKA-DOCZEKALSKA, Thermal decomposition of the 2,2′-bipyridine and 4,4′-bipyridine compounds with some bismuth, antimony and tin chlorides 1105

D.

DANEȘ F., voir GEANĂ D. 1009
DĂNEȚ A. F. and ANCA MARIANA BERCARU, Extraction, complexing and determination of phenyl-mercuric ion with diazoaminobenzene 459
DAVID V., voir MOLDOVEANU Ș. 325
—, voir MOLDOVEANU Ș. 471
DAYAL R., voir VARMA R. P. 257
DENGEL H., voir CONSTANTINESCU E. 47
DEV B. R., voir PATI S. C.. 523
DEYA P. M. and A. COSTA, J. V. SINISTERRA, J. M. MARINAS, The $AlPO_4$ and related systems as catalysts in organic reactions. I. Tertbutylbenzene cracking 401
DIMA L., voir RADOVICI O. 115
DIMITRIU E., voir VÎLCU R. 169
— , voir VÎLCU R. 719
DIMONIE M., voir CARACHEORGHEOPOL A. 969
— , voir DRĂGAN GH. 585
— , voir HUBCA GH. 433
— , voir HUBCA GH. 659
DWIVEDI V., voir AGARWAL S. C.. 265
DOCA N. and F. KLEPP, E. SEGAL, Reactant-catalyst interaction parametrisation 365
DOMKA F. and W. ZMIERCZAK, J. MICIUKIEWICZ, Catalytic properties of iron chromite, activated by alkali oxides (in French) 381
DONIGA E., voir CALU C. 667
DRĂGAN GH., voir HUBCA GH. 433
— and GH. HUBCA, CR. OPRESCU, M. DIMONIE, Synthesis and polymerization of polyethylene glycol dimethacrylates. V. Analysis of kinetic data obtained at polymerization based on topoenergetic principles 585

DRĂGHICI C., voir BANCIU M. 19

— , voir BANCIU M. 1037

DUCA AL., voir IONESCU GH. 1141

DUMITRIU E., voir OPREA S. 651

E.

El-BASIL S., On the cyclization of 3-α-naphtyl-propenoyl carbonium ion (An intramolecular perturbation) 557

— and B. ABD El-FATTAH, M. M. El-ENANY and N. BOULOS, Cation-anion combination reactions. Molecular orbital calculations 905

El-ENANY M. M., voir El-BASIL S. 905

El-EZBAWY S. R. and A. A. ABDEL-WAHAB, A. A., KHALAF, Synthesis of some new biologically active 2-aminopyridine derivatives 537

El-HASHASH M. A., voir MOHAMED M. M. 865

El-KAFRAWY A. F., voir HASHEM A. I. 835

— , voir MOUSSA G. E. M. 549

El-SHERIEF H. A., voir ABDEL-RAHMAN A. E. 781

ELIAN M., voir BANCIU M. 19

ENE R. and I. BICĂ, D. SĂNDULESCU, Determination of hydrogen solubility in liquid hydrocarbons at atmospheric pressure 609

ELROD L. W., voir ROBERTS R. M. 761

ESSAWY A., Synthesis and reactions of 2-furyl-3, 1-benzothiazine-4(*H*)-thione, 2-furyl-4(3H)-quinazolinone and 2-furyl-3,1-benzoxazin-4(*H*)-one 415

F.

FAZAKAS J., Determination of gold by graphite furnace. Atomic absorption spectrometry with atomization under pressure 685

— , voir KALYUZHYI A. 503

FERNANDEZ F. M., voir CASTRO E. A. 1025

FERRI T., voir CAMPANELLA L. 681

FINTA Z. and E. CHIFU, EUGENIA GAVRILA, M. SALAJAN, Surface oxidation of some sulphurous minerals by the hypochlorite ion 191

G.

GABRIELLI M., voir CAMPANELLA L. 681

GARCIA DE MARIA C., voir MÉNDEZ J. H. 981

GAVRILA E., voir FINTA Z. 191

GEANĂ D. and F. DANEȘ, Application of Kuhn-Tucker conditions to the problem of chemical and phase equilibrium 1009

GEORGESCU E. I., voir GEORGESCU F. 635

GEORGESCU F. and E. I. GEORGESCU, F. CHIRALEU, I. ZUGRĂVESCU, Pyrimidinium-ylids. III. Synthesis of carbanion-disubstituted pyrimidinium-ylids (in French) 635

GHATTAS A. G., voir ABDEL-RAHMAN A. E. 781

GHINEA S., voir VLĂDESCU L. 569

GHIRVU C. and ANA ONU, GH. IONITA, Spectral study of the influence of polystyrene in benzene solutions on the α, α′-diphenyl-β-picrylhydrazyl (DPPH) radical . . 1029

GLATZ A.-M., voir RĂZUȘ A. C. 423

GOYAL A. R., voir ANAND M. 939

GRECU N., voir HERDAN J. 69

GUPTA B. K., voir SYAMAL A.. 927

GUPTA R. P. and A. K. SRIVASTAVA, Thiosemicarbazones as ligands and evaluation of their virus inhibitory behaviour. I. Some transition metal complexes of substituted isatin β-thiosemicarbazones 393

GUPTA S. P., voir ANAND M. 939

GUȚUL M., voir MINCU V. 931

H.

HAIDUC I., voir ŞILAGHI-DUMITRESCU I. 911
HAMED A. A., voir HASSAN M.A. 963
HANNA M. T., voir KHALIL F. Y. 357
HARLES A., voir VLĂDESCU L. 301
— , voir VLĂDESCU L. 453
HASHEM A. F,. voir ANWAR M. 839
HASHEM A. I., Replacement of the nitro group in pentachloronitrobenzene by nucleophiles 429
— and M. E. SHABAN, A. F. El-KAFRAWY, Reactions of some 5-oxo-2-pyrrolines 835
HASSAN M. A. and E. A. SOLIMAN, A. A. HAMED, Synthesis and reactions of polysubstituted 2(1*H*)pyridones and pyridines 963
HERDAN J. and G. IORDACHE, N. NEGOIŢĂ, N. GRECU, A. T. BALABAN, New 2, 4, 6-trisubstituted phenols and their corresponding aroxyls 69
HERŢIA D. I., voir IVANOV AL. 243
HODOŞAN F., voir POP L. 545
HOLBAN S., voir CHIRIAC A. 561
HUBCA GH., voir CARAGHEORGHEOPOL A. 969
— , voir DRĂGAN GH. 585
— and C. OPRESCU, A. CARAGHEORGHEOPOL, H. CĂLDĂRARU, D. RACOŢI, M. DIMONIE, Synthesis and polymerization of polyethylene glycol dimethacrylates. VI. Study of copolymerization process of polyethylene glycol dimethacrylates with styrene 659
— and CR. OPRESCU, GH. DRĂGAN, M. DIMONIE, Synthesis and polymerization of polyethylene glycol dimethacrylates. IV. Study of the polymerization process of polyethylene glycol dimethacrylates 433

I.

IBRAHIM M. G., voir OSMAN A. N. 859
IONESCU GH. and F. MATEI, AL. DUCA, Contributions to the kinetical-analytical study regarding CN^--traces determination based on its inhibitory effect (in German) 1141
IONESCU N. I. and M. CĂLDĂRARU, Propylene oxidation on MoO_3/SiO_2 and Bi_2O_3/SiO_2 catalysts 75
— and D. POPESCU, Oxidation of methanol on copper phthalocyanine 481
IONESCU S. G., voir ONCESCU T. 95
IONIŢĂ GH., voir GHIRVU C. 1029
IORDACHE G., voir HERDAN J. 69
IOVU M. and E M. VASILESCU, New vibration modes made evident in the IR spectra of a class of alkyl aryl ethers 629
IRINEI F., voir VÎLCU R. 155
ISLAM I., voir MOHAMED M. M. 865
ISMAIL M. A., voir OSMAN A. N. 859
ISMAIL M. T., voir KASEM K. K. 475
ISUF A., voir VLĂDESCU L. 673
IULIAN O., voir LANDAUER O. 603
— , voir LANDAUER O. 351
IVANA E., voir MURGULESCU I. G. 695
— , voir MURGULESCU I. G. 799
IVANOV AL. and D. I. HERŢIA, Stationarity in quantum theory of molecules. I. General formalism 243

J.

JAIN P. K., voir VARMA R. P. 1117
JAIN S. K., Surface properties of solutions of lithium nitrate in some molten hydrates 713
JIMENEZ C., voir ARAMENDIA M. A. 853
JITARU I., voir MINCU V. 931

K.

KALYUZHNYI A. and V. MILYUTIN, J. FAZAKAS, M. NEGOIU, On the extraction of palladium (II) and gold(III) from solution on inorganic electron exchangers (in Russian) 503

KASEM K. K. and M. T. ISMAIL, Additional physical properties for butyrate and isobutyrate anions 475

KHALAF A. A., voir El-EZBAWY S. R. 537

KHALIFA M., voir OSMAN A. N. 859

KHALIL F. Y. and M. T. HANNA, Kinetic and thermodynamic parameters of the reversible acid hydrolysis of benzyl acetate in water-methanol mixtures 357

KHAN A. R., voir LODHI S. A. K. 509

KHAN S. A. and M. STONE, Spectrophotometric determination of fluorine in silicate rocks and minerals using zirconium-cyanine R. system 885

KLEPP F., voir COCHECI V. 27

— , voir DOCA N. 365

KRYACHKO E. S., On water dimer structure in Coulson-Eisenberg model 901

KULKARNI M. V. and V. D. PATIL, Synthesis of pharmacologically active benzimidazoles 1131

KUMAR S., voir SENGUPTA S. K. 741

L.

LANDAUER O. and C. MATEESCU, O. IULIAN, The influence of the solvent on the reaction rate. The alkaline hydrolysis of the n-butyl acetate, propionate and butyrate in the mixed solvent waterdimethylsulphoxide (in French) 351

— and C. MATEESCU, O. IULIAN, G. COSTEANU, On the viscosity of the mixed system tetrahydrofuranwater (in French) 603

LECA M., A new route for determining the nonpolar solubility parameters of organic solvents by gas-liquid chromatography 987

LEPĂDATU C. I., The concept of electronegativity and the interelectronic repulsion energy in the vector model of the atom 897

— , On a formula of Racah and Shadmi for the interelectronic repulsion parameters 1035

— , voir MINCU V. 931

— , voir MUNTEANU G. 727

LINGWAY I., voir STERNBERG S. 1085

LODHI S. A. K. and A. R. KHAN, Vinyl monomer complexes. I. The complexes of acryl nitrile with some inorganic salts 509

LUCA C., voir QILONG L. 443

— , voir QILONG L. 615

M.

MACAROVICI C. GH., voir MARTA L. 87

MADHURI M., voir SINGH S. P. 803

MAHMOUD A. M., voir ABDEL-RAHMAN A. E. 781

MARCHIDAN D. I., voir CONTINEANU I. 55

— , voir CONTINEANU I. 205

MARCHIDAN S. and I. VARTIRES, N. D. TOTIR, Determination of trace quantities of the group V—A elements by anodic stripping voltammetry. II. Trace analysis of antimony 81

MARCU GH., voir ABDEL SALAM El ABSY M. 917

— , voir ZSAKÓ J. 815

MĂRIE A., voir SIMITI I. 273

MARINAS J. M., voir ARAMENDIA M. A. 853

— , voir DEYA P. M. 401

— , voir RASO A. G. 1047

MARKOV P., voir PETKOV I. 847

MARTA L. and M. ZAHARESCU, C. GH. MACAROVICI, Thermal and structural investigation of some oxalato-niobic complexes. II. Barium tris (oxalato)niobate 87

MASCAŞ A., voir STERNBERG S. 147

MASOUD M. S. and T. M. SALEM, M. H. AMER, Studies on iron (III), cobalt (II) and nickel(II) azido complexes 235

MATEESCU C., voir LANDAUER O. 351

— , voir LANDAUER O. 603

MATEI F., voir IONESCU GH. 1141

MATEI V., voir BANERJEE D. K. 621

MATEOS A. A., voir MÉNDEZ J. H. 491

— , voir MÉNDEZ J. H. 981

MATEOS E. J. M., voir MÉNDEZ J. H. 981

MÉNDEZ J. H. and G. LOPEZ CUETO, A. ALONSO MATEOS, C. SANCHEZ BURON, Kinetics of the reaction between oxygen and tin(II) : stabilization of Sn(II) solutions and their utilization in reductometry (in Spanish) 491

— and A. ALONSO MATEOS, E. J. MARTÍN MATEOS, C. GARCÍA DE MARÍA, Gravimetric determination of gold by means of the ion pair $[AuI_4^-]$ $(C_4H_9)_4N^+]$ (in Spanish) 981

MICIUKIEWICZ J., voir DOMKA F. 381

MILYUTIN V., voir KALYUZHNYI A. 503

MINCU V. and C. LEPĂDATU, M. GUȚUL, M. BREZEANU, I. JITARU, Optical and magnetic studies of some heteronuclear complexes of nickel and zinc with hydrazine 931

MISHRA R., Excess surface tension of binary liquid mixtures 199

MITAL R. L., voir ANAND M. 939

MOHAMED M. M. and M. A. El HASHASH, I. ISLAM and O. A. ABO-BAKER, 1,4-Arylation of β-(4-chloro-3-methylbenzoyl)-acrylic acid with activated hydrocarbons under Friedel-Crafts conditions and some studies on the products 865

MOLDOVAN V., voir TEOREANU I. 1091

MOLDOVEANU Ș. and V. DAVID, An extended Hückel FORTRAN program for molecules including the elements from hydrogen to xenon except the transition metals 325

— and V. DAVID, The generalization of Beveridge-Schnuelle solvating model 471

MOȚOC I. and A. T. BALABAN, Testing the geometrical meaning of Taft type steric constants 735

— , voir CHIRIAC A. 561

— , voir VÂLCEANU R. 225

MOUSSA G. E. M. and M. N. BASYOUNI, M. E. SHABAN, A. F. El-KAFRAWY, N. K. Al-AASAR, Synthesis and some reactions of 1-arylisoindoles 549

MRACEC M., voir RADULY S. 121

MUNTEANU G. and C. I. LEPĂDATU, L. PATRON, M. BREZEANU, Electronic spectra, magnetic properties and structure of polynuclear complexes $[Fe_2^{III}M^{II}Cl_{12}]^{4-}$ of manganese (II) and cobalt (II) 727

MURGULESCU I. G. and E. IVANA, E. POPA, Absorption spectrum and composition of SnI_2 vapour 695

— and E. POPA, E. IVANA, Optical properties of molten SnI_2 799

— and M. ȘERBAN, Viscosity of liquids with quasispherical molecules. Checking Eyring's equation 597

MUSTE A., voir RADULY S. 121

N.

NATANSOHN A., voir PERCEC S. 775

NEGOIU M., voir KALYUZJNYI A. 503

NEGOIȚĂ N., voir HERDAN J. 69

NEGULESCU L., voir COCHECI V. 37

NEGULIANU CL., voir SIMIONESCU CR. 1055

O.

ONCESCU T. and M. CONTINEANU, S. G. IONESCU, Model system to obtain photohydrogen 95

ONICIU L. and V. A. TOPAN, Investigation methods of the electrode processes 103

ONU A., voir GHIRVU C. 1029

OPREA S. and E. DUMITRIU, Reactivity of acrylic monomers. XI. Synthesis and copolymerization of 3-chloro-2-hydroxypropylacrylate 651

OPRESCU CR., voir CARAGHEORGHEOPOL 969

— , voir DRĂGAN GH. 585

— , voir HUBCA GH. 433

— , voir HUBCA GH. 659

OSMAN A. E., voir OSMAN A. N. 859

OSMAN A. N. and M. KHALIFA, M. A. ISMAIL, A. E. OSSMAN and M. G. IBRAHIM, Synthesis and biological activity of certain derivatives of 2,4-dioxo-1,2,3,4-tetrahydroquinazoline. I. 859

P.

PANDEY J. D. and R. P. PANDEY, On gneralized pair potential. Evaluation of crystal properties 211

PARASCHIV M., voir BALABAN A. T. 513

PATI S. C. and B. R. DEV, Kinetics and mechanism of Ru(III) catalyzed oxidation of aliphatic diols and cyclanols by phenyliodoso acetate 523

PATIL V. D., voir KULKARNI M. V. 1131

PATRON L., voir MUNTEANU G. 727

— , voir SEGAL E. 137

PERCEC S. and A. NATANSOHN, FL. POPESCU, ^{1}H-NMR spectra of some flame-retardant polymers 775

— , voir POPESCU FL. 291

PETKOV I. and P. MARKOV, Influence of substituents on the photoketonization of some enolizable β-ketoesters in solution 847

PETREUŞ O., voir POPESCU FL. 291

PLATH P. J., voir TAUSCH M. W. 953

POP L. and F. HODOŞAN, Synthesis of (Z)-9-tricosene (Muscalure) 545

POPA E., voir MURGULESCU I. G. 695

— , voir MURGULESCU I. G. 799

POPESCU B., voir RADOVICI O. 115

POPESCU D., voir IONESCU N. I. 481

POPESCU F., voir PERCEC S. 775

POPESCU FL. and L. ROSESCU, S. PERCEC, O. PETREUŞ, Study of hydrolytic behaviour of certain polyesters and polyamides containing phosphorus in the chain (in French) 291

POPOVICI T., voir CALU N. 385

PURANIK G. S., voir BADAMI B. V. 281

Q.

QILONG L. and C. LUCA, A. CĂLUŞARU, F. G. BĂNICĂ, Catalytic hydrogen discharge by cycloserine in metal-ion containing ammonia buffer 443

— and C. LUCA, A. CĂLUŞARU, F. G. BĂNICĂ, Catalytic hydrogen discharge by cycloserine in nickel ion containing phosphate buffer 615

R.

RACOŢI D., voir HUBCA GH. 659

RADOVICI O. and B. POPESCU, L. DIMA, The anodic oxidation of *n*-decane on platinum electrode in acid electrolyte 115

RADULY S. and M. MRACEC, D. CIUBOTARIU, A. MUSTE, Z. SIMON, Arylamides of oxalic acid. III. Hückel molecular orbital and Del Ré calculations 121

RADWANSKA-DOCZEKALSKA J., voir CZAKIS-SULIKOWSKA D. M. 1105

RASO A. G. and J. V. SINISTERRA, J. M. MARINAS, Hydrolysis of n-alkyl salicilates catalysed by activated barium hydroxides (in Spanish) 1047

RĂZUŞ A. C. and ZS. ARVAY, A. M. GLATZ, Aluminium chloride catalyzed reactions of unsaturated acids with benzene. XIV. Reaction of *t*-butyl acrylic acid 423
ROBERTS R. M. and L. W. ELROD, Friedel-Crafts dealkylations of secondary heptylbenzenes 761
ROBU T., voir SEGAL E. 137
ROSESCU L, voir POPESCU FL. 291
RUBIO M. and R. CETINA, M. SALMÓN, Conformational calculations of some azobilirubin isomers. II. 3′-Methyl-4′-vinyl derivative (in Spanish) 285

S.

SAFARICA E., voir SEGAL E. 137
SAHINI V. E. and C. BENDIC, L. VIRAG, Reactivity of *m*-nitrophenyl acetate in excited state 129
SALAJAN M., voir FINTA Z. 191
SALEM T. M., voir MASOUD M. S. 235
SALMÓN M., voir RUBIO M. 285
SĂNDULESCU D., voir ENE R. 609
SAVIUC E., voir CALU N.. 385
SCHIKETANZ I. and A. T. BALABAN, E. CIORĂNESCU, Aminoketone and oxazole synthesis. VII. Conversion of bis-azlactones into bis-oxazoles 1125
SEGAL E. and M. BREZEANU, E. SAFARICA, L. PATRON, T. ROBU, An analysis of thermal decomposition of coordination polynuclear compounds in Fe(III), Mn(II), Ni(II) systems 137
— , voir DOGA N. 365
SENGUPTA S. K. and S. KUMAR, Five- and six-coordinated complexes of hafnium (IV) with triazoline thione 741
ŞERBAN M., voir MURGULESCU I. G. 597
SHABAN M. E., voir HASHEM A. I. 835
— , voir MOUSSA G. E. M. 549
SHAHEEN N., voir BARAKAT N. 261
SHOUKRY A. F. and A. I. ABDEL-RAHMAN, N. T. ABDEL-GHANI, Analysis of ternary alloys containing Co(II), Ni(II), and Cu(II) 993
SHUKLA J. P., Vanadium (V) chelates of N-substitued phenylhydroxylamines. A spectrophotometric study 751
SILAGHI-DUMITRESCU I. and L. SILAGHI-DUMITRESCU, I. HAIDUC, Normal coordinate analysis of the vibrational spectrum of dimethyldithioarsinato anion, $(CH_3)_2AsS_2^-$ 911
SILAGHI-DUMITRESCU L., voir SILAGHI-DUMITRESCU I. 911
SIMIONESCU B. C., voir SIMIONESCU CR. I. 141
SIMIONESCU CR. I. and B. C. SIMIONESCU, Plasma-induced polymerization. VII. Some characteristics of this new method of polymer synthesis 141
— and C. VASILIU-OPREA, C. NEGULIANU, The mechanochemical synthesis of some polychelates on polyamidic support (in Russian) 1055
SIMITI I. and A. MĂRIE, Contribution to the study of some heterocycles. LI. Preparation of some 2-phenyl-5-R-thiazolo [3,2-*b*]—1,2,4-triazoles (in French) 273
SIMON Z., voir CHIRIAC A 561
— , voir RADULY S. 121
SINGH K., voir BAHADUR P. 485
SINGH S. P. and M. MADHURI, P. BAHADUR, Stabilization of emulsions by surface active agents 803
SINISTERRA J. V., voir DEYA P. M. 401
— , voir RASO A. G. 1047
SITARU S., voir CRISTESCU C 943
SOLIMAN E. A., voir HASSAN M. A. 963
SRIVASTAVA A. K., voir GUPTA R. P. 393
ŞTAN I., voir CHIFU E. 703
ŞTĂNESCU L., voir CONTINEANU I. 205
STERNBERG S. and V. BRÂNZOI, Polarization behaviour of Armco iron in anhydrous solution of R-OH + HCl 217

— and V. BRÂNZOI, Polarization behaviour of stainless steel, type W.1.4541 in R—OH + HCl anhydrous solution . . . 1003

— and I. LINGVAY, T. VIŞAN, The cathodic reactions on silicon electrode in molten potassium nitrate . . . 1085

— and A. MASCAS, Thermal conductivity in $Ca(NO_3)_2 \cdot 4H_2O - nH_2O$ system . . . 147

— and T. VIŞAN, Electroreduction of nitrate ions in molten alkali nitrates . . . 345

STONE M., voir KHAN S. A. . . . 885

SYAMAL A. and B. K. GUPTA, New nickel (II) complexes with dibasic tridentate ONO donor ligands . . . 927

T.

TAUSCH M. W. and P. J. PLATH, Rearrangements of $(CH)_7^{\neq}$ ions (in German) . . . 953

TEOREANU I. and V. MOLDOVAN, On the hardening structures developed in the system Portland cement-water . . . 1091

THUY F. L., voir BANCIU M. . . . 19

TOMOAIA-COTIŞEL M., voir CHIFU E. . . . 27

TOPAN V. A., voir ONICIU L. . . . 103

TOTIR N. D., voir MARCHIDAN S. . . . 81

TOWNSHEND A., voir BURGUERA J. L. . . . 879

V.

VÂLCEANU R. and I. MOŢOC, Steric effects in effector-receptor interactions. The steric difference method and applications (in German) . . . 225

VANTU V., voir BANERJEE D. K. . . . 621

VARHELYI CS., voir ABDEL SALAM El ABDY M. . . . 917

VÁRHELYI M., voir ZSAKŐ J. . . . 815

VARMA R. P. and R. DAYAL, Characterization of strontium soaps and studies of their viscosity in aqueous isopropanol . . . 257

— and P. K. JAIN, Studies on the behaviour of cobalt and calcium soaps. III. Viscosity and surface tension studies in alcohols . . . 1117

— and A. K. VIRMANI, Studies on physical properties of cadmium soaps. I. Infrared, solubility, conductivity and viscosity studies in water . . . 1109

VARTIRES I., voir MARCHIDAN S. . . . 81

VASILESCU D. S., Alternating tendency in copolymerization. IV. Simultaneous cationic polymerization and radical terpolymerization . . . 575

VASILESCU E. M., voir IOVU M. . . . 629

VASILIU-OPREA CL., voir SIMIONESCU CR. . . . 1055

VASS M. I., voir CONŢESCU C. R. . . . 59

VASU GH., voir VÎLCU R. . . . 313

VIDAL B., Influence on the UV spectrum, of an aliphatic chain included between a benzenic chromophore and an electron-withdrawing auxochrome (in French) 823

VÎLCU R. and A. CIOCHINA, GH. VASU, Absolute measurement of thermal conductivity and thermal diffusivity of gases by the classical procedure of the transient hot wire method . . . 313

— and E. DIMITRIU, Nickel electroless plating in ultrasonic field . . . 169

— and E. DIMITRIU, Microstructure of electroless deposited nickel in an ultrasonic field . . . 719

— and FL. IRINEI, Thermodynamics of multicomponent electrolyte solutions. III. Ammonium persulfate activity coefficients in quaternary system, in solubility measurements . . . 155

VIRAG L., voir SAHINI V. E. . . . 129

VIRMANI A. K., voir VARMA R. P. . . . 1109

VIŞAN T., voir STERNBERG S. . . . 345

— , voir STERNBERG S. . . . 1085

VLAD R., voir BANCIU M. . . . 1 037

VLĂDESCU L. and S. GHINEA, Utilization of Tiron in the separation and concentration of titanium with ion exchange resins 569
— and A. HARLES, Utilization of chromotropic acid in separation of titanium with ion exchange resins. I. Cation exchange behaviour 301
— and A. HARLES, Utilization of chromotropic acid in separation of titanium with ion exchange resins. II. Anion exchange behaviour 453
— and A. ISUF, Ion excange procedure for the elimination of interferences in the spectrophotometric determination of magnesium with Eriochrome black T 673
VOLCEANOV A. and A. BĂRBULESCU, Effective hybridization of oxygen orbitals in SiO_2 1099

W.

WAGNER L., voir CONTINEANU I. 205

Z.

ZMIERCZAK W., voir DOMKA F. 381
ZSAKÓ J., voir ABDEL SALAM EL ABSY M. 917
— and GH. MARCU, M. VÁRHELYI, Kinetic analysis of thermogravimetric data. XV. Thermal decomposition of $[Co(en)_2(pyridine)Br]X_2$ type complexes 815
ZUCA ŞT. and M. CONSTANTINESCU, Cationic self-diffusion coefficients in molten $(Tl\text{-}Ag)NO_3$ system 161
ZAHARESCU M., vor MARTA L. 87
ZUGRĂVESCU I., voir GEORGESCU F. 635

INDEX DES SUJETS

1982

Absorption spectrum and composition of SnI_2 vapour, I. G. MURGULESCU, E. IVANA and E. POPA . . . 695

Acetone by the peroxodisulphate ion, Kinetics and mechanism of Cu(II) – catalysed oxidation of –, S. C. AGARWAL, SMT. P. L. AGARWAL, V. B. AGARWAL and V. DWIVEDI . . . 265

Acrylic monomers. XI. Synthesis and copolymerization of 3-chloro-2-hydroxypropyl acrylate, Reactivity of –, S. OPREA and E. DUMITRIU . . . 651

Aliphatic chain included between a benzenic chromophore and an electron-withdrawing auxochrome, Influence on the UV spectrum, of an –, B. VIDAL . . . 823

Alkaline hydrolysis of the n-butyl acetate, propionate and butyrate in the mixed solvent water-dimethylsulphoxide, The – in French, O. LANDAUER, C. MATEESCU and O. IULIAN . . . 351

Alkanols in the presence of alkaline earth metal soaps, Solubilization of –, P. BAHADUR and K. SINGH . . . 485

Alkyl aryl ethers, New vibration modes made evident in the IR spectra of a class of –, M. IOVU and E. M. VASILESCU . . . 629

Aluminium chloride catalyzed reactions of unsaturated acids with benzene. XIV. Reaction of *t*-butyl acrylic acid, A. C. RĂZUȘ, ZS. ARVAY and A. M. GLATZ 423

Aminoketone and oxazole synthesis. VII. Conversion of bis-azlactones into bis-oxazoles, I. SCHIKETANZ, A. T. BALABAN and E. CIORĂNESCU . . . 1125

2-Aminopyridine derivatives, Synthesis of some new biologically active –, S. R. El-EZBAWY, A. A. ABDEL-WAHAB and A. A. KHALAF . . . 537

Anodic oxidation of *n*-decane on platinum electrode in acid electrolyte, The –, O. RADOVICI, B. POPESCU and L. DIMA . . . 115

Anodic stripping voltammetry. II. Trace analysis of antimony, Determination of trace quantities of the group V–A elements by –, S. MARCHIDAN, I. VARTIRES and N. D. TOTIR . . . 81

Aromatic amides directly from acids, A new method for the synthesis of –, C. I. CHIRIAC . . . 747

Aromatic esters by a new direct condensation reaction, C. I. CHIRIAC . . . 831

Aromatic esters by a new direct condensation reaction using triaryl borates, C. I. CHIRIAC 533

5-Aryl-3-chloromethyl-2-thiono-1,3,4-oxadiazoles, Action of hydrazines, hydroxylamine and urea on –, M. ANWAR, F. I. ABDEL-HAY and A. F. HASHEM . . . 839

Arylamides of oxalic acid. III. Hückel molecular orbital and Del Ré calculations, S. RADULY, M. MRACEC, D. CIUBOTARIU, A. MUSTE and Z. SIMON . . . 121

1-Arylisoindoles, Synthesis and some reactions of –, G. E. M. MOUSSA, M. N. BASYOUNI, M. E. SHABAN, A. F. El-KAFRAWY and N. K. Al-AASAR . . . 549

Azido complexes, Studies on iron(III), cobalt(II) and nichel(II) –, M. S. MASOUD, T. M. SALEM and M. H. AMER . . . 235

Azobilirubin isomers. II.3′-Methyl-4′-vinyl derivative, Conformational calculations of some – (in Spanish), M. RUBIO, R. CETINA and M. SALMÓN . . . 285

Benzimidazoles, Synthesis of pharmacologically active benzimidazoles, Synthesis of pharmacologically active –, M. V. KULKARNI and V. D. PATIL . . . 1131

Benzyl acetate in water-methanol mixtures, Kinetic and thermodynamic parameters of the reversible acid hydrolysis of –, F. Y. KHALIL and M. T. HANNA . . . 357

BOOK REVIEWS 305, 305, 306, 307, 308, 467, 468, 591, 591, 592, 691, 692, 787, 1079, 1151

Butyrate and *iso*butyrate anions, Additional physical properties for –, K. K. KASEM and M. T. ISMAIL . . . 475

Cadmium soaps. I. Infrared, solubility, conductivity and viscosity studies in water, Studies on physical properties of –, R. P. VARMA and A. K. VIRMANI . . . 1109

Catalytic hydrogen discharge by cycloserine in metal-ion containing ammonia buffer, Li QILONG, C. LUCA, A. CĂLUŞARU and F. G. BĂNICĂ 443

Catalytic hydrogen discharge by cycloserine in nickel ion containing phosphate buffer, LI QILONG, C. LUCA, A. CĂLUŞARU and F. G. BĂNICĂ 615

Catalytic properties of iron chromite, activated by alkali oxides (in French), F. DOMKA, W. ZMIERCZAK and J. MICIUKIEWICZ 381

Cationic self-diffusion coefficients in molten $(Tl\text{-}Ag)NO_3$ system, ŞT. ZUCA and M. CONSTANTINESCU 161

Charge transfer by quantum tunneling across the separation interface of two media using perturbation formalism, A. CĂLUŞARU and M. APOSTOL 175

Chemiluminescent reactions, The principles, applications and trends of flow injection analysis for monitoring —, J. L. BURGUERA, M. BURGUERA and A. TOWNSHEND 879

β-(4-Chloro-3-methylbenzoyl)-acrylic acid with activated hydrocarbons under Friedel-Crafts conditions and some studies on the products, 1,4-Arylation of —, M. M. MOHAMED, M. A. El-HASHASH, I. ISLAM and O. A. ABO-BAKER 865

CN-traces determination based on its inhibitory effect, Contributions to the kinetical-analytical study regarding — (in German) GH. IONESCU, F. MATEI and AL. LUCA 1141

Cobalt and calcium soaps. III. Viscosity and surface tension studies in alcohols, Studies on the behaviour of —, R. P. VARMA and P. K. JAIN 1117

Cobalt(III) with acetylacetone derivatives, Spectrophotometric and derivatographic study on some new tetradentate mixed chelates of —, M. ABDEL SALAM El ABSY, GH. MARCU, J. ZSAKÓ and CS. VÁRHELYI 917

Coordination polynuclear compounds in Fe(III), Mn(II), Ni(II) systems, An analysis of thermal decomposition of —, E. SEGAL, M. BREZEANU, E. SAFARICA, L. PATRON and T. ROBU 137

Copolymerization. IV. Simultaneous cationic polymerization and radical terpolymerization, Alternating tendency in —, D. S. VASILESCU 575

Cyclodehydrations with phenyldichlorophosphite-dimethyl-formamide. A new convenient method for the synthesis of 1,3,4-oxadiazoles from diaroylhydrazines, C. I. CHIRIAC. 935

Dealkylations of secondary heptylbenzenes, Friedel-Crafts —, R. M. ROBERTS and L. W. ERLROD 761

Dibenzo[*c*, *e*] tricyclo $[5.3.0.0^{2,10}]$ deca-3,5,8-triene, a new dibenzo $(CH)_{10}$ hydrocarbon, Synthesis and pyrolysis of —, M. BANCIU, M. ELIAN, PHAN LE THUY, C. DRĂGHICI and E. CIORĂNESCU 19

Dimer structure in Coulson-Eisenberg model, On water —, E. S. KRYACHKO . . . 901

Dimethyldithioarsinato anion, $(CH_3)_2\ AsS_2^-$, Normal coordinate analysis of the vibrational spectrum of —, I. SILAGHI-DUMITRESCU, L. SILAGHI-DUMITRESCU and I. HAIDUC 911

2,4-Dioxo-1,2,3,4-tetrahydroquinazoline. I., Synthesis and biological activity of certain derivatives of —, A. N. OSMAN, M. KHALIFA, M. A. ISMAIL, A. E. OSSMAN and M. G. IBRAHIM 859

Dipole moment of Cu, Ag and Au atoms adsorbed on different tungsten planes, On the —, CR. CONŢESCU and M. I. VASS 59

Electrode processes, Investigation methods of the —, L. ONICIU and V. A. TOPAN 103

Electron acceptors V. Inter- and intramolecular charge transfer of amino-substituted pyridinium salts evidenced by electronic absorption spectra, Molecular complexes with aromatic cations as —, A. T. BALABAN and M. PARASCHIV 513

Electronegativity and the interelectronic repulsion energy in the vector model of the atom, The concept of —, C. I. LEPĂDATU 897

Electroreduction of nitrate ions in molten alkali nitrates, S. STERNBERG and T. VIŞAN 345

Emulsions by surface active agents, Stabilization of —, S. P. SINGH, M. MADHURI and P. BAHADUR 803

Enthalpies of combustion and formation of 3-amino-4-methoxyacetanilide and 3-(N-β-cyanoethyl)-amino-4-methoxyacetanilide, The —, I. CONTINEANU, DAN BREŢCANU and D. I. MARCHIDAN 55

Enthalpies of combustion and formation of *o*-phenylenediamine urea, and 2-hydroxy benzimidazole, The —, I. CONTINEANU, L. WAGNER, L. STĂNESCU and D. I. MARCHIDAN 205

Excess surface tension of binary liquid mixtures, R. MISHRA Fe(III)-3-hydroxypyridine N-oxide system, Study of the —, N. CALU, E. SAVIUC and T. POPOVICI . . 385

Fluorine in silicate rocks and minerals using zirconium-cyanine R. System, Spectrophotometric determination of —, S. A. KHAN and M. STONE 885

2-Furyl-3,1-benzothiazine-4(*H*)-thione, 2-furyl-4(3H)-quinazolinone and 2-furyl-3,1-benzoxazin-4(*H*)-one, Synthesis and reactions of —, A. ESSAWY 415

Gold by graphite furnace — Atomic absorption spectrometry with atomization under pressure, J. FAZAKAŞ 685

Gold by means of the ion pair $[AuI_4^-]$ $[(C_4H_9)_4N^+]$, Gravimetric determination of — (in Spanish), J. HERNÁNDEZ MÉNDEZ, A. ALONSO MATEOS, E. J. MARTÍN MATEOS and C. GARCÍA DE MARÍA 981

Hafnium (IV) with triazoline thione, Five- and six-coordinated complexes of —, S. K. SENGUPTA and S. KUMAR 741

Hardening structures developed in the system Portland cement-water, On the —, I. TEOREANU and V. MOLDOVAN 1091

Heterocycles. LI. Preparation of some 2-phenyl-5-R-thiazolo [3,2-*b*]-1,2,4-triazoles, Contribution to the study of some — (in French), I. SIMITI and A. MĂRIE 273

Hückel FORTRAN program for molecules including the elements from hydrogen to xenon except the transition metals, An extended —, Ş. MOLDOVEANU and V. DAVID 325

Hydrazides by a direct condensation reaction, A new synthesis of —, C. I. CHIRIAC . . 411

Hydrogen solubility in liquid hydrocarbons at atmospheric pressure, Determination of —, R. ENE, I. BICĂ and D. SĂNDULESCU 609

Indium determination in aluminium alloys by atomic absorption and emission spectrometry, A. J. ALLER . . . .

Interelectronic repulsion parameters, On a formula of Racah and Shadmi for the —, C. I. LEPĂDATU . . . .

Ion exchange equilibrium in water dimineralization process, Contributions to the calculation of —, V. COCHECI, L. NEGULESCU and F. KLEPP 37

Ionization potential, Semiempirical prediction of —, E. A. CASTRO and F. M. FERNANDEZ . . . .

Quantum theory of molecules. I. General formalism, Stationarity in —, Al. IVANOV and D. I. HERŢIA 243

Liquid membrane electrodes for benzoic acid determination, L. CAMPANELLA, T. FERRI, M. GABRIELLI 681

Lutidinic acid, Polarographic behaviour of —, L. CAMPANELLA and G. DE ANGELIS 973

Magnesium with Eriochrome black T, Ion exchange procedure for the elimination of interferences in the spectrophotometric determination of —, L. VLĂDESCU and A. ISUF 673

Microstructure of electroless deposited nickel in an ultrasonic field, R. VÎLCU and E. DIMITRIU 719

Mixed films of retinyl palmitate with lipids at the air-water interface, E. CHIFU and M. TOMOAIA-COTIŞEL 27

Molecular orbital calculations, Cation-anion combination reactions, S. EL-BASIL, B. ABD EL-FATTAH, M. M. EL-ENANY and N. BOULOS . . . .

Molten potassium nitrate, The cathodic reactions on silicon electrode in —, S. STERNBERG, I. LINGVAY and T. VIŞAN 1085

3-α-Napthayl-propenoyl carbonium ion (An intramolecular perturbation), On the cyclization of —, S. El-BASIL 557

Nickel (II) complexes with dibasic tridentate ONO donor ligands, New —, A. SYAMAL and B. K. GUPTA 927

Nickel electroless plating in ultrasonic field, R. VÎLCU and E. DIMITRIU 169

Nickel and zinc with hydrazine, Optical and magnetic studies of some heteronuclear complexes of —, V. MINCU, C. LEPĂDATU, M. GUŢUL, M. BREZEANU and I. JITARU 931

Nitrobenzenes by hydrogen. Transfer from cyclohexene, Pd/SiO_2-AlPO_4 catalyzed reduction of —, M. A. ARAMENDIA, V. BORAU, C. JIMENEZ and J. M. MARINAS 853

m-Nitrophenyl acetate in excited state, Reactivity of —, V. E. SAHINI, C. BENDIC and L. VIRAG 129

Optical properties of molten SnI_2, I. G. MURGULESCU, E. POPA and E. IVANA . . 799

Organic solvents by gas-liquid chromatography, A new route for determining the nonpolar solubility parameters of —, M. LECA 987

Oxalato-niobic complexes. II. Barium tris (oxalato) niobate, Thermal and structural investigation of some —, L. MARTA, M. ZAHARESCU and C. GH. MACAROVICI 87

5-Oxo-2-pyrrolines, Reactions of some —, A. I. HASHEM, M. E. SHABAN and A. F. El-KAFRAWY 835

Oxygen orbitals in SiO_2, Effective hybridization of —, A. VOLCEANOV and A. BĂRBULESCU 1099

Pair potential. Evaluation of cyrstal properties, On generalized — - J. D. PANDEY and R. P. PANDEY 211

Palladium (II) and gold (III) from solution on inorganic electron exchangers, On the extraction of —, A. KALYUZHNYI, V. MILYUTIN, J. FAZAKAS and M. NEGOIU 503

Phase equilibrium, Application of Kuhb-Tucker conditions to the problem of chemical and —, D. GEANA and F. DANES 1009

Phenolys and their corresponding aroxyls, New 2,4,6-trisubstituted —, J. HERDAN, G. IORDACHE, N. NEGOIŢĂ, N. GRECU and A. T. BALABAN 69

Phenothiazines and their oxidation products, Synthesis of some substituted trifluoromethyl —, M. ANAND, S. P. GUPTA, A. R. GOYAL and R. L. MITAL . . . 939

Phenyl-mercuric ion with diazoaminobenzene, Extraction, complexing and determination of —, A. F. DĂNEŢ and A. M. BERCARU 459

Photochemical ring contraction of 3-diazo-dibenzo [*f*, *i*] bicyclo [3.2.2] nona-6 8-dien-2-one, M. BANCIU 769

Photohydrogen, Model system to obtain —, T. ONCESCU, M. CONTINEANU and S. G. IONESCU 95

Photoketonization of some enolizable β-ketoesters in solution, Influence of substituents on the —, I. PETKOV and P. MARKOV 847

Phthalocyanine, Oxidation of methanol on copper —, N. I. IONESCU and D. POPESCU 481

Plant growth regulating optically active acetic acid derivatives, Quantitative structure-activity relations with the MTD-procedure for —, A. CHIRIAC, V. CHIRIAC, S. HOLBAN, I. MOŢOC and Z. SIMON 561

Plasma-induced polymerization. VII. Some characteristics of this new method of polymer synthesis, CR. I. SIMIONESCU and B. C. SIMIONESCU 141

Polarization behaviour of Armco iron in ahydrous solution of R—OH+HCl, S. STERNBERG and V. BRÂNZOI 217

Polichelates on poliamidic support, The mechanochemical synthesis of some —, CR. SIMIONESCU, CL. VASILIU-OPREA and CL. NEGULIANU 1005

Polyesters and polyamides containing phosphorus in the chain, Study of hydrolytic behaviour of certain — (in French), FL. POPESCU, L. ROSESCU, S. PERCEC and O. PETREUŞ 291

Polyethylene glycol dimethacrylates. IV. Study of the polymerization process of polyethylene glycol dimethacrylate, Synthesis and polymerization of —, GH. HUBCA, CR. OPRESCU, GH. DRĂGAN and M. DIMONIE 433

Polyethylene glycol dimethacrylates. V. Analysis of kinetic data obtained at polymerization based on topoenergetic principles, Synthesis and polymerization of —, GH. DRĂGAN, GH. HUBCA, CR. OPRESCU and M. DIMONIE 585

Polyethylene glycol dimethacrylates. VI. Study of copolymerization process of polyethylene glycol dimethacrylates with styrene, Synthesis and polymerization of —, GH, HUBCA, C. OPRESCU, A. CARACHEORGHEOPOL, H. CĂLDĂRARU, D. RACOTI and M. SIMONIE 659

Polyethylene glycol dimethacrylates. VII. E SR study of ethylene glycol dimethacrylate-Styren copolymers, Synthesis and polymerization of — , A. CARAGHEORGHEOPOL, M. CĂLDĂRARU, GH. HUBCA, CR. OPRESCU and M. DIMONIE 969

Polymers, ^{1}H-NMR spectra of some flame-retardant —, S. PERCEC, A. NATANSOHN and F. POPESCU 775

Polynuclear complexes $[Fe_2^{III}M^{II}Cl_{12}]^{4-}$ of manganese (II) and cobalt (II), Electronic spectra, magnetic properties and structure of —, G. MUNTEANU, C. I. LEPĂDATU, L. PATRON and M. BREZEANU 727

Polystyrene in benzene solutions on the, α, α′-diphenyl-β-picrylhydrazyl (DPPH) radical, Spectral study of the influence of —, C. GHIRVU, A. ONU and GH. IONIŢA 1029

Propylene oxidation on MoO_3/SiO_2 and Bi_2O_3/SiO_2 catalysts, N. I. IONESCU and M. CĂLDĂRARU 75

Publications of Professor I. G. Murgulescu 7

2(1H) Pyridones and pyridines, Synthesis and reactions of polysubstituted —, M. A. HASSAN, E. A. SOLIMAN and A. A. HAMED 963

Pyrimidinium-ylids. III. Synthesis of carbanion-disubstituted pyrimidinium-ylids (in French), F. GEORGESCU, E. I. GEORGESCU, F. CHIRALEU and I. ZUGRĂVESCU 635

Pyrolysis of some alkylbenzenes, Kinetic studies of the —, D. K. BANERJEE, V. MATEI and I. VÂNTU 621

Pyrylium salts with an annelated dibenzo *[f, i]* bicyclo [3.2.2.] nona-6,8-diene skeleton (oxonia-hornotripticenes) and their reactions with nucleophiles, Synthesis of —, M. BANCIU, A. T. BALABAN, C. DRĂGHICI and R. VLAD 1037

Reactant-catalyst interaction parametrisation, N. DOCA, F. KLEPP and E. SEGAL 365

Rearrangements of $(CH)_7^+$ ions, M. W. TAUSCH and P. J. PLATH 953

Reductimetry, Kinetics of the reaction between oxygen and tin(II) : stabilization of Sn (II) solutions and their utilization in —, J. HERNANDEZ MENDEZ, G. LOPEZ CUETO, A. ALONSO MATEOS and C. SANCHEZ BURON 491

Ru (III) catalysed oxidation of aliphatic diols and cyclanols by phenyliodoso acetate, Kinetics and mechanism of —, S. C. PATI and B. R. DEV 523

Salicilates catalysed by activated barium hydroxides, Hydrolysis of n-alkyl- —, A. GARCIA RASO, J. V. SINISTERRA y J. M. MARINAS 1047

Solvating model, The generalization of Beveridge-Schnuelle —, Ș. MOLDOVEANU and V. DAVID 471

Stainless steel, type W. 1.4541 in R—OH + HCl anhydrous solution, Polarization behaviour of —, S. STERNBERG and V. BRANZOI 1003

Steric constants, Testing the geometrical meaning of Taft type —, I. MOȚOC and A. T. BALABAN 735

Steric effects in effector — receptor interactions. The steric difference method and applications (in German), R. VÂLCEANU and I. MOȚOC 225

Strontium soaps and studies of their viscosity in aqueous isopropanol, Characterization of —, R. P. VARMA and R. DAYAL 257

Surface mobility of surfactant solutions. X. Marangoni flow against gravity forces, E. CHIFU and I. STAN 703

Surface oxidation of some sulphurous minerals by the hypochlorite ion, Z. FINTA, E. CHIFU, E. GAVRILA and M. SALAJAN 191

Surface properties of solutions of lithium nitrate in some molten hydrates, S. K. JAIN 713

Sydnones ; Reactions of —, B. V. BADAMI and G. S. PURANIK 281

Ternary alloys containing Co(II), Ni(II) and Cu(II), Analysis of —, A. F. SHOUKRY, A. I. ABDEL-RAHMAN and N. T. ABBEL-GHANI 993

Tertbutylbenzene cracking, The $AlPO_4$ and related systems as catalysts in organic reactions. I., P. M. DEYA, A. COSTA, J. V. SINISTERRA and J. M. MARINAS 401

Thermal conductivity in $Ca(NO_3)_2 \cdot 4H_2O - nH_2O$ system, S. STERNBERG and A. MASCAȘ 147

Thermal conductivity and thermal diffusivity of gases by the classical procedure of the transient hot wire method, Absolute measurement of —, R. VÎLCU, A. CIOCHINĂ and GH. VASU 313

Thermal decomposition of the 2,2′-bipyridine and 4,4′-bipyridine compounds with some bismuth, antimony and tin chlorides, D. M. CZAKIS-SULIKOWSKA and J. RADWANSKA-DOCZEKALSKA 1105

Thermodynamic of multicomponent electrolyte solutions. III. Ammonium persulfate activity coefficients in quaternary system, in solubility measurements, R. VÎLCU and F. IRINEI 155

Thermogalvanic cells with aqueous rubidium chloride solutions (in German), E. CONSTANTINESCU and H. DENGEL 47

Thermogravimetric data. XV. Thermal decomposition of $[Co(en)_2$ (pyridine) $Br]\ X_2$ type complexes, Kinetic analysis of —, J. ZSAKÓ, GH. MARCU and M. VÁRHELYI 815

1,3,4-Thiadiazole derivatives with antibacterial activity, Synthesis of some —, A. E. ABDEL-RAHMAN, A. M. MAHMOUD, H. A. El-SHERIEF and A. G. GHATTAS 781

Thiamine, Amperometric determination of —, C. CALU and E. DONIGA 667

Thiosemicarbazones as ligands and evaluation of their virus inhibitory behaviour. I. Some transition metal complexes of substituted isatin β-thiosemicarbazones, R. P. GUPTA and A. K. SRIVASTAVA 393

Titanium with ion exchange resins. I. Cation exchange behaviour, Utilization of chromotropic acid in separation of —, L. VLĂDESCU and A. HARLES 301

Titanium with ion exchange resins. II. Anion exchange behaviour, Utilization of chromotropic acid in separation of —, L. VLĂDESCU and A. HARLES 453

Titanium with ion exchange resins, Utilization of Tiron in the separation and concentration of —, L. VLĂDESCU and S. GHINEA 569

Triaryl-*s*-triazoles from diaroylhydrazines, A new method for the preparation of —, C. I. CHIRIAC 645

as-Triazine derivatives with potential therapeutic action. XVI. Synthesis of 5(ω-carboxyalkyl) mercapto-6-azauridines, C. CRISTESCU and S. SITARU 943

Tribute to Professor I. G. Murgulescu on his 80th birthday, 27th January 1982 3

Vanadium (V) chelates of N-substituted phenylhydroxylamines. A spectrophotometric study, J. P. SHUKLA 751

Vinyl monomer complexes. I. The complexes of acrylonitrile with some inorganic salts, S. A. K. LODHI and A. R. KHAN 509

Viscosity of liquids with quasispherical molecules. Checking Eyring's equation, I. G. MURGULESCU and M. ȘERBAN 597

Viscosity of the mixed system tetrahydrofuran-water, On the —, (in French) O. LANDAUER, C. MATEESCU, O. IULIAN and G. COSTEANU 603

(Z)-9-tricosene (Muscalure), Synthesis of —, L. POP and F. HODOȘAN 545

Zirconium by chemical enrichment, Quantitative spectrographic estimation of —, N. BARAKAT, F. ABOU El-NOUR and N. SHAHEEN 261

NOTE POUR LES AUTEURS

La Revue Roumaine de Chimie publie des articles en anglais français, russe, allemand ou espagnol. Les auteurs sont priés d'envoyer des articles et des comptes rendus inédits.

Les manuscrits seront dactylographiés à double interligne. La bibliographie, les tableaux et la légende des figures seront placés après le texte.

Si l'article fait partie d'une série numérotée, la partie précédente sera donnée comme première référence.

Chaque article sera précédé d'un résumé comprenant quinze lignes au maximum.

Les références bibliographiques dans le texte seront faites par des exposants sans parenthèses et paraîtront à la fin de l'ouvrage.

Les publications périodiques mentionnées dans la bibliographie seront présentées suivant les prescriptions internationales : le nom de l'auteur précédé de l'initiale du prénom, le titre du périodique abrégé conformément à « Chemical Abstracts » et souligné par une ligne, le numéro du tome indiqué par des chiffres arabes et souligné par deux lignes, suivi de la première page de l'article ; à la fin, l'année de la parution sera placée entre parenthèses. Le numéro de la revue ne sera pas indiqué si les pages du volume sont numérotées consécutivement.

Les textes des livres ou traités incluеront : le nom des auteurs, l'initiale du prénom, le titre du livre entre guillemets et sans être souligné, le numéro du tome précédé par l'abréviation « vol. » (ou « Bd. »), le numéro de l'édition, les éditions (the publisher), la localité de la parution du livre, l'année de la parution et la page de la référence précédée(s) par l'abréviation « p » (ou « S »).

Les brevets seront indiqués comme suit : l'auteur ou la firme, le pays et le numéro du brevet, la date et la revue *(Chem. Abstr.)*. Par ex. : M. Jones (to Union Carbide Co.), Brit. Pat. 601 238, 2 sept. 1959 ; cf. *Chem. Abstr.*, **54**, 12808 (1960).

Si la référence n'a pas été lue en original, on indiquera aussi la revue de références consultée.

Les diagrammes seront tracés à l'encre de Chine sur papier calque. Les tableaux et les figures (en nombre strictement nécessaire), ainsi que les courbes dans les figures seront numérotés par des chiffres arabes. Leur explication sera donnée dans la légende des figures. Prière de ne pas inscrire les mêmes données dans les tableaux et les figures. Chaque tableau aura un titre. On indiquera dans le texte la place approximative des tableaux et des figures. Les formules chimiques seront incluses dans le texte ; en outre, elles seront transcrites sur papier calque, à l'encre de Chine.

Les auteurs sont priés d'indiquer les caractères italiques (en soulignant les lettres au crayon), ainsi que tout autre caractère spécial ; les préfixes *ortho, meta, para, cis, trans,* etc. seront soulignés pour indiquer leurs caractères italiques et ne seront jamais écrits avec des majuscules.

Aucune correction à la main ne sera admise sur le manuscrit. Les corrections seront tapées à la machine. Les lettres grecques ou d'autres symboles spéciaux seront insérés à la main à l'encre clairement.

Le manuscrit sera signé par l'auteur.

Le titre-courant aura 50 lettres au maximum.

L'entière responsabilité du contenu des articles appartient aux auteurs.

Sur demande on peut obtenir une note plus complète.

PRINTED IN ROMANIA

TRAVAUX PARUS AUX ÉDITIONS DE L'ACADÉMIE DE LA RÉPUBLIQUE SOCIALISTE DE ROUMANIE

ELENA CEAUŞESCU, **Noi cercetări în domeniul compuşilor macromoleculari** (Nouvelles recherches dans le domaine des composés macromoléculaires), 1981, 536 p.

I. G. MURGULESCU, RODICA VÎLCU, **Introducere în chimia fizică, Vol. III. Termodinamica chimică** (Introduction à la chimie physique, Vol. III, Thermodynamique chimique), 1982, p. 624.

I. G. MURGULESCU, J. PĂUN, **Introducere în chimia fizică. Vol. I.3. Nucleul atomic, reacţii nucleare, particule elementare** (Introduction à la chimie physique. Vol. I.3. Noyau atomique, réactions nucléaires, particules élémentaires), 1982, 606 p.

ELENA JERCAN, **Analiza cromatografică** (Analyse chromatographique), 1982, 286 p.

I. G. MURGULESCU, TATIANA ONCESCU, E. SEGAL, **Introducere în chimia fizică. Vol. II.2. Cinetică chimică şi cataliză** (Introduction à la chimie physique. Vol. II.2. Cinétique chimique et catalyse), 1981, 1024 p.

V. DRĂGUŢAN, A. T. BALABAN, M. DIMONIE, **Metateza olefinelor şi polimerizarea prin deschidere de inel a cicloolefinelor** (La métathèse des oléfines et la polymérisation par ouverture annulaire des cyclooléfines), 1981, 254 p.

LYDIA-MARIA VAICUM, **Epurarea apelor uzate cu nămol activ. Bazele biochimice** (L'épuration des eaux résiduelles à boue active. Les bases biochimiques), 1981, 218 p.

I. GĂLĂŢEANU, **Procese şi metode radiochimice în energetica nucleară** (Processus et méthodes radiochimiques dans l'énergétique nucléaire), 1981, 234 p.

O. IORDACHE, **Procese polistocastice aplicate în fenomenele de transfer** (Processus polystochastiques appliqués aux phénomènes de transfert), 1981, 187 p.

CR. SIMIONESCU, VALERIA GORDUZA, **Polimeri biocompatibili şi biologic activi** (Polymères biocompatibles et biologiquement actifs), 1980, 497 p.

ELENA CEAUŞESCU, **Polimerizarea stereospecifică a izoprenului** (La polymérisation stéréospécifique de l'isoprène), 1979, 307 p.

M. FLORESCU, **Metode ştiinţifice în dezvoltarea industriei chimice moderne** (Méthodes scientifiques dans le développement de l'industrie chimique moderne), 1979, 256 p.

A. T. BALABAN, I. GĂLĂŢEANU, G. GEORGESCU, LIGIA SIMIONESCU, **Compuşi marcaţi şi radiofarmaceutici cu aplicaţii în medicina nucleară** (Composés marqués et radiopharmaceutiques à application en médecine nucléaire), 1979, 495 p.

CONST. GH. MACAROVICI, **Analiza chimică cantitativă anorganică** (L'analyse chimique quantitative inorganique), 1979, 457 p.

I. G. MURGULESCU, E. SEGAL, **Introducere în chimia fizică. Vol. II.1. Teoria molecular cinetică a materiei** (Introduction à la chimie physique. Vol. II.1. La théorie moléculaire-cinétique de la matière), 1979, 1036 p.

S. STERNBERG, FL. DANEŞ, **Termodinamica chimică aplicată** (La thermodynamique chimique appliquée), 1978, 400 p.

I. G. MURGULESCU, V. EM. SAHINI, **Introducere în chimia fizică. Vol. I.2. Structura şi proprietăţile moleculelor** (Introduction à la chimie physique. Vol. I.2. La structure et les propriétés des molécules), 1978, 604 p.

I. ZUGRĂVESCU, MAGDA PETROVANU, **N-ylid chemistry**, coédition avec McGraw-Hill International Book Company, U.S.A., 1977, 396 p.

I. G. MURGULESCU, **Introducere în chimia fizică. Vol.I.1. Atomi, molecule, legătură chimică** (Introduction à la chimie physique. Vol. I.1. Atomes, molécules, liaison chimique), 1976, 560 p.

ELENA CEAUŞESCU, **Research work on synthesis and characterization of macromolecular compounds. Contributions.** 1974, 251 p.

CR. SIMIONESCU, VIORICA RUSAN, V. POPA, **Chimia algelor marine** (La chimie des algues marines), 1974, 212 p., 1 pl.

1983 APR 1

I. P. Informaţia c. 2464

43 426

Lei 40

$ 70 (pour un abonnement annuel)